

# Proceedings of the IV Ibero-American Conference on Smart Cities (ICSC-CITIES 2021)

Cancun, Mexico, November 29th to December 1st



## **Editors:**

Ponciano Jorge Escamilla-Ambrosio

Luis Hernández-Callejo

Sergio Nesmachnow

Pedro Moreno

Diego Rossit



CIUDADES INTELIGENTES TOTALMENTE INTEGRALES, EFICIENTES Y SOSTENIBLES



Elaborated by the organizing committee of the IV Ibero-American Conference on Smart Cities (ICSC-CITIES 2021).

**Disclaimer:** The information in this book is true and complete to the best of the editor's knowledge. All recommendations are made without a guarantee on the part of the editors. The editors disclaim any liability in connection with the use of this information.

**Editors:** Ponciano J. Escamilla-Ambrosio, Luis Hernández-Callejo, Sergio Nesmachnow, Pedro Moreno, Diego Rossit.

How to cite this book:

Escamilla-Ambrosio, P.J., Hernández-Callejo, L., Nesmachnow, S., Moreno, P. & Rossit, D. (Eds.). (2021). *Proceedings of the IV Ibero-American Conference on Smart Cities*. CITIES.

**ISBN:** 978-607-99960-0-0



This work is licensed under a Creative Commons Attribution 4.0 International License.

## ABOUT THE EVENT

A Smart City is a framework composed mainly of Internet of Things systems and Information and Communication Technologies (ICT), integrated to develop, implement and promote sustainable development practices and face the challenges of urbanization.

The Ibero-American Conference on Smart Cities (ICSC-CITIES) is a discussion forum that aims to create synergies among different research groups to promote the development of Smart Cities, and contribute to their knowledge and integration in different scenarios. The conference is held yearly since 2018 and is sponsored by the Ibero-American Program of Science and Technology for Development (CYTED). The first and the second editions, i.e., 2018 and 2019, were celebrated in Soria, Spain. The third edition was celebrated virtually, but hosted by the Costa Rica Institute of Technology.

The Fourth Ibero-American Conference on Smart Cities (ICSC-CITIES 2021) was held in a hybrid way (face-to-face and virtual) from November 29th to 30th and December 1st, 2021, in Cancun, Quintana Roo, Mexico, with the sponsorship of the Ibero-American Program of Science and Technology for Development (CYTED) and the support of the National Polytechnic Institute through the Computer Research Center (CIC) and the Cancun Regional Development and Linkage Center (CVDR-Cancun). Seventy technical presentations were given by researchers from 20 different countries during the ICSC-CITIES 2021. Fifteen papers were included as posters. Papers were divided into four topics, i.e., Governance and Citizenship, Mobility and IoT, Infrastructures, Energy and the Environment and Energy Efficiency. Those contributions were selected from a pool of 112 submitted papers, yielding an acceptance rate of 75%.

ICSC-CITIES 2021 program also included the participation of government representatives from several American countries. More specifically, two panel discussion sessions were held. The first one was related to Governance and Sustainability in Smart Cities. In this panel participated Paola Vega Castillo, Minister of Science, Innovation, Technology and Telecommunications of the Republic of Costa Rica, Pablo De Chiara, Minister of Science and Technology of the Government of the Province of Córdoba, Argentina, Marco A. Moreno Ibarra, Director of the Computer Research Center of the National Polytechnic Institute, Mexico, and Juan Leonardo Espinoza, Vice Chancellor of the University of Cuenca, Ecuador. A second discussion panel was held which was related to the Role of Smart Tourist Destinations and Sustainability within the Smart Cities framework. In this panel participated Alejandro del Amo, CEO of Abora Solar, Oscar Torrecilla Representative of the Quintana Roo Office of CANIETI, Margarita Carbajal Carmona, National President of the Federation of Tourism Entrepreneurs, A.C. (FETUR), and Marco Antoni Bravo Fabian, General Director of the Quintanarroense Institute of Innovation and Technology (IQIT).

## COMMITTEE

### General Chairs

Luis Hernández Callejo, Universidad de Valladolid, Spain

Sergio Nesmachnow, Universidad de la República, Uruguay

### Organizing Committee

Luis Hernández Callejo, Universidad de Valladolid (España)

Sergio Nesmachnow, Universidad de la República (Uruguay)

Ponciano Jorge Escamilla-Ambrosio, Centro de Investigación en Computación, Instituto Politécnico Nacional (México)

Marco Antonio Moreno Ibarra, Centro de Investigación en Computación, Instituto Politécnico Nacional (México)

Hirma Valdez Flores, Centro de Vinculación y Desarrollo Regional, Instituto Politécnico Nacional (México)

Carlos Meza Benavides, Instituto Tecnológico de Costa Rica (Costa Rica)

Ángel L. Zorita, Universidad de Valladolid (España)  
Adriana Correa, Universidad de Valladolid (España)  
Epifanio Díez, Universidad de Valladolid (España)  
Manuel A González, Universidad de Valladolid (España)  
Jesús M. Vegas, Universidad de Valladolid (España)  
Teodoro Calonge, Universidad de Valladolid (España)  
Oscar Duque, Universidad de Valladolid (España)  
Lilian J. Obregón, Universidad de Valladolid (España)

### **Publication Chairs**

Luis Hernández Callejo, Universidad de Valladolid, Spain  
Sergio Nesmachnow, Universidad de la República, Uruguay

### **Submission and Conference Management Chair**

Santiago Iturriaga, Universidad de la República, Uruguay

### **Track Chairs:**

Adriana	Correa-Guimaraes	Universidad de Valladolid
Alfredo	Cristobal-Salas	Universidad Veracruzana
Ana	Ruiz	San Jorge University
Ana Carolina	Olivera	Universidad Nacional de Cuyo
Andrés Adolfo	Navarro Newball	Pontificia Universidad Javeriana, Cali
Bernabe	Dorronsoro	University of Cadiz
Daniel	Rossit	Departamento Ingeniería, Universidad Nacional del Sur
Diego Gabriel	Rossit	DI, Universidad Nacional del Sur (UNS) and CONICET
Fabian	Castillo Peña	Universidad Libre, Cali
Irene	Lebrusán	Harvard University
Jamal	Toutouh	Massachusetts Institute of Technology
Jorge	Mírez	Universidad Nacional de Ingeniería
Lorena	Parra	Universitat Politècnica de València
Luis	Tobon	Pontificia Universidad Javeriana Cali
Luis Manuel	Navas-Gracia	Universidad de Valladolid
Luiz Angelo	Steffenel	Université de Reims Champagne-Ardenne
Óscar	Duque-Pérez	University of Valladolid
Paulo	Gondim	Universidade de Brasilia
Pedro	Moreno	Universidad Autónoma del Estado de Morelos
Ponciano Jorge	Escamilla-Ambrosio	Centro de Investigación en Computación, Instituto Politécnico Nacional
Renzo	Massobrio	Universidad de la República
Roberto	Villafafila	Universitat Politècnica de Catalunya
Sara	Gallardo-Saavedra	Universidad de Valladolid
Teodoro	Calonge	Universidad de Valladolid
Víctor	Alonso Gómez	Universidad de Valladolid

**Program Committee:**

Abigail	Parra Parra	Universidad Autónoma del Estado de Morelos
Adrian	Toncovich	Universidad Nacional del Sur
Adriana	Correa-Guimaraes	Universidad de Valladolid
Agustín	Laguarda	Universidad de la República, Laboratorio de Energía Solar
Alberto	López Casillas	Diputación de Ávila
Alejandro	Otero	FIUBA / CSC-CONICET
Alejandro	Paz Parra	Pontificia Universidad Javeriana - Cali
Alessandra	Bussador	UDC
Alex	Cano	Universidad de Quintana Roo
Alexander	Shemetev	VSE
Alexander	Vallejo Díaz	Santo Domingo Institute of Technology
Alfredo	Cristobal-Salas	Universidad Veracruzana
Alice	Monteiro	UFMG
Alicia	Martínez	CENIDET
Ana	Ruiz	San Jorge University
Ana Carolina	Olivera	Universidad Nacional de Cuyo
Andrés Adolfo	Navarro Newball	Pontificia Universidad Javeriana, Cali
Andres Felipe	Fuentes Vasquez	Pontificia Universidad Javeriana
Ángel L	Zorita Lamadrid	Universidad de Valladolid
Angela	Ferreira	Polytechnic Institute of Bragança
Antonio	Mauttone	Universidad de la República
Antonio	Muñoz	University of Malaga
Armando	Huicochea	Research center for Engineering and Applied Science, Autonomous University of Morelos State
Belén	Carro	Universidad de Valladolid
Bernabe	Dorrnsoro	University of Cadiz
Bouras	Abdelkarim	Electromechanical Systems Laboratory, Department of Electromechanical
Carlos	Grande	Universidad Centroamericana "José Simeón Cañas"
Carlos	Meza Benavides	Anhalt University of Applied Sciences
Carlos	Torres	CENIDET
Carmen	Vásquez	UNEXPO
Carolina	Solis Maldonado	Universidad Veracruzana
César	Varela	CENIDET
Christian	Cintrano	Universidad de Málaga
Claudio	Paz	UTN FRC
Claudio	Risso	InCo - Facultad de Ingeniería - Universidad de la República
Cleonilson	Protasio	Federal University of Paraíba
Cristina	Sáez Blázquez	Department of Cartographic and Land Engineering, University of Salamanca, Higher Polytechnic School of Avila
Daniel	Morinigo-Sotelo	Universidad de Valladolid
Daniel	Rossit	Departamento de Ingeniería, Universidad Nacional del Sur

Daniel H.	Stolfi	University of Luxembourg
David	Peña Morales	UNIVERSITY OF CADIZ
Deyslen	Mariano	Instituto Tecnológico de Santo Domingo
Diana	Sánchez-Partida	UPAEP
Diego	Arcos-Aviles	Universidad de las Fuerzas Armadas ESPE
Diego	González-Aguilera	University of Salamanca
Diego Alberto	Godoy	Universidad Gastón Dachary
Diego Gabriel	Rossit	DI, Universidad Nacional del Sur (UNS) and CONICET
Edgardo Aníbal	Belloni	Universidad Gastón Dachary
Edith Gabriela	Manchego Huaquipaco	Universidad Nacional de San Agustín de Arequipa
Eduardo	Fernández	Universidad de la República, INCO
Elina	Pacini	ITIC - Universidad Nacional de Cuyo
Emmanuel	Millán	Universidad Nacional de Cuyo
Enrique	González	Universidad de Salamanca
Enrique Gabriel	Baquela	GISOI - F.R.S.N. - U.T.N.
Esteban	Mocskos	UBA
Fabián	Castillo Peña	Universidad Libre, Cali
Fermin	Armenta	Centro de Enseñanza Técnica y Superior (CETYS Universidad)
Fernando	Velez Varela	Universidad Libre seccional Cali, Universidad Santiago de Cali / Universidad del Cauca
Francisco	Valbuena	Univesridad de Valladolid
Franco	Robledo	Facultad de Ingenier UDELAR
Gabriel	Bayá	Facultad de Ingeniería UDELAR
Gilberto	Martínez	CIC-IPN
Gina Paola	Maestre Gongora	Universidad Cooperativa de Colombia
Harrison Oluwaseyi	Ogunkalu	Niğde Ömer Halisdemir Üniversitesi
Ignacio	De Godos Crespo	Universidad de Valladolid
Ignacio	Martín Nieto	Universidad de Salamanca, Departamento de Ingeniería Cartográfica y del Terreno, Escuela Politécnica Superior de Ávila
Ignacio	Turias	Universidad de Cádiz
Irene	Lebrusán	Harvard University
Ivett	Zavala Guillén	Centro de Investigación Científica y de Educación Superior de Ensenada
Jamal	Toutouh	Massachusetts Institute of Technology
Javier	Rocher	Universitat Politècnica de València
Jennifer	Kim	University of Mons
Joao	Coelho	Instituto Politécnico de Bragança
Jonathan	Muraña	UDELAR
Jorge	Caramés	UTE
Jorge	Mírez	Universidad Nacional de Ingeniería
Jorge	Nájera	Centro de Investigaciones Energéticas, Medioambientales y Tecnológicas
Jorge	Pérez Martínez	Universidad de Concepción, Chile
Jorge Mario	Cortés-Mendoza	South Ural State University

José	Aguerre	Facultad de Ingeniería, Universidad de la República Uruguay
Jose	Lizardi	Autonomous University of Mexico City
José Alberto	Hernández	Universidad Autónoma del Estado de Morelos
José Ángel	Morell Martínez	UMA
José Antonio	Martín-Jiménez	Universidad de Salamanca, España
José Antonio	Ferrer	CIEMAT
José-Ramón	Aira	Universidad Politécnica de Madrid
Juan	Chavat	Universidad de la República
Juan	Espinoza	Universidad de Cuenca
Juan	Pavón	Universidad Complutense de Madrid
Juan	R. Coca	Universidad de Valladolid
Juan Francisco	Cabrera Sánchez	Universidad de Cádiz
Juan José	Tarrio	CNEA
Leonardo	Cardinale	Instituto Tecnológico de Costa Rica
Lilian	Obregón	Universidad de Valladolid
Lorena	Parra	Universitat Politècnica de València
Lucas	Iacono	Know-Center GmbH
Lucas	Mohimont	Université de Reims
Luis	García	Universidad de Concepción
Luis	Hernández Callejo	Universidad de Valladolid
Luis	Marrone	UNLP
Luis	Tobon	Pontificia Universidad Javeriana Cali
Luis Bernardo	Pulido-Gaytan	CICESE Research Center
Luis G.	Montané Jiménez	Universidad Veracruzana
Luis Manuel	Navas-Gracia	Universidad de Valladolid
Luis Omar	Jamed Boza	Universidad Veracruzana
Luis Ricardo	Delgado Cortés	CIATEQ (Centro de Investigación y Asesoría Técnica del Estado de Querétaro)
Luisena	Fernández	LUZ
Luiz Angelo	Steffenel	Université de Reims Champagne-Ardenne
Manuel	González	Universidad de Valladolid
Marcela	Quiroz Castellanos	Instituto Tecnológico de Ciudad Madero
Marcin	Seredynski	E-Bus Competence Center
Mariano	Frutos	Department of Engineering, Universidad Nacional del Sur and CONICET
Mario	Vignolo	Universidad de la República, Uruguay
Marta	Pons Nieto	University of the Balearic Islands
Martín	Draper	Universidad de la República
Mauro	D'Angelo	Facultad de Ingeniería - UdelaR
Melva Inés	Gómez Caicedo	Fundación Universitaria Los Libertadores
Mercedes	Gaitán	Universidad Konrad Lorenz
Miguel	Davila	Universidad Politécnica Salesiana
Mónica	Alonso	University Carlos III de Madrid
Mónica	Montoya Giraldo	CIDET

Mónica Fátima	Díaz	Universidad Nacional del Sur y PLAPIQUI UNS-CONICET, Argentina
Neiel Israel	Leyva Santes	Barcelona Supercomputing Center - Centro Nacional de Supercomputación
Nestor	Rocchetti	Facultad de Ingeniería, Universidad de la República, Uruguay
Noelia	Uribe-Pérez	Tecnalia Research & Innovation
Noelia Soledad	Pinto	UTN FRRe
Norela Vanessa	Mora Ceron	Universidad Politécnica de Valencia
Olalla	García Pérez	Universidad Europea de Madrid
Óscar	Duque-Pérez	University of Valladolid
Óscar	Izquierdo	CEDER-CIEMAT
Pablo	Monzón	Universidad de la República, Uruguay
Pablo	Rodríguez-Bocca	Universidad de la República, Uruguay
Pablo	Vidal	Universidad Nacional de Cuyo
Pablo Daniel	Godoy	ITIC - Universidad Nacional de Cuyo
Pablo Javier	Vidal	Universidad Nacional de Cuyo - Consejo Nacional de Investigaciones Científicas y Técnicas
Patricia	Ruiz	Universidad de Cádiz
Paul	Ayala	Universidad de las Fuerzas Armadas
Paula	de Andrés Anaya	Escuela Politécnica Superior de Ávila (USAL)
Paulo	Gondim	Universidade de Brasilia
Pedro	Curto	Universidad de la República
Pedro	Moreno	Universidad Autónoma del Estado de Morelos
Pedro	Piñeyro	Facultad de Ingeniería - Universidad de la República
Ponciano Jorge	Escamilla-Ambrosio	Centro de Investigación en Computación, Instituto Politécnico Nacional
Rallou	Taratori	University of Mons
Ramiro	Martins	Polytechnic Institute of Bragança
Raúl	Luna	Universidad Veracruzana
Raúl Alberto	López Meraz	Universidad Veracruzana
Renato	Andara	Universidad Nacional Experimental Politécnica Antonio José de Sucre
Renzo	Massobrio	Universidad de la República
Rhonmer	Pérez	UNEXPO
Roberto	Villafafila	Universitat Politècnica de Catalunya
Rodrigo	Alonso-Suárez	Universidad de la República, Laboratorio de Energía Solar
Rodrigo	Porteiro	Udelar
Santiago	Iturriaga	Universidad de la República, Uruguay
Sara	Gallardo-Saavedra	Universidad de Valladolid
Saúl	Esquivel García	CIATEQ
Sergio	Nesmachnow	Universidad de la República, Uruguay
Sesil	Koutra	UMONS
Silvia	Soutullo	CIEMAT
Susana	del Pozo	University of Salamanca
Teodoro	Calonge	Universidad de Valladolid
Teresa	Batista	Universidade de Évora

Tiago	Carneiro Pessoa	INRIA
Vanessa	Guimarães	CEFET/RJ
Vicente	Canals	Universidad de las Islas Baleares
Vicente	Leite	Instituto Politécnico de Bragança
Víctor	Alonso Gómez	Universidad de Valladolid
Víctor Manuel	Padrón Nápoles	Universidad Europea de Madrid
Yamila Soledad	Grassi	Universidad Nacional del Sur y PLAPIQUI UNS-CONICET, Argentina
Yuri	Molina	UFPB
Zacharie	De Greve	Power electrical engineering department, University of Mons

## PROGRAM

ICSC-CITIES 2021 took place simultaneously in more than 12 countries throughout Latin America, Spain, and Portugal. To facilitate the attendance of students, researchers and professionals from these countries, the event was scheduled in such a way that it was in a suitable period of the day for everyone. The conference program is shown below at the local time of the hosting institution (UTC-5).

### Monday, November 29th

Hour (UTC-5)	Activity	Speaker	
8:00 a 8:30	Opening Ceremony Moderator Lic. Hiram Valdez Flores	Dr. Heberto Antonio M. Balmori Ramírez (Virtual)	Secretario de Investigación y Posgrado del Instituto Politécnico Nacional
		Dr. Marco Antonio Moreno Ibarra (Virtual)	Director del Centro de Investigación en Computación del Instituto Politécnico Nacional
		Lic. Hiram Valdez Flores	Director CVDR Cancún
		Ing. Pablo De Chiara	Ministro de Ciencia y Tecnología del Gobierno de la Provincia de Córdoba, Argentina
		Dr. Luis Hernández Callejo	Coordinador Red CITIES CYTED
8:30 a 10:00	Discussion Panel: Governance and Sustainability in Smart Cities Moderator Dr. Luis Hernández Callejo	Dra. Paola Vega Castillo (virtual)	Ministra de Ciencia, Innovación, Tecnología y Telecomunicaciones de la República de Costa Rica
		Ing. Pablo De Chiara	Ministro de Ciencia y Tecnología del Gobierno de la Provincia de Córdoba, Argentina
		Dr. Marco A. Moreno Ibarra	Director del Centro de Investigación en Computación del Instituto Politécnico Nacional, México
		Dr. Juan Leonardo Espinoza	Vicerrector de la Universidad de Cuenca, Ecuador
10:00 a 10:30	Coffee break		
10:30 a 12:15	(21) Modelo para evaluación de calidad de datos abiertos de gobierno: Caso Colombia.	Gina Maestre-Gongora, Adriana Milena Rangel-Carrillo and Mariutsi Osorio-Sanabria	S1. Governance and Citizen Management Moderator Dr. Ponciano Jorge Escamilla-Ambrosio
	(25) How Smart Furniture can help improve the quality of life of the elderly? Extended Interconnected Public Spaces.	Víctor Manuel Padrón Nápoles, Olalla García Pérez, José Luis Esteban Penelas, Sonia Escorial Santa Marina and María José García Santacruz	
	(31) Indicadores de Destinos Turísticos e Normas Brasileiras de Cidades Inteligentes para a concepção de um Smart Destination	Alessandra Bussador, Katya Regina de Freitas Zara and Janine Carvalho Padilha	
	(38) El modelo de destino turístico inteligente y la relación de la gestión pública en su impulso, caso Cozumel, México 2015-2019	Alex Adiel Cano Heredia and Crucita Aurora Ken Rodríguez	
	(62) Smart Governance for Collaborative Ecosystems	Rallou Taratori, Sesil Koutra, Montserrat Pareja-Eastaway and Nikolaos Al. Papadopoulos	

(33) Badajoz Es Más – Smart Provincia: Tecnología al servicio de la Gobernanza y la Ciudadanía	Ulises Gamero Rodríguez and Roberto Gallego Delgado
(75) Using open data to analyze public bus service from an age perspective: Melilla case	Jamal Toutouh, Irene Lebrusán and Christian Cintrano
(74) A Technical-Economic Study of the Implementation of Renewable Energies in a Train-based Mass Transportation System using RETScreen Software	Jorge Luis Mirez Tarrillo and Estefani Gabriela Mendoza Guerra
(47) The ethics of artificial intelligence and virtual reality in the construction of society 5.0 - Society 5.0 and artificial affairs and virtual reality	Roberto Ramírez Basterrechea, Viviana Polisená and Katherine Hoolahan
(59) Optimization of a Hybrid Echo State Network methodology for forecasting the spot price of Iberian electricity market	Murti Bär, Marta Pons, Miquel Roca, Eugeni Isern, Josep L. Rosselló and Vincent Canals

## Monday, November 29th

Hour (UTC-5)	Activity	Speaker	Session
12:15 a 14:00	(15) Study for the improvement of a mini-hydraulic installation in a smart microgrid	Oscar Izquierdo-Monge, Paula Peña-Carro, Siro Soria Franco, Gonzalo Martín Jiménez and Alejandro Carballo Ruiz	S2. Energy Efficiency and Sustainability Moderator Dr. Vicente Leite
	(23) A Framework for preliminary urban wind energy potential assessment with resilience approach in Dominican Republic	Alexander Vallejo-Díaz, Idalberto Herrera-Moya and Alexeis Fernández-Bonilla	
	(24) Comparison of Electric Vehicle Types Considering Tank-to-Wheel Emissions and Energy-Ecological Efficiency	Laene Oliveira Soares, Vanessa de Almeida Guimarães, Danielle Rodrigues de Moraes and Ronney Arismel Mancebo Boly	
	(28) Comparative performance analysis between static solar panels and single-axis tracking systems	Natalia Andrea Barros Barrera, Ana María Arbeláez Marulanda, Freddy Bolaños Martínez and Nicolás Villegas	
	(32) Building design strategies adapted to climate changes in arid regions	Cristina Sanz Cuadrado, Emanuela Giancola, Silvia Soutullo, María José Jiménez, José Antonio Ferrer and María Nuria Sánchez	
	(41) Potential of biogas generation the Waste Treatment Center Santa Rosa in Rio de Janeiro: a theoretical estimation	Gardênia Mendes de Assunção and Ronney Arismel Mancebo Boly	
	(42) A practical approach for sustainable Transit Oriented Development in Montevideo, Uruguay	Silvina Hipogrosso and Sergio Nesmachnow	
	(43) Outdoor efficiency model for photovoltaic modules and its experimental validation	Luis Diego Murillo-Soto and Carlos Meza Benavides	
	(58) Analysis about the hybridization of PV solar and low enthalpy geothermal energies by using green hydrogen as energy vector	Cristina Sáez Blázquez, Ignacio Martín Nieto, Arturo Farfán Martín and Diego Gonzalez-Aguilera	
(61) Off-grid photovoltaic system in an existing urban building. Case of the library at the ETSEIB	Roberto Villafila		

## Tuesday, November 30th

Hour (UTC-5)	Activity	Speaker	Session
08:00 a 10:00	(63) Ahorro de Energía: Acoplamiento directo de sistemas de absorción para enfriamiento y calentamiento	Valente Cano Garcia and Armando Huicochea Rodriguez	
	(65) Upgrading urban services through BPL: practical applications for Smart Cities	Noelia Uribe-Perez, Igor Fernández and David de la Vega	
	(71) Design and Installation of an IoT Electricity and Water Technological and Monitoring Solution	Ponciano Jorge Escamilla-Ambrosio, María Guadalupe Pulido-Navarro, Marco Antonio Ramírez-Salinas, Marco Antonio Moreno-Ibarra and Juan Humberto Sossa-Azuela	

	(82) A review of the role of electric vehicles in carbon regulation policies related to the transport sector	Rayssa Paula Correia Lima and Vanessa de Almeida Guimarães	S3. Energy Efficiency and Sustainability Moderator Dr. Víctor Alonso
	(84) Educación en eficiencia energética para el desarrollo de ciudades inteligentes: fortaleciendo la conciencia ambiental ciudadana	José Gabriel Pérez Canencio, Mary Luz Ojeda Solarte, Andres Rey Piedrahita and Daniel Hernán Moreno Gutiérrez	
	(112) Integration of PV technologies for rural sustainable tourism	María Sánchez-Aparicio, Enrique González-González, Jose Martín-Jiménez, Susana Del Pozo, Paula De Andrés and Susana Lagüela	
	(20) El Hidrógeno Verde en Costa Rica: una revisión	Rhonmer Orlando Pérez Cedeño, Leonardo Suárez Matarrita, Carmen Luisa Vásquez Stanesco and Valeria Vargas Torres	
	(29) LTSpice Polynomial Modeling of Peltier-Seebeck Thermoelectric Module	Miguel Antonio Baldera Arvelo, Miguel Antonio Baldera Echavarría and Juan Castellanos	
	(100) Effectiveness of PV string current measurements to detect fault in PV systems	Bryan Rodriguez, Leonardo Cardinale-Villalobos, Carlos Meza Benavides, Luis Diego Murillo-Soto and Hugo Sanchez	
	(18) Hybrid AC/DC Architecture in CEDER-CIEMAT Microgrid: a case study	Oscar Izquierdo-Monge, Paula Peña-Carro, Siro Soria Franco, Gonzalo Martín Jiménez and Mariano Martín Martínez	
	(78) Alocação Ótima de Sistemas de Armazenamento de Energia Visando o Despacho Econômico	Raphael van der Linden, Lucas Carlos da Silva and Yuri Percy Molina Rodriguez	
10:00 a 10:30	Coffee break		

## Tuesday, November 30th

Hour (UTC-5)	Activity	Speaker	Session
10:30 a 12:15	Discussion Panel: The Role of Smart Tourist Destinations and Sustainability in the Framework of Smart Cities Moderator Dr. Ponciano Escamilla	Dr. Alejandro del Amo (virtual)	CEO of Abora Solar
		Ing. Oscar Torrecilla	Representative of the Quintana Roo Office of CANIETI
		Mtro. Marco Antonio Bravo Fabian	General Director of the Quintanarroense Institute of Innovation and Technology, IQIT
		Lic. Margarita Carbajal Carmona	National President of the Federation of Tourism Entrepreneurs, A.C. (FETUR)
12:15 a 14:00	(97) A Multi-Lens Approach to Smart City Planning: Philadelphia	Jennifer Kim, Sesil Koutra and Zacharie De Grève	S4. Mobility and Smart Public Services Moderator Dr. Luis Manuel Navas
	(99) Análisis de la evolución del uso del transporte urbano público en ciudades de Latinoamérica, Europa y Asia durante la pandemia del COVID-19 electric mobility	Melva Gómez-Cacedo, Anderson Quintero, Rodrigo Ramírez-Pisco, Mercedes Gaitan-Angulo, Renato Andara, Jesús Ortego-Osa, Luis Manuel Navas and Carmen Luisa Vásquez Stanesco	
	(19) Análisis Multiobjetivo de la Degradación del Acetaminofén usando TiO2 Degussa P25	Alfredo Cristóbal Salas, Bardo Santiago Vicente, Neiel Israel Leyva Santes, Raúl Alejandro Luna Sánchez and Carolina Solis Maldonado	
	(37) Energy-aware smart home planning: a real case study in Montevideo, Uruguay	Diego Gabriel Rossit and Sergio Nesmachnow	
	(40) A Covid-19 Vaccination Tracking and Control Platform in Santiago de Cali	Andres Felipe Fuentes Vasquez, Diego Fernando Botero Henao and Cristhian Torres Ramirez	
(48) Solar E-bikes share system design in the city of Ávila.	Enrique González-González, María Sánchez-Aparicio, Susana Lagüela, José Martín-Jiménez, Susana Del Pozo		

		and Paula de Andrés	
	(54) Smart technologies for monitoring older adults with dementia	Jessica Beltrán-Márquez, Omar A. Montoya-Valdivia, Ricardo Bañuelos-De La Torre, Leonardo Melendez-Lineros, Gabriel Parada-Picos, Cynthia B. Pérez and Ciro Martínez-García-Moreno	
	(96) Análisis inteligente de oferta de estacionamientos de bicicletas potenciales aplicando diagrama de Voronoi y densidad Kernel: Caso Centro Histórico de Arequipa	Edith Gabriela Manchego Huaquipaco, Belén Arlett Flores Chambí, Ernesto Mauro Suarez Lopez, Cinthya Lady Butron Revilla and Ursula Estefany Pinto Enriquez	
	(103) Análisis histórico de la movilidad individual ECOBICI en la Ciudad de México	Gilberto Lorenzo Martinez Luna, Adolfo Guzmán Arenas and Eduardo Varas Reyes	
	(105) Travel time estimation in public transportation using bus location data	Renzo Massobrio and Sergio Nesmachnow	

### Wednesday, December 1st

Hour (UTC-5)	Activity	Speaker	Session
08:00 a 10:00	(5) Methodology for inspection of defects in photovoltaic plants by drone and electroluminescence	Luis Hernández-Callejo, Sara Gallardo-Saavedra, José Ignacio Morales-Aragonés, Víctor Alonso-Gómez, Alberto Redondo Plaza and Diego Fernández Martínez	S5. Energy, Urban Computing, Big Data and Data Management Moderator Dr. Sergio Nesmachnow
	(8) Second life for LiFePo4 batteries as energy storage system in a smart microgrid	Oscar Izquierdo Monge, Nicolas Alonso Gonzalez, Paula Peña Carro, Gonzalo Martín Jiménez, Oscar Duque Perez, Angel Zorita-Lamadrid and Victor Alonso Gómez	
	(13) Renewable potential in urban environments: case study of the solar potential in municipal buildings in the city of Soria (Spain)	Sara Gallardo-Saavedra, Alberto Redondo-Plaza, Diego Fernández-Martínez, Víctor Alonso-Gómez, José Ignacio Morales-Aragonés and Luis Hernández-Callejo	
	(16) Overshot waterwheel based grid-connected pico-hydro system	Vicente Leite	
	(56) Photovoltaic cells defects classification by means of Artificial Intelligence and electroluminescence images	Héctor Felipe Mateo-Romero, Álvaro Pérez-Romero, Luis Hernández Callejo, Sara Gallardo-Saavedra, Víctor Alonso-Gómez, José Ignacio Morales-Aragonés, Alberto Redondo Plaza and Diego Fernández Martínez	
	(57) Dependence on solar activity as a factor in the energy consumption of supermarkets	R. A. López-Meraz, Luis Hernández Callejo, J. A. Del Ángel-Ramos, L. O. Jamed-Boza, J. J. Marín-Hernández, J. L. Arenas-Del Ángel and V. Alonso-Gómez	
	(60) The current and future role of hydrogen in the EU Energy Transition	Marta Pons, Murti Bär, Eugeni Isern, Miquel Roca, Josep L. Rosselló, Víctor Martínez-Moll and Vincent Canals	
	(80) Redes descentralizadas em sistemas conjugados de chaminés solares e trocadores de calor terra-ar	Erick S. Oliveira, Daduí C. Guerrieri, Igor L. Santos and José L. Z. Zotin	
	(26) Prescriptive Analytics in Rescue Operations: A Combinatorial Optimization approach	Igor Morais, Vanessa de Almeida Guimarães, Eduardo Bezerra da Silva and Pedro Henrique González	
	(68) Clasificación de perfiles de comportamiento para clientes no-residenciales considerando variable de consumo de energía eléctrica con/sin presencia de sistema de generación distribuida.	Jerson San Martin, Luis García García Santander, Dante Carrizo and Fernando Ulloa Vasquéz	
	(70) Open source big data platform for real-time geolocation in smart cities	Pedro Moreno-Bernal, Carlos Alan Cervantes-Salazar, Sergio Nesmachnow, Juan Manuel Hurtado-Ramírez and Jose Alberto Hernández-Aguilar	
10:00 a 10:30	Coffee break		

### Wednesday, December 1st

Hour (UTC-5)	Activity	Speaker	Session
10:30 a 12:15	(83) Techno-Economic Dimensioning Methodology for Battery Energy Storage Systems: Electricity Access Fee Reduction in Industrial Consumptions	Jorge Nájera, Miguel Santos, Marcos Blanco, Gustavo Navarro, Jorge Torres and Marcos Lafoz	

	(94) Methodology to design a polygeneration system (CCHP) in a hotel complex in Xalapa City, Veracruz	Jorge Arturo Del Ángel Ramos, Raúl Alberto López Meraz and Jazmín Rivera Peña	S6. Energy and Smart Grid Moderator Dr. Juan Leonardo Espinoza
	(107) A low-cost device for measuring the complete I-V curve of solar cells integrated into a modular platform suitable for other techniques such as electroluminescence.	Víctor Alonso-Gómez, José Ignacio Morales-Aragoneses, Sara Gallardo-Saavedra, Alberto Redondo Plaza, Diego Fernández Martínez and Luis Hernández Callejo	
	(6) Charge management of electric vehicles from undesired dynamics in solar photovoltaic generation	Ivania Aguirre, Miguel Davila, Luis Gonzalez, Luis Hernández Callejo and Juan Espinoza	
	(7) Charging control of electric vehicles in microgrids with high penetration of photovoltaic generation: an integrated simulation method with Python and OpenDSS	Miguel Davila, Oscar Duque Perez, Luis Hernández Callejo, Luis Gonzalez, Angel Zorita Lamadrid and Juan Espinoza	
	(10) P2P Energy Trading Model for a Local Electricity Community Considering Technical Constraints	Fernando García, Francisco Díaz González and Cristina Corchero	
	(22) Development and improvement of a data storage system in a microgrid environment with HomeAssistant and MariaDB	Oscar Izquierdo-Monge, Gonzalo Martín Jiménez and Paula Peña-Carro	
	(104) Wide-range time-domain simulation environment for stand-alone microgrids	Mario Araya-Carillos and Carlos Meza Benavides	
12:15 a 14:00	(39) A machine learning approach for detecting traffic incidents from video cameras	Guillermo Gabrielli, Ignacio Ferreira, Pablo Dalchiele, Andrei Tchernykh and Sergio Nesmachnow	S7. AI for Smart Cities, IoT, other SC Developments, Smart Industry Moderator Dr. Humberto Sossa
	(98) Exact approach for electric vehicle charging infrastructure location: a real case study in Málaga, Spain	Claudio Riso, Christian Cintrano, Jamal Toutouh and Sergio Nesmachnow	
	(46) Integration of Internet of Things Technologies in Government Buildings through Low-cost Solutions	Miguel Aybar-Mejía, Deyslen Mariano-Hernández, Jesús Coronado Marte, Adrián Contreras Gomez and Jimmy Arias Peña	
	(27) Propuesta de Nuevas Tarifas con Opción de Precios por Tiempo de Uso para Clientes de la Cooperativa Eléctrica de San Pedro de Atacama en Chile	Jorge Pérez Martínez and Luis García Santander	
	(45) Smart Campus CIC-IPN	Ponciano Jorge Escamilla-Ambrosio, Marco Antonio Ramírez-Salinas, Jorge Iván Martínez-Badillo, Hugo Enrique Vega-Rivera and Maria Guadalupe Pulido-Navarro	
	(89) Visualization in Smart City Technologies	M. Teresa Cepero, Luis G. Montané-Jiménez, Edgard Benítez-Guerrero and Carmen Mezura-Godoy	
	(101) Smart City Vienna – Factors Driving Location Attractiveness	Pablo Collazzo and Velislava Stoyanova	
	(14) VIA: A Virtual Informative Assistant for Smart Tourism	María Camila López, David Hernández, Andrés A. Navarro-Newball and Edmond C. Prakash	
	(11) A case study of smart industry in Uruguay: grain production facility optimization	Gabriel Bayá, Pablo Sartor, Franco Robledo, Eduardo Canale and Sergio Nesmachnow	
	(85) Hybrid GRASP+VND for flexible vehicle routing in smart cities	Lucía Barrero, Rodrigo Viera, Claudio Riso, Franco Robledo and Sergio Nesmachnow	

## Posters

	(12) Reactive power optimization on a smart microgrid	Oscar Izquierdo-Monge, Elgar Lloret Pérez, Paula Peña-Carro, Gonzalo Martín Jiménez, Luis Hernandez-Callejo, Angel Zorita-Lamadrid and Oscar Duque Perez	Posters
	(53) Modelado de llamado masivo remoto de medidor con requerimientos de alta disponibilidad para la operación de un CGM	Fernando Velez Varela and Jorge Junior Garcia Ledesma	
	(69) Cooling effect of urban green infrastructures by remote sensing data: case study in 7 cities of the northern hemisphere	Paula Andrés-Anaya, Susana del Pozo, María Sánchez-Aparicio, Enrique González-González, Jose Martín-Jiménez and Susana Lagüela	
	(72) A mathematical model to regulate the density of natural gas based on its composition	Jorge Luis Mirez Tarrillo and Eduardo Calle	
	(111) Microclimatic Studies and Scenarios Simulation with ENVI-Met – A Case Study from a Residential	Marcos Costa, Artur Gonçalves, António Castro Ribeiro and Felipe Romero	

Neighbor-hood in Bragança (Portugal)	
(92) Analysis of mathematical models for location of electric vehicle charging stations: state of the art	Fernanda Verneque, Vanessa Guimarães and Pedro Henrique González
(66) Solar-driven drinking water supply in rural areas: Jutiapa (El Salvador) experience	Alfonso García Álvaro, Sara Gallardo Saavedra, Raúl Muñoz Torre, Alberto Redondo Plaza, Diego Fernández Martínez, Víctor Alonso Gómez and Ignacio De Godos Crespo
(76) A study of polystyrene biodegradation through the use of mealworm larvae with application in waste treatment in cities	Jorge Luis Mirez Tarrillo and Maura Arminda Jara Ramos
(81) Analysis of the orography for the study of the technical feasibility of urban electric buses in Ávila	Jose Antonio Martín-Jimenez, Susana Del Pozo Aguilera, María Sánchez Aparicio, Enrique González, Paula de Andrés Anaya and Susana Lagüela
(102) Embedded System for automating manual inventory survey process of street lighting with a I2C photometric sensor network	Luis Ricardo Delgado Cortés and Saúl Esquivel-García
(110) Building Smart City Based on the Big Data, Computer Analytics, Public Demand, and Governance	Alexander Shemetev and Martin Pelucha
(34) Diseño colaborativo de servicios inclusivos en ciudades inteligentes con mapas interactivos	Iván García-Magariño, Juan Pavón, Rubén Fuentes-Fernández and Jorge J. Gómez-Sanz
(17) Post-pandemic redesign of downtown streets for people. The Bahía Blanca city experience	Yamila Soledad Grassi and Mónica Fátima Díaz
(64) Technological Intelligence in Small Cities	Norela Vanessa Mora Ceron
(90) Desarrollo de un sistema tecnológico para el monitoreo de cultivos de agricultura familiar en transición agroecológica de la provincia del Sumapaz Colombiano	Roberto Ferro Escobar and Danilo Alberto Vera Parra

## TABLE OF CONTENTS

(21) Modelo para evaluación de calidad de datos abiertos de gobierno: Caso Colombia	1
(25) How Smart Furniture can help improve the quality of life of the elderly? Extended Interconnected Public Spaces	16
(31) Indicadores de Destinos Turísticos e Normas Brasileiras de Cidades Inteligentes para a concepção de um Smart Destination	28
(38) El modelo de destino turístico inteligente y la relación de la gestión pública en su impulso, caso Cozumel, México 2015-2019	43
(62) Smart Governance for Collaborative Ecosystems	57
(33) Badajoz Es Más – Smart Provincia: Tecnología al servicio de la Gobernanza y la Ciudadanía	81
(75) Using open data to analyze public bus service from an age perspective: Melilla case	94
(74) A Technical-Economic Study of the Implementation of Renewable Energies in a Train-based Mass Transportation System using RETScreen Software	109
(47) The ethics of artificial intelligence and virtual reality in the construction of society 5.0 - Society 5.0 and artificial affairs and virtual reality	119
(59) Optimization of a Hybrid Echo State Network methodology for forecasting the spot price of Iberian electricity market	137
(15) Study for the improvement of a mini-hydraulic installation in a smart microgrid	152
(23) A Framework for preliminary urban wind energy potential assessment with resilience approach in Dominican Republic	167
(24) Comparison of Electric Vehicle Types Considering Tank-to-Wheel Emissions and Energy-Ecological Efficiency	189
(28) Comparative performance analysis between static solar panels and single-axis tracking systems	205
(32) Building design strategies adapted to climate changes in arid regions	214
(41) Potential of biogas generation the Waste Treatment Center Santa Rosa in Rio de Janeiro: a theoretical estimation	230
(42) A practical approach for sustainable Transit Oriented Development in Montevideo, Uruguay	245
(43) Outdoor efficiency model for photovoltaic modules and its experimental validation	260
(58) Analysis about the hybridization of PV solar and low en-thalpy geothermal energies by using green hydrogen as energy vector	277
(61) Off-grid photovoltaic system in an existing urban building. Case of the library at the ETSEIB	292
(63) Ahorro de Energía: Acoplamiento directo de sistemas de absorción para enfriamiento y calentamiento	305
(65) Upgrading urban services through BPL: practical applications for Smart Cities	320
(71) Design and Installation of an IoT Electricity and Water Technological and Monitoring Solution	333
(82) A review of the role of electric vehicles in carbon regulation policies related to the transport sector	347
(84) Educación en eficiencia energética para el desarrollo de ciudades inteligentes: fortaleciendo la conciencia ambiental ciudadana	362
(112) Integration of PV technologies for rural sustainable tourism	378
(20) El Hidrógeno Verde en Costa Rica: una revisión	392
(29) LTSpice Polynomial Modeling of Peltier-Seebeck Thermoelectric Module	405
(100) Efectiveness of PV string current measurements to detect fault in PV systems	418

(18) Hybrid AC/DC Architecture in CEDER-CIEMAT Microgrid: a case study	427
(78) Alocação Ótima de Sistemas de Armazenamento de Energia Visando o Despacho Econômico	439
(97) A Multi-Lens Approach to Smart City Planning: Philadelphia	456
(99) Análisis de la evolución del uso del transporte urbano público en ciudades de Latinoamérica, Europa y Asia durante la pandemia del COVID-19	471
(19) Análisis Multiobjetivo de la Degradación del Acetaminofén usando TiO2 Degussa P25	484
(37) Energy-aware smart home planning: a real case study in Montevideo, Uruguay	499
(40) A Covid-19 Vaccination Tracking and Control Platform in Santiago de Cali	514
(48) Smart Mobility in Cities: Solar E-bikes share system design in the city of Ávila	528
(54) Smart technologies for monitoring older adults with dementia	539
(96) Análisis inteligente de oferta de estacionamientos de bicicletas potenciales aplicando diagrama de Voronoi y densidad Kernel: Caso Centro Histórico de Arequipa	551
(103) Análisis histórico de la movilidad individual ECOBICI en la Ciudad de México	565
(105) Travel time estimation in public transportation using bus location data	578
(5) Methodology for inspection of defects in photovoltaic plants by drone and electroluminescence	593
(8) Second life for LiFePo4 batteries as energy storage system in a smart microgrid	606
(13) Renewable potential in urban environments: case study of the solar potential in municipal buildings in the city of Soria (Spain)	623
(16) Overshot waterwheel based grid-connected pico-hydro system	640
(56) Photovoltaic cells defects classification by means of Artificial Intelligence and electroluminescence images	652
(57) Dependence on solar activity as a factor in the energy consumption of supermarkets	664
(60) The current and future role of hydrogen in the EU Energy Transition	679
(80) Redes descentralizadas em sistemas conjugados de chaminés solares e trocadores de calor terra-ar	694
(26) Prescriptive Analytics in Rescue Operations: A Combinatorial Optimization approach	706
(68) Clasificación de perfiles de comportamiento para clientes no-residenciales considerando variable de consumo de energía eléctrica con/sin presencia de sistema de generación distribuida	721
(70) Open-source big data platform for real-time geolocation in smart cities	735
(83) Techno-Economic Dimensioning Methodology for Battery Energy Storage Systems: Electricity Access Fee Reduction in Industrial Consumptions	750
(94) Metodology to design a polygeneration system (CCHP) in a hotel complex in Xalapa City, Veracruz	769
(107) A low-cost device for measuring the complete I-V curve of solar cells integrated into a modular platform suitable for other techniques such as electroluminescence	779
(6) Charge management of electric vehicles from undesired dynamics in solar photovoltaic generation	802
(7) Charging control of electric vehicles in microgrids with high penetration of photovoltaic generation: an integrated simulation method with Python and OpenDSS	817
(10) P2P Energy Trading Model for a Local Electricity Community Considering Technical Constraints	832
(22) Development and improvement of a data storage system in a microgrid environment with HomeAssistant and MariaDB	844
(104) Wide-range time-domain simulation environment for stand-alone microgrids	856
(39) A machine learning approach for detecting traffic incidents from video cameras	871

(98) Exact approach for electric vehicle charging infrastructure location: a real case study in Málaga, Spain	886
(46) Integration of Internet of Things Technologies in Government Buildings through Low-cost Solutions	901
(27) Propuesta de Nuevas Tarifas con Opción de Precios por Tiempo de Uso para Clientes de la Cooperativa Eléctrica de San Pedro de Atacama en Chile	911
(45) Smart Campus CIC-IPN	926
(89) Visualization in Smart City Technologies	938
(101) Smart City Vienna – Factors Driving Location Attractiveness	953
(14) VIA: A Virtual Informative Assistant for Smart Tourism	962
(11) A case study of smart industry in Uruguay: grain production facility optimization	977
(85) Hybrid GRASP+VND for flexible vehicle routing in smart cities	992
(12) Reactive power optimization on a smart microgrid	1007
(53) Modelado de llamado masivo remoto de medidor con requerimientos de alta disponibilidad para la operación de un CGM	1022
(69) Cooling effect of urban green infrastructures by remote sensing data: case study in 7 cities of the northern hemisphere	1043
(72) A mathematical model to regulate the density of natural gas based on its composition	1056
(111) Microclimatic Studies and Scenarios Simulation with ENVI-Met – A Case Study from a Residential Neighborhood in Bragança (Portugal)	1068
(92) Analysis of mathematical models for location of electric vehicle charging stations: state of the art	1081
(66) Solar-driven drinking water supply in rural areas: Jutiapa (El Salvador) experience	1094
(76) A study of polystyrene biodegradation through the use of mealworm larvae with application in waste treatment in cities	1105
(81) Analysis of the orography for the study of the technical feasibility of urban electric buses in Ávila	1115
(102) Embedded System for automating manual inventory survey process of street lighting with a I2C photometric sensor network	1125
(110) Building Smart City Based on the Big Data, Computer Analytics, Public Demand, and Governance	1140
(34) Diseño colaborativo de servicios inclusivos en ciudades inteligentes con mapas interactivos	1153
(17) Post-pandemic redesign of downtown streets for people. The Bahía Blanca city experience	1163
(64) Technological Intelligence in Small Cities	1175
(90) Desarrollo de un sistema tecnológico para el monitoreo de cultivos de agricultura familiar en transición agroecológica de la provincia del Sumapaz Colombiano	1189

## Modelo para evaluación de calidad de datos abiertos de gobierno: Caso Colombia.

Gina Maestre-Góngora<sup>1</sup>[0000-0002-2880-9245], Adriana Rangel-Carrillo<sup>1</sup> [0000-0002-2206-748X]  
and Mariutsi Osorio-Sanabria<sup>2</sup>[0000-0001-7375-3052]

<sup>1</sup> Universidad Cooperativa de Colombia, Medellín, Colombia

<sup>2</sup> Fundación Universitaria María Cano, Medellín, Colombia

{gina.maestre, adriana.rangel}@campusucc.edu.co,  
mariutsialexandraosoriosanabria@fumc.edu.co

**Abstract.** En Colombia para promover el desarrollo de ciudades inteligentes y gobierno abierto se han generado políticas con el fin de garantizar la transparencia y accesibilidad de la información pública. Si bien el país ha definido orientaciones para avanzar en la apertura y uso de datos abiertos, estas se asumen de una manera aislada y son escasas las metodologías integradas que les permitan a las oficinas de Tecnologías de la Información (TI) de las entidades públicas abordar el proceso identificando claramente herramientas e instrumentos para generar datos abiertos de calidad. Este artículo tiene como objetivo presentar un modelo usando BPMN (Business Process Model and Notation) que facilite el proceso de implementación de datos abiertos de gobierno (DAG) en entidades públicas colombianas hacia un enfoque de calidad. Se proponen cuatro fases: Planear y Obtener, Estructurar y Publicar, Promover el uso y Monitorear la calidad, uso e impacto. En cada fase se establecen los subprocesos y tareas y se relacionan los documentos de política pública, las herramientas y artefactos que soportan del desarrollo de las tareas propuestas. Esta propuesta se validó con 16 funcionarios públicos de Colombia donde se concluye que el modelo presenta los procesos claves para realizar la implementación de DAG, es fácil de comprender, presenta un nivel adecuado de abstracción y es pertinente ya que se ajusta a las necesidades de las entidades públicas, aunque requiere un nivel de experticia para su aplicación.

**Keywords:** Datos abiertos, BPMN, Calidad de datos, Ciudades Inteligentes, Gobernanza, Gobierno Abierto

### 1 Introducción

Las entidades públicas cada día generan, gestionan y comparten altos volúmenes de datos, en diversos formatos, a gran velocidad y variedad, que deben ser publicados de manera abierta para facilitar el acceso por los ciudadanos y facilitar su uso, dichos datos se denominan datos abiertos de gobierno(DAG) [1]. Uno de los desafíos que se evidencian en los DAG, es el asociado con la calidad de los datos, dado que se genera

resistencia por parte de los involucrados en trabajar este proceso; debido a que buscar, encontrar, corregir errores en gran cantidad y variedad de datos, y rastrear fuentes de confirmación para aquellos no confiables, requiere un 50% de tiempo del proceso de análisis de grandes cantidades de datos (Big data), un 60% de tiempo para limpiar y organizar, y además tiene un costo total asociado del 75% del presupuesto destinado para el análisis de datos [2].

En este propósito, surge la necesidad de identificar factores relevantes y su relación para la evaluación de calidad de DAG que faciliten la implementación de estrategias de ciudades inteligentes [34] para potencializar la capacidad de los datos abiertos para satisfacer las necesidades de los diferentes interesados, promover su uso y explotación orientados a generar valor agregado a la academia, la industria, la ciudadanía y los gobiernos a partir de requerimientos específicos de uso [3].

Con el fin de garantizar la transparencia y accesibilidad de la información pública, en Colombia se estableció la Ley 1712 de 2014 [4], a través de la cual se reguló la obligatoriedad de divulgación de la información pública (sin carácter clasificado o reservado), para todas las instituciones estatales, en el sitio web oficial dispuesto por el gobierno nacional para datos abiertos ([www.datos.gov.co](http://www.datos.gov.co)). En 2018, se aprobó en el Consejo Nacional de Política Económica y Social — CONPES, el documento CONPES 3920 sobre la política nacional de explotación de datos (Big Data), el cual está enfocado en fomentar el desarrollo de proyectos de Big Data bajo una política pública integral. Por medio de este CONPES se busca aprovechar los datos digitales y generar a su vez desarrollo social y económico. Además, se define una política pública para fomentar la formación de capital humano que apoye la generación y explotación de datos, y se proyecta el establecimiento de un marco jurídico para proteger a los colombianos con la disponibilidad y explotación masiva de la información, sin degradar la generación de valor [5].

Si bien el país ha avanzado en las orientaciones y en el desarrollo de una política pública que ha permitido avanzar en la apertura y uso de datos abiertos [6]- [7], estos se asumen de una manera aislada y no se ha promovido una metodología integrada que les permita abordar el proceso como un todo desde la apertura de datos hasta la explotación y uso a mediano y a largo plazo. Abordar este tema, es oportuno para facilitar la identificación de datos relevantes y por ende, es útil para establecer aplicaciones con dichos datos [8], con lo cual se pueda obtener una comprensión razonable de los mismos [9], debido a que una calificación buena de los datos como materia prima, depende de la manera en que se usan y el impacto de los resultados que generan.

Considerando lo anterior, este artículo tiene como objetivo proponer un modelo usando BPMN (Business Process Model and Notation) que facilite el proceso de implementación datos abiertos de gobierno en entidades públicas de Colombia hacia un

enfoque de calidad. Se presenta en la sección dos conceptos relacionados con DAG, en la sección tres la metodología para el diseño del modelo. Posteriormente, en la sección cuatro se describen los principios, lineamientos y atributos que soportan el modelo, así como las fases y procesos definidos para la evaluación de calidad de datos junto con la validación de este, en entidades públicas de Colombia. Finalmente, en la sección cinco se exponen las conclusiones y el trabajo futuro.

## 2 Antecedentes

Dado el crecimiento exponencial de los datos generados, se encuentran aquellos que son considerados de carácter público, los cuales pueden ser usados y reutilizados por cualquier persona de manera libre; estos han sido denominados datos abiertos y se estiman como factores claves que proveen una plataforma de transformación global para que los gobiernos, empresas privadas y públicas y los ciudadanos en general, tengan bases claras e información real para tomar decisiones que permitan el desarrollo de sus áreas de desempeño laboral, profesional e intelectual [6].

El principal objetivo de los proyectos e iniciativas de DAG es dar apertura de dichos datos de manera libre, permitiendo que sean reutilizados por la ciudadanía en general, la comunidad académica y el sector empresarial, para facilitar la cooperación entre la administración pública, la política, la industria y la ciudadanía, fortaleciendo la transparencia, la democracia, la participación y el trabajo colaborativo [10]. Los DAG se rigen por una serie de principios que están enfocados en facilitar el uso, acceso y la reutilización de dichos datos, entre ellos tenemos: procesables por máquinas, accesibles, completos, deben obtenerse de la fuente de origen, no propietarios, oportunos, actualizados, con licenciamiento abierto y deben estar disponibles para cualquier persona sin discriminación [10].

En lo referente a la calidad es un concepto interdisciplinario que se construye con diferentes perspectivas y mediciones [11]. Por ello, es requerido un proceso definido y sistemático que aporte en la producción de DAG con alta calidad [12], a través de la validación enfocada en procesos de mejoramiento en todo el proceso del ciclo de vida de los datos [13], y así, transformar los datos en información y conocimiento e innovación [14]. La evaluación de calidad de los DAG es un proceso que requiere identificar y acondicionar factores relevantes que faciliten el análisis de Big Data como iniciativa estratégica, para potencializar la capacidad de los datos de satisfacer las necesidades declaradas e implícitas según las condiciones específicas de uso de los datos [3].

Para el caso de Colombia, actualmente los documentos técnicos emitidos por el Ministerio de Tecnologías e Información (MinTIC) han generado una política pública relacionados con DAG, entre los cuales se encuentran: Guía para el uso y aprovechamiento de Datos Abiertos en Colombia[16], Guía de estándares de calidad e interoperabilidad de los datos abiertos del gobierno de Colombia[15], Requisitos de datos abiertos[17] y Ficha Técnica de Calidad de Datos Abiertos de Colombia [7].

Estos documentos trazan la ruta para promover la transparencia y el control social, Facilitar la innovación de productos y la creación de nuevos modelos de negocio, la planeación y prospectiva de escenarios futuros para la sociedad y ayudar a que las personas puedan asumir un rol más activo en la sociedad al tomar sus decisiones individuales y comunitarias con información real [6].

### **3 Metodología**

Este trabajo tiene rasgos de investigación exploratoria y descriptiva ya que pretende formular un marco de referencia que parte de la revisión bibliográfica alrededor de los temas relevantes de la investigación, una recopilación de metodologías de evaluación de calidad de datos, las cuales serán la base para identificar los lineamientos conceptuales y proponer una guía metodológica aplicable al contexto colombiano a través de las siguientes etapas:

#### **3.1 Diseño del Modelo**

La arquitectura del modelo se propone a partir de la revisión de literatura proponiendo principios, lineamientos, dimensiones y atributos que serán la guía para el diseño del modelo.

#### **3.2 Modelado en BPMN:**

En esta fase se definen actores, fases, y procesos, así como los documentos de política pública que soportan las actividades y tareas. Se adopta un enfoque de modelado iterativo e incremental por versiones las cuales se resumen a continuación: a) Versión 1: Se propone ajustes de inclusión de fases. b) Versión 2: Se describen los subprocesos de cada etapa y fase. c) Versión 3: Se ajustan nombres de procesos y descripción de cada subproceso y tareas. d) Versión 4: Se incluye la relación de los documentos técnicos del MinTIC en cada proceso y se especifican salidas.

#### **3.3 Validación**

El modelo se socializó y se evaluó mediante una encuesta aspectos como completitud, comprensión, abstracción, claridad, pertinencia y aplicabilidad. Fue aplicada a 16 funcionarios de entidades públicas de Colombia.

## 4 Resultados

El Modelo propone una hoja de ruta para implementar DAG bajo un enfoque de calidad adaptado para su aplicación en Colombia, basado en los documentos técnicos y lineamientos dados por el MinTIC, los cuales son una guía para las entidades públicas, pero no un procedimiento definido que indique las acciones requeridas para su implementación.

Este modelo presenta principios, lineamientos y dimensiones desde lo conceptual y las fases, actores, procesos, subprocesos, actividades y su respectiva relación con los documentos técnicos de MinTIC para la puesta en operación en las Entidades públicas desde lo metodológico.

### 4.1 Aspectos conceptuales

Se presenta a partir de la revisión de literatura los principios, lineamientos, dimensiones propuestas [32], y el valor de los datos [33] que serán el insumo principal para la definición del modelo para la evaluación de calidad de DAG en el contexto colombiano (Fig. 1). A continuación, se describen cada uno de sus elementos.

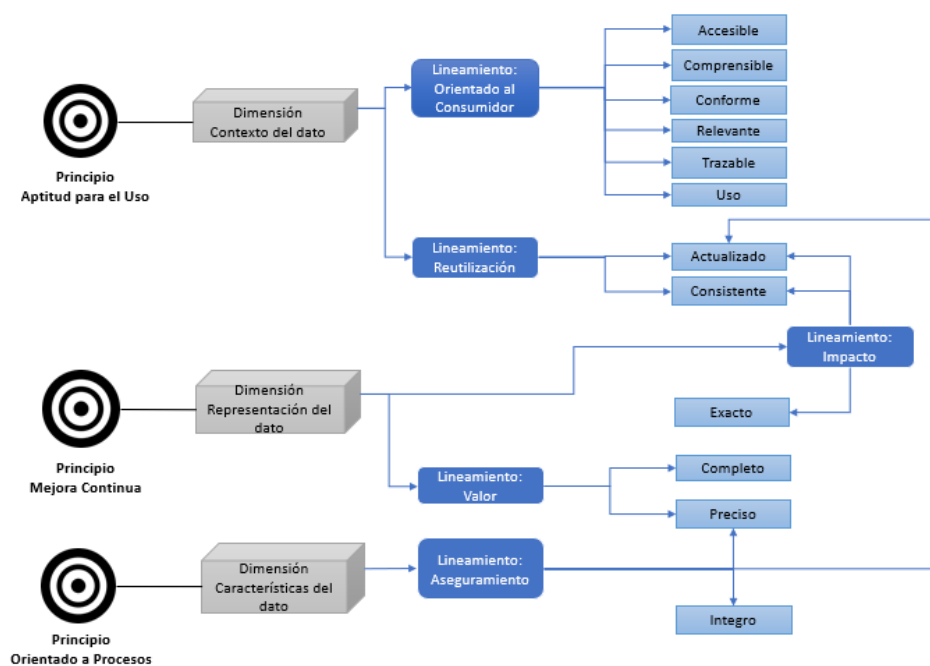


Fig. 1. Propuesta Modelo Conceptual

**Principios.**

Aptitud para el uso: Asegurar la capacidad del dato para servir a un propósito definido. [4], [10], [21],

Orientado a procesos: Gestionar la calidad de los datos, a través de procesos que permitan implementar la estrategia de calidad de forma efectiva, con actividades interrelacionadas para una ejecución sistemática. [11], [14], [18]–[21].

Mejora continua: Garantizar la calidad de los datos a través de la planeación, ejecución de acciones concretas y verificación periódica. [11], [14], [18]–[24].

**Lineamientos.**

Reutilización: Habilitar el uso de los datos en varios contextos. [11], [25]

Impacto: Generar valor para los consumidores, según el uso de los datos en un contexto específico [15].

Orientado al consumidor: Facilitar al consumidor del dato el conocimiento contextual y acceso a los datos [25], [26].

Aseguramiento: Realizar actividades planificadas y sistemáticas con el fin de alcanzar requisitos de calidad para las propiedades inherentes de los datos [7], [27], [28]

Adecuación: Acondicionar los datos para cumplir con los requisitos de calidad relacionados a sus propiedades inherentes. [6], [12], [14], [28]

Valor: Garantizar la representación de los datos como una unidad de valor para sus consumidores. [5], [14], [28]–[31].

**Dimensiones.**

Contexto del dato: Corresponde al contexto del dato. [19], [21].

Características del dato: Propiedades inherentes del dato [19], [21], [22].

Representación del dato: Corresponde a la representación del dato en su contexto o en sus usos potenciales [19], [21].

**4.2 Aspectos Metodológicos**

En la Fig. 2 se muestra el modelo general de implementación de DAG usando BPMN y el software Bizagi Modeler. Para el proceso general, se proponen cuatro fases: Planear y Obtener DAG, Estructurar y Publicar los DAG, Promover el uso de los DAG y Monitorear la calidad, uso e impacto. En cada fase se establecen los subprocesos y tareas y se relacionan los documentos de política pública, las herramientas y artefactos que soportan del desarrollo de las tareas propuestas. Adicionalmente, se identifican los siguientes actores del proceso:

- Tomadores de decisiones: Encargados de realizar la planeación de apertura de los datos.

- Responsables de procesos de DAG: Encargados de estructurar y preparar los datos para la publicación.
- MinTIC: Actores que se encargan de validar la adecuación de los datos y su posterior publicación.
- Gestores de DAG: Estos actores aúnan esfuerzos para promover el uso de los datos y realizar el proceso de monitoreo de calidad, uso e impacto.

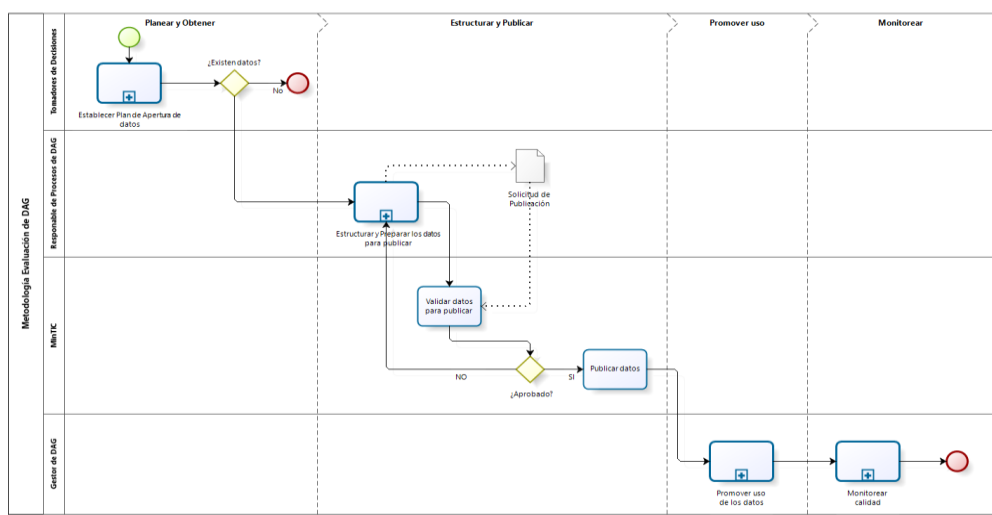


Fig. 2. Modelo General de la implementación de DAG bajo un enfoque de calidad

Fuente: Elaboración propia.

**Fase Planear.**

Esta fase tiene por objetivo identificar la necesidad de publicación o actualización de los datos, los cuales se seleccionan, analizan y priorizan según la estimación de impacto y valor que genere en los actores del ecosistema (Fig. 3).

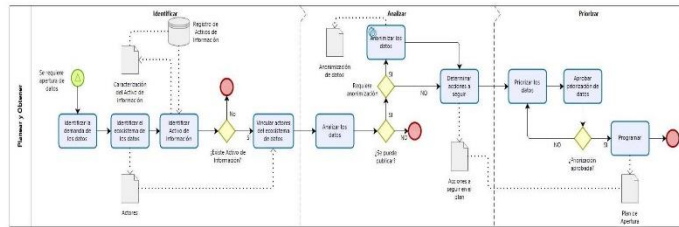


Fig. 3. Procesos Fase Planear

Fuente: Elaboración propia.

Algunos de los aspectos para tener en cuenta en esta fase son: i) Identificar la demanda de los datos, ii) Verificar las solicitudes de información más recurrente para la entidad. iii) Identificar los tipos de actores que son considerados de interés, normativas y regulaciones, restricciones y dinamizadores del ecosistema, tendencias a nivel nacional e internacional, herramientas hardware y software; y iv) Realizar un diagnóstico, levantamiento y clasificación de la información pública. Tener en cuenta los datos de la entidad clasificados como datos abiertos, los datos públicos generados por los sistemas de la entidad, los datos más solicitados por la ciudadanía y los datos de otras entidades o dependencias para evitar duplicidad y finalmente priorizar los datos con potencial de generar impacto en la ciudadanía y solucionar problemas públicos, tal como cumplimiento de metas institucionales, transparencia, participación, control social y colaboración.

**Fase Estructurar y Publicar.**

En esta fase se definen los metadatos que tendrá cada uno de los conjuntos de los datos a publicar. Son una herramienta fundamental para organizar, clasificar, relacionar y encontrar datos. Posteriormente, se verifican, estructuran y se estandarizan los datos a publicar (Fig. 4).

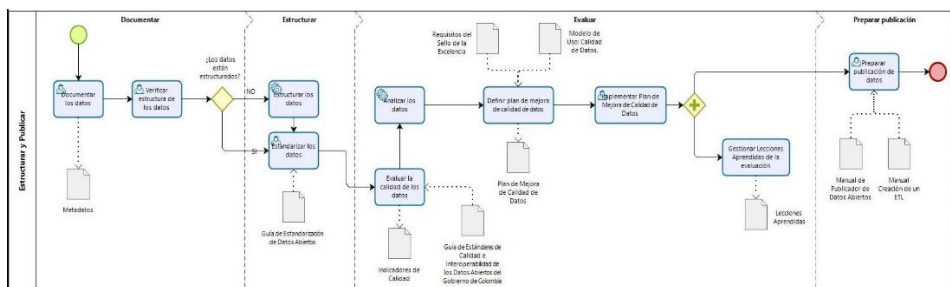


Fig. 4. Procesos Fase Estructurar y Publicar los DAG

Fuente: Elaboración propia.

Seguidamente, se evalúa la calidad de los datos con base en las dimensiones y atributos aplicables para los activos de información seleccionados, se busca detallar los tipos de datos y ordenarlos por grupos. Para cada grupo relacionar los atributos de evaluación correspondientes. Medir indicadores según la aplicación de métricas y herramientas en los datos. Al obtener el resultado se realiza análisis de cada dato (nivel de calidad y acciones requeridas) para definir un plan teniendo en cuenta: Alcance, Objetivo, Errores que resuelve, Causas a prevenir, Recursos, Tiempo y Costos.

Finalmente, desde el análisis de los datos, especificar los errores e identificar la causa de cada error y gestionar lecciones aprendidas para poner a disposición de los usuarios el conjunto de datos abiertos a través del cargue de datos en una plataforma que permita la organización y fácil consulta por parte de quienes van a reutilizar los datos.

**Fase Promover uso de los datos.**

Esta fase permite conocer los datos para su reutilización, por lo cual se deben vincular los actores e interesados, así como definir estrategias para consolidarlos y posicionarlos ante los actores como academia, industria, gobierno y ciudadanos (Fig. 5).

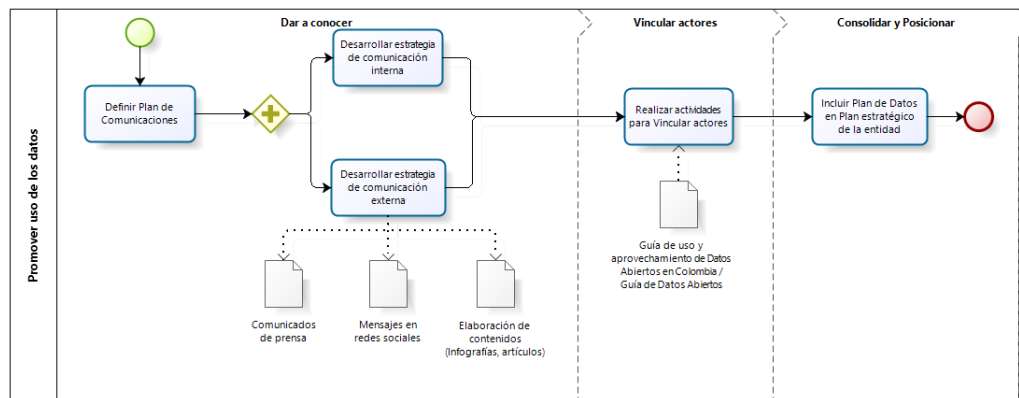


**Fig. 5.** Procesos Fase Promover uso de los DAG

Fuente: Elaboración propia.

Para ello es importante desarrollar una estrategia de comunicación interna informando a los servidores públicos, a fin de transformar el manejo tradicional de los datos públicos e implementar una estrategia de comunicación externa mediante comunicados de prensa, mensajes en redes sociales, elaboración de contenidos como infografías, artículos o videos que promuevan el uso de datos para la ciudadanía. Por otra parte, se sugiere adelantar proyectos para vincular a diferentes actores como academia e industria que promuevan la reutilización de la información disponible es una recomendación para esta fase.

### Fase Monitorear.

La mejora continua es el resultado de la aplicación de estrategias que se obtienen del análisis de indicadores que proveen una perspectiva del impacto y valor de los datos, por lo que esta fase se enfoca en el nivel de publicación y consulta de los datos, medir el uso e impacto generado por estos (Fig. 6).

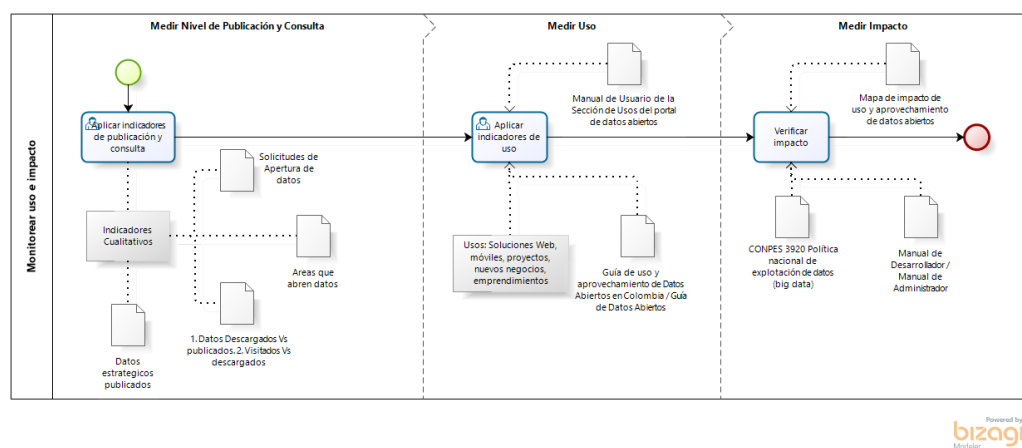


Fig. 6. Proceso Fase Monitorear

Fuente: Elaboración propia.

En esta fase, se recomienda aplicar indicadores de tipo cuantitativo como: solicitudes de apertura de datos, dependencias o áreas estratégicas de la entidad que abren datos, número de conjuntos de datos descargados vs. publicados, número de conjuntos de datos visitados vs. descargados y aplicar indicadores de uso como: número de soluciones web o móviles generadas a partir de datos abiertos, número de proyectos que hicieron uso de los conjuntos de datos abiertos, número de proyectos de emprendimiento o nuevos negocios generados a partir del uso de datos abiertos.

Para la verificación del impacto se propone mapear los distintos usos de los datos, introducir de forma gradual más parámetros de medición impulsados por ciudadanos, que representen las experiencias reales del usuario para pasar de una perspectiva institucional a una ciudadana sobre los resultados e impactos de los datos abiertos.

Finalmente, se establece adelantar, financiar o participar en estudios que permitan cuantificar el valor económico de los datos abiertos y establecer alianzas con entidades públicas y privadas, así como organizaciones de la sociedad civil, academia, ONG para proyectos de explotación de datos son acciones deseables a mediano y largo plazo.

### 4.3 Validación

Para la validación se elaboró como instrumento una encuesta (<https://www.surveio.com/survey/d/F0G5L0A6Q3U6A1C6K>) con el fin de validar el modelo BPMN que describe la hoja de ruta para implementar DAG bajo el enfoque de calidad y verificar la pertinencia y correlación de las fases, procesos, subprocesos y responsables.

En esta encuesta participaron 16 funcionarios públicos pertenecientes a las siguientes entidades: Ministerio de Hacienda y Crédito Público con una participación del 38%, Gobernación de Cundinamarca con una participación del 25%, Instituto Nacional de Vías con una participación del 13% y Dirección Nacional de Aduanas Nacionales, Instituto Nacional de Vigilancia de Medicamentos y Alimentos, Colombia Compra Eficiente y Fondo Nacional del Ahorro con una participación de un 6% cada una.

Los participantes estuvieron de acuerdo en que el modelo BPMN incluye los procesos claves para realizar la evaluación de calidad de DAG, es fácil de comprender, presenta un nivel adecuado de abstracción, es claro, pertinente ya que se ajusta a las necesidades de las entidades públicas, aunque requiere un nivel de experticia para su aplicación. El 94% de los participantes concuerdan en que las fases "Planear y Obtener", "Evaluar y Publicar" y "Promover uso" de la Metodología de evaluación de calidad de DAG facilitan la implementación del proceso en las Entidades Públicas, respecto a la fase "Monitorear", sólo el 81% de los participantes se encuentra de acuerdo con su facilidad de implementación en las entidades públicas, mostrando una diferencia del -13% con respecto de las otras fases del modelo.

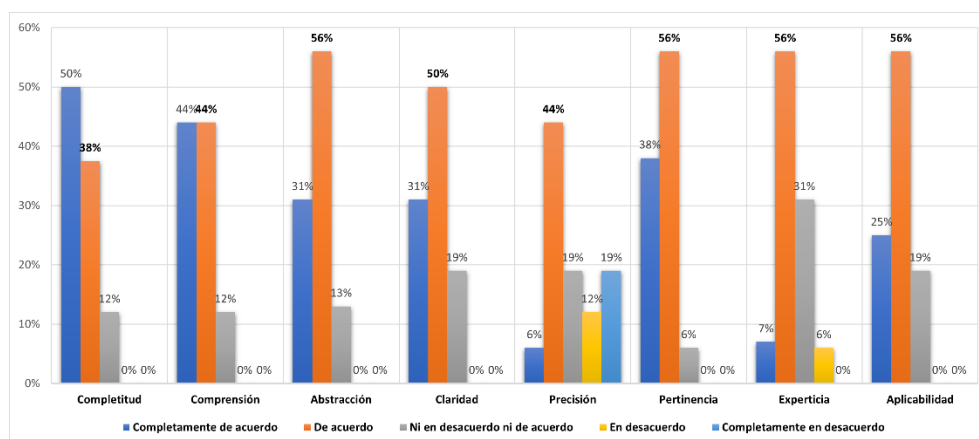


Fig. 7. Resultados encuesta expertos

El atributo más aceptado es el de complejidad y comprensión, identificando oportunidades de mejora en lo relacionado a la precisión. En relación con el atributo de Precisión el 50% de los participantes opinan que el modelo BPMN no presenta ambigüedad en sus procesos y actividades, el 19% no está de acuerdo ni en desacuerdo y el 32% opina que el modelo BPMN si presenta ambigüedad en alguna de sus fases como se muestra en la fig 7.

## 5 Conclusiones y trabajo futuro

El modelo para orientar la implementación de DAG desde el enfoque de calidad provee una perspectiva para establecer oportunidades de publicación de datos estratégicos que se encuentren estructurados según los lineamientos establecidos para el ámbito colombiano y que presenten un nivel de calidad favorable para promover su uso y motivar la explotación pública y privada con un enfoque que varíe desde lo académico hasta lo comercial. Las fases, procesos, subprocesos y actores del modelo presentan el detalle requerido para facilitar su implementación y estructurar las actividades según las necesidades propias de cada entidad pública. El modelo propuesto puede ser utilizado por los interesados de las entidades públicas para proponer nuevas estrategias de uso, mejorar la formulación y medición de indicadores de impacto y calidad. Además, como una hoja de ruta para evaluar el progreso de publicación y explotación de los DAG en Colombia.

El trabajo futuro se puede enfocar en definir una estrategia de acompañamiento para implementar el modelo en entidades públicas, basada en el aprovechamiento de los datos y la explotación de la información con potencial de valor para terceras partes. Algunas de las recomendaciones para fortalecer el trabajo futuro son: realizar acompañamiento en la implementación o realización de pilotos para validar la metodología en la práctica, tener presente el nivel de incertidumbre, propio de una entidad pública, por temas de talento humano y objetivos a largo plazo por ello el detalle entre las fases es necesario, empoderar a la alta dirección e involucrar a todas las áreas del negocio en la adopción de la metodología. Así mismo se deben fortalecer las dimensiones humanas en cuanto dan cuenta de la relación de los gobiernos con el ciudadano y la generación de capacidad de capital humano y los ciudadanos en competencias de uso y apropiación de TI, como recurso crítico para dinamizar el crecimiento de ciudades inteligentes.

## Referencias

1. López, N; Mahecha, J: Prototipo de software para la evaluación de la calidad de datos abiertos, Tesis de Pregrado, Colombia (2017).
2. Bad Data Costs the U.S. \$3 Trillion Per Year, <https://hbr.org/2016/09/bad-data-costs-the-u-s-3-trillion-per-year>, last accessed 14-jul-2020].
3. ISO/IEC 25012, <https://iso25000.com/index.php/normas-iso-25000/iso-25012>. ,last accessed 14-jul-2020.
4. Ley 1712 DE 2014, <http://suin.gov.co/viewDocument.asp?ruta=Leyes/1687091>. ,last accessed 04/05/2020.
5. Política Nacional de Explotación de Datos, <https://colaboracion.dnp.gov.co/CDT/Conpes/Econ%c3%b3micos/3920.pdf>, last accessed 15/09/2020.
6. Guía de Datos Abiertos en Colombia”, [https://estrategia.gobiernoenlinea.gov.co/623/articulos-9407\\_brief\\_guia\\_datos.pdf](https://estrategia.gobiernoenlinea.gov.co/623/articulos-9407_brief_guia_datos.pdf), last accessed 15/09/2020.
7. Ficha calidad Datos Abiertos Colombia, <https://herramientas.datos.gov.co/es/fichatecnica-calidad>. ,last accessed 29/04/20200.
8. 10 Challenges for Open Data – Open State Foundation, <https://openstate.eu/en/2015/08/english-10-challenges-for-open-data/>. ,last accessed 20/10/2020].
9. Dvir, N.: Mitigating Challenges of Open Government Data. Preprints 1(82). doi: 10.20944/preprints201712.0182.v4 (2017)
10. Kucera, J.: Open Government Data Publication Methodology: J. Syst. Integr., 6(2)52–61, (2015). doi: <https://doi.org/10.20470/jsi.v6i2.231>.
11. Attard, J., Orlandi, F., Scerri, S., Auer, S.: A systematic review of open government data initiatives, Gov. Inf. Q., 32(4) 399–418, (2015). doi: 10.1016/j.giq.2015.07.006.
12. Martin, S., Foulonneau, M., Turki, S., Iahadjadene, M.: Open Data: Barriers, Risks and Opportunities In: ECEG2013- 13th European Conference on eGovernment: ECEG 2013, Luxemburgo, 301-309 (2013).
13. Cadena-Vela, S., Fuster-Guilló, A., Mazón, J.: Publicando datos abiertos considerando criterios de calidad. RISTI 22 (8) 295-306 (2019).
14. Kucera, J., Chlapek, D.: “Benefits and Risks of Open Government Data”, J. Syst. Integr., 5(1) 30–41, (2014). doi: <http://dx.doi.org/10.20470/jsi.v5i1.185>,

15. Guía de estándares de Calidad e interoperabilidad de los Datos Abiertos del Gobierno de Colombia, [https://herramientas.datos.gov.co/sites/default/files/2020-11/A\\_guia\\_de\\_estandares\\_final\\_0.pdf](https://herramientas.datos.gov.co/sites/default/files/2020-11/A_guia_de_estandares_final_0.pdf) 2016, last accessed 15/09/2020.
16. Guía para el uso y aprovechamiento de Datos Abiertos en Colombia, [https://estrategia.gobiernoenlinea.gov.co/623/articulos-9407\\_brief\\_guia\\_datos.pdf](https://estrategia.gobiernoenlinea.gov.co/623/articulos-9407_brief_guia_datos.pdf), last accessed 15/09/2020.
17. Requisitos de calidad para Datos Abiertos, [https://sellodeexcelencia.gov.co/documents/UTSF\\_SDE\\_Requisitos\\_de\\_calidad\\_para\\_datos\\_abiertos\\_2019\\_12\\_02\\_v\\_2\\_0.pdf](https://sellodeexcelencia.gov.co/documents/UTSF_SDE_Requisitos_de_calidad_para_datos_abiertos_2019_12_02_v_2_0.pdf), last accessed 15/09/2020.
18. Cai, L., Zhu, Y.: The Challenges of Data Quality and Data Quality Assessment in the Big Data Era, *Data Sci. J.*, 14(0)) 2-10, (2015). doi: 10.5334/dsj-2015-002,
19. Wahyudi, A., Kuk, G. & Janssen, M. A Process Pattern Model for Tackling and Improving Big Data Quality. *Inf Syst Front* 20, 457–469 (2018). <https://doi.org/10.1007/s10796-017-9822-7>
20. Data Quality Management for Industry 4.0: A survey”, <https://asq.org/quality-resources/articles/data-quality-management-for-industry?id=0c3073f0489d45a6891309b94261efab>, last accessed 15/09/2020.
21. Koltay, T.: Quality of Open Research Data: Values, Convergences and Governance, *Information*, 11(4), 2020, doi: 10.3390/info11040175.
22. A Suggested Framework for the Quality of Big Data Deliverables. <https://statswiki.unece.org/download/attachments/108102944/Big%20Data%20Quality%20Framework%20-%20final-%20Jan08-2015.pdf?version=1&modificationDate=1420725063663&api=v2>, last accessed 15/09/2020.
23. Merino, J., Caballero, I., Rivas, B., Serrano, M., M. Piattini, M.: A Data Quality in Use model for Big Data, *Futur. Gener. Comput. Syst.*, 63, 123–130, (2016), doi: 10.1016/j.future.2015.11.024.
24. Yi, M.: Exploring the quality of government open data Comparison study of the UK, the USA and Korea, *Electron. Libr.*, 37 (1) 35–48, (2019), doi: 10.1108/EL-06-2018-0124.
25. J. Attard, J., Orlandi, F., Auer, S.: Value Creation on Open Government Data, In 2016 49th Hawaii International Conference on System Sciences (HICSS), 2605–2614, (2016) doi: 10.1109/HICSS.2016.326.
26. Talukder, M., Shen, L., Hossain Talukder, M., Bao, Y.: Determinants of user acceptance and use of open government data (DAG): An empirical investigation in Bangladesh, *Technol. Soc.*, 56, 147–156, (2019), doi: 10.1016/j.techsoc.2018.09.013.
27. Guía de Implementación de la Política de Datos Abiertos - México”, <https://datos.gob.mx/guia/>, last accessed 15/09/2020.
28. Muentke-Kunigami, A., Serale, F.: Los datos abiertos en América Latina y el Caribe, *Los datos abiertos en América Lat. y el Caribe*, (2018), doi: 10.18235/0001202.
29. Kalampokis, E., Tambouris, E., Tarabanis, K.: Open government data: A stage model, en *Lecture Notes in Computer Science*, 6846 ,235–246, (2009) doi: 10.1007/978-3-642-22878-0\_20.
30. Sabri, N., Emran, N., Harum, N.: Government open data portals: A measurement of data veracity coverage, *Int. J. Innov. Technol. Explor.* 8(12), 1975–1983, (2019), doi: 10.35940/ijitee.L2908.1081219.
31. El análisis predictivo: impulsando la mejora a partir de los datos, <https://blogs.iadb.org/administracion-publica/es/analisis-predictivo-impulsar-mejoras-mediante-uso-datos/>, last accessed 15/09/2020.

32. Rangel, A., Maestre-Gongora G., Osorio, M., Principios, lineamientos, dimensiones y atributos para la evaluación de calidad de Datos Abiertos de Gobierno. *Aibi Revista De investigación, administración E ingeniería*, 8(S1), 54-65.(2020) <https://doi.org/10.15649/2346030X.950>
33. Maestre-Gongora, G., Rangel-Carrillo, A., & Osorio-Sanabria, M. The value of open data government: a quality assessment approach. *Revista de Investigación, Desarrollo e Innovación*, 11(3), 507–518(2021) <https://doi.org/10.19053/20278306.v11.n3.2021.13348>
34. Maestre-Gongora, G. P., & Bernal, W. N. Conceptual model of information technology management for smart cities: SmarTICity. *Journal of Global Information Management (JGIM)*, 27(2), 159-175.2, (2019) <https://doi.org/10.4018/JGIM.2019040109>

# How Smart Furniture can help improve the quality of life of the elderly? Extended Interconnected Public Spaces: A preliminary proposal

Víctor Manuel Padrón Nápoles<sup>1</sup>, Olalla García Pérez<sup>1</sup>, José Luis Esteban Penelas<sup>1</sup>,  
Sonia Escorial Santa Marina<sup>2</sup>, María José García Santacruz<sup>2</sup>

<sup>1</sup>Escuela de Arquitectura, Ingeniería y Diseño

<sup>2</sup>Facultad de Ciencias Sociales y de la Comunicación

Universidad Europea de Madrid. c/ Tajo s/n, Villaviciosa de Odón, Madrid

victor.padron@universidadeuropea.es, olalla.garpe@gmail.com,  
jluis.esteban@universidadeuropea.es, sonia.escorial@universidadeuropea.es, mariajose.garcia3@universidadeuropea.es

**Abstract.** Smart cities, and particularly public smart furniture, change the meaning and the use of cities' public spaces. Transforming them from just physical meeting places to a mixture of physical and virtual spaces. Most of the smart furniture or smart kiosks are used to require information, or to require economic-related services. However, according to the concept of Interconnected Public Space, this infrastructure can be used to attract elderly people for collectively sharing outdoor experiences in parks, squares, bus stops or other public spaces. Connecting the elderly beyond the physical barriers of space (to any other city or town on our planet), creating bigger communities and stimulating them physically, mentally, socially and emotionally. This paper develops the Extended Interconnect Public Space, a concept that can help to achieve the same objectives faster and at a lower cost.

**Keywords:** Smart Cities, quality of life of the elderly, smart furniture, extended interconnected public spaces.

## 1 Introduction

In recent years, developed societies have shown progressive aging and displacement towards urban environments, as well as growing needs and interest in health. The post-pandemic era, on the other hand, is expected to produce a substantial change in general behavior and be accompanied by a great growth of the Web of data and collaborative activities between communities (forums and social networks) [1]–[4]. These elements are part of the Smart Cities, considered as environments that use technologies to improve the quality of life of their population.

Unmanned digital kiosks are a key component of the Smart Cities' services. They can be integrated with 24/7 IP surveillance cameras and smart sensors, provide free Wi-

Fi and video calls, mobile charging points, etc. Kiosks can provide visitors and citizens with local government information, as well as information about places, retail stores, restaurants, events, etc.

In addition, smart furniture can be used for improving the quality of life of the elderly using the Interconnected Public Space (IP-Space or IPS) concept [5, 6]. Nevertheless, its direct implementation is relatively complex, costly and time-consuming. It requires the design, construction, test and deployment of the outdoor equipment, shelter and external infrastructure; simultaneously with the development of software components, and the design and research of activities suitable for the elderly.

This paper describes a new approach for overcoming these limitations, the Extended Interconnected Public Space concept (Extended IP-Space or EIPS) [7]. It focuses, first, on the development of activities, attracting elderly communities and constructing the basic software, before proceeding to more expensive external and sophisticated tasks.

Next section introduces the needs of the elderly population and the state-of-the-art of smart furniture. Then, the extended IP-Space is described and discussed, to finally present the conclusions and future work.

## **2 Related Work and Background**

The number of elderly is estimated to double to 1.5 billion in 2050, growing from current 9% to 16% of the population [8]. Part of this growing sector of population has special needs to maintain good physical and mental wellbeing. These needs include physical exercise, social interaction and mental stimulation. Research into ageing and cognition has demonstrated the close relationship of sensory functioning and social communication to maintaining cognitive performance and mood in the elderly, yet in modern societies elderly people are increasingly isolated and under-stimulated, both physically and psychosocially [9]. This situation results in accelerated cognitive decline and the suffering associated with loneliness and confusion. Social interaction and intellectual stimulation may be relevant to preserving mental functioning in the elderly [10]. Some studies report that subjects, who participated in senior citizen clubs or senior centers, can have a lower risk of cognitive decline, especially if this interaction is realized with young adults [11]. Other studies highlight the potential of video games for developing physical skills, creating mental and social interactions for elderly people. Particularly if these video or computer games are designed with engaging content and provided through an easy and pleasurable interface [12].

### **2.1 Smart furniture and Smart Cities**

Many cities are using Smart Furniture as elements of their Smart City concept and deployment. Two of the main types of this furniture are Smart Kiosks and Smart Bus Stops.

#### **Smart Kiosks.**

Among the outstanding examples of cities employing Smart Kiosks are the cities of Daegu, in South Korea, and Philadelphia, in the US.

Daegu, the third-largest city in South Korea, has deployed unmanned kiosks as key components for disaster management. They transmit crucial information during disasters (earthquakes, floods, or fires) and provide local guidance to people. City authorities consider these kiosks as essential instruments to maintain communication with citizens even in the most complex circumstances while guiding and informing citizens and visitors daily [13].

Philadelphia, one of the largest cities in the USA, created the LinkPHL infrastructure, 100 smart kiosks in central areas with high pedestrian traffic. These kiosks provide free services such as recharging points, Wi-Fi service, emergency services, city social services, and cultural information (news, weather, events, public initiatives, etc.). Besides, its interactive maps will help locate the closest available LinkPHL access points while guiding visitors with routes. Installation and maintenance costs are offset by revenue earned from electronic advertisements. LinkPHL shows how digital kiosks can connect communities, people, and businesses [14].

Another outstanding example is the Portuguese manufacturer TOMI, which produces smart furniture adapted to people with disabilities (Fig. 1).



**Fig. 1.** Outdoor TOMI accessible information kiosk (Courtesy TOMI World).

### **Smart Bus Stops.**

Several European cities have launched smart bus stop pilot projects. That is the case of Paris (one-stop, Boulevard Diderot, 85 m<sup>2</sup>, accessible to persons with disabilities, and providing free Wi-Fi and USB charge, among other services), London (100 Clear Channel bus shelters, using Google Outside service to provide information), and Barcelona (around 10 stops, with mobile-based payment system).

The interfaces of the Smart Bus Stop are increasing in technical sophistication. Figure 2 shows the use of directional sound and big screens for publicity campaigns [15].



**Fig. 2.** Bus Stops using Directional Sound [<https://www.holosonics.com/applications-1>].

### 3 Description of the Extended IP-Spaces

As shown in the previous section, Smart Furniture is a mature technology, which can be applied for increasing or maintaining the quality of life of elderly people developing Interconnect Public Spaces. Nevertheless, to this development succeed it should be economically viable and have the acceptance of the elder community. The introduction of the Extended Interconnect Public Spaces helps in reducing costs and facilitates an agile development in closer collaboration with the elders.

This section first reviews the concept of Interconnected Public Space and then describes its generalization, the Extended Interconnected Public Space (EIPS). Next, a high-level architecture for EIPS implementation is proposed, to finally proceed to describe some of the potential activities that can be performed in these spaces.

#### 3.1 The Interconnected Public Spaces concept

An “Interconnected Public Space” or IP-Space [7] i.e. an outdoor space provided with an ICT equipment that can connect only with a similar space in another part of the world. Therefore, an IP-Space becomes a node in a network of IP-Spaces. An IP-Space node can be established in a bus stop, in a park, in a square or any other outdoor spot in the city, in which a group of persons could potentially interact with it. Therefore, IP-Spaces allow the sharing of collective experiences.

These nodes can be used to connect with persons from other regions or countries, using the *same or different languages*. They can be used to participate remotely in different sports, physical, cultural and playful activities (such as intellectual games or video games, physical exercises, dancing competitions and many more) engaging elderly people in remote communities and stimulating them mentally, physically, socially and intellectually.

Specifically for the elderly, promoting participation in cultural and sportive activities contributes to emotional, physical health and social cohesion [16]–[23]. The positive impact of participation in cultural activities –no matter what the level of ‘artistic competence’ of the people involved –on the perception of one’s own psycho-physic well-

being has been acknowledged for around 40 years and confirmed by a scientific measurement scale, the psychological general wellbeing index. As conclusion, the connection between culture and subjective wellbeing may often seem obvious although scientific evidence is much harder to get [24]. Interconnected public spaces can help create the conditions under which well-being is more likely to improve.

Figure 3 describes a potential implementation of IP-Spaces in the context of Smart Cities. Two sets of people from two different countries are sharing a dancing experience. Another group of people is sharing a yoga experience with remote people that could be in a third country.

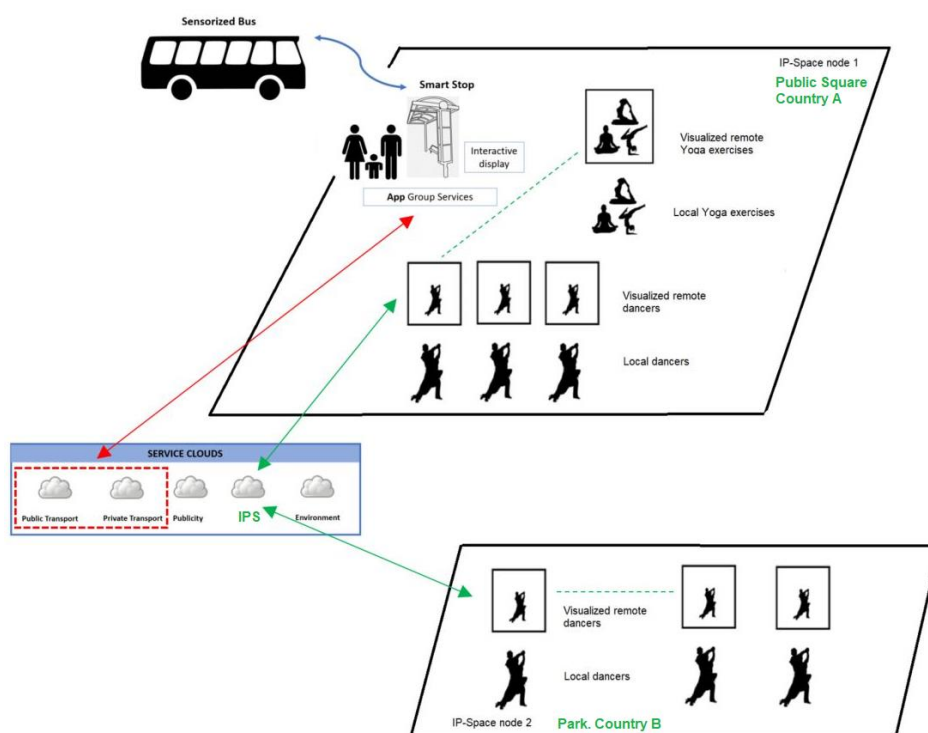


Fig. 3. IP-Spaces in the context of Smart Cities.

The surfaces for interaction are shown as walls, however, they can be implemented in floors, ceilings or using holograms. For another activity, the use of virtual reality glasses or augmented reality techniques, could complement the user interface.

A particular mention, it deserves the case when a bus smart stop (or another Smart Furniture) shares its infrastructure with an IP-Space. This is economically advantageous, reducing ICT deployment costs.

### 3.2 The Extended Interconnected Public Spaces concept

Sometimes economic and technological resources constraints can prevent the implementation of IP-Spaces in their original concept as an outdoor space. For those cases, the concept of “Extended Interconnected Public Space” (EIPS) was introduced [7], that is, a public outdoor or indoor IP-Space.

Indoor public implementation reduces the requirements on electronic system capability to withstand harsh environmental conditions (reduced costs) while keeping the requirements of being *outside home and sharing collective experiences*. This extended concept or implementation allows using existing non-digitalized locations as dancing clubs, elder people associations’, etc., as extended IP-Spaces (Fig. 4).

Therefore, applying the EIPS concept allows fast prototyping using low-cost hardware and getting close to already established elders’ local communities.

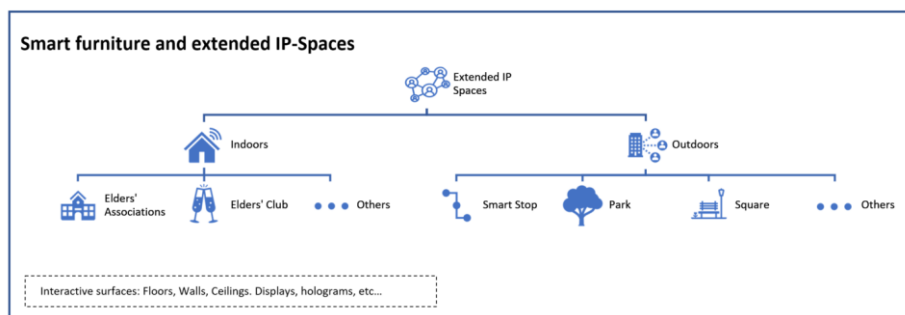
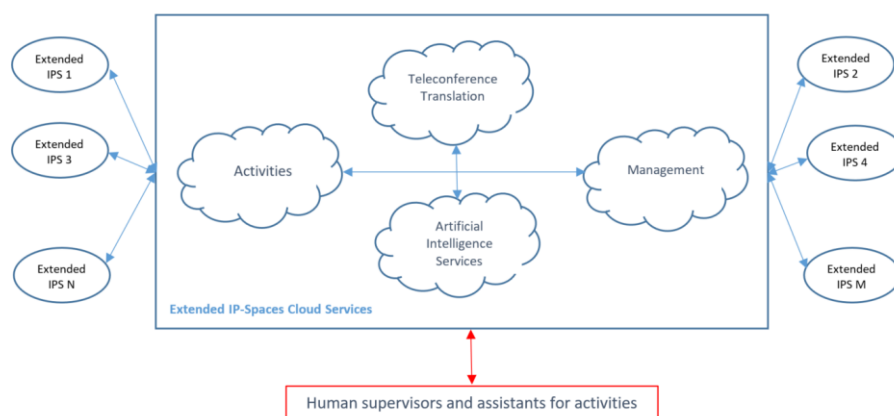


Fig. 4. The extended IP-Space possible implementations.

### 3.3 Extended IP-Spaces architecture

The proposed high-level architecture for the implementation of the extended IP-Spaces, is the same for outdoor and indoor implementations. Its functional description [25] is described below. The different extended IP-Spaces, as well as the staff for supervising and assisting elders’ activities, connect to the Extended IP-Spaces Cloud Services (Fig. 5).



**Fig. 5.** High-level Architecture of the Extended IP-Spaces.

This Cloud architecture contains four main services:

1. **Activities.** It provides the access to digital activities or required digital support for activities: electronic games, education services, artistic activities, sports and physical activities, workshops, etc. A more exhaustive list of activities is provided in section 3.4 of this paper.
2. **Teleconference and translation services.** It is a key component that ensures not only physical communication, but also overcomes the language barrier. One example of such existing services is Skype Translator.
3. **Management services.** It ensures the organization of the activities, including services such as: appointments and calendar, authentication of users and supervision staff, interface customization settings, catalog of Spaces (“Addresses’ Book”) and catalog of activities (“Activities’ Book”) among other related tasks.
4. **Artificial Intelligence Services.** This is an optional service, which works on consent of the users, respecting their anonymity. Its main task is the analysis of the activities to reinforce learning and help supervision staff and users, to improve the activities’ outcomes.

**Human supervisor and assistants.** Staff such as teachers, coaches, and any other assistant personnel that helps or supervise elders’ activities. Dance teachers, yoga teachers, language teachers, health services related personnel, university course professors are some of the potential examples.

The Extended IP-Spaces’ interfaces can be complemented with different sensors (360° cameras, Virtual Reality glasses, biosensors, movement sensors, etc.), and mobile apps (e.g. outdoor individual translation), which allow improve the communication or obtain information enriching the interaction.

### 3.4 Extended IP-Spaces activities

Extended IP-Spaces (EIPS) introduce new conditions into elders’ traditional activities such as remote connections, the interaction with bigger electronic devices and multi-language communication.

The number of EIPS activities is almost endless. It can cover many aspects of the elderly’s life: education, arts, games, sports, economic activities, volunteering, aid campaigns with ecological and social purposes, etc. [7]. A short list of these activities is shown in Table 1.

**Table 1.** A brief list of EIPS activities.

Field	Activities	Description
<b>Education</b>	Languages	Provides the ability to learn and practice a language individually or in groups.
	Courses	Offers the possibility of learning different kinds of skills and knowledge, such as handcrafts, programming, culture, up to date learning pills, etc.
<b>Arts</b>	Painting	Painting lessons individually or in groups
	Music	Option to create, share or listen to music with other users.
	Reading	Allows book sharing, exchanging recommendations and book presentations reaching people all over the globe.
<b>Games</b>	Brain trainers	Games that improve your memory and also that provide the opportunity to challenge other users.
	Games	Electronic dominoes, checkers, chess, video games, etc.
<b>Sports</b>	Dances, Yoga, Gymnastics	Healthy activities that can be performed individually or in groups formed in different locations.

## 4 Discussion

It is very important to design activities and assess them to ensure the improvement (or the maintenance) of the quality of life of the involved persons. A list of parameters has been defined to evaluate this assessment (Table 2).

**Table 2.** A non-exhaustive list of parameters to assess activities effectiveness

Parameters
Physical well-being
Mental well-being
Social interaction
Mental stimulation

Cognitive performance

Good mood

Loneliness

Mental confusion

To collect data about the activities' performance and their impact on these parameters, five methods are going to be used:

1. An initial interview before exposing the person to any activity on the EIPS. A reference for evaluating the impact of the activities on his/her quality of life.
2. Periodic surveys and interviews to obtain feedback from users, supervisors and assistants.
3. Direct observation and communication between supervisors and human assistants, during the realization of the activities.
4. Observation and direct communication between the users involved in a certain activity.
5. The consented use of cameras and sensors to obtain information on the performance of activities.

All these data will feed artificial intelligence algorithms for detecting patterns and suggesting improvements in the design and execution of the activities. For example, the automatic suggestion of the best activities matching the mood of a given person, or the modifications of some activities to match the individual physical status of a person.

Older adults are a heterogeneous age group, and therefore they require different strategies than other age groups to successfully participate in sports and physical activities [26], [27]. In this sense, assistance using Artificial Intelligence can help to customized and personalize activities for individual specific conditions promoting an effective participation.

Initial experiments will be conducted using three groups of a minimum of four persons. Two of these groups will be able to speak the same language. This will allow evaluating the influence of using different languages during the activities. The autochthonous groups are expected to come from two cities in two different regions of Spain. Currently, coordination is progressing with two associations of elderly people belonging to the municipalities of the cities. This collaboration will help to initially select persons with similar interests and abilities, over 60 years of age.

The initial use of reduced groups will enable a gradual study about the development of the activities, and the realization of qualitative research, before proceeding to involve greater groups and collect significant sample data for complementing the studies with quantitative studies.

## 5 Conclusions

Nowadays, due to the increasing use of technology in society, older adults have begun to lag behind, since many of these smart devices are aimed at the vast majority of the population, but do not take into account the inclusion of this population sector.

The concepts of the "Interconnected Public Space" and the "Extended Interconnected Public Space" not only can allow overcoming this generational and technological barrier. They can engage elders in exciting activities that help them to maintain or increase their quality of life, counteracting the effects of ageism and age segregation in our societies.

Problems of isolation and loneliness [28], are getting serious attention from governments, due to their social and financial costs [29]. The UK and Japan appointed even Ministers of Loneliness to alleviate these issues, especially in a pandemic era. The health and active participation of an ever ageing population can promote the benefits of transmitting the experience and knowledge accumulated, as well as promote a thriving 'silver economy'.

Smart Cities' technologies can be applied for such purposes. In this sense, Extended Interconnected Public Spaces is an agile path that helps to reduce costs and involve elder communities in these developments.

**Acknowledgments:** This research was funded by Universidad Europea de Madrid grant number 2019/UEM19.

## References

1. Manzini, E. & Menichinelli, M.: Platforms for re-localization. Communities and places in the post-pandemic hybrid spaces. *Strategic Design Research Journal* 4 (1). 351-360 (2021). <https://doi.org/10.4013/sdrj.2021.141.2>.
2. Mangla, N.: Working in a pandemic and post-pandemic period – Cultural intelligence is the key. *International Journal of Cross-Cultural Management* 21 (1), 53-69 (2021). <https://doi.org/10.1177/14705958211002877>.
3. Mitchell, A.: Collaboration technology affordances from virtual collaboration in the time of COVID-19 and post-pandemic strategies. *Information Technology & People*, (2021). <https://doi.org/10.1108/ITP-01-2021-0003>.
4. Robinson, W. I.: Global capitalism post-pandemic. *Race & Class* 62 (2), 3-13 (2020). <https://doi.org/10.1177/0306396820951999>.
5. Nápoles V.M.P., Páez D.G., Penelas J.L.E., García G.G., Santacruz M.J.G.: Bus Stops as a Tool for Increasing Social Inclusiveness in Smart Cities. In: Nesmachnow S., Hernández Callejo L. (eds.) *Smart Cities. ICSC-CITIES 2019. Communications in Computer and Information Science*, vol. 1152. Springer, Cham (2019). [https://doi.org/10.1007/978-3-030-38889-8\\_17](https://doi.org/10.1007/978-3-030-38889-8_17).
6. Padrón-Nápoles, V. M., Gachet Páez, D., Esteban Penelas, J. L., García Pérez, O., García Santacruz, M. J., Martín de Pablos, F.: Smart bus stops as interconnected public spaces for increasing social inclusiveness and quality of life of elder users. *Smart Cities*, 3, 430–443 (2020).

7. Padrón Nápoles, V. M., Gachet Páez, D., Esteban Penelas, J. L., García Pérez, O., Martín de Pablos, F., Muñoz Gil, R.: Social inclusion in smart cities. In: J. C. Augusto (eds.), *Handbook of smart cities*. Cham: Springer (2020). [https://doi.org/10.1007/978-3-030-15145-4\\_42-1](https://doi.org/10.1007/978-3-030-15145-4_42-1).
8. Department of Economic and Social Affairs, United Nations. *World Population Ageing 2019: Highlights*; United Nations: New York, NY, USA, pp. 1–2 (2019).
9. Waterworth, J.; Ballesteros, S.; Christian, P.; Bieber, G.; Kreiner, A.; Wiratanaya, A.; Polymenakos, L.; Wanche-Politis, S.; Capobianco, M.; Etxeberria, I.; et al. Ageing in a networked society—Social inclusion and mental stimulation. In *Proceedings of the 2nd International Conference on Pervasive Technologies Related to Assistive Environments (PETRA 2009)*, Corfu, Greece, (2009).
10. Wang, H.; Karp, A.; Winblad, B.; Fratiglioni, L. Late-Life Engagement in Social and Leisure Activities Is Associated with a Decreased Risk of Dementia: A Longitudinal Study from the Kungsholmen Project. *Am. J. Epidemiol.* 155, 1081–1087, (2002).
11. Lee, S.H.; Kim, Y.B. Which type of social activities may reduce cognitive decline in the elderly?: A longitudinal population-based study. *BMC Geriatr.* 16, 165, (2016).
12. IJsselsteijn, W.; Nap, H.H.; de Kort, Y.; Poels, K. Digital Game Design for Elderly Users. In *Proceedings of the Conference on Future Play—Future Play '07*, Toronto, ON, Canada, (2007).
13. Smart City Press. Unmanned kiosks – the most effective stand to connect citizens with cities, <https://smartcity.press/digital-kiosks-benefits/>, last accessed 2021/11/24.
14. City of Philadelphia. 10 Ways to use the new LinkPHL kiosks, <https://www.phila.gov/2018-12-06-10-ways-to-use-the-new-linkphl-kiosks/>, last accessed 2021/11/24.
15. Martín de Pablos, F., Padrón Nápoles, V.M., Gachet Páez, D., Esteban Penelas, J.L., García Pérez, O., Muñoz Gil, R., García González, J., Escorial Santa Marina, S.: Human-Computer Interfaces for Smart Bus Stops as Interconnected Public Spaces (IP-Spaces) elements in Smart Cities. In: Meza, C., Hernandez-Callejo, L., Nesmachnow, S., Ferreira, A., Leite, V. (Eds.). *Proceedings of the III Ibero-American Conference on Smart Cities*. Instituto Tecnológico de Costa Rica (2020).
16. Bacon, N.; M. Brophy, N. Mguni, G. Mulgan and A. Shandro. *The State of Happiness: Can Public Policy Shape People’s Wellbeing and Resilience?* The Young Foundation: London, UK, 2010. Available online: <https://youngfoundation.org/wp-content/uploads/2012/10/The-State-of-Happiness.pdf>, last accessed 2021/11/24.
17. WHO. Regional Office for Europe: Active ageing: physical activity promotion in elderly, <https://www.euro.who.int/en/health-topics/disease-prevention/physical-activity/activities/hepa-europe/hepa-europe-projects-and-working-groups/active-ageing-physical-activity-promotion-in-elderly>, last accessed 2021/11/17.
18. Archer, L., Davidson, S., Iparraguirre, J., Kohler, M., Pursch, B., Vass, J., Curran, F.: Creative and Cultural Activities and Wellbeing in Later Life. Age UK Policy and Research Department and Age UK Oxfordshire, <https://www.ageuk.org.uk/creativewellbeing>, last accessed 2021/11/17.
19. UNESCO. Diversity of Cultural Expressions. Promoting participation in arts and cultural activities by the elderly. <https://en.unesco.org/creativity/policy-monitoring-platform/promoting-participation-arts>, <https://www.ageuk.org.uk/creativewellbeing>, last accessed 2021/11/17.
20. Ryu, J., Heo, J.: Relationships between leisure activity types and well-being in older adults. *Leisure Studies* 37 (3), 331–342 (2018).

21. Toepoel, V.: Cultural participation of older adults: Investigating the contribution of lowbrow and highbrow activities to social integration and satisfaction with life. *Int J Disabil Hum Dev* 10(2), 123–129 (2011).
22. Sheppard, A., Broughton, M. C.: Promoting wellbeing and health through active participation in music and dance: a systematic review. *International Journal of Qualitative Studies on Health and Well-being* 15(1), (2020).
23. Popovic S, Masanovic B.: Effects of Physical and Social Activity on Physical Health and Social Inclusion of Elderly People. *Iran J Public Health*, 48(10), 1922-1923, 2019.
24. Diener, E. *The Science of Well-Being: The Collected Works of Ed Diener*; Social Indicators Research Series; Springer: London, UK, Volume 37 (2009).
25. Grey, T.: Five principles for cloud-native architecture—what it is and how to master it. Google Cloud (2019). <https://cloud.google.com/blog/products/application-development/5-principles-for-cloud-native-architecture-what-it-is-and-how-to-master-it>, last accessed 2021/11/24.
26. Jenkin, C.R., Eime, R.M., Westerbeek, H., O’Sullivan, G. and van Uffelen, J. G. Z.: Sport and ageing: a systematic review of the determinants and trends of participation in sport for older adults. *BMC Public Health* 17 (976), (2017). <https://doi.org/10.1186/s12889-017-4970-8>.
27. Brawley, L.: Promoting physical activity for older adults. The challenges for changing behavior. *American Journal of Preventive Medicine*, 25(3), 172–183 (2003). doi:10.1016/s0749-3797(03)00182-x.
28. Fried, L. P.: Designing a new social infrastructure to combat loneliness in aging adults. *Generations* (2020).
29. Mihalopoulos, C., Le, L. KD., Chatterton, M.L., Bucholc, J., Holt-Lunstad, J., H. Lim, M., Engel, L.: The economic costs of loneliness: a review of cost-of-illness and economic evaluation studies. *Social Psychiatry and Psychiatric Epidemiology* (55), 823–836 (2020). <https://doi.org/10.1007/s00127-019-01733-7>.

## Indicadores de Destinos Turísticos e Normas Brasileiras de Cidades Inteligentes para a concepção de um *Smart Destination*

Alessandra Bussador<sup>1</sup>[0000-0002-5900-9398], Katya Regina de Freitas Zara<sup>2</sup>[0000-0002-1172-7729] e Janine Carvalho Padilha<sup>3</sup>[0000-0002-7404-6568]

<sup>1</sup> Universidade Federal da Integração Latino-Americana, Av. Tancredo Neves, 3838, Foz do Iguaçu, Paraná, BR  
alebussador@gmail.com

<sup>2</sup> Universidade Federal da Integração Latino-Americana, Av. Tancredo Neves, 3838, Foz do Iguaçu, Paraná, BR  
katya.freitas@unila.edu.br

<sup>3</sup> Universidade Federal da Integração Latino-Americana, Av. Tancredo Neves, 3838, Foz do Iguaçu, Paraná, BR  
janine.padilha@unila.edu.br

**Resumo.** Em resposta à necessidade de eficiência e sustentabilidade, no século XXI, surgiu uma nova tendência de desenvolvimento e gestão urbana em que há integração das tecnologias de informação para otimizar e auxiliar na tomada de decisões na gestão dos serviços públicos. Como as cidades inteligentes integram o sistema humano, físico e digital, elas permitem um modelo de gestão governamental participativo. Proporcionam experiências diferenciadas para seus moradores por meio da infraestrutura tecnológica disponível. Cidades turísticas que incluem indicadores de Cidades Inteligentes e integram a sustentabilidade e tecnologia nas fases da cadeia de valor do turismo como estratégia, criam um desenvolvimento sustentável baseado nas capacidades locais e potencializam a inserção da tecnologia em toda a relação de valor do destino turístico. O objetivo desse artigo foi averiguar quais são os indicadores dos Destinos Turísticos Inteligentes e das normas brasileiras para cidades inteligentes que são identificados nos principais destinos turísticos brasileiros, com mais de 50.000 habitantes, que caracterizariam estes municípios como *Smart Destination*. Como resultado, observou-se que a cidade do Rio de Janeiro foi a única que se apresentou entre as 100 primeiras cidades em todos os indicadores analisados e Natal foi a que menos se destacou, estando apenas com evidência em Mobilidade e Inovação. A identificação desses indicadores nos destinos turísticos poderá auxiliar em um melhor planejamento e gestão da atividade turística, procurando investir no desenvolvimento desses indicadores para transformar essas cidades em *Smart Destination*.

**Palavras-chave:** Cidades Inteligentes, Turismo, *Smart Destination*, Indicadores, Sustentabilidade, Governança.

## 1 Introdução

O crescimento populacional requer mudanças substanciais em termos de comportamento e estratégias de investimento em tecnologia, inovação e sustentabilidade para atender o desenvolvimento sustentável. O processo de urbanização, sem o devido planejamento, gera uma série de problemas sociais, tais como falta de acesso à moradia, violência, ausência de gestão de resíduos e exclusão social.

No mundo, 55% da população vive em áreas urbanas e a expectativa é de que esta proporção aumente para 70% até 2050 [1]. No Brasil, de acordo com dados da Pesquisa Nacional por Amostra de Domicílios, a maior parte da população, 84,72%, vive em áreas urbanas e somente 15,28% dos brasileiros vivem em áreas rurais [2].

Pelo crescimento da população urbana, as estratégias das cidades influenciam no engajamento dos cidadãos, os negócios, os investidores, ou seja, impactam o futuro da cidade [3]. Por esse motivo, o desenvolvimento sustentável é um dos temas de grande relevância em uma gestão municipal, pois ao se tornarem sustentáveis, as áreas urbanas devem preservar melhor os ecossistemas dos quais elas dependem. Além da preservação ambiental, os cidadãos poderão ter melhor qualidade de vida. Para isto, algumas ferramentas podem ser utilizadas, como as Tecnologias de Informação e Comunicação (TIC).

As cidades que utilizam TIC visam a gestão eficiente no uso de recursos e maior participação cidadã, onde a sustentabilidade é um dos seus objetivos, e utiliza indicadores para direcionar as políticas públicas e investimentos. Essas, são consideradas cidades inteligentes e sustentáveis. Ribeiro dos Santos e Gândara afirmam que as Cidades Inteligentes (CI) têm proporcionado experiências diferenciadas a seus moradores através da infraestrutura tecnológica disponível, contribuindo para a melhoria da qualidade de vida e um crescimento econômico sustentável, por meio de um modelo de gestão governamental participativo, a fim de impulsionar o crescimento econômico local [4, 5].

Os indicadores, além de contribuir para comparações entre cidades, podem embasar políticas integradas que auxiliam na tomada de decisões através do monitoramento de seu desempenho. A referência no Brasil para CI são as Normas de Cidades e Comunidades Sustentáveis NBR<sup>1</sup> ISO 37120:2021 e NBR ISO 37122:2019 [6, 7]. Cidades turísticas que incluem indicadores de CI e integram a sustentabilidade e tecnologia nas fases da cadeia de valor do turismo como estratégia, criam um desenvolvimento sustentável baseado nas limitações e capacidades locais e potencializam a inserção da tecnologia em toda a relação de valor do destino turístico, definindo, assim, um *Smart Destination* [4, 8].

Dada a transversalidade da atividade turística, os Destinos Inteligentes caracterizam-se nos eixos que exercem a gestão do turismo: governança, inovação, sustentabilidade, tecnologia e acessibilidade. A cidade e destino inteligentes apresentam sinergias porque compartilham o mesmo objetivo: melhorar a qualidade de vida dos cidadãos [9].

Considerando que o Brasil está investindo na construção de cidades inteligentes, e muitas têm a característica turística, percebeu-se a importância de verificar a relação

<sup>1</sup> Norma Brasileira [6].

existente entre os indicadores de Destinos Turísticos Inteligentes (DTI) e as normas nacionais relacionadas à CI. Neste contexto, a proposta deste trabalho é responder a seguinte questão: quais são as categorias dos DTI e das normas brasileiras para cidades inteligentes que são identificados nos principais destinos turísticos brasileiros, acima de 50.000 habitantes, que caracterizariam estes municípios como *Smart Destination*?

## **2 Breve Approach sobre Cidades Inteligentes e Smart Destination**

O conceito de cidade tem se modificado com o tempo, com diferentes termos e perspectivas como meio de definir a evolução urbana, de acordo com as experiências individuais. A abrangência das cidades é de acordo com sua aglomeração, podendo ser definidas como comunidades de 1.000 a 2.500 pessoas; cidades com uma população mais de 10.000 e 1,5 milhões de habitantes; e megacidades com uma população que excede 1,5 milhão de pessoas. Algumas cidades também são chamadas de globais ou internacionais devido a sua localização geográfica, riquezas naturais, oportunidades de emprego, ou outros fatores considerados de impacto. Essas cidades atraem habitantes de fora do país ou mesmo de todas as partes do mundo [10].

Além de seu tamanho e impacto, as cidades podem ser classificadas de acordo com seu estágio de desenvolvimento. Para encontrar o significado de "cidade inteligente", podemos definir que é a combinação de "cidade inteligente" e "cidade", representada como uma área urbana que utiliza sistemas inteligentes para facilitar o dia a dia. [11]. Estes sistemas consistem na utilização de tecnologias informáticas e de comunicações que proporciona maior profundidade e alcance ao sistema de inovação, tornando ao mesmo tempo suas funções mais transparentes e eficazes. Com isto, a cidade obtém maior capacidade de inovação, fato que resulta em incrementação da competitividade e do bem-estar [12].

O conceito de cidades inteligentes passou por um processo histórico evolutivo que deu início em 1994 com o uso de tecnologia e inovação nas áreas urbanas, na cidade digital em Amsterdã. Em 1997, surgiram as áreas urbanas virtuais. Estas foram definidas como representações eletrônicas e baseadas na web das áreas urbanas reais e foram abrigadas com a ajuda da rede mundial de computadores. As cidades virtuais foram tratadas como o primeiro esforço para fazer uso da Internet para apoiar a democracia e permitiram promoção urbana e desenvolvimento social nas cidades. Após a introdução da cidade virtual, o conceito de comunidade virtual passou a existir em 1998, permitindo a comunicação entre indivíduos por meio de normas compartilhadas. Essa rede de comunidade virtual tinha um escopo estreito de digitalização, porque estava associada a uma comunidade. Pessoas de fora da comunidade não tinham acesso direto à rede comunitária [11].

Em 1999, a primeira definição de cidade inteligente foi considerada em Dubai, onde os moradores e os governos locais criaram comunidades a partir do uso da TIC e sensores para compartilhamento de informações. Com o início da década de 2000, os tipos de cidades inteligentes evoluíram para ecossistemas mais “sofisticados”, cujo nível de

integração ampliou da simples entrega de informações incorporados em sistemas sociais para a entrega de serviços inteligentes (*EcoCity*) [10].

A caracterização de cidade digital tornou-se sinônimo de cidade da informação, e posteriormente avançou para a cidade ubíqua, onde a integração humano-computador torna-se invisível, integrando a informática com as ações e comportamentos naturais das pessoas (2006) por meio da computação pervasiva. A partir de 2007, foram criados grupos em diversos países para estudar e colaborar com o tema de Cidades Inteligentes [11].

Em 2012, foi definido o conceito de Cidade Digitais Estratégicas por Rezende [13]. Neste mesmo ano, conceituou-se Destinos Turísticos Inteligentes, suprimindo demandas específicas de governo e turismo para as cidades [14]. Para criar um ponto de referência de Cidades Sustentáveis no Brasil, é publicada em 2014 a norma técnica NBR ISO 37120:2021 [6]. Esta norma considera a sustentabilidade como o seu princípio geral, e a cidade inteligente como um conceito orientador no desenvolvimento das cidades. Em 2015 é criado o grupo *Smart City* IEEE com a missão de ser a fonte principal de informações técnicas sobre Cidades Inteligentes e desenvolver as melhores práticas técnicas aplicados no contexto de infraestrutura urbana [15].

Em 2019, um grupo financeiro formado pelas 19 maiores economias do mundo (G20), elegeu o secretariado da Aliança Global de Cidades Inteligentes durante o Fórum Econômico Mundial para auxiliar na transformação digital das cidades e combater desigualdades sociais [16]. A evolução de conceitos e os acontecimentos descritos acima ajudaram na formalização de cidades inteligentes está representada na Figura 1.

Atualmente, cidades que possuem um projeto base para análise de indicadores, ou mesmo que buscam inovar e propor melhoria na vida dos cidadãos podem ser consideradas precursoras de inteligência no tocante à utilização de tecnologias para gerar eficiência em seus serviços. Rampazzo e Vasconcelos [17] afirmam que as cidades inteligentes são aquelas que desenvolvem políticas, estratégias e abordagens de planejamento, finanças, construção, governança e operação das infraestruturas e serviços urbanos que se utilizam das TIC como elemento central. Existem, contudo, diversas definições do que é uma cidade inteligente.

Buhalis e Amaranggana [18] apresentaram em seu trabalho aspectos para cada um dos indicadores de inteligência:

- Governança inteligente, que se relaciona com o aspecto da transparência dentro dos sistemas de governança por meio da modernização da administração da cidade, apoiando a abertura de dados e o envolvimento público;
- Ambiente Inteligente, que está relacionado à otimização de energia que leva ao gerenciamento sustentável dos recursos disponíveis;
- Mobilidade Inteligente, que se refere à acessibilidade dentro e fora da cidade e disponibilidade de sistemas de transporte modernos;
- Economia Inteligente, que está relacionada à implementação de estratégias econômicas baseadas na tecnologia digital;
- Pessoas Inteligentes, relacionadas ao nível de qualificação do capital humano da cidade; e

- Vida Inteligente, que envolve a qualidade de vida medida em termos de meio ambiente saudável, coesão social, atração turística e disponibilidade de serviços culturais e educacionais.

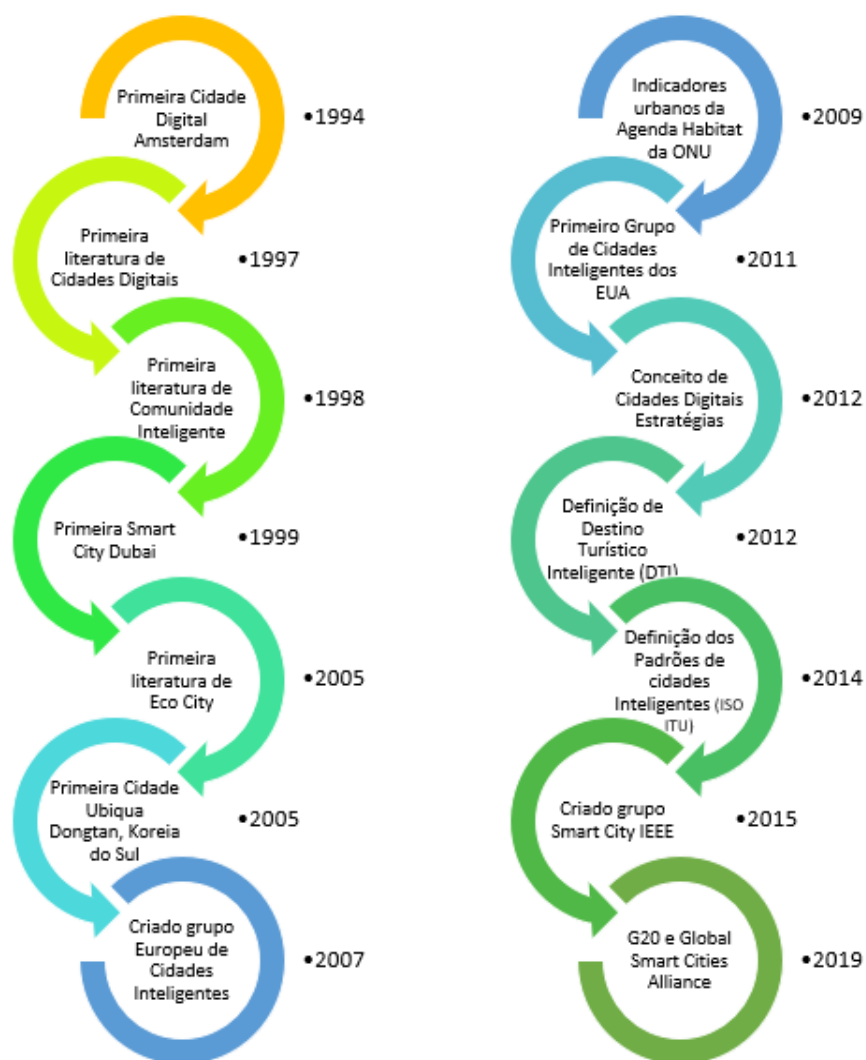


Fig. 1. Linha do tempo de Cidades Inteligentes.

Estes indicadores contribuem para a transformação de uma cidade em cidade inteligente, havendo a necessidade da inclusão do fator humano além de oferecer uma estrutura tecnológica para a cidade. Com base nos indicadores são criadas as normas que auxiliam no gerenciamento e boas práticas das cidades inteligentes. Neste contexto, o Brasil também possui as suas normas.

## 2.1 Normas Brasileiras para Cidades e Comunidades Sustentáveis

A Associação Brasileira de Normas Técnicas (ABNT) é o órgão responsável pela normalização técnica no Brasil, que fornece insumos ao desenvolvimento tecnológico brasileiro. Trata-se de uma entidade privada e sem fins lucrativos e de utilidade pública, fundada em 1940.

A NBR ISO 37120:2021 publicada em 2017 e revisada em 2021, tem como objetivo primordial a sustentabilidade, onde define e estabelece metodologias para um conjunto de indicadores, a fim de orientar e medir o desempenho de serviços urbanos e qualidade de vida. Ela segue princípios estabelecidos e pode ser utilizada em conjunto com a norma internacional ISO 37101, *Sustainable Development in Communities – Management System for Sustainable Development – Requirements with Guidance for Use* [6, 7].

De acordo com a ABNT (2021), estar em conformidade não garante à cidade o propósito de ser inteligente, mas sim a conformidade com os indicadores para serviços urbanos e qualidade de vida definidos. Estes indicadores podem ser utilizados para rastrear e monitorar o progresso do desempenho da cidade para que esta possa atingir o desenvolvimento sustentável.

A NBR ISO 37122:2019, publicada em 2020, especifica definições e metodologias para um conjunto de indicadores para medir e considerar aspectos e práticas que aumentem o ritmo em que as cidades melhoram os seus resultados de sustentabilidade social econômica e ambiental [6, 7]. Esta norma considera a sustentabilidade como o seu princípio geral, e a cidade inteligente como um conceito orientador no desenvolvimento das cidades. Sugere-se a implementação da norma em conjunto com a NBR ISO 37120:2021 para medir o progresso em direção às cidades inteligentes e sustentáveis. A lista de indicadores das normas brasileiras contempla 19 temas: economia, educação, energia, meio ambiente e mudanças climáticas, finanças, governança, saúde, habitação, população e condições sociais, recreação, segurança, resíduos sólidos, esporte e cultura, telecomunicação, transporte, agricultura local/urbana e segurança alimentar, planejamento urbano, esgotos e água. Estes indicadores são de grande importância para qualquer cidade, entretanto, alguns precisam ser adicionados, quando se trata de uma cidade turística.

## 2.2 Destinos Turísticos Inteligentes

Com a tecnologia integrada a todas as organizações e entidades, os destinos aproveitam as sinergias entre a tecnologia e seus componentes sociais para apoiar o enriquecimento das experiências turísticas. Ao aplicar o conceito de inteligência para atender às necessidades dos viajantes antes, durante e depois da viagem, os destinos podem aumentar seu nível de competitividade. Este é um dos principais desafios para a gestão do turismo urbano [9].

O conceito de DTI criado pela *Sociedad Mercantil Estatal para la Gestión de la Innovación y las Tecnologías Turísticas* (SEGITTUR) foi adotado como base conceitual e ferramenta estratégica que busca criar experiências turísticas e aprimorar a gestão do destino por meio do conhecimento. Tem como objetivo principal prestar serviços

aos turistas em tempo real, criando um ambiente de cooperação e compartilhamento de dados, informação e conhecimento. O modelo espanhol utiliza uma visão sistêmica para a conversão de destinos em destinos inteligentes, por meio de cinco eixos fundamentais: inovação, sustentabilidade, competitividade, acessibilidade e governança [19]. O entendimento das diferenças descritivas entre uma cidade inteligente e um destino inteligente permitem um domínio maior das necessidades da cidade, além das contribuições que um modelo de turismo inteligente pode gerar em aspectos não incluídos nos modelos de cidade inteligente e ainda assim estão presentes na estrutura da cidade [9].

Com base em pesquisas e metodologias de CI, um DTI implementa com sucesso a inteligência que é fomentada pela inovação aberta, apoiada por investimentos em capital humano e social, e sustentada por governança participativa. Estas características desenvolvem a competitividade coletiva dos destinos turísticos para melhorar o social e a prosperidade econômica e ambiental para todas as partes interessadas criando um habitat ideal para o *Smart Destination* [22].

SEGITTUR [20] aborda o fenômeno considerando o paralelismo inegável com as cidades inteligentes, identificando uma série de aspectos que se diferem quando é aplicado para destinos inteligentes (Tabela 1):

**Tabela 1** – Diferenças entre cidades inteligentes e destinos inteligentes. (Fonte: [9])

<b>Cidade Inteligente</b>	<b>Características</b>	<b>Destino Inteligente</b>
Jurisdição	Limites Geográficos	Município, rede de cidades, Regiões
Cidadão	Público-alvo	Visitante
Área do Governo em Gestão de Cidades Inteligentes	Atores que impulsionam	Área do Governo em Gestão Turística
Constante	Temporalidade	Ciclo de viagem do turista
Melhorar a qualidade de vida dos cidadãos	Finalidade	Melhorar a qualidade das experiências turísticas e da qualidade de vida dos cidadãos

Apesar de terem algumas características diferentes, tanto a CI, quanto o DTI têm como objetivo o bem maior que é um ambiente melhor, tanto para o morador do local, quanto para o visitante, independente do tempo de estadia.

Ivars-Baidal et al. [9, 22] desenvolveram a partir do conceito de *Smart Destination* um sistema de indicadores para destinos turísticos inteligentes adaptando os indicadores existentes na literatura de gestão de destinos turísticos e de cidades inteligentes para destinos da região de Valência, Espanha (INVAT.TUR<sup>2</sup>). Os padrões foram analisados para identificar aqueles que se enquadram no modelo Destinos Inteligentes, derivados de índices de cidades inteligentes e ajustados ao contexto do turismo. Os autores identificaram nove categorias (governança, sustentabilidade, inovação, acessibilidade, conectividade, informação inteligente, marketing online e indicadores de performance), obtendo um conjunto de 72 indicadores. Estes indicadores foram utilizados em conjunto

<sup>2</sup> Instituto Valenciano de Tecnologias Turísticas [21].

com as normas brasileiras de CI para definir as características necessárias de *Smart Destination* adaptado para a realidade brasileira.

### 2.3 Cidades turísticas brasileiras

De acordo com o Ministério Brasileiro do Turismo, as dez principais cidades brasileiras turísticas são Rio de Janeiro (RJ), São Paulo (SP), Maceió (AL), Gramado (RS), Fortaleza (CE), Natal (RN), Foz do Iguaçu (PR), Porto de Galinhas (PE), Salvador (BA) e Florianópolis (SC) [22]. Dessas cidades, Gramado e Porto de Galinhas possuem menos de 50.000 habitantes. A Figura 2 mostra estes destinos, com exceção de Porto de Galinhas, que é uma vila pertencente ao município de Ipojuca (PE). A maioria dos destinos turísticos são cidades litorâneas. A seguir apresentam-se algumas características desses principais destinos, conforme o Instituto Brasileiro de Geografia e Estatística (IBGE Cidades) [23].

O destino mais procurado é a cidade do Rio de Janeiro que possui 6,8 milhões de habitantes, com taxa de escolarização de 96,9%. A taxa de urbanização de vias públicas de 78,4% e o Índice de Desenvolvimento Humano Municipal (IDHM) de 0,799. O segundo destino, São Paulo, tem a população de 12,4 milhões de pessoas, taxa de escolarização de 96% e urbanização de vias públicas de 50,3% e IDHM 0,805. Em terceiro lugar, tem-se a cidade de Maceió, cuja população é de pouco mais de 1 milhão de pessoas, com taxa de escolaridade de 95% e taxa de urbanização de 32,7% e IDHM de 0,721. Gramado, destino turístico que ocupa a quarta posição, tem 36,9 mil habitantes, com taxa de escolarização de 96,9% e taxa de urbanização de 23,5% e IDHM de 0,764.

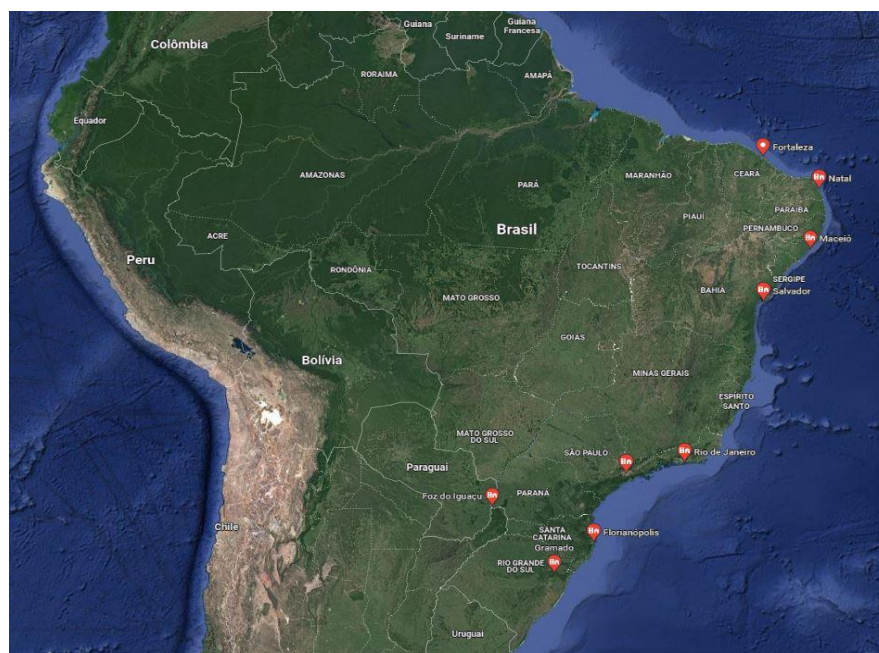


Fig. 2. Mapa do Brasil com destaque nos destinos turísticos (Fonte: Google Maps)

Fortaleza com população de 2,7 milhões, está em quinto lugar e possui uma taxa de escolarização de 96,1% e de urbanização de 13,2% e IDHM de 0,754. Em sexto lugar, está a cidade de Natal com 896,7 mil habitantes, com taxa de escolarização de 96%, taxa de urbanização de 16,5% e IDHM de 0,763.

O município de Foz do Iguaçu ocupa a sétima posição, com cerca de 258 mil habitantes, taxa de escolarização de 96,4%, taxa de urbanização de 50% e IDHM de 0,751. O próximo destino, Salvador, está em oitavo lugar e possui 2,9 milhões de habitantes, com taxa de escolaridade de 95,9%, taxa de urbanização de 39,5% e IDHM de 0,759. O último destino, dos apresentados no mapa, é a cidade de Florianópolis, com uma população de 516,5 mil, taxa de escolarização de 98,4%, taxa de urbanização de 54,4% e IDHM de 0,847.

### 3 Metodologia

Para realização desta pesquisa e seleção dos indicadores foi realizado um estudo descritivo por meio do levantamento bibliográfico e documental das normas brasileiras de cidades inteligentes e o modelo de indicadores proposto pela SEGITTUR e que definiu o conceito de DTI. O processo descritivo visa a identificação, registro e análise das características, fatores ou variáveis que se relacionam com o fenômeno ou processo [24].

A pesquisa analisou a literatura sobre a contribuição de serviços digitais das cidades inteligentes para o desenvolvimento de cidades sustentáveis. Concomitante foram analisadas as normas ABNT para Cidades Inteligentes NBR ISO 37120:2021 – Desenvolvimento Sustentável de Comunidades: Indicadores para Serviços Urbanos e Qualidade de Vida e NBR ISO 37122:2019 – Cidades e Comunidades Sustentáveis: Indicadores para Cidades Inteligentes que resultou na seleção dos critérios avaliados entre CI e DTI.

Para a definição dos indicadores para os destinos turísticos, foram selecionados os indicadores de inteligência do modelo desenvolvido por Buhalis e Amaranggna [18] e relacionados com os indicadores de DTI propostos por Ivars-Baidal et al. [9] e destacados pela SEGITTUR. Posteriormente, o conjunto dessas categorias foram comparadas e observadas a luz das normas ABNT ISO supracitadas para adequação às características dos destinos turísticos brasileiros.

### 4 Resultados

Os resultados deste trabalho foram obtidos a partir dos destinos turísticos brasileiros, procurando identificar uma relação dos indicadores de cidades inteligentes, normas brasileiras de cidades inteligentes e as categorias dos destinos inteligentes, confrontando-as com os indicadores obtidos no ranking do *Connected Smart Cities (CSC) 2020*<sup>3</sup> [25].

<sup>3</sup> Estudo desenvolvido desde 2015 pela empresa Urban Systems que analisa 75 indicadores em todas as cidades brasileiras com mais de 50 mil habitantes em 11 eixos temáticos, criando um ranking e uma plataforma de discussão sobre Cidades Inteligentes [25].

Primeiramente, associou-se os indicadores de inteligência (Economia Inteligente, Pessoas Inteligentes, Governança Inteligente, Mobilidade Inteligente, Ambiente Inteligente e Vida Inteligente) definidos por Buhalis e Amaranggna [18] e as 19 categorias das normas ABNT NBR ISO 37120 e NBR ISO 37122 [7, 8] agregados conforme os indicadores de cidades inteligentes (Tabela 2).

**Tabela 2.** Relação entre os indicadores de Inteligência e as categorias das normas de CI

<b>Indicadores de Inteligência</b>	<b>Categorias das Normas Brasileiras de CI</b>
Ambiente Inteligente	Resíduos Sólidos, Meio Ambiente, Agricultura, Água, Esgoto e Energia
Economia Inteligente	Economia, Finanças
Governança Inteligente	Planejamento Urbano e Governança
Mobilidade Inteligente	Telecomunicação, Transporte
Pessoas Inteligente	Educação, População
Vida Inteligente	Saúde, Segurança Pública, Esporte e Cultura, Recreação e Habitação

Os dados de relacionamento entre indicadores de inteligência e as categorias das normas brasileiras mostram a presença de grupos que assinalam uma maior complexidade de análise. Isto consiste em uma maior quantidade de dados e relevância para a determinação de atendimento dos serviços urbanos, além da qualidade de vida almejada para a cidade. Esta situação fica mais evidente nas categorias relacionadas aos indicadores de Ambiente Inteligente (6) e Vida Inteligente com 5 categorias. Nota-se que nestas categorias estão desde o levantamento de infraestrutura, condições ambientais, necessidade de atendimento médico/hospitalar, até as percepções do próprio cidadão ao se sentir atendido, ou não, no que está relacionado com suas necessidades básicas.

Em um estudo comparativo, foram relacionados os indicadores de inteligência definidos por Buhalis e Amaranggna [18] e as categorias de destinos turísticos inteligentes em Ivars-Baidal [8] (Tabela 3).

**Tabela 3.** Relação entre os indicadores de Inteligência e DTI

<b>Indicadores de Inteligência</b>	<b>Categorias de Destinos Turísticos Inteligentes</b>
Ambiente Inteligente	Sustentabilidade
Economia Inteligente	Indicadores de Performance, Marketing Online, Turismo Inteligente
Governança inteligente	Governança, Sistemas de Informação
Mobilidade Inteligente	Acessibilidade
Pessoas Inteligentes	Inovação
Vida Inteligente	Conectividade e Sensoriamento

Considerando as relações entre os indicadores de inteligência e as categorias de destinos turísticos inteligentes percebe-se maior homogeneidade, com exceção dos indicadores para Economia Inteligente e Governança Inteligente, que se relacionam com 3 e 2 categorias de destinos turísticos inteligentes, respectivamente. Estes itens estão

diretamente relacionados, pois não basta o local ter atrativos naturais ou construídos, se não houver boa divulgação, busca de melhorias locais e utilização das tecnologias existentes.

Os turistas precisam de informações sobre o local de onde pretendem visitar, outrossim, eles serão os próprios que poderão ajudar nesta divulgação ao publicarem nas redes de comunicação sobre os serviços que fizeram uso, bem como as impressões que tiveram do local. Neste contexto, a visão de satisfação do morador local influenciará enormemente nas impressões que o turista levará da cidade e afetará a economia local. Porém, o sucesso da Economia Inteligente está diretamente relacionado com a Governança Inteligente.

Os padrões analisados identificaram aqueles que se enquadram no modelo destinos inteligentes, derivados de índices de cidades inteligentes e ajustados ao contexto do turismo. A partir dessa relação, foi realizada uma correspondência de indicadores de cidades inteligentes e destinos turísticos inteligentes utilizando o modelo DTI espanhol, com os temas existentes nas normas brasileiras para a seleção das categorias a serem aplicadas neste estudo [7, 9] (Tabela 4).

**Tabela 4.** Relação entre os indicadores de Inteligência e as categorias de CI e DTI

Indicadores de Inteligência	Categorias	
	Destinos Turísticos Inteligentes	Normas Brasileiras de CI
<b>Ambiente Inteligente</b>	Sustentabilidade	Ações de Sustentabilidade Territorial e Urbana (Resíduos Sólidos, Meio Ambiente, Agricultura, Água, Esgoto e Energia)
<b>Economia Inteligente</b>	Indicadores de Performance, Marketing Online, Turismo Inteligente	Economia e Finanças
<b>Governança Inteligente</b>	Sistemas de Informação, Governança	Governança, Planejamento urbano
<b>Mobilidade Inteligente</b>	Acessibilidade	Telecomunicação, Transporte
<b>Pessoas Inteligentes</b>	Inovação	Educação, População
<b>Vida Inteligente</b>	Conectividade e Sensoriamento	Serviços Públicos e Sociais (Saúde, Segurança Pública, Esporte e Cultura, Recreação e Habitação)

Como forma de interpretação da tabela 4, que apresenta a relação dos indicadores de CI e DTI, foram identificadas as oito cidades turísticas mais visitadas em 2020 citadas pelo Ministério do Turismo [22], acima de 50.000 habitantes e destacadas entre as 100 melhores no ranking CSC 2020 [25] para cada um dos indicadores supracitados. As cidades são: Rio de Janeiro (RJ), São Paulo (SP), Maceió (AL), Fortaleza (CE), Natal (RN), Foz do Iguaçu (PR), Salvador (BA) e Florianópolis (SC).

O indicador Ambiente Inteligente é referente aos temas meio ambiente, água e energia e gestão sustentável. As cinco cidades em destaque são: Foz do Iguaçu (24<sup>a</sup>), São Paulo (35<sup>a</sup>), Florianópolis (45<sup>a</sup>), Salvador (47<sup>a</sup>), e Rio de Janeiro (75<sup>a</sup>).

Economia Inteligente foca na produtividade, empreendedorismo, inovação e no mercado de trabalho, destacando as cidades Florianópolis (4<sup>a</sup>), São Paulo (8<sup>a</sup>), Foz do Iguaçu (37<sup>a</sup>) e Rio de Janeiro (60<sup>a</sup>).

Governança Inteligente está ligado à eficiência dos serviços públicos prestados e a existência de canais de transparência das ações da prefeitura. Prevalece as cidades de Fortaleza (15<sup>a</sup>), Salvador (16<sup>a</sup>), Florianópolis (53<sup>a</sup>), São Paulo (60<sup>a</sup>), Rio de Janeiro (61<sup>a</sup>) e Foz do Iguaçu (95<sup>a</sup>).

O indicador Mobilidade Inteligente relaciona-se às iniciativas de transporte, segurança do transporte, uso de veículos não poluentes e o acesso da população à internet. Destacam-se São Paulo (1<sup>a</sup>), Florianópolis (3<sup>a</sup>), Rio de Janeiro (4<sup>a</sup>), Salvador (10<sup>a</sup>), Fortaleza (18<sup>a</sup>), Natal (28<sup>a</sup>), Foz do Iguaçu (63<sup>a</sup>) e Maceió (89<sup>a</sup>).

Pessoas Inteligentes têm relação ao nível de qualificação oferecido ao cidadão e a sua qualidade, bem como a participação do cidadão na vida pública do município. Na Educação, as cidades são Florianópolis (5<sup>a</sup>), Rio de Janeiro (44<sup>a</sup>) e Maceió (67<sup>a</sup>). Na categoria Inovação, as cidades que se destacam são Rio de Janeiro (1<sup>a</sup>), Salvador (4<sup>a</sup>), Fortaleza (7<sup>a</sup>), São Paulo (8<sup>a</sup>), Florianópolis (34<sup>a</sup>), Natal (36<sup>a</sup>) e Maceió (62<sup>a</sup>).

O indicador Vida Inteligente diz respeito à gestão da saúde, da segurança pública, condições das habitações, bem como o nível de qualidade de vida dos cidadãos. Nas questões urbanas, se destacam as cidades São Paulo (10<sup>a</sup>), Salvador (14<sup>a</sup>), Rio de Janeiro (47<sup>a</sup>) e Fortaleza (93<sup>a</sup>).

Na Tabela 5 é apresentado o resumo da colocação das cidades avaliadas neste estudo, considerando o total de habitantes, posição no ranking *Connected Smart Cities 2020* e as 10 cidades turísticas mais visitadas em 2020 segundo o Ministério do Turismo.

**Tabela 5.** Relação entre as cidades mais visitadas com o ranking CSC 2020

Cidades	Ranking Cidades Visitadas	CSC 2020	Total de Habitantes (x1000)
Rio de Janeiro	1 <sup>a</sup>	7 <sup>a</sup>	6.800
São Paulo	2 <sup>a</sup>	1 <sup>a</sup>	12.400
Maceió	3 <sup>a</sup>	85 <sup>a</sup>	1.000
Gramado	4 <sup>a</sup>	-	37
Fortaleza	5 <sup>a</sup>	22 <sup>a</sup>	2.700
Natal	6 <sup>a</sup>	-	896
Foz do Iguaçu	7 <sup>a</sup>	44 <sup>a</sup>	258
Porto de Galinhas	8 <sup>a</sup>	-	4
Salvador	9 <sup>a</sup>	10 <sup>a</sup>	2.900
Florianópolis	10 <sup>a</sup>	2 <sup>a</sup>	516

De acordo com esses dados, não se tem uma relação direta entre as posições de visitantes com o ranking de Cidades Inteligentes. Isto evidencia a necessidade de um estudo específico para avaliar indicadores que representem as características de cidades inteligentes com o perfil de cidade turística.

## 5 Considerações finais

O objetivo desse artigo foi averiguar quais são as categorias do DTI e das normas brasileiras para cidades inteligentes que são identificadas nos principais destinos turísticos brasileiros, com mais de 50.000 habitantes, que caracterizariam estes municípios como *Smart Destination*.

Ao estudar as relações entre os indicadores de inteligência e as categorias presentes nas normas brasileiras para a definição de destinos turísticos inteligentes, destacaram-se os itens relacionados ao meio ambiente e vida. Paralelamente são evidenciadas as normas e economia para destinos turísticos. Esses elementos deixam claro que os indicadores de cidades inteligentes têm pesos distintos ao se considerar a avaliação e categorização de dados.

Chama a atenção também o fato de que nas categorias de DTI existe uma predominância dos indicadores de Economia. Isto dá a entender que são necessárias ações direcionadas ao fortalecimento do ecossistema empreendedor da cidade para melhorar os serviços turísticos ofertados.

Em relação ao ranking CSC 2020, nacional, São Paulo ocupa a primeira posição, seguido por Florianópolis (2<sup>a</sup>), Rio de Janeiro (7<sup>a</sup>), Salvador (10<sup>a</sup>), Fortaleza (22<sup>a</sup>), Foz do Iguaçu (44<sup>a</sup>) e Maceió (85<sup>a</sup>). A cidade de Natal, neste ranking, está fora das 100 primeiras posições do ranking CSC 2020, não sendo, portanto, avaliada neste estudo, e o mesmo para a vila de Porto de Galinhas e a cidade de Gramado, por não possuírem pelo menos 50.000 habitantes. Observou-se que os principais destinos se encontram nas regiões Nordeste (5), Sul (3) e Sudeste (2).

Em termos regionais para o CSC 2020, no Nordeste, Salvador ocupa a primeira posição, seguido por Fortaleza (2<sup>a</sup>), Maceió (9<sup>a</sup>) e Natal (13<sup>a</sup>). Na região Sul, Florianópolis está em primeiro lugar, seguido de Foz do Iguaçu (13<sup>a</sup>) e na região Sudeste, São Paulo encontra-se na primeira posição, seguido por Rio de Janeiro (4<sup>a</sup>).

A cidade do Rio de Janeiro foi a única que apresentou avaliação entre as 100 primeiras cidades em todos os indicadores analisados e Natal foi a que menos se destacou, com avaliação somente nos indicadores de Mobilidade e Inovação. Por outro lado, analisando os indicadores individualmente, percebeu-se que a Mobilidade é a única que os destinos turísticos se destacam dentro dos 100 principais no ranking. Uma das razões pode ser o fato de a maioria ser capital de estado.

A identificação desses indicadores nesses destinos turísticos poderá auxiliar na melhoria do planejamento e gestão da atividade turística. Com o investimento no desenvolvimento e aplicação dos indicadores, nessas cidades, elas poderão ser transformadas em *Smart Destination*, conforme explicitado nos dados apresentados na Tabela 5.

Esta progressiva transformação será possível a partir do desenvolvimento de parâmetros para cada um dos indicadores, com intuito de ranquear a sua importância para os destinos turísticos brasileiros. Tais ações consistem nos próximos passos deste trabalho.

## Referências

1. ONU (2019) ONU prevê que cidades abriguem 70% da população mundial até 2050. Organ das Nações Unidas(ONU) 2019:1–4
2. PNAD (2015) População rural e urbana - IBGE. In: *Pesqui. Nac. por Amostra Domicílios*. <https://educa.ibge.gov.br/jovens/conheca-o-brasil/populacao/18313-populacao-rural-e-urbana.html>. Accessed 4 Sep 2021
3. Brorström S (2017) The paradoxes of city strategy practice: Why some issues become strategically important and others do not. *Scand J Manag* 33:213–221
4. Ribeiro dos Santos S, Gândara J (2016) Destino turístico inteligente: construção de um modelo de avaliação com base em indicadores para planejamento, gestão e controle de destinos histórico-culturais patrimônio da humanidade, analisando o caso de São Luís (Maranhão, Brasil). *Cult - Rev Cult e Tur* 10:69–79
5. Grimaldi D, Fernandez V (2017) The alignment of University curricula with the building of a Smart City: A case study from Barcelona. *Technol Forecast Soc Change* 123:298–306
6. ABNT (2021) NBR ISO 37120 - Cidades e comunidades sustentáveis – Indicadores para serviços urbanos e qualidade de vida. 146
7. ABNT (2020) NBR ISO 37122 - Cidades e comunidades sustentáveis - indicadores para cidades inteligentes. 112
8. Ivars-Baidal JA, Celdrán-Bernabeu MA, Femenia-Serra F, Perles-Ribes JF, Giner-Sánchez D (2021) Measuring the progress of smart destinations: The use of indicators as a management tool. *J Destin Mark Manag* 19:100531
9. Guerrero G, Acosta D (2019) Destinos turísticos inteligentes en Latinoamérica: tendencias y retos para el desarrollo inteligente de destinos. IV Congr. Ciudad. Intel.
10. Anthopoulos LG (2017) The Rise of the Smart City. In: *Public Adm. Inf. Technol*. Springer, Cham, Online, pp 5–45
11. Das A, Sharma SCM, Ratha BK (2018) The new era of smart cities, from the perspective of the internet of things. In: Danda B, Rawat, Kayhan Zrar Ghafoor (eds) *Smart Cities Cybersecurity Priv*. Elsevier Inc., Amsterdam, Netherlands, pp 1–9
12. Komninos N (2007) Cidades Inteligentes. *Sistemas de Inovação e Tecnologias da Informação ao serviço do Desenvolvimento das Cidades*. 5–9
13. Rezende DA (2012) *Planejamento de estratégias e informações municipais para cidade digital: guia para projetos em prefeituras e organizações públicas*, 1 Edição. Atlas, Sao Paulo, SP
14. Jovicic DZ (2019) From the traditional understanding of tourism destination to the smart tourism destination. *Curr Issues Tour* 22:276–282
15. (2021) IEEE Smart Cities. *IEEE Power Energy Soc*. <https://doi.org/10.1109/tpwrs.2017.2758639>
16. GlobalData Thematic Research (2020) History of smart cities: Timeline. *Digit Distruption Internet Things Technol* 1–2
17. Rampazzo R de FP, Vasconcelos FN (2019) Cidades Inteligentes e (Quase) Humanas. *Rev Políticas Públicas Cid* 8:27–39
18. Buhalis D, Amaranggana A (2013) Smart Tourism Destinations. *Inf Commun Technol Tour* 2014 553–564
19. Muniz ECL, Dandolini GA, Biz AA, Ribeiro AC (2020) Customer knowledge management

- and smart tourism destinations: a framework for the smart management of the tourist experience – SMARTUR. *J Knowl Manag* 25:1336–1361
20. SEGITTUR (2021) Destinos Turísticos Inteligentes. In: SEGITTUR. <https://www.segittur.es/destinos-turisticos-inteligentes/proyectos-destinos/destinos-turisticos-inteligentes/>. Accessed 31 Jul 2021
  21. Femenia F, Celdrán M, Ivars-Baidal JA (2017) Guía de Implantación de Destinos Turísticos Inteligentes de la Comunitat Valenciana. Agencia Valencia del Tur Invariantur 116
  22. Turismo M do (2021) Rio de Janeiro foi a cidade mais procurada por brasileiros em 2020. In: Gov. Fed. <https://www.gov.br/turismo/pt-br/assuntos/noticias/rio-de-janeiro-foi-a-cidade-mais-procurada-por-brasileiros-em-2020-diz-decolar>. Accessed 31 Jul 2021
  23. IBGE (2010) IBGE Cidades. In: Censo. <https://cidades.ibge.gov.br/>. Accessed 25 Sep 2021
  24. Gil AC (2017) Como elaborar projetos de pesquisa, 6th ed. Atlas, São Paulo
  25. Urban Systems (2020) Ranking Connected Smart Cities. Urban Systems

## El modelo de destino turístico inteligente y la relación de la gestión pública en su impulso, caso Cozumel, México 2015-2019

Alex Adiel Cano Heredia<sup>1</sup>[0000-0003-2623-7092] y Crucita Aurora Ken Rodríguez<sup>2</sup>[0000-0002-9673-2745]

<sup>1</sup> Universidad de Quintana Roo, México

<sup>2</sup> Universidad de Quintana Roo, México

**Resumen.** El modelo de los destinos turísticos inteligentes se ha transformado en una herramienta con grandes ventajas para analizar la gestión pública de los destinos turísticos, resaltando el progreso de la sostenibilidad del sector, la adaptación a la digitalización y conectividad del destino, el avance hacia un destino inclusivo, el nivel de desarrollo del destino turístico y el impulso de otras dimensiones. En estas otras dimensiones se incorporan a este concepto, de forma más amplia, los beneficios a la población local del destino y el papel que juega la gestión pública. Siguiendo una metodología basada en la revisión bibliográfica y documental de los fundamentos teóricos en los que se sustenta esta investigación. Dentro de este proceso se logró el diseño del modelo de Destino Turístico Inteligente, sus dimensiones y sus variables adaptados para el destino de Cozumel, Quintana Roo, el cual, mediante la aplicación de la instrumentación necesaria a cada criterio, se obtuvo el grado de aplicación de cada una de las dimensiones del modelo de DTI en Cozumel. En este artículo se pretende plasmar un panorama actual del modelo inteligente, en Cozumel. Esto nos permite señalar los retos que este destino turístico insular enfrenta para convertirse en un DTI y sobre todo midiendo el desempeño de la gestión pública en el logro de este objetivo. El análisis se concentró en la situación actual de Cozumel en cuanto a las características que la clasificarían como destino turístico inteligente y haciendo a referencia del papel que juega la gestión pública en alcanzar esta clasificación.

**Palabras Clave:** Turismo, tecnología, gestión turística, destinos turísticos inteligentes.

### 1 Introducción

Se seleccionó el destino turístico de Cozumel, Quintana Roo, por los antecedentes del modelo en el destino ya que la isla de Cozumel se incorporó al proyecto Destinos Inteligentes mediante la elaboración del Informe de Evaluación y Plan de Acción para la transformación de Cozumel en Destino Turístico Inteligente (DTI) realizado entre abril y julio de 2015. Los técnicos de la sociedad estatal española dedicada a la gestión de la innovación y las tecnologías turísticas (SEGITTUR) se trasladaron a México para

entrevistarse con funcionarios de la Secretaría de Turismo (SECTUR), de la Secretaría de Turismo del Estado de Quintana Roo (SEDETUR) y del Fondo Nacional de Fomento al Turismo (FONATUR) (Rodríguez y Aguirre, 2018).

De igual forma se tomó en cuenta a la potencialidad que supone este caso de estudio para indagar los fenómenos a escala local, determinan la importancia de visibilizar los resultados de esta evaluación, analizar el diagnóstico actual del modelo y sentar las bases para que abra el camino a la formulación de estrategias de gestión pública, la toma de decisiones en el desarrollo de la zona, la planeación estratégica en materia de políticas públicas, que conecten a todos los actores del sector hacia un bien común: el fortalecimiento de la industria del turismo en Cozumel.

## 2 Definición de las dimensiones para la evaluación del modelo de destino turístico inteligente en Cozumel

Se ha denominado modelo DTI al diagrama multidimensional y los índices respectivos que representan al estado del modelo. Dicho cuadro revela el grado de desarrollo del modelo de la unidad de análisis en cuestión, los aparentes desequilibrios entre las dimensiones y los problemas que se sobrelleva el modelo (Schuschny y Soto,2009). De esta manera se pudieron operacionalizar las siguientes 5 dimensiones analíticas dentro del modelo teórico en el marco del modelo de DTI (véase figura 1).

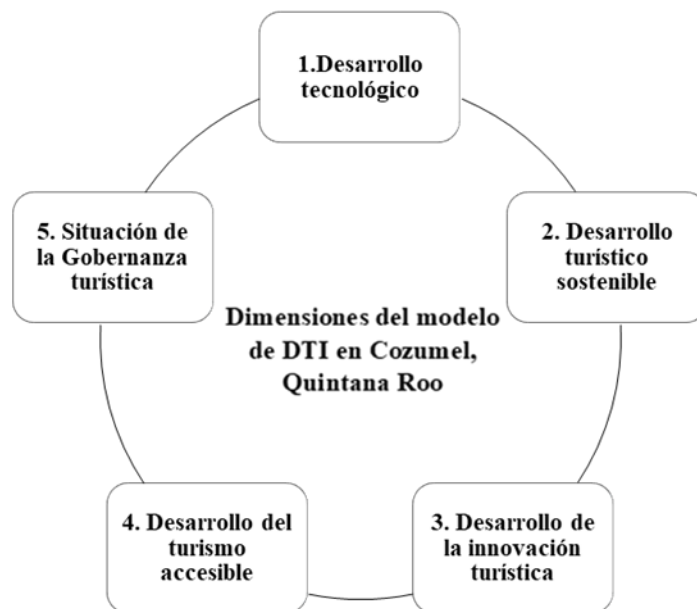


Fig. 1. Dimensiones analíticas del modelo teórico en el marco del modelo de DTI en Cozumel, Quintana Roo

Dentro del modelo es relevante mencionar que cada dimensión analítica es una construcción con la capacidad de capturar con coherencia dentro del modelo teórico de DTI, los componentes principales que permiten evaluar y definir el grado en el que se encuentran desarrolladas las dimensiones del modelo de DTI, respecto a la gestión pública y su atención a las necesidades de impulso de estas dimensiones en el destino turístico de Cozumel. De acuerdo con la precisión y grado de complejidad de cada dimensión se determinaron 3 variables específicas para cada dimensión, dando un total de 15 variables dentro del modelo teórico basado el modelo de DTI.

### **3 Método del análisis de las dimensiones del modelo de destino turístico inteligente en Cozumel**

En este sentido el modelo DTI y sus dimensiones se representan mediante un gráfico de radial o telaraña, en el cual cada eje (radio) simboliza una variable. Por lo tanto, cada uno de los radios del círculo o tiene un valor de 1, por lo tanto cada puntuación de cada variable oscilará entre 0 y 1. Donde 1 representa un nivel máximo de desarrollo y 0 un mínimo.

De igual forma, se representa cada una de las dimensiones del modelo, lo cual permite establecer el grado de desempeño de cada una, facilitando una primera aproximación del grado de desarrollo de cada dimensión en forma individual, así como, permite formarse una idea de la contribución de cada dimensión al desarrollo del modelo de DTI en Cozumel. Visualizar en una sola imagen las inestabilidades del modelo, permite la identificación de la dimensión para la cual se requiere aplicar políticas, inversiones u otros instrumentos específicos, para solucionar los problemas del modelo en Cozumel.

Se utilizan 3 colores para caracterizar fácilmente el estado de desarrollo del modelo en Cozumel. Cuando el valor alcanzado equivale a un índice por debajo de 0.33, este se representa con rojo, simboliza un estado crítico del modelo o dimensión. Para valores entre 0.33 y 0.66 el color es amarillo e indica un estado inestable del modelo o dimensión. Finalmente, de 0.66 a 1 el color es verde y se considera como un estado óptimo del modelo.

Es necesario explicar que el método e índice desarrollado en este estudio están basados, parcialmente, en la metodología del índice integrado de desarrollo sostenible, propuesto por Sergio Sepúlveda (2008) donde el índice es un valor específico de desempeño del desarrollo sostenible, con el cual se puede comparar la evolución de una unidad de análisis. De igual forma, es posible generar índices específicos para cada dimensión, en cuyo caso este indicador por dimensión representa el estado o desarrollo de cada una. Para el cálculo de los índices de desarrollo del modelo DTI, se utiliza una fórmula que primero calcula el promedio ponderado de las variables de cada una de las dimensiones, previamente relativizados. Después de calcular el promedio de cada dimensión, estas se ponderan de acuerdo con el nivel de importancia (priorización)

estipulado por los actores claves. La fórmula para calcular el Índice de cada dimensión puede observar a continuación:

$$I_D = \frac{1}{n_D} \sum_{i=1}^{n_D} V_i^D$$

En donde  $V_i^D$  es la variable de la dimensión D y se entiende que esa dimensión tiene  $n_D$  variables. Por tanto  $I_D$  es un promedio de las variables de la dimensión, los cuales han sido previamente estandarizados, para que tomen valores entre 0 y 1.

Posteriormente los índices de todas las dimensiones se agregan para obtener el índice integral de desarrollo del modelo de destino turístico inteligente (IIMDTI). La agregación se hace ponderando cada dimensión por un porcentaje de importancia  $\beta_D$ , obtenido mediante el cálculo de la priorización relativa. La siguiente fórmula muestra el método para calcular el IIMDTI:

$$IIMDTI = \sum_1^M = \left( \frac{\beta_D}{100} \right) I_D$$

Este proceso metodológico permite representar la evaluación y situación determinada del modelo DTI, mediante un índice proxy de desarrollo. Estos índices simbolizan el estado de desarrollo del modelo DTI y permite una primera aproximación a la situación del destino.

Parte del diseño del instrumento se sirve de la propuesta presentada por Acosta G. D. (2017) en su investigación Smart City, el puntapié para el desarrollo inteligente del turismo en un destino urbano. Si bien, el contexto es diferente es perfectamente aplicable a la región de estudio con las adaptaciones pertinentes. En total se aplicaron 40 instrumentos: 20 al sector público y 20 al sector privado.

El instrumento cuenta con dos secciones, la sección A, se basa en las valoraciones respecto a las iniciativas o acciones de la gestión pública en cada una de las dimensiones y variables del modelo de destino turístico inteligente en Cozumel, Quintana Roo durante el periodo de 2015 al 2019. La sección B consta de valoraciones respecto a la importancia relativa que tienen las diferentes dimensiones y variables que hacen a la inteligencia, o no, de un destino turístico.

La selección de los criterios de evaluación y diagnóstico cualitativo se basaron en una valoración y semaforización de los indicadores respecto al grado de aplicación de las iniciativas, con valores de 0, 0.5 y 1. Siendo 1 la existencia de iniciativas aplicadas exitosamente, 0.5 iniciativas en fase de proyecto (ideación o aplicación parcial) y 0 si no tiene ideadas iniciativas en relación con el indicador. Esta es una adecuación de la forma básica de la escala tipo Likert (1932), como es el caso de la adaptación realizada en esta investigación dado que la escala se ordenó de lo mínimo a lo máximo y se redactó según la pregunta. Es importante mencionar que la escala Likert es ordinal, aunque su uso más común es como intervalos, por lo que las medidas estadísticas usuales son la mediana y la moda para describir la tendencia central de los datos. En esta encuesta se busca el criterio más votado o la moda. Las preguntas que se formularon con esta escala permitieron al encuestado hacer un juicio de valor entre estas 3 alternativas, y no meramente exponer estrictamente su juicio sobre el hecho.

El muestreo fue no estadístico considerando el perfil preponderantemente cualitativo del estudio, por lo que la selección de los actores claves se procedió a través de la

identificación y clasificación de los principales agentes del desarrollo regional dentro de las dimensiones del modelo de DTI, estando éstos integrados en el sector público y privado.

Para la captura, sistematización de la información y la generación de resultados se optó por usar el programa estadístico IBM SPSS que ofició las herramientas necesarias para la captura y análisis de datos. De igual formas se utilizó la plataforma de cálculo y diseño EXCEL, que sirvió para la comprobación de resultados y realización del modelo radial.

#### 4 Resultados de la evaluación del grado en el que se encuentran desarrolladas las dimensiones del Modelo de Destino Turístico Inteligente en Cozumel, Quintana Roo.

##### 4.1 Índice integral del modelo de destino turístico inteligente Cozumel, Quintana Roo (IIMDTI)

En la siguiente tabla, se observa la evaluación integral del modelo mediante el índice obtenido por cada una de las 5 dimensiones que componen el modelo DTI. El resultado del modelo DTI en el Cozumel logró un IIMDTI de 0.44. Seguidamente podemos observar en la figura\_ el modelo radial y los valores alcanzados por las dimensiones del modelo DTI: 1. Desarrollo turístico sostenible;2. Desarrollo tecnológico;3. Desarrollo del turismo accesible;4. Desarrollo de la innovación turística y 5. Situación de la gobernanza turística.

Tabla 1. Índice integral del modelo de destino turístico inteligente Cozumel, Quintana

	ID	
 Índice integral de desarrollo del modelo de destino turístico inteligente Cozumel, Quintana Roo (IIMDTI)	0.44	
 Desarrollo turístico sostenible	0.55	
 Desarrollo tecnológico	0.28	
 Desarrollo de la innovación turística	0.30	
 Desarrollo del turismo accesible	0.56	
 Situación de la gobernanza turística	0.33	

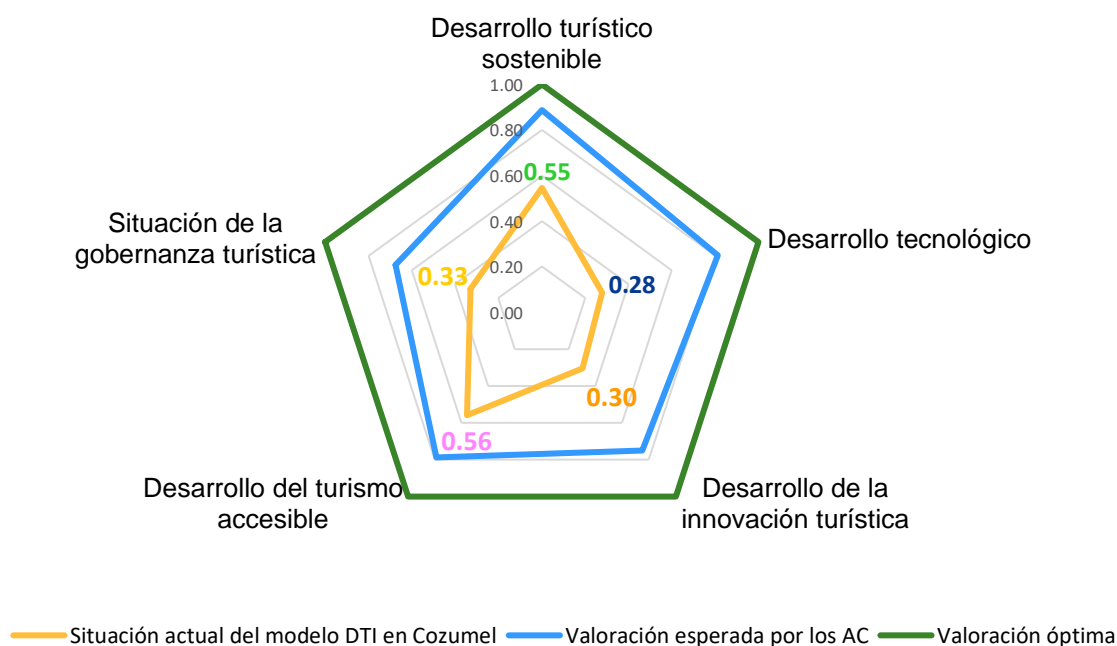


Fig. 2. Índices por dimensión del modelo DTI en Cozumel

Este índice integral representa una situación inestable para el modelo en el destino, de manera general podemos constatar que los actores clave de los diferentes sectores tienen el conocimiento de que las iniciativas o acciones implementadas o promovidas por la gestión pública muestran que Cozumel se encuentra deficiente en tecnología e innovación, e incluso en sostenibilidad y accesibilidad, que han sido los aspectos más sobresalientes en el destino. De igual forma, se comprueba que la situación de la gobernanza turística se encuentra en una situación crítica, a pesar de representar el eje transversal de las demás dimensiones como ente impulsor del modelo DTI en el destino, reafirmando el estado débil e inestable de las dimensiones y variables. Al respecto, hace falta como punto especialmente importante la participación de todos los actores turísticos: gestión pública, sector empresarial y sociedad civil, para incidir de manera positiva en todas las variables posibles del modelo en Cozumel.

#### 4.2 Índices por dimensión

El índice de desarrollo de la dimensión Tecnología (IDT) para el municipio Cozumel alcanzó un valor de 0.28. Esto significa que los componentes de desarrollo tecnológico en el municipio se encuentran en un estado crítico y tienen un impacto relativamente negativo en la prosperidad del destino y en su objetivo de implementar el modelo de DTI.

De acuerdo con el valor obtenido para cada variable e indicador, en la tabla 1 se revelan los factores determinantes en el desarrollo de la dimensión tecnología del

municipio. Los resultados cercanos a uno tienen un impacto positivo en el desarrollo del modelo DTI en el destino, mientras que los cercanos a cero requieren priorizarse para su mejora.

**Tabla 2.** Índice de desarrollo de la dimensión Tecnología (IDT)

Dimensión y variables	ID	
 <b>1 Índice de desarrollo de la dimensión Tecnología (IDT)</b>	<b>0.28</b>	
<b>1.1 Conectividad</b>	<b>0.46</b>	
<b>1.2 Sensorización del destino</b>	<b>0.30</b>	
<b>1.3 Sistema de información turística</b>	<b>0.08</b>	

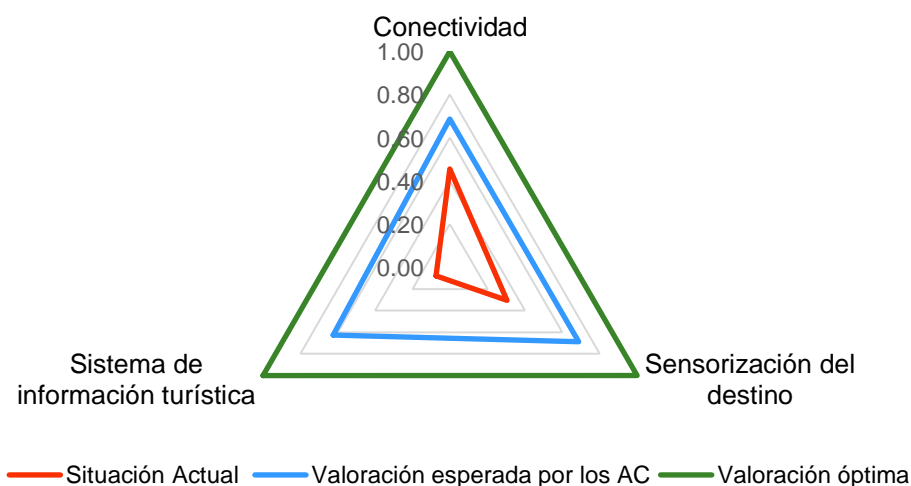


**Fig. 3.** Variables del Índice de desarrollo de la dimensión Tecnología (IDT)

En la figura 3 se muestra la dimensión de tecnología en Cozumel. La situación actual evidencia una muy baja calificación para el subdimensión sistema de información turística, seguida por una calificación baja para la sensorización del destino. El problema manifestado es que en el destino no se tiene evidencia de la existencia de un sistema de

información o captación de datos del sector turístico, lo que ocasiona el bajo grado de digitalización del turismo en el municipio.

Para evaluar las condiciones del municipio con relación a la dimensión de sostenibilidad, esta se integra por 3 variables. El resultado de la dimensión para Cozumel alcanzó un valor de 0.55. Esto significa que existe un avance moderado en la gestión de la sostenibilidad e infraestructura física y de servicios en la recolecta y tratamiento de residuos en el destino, logrando un impacto relativamente positivo en el desarrollo urbano del municipio, consiguiendo una situación general inestable de la dimensión.

En la siguiente tabla 2 se muestran los valores de las variables determinantes en el desarrollo de la dimensión sostenibilidad en el municipio, dentro de los márgenes del modelo DTI. Los resultados cercanos a uno tienen un impacto positivo, mientras que los cercanos a cero requieren atención.

**Tabla 3.** Índice de desarrollo de la dimensión sostenibilidad (IDS)

Dimensión y variables	ID	
 <b>2 Índice de desarrollo de la dimensión sostenibilidad (IDS)</b>	<b>0.55</b>	
<b>2.1 Planeamiento urbanístico sostenible</b>	<b>0.66</b>	
<b>2.2 Fomento de la eficiencia energética</b>	<b>0.26</b>	
<b>2.3 Recogida y tratamiento de residuos</b>	<b>0.71</b>	

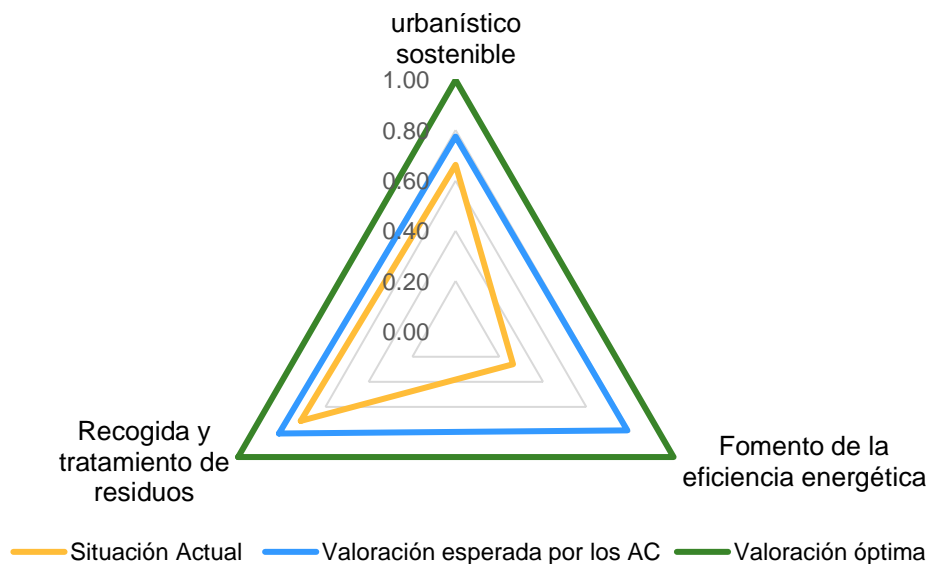


**Fig. 4.** Variables del Índice de desarrollo de la dimensión sostenibilidad (IDS)

La dimensión de sostenibilidad puede considerarse como una de las dimensiones con avance evidente en Cozumel, dentro del contexto del modelo de DTI. La gestión pública tanto federal como estatal define a la sostenibilidad como el eje rector de la política turística, con la adecuación de la Ley Estatal de Turismo que cimentaron las disposiciones legales que permiten desarrollar, promover y detonar destinos del estado en términos de sostenibilidad (GMC, 2019). En este contexto podemos evidenciar lo anterior en la figura 4 donde observamos una valoración considerable en la variable planeamiento urbanístico y seguida por la variable recogida y tratamiento de residuos, factores que están principalmente administrados por el sector público.

El índice de desarrollo de la dimensión innovación turística (IDI) para el municipio Cozumel obtuvo un valor de 0.30. Esto significa que los factores de desarrollo de la innovación turística en el destino se encuentran en un estado crítico y tienen un impacto relativamente negativo en la prosperidad empresarial y oferta de productos turísticos del destino. De acuerdo con el valor obtenido para cada variable e indicador, en la tabla 3 se revelan los factores determinantes en el desarrollo de la innovación turística. Los resultados cercanos a uno tienen un impacto positivo en el desarrollo del modelo DTI en el destino, mientras que los cercanos a cero requieren priorizarse para su mejora.

**Table 4.** Índice de desarrollo de la dimensión innovación turística (IDI)

Dimensión y variables	ID	
 <b>3 Índice de desarrollo de la dimensión innovación turística (IDI)</b>	<b>0.30</b>	
<b>3.1 Innovación en productos y servicios</b>	<b>0.39</b>	
<b>3.2 Innovación en la gestión turística</b>	<b>0.20</b>	
<b>3.3 Emprendimiento</b>	<b>0.33</b>	

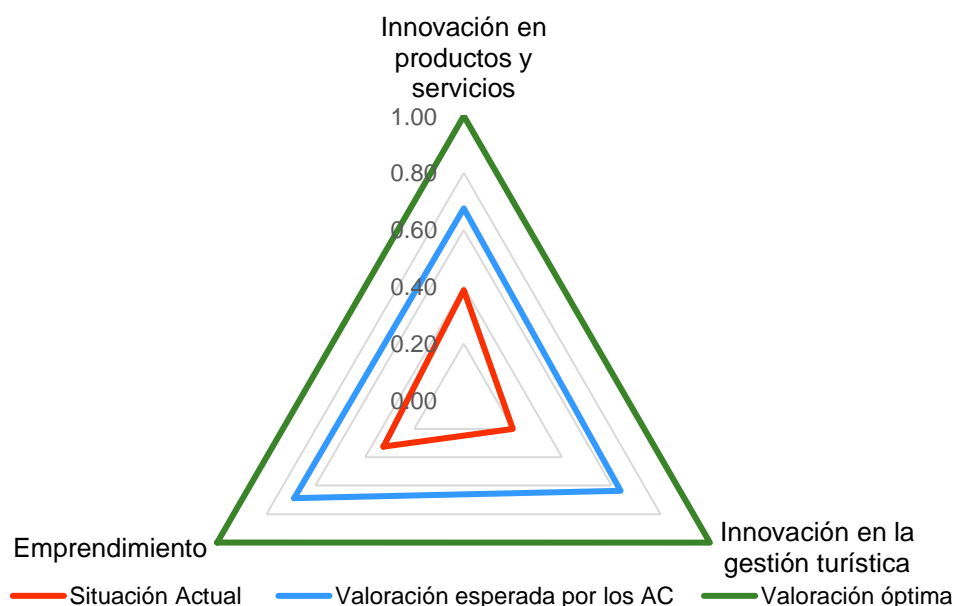


Fig. 5. Variables del Índice de desarrollo de la dimensión innovación turística (IDI)

En el modelo radial podemos observar que Cozumel presenta un grado moderado en la implementación de iniciativas enfocadas a la innovación en productos y servicios turísticos, a diferencia de aquellas iniciativas de innovación en la gestión turística. Se evidencia el enfoque de la gestión pública, mediante la Secretaría de Turismo, que lleva a cabo sus responsabilidades a través de la Dirección General de Innovación del Producto Turístico, como unidad promotora del desarrollo, consolidación y competitividad de la oferta turística a través del impulso a la innovación y diversificación de los productos turísticos (SECTUR, 2015).

Para evaluar las condiciones del destino de Cozumel con relación a la accesibilidad, esta dimensión se compone por 3 variables. El resultado para el destino logró un valor de 0.56. Esto representa que la provisión y ejecución de iniciativas que fomentan la infraestructura física y redes urbana en el destino es inestable, sin embargo, podemos considerar que esta dimensión tiene un impacto relativamente positivo en la prosperidad urbana del destino. En la siguiente tabla 5 se exponen los factores determinantes en el desarrollo de la accesibilidad turística en el municipio. Los resultados cercanos a uno tienen un impacto positivo, mientras que los cercanos a cero requieren priorizarse.

Table 5. Índice de desarrollo de la dimensión turismo accesible (IDA)

Dimensión y variables	ID	
 <b>4 Índice de desarrollo de la dimensión turismo accesible (IDA)</b>	<b>0.56</b>	
<b>4.1 Recursos/atractivos turísticos accesibles</b>	<b>0.63</b>	
<b>4.2 Sistema de certificaciones de accesibilidad turística</b>	<b>0.41</b>	
<b>4.3Accesibilidad mediante rampas en los atractivos turísticos</b>	<b>0.64</b>	

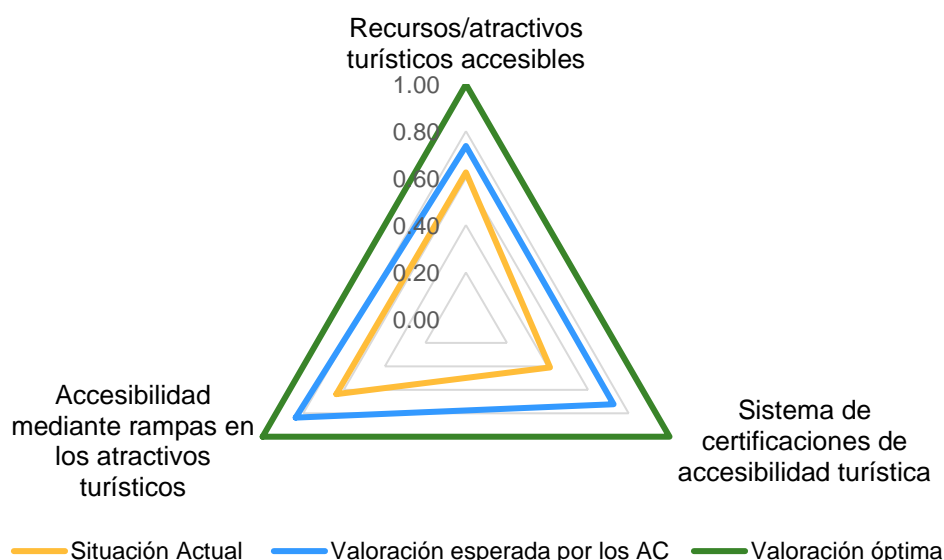


Fig. 6. Variables del Índice de desarrollo de la dimensión gobernanza turística (IDG)

El destino inteligente también sienta sus bases para asegurar un turismo inclusivo, que trabaja la accesibilidad desde una perspectiva integral, impulsando la creación de ambientes accesibles. En este marco podemos observar que las variables, recursos/atractivos turísticos accesibles y accesibilidad mediante rampas en los atractivos turísticos, que están basadas en infraestructura física, alcanzaron un puntaje considerable, revelando que de acuerdo con la percepción de los actores clave, en Cozumel existen iniciativas enfocadas al desarrollo de la accesibilidad física. Por otro lado la implementación de otros instrumentos que fomentan la accesibilidad en el sector, como un sistema de certificaciones de accesibilidad turística, aún se encuentra en un estado incierto y con acciones poco concretas para lograr una implementación de este instrumento, contar con una normativa específica de turismo accesible, es una herramienta de impulso al sector en el destino. A pesar de ciertos avances en el municipio, aún no asegura un diseño o propuestas aceptables para generar un entorno accesible tanto a locales como a turistas.

Para medir las condiciones de gobernanza, esta dimensión se integra por tres variables. El resultado para el municipio de Cozumel alcanzó un valor de 0.33. Esto representa que la situación de la gobernanza turística está en un estado crítico y tiene un impacto congruentemente negativo en el desarrollo del modelo DTI en el destino. De acuerdo con el valor conseguido para cada variable, en la siguiente tabla 6 se exponen los factores que se consideraron precisos en el desarrollo de la gobernanza turística en el municipio. Los resultados cercanos a uno tienen un impacto positivo, mientras que los cercanos a cero requieren atenderse.

Tabla 6. Índice de desarrollo de la dimensión gobernanza turística (IDG)

Dimensión y variables	ID	
5 Índice de desarrollo de la dimensión gobernanza turística (IDG)	<b>0.33</b>	
5.1 Aplicación de un Plan Estratégico de Turismo con perspectiva de DTI	<b>0.19</b>	
5.2 Departamento para el desarrollo del DTI	<b>0.16</b>	
5.3 Desarrollo del Gobierno Abierto	<b>0.64</b>	

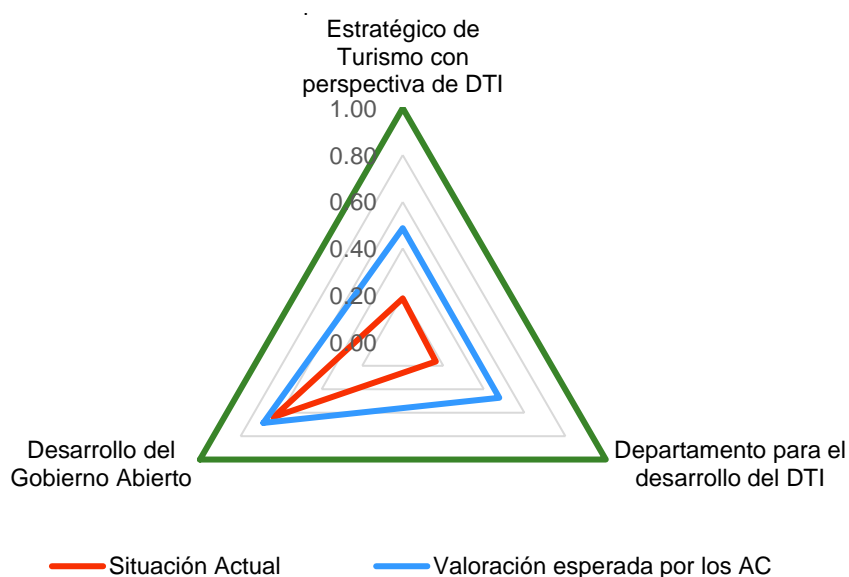


Fig. 7. Variables del Índice de desarrollo de la dimensión gobernanza turística (IDG)

Se evidencia en la figura 7, la débil valoración y la ausencia aparente de un Plan Estratégico de Turismo con perspectiva de DTI que contemple la participación de los diferentes actores del sistema turístico. En consecuencia, no se logró evidenciar en la evaluación la presencia de un departamento para el desarrollo del DTI o iniciativas públicas en proceso para su impulso en la gestión turística. La única variable que alcanzó un valor destacado fue la del desarrollo del Gobierno Abierto, y puntaje logrado mayormente por la valoración de los actores del sector público, esto debido a la legislación sobre la rendición de cuentas y datos abiertos que existe en la administración federal actual. Sin embargo, esta débil valoración de la dimensión logra colocarla en una situación crítica para el destino, siendo necesario un liderazgo político, compromiso entre los agentes turísticos, y visión estratégica para transformar la gestión pública turística habitual. Se trata de un cambio que requiere un esfuerzo continuo y que puede impulsarse con el desarrollo de una estrategia DTI por parte de la gestión pública, con fin de acercar cada vez más a Cozumel en su objetivo de ser definido como un destino turístico inteligente.

## 5 Conclusiones

Si bien la isla de Cozumel es uno de los destinos turísticos pioneros en subscribirse al modelo de destino turístico inteligente, la implementación de las características que componen al modelo no fue impulsado lo suficientemente eficaz para lograr un índice, en este estudio, que sea estable. El índice de 0.44 demuestra que la gestión pública no

ha acompañado a este modelo lo suficiente para ostentar los grados de tecnología, de sustentabilidad, de acceso incluyente y gobernanza.

El panorama presentado mediante esta evaluación toma en cuenta el quehacer de la gestión pública dentro de las dimensiones del modelo con el fin de sostener la posibilidad de entender al destino turístico inteligente como esquema social y técnico con voluntad de constituirse en un nuevo marco dominante respecto al futuro de las ciudades turísticas. Las acciones disponibles implementadas o promovidas por la gestión pública muestran que Cozumel se encuentra deficiente en accesibilidad, tecnología e innovación, e incluso en sostenibilidad, que ha sido uno de los aspectos más atendidos en el destino. Al respecto, hace falta como punto especialmente importante la participación de todos los actores de la sociedad: gobierno, sector empresarial, academia y sociedad civil, para incidir de manera positiva en todos los indicadores posibles.

Con todas las reflexiones anteriores se puede llegar a una conclusión que es la siguiente: el municipio de Cozumel precisa seguir avanzando en la definición de un modelo de referencia que contemple a la actividad turística como estratégica y no solo operativa. Este cambio de mejora del sector turístico puede ser potenciado a través de las iniciativas y proyectos llevados a cabo por las diferentes áreas de la gestión pública. Dado que el destino tiene ciertos avances en las dimensiones del modelo de DTI, es posible que ese cambio permita generar la plataforma necesaria para convertirse en un destino turístico inteligente. Por lo tanto, se concluye que definitivamente se tiene avanzar más en cada una de las dimensiones del modelo de DTI dentro del contexto local del destino y seguir realizando evaluaciones tanto cuantitativa como cualitativa para determinar grado de progreso de cada dimensión con el afán de poder tener deficiencias específicas del destino y poder solucionarlas con propuestas de política pública, para acercar cada vez más al destino en su objetivo de ser definido un destino turístico inteligente.

## 6 Referencias

1. Acosta G. D. (2017). Smart City, el puntapié para el desarrollo inteligente del turismo en un destino urbano. Buenos Aires, Argentina: Universidad Nacional de la Plata.
2. Rodríguez, A., y Aguirre, F. (2018). Modelo de Destino Turístico Inteligente. Estudios sobre geografía y territorio.
3. Schuschny, A., y Soto, H. (2009). Guía metodológica Diseño de indicadores compuestos de desarrollo sostenible. CEPAL.
4. SECTUR. (2015). Plan de trabajo de desarrollo institucional 2015. México.
5. Sepúlveda S. (2008) Biograma: metodología para estimar el nivel de desarrollo sostenible de territorios. San José, Costa Rica.

## Smart Governance for Collaborative Ecosystems

Rallou Taratori<sup>1</sup>, Sesil Koutra<sup>1</sup>, Montserrat Pareja-Eastaway<sup>2</sup>, and Nikolaos Al. Papadopoulos<sup>3</sup>

<sup>1</sup> University of Mons, 7000 Mons, Belgium

<sup>2</sup> University of Barcelona, Avinguda Diagonal, 696, 08034 Barcelona, Spain

<sup>3</sup> University of Macedonia, 156 Egnatia Street, GR-54636 Thessaloniki, Greece

**Abstract.** Hitherto, a plethora of theoretical and empirical studies have attempted to explore and unveil the evolution of (smart) governance mechanisms in the smart city era. Several different categories have emerged, such as but not limited to e-/open/participatory/smart/transition governance, nonetheless, no specific and comprehensive conceptualization of smart governance is unanimously accepted nor adopted by scholars and practitioners. Moreover, it ought to be mentioned that smart governance's evolution is significantly influenced by and aligned with the evolutionary waves of innovation ecosystem models.

Therefore, this review aims to address the question of what may literature reveal about the conceptualization of smart governance organizational mechanisms and collaborative ecosystems within the broad context of smart cities. This study contributes towards the framing of the multiple theories upon smart cities, smart governance, and the conceptualization of those under the collaborative ecosystem context. Additionally, the presentation of the evolution of innovation ecosystems models and theories will reveal the maturity of the Quintuple Helix Innovation Ecosystems model, and its significance while striving for achieving SDGs.

**Keywords:** Collaborative Ecosystems, Innovation Ecosystems, Smart City, Smart Governance

### 1 Introduction

The global standards that were lately set by the United Nations, yield for the reinforcement, or even emergence, of evolutionary models to secure sustainable development at a global level, with cities playing a significant role for this transition ([1–3]). Specifically, and according to the United Nations' *2030 Agenda for Sustainable Development* and *New Urban Agenda* ([2–3]), a smart-city approach should *ameliorate the whole sustainable urban development*.

The contribution of technological innovations towards the transition of conventional cities to modern ones has been significant and obvious in the domains of development, growth, well-being, and quality of life [4]. Nowadays, this interaction between technologies and cities' transformation towards sustainable development is being reinforced and revolutionized by the new wave of ICT [5], in most of the distinct fields of

a city and by allowing customized ICT solutions for major sustainability challenges. Multiple scholars and researchers (e.g. [6–11]), pursued to explore and reveal the different mechanisms associated with the design and realization of smart development projects. Nevertheless, despite the majority of such research that focuses on the possible ways to facilitate smart city development, there are still no solid definitions and methodologies that secure the success of a city into becoming smart. This work emerges from the interest of how reinforced organizational theories and mechanisms may effectively contribute towards and perhaps secure the aforementioned success, in smart city governance and collaborative ecosystems.

Yet, the concept of smart cities is highly related to ICT-led urban innovation, which may be exploited for ameliorating the well-being of citizens [12]. Testoni et al. [13] suggest that novel models of governance need to emerge in combination with appropriate coordination by the local government to efficiently manage the demanding dynamics of smart cities and complex cooperation procedures with a plethora of different social actors (especially citizens). For such a scenario to be achieved successfully, the role of governments, citizens, academia, industries, and other stakeholders should be reconstructed, while the most proper ICTs should be used per goal. These will subsequently lead to new governance models, which will be framed with new relationships, balances, processes, and forms of government [14].

The scope of this work aims to answer the question of what may literature reveal about the conceptualization of smart governance organizational mechanisms and collaborative ecosystems within the broad context of smart cities. Our contribution by answering this research question is the review of the plethora of theories and concepts upon smart cities, smart governance, and the conceptualization of those under the collaborative ecosystem context. Moreover, the presentation of the evolution of innovation ecosystems models and theories will reveal the maturity of the Quintuple Helix Innovation Ecosystems model, and its significance while striving for achieving SDGs.

In this review's chapters, the following issues will be addressed: i. conceptualization of SCs under the collaborative smart governance scope; ii. evolution of smart governance theory; iii. exploration of whether smart governance can be solely technocratic and corporate-driven; iv. introduction to smart collaborative ecosystems and conceptualization of both SCs and SCGs under this frame; and finally, v. evolution of the collaborative innovation models: Triple, Quadruple and Quintuple Helix models of innovation in ecosystem.

## **2 Smart City Conceptualization**

Gibson et al. [15] were a team of recognized professionals from government, academia and industry that in 1992 bibliographically placed first the term 'smart' within the urban framework. They discussed information, ideas, projects and initiatives that reinforce the development of SCs, fast systems and global networks, thus, they formulated a technological-oriented SC framework. Nowadays, there is a variety of literature definitions for the term 'smart city', thus, the lack of a universally accepted definition (e.g. [16–19]) is giving the label of SC a fuzzy concept and a broad frame for interpretation,

implementation and governing [16]. However, it is a fact that a growing number of cities globally, recognize the potential of addressing modern urban challenges by introducing the SC concept in their policy agendas and strategies [20]. More specifically, the '2020 Smart City Index' report ranked the 109 top major global cities that were considered as 'smart', based on economic and technological data, along with their citizens' perceptions of how 'smart' their cities are (e.g., transport and mobility, sustainability, governance, innovation economy, digitalization, living standard) [21].

Multiple terms and theories have emerged on the basis of SCs, and one of them was given by Mitchell [22], in relation with the advantages offered by ICTs and modern infrastructures, who defined the term 'smart growth' as "...attractive combinations of economic and cultural vibrancy, social equity and long-term environmental responsibility". Additional importance is given to the education of a new generation of citizens that will be able to contribute towards urban smartness via their knowledge expertise in a variety of fields (technological, social, environmental, etc.) and their generation of innovative ideas ([23–25]). More generally, for cities to achieve 'smartness', continuous learning and innovation must be established, a process that can be accelerated from openness and collaboration both between cities' best practices [26] and within each city for community-driven approaches [27].

The focus on ICT's importance within a city was the major component of the research on the field of smart cities for several years, yet, some years later different aspects of the SC started emerging and focusing on communities and governance. The California Institute for Smart Communities was one of the pioneers in that essence, as they investigated the possible ways that a community can transition to a smart state. They also examined the alternative ways of city planning that could benefit from the advantages of ICTs [28]. Moving forward, the interest of scholars and governments was shifted from the vastly criticized technology-driven smart city framework to more holistic approaches that included multiple pillars and presented governance-oriented approaches (e.g., [17, 29–31]). Specifically, Lee et al [32] proposed six dimensions for the analysis of SC's concept: i. urban openness, ii. service innovation, iii. partnership and collaboration, iv. proactiveness, v. infrastructure integration, and vi. governance.

Collectively, when examining the bibliography for SC definitions, three typical conceptualizations are formulated: i. Technologically-led, ii. Smart human-oriented, and iii. Smart collaboration and smart governance-focused SCs [33]. Literature (e.g., [18, 34–35]) suggests that there are still substantial challenges for cities to fully exploit the potential benefits associated with the SC concept; if cities want to become smarter, they require to question and reconstruct their conventional governance structures and organizational planning.

For the purposes of this review, the governance focus will be addressed in an attempt to stress the need for the emergence of sophisticated models and solutions, in the SC context, that may efficiently exploit ICTs for the facilitation of the collaboration among a variety of city actors and stakeholders, whilst in the pursuit of novel and comprehensive sustainable strategies, policies and overall transitions [36].

On these grounds, the SC definition of Ruhlandt [37] (as it was composed with the combination of segments of other relevant definitions and discussions of Kourtit et al. [38], Kitchin [39], Batty et al. [40], Townsend [27] and Paskaleva [41]) will be

followed. It states that “smart cities are a multi-dimensional mix of human (e.g., skilled labor), infrastructural (e.g., high-tech facilities), social (e.g., open network linkages) and entrepreneurial capital (e.g., creative business activities), that are merged, coordinated and integrated (into the fabrics of the city) using new technologies, to address social, economic and environmental problems, involving multi-actor, multi-sector and multi-level perspectives” [37].

It is worth mentioning that even though multiple researchers have stressed the significance of framing a functional, organized and comprehensive governance structure for securing a SC development (e.g. [17, 29, 31, 42–44]), there are still plenty of questions to be addressed regarding the indispensable components of a successful SCG and the ways it can be achieved via the appropriate tools and models to be defined.

### **3 Evolution of Governance Concept**

To understand and define modern forms of governance, a brief presentation of its basic evolution hitherto will follow in the next paragraphs.

#### **3.1 From the Government to the Governance**

Government is defined as the “political system by which a country or community is administered and regulated” [45]. The evolution of the whole concept has been traditionally formulated from top-down approaches for the policymaking and general governing processes; inevitably these approaches synthesized the amalgam of the 20th century’s political science literature [45]. However, the emerging needs of contemporary communities yield for new forms of government, if people, as political animals, are to advance further [45]. This whole conventional concept of government seems that has lost its descriptive and normative power for policymaking, and governance is considered a more appealing concept to achieve reinforced and sustainable development goals [46].

The wave of digital transformation is modifying governance models in a multidimensional, multifactorial and complex manner. Governance is a genuinely broad concept and a universal solid definition is not easily attainable. According to the UN-Habitat [47], governance is considered “an enabling environment that yields for appropriate legal contexts and effective processes to allow a government’s responsiveness to the citizens’ demands and interests”. Additionally, governance may also be described through the interaction and the cooperation of divergent actors and stakeholders during decision-making procedures ([48–49]). A part of the population interlaces the concepts of governance and government, while they are indeed associated, their difference lies in the former's conceptualization as it refers to “...all of processes of governing, whether undertaken by a government, market or network, whether over a family, tribe, formal or informal organization or territory and whether through the laws, norms, power or language ” [50].

Societal and political transformations over the last decades have allowed for new governance concepts, frameworks and models to emerge (e.g., e-governance, open

governance, participatory governance, etc.). New relations amongst the society and individuals, as well as new challenges that result from the increasingly complex systems of contemporary cities, are being observed; multicultural environments are a common phenomenon especially in metropolises, while human rights, environmental policies, democracy, and more, are being reclaimed and redefined from different populations as a response to different issues (e.g., climate change, inequalities) and because modern times allow for these degrees of freedom. As a result, more and enhanced participatory processes along with the empowerment of citizens are required in public decision making to satisfy the emerging needs of these liquid societies, with a horizontal integration throughout policy fields and a vertical integration among divergent stakeholders' groups, in order to deal with contemporary governance matters [46].

**e-Governance.** The core concept of e-Governance is revolving around creating multiple positive impacts on society, by exploiting technological advancement by governments, for reinforcing their inner structures, their relationships and interactions with state and non-state city actors ([51–52]).

**Smart governance.** Smart Governance is “... *the capacity of employing intelligent and adaptive acts and activities of looking after and making decisions about something*” [53]. Additionally, it is considered a base whilst in the pursuit of achieving a smart, open and participatory government [54]. The aforementioned concepts have a significant role when examining the smart city framework, while the role of ICT is of high importance as well for smart government as a section of broader smart governance models [12]. The role of ICT in contemporary urban governance is highlighted, as it has the prospect of offering effective solutions in highly complex city problems, while it presents the potential of enabling *public sector innovation* [55] and ICT-led urban innovation in general and in alignment with the smart city concept. It furthermore totally transforms the conventional forms of governance and government into the respective electronic versions (i.e. e-governance, e-government) [51].

According to Pereira et al. [12], smart governance may be defined as the “*capability of governments to proceed with more robust and reinforced decisions, while exploiting the integration of collaborative governance and ICT- facilitated urban innovation*”. Essentially, the available evidence (i.e., data) should be utilized in order to ameliorate the decision-making and instant democracy processes and outcomes, that in the end will serve the interests of the citizens. Moreover, Alawadhi et al. [53] identified some highly important smart-city initiatives factors, such as the reforming of administrative processes and structures at and across different levels of government, along with the integration of stakeholders' (including citizens) engagement in governance. By constructing new smart governance frames for urban policymaking, the whole decision-making procedures and the public services quality can be ameliorated [56].

**Open governance.** As discussed on previous sections, a main characteristic of the modern era is the great extent to which technology is being used, something that consequently leads to the generation of vast amounts of information and data (as created by

sensors, government, industries, academia, stakeholders, users of social media, citizens' feedback and more). The quantity and quality of the available data have the potential to improve governance practices and strategies, as well as enhance evidence-based policy and decision making, while ameliorating the knowledge management methodologies ([57–58]). It is a fact that governments attempt to base their decision-making processes on data-led and crowdsourced solutions realized via digital applications and platforms [59], by promoting and incorporating open government data practices in their agendas [60].

Thus, open governance can be conceptualized by accepting that data and information, in general, belong to the public, and when combined with e-democracy approaches it has the potential to transform e-Government to electronic open Governance ([61–62]). It should also be highlighted that in order to boost participatory governance practices, the transparency of governance processes is a prerequisite in order to secure the trust of the public towards the government authorities; a notion that yields for the integration of open governance features (i.e. big and open data, open government) [63].

**Participatory governance.** Participatory governance focuses on the “*interplay between sectors and territories*” [64], and particularly in ensuring the participation and inclusion of the civil society in policy-making processes [65]. The principal interest of such models is on maximizing transparency and accountability in the governance processes via the creation of synergies between the state and the civil society [66]. There are numerous studies that analyze how the participation in governance models work and the ways that may potentially lead to successful implementations (e.g., [67–71]). On the other hand, participatory governance has received criticism as in some cases fails to become something further than attending consultations (e.g., ([66, 72–73]), or even ensure that government-driven negotiations [74] are capable of improving the meaningful engagement of the civil society within governance processes [75]. Nonetheless, the research of Shin et al. [76], revealed that a key element that should be harvested during participation schemes is the consideration of ‘*adaptive preferences*’ (i.e., “*adjustment of people's aspirations to feasible possibilities*” [77]), especially of marginalized actors, as it increases the possibility of collaboration between various actors with conflicting interests.

**Transition governance.** Transition governance's main goal is to effectively facilitate sustainability transitions, whilst exploiting the utmost potential of appropriate societal processes [78]. It ensures that such transitions will not emerge to serve a single authority's agenda [79]; on the contrary, they should be achieved via the societal interactions and transformations of a plethora of stakeholders with a variety of differentiated or even conflicting interests, values and perspectives ([80–81]), along with the exploitation of appropriate decision-making societal approaches [82], all in the pursuit of striving for sustainable development. Even though a significant literature body for a variety of tools, methodologies and frameworks to boost stakeholder engagement does exist (e.g., ([83–87]), the need for specific participatory modeling is yielded from sustainability transitions' complex nature [88]. This is because, on the one hand models have

the advantage of offering clarity over frameworks, concepts, processes and even system dynamics, when they encourage systematic experiments that perhaps would not be feasible with another approach [88], while on the other hand they encourage the engagement of multi-actors in the development and realization of models [78].

Halbe et al. [78] synthesized the following six process phases of transition governance: i. Process phase 1: integrated knowledge production and problem definition; ii. Process phase 2: stakeholder analysis and selection; iii. Process phase 3: participatory visioning and goal formulation; iv. Process phase 4: interactive strategy development that anticipates long-term systemic effects; v. Process phase 5: coordination of the implementation of experimental actions; and vi. Process phase 6: systematic monitoring and assessment of actions.

### **3.2 The problems with a solely technocratic and corporate-driven smart governance**

According to Gil-Garcia [89], smart governance is capable of utilizing sophisticated ICTs to link and combine information, processes, organizations, and modern city infrastructure to facilitate the satisfaction of citizens' and communities' needs. In a relative literature review of Meijer et al. [33], four typical conceptualizations of smart governance were identified as following: i. smart city government, ii. smart decision-making, iii. smart administration, and iv. smart urban collaboration. These categories depict the gradual transition from a more stable and conventional form of government to a more dynamic, efficient and open form of governance that allows multi-actor, multi-sector and multi-level collaboration among government and a variety of stakeholders for multiple governance processes, policies and city strategies, and with the use of ICTs [33].

However, regardless of the opportunities of collaboration that smart governance allows, the literature reveals a more technocratic way in the governing of cities ([90–92]). In this context, the smart urban governance is facilitated by the reinforced government capabilities in regards to being able to gather and exploit great amounts of city information, that will allow for a more coherent understanding of urban challenges, and eventually lead to more robust, analytic and accurate administrative decision-making processes ([12, 93]). When a technologically-oriented approach is realized for the smart governance, then technology and ICT companies take the lead to the smart city transition by being the major providers of efficient digital solutions to urban large scale challenges, as perceived by them, contributing, if not formulating to the greatest extent, to the technocratic and corporate-led policy development in smart governance in cities [92].

This type of technocratic and technologically-led 'smart' governance has received a considerable amount of criticism, as it fails to incorporate the collective intelligence, an element that ought to be indispensable from the decision-making procedures that drive smart societal innovation and city development, while it is also not capable to fully manage the intricacy imposed by the socio-technical transformation any city is going through whilst attempting to become smart [94]. It is said that in practice, this approach simplifies urban problems into technological ones [95], while it neglects to include the vital aspect of citizens' participation for policy-making processes. In simpler

words, and as Plato quoted: “This City is what it is because our citizens are what they are”. The importance of the aforementioned point is stressed out, as it furthermore reflects the exclusion of unprivileged groups or individuals that are incapable of engaging in any policymaking that requires digital means and a certain degree of wealth or education [96]. This is the basic reason why the majority of such technological solutions formulated fail to include all possible related urban aspects involved, from the government agendas [92] to the public needs and requests [90] and the deeper social and inequality urban issues [8]. In addition, the technocratic, corporate-driven governance examples have revealed numerous negative impacts; government control and privacy issues [97], absence of citizen - all-inclusive- engagement [98], and nescience of place-based information [99].

Those reasons yield for collaborative ecosystems that ensure openness, inclusiveness and transparency amongst all the city stakeholders (i.e., state/government, industry/businesses, academia/universities, etc.), citizens and civil society organizations/unions; something that could be achieved via a collaborative model. Models like this demand the systematic review and redefinition of conventional bureaucratic organizations into contemporary collaborative ecosystems that ensure the above-wanted features and interact with the external environment ([100–101]).

## 4 Collaborative and ‘Smart’ Ecosystems

The term ecosystem has been typically used to describe biological systems. Nonetheless, the evolution of innovation concept within SCs and the reinforcement of organizational mechanisms in SCGs with the engagement of multiple stakeholders, has led to the conceptualization of those two as collaborative and ‘smart’ ecosystems.

### 4.1 Smart cities as ‘ecosystems’

The term ‘ecosystem’ in relation to SCs is no new within the body of the available literature. According to AFNOR [102], the main three elements that classify the city as an ecosystem are its: i. physical structure (i.e., natural environment, location, topography), ii. contained living entities, and iii. interactions’ flow layers (i.e., functions, economy, society, and information). Complementary, it has been used for the analysis of SCs for three key reasons: i. the resemblance that a plethora of SCs’ components (e.g., diversity of involved stakeholders) share with various ecosystems (e.g., knowledge, innovation), ii. it reveals exploitable insights for governance, and iii. it assists in the designing, development and implementation of sustainable solutions for the long-term horizon from the involved urban stakeholders and policymakers [103].

The SC could be regarded as a “complex system of people, processes, policies, technology and other enablers working together to deliver outcomes to specific ‘smart’ objectives, where ensuring QoL is an important concern as cities and urban environments are facing challenges to establish efficient, effective, open and participative processes to jointly create applications that meet the citizens demands” [104]. In these ‘ecosystems’, conventional partnerships between public and private organizations are

not adequate solely by themselves [105], and thus different forms of collaboration among the various stakeholders are emerging as a response to deal 'smartly' with the urban challenges [106]. Also, social and technological innovations are facilitated within 'ecosystems' for collaboration purposes [107]. Nonetheless, the development and realization of effective collaboration models amongst the stakeholders remain one of the key challenges that SCs are facing nowadays [108].

A SC can also be described as "a well-defined geographical area, in which high technologies, such as ICT, logistic, energy production, and so on, cooperate to create benefits for citizens in terms of well-being, inclusion and participation, environmental quality, and intelligent development" [109]. In this scope and while examining the term 'ecosystem' in relation to 'smartness', various meanings are detected among both technical and human capital systems, where the connection is towards the 'smart' urban transformation via schemes of typically open and driven innovation [110] and stimulated learning [111]. To understand the enabling of the 'smartness' element within ecosystems for SC development, a more holistic approach towards the similar incorporated ecosystems formatting, such as those of innovation or knowledge, should be adopted [112]. Additionally, taking into consideration the resemblance of the emerging 'smart needs' as an organizational structure of an 'ecosystem', the updating and redefining of SCs' practices and applications for sustainable economic growth are considered necessary [109].

What is more, the 'ecosystem' concept is used when assessing SC urban challenges that involve a variety of city actors, where the required 'ecosystem' management is framed via the identification of the different elements impacting its development (i.e., understanding, scoping, activating, managing and servicing) [113]. With the appropriate and efficient enabling of target urban groups via updated available services (i.e., innovation in information processing or integration of external digital assets) the 'ecosystem' approach shares the greater potential for more robust outcomes [114].

Chan [115] conceptualizes SCs as adaptive ecosystems that strive for sustainable development with the assistance of technological evolution, and whose structures are based on capability layers with equitable importance for the support and improvement of the SC 'ecosystem'. The bottom three layers are about the exploitation of technology and ICT, with accessible and secure portals for the dissemination of open information and knowledge. This basis ensures the creation of a fruitful environment for the furthermore exploitation of such knowledge by the respective and appropriate co-creation synergies between stakeholders, where collaboration amongst all involved actors (e.g., municipality, public, industry) is considered pivotal. The significance of such synergies for SC 'ecosystems' lies with the potential they create for resources' sharing (e.g., empirical knowledge, tools) and for practical (technological) experimentation for the enabling of smart objectives (i.e., technology-led contribution to the SC 'ecosystem', SC development policies and strategies, and creation of models for enabling social participation) [112]. Through these synergies, the governance could be reconstructed into collaborative smart governance with updated relationships and assignment of roles and responsibilities among the involved stakeholders, while allowing for the enabling of innovation to emerge and accelerate SCs' transformation with the resulting new 'smart' and varyingly-driven services (i.e. city-led, corporate-led, community-led, and private

citizen-led). Stam [116] adds that the opportunities to create value within an ecosystem require strong models of governance as the systemic conditions.

#### 4.2 Smart city governance conceptualization as ‘collaborative ecosystem’

A substantial amount of progress has been made over the last decades for the transformation of cities into smarter ones, something noticeably accelerated with the technological-led breakthroughs (e.g., ICTs) [117], however, it seems that the absence of established sufficient governance arrangements is significantly slowing down the whole transition [118]. City governance may be captured as a highly complex ecosystem that includes a plethora of stakeholders (e.g., citizens, organizations, local governments, city planners) who frequently present a conflict of interests in a variety of different perspectives of the prospective smart city projects. Therefore, a SCG should be highly customized to the specific amalgam of a city’s socio-economic and environmental components and drives, as well as substantially dynamic to the inner and outer eco-systemic balances and transformations, and the liquid city’s smart aspirations.

As discussed in previous paragraphs, smart and collaborative models of urban governance with an increased level of interaction, participation and cooperation among a variety of stakeholders and a user/citizen-centric approach, are considered vital for optimized outcomes and better smart city government and administrative services, as they depict more accurately the urban problems and determine holistically their importance ([119–120]). More specifically, it seems that these types of smart collaborative governance pursue the promotion and establishment of productive and strong relationships and interactions among networks of city actors [121], focusing thus on the development of collaborative ecosystems-oriented approaches for governing a city.

Based on an extensive literature review, Ruhlandt [37] identified the principle research emphasis pillars on SCG, revealing an eco-systemic and transdisciplinary approach. The collaboration element is a vital structure for his SCG conceptualization, while the categories that emerged (with their subcategories) from the literature review are presented in **Fig. 1** **Σφάλμα! Το αρχείο προέλευσης της αναφοράς δεν βρέθηκε.** below:

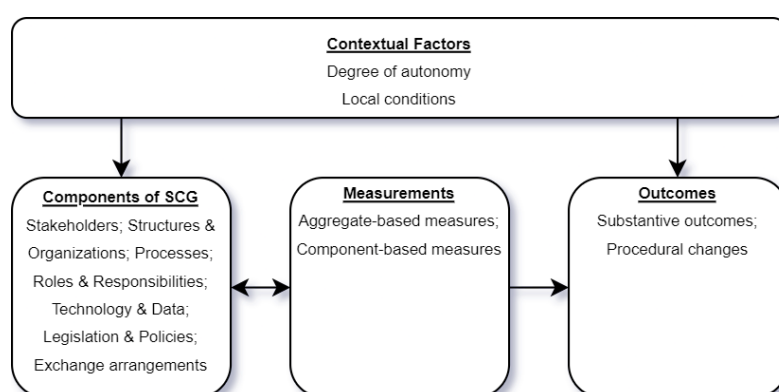


**Fig. 1.** Adaptation of Ruhlandt’s smart city governance research scheme [37]

The literature review of Ruhlandt [37] led to some significant findings and discussions about SCG, as summarized and presented below (Table 1):

**Table 1.** Ruhlandt's [37] findings and discussion on the literature review of SCG

Domain of SCG	Findings
Components	There are no specific component or combination of components that can grant if and to what extent a city maintains or is on the pursuit of achieving a SCG, neither if there exists a model of the <u>underlying causal relationship</u>
Measurements	A currently low scientific interest and a lack of agreement for the SCG's measurement unit for the analysis Any combination of available and suitable measurement techniques, is expected to provide a more holistic analysis of the component or sub-component measured in comparison with any technique applied independently
Contextual factors	The potential types and magnitude of influence of contextual factors on SCGs is still to be fully investigated and clearly understood due to the absence of adequate research papers and solid empirical proof <u>The ways that contextual factors may impact smart governance should be furthermore and thoroughly investigated, along with certain specifications for analysis of smart city governance in context</u>
Outcomes	Further research should be conducted on the understanding of the causal connections between SCG components and the achievements of SCG outcomes

## 5 Evolution of Innovation Models: Triple, Quadruple and Quintuple Helix Innovation Systems

Taratori et al. [122] in their work conclude that the evolution of smart governance mechanisms and processes demands the parallel evolution of innovation models for collaborative ecosystems. Thus, this chapter will attempt to present briefly the evolution of such models and their respective core elements and attributes.

To begin with, Etzkowitz et al. ([123–124]) came up with the term ‘Triple Helix’ to describe and define a model that focuses on the interaction of three helices, namely: state (i.e., the government sector), academia (i.e., the higher education sector) and industry (i.e., the business enterprise sector). The authors stressed the pivotal importance of these three helices interaction, while identified universities as core institutions and with significant innovation roles within the knowledge societies [123]. With this model, they propose that the central functions of universities should expand from teaching and research excellence to supporting economic and social development [123]. Practically, the overlap and cross-helix communication of the three different sectors are considered crucial in a knowledge society and economy [123].

Some key points of the 'Triple Helix' model are: i. the level for arrangements between government and industrial sectors is not solely defined by the nation-state; ii. economic benefits are considered a significant motivation; iii. institutions' opportunity structure is updated with successful innovations; iv. the importance of the human capital factor is raised (enabling thus the pillar of 'smart economy' [107]); v. tensions generate new dynamics within the system, which might have a positive impact and not always require resolving; vi. the communication density within each helix is higher than across the helices, without that meaning that the cross-helix communication is low or insignificant, on the contrary [123].

Nonetheless, this model has received criticism over the years, and perhaps the most important is validated via the unsuccessful applications due to the influence of barriers amongst the various stakeholders involved and to the absence of appropriate interfaces that could facilitate its use ([125–126]).

The 'Quadruple Helix' was conceptualized as a human-centered response to the emerging need of incorporating a fourth helix that greatly influences national innovation systems; the public [127]. Specifically, this model includes and connects the helices of government, academia, industry and the media-based and culture-based public [127]. The fourth sphere that enters the innovation ecosystem introduces the concepts of media, creative industries, (innovation) culture (e.g. [128]), values, lifestyles and 'creative class' (e.g. [129–130]). It seems that this helix adds the elements of arts, artistic research and arts-based innovation, that act as a source of creativity for the reinforcement of innovation production, and extend the disciplines of the sciences, social sciences, and humanities, thus promoting a broader understanding and applications of interdisciplinarity and transdisciplinarity [129]. Moreover, "the 'Quadruple Helix' also could be emphasized as the perspective that specifically brings in the "dimension of democracy" or the "context of democracy" for knowledge, knowledge production, and innovation" [129].

This model, which frames the 'Triple Helix' in a context of media-based and culture-based public, is capable of investigating and understanding phenomena and relationships that the former model couldn't (i.e., media-based democracy, multi-media information society [131]). In addition, it has the potential of exploiting the mass media for supporting and reinforcing knowledge and innovation policies and strategies, via the proper dissemination to the general public [129] and via a system approach that focuses on the infrastructure of mass media and various means of mass communication [132]. All in all, this model can incorporate the principles of social accountability and reflexivity of 'Mode 2', as it creates the grounds for recognizing and capturing the culture and values of both society as a whole, and individuals and target groups. This way, and during the knowledge production via application, the problem-solving reflects the societal demands and the civil societal goals [133] and therefore has greater potential for successful implementations [129]. However, a methodological gap exists in the ways of securing the public perspective via citizens engagement schemes, and in the ways that the various actors will claim their functional role of the society as a fourth pillar under the context of innovation ecosystems.

In an attempt to answer "How do knowledge, innovation, and the environment relate to each other?", Carayannis et al. [129] proposed and conceptualized the 'Quintuple

Helix' which expand the 'Quadruple Helix' (and thus the 'Triple Helix' as well) by introducing the environment or the natural environment's context (**Fig. 2**). This model embeds simultaneously two natures: an interdisciplinary analysis one and a transdisciplinary problem-solving one [129]. The former is expressed via the understanding of the helices context and the relationships and cross-linkages formatting amongst them (e.g., natural sciences because of the natural environment sphere, social sciences and humanities because of the society, democracy and economy spheres, etc.) [129]. The latter is captured via the potential it presents (via the combination of knowledge, innovation and the natural environment) for acting as a reference for the decision-making processes [129].

The current ecological status of the world yields immediate actions for sustainable development (e.g. [134–135]). Thus, and complementary to conceptualize more thoroughly the 'Quintuple Helix' model, Carayannis et al [129] elaborated on the term sustainable development and introduced the term 'social ecology'. They specifically stated that "...we could also define sustainable development as a coevolution of the different systems of society, based on knowledge and a mutual cross-learning that is socially and environmentally sensitive and that is receptive for concepts of a quality of democracy" [129]. Additionally, 'social ecology' focuses on the interactions of society and nature between 'human society' (i.e. the cultural (symbolic) sphere of causation) and the 'material world' (i.e. the natural (biophysical) sphere of causation) [129].

To gain a better insight into the last sentence, a better understanding of 'innovation ecosystem' should precede, as an example of social ecosystems. The science-based biological ecosystems might be reconceptualized as 'social (or societal) ecosystems' with certain components (e.g. stakeholders, organizations, processes and structures) and their complex causal relationships, under the social environments of the various society's systems and into the contextualization of the natural environment of the whole society [129]. The focus of 'innovation ecosystems' is the complexity of non-linear innovation systems within the framework of social and natural environments [127]. Carayannis et al. [129] suggest that biological and social (or societal) ecosystems could be embedded within a transdisciplinary framework based on 'social ecology'.

The 'Quintuple Helix' concentrates the potential for integrating 'social ecology' on 'Mode 3' knowledge and innovation systems; thus, this model "has the potential to serve as an analytical framework for sustainable development and social ecology, by conceptually relating knowledge and innovation to the environment" [129]. Also, Carayannis et al. [129] address the fact that long-term economic and sustainable development are associated with environmental sensitivity and social ecology, while they may stabilize or even increase the economic growth rates. Finally, by supporting the coevolution of knowledge, innovation and ecology, this model creates crucial synergies among the society, the democracy and the economy [136].

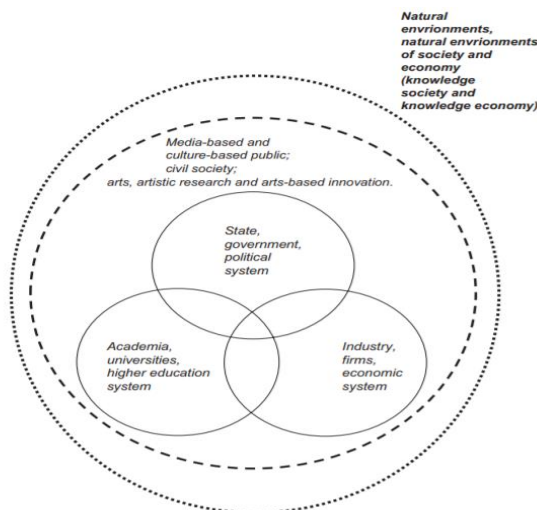


Fig. 2. The ‘Quintuple Helix’ innovation system [129]

## 6 Conclusions and Discussion

The starting point for answering the set research question was the conceptualization of SC. The literature revealed that cities, whilst in the pursuit to become smarter and sustainable, have to appropriately manage the complexity imposed by the socio-technical transformation. To do so, it should be made clear that SCs “are a multi-dimensional mix of human (e.g. skilled labor), infrastructural (e.g., high-tech facilities), social (e.g., open network linkages) and entrepreneurial capital (e.g., creative business activities), that are merged, coordinated and integrated (into the fabrics of the city) using new technologies, to address social, economic and environmental problems, involving multi-actor, multi-sector and multi-level perspectives” [37]. The collaborative context that emerged via the aforementioned definition made purposeful the further investigation of how these systems organize simply said: their governance mechanisms.

To fully grasp the extent and potential of governance in SCs, its evolution was explored. In the beginning, cities were governed by governments, however as cities and communities evolved and expanded, they also became more complex. The first evolutionary wave came with the exploitation of new ICT technologies and the mentality for openness in data, that allowed for improved services, administrative efficiency and interoperability, as well as citizen centrality (e.g., e-government, smart-government). Nonetheless, societal and political transformations over the last decades have yielded the development of the governance theory, concepts, frameworks and models. Smart governance promotes participation, collaboration amongst various stakeholders, co-creation, co-decision-making, co-production, community-led development, open innovation, user-driven innovation, and crowdsourcing. In general, it strives for the development of sophisticated models and solutions that may efficiently exploit ICTs for the facilitation of the open collaboration among a variety of city actors and stakeholders,

whilst in the pursuit of novel, comprehensive and reinforced adaptive sustainable strategies, policies, decisions and overall transitions. Nevertheless, it ought to be highlighted that it cannot be solely technocratic and corporate-driven, as such an approach would fail to serve the collective interests and public value.

The need to address SCs and SCG as collaborative ecosystems is vital for achieving smart and sustainable development. This is because a SC is regarded as a “complex system of people, processes, policies, technology and other enablers working together to deliver outcomes to specific ‘smart’ objectives, where ensuring QoL is an important concern as cities and urban environments are facing challenges to establish efficient, effective, open and participative processes to jointly create applications that meet the citizens demands” [104]. By contemplating upon this definition, it is clear that SCGs, as the organizational mechanisms of SCs, have to be also regarded as collaborative ecosystems that have several components, exploit measures and indicators, based on their unique contextual factors, in order to reach impactful outcomes and the envisaged smart and sustainable transitions.

The literature review of Ruhlandt [37] led to some significant findings and discussions about SCG. It is observed that even though the smart governance concept has been broadly utilized for some time, there is still a substantial lack of investigation and clear understanding of its different domains, as well as an overall liquid approach of which practices per domain are best and why. Most importantly the observation that there are no specific solidly defined prerequisites that secure that a smart governance will be successful, nor how we can measure this success, or even how to customize approaches based on set contextual factors, is underlined. For all these reasons, it is considered that future work should target these directions if the acceleration of smart and sustainable transitions via effective smart governance processes is to be attained.

Moving forward, by investigating the evolution of innovative ecosystems it is concluded that the mode and extend of stakeholders' collaboration evolved accordingly. Evolving from Triple to Quadruple and finally Quintuple Innovation (eco)Systems, it is understood that the initial need for cooperation among government, academia and industry for more robust results, innovation and knowledge production, was expanded because of the need to secure the trust and acceptance of people for sustainability transitions. Broad public acceptance is a prerequisite for smart and sustainable development, as the citizens are the end-users. Therefore, a deep behavioral transformation has to take place if real change is to come, and the way to smooth this transformation is via the inclusion, education and empowerment of the general public to become an active member of this ecosystem and have a saying in the designing and decision upon their future. Finally, the attention is drawn to the fact that long-term economic and sustainable development, as well as people's well-being, are indispensably connected and based on both ecological and environmental sensitivity, as well as a knowledge economy, knowledge society and knowledge democracy. It is firmly trusted that the adoption of a ‘social ecology’ mentality and the building of an educated environmental-sensitive community, is the fastest and most effective way to opt for a holistic smart and sustainable development from local to global levels, and the creation of impactful public value. This is the reason why the significance of adopting a Quintuple Helix model approach in the collaborative ecosystems that strive for achieving SDGs, ought to be established.

**Nomenclature**

<b>Acronym</b>	<b>Definition</b>
SDG	Sustainable Development Goal
ICT	Information and Communication Technologies
QoL	Quality of Life
SC	Smart City

**References**

1. United Nations: Addis Ababa Action Agenda of the Third International Conference on Financing for Development (Addis Ababa Action Agenda), [https://www.un.org/esa/ffd/wp-content/uploads/2015/08/AAAA\\_Outcome.pdf](https://www.un.org/esa/ffd/wp-content/uploads/2015/08/AAAA_Outcome.pdf), last accessed 2020/05/20.
2. United Nations: Transforming Our World: The 2030 Agenda for Sustainable Development, <https://sustainabledevelopment.un.org>, last accessed 2020/05/20.
3. United Nations: New Urban Agenda, <http://habitat3.org>, last accessed 2020/05/20.
4. Benevolo, L.: *The European City*. Blackwell Publishing Ltd., Oxford (1993).
5. Mitchell, W.J.: *The City of Bits: Space, Place, and the Infobahn*. MIT Press, Cambridge, MA (1995).
6. Angelidou, M.: The Role of Smart City Characteristics in the Plans of Fifteen Cities. *J. Urban Technol.* 24, 3–28 (2017). <https://doi.org/10.1080/10630732.2017.1348880>.
7. Appio, F.P., Lima, M., Paroutis, S.: Understanding Smart Cities: Innovation ecosystems, technological advancements, and societal challenges. *Technol. Forecast. Soc. Change.* 142, 1–14 (2019). <https://doi.org/10.1016/j.techfore.2018.12.018>.
8. Datta, A.: New urban utopias of postcolonial India: ‘Entrepreneurial urbanization’ in Dholera smart city, Gujarat. *Dialogues Hum. Geogr.* 5, 3–22 (2015). <https://doi.org/10.1177/2043820614565748>.
9. Lee, J. H., Hancock, M.G., Hu, M.: Towards an effective framework for building smart cities: Lessons from Seoul and San Francisco. *Technol. Forecast. Soc. Change.* 89, 80–99 (2014).
10. Mora, L., Deakin, M., Reid, A.: Strategic principles for smart city development: A multiple case study analysis of European best practices. *Technol. Forecast. Soc. Change.* 142, 70–97 (2019). <https://doi.org/10.1016/j.techfore.2018.07.035>.
11. Vanolo, A.: Smartmentality: The Smart City as Disciplinary Strategy. *Urban Stud.* 51, 883–898 (2014). <https://doi.org/10.1177/0042098013494427>.
12. Pereira, G.V., Parycek, P., Falco, E., Kleinhans, R.: Smart governance in the context of smart cities: A literature review. *Inf. Polity.* 23, 143–162 (2018). <https://doi.org/10.3233/IP-170067>.
13. Testoni, C., Boeri, A.: Smart Governance: urban regeneration and integration policies in Europe. Turin and Malmö case studies. *City community.* 26, 28 (2015).
14. Gil-Garcia, J.R.: Towards a smart State? Inter-agency collaboration, information integration, and beyond. *Inf. Polity.* 17, 269–280 (2012). <https://doi.org/10.3233/IP-2012-000287>.

15. Gibson, D. V., Kozmetsky, G., Smilor, R.W.: The Technopolis Phenomenon: Smart Cities, Fast Systems, Global Networks. *Behav. Sci.* 38, 216 (1992).
16. Vito Albino, Umberto Berardi, Rosa Maria Dangelico: Smart Cities: Definitions, Dimensions, Performance, and Initiatives. *J. Urban Technol.* 22, 3–21 (2015).
17. Chourabi, H., Nam, T., Walker, S., Gil-Garcia, J.R., Mellouli, S., Nahon, K., Pardo, T.A., Scholl, H.J.: Understanding smart cities: An integrative framework. *Proc. Annu. Hawaii Int. Conf. Syst. Sci.* 2289–2297 (2012). <https://doi.org/10.1109/HICSS.2012.615>.
18. Gil-Garcia, J.R., Pardo, T.A., Nam, T.: What makes a city smart? Identifying core components and proposing an integrative and comprehensive conceptualization. *Inf. Polity.* 20, 61–87 (2015). <https://doi.org/10.3233/IP-150354>.
19. O’Grady, M., O’Hare, G.: How Smart Is Your City? *Science* (80-. ). 335, 1581–1582 (2012). <https://doi.org/10.1126/science.1217637>.
20. Allwinkle, S., Cruickshank, P.: Creating smart-er cities: An overview. *J. Urban Technol.* 18, 1–16 (2011). <https://doi.org/10.1080/10630732.2011.601103>.
21. IMD: Smart City Index 2020. (2020).
22. Mitchell, W.J.: Electronic cottages, wired neighborhoods and smart cities. *Smart Growth Form Consequences.* 66–81 (2002).
23. Winters, J. V.: Why are Smart Cities Growing? Who Moves and Who Stays. *SSRN Electron. J.* (2011). <https://doi.org/10.2139/ssrn.1284586>.
24. Caragliu, A., del Bo, C., Nijkamp, P.: Smart cities in Europe. *J. Urban Technol.* 18, 65–82 (2011). <https://doi.org/10.1080/10630732.2011.601117>.
25. Neirotti, P., De Marco, A., Cagliano, A.C., Mangano, G., Scorrano, F.: Current trends in Smart City initiatives: Some stylised facts. *Cities.* 38, 25–36 (2014). <https://doi.org/10.1016/j.cities.2013.12.010>.
26. Campbell, T.: *Beyond smart cities: How cities network, learn and innovate.* Taylor and Francis, London-New York (2013). <https://doi.org/10.4324/9780203137680>.
27. Townsend, A.M.: *Smart Cities: Big Data, Civic Hackers, and the Quest for a New Utopia.* , New York (2013).
28. Alawadhi, S., Aldama-Nalda, A., Chourabi, H., Gil-Garcia, J.R., Leung, S., Mellouli, S., Nam, T., Pardo, T.A., Scholl, H.J., Walker, S.: Building understanding of smart city initiatives. *Lect. Notes Comput. Sci. (including Subser. Lect. Notes Artif. Intell. Lect. Notes Bioinformatics).* 7443 LNCS, 40–53 (2012). [https://doi.org/10.1007/978-3-642-33489-4\\_4](https://doi.org/10.1007/978-3-642-33489-4_4).
29. Giffinger, R., Fertner, C., Kramar, H., Kalasek, R., Pichler-Milanović, N., Meijers, E.: Smart cities Ranking of European medium-sized cities. *October.* 16, 13–18 (2007). [https://doi.org/10.1016/S0264-2751\(98\)00050-X](https://doi.org/10.1016/S0264-2751(98)00050-X).
30. Thuzar, M.: Urbanization in Southeast Asia: Developing Smart Cities for the Future? *Reg. Outlook.* 96–100 (2011). <https://doi.org/10.1355/9789814311694-022>.
31. Nam, T., Pardo, T.: Conceptualizing Smart City with Dimensions of Technology, People , and Institutions. In: *The Proceedings of the 12th Annual International Conference on Digital Government Research.* pp. 282–291 (2011).
32. Lee, J.H., Hancock, M.G., Hu, M.C.: Towards an effective framework for building smart cities: Lessons from Seoul and San Francisco. *Technol. Forecast. Soc. Change.* 89, 80–99 (2014). <https://doi.org/10.1016/j.techfore.2013.08.033>.

33. Meijer, A., Bolívar, M.P.R.: Governing the smart city: a review of the literature on smart urban governance. *Int. Rev. Adm. Sci.* 82, 392–408 (2016). <https://doi.org/10.1177/0020852314564308>.
34. Bolívar, M.P.R.: Mapping Dimensions of Governance in Smart Cities. 312–324 (2016). <https://doi.org/10.1145/2912160.2912176>.
35. Caragliu, A., Del Bo, C.: Smartness and European urban performance: Assessing the local impacts of smart urban attributes. *Innovation*. 25, 97–113 (2012). <https://doi.org/10.1080/13511610.2012.660323>.
36. Visvizi, A., Lytras, M.D.: Rescaling and refocusing smart cities research: from mega cities to smart villages. *J. Sci. Technol. Policy Manag.* 9, 134–145 (2018). <https://doi.org/10.1108/JSTPM-02-2018-0020>.
37. Ruhlandt, R.W.S.: The governance of smart cities: A systematic literature review. *Cities*. 81, 1–23 (2018). <https://doi.org/10.1016/j.cities.2018.02.014>.
38. Kourtit, K., Nijkamp, P.: Smart cities in the innovation age. *Innovation*. 25, 93–95 (2012). <https://doi.org/10.1080/13511610.2012.660331>.
39. Kitchin, R.: The Real-Time City? Big Data and Smart Urbanism. *SSRN Electron. J.* (2013). <https://doi.org/10.2139/ssrn.2289141>.
40. Batty, M., Axhausen, K.W., Giannotti, F., Pozdnoukhov, A., Bazzani, A., Wachowicz, M., Ouzounis, G., Portugali, Y.: Smart cities of the future. *Eur. Phys. J. Spec. Top.* 214, 481–518 (2012). <https://doi.org/10.1140/epjst/e2012-01703-3>.
41. Paskaleva, K.A.: Enabling the smart city: the progress of city e-governance in Europe. *Int. J. Innov. Reg. Dev.* 1, 405 (2009). <https://doi.org/10.1504/ijird.2009.022730>.
42. Dameri, R.P., Benevolo, C.: Governing Smart Cities: An Empirical Analysis. *Soc. Sci. Comput. Rev.* 34, 693–707 (2016). <https://doi.org/10.1177/0894439315611093>.
43. Hollands, R.G.: Will the real smart city please stand up? Intelligent, progressive or entrepreneurial? *City*. 12, 303–320 (2008). <https://doi.org/10.1080/13604810802479126>.
44. Ben Yahia, N., Eljaoued, W., Bellamine Ben Saoud, N., Colomo-Palacios, R.: Towards sustainable collaborative networks for smart cities co-governance. *Int. J. Inf. Manage.* 56, (2021). <https://doi.org/10.1016/j.ijinfomgt.2019.11.005>.
45. Brogan, H.: Government, <https://www.britannica.com/topic/government>, (2020).
46. Ulrich, P., Marshment-Howell, J., & van Geest, T.: Open governance in the smart city - A scoping Report. (2017).
47. Un-Habitat: State of the world's cities 2008/2009: Harmonious cities. *State World's Cities 2008/2009 Harmon. Cities.* 9781849772, 1–264 (2012). <https://doi.org/10.4324/9781849772624>.
48. Garcia Alonso, R., Lippez-De Castro, S.: Technology Helps, People Make: A Smart City Governance Framework Grounded in Deliberative Democracy. *Public Adm. Inf. Technol.* 11, 333–347 (2016). [https://doi.org/10.1007/978-3-319-17620-8\\_18](https://doi.org/10.1007/978-3-319-17620-8_18).
49. Albino, V., Berardi, U., Dangelico, R.M.: Smart Cities: Definitions, Dimensions, Performance, and Initiatives. *J. Urban Technol.* 22, 3–21 (2015). <https://doi.org/10.1080/10630732.2014.942092>.
50. Bevir, M.: Governance: A Very Short Introduction. 144 (2012).
51. Estevez, E., Janowski, T.: Electronic Governance for Sustainable Development - Conceptual framework and state of research. *Gov. Inf. Q.* 30, (2013).

- <https://doi.org/10.1016/j.giq.2012.11.001>.
52. Janowski, T., Pardo, T.A., Davies, J.: Government Information Networks - Mapping Electronic Governance cases through Public Administration concepts. *Gov. Inf. Q.* 29, S1–S10 (2012). <https://doi.org/10.1016/j.giq.2011.11.003>.
  53. Alawadhi, S., Scholl, H.J.: Smart governance: A cross-case analysis of smart city initiatives. *Proc. Annu. Hawaii Int. Conf. Syst. Sci.* 2016-March, 2953–2963 (2016). <https://doi.org/10.1109/HICSS.2016.370>.
  54. Scholl, H.J., Scholl, M.C.: Smart Governance: A Roadmap for Research and Practice. In: *iConference 2014 Proceedings*. pp. 163–176 (2014). <https://doi.org/10.9776/14060>.
  55. European Commission: Overview of Horizon 2020 projects on “ICT-enabled Public Sector Innovation” | Shaping Europe’s digital future. (2019).
  56. Elisei, P., Orazio, A.D., Prezioso, M.: Smart Governance Answers to Metropolitan Peripheries: Regenerating the Deprived Area of the Morandi Block in the Tor Sapienza Neighbourhood (Rome) Pietro Elisei, Angela D’Orazio, Maria Prezioso. 8, 1051–1061 (2014).
  57. Misuraca, G., Broster, D., Centeno, C.: Digital Europe 2030: Designing scenarios for ICT in future governance and policy making. *Gov. Inf. Q.* 29, S121–S131 (2012).
  58. Ubaldi, B.: Open Government Data: Towards Empirical Analysis of Open Government Data Initiatives. *OECD Work. Pap. Public Gov.* 22, 61 (2013).
  59. Silva, C.N.: Open source urban governance: Crowdsourcing, neogeography, VGI, and citizen science. *Open Source Technol. Concepts, Methodol. Tools, Appl.* 1–4, 209–226 (2014). <https://doi.org/10.4018/978-1-4666-7230-7.ch012>.
  60. Peled, A.: Traversing digital babel: Information, E-government, and exchange, (2014). <https://doi.org/10.1111/padm.12196>.
  61. Wijnhoven, F., Ehrenhard, M., Kuhn, J.: Open government objectives and participation motivations. *Gov. Inf. Q.* 32, 30–42 (2015). <https://doi.org/10.1016/j.giq.2014.10.002>.
  62. Klaus, L.C.O.: Transforming armed forces through military transparency: Open government challenges in a world of secrecy. *Transform. Gov. People, Process Policy.* 10, 99–119 (2016). <https://doi.org/10.1108/TG-01-2015-0002>.
  63. Bonsón, E., Royo, S., Ratkai, M.: Citizens’ engagement on local governments’ Facebook sites. An empirical analysis: The impact of different media and content types in Western Europe. *Gov. Inf. Q.* 32, 52–62 (2015).
  64. Debrie, J., Raimbault, N.: The port-city relationships in two European inland ports: A geographical perspective on urban governance. *Cities.* 50, 180–187 (2016). <https://doi.org/10.1016/j.cities.2015.10.004>.
  65. Jeong, M.G., Oh, S.G.: Searching for participatory governance in Korea. *J. Contemp. Asia.* 40, 275–290 (2010). <https://doi.org/10.1080/00472331003600481>.
  66. Postigo, A.: Accounting for outcomes in participatory Urban governance through state-civil-society synergies. *Urban Stud.* 48, 1945–1967 (2011). <https://doi.org/10.1177/0042098010379272>.
  67. Forester, J.: Making Participation Work When Interests Conflict. *J. Am. Plan. Assoc.* 72, 447–457 (2006).
  68. Forester, J.: *The Deliberative Practitioner*. (1999).
  69. Innes, J.E.: Consensus building: Clarifications for the critics. *Plan. Theory.* 3, 5–20 (2004). <https://doi.org/10.1177/1473095204042315>.

70. Booher, D.E., Innes, J.E.: Network power in collaborative planning. *J. Plan. Educ. Res.* 21, 221–236 (2002). <https://doi.org/10.1177/0739456X0202100301>.
71. Susskind, L., Field, P.: Dealing with an Angry Public: The Mutual Gains Approach. 1–14; 152–197 (1997).
72. Blakeley, G.: Local governance and local democracy: The Barcelona model. *Local Gov. Stud.* 31, 149–165 (2005). <https://doi.org/10.1080/03003930500031959>.
73. Blakeley, G.: Governing ourselves: Citizen participation and governance in Barcelona and Manchester. *Int. J. Urban Reg. Res.* 34, 130–145 (2010). <https://doi.org/10.1111/j.1468-2427.2010.00953.x>.
74. Lijphart, A.: Negotiation Democracy versus Consensus Democracy: Parallel Conclusions and Recommendations. *Eur. J. Polit. Res.* 41, 107–113 (2002).
75. Smith, H.: El Triángulo de Solidaridad en Costa Rica: ¿es posible que espacios de negociación creados por el Estado promuevan una mayor injerencia de la sociedad civil en la gobernanza política? *Environ. Urban.* 16, 63–78 (2004). <https://doi.org/10.1630/095624704323026151>.
76. Shin, H.R., Lee, K.: Participatory governance and trans-sectoral mobilities: The new dynamics of adaptive preferences in the case of transport planning in Seoul, South Korea. *Cities.* 65, 87–93 (2017). <https://doi.org/10.1016/j.cities.2017.01.012>.
77. Elster, J.: *Sour Grapes. Studies in the Subversion of Rationality.* Cambridge University Press, Cambridge (1983).
78. Halbe, J., Holtz, G., Ruutu, S.: Participatory modeling for transition governance: Linking methods to process phases. *Environ. Innov. Soc. Transitions.* 35, 60–76 (2020). <https://doi.org/10.1016/j.eist.2020.01.008>.
79. Voß, J.P., Bauknecht, D., Kemp, R.: Reflexive governance for sustainable development. *Reflexive Gov. Sustain. Dev.* (2006).
80. Loorbach, D.: Transition management for sustainable development: A prescriptive, complexity-based governance framework. *Governance.* 23, 161–183 (2010). <https://doi.org/10.1111/j.1468-0491.2009.01471.x>.
81. Halbe, J.: Governance of Transformations towards Sustainable Water, Food and Energy Supply Systems Facilitating Sustainability Innovations through Multi-Level Learning Processes. 194 (2016).
82. Ardoin, N.M., Gould, R.K., Kelsey, E., Fielding-Singh, P.: Collaborative and Transformational Leadership in the Environmental Realm. *J. Environ. Policy Plan.* 17, 360–380 (2015). <https://doi.org/10.1080/1523908X.2014.954075>.
83. Sinfonia: Toolkit for stakeholder involvement in smart city projects, <http://www.sinfonia-smartcities.eu/en/stakeholder-engagement-toolkit/>, last accessed 2021/05/05.
84. European Institute of Innovation and Technology (EIT): EIT Urban Mobility | STRATEGIC AGENDA 2021 – 2027. , Barcelona (2021).
85. García, J.B., Mora, M.S.: +CityxChange | Work Package 3, Task 3.2\_D3.2: Delivery of the citizen participation playbook. (2020).
86. Mee, A., Crowe, P.: +CityxChange | Work Package 3, Task 3.6\_D3.3 Framework for Innovation Playgrounds. (2020).
87. Tanum, Ø., Mjøen, K., Berthelsen, B.O., Reeves, K., Næss, K.: +CityxChange | Work Package 3, Task 3.1\_D3.1 Framework for Bold City Vision, Guidelines, and Incentive

- Schemes. (2020).
88. Holtz, G., Alkemade, F., De Haan, F., Köhler, J., Trutnevyte, E., Luthe, T., Halbe, J., Papachristos, G., Chappin, E., Kwakkel, J., Ruutu, S.: Prospects of modelling societal transitions: Position paper of an emerging community. *Environ. Innov. Soc. Transitions*. 17, 41–58 (2015). <https://doi.org/10.1016/j.eist.2015.05.006>.
  89. Ramon, G.J.: Enacting Electronic Government Success: An Integrative Study of Government-wide Websites, Organizational Capabilities, and Institutions. *Integr. Ser. Inf. Syst.* 31, (2012).
  90. Grossi, G., Meijer, A., Sargiacomo, M.: A public management perspective on smart cities: ‘Urban auditing’ for management, governance and accountability. *Public Manag. Rev.* 22, 633–647 (2020). <https://doi.org/10.1080/14719037.2020.1733056>.
  91. Jiang, H., Geertman, S., Witte, P.: Avoiding the planning support system pitfalls? What smart governance can learn from the planning support system implementation gap. *Environ. Plan. B Urban Anal. City Sci.* 47, 1343–1360 (2020). <https://doi.org/10.1177/2399808320934824>.
  92. Verrest, H., Pfeffer, K.: Elaborating the urbanism in smart urbanism: distilling relevant dimensions for a comprehensive analysis of Smart City approaches. *Inf. Commun. Soc.* 22, 1328–1342 (2019). <https://doi.org/10.1080/1369118X.2018.1424921>.
  93. Barns, S.: Smart cities and urban data platforms: Designing interfaces for smart governance. *City, Cult. Soc.* 12, 5–12 (2018). <https://doi.org/10.1016/j.ccs.2017.09.006>.
  94. Malone, W., Bernstein, M.S.: *Handbook of Collective Intelligence*. The MIT Press, Cambridge, MA (2015).
  95. León, L.F.A., Rosen, J.: Technology as Ideology in Urban Governance. *Ann. Am. Assoc. Geogr.* 110, 497–506 (2020). <https://doi.org/10.1080/24694452.2019.1660139>.
  96. Lam, P.T.I., Ma, R.: Potential pitfalls in the development of smart cities and mitigation measures: An exploratory study. *Cities*. 91, 146–156 (2019). <https://doi.org/10.1016/j.cities.2018.11.014>.
  97. Pasquale, F., Sadowski, J.: The spectrum of control: A social theory of the smart city. *First Monday*. 20, 1–13 (2015).
  98. Hollands, R.G.: Critical interventions into the corporate smart city. *Cambridge J. Reg. Econ. Soc.* 8, 61–77 (2015). <https://doi.org/10.1093/cjres/rsu011>.
  99. McFarlane, C., Söderström, O.: On alternative smart cities: From a technology-intensive to a knowledge-intensive smart urbanism. *City*. 21, 312–328 (2017). <https://doi.org/10.1080/13604813.2017.1327166>.
  100. Kornberger, M., Meyer, R.E., Brandtner, C., Höllerer, M.A.: When Bureaucracy Meets the Crowd: Studying “Open Government” in the Vienna City Administration. *Organ. Stud.* 38, 179–200 (2017). <https://doi.org/10.1177/0170840616655496>.
  101. Arellano-Gault, D., Demortain, D., Rouillard, C., Jean-Claude, T.: “Bringing Public Organization and Organizing Back In.” *Organ. Stud.* 32, 1302–1304 (2011). <https://doi.org/10.1177/0170840611424017>.
  102. AFNOR: ISO 37105:2019 Sustainable cities and communities - Descriptive framework for cities and communities. (2019).
  103. Ooms, W., Caniëls, M.C.J., Roijackers, N., Cobben, D.: Ecosystems for smart cities: tracing the evolution of governance structures in a dutch smart city initiative. *Int. Entrep. Manag. J.* 16, 1225–1258 (2020). <https://doi.org/10.1007/s11365-020-00640-7>.

104. Koutra, S., Fiscal, P.R., Pacho, M.A., Taratori, R.: The Importance of Collaborative Ecosystems to Boost 'Smartness' in Cities. (2020).
105. Pellicano, M., Calabrese, M., Loia, F., Maione, G.: Value Co-Creation Practices in Smart City Ecosystem. *J. Serv. Sci. Manag.* 12, 34–57 (2019). <https://doi.org/10.4236/jssm.2019.121003>.
106. Fernandez-Anez, V., Fernández-Güell, J.M., Giffinger, R.: Smart City implementation and discourses: An integrated conceptual model. The case of Vienna. *Cities*. 78, 4–16 (2018). <https://doi.org/10.1016/j.cities.2017.12.004>.
107. Appio, F.P., Lima, M., Paroutis, S.: Understanding Smart Cities: Innovation ecosystems, technological advancements, and societal challenges. *Technol. Forecast. Soc. Change*. 142, 1–14 (2019). <https://doi.org/10.1016/j.techfore.2018.12.018>.
108. Meijer, A., Rodriguez Bolivar, M.: Governing the smart city: a review of the literature on smart urban governance. *Int. Rev. Adm. Sci.* 82, 392–408 (2016). <https://doi.org/10.1177/0020852314564308>.
109. Dameri, R.P.: Searching for Smart City definition: a comprehensive proposal. *Int. J. Comput. Technol.* 11, 2544–2551 (2013). <https://doi.org/10.24297/ijct.v11i5.1142>.
110. Hefnawy, A., Lyon, U.L., Lyon, U.L., Hefnawy, A., Bouras, A., Cherifi, C.: Lifecycle Based Modeling of Smart City Ecosystem Lifecycle Based Modeling of Smart City Ecosystem. 14th Int. Conf. Inf. Knowl. Eng. (2015).
111. Nam, T., Pardo, T.A.: Conceptualizing smart city with dimensions of technology, people, and institutions. *ACM Int. Conf. Proceeding Ser.* 282–291 (2011). <https://doi.org/10.1145/2037556.2037602>.
112. Schaffers, H., Komminos, N., Pallot, M.: Smart Cities as Innovation Ecosystems Sustained by the Future Internet. 65 (2012).
113. Van den Bergh, J., Danneels, L., Viaene, S., Bergh, J. Van Den, Danneels, L., Viane, S.: Raising the Bar for Smart City Ecosystems. *Int. Conf. eDemocracy Open Gov. Locat. Proceeding*, 7–12 (2017).
114. Abellá-García, A., Ortiz-De-Urbina-Criado, M., De-Pablos-Heredero, C.: The Ecosystem of Services Around Smart Cities: An Exploratory Analysis. *Procedia Comput. Sci.* 64, 1075–1080 (2015). <https://doi.org/10.1016/j.procs.2015.08.554>.
115. Chan, B.: Planning Sustainable Smart Cities with the Smart City Ecosystem Framework. *Strateg. Things*. (2018).
116. Stam, S.: Entrepreneurial ecosystems and regional policy: A sympathetic critique. *Eur. Plan. Stud.* 23, 1759–1769 (2015).
117. Cosgrave, E., Doody, L.: DELIVERING THE SMART CITY. *Governing Cities in the Digital Age*. (2014).
118. Manville, C., Cochrane, G., Cave, J., Millard, J., Pederson, J., Thaarup, R., Liebe, A., Wissner, M., Massink, R., Kotterink, B.: Mapping Smart Cities in the EU European Union, [https://www.europarl.europa.eu/RegData/etudes/etudes/join/2014/507480/IPOL-ITRE\\_ET\(2014\)507480\\_EN.pdf](https://www.europarl.europa.eu/RegData/etudes/etudes/join/2014/507480/IPOL-ITRE_ET(2014)507480_EN.pdf), last accessed 2020/05/18.
119. Viale Pereira, G., Cunha, M.A., Lampoltshammer, T.J., Parycek, P., Testa, M.G.: Increasing collaboration and participation in smart city governance: a cross-case analysis of smart city initiatives. *Inf. Technol. Dev.* 23, 526–553 (2017). <https://doi.org/10.1080/02681102.2017.1353946>.

120. Lytras, M.D., Visvizi, A.: Who uses smart city services and what to make of it: Toward interdisciplinary smart cities research. *Sustain.* 10, (2018). <https://doi.org/10.3390/su10061998>.
121. Kourtit, K., Nijkamp, P., Arribas, D.: Smart cities in perspective - a comparative European study by means of self-organizing maps. *Innovation.* 25, 229–246 (2012). <https://doi.org/10.1080/13511610.2012.660330>.
122. Taratori, R., Rodriguez-Fiscal, P., Pacho, M.A., Koutra, S., Pareja-Eastaway, M., Thomas, D.: Unveiling the evolution of innovation ecosystems: An analysis of triple, quadruple, and quintuple helix model innovation systems in european case studies. *Sustain.* 13, (2021). <https://doi.org/10.3390/su13147582>.
123. Etzkowitz, H., Leydesdorff, L.: The dynamics of innovation: From National Systems and “mode 2” to a Triple Helix of university-industry-government relations. *Res. Policy.* 29, 109–123 (2000). [https://doi.org/10.1016/S0048-7333\(99\)00055-4](https://doi.org/10.1016/S0048-7333(99)00055-4).
124. Etzkowitz, H.: Innovation in innovation: The Triple Helix of university-industry-government relations. *Soc. Sci. Inf.* 42, 293–337 (2003). <https://doi.org/10.1177/05390184030423002>.
125. Bruneel, J., D’Este, P., Salter, A.: Investigating the factors that diminish the barriers to university-industry collaboration. *Res. Policy.* 39, 858–868 (2010). <https://doi.org/10.1016/j.respol.2010.03.006>.
126. Geuna, A., Muscio, A.: The governance of university knowledge transfer: A critical review of the literature. *Minerva.* 47, 93–114 (2009). <https://doi.org/10.1007/s11024-009-9118-2>.
127. Carayannis, E.G., Campbell, D.F.J.: “Mode 3” and “Quadruple Helix”: Toward a 21st century fractal innovation ecosystem. *Int. J. Technol. Manag.* 46, 201–234 (2009). <https://doi.org/10.1504/ijtm.2009.023374>.
128. Kuhlmann, S.: Future governance of innovation policy in Europe - Three scenarios. *Res. Policy.* 30, 953–976 (2001). [https://doi.org/10.1016/S0048-7333\(00\)00167-0](https://doi.org/10.1016/S0048-7333(00)00167-0).
129. Carayannis, E.G., Campbell, D.F.J.: *Smart Quintuple Helix Innovation Systems.* Springer International Publishing, Cham (2019). <https://doi.org/10.1007/978-3-030-01517-6>.
130. Naylor, T.D., Florida, R.: The Rise of the Creative Class: And How It’s Transforming Work, Leisure, Community and Everyday Life. *Can. Public Policy / Anal. Polit.* 29, 378 (2003). <https://doi.org/10.2307/3552294>.
131. Plasser, F. and Plasser, G.: Global political campaigning: a worldwide analysis of campaign professionals and their practices. 69–103 (2002).
132. Ivanova, I.: Quadruple Helix Systems and Symmetry: A Step Towards Helix Innovation System Classification. *J. Knowl. Econ.* 5, 357–369 (2014). <https://doi.org/10.1007/s13132-014-0201-z>.
133. Höglund, L., Linton, G.: Smart specialization in regional innovation systems: a quadruple helix perspective. *R D Manag.* 48, 60–72 (2018). <https://doi.org/10.1111/radm.12306>.
134. UN General Assembly: *Transforming our world: the 2030 Agenda for Sustainable Development.* (2015).
135. Philip J Landrigan, Richard Fuller, Nereus J R Acosta, Olusoji Adeyi, Robert Arnold, Niladri (Nil) Basu, Abdoulaye Bibi Baldé, R.B., Stephan Bose-O’Reilly, Jo Ivey

- Boufford, Patrick N Breysse, Thomas Chiles, Chulabhorn Mahidol, Awa M Coll-Seck, Maureen L Cropper, J.F., Valentin Fuster, Michael Greenstone, Andy Haines, David Hanrahan, David Hunter, Mukesh Khare, Alan Krupnick, Bruce Lanphear, B.L., Keith Martin, Karen V Mathiasen, Maureen A McTeer, Christopher J L Murray, Johanita D Ndahimananjara, Frederica Perera, J.P., Alexander S Preker, Jairam Ramesh, Johan Rockström, Carlos Salinas, Leona D Samson, Karti Sandilya, Peter D Sly, Kirk R Smith, A.S., Richard B Stewart, William A Suk, Onno C P van Schayck, Gautam N Yadama, Kandeh Yumkella, M.Z.: The Lancet Commission on pollution and health. *Lancet*. 391, 462–512 (2018).
136. Carayannis, E., Campbell, D.F.J.: Triple Helix, Quadruple Helix and Quintuple Helix and How Do Knowledge, Innovation and the Environment Relate To Each Other? *Reg. Dev.* 535–565 (2012). <https://doi.org/10.4018/978-1-4666-0882-5.ch308>.

## **Badajoz Es Más – Smart Provincia: Tecnología al Servicio de la Gobernanza y la Ciudadanía**

Ulises Gamero Rodríguez<sup>1</sup> y Roberto Gallego Delgado<sup>2</sup>

<sup>1</sup> Diputación de Badajoz, Badajoz, España  
ugamero@dip-badajoz.es

<sup>2</sup> Diputación de Badajoz, Badajoz, España  
rgallego@dip-badajoz.es

**Resumen.** Con una clara determinación de adaptarse a la llegada de las TIC y de incorporar estas nuevas tecnologías en la estrategia de innovación y transformación digital del territorio, y con el foco en los retos rurales a afrontar como la despoblación, la brecha digital, la retención de talento o la dispersión de los servicios, la Diputación Provincial de Badajoz pone en marcha el proyecto “Badajoz Es Más” para liderar y abanderar esta transformación digital poniendo a disposición de los municipios, empresas y ciudadanos servicios e infraestructura que utilicen el IoT, el Big Data, la Inteligencia Artificial, etc. para conseguir unos servicios públicos más eficientes, disponer de la información necesaria para una mejor toma de decisiones y dinamizar el territorio impulsando una serie de actividades y programas para fomentar el emprendimiento y el conocimiento de estas nuevas tecnologías.

Para ello implementa la Plataforma Provincial de Gestión Inteligente de los Servicios Públicos como elemento principal sobre el que gira todo el proyecto, y se apoya en una Oficina Técnica del proyecto, cuya labor principal es la de integrar los datos de los distintos servicios y desarrollar cuadros de mando, indicadores e informes que hagan más eficiente la gestión de los mismos, y en un centro de innovación para llevar el conocimiento de estas tecnologías al ecosistema de empresas, emprendedores, Entidades Locales, Universidad, etc. del territorio con el consiguiente aumento en su competitividad, incentivación del emprendimiento y el aumento en la generación de empleo.

**Palabras clave:** Ciudadanía, Gobernanza, Territorio

### **1 El Gobierno del Dato para la Mejora de los Servicios Públicos**

#### **1.1 De la Filosofía a la Práctica**

El proyecto “Badajoz Es Más” es una iniciativa llevada a cabo por la Diputación Provincial de Badajoz cuyo objetivo es hacer más eficientes los servicios públicos, mejorar la calidad de vida de sus ciudadanos y fomentar el emprendimiento y la innova-

ción a través de las tecnologías y el gobierno del dato dentro de la provincia de Badajoz.

El avance imparable de las TIC en las ciudades y territorios rurales, y el contexto social, económico y cultural que lo sustenta, exige habilidades y competencias que nos posicionen de forma ventajosa ante nuevos escenarios y entornos de innovación territorial. En este contexto, la Diputación Provincial de Badajoz ha sabido adaptarse y adelantarse a las circunstancias, y a partir del año 2018 puso en marcha la iniciativa “Badajoz Es Más – Smart Provincia”.

La estrategia de transformación digital de la planificación y actuaciones de la Diputación en la provincia de Badajoz, que cuenta con 165 municipios, debe ponerse en valor bajo una visión de transformación digital del territorio, incorporando cada una de ellas a aquellos elementos que favorezcan la creación de oportunidades de negocio, de mejora social y de asentamiento de la población.

Es justo este enfoque más transversal con ámbito territorial digital, inteligente y tecnológico el que hace tan particular este proyecto, alejado de conceptos más tradicionales de “Smart Cities” que ponían sus esfuerzos en las ciudades, renovación de centros históricos, etc. y enfocado en la transformación de las zonas rurales, pueblos inteligentes y sus ciudadanos.

En abril de 2017, la Comisión Europea presentó la acción de la UE «Smart Villages» [1] y en dicho plan se incluía una definición pragmática de los pueblos inteligentes y se hace referencia específicamente a la necesidad de ir más allá de las iniciativas individuales aisladas. La Agenda Digital reconocía a los Territorios un importante papel a través del Plan Nacional de Ciudades Inteligentes (Hoy y desde Diciembre de 2017 denominado Plan Nacional de Territorios Inteligentes [2]).

Y esta es la estrategia de la Diputación Provincial de Badajoz, poner el foco en los retos rurales como la despoblación de los municipios rurales, la brecha digital, la retención de talento o la dispersión de los servicios, evitando los “silos” aislados y transformar estos retos en oportunidades mediante la mejora de la gestión de la información y a través de la explotación de los datos de una manera productiva y eficiente.

## 1.2 El Ciudadano, en el Centro

El proyecto “Badajoz es Más” persigue llevar a cabo la transformación digital del territorio poniendo a disposición de los municipios, empresas y ciudadanos las nuevas tecnologías del IoT, Big Data, Inteligencia Artificial, etc. para conseguir unos servicios públicos más eficientes, simplificar y modernizar dichos servicios y dinamizar el territorio impulsando una serie de actividades y programas para fomentar el emprendimiento y el conocimiento de estas tecnologías.

A continuación, se exponen las líneas maestras del proyecto.

**Plataforma Provincial de Gestión Inteligente de Servicios Públicos.** Es el componente nuclear de la iniciativa, ya que permite la integración de la información de cualquier dispositivo IoT, sistema de información o fuente de datos en un único lugar para

su almacenamiento, visualización y análisis posterior a través de cuadros de mando e indicadores.

Es una Plataforma horizontal y abierta. Está basada en estándares (cuestión fundamental para el desarrollo del ecosistema innovador en el territorio) y ofrece la capacidad de monitorizar y gestionar de forma centralizada un conjunto ampliable de servicios públicos.

Construido siguiendo las directrices marcadas por CTN 178 de AENOR (UNE 178104 [3]), cuenta con un módulo central Orion Context Broker (OCB) [4] que permite administrar todo el ciclo de vida de la información.

Su enfoque “multientidad” permite proveer de información, conocimiento y servicios tanto a la propia Diputación Provincial como al conjunto de los municipios de la provincia.

Los desarrollos implementados están basados en licencias de código abierto (principalmente GNU Affero GPL v3, GNU GPL v2, Apache 2.0 y Licencia BSD).

Su interoperabilidad está garantizada gracias al uso de sus API NGSI, sus Agentes IoT, su bidireccionalidad con Portales de Datos abiertos y el uso del estándar de código abierto FIWARE [5], entre otros.

FIWARE es una iniciativa promovida por la Comisión Europea que cuenta con el apoyo de diversas asociaciones internacionales OASIS, ETSI, GSMA y TM Forum que aporta la capacidad de homogeneizar los datos (FIWARE Data Model [6]) y definir un estándar para la publicación y compartición de los mismos.

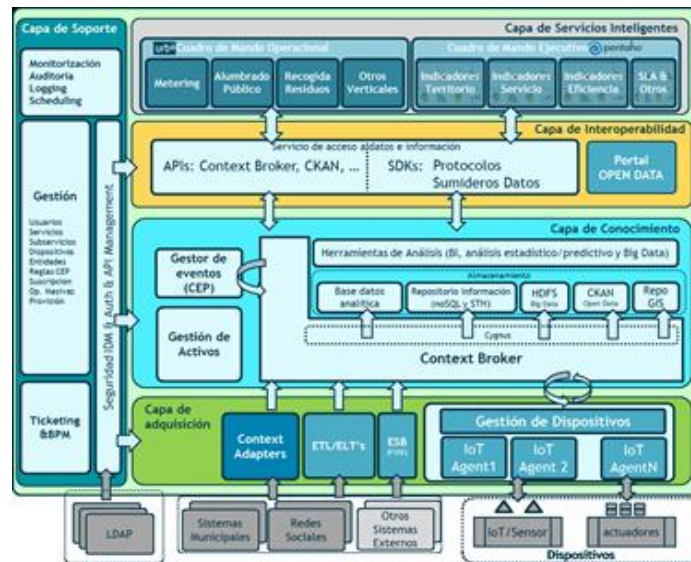


Fig. 1. Arquitectura de la Plataforma Provincial de Gestión Inteligente de Servicios Públicos

**Alineación con proyectos de Territorio Inteligente/Smart Cities.** Este proyecto se encuentra alineado con la Agenda Digital para España [7] (ADpE, “hoja de ruta en

matéria de Tecnologías de la Información y las Comunicaciones”). La Agenda Digital para España se encuentra incluida dentro de la Agenda Digital Europea, que a su vez están centrados en los Objetivos de Desarrollo Sostenible de las Naciones Unidas.

Está alineado con las normas del Plan Nacional de Territorios Inteligentes (incluido en la ADpE, cuyo principal objetivo es "impulsar la industria tecnológica en las ciudades y ayudar a las entidades locales en los procesos de transformación hacia ciudades y destinos inteligentes”).

También estará alineado, aun no estando publicada aún, con el PNE 178601: Territorios Rurales Inteligentes [8], cuyas principales directrices serán la sensorización de los territorios rurales y aplicación de la IoT a la monitorización y evaluación del ámbito de políticas de la EELL o la mejora de los Servicios públicos 4.0.

La Plataforma Provincial, como se ha indicado anteriormente, es compatible con la norma UNE 178104 y las recomendaciones OASC [9]. Además de aportar a todo el ecosistema de servicios inteligentes el estándar FIWARE.

Dentro del esquema FIWARE, el centro de innovación del Proyecto FIWARE Space [10] cuenta actualmente con 2 estrellas. También cuenta con una solución “Powered By FIWARE Platform”, el Proyecto RESPIRA [11].

Dicho Centro además ha sido reconocido por la RED “DIGITAL INNOVATION HUBS” de la COMISIÓN EUROPEA como DIH [12].

Por último, dado el carácter abierto e interoperable del proyecto, se encuentra alineado con el Esquema Nacional de Seguridad [13] e Interoperabilidad [14].

**Servicios públicos 4.0.** Actualmente, la Diputación Provincial de Badajoz ya ha implantado a algunos de sus ejes / verticales previstos en los municipios de la provincia como pueden ser la gestión inteligente de las instalaciones deportivas en Medellín o Castuera, el control de la contaminación sonora en varios municipios, la implantación de parking inteligente en Olivenza, la monitorización de la calidad medioambiental en varios puntos de la provincia, la gestión inteligente de paso de peatones en Valdelacalzada y Olivenza, el control de aforo en el Museo de Bellas Artes de Badajoz, o incluso la gestión de playas inteligente en las playas de agua dulce de los municipios de Chales y Orellana. La información de las soluciones “Smart” distribuidas por todo el territorio ha sido integrada por parte de la Oficina Técnica del proyecto (PMO), equipo de trabajo del proyecto.



**Fig. 2.** Paso de peatones inteligente de Valdelacalzada

Además de iniciativas propias, este proyecto integra ya distintos servicios o “verticales” existentes dentro del Territorio. Para ello se trabaja con Promedio, consorcio de la Diputación de Badajoz orientado a la gestión supramunicipal de los servicios medioambientales de carácter local, y con la delegación de Desarrollo Rural y Sostenibilidad de la Diputación de Badajoz, integrando los servicios o “verticales” de su responsabilidad como la Gestión Inteligente de Residuos (análisis automático de la información proveniente de los distintos contenedores de residuos y camiones de recogida), Gestión del Ciclo Integral del Agua (monitorizando el estado general de los sistemas de abastecimiento / saneamiento / reutilización de agua) o medición de la Eficiencia Energética (visualiza información del sistema de alumbrado público, implantación de tecnología LED y datos de consumo).



**Fig. 3.** Esquema de las soluciones “Smart” implantadas en la Provincia

### 1.3 Ejes Principales de Actuación

Más de treinta soluciones o verticales Smart distribuidas por el Territorio (tanto internas como externas) ya han sido incluidas en este proyecto, sus datos procesados y analizados mediante diferentes tecnologías (Business Intelligence, Big Data, AI, etc.) y representados en diferentes visualizaciones para su uso interno (Cuadros de Mando e Informes) o externo (Portal de Datos Abiertos, iniciativa RESPIRA, Cuadro de mando Abierto).

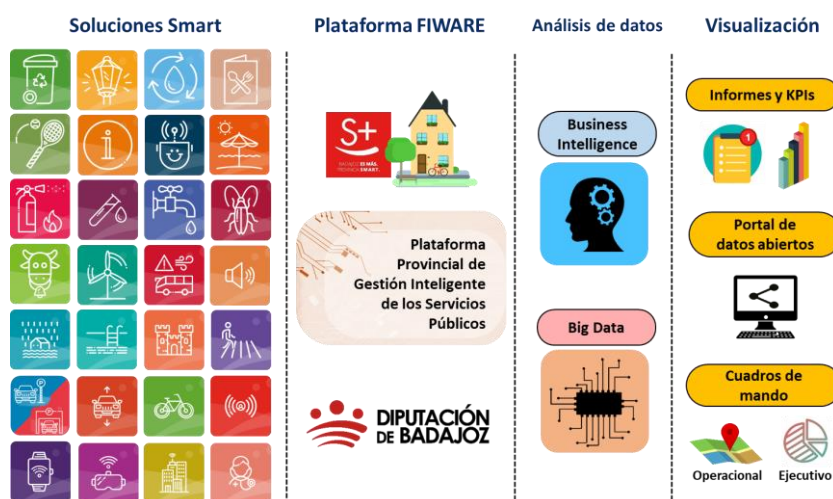


Fig. 4. Metodología de trabajo del proyecto "Badajoz Es Más"

La representación de la información está basada en la construcción de un Catálogo de Indicadores de Territorio Inteligente. Los Indicadores obtenidos son sencillos, cuantificables, representativos e históricos, seleccionando solo aquellos Indicadores que son "rentables", es decir, aquellos para los cuales la importancia de la información que simbolizan justifica el esfuerzo necesario para su obtención.

La clave para representar la información y que sea válida para diferentes entidades y roles es la Multientidad, lo que permite generar información de manera independiente para diferentes servicios a partir de la Plataforma Provincial única.

A continuación, se desarrollan alguna de las iniciativas / soluciones / verticales más destacadas hasta la fecha dentro del proyecto, clasificadas según la naturaleza de su actuación. Cada una responde a necesidades específicas de los municipios o la propia Diputación de Badajoz, y siempre se busca con el desarrollo de estas soluciones la mejora de los servicios a través del análisis del dato y la iteración continua con el usuario final.

**Eje Estratégico** Iniciativas asociadas a un enfoque más estratégico, cuya visión es más holística y su objetivo es representar información a alto nivel. Se pueden mencionar las siguientes actuaciones:

*Cuadro de Mando para el seguimiento de la I Estrategia de Desarrollo Sostenible.* El objetivo de la Diputación Provincial de Badajoz es promover un modelo de provincial más sostenible, cohesionada y acorde con el entorno, que garantice el futuro, el bienestar, la protección del medio ambiente y la calidad de vida. Basado en esta filosofía que promueven los Objetivos de Desarrollo Sostenible y la Agenda 2030, la Diputación ha diseñado la I Estrategia de Desarrollo Sostenible para el horizonte temporal 2020-2023, que pretende dar respuesta a los principales retos a los que se enfrentan los municipios mediante la aplicación de 121 medidas. El objetivo de este Cuadro de Mando es realizar el seguimiento del cumplimiento de dicha Estrategia a través de sus Acciones asociadas.

*Cuadro de Mando Municipal.* Este Cuadro de Mando está construido con el objetivo de proporcionar información individualizada y particularizada para cada uno de los municipios asociados de la Provincia. La Diputación Provincial proporciona este servicio de manera gratuita permitiendo a los municipios asociados convertirse en Pueblos Inteligentes.

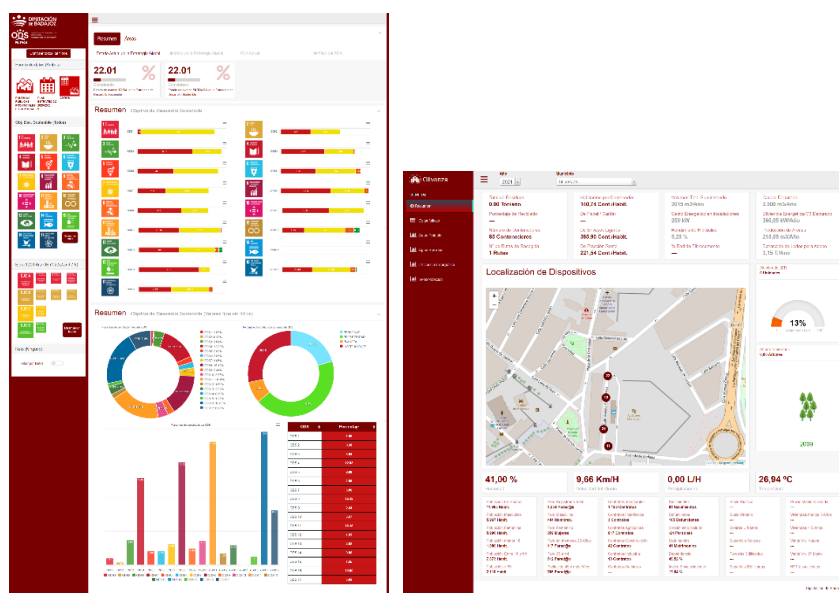


**Fig. 5.** Cuadro de Mando para el seguimiento de la I Estrategia de Desarrollo Sostenible y Cuadro de Mando Municipal

**Eje Operacional.** Dentro del proyecto también tienen cabida Cuadros de Mando con información más operacional, útil para el día a día y enfocado a un personal más téc-

nico. Estos Cuadros suelen contener información en tiempo real y permiten monitorizar los servicios con el objetivo de obtener alertas o alarmas sobre el funcionamiento de alguno de ellos. Dentro de este grupo, se pueden mencionar las siguientes actuaciones:

*Cuadro de Mando para la Gestión Inteligente de Residuos.* Proporciona la información del funcionamiento del servicio mediante el análisis automático de la información proveniente de los distintos contenedores de residuos y camiones de recogida. Desde el visor principal cualquier usuario de la plataforma puede acceder a la información general del servicio permitiendo de un vistazo y gracias a los indicadores generales conocer cómo se está llevando a cabo la recogida de los distintos tipos de residuos.

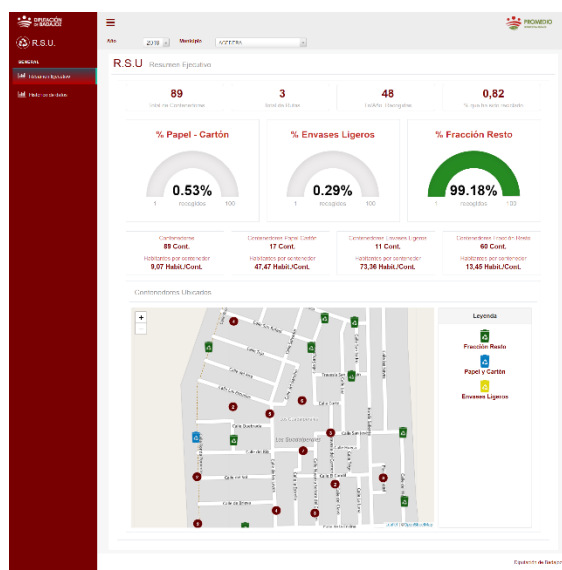


Fig. 6. Cuadro de Mando para la Gestión Inteligente de Residuos

*Cuadros de Mando para la Gestión Inteligente del Ciclo del Agua.* Muestra el estado general de los sistemas de abastecimiento/ saneamiento/ reutilización de agua permitiendo la monitorización de diversos parámetros y la integración con sistemas industriales existentes de los que obtiene la información.

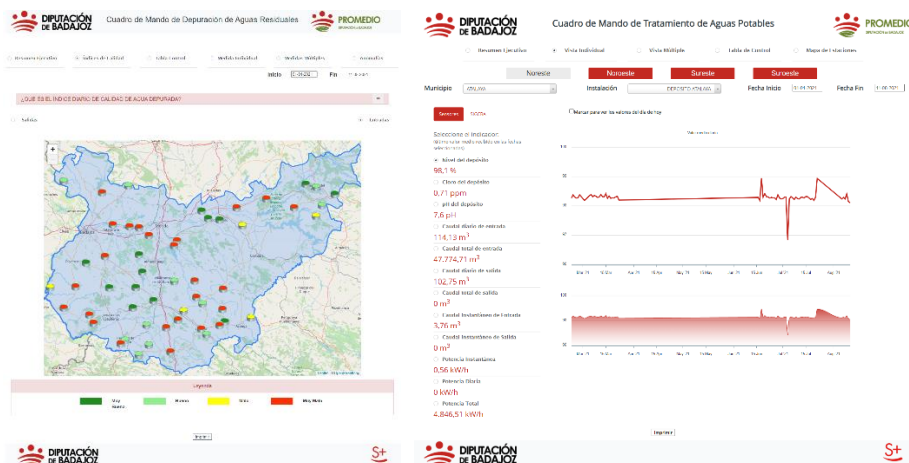


Fig. 7. Cuadro de Mando para la Gestión Inteligente del Ciclo del Agua

*Cuadro de Mando de Desarrollo Sostenible.* Visualiza información del sistema de alumbrado público mostrando un resumen de la situación general del alumbrado de la provincia, consumo en las últimas 24 horas, consumo actual, total de energía activa, energía reactiva, etc. así como detalla el estado de la implantación de iluminación LED en los municipios, la monitorización del consumo energético de edificios, datos de uso y consumo de las electrolineras instaladas, etc.

**Eje Ciudadano.** El Eje Estratégico y Eje Operacional tienen una visión enfocada en proporcionar conocimiento de carácter interno para la propia Diputación Provincial y sus municipios asociados, en cambio, este Eje tiene como objetivo proporcionar información al ciudadano, convirtiendo a la provincia en un Territorio abierto, transparente e interoperable, donde cualquier persona y/o asociación y/o empresa pueda consultar, descargar y reutilizar los datos publicados a través de esta iniciativa. A continuación, se muestran un par de ejemplos relacionados, aunque la información abierta es volcada en otros repositorios, como por ejemplo en el Portal de Datos Abiertos de la Diputación de Badajoz (basado en CKAN):

*Cuadro de Mando público.* Este proyecto conocido como “Badajoz Es Más - Provincia abierta” se encuentra actualmente en fase de despliegue y proporcionará información en tiempo real al ciudadano de cada uno de los servicios “Smart” con los que cuenta actualmente la Diputación de Badajoz. Permite al ciudadano saber el estado de la calidad medioambiental de su municipio, conocer la afluencia en sus playas de interior, o encontrar un aparcamiento libre en los parkings monitorizados dentro de la provincial.



Fig. 8. Cuadro de Mando público “Provincia abierta”

*Proyecto RESPIRA*. RESPIRA fue el proyecto ganador de una convocatoria a un Reto lanzado desde FIWARE Space. Es una plataforma abierta que permite monitorizar la calidad del aire de los municipios de la provincia a través de la instalación de varias estaciones meteorológicas de código abierto (<http://www.calidadmedioambiental.org/>). Este proyecto, además de proporcionar una plataforma de gestión medioambiental para el control y gestión de la contaminación medioambiental en el territorio, es una plataforma abierta en la que cualquier interesado puede implementar e integrar sus dispositivos de medición medioambiental, promoviendo la cultura “Maker” y “DIY” e implicando de primera mano al ciudadano dentro de este proceso de transformación digital.

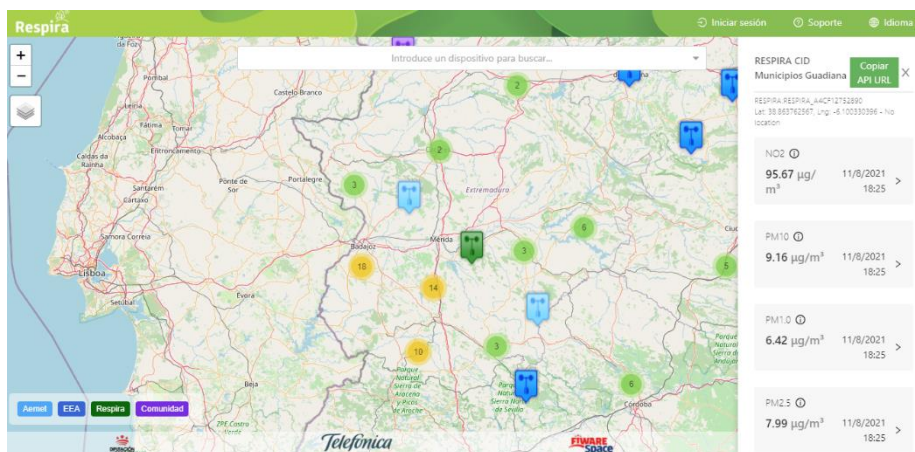


Fig. 9. Plataforma RESPIRA

#### 1.4 Ecosistema de Innovación

Para conseguir que la iniciativa llegue a los ciudadanos, empresas, entidades públicas y resto de organizaciones la Diputación Provincial de Badajoz ha desarrollado un ecosistema de innovación que sirve de punto de encuentro entre los ciudadanos (que demandan estos servicios), emprendedores y entidades educativas (que tienen interés en estas tecnologías), empresas (que tienen la capacidad de implantar estas soluciones) y entidades públicas (los que pueden poner en marcha este tipo de proyectos) y que facilita y provee las herramientas, conocimientos y asesoramiento necesario para que los proyectos que surjan de este encuentro puedan llevarse a cabo.

Este ecosistema tiene como elemento central un centro de innovación físico llamado FIWARE Space.

FIWARE Space lleva a cabo labores como la organización de eventos para la divulgación de las tecnologías y conceptos Smart, talleres demostrativos y formativos, hackathones, cuenta con un showroom para la exposición de soluciones, tiene presencia en congresos nacionales e internacionales como Greencities, Fiware Global Summit, etc. y realiza mentorizaciones a empresas y otras entidades.

Dentro de su “Programa de Mentorización” acompaña a empresas en su proceso de adaptación a la tecnología FIWARE y el desarrollo de soluciones compatibles con este estándar, y actualmente han cursado este programa un total de 9 empresas, de las cuales 7 de ellas ya aparecen en el “FIWARE Marketplace” como empresas con soluciones certificadas en la tecnología FIWARE.

Además, el centro consiguió ascender de categoría consiguiendo la distinción de iHub de dos estrellas por la Fundación FIWARE [15], y ha sido reconocido como miembro DIH dentro del selecto club de HUBs reconocidos por la Comisión Europea que destinan su esfuerzo diario al desarrollo tecnológico de las empresas que componen su ecosistema de innovación.



**Fig. 10.** Centro de Innovación FIWARE Space

Toda la información de los servicios que se ofrecen, actividades que se realizan y cómo poder contactar y comenzar a trabajar con el equipo del centro está disponible en la página web [10] del mismo.

## 2 Resultados Obtenidos y Conclusiones

Con el proyecto “Badajoz Es Más” se pretende que cada vez más municipios, empresas, ciudadanos y otros grupos de interés se incorporen al proyecto y comiencen a desarrollar soluciones, a través del tratamiento y el análisis de datos, que les aporten valor y aporten valor a la sociedad, buscando mejorar la calidad de vida de nuestros pueblos y territorios a través de las nuevas tecnologías. A día de hoy, el proyecto ha alcanzado los siguientes resultados:

- Más de 20 municipios disponen ya de soluciones “Smart” implantadas
- Más de 22 empresas están enviando datos a la Plataforma Provincial
- Disponemos de más de 40 fuentes de datos integradas
- Más de 600 elementos y dispositivos conectados
- Más de 500 transacciones por minuto
- 18 Cuadros de Mando desarrollados
- 228 Indicadores de Territorio Inteligente implementados

Sin duda son avances importantes, pero aún queda mucho camino por recorrer. El proyecto va a seguir trabajando en alinear todas las necesidades de transformación digital y digitalización de los municipios de la provincia con los servicios del tejido empresarial local y regional y las capacidades de nuestros estudiantes, emprendedores y trabajadores para seguir generando valor en la región y poco a poco disminuir la brecha digital, la despoblación y la falta de oportunidades que sufren muchos de los municipios de la provincia.

Podemos concluir que la Diputación de Badajoz hace posible a través de este proyecto el proveer de las herramientas y servicios tecnológicos a los municipios, empresas, entidades educativas y ciudadanos que conforman el entorno de Smart Provincia para poder llevar a cabo este tipo de proyectos y aporta las capacidades técnicas y de gestión que resulta enormemente difícil de acometer por parte de los municipios de escasa población, convirtiéndose en la precursora de la transformación digital de la región en cuanto a servicios públicos se refiere y sentando la primera piedra de la conversión de la provincia pacense de un Territorio Eficiente a un Territorio Inteligente.

## Referencias

1. Smart Villages. [https://enrd.ec.europa.eu/smart-and-competitive-rural-areas/smart-villages/smart-villages-portal\\_es](https://enrd.ec.europa.eu/smart-and-competitive-rural-areas/smart-villages/smart-villages-portal_es)
2. Plan Nacional de Territorios Inteligentes. [https://avancedigital.mineco.gob.es/es-es/Novedades/Documents/Plan\\_Nacional\\_Territorios\\_Inteligentes.pdf](https://avancedigital.mineco.gob.es/es-es/Novedades/Documents/Plan_Nacional_Territorios_Inteligentes.pdf)
3. Sistemas Integrales de Gestión de la Ciudad Inteligente. Requisitos de interoperabilidad para una Plataforma de Ciudad Inteligente. <https://www.une.org/encuentra-tu-norma/busca-tu-norma/norma?c=N0059471>
4. Orion Context Broker. <https://ec.europa.eu/cefdigital/wiki/display/CEFDIGITAL/Orion+Context+Broker>
5. FIWARE. <https://www.fiware.org/>
6. Smart Data Models. <https://smartdatamodels.org/>
7. España Digital 2025. [https://portal.mineco.gob.es/ca-es/ministerio/estrategias/Paginas/00\\_Espana\\_Digital\\_2025.aspx](https://portal.mineco.gob.es/ca-es/ministerio/estrategias/Paginas/00_Espana_Digital_2025.aspx)
8. Territorios Rurales Inteligentes. Definición, atributos y requisitos, <https://www.une.org/encuentra-tu-norma/busca-tu-norma/proyecto?c=P0050234>
9. Open & Agile Smart Cities. <https://oascities.org/>
10. FIWARE SPACE. <https://www.fiware.space/>
11. RESPIRA IoT Platform. <https://marketplace.fiware.org/pages/solutions/86f65987f33c2c5d365e9fb5>
12. Digital Innovation Hubs. <https://s3platform.jrc.ec.europa.eu/web/guest/digital-innovation-hubs-tool>
13. ENS. [https://administracionelectronica.gob.es/pae\\_Home/pae\\_Estrategias/pae\\_Seguridad\\_Inicio/pae\\_Esquema\\_Nacional\\_de\\_Seguridad.html](https://administracionelectronica.gob.es/pae_Home/pae_Estrategias/pae_Seguridad_Inicio/pae_Esquema_Nacional_de_Seguridad.html)
14. ENI. <https://administracionelectronica.gob.es/ctt/eni#.YVHzfJpBxPY>
15. FIWARE iHubs. <https://www.fiware.org/community/fiware-ihubs/>

# Using open data to analyze public bus service from an age perspective: Melilla case

Jamal Toutouh<sup>1</sup>[0000–0003–1152–0346], Irene Lebrusán<sup>2</sup>[0000–0003–3445–0651], and Christian Cintrano<sup>1</sup>[0000–0003–2346–2198]

<sup>1</sup> University of Málaga, Spain  
{cintrano, jamal}@lcc.uma.es

<sup>2</sup> GISMAT, University Complutense of Madrid, Spain  
{ilebrusan}@ucm.es,

**Abstract.** The increase in life expectancy is undoubtedly a social achievement. If we want an inclusive and integrating society, the inclusion of the age perspective is key when planning the city and its services. Accordingly, this is reflected in the Sustainable Development Goals (SDGs), especially in SDG 11.2, which aims to provide and expand access to public transport with special attention to the needs of the elderly. In general, the data required to evaluate public transportation is managed by the bus operators and/or other entities that decide whether (or not) to share it. This hampers the independent evaluation of the bus service by third-party stakeholders. Thus, this article aims to objectively assess the bus network's quality of service, relying exclusively on available socio-demographic and mobility open data, highlighting the elderly as target users in the city of Melilla (Spain). The open data available allowed the computation of indicators, such as journey times estimation or bus stop distribution to evaluate the universality in access to public transport. However, it has been noted that the lack of available data prevents the calculation of other age-friendly indicators. The main result of this research is that bus service provides a considerable reduction in journey times for the elderly than for non-elderly.

**Keywords:** Open data · Public transport · Bus service · Elderly

## 1 Introduction

The most commonly used mean of transportation in modern cities is the private vehicle, which is causing major environmental problems [9]. The noise and polluting gases associated with road transportation are having a direct impact on people's health [24, 33]. According to the European Commission, air pollution is the principal health hazard for European citizens [12]. Besides, according to the European Environment Agency, exposure to high noise levels generates a health risk, causing some 12,100 premature deaths per year on the continent [13].

Reducing road traffic in urban areas is a relevant issue, which can be addressed by improving the quality of public transport system, such as urban buses [15]. It is necessary to have a public transport network that allows moving along the urban

areas minimizing the use of private transport. However, citizens often perceive the bus service as unreliable, with unpredictable travel times and schedules [5].

Different studies have been published identifying causes that impact the quality of the public urban bus system, such as poor design. The quality of bus service can be measured in terms of travel time, frequency, passenger comfort, price, and vehicle safety [4, 8, 18, 28]. Besides, providing a high quality, efficient, and effective bus service is a very complex problem. Thus, several authors have applied computational intelligence to bus network/service design [14, 20, 22, 30, 32].

Open data is becoming essential in the development of Smart Cities [1]. Open data allows the evaluation of different aspects of the city and the quality of life of its inhabitants [23–25]. Besides, it can be used to design applications that assist both citizens and managers to improve dwellers life [3, 11]. This paper explores the use of open data to perform an independent evaluation of the bus service in a city, focusing on elderly citizens' perspective. The case of study is Melilla in Spain. Our main motivation is that having a high quality bus system positively impacts on the relationship between the elderly and the urban spaces [26].

The main contributions of this work are: *i*) selecting and proposing a set of indicators to evaluate the quality of bus service that only rely on available open data, *ii*) analyzing the public bus service in Melilla with special emphasis on the service provided to the elderly, and *iii*) pointing out the main issues faced on performing the bus network evaluation using only open data.

The rest of this manuscript is organized as follows. Next section explores the importance of public transport to remain independent and participate in society for the elderly, as well as the international compromise to do so. Section 3 introduces the context of the use case taken into account in this paper, the city of Melilla and the public bus service provided there. Section 4 presents the materials and methods applied in the analysis of the bus service. Section 5 evaluates the public bus transport service according to the shared open data. Section 6 discusses the main limitations of this study due to the open data scarcity. Finally, Section 7 presents the conclusions and the main lines of future work.

## 2 Towards inclusive aging: public transport matters

Access to public transport is key to the establishment of social connections, especially of fundamental age-related connections during old age [34] contributing to maintaining independence when age-related constraints make driving difficult in later life. However, the prioritization of the use of public vehicles over public transport is one of the problems detected in the process of integrated aging in our cities [26, 27] which can limit social interactions and have negative consequences on their health [2] and may even produce undesired mobility (expulsion) from the urban area in which they wish to live [26].

These issues, and especially the need to pay attention to public transport from an age perspective, have begun to receive attention in international agreements: The 2030 Agenda for Sustainable Development established the importance of transport to make cities and human settlements inclusive, safe, resilient, and sustainable (Goal 11), pointing specifically that by 2030, cities should provide

access to safe, affordable, accessible and sustainable transport systems for all, improving road safety, notably by expanding public transport, with special attention to the needs of those in vulnerable situations, women, children, people with disabilities and elderly (target 11.2).

### 3 Use case: public bus service in Melilla

This section introduces the use case of this study: Melilla city in Spain and the public bus network provided in the city.

#### 3.1 Melilla city

The city of Melilla is the smallest autonomous territory in extension of Spain with a surface of 12 km<sup>2</sup> and a population of 87076 inhabitants in the year 2020. These numbers make its population density (6035 inhabitants per square kilometer) superior to population densities of cities like Madrid (5518 people per square kilometer). This is especially relevant in Spain with low density (national average of 91.4 inhabitants per square kilometer) [16].

Melilla is located in the north of Morocco (Africa). It is bordered by Morocco (by land) and by the Alboran Sea. The administrative division is composed of eight districts, 25 neighborhoods and 35 census segments. Fig. 1 shows the location of the districts and their segments.

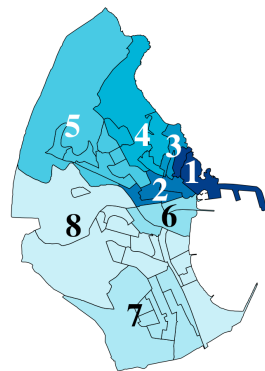


Fig. 1: Location of the districts and sections in Melilla.

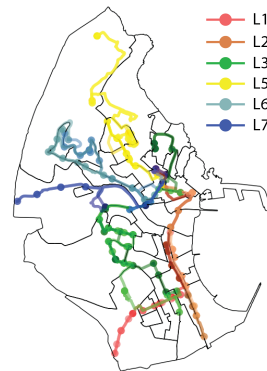


Fig. 2: Bus stops and lines distributed through the city.

Table 1 summarizes the main socioeconomic variables taken into account in this study. The metrics are aggregated by district because we have not been able to access to the same in other resolution (i.e., grouped by census segments). The table shows the area, the number of houses (housing), the number of inhabitants (population), the ratio of elderly population, i.e., citizens with age greater than 65, (elderly ratio), and the number of inhabitants per km<sup>2</sup> (pop. density)

If we analyze the ratio between the number of people over 65 and the number of people under 16 in provincial capitals and/or municipalities with more than 50,000 inhabitants, Melilla is the second city in Spain with the lowest aging ratio (44.05% compared to 254.43% in El Ferrol and a national average of 129.17%).

Table 1: Socioeconomic data evaluated per district (# indicates *number of*).

district id	area (km <sup>2</sup> )	housing (# houses)	population (# people)	elderly ratio (% of elderly)	pop. density (people/km <sup>2</sup> )	poverty ratio (% of people)
1	0.30	770	3117	11.3	10390.0	34.4
2	0.46	1455	5517	16.8	11993.5	48.1
3	0.06	676	2744	13.7	45733.3	48.1
4	0.56	1665	8941	8.6	15966.1	50.1
5	1.14	3206	15484	8.6	13582.5	69.5
6	0.58	1113	4782	12.6	8244.8	34.3
7	1.46	2025	12943	9.5	8865.1	29.6
8	3.25	7016	30229	10.6	9301.2	17.1

### 3.2 Public bus service

Public passenger transport in Melilla is provided only by the taxi service (run by various private companies) and the public bus network provided by the *Cooperativa Omnibus de Autobuses* (COA). COA provides six urban bus lines, articulated by a fleet of 21 vehicles plus reserve vehicles for special needs.

Table 2 summarizes the data for the main bus service during the weekdays when the bus usage is the highest. The distance that the line travels (distance in kilometers), the number of installed bus stops (bus stops), and the frequency in terms of time between the departure from the first stop of two consecutive buses of the same line (bus departure frequency), and the service time. Fig. 2 shows the bus lines and stops distribution along the districts of Melilla.

As Table 2 shows, COA offers six bus lines that operate mostly from 7:00h to 22:00h. Line L2, which connects the Central Market with the Benienzar Border, is the one that offers the highest frequency. Line L1, which connects the Central Market with Barrio Chino Border, is the longest route (it has 40 stops) and runs along the roads of districts 2, 6, 8, and 7. It should be noted that both L1 and L2 are mainly used by cross-border visitors that enter the city every day.

Table 2: Melilla bus service summary.

line	distance (km)	bus stops	bus departure frequency	service time
L1	9.6	37	every 20/30 minutes	7:00-22:00
L2	7.6	21	every 10/15 minutes	7:00-22:00
L3	14.3	43	every 20/30 minutes	7:00-22:00
L5	8.8	20	every 30 minutes	7:00-22:00
L6	7.0	29	every 40 minutes	7:00-22:00
L7	7.1	15	every 15/20 minutes	7:00-21:00

Although Melilla is a small territory, the bus service suffers from deficiencies related to the regularity of service and accessibility of the buses (on which we have not obtained information). One of the biggest challenges is that the buses do not have their bus lanes, so the buses suffer from traffic jams during rush hour, which limits the quality of the bus service. This causes the vast majority of the population to opt for private transport (93%), with only 7% of the population using the bus service regularly [7].

The main aim of this paper is to evaluate the bus service provided by COA using open data. The idea is to become aware of how important it is to have this type of data available to get objective measures about the quality of the bus service, without having to conduct extensive user survey campaigns or employ expensive monitoring systems. In turn, this paper research on elderly citizens, a segment of the population in cities that is particularly vulnerable.

## 4 Materials and methods

This section is organized as follows: first, it describes the open data used to perform the analysis of the public bus service of Melilla; second, it presents the metrics evaluated in study study; and third, it introduces the methods applied to evaluate the metrics and the computational tools used.

### 4.1 Open data used to evaluate the public bus service of Melilla

When carrying out any study on mobility over a given city, it is necessary to have real data. Nowadays, municipalities have developed portals where they publish a multitude of open data. In addition to the official open data portals, there are several initiatives in which a community of users is responsible for collecting and publishing open data, e.g., Open Street Maps (OSM) [31]. We now describe the open data sources used in this research.

The data reported in Table 1 was obtained from the municipal census of the National Institute of Statistics and the open reports published by the European Network for the Fight against Poverty and Social Exclusion in Melilla [10]. The areas covered by the districts (and segments) in Melilla were obtained from the geographic information systems (GIS) provided by the National Institute of Statistics [17] (see Fig. 1). The information about the bus transport reported in Table 2 and Fig. 2 is freely available on the official website of COA [6].

There is no available open data on mobility (e.g., roads average speeds, pedestrian paths or affluence, etc.) or on bus network (e.g., the average time a bus needs to perform one whole cycle per bus line or the number of buses per line). This information would be handy for calculations on different bus mobility indicators. The OSM data was used to estimate several mobility metrics useful to compute the bus quality of service indicators to mitigate the lack of data.

### 4.2 Metrics evaluated

This article aims to use open data to study the quality of service of the Melilla bus system, emphasizing the service provided to elderly users. Even though the indicators exist in the literature [18, 28], they have been computed/estimated by relying only on available open data. The metrics evaluated are presented below:

- *Travel time*: It evaluates the travel time in minutes when the inhabitants travel between any pairs of census segments. Two travel times are computed: *a)* citizens move only by foot and *b)* the users use the public bus service.
- *Improvement when using public bus service*: It represents the reduction ratio in travel time required when using the bus service compared to walking.

- *Travel times difference between elderly and non-elderly*: It compares the travel times of these two types of citizens by computing the ratio of travel time increase of the elderly over non-elderly.
- *Walking distance during the bus trip*: It measures the length of the walking part of a bus trip. This distance includes walking from/to bus stops when starting and finishing the travel. But it also considers the walking required to perform bus transfers, if it is needed.
- *Bus stops density*: It is computed as the number of bus stops installed per square kilometer for each district. This metric allows studying the accessibility of the bus system. In turn, the bus stops density gives an overview of how effectively the bus network is distributed throughout the city.
- *Walking distance to the closest bus stop*: It measures how long (in meters) a citizen has to walk to access the bus network. This walking distance is important because it may impact the use of the bus system, especially for people with mobility difficulties, such as elderly people.

Travel time, bus stop density, and walking distance to the closest bus stop are metrics found in the literature. The improvements when using the bus, the travel times difference between elderly and non-elderly, and the walking distance during the bus trip have not been found in previous research works.

### 4.3 Methods and tools for the evaluation

Most of the evaluated metrics rely on the computation of routes between the segments. The lack of mobility data has motivated the development of a method to model the citizens' trips to estimate the required metrics for our analysis. The routes are computed between the centroids of all the census segments. There are two types of trips: *a)* on foot-only and *b)* getting on the bus. These computations rely on a graph created by using OSM data, which represent the whole city of Melilla including all the walking paths, roads, bus stop locations, etc.

When computing on foot-only trips, the street network of the city is modeled as an undirected graph (named walking graph), in which the edge weights represent the walking time between the nodes (i.e., computed as distance divided by walking speed). The pedestrian trips between two segments are modeled by selecting the shortest path between the centroids of the segments according to the Dijkstra algorithm (minimizing travel time). According to the literature, the walking speed is 1.25 meters per second (m/s) for non-elderly people, and the walking speed is 0.97 m/s for the elderly [19].

To compute the getting on the bus travel, new directional edges that link bus stops are added to the walking graph to represent the bus itinerary (named bus edges). The directionality of the bus edges depends on the direction in which the bus travels, and the weight is the trip time between the bus stops (the bus speed is considered 14.5 km/h [29]). Thus, the algorithm may select walking or bus edges when applying Dijkstra to compute the shortest path between the segments, considering the route by foot from/to the bus stop plus the journey using the bus. Besides, Dijkstra takes into account trips that the user may change the bus or even walk from a given bus stop to the other while on the move (to represent the case of bus transfer).

The bus travel times are affected by the number of bus stops (because they have to wait for passengers to get on or off) and by the frequency (i.e., the time between the departure of two consecutive buses) that impacts the waiting time to get on bus. Thus, the Dijkstra algorithm has been modified to add these times when computing the trips. Each bus stop during the journey adds a travel time of 30 seconds. This time value has been set after meetings with 12 bus drivers. Besides, every time the user has to get on the bus (either for starting the trip or transfer to another line), a random amount of time (modeled applying a Poisson process of intensity equal to the frequency of the bus line) is also added.

Fig. 3 illustrates an example of how the trips are computed. The algorithm consider two trips (among others): *Trip 1* and *Trip 2*. On the one hand, the *Trip 1* time considers the walking time to the bus stop, the random waiting time to get on the bus, the bus trip time to the closest bus stop to the end of the trip, and the walking time from the bus stop to the end. On the other hand, the *Trip 2* time considers the time required to walk to the endpoint of the trip.

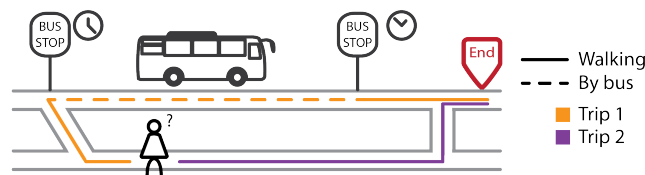


Fig. 3: An example of two trips to compute the routes.

The walking parts of the bus routes make the main difference between the non-elderly and elderly people computations. This is because the criterion applied by the devised method to select the trips minimizes the total required time without considering the path length. Thus, for the same origin and destination, there are cases that non-elderly do not use the bus service because they walk at enough speed to make the travel times shorter than when using the bus. Still, the elderly take the bus because their walking speed is slower.

In order to compute the bus stop density, the information about the polygons provided by the National Institute of Statistics and the information about the location of the buses is used.

The software required for the computations has been developed by using Python. The data analysis has been implemented using Numpy, scikit-learn, and Pandas. The GIS computations rely on Geopandas and Arcpy. Finally, the routes are computed by using libraries for working with graphs OSMnx and NetworkX.

## 5 Analysis

This section evaluates walking trips, analyzes bus travels, examines the bus stop distribution through the city.

### 5.1 Walking through the city

This section evaluates the walking mobility in the city of Melilla. The main goal is to realize the importance of having a public bus transportation service, even

for small-sized urban areas. Table 3 presents the mean and standard deviation (mean±std) and maximum (max) of the length in meters and the times in min for the trips on foot between all census sections (grouped by district).

Table 3: Distances in meters between the districts and walking times in minutes.

district	distance		non-elderly walking time		elderly walking time	
	mean±std	max	mean±std	max	mean±std	max
1	2072.6±849.3	4258.4	32.8±14	69.5	42.2±19	89.6
2	1589.9±759.1	3680.5	26.6±13	60.9	34.3±17	78.5
3	1946.3±902.0	4080.1	30.9±15	67.3	39.8±20	86.8
4	2278.9±1073.5	5114.9	37.8±18	80.0	48.7±23	103.1
5	2274.5±1080.2	5110.8	40.7±19	92.8	52.4±24	119.6
6	1606.4±705.1	3721.4	27.5±13	62.7	35.4±16	80.9
7	2389.8±1171.0	5043.7	41.0±20	92.8	52.8±26	119.6
8	1951.7±936.2	5114.9	34.1±16	82.2	44.0±20	105.9

The inhabitants of district 7 are farthest away (longer walking distances with an average of 2389.8 meters), and therefore need more time to move through the city. Districts 2 and 6 located in the city downtown (see Fig. 1) are those whose residents have the shortest walking distances, average distances of 1589.9 and 1606.4 meters, respectively.

There is a remarkable difference in the walking times between elderly and non-elderly people, even for a small-sized city (see Table 3). The longest trips are the ones between district 5 and district 7, which are the most separated peripheral ones (see Fig. 1). The non-elderly citizens require up to 92.8 min to walk between these two districts. The elderly need up to almost two hours for the exact travel (119.6 min).

According to the walking speed considered, elderly people require 22.39% longer times to travel between the census sections. Thus, one would expect the bus service to provide competitive solutions to mitigate this travel time difference with non-elderly while reducing the walking distances.

## 5.2 Travel times when using the bus service

This section discusses the quality of bus service in terms of travel time improvement compared to walking. Thus, the travel time using bus transport between all the census sections of the city is estimated for both non-elderly and elderly users by using the method presented in Section 4.3. The trip through the city considers *walking-bus multi-modal* and bus transfers, i.e., the user can walk, get on a bus, walk again and get on another bus at another stop, etc. The simulated bus users select the route to minimize the travel time over all possible combinations that may exist from the origin to the destination (including walking to/from several different bus stops, using various bus lines, etc.).

Tables 4 and 5 presents the travel times between all the sections of the city in terms of mean and standard deviation (mean±std) grouped by districts. These two tables are non-symmetric because parts of the bus trips are carried out through different (one-way) roads depending on the direction of the line.

Table 4: Bus travel times between districts in min for the non-elderly (mean±std).

Dest.	Origin							
	1	2	3	4	5	6	7	8
1	15.4±0	20.8±8	13.0±7	27.7±8	29.1±4	27.3±3	31.6±4	32.1±8
2	22.9±6	20.3±1	19.1±6	26.0±4	23.4±3	22.4±2	26.9±3	27.0±8
3	16.0±9	19.1±6	3.8±0	21.4±10	25.1±3	23.5±2	28.2±3	27.9±8
4	29.3±7	26.0±4	23.3±9	26.2±5	26.8±6	28.2±5	32.9±5	32.6±9
5	30.4±3	24.1±2	26.6±2	27.8±6	24.0±6	27.2±2	32.0±4	31.7±8
6	25.3±8	20.3±4	24.0±2	27.6±5	25.5±3	18.9±9	27.5±4	26.9±10
7	32.8±4	27.1±3	29.0±3	32.2±5	29.8±4	27.7±4	16.8±10	29.4±8
8	32.5±8	26.7±8	28.7±8	32.6±9	30.7±9	27.2±9	29.5±8	29.2±13

Table 5: Bus travel times between districts in min for the elderly (mean±std).

Dest.	Origin							
	1	2	3	4	5	6	7	8
1	19.9±0	23.6±8	19.1±10	33.5±7	32.3±4	30.5±4	34.8±5	36.2±11
2	25.6±6	21.7±1	20.6±6	28.4±5	25.1±3	24.1±2	28.6±4	29.5±10
3	18.3±9	20.6±6	4.8±0	26.1±10	27.2±4	25.5±3	30.3±4	30.7±10
4	33.1±7	28.3±5	25.9±10	33.4±5	29.9±6	30.9±6	36.7±7	36.1±11
5	33.8±4	25.9±3	28.8±3	30.6±7	26.4±6	29.5±3	34.3±4	34.7±10
6	28.6±8	22.2±4	26.1±2	30.5±6	27.7±4	21.1±10	29.7±5	30.7±11
7	36.2±5	29.1±4	31.2±4	35.1±6	32.0±5	30.0±5	19.1±11	32.5±11
8	36.5±11	29.4±10	31.5±10	36.3±12	33.7±11	30.1±11	32.6±11	32.9±16

Results in tables 4 and 5 show that in general, there is an improvement (travel time reduction) when the citizen uses the bus to travel through the city. The maximum mean travel time occurs when the users move from district 7 to district 4, which is 32.9 min and 36.7 min for non-elderly and elderly, respectively.

Focusing on the trips between districts 5 and 7 (which represent the furthest districts), there is a significant reduction in the travel time when the bus is taken. For example, elderly users go down from requiring 83.8 min to walk from district 5 to district 7 to only 32.0 min, which implies a time reduction of 62%.

In order to have a global view of the quality of service (in terms of travel time improvements regarding walking time) provided by the public bus transport, Table 6 summarizes the bus trip time and the percentage of travel time reduction (i.e., the improvement) by showing the mean and standard deviation (mean±std) and maximum (max) values, for non-elderly and elderly people.

Table 6 shows that trips from peripheral districts (i.e., districts 5 and 7) are the ones that reduce travel times the most. For example, elderly mean improvements for districts 5 and 7 are 30.7% and 30.4%, respectively. In contrast, trips from districts 1, 2, and 6 (located in the city’s downtown) reduce the travel times least. This lower travel time improvement is mainly because their geographical location makes that moving by foot requires less than 35 minutes on average.

Fig. 4 illustrates the percentage of travel time reduction when using the bus services to travel between all the census sections in a heat map. Darker blues represent higher reductions. The labels in the ticks of the x-axis and y-axis are different. But the two axes have the same ticks and are symmetrical, i.e. the x-axis represents the same census segments as the y-axis. The black axis tick labels represent the segment ids, while the bold red labels the district ids.

Table 6: Travel times between districts when the citizens use the bus (in min) and the time reduction (% of improvement) regarding the same trip by foot.

district	non-elderly users				elderly users			
	travel time		improvement (%)		travel time		improvement (%)	
	mean±std	max	mean±std	max	mean±std	max	mean±std	max
1	27.7±9	63.1	12.9±14	47.6	31.9±10	76.0	20.3±17	56.1
2	22.3±8	55.1	12.9±17	48.5	25.6±9	67.6	20.6±20	57.6
3	24.4±8	58.2	17.1±17	52.9	27.5±9	69.8	25.5±20	61.4
4	28.5±9	69.8	20.7±19	58.1	32.4±10	83.3	28.7±21	65.3
5	27.7±7	65.7	30.7±22	66.9	30.7±9	78.4	39.3±22	73.2
6	23.8±8	58.7	11.6±15	50.5	27.4±9	70.1	19.1±18	59.5
7	29.1±6	61.5	30.4±20	60.9	32.2±8	79.2	39.3±21	67.8
8	28.5±9	68.5	17.8±17	57.9	32.3±11	81.8	26.9±19	65.4

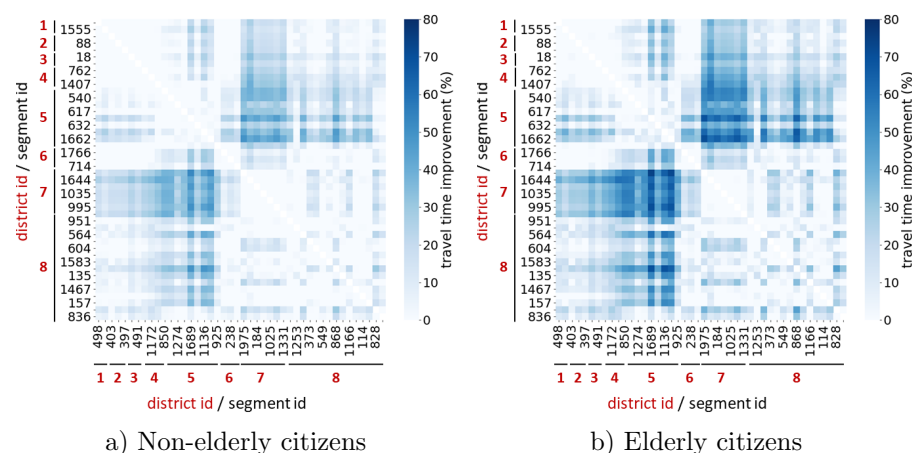


Fig. 4: Travel time improvements on trips between city sections.

In general, when comparing Fig. 4.a (non-elderly users) against Fig. 4.b (elderly users), the second one shows darker blue, which indicates more improvements (higher time reduction). There is not any cell in the heat-map in Fig. 4.a that contains a darker blue than the same cell in the heat map Fig. 4.b. Besides, two dark areas (located at the left-bottom and right-top) represent the improvements when travelling between the census segments in the district 5 and 7.

The results in Fig. 4 are in line with the improvement columns in Table 6. The quality of the bus service in terms of travel time reductions is higher for the elderly users and for travelling between the peripheral districts.

When comparing the improvements in Table 6, it is observed that elderly citizens reduce their travel times more than non-elderly ones. The mean time reductions are 29.90% and 21.41% for elderly and non-elderly, respectively. This is a significant outcome because the bus network is expected to improve the most those users who have more limitations getting around the city. Focusing on elderly, districts 7, 5, and 4 show the most significant improvements, which are the districts with the lowest elderly ratio in the city.

Table 7 presents the percentage of additional time required by the elderly citizens to move from a given district regarding the same by the non-elderly people when both types of evaluated users take the bus. According to the results in Section 5.1, elderly people require 22.39% longer times to walk among the census segments than the non-elderly. The results in Table 7 show that percentage is significantly reduced when the bus system is used. On average, when the bus is taken elderly spend 9.97% longer times than non-elderly. Thus, it can be seen that the improvements over the travel time when using the bus network mitigate the mobility differences between the travel times of the two types of users studied.

Table 7: Travel time difference between non-elderly and elderly users when using the bus (percentage of additional time required by the elderly).

District	1	2	3	4	5	6	7	8
Time difference	12.2%	9.0%	11.3%	12.2%	9.4%	9.2%	8.4%	10.3%

Focusing on the walking part of the trip, it has been observed that elderly users select routes that require walking shorter distances than non-elderly. Table 8 presents the percentage of reduction of the length traveled on foot of the elderly over non-elderly users grouped by the origin district of the route.

Table 8: Length of the walking part difference between non-elderly and elderly when using the bus (reduction percentage of the walking distance by the elderly).

District	1	2	3	4	5	6	7	8
Walking distance reduction	2.3%	3.9%	3.8%	3.1%	6.4%	2.1%	2.1%	1.0%

Thus, results in tables 7 and 8 show that the bus system mitigates the differences in travel times that exist between non-elderly and elderly citizens while offering more comfortable routes (i.e., needing shorter walks) to the elderly.

### 5.3 Bus stops distribution

The distribution of the bus stops has a direct impact on the distance users have to walk to get the bus network, travel times (more stops longer times because the buses stop more often), and the cost of operations (more stops increases costs) [14, 32]. This section is focused on the first aspect of the bus stop distribution, the walking distance because it is essential for elderly users.

Table 9 shows that as the districts increase in size (see Table 1), the number of bus stops installed in them also increases. Pearson’s correlation analysis confirms this statement with a resulting correlation of 0.86 (i.e., high correlation). A similar correlation can be seen between the number of inhabitants of the districts and the number of stops installed, obtaining a Pearson coefficient of 0.91 (i.e., high correlation). This may lead us to realize better access to the bus system in the larger and more populated districts. However, considering elderly people (i.e., the number of elderly citizens in the district) and the density of bus stops, the Pearson coefficient is -0.02, which indicates that the distribution of the bus stops does not take into account where the elderly population of Melilla live.

Table 9 summarizes the bus stop distribution by including the number of bus stops per square kilometer for each district and the distance in meters to the closest bus stops for all the segments for each district.

Table 9: Density of bus stops and walking distance to the closest stop (meters).

district id	bus stops per km <sup>2</sup>	distance to the closest bus stop		
		mean±std	min	max
1	0.0	489.7±205.6	284.1	695.3
2	34.8	131.2±49.6	62.5	178.1
3	16.7	197.7±133.2	64.4	330.9
4	26.8	339.5±243.1	132.5	748.2
5	24.6	176.5±125.5	24.2	456.1
6	10.3	231.4±85.8	127.4	337.6
7	17.8	201.3±51.8	121.5	299.8
8	11.1	354.1±466.6	89.5	424.4

There is significant variability in the density of bus stops installed in the different districts (see Table 9). District 1 has no bus stops, and district 2 has 34.8 bus stops per km<sup>2</sup>. Thus, when the citizens of district 1 need to take a bus have to walk about 500 meters to find the closest bus stop (district 1 is the smallest district with the lowest population size). However, inhabitants of district 2 need to walk only 131 meters. This is because district 2 is located in the city's downtown, and most bus lines operate through the downtown.

Considering this quality of service metric, the peripheral districts (districts 5 and 7) are ranked in the middle with 24.6 and 17.8 bus stops per km<sup>2</sup>. However, this does not affect travel times, because as it has been discussed in Section 5.2, they are the districts with the most significant improvement when using the bus.

## 6 Analysis limitations due to lack of open data

This research tries to propose evaluating the public bus system in a city from an age perspective based solely and exclusively on open data. The idea is to show the results and the challenges found when carrying out this independent analysis by third parties (other than the concessionary bus company itself or the public bodies involved that manage valuable information about the bus service).

A comprehensive assessment of the bus network would require metrics and indicators such as comfort, cleanliness, and crowding of the bus, ease of access stops, noise, vibration, and temperature on the bus, security against crimes on the bus and at stops, among others [28]. However, these indicators usually are private or difficult to calculate. The indicators selected in this article have the particularity of using only open data (one of the objectives of this study) rather than private or on-site collected data [18].

The evaluation presented in Section 5 has been performed by using data found on various websites (e.g., the COA official website) and official reports (e.g., the census of the National Institute of Statistics), but anything from official open data portals. This absence of data on official portals shows the lack of concern of public institutions for making relevant information about public transport available to citizens, which limits the task of an independent evaluation.

Estimating travel times and distances rely on the calculation of routes (on foot and by bus), which suffer from the lack of information on urban mobility (e.g., speeds at which buses move in different situations, use of private transport in the city, what are the most common mobility patterns of citizens, etc.). Therefore, a method for route estimation had to be implemented (see Section 4.3). The accuracy of the method is limited because it considers that the buses and citizens move with constant speed, the time waiting for the next bus is modeled by using Poisson processes, the time stop time does not depend on the bus stop or the hour of the day, etc. Besides, the indicators computations consider all possible trips between any census segments for the computations of the indicators. Having information on the mobility and affluence (e.g., most typical trips) would allow the weighting of trips by importance to provide a fairer indicator evaluation. Therefore, incorporating new real data and using a realistic urban simulator such as SUMO [21] may improve the computation of these indicators.

Incorporating information on the distances users are willing to walk to get a bus would allow knowing if there are disconnected users. Getting data on the bus service fares and the cost of operating the bus system would allow an economic evaluation of the system by getting information on the costs of using the service and the efficiency of the service maintenance. Finally, knowing whether buses are adapted for users with special needs (such as the elderly) would improve the evaluation of the system from an aging perspective.

## 7 Conclusion and future work

This work is motivated by the need to provide an efficient and effective public bus system that represents an alternative to private transport, emphasizing the service provided to the elderly because public transport allows independence, enhances well-being, and improves their relationship with urban spaces. Specifically, we analyze the case of Melilla. The main aim is to perform an objective and independent assessment of the bus network relying only on available open data. Thus, the main limitations of such analysis because of the lack of valuable open data have been discussed.

According to the results, the public bus service reduces travel times more for the elderly than non-elderly. This reduction in trip times is higher for districts with the lowest elderly ratio. In turn, it has been shown that the bus system mitigates the differences in travel times between non-elderly and elderly citizens while offering more comfortable routes (i.e., needing shorter walks). However, the distribution of the bus stops does not consider the areas where the most elderly people live, making the elderly have to walk long distances to reach the nearest bus stop. These results indicate that the bus service of Melilla provides a competitive service, but a new distribution of bus stops (or lines) may improve the service with an aging perspective.

The limitation of the proposed study due to the scarcity of open data dictates some of the future research lines. These future works include: *i*) including socioeconomic aspects, bus fares, and cost of operating to extend the analysis; *ii*) considering a collaboration with other stakeholders (such as the COA bus

company) to get new (not-open) data such as the types of buses, the bus mobility, the influx on the different bus lines, the number of buses per line, etc. to include new indicators; *iii*) getting information about the location of the most used facilities and ordinary trips of elderly for social/recreational reasons to evaluate the service provided to that specific travels; *iv*) taking into account mobility limitations to find possible disconnected passengers; and *v*) using SUMO urban simulator to improve the accuracy of the evaluated travels.

*Acknowledgments* The research of J. Toutouh and C. Cintrano is partially funded by the Universidad de Málaga and MCIN/AEI/10.13039/501100011033 under grant number PID 2020-116727RB-I00 (HUmOve) .

## References

1. Barns, S.: Smart cities and urban data platforms: Designing interfaces for smart governance. *City, culture and society* **12**, 5–12 (2018)
2. Buffel, T., Phillipson, C., Scharf, T.: Ageing in urban environments: Developing ‘age-friendly’ cities. *Critical social policy* **32**(4), 597–617 (2012)
3. Camero, A., Toutouh, J., Stolfi, D.H., Alba, E.: Evolutionary deep learning for car park occupancy prediction in smart cities. In: *International Conference on Learning and Intelligent Optimization*. pp. 386–401. Springer (2018)
4. Carrion, C., Levinson, D.: Value of travel time reliability: A review of current evidence. *Transp. research part A: policy and practice* **46**(4), 720–741 (2012)
5. Chen, X., Yu, L., Zhang, Y., Guo, J.: Analyzing urban bus service reliability at the stop, route, and network levels. *Transp. research part A: policy and practice* **43**(8), 722–734 (2009)
6. COA Melilla: Cooperativa Omnibus de Autobuses de Melilla. <https://coamelilla.com/> (2021), Accessed: 2021-01-05
7. Conserjería de Medio Ambiente y Sostenibilidad. Ciudad autónoma de Melilla.: El sistema de transporte público de Melilla. <https://medioambientemelilla.es/el-sistema-de-transporte-publico/> (2020)
8. Diab, E.I., Badami, M.G., El-Geneidy, A.M.: Bus transit service reliability and improvement strategies: Integrating the perspectives of passengers and transit agencies in north america. *Transport Reviews* **35**(3), 292–328 (2015)
9. Dirección General de Tráfico (DGT): El impacto medioambiental del tráfico. [https://www.dgt.es/PEVI/documentos/catalogo\\_recursos/didacticos/did\\_adultas/impacto.pdf](https://www.dgt.es/PEVI/documentos/catalogo_recursos/didacticos/did_adultas/impacto.pdf) (2014)
10. EAPN Melilla: Red Europea de Lucha contra la Pobreza y la Exclusión Social en Melilla. <https://eapnmelilla.wordpress.com/> (2021), Accessed: 2021-01-05
11. Estrada, E., Maciel, R., Negrón, A.P.P., López, G.L., Larios, V., Ochoa, A.: Framework for the analysis of smart cities models. In: *International Conference on Software Process Improvement*. pp. 261–269. Springer (2018)
12. European Environment Agency: Noise pollution is a major environmental health concern in europe. Collection - Environment and health (2018), <https://www.eea.europa.eu/themes/human/noise/noise-2>
13. European Environment Agency: Health risks caused by environmental noise in Europe. <https://www.eea.europa.eu/publications/health-risks-caused-by-environmental> (2020)
14. Fabbiani, E., Neschachnow, S., Toutouh, J., Tchernykh, A., Avetisyan, A., Radchenko, G.: Analysis of mobility patterns for public transportation and bus stops relocation. *Programming and Computer Software* **44**(6), 508–525 (2018)

15. González, F., Valdivieso, V., De Grange, L., Troncoso, R.: Impact of the dedicated infrastructure on bus service quality: an empirical analysis. *Applied Economics* **51**(55), 5961–5971 (2019)
16. Instituto Nacional de Estadística: Padrón, población por municipios (2021). <https://www.ine.es> (2021), Accessed: 2021-10-05
17. Instituto Nacional de Estadística (INE): Melilla: Población por municipios y sexo. <https://www.ine.es/jaxiT3/Datos.htm?t=2909> (2020)
18. Jomnonkwo, S., Ratanavaraha, V.: Measurement modelling of the perceived service quality of a sightseeing bus service: An application of hierarchical confirmatory factor analysis. *Transport Policy* **45**, 240–252 (2016)
19. Knoblauch, R.L., Pietrucha, M.T., Nitzburg, M.: Field studies of pedestrian walking speed and start-up time. *Transportation Research Record* **1538**(1), 27–38 (1996)
20. Köksal Ahmed, E., Li, Z., Veeravalli, B., Ren, S.: Reinforcement learning-enabled genetic algorithm for school bus scheduling. *Journal of Intelligent Transportation Systems* pp. 1–19 (2020)
21. Krajzewicz, D.: Traffic simulation with sumo—simulation of urban mobility. In: *Fundamentals of traffic simulation*, pp. 269–293. Springer (2010)
22. Kumar, A., Srikanth, P., Nayyar, A., Sharma, G., Krishnamurthi, R., Alazab, M.: A novel simulated-annealing based electric bus system design, simulation, and analysis for dehradun smart city. *IEEE Access* **8**, 89395–89424 (2020)
23. Lebrusán, I., Toutouh, J.: Car restriction policies for better urban health: a low emission zone in madrid, spain. *AQAH* **14**, 333–342 (2020)
24. Lebrusán, I., Toutouh, J.: Using Smart City Tools to Evaluate the Effectiveness of a Low Emissions Zone in Spain: Madrid Central. *Smart Cities* **3**(2), 456–478 (2020)
25. Lebrusán, I., Toutouh, J.: Smart city tools to evaluate age-healthy environments. In: Nesmachnow, S., Hernández Callejo, L. (eds.) *Smart Cities*. pp. 285–301. Springer International Publishing, Cham (2021)
26. Lebrusán Murillo, I.: La vivienda en la vejez: problemas y estrategias para envejecer en sociedad. *La vivienda en la vejez* pp. 1–243 (2019)
27. Lebrusán Murillo, I.: Las dificultades para habitar en la vejez. *Documentación Social* **1**(1), 1 (2020)
28. Mahmoud, M., Hine, J.: Measuring the influence of bus service quality on the perception of users. *Transportation Planning and Technology* **39**(3), 284–299 (2016)
29. Nesmachnow, S., Massobrio, R., Arreche, E., Mumford, C., Olivera, A.C., Vidal, P.J., Tchernykh, A.: Traffic lights synchronization for bus rapid transit using a parallel evolutionary algorithm. *International Journal of Transportation Science and Technology* **8**(1), 53–67 (2019)
30. Nguyen, T., Nguyen-Phuoc, D.Q., Wong, Y.: Developing artificial neural networks to estimate real-time onboard bus ride comfort. *Neural Computing and Applications* **33**(10), 5287–5299 (2021)
31. OpenStreetMap contributors: Planet dump retrieved from <https://planet.osm.org>. <https://www.openstreetmap.org> (2017)
32. Rossit, D.G., Nesmachnow, S., Toutouh, J.: Multiobjective design of sustainable public transportation systems. In: *1st Int Workshop on Advanced Information and Computation Technologies and Systems*. pp. 152–159. CEUR-WS (2021)
33. Soni, N., Soni, N.: Benefits of pedestrianization and warrants to pedestrianize an area. *Land use policy* **57**, 139–150 (2016)
34. Walters, P., Bartlett, H.: Growing old in a new estate: establishing new social networks in retirement. *Ageing & Society* **29**(2), 217–236 (2009)

# A Technical-Economic Study of the Implementation of Renewable Energies in a Train-based Mass Transportation System using RETScreen Software

Estefani Gabriela Mendoza Guerra<sup>1</sup> [0000-0001-5028-9816] and Jorge Mirez<sup>2</sup> [0000-0002-5614-5853]

<sup>1,2</sup> Universidad Nacional de Ingeniería, Lima, Peru

<sup>1</sup>estefani.mendoza.g@uni.pe

<sup>2</sup>jmirez@uni.edu.pe

**Abstract.** This paper reports a proposal for the implementation of renewable energies in the mass transportation system of the Lima City, Peru. For this, a compilation of information has been made from cities of interest that have committed and carried out management for the development of mass transport in an efficient way to reduce the impacts of the great urban traffic problems (congestion, delays, accidents and environmental problems), which is the product of population growth and poor urban planning. It is of special interest, the cases with greater technological development and/or large number of population. The implementation is done through the simulation of photovoltaic solar energy, wind and hybrid sources in the RETScreen Expert program to supply electricity to the Alstom Metropolis 9000 trains in Lima. As a result, an arrangement of a 3 MW wind power plant and two photovoltaic plant of 0.5 MW each one (Scenario 3) represents the best option from the point of view of greenhouse gas emission analysis at a initial cost of US\$ 4,669,279, while the cheapest option is a 4 MW photovoltaic solar plant (Scenario 2) with a initial cost of US\$ 3,484,000. RETScreen Expert program has been verified in its application in Peru through validation simulations of the Rubí Solar Photovoltaic Plant. Economically, Scenario 2 implies initial costs of US\$ 3,484,000, which is lower than Scenario 3 and Scenario 1 (four wind turbines with nominal power of 1 MW per wind turbine).

**Keywords:** Renewable energies, mass public transport, trains, environmental pollution, energy efficiency.

## 1 Introduction

Transport and energy have been a central part of the economic history of mankind for the mobility of people and goods. An efficient and sustainable transport system is synonymous with economic development and well-being, as well as a qualified thermometer on the degree of advancement of a society. Mobility and energy are two sides of the same coin, for the following reasons: The first, due to the impact of international, European and domestic policies on decarbonization, with the consequent legal heritage regarding urban mobility. The second, due to the digital revolution

currently underway and which is affecting the way and the way of organizing and living in modern urban societies; The third, due to the technological evolution that is energetically transforming mobility and energy management in the urban habitat [1].

The greenhouse gases (GHG), a growing world population that will reach 9.7 billion in 2050 and 11.2 billion around 2100 [2] and the need to move over longer distances; what has caused a triggering accelerated pace of life, with the use of cars, motorcycles, trains and bicycles.

In the most populated and extensive cities [3] they have opted for the train lines to be able to meet all the requested demand, however; there are still many places in the world that need to implement solutions to the transport of goods and people according to the characteristics of their territory.

Already in 2014, the transport sector alone consumed around 2.5 billion tonnes of oil equivalent (MTEP), almost a third of the final energy consumption, supplied mainly by oil derivatives [4].

Global emissions from transportation increased 0.5% in 2019 (compared to 1.9% annually since 2000) due to efficiency improvements, electrification, and increased use of biofuels. Transport continues to be responsible for 24% of direct CO<sub>2</sub> emissions from fuel combustion. Road vehicles (cars, trucks, buses, and two- and three-wheelers) account for almost three-quarters of the CO<sub>2</sub> emissions from transport, and emissions from aviation and shipping continue to rise [5].

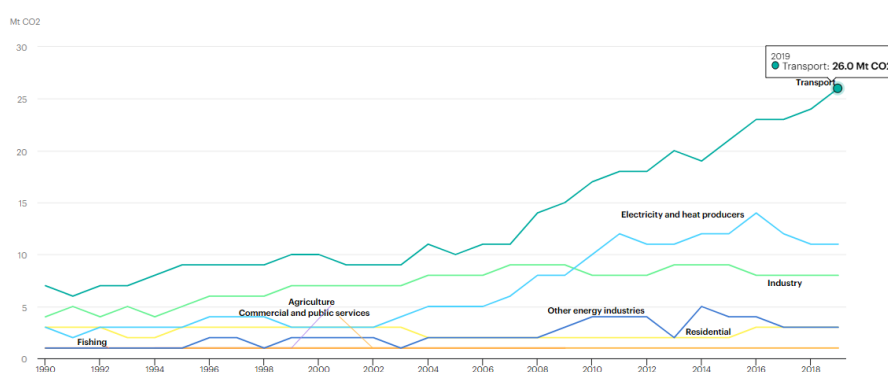


Fig. 1. CO<sub>2</sub> emissions by sector, Peru 1990-2019 [29].

Those with more than half the population of the entire planet and around 80% of the world gross domestic product (GDP) in 2013, it's two-thirds (2/3) of the demand for primary energy and 70% of total emissions CO<sub>2</sub> related to energy. The energy and carbon footprint of urban areas will increase with urbanization and the increasing economic activity of urban citizens. By 2050, the urban population will increase to two-thirds (2/3) of the world's population and the urban share of world GDP will be around 85%. The continuation of current trends in the energy system, driven by existing policies such as the 6°C Scenario (6DS), will increase urban demand for primary energy in the order of 70%, from 2013 levels, to about 620 EJ in 2050, the year in which said demand will represent 66% of the total. Furthermore, carbon emissions

from energy use in cities (including indirect emissions related to electricity and heat generation) would increase by 50% [6].

Cities are the main drivers of global mobility demand. Urban transport activity accounted for around 40% of total transport energy consumption in 2013. Furthermore, an important part of non-urban transport activity comes from demand for products and materials by urban businesses and households. The role of public transport is just as relevant in non-Organization for Economic Cooperation and Development (OECD) economies to avoid disorderly urban sprawl and the consequent high share of personal transport, characteristic of some cities in the developed world. Therefore, low-carbon mobility can generate additional sustainability benefits such as less environmental pollution, less traffic congestion, and increased safety [6].

Lima, capital of Peru, is the second city with the worst traffic in South America, and in position 15 of 416 cities evaluated worldwide [7]. The transport sector in Peru is the largest GHG emitter (see Fig. 1)

When conducting the respective bibliographic search, a proposal for the city of Lima for the application of renewable energy technologies in urban transport systems has not been found, therefore, it is an interesting topic to investigate, also considering that the implementation of transport massive urban through trains is growing; the Line 1 subway is in operation, with progress in the construction of the Lima Line 2 subway [8], pre-investment studies for the future Line 3 subway [9]. Line 1 is fed from the grid and the proposal for the implementation of renewable energy would serve to reduce the bill and consumption of the grid that uses conventional energy.

## **2 Theoretical Framework**

### **2.1 About existing mass transport systems**

At the regional level, a comparison is made between the cities of Buenos Aires (Argentina), Santiago de Chile and Medellin (Colombia), which is shown in Table 1 in terms of technical-economic details of the investments in their respective public transport systems.

### **2.2 Technical specifications of the Alstom Metropolis 9000 Train.**

Each of the Alstom Metropolis 9000 trains that run through the Lima Metro is made up of six cars called Ma1-Mb1-RR-Mb2-Ma2, which can be classified by two types of trailer and motor car, where: Ma1 and Ma2 are motor cars (each car has four motors, that is to say: one motor per axle) with a driving position. Each motor car has an automatic coupling at the end of the cabin (to carry out the mechanical, pneumatic and electrical connection with another train unit of the same series supplied by Alstom Metropolis 9000 or mechanical and pneumatic with existing trains; Mb1 and Mb2 are intermediate motor cars with pantograph (in charge of receiving the 1,500 Vdc from the catenary); R is an intermediate trailer car (without motor, it does not have traction) [16].

**Table 1.** : Comparison between the cities of Buenos Aires, Santiago de Chile and Bogotá.

Feature / City	Buenos Aires	Santiago de Chile	Medellin	Lima
Metro / Start year	Metro Bs.As., 1913	First line 1975	Metro Medellin, 1995 [12]	Metro of Lima, 2021 [13]
Bus/ Start year	Metrobus 2011	Transantiago 2007	Transmilenio 2010	Metropolitano
Investment BTR (US\$)	124 millions			241 millions [14]
Supervisory Office		Ministry of Transport		OSITRAN, AATE, ATU, INVERMET
Mileage Metro	6 lines	7 lines, 140 km [11]	Mileage Metro	6 lines
Mileage bus	59.7 km [10]	Mileage bus	59.7 km [10]	Mileage bus
Pasajeros año/metro		985 millions		
Pasajeros año/bus		1,200 millions		
Pasajeros día/metro		2.6 millions [11]		692,000 [13]
Pasajeros día/bus		3.3 millions		700,000 [15]
Project executor BTR	Local	Local	Local/National	Local [15]
Project executor Metro	National	National	Local/National	National

The Alstom Metropolis 9000 train requires a line voltage of 1,500 Vdc; In addition, it has a redundant communication system, in master mode and slave mode that allows the cars to be connected and if it is detected that a device is not working, the backup system enters or depending on the type and number of devices that do not work, train traction is prevented [16].

**Table 2.** : Dimensions of the Alstom Metropolis 9000 train [16]

Description	Driving	Trailer
Number of bogies	2	2
Number of wagons	4	2
Number of motors	4	0
Number of axles	16	8
Wheels quantity	32	16
Brake pad quantity	32	16
Wheelbase [mm]	2,000	2,000
New wheel diameter [mm]	840	840
Minimum wheel diameter [mm]	770	770
Track width (gauge) [mm]	1,435	1,485
Wheel spacing [mm]	1,360	1,360
Total length [mm]	3,440	3,440
Total width [mm]	2,550	2,550

To start the train traction, the pantograph is raised through the auxiliary compressor, supplying a voltage of 1,500 Vdc to the static converters which deliver a voltage of 400 Vac, 220 Vac and 72 Vdc by supplied to the train equipment, such as: the main compressor (works at 400 Vac) that generates a pressure of 8 to 10 bar to supply air to the braking and suspension system; ventilation systems (works at 400 Vac) of power electronic equipment (of brand: ONIX); 220 Vac car lighting, 400 Vac air conditioning, and 72 Vdc battery charging. Once the equipment has been fed with the static converter and having compressed air, the operation test is carried out, which consists of a series of tests on: doors, lighting, braking levels, air conditioning, communication, etc. If no faults are registered during the operational tests, is able to travel the line and that during its operation it has a nominal consumption of 4 MW [16].

**2.3 Wind Energy.**

Eq. (1) expresses the mechanical power output, where  $r$  is the radius of the wind turbine blade (m);  $V$  is the wind speed (m/s),  $C_p$  is the Power Coefficient, and  $\rho$  is the air density ( $\text{kg/m}^3$ ) [17].

$$P = \frac{1}{2} C_p \rho A V^3 \tag{1}$$

In Eq. (2), the air density is expressed as a function of the air pressure, the air temperature and the height above sea level, where  $\rho_0$  is the air density as a function of the altitude ( $\text{kg/m}^3$ );  $\rho_0$  is the standard atmospheric density at sea level ( $1.225 \text{ kg/m}^3$ );  $R$  is the gas-specific constant for air ( $287.05 \text{ J/kg}\cdot\text{K}$ );  $g$  is constant gravity ( $9.81 \text{ m/s}^2$ );  $T$  is the temperature (K), and;  $z$  is the altitude above sea level (m) [18].

$$\rho = \frac{p}{R(T + z)} \tag{2}$$

The power law represents a model for the vertical wind speed profile, expressed in Eq. (3) where  $U(z)$  is the wind speed in height  $z$ ;  $U(z_r)$  is the referential wind speed at height  $z_r$ , and;  $\alpha$  is the exponent of the power law [19].

$$U(z) = U(z_r) \left[ \frac{z}{z_r} \right]^\alpha \tag{3}$$

**2.4 Photovoltaic solar energy.**

The power generation of the photovoltaic cell can be using Eq. (4) where  $P$  is the power generated by the photovoltaic solar panel;  $P_{STC}$  is the nominal power of the photovoltaic solar panel under standard test conditions;  $G$  is the instantaneous solar irradiance;  $G_{STC}$  is the solar irradiance under standard test conditions;  $k$  is the temperature coefficient of the silicon (Si) with which the photovoltaic cell is manufactured;  $T_{ref}$  is the reference temperature of the cell,  $y$ ;  $T_c$  is the cell temperature under standard test conditions standard [20].

$$\text{---} \tag{4}$$

### 3 Simulations and Results

The simulations have been developed in the RETScreen® Clean Energy Management Software platform enables low-carbon planning, implementation, monitoring and reporting [21].

#### 3.1 Scenario 1.

For this Scenario, four wind turbines with a nominal power of 1 MW per wind turbine have been considered, from the manufacturer Vestas with model NEDWIND NW55/2/1000-240-70m. Has been considered 1,266 US\$/kW as initial cost according to [22], also the operation and maintenance costs of wind installations in onshore areas are 46 US\$/kW-year [23]. For the capacity factor, 30% is considered according to [24]. From the analysis of GHG emissions, a reduction of 3,125.9 T of CO<sub>2</sub> is obtained, which is equivalent to 1,343,133.4 liters of gasoline. From the economic analysis, is obtained that the return on investment occurs in year N° 4 (see Fig. 1) with a debt ratio of 50%.

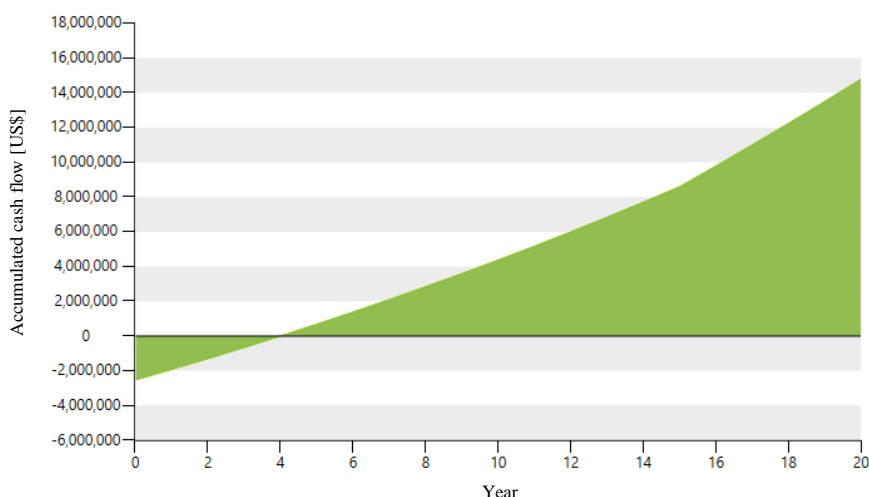


**Fig. 2.** Economic analysis with wind turbine plant according to Scenario 1 using RETScreen Expert software.

#### 3.2 Scenario 2.

For Scenario 2, a 4 MW photovoltaic solar plant is considered, consisting of 12,500 units of 320 W mono-Si photovoltaic solar panels, from the manufacturer SunPower

with the mono-Si model SPR-320E-WHT. According to [22] 871 US\$/kW is considered as initial costs, also the operation and maintenance costs of photovoltaic plants with 25 US\$/kW-year [23]. For the capacity factor, 30% is considered according to [24]. The analysis of the amount of GHG emissions describes a reduction of 3,125.9 T of CO<sub>2</sub>, which is equivalent to 1,343,133.4 liters of diesel, and the economic analysis shows a return on investment in approximately 2.2 years.

### 3.3 Scenario 3.

In this Scenario, a wind power plant and two photovoltaic solar panel plants are considered. The wind power plant consists of three wind turbines with a nominal power of 1 MW per wind turbine from the manufacturer Vestas with model NEDWIND NW55/2/1000-240-70m; with 1,266 US\$/kW as initial cost and 46 US\$/kW-year for costs operation and maintenance [23]. Each of the photovoltaic solar plants consists of 1,563 units of 320 W mono-Si photovoltaic solar panels from the manufacturer SunPower with the mono-Si model SPR-320E-WHT, which allow a total of 1 MW to be obtained; according to [22] 871 US\$/kW is considered as initial costs and the operation and maintenance costs of photovoltaic plants with 25 US\$/kW-year [23]. For the capacity factor, 30% is considered according to [24].

Performing the analysis of the amount of GHG emission in Scenario 3, a reduction of 3,126.2 T of CO<sub>2</sub> is obtained, which is equivalent to 1,343,240.8 liters of gasoline, and in the economic analysis a return is obtained investment in year N° 3.5 (see Fig. 3), being similar to Scenario 1, but involves twice as many years compared to Scenario 2.

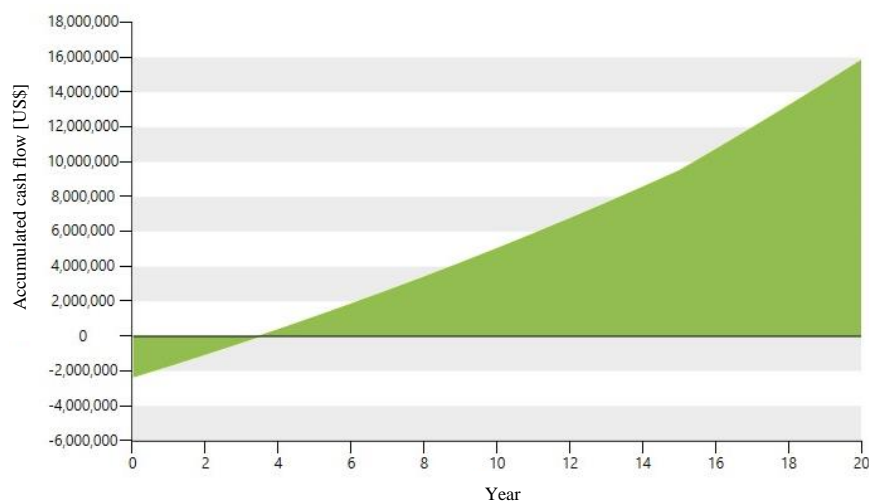


**Fig.3.** Economic analysis with wind turbine plant according to Scenario 3 using RETScreen Expert software.

### 3.4 Simulation of Rubí Solar Power Plant.

The Rubí Solar Power Plant is located at the coordinates: Latitude  $-7.050^{\circ}$  and longitude  $-76.55^{\circ}$ . The location data were entered in the RETScreen Expert, the technical data [25] and then the simulation was carried out. Data was downloaded from NASA [26] on solar radiation at the coordinates of the Central. In addition, polycrystalline photovoltaic modules, the number of photovoltaic modules, initial investment [27], capacity factor (= 34.76%), operating expenses (OPEX) cost and maintenance cost, have been considered.

Form factor [28] was calculated from the data: Generation power 144.48 MW, energy produced annually 440 GW-h/year, hours per year 8,760 hours/year, plant factor 34.76%. An initial cost of US\$ 165,123,072 was considered. In the analysis of the amount of GHG emissions, an emission reduction of 162,517.6 T of CO<sub>2</sub> is obtained, which is equivalent to 69,829,285.2 liters of gasoline. This shows that the Rubí photovoltaic plant is technically and economically viable, with a return on investment in the year N° 2.

## 4 Discussion

Three (03) study scenarios have been developed using RETScreen Expert [21] for the integration of renewable energies in the Alstom Metropolis 9000 trains that belong to Lima Metro Line 1. Of these, it is determined that it is feasible to implement Scenario 2 with a return on investment in year 2; Scenario 3 has a return on investment in year 3.5 and Scenario 1 has a return on investment in year 4. Economically, Scenario 2 implies initial costs of US\$ 3,484,000, which is lower than Scenario 3 with US\$ 4,669,279 (by -25.38%) and Scenario 1 with US\$ 5,064,000 (by -31.20%).

In the environmental aspect, Scenario 3 represents the best option from the point of view of the GHG emission analysis, in which an annual reduction of 3,126.2 T of CO<sub>2</sub> is obtained, and closely, with a difference of 0.00959% is Scenario 2 (3,125.9 T of CO<sub>2</sub> per year), which makes a difference of 300 kg CO<sub>2</sub> per year.

For the case studies in Lima, Peru, the implementation of a central photovoltaic plant has a better economic feasibility as a source of electrical energy for mass public transportation.

## Acknowledgment

The authors thank the following projects and institutions: (a) CYTED Thematic Network “Ciudades Inteligentes Totalmente Integrales, Eficientes y Sostenibles (CITIES)” N° 518RT0558; too, (b) thanks to the support and motivation provided by the Federal University of Maranhão (UFMA), CEMAR, CP ELETÔNICA, CNPq – Brazil, and MEIHAPER CYTED; (c) Group of Mathematical Modeling and Numerical Simulation (GMMNS) y Center of Communications and Information Technologies (CTIC) in National University of Engineering (UNI), Lima, Peru, for the use of

facilities for research development, and to; (e) Miss Fabiola García Herrera by technical support

## References

1. Á. Pelegrý y M. Sánchez, «Energías alternativas para el transporte de pasajeros.», p. 231, 2017. Cuadernos Orkestra, 2017/25, ISSN 2340-7638. Available in: [https://www.orkestra.deusto.es/images/investigacion/publicaciones/informes/cuadernos-orkestra/Informe\\_transporte.pdf](https://www.orkestra.deusto.es/images/investigacion/publicaciones/informes/cuadernos-orkestra/Informe_transporte.pdf)
2. Habibur Rahman y Hoong Chor Chin, «“A balanced scorecard for performance evaluation of sustainable urban transport”», International Society for Development and Sustainability, Online ISSN: 2168-8662. Volume 2 Number 3 (2013): Pages 1671-1702 ISDS Article ID: IJDS13032501. Available in: <https://isdsnet.com/ijds-v2n3-3.pdf>
3. GTZ, «Proyecto sectorial Servicio de Asesoría en Política de Transporte. “Opciones de transporte público masivo”. Módulo 3a. Transporte sostenible: Texto de Referencia para formuladores de políticas públicas en ciudades de desarrollo”». Available in: [https://www.sutp.org/files/contents/documents/resources/A\\_Sourcebook/SB3\\_Transit-Walking-and-Cycling/GIZ\\_SUTP\\_SB3a\\_Mass-Transit-Options\\_ES.pdf](https://www.sutp.org/files/contents/documents/resources/A_Sourcebook/SB3_Transit-Walking-and-Cycling/GIZ_SUTP_SB3a_Mass-Transit-Options_ES.pdf)
4. Purvis, Charles; Turner, Shawn; Limoges, Edward; et. al. The Future of Urban Transportation Data: Transportation in the New Millennium – A Look Forward. A1D08: Committee on Urban Transportation Data and Information System. Transportation Research Record Journal of the Transportation Research Board. Available in: [https://www.researchgate.net/publication/252223235\\_The\\_Future\\_of\\_Urban\\_Transportation\\_Data\\_Transportation\\_in\\_the\\_New\\_Millennium\\_-\\_A\\_Look\\_Forward](https://www.researchgate.net/publication/252223235_The_Future_of_Urban_Transportation_Data_Transportation_in_the_New_Millennium_-_A_Look_Forward)
5. International Energy Agency. «Fuels & Technologies», Available in: <https://www.iea.org/reports/key-world-energy-statistics-2021/final-consumption>
6. United Nations - Department of Public Information. «Creciendo a un ritmo menor, se espera que la población mundial alcanzará 9.700 millones en 2050 y un máximo de casi 11.000 millones alrededor de 2100: Informe de la ONU». Accedido: oct. 04, 2021. Available in: [https://population.un.org/wpp/Publications/Files/WPP2019\\_PressRelease\\_ES.pdf](https://population.un.org/wpp/Publications/Files/WPP2019_PressRelease_ES.pdf)
7. Tomtom. Traffic Index ranking. Available in: [https://www.tomtom.com/en\\_gb/traffic-index/ranking/](https://www.tomtom.com/en_gb/traffic-index/ranking/)
8. Agencia de Promoción de la Inversión Privada del Perú. «Línea 2 y Ramal Av. Faucett - Av. Gambetta de la Red Básica del Metro de Lima y Callao». Available in: <https://www.proyectosapp.pe/modulos/JER/PlantillaProyecto.aspx?ARE=0&PFL=2&JER=5695&SEC=22>.
9. Agencia de Promoción de la Inversión Privada del Perú. «Inversiones Estratégicas - Cartera de Proyectos: Línea 3 del Metro de Lima y Callao». Available in: <https://www.proyectosapp.pe/modulos/JER/PlantillaProyecto.aspx?ARE=0&PFL=2&JER=8162>
10. Carlos Posada. «Comercio Exterior: Aumento continuo del parque automotor, Un problema que urge solucionar», La Cámara. Febrero 26, 2018. p. 3. Available in: [https://apps.camaralima.org.pe/repositorioaps/0/0/par/r816\\_3/comercio%20exterior.pdf](https://apps.camaralima.org.pe/repositorioaps/0/0/par/r816_3/comercio%20exterior.pdf)
11. Metro de Santiago «Metro de Santiago». Available in: <https://www.metro.cl/>
12. Metro Medellín «Metro Medellín» Available in: <https://www.metrodemedellin.gov.co/>
13. Línea 1 del Metro de Lima « Nuevo récord de 692 mil pasajeros », Disponible en: <https://www.lineauno.pe/noticias/comunicado-22/> (accessed on oct. 04, 2021).

14. Andina Agencia Peruana de Noticias, «Presupuesto de El Metropolitano se incrementó de US\$ 134 a 241 millones, informa Protransporte». Online Edition. Available in: <https://andina.pe/agencia/noticia-presupuesto-de-metropolitano-se-incremento-134-a-241-millones-informa-protransporte-199829.aspx> (accessed oct. 04, 2021).
15. Instituto Metropolitano PROTRANSPORTE de Lima. «Sistema». Available in: <http://www.metropolitano.gob.pe/conocenos/sistema/> (accessed on oct. 04, 2021).
16. Alstom, «Manual de generalidades», Lima, Perú, 2016. Documento interno de trabajo.
17. S. M. Muyeen, Stability Augmentation of a Grid-connected Wind Farm. Kitami Institute of Technology. Abu Dhabi: Springer, 2009.
18. T. Ackermann, Wind Power in Power Systems. Stockholm: John Wiley & Sons, 2005.
19. JF Manguel y J. G. McGowan, Energía Eólica Explicado Teoría, Diseño y Aplicación, Segunda Edición. Wiley, 2009.
20. A. Niinisto, «Simulation of the Management of a Micro Grid with Wind, Solar and Gas Generators.», Master's Thesis of Engineering. Faculty of Electronics, Communications and Automation, School of Science and Technology. Aalto University, Espoo, 2019.
21. Government of Canada. RETScreen® Clean Energy Management Software. Available in: <https://www.nrcan.gc.ca/maps-tools-and-publications/tools/modelling-tools/retscreen/7465>
22. Comisión Nacional de Energía (CNE) Chile «Informe de Costos de Tecnologías de Generación - Informe Anual 2020». [On line]. Available in: <https://www.cne.cl/wp-content/uploads/2020/03/ICTG-Marzo-2020.pdf>
23. Revistel – Energía para las Industrias «Operación y Mantenimiento es fundamental para rentabilidad del negocio eléctrico», [En línea]. Available in: <https://revistel.pe/operacion-y-mantenimiento-es-fundamental-para-rentabilidad-del-negocio-electrico/> (accessed on oct. 04, 2021).
24. C. A. A. Fernández Vázquez y M. Fernández Fuentes, «Inventario, evaluación y proyección de las emisiones de carbono provenientes del sector eléctrico nacional. Bolivia 2025», Acta Nova, vol. 8, n.o 3, pp. 354-375, mar. 2018.
25. División de Supervisión de Electricidad, «Proyectos relevantes de generación y transmisión de energía eléctrica en construcción.», OSINERGMIN, Lima, Perú, Técnico Ingeniería, 2018. Accedido: jul. 08, 2021. [En línea]. Available in: <https://www.osinergmin.gob.pe/newweb/uploads/Publico/MapaSEIN/informes/proyectos/construccion/201801.pdf>
26. National Aeronautics and Space Administration «POWER Data Access Viewer». Available in: <https://power.larc.nasa.gov/data-access-viewer/>.
27. Ministerio de Energías de Bolivia «Estudio de determinación de Costos de Operación, Mantenimiento y Administración Fijos de Generación con base en Energías Alternativas. Tomo I: Generación Solar Fotovoltaica» Accedido: oct. 04, 2021. Available in: [https://energypedia.info/images/e/e2/Estudio\\_Costos\\_Fijos\\_OMA-Generacion\\_SOLAR\\_FV.pdf](https://energypedia.info/images/e/e2/Estudio_Costos_Fijos_OMA-Generacion_SOLAR_FV.pdf)
28. Jean Pool Genaro Rojas Bismarck, «Diseño de una central solar fotovoltaica de 30MW, para su análisis técnico, operativo y económico en el SEIN; ubicada en Tacna - 2017», Universidad Señor de Sipan, Pimentel, Perú, 2018. [En línea]. Available in: <https://repositorio.uss.edu.pe/bitstream/handle/20.500.12802/4873/Rojas%20Bismarck.pdf?sequence=1>
29. International Energy Agency. «Data and statistics: Data Tools; Energy topic: CO<sub>2</sub> emissions; Indicator: CO<sub>2</sub> emissions by sector; Country: Peru», Available in: <https://www.iea.org/data-and-statistics/data-browser?country=PERU&fuel=CO2%20emissions&indicator=CO2BySector>

# The ethics of artificial intelligence and virtual reality in the construction of society 5.0

## Society 5.0 and artificial affairs and virtual reality

Roberto Ramirez Basterrechea<sup>1</sup> and Viviana Polisena<sup>2</sup> and Katherine Hoolahan<sup>3</sup>

<sup>1</sup> Co-founder of CivesSolutions, expert in Smart City and society 5.0

<sup>2</sup> Catholic University of Córdoba - UCC

<sup>3</sup> Managing director. [virtuallyhealthy.co.uk/](http://virtuallyhealthy.co.uk/)

**Abstract.** Developing ethical axioms for the governance of Society 5.0 is one of our greatest challenges, because we are not only laying the foundations for future ethics but we are building the new society. Correctly integrating the data is part of this edification, since a correct interaction will avoid an immense network of falsehoods and their consequent bad decision-making that will affect present and future public affairs. By taking into account the correct fusion and integration of data, Big Data will instill greater trust and artificial intelligence and virtual reality will be more solid, this will lead to its development being collaborative. For artificial intelligence and the virtual world to flourish, a well-connected and ethically integrated data set is needed. We are proposing an ethical integration of data so that a global sustainable collaborative governance of public affairs emerges that encompasses insights from economics and organizational behavior psychology to generate common decisions. The objective is that the artificial and the virtual collaborate with the proper functioning of human life. Artificial intelligence (AI) and virtual reality (VR) has enormous potential to accelerate and support the global energy transition, but several key barriers prevent rapid adoption of that global scale. This document attempts to explore the potential of AI and VR for the transition to the artificial and establishes a set of ethical principles to help governments to scale AI and VR technology in a fast, safe and fair way.

**Keywords:** Ethical governance. Artificial intelligence. Virtual reality. society 5.0.

## 1 Introduction

In this paper we will present three fundamental ethical principles to take into account when building and putting into practice new integrated technologies, focusing specifically on the ethical impact of artificial intelligence (AI) and virtual reality (VR) in Society 5.0. The explosion of society 5.0 has begun, it is time to reflect on the ethics that will regulate new technologies in education, science and culture.

We do not know where we are going with our own creations, but if we know that we have to regulate their development, teamwork and the agreement of interests will lead us to a consensus on the use of technology both in the private sphere and in the field. Public ambit. Although progress has been made in this task, most of it comes from more developed countries; Why aren't the least developed countries involved? If new technologies will boost productivity and performance in all areas; it is fair that the consensus for ethical regulation is global; In other words, all countries intervene in some way; The first point to correctly regulate the new technology is precisely to listen to all voices and thus avoid discrimination and absences from the starting point. Participation and consensus must be global because the playing field is global.

We propose that the ethics of artificial intelligence and virtual reality be based on three fundamental principles:

2

- 1) The artificial must always collaborate with the support of natural and human life.
- 2) All artificial devices must promote the development of critical-reflective thinking, that is to say, the artificial can never prevent the human being from thinking, the artificial and the virtual can never prevent the human being from philosophizing. Free will must never be annulled.
- 3) All technology must respect the human values of health, education, freedom of thought, happiness and progress.



Integrated technologies present us with a host of solutions to unsolved issues from science; The integration of technologies unleashes new philosophical and ethical debates, but it also proposes a certain new cultural dimension that we cannot ignore because it presents an innovative relationship between the philosophy of science and the philosophy of technology, from which multiple realities emerge that require a social contract updated. In this contract a different way of understanding science, technology, philosophy and their interactions is crystallized, it forms a model in neural network format; in which, the interactions produce an increase in collective synapses. This context has new techno-ethical results since there is a displacement of moral and legal borders. The aforementioned will unleash new collective neuronal synapses, which will lead the human to a higher state of reasoning and empathy; Hence the relevance of the proper use of these technologies since they not only enable the implementation of the principle of non-locality, but will also have an impact on medicine, food production, education, transportation and the mode of transportation. conceive and build smart cities.

All this founds a reality so new that it makes visible what was previously invisible and suggests another interpretation and another perception of forces; in this way the notion of applying matter to form is broken and a new meaning of the data emerges. Data are also technical objects. We live in a handmade reality, a reality that is woven and in the act of weaving the surface on which an idea can be applied is produced. From the

3

muscle-building of the tissue as a struggle and an alliance, as a play of forces from which matter lets itself be, the culture of the bio-artifact arises, which embraces both the artificial and the data. The division of forces no longer corresponds because from a fundamental analysis, all the forces are a single block that records and disaggregates all possible information as a blockchain. In this way, data integration is achieved as a symptom of the great digital transformation.

In making good decisions-actions, individual-collective ethical reflection is necessary because it is the only way to know ourselves and ensure a free and fair future.

*“The urgency to examine life corresponds to the urgent need to lay the foundations of contemporary Demos: a society of thinkers committed to the collective restoration of knowledge and the social fabric, because a society founded on well-being results in a more benevolent shared existence”.* [1]

These times of crisis require citizens who are aware of the responsibility that they must apply to all their activities with non-transferable values. The successful solution is precisely teamwork thinking of each of the participants, since the entire team takes care of each of the members, maintaining codes of conduct over time. Honesty is needed for the conditions of possibility of the novel to emerge. The novelty only arises in an environment of trust and trust is fostered when the group gives the best of itself, thinking of the other.

The cultural disruption of society 5.0 in smart cities is maximized through the triple helix mechanism, identifying and processing the intellectual capital that sustains the development of a cultural reconstruction and reveals how it is possible that cultural reinvention works as a stabilizing mechanism. that integrate cities into emerging innovation systems. We focus on intellectual capital and this begins with a limitation, which is that knowledge becomes obsolete and must be replaced with techno-scientific knowledge generated in "transdisciplinary" projects. The reinvention of smart cities and society 5.0 is defined by Systematically elaborated innovations such as the educational content of the social and cultural processes that operate at the local level, this generates a rectification in the global perspective since the localities do not have to go to the regional, then to the national and then to the international. do it directly. [2].

## **2 The ethical for the Development of the artificial**

Where are we going? We are building a fabric of people, which will build a fabric of technology, which will do everything possible to weave a new society. And, if we succeed, we will use the most transformative technology in human history to build a more trustworthy 5.0 society. Society 5.0 develops from its own reality through a cultural transformation, in a continuous process of autonomy, freedom, communication, values, use of technology and constant social development. Since ancient times, philosophers have dreamed of deducing ethics from scratch, using only unquestionable principles and logic. After thousands of years, the only consensus that has been reached is that there is no consensus [3].

Developing ethical axioms for the governance of Society 5.0 is one of our greatest challenges. The manipulated information lays down ethical axioms with social values that are transformed as a result of the latent threats existing in social networks [4]; because

4

we are not only laying the foundations of the future ethics but we are building the new society. Artificial Intelligence (AI) is a fast evolving family of technologies that can bring a wide array of economic and societal benefits across the entire spectrum of industries and social activities [.....] However, the same elements and techniques that power the socio-economic benefits of AI can also bring about new risks or negative consequences for individuals or the society[5].

Correctly integrating the technology is part of this edification, since a correct interaction will avoid an immense network of falsehoods and their consequent bad decision-making that will affect present and future public affairs. By taking into account the correct fusion and integration of data, Big Data will instill greater trust and artificial intelligence and virtual reality will be more solid, this will lead to its development being collaborative. For artificial intelligence and the virtual world to flourish, a well-connected and ethically integrated data set is needed. We are proposing an ethical integration of data so that a global sustainable collaborative governance of public affairs emerges that encompasses insights from economics and organizational behavior psychology to generate common decisions. The objective is that the artificial and the virtual collaborate with the proper functioning of human life.

*“Innovation is not that which only gives immediate economic results but an end at the service of being and an existence oriented to the quality of shared work, thus an Ethics of Contemporary Innovation must contemplate an eminently social, sustainable character; promote an essentially humanistic attitude, include the concepts: commitment, dignity and virtue; generate creative competitiveness, eliminate the meaning of error as failure, move to all areas and be communicable to provoke debate”.[6]*

### 3 Conceptualizing ethics in society 5.0 - Education blockchain

It is necessary to consider again the Aristotelian legacy, that is to say, the right of the citizens of the polis to an education that could guarantee their freedom and continue with it in the third millennium. Human beings try to explain and understand physis and lay down its founding principles in order to form the polis. Both tasks could only be carried out by free human beings, and this freedom is only possible with an education based on paideia principles. This is an integral education, which allows a broad development of personality traits so that each individual could develop ethos towards excellence in the acquisition of personal values and qualities. Ethos should be developed as a morality that can allow us to create laws and participate in the res publica since this is the best way of becoming virtuous human beings.

Education could also be seen as an opportunity for the creation of new jobs, however, if the challenges are undressed, this disparity between supply and demand will may intensify and the outcomes are likely to worsen between those who are prepared for the Education blockchain and those who are not. Impacting not only to the 1.8 billion global youth between the ages of 15 and 29, to whom this revolution will significantly determine their roles as workers and competitors, but also to the millions of workers currently active in the workforce”. In light of technological trends such as the ones outlined before, in recent years many countries have undertaken significant efforts to increase

5

the amount of STEM (science, technology, engineering and mathematics) graduates produced by their national education systems. For example South Korea's Meister schools. These schools collaborate with industry to deliver curricula that provide hands-on training and direct employment. Other systems, such as the Philippines' K-to-12 Program, have redesigned their secondary education systems to encourage specialization in skills development, and align formal education with technical and vocational education and training (TVET). Other examples include the European Qualifications Framework, India's National Skills Qualifications Framework, the Skills Initiative for Africa, and countries like Denmark allocates funding for two weeks' certified skills training per year for adults.

The practice of virtues and the development of telos not only implies to observe the law but also to observe a common way of being that can be carried out in the polis. This should be fostered by education since virtues and values are acquired by practicing them, which is why learning through example is crucial. Education should offer an exemplary ethos so that it could be worth emulating. Courage and boldness are needed to educate, but philosophy is also needed because human's beings naturally seek knowledge, and, in this sense, contemplation is inherent to human beings. Knowledge and contemplation are biological conditions of personal realization. If we are deprived of these conditions, the essence of our being is curtailed; in other words, cognitive pleasure is curtailed. Therefore, philosophy is so important for education in the polis, and this is why the polis should be formed in freedom due to the fact that philosophical questioning is only possible among free human beings. Therefore, philosophy has a liberating role. Philosophy helps to develop, on the one hand, the spontaneous disposition to learn, on the other hand, the mental and spiritual empowerment to transform the citizens of the world. Empowerment is a process by which human beings increase their strength and confidence in their own capacities and actions which results in self-control, development of new ideas and global new ideology to improve the welfare of the polis, which, in turn, contributes to the resolution of common existential issues and to the appropriate use of new technologies. Empowerment does not relinquish the power of decision to anyone but to oneself, which is why the outputs of the economy of the new millennium will result from that empowerment. One of those goods will be knowledge and information transference in physis, which will allow us to enlarge or broaden the borders of the present.

Our objective is to create a paideia based on the enhancement of enthusiasm by questioning. This may lead to the appropriate use of technology and information, which in turn will change the topology of the polis and will consequently innovate the democratic attitude and will guarantee creativity in the humanistic construction of the knowledge of the 21st century. Paideia ensures development, innovation and empowerment because it has to do with the various ways in which a free citizen deals with common matters of the polis. This implies taking knowledge of physis to the agora, that is to say to the res publica, to expand it. However not only knowledge should be expanded or globalized, but also the ideas of truth, justice, and supreme good. In fact, the free citizen globalizes culture as an example, which indicates that a successful, efficient and legitimate progress could be attainable by everybody. Therefore, the notion of governance shows a new way of managing pedagogic strategies of the polis in terms of educational innovation, taking into account that there is nothing more important than education as a common good. Thus, we can observe that the paideia governance, as an integral civic humanism, can improve our common environment, and can unfold individual capacities to reach the status of free citizens that encourage the social dynamics

6

of the polis. This process may surely arise from a participative and cooperative ethics with an educational instruction that aims at conflict resolution by means of cooperative actions.

*“Physis, Polis, kai Paideia (Nature, City, and Education), a scientific-political-cultural project in the age of globalization, has as its purpose to address the phenomena of nature in order to lay the foundation for a new way of life. This project can be successful only within the framework of free and rational citizens, people whose education has guaranteed the full development of personality. With that education, they are able to contribute ethically to the enrichment of thought and language. In this way, culture (communication, knowledge, learning, and transfer) as paideia is the property of the polis because in it are generated customs and habits that transmit to subsequent generations the practice of ethical wisdom and the axiom of the spiritual development of humanity”. [7].*

Education is a blockchain ecosystem, said ecosystem optimizes processes to take advantage of expanding knowledge in developing countries, and the impact of said application, from different perspectives and at different stages of the educational process, will allow the recording of virtual data shielding the information in real time so that the chain of knowledge reaches the citizen-users. We are talking about an unalterable, encrypted, secure, transparent and accessible record for all participants and students. Although it emerged in the financial system with the launch of the virtual currency bitcoin, nowadays the concept of blockchain is used in a wide range of activities, such as, for example, it can be applied to education and transmission of knowledge. This tool, which had already been developed, has become much more important in the context of the COVID-19 health crisis and predictably in the post-pandemic world.

A concrete example of how this process works in practice can be seen from the experience of the French company Auchan Retail, which has implemented food traceability based on blockchain technology on an international scale throughout its entire supply chain. After tests in Vietnam, together with Te-Food, it has already applied this technology to track goods and services originating in France, Italy, Spain, Portugal and Senegal. This system allows the tracking of different types of products "from farm to table", as well as the registration of food quality data and related logistics information through a QR code.

The same can be done with the knowledge process, we must bear in mind that there are three groups of challenges to improve the implementation of this technology: technical, management and governance, and large-scale implementation. The former include technological infrastructure development challenges. The second, the need for open standards and sectoral and business coalitions of the different countries that allow the development of knowledge of scale and interoperability. The last group includes data quality, the participation of all stakeholders, the development of inclusive systems and secure interfaces. New technologies for a greater and better international insertion cannot be left out of this new challenge to increase the quantity and quality of knowledge. Blockchain technology does not discriminate between color, gender, age, nationality, or background (education). This new technology presents an opportunity for all who want to take advantage of it. Political freedom must be accompanied by economic

7

freedom for people to be truly free. Blockchain technology is a new frontier in the educational landscape and provides a framework in which trust and transparency can underpin financial institutions, electoral systems, and communication platforms. The Blockchain process can be the great equalizer between races, genders, economic status and even educational levels; this technology can restore public trust in our educational institutions.

#### **4 Humanization of the digital economy in society 5.0**

If we conceive of education as a blockchain, we must not forget the economy only as circular but as a network, since the circular economy continues to be linear so it is not innovative or inclusive. The economy must be conceived as a rhizome, re-think the use of technology-models-simulations from a new Ethics, the notion of rhizome leaves the rigid-binary logic to immerse itself in the ramification of ideas, interconnect models-concepts- categories in the same way that nature does. The rhizome provides a strategy compatible with complex thinking: an enveloping dimension. In biology, the rhizome is a horizontal underground stem that grows indefinitely, the flora is rhizomorphic when it forms tubers with a plurality of exits-entrances. In zoology, animals move like rhizomes: migratory birds, rodents. The cities are rhizomatic: Venice, Favelas, Villas Miseria, Paris. In Philosophy, rhizome is an epistemic model in whose structure any predicate of one element can affect the conception of other elements [8].

The digital economy has the principles of the rhizome: (i) Connection and Heterogeneity: all points are connected to each other. You can get to any point without following a hierarchically determined path; (ii) Multiplicity: there are no positions, it has no beginning or end. Combination increases with multiplicity; (iii) Breakdown of the Significant: it can be decomposed at each stage and start over; (iv) Cartography and Decal: the structure is changeable. It is a detachable-pluggable multi-input map.

On 07-22-2013, the results of an investigation at the University of Barcelona were published in Nature Physics: "Cultured neurons do not need biological help to order, interconnect and organize among themselves. They are activated and evolve towards a state of coherent activity simultaneously following a harmonic pattern. Spontaneously emerging a self-organized collective behavior orchestrated without the need for a director, that is, without any element that acts as a leader, similar to the spread of rumors through social networks". [9].

These cultures are prepared from neurons in the early stages of their development, within a few days the neurons spontaneously form a network of connections with great electrical activity. It is concluded that this phenomenon may be key when establishing spontaneous activity patterns in different neuronal tissues; Like the functioning of neurons and the development of the rhizome, it becomes a natural activity, where the units bifurcate and interact, gaining in multiplicity. The multiple is built and points to social transformation, we need an economy that leads us to an encounter with the other, so it will be an economy focused on the development of the citizen and not on the growth of the finances of a few.

The global lockdown due to COVID-19 has had a seismic effect on the global economy. Some sectors have been especially vulnerable, while others, such as streaming platforms and online commerce, linked to digitization, have been reinforced. Digitization, aligned with scrupulous respect for the environment, will shape the economy of the future. A good example of this synergy is smart farming, which allows farmers to

8

maximize their resources and irrigate, fertilize and fumigate each piece of land with surgical precision according to its particularities and weather forecasts. Thus, this revitalization, which is already a reality in cities (smart cities), will make the leap to towns (smart villages). Tools such as big data and its ability to squeeze the juice out of massive amounts of information, the Internet of Things (IoT), artificial intelligence or machine learning have revolutionized the business and industrial world, favoring both the efficiency and quality of processes productive as the optimization of decision making. The evolution of the economy will generate many opportunities for businesses, which will arise as we move towards new industries and their interaction with the markets; This will develop each place according to its own talents. We are talking about the human economy and how to create decent livelihoods in the digital decade based on social security. The human economy will be built around the recognition of human contributions to the common good. Building the digital human economy is not a technical task but the result of public policies and fair alliances in smart governments so that cities can evolve.

*“The dynamics of the selection process from a current city to a smart city is not inherited biologically, but is a cultural process, that is, it depends on the development of interaction and communication skills, which is represented in the knowledge of citizens. Interactions between dynamics can be intensified by communication technologies (ICT), which are being used to generate the notion of “creative cities”. The intelligent governments that integrate this dynamic as well as the citizens are generators of values of a community, their transforming ideas and intelligent services turn individual actions into reciprocal interactions, and in it there is no cavity for the repetition of previous erroneous models”. [10].*

## 5 Ethics of digital in Society 5.0

The governance of AI and VR cannot be done in isolation, but requires an international approach that provides a common direction that addresses the challenges and risks that technological tools pose to future generations.

After the pandemic, society has become more aware than ever of the impact its actions have on the environment. We have become aware of the need to move towards sustainable development guided by environmental, social and good governance criteria. Although we need quick responses, they must also be slow because entrepreneurs seal a cultural change and companies need to adapt to processes and decision-making. Within the new ethical-system we find key requirements that AI systems must meet to be considered reliable: human agency and supervision; technical robustness and safety; privacy and data governance; transparency; diversity, non-discrimination and equity; social and environmental well-being; and accountability.



10

axioms of freedom are eroding. "People will no longer see themselves as autonomous beings who lead their lives according to their own wishes, but rather as a collection of biochemical mechanisms that are constantly monitored and controlled by a network of electronic algorithms." Freedom "will collapse the day the system knows me better than myself."

Now, as a society, the reciprocity of ethical behavior is inserted and developed in the first place within a given social system, and encompasses attitudes and symbolic manifestations, so that algorithms can be understood as a validator of social behavior. In this regard, we consider relevant what [17] "Public space is our common space and our common future depends on it. And we also know that the successful ways of governance do not go through authoritarian, elitist or autistic forms of leadership, but through leadership with high human quality, based on integrity, commitment and the cultivation of certain values of service to the community".

Human beings today are aware of the consequences of unethical public management and the danger that hangs over technology, since, while humans are technologically limited, technical devices such as robots and artificial intelligence are enabled. According to [18]. "In this context of transition from traditional government to a model based on governance, the need to manage the social responsibility of public administrations appears as a central challenge to improve the capacity to create social value". Society 5.0 currently seeks that its leaders are ethically responsible, to eradicate corruption, bureaucracy, the misuse of technology, government negligence and political indifference on matters that concern the same society.

According to Bilbeny, N. "The use of the ethical is concerned, instead of the good end, for which it happens to adopt categorical imperatives that, as conditioned to ends, come to be recommendations, rather than mandates unconditional" [19]. In this sense, the recommendations are given through participation, which would be framed as an ethical principle in the decision-making of city councils.

The reality of cultural transformation in society 5.0 involves cultures with different ways of understanding and implementing ethics. The social, political, economic and historical reality of each region influences the ethics with which governments manage decision-making, although, nowadays, algorithms increasingly take actions for us and on our behalf, that is, intervention human is becoming unnecessary. According to Escudero P., [20] "The context of relationships between people, [...] ethics appears when an action of one person affects in some way the projects of another, which implies conflict; therefore, ethics becomes a civilized way of conflict resolution. And the actions of people cause conflict with others when they produce significant benefits or harm or when they prevent others from carrying out their projects". The dangerous difference from what Escudero points out is that now it is not people who drive decisions but rather intelligent machines that collect and analyze data to decide what to do.

It is necessary to identify common values and principles that are based on a universal ethic, since what we are building are global technologies and the technological euphoria does not show the risk to which we are exposed. The vision is that people will no longer be a machine among machines but an obsolete part of the system. Therefore, it is necessary to build a universal ethical model that facilitates adherence and promotes values in modern society "Modern societies live from moral presuppositions that it cannot guarantee", and in fact, it can only provide some social conditions of participation [21]. The issue corresponds to individual and group voluntary behavior in society that can be questioned in the same way by the same society. Based on the words of Escudero P., "Ethics, in short, comes to consist of the establishment of rights and duties whose

11

respect and fulfillment allow conflicts to be resolved through the allocation or distribution of damages and benefits that human actions generate in others”.

It is not a question of establishing a utopian behavior of ethics in society 5.0, but of laying the foundations for a behavior that adapts to the demands on the ethical use of technology in the face of the demands of future generations. In this regard, Leyva, G. points out that the growing burden on institutions deteriorates the social infrastructure of future generations.

For this we propose three fundamental principles as a basis for the development of ethics in society 5.0. They are: 1) The artificial must always collaborate with the support of natural and human life; 2) Any artificial device must promote the development of critical-reflective thinking, that is, the artificial can never prevent the human being from thinking, the artificial and the virtual can never prevent the human being from philosophizing. Free will must never be annulled; 3) All technology must respect the human values of health, education, progress.

We will have to build new social contracts and new ethics treaties; everything can be modifiable and improvable but these three fundamental principles must be permanent in society and in the relationship between people and artifacts.

## **6 The ethical in the use of virtual reality as a motor of our brain activity**

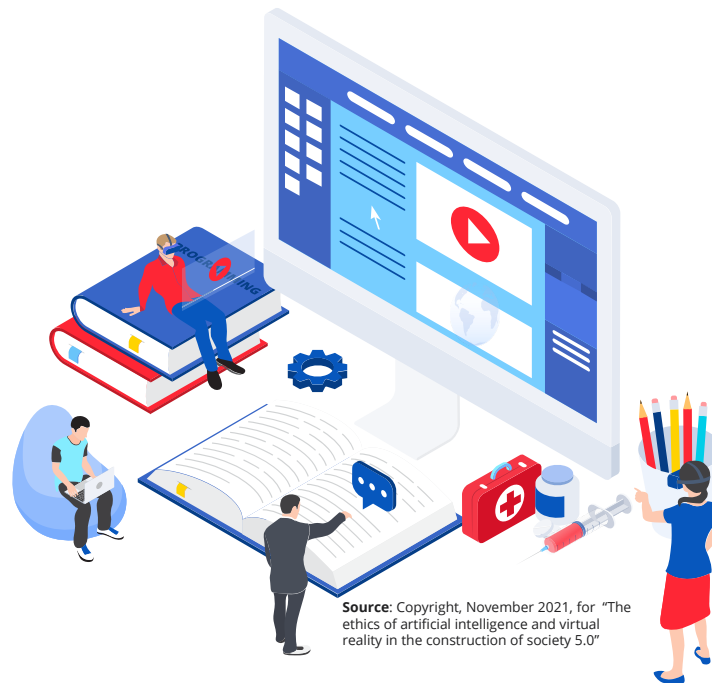
A central issue is addressing the question of whether VR as a tool enhances or diminishes our free will. VR can not only transform where the user is, but who the user is. The idea that in VR, our brains can quickly absorb new virtual bodies as if they were our own and trick our brain into becoming someone else can, apparently, make us a smarter and more lovable person; even unconsciously reducing racial prejudice. But how do we trick our brain into becoming someone else?

The promises of the "connected world", a programmable world with the ubiquitous internet and sensors in all kinds of objects that behave in a coordinated way with us, are immeasurable; also, the opportunities to innovate and improve countless everyday issues, but the promises of the programmable and connected world, which constitutes the new context, arouses as much hope as suspicion.

As with the nature of gaming, there tends to be a set path for the user to follow in the virtual experience. Although there can be a large element of choice within the virtual world, it is not simply possible for the user to do anything without first programming that into the experience. This therefore limits our free will within the virtual environment. As AI progresses, we will inevitably create more dynamic experiences, with more options for choice and free will within the virtual world. Although, the question remains - will we ever truly be able to reach a point where we have as much control over the virtual world as we do the real world? Or perhaps we should also consider the limitations of the real world and how we can step outside of those whilst in VR. In VR you can defy physics and gravity, therefore, will it instead provide different options for choice and free will due to the fact that we are able to do things that we cannot in the real world, which is bound by the laws of physics and the risks that some experiences come with.

The description of the kinder future, focused on the collection and analysis of all kinds of information from the real world, including ourselves, produced both excitement and concern; precisely because we ourselves are real world data.

12



Our ideas and our thoughts are data with which the virtual world is fed, our conscience and everything that happens in our brain are simple data to develop the virtual world. Our ethical approach goes beyond that the actions of each citizen are monitored, we are talking about a guided and planned neural interference, which not only diminishes free will but also implants other people's ideas so that each individual or group considers them their own and acts accordingly. consequence. This risk goes beyond an intrusion, it is a penetration into the depths of the neurological ethical processing. It is no longer about manipulating acts or decisions; it is about manipulating the scale of ethical values in the collective consciousness so that our technology is acted in a certain way. Our concern is very deep; hence, our fundamental ethical principles are inalienable and unchangeable since they are the guarantee that technology does not sow collective neurological modifications that can disrupt our most essential human values.

*"The Smart Governors act with political ethics and public morality because they are made up of people committed to the common good, generosity and solidarity; Hence, it requires not only the incorporation of state-of-the-art technologies, but also the ability to build a governance oriented towards the good living of the citizen, for this it reconfigures the management of solutions. In short, the Smart Governments are based on a transparent and non-bureaucratic administration that integrates the public and the private for the privilege of entrepreneurship and civil empowerment, and increase interaction with citizens, companies and educational organizations. Smart Governments require their citizens to develop new skills, especially mental skills*

*that will have social consequences. Preparing ourselves for the era of automation implies understanding the importance of awareness and interaction with nature through thought "[22].*

VR remains a technology limited by the difficulties in creating a sensory experience almost identical to reality. Smell and taste, two fairly important components of ordinary reality - keys to memory, enjoyment of the present moment, and more - are not taken into account in VR devices on the market today. Although there are devices that allow scent to be part of the VR experience, this requires the purchase of an additional component and is not common.

The introduction of affordable, immersive VR headsets with 6 degrees of freedom (i.e. tracking three dimensional movement and rotation within a space), starting with the Oculus Rift and HTC Vive in 2016, opened a whole new world of possibilities for society. It currently has applications within healthcare; fitness; sport; education; military; training; scientific visualisation; sales; entertainment; film; media; engineering; fashion and telecommunications sectors [23]. VR has a massive part to play within society 5.0 and with the appropriate ethical considerations it can push us forward and connect us like never before.

Although VR has been around since the 1930's, development of the technology was expensive and the immersion, graphics and interaction were nowhere near the standards of today's modern headsets. VR was initially developed for military purposes, with the first application of VR being a flight simulator to safely train military pilots in 1930 [24]. It soon branched out into the entertainment sector in the 1950s and was picked up by Hollywood for use in the film industry in the 1970s [25]. However it wasn't until the release of the HTC Vive and Oculus Rift in 2016 that VR started to grow exponentially and many more applications came to fruition.

Modern, immersive VR simulates a completely virtual environment and allows the user to move around in, and interact with, the virtual world using body movement sensors; usually in the form of a head-mounted display (headset) and handheld controllers. Recent advances have also seen the introduction of hand tracking - allowing more interaction without the need for physical handheld controllers. VR has already positively impacted many industries, however more research and development is required for it to reach its full potential.

The ability to be able to practice skills without the risk of harm is one of the major benefits of VR. It allows us to train in dangerous conditions to improve our chances of success when it comes to the real thing. As mentioned previously, the first use cases of VR were flight simulations to train pilots without risk of harm to them or others. Along with other military training applications, VR is also being used to train surgeons - providing the necessary practice that could save a patient's life. As VR has become more precise with better tracking and graphics, it has become better able to replicate intricate parts of the human body which could be key to proper training in the medical field. Not only just to practice aspects such as surgery, but to better educate our medical professionals, both generally and more specifically, through visualisation. Combined with scanning technology, medical professionals are able to view detailed images of patients and use that information to make better decisions regarding treatment and surgery. This technology can also be used to educate the patient about the ailment for them to better understand it, as well as to virtually walk them through the procedures and technology used within treatments. This can help to provide a different perspective for the patient and help to put their mind at ease about the process of treatment [26].

14

This platform which allows us to embody a virtual being in any virtual environment allows us to become closer to those who are far away. We can walk and talk in the same 3D space, wave and shake virtual hands with real movements in real-time; and it won't be long before we can feel those interactions as well. There are already devices, such as gloves and vests which allow more immersive haptic feedback - soon we will be able to feel the hug of a loved one from the other side of the world. As we use this technology to become more connected, we must consider not only the benefits, but the risks as well, and minimize any potential misuse and harm which may come from that.

One of the most common ethical questions that comes up for VR is the question of age. At what age is VR okay to use? Is it ok for children to be using VR? Are there limitations we should implement for young people using VR? Mostly, VR headsets have an age limit of 13, although there is variation between headsets, with the Playstation VR having an age limit of 12 and HTC Vive not having an age limit at all - simply a warning that it should not be used with young children. These VR companies also provide little basis for why these ages are chosen. For the Oculus Quest (owned by Facebook) it is the same age as a user must be to have a Facebook account - is that merely coincidence? Or does the age that a child can use social media link well with the age they should be allowed to use VR? Whilst a couple of studies have been completed into the short term effects of VR on children, there is not yet any research investigating the long term effects. Because of this, there is no consensus on what age children should be allowed to use VR, and little scientifically backed professional advice to allow parents to make informed decisions about its safety for their children. Generally, research suggests that time limits should be put in place for VR use by young people [27]. Let us delve into the theory behind the potential risks for children. One of the main things that comes up in the argument against children using VR is that VR is thought to negatively affect eyesight. There have been various studies linking screen time to increased prevalence of Myopia [28], [29], particularly in children. There are two aspects of the risks to eyesight - the first is close work (i.e. looking at things close to your face) and the second is blink rate. [30], showed that blink rate decreased whilst in VR, as users are so focused on the immersive content. Lower blink rate has been linked to ophthalmic diseases, such as keratitis and dry eye. Again, this is not limited to VR - screen time in general has been shown to reduce blink rate. This is not only a risk for young people using VR, but for adults as well. Therefore it should be taken into consideration when using VR in general, with an aim to take regular breaks during VR sessions and limit the amount of time spent in VR each day.

Another argument against children being allowed to use VR is that it is unclear how it affects brain development. There are worries about the largely unexplored psychological effects on children, especially due to the increased neuroplasticity of the brain at a young age. A study on mice by [31] showed that the region of the brain responsible for spatial learning reacted differently whilst in a virtual environment compared to the real world, with spatial learning and navigation impaired whilst in VR. Whether this also has the same effect on humans is unknown, but whilst research into this is still in its infancy, we should proceed with caution.

As children, we are on a quest to discover who we are and how we fit into this world - why we are here, and what our purpose is. By spending time in another reality in which we embody another body in the form of a virtual being, could that affect the process of understanding who we are? Could VR affect our development as social beings in the real world - or could it perhaps be an enhancement to this process, to prepare for the

future of technology and how the world is inevitably progressing. Could it be a vital step that is part of our modern day evolution?

It is known that young children under the age of 5 generally have difficulty distinguishing reality from fantasy [32], which adds another psychological risk of young children using VR. Anything experienced in VR is going to be real to young children. This leads to the ethical question of appropriate content. VR content is not yet as legally regulated as films and video games are - the age ratings in films and video games have well established criteria, however this is not the same with VR content, VR does not need to undergo rating before its release. This will likely come in time, but not only should content such as profanity and violence be taken into consideration for this, but the social elements as well. The embodiment of an avatar in the virtual world adds another element to virtual social interaction. Many parents are aware of the dangers of chat rooms on the internet, but may not be aware that the multiplayer VR games they allow their child to play, double as a 3D chat room - with somebody embodying a virtual being who moves and interacts just as the person on the other end does in real life. This combined with the lack of parental control options as are available on other devices and the likelihood that parents are not watching what their child is doing in VR - this poses a psychosocial risk to young children in VR. There are, however, also many benefits of using VR. Childhood obesity (and obesity as a whole) is a major problem in many first world countries. Many VR games provide a physically active experience which is both fun and motivational whilst reducing perception of exertion [33]. These VR games can provide an effective solution to increase engagement in physical activity to improve health - not only to reduce obesity, but to prevent a wide range of health conditions linked to a lack of physical activity. Not only has VR been shown to help with physical health, but mental health as well [34], which is particularly important with the growing worldwide mental health epidemic [35].

At what point do the benefits outweigh the risks and who is to make that decision? There is an argument for parents to be allowed to make that decision, however if parents are not provided with the appropriate information to make an informed decision, this could end up with harm coming to the child. Even when provided with the information, who's to say that they will actively seek it out or may simply ignore the advice altogether - then should it become the responsibility of the companies developing this technology to restrict its use? As the VR industry is still in its infancy, along with the research behind the potential risks and benefits, there is little in the form of ethical bodies to draw up guidelines to answer questions such as these. There are ethical groups which have formed recently to begin to address these ethical problems, however the approach to ethics in VR is still scattered, with no one group responsible. As the industry progresses, there will need to be a consensus upon the rules and regulations to prevent harm, whilst also pushing VR forward to reach its potential.

## 7 Conclusion

We consider that our proposal of basic principles or ethical axioms for the governance of Society 5.0 is one of our greatest challenges, because we are not only laying the foundations for future ethics but we are building the new society; Therefore, these principles must be included in any treaty or Law on Artificial Intelligence and Virtual Reality and must become the world standard to be effective, taking into account the potential impacts of said applications. We need a balance so that the approach is horizontal

16

and that all voices are heard, in order to create rules that last and are global technology regulators. In this way, the new Law will work in practice; Since protecting people is protecting data, protecting the smooth running of public affairs, protecting development and progress to be collaborative, protecting common decisions, protecting the governance of the world, the well-being of the planet and democratic functioning. Our proposal advocates a human-centered approach at the international level.

Designing and modeling the relationships between technology and society leads us to anticipate needs and problems and to understand the social and ethical implications of technological application. Debating the ethical limits of the design of technologies that influence our thinking and analyzing the ethical dimensions of artificial intelligence and virtual reality is the challenge and commitment of our time and our generation.

The objective is that the artificial and the virtual collaborate with the proper functioning of human life. The field of AI can respond to the need for inclusive and diverse perspectives, it can address issues related to the protection of vulnerable children around the world and to health care.

Artificial Intelligence and Virtual Reality are a rapidly evolving family of technologies that can deliver a wide range of economic and social benefits across the spectrum of industries and human activities, supporting productive environmental outcomes and providing advantages for businesses and economies.

The human being must become trustworthy for the human being, so that our own innovations will be safe for ourselves.

## References

1. Polisena, V.: Importancia de la ética en la ingeniería contemporánea. In *itinere*. Revista Digital de Estudios Humanísticos. Universidad Fasta, Argentina, pp. 55. (2014). Homepage, <http://revistas.ufasta.edu.ar/index.php/initinere/article/view/25>, last accessed 2021/08/21.
2. Ramírez, B. R.: Expo congreso internacional smart cities. pp.23. Lima, Perú, (2019). Homepage, <https://robertoramirezbasterrechea.com>, last accessed 2021/08/21.
3. Tegmark, M.: *Life 3.0: Being Human in the Age of Artificial Intelligence*. pp.310. Publisher Taurus. Madrid, Spain. (2018).
4. Ramírez, B. R.: *Desafíos globales en tiempos de esclavitud del liderazgo con pensamiento binario: posliderazgo*. pp. 2. Publisher El Nacional. Venezuela, (2021). Homepage, <https://www.elnacional.com/opinion/desafios-globales-en-tiempos-de-esclavitud-del-liderazgo-con-pensamiento-binario-posliderazgo/>, last accessed 2021/08/21.
5. Regulation of the European Parliament and of the council: Laying down harmonised rules on artificial intelligence (artificial intelligence act) and amending certain union legislative acts. (Nº 2021/0106(COD) Belgium, Brussels, (2021).
6. Polisena, V.: Importancia de la ética en la ingeniería contemporánea. In *itinere*. pp. 57. Publisher Revista Digital de Estudios Humanísticos. Universidad Fasta, Argentina, (2014). Homepage, <http://revistas.ufasta.edu.ar/index.php/initinere/article/view/25> last accessed 2021/08/05.
7. Polisena, V.: *Physis, Polis, kai Paideia in the Era of Globalization*. Publisher Apeiron Centre. France. (2018). Homepage, <https://apeironcentre.org/physis-polis-kai-paideia-in-the-era-of-globalization/>, last accessed 2021/08/05.
8. Deleuze, g.; Guattari, F.: *Rizoma (Mil Mesetas 1980)*. trad. Vázquez, J. P. pp 48. Paris: Minuit, (1976).

17

9. Orlandi, J.: Un nuevo mecanismo de comportamiento colectivo neuronal autoorganizado. Publisher Revista Universitaria. Barcelona, España. (2013). Homepage, [http://www.ub.edu/web/ub/ca/menu\\_eines/noticies/2013/07/058.html](http://www.ub.edu/web/ub/ca/menu_eines/noticies/2013/07/058.html), last accessed 2021/09/10.
10. Ramírez B. R.; Polisená, V. Smart City et Géométrie de la Nature: la capacité d'un smart government à modéliser les affaires publiques comme une itération quantique. IMODEV: Improving Public Policies in a Digital World. Publisher International Review of Open Governments. France. (2020). Homepage, <https://ojs3.imodev.org/?journal=RIGO&page=article&op=view&path%5B%5D=331>, last accessed 2021/08/21.
11. European Parliament Resolution: Framework of ethical aspects of artificial intelligence, robotics and related technologies. (2020). Homepage, [https://oeil.secure.europarl.europa.eu/oeil/popups/ficheprocedure.do?lang=en&reference=2020/2012\(INL\)](https://oeil.secure.europarl.europa.eu/oeil/popups/ficheprocedure.do?lang=en&reference=2020/2012(INL))
12. European Parliament resolution: Civil liability regime for artificial intelligence. (2020). Homepage, [https://www.europarl.europa.eu/doceo/document/TA-9-2020-0276\\_EN.html](https://www.europarl.europa.eu/doceo/document/TA-9-2020-0276_EN.html)
13. European Parliament resolution: Intellectual property rights for the development of artificial intelligence technologies. (2020). Homepage, [https://www.europarl.europa.eu/doceo/document/A-9-2020-0176\\_EN.html](https://www.europarl.europa.eu/doceo/document/A-9-2020-0176_EN.html)
14. European Parliament Draft Report, Artificial intelligence in criminal law and its use by the police and judicial authorities in criminal matters. (2020). Homepage, [https://oeil.secure.europarl.europa.eu/oeil/popups/ficheprocedure.do?lang=en&reference=2020/2016\(INI\)](https://oeil.secure.europarl.europa.eu/oeil/popups/ficheprocedure.do?lang=en&reference=2020/2016(INI))
15. European Parliament Draft Report, Artificial intelligence in education, culture and the audiovisual sector. (2021). Homepage, [https://www.europarl.europa.eu/doceo/document/A-9-2021-0127\\_EN.html](https://www.europarl.europa.eu/doceo/document/A-9-2021-0127_EN.html)
16. Daft, R.: La experiencia del liderazgo. Publisher Thomson. 3ª edición. Distrito Federal, México. (2006).
17. Canyelles, J.M.: Responsabilidad social de las administraciones públicas. Nuevas tendencias en gestión pública, Contabilidad y dirección. pp. 85. Publisher Editorial Bresca S.L. Barcelona, España. (2011)
18. Castiñeira, À. y Lozano, J. M.: "El poliedro del liderazgo". [e-Book]. Publisher Editorial Virtuts Angulo y Paco López (2012). 1ª Edición. Barcelona, España. (2012).
19. Bilbeny, N. S.: El saber como ética. pp. 30. Publisher Ediciones Península. Barcelona, España. (1998)
20. Escudero P. G.: Bien Común y Stakeholders, La propuesta de Edward Freeman. Publisher Editorial Universidad de Navarra. Navarra, España. (2010). ISBN 978-84-313-2739-1
21. Leyva, G.: El proyecto político de la modernidad. Publisher Editorial Fondo de Cultura Económica de Argentina, S. A. 1ª edición. Buenos Aires, Argentina. (2008).
22. Ramírez B. R.; Polisená, V.: Smart City et Géométrie de la Nature: la capacité d'un smart government à modéliser les affaires publiques comme une itération quantique. IMODEV: Improving Public Policies in a Digital World. International Review of Open Governments. France. (2020). Homepage, <https://ojs3.imodev.org/?journal=RIGO&page=article&op=view&path%5B%5D=331>, last accessed 2021/09/07.

18

23. Virtual Reality Society.: Applications Of Virtual Reality - Virtual Reality Society. (2017). Homepage, <https://www.vrs.org.uk/virtual-reality-applications/>, last accessed 2021/09/28.
24. Jeon, C.: The Virtual Flier: The Link Trainer, Flight Simulation, and Pilot Identity. 56(1), pp. 22–53. *Technology and Culture*, (2015). Homepage, <https://www.jstor.org/stable/24468693>, last accessed 2021/09/28.
25. Lovaglio, E. (n.d.): Exploring Virtual Reality: Historical Overview. Homepage, <https://www.mat.ucsb.edu/~g.legrady/academic/courses/01sp200a/students/enricaLovaglio/VRsite/history.html>, last accessed 2021/09/28.
26. Davis, J.: Going virtual, How VR is guiding interventional radiology. (2018). Homepage, <https://www.elsevier.com/connect/going-virtual-how-vr-is-guiding-interventional-radiology>, last accessed 2021/10/15.
27. Kaimara, P., Oikonomou, A., & Deliyannis, I.: Could virtual reality applications pose real risks to children and adolescents? A systematic review of ethical issues and concerns. pp. 1–39. (2021). Homepage, <https://doi.org/10.1007/S10055-021-00563-W>, last accessed 2021/09/01.
28. Pärssinen, O., & Kauppinen, M.: Risk factors for high myopia: a 22-year follow-up study from childhood to adulthood. *Acta Ophthalmologica*, 97(5), pp. 510–518. (2019). Homepage, <https://doi.org/10.1111/AOS.13964>, last accessed 2021/09/01.
29. Webster, M.: Sitting Too Close to the Computer Screen Can Make You Go Blind - Scientific American. (2007). Homepage, <https://www.scientificamerican.com/article/is-sitting-too-close-to-screen-making-you-blind/>, last accessed 2021/09/28.
30. Kim, Kumar, Yoo & Kwon: Change of Blink Rate in Viewing Virtual Reality with HMD. *Symmetry*, 10(400). doi:10.3390/sym10090400. (2018).
31. Sato, M., Kawano, M., Mizuta, K., Islam, T., Lee, M. G., & Hayashi, Y.: Hippocampus-Dependent Goal Localization by Head-Fixed Mice in Virtual Reality. *ENeuro*, 4(3). (2017). Homepage, <https://doi.org/10.1523/ENEURO.0369-16.2017>, last accessed 2021/09/25.
32. Woolley, J. D., & Ghossainy, M.: Revisiting the Fantasy-Reality Distinction: Children as Naïve Skeptics. *Child Development*, 84(5), 1496. (2013). Homepage, <https://doi.org/10.1111/CDEV.12081>, last accessed 2021/09/28.
33. Hoolahan, K. J.: A Preliminary Investigation Into the Effects of Gamified Virtual Reality on Exercise Adherence, Perceived Exertion, and Health. *Publisher International Journal of Virtual and Augmented Reality (IJVAR)*, 4(2), pp. 14–31. (2020). Homepage, <http://doi.org/10.4018/IJVAR.2020070102>, last accessed 2021/09/25.
34. Jerdan, S. W., Grindle, M., Woerden, H. C. van, & Boulos, M. N. K.: Head-Mounted Virtual Reality and Mental Health: Critical Review of Current Research. *Publisher JMIR Serious Games*, 6(3). (2018). Homepage, <https://doi.org/10.2196/GAMES.9226>, last accessed 2021/09/28.
35. Tucci, V., & Moukaddam, N.: We are the hollow men: The worldwide epidemic of mental illness, psychiatric and behavioral emergencies, and its impact on patients and providers. *Publisher Journal of Emergencies, Trauma, and Shock*, 10(1), 4. (2017). Homepage, <https://doi.org/10.4103/0974-2700.199517>, last accessed 2021/09/28.

# Optimization of a Hybrid Echo State Network methodology for forecasting the spot price of Iberian electricity market

D.M. Baer, M. Pons, M. Roca, E.Isern, J.L. Rosselló, and V. Canals

University of the Balearic Islands, Palma, Ctra. Valldemossa km 7.5, Campus UIB,  
Balearic Islands E-07122, Spain

Phone/Fax number: +34971173426, e-mail: [deva.baer1@estudiant.uib.cat](mailto:deva.baer1@estudiant.uib.cat)

**Abstract.** In the vast majority of UE countries, the electricity market is structured into day-ahead, an Intraday auction market and an Intraday continuous market. As an integral part of the electrical energy production market, the single day-ahead coupling (SDAC), aims to carry out electrical energy transactions by submitting selling and takeover bids for electrical energy on behalf of the market agents for the twenty-four hours of the next day. The electricity price forecast is a key information to help producers and purchasers involved in the electricity market to prepare their bidding strategies in order to maximize the profits and avoid penalties due to overconsumption or lack of generation. This work proposes a novel methodology to forecast day-ahead electricity based on Self-Organizing Map (SOM) and a set of Echo State Network (ESN) models. The SOM is in charge to cluster the input data automatically according to their similarity to train/infer the ESNs. The ESN models for regression are built on the categories clustered by SOM separately. ESN model parameters (leak rate and spectral radius) are automatically chosen by a genetic algorithm (GA) to improve prediction accuracy by up to 15%. The results suggest that SOM-ESN-GA provides a considerable improvement in the forecast of the daily price in the Iberian electricity market, archiving MAPE results lower than the best forecasting works in the literature.

**Keywords:** Artificial neural networks, Recurrent neural network, Self-organizing map, Genetic algorithm, Electricity price forecasting, Echo state network.

## 1 Introduction

The widespread use of electricity in society led to a series of profound transformations, causing that since the beginning of the generation of electricity as an industrial activity, at the XX century, the "lifestyle" of the society changed radically compared to previous centuries. Electric power has been the engine of progress of the modern society, and nowadays it is indispensable for a large number of activities and it is considered as a basic service. Since the process of regulatory reform, restructuring, liberalization, and privatization of the electricity sector in Europe, at the beginning of the 1990s, different countries have selected different pool market structures.

In the Spanish electricity market, the electricity price is set by auction. First, the cheapest electricity generation technologies enter the pool, followed by the next cheapest technology and so on until demand is met. The final pool price is set to the last generator price that enters the pool.

Since electric energy cannot be stored in large enough quantities to be able to satisfy the demand of the loads connected to the grid, the energy produced at every moment has to be equal to the demanded power. If it is taken into account that the supplied energy must conform with a certain level of safety, reliability and quality, and that the demand presents enormous variability (it varies throughout the day, the month and the year) keeping the balance is very challenging. This difficulty has made that maintaining a reliable electricity system is one of the main objectives of energy market regulators. Great efforts and investments have been made to develop tools to facilitate this task, such as energy demand forecasting models. Similarly, the agents that participate in the electricity market in electricity purchase and sale operations have developed price forecast tools in order to maximize their profit margin and to avoid penalizations, having an enormous importance at the corporate level as an input to energy companies' decision-making mechanisms.

According to the methodology or approach followed, in general terms the prediction models can be classified into methods based on statistical systems or based on artificial intelligence, and the different forecasting methodologies can be organized as [1]:

- **Multi-agent models** try to recreate the functioning of the market, generating agents and building the pricing process. Suitable for markets with little uncertainty.
- **Fundamental models** try to model the price of electricity based on physical and economical parameters. These models are adapted to medium-term predictions since they require data that is usually obtained at monthly intervals.
- **Reduced models** try to reproduce the properties of the electricity price using statistical parameters distributed over time. They are very useful for long-term predictions.
- **Statistical models** use statistical techniques to make forecasts, and are usually used in combination with models such as: ARIMA, ARFIMA, SARIMA, ARMA, ARMAX, ARIMAX, etc. These models are based on mathematical algorithms that use historical data and other explanatory parameters selected by the user.
- **Artificial intelligence models** use machine learning techniques to replicate complex dynamic systems that allow finding non-linear relationships between the input data. The use of this type of models for electricity price forecasting applications is relatively recent, but they should be highlighted due to their capacity to work with low quality data.

According to the time-scale of application, the different artificial intelligence models can be classified in:

- **Short-term models** are useful for day trading, i.e. to intervene in the daily market. On this time scale, various artificial neural network approaches have been proposed in literature. Singhal and Swarup [2] proposed a neural network approach to predict the electric market behaviors based on the historical prices, quantities

and other information to forecast the future prices and quantities. Panapakidis and Dagoumas [3] proposed to combine multiple neural networks, that allowed the user to realize an optimization search in order to select the model that best fits the input data, for one-day ahead forecasts.

- **Mid-term models** allows to make forecasts with a time horizon from a few days to one or two months. These models are useful for risk management evaluations and operations with products derived from electricity prices. Whei-Min, Lin et al.[4] proposed a neural network based model which allows the user to make EPF one week in advance.
- **Long-term** are useful to carry out analyses for investment planning, from a cost effectiveness standpoint perspective for months, quarters of year or years ahead. Villada et al. [5] proposed a neural network to make one-month ahead electricity price forecasts for the Colombian market.

In this work, a novel electricity price forecast model is presented, based on the combination of a neural network of the SOM type with a series of ESN whose parameters are optimized using a GA. The objective of this work is to analyze the feasibility of being able to predict time series from a model architecture inspired by multi-agent systems, where daily data are classified by a SOM. This implies that the model does not require a temporal correlation between the different days to work properly. Moreover, the clustering of data by the SOM allows training and inferring the set of ESNs, whose parameters have been optimized by a GA, in an optimal way.

The results show that this optimization methodology improves the forecasting behavior of the model reaching forecast errors of the same order of magnitude and even with absolute values lower than traditional time series forecasting methodologies. The document is structured as follows. Section 2.1 presents the data preprocessing stage and the SOM implementation. Section 2.2 introduces the set of echo state networks and presents price forecasting reference results. Section 2.2.1 introduces the genetic algorithm (GA) developed to improve the ESN internal parameters basis in order to improve the forecast accuracy. Section 3 presents a comparison between the price forecasting reference results and the improved ones. Finally, section 4 introduces the conclusions of this work.

## 2 Materials and Methods

Day-ahead electricity price forecast proposed in this work is based on Self-Organizing Map (SOM) and a set of  $n$  Echo State Network (ESN) units, as presented in **Fig.1**. The SOM stage is responsible for grouping similar days (24h) automatically to improve the training and inference phases of the Echo State Network (ESN) units. The ESN units for forecasting the price of electricity are based on the categories of days previously grouped by SOM. Finally, ESN models parameters (Leak Rate and Spectral Radius) are chosen by a Genetic Algorithm (GA) automatically in order to improve the forecasting accuracy.

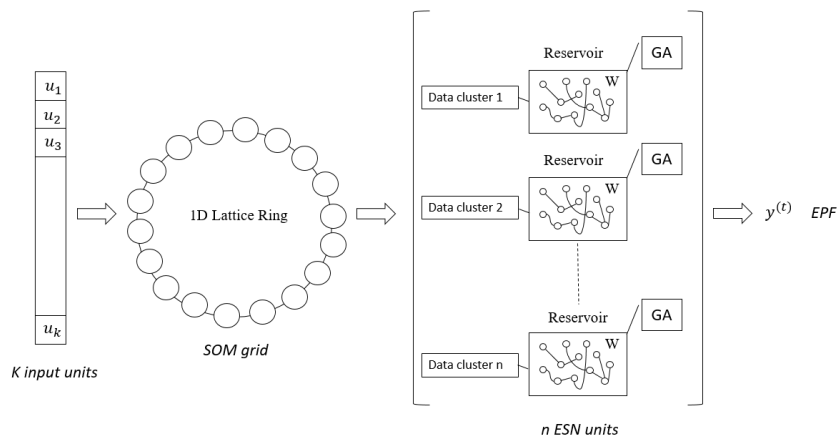


**Fig. 1.** Architecture of the electricity price forecast model (EPF).

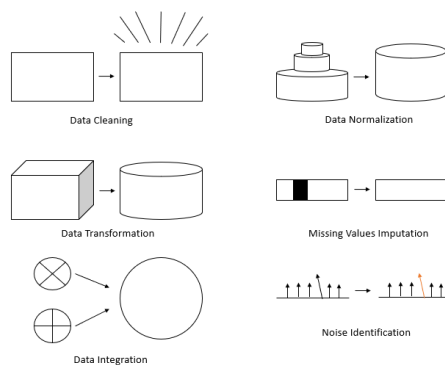


**Fig. 2.** Stages of the pre-processing phase.

## 2.1 Input data

Any price forecast model based on Machine Learning methods needs of a set of reliable historical data to work properly. Whereas, the data preprocessing is an important part of any machine learning application since having a good quality data is essential to obtain good results. This task is responsible for normalizing, standardizing and coding characteristics of the input model data in order to improve the learning process, such as: eliminating extreme or noisy values, filling data gaps, coding data, etc. The **Fig. 2** depicts the different stages of a pre-processing task.

Specifically, the input data of the novel machine learning model proposed in this work will be the historical data of the spot price of Iberian electricity and the generation mix, for the period 2019-2021. The data is available to download through the Iberian Transport System Operator, *Red Eléctrica de España* (REE), Information System (eSIOS) website. The time series of the downloaded data from spot prices (period of ten minutes) is integrated by hourly periods, normalized using the Min-Max method,

and stored in rows. Later, they are integrated into a global database and new variables are created. After the preprocessing phase is complete, the following variables are available:

- a. Actual hourly electricity price [€/MW]
- b. Festivity factor.
- c. Hourly data of the generation mix and demand: load demand, wind power generation, hydropower generation, nuclear power generation, solar generation.
- d. Chronological variables: date, day category, hour category.
- e. Continuous chronological variables: day\_of\_year\_sinus, day\_of\_year\_cosinus, hour\_of\_day\_sinus, hour\_of\_day\_cosinus.

### 2.2 Data clustering

After the pre-processing task is completed, the data is grouped according to the characteristics of the daily electricity price curve. A Self Organizing Map neural network is used for this purpose. SOM is a type of Artificial Neural Network (ANN) related to a feed-forward architecture composed by only two layers [6]. However, this type of ANN architecture is fundamentally different in arrangement and motivation to the feed-forward ANN. These ANNs apply a competitive and unsupervised learning method to train the network, based on a grid of artificial neurons whose weights are adapted to match the input vectors of a training set. Specifically, it approximates an unlimited number of inputs by a finite set of clusters/neurons arranged in a  $n$ -dimensional lattice (generally 1-D or 2-D), where neighboring nodes correspond to similar data (daily spot price shape). The SOM network input layer given a set of  $n$  input vectors  $\{x_i \in \mathbb{R}^k, i = 1, \dots, n\}$   $k$ -dimensional has  $k$  units. The output layer or the visible part of the SOM is the feature space, which consist of  $m$  nodes or neurons. The feature map space is defined beforehand, usually ranged in a  $n$ -dimensional region where nodes are arranged in a regular hexagonal or rectangular grid [7]. In this work, a computationally efficient one-dimensional cyclic topology is proposed, similar to **Fig. 3**.

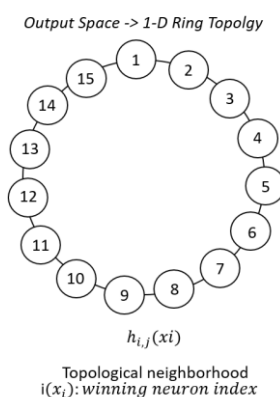


**Fig. 3.** 1D Lattice Ring Topology with 15 neurons.

SOM perform competitive training, in which the position of the neurons is kept fixed. Each neuron has an associated weight vector of the same size as the input vectors. Throughout training, these weight vectors are adjusted to be more similar to the input vectors, thus becoming winners [8].

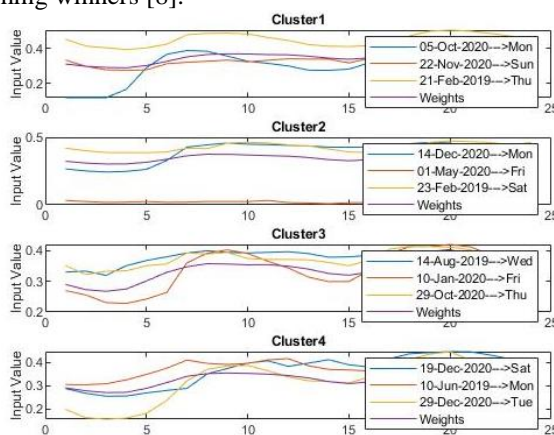


**Fig. 4.** Shape of the daily spot price curves for each data set according to Kendall's rank correlation.

- **SOM algorithm**

Let N be the number of input neurons and M the number of output neurons, the algorithm consists of:

1. Initialization of the weights  $w_{ij}$  with uniformly distributed random values.
2. Presentation of the input data as a vector  $E_k = (e_1, \dots, e_N)$  whose components are continuous values.

Determination of the winning neuron of the output layer. The winning neuron will be the one whose vector of weights,  $w_{ij}$ , is most similar to the input data  $E_k$ . To do this, the distances between the vectors  $E_k$  and  $W_i$  are calculated for each output neuron. Since the objective is to classify the data according the shape of the daily curve, in this work the Kendall rank correlation will be used as the SOM distance metric.

- Kendall rank correlation  $r_K$  is defined as [9]:

$$r_K = \frac{((\text{number of concordant pairs}) - \text{number of discordant pairs})}{\frac{1}{2} \cdot n(n-1)} \tag{1}$$

- Where  $\frac{1}{2} \cdot n(n-1)$  is the binomial coefficient related to the number of ways to choose two items from a set of  $n$  items. Any pair of observations  $(e_i, w_i)$  and  $(e_j, w_j)$  where  $i < j$ , are said to be concordant if the following two conditions are met,  $e_i > e_j$  and  $w_i > w_j$  or both  $e_i < e_j$  and  $w_i < w_j$ .
3. Once the winning neuron,  $j^*$ , is located, the weights of its input connections are updated, as well as those of the neighboring neurons (those belonging to its

neighborhood zone, Zone  $j(t)$ ). The goal is to associate the input information with a certain zone of the output layer.

$$w_{ij}(t + 1) = w_{ij}(t) + \beta(t) \cdot [e_i^{(k)} - w_{j^*i}(t)] \quad (2)$$

For  $j$  belonging to zone  $j$  at the instant  $t$ . The term  $\beta(t)$  is a gain parameter or learning coefficient, with a value between 0 and 1 that decreases with the number of iterations of the training process. The expression  $\beta(t) = 1/t$  can be used.

The best clustering results have been obtained using 4 neurons and taking into account the different generation variables, the price of electricity, the electricity demand and the chronological variables. The **Fig. 4** shows an example of clustering daily spot price data.

• **Echo State Networks.**

Once the SOM data pooling stage has been completed, four independent daily spot price databases are available, whose daily electricity price curves have similar shapes. Echo State Networks (ESN) are a kind of Recurrent Neural Networks (RNN) in which the training and processing of the recurring part of the network is done in a different way. The ESN over other RNN is the ability to manage cyclical RNN dependencies, where very small changes in network parameters can cause abrupt variations in output. This implies that traditional training methods such as gradient descent or backpropagation, which are very costly from a computational point of view, sometimes cannot provide an adequate result or achieve a local minimum [10], [11], [12]. ESNs are composed of an input layer and a hidden layer where synaptic weights are set randomly, where the only neurons that are trained are the connection weights between the reservoir and the output layer. In addition, the neurons in the hidden layer are sparsely connected and their weights are scaled according to a spectral radius. The generic formulation of the reservoir and network outlet (4) as well as the state update equation (3) are [10],[11], [12]:

$$x(n + 1) = f(W^{in} \cdot u(n + 1)) + Wx(n) + W^{back}y(n) + W^{bias} \quad (3)$$

$$y(n + 1) = f^{out}(W^{inout} \cdot u(n + 1)) + W^{out}x(n + 1) + W^{outout}y(n) + W^{biasout} \quad (4)$$

Where:

- $u(n)$  is the input at time  $n$ .
- $x(n)$  is the reservoir state at time  $n$ .
- $y(n)$  is the output at time  $n$ .
- $f(\ )$  is the activation function (in this work we use the tangent sigmoidal).

As stated, the weights connected to the output layer are trained ( $W^{inout}$ ,  $W^{out}$  and  $W^{biasout}$ ) using ridge regression [13]. This makes it possible to reduce the slope of the regression so that changes in the values of the weights have less effect. In this way, the weights are less fit to the input data and overfitting is avoided.

As mentioned above, the weight arrays attached to the reservoir are randomly initialized, then scaled using the spectral radius (to the absolute value of the largest eigenvalue) and multiplied by a choice factor. The value of this factor is related to the variable length of the memory and the degree of contractivity of the reservoir dynamics, larger values resulting in a greater length of the memory [14]. By incorporating a leak rate factor into the equation of state and adjusting its value, the velocity of reservoir dynamics in response to input can be optimized. The higher its value, the faster it will react to input [15]. Adding the leaky parameter to Eq. (3), is called leaky integrator neurons [16], and results in Eq. (5):

$$x(n + 1) = f \left( (1 - \alpha) \cdot x(n) + \alpha(Wx(n) + W^{in} \cdot u(n) + W^{bias}) \right) \quad (5)$$

Where  $\alpha$  is the leaky rate parameter. **Fig. 5** shows the general purpose architecture of ESN units (dotted arrows indicate connections that are possible but not required).

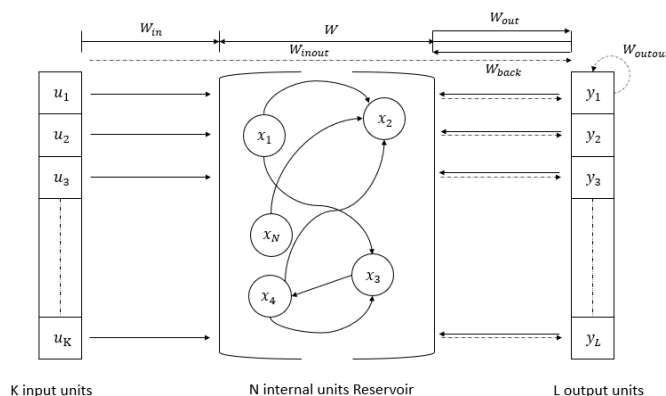


**Fig. 5.** The general purpose ESN architecture.

In this work, the ESN units consists of 14 data inputs, 1000 neurons in the inner layer and one output that represents the prediction of the spot electricity price.

The general methodology to follow when using ESNs can be summarized in the following steps:

1. Generate randomly a large reservoir.
2. Set values for the leaky parameter, the spectral radius scaling factor and initialize all weights except the output ones.
3. Run the network using the training data and store the reservoir activation states and the output weights.
4. Use the trained network with new data  $u(n)$  and perform the  $y(n)$  prediction, using the trained output weights.
5. Interpret the results in base of the prediction errors. The prediction error is generally defined as the difference between the measured value and the predicted value.

For example, let  $P$  be the price of electricity at a time "k", the prediction error is defined as [17]:

$$e(t + k|t) = P(t + k) - \hat{P}(t + k|t) \tag{6}$$

To evaluate the relative errors of the price forecasting, the following numerical indexes are calculated [13], [18], [19]:

- MSE (Mean Squared Error): the sum of the squared forecast errors:

$$MSE(k) = \frac{1}{N} \cdot \sum_{t=1}^N (e(t + k|t))^2 \tag{7}$$

- RMSE (Root Mean Square Error), or square root of the root mean square error:

$$RMSE(k) = \sqrt{MSE} = \sqrt{\frac{1}{N} \cdot \sum_{t=1}^N (e(t + k|t))^2} \tag{8}$$

Once the ESN units have been initialized and the input variables have been pooled, four independent ESNs (related to the data in each group) are trained. At this point, the proposed electricity price forecast model is ready to be tested and its accuracy verified. **Fig. 6** presents the electricity hourly-price forecast through the proposed architecture, for the period 9/12/2020 00:00:00 - 11/12/2020 00:00:00, i.e. for a 72-hour horizon. These results have been obtained by assigning a value of 1 to the leak rate and using a spectral radius scale factor of 1.25. In this way, a network is defined that complies with the Echo State Property of ESNs and that will quickly converge due to the high value of the leakage parameter.

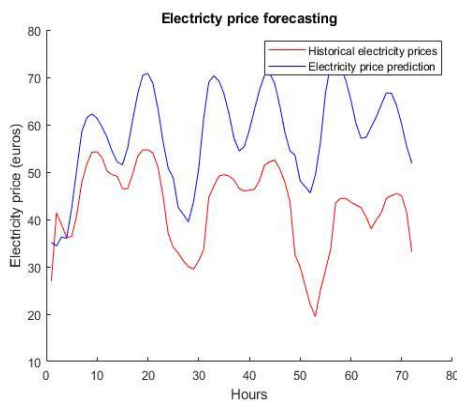


**Fig. 6.** Results of the electricity price forecast model (EPF) proposed for a horizon of 72 hours, period 12/9/2020 00:00:00 - 12/11/2020 00:00:00.

The blue curve in **Fig. 6** represents the expected value of the electricity price, while the red curve represents the real spot price curve. The proposed model forecasts the

price of electricity per hour with a good performance during this period reaching an RMSE of 0.28942.

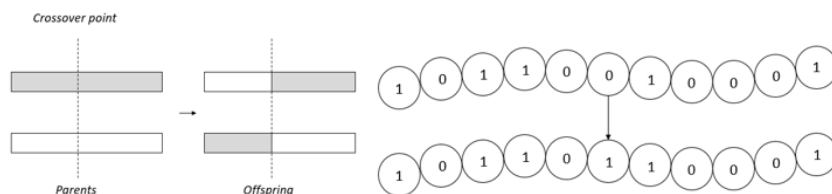


**Fig. 7.** One-point crossover (left) and bit mutation (right).

### 2.2.1 Evolutionary Optimization of Echo State Networks.

Generally, ESN structural parameters, such as reservoir size, weight initialization method, number and type of inputs, and internal connectivity, are set based on user experience. This can result in a suboptimal network configuration. In this work, a genetic algorithm will be used to optimize the scale value of the spectral radius and the leakage parameter.

- **Leak Rate.** The contribution of the leakage parameter to the reservoir can be verified in the equation (5). This parameter acts as a frequency factor, since it establishes the speed at which the firing capacity of neurons decreases with each iteration of the algorithm. The higher the value of the leakage parameter, the fewer the number of patterns the network will have to detect in the input data for the network to converge and set the output weights during training [20].
- **Spectral Radius.** In a conventional ESN, the spectral radius affects the short-term memory of the network, which increases with the size of the spectral radius.

## 2.3 Genetic Algorithm

Genetic algorithms (GA) are inspired by the mechanisms of biological natural selection, a process in which only the strongest, best adapted individuals survive. Similarly, only those parameters that provide the best solutions are kept in genetic algorithms. These parameters are encoded in the form of chromosomes, strings of binary numbers where each value represents a gene [21].

An initial population of chromosomes is randomly generated and, subsequently, following an evolutionary process, a new population is created from the previous one, iteration by iteration. A recombination between the "parents" takes place, giving rise to a litter of offspring. Parents and offspring are then ordered according to the fitness score obtained using a cost function, and the worst performers are discarded. This evolutionary cycle is repeated until a certain termination criterion is reached. To accelerate the evolutionary process, two operations are incorporated: crossing over (**Fig. 7, left**) and mutations (**Fig. 7, right**).

- **Generic Genetic Algorithm [22]**

1. Initialize a random population of individuals  $P(t)$ .
2. Evaluate fitness of all individuals from the population.
3. Test for termination criterion (iterations, fitness, etc.).
4. While the termination criterion is not reached:
  - Select a sub-population for offspring production.
  - Recombine the “genes” of selected parents.
  - Perturb a portion of the mated population by mutation.
  - Evaluate its new fitness.
  - Select the survivors from actual fitness.
5. Begin again.

In this work, each chromosome has been encoded with 16-bit, where the 8 most significant bits represent the leak rate and the 8 least significant bits represent the scale factor of the spectral radius. The search range of the algorithm was constrained to  $[0,1]$  for the leaking rate and to  $[0.1,2]$  for the spectral radius factor. The optimization process was started with a population size of 100 chromosomes and converged after around 60 iterations. In each iteration 100 evolutionary cycles are carried out.

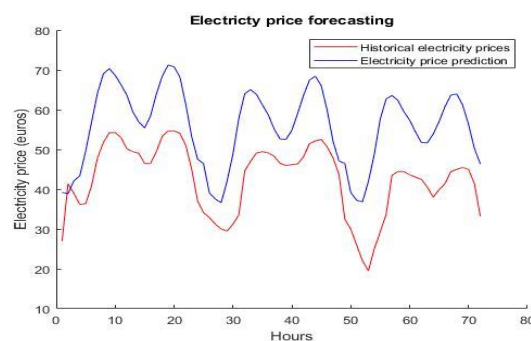


**Fig. 8.** ESN unit price forecast results optimized by GA, period 9/12/2020 00:00:00 - 11/12/2020 00:00:00.

- **GA Validation**

**Fig.6** presents an example of an electricity price forecast, using a set leak rate and spectral radius. Meanwhile, **Fig. 8** presents the prediction results for the same period, but with the values of the leak rate and the spectral radius optimized by the GA. In the optimized case, the prediction error was reduced to an RMSE of 0.23716. This means that optimizing the values of these parameters using a genetic algorithm has reduced the error by 15%.

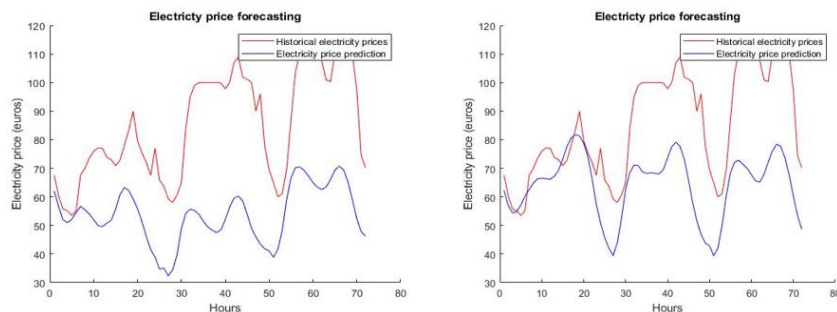


**Fig. 9.** Electricity price forecasting (EPF) model results, period 6/01/2020 – 8/01/2020. **Left:** without GA optimization. **Right:** with GA optimization.

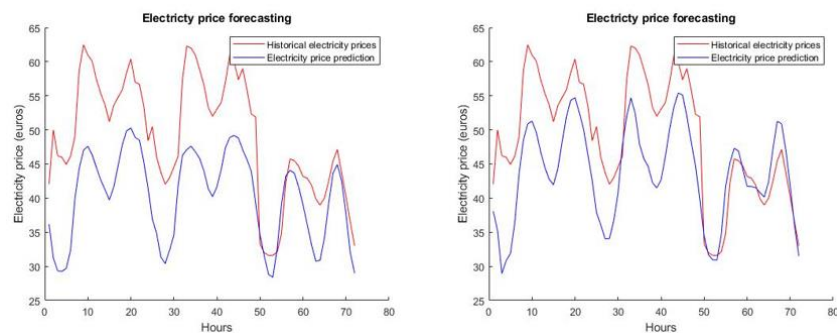


**Fig. 10.** Electricity price forecasting (EPF) model results, period 28/03/2019 – 30/03/2019. **Left:** no GA optimization. **Right:** with GA optimization.

### 3 Results

In order to evaluate the improvements provided by the GA-based optimization methodology, we will make a comparison of the results obtained with the Electricity price forecasting (EPF) model proposed with and without the GA optimization.

To make this comparison we will choose a period in which electricity prices undergo drastic changes to show how difficult it is to predict the price of electricity due to its great variability, presenting a non-constant mean and variance, and a significant number of outliers. Specifically, the chosen period is the second week of January 2020. The prediction will start on January 6, Three Kings Day, a Spanish national holiday in which the price was relatively low compared to the general trend for the month. The results of the electricity price forecast model (EPF) for a horizon of 72 h, period 06/01/2020 - 8/01/2020, with the GA optimization deactivated are not good (**Fig. 9, left**), while the optimized results are quite better but not optimal (**Fig. 9, right**). Although in both cases the model is capable of reproducing to a greater or lesser extent the shape of the price.

It is worth noting that the precision of the introduced price forecasting approach can be higher if a period during which the electricity price is more stable is selected. To verify this statement, we have chosen a weekday in the last week of March 2019. The

results of the electricity price forecast model (EPF) for a horizon of 72 h, period 28/03/2019 - 30/03/2019, with the GA optimization deactivated are quite good (**Fig. 10, left**), while the optimized results are optimal (**Fig. 10, right**). Finally, the errors (RMSE and MAE) associated with the forecasts are presented in **Table 1**.

**Table 1.** forecasting errors.

Figure	RMSE	MAE
Fig 9, left	0.5681	0.5139
Fig 9, right	0.4203	0.3423
Fig 10, left	0.1673	0.1455
Fig 10, right	0.1293	0.0890

**Table 2** shows the MAPE corresponding to a 24-hour forecast of the price of electricity for the Spanish electricity market, obtained with the proposed model and by other research works.

**Table 2.** forecasting errors.

Model	Forecasting horizon	MAPE (%)
This work	24 h	7.85
M18 Ref. [23]	24 h	10.69
EMPF Ref. [24]	24 h	13.36

In order to correctly compare these models, the same input data should be used. However, it can be observed that the 24-hour horizon forecast errors obtained by the proposed model and the other models have the same order of magnitude, even those obtained by our methodology being slightly better.

## 4 Conclusions

In this work, a new model for forecasting the price of electricity per hour for a 72-hour horizon based on a Self-Organizing Map (SOM) and a set of Echo State Network (ESN) models has been presented and evaluated. The SOM is in charge to cluster the input data automatically according to their similarity to train/infer the ESNs. The ESN models for regression are built on the categories clustered by SOM separately. While the ESN models parameters (Leak Rate and Spectral Radius) are chosen by Genetic Algorithm (GA) automatically in order to improve the forecasting accuracy. The results obtained show how GA improves the precision of the proposed model by up to 15%. It should be noted that the proposed model achieves lower MAPE results compared to the best forecasting works for hourly spot price of Iberian electricity.

## 5 Acknowledge

This work has been funded in part by a research grant from *Cátedra Endesa-Red de Innovación Energética of the University of the Balearic Islands* and by the Spanish

Ministry of Economy and competitiveness and the EU with Regional European Development Funds under Grants *PID2020-120075RB-I00* and *PDC2021-121847-I00*.

## References

- [1] S. K. Aggarwal, L. M. Saini, and A. Kumar, "Electricity price forecasting in deregulated markets: A review and evaluation," *Int. J. Electr. Power Energy Syst.*, vol. 31, no. 1, pp. 13–22, Jan. 2009, doi: 10.1016/j.ijepes.2008.09.003.
- [2] D. Singhal and K. S. Swarup, "Electricity price forecasting using artificial neural networks," *Int. J. Electr. Power Energy Syst.*, vol. 33, no. 3, pp. 550–555, Mar. 2011, doi: 10.1016/j.ijepes.2010.12.009.
- [3] I. P. Panapakidis and A. S. Dagoumas, "Day-ahead electricity price forecasting via the application of artificial neural network based models," *Appl. Energy*, vol. 172, pp. 132–151, Jun. 2016, doi: 10.1016/j.apenergy.2016.03.089.
- [4] W.-M. Lin, H.-J. Gow, and M.-T. Tsai, "Electricity price forecasting using Enhanced Probability Neural Network," *Energy Convers. Manag.*, vol. 51, no. 12, pp. 2707–2714, Dec. 2010, doi: 10.1016/j.enconman.2010.06.006.
- [5] F. Villada, E. García, and J. D. Molina, "Pronóstico del Precio de la Energía Eléctrica usando Redes Neuro-Difusas," *Inf. tecnológica*, vol. 22, no. 6, pp. 111–120, 2011, doi: 10.4067/S0718-07642011000600012.
- [6] T. Kohonen, "Self-organized formation of topologically correct feature maps," *Biol. Cybern.*, vol. 43, no. 1, pp. 59–69, 1982, doi: 10.1007/BF00337288.
- [7] S. Ray, "A Quick Review of Machine Learning Algorithms," in *2019 International Conference on Machine Learning, Big Data, Cloud and Parallel Computing (COMITCon)*, Feb. 2019, pp. 35–39, doi: 10.1109/COMITCon.2019.8862451.
- [8] A. Moran, J. L. Rossello, M. Roca, and V. Canals, "SoC Kohonen Maps Based on Stochastic Computing," in *2020 International Joint Conference on Neural Networks (IJCNN)*, Jul. 2020, pp. 1–7, doi: 10.1109/IJCNN48605.2020.9207476.
- [9] D. Gao, Y. Zhou, T. Wang, and Y. Wang, "A Method for Predicting the Remaining Useful Life of Lithium-Ion Batteries Based on Particle Filter Using Kendall Rank Correlation Coefficient," *Energies*, vol. 13, no. 16, p. 4183, Aug. 2020, doi: 10.3390/en13164183.
- [10] H. Soh and Y. Demiris, "Spatio-Temporal Learning With the Online Finite and Infinite Echo-State Gaussian Processes," *IEEE Trans. Neural Networks Learn. Syst.*, vol. 26, no. 3, pp. 522–536, Mar. 2015, doi: 10.1109/TNNLS.2014.2316291.
- [11] S. Scardapane, D. Wang, and M. Panella, "A decentralized training algorithm for Echo State Networks in distributed big data applications," *Neural Networks*, vol. 78, pp. 65–74, Jun. 2016, doi: 10.1016/j.neunet.2015.07.006.
- [12] C. Venugopal, S. P. Devi, and K. S. Rao, "Predicting ERP User Satisfaction—an Adaptive Neuro Fuzzy Inference System (ANFIS) Approach," *Intell. Inf. Manag.*, vol. 02, no. 07, pp. 422–430, 2010, doi: 10.4236/iim.2010.27052.
- [13] A. A. Ferreira, T. B. Ludermir, and R. R. B. de Aquino, "An approach to reservoir computing design and training," *Expert Syst. Appl.*, vol. 40, no. 10, pp. 4172–4182, Aug. 2013, doi: 10.1016/j.eswa.2013.01.029.

- [14] C. Gallicchio and A. Micheli, “Architectural and Markovian factors of echo state networks,” *Neural Networks*, vol. 24, no. 5, pp. 440–456, Jun. 2011, doi: 10.1016/j.neunet.2011.02.002.
- [15] H. Jaeger, M. Lukoševičius, D. Popovici, and U. Siewert, “Optimization and applications of echo state networks with leaky- integrator neurons,” *Neural Networks*, vol. 20, no. 3, pp. 335–352, Apr. 2007, doi: 10.1016/j.neunet.2007.04.016.
- [16] M. Lukoševičius and H. Jaeger, “Reservoir computing approaches to recurrent neural network training,” *Comput. Sci. Rev.*, vol. 3, no. 3, pp. 127–149, Aug. 2009, doi: 10.1016/j.cosrev.2009.03.005.
- [17] H. Madsen, P. Pinson, G. Kariniotakis, H. A. Nielsen, and T. S. Nielsen, “Standardizing the Performance Evaluation of Short-Term Wind Power Prediction Models,” *Wind Eng.*, vol. 29, no. 6, pp. 475–489, Dec. 2005, doi: 10.1260/030952405776234599.
- [18] M. P. Clements and D. F. Hendry, “On the limitations of comparing mean square forecast errors,” *J. Forecast.*, vol. 12, no. 8, pp. 617–637, Dec. 1993, doi: 10.1002/for.3980120802.
- [19] P. S. A. Freitas and A. J. L. Rodrigues, “Model combination in neural-based forecasting,” *Eur. J. Oper. Res.*, vol. 173, no. 3, pp. 801–814, Sep. 2006, doi: 10.1016/j.ejor.2005.06.057.
- [20] A. J. Wootton, S. L. Taylor, C. R. Day, and P. W. Haycock, “Optimizing Echo State Networks for Static Pattern Recognition,” *Cognit. Comput.*, vol. 9, no. 3, pp. 391–399, Jun. 2017, doi: 10.1007/s12559-017-9468-2.
- [21] J. WANG, “A new method for estimating effective population sizes from a single sample of multilocus genotypes,” *Mol. Ecol.*, vol. 18, no. 10, pp. 2148–2164, May 2009, doi: 10.1111/j.1365-294X.2009.04175.x.
- [22] L. Min and W. Cheng, “A genetic algorithm for minimizing the makespan in the case of scheduling identical parallel machines,” *Artif. Intell. Eng.*, vol. 13, no. 4, pp. 399–403, Oct. 1999, doi: 10.1016/S0954-1810(99)00021-7.
- [23] C. Monteiro, I. Ramirez-Rosado, L. Fernandez-Jimenez, and P. Conde, “Short-Term Price Forecasting Models Based on Artificial Neural Networks for Intraday Sessions in the Iberian Electricity Market,” *Energies*, vol. 9, no. 9, p. 721, Sep. 2016, doi: 10.3390/en9090721.
- [24] C. Monteiro, L. Fernandez-Jimenez, and I. Ramirez-Rosado, “Explanatory Information Analysis for Day-Ahead Price Forecasting in the Iberian Electricity Market,” *Energies*, vol. 8, no. 9, pp. 10464–10486, Sep. 2015, doi: 10.3390/en80910464.

## Study for the improvement of a mini-hydraulic installation in a smart microgrid

Alejandro Carballo Ruiz<sup>1</sup>, Siro Soria Franco<sup>1</sup>, Gonzalo Martin Jimenez<sup>1</sup>, Paula Peña Carro<sup>1</sup>, Oscar Izquierdo Monge<sup>1</sup>

<sup>1</sup> CEDER-CIEMAT, Autovía de Navarra A15 salida 56, 422290 Lubia (Soria), Spain, A.C.R.: alejandroc775n@gmail.com; S.S.F.: siro.soria@ciemat.es; G.M.J.: gonzalomj96@gmail.com; P.P.C.: paula.pena@ciemat.es; O.I.M.: oscar.izquierdo@ciemat.es;

**Abstract:** This paper presents a study to improve a hydraulic installation (Turbine and pump system) integrated in CEDER smart microgrid. Different options have been studied trying to find the best solution such as the replacement of the Pelton turbine and pumps by a reversible Francis turbine, the installation of intermediate pumps, modifications on water conductions to reduce losses of the installation, etc. Once the different options have been studied and the degree to which they improve the system has been determined, the next step will be the implementation of these measures, which will be developed later.

**Keywords:** Smart microgrid, Turbine, Pumping system, reversible hydraulic installation.

### 1 Introduction

Energy has become a key factor in the development of our lives, leading us to an increment in the global necessities of energy, presenting a challenge for the electric traditional system [1].

A microgrid is a group of different energies that are placed at the same level as the electric distribution system. The main part of control of a microgrid is the one that manages all the energies along with the microgrid. Its principal objective is to achieve an ideal behavior by producing some values for local control agents of each of the energies, so we can achieve the balance of power in the microgrid [2].

Little by little, more renewable sources of energy have been introduced in the electric systems, such as wind generators and photovoltaic panels. Due to its intermittent nature, because of its location in places where there is a lack of electric infrastructure and because of is a type of energy which is no concentrated, they need the use of storage technologies [3].

In figure 1, there is an image of an electric smart microgrid, distinguishing all the components that are part of it.



Fig. 1. CEDER Smart microgrid.

An important part of microgrids are the storage systems. These can counteract the energy imbalances [4] managing to fit the generation and the total load of the microgrid curve [5], which is affected by the uncontrollable generation associated to these systems [6-9].

The installation of a storage system is essential in a microgrid to achieve the balance between the demand and the production. The storage systems are important, like the systems that allow the generation control of demand to be as better as possible. The most useful storage systems in the past were the batteries, and above all, the hydraulic power plants [3].

In the long term, the hydraulic storage is the storage system that has the better properties. Between all the types of renewable energies, the hydroelectric plants have an important advantage, they are plants that have a long last life:

There are some examples of hydroelectric plants that have lasted over one hundred years. In addition to this, the hydroelectric plants use clean energy and have little emissions. There are two types of hydraulic pumping systems: river or no river, with the installation of water tanks at different heights. For example, in no river installations, you work with artificial water reservoirs at different heights with the purpose of leading water in a close circuit. Thanks to this water reservoirs and to the turbine and the pumping system, we can both storage and produce energy.

Hydraulic energy is a type of energy that has some advantages over conventional energies and over other renewable energies [10, 11]. Hydraulic installations are an economic way of storage energy by the form of retaining water in a higher water reservoir [12].

There is a problem because the hydroelectric generation is usually away from the consume centres, what fore us to have transport lines and this produces energy losses and an important impact in the environment.

The main aim of the study in this article is to improve the efficiency of an electric smart microgrid, trying to find the cheapest and the most efficient way.

The article is divided in some different sections. Section 2 shows the microgrid and the hydraulic installation, section 3 present an explanation of the different improvements of the installation, section 4 present the selection of the best improvement, and section 5 show future plans.

## 2 Material and methods

This CEDER’s microgrid is supplied by 45 kV from the distribution network and it transforms this amount of tension into 15 kV at the start. It is composed of different sources of generation (wind turbines of low power and photovoltaic panels). Storage systems (hydraulic installations and batteries) and loads that are the buildings connected to the microgrid.

The microgrid has a control system which manages and monitors all the components that are connected to it and also it allows managing the components in an efficient way.

What really matters to us about this microgrid is the hydraulic installation, and now we are going to explain it:

In this installation, we have 3 water tanks where the water is in rest and in contact with the atmosphere. These water tanks are built at different heights, so there is a high jump between them. We are going to take advantage of this jump so we can transform the potential energy into electric energy.

The water tanks are connected each other thanks to a group of pipes which have some load losses.

In figure 2, we can see the magnitude of the jump between the water tanks.

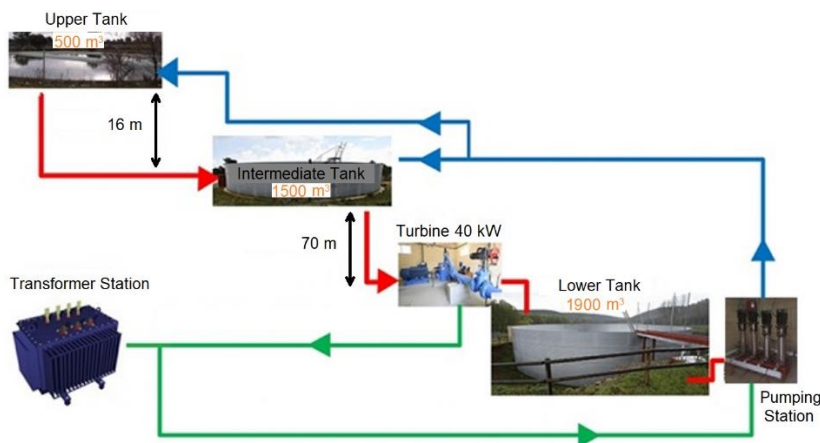


Fig. 2. Drawing of the hydraulic installation.

There is installed a Pelton turbine with 60 kW of nominal power whose objective is to take advantage of the jump between the water tanks. We are also going to have a

group of four parallel pumps, which are built in a vertical position. The main aim of this pumps is to pump water from the lowest water tank to the highest water tank.

The main aim of this hydraulic installation is to turbine when there is shortage of energy and to pump when there is excess. However, due to the high load losses in the pipes and to the low efficiency of the actual pumps (about 30% of efficiency), the efficiency of this installation is really low.

In this article, what we are trying to find out which is the best way for improving our installation. It is also important to choose the way that consumes the less and produces the cleanest energy so we can reduce the amount of excess energy that we are losing.

In the hydraulic installation, we have:

- Three water tanks
- A Pelton turbine
- Four pumps with a power of 7,5 kW each one
- 693 meters of a drainpipe with a diameter of 250 mm
- 725 meters of a riser pipe with a diameter of 100 mm

It is really important to comment that most of all the components of the hydraulic installation have been used previously, so these components used to be in another places and with other functions, and now are installed in our hydraulic installation.

With the purpose of doing some operations, we have calculated how much the friction coefficient is for the pipe losses. This friction coefficient depends on the diameter of the pipe and its relative roughness.

We can obtain the coefficient by using Moody's diagram.

- $f_{descent}=0.016$
- $f_{ascent}=0.0148$

In figure 3, there is an image of the Pelton turbine along with its characteristics.



**Fig. 3.** Pelton turbine and its nominal characteristics of the turbine.

In table 1, we have the results from the turbine at different powers.

Table 1, Results from the turbine. Source: CEDER documents

Power generated (kW)	Pumping water (mm/hour)	Pumping water (liters/hour)	mm/kW
5	160	88357	32.0
10	220	117810	22.0
15	300	147262	20.0
20	370	181623	18.5
25	450	211076	18.0
30	540	265072	18.0
35	700	311705	20.0
40	900	441786	22.5

Thanks to a previous study of the turbine, we know that, although the nominal power of the turbine is 60 kW, only 40 kW are entering into the turbine, due to different power losses throughout all the drainpipes. This is produced thanks to the wrong installation of the pipe and thanks to other important factors that affect the efficiency of the hydraulic system.

Like we did with the turbine, we also did a previous study of the pumping system of the company.

In figure 4, there are some images of the pumps and its nominal characteristics.



Fig. 4. Pumps of 7.5 kW of power each one and its nominal characteristics.

Thanks to these studies, the efficiency of the hydraulic installation can be calculated by the ratio between the liters of pumping water in an hour and the liters of turbine water in an hour.

In table 2, we have the results of the pumps in relation with power.

Table 2, Pump results. Source: CEDER documents

Number of pumps	Power consumed (kW)	Pumping water (mm/hour)	Pumping water (liters/hour)	mm/kW
1	7.5	44.08	21640	5.87
2	15	88.2	43308	5.88
3	22.5	135.6	64876	5.87
4	30	179.64	86520	5.86

Now, we are going to calculate the efficiency of the installation.

$$\eta = \frac{E_{generated}}{E_{consumed}} = \frac{43308}{147262} = 0.294$$

### 3 Results

The objective of this section is to analyze different improvements in the installation.

#### 3.1- Reversible Francis turbine

Here, the idea is to substitute our Pelton turbine into a reversible hydraulic turbine. First of all, we must calculate the specific velocity in our installation. And after that, we will change some properties, so we can have the specific velocity that we need to install the new turbine.

Each turbine has a design constant value. This constant value is known as the specific velocity:

$$Ns = N \times (Pt)^{0.5} \times (Hd)^{-1.25} \tag{1}$$

Ns is the specific velocity. N is the rotation velocity, which is measured in rpm. Pt is the turbine power measured in kW. And finally, Hd which is the load design of the turbine, in meters.

In our case, these variables are equal to:

- $N = 750$  rpm. This value is determined from the generator characteristics.
- $Pt = 60$  kW
- $Hd = 70$  meters

With these values, we obtain a specific velocity of 28. For this velocity, a Pelton turbine is well-built.

If we had wanted to install a Kaplan turbine, we would have had a specific velocity of 300. In case of a Francis turbine, we must have a specific velocity value between 350 and 50.

For a Francis turbine, we have different range of values depending on the type of Francis turbine you want to install. There are three types of Francis turbine: slow, normal and fast.

The principal idea was to install a reversible Kaplan turbine. However, is almost impossible reaching so higher values of specific velocity with our characteristics.

Thanks to this, we are going to try to install a more adaptable turbine for our characteristics.

The reversible turbine we are going to install is a slow Francis turbine, with a specific velocity of 120. To choose the type of Francis turbine, we have a range of specific velocity values from 50 to 350 [13].

In table 3, we have the different types of turbines according to its specific velocity values.

Table 3. Specific velocity for each type of turbine. Source: Nava Mastache, Arturo. Selection and sizing of hydraulic turbines for hydroelectric power plants.

<i>Pelton Turbine</i>	$Ns \leq 100$
<i>Francis Turbine</i>	$50 \leq Ns \leq 350$
<i>Kaplan Turbine</i>	$Ns \geq 300$

In table 4, we have in a more specific way the specific velocity values for each type of Francis turbine.

Table 4. Specific velocity for each type of Francis turbine. Source: Nava Mastache, Arturo. Selection and sizing of hydraulic turbines for hydroelectric power plants.

<i>Slow Francis Turbine</i>	$50 \leq Ns \leq 150$
<i>Normal Francis Turbine</i>	$150 \leq Ns \leq 250$
<i>Fast Francis Turbine</i>	$250 \leq Ns \leq 350$

Francis turbines have many applications in a large range of specific velocities. This range of applicability and its structural easiness in designs, allows Francis turbines to have more advantages than other hydraulic turbines [14].

The idea is to install a slow Francis turbine with a specific velocity of 120. To reach this velocity, we must use a generator of 3000 rpm of nominal speed.

$$Ns = N \times (Pt)^{0.5} \times (Hd)^{-1.25} \tag{2}$$

$$120 = 3000 \times Pt^{0.5} \times 70^{-1.25} \tag{3}$$

$$\frac{120}{14,82} = Pt^{0.5} \tag{4}$$

$$Pt = 65.65 \text{ kW} \tag{5}$$

Once we have calculated the turbine power (Pt), we are going to calculate the real power of the turbine for its nominal properties. Before this, we have to suppose that the efficiency of the turbine is the same as in the Pelton turbine.

$$Ph = \frac{Pt}{0.7289} = \frac{65.56}{0.7289} = 89.95 \text{ kW} \tag{6}$$

Finally, we are going to calculate the nominal flow for the new turbine.

$$PH = \rho \times g \times Q \times H \tag{7}$$

$$P 89.95 = 1 \times 9.8 \times 70 \times Q \tag{8}$$

As we can see, we have obtained a similar flow in both turbines. The main advantages of this idea are:

- Now, we can pump and turbine in the same pipe. This produces an improvement in the efficiency of the installation.
- We can pump in both pipes, so we are going to consume less energy. This produces a reduction in the amount of excess energy that we are going to lose in the net.

The disadvantages are:

- The high initial inversion to install the new turbine.
- In case of using both turbines, there will be an increment in the costs, because of the installation of another pipe for the new turbine.

### 3.2- Intermediate Pumps

Installation of a group of pumps in the middle pump of the ascent pipe. This group of pumps could it be reused by CEDER or can be bought.

The main aim of this idea is to relaunch the fluid from the middle point to the higher water tank, so the fluid will arrive with more energy. It is also important to improve the efficiency of the pumps because, as it is explained before, the efficiency of our pumps is really low.

If we want to calculate the efficiency, we must do:

$$H3 - H1 = HBeq1 + HBeq2 - hp \tag{9}$$

$$HBeq1 = HB1 = HB2 \tag{10}$$

$$HBeq2 = HB3 = HB4 \tag{11}$$

$$Qeq1 = Q1 + Q2 \tag{12}$$

$$Qeq2 = Q3 + Q4 \tag{11}$$

$$D1 = D2 \tag{14}$$

$$hp = f \times \frac{L1 \times 8 \times Qeq1^2}{D1 \times g \times \pi^2 \times D1^4} + k1 \times \frac{8 \times Qeq1^2}{g \times \pi^2 \times D1^4} + f \times \frac{L2 \times 8 \times Qeq2^2}{D2 \times g \times \pi^2 \times D2^4} + k2 \times \frac{8 \times Qeq2^2}{g \times \pi^2 \times D2^4} \tag{15}$$

L1=363 meters. Length between lower water tank and the middle point, where the new pumps are located.

L2=362 meters. Length between the higher water tank and the middle point.

These lengths have been obtained by the study of some Topographic designs. In these designs, we can see the distance between the water tanks and its inclination.

$$Q_{4pumps} = 0.026 \text{ m}^3/\text{s}$$

$$Q_{2pumps} = 0.013 \text{ m}^3/\text{s}$$

These pump flows have been obtained thanks to knowing the characteristics of the pumps and thanks to the height of the equivalent pump.

We are arranging two pumps in series, so the flow is constant, and it is the height of the pumps what is multiplied by two.

$$hp1 = 1.07 \times \frac{0.016 \times 363 \times 8 \times 0.013^2}{9.8 \times 0.1^5 \times \pi^2} = 8.68 \text{ m} \tag{16}$$

$$hp2 = 1.07 \times \frac{0.016 \times 362 \times 8 \times 0.013^2}{9.8 \times 0.1^5 \times \pi^2} = 8.68 \text{ m} \tag{17}$$

$$70 = 2 \times HBeq - 2 \times 8.68 \tag{18}$$

$$HBeq = 43.68 \text{ m} \tag{19}$$

Now, we are going to study the case in which any of our four pumps is moved. In this case, we are going to install two new pumps with similar characteristics to the old ones.

$$hp1 = \frac{1.07 \times 0.016 \times 363 \times 8 \times 0.026^2}{9.8 \times 0.1^5 \times \pi^2} = 34.64 \tag{20}$$

$$hp2 = \frac{1.07 \times 0.016 \times 362 \times 8 \times 0.026^2}{9.8 \times 0.1^5 \times \pi^2} = 34.64 \tag{21}$$

$$70 = 2 \times HBeq - 2 \times 34.64 \tag{22}$$

$$HBeq = 69.64 \text{ m} \tag{23}$$

Efficiency:

$$W_{pump} = \rho \times g \times Q \times HB \quad (24)$$

$$W_{acc} = 30kW \quad (25)$$

$$pump\ efficiency = \frac{W_{pump}}{W_{acc}} \quad (26)$$

- With four pumps only:

$$W_{pump} = 9.8 \times 1 \times 0.013 \times 2 \times 43.68 = 11.13\ kW \quad (27)$$

$$\eta = \frac{11,13}{30} = 37.1\% \quad (28)$$

- With six pumps (adding two new pumps to the system):

$$W_{pump} = 1 \times 9.8 \times 0.026 \times 69.64 \times 2 = 35.49\ kW \quad (29)$$

$$\eta = \frac{35,49}{45} = 78.87\% \quad (30)$$

### 3.3- Losses:

Although this part is not a way of improvement, we are going to analyze it as it was. The aim of this section is to solve the problem of the load losses and to find out a way to reduce these losses. Almost all of the losses come from the evaporation and the pipes.

#### 3.3.1- Evaporation losses:

This type depends on the relative humidity of the place where the water tanks are located, the air temperature, the wind speed and solar radiation [15][16].

As we can see, most of these factors are uncontrollable because of its nature.

Since a long time ago, Scientifics from all over the world have tried to develop different methods for reducing the evaporation. The idea is to lose the less amount of water at the cheapest way [8].

The equation we are going to use to calculate the losses is:

$$E = P \pm \Delta D \quad (31)$$

- $E$ = evaporation losses
- $P$ = the precipitation height between two measurements
- $\Delta D$ = the water that is added (+) or removed (-) from the water tank

Figures 5 and 6 show evaporation effects in water tanks in two seasons of the year.

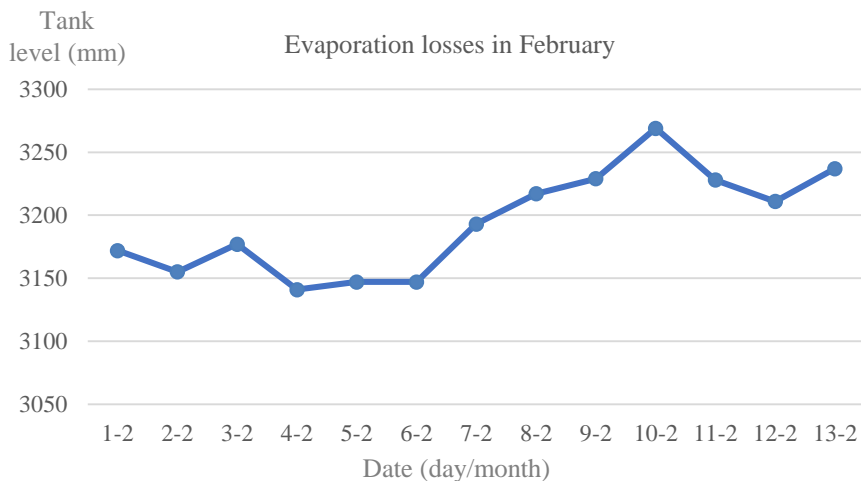


**Fig. 5.** Losses in the tank in February

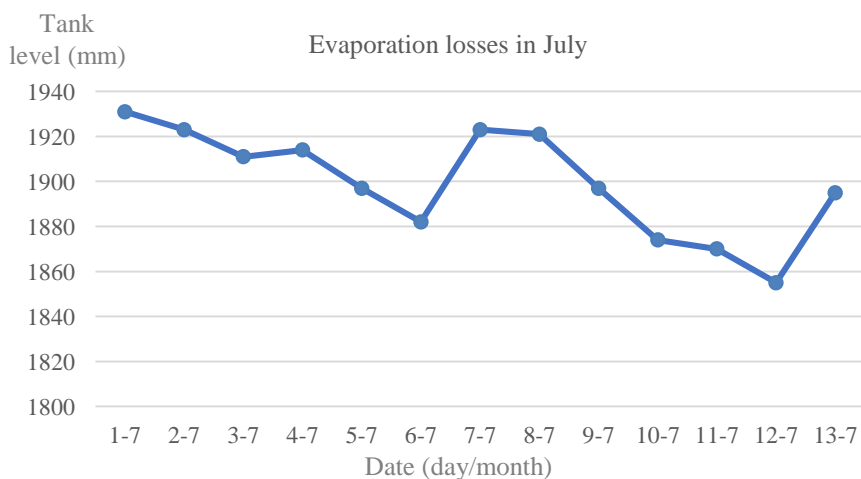


**Fig. 6.** Losses in the tank in July

In figure 6 we can see the losses produced in the water tank in a day. If we want to see only the evaporation losses, we must analyze a day without pumping and turbine.

The measurement of this process has made by an ultrasound sensor from CEDER-CIEMAT.

**Different ways of solving the evaporation losses**

Now we are going to mention some ways of reducing the evaporation losses [8]:

- 1- Oily alcohols: When this compound touches the water, it forms like monomolecular layer over the surface. This layer creates a type of barrier which difficult the evaporation.
- 2- Floating modulate systems: This method consists in putting a type of barrier over the water surface.
- 3- Shade balls: This method consists in filling the water tank with dark balls, so these balls can absorb all the solar radiation. However, this method can produce a problem of blockage at the entrance of the turbine.
- 4- Anti-evaporation panels: These are a floating system with geometric forms that are trying to avoid the incidence of the sun into the water and to avoid the wind effect.
- 5- Canvas: The canvas is going to cover up the water surface. Canvas are too big, due to this, we have to use structures for supporting its weight.
- 6- Floating photovoltaic panels: With this method we can avoid the evaporation and also, we can storage solar energy in it.



**Fig. 7.** Floating photovoltaic panels.

### 3.3.2- Pipe losses:

The load loss that takes place in a conduction, is the dynamic energy loss. This dynamic loss is due to the friction between the fluid particles and the walls of the pipe.

First of all, we must calculate the linear losses, the ones that depends on the friction coefficient:

We have two pipes; one is made of PVC and the other of fiber cement. These pipes are going to produce some losses in the pipes that depend on the pipes' material.

The pipes' diameter is:

- 250 mm for the PVC pipe
- 100 mm for the fiber cement pipe

Now we must calculate the friction coefficients of our pipes:

- Initial details
  - $D_{PVC}$ : 250 mm
  - $\epsilon_{PVC}$ : 0.0015 mm
  - $D_{fiber\ cement}$ : 100 mm
  - $\epsilon_{fiber\ cement}$ : 0,025 mm

By using Moody's diagram, we are going to calculate our friction coefficient:

We are supposing we are working with a normal temperature of 20 °C. This leads us to a water viscosity of 1.004 mm<sup>2</sup>/s. We are also going to suppose that we are working with nominal conditions of flow, about 0.12 m<sup>3</sup>/s.

$$\frac{\epsilon}{D} = \frac{0,025}{100} = 2.5 \times 10^{-4} \quad (32)$$

$$Re = \frac{v \times D}{\nu} \quad (33)$$

$$Re_{fiber\ cement} = 1522094$$

Therefore, we are having a turbulent system in this pipe with an average speed of 15.28 m/s.

Knowing the Reynolds number and the relative roughness, we get that  $f=0.016$  for the fiber cement pipe.

$$\frac{\epsilon}{D} = \frac{0,0015}{250} = 6 \times 10^{-5} \quad (34)$$

$$Re = \frac{v \times D}{\nu} \quad (35)$$

$$Re_{PVC} = 608838$$

We also have a turbulent system in the PVC pipe with an average speed of 2,44 m/s.

Knowing the Reynolds number and the relative roughness, we get that  $f=0,0148$  for the PVC pipe.

Singular losses:

Due to the impossibility of knowing with accuracy the elbows and the direction changes of our pipes, we have supposed that the singular losses in our case are about 7% of our total linear losses. That is because we know that the singular losses of an installation are in a range between the 5 and the 10% of the total linear losses.

## 4 Conclusions

The objective of the paper is to study different options to improve the efficiency of a hydraulic installation in a smart electric microgrid. To choose the best option to improve the installation, some factors must be taken into account as costs and efficiency.

The best solution, from a cost point of view, is the improvement of water pipelines to reduce turbine head losses and pumping friction losses.

Another good option from this point of view is the installation of new pumps, in the middle of the conduction to improve pumping system efficiency.

The best option from an efficiency point of view is the replacement of the existing Pelton turbine with a reversible Francis turbine of similar power, although it is the most expensive and the most difficult to implement of the solutions.

## 5 Future plans

1. Installation of different methods with the aim of reducing the evaporation losses and study of its costs and its efficiency.
2. Study of the ability of the current conductions to put up with the installation new changes.
3. Setting up the new pipes and changes of the installation, and study of the reduction of the losses with these changes.

## References

1. O. Izquierdo-Monge, P. Peña-Carro, R. Villafafila-Robles, O. Duque-Perez, A. Zorita-Lamadrid, and L. Hernandez-Callejo, "Conversion of a Network Section with Loads, Storage Systems and Renewable Generation Sources into a Smart Microgrid," *Applied Sciences*, vol. 11, no. 11, 2021, doi: 10.3390/app11115012.
2. T. (1) Sachs, G. (1) Fridgen, A. (2) Gründler, and M. (2) Rusic, "Framing Microgrid Design from a Business and Information Systems Engineering Perspective," *Bus. Inf. Syst. Eng.*, vol. 61, no. 6, pp. 729–744, D2019, doi: 10.1007/s12599-018-00573-0.
3. R. A. Vicini and O. M. Micheloud, *Smart grid: fundamentos, tecnologías y aplicaciones*. Cengage Learning, 2012.
4. K. C. Divya and J. Astergaard, "Battery energy storage technology for power systems -- An overview," *Electr. Power Syst. Res.*, vol. 79, no. 4, p. 511, Apr. 2009, [Online]. Available: <https://search.ebscohost.com/login.aspx?direct=true&AuthType=sso&db=edsgao&AN=edsgcl.193579573&lang=es&site=eds-live&scope=site&custid=s1132340>.
5. M. A. Jirdehi, V. S. Tabar, S. Ghassemzadeh, and S. Tohidi, "Different aspects of microgrid management: A comprehensive review," *J. Energy Storage*, vol. 30, p. 101457, 2020, doi: <https://doi.org/10.1016/j.est.2020.101457>.

6. Q. LI, Z. XU, and L. YANG, “Recent advancements on the development of microgrids,” *J. Mod. Power Syst. Clean Energy*, vol. 2, no. 3, pp. 206–211, 2014, doi: 10.1007/s40565-014-0069-8.
7. Y. JIA, X. LYU, C. S. LAI, Z. XU, and M. CHEN, “A retroactive approach to microgrid real-time scheduling in quest of perfect dispatch solution,” *J. Mod. Power Syst. Clean Energy*, vol. 7, no. 6, pp. 1608–1618, 2019, doi: 10.1007/s40565-019-00574-2.
8. A. Kaur, J. Kaushal, and P. Basak, “A review on microgrid central controller,” *Renew. Sustain. Energy Rev.*, vol. 55, pp. 338–345, 2016, doi: <https://doi.org/10.1016/j.rser.2015.10.141>.
9. A. Ahmad Khan, M. Naeem, M. Iqbal, S. Qaisar, and A. Anpalagan, “A compendium of optimization objectives, constraints, tools and algorithms for energy management in microgrids,” *Renew. Sustain. Energy Rev.*, vol. 58, pp. 1664–1683, 2016, doi: <https://doi.org/10.1016/j.rser.2015.12.259>.
10. I. y C. Agencia Andaluza de la Energía Consejería de Economía, “Estudio de Potencial y Viabilidad para la Recuperación de Centrales Minihidráulicas en Andalucía,” 2009.
11. J. Uche, “Análisis prospectivo sobre la interrelación agua y energía en la Cuenca del Ebro.”
12. J. M. Marcos Fano, “La generación de energía hidroeléctrica,” *Anales de mecánica y electricidad*, vol. 83, pp. 35–40, Jan. 01, 2006, [Online]. Available: <https://search.ebscohost.com/login.aspx?direct=true&AuthType=sso&db=eds-dnp&AN=edsdnp.1448362ART&lang=es&site=eds-live&scope=site&custid=s1132340>.
13. “Selección de turbinas hidráulicas.” [https://www.ingenieria.unam.mx/deptohidraulica/publicaciones/pdf\\_publicaciones/SELECYDIMENSIONAMIENTO-deTURBINAS.pdf](https://www.ingenieria.unam.mx/deptohidraulica/publicaciones/pdf_publicaciones/SELECYDIMENSIONAMIENTO-deTURBINAS.pdf) (accessed Jun. 10, 2021).
14. R. P. Dewi, B. Anggoro, and B. Halimi, “Francis Turbine Design on Malabar Mini Hydropower Plant,” in *2018 Conference on Power Engineering and Renewable Energy (ICPERE)*, 2018, pp. 1–4, doi: 10.1109/ICPERE.2018.8739449.
15. “Pérdidas por evaporación.” <https://agro.iberf.es/evitar-evaporacion-embalses/> (accessed Jul. 10, 2021).
16. J. I. LÓPEZ MORENO, “ESTIMACIÓN DE PÉRDIDAS DE AGUA POR EVAPORACIÓN EN EMBALSES DEL PIRINEO,” [Online]. Available: <file:///C:/Users/usuario/Downloads/Dialnet-EstimacionDePerdidasDeAguaPorEvaporacionEnEmbalses-2762772.pdf>
17. C. Marín Peralta, J. J. Marcuello Pablo, and M. Zajkowski, “Estudio de la tecnología de módulos fotovoltaicos flotantes en superficies de agua,” Universidad de Zaragoza, 2016.

# A Framework for Preliminary Urban Wind Energy Potential Assessment with Resilience Approach in Dominican Republic

A. Vallejo-Díaz<sup>1-2</sup>[0000-0003-3215-6352], I. Herrera-Moya<sup>1</sup>[0000-0003-1407-5962] and A. Fernández-Bonilla<sup>1</sup>[0000-0003-3071-287X]

<sup>1</sup> Instituto Tecnológico de Santo Domingo, SD 10602, Dominican Republic

<sup>2</sup> Instituto Especializado de Estudios Superiores Loyola, SC 91000, Dominican Republic  
alexander.vallejo@intec.edu.do

**Abstract.** Climate changes pose big challenges to scientists, engineers and decision makers to provide sustainable energy services to the cities. Innovative energy solutions are required in order to fulfil the growing energy demand in a sustainable and resilient way, especially in developing countries. The concept of small-scale energy systems integrated by several renewable sources such as wind and solar photovoltaic is a promising technological approach, in this direction urban wind energy should play an important role. A preliminary assessment of urban wind energy is needed by turbine developers, investors and decision makers. The present work, aims to present an assessment of wind energy potential of selected locations at two major cities in Dominican Republic, for this purpose was developed a simple but robust framework to provide a preliminary and city-environment assessment of the wind energy potential in a tropical area, i.e. at city selected locations, for roof-mounted turbines. The framework is based on six main steps: (1) site selection, (2) resource prospecting/analysis, (3) turbine selection, (4) estimation of currently produced energy, (5) environmental evaluation and (6) resilience assessment. The methodology was applied in San Cristóbal and Santo Domingo, two major cities in the Dominican Republic. In this case, the urban wind energy potential was assessed considering the installation of 1075 small two-blade Darrieus H-type vertical axis wind turbines (VAWTs) on the roofs of 275 existing high-rise buildings, yielding an annual energy production of about 317 MWh with a potential CO<sub>2</sub> emission reduction of 197 Ton/yr.

**Keywords:** Urban Wind Energy Assessment, Small Wind Turbine, Tropical Zone.

## 1 Introduction

The world is undergoing an energy transition to limit climate change, the main base of such transition is to accelerate the use of clean energy. Several of the United Nations Sustainable Development Goals until 2030 are set in this direction, especially Goal 7, which sets out the challenge of Affordable and Clean Energy for All [1]. For this purpose, it is necessary to reduce the costs of renewable energies and take full advantage

of the potential of energy efficiency, digitalization, smart technologies and sustainable solutions for electrification [2]. This paper proposes the use of urban wind energy as one of the alternatives to decouple the necessary economic expansion from the intensive use of fossil fuels. The goal is to promote the idea of providing energy accessibility in a sustainable way for humanity, taking the Dominican Republic (DR) as a case study. In that way, the DR, in the frame of the Paris agreement has the commitment to reduce by 25% the estimated per capita emissions of 3.6 tCO<sub>2</sub>e by 2030, with respect to 2010 [3].

Due to the high population density in urban areas, both in emerging and developed countries, tailor-made energy solutions close to the area where demand is generated are required. Globally, consumption in buildings accounts for 30% of primary energy consumption [4]. With the implementation of energy efficiency measures, savings about 20 - 40% can be achieved. Small wind turbine (SWT) installations are expected to contribute to the energy transition towards low carbon and high efficiency services in cities [5].

Decentralized generation in urban environments is a possible solution, involving technologies such as solar photovoltaic and SWT [6]. In this direction, a full understanding of the renewable resources available in urban environments is needed. This research, rather novel in the Caribbean region and especially in the DR, aims to contribute to the characterization of wind in urban environments for the proper assessment of the technology to be used. The wind characteristics and the orography (existing buildings, environment, etc.) are crucial elements for the deployment of SWT in urban environment, and the consideration of the atmospheric events to predict the system's risks. Another expectation of this work is to influence the architecture and urban planning to facilitate the use of the wind resource in the future. In section 3.1, the proposed methodology is applied in a case study, focuses on the potential of two major cities in the DR, Santo Domingo and San Cristóbal.

## 2 Methodology

The methodology presented in this research have the purpose to perform with adequate precision a characterization of the urban wind energy potential in the Caribbean area, especially in the DR. It is important to highlight the efforts made to combine the current state of the art in the subject and the data available in the context of the region.

A suitable methodology was presented by Bekele to evaluate the wind energy potential in specific location in Ethiopia [7], the most important contribution of this work was the methods developed to complete the lapses with wind records unavailability by using a Georeferenced Information Systems (GIS) database. This allows to covert three horary existing database to horary database to study the wind energy potential minimizing the energy estimation error. Similar works was carried out by Ashtine, also presents a way to determine the wind trend with GIS system databases with time lag (records every 3 hours) over Ontario and Great Lakes, and in that sense the atmospheric stability [8]. Gagliano presented an interesting methodology consisting of Computational Fluid Dynamics (CFD) simulations from the integration from GIS platform, in

order to provide easy way to evaluate the potential wind energy production for non-specialized users, and that methodology was validated by on-site measurement [9].

The accuracy of methodologies containing wind tunnels is highly dependent on the complexity of the upstream terrain. Furthermore, to it is very difficult to measure turbulence in the wind tunnel due to the scalability of the model, and it is relatively more expensive [9]. Al-Quraan reported estimation errors in the order of 5 - 20%, through validation of wind tunnel methods and on-site measurements [10]. According to Wang's methodology, CDF simulation is used for optimal placement of SWTs on the building, which are validated with on-site measurements [11]. Similar to the wind tunnel method, the computational simulations must be validated with on-site wind measurements [12].

Methodologies using the analytical method present a simplified version of the multiple factors involved in urban wind flow. Based on cross-sectional pressure differentials in vertical axis turbines, theoretical efficiencies have been reported between 48 and 61%, based on fluid flow theory, which is in excess of the Betz Limit, which is the upper limit of power that can be extracted from the wind [13], [14].

The methodology presented by Rezaeiha [15] is one of the most comprehensive and feasible in terms of cost and time, according to the author's consideration. Especially in emerging countries, where resources are limited. Rezaeiha presents preliminary estimation for the study of urban wind potential on the roofs of buildings in a city or a country, using a combination of GIS and CFD methods. However, many site measurements are needed to corroborate the country-scale estimation of GIS and field measured data. In addition, dynamic loads, available areas, and other physical aspects of the buildings that are supposed to be used to harness urban wind energy need to be considered.

Based on the above mentioned, the author recommends for wind energy assessment to combine the methods: GIS, on-site measurement, and CFD, to have a spatial approach from meso-scale to micro-scale. On the other hand, is recommended to validate the results of the GIS using on-site measurement method, in order to obtain the real physical parameters for the numerical simulation in CFD. Only a few research has been conducted in the tropical zone around the world, so far no precedents in the Caribbean region has been found, as shown in [16].

In this work a novel methodology is proposed to analyze the energy potential of urban wind. This methodology adopts several steps from some existing ones and proposes to incorporate an environmental evaluation for a more complete study, taking into account the need to reduce the CO<sub>2</sub> emissions. The methodology includes five steps: (1) site selection, (2) resource prospecting/analysis, (3) turbine selection, (4) estimation of currently produced energy, (5) Environmental evaluation and (6) Resilience assessment, as shown synthetically in Fig. 1. The step presented in Fig. 1 are described in the sections 2.1 to 2.6.



Fig. 1. Schematic illustration of the steps of the proposed methodology.

## 2.1 Characterization of the study area and selected cities

There is great potential in the use of urban wind for distributed electricity generation in densely populated urban areas [17], [18]. In these environments, small wind turbines can be conceived as building-integrated from the design phase or installed on rooftops of existing buildings or surrounding areas. Distributed wind energy in cities has the advantage of its proximity to the point of electricity demand, which means reduced costs for high-voltage transmission lines as well as for the necessary devices of such a system [19].

Trees, buildings and other obstacles on the ground influence wind speed and turbulence, especially in sites with low wind speed and high turbulence levels [11]. This significantly reduces the resource utilization using small wind turbines, obstacles extract wind flow momentum, resulting in lower average wind speed [20].

In order to identify potentially usable buildings for SWT siting, parameters such as height, available roof area and structural integrity need to be assessed. A possible method for this purpose was identified in the work performed by Rezaeiha [15]. In this research, buildings in cities were identified and classified using GIS databases available on freely accessible websites, such as: <https://skyscraperpage.com/> [21]. These tools serve as a starting point to stratify buildings that meet the criteria for SWT installation.

## 2.2 Wind energy assessment

In the literature several methods can be found for site-specific urban wind forecasting for energy purposes. The most commonly used methods are: on-site measurement, wind tunnel, georeferenced information systems (also well known as numerical climate prediction), computational fluid dynamics and analytical methods.

According to Al-Quraan [10], the wind tunnel tests are used to give a more accurate estimate of wind without actually undertaking a wind measurement campaign. Wind tunnels have been a key element in scientific research in several fields. Wind tunnel experiments can even provide approximate values for variables that might be difficult to obtain with experimental instrumentation and offer great potential for understanding a wide range of phenomena [22], [23].

Georeferenced information software (GIS) involves the use of a combination of digital maps and georeferenced data that write various features of a given area at different scales. They are used for various purposes, from urban planning to, more recently, the study of renewable energy penetration. Both at micro and macro scales [9]. CFD programs solve the complex Navier-Stokes equations in three dimensions to describe the actual fluid motion [9]. The Reynolds-averaged Navier-Stokes (RANS) solution using CFD has become the most common technique because it requires less computational performance, i.e., cost and time [24].

Mathematical methods present a simplified version of the multiple factors involved in urban wind flow. Based on cross-sectional pressure differentials in vertical axis turbines, theoretical efficiencies have been reported between 48 and 61%, based on fluid flow theory, which is in excess of the Betz Limit, which is the upper limit of power that can be extracted from the wind [13], [14].

In any case, the main objective is to perform a wind characterization that includes the determination of parameters such as: average speed, direction, turbulence, energy density, etc. In this work, on-site measurements are used to evaluate the urban wind potential in the cities. A brief description of this method is presented below.

Wind speed and direction are the main parameters for the characterization of the urban wind for energy purposes. The reference wind speed is established on the basis of measurements averaged every 10 minutes, according to the International Electrotechnical Commission Standard. For the measurement of these parameters, an anemometer installed according to the aforementioned standard at the measurement site is needed [25].

Usually, the wind speed and direction are statistically processed and plotted on a polar diagram called a wind rose, where the radial axis indicates the magnitude and frequency of the wind, showing the prevailing wind direction. It can also be displayed in a Cartesian coordinate diagram [18], [26], [27].

The accumulated records of wind parameters allow the construction of probability functions and predict the energy potential. The Weibull, Rayleigh and Lognormal distributions are widely used to predict wind speed. The most widely used is the Weibull distribution because of its flexibility and simplicity. However, limitations have been observed in this function for average wind speed lower than 2 m/s or close to zero, in this speed range the density distribution estimation can be very inconsistent [28]. This limitation is not relevant to use this function evaluating the potential for SWT, because typically the cut-out speed of this machines is 2 m/s. In this work, the Rayleigh Distribution, a variant of the Weibull distribution with a form factor equal to 2 is adopted [25].

Weibull distribution  $p(V_{avg})$  is the probability distribution function used to describe the distribution of wind speeds over time duration. The Weibull probability function is given by Eq. 1:

$$p(V_{avg}) = \left(\frac{k}{c}\right) * \left(\frac{V_{avg}}{c}\right)^{k-1} e^{-\left(\frac{V_{avg}}{c}\right)^k} \quad (1)$$

Where:  $k$ , is the shape factor, a parameter that controls the width of the distribution and  $c$  is the scale factor in m/s, this parameter controls the average wind speed and is defined in Eq. 2.

$$c = \frac{V_{avg}}{\sqrt{\pi}} \quad (2)$$

Where:  $V_{avg}$ , is the average wind speed.

The parameters  $k$  and  $c$  can be estimated by several methods, being the method of maximum likelihood the most commonly used [6], [28].

Another important characteristic of the wind is the Turbulence Intensity (TI), it is defined as the ratio of standard deviation of fluctuating wind velocity to the mean wind speed, and it represents the intensity of wind velocity fluctuation. This index should be calculated at 15 m/s, as it is one of the characteristic parameters included in the classification (classes) of small wind turbines according to the International Electrotechnical Commission [25]. At presents four SWT classes has been defined, for all classed the turbulence intensity should be 0.18 or less, and for the "S" class, it should be determined according to the referred standard. A turbine should not be exposed to wind turbulence intensity higher than 25%, so this parameter is essential for determining the installation of small wind turbines [11]. Small wind turbines must be able to respond to frequent urban wind fluctuations and the site and system characteristics [29]. According to the National Renewable Energy Laboratory (NREL) of the United States, turbulence levels can be categorized as follows: low, if TI have values less than or equal to 10%; moderate, if TI have values between 10% to 25%; and high, if TI have values greater than 25% [30]. The TI calculation is given by Eq. 3.

$$TI = \frac{\sigma}{V_{avg}} \quad (3)$$

Where:  $\sigma$  is the 10-min standard deviation,  $V_{avg}$  is 10-min average wind speed.

### 2.3 Selection of small turbines

SWTs are aerodynamic machines, used to convert wind energy into electricity. Electricity production is a function of air density, the sweep area of the turbine blades, and the speed cube [31].

There is a wide variety of designs and types of small wind turbines. Commonly, highly efficient developments are considerably influenced by criteria related to the operation and location of the machine. In the wind turbine industry, there are mainly two designs, horizontal axis wind turbines (HAWTs) and vertical axis wind turbines (VAWTs) [9], [32], [33].

HAWTs are generally installed in areas relatively separated from cities, and with considerable heights above ground level, according to local policies and regulations. These machines must always be oriented with the rotor perpendicular to the wind direction, which makes it unappropriated to be installed in places with frequent changes in wind direction or high turbulence [34], [35].

VAWTs can be classified into two main categories, Darrieus and Savonius rotor. Darrieus VAWTs are usually considered a lift rotor, since the torque is generated by

the average lift force. On the other hand, Savonius rotors operate normally by the action of drag force. H-type rotor VAWTs are a combination of lift and drag forces. VAWTs are more used in urban environments because they are less vulnerable to changes in wind directions.

According to the International Electrotechnical Commission (IEC), SWTs are those with a capacity  $\leq 50$  kW and a rotor swept area  $\leq 200$  m<sup>2</sup> [25]. Different classifications, according to power, hub height, and swept exist in different countries. In this work we adopt IEC classification.

According to Rezaeiha [15], urban wind energy harvesting systems can be categorized as follow: (i) Stand-alone near building, (ii) Retrofitted to existing building, and (iii) Fully integrated into building architectural form.

#### 2.4 Annual Energy Production Estimation

For the estimation of the annual energy production (AEP), the methodology proposed by Rezaeiha [15] is adopted.

The equation to estimate the AEP is shown in Eq. 4:

$$AEP = 8760 * \int_0^{\infty} P(V_{avg}; c; k) * P(V_{avg}) dv \quad (4)$$

Where: 8760 are the hours during a year, is  $P(V_{avg}; c; k)$  is the probability of occurrence of a given speed based on the Weibull distribution, and  $P(V_{avg})$  is the power produced by the wind turbine at that speed.

The power extracted by the wind turbine is described according to Eq. 5:

$$P(V) = 0.5 * C_p * \rho * A * V_{avg}^3 \quad (5)$$

Where:  $A$  is rotor area,  $C_p$  is the power coefficient of the rotor,  $V_{avg}$  is the mean wind speed and  $\rho$  is the air density.

#### 2.5 Environmental evaluation

To assess the potential environmental benefit from the installation of the SWTs the evaluation of mitigation outcome in terms of Greenhouse Gas (GHG) emission reduction is performed. Fossil fuels prevail in DR electricity sector, according to Guerrero-Liquet: oil (46.27%), natural gas (25.92%) and coal (14.03%), represented 86% of electricity generation in the country. Only 10% of electricity generation is based on renewable sources, particularly hydropower (6.26%) and wind energy (1.90%) [36]. Is it important to highlight that oil and coal are the higher CO<sub>2</sub> emitters, in DR the total electricity generation based on this fuels is the 72.2%. With data from The Coordinating Entity of the National Interconnected Electrical System (OC) <https://www.oc.do/> an estimation of the emission factors for these fuels have been done. It was found that emissions factors expressed in tCO<sub>2</sub>eq/MWh for oil and coal are about 0.75 and 0.98 respectively. Base on that a significant contribution to the electric sector decarbonization can be expected with the deployment of renewables energies such as SWTs.

To determine the mitigation of CO<sub>2</sub> emissions in this research the Standardized Baselines (SB) set by the United Nations Framework Convention on Climate Change is adopted [37]. A SB simplifies the evaluation of Greenhouse Gas (GHG) emission reduction, defining a baseline emission factor for a sector, which could potentially be applicable to all mitigation activities in this sector. The SB for DR, published by UNFCCC on February 3rd, 2020, is valid until February 2nd, 2023. In this base lines is stablished the CO<sub>2</sub> emission factor for the National Interconnected Electrical System (SENI), including the specific value for wind and solar power generation projects. This SB was derived using the ex-ante data vintage option of the “TOOL07: Tool to calculate the emission factor for an electricity system”, version 7.0 (hereinafter referred to as “the grid tool”) based on 2014 – 2016 data vintage. This standardized baseline can apply to projects implemented in the Dominican Republic and connected to the SENI, it was approved by CDM Executive Board in accordance with the “Procedure for development, revision, clarification and update of standardized baselines” (CDM-EB63-A28-PROC). The emission factor in this SB includes both, the operating and build margin grid emissions, as described in the grid tool [37], taking into account the life cycle of the project.

For wind and solar power generation projects a combined margin (Operating&Build) CO<sub>2</sub> emission factor for the SENI of 0.6216 tCO<sub>2</sub>/MWh is established in the so call SB ASB0047-2020 [37].

The avoided emission can be calculated by Eq. 6.

$$\text{Avoided annual emission (tCO}_2\text{eq/yr)} = \text{AEP (MWh/yr)} * \text{emissions factor (tCO}_2\text{eq/MWh)} \quad (6)$$

## 2.6 Resilience assessment

Resilience as a concept has gained much attention in recent years, researchers have defined resilience in various disciplines and systems, such as ecosystems and infrastructure (power plants, water and transport), seismic, ecological, economic and community. In general, resilience refers to the ability of an object to return to its original shape or position after being stressed.

The "resilience triangle" is the fundamental basis of many studies, in which one wants to measure a high-impact, low-frequency event, mainly in power systems [38]. The geometric shape evolved to a trapezoid, because this shape cannot capture other highly critical dimensions of resilience in an electrical power system, such as the time the system or an element remains in the degraded state [39].

The resilience of a system is determined by the combination of capacities in three phases, which are (1) the ability to prevent possible threats and mitigate the initial damage should it occur, (2) the absorption capacity in terms of when the system withstands the initial damage and minimizes the consequences, and (3) the restoration capacity as the ability to recover quickly and effectively [40]. Ahmadi et al., defines four phases of the resilience of an energy system, consisting of anticipation, absorption, adaptation and restoration; the adaptation phase is the level of system performance after the propagation of the event has reached its peak [41].

Caribbean countries are at high risk from hurricanes, so it is vital that energy supply solutions are resilient to such adverse phenomena. The two DR provinces taken as case studies in this work, with high population density, are frequently affected by deteriorating atmospheric conditions associated with hurricanes. As all renewable energy systems are climate-dependent, metrics for assessing the resilience of these systems should include the phases of preparedness, resistance, adaptation and recovery, as proposed by Ahmadi et al. [41].

Understanding hazards is crucial for designing and preparing for weather events, which can be very different from one another in terms of impact, frequency, geographic probability, duration, etc. Changing weather conditions require dynamic responses with both qualitative and quantitative performance criteria and metrics that can anticipate and enable energy supply systems to adjust or recover quickly. According to Charani Shandiz, the time to anticipate the extreme event and the extra resilience capacity (>100%) will depend on the predictive ability, system performance and the type of extreme event [42].

In this paper the author adopts Charani's conceptual phases of the resilience trapezoid, which correspond to the following states: (1) robust state (pre-event), (2) post-event state (including event occurrence state), (3) recovery state and (4) post-recovery state, as shown in Fig. 2. In all states and phases of the resilience trapezoid, the shape (slope, areas, etc.) depends mainly on the performance of the system and the type of disruptive event, well described in [42].

An energy system must have the ability to handle the adversities of the event, and not fail at all to withstand the disturbance. There are three subsequent resilience capabilities, which are: a) engineering design resilience; b) operational resilience; and c) community and social resilience.

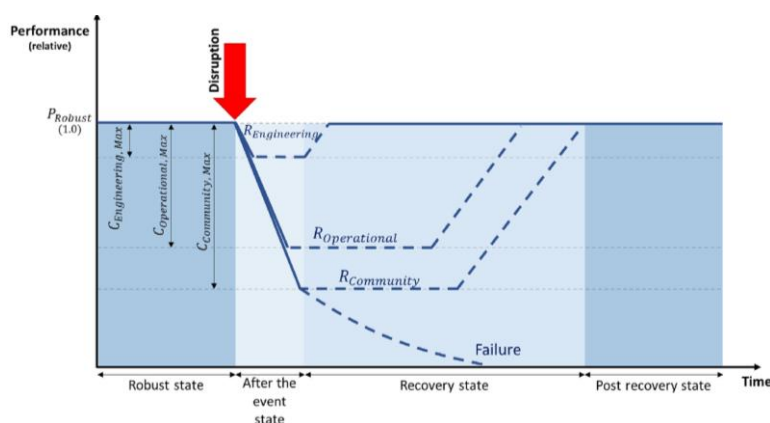


Fig. 2. Conceptual multi-phase energy resilience trapezoidal, presented [42].

As a novel part of this proposed methodology, the author identifies three possible scenarios to hypothesize the resilience analysis of these building-integrated energy systems to capture the kinetic energy of the wind, which are highly dependent of the atmospheric conditions of the tropics, especially in the Caribbean.

- **Scenario 1:** Energy not produced when the SWT is taken out of service due to high wind speed, without decommissioning and damage during the interim in which the wind exceeds the maximum operating speed, as shown in the Fig. 3.

- **Scenario 2:** Energy not produced when the SWT is out of operation: due to the forecast of high wind speed due to atmospheric events exceeding the nominal maximum operating speed, plus the inclusion of disassembly and reassembly time to avoid serious damage to the system. This forecast time is important to dismantle the SWTs in a timely manner and to return the system to its optimal operation, as shown in Fig. 4.

- **Scenario 3:** Energy not produced when the SWT is out of operation due to high wind speed and severe structural damage due to failure caused by an atmospheric event. In this case a capital investment is required, as shown in Fig. 5.

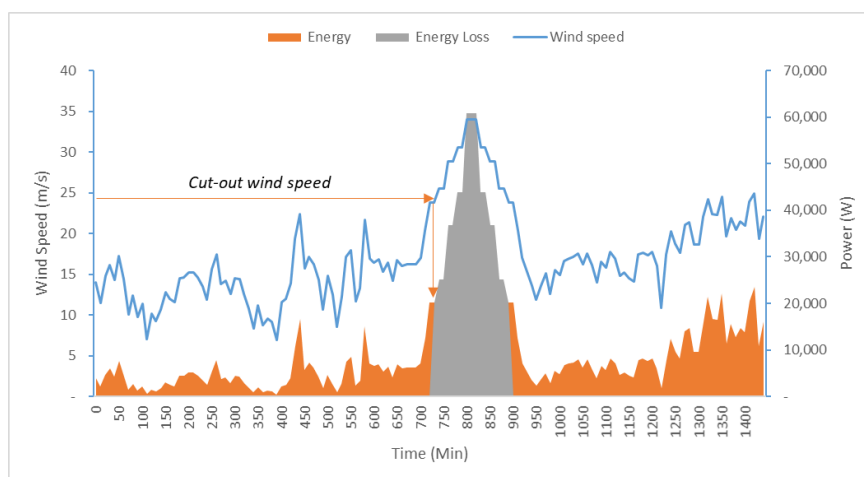
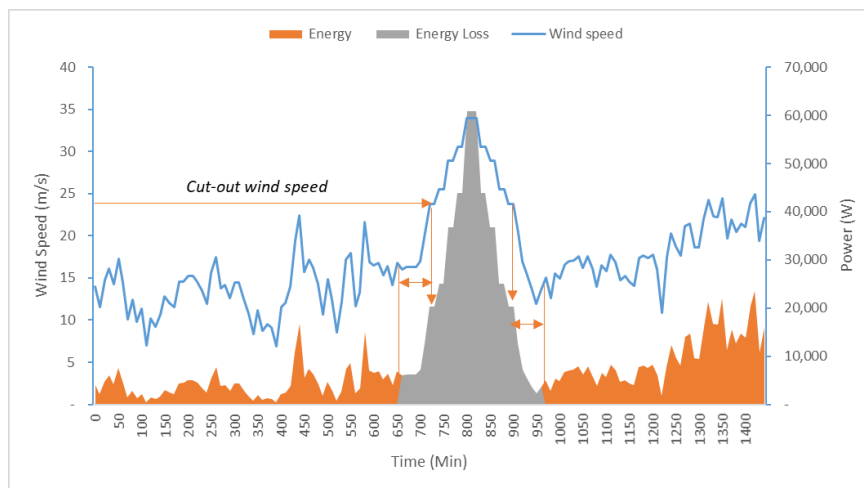
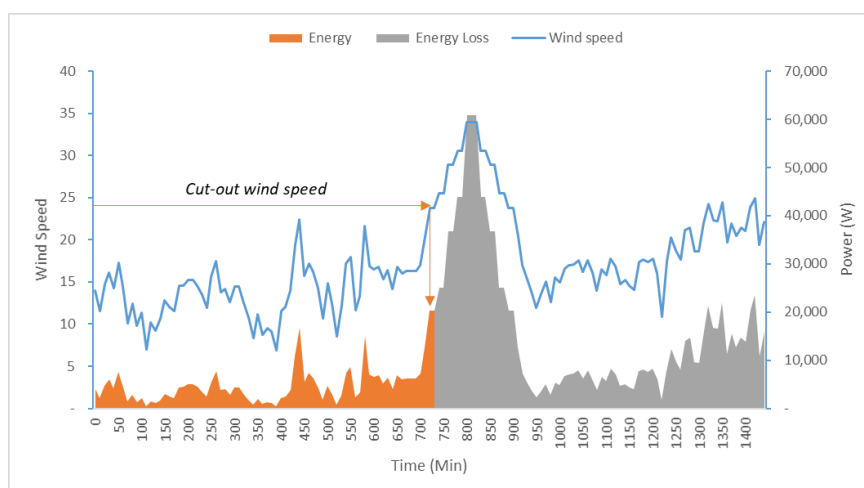


Fig.

3. Scenario 1: Energy not produced when the SWT is taken out of service due to high.



**Fig. 4.** Scenario 2: Disassembly and reassembly time to avoid serious damage in advance of atmospheric event.



**Fig. 5.** Scenario 3: Severe structural damage due to failure.

### 3 Results and discussion

This methodology has been developed to determine the urban wind potential in the tropical area, for the purpose of using it to generate electricity and contribute to the decarbonization of the country. In this sense, it has the novel integration of an environmental assessment. In the following subsection, it will be applied to a case study in the DR, followed by the results, discussion, and future work.

### 3.1 Case study

This case study has been developed to determine the urban wind energy potential in two densely populated cities of the Dominican Republic. The most important findings are presented from survey campaigns carried out at the Technological Institute of Santo Domingo (INTEC) and the Specialized Institute of Higher Studies Loyola (IEESL), located in Santo Domingo and San Cristóbal, respectively. Two anemometers were installed for data recording at INTEC and one at IEESL, which are identified with the following nomenclature: Aem1-INTEC, Anem2-INTEC and Anem1-IEESL.

Based on the section 2.1, in order to estimate the urban wind potential in the two cities of interest, high and structurally suitable buildings for the installation of VAWTs were identified. Buildings in Santo Domingo were identified and classified using the GIS database available on the freely accessible website <https://skyscraperpage.com/>. In the case of San Cristóbal, no information was found available on the web pages, so an inspection of the main buildings of the city was carried out. In total, 190 high and structurally suitable buildings were identified in Santo Domingo. A scenario was modelled in which 95 buildings in the city were characterized by the wind regimes recorded by Anem1-INTEC and another 95 by Anem2-INTEC. In the case of San Cristóbal, 25 high and structurally suitable buildings were identified for the installation of VAWTs. For a total of 215 buildings in both cities.

To perform a wind characterization that includes the determination of parameters such as: average speed, direction, turbulence, energy density, etc., a wind energy assessment according to section 2.2 is carried out. In this work, on-site measurements are used to evaluate the urban wind potential in the cities of Santo Domingo and San Cristóbal, in DR. The data set collected from three anemometers installed in representative building in Santo Domingo and San Cristóbal were used.

The Anem1-INTEC and Anem2-INTEC registered data during the period May-December and June-December 2017 respectively. The Anem1-IEESL has been operational since May 2020, the period May - December 2020 was taken in account for this study. The sensors were installed in buildings with heights of 20 m. A total of 208 881, 152 816 and 308 803 records were taken from Anem1-INTEC, Anem2-INTEC and Anem1-IEESL, with an availability of 71%, 77% and 92%, respectively. In 2017 the country was hit by several meteorological adverse events which affected the data collection.

Fig. 6a) shows the behavior of the monthly average wins speed. The mean speed for the periods were 2.32, 2.48 and 2.07 m/s respectively.

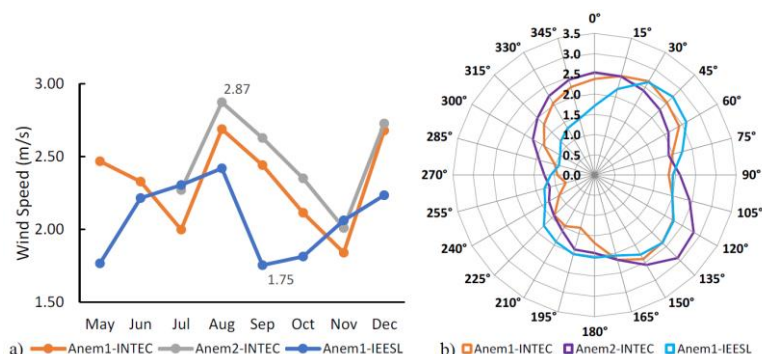


Fig. 6. a) Average monthly wind speed, b) Period average wind rose.

Fig. 6b) shows the wind rose for the three sensors during the study period. The predominant wind direction is North-East, with a strong correlation with the data records of the meteorological services for both cities. The predominant wind direction with the highest intensity was recorded between 15°-60°, respect to North.

Table 1 shows the hourly variation of wind speed for one day. The Table 1 has a color scale, where red represents unfavorable speeds and green favorable. Note that in the interval from 13:00 to 15:00 the highest energy potential occurs. This is very positive, since the energy consumption associated with air conditioning in this horary is considerable in tropical areas. Note that in Santo Domingo there are wind speeds higher than 2 m/s during approximately 18h every day.

Table 1. Diurnal average variation of wind speed at both cities for the period.

Table 1. Diurnal average variation of wind speed at both cities for the period.

Hours	1	2	3	4	5	6	7	8	9	10	11	12	
Anem1-INTEC	1.9	1.9	1.8	1.8	1.8	1.8	2.0	2.4	2.8	2.8	2.8	2.8	
Anem2-INTEC	2.0	2.0	1.9	1.9	1.9	1.9	2.1	2.5	2.8	2.9	3.0	3.1	
Anem1-IEESL	1.6	1.6	1.6	1.6	1.6	1.6	1.8	2.3	2.7	2.9	2.9	2.9	
Hours	13	14	15	16	17	18	19	20	21	22	23	24	Avg.
Anem1-INTEC	2.8	3.0	2.8	2.7	2.6	2.4	2.4	2.2	2.2	2.1	2.0	2.0	2.32
Anem2-INTEC	3.2	3.4	3.3	3.1	2.9	2.7	2.5	2.4	2.3	2.1	2.1	2.1	2.50
Anem1-IEESL	2.9	2.8	2.7	2.5	2.2	1.8	1.6	1.6	1.7	1.7	1.7	1.7	2.08

From the minute-by-minute recordings, the average speed was calculated for 10-minute intervals. A normal distribution of average wind speed calculated for 10-minute intervals is shown in Fig. 7a). Note from this graph that in the city of San Cristóbal there is a higher probability of occurrence of slightly lower speeds than in Santo Domingo, note the leftward bias in the Anem1-IEESL curve. This indicates more favorable wind speed regimes in Santo Domingo than in San Cristóbal for SWTs installation. The most probable speed recorded in all instruments was 2 m/s, with probabilities of occurrence of 37%, 33% and 38% respectively.

Fig. 7b) shows the Weibull distribution for the parameters given in Table 2. The same proportionality is observed in the leftward bias for lower wind speeds in the anemometer installed at IEESL. Slightly lower velocities were recorded at this instrument than those recorded at Anem1-INTEC and Anem2-INTEC in the order of 11% and 20%, respectively.

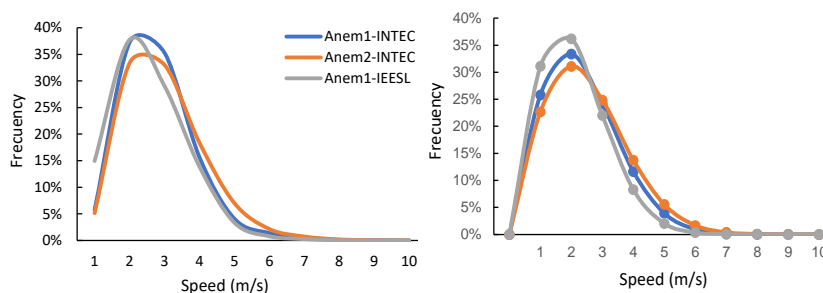


Fig. 7. Monthly average wind speed a) with normal distribution, b) Weibull distribution.

Table 2. Weibull distribution parameters at both cities.

Anemometer	Mean Wind Speed (m/s)	Scale Factor	Shape Factor (m/s)
Anem1-INTEC	2.322	2	2.621
Anem2-INTEC	2.498	2	2.819
Anem1-IEESL	2.085	2	2.353

Turbulence intensity (TI) was categorized binned in the histograms shown in Fig. 8. According to NREL, TI below 10% is considered low, between 10% and 25% moderate and above 25% as high. From Figure 4 it can be seen that on average 35% of the records correspond to high turbulence intensity. This may be mainly associated with the terrain orography, taking into account that these measurements were made in buildings in urban environments.

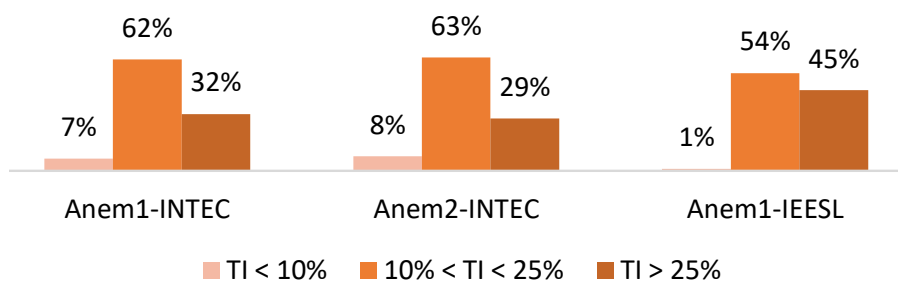


Fig. 8. TI categorization.

Given the wind characteristics described above, VAWT technology was chosen in this study, since this type of turbine have a good performance in urban locations with

low wind speeds and high TI. A turbine similar to the one selected by Rezaeiha in the wind potential studies in 12 cities in the Netherlands was selected [15]. The selected turbine is a Darrieus Type-H rotor with a rated power of 2.4 kW at a wind speed of 12.5 m/s and a swept area of 5 m<sup>2</sup>. From the power curve of the two-blade Darrieus Type-H turbine, the energy produced during the year can be estimated as a function of wind speed regimes. The equation that best fit to the power curve for this machine was estimated using the potential regression method, with a correlation of R<sup>2</sup> = 0.9944, the function is:

$$y = 1.1501 * V_{avg}^{3.0842} \tag{7}$$

Where: y, is the power delivered by the machine in Watt; V, is the wind speed in (m/s).

Table 3 shows the estimated annual power and energy generated for the given speed ranges of a VAWT installed at each sensor position, the energy that could potentially be generated at the Anem1-INTEC, Anem2-INTEC and Anem1-IEESL positions would be 274, 342, and 196 kWh/year, respectively.

**Table 3.** AEP estimation for each binned wind speed.

Wind Speed (m/s)	Power (W)	Anem1-INTEC	Anem2-INTEC	Anem1-IEESL
		Energy (W-h/yr)		
2	10	28,496	26,559	30,919
3	34	72,072	74,161	65,644
4	83	84,206	99,525	60,029
5	165	56,489	79,785	29,387
6	289	2,3971	42,093	8,485
7	465	6,776	15,390	1,522
8	701	1,316	4,022	175
9	1,009	179	766	13
10	1,396	17	108	1
11	1,873	1	11	0
12	2,450	0	1	0
13	3,136	0	0	0
14	3,941	0	0	0
15	4,875	0	0	0
Annual energy production		273,523	342,421	196,174

With an initial cautious prediction, it is considered that according to the characteristics of the buildings it is possible to install 5 VAWTs per building, for a total of 1075 in 215 buildings in both cities. Table 4 shows that the estimated annual energy production is 317 MWh/yr. With this energy generation 106 houses with an energy demand of 250 kWh/month or 3 MWh/yr could cover 100% of their energy needs. Base on the scenario modelled in this study, approximately 10 VAWTs are required to satisfy the energy demand for a house.

The electricity produced by SWTs can be exported to the grid distribution lines. This will reduce capital costs and investment in battery energy storage. Based on DR regulations, the project can be enrolled in net metering program [43].

Based on the estimated annual energy production with an emission factor of 0.6216 TonCO<sub>2</sub>/MWh, it can be determined that 197 tonnes of CO<sub>2</sub> emissions into the atmosphere could be avoided annually.

**Table 4.** AEP estimation for both cities.

City	Santo Domingo		San Cristóbal
	Anem1- INTEC	Anem2- INTEC	Anem1- IEESL
Annual energy per SWT (kWh)	274	342	196
Number of VAWTs per building	5	5	5
Number of buildings	95	95	25
Total VAWTs	475	475	125
Total Annual Energy Estimated (kWh)	129,923	162,650	24,522
Total Annual Energy Estimated (MWh)		317	
Avoided CO <sub>2</sub> emissions (Ton/yr)		197	

### 3.2 Economic considerations

The cost of generating electricity with urban wind is a key factor, urban wind generation systems effectively contribute to the future diversification of the urban energy mix, which requires optimal consideration of the physical and financial leverage for the entire system [44]. In this regard, it is recommended to assess the estimated economic viability of these projects, considering the total costs of the central generation system, such as energy costs, capacity, auxiliary services (balancing power), transmission and distribution costs, energy losses, and, if applicable, subsidies to the electricity sector, as well as financial consideration well described by [45]. The cost of energy in the DR during 2020 was 0.1314 USD/kWh, considering the drop in fossil fuel prices during the pandemic, which represented a cost to the government of USD 700 million in subsidies to the electricity sub-sector [46]. A preliminary assessment of the levelized costs of energy (LCOE) for the deployment of SWTs as it is presented in this work indicate a LCOE of 0.9057 USD/kWh, this is 6.9 times the price of the energy in the DR electric grid in 2020. The assumptions adopted for this calculation are shown in Table 5:

**Table 5.** Assumptions for LCOE calculation for one commercial VAWT Darrieus Type-H.

AEP (kWh/y)	Investment (US\$)	Operation and maintenance (US\$/y)	Interest Rate (%)	Life- time (y)	AEP (kWh/y)	Investment (US\$)
342	3,000	91.66	8.00	20	342	3,000

### 3.3 Resilience assessment

In the last 20 years in the DR there have been approximately 17 atmospheric events according to Historical Hurricane Tracks tool provided by [47], which have posed risks to the national energy system, as well as to other systems / ecosystems. Fig. 9 shows a dispersion of events classified according to the Saffir-Simpson scale, from tropical storms (TS) to hurricanes of categories 1 to 5 (H1 - H5). The probability of occurrence of TS, H1 and H3 - H5 was 47%, 18% and 12% respectively.

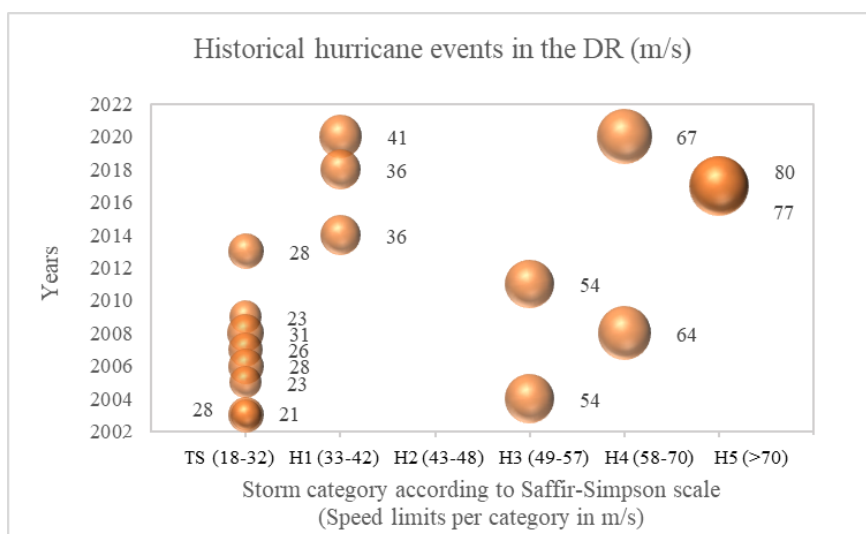


Fig. 9. Historical hurricane events in the Dominican Republic over last 20 year.

The VAWT, Darrieus H-Type adopted in this research has a shear velocity of 24 m/s, as mentioned earlier in Ref. [15]. This implies that 53% of the events in the last 20 years exceed the maximum wind speed at which the SWT.

Other considerations to take into account are the logistics of dismantling and erecting SWTs if necessary, before problematic events are foreseen. Adequate estimation of the associated costs and skilled manpower must be analyzed in depth in order to make the right decisions.

## 4 Conclusions

This research is a starting point for assessing the urban wind potential for electricity generation in urban environment and contribute to the decarbonization of the Dominican Republic energy matrix. The wind generation potential in two large, densely populated cities, Santo Domingo and San Cristóbal, has been assessed in an initial cautious scenario. Data from on-site measurement campaigns conducted at INTEC and IEESL in 2017 and 2020 respectively were used.

The mean wind speed in Anem1-INTEC, Anem2-INTEC and Anem1-IEESL was 2.32, 2.5 and 2.08 m/s respectively, which is considered a relatively low. It was identified that the highest values are observed during the summer, specifically in August; and the lowest values in autumn specifically in November, a trend that has been verified in 2017 and 2020.

The trend of the prevailing wind direction for both case studies is similar. The prevailing wind direction with the highest intensity was recorded between  $15^{\circ}$  -  $60^{\circ}$  respect to North. The wind roses for each case correlate with freely available GIS databases.

There is a daily similar pattern in the wind intensity variation for both sites. For the whole period studied between 13:00h to 15:00h the higher wind intensity occurs. It was observed that wind intensity decreases towards dawn and dusk, beginning the rising cycle around 9h.

A methodology was presented to estimate the urban wind potential taking into account the number of available buildings in Santo Domingo and San Cristóbal. In a cautious scenario, 190 and 25 buildings were identified as suitable for VAWTs, for a total of 215 buildings. The selected turbine was VAWT Darrieus Type-H, with good performance at low speed and very turbulent environments. The estimated AEP was 317 MWh/yr with a potential CO<sub>2</sub> emission reduction of 197 Ton/yr, this potential is still cautious and needs to be systematically reviewed as more efficient technology and more survey data become available. With this energy generation 106 houses with an energy demand of 250 kWh/month or 3 MWh/yr could cover 100% of their energy needs. Base on the scenario modelled in this study, approximately 10 VAWTs are required to satisfy the energy demand for a house.

Future research should quantify 100% of the available potential in buildings with a detailed estimate of the number of buildings and the area available for VAWT installation. In addition, survey studies should be extended both spatially and temporally in the selected cities.

A preliminary economic analysis shows that urban wind energy solution at present seems to be about seven times more expensive than current energy services, influence by factors such as low utilization factor associated to a low wind speed and the technology characteristics, however the CO<sub>2</sub> emissions should be included as added value in future assessments. A more detailed estimation of the levelized costs of energy for the assessment of economic feasibility, which is a key aspect, as well as another sustainability indicator.

A novel part of this proposed methodology is to assess resilience with the metrics well established so far for other systems or ecosystems. In this sense, the author proposes three possible scenarios as a starting point to quantify the resilience of building-integrated SWT systems in Caribbean cities. Mainly atmospheric events are the ones that can compromise SWT systems, as other hazards (earthquakes, dust storms, etc.) are not identified as an imminent risk.

## 5 References

- [1] “Objetivo 7: Energía asequible y No contaminante | PNUD,” *UNDP*, Jun. 11, 2020. <https://www.undp.org/content/undp/es/home/sustainable-development-goals/goal-7-affordable-and-clean-energy.html> (accessed Jun. 11, 2020).
- [2] “Global energy transformation: A roadmap to 2050 (2019 edition),” */publications/2019/Apr/Global-energy-transformation-A-roadmap-to-2050-2019Edition*, Mar. 15, 2020. */publications/2019/Apr/Global-energy-transformation-A-roadmap-to-2050-2019Edition* (accessed Mar. 15, 2020).
- [3] Á. Estévez Bourdierd, E. Peña Acosta, and I. Mattila, “Primer Informe Bienal de Actualización (‘fBUR’),” no. 1, p. 267, Feb. 2020.
- [4] S. Chen, G. Zhang, X. Xia, S. Setunge, and L. Shi, “A review of internal and external influencing factors on energy efficiency design of buildings,” *Energy and Buildings*, vol. 216, p. 109944, Jun. 2020, doi: 10.1016/j.enbuild.2020.109944.
- [5] J. T. Millward-Hopkins, A. S. Tomlin, L. Ma, D. B. Ingham, and M. Pourkashanian, “Assessing the potential of urban wind energy in a major UK city using an analytical model,” *Renewable Energy*, vol. 60, pp. 701–710, Dec. 2013, doi: 10.1016/j.renene.2013.06.020.
- [6] B. R. Karthikeya, P. S. Negi, and N. Srikanth, “Wind resource assessment for urban renewable energy application in Singapore,” *Renewable Energy*, vol. 87, pp. 403–414, Mar. 2016, doi: 10.1016/j.renene.2015.10.010.
- [7] G. Bekele and B. Palm, “Wind energy potential assessment at four typical locations in Ethiopia,” *Applied Energy*, vol. 86, no. 3, pp. 388–396, Mar. 2009, doi: 10.1016/j.apenergy.2008.05.012.
- [8] M. Ashtine, R. Bello, and K. Higuchi, “Assessment of wind energy potential over Ontario and Great Lakes using the NARR data: 1980–2012,” *Renewable and Sustainable Energy Reviews*, vol. 56, pp. 272–282, Apr. 2016, doi: 10.1016/j.rser.2015.11.019.
- [9] A. Gagliano, F. Nocera, F. Patania, and A. Capizzi, “Assessment of micro-wind turbines performance in the urban environments: an aided methodology through geographical information systems,” *Int J Energy Environ Eng*, vol. 4, no. 1, p. 43, Nov. 2013, doi: 10.1186/2251-6832-4-43.
- [10] A. Al-Quraan, T. Stathopoulos, and P. Pillay, “Comparison of wind tunnel and on site measurements for urban wind energy estimation of potential yield,” *Journal of Wind Engineering and Industrial Aerodynamics*, vol. 158, pp. 1–10, Nov. 2016, doi: 10.1016/j.jweia.2016.08.011.
- [11] Q. Wang, J. Wang, Y. Hou, R. Yuan, K. Luo, and J. Fan, “Micrositing of roof mounting wind turbine in urban environment: CFD simulations and lidar measurements,” *Renewable Energy*, vol. 115, pp. 1118–1133, Jan. 2018, doi: 10.1016/j.renene.2017.09.045.
- [12] M. A. Heath, J. D. Walshe, and S. J. Watson, “Estimating the potential yield of small building-mounted wind turbines,” *Wind Energy*, vol. 10, no. 3, pp. 271–287, 2007, doi: 10.1002/we.222.
- [13] S. V. Mikhailuta, A. A. Lezhenin, A. Pitt, and O. V. Taseiko, “Urban wind fields: Phenomena in transformation,” *Urban Climate*, vol. 19, pp. 122–140, Jan. 2017, doi: 10.1016/j.uclim.2016.12.005.

- [14] S. L. Walker, “Building mounted wind turbines and their suitability for the urban scale— A review of methods of estimating urban wind resource,” *Energy and Buildings*, vol. 43, no. 8, pp. 1852–1862, 2011, doi: <https://doi.org/10.1016/j.enbuild.2011.03.032>.
- [15] A. Rezaeiha, H. Montazeri, and B. Blocken, “A framework for preliminary large-scale urban wind energy potential assessment: Roof-mounted wind turbines,” *Energy Conversion and Management*, vol. 214, p. 112770, Jun. 2020, doi: [10.1016/j.enconman.2020.112770](https://doi.org/10.1016/j.enconman.2020.112770).
- [16] Y. Toparlar, B. Blocken, B. Maiheu, and G. J. F. van Heijst, “A review on the CFD analysis of urban microclimate,” *Renewable and Sustainable Energy Reviews*, vol. 80, pp. 1613–1640, Dec. 2017, doi: [10.1016/j.rser.2017.05.248](https://doi.org/10.1016/j.rser.2017.05.248).
- [17] T. Simões and A. Estanqueiro, “A new methodology for urban wind resource assessment,” *Renewable Energy*, vol. 89, pp. 598–605, 2016, doi: <https://doi.org/10.1016/j.renene.2015.12.008>.
- [18] A.-S. Yang, Y.-M. Su, C.-Y. Wen, Y.-H. Juan, W.-S. Wang, and C.-H. Cheng, “Estimation of wind power generation in dense urban area,” *Applied Energy*, vol. 171, pp. 213–230, Jun. 2016, doi: [10.1016/j.apenergy.2016.03.007](https://doi.org/10.1016/j.apenergy.2016.03.007).
- [19] F. Toja-Silva, A. Colmenar-Santos, and M. Castro-Gil, “Urban wind energy exploitation systems: Behaviour under multidirectional flow conditions—Opportunities and challenges,” *Renewable and Sustainable Energy Reviews*, vol. 24, pp. 364–378, Aug. 2013, doi: [10.1016/j.rser.2013.03.052](https://doi.org/10.1016/j.rser.2013.03.052).
- [20] J. Fields, F. Oteri, R. Preus, and I. Baring-Gould, “Deployment of Wind Turbines in the Built Environment: Risks, Lessons, and Recommended Practices,” NREL/TP--5000-65622, 1260340, Jun. 2016. doi: [10.2172/1260340](https://doi.org/10.2172/1260340).
- [21] SkyscraperPage, “Database - SkyscraperPage.com,” *SkyscraperPage*, May 02, 2021. <https://skyscraperpage.com/cities/> (accessed May 02, 2021).
- [22] K. Ahmad, “06/01841 Wind tunnel simulation studies on dispersion at urban street canyons and intersections — a review: Ahmad, K. et al. Journal of Wind Engineering and Industrial Aerodynamics, 2005, 93, (9), 697–717,” *Fuel and Energy Abstracts*, vol. 47, no. 4, p. 279, Jul. 2006, doi: [10.1016/S0140-6701\(06\)81847-3](https://doi.org/10.1016/S0140-6701(06)81847-3).
- [23] G. F. Garuma, “Review of urban surface parameterizations for numerical climate models,” *Urban Climate*, vol. 24, pp. 830–851, Jun. 2018, doi: [10.1016/j.uclim.2017.10.006](https://doi.org/10.1016/j.uclim.2017.10.006).
- [24] H. Mittal, A. Sharma, and A. Gairola, “A review on the study of urban wind at the pedestrian level around buildings,” *Journal of Building Engineering*, vol. 18, pp. 154–163, Jul. 2018, doi: [10.1016/j.jobbe.2018.03.006](https://doi.org/10.1016/j.jobbe.2018.03.006).
- [25] *IEC 61400-2:2013*. 2013. [Online]. Available: <https://webstore.iec.ch/publication/5433>
- [26] E. Arteaga-López, C. Ángeles-Camacho, and F. Bañuelos-Ruedas, “Advanced methodology for feasibility studies on building-mounted wind turbines installation in urban environment: Applying CFD analysis,” *Energy*, vol. 167, pp. 181–188, 2019, doi: <https://doi.org/10.1016/j.energy.2018.10.191>.
- [27] A. Vallejo, “Procedimiento para la Caracterización del Viento Urbano como Fuente Energética en la Ciudad de Santo Domingo,” Instituto Tecnológico de Santo Domingo, Santo Domingo, 2018.
- [28] M. R. Islam, R. Saidur, and N. A. Rahim, “Assessment of wind energy potentiality at Kudat and Labuan, Malaysia using Weibull distribution function,” *Energy*, vol. 36, no. 2, pp. 985–992, Feb. 2011, doi: [10.1016/j.energy.2010.12.011](https://doi.org/10.1016/j.energy.2010.12.011).

- [29] F. C. Emejeamara and A. S. Tomlin, "A method for estimating the potential power available to building mounted wind turbines within turbulent urban air flows," *Renewable Energy*, vol. 153, pp. 787–800, Jun. 2020, doi: 10.1016/j.renene.2020.01.123.
- [30] J. Blackledge, E. Coyle, D. Kearney, E. Murphy, and M.-J. R. Duarte, "Wind Resource in the Urban Environment," *Forthcoming in The Journal of Applied Research in Innovative Engineering of the Built Environment*, 2013, Jan. 2012, doi: 10.21427/D70P7R.
- [31] K. Dai, A. Bergot, C. Liang, W.-N. Xiang, and Z. Huang, "Environmental issues associated with wind energy – A review," *Renewable Energy*, vol. 75, pp. 911–921, Mar. 2015, doi: 10.1016/j.renene.2014.10.074.
- [32] I. Paraschivoiu, "Wind Turbine Design: With Emphasis on Darrieus Concept - Ion Paraschivoiu," *Polytechnic International Press, Canada*, 2002. [https://books.google.com.do/books?hl=es&lr=&id=sefVtnVgso0C&oi=fnd&pg=PR13&ots=HmDYuSgz1d&sig=8Ef1nSjDDSp1SDRWbmPZiX\\_F\\_Go&redir\\_esc=y#v=onepage&q&f=false](https://books.google.com.do/books?hl=es&lr=&id=sefVtnVgso0C&oi=fnd&pg=PR13&ots=HmDYuSgz1d&sig=8Ef1nSjDDSp1SDRWbmPZiX_F_Go&redir_esc=y#v=onepage&q&f=false) (accessed Jul. 17, 2020).
- [33] T. Stathopoulos *et al.*, "Urban wind energy: Some views on potential and challenges," *Journal of Wind Engineering and Industrial Aerodynamics*, vol. 179, pp. 146–157, Aug. 2018, doi: 10.1016/j.jweia.2018.05.018.
- [34] D. Micallef and G. Van Bussel, "A Review of Urban Wind Energy Research: Aerodynamics and Other Challenges," *Energies*, vol. 11, no. 9, Art. no. 9, Sep. 2018, doi: 10.3390/en11092204.
- [35] Z. Tasneem *et al.*, "An analytical review on the evaluation of wind resource and wind turbine for urban application: Prospect and challenges," *Developments in the Built Environment*, vol. 4, p. 100033, Nov. 2020, doi: 10.1016/j.dibe.2020.100033.
- [36] G. C. Guerrero-Liquet, J. M. Sánchez-Lozano, M. S. García-Cascales, M. T. Lamata, and J. L. Verdegay, "Decision-Making for Risk Management in Sustainable Renewable Energy Facilities: A Case Study in the Dominican Republic," *Sustainability*, vol. 8, no. 5, Art. no. 5, May 2016, doi: 10.3390/su8050455.
- [37] UNFCCC, "Grid emission factor for the Dominican Republic (version 01.0)," May 15, 2021. [https://cdm.unfccc.int/methodologies/standard\\_base/2015/sb143.html](https://cdm.unfccc.int/methodologies/standard_base/2015/sb143.html) (accessed May 15, 2021).
- [38] K. Tierney and M. Bruneau, "Conceptualizing and Measuring Resilience: A Key to Disaster Loss Reduction," *TR News*, no. 250, May 2007, Accessed: Sep. 12, 2021. [Online]. Available: <https://trid.trb.org/view/813539>
- [39] M. Panteli, P. Mancarella, D. N. Trakas, E. Kyriakides, and N. D. Hatziargyriou, "Metrics and Quantification of Operational and Infrastructure Resilience in Power Systems," *IEEE Transactions on Power Systems*, vol. 32, no. 6, pp. 4732–4742, Nov. 2017, doi: 10.1109/TPWRS.2017.2664141.
- [40] M. Ouyang and L. Dueñas-Osorio, "Time-dependent resilience assessment and improvement of urban infrastructure systems," *Chaos: An Interdisciplinary Journal of Nonlinear Science*, vol. 22, no. 3, p. 033122, Aug. 2012, doi: 10.1063/1.4737204.
- [41] S. Ahmadi, Y. Saboohi, and A. Vakili, "Frameworks, quantitative indicators, characters, and modeling approaches to analysis of energy system resilience: A review," *Renewable and Sustainable Energy Reviews*, vol. 144, p. 110988, Jul. 2021, doi: 10.1016/j.rser.2021.110988.



# Comparison of Electric Vehicle Types Considering Tank-to-Wheel Emissions and Energy-Ecological Efficiency

Laene Oliveira Soares<sup>1</sup>, Vanessa de Almeida Guimarães<sup>1</sup>, Danielle Rodrigues de Moraes<sup>1</sup>, Ronney Arismel Mancebo Boloy<sup>1</sup>

<sup>1</sup> Group of Entrepreneurship, Energy, Environment and Technology – GEEMAT, Federal Centre of Technological Education Celso Suckow da Fonseca, Rio de Janeiro, Brazil

## Abstract

The present study compares the Tank-to-Wheel (TTW) emissions of the Plug-in Electric Vehicle (PEV), the Hybrid Electric Vehicle (HEV) and the Plug-in Hybrid Electric Vehicle (PHEV), considering the Brazilian scenario. For HEV and PHEV, an internal combustion engine in single-fuel mode (ICE-SF) fuelled with biogas, bioethanol, gasoline A, and Brazilian gasoline, and an internal combustion engine in dual-fuel mode (ICE-DF) fuelled with biogas and bioethanol were considered. Moreover, the energy-ecological efficiency of the ICE-SF and ICE-DF was measured to analyse the negative impacts on human and environmental health. The PEV presented lower TTW emissions, however, due to the lack of recharging infrastructure, the national biofuel market, and the possibility of reducing the vehicle carbon footprint based on savings in carbon fixation, the HEV fuelled with bioethanol or bioethanol-biogas blends is most appropriate to the current Brazilian scenario. Furthermore, the use of biomass for biofuel production shows potential to perform well in the carbon pricing market, already established in Brazil through RenovaBio program. The findings presented address topics that will help in policies to achieve zero carbon dioxide emissions in transport sector.

**Keywords.** Electric vehicles; Emissions; Energy-ecological efficiency; Tank-to-Wheel.

## 1. Introduction

The use of biofuels in the internal combustion engines (ICE) can be an alternative to reduce the emissions of pollutants that aggravates the climate changes and problems related to the human health. The biofuels are produced from lignocellulosic or cellulosic biomasses, urban or agroindustry wastes, etc, and can be classified as first-generation or second-generation biofuel, depending on their sources.

One common drawback of the ICE when fuelled with non-renewable fuels is the high level of negative environmental impact caused by the emissions of pollutant gases, such as: carbon dioxide (CO<sub>2</sub>), particulate matter (PM), nitric oxides (NO<sub>x</sub>), hydrocarbons (HC), etc, which increase the global warming and the human toxicity. Some types of electric vehicles have an internal combustion ICE, such as the hybrid electric vehicle (HEV) and the plug-in hybrid electric vehicle (PHEV), which is an important component to analyse in studies focused on the tailpipe emissions.

The ICE can operate in single-fuel mode, which only one fuel is injected in the chamber, or in dual-fuel mode, with the necessary adaptations, which two fuels are injected in the chamber. The internal combustion engine in dual-fuel mode (ICE-DF) is a technology projected to burn two fuels at the same time during the combustion process, when a gaseous fuel is burned predominantly with a percentual of liquid fuel, which is used to start the ignition [1]. The use of the ICE fuelled with biofuels contributes to the independence of the use of fossil fuels and to the reduction of greenhouse gases (GHG) emission, and the consequent decrease of the negative environmental impacts caused by non-renewable fuels combustion [2]. Understand the use of biofuels in the ICE is necessary to reduce the GHG and develop sustainable options of urban mobility transport, which is necessary to the criteria to be achieved in the smart, efficiency, and sustainable cities [3].

Finding an alternative to replace fossil fuels, Brazilian governmental agencies created incentives policies, as RenovaBio and Route 2030. The RenovaBio is a national biofuels policy established in 2017 by ANP (National Agency for Oil – in portuguese, Agência Nacional do Petróleo, Gás Natural e

Biocombustíveis) with the aim of: provide contributions to the fulfilment of the commitments determined by the country under the Paris Agreement; promote an expansion of biofuels in the energy matrix; and ensure predictability for the fuel market, inducing gains in energy efficiency and reduction of GHG emissions during the entire production process, availability and use of biofuels. The Route 2030 is the label given to law 13.755 that encourages research and development projects in the automotive area, extending to the auto parts sector and strategic vehicle production systems. Among the main directions of this program is the promotion of the use of biofuels and alternative forms of propulsion and valuing the Brazilian energy matrix. Brazil presents a relevant potential to produce biofuels from biomass, such as bioethanol, biogas, and hydrogen (green or blue), due to its rank position in world producer of sugarcane and cassava, for example, and the possibility of conversion of many organic wastes generated in the agroindustry.

The vehicles powered by an ICE are responsible for the majority fleet of light-duty vehicles in Brazil, which corresponded to almost 44,639,000 in 2020 [4], and the transport sector is the main source of emissions related to the Brazilian energy matrix, totalizing 49% equivalent carbon dioxide ( $\text{CO}_2_{\text{eq}}$ ) emitted in 2018 (SEEG, 2019). Thus, it is necessary to apply methods such as policies and government incentives to mitigate the emissions caused by this sector, such as: carbon regulations (e.g., carbon tax, carbon cap, carbon cap-and-trade etc.); the use of biofuels; the use of electric vehicles; actions to increase the energy efficiency; and the elaboration of emissions inventory (Guimarães, 2019).

### 1.1. State of Art

Most studies have used fossil fuels to power the ICE-DF, such as hydrogen and gasoline [7,8]. However, in many scenarios, the costs related to the hydrogen production, logistics, and storage, become the use of this fuel unfeasible [9]. Therefore, the use of biofuels can be an alternative to reduce the GHG emissions, as well as contributing to an eco-friendly urban mobility [3]. Recently, an investigation was published about the use of bioethanol and biogas in dual-fuel mode in three different conventional vehicles, where the Tank-to-Wheel (TTW) emissions were calculated for each vehicle category, such as 1.0, 1.6, and 2.0 [3]. The results showed that the use of 80% and 20% biogas in the mixture can reduce the TTW emissions, reaching values lower than gasoline A and liquefied petroleum gas (LPG). According to the authors, the energy-ecological efficiency of the mixture of 50% biogas and 50% bioethanol reached 47%, while the gasoline with 20% ethanol reached 41% and the gasoline with 27% ethanol, nowadays available in Brazilian refuelling stations, achieved 40%.

The focus of the studies available in the literature was around fuel economy applied mainly in the PHEV. This is because of the energy management system of the PHEV, which is a component to achieve better fuel economy in this type of electric vehicle [10]. Due to the fuel economy, the PHEV can be an alternative to reduce the tailpipe emissions, and this vehicle needs a medium or large battery size, ensuring an autonomy in pure electric mode; that means zero pollutant emissions.

The emissions of the electric vehicles were analysed to investigate the number of pollutants that aggravate global warming and/or human toxicity are emitted. Otherwise, the battery degradation also was the focus of many studies. Hu et al. (2016) analysed the usefulness of wind power to reduce the  $\text{CO}_2$  emissions of PHEV. The  $\text{CO}_2$  optimal scenario was compared with heuristics scenarios, considering daily battery degradation. The results showed that as wind power increases, the  $\text{CO}_2$  in an optimal scenario uses more electricity from the grid, which worsens the battery stress (Hu et al., 2016). On the other hand, the battery aging is “smaller under low and average wind power” (Hu et al., 2016). Silva et al. (2021) proposed a powertrain configuration and sizing optimization of the PHEV to improve the battery state of health and decrease its degradation through a multi-objective optimization design and control. According to the results, the best configuration was able to keep advantages as low fuel consumption and emissions, and the configuration proposed is robust to be used under different driving conditions.

Recently, the studies were directed to the life cycle assessment of the electric and conventional vehicles, considering alternative fuels. Yang et al. (2021) conducted an adopted life cycle assessment of electric and internal combustion engine vehicles in China to evaluate the  $\text{CO}_2$  and pollutant emissions since the vehicle production until its end-life. According to the authors, the PM and sulphur dioxide ( $\text{SO}_2$ ) emissions found for electric vehicles were higher than that found for conventional vehicles in their high renewable energy scenario. The emissions of different electric vehicle types still are the focus of recent studies around the world, aiming to find a way to decrease the negative impacts to environment and human health. Andersson and Börjesson (2021) conducted a study about GHG emissions of different electric vehicle types fuelled with renewable fuels, such as first-generation and second-generation biofuels. According to the results, the PHEV can reach more ambitious climate goals than the battery electric vehicle (BEV) [14].

## 1.2. Importance of the Study

The use of electric vehicle fuelled with biofuels can decrease significantly the emissions caused by the conventional vehicles fuelled with fossil fuels. Moreover, the dual-fuel mode can also contribute to reducing air pollution, once two fuels can be used and the most pollutant one can be replaced by a percentage of a less pollutant fuel, or use two biofuels, which can contribute even more to the environment. The Brazilian scenario, for example, presents an electric matrix mainly renewable and a great possibility to produce biofuels from biomass, such as sugarcane. It would be good to note that, in the last years, while there are efforts in the multiple topics such as fuel economy, emissions, life cycle assessment, none of the studies found investigated the use of biofuels in dual-fuel mode in electric vehicles. Also, up to date, no scientific works were found analysing the energy-ecological efficiency and TTW emissions of hybrid electric vehicles with biofuels inserted into the ICE-DF. In order to address this research gap, this paper applies a method based on pollutant indicators that considers negative impacts to human toxicity and climate change to evaluate the energy-ecological efficiency and mensurates the TTW emissions of the ICE powered by different fuels, including biofuels from sugarcane, in dual-fuel mode and single-fuel mode.

## 1.3. Purpose of the Study

With the considerations above, this study compares the Tank-to-Wheel (TTW) emissions of the Plug-in Electric Vehicle (PEV), the Hybrid Electric Vehicle (HEV) and the Plug-in Hybrid Electric Vehicle (PHEV), considering the Brazilian scenario. For HEV and PHEV, an internal combustion engine in single-fuel mode (ICE-SF) fuelled with biogas, bioethanol, gasoline A, and Brazilian gasoline, and an internal combustion engine in dual-fuel mode (ICE-DF) fuelled with biogas and bioethanol were considered. For this purpose, the pollution factors that consider the human toxicity and the global warming, and the pollution indicator were measured, and the emissions related to the Brazilian electricity mix were calculated. Moreover, the energy-ecological efficiency of the ICE-SF and ICE-DF was measured to analyse the negative impacts on human and environmental health.

Finally, this study was divided into four topics. First, the methodological procedures will be presented in Section 2, which will show three electric vehicle types analysed, the simulation of combustion of different fuels, and the calculation of the TTW emissions and the energy-ecological efficiency. In Section 3, the results about the calculations and simulation made will be discussed. In Section 4, the conclusions will be made aiming to highlight the results found.

## 2. Methodological Procedures

In this section, the equations to calculate the TTW emissions of the electric vehicles will be showed. Therefore, one electric vehicle was chosen for each category, such as: PHEV, HEV and Plug-in Electric (PEV). The TTW emissions will be measured considering the electric matrix, and the ICE-SF and ICE-DF fuelled with fossil fuels and biofuels from sugarcane. For the energy-ecological efficiency, the method elaborated by Carneiro and Gomes (2019) will be applied to estimate the negative impacts caused to human and environment health. Thus, this section will be divided in 5 items: Section 2.1 shows the three electric vehicles chosen to this study; Section 2.2 demonstrates the simulation of gasoline A, bioethanol, and biogas on GASEQ; Section 2.3 shows the TTW emissions measurement of the electric vehicles chosen, considering the emissions related to the Brazilian electricity mix; Section 2.4 demonstrates the method used to calculate the energy-ecological efficiency of the HEV and PHEV in ICE-SF and ICE-DF; Section 2.5 presents the parameters used in this study.

### 2.1. Electric Vehicles Analysed

For the analysis purpose in this study, three electric vehicles were chosen, as can be seen in Table 1, considering different types of electric vehicles: PEV, HEV and PHEV. The PEV is a type of electric vehicle that only operates with the energy provided by the grid through the plug and when the energy is over, this type needs to be connected in a recharge station. Different of the PEV, the HEV does not operate with the electricity provided by the grid, but by the energy generated through the conversion of the fuel consumed in the ICE into electricity to power the electric motor. Finally, the PHEV is a combination of the two types explained before, operating in two modes basically: electric mode, using the electricity provided by the grid; and conventional mode, using the ICE to provide energy needed to power the electric motor. When

the battery charge of the PHEV is over, this vehicle only will operate in 100% electric mode when plugged in a recharge station. When the PHEV operates in conventional mode, the battery is recharged by the spare energy that comes through the electric motor. These vehicle models were chosen because they are available in Brazil market, as the Zoe E-Tech and the Corolla Altis Hybrid, or already was available in Brazil, as the Volt II Generation, with some vehicles in the fleet.

**Table 1.** Types of electric vehicles analysed (Data based on their manufacturer manual).

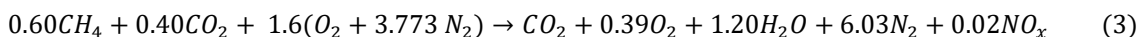
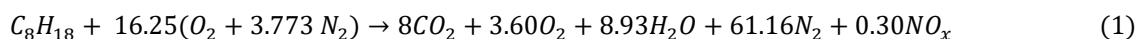
PEV		HEV		PHEV	
					
Brand	Renault	Brand	Toyota	Brand	Chevrolet
Model	Zoe E-Tech	Model	Corolla Altis Hybrid	Model	Volt II Generation
EM power	181 kW	EM power	96.6 kW	EM power	111 kW
EA	385 km	ICE power	135 kW	ICE power	75 kW
Battery capacity	52 kWh	FC	16.3 km/l	EA	85 km
				Battery capacity	18.4 kWh
				FC	15.87 km/l

EA – electric autonomy; FC – fuel consumption; EM – electric motor; ICE – internal combustion engine.

### 2.2. Simulation of the Combustion Process on GASEQ

The GASEQ software is a tool used to simulate applications in different thermodynamic scenarios, considering their stoichiometric equilibrium. In this study, equilibrium air-fuel mixtures were simulated, at a specific temperature of 300K and a pressure of 1 atm., corresponding to the combustion process of the MCI. For such simulation, this software uses as basis a Lagrange equation and Taylor series.

The combustion of gasoline A, bioethanol, and biogas (60% CH<sub>4</sub>) were simulated through the GASEQ software to quantify the emission factors and, finally, calculate the TTW emissions and the energy-ecological efficiency of the chosen electric vehicles. For these analyses, two ICE types were considered, the ICE-SF and the ICE-DF. The ICE-SF was fuelled with gasoline A, Brazilian gasoline (with 27% ethanol, in volume basis), bioethanol, and biogas; and the ICE-DF was fuelled with 50% bioethanol and 50% biogas. For the simulation, an air excess coefficient equal to 30%, was adopted to gasoline A and bioethanol, and 40% was adopted to biogas. The reaction combustion of gasoline A, bioethanol, and biogas are respectively presented in Eq. (1-3), which were calculated by the authors through the universal equation:  $Fuel + (O_2 + 3.773 N_2) \rightarrow CO_2 + H_2O$ . The other elements were taken from the simulation results, to make an equation more complete.



### 2.3. Tank-to-Wheel Emissions

The TTW emissions consider the instant since the vehicle refuel in the refuelling station until the disposal of exhaust gases, resulted from the fuel combustion. In this paper, the TTW emissions of the ICE-SF fuelled with gasoline A, Brazilian gasoline, bioethanol, and biogas, and the ICE-DF fuelled with 50% biogas and 50% bioethanol were analysed. Thus, The TTW for the ICE-SF and ICE-DF can be calculated through Eq. (4) and (5), respectively, as provided by [3]. The TTW for the Brazilian gasoline considers 27% bioethanol and 73% gasoline A, being calculated as can be seen in Eq. (6).

$$TTW_{ICE-SF} = \left( \frac{f_{CO_2 eq fuel} \times \rho_{fuel}}{FC_{fuel}} \right) \quad (4)$$

$$TTW_{ICE-DF} = z \left( \frac{f_{CO_2 \text{ eq biogas}} \times \rho_{biogas}}{FC_{biogas}} \right) + y \left( \frac{f_{CO_2 \text{ eq bioethanol}} \times \rho_{bioethanol}}{FC_{bioethanol}} \right) \quad (5)$$

$$TTW_{BR \text{ gasoline}} = \% e \left( \frac{f_{CO_2 \text{ eq bioethanol}} \times \rho_{bioethanol}}{FC_{bioethanol}} \right) + \% g \left( \frac{f_{CO_2 \text{ eq gasoline A}} \times \rho_{gasoline A}}{FC_{gasoline A}} \right) \quad (6)$$

Where,  $f_{CO_2 \text{ eq fuel}}$  is the  $CO_2 \text{ eq}$  emission factor resulted from the fuel combustion, in  $kg \text{ CO}_2 \text{ eq/kg fuel}$ ;  $\rho_{fuel}$  is the fuel density, in  $kg / m^3$ ;  $FC_{fuel}$  is the fuel consumption, in  $km/l$ ;  $f_{CO_2 \text{ eq biogas}}$  is the  $CO_2 \text{ eq}$  emission factor resulted from the biogas combustion, in  $kg \text{ CO}_2 \text{ eq/kg biogas}$ ;  $\rho_{biogas}$  is the biogas density, in  $kg/m^3$ ;  $FC_{biogas}$  is the biogas consumption, in  $km / l$ ;  $f_{CO_2 \text{ eq bioethanol}}$  is the  $CO_2 \text{ eq}$  emission factor resulted from the bioethanol combustion, in  $kg \text{ CO}_2 \text{ eq/kg bioethanol}$ ;  $\rho_{bioethanol}$  is the bioethanol density, in  $kg/m^3$ ;  $FC_{bioethanol}$  is the bioethanol consumption, in  $km/l$ ;  $z$  is the proportion of biogas in the mixture, where  $z = 0$  indicates operation with bioethanol only and  $z > 1$  indicates operation in dual mode with biogas;  $y$  is the proportion of bioethanol ( $1 - z$ );  $\% e$  is the percentual of ethanol;  $\% g$  is the percentual of gasoline A;  $f_{CO_2 \text{ eq gasoline A}}$  is the  $CO_2 \text{ eq}$  emission factor resulted from the gasoline A combustion, in  $kg \text{ CO}_2 \text{ eq/kg gasoline A}$ ;  $\rho_{gasoline A}$  is the gasoline A density, in  $kg/ m^3$ ;  $FC_{gasoline A}$  is the gasoline A consumption, in  $km/l$ .

In the Chevrolet and Toyota manuals, the fuel consumption provided for the PHEV and PEV models refers to the gasoline A consumption. So, the energy consumption will be calculated, through the Eq. (7), to mensurate the energy consumption needed in the ICE. Thus, the fuel consumption can be calculated through the Eq. (8), considering the energy consumption found [3].

$$E_{consump} = \frac{LHV_{gasoline A} \times \rho_{gasoline A}}{1000 \times FC_{gasoline A}} \quad (7)$$

$$FC_{fuel} = \frac{LHV_{fuel} \times \rho_{fuel}}{E_{consump} \times 1000} \quad (8)$$

Where,  $E_{consump}$  is the energy consumption needed in the ICE, in  $MJ/km$ ;  $LHV_{gasoline A}$  is the low heating value of the gasoline A, in  $MJ/kg \text{ gasoline A}$ ,  $FC_{fuel}$  is the fuel consumption, in  $km/l$ ;  $LHV_{fuel}$  is the low heating power of the fuel, in  $MJ/kg \text{ fuel}$ .

The emissions related to the electricity consumption will be calculated for the PEV and PHEV, as shown in Eq. (9), once the HEV is a type of electric vehicle that only consumes energy provided by the ICE.

$$E_{electric mode} = \frac{C_b \times E_{Brazilian mix}}{A_{electric}} \quad (9)$$

Where,  $E_{electric mode}$  is the emission related to the electricity consumption, when operating in electric mode, in  $gCO_2 \text{ eq/km}$ ;  $C_b$  is the battery capacity, in  $kWh$ ;  $E_{Brazilian mix}$  is the emission related to the Brazilian electricity mix;  $A_{electric}$  is the electric autonomy of the vehicle, when operating in electric mode, in  $km$ .

#### 2.4. Energy-Ecological Efficiency

The energy-ecological efficiency is a method that makes a comparison between the pollutant emissions issued by this process and the air quality standards [16], to evaluate the potential of pollution of the fuels used and their efficacy [15]. Thus, applying this method to the ICE fuelled with biogas, bioethanol, gasoline A, and Brazilian gasoline will be easy to compare their environmental impacts with other vehicle technologies, as well single-fuel or dual-fuel mode. From this method, it is possible to estimate the negative impacts to the human and environmental health. According to Carneiro and Gomes (2019), the energy-ecological efficiency is calculated as shown in Eq. (10).

$$\varepsilon = \left[ 2.01 \frac{\eta}{\eta + \Pi} \ln(1.645 \pm \Pi) \right]^{1.7} \quad (10)$$

Where,  $\varepsilon$  is the energy-ecological efficiency;  $\eta$  is the brake thermal efficiency of the ICE; and  $\Pi$  is the pollution indicator, in  $\text{kg}_{\text{eq pollutant}}/\text{MJ}_{\text{fuel}}$ . The pollution indicator  $\Pi$  consists in two pollution factors and can be expressed through the Eq. (11).

$$\Pi = 0.742 \Pi_{HT} + 0.258 \Pi_{GW} \quad (11)$$

Where,  $\Pi_{GW}$  (in  $\text{kg}_{\text{eq pollutant}}/\text{MJ}_{\text{fuel}}$ ) and  $\Pi_{HT}$  (in  $\text{kg}_{1.4\text{DCB}_{\text{eq}}}/\text{kg}_{\text{fuel}}$ ) are pollution factors that considers the emissions that contribute to the global warming and human toxicity, respectively. These pollution factors and their respective equivalent emission factors can be calculated through the Eq. (12-15).

$$\Pi_{GW} = \frac{f_{CO2\text{eq}}}{LHV_{fuel}} \quad (12)$$

$$\Pi_{HT} = \frac{f_{1,4\text{DCB}_{\text{eq}}}}{LHV_{fuel}} \quad (13)$$

$$f_{CO2\text{eq}} = f_{CO2} + 28f_{CH4} + 265f_{N2O} \quad (14)$$

$$f_{1,4\text{DCB}_{\text{eq}}} = 4.54f_{SO2} + 56.71f_{NOx} + 38.75f_{PM} \quad (15)$$

Where,  $f_{CO2\text{eq}}$  is the equivalent carbon dioxide emission factor, in  $\text{kg}_{CO2\text{eq}}/\text{kg}_{\text{fuel}}$ ;  $f_{1,4\text{DCB}_{\text{eq}}}$  is the equivalent 1,4-dichlorobenzene emission factor, in  $\text{kg}_{1,4\text{-DCB}_{\text{eq}}}/\text{kg}_{\text{fuel}}$ ;  $LHV_{fuel}$  is the low heating value of the fuel, in  $\text{MJ}/\text{kg}_{\text{fuel}}$ . The  $f_{specie}$  is the specie emission factor and can be calculated as can be seen in Eq. (16).

$$f_{specie} = \frac{(n_{specie} \times W_{specie})}{(n_{fuel} \times W_{fuel})} \quad (16)$$

Where,  $n_{specie}$  is the number of mols of the specie;  $W_{specie}$  is the molecular weight of the specie;  $n_{fuel}$  is the number of mols of the fuel;  $W_{fuel}$  the molecular weight of the fuel.

## 2.5. Parameters and Considerations Adopted in this Study

The parameters and considerations adopted to the TTW emissions of the ICE-SF and the ICE-DF, and the energy-ecological efficiency of different fuels are presented in Table 2.

**Table 2.** Parameters and considerations adopted.

Parameter	Value	Unit	Source
Electric motor power – PEV	181	kW	Renault
Electric autonomy – PEV	385	km	Renault
Battery capacity - PEV	52	kWh	Renault
Electric motor power – HEV	96.6	kW	Toyota
ICE power – HEV	135	kW	Toyota
Fuel consumption - HEV	16.3	km/l	Toyota
Electric motor power – PHEV	111	kW	Chevrolet
ICE power – PHEV	75	kW	Chevrolet
EA – PHEV	85	Km	Chevrolet
Battery capacity – PHEV	18.4	kWh	Chevrolet
Fuel consumption – PHEV	15.87	km/l	Chevrolet
Gasoline molecular weight	114	g	Calculated by the authors
Ethanol molecular weight	46	g	Calculated by the authors
Biogas molecular weight	60	g	Calculated by the authors
Air excess coefficient – Biogas	40	%	Coronado et al. (2009)
Air excess coefficient – Bioethanol	30	%	Coronado et al. (2009)
Air excess coefficient – Gasoline	30	%	Coronado et al. (2009)
Density - Anhydrous ethanol	791	kg/m <sup>3</sup>	ANP (2019)
Density - Sugarcane vinasse	1,031	kg/m <sup>3</sup>	Prasad & Shih (2016)
Density – Vinasse biogas	0.784	kg/m <sup>3</sup>	Neto et al. (2017)
Density – Gasoline A	742	kg/m <sup>3</sup>	ANP (2019)
Density – Brazilian gasoline	754	kg/m <sup>3</sup>	ANP (2019)
Density - Anhydrous ethanol	791	kg/m <sup>3</sup>	ANP (2019)
LHV – Anhydrous ethanol	28,242	kJ/kg	ANP (2019)
LHV – Vinasse biogas	23,200	kJ/kg	Lima. and Passamani. (2012)
LHV – Gasoline A	43,543	kJ/kg	ANP (2019)
LHV – Brazilian gasoline	39,356	kJ/kg	ANP (2019)
Z	50	%	da Costa et al. (2020)
BTE <sub>dual-fuel</sub> (for z = 50%)	36.1	%	da Costa et al. (2020)
BTE <sub>bioethanol</sub>	25	%	Balki et al. (2014)
BTE <sub>gasoline</sub>	23	%	Balki et al. (2014)
Brazil electricity mix	416.3	gCO <sub>2eq</sub> /kWh	EPE (2020b)

### 3. Results and Discussion

In this study, the TTW emissions of the ICE-SF and ICE-DF fuelled with fossil fuels and biofuels from sugarcane were mensurated, as well as their energy-ecological efficiency. Then, the pollutant emitted through the combustion process were simulated using the GASEQ software, which values found were used to calculate the energy-ecological efficiency. The comparison of three types of electric vehicle (i.e., PEV, HEV and PHEV) was made to investigate the most appropriate electric vehicle for the Brazilian context, considering the electricity mix, the biofuels production, and the country infrastructure.

### 3.1. Tank-to-Wheel Emissions

The TTW emissions of the ICE-SF powered by gasoline A, Brazilian gasoline, bioethanol and biogas and the ICE-DF powered by bioethanol and biogas were determined. For the calculation, a 15 m<sup>3</sup> cylinder was considered for biogas storage, stipulating a vehicle consumption of 12 km/m<sup>3</sup> [3]. The fuel consumption of the vehicles, in km/l, were calculated and the results are shown in Table 2. The Brazilian gasoline consumption was not calculated because the TTW emissions was determined by applying the percentage of 73% gasoline and 27% bioethanol.

**Table 3.** Consumption found for different fuels.

HEV – Toyota – Corolla Altis Hybrid		
Fuel	Consumption	Reference
Gasoline A	23.57 km/l	Calculated by the authors (Eq. F)
Bioethanol	16.30 km/l	Toyota
Biogas	0.013 km/l	Calculated by the authors (Eq. F)
PHEV – Chevrolet – Volt II Generation		
Fuel	Consumption	Reference
Gasoline A	15.87 km/l	Chevrolet
Bioethanol	10.97 km/l	Calculated by the authors (Eq. F)
Biogas	0.0089 km/l	Calculated by the authors (Eq. F)

Through the Eq. (4-6) was possible to calculate the TTW emissions for the ICE-SF and the ICE-DF, and the TTW emissions related to Brazilian gasoline. In addition to the emissions related to the combustion in the ICE, the emissions related to the electricity mix was analysed. The emissions related to the Brazilian electricity mix considered only fossil fuels as source, such as: coal, natural gas, fuel oil and diesel oil once the annual information considers them. This analysis is necessary because the grid provides electricity to be storage in the PEV and PHEV batteries. The results are shown in Fig. 1.

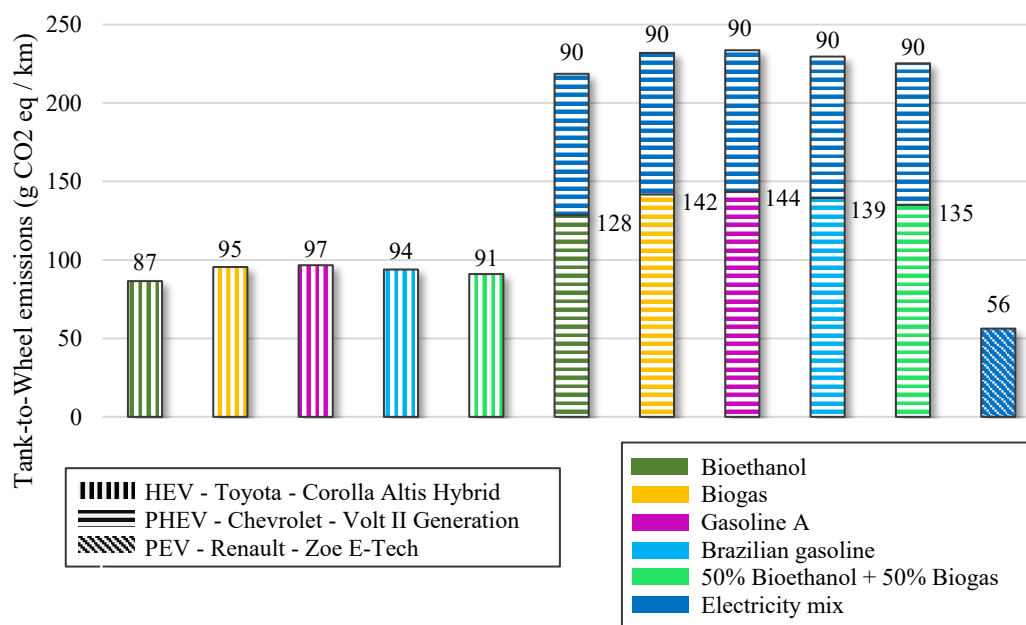


**Figure 1.** Tank-to-Wheel emissions of the three electric vehicle types analysed.

The highest values found were related to the PHEV, because this type of vehicle operates using the ICE and the energy provided from the grid. Firstly, the PHEV chosen to this analysis presented lower mileage per litre of fuel than the HEV and, secondly, the PHEV presented electric autonomy and battery capacity

78% and 65% lower, respectively, than the PEV analysed in this study. It means that the PEV can storage more energy and travel more mileage in electric mode, presenting lower electric consumption, and consequently emitting less  $\text{g CO}_2_{\text{eq}}$  per kilometre than the PHEV.

Considering that the electricity mix in Brazil is mostly compound by renewable sources, which according to the Energy Research Company (in Portuguese, Empresa de Pesquisa Energética – EPE) (EPE, 2020a) only 6.4% of the electricity is generated provided by coal and fossil fuels, the emissions related to the electricity consumption can be drastically reduced or tend to zero once the renewable sources do not emit  $\text{CO}_2_{\text{eq}}$ , when compared to the TTW emissions caused by burning fuels. Thus, Brazil would present an advantage in using electric vehicle in the transport sector.

In the scope of the infrastructure, the PEV and the PHEV have a disadvantage, once the recharge stations are not available in large scale in Brazil and the fewer number of electric vehicles to charge. In 2018, ANEEL approved a Normative Resolution that is the first regulation about the recharging of electric vehicles by those interested in providing this service in any location, such as gas stations, shopping centers etc. any interested party is allowed to carry out electric vehicle recharge activities, including for the purpose of commercial exploitation are freely negotiated prices, the so-called public recharge. Thus, the local distributors can install charging stations in their areas of operation for public or private charging. For this purpose, the agency requests some data from the interested party, such as the installation location, number of recharging points per station, and supply voltage. It is possible that more government incentives are needed to implement large-scale recharging stations.

In view of the fuel options, Brazil presents high potential for biofuel production, once it is the major sugarcane producer in the world, being able to produce bioethanol and biogas from sugarcane biomasses. Besides that, bioethanol from sugarcane is available in the refuelling stations across the country. The advantage of using biofuels is that the  $\text{CO}_2$  fixed in the biomass during the photosynthetic reaction returns to the atmosphere when the plant is processed. Thus, TTW emissions issued by biofuels would be deducted, reducing the negative environmental impacts. When the emissions are considered, PEV was found as the best choice since the model chosen presented lower TTW emissions than the other models analysed. However, considering the lack of infrastructure, the national use of biofuels, and the possibility of deduction of the carbon fixed from the vehicle carbon footprint, the HEV fuelled with bioethanol or bioethanol-biogas blends is most appropriate to the Brazilian scenario.

Furthermore, the use of biomass for biofuel production shows potential to perform well in the carbon pricing market. Carbon pricing is a regulatory instrument that generates cost-effectiveness gains, i.e., it demonstrates mitigation potential by directing consumer demands and investments to services and technologies with a lower carbon footprint (CEBDS, 2016). The RenovaBio program plays an important role through the implementation of Decarbonization Credits (CBIO), applied to certified Brazilian producers and importers of biofuels. This instrument aims to value efficient agents in the biofuels market and generate incentives to reduce the carbon intensity of their production process each year. According to projections by the International Council on Clean Transportation, the CBIO provide incentives for better performing sugarcane ethanol producers, with an emphasis on bagasse ethanol (i.e., second-generation ethanol) producers which generates 95% carbon savings over fossil gasoline (ICCT, 2019).

### 3.2. Calculation of Emission Factors and Pollutant Indicators

In this section, the emission factors and pollutant indicators were simulated to calculate the energy-ecological efficiency of different fuels powering the ICE of the PHEV and the HEV. The combustion of gasoline A, bioethanol and biogas was simulated through the GASEQ software, considering the values of  $\text{CO}_2$ ,  $\text{CH}_4$ ,  $\text{N}_2\text{O}$ ,  $\text{SO}_2$ ,  $\text{NO}_x$  and PM, once these are the incognitos visualized in Eq. (14-15) to mensurate the carbon dioxide and the 1,4-Dichlorobenzene emission factors and the pollutant indicators that contributes to global warming and human toxicity, respectively. Table 3-5 show the reactants and products of the bioethanol, gasoline A and biogas combustion, and the number of moles, molecular weight, and equivalent emission factor of each product specie. The results shown in the Tables were compared to that simulated in previous study from [3].

**Table 4.** Reactants and products of the bioethanol combustion, and the emission factor of the resultant species.

Reactants	No. Moles	Mol. Weight	
C <sub>2</sub> H <sub>5</sub>	1,00000	29	
OH	1,00000	17	
O <sub>2</sub>	3,90000	32	
N <sub>2</sub>	14,71470	28	
Products	No. Moles	Mol. Weight	<i>f<sub>specie</sub></i>
CO <sub>2</sub>	1,86156	44	1,7806226
CH <sub>4</sub>	0,00000	16	1,335E-17
N <sub>2</sub> O	0,00001	44	7,17E-06
SO <sub>2</sub>	0,00000	64	0
NO <sub>x</sub>	0,15834	30	0,1032641
PM	0,00000	12	0

**Table 5.** Reactants and products of the biogas combustion, and the emission factor of the resultant species.

Reactants	No. Moles	Mol. Weight	
CH <sub>4</sub>	0,60000	16	
CO <sub>2</sub>	0,40000	44	
O <sub>2</sub>	1,60000	32	
N <sub>2</sub>	6,03680	28	
Products	No. Moles	Mol. Weight	<i>f<sub>specie</sub></i>
CO <sub>2</sub>	0,99880	44	1,615705882
CH <sub>4</sub>	0,00000	16	6,96471E-23
N <sub>2</sub> O	0,00000	44	1,40849E-06
SO <sub>2</sub>	0,00000	64	0
NO <sub>x</sub>	0,01807	30	0,019928923
PM	0,00000	12	0

**Table 6.** Reactants and products of the gasoline A combustion, and the emission factor of the resultant species.

Reactants	No. Moles	Mol. Weight	
C <sub>8</sub> H <sub>18</sub>	1,00000	114	
O <sub>2</sub>	16,25000	32	
N <sub>2</sub>	61,31100	28	
Products	No. Moles	Mol. Weight	<i>f<sub>specie</sub></i>
CO <sub>2</sub>	7,94998	44	3,068413333
CH <sub>4</sub>	0,00000	16	1,00281E-20
N <sub>2</sub> O	0,00001	44	5,63895E-06
SO <sub>2</sub>	0,00000	64	0
NO <sub>x</sub>	0,29759	30	0,078313158
PM	0,00000	12	0

To calculate the equivalent emission factors of the Brazilian gasoline, the percentage of 27% ethanol needed to be added to the gasoline A. Thus, 27% of the equivalent emission factors found for bioethanol were added to 73% of the equivalent emission factors found for gasoline A. The same was done to the ICE-DF powered by 50% bioethanol and 50% biogas. The equivalent emission factors of the ICE-SF fuelled with bioethanol, biogas, gasoline A, Brazilian gasoline and the ICE-DF fuelled with biogas and bioethanol

are presented in Table 7. The CO<sub>2</sub>, CH<sub>4</sub> and N<sub>2</sub>O emission factors were considered to calculate the  $f_{CO_2 \text{ eq}}$ , and the SO<sub>2</sub>, NO<sub>x</sub> and PM were considered to measure the  $f_{1.4\text{-DCB eq}}$ .

**Table 7.** Equivalent emission factors found for different fuels.

Equivalent Emission Factors	Fuels				
	Bioethanol	Biogas	Gasoline A	BR Gasoline <sup>1</sup>	Dual-Fuel <sup>2</sup>
$f_{CO_2 \text{ eq}}$ (kgCO <sub>2eq</sub> / kg <sub>fuel</sub> )	1,7825	1,6160	3,0699	2,7223	1,6993
$f_{1.4\text{-DCB eq}}$ (kg 1.4DCB <sub>eq</sub> / kg <sub>fuel</sub> )	5,8561	1,1301	4,4411	4,8231	3,4931

<sup>1</sup>Brazilian gasoline – 27% bioethanol + 73% gasoline A; <sup>2</sup>ICE fuelled with 50% bioethanol and 50% biogas.

As can be seen, the combustion of gasoline A presented the highest  $f_{CO_2 \text{ eq}}$  value between the fuels analysed due to its highest value of CO<sub>2</sub> produced during its combustion. This value is approximately 12.8% higher than that found for Brazilian gasoline. On the other hand, the Brazilian gasoline resulted in 8.6% more  $f_{1.4\text{-DCB eq}}$  than gasoline A. It can be explained by the percentage of bioethanol, nowadays available in the refuelling stations in Brazil, that compounds the Brazilian gasoline, which presented the highest  $f_{1.4\text{-DCB eq}}$  value. The ICE-DF presented  $f_{CO_2 \text{ eq}}$  value 44.6% and 37.6% lower than that found for gasoline A and Brazilian gasoline, respectively.

The pollution factors that consider the global warming ( $\Pi_{GW}$ ) and the human toxicity ( $\Pi_{HT}$ ), and pollution indicators ( $\Pi$ ) were calculated. It is important to highlight that the  $\Pi$  is mainly compound by  $\Pi_{HT}$ , which represents 74,2% of its total. The results are shown in Fig. 2. As can be seen, the gasoline A presented the highest  $\Pi_{GW}$  among the fuels analysed, due to its highest  $f_{CO_2 \text{ eq}}$  value. In the same way, the bioethanol resulted in the highest  $\Pi_{HT}$ , due to its highest  $f_{1.4\text{-DCB eq}}$  value. It increases the  $\Pi_{HT}$  value found for Brazilian gasoline and the bioethanol + biogas in dual-fuel mode, because of the percentage of bioethanol in these mixtures. The 50% bioethanol and 50% biogas powering the ICE-DF presented  $\Pi_{GW}$  value 5.2% higher than that found for bioethanol. It can be explained by the percentage of biogas in the mixture, which presented  $\Pi_{GW}$  value 10.4% higher than that found for biogas, aggravating the  $\Pi_{GW}$  value for the mixture in dual-fuel mode. Finally, the highest  $\Pi$  value was found for bioethanol, which presented a result 51.7% higher than that found for the mixture of biogas and bioethanol in dual-fuel mode. The Brazilian gasoline presented a  $\Pi$  value 2.1% higher than that found for biogas and bioethanol in dual-fuel mode.

The elevated NO<sub>x</sub> emission is the main reason for the high human toxicity potential of ethanol. Studies have been carried out in order to achieve an optimal spark-ignition engine performance concerning NO<sub>x</sub> control. Najafi et al. (2015) considered an ICE powered by gasoline with 5-15% of ethanol blends for performance optimization using response surface methodology. The authors have found that the concentration of NO<sub>x</sub> emissions increased by introducing ethanol blends and, for an engine speed of 3000 rpm, a blend of 10% bioethanol and 90% gasoline was the best scenario. Al-Harbi et al. (2022) also analysed the NO<sub>x</sub> emissions from ethanol-gasoline blends to enhance spark-ignition engines. The results indicated a decrease in NO<sub>x</sub> emissions by increasing the air-fuel ratio to reach the minimum at the highest lean condition, however, this solution was followed by an increase in fuel consumption.

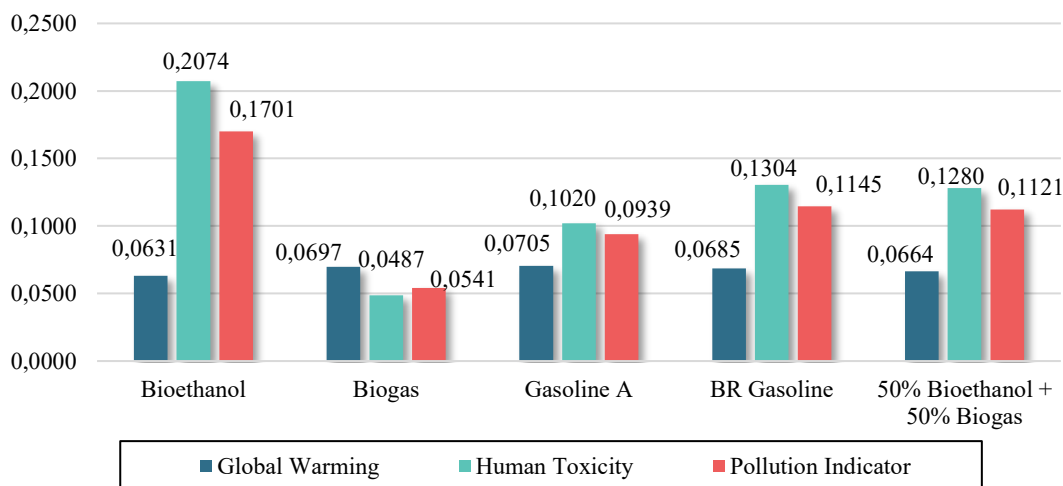


Figure 2. Pollution factors and pollution indicators found for different fuels.

### 3.3. Energy-Ecological Efficiency

The energy-ecological efficiency ( $\epsilon$ ) was calculated for the ICE-SF fuelled with biogas, bioethanol, gasoline A and Brazilian gasoline, and for the ICE-DF powered by 50% bioethanol and 50% biogas. As can be seen in Fig. 3, the ICE-SF fuelled with biogas presented the highest  $\epsilon$  because of the lowest pollution indicator and pollution factors found for this biofuel. Besides that, the percentage of biogas in the ICE-DF increased its  $\epsilon$  value, resulting in  $\epsilon$  25.6% higher than that found for Brazilian gasoline. The lowest  $\epsilon$  was found for bioethanol because of its human toxicity pollution factor and pollution indicator, which presented the highest value between the fuels analysed. Thus, the best choices to power the HEV and PHEV, which are the electric vehicle types that operates with an ICE, are fuelling the ICE-SF with biogas or fuelling the ICE-DF with bioethanol and biogas.

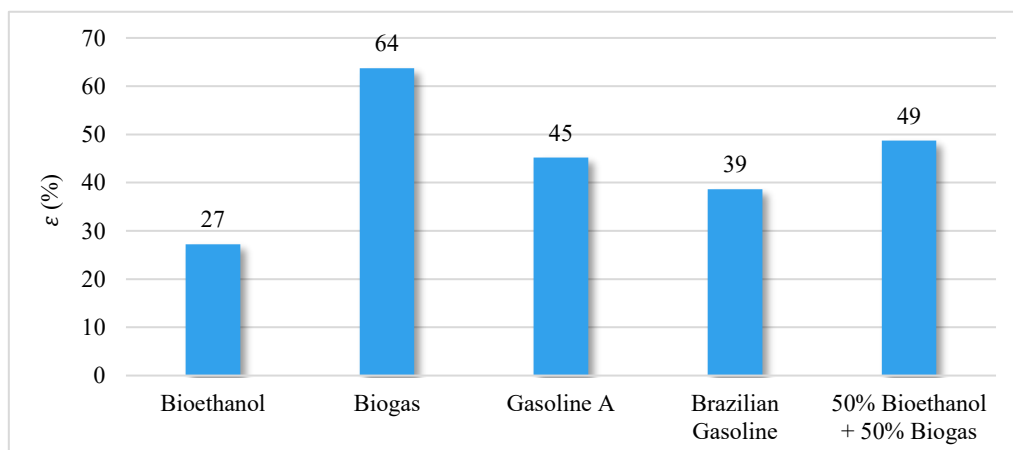


Figure 3. Energy-ecological efficiency for different fuels.

The ICE-DF fuelled with bioethanol and biogas presented an  $\epsilon$  value higher than that found for gasoline A, bioethanol, and Brazilian gasoline. Even though the  $\epsilon$  value found for the dual-fuel mode is a little smaller than that found for gasoline A, three points must be considered to make advantage to the dual-fuel fuelled with biofuels: first, the gasoline A is a fossil fuel, which means that its use should be reduced along the year (as well as Brazilian gasoline), and is a fuel that is not available in Brazil; second, the biofuel from sugarcane or any other biomass, present fixed  $\text{CO}_2$  rate that must be deducted from the biofuel emissions; three, the  $\epsilon$  value can be even bigger if the percentual of biogas is higher. Thus, the  $\epsilon$  value of the ICE-DF

fuelled with bioethanol and biogas will be increased, as much as the  $\epsilon$  value for bioethanol and for biogas in the ICE-SF, once these biofuels present a percentual of carbon fixed on their biomass.

#### 4. Conclusions and Further Work

In summary, through the results, the PEV presented less TTW emissions between the vehicles analysed. However, considering the infrastructure and the use of biofuels, the HEV fuelled with bioethanol, in single-fuel mode, or bioethanol and biogas, in dual-fuel mode, would be most appropriate to the Brazilian scenario due to the Brazilian infrastructure, its electricity mix, which is mainly renewable, and its potential to produce biofuels. Besides that, the results showed that the ICE-SF fuelled with bioethanol presented the lowest energy-ecological efficiency ( $\epsilon$ ) between the fuels analysed, and the ICE-DF powered by bioethanol and biogas presented a higher  $\epsilon$  value than that found for gasoline A, Brazilian gasoline, and bioethanol.

However, three points must be considered to make advantage to the dual-fuel fuelled with biofuels: first, the gasoline A is a fossil fuel, which means that its use should be disincentivised, and is a fuel that is not available in Brazil; second, the biofuel from biomass, as sugarcane, presents fixed CO<sub>2</sub> rate that must be deducted from the biofuel emissions, been a positive point to replace the fossil fuels; three, the  $\epsilon$  value can be even bigger if the percentual of biogas is higher, which presented the lower  $\epsilon$  value between the fuels analysed.

The dual-fuel technology fuelled with biofuels offers a less environmental impact when compared to single-fuel mode for use of a wide range of PHEV and HEV. The findings presented address topics that will help in policies to achieve zero carbon dioxide emissions in transport sector. But, the dissemination of the electric vehicles depends on many factors, including government interest and investments.

The electric vehicles analysed in this study were chosen considering the vehicles available in Brazil, as well as bioethanol and biogas from sugarcane, once bioethanol from sugarcane is nowadays available in the refuelling stations, and due to the ranking that Brazil occupies between the sugarcane productors.

For further work, vehicles that make up the collective vehicle fleet will be analysed fuelled with different biofuels and alternative fuel, as hydrogen. Moreover, the carbon fixed by the sugarcane plantations will be considered and the life cycle cost of the electric vehicle types will be analysed. An analysis is suggested considering other countries scenarios and their public policies that encourage the implementation of large-scale electric vehicles.

**Acknowledgment:** The authors are very grateful to the financial support provided by the Brazilian National Council for Scientific and Technological Development (CNPq) with the project, title in Portuguese “Misturas Biogás-Biodiesel utilizadas em sistemas de injeção dual-fuel dos Motores de Combustão Interna a Compressão” [406789/2018-5]; the Iberoamerican Program of Science and Technology for Development (CYTED) with the project Smart Cities Totally Comprehensive, Efficient and Sustainable (CITIES) – CODE 518RT0557; and was financed in part by the Coordenação de Aperfeiçoamento de Pessoal de Nível Superior - Brasil (CAPES) - Finance Code 001.

## References

1. Liu H, Wang Z, Long Y, Wang J. Dual-Fuel Spark Ignition (DFSI) combustion fuelled with different alcohols and gasoline for fuel efficiency. *Fuel* 2015;157:255–60. <https://doi.org/10.1016/j.fuel.2015.04.042>.
2. Ramachandran S, Stimming U. Well to wheel analysis of low carbon alternatives for road traffic. *Energy Environ Sci* 2015;8:3313–24. <https://doi.org/10.1039/c5ee01512j>.
3. Soares LO, de Moraes DR, Boloy RAM. Energy-Ecological Efficiency and TTW Emissions of the DFSIE Fuelled with Biofuels. *Bioenergy Res* 2021;14:623–33. <https://doi.org/10.1007/s12155-020-10229-1>.
4. Sindipeças, Abipeças. Relatório da Frota Circulante - Edição 2019 2019:13.
5. System Gas Emissions Estimation (SEEG). *Análise das Emissões Brasileiras de Gases de Efeito Estufa*. 2019.
6. Guimarães V de A. Localização-alocação de centros de integração logística considerando critérios econômicos e ambientais. UFRJ, 2019.
7. Wu H, Yu X, Du Y, Ji X, Niu R, Sun Y, et al. Study on cold start characteristics of dual fuel SI engine with hydrogen direct-injection. *Appl Therm Eng* 2016;100:829–39. <https://doi.org/10.1016/j.applthermaleng.2016.02.097>.
8. Sun P, Liu Z, Yu X, Yao C, Guo Z, Yang S. Experimental study on heat and exergy balance of a dual-fuel combined injection engine with hydrogen and gasoline. *Int J Hydrogen Energy* 2019;44:22301–15. <https://doi.org/10.1016/j.ijhydene.2019.06.149>.
9. da Silva César A, da Silva Veras T, Mozer TS, da Costa Rubim Messeder dos Santos D, Conejero MA. Hydrogen productive chain in Brazil: An analysis of the competitiveness' drivers. *J Clean Prod* 2019;207:751–63. <https://doi.org/10.1016/j.jclepro.2018.09.157>.
10. Qi X, Luo Y, Wu G, Boriboonsomsin K, Barth MJ. Deep reinforcement learning-based vehicle energy efficiency autonomous learning system. *IEEE Intell Veh Symp Proc* 2017:1228–33. <https://doi.org/10.1109/IVS.2017.7995880>.
11. Hu X, Zou Y, Yang Y. Greener plug-in hybrid electric vehicles incorporating renewable energy and rapid system optimization. *Energy* 2016;111:971–80. <https://doi.org/10.1016/j.energy.2016.06.037>.
12. Silva SF da, Eckert JJ, Silva FL, Silva LCA, Dedini FG. Multi-objective optimization design and control of plug-in hybrid electric vehicle powertrain for minimization of energy consumption, exhaust emissions and battery degradation. *Energy Convers Manag* 2021;234:113909. <https://doi.org/10.1016/j.enconman.2021.113909>.
13. Yang L, Yu B, Yang B, Chen H, Malima G, Wei YM. Life cycle environmental assessment of electric and internal combustion engine vehicles in China. *J Clean Prod* 2021;285:124899. <https://doi.org/10.1016/j.jclepro.2020.124899>.
14. Andersson Ö, Börjesson P. The greenhouse gas emissions of an electrified vehicle combined with renewable fuels: Life cycle assessment and policy implications. *Appl Energy* 2021;289. <https://doi.org/10.1016/j.apenergy.2021.116621>.
15. Carneiro MLNM, Gomes MSP. Energy-ecologic efficiency of waste-to-energy plants. *Energy Convers Manag* 2019;195:1359–70. <https://doi.org/10.1016/j.enconman.2019.05.098>.
16. Cârdu M, Baica M. A seismic vision regarding a methodology to estimate globally the energy-ecologic efficiency of thermopower plants (TPPs). *Energy Convers Manag* 2001;42:1317–25. [https://doi.org/10.1016/S0196-8904\(00\)00138-2](https://doi.org/10.1016/S0196-8904(00)00138-2).
17. Coronado CR, de Carvalho JA, Yoshioka JT, Silveira JL. Determination of ecological efficiency in internal combustion engines: The use of biodiesel. *Appl Therm Eng* 2009;29:1887–92. <https://doi.org/10.1016/j.applthermaleng.2008.10.012>.
18. ANP. *Anuário Estatístico Brasileiro* 2019:1–264.
19. Neto, A. E.; Shintaku, A.; Pio, A. A. B.; Conde, A. J.; Giannetti, F.; Donzelli JL. *Manual de Conservação e Reuso de Água na Agroindústria Sucroenergética*. vol. 5. 2017.
20. Lima. ACG, Passamani. FC. Universidade Federal do Espírito Santo, dissertation of graduation in portuguese - Vitória. *Avaliação Do Potencial Energético Do Biogás Produzido No Reator Uasb Da Ete-Ufes* 2012:106.
21. da Costa RBR, Valle RM, Hernández JJ, Malaquias ACT, Coronado CJR, Pujatti FJP. Experimental investigation on the potential of biogas/ethanol dual-fuel spark-ignition engine for power generation: Combustion, performance and pollutant emission analysis. *Appl Energy* 2020;261:114438.

- <https://doi.org/10.1016/j.apenergy.2019.114438>.
22. Balki MK, Sayin C, Canakci M. The effect of different alcohol fuels on the performance, emission and combustion characteristics of a gasoline engine. *Fuel* 2014;115:901–6. <https://doi.org/10.1016/j.fuel.2012.09.020>.
  23. EPE. Anuário Estatístico de Energia Elétrica 2020.
  24. Brazilian Business Council for Sustainable Development (CEBDS). Precificação de carbono: o que o setor empresarial precisa saber para se posicionar. 2016.
  25. International Council on Clean Transportation (ICCT). Opportunities and risks for continued biofuel expansion in Brazil 2019.
  26. Najafi G, Ghobadian B, Yusaf T, Ardebili SMS, Mamat R. Optimization of performance and exhaust emission parameters of a SI (spark ignition) engine with gasolineethanol blended fuels using response surface methodology. *Energy* 2015;90:1815–29. <https://doi.org/10.1016/j.energy.2015.07.004>.
  27. Al-Harbi AA, Alabduly AJ, Alkhedhair AM, Alqahtani NB, Albishi MS. Effect of operation under lean conditions on NOx emissions and fuel consumption fueling an SI engine with hydrous ethanol–gasoline blends enhanced with synthesis gas. *Energy* 2022;238:121694. <https://doi.org/10.1016/j.energy.2021.121694>.

## NOMENCLATURES

$% e$	Percentual of ethanol
$% g$	Percentual of gasoline A
1,4-DCB <sub>eq</sub>	1,4-Dichlorobenzene, substance used to calculate the level of human toxicity
$A_{electric}$	Electric autonomy
$BTE_{bioethanol}$	Brake thermal efficiency of the internal combustion engine when fuelled with bioethanol
$BTE_{gasoline}$	Brake thermal efficiency of the internal combustion engine when fuelled with gasoline A
$C_2H_5OH$	Gasoline
$C_b$	Battery capacity
$CH_4$	Methane
$CO_2$	Carbon dioxide
$CO_2_{eq}$	Equivalent carbon dioxide
$E_{Brazilian\ mix}$	Emission related to the Brazilian electricity mix
$E_{consump}$	Energy consumption needed in the internal combustion engine
$E_{electric\ mode}$	Emission related to the electricity consumption
$FC_{bioethanol}$	Bioethanol consumption
$FC_{biogas}$	Biogas consumption
$FC_{fuel}$	Fuel consumption
$FC_{gasoline\ A}$	Gasoline A consumption
$f_{1,4DCBeq}$	Equivalent 1,4-dichlorobenzene emission factor
$f_{CO_2\ eq\ bioethanol}$	Equivalent carbon dioxide emission factor resulted from the bioethanol combustion
$f_{CO_2\ eq\ biogas}$	Equivalent carbon dioxide emission factor resulted from the biogas combustion
$f_{CO_2\ eq\ fuel}$	Equivalent carbon dioxide emission factor
$f_{CO_2\ eq\ gasoline\ A}$	Equivalent carbon dioxide emission factor resulted from the gasoline A combustion
$f_{specie}$	Specie emission factor
$H_2O$	Water steam
$LHV_{fuel}$	Low heating power of the fuel
$LHV_{gasoline\ A}$	Low heating value of the gasoline A
$N_2$	Nitrogen
$NO_x$	Nitric oxides
$n_{fuel}$	Number of mols of the fuel
$n_{specie}$	Number of mols of the specie
$O_2$	Oxygen
$TTW_{BR\ gasoline}$	Tank-to-Wheel for the Brazilian gasoline
$TTW_{ICE-DF}$	Tank-to-Wheel for the internal combustion engine in dual-fuel mode
$TTW_{ICE-SF}$	Tank-to-Wheel for the internal combustion engine in single-fuel mode

$W_{fuel}$	Molecular weight of the fuel
$W_{specie}$	Molecular weight of the specie
$z$	Proportion of biogas in the mixture
$y$	Proportion of bioethanol in the mixture

### GREEK CHARACTERS

$\varepsilon$	Energy-ecological efficiency
$\eta$	Brake thermal efficiency of the internal combustion engine
$\Pi$	Pollution indicator
$\Pi_{GW}$	Pollution factor that considers the emissions that contribute to the global warming
$\Pi_{HT}$	Pollution factor that considers the emissions that contribute to human toxicity
$\rho_{bioethanol}$	Bioethanol density
$\rho_{biogas}$	Biogas density
$\rho_{fuel}$	Fuel density
$\rho_{gasoline A}$	Gasoline A density

### ABBREVIATIONS

BEV	Battery electric vehicle
EA	Electric autonomy
EM	Electric motor
FC	Fuel consumption
GHGs	Greenhouse gases
HC	Hydrocarbons
HEV	Hybrid electric vehicle
ICE	Internal combustion engine
ICE-DF	Internal combustion engine in dual-fuel mode
ICE-SF	Internal combustion engine in single-fuel mode
LPG	Liquefied petroleum gas
PEV	Plug-in electric vehicle
PHEV	Plug-in hybrid electric vehicle
PM	Particulate matter
TTW	Thank-to-Wheel

## Comparative performance analysis between static solar panels and single-axis tracking systems

Ana María Arbeláez<sup>1</sup>[0000-0003-3214-655X], Natalia Barros<sup>2</sup>✉[0000-0002-9288-3431], Freddy Bolaños<sup>3</sup>[0000-0002-3123-5481] and Nicolás Villegas<sup>4</sup>[0000-0001-5877-6328]

<sup>1,2,3</sup> Universidad Nacional de Colombia, Medellín, Colombia

<sup>1,4</sup>Solenium, Medellín, Colombia

nabarrosb@unal.edu.co

anmarbelaezma@unal.edu.co

fbolanosm@unal.edu.co

nicolas.villegas@solenium.co

**Abstract.** This paper explores the advantages of the implementation of solar tracker systems and bifacial panels, when compared to fixed conventional photovoltaic systems. Three systems consisting of a fixed conventional solar system, a conventional panel connected to a solar tracking device and a bifacial panel connected to a solar tracker are compared. Such systems are installed on the rooftop of Ruta N Building, in Medellín, Colombia. Generation data of all three systems is collected through a micro-inverter and can be retrieved using the Energy Monitoring & Analysis (EMA), an APSystems Software. A daily and monthly comparison of the produced energy, the economic savings and the carbon emission reduction is performed. It is concluded that the implementation of a bifacial solar panel connected to a tracking system could provide a significant increase in power production that can be of use in designs where installation space is a constraint and should be studied further to make optimal use of the advantages these systems can offer.

**Keywords:** Photovoltaic System · Solar Tracker · Renewable Energy · Bifacial Panels

### 1 Introduction

In recent years there has been a growing concern about the effects of climate change and how to mitigate them. Some efforts to achieve a more sustainable society are the Paris Agreement, in which 195 nations, including Colombia, made the commitment to keep the increase in global average temperature below 2°C [1]. In that sense, the integration of Renewable Energy Resources is key to reduce emissions and increase energy efficiency.

According to the Renewables 2020 Global Status Report, hydro, wind and solar are the resources with the highest installed capacity worldwide [2]. Colombia has largely used hydro power and is recently integrating new renewable resources to its energy matrix. Even though Colombia shows high potential for the integration of wind energy, this potential is only found in certain regions of the country. While the average for solar energy is higher than the world's average [3].

While photovoltaic solar energy has shown important improvements in the last years, such as increased efficiency and reduction of costs, it is still mostly useful during the hours the sunlight hits the surface of the solar panel with an incidence angle close to  $0^\circ$  [4].

The use of solar tracker systems has been studied as an alternative to increase the amount of sun hours, thus increasing the amount of energy produced and lowering the cost per kWh [5].

In [6] the authors design and implement a low-cost single axis solar tracker system and then compare the performance of this system with that of a fixed panel system. They find that the solar tracking system produces 30 % more energy than the fixed array.

The authors of [7] propose a low-cost prototype of a dual axis solar tracking system and compare the performance of this system and a fixed-position photovoltaic system in tropical weather conditions. The authors find that the use of a dual-axis solar tracking system poses an alternative solution to increase the energy output of a solar energy system. Also, they find that there is an important relation between the clearness of the day and the performance of the tracking system. The authors conclude that the use of a dual-axis tracking system is an approach to increase the production of energy without enlarging the solar system.

In [8] the authors perform a comparative analysis between a fixed photovoltaic solar panel and a one-axis tracking system located in a dry climate region of Brazil. The authors compare the performance of both systems and find that the tracking system has a small gain (only 11 %) in produced power compared with the fixed solar system. They attribute this behavior to the angle of incidence of sunlight through the day, due to the proximity to the Equator.

A performance comparison between a grid-tied fixed solar array and a grid tied tracking photovoltaic array is described in [9]. The authors compare power production and CO<sub>2</sub> emission reduction and conclude that the implementation of a single-axis tracking system in Florida has a moderate effect in the increase of energy production - 15 % more power production than with the fixed solar panel, and thus there is need for improvement and further study of the tracking system.

The previous works are mainly focused on single axis tracking systems using conventional solar panels. The use of bifacial solar panels combined with tracking has not been explored and in this paper, we plan to analyze if this technology poses any significant improvement in energy generation in the studied region.

In this paper we compare the performance of three systems: a fixed conventional photovoltaic panel, a conventional photovoltaic panel, and a bifacial panel both connected to a single-axis tracking system. The document is divided into six sections. Following the introduction, the second section, Materials and Methods provides a description of the studied systems. The third section, Results, presents the findings of our study and a detailed analysis of those findings. Then, we discuss those results and present our conclusions. Finally, the last section, acknowledgements.

## 1 Materials and Methods

As mentioned earlier, three systems are used in this study: a static solar system with a conventional photovoltaic panel, a single axis solar tracking system with a conventional panel and a single axis solar tracking system with a bifacial panel. The used panels are TSM-385DE15H(II), JKM395M-72H and JKM390M-72H-TV respectively and have the technical specification listed in table 1. The used tracker technology for both the conventional and bifacial systems is the Zentrack, which uses an 80jbx+76zyt-10 HH Motor, whose characteristics are found in table 2.

**Table 1.** Technical specifications of the used panels.

Module Type	TSM-385DE15H(II) [10]	JKM395M-72H [11]	JKM390M-72H-TV [12]
Maximum Power ( $P_{max}$ )	385W	395W	390W
Maximum Power Voltage ( $V_{mp}$ )	40.10V	41.40V	39.70V
Maximum Power Current ( $I_{mp}$ )	9.61A	9.55A	9.85A
Open-circuit Voltage ( $V_{oc}$ )	48.50V	49.50V	48.20V
Short-circuit Current ( $I_{sc}$ )	10.03A	10.23A	10.15A
Module Efficiency STC (%)	18.9	19.63	19.05
Temperature coefficients of $P_{max}$	-0.37%/°C	-0.36%/°C	-0.35%/°C
Temperature coefficients of $V_{oc}$	-0.29%/°C	-0.28%/°C	-0.29%/°C
Temperature coefficients of $I_{sc}$	0.05%/°C	0.048%/°C	0.048%/°C
Bifacial Factor	-	-	70%

**Table 2.** Technical specifications of the used motor.

<b>Specifications 80JBX+76ZYT-10 [13]</b>	
Voltage ( $V_{DC}$ )	24
No Load Current (mA)	1730
No Load Speed (r/min)	7
Rated Load Current (mA)	7480
Rated Load Speed (r/min)	6
Torque ( $N \times m$ )	138.1

Ratio	531
Stage	4
Power (W)	82
Length (mm)	233

These systems were installed in the roof of Ruta N building in Medellín, Colombia.

All three systems are connected to a QS1A APSystems micro-inverter. All the gathered information was retrieved from the Energy Monitoring & Analysis, an APSystems Software.

For each system, daily generation measurements from December 2020 through February 2021 were collected and processed in excel. Then, the total monthly generation was calculated as the sum of the daily generation in each scenario.

As all three panels have a different peak power, we implemented a normalization of the data dividing the average power generation of each system by the peak power of the respective module. Then, we performed a comparison of the resulting values, as well as the cost saving that implementing these systems would represent. Also, we calculated the emission reduction resulting from the power generation using the fixed conventional photovoltaic panel, the single-axis tracking system with the conventional photovoltaic and the single-axis tracking system with the bifacial panel. To estimate these reductions, we used the expression (1):

$$\text{Emission Reduction [tonCO}_{2\text{eq}}] = \text{Generated Energy [MWh]} * \text{Greenhouse Emission Factor [tonCO}_{2\text{eq}}/\text{MWh}] \tag{1}$$

The greenhouse emission factor is determined by the Unidad de Planeación Minero Energética (UPME) of Colombia through an official yearly resolution. For 2020, the emission factor for photovoltaic and wind farm projects connected to the national interconnected grid of Colombia is 0.591 tonCO<sub>2eq</sub>/MWh [14].

Finally, the monthly economic savings resulting from the generated energy with each of the systems matter of this study were calculated. To calculate said savings, we used the average price of traded energy for Medellín’s energy provider – Empresas Públicas de Medellín – in the month of May 2021, \$ 541.9478 COP/ kWh [15]. The economic savings were calculated according to equation 2.

$$\text{Monthly savings [COP]} = \text{Generated energy [kWh]} * \text{Average Energy Price [COP/kWh]} \tag{2}$$

As shown in Table 2, the power consumption of the motor is not relevant compared to the total production of the systems, so it won’t be considered in the performed calculations.

The results of the performed comparisons are presented in the next section.

## 2 Results

### 2.1 Energy generation

As mentioned in section 2, the energy produced by each system was measured and recorded daily through the months of December 2020 to February 2021. In figure 1 a visual comparison of the generation for the month of January is presented. As shown in this Figure, it's evident that the single axis tracking system with the bifacial panel (System 3 from here on) is the one with the highest energy production every day of the three months that were studied. Also, it can be observed that most days the single axis tracking system with the conventional panel (System 2) produces more energy than the fixed system with the conventional panel (System 1), except for some days where System 2 generated less than System 1.

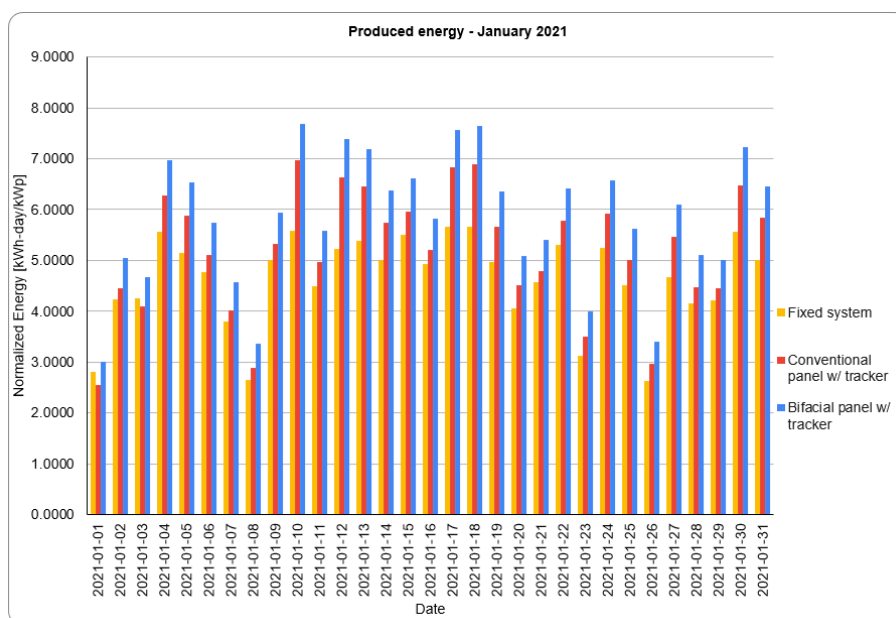


**Fig. 1.** Comparison between the daily generated energy of each system for the month of January 2021.

Figure 2 depicts the monthly comparison of the energy generated by all three systems. As could be predicted by the daily behavior, each month System 3 produced the most energy out of the three studied systems. Followed by System 2, being System 1 the one that generated the least.

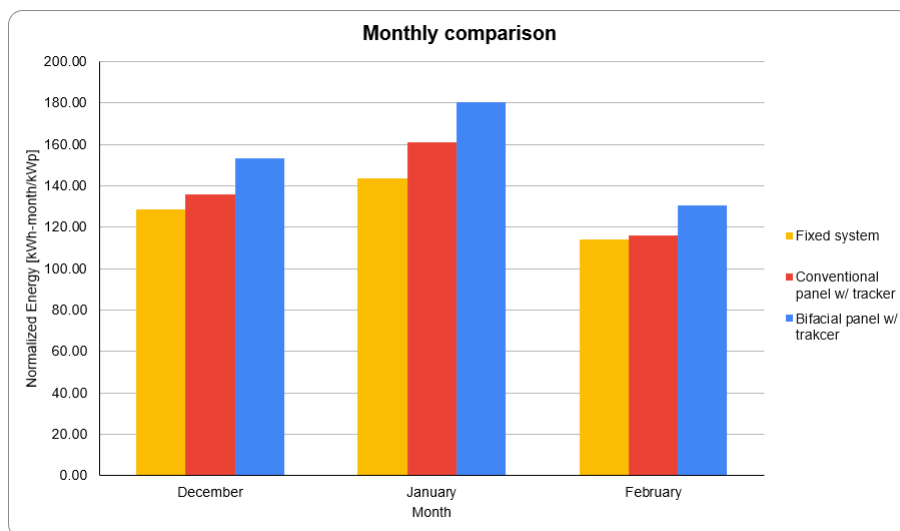


Fig. 2. Comparison between the monthly generated energy of each system.

In Figure 3, a comparison between the production of each system relative to System 1 is presented. Using System 1 as reference, we compare the percentage differences of the daily energy generation of the systems, dividing the generated energy of each system by the generated energy of the reference system. The same trend found in the previous comparison is evident in this Figure as well.

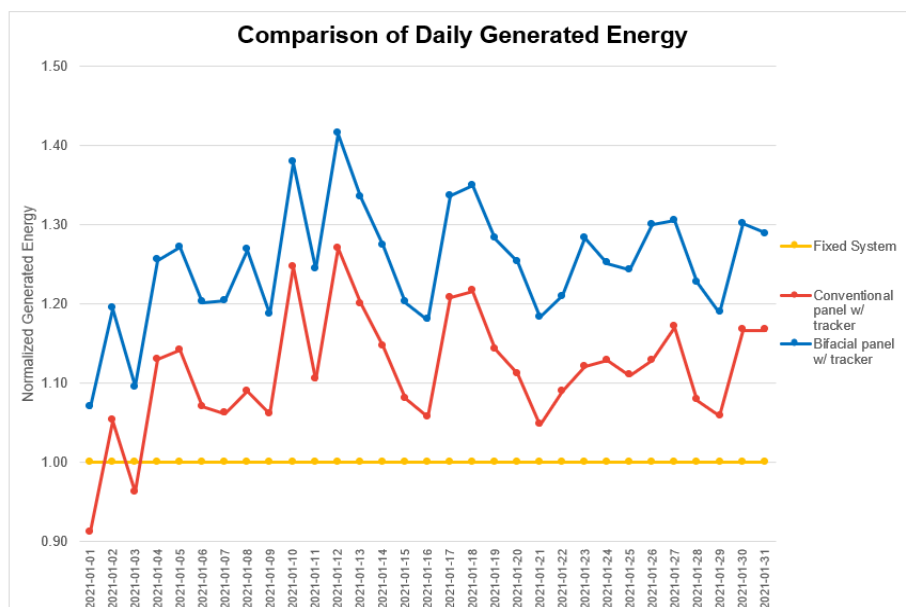


Fig. 3. Daily energy production comparison.

In table 3, we present a summarized comparison between each system using System 1 as reference. When the energy produced by System 1 is compared with that from System 2, it can be noted that System 2 produces 9.71 % more energy than System 1 under the same conditions. When the fixed system is compared with the single-axis tracking system with the bifacial panel it's found that the latter produces 21.85 % more energy than the fixed conventional panel.

**Table 3.** Monthly comparison of the energy generated by the studied systems.

<b>Generated Energy Comparison</b>	
Conventional panel with tracker - Fixed system	9.71%
Bifacial panel with tracker - Fixed system	21.85%

### 1.1 Emission reduction

The monthly emission reduction for each system was calculated according to equation 1, as explained in section 2. The results of these calculations are presented in table 4. As each system only has one solar panel, we performed another comparison between each system to give a better understanding of the effect of implementing each of the proposed systems, presented in table 5. As expected, the percentage variation between each pair of systems is the same as the obtained in the previous comparison, as the carbon dioxide emission reduction is proportional to the amount of energy generated.

**Table 4.** Monthly Emission Reduction

<b>Monthly Emission Reduction [tonCO<sub>2</sub>eq/MWh]</b>			
<b>Month</b>	<b>Fixed system</b>	<b>Conventional panel w/ tracker</b>	<b>Bifacial panel w/ tracker</b>
December	0.0292	0.0317	0.0353
January	0.0327	0.0376	0.0416
February	0.0259	0.0271	0.0301
<b>Average</b>	<b>0.0293</b>	<b>0.0321</b>	<b>0.0357</b>

**Table 5.** CO<sub>2</sub> Emission Reduction Comparison.

<b>CO<sub>2</sub> Emission Reduction Comparison</b>	
Conventional panel with tracker - Fixed system	9.71%
Bifacial panel with tracker - Fixed system	21.85%

### 1.2 Monthly economic savings

The monthly economic savings due to the implementation of the studied systems were calculated using the monthly average price for the traded energy for Medellín's largest energy provider, according to equation 2. These savings are presented in table 6. We compared the economic savings between each pair of systems in this case as well and present the percentage variation in table 7. As in the case of the emission reduction, this variation is again the same as in the energy production, due to the linearity of equation 2.

**Table 6.** Monthly Economic Savings due to the implementation of the studied systems.

<b>Monthly Economic Savings [COP]</b>			
<b>Month</b>	<b>Fixed system</b>	<b>Conventional panel w/ tracker</b>	<b>Bifacial panel w/ tracker</b>
December	\$26,794	\$29,027	\$32,365
January	\$29,981	\$34,490	\$38,142
February	\$23,754	\$24,832	\$27,618
<b>Average</b>	<b>\$26,843</b>	<b>\$29,449</b>	<b>\$32,708</b>

**Table 7.** Economic Savings Comparison.

<b>Economic Savings Comparison</b>	
Conventional panel with tracker - Fixed system	9.71%
Bifacial panel with tracker - Fixed system	21.85%

## 2 Conclusions

As presented in section 3, it is evident that there is a benefit in the use of solar tracking systems. Both the system using a conventional panel and the one with the bifacial panel show an evident gain in the production of energy when compared with the fixed conventional solar panel. Bifacial technology provides an advantage over conventional panels, as it can capture sun rays from both sides. In that sense, bifacial panels provide a higher improvement, as they produce even more energy than the conventional solar panel connected to the tracking system.

The use of solar trackers combined with bifacial solar panels represent a gain in generated energy of up to 22 % when compared with the fixed conventional system. This is an asset that should be considered in designs where space is a constraint, as it not only provides greater energy production but also increases the economic savings and emission reduction associated with the implementation of photovoltaic power plants. However, it should be noted that in order to be able to take advantage of the tracking during the day without requiring backtracking and to reduce shadows casted by other rows of panels, an additional distance between rows could be needed.

As discussed in section 2, the power consumption of the motor used by the tracker is not significant when compared to the power production of the studied systems, taking into account that this type of motor is designed to move dozens of modules. Considering that the motor won't be on continuously, but rather when the tracker is activated, a calculation of the effective working hours and the load the motor carries must be evaluated to estimate the actual power consumption of the motor. Further studies should be carried out considering the motor's power consumption in order to analyze if the extra amount of power the trackers help produce would be significant when compared to the energy that would be consumed by the system itself.

### 3 Acknowledgements

The authors would like to thank Universidad Nacional de Colombia, and Solenium, by its support in the development of this work.

### References

1. Paris Agreement, [https://ec.europa.eu/clima/policies/international/negotiations/paris\\_en](https://ec.europa.eu/clima/policies/international/negotiations/paris_en), last accessed 2021/03/22.
2. REN21.: Renewables 2020 Global Status Report. Paris (2021).
3. UPME.: Integración de las energías renovables no convencionales en Colombia. Bogotá (2015).
4. Solar Radiation Basics, <https://www.energy.gov/eere/solar/solar-radiation-basics>, last accessed 2021/03/22.
5. A. Awasthi et al.: Review on sun tracking technology in solar PV systems. Energy Reports (6), 392-405 (2020). doi: 10.1016/j.egy.2020.02.004
6. Rizk, J., Chaiko, Y.: Solar Tracking System: More Efficient Use of Solar Panels. World Academy of Science, Engineering and Technology 2(5), 784-786 (2008).
7. Lee, J.F., Rahim, N.A.: Performance Comparison of Dual-Axis Solar Tracker vs Static Solar System in Malaysia. IEEE Conference on Clean Energy and Technology (CEAT), 102-107 (2013). doi:10.1109/CEAT.2013.6775608
8. Vieira, R.G., Guerra, F.K.O.M.V., Vale, M.R.B.G., Araújo, M.M.: Comparative performance analysis between static solar panels and single-axis tracking system on a hot climate region near to the equator. Renewable and Sustainable Energy Reviews 64, 672-681 (2016). doi: 10.1016/j.rser.2016.06.089
9. Moradi, H., Abtahi, A., Messenger, R.: Annual Performance Comparison Between Tracking and Fixed Photovoltaic Arrays. IEEE 44th Photovoltaic Specialist Conference (PVSC), 1-5 (2017). doi:10.1109/PVSC.2017.8366750
10. Trina Solar TSM-385DE15H(II) (385W) Solar Panel, <http://www.solardesigntool.com/components/module-panel-solar/Trina-Solar/5793/TSM-385DE15H-II-/specification-data-sheet.html>, last accessed 2021/08/01.
11. Jinko JKM395M-72H (395W) Solar Panel, <http://www.solardesigntool.com/components/module-panel-solar/Jinko/5626/JKM395M-72H/specification-data-sheet.html>, last accessed 2021/08/01.
12. Swan Bifacial HC 72M 385-405W, <https://es.enfsolar.com/pv/panel-datasheet/crystalline/41584>, last accessed 2021/08/01.
13. BPM-80JBX+76ZYT 24V High Torque DC Planetary Reduction Gear Motor, <https://www.belmont-tech.com/BPM-80JBX-76ZYT-24V-High-Torque-DC-Planetary-Reduction-Gear-Motor-pd47736517.html>, last accessed 2021/08/01.
14. UNIDAD DE PLANEACIÓN MINERO ENERGÉTICA - UPME, "RESOLUCIÓN No. 000385 de 2020", Bogotá, 2020.
15. Precio promedio y energía transada, <https://www.xm.com.co/Paginas/Mercado-de-energia/precio-promedio-y-energia-transada.aspx?GroupString=%3B%23Precio%20Promedio%20y%20Energ%C3%ADa%20Transada%202021%3B%23&IsGroupRender=TRUE>, last accessed 2021/07/10.

## Building design strategies adapted to climate changes in arid regions

Sanz C.<sup>1</sup>, Giancola E.<sup>2</sup>, Soutullo S.<sup>2</sup>, Jiménez M.J.<sup>2</sup>, Ferrer J.A.<sup>2</sup>, Sánchez M.N.<sup>2</sup>

<sup>1</sup> Facultad de Ciencias, Universidad Autónoma de Madrid, 28049 Madrid, Spain

<sup>2</sup> Energy Efficiency in Buildings Unit, CIEMAT, 28040 Madrid, Spain  
cristina.sanzcuadrado@estudiante.uam.es

**Abstract.** Cities present one of the greatest challenges at an international and European level in the fundamental transformation of economies and societies. The building sector is responsible for a high percentage of greenhouse gas emissions and global energy consumption. In order to carry out actions that have a relevant impact on the reduction of energy consumption in the thermal conditioning of buildings, an exhaustive knowledge of the energy performance of buildings and their boundary conditions is required. In addition, the reduction of the gap that currently exists between the energy performance based on theoretical calculations and the real one is also very important. In this work, the impact of climatic conditions on the energy performance of buildings is evaluated by analyzing the bioclimatic strategies with the greatest potential in thermal conditioning. First, an analysis of climatic trends is carried out by studying the most representative climatic variables in arid regions. Secondly, a comparative analysis of three climatic databases is done: two synthetic databases commonly used in building energy simulation tools and a Typical Meteorological Year experimental file. Then, the energy needs of the buildings are estimated, both seasonally and annually. In addition, Givoni diagrams are developed to determine the representative climate strategies that are necessary to achieve indoor thermal comfort. All results for the three analyzed databases have been compared in order to observe the variability and to minimize the impacts derived from evaluating buildings in different climatic scenarios.

**Keywords:** Climate trends, Long-term monitoring, Building energy demand, Building energy performance.

2

## 1 Introduction

Climate change is a global problem caused by the increase in greenhouse gas (GHG) emissions, which leads to a gradual increase in the Earth's surface temperature [1]. The Intergovernmental Panel on Climate Change (IPCC) defines various scenarios in which the Earth's average temperature rises 1-2°C by 2050 and 1.5-3.5°C by 2085 [2].

In this context, according to the International Energy Agency (IEA), the building sector accounts for one third of total energy consumption and is responsible for about 25-40% of GHG emissions into the atmosphere [3]. In the case of the European Union (EU), the aforementioned sector accounts for 40% of total energy consumption and 36% of CO<sub>2</sub> emissions [4]. For this reason, reducing the energy demand of buildings is an important issue. This mitigation would reduce the expected temperature increase [2], which has direct implications on the energy demand of buildings, determined among other factors by the climatic conditions of the outdoor location [5], [6]. Several studies predict that the increase in temperature will lead to a higher cooling demand and a decrease in heating demand in the future [3], [7].

The analysis of climatic variables and boundary conditions, as indicated in the SET-plan 3.2 [8] of Positive Energy Districts (PED), will be decisive in optimizing the energy demand of buildings. Although global climate classifications exist, the identification of energy efficient design strategies and the development of solar systems require a reliable climate characterization that is representative of the local climatology. This point represents therefore one of the most critical elements when theoretically analyzing the behavior of a given system, being fundamental the interaction of the system with the surrounding environment.

The climate of an area can be characterized by analyzing the most representative meteorological variables recorded over the years in that area. If records are available over a long period of time, there is the possibility of generating a typical meteorological year (TMY), which is representative of the climate of a region [9]. The TMY is in fact a tool used to model the weather patterns that characterize a certain area over a long period of time. This file can be used as input information to calculate the energy consumption of a building and predict its long-term thermal behavior [10]. Based on literature, the minimum time period considered should be ten years [11]. The creation of updated TMYs is relevant since it allows to consider the impact of climate evolution on building performance. This aspect has been addressed in several studies that show the importance of assessing how climate change affects the different climate databases used in simulation models [4] to obtain meaningful data to carry out a correct assessment of the energy performance of buildings [12], [13].

In this work, an empirical analysis of the climatic representativeness in the arid area of Tabernas is carried out. The Tabernas Desert is one of Spain's semi-arid deserts, located within Spain's southeastern province of Almería. The study identified the climate change patterns in this zone by comparing the climate data monitored in the last twelve years in this location and two existing reference climate databases. For this purpose, the following climatic variables have been evaluated: temperature (maximum, minimum and average), relative humidity (maximum, minimum and average), wind

speed and direction, and global horizontal solar radiation [14]. An analysis of the climatic severity of the area was also carried out using a Givoni diagram, and the bioclimatic design of the buildings in this location was optimized by identifying the heating and cooling conditioning measures that ensure indoor thermal comfort.

## **2 Methodology**

The methodology developed in this work assesses the impact of climate change on the energy performance of buildings based on long-term monitoring campaigns. This methodology can be applied in both new developments and urban area retrofit plans, in order to optimize the energy conservation, the use of energy resources and the reduction of environmental pollution and energy poverty.

The location studied in this work is the Tabernas Desert in Almeria. It is an arid area characterized by dry cold desert climate, corresponding to a BWk zone in the Köppen-Geiger classification [15]. These types of climatic classifications make it possible to obtain a general idea of the behavior of climatology in large geographical areas. However, factors such as orography, proximity to large bodies of water, vegetation or wind regime, among others, cause large deviations between the general climatic characteristics of the area and those of the specific location within that climatic zone. To perform an analysis of the main climatic variables affecting the energy consumption of buildings for the Tabernas site, the experimental methodology explained below has been developed [16].

### **2.1 Experimental Monitoring**

The Research Centre for Energy, Environment and Technology (CIEMAT) is a public research body assigned to the Spanish Ministry of Science and Innovation. CIEMAT has experimental monitoring facilities for the characterization under real conditions of use of various buildings and their boundary conditions. Long-term campaigns have been carried out for the experimental measurement of the main climatic variables over the years: air temperature and relative humidity, global horizontal solar radiation and wind direction and speed [17]. Two weather stations installed in the same location simultaneously record climatic data in order to minimize the existence of gaps in the climatic data files [18].

### **2.2 Data processing**

Data processing is based on the creation of a multi-annual database. Erroneous or statistically unrepresentative minute values of the general behavior of the measured variables are identified for each one of the monitored meteorological variables. First, data belonging to the valid range of measurement of the respective sensor is checked, otherwise the value is deleted from the database. Then, for each of the variables, time series in which the minute value of the variable is exactly the same are identified. This would indicate that there was an error in the recording of this variable, and the repetitive values

4

are deleted from the minute database. Finally, a statistical analysis is performed by calculating the 25th percentile (q1) and 75th percentile (q3) of the data on an hourly basis, and values out of range are discarded. With the aim of having the longest data time series possible, the data gaps will be filled from the minute data recorded at the second meteorological station where the same methodology is applied to generate the climate data files. Finally, the climatic data files (minute, hourly, daily, monthly, annual) are generated.

### **2.3 Climatic analysis**

A typical meteorological year (TMY) is generated from the experimental climate files [19] and compared with the synthetic EPW and MET climate years. In this case, the TMY is elaborated following the PASCOOL methodology [20] from the experimental campaign indicated in section 2.1, which has allowed evaluating the climatic conditions in the Tabernas area during the last twelve years. Using these measurements from the available climatic variables, and considering each month separately, the annual representativeness has been obtained as the minimum value of a weighted sum that takes into account the following variables: average, maximum and minimum temperature, average, maximum and minimum relative humidity, average, maximum and minimum wind speed and average global solar radiation. In this case the outdoor temperature and solar radiation are the most weighted variables with a value of 0.25 [21].

In Spain, the EPW and MET synthetic years are often used as climatic input hourly files in many building simulation and certification programs. The climatic databases used to create these Synthetic Years come from the World Meteorological Organization (WMO) and the Spanish Technical Building Code (CTE) respectively.

In this study, the variability and tendency of the climate over a long period is assessed. In addition, a series of hourly distribution maps of the three main climatic variables are generated [15]. Also, a qualitative study of the climate influence on the building energy demand based on Degree-Days method is done. Finally, bioclimatic charts are used to evaluate the thermal severity of the area and to determine the bioclimatic strategies best adapted to climate change to achieve thermal comfort inside the building.

## **3 Results**

### **3.1 Determination of the Typical Meteorological Year (TMY)**

The experimental TMY has been created following the methodology described in section 3.3. As mentioned above, the PASCOOL methodology has been followed using weighting factors optimized for its use in buildings, and adapted to the Mediterranean climate. The most representative years of the 2009-2020 period, are identified each month generating a climate data file of 8760 hourly values (TMY). This data file is used in the comparative study with the synthetic files EPW and MET.

### 3.2 Comparison of representative climate variables

This section quantifies the climatic trends in three climatic scenarios: one experimental and two synthetics. A seasonal comparison of the temperature (T), relative humidity (RH) and solar radiation (Ig) variables is made (see Fig. 1). The main conclusion that can be drawn from these comparisons is a better understanding of the gap that exists in the energy assessment of buildings, by characterizing and quantifying the magnitude of possible biases arising from the use of different meteorological databases.

The TMY (black) shows mean temperature values similar to those of the MET (green), which differ by only 1-2°C in the winter, summer and autumn seasons, while during spring, these mean temperature differences increase to 3°C. The EPW file (orange) shows that the temperature values in spring and summer are only 0.5°C below the mean value for the TMY, while in the rest of the seasons this difference is around 2-3°C. On the other hand, relative humidity shows large variations between the files. TMY has the lowest mean RH compared to EPW and MET, where the mean values in winter are about 10% higher than the experimental values. The same pattern in spring, although in this case, MET values decrease by 5% compared to EPW. In summer and autumn, relative humidity values of TMY and MET are similar, 20% below EPW in summer and 8% in the case of autumn. Finally, the average irradiance for TMY is higher than for the synthetic files, this difference is about 10 W/m<sup>2</sup> higher for TMY than for EPW during winter and about 15 W/m<sup>2</sup> in spring and summer, while in autumn, the difference is negligible. However, the difference in irradiance for TMY and MET is around 50 W/m<sup>2</sup> in winter and spring and 30 W/m<sup>2</sup> in summer and fall.

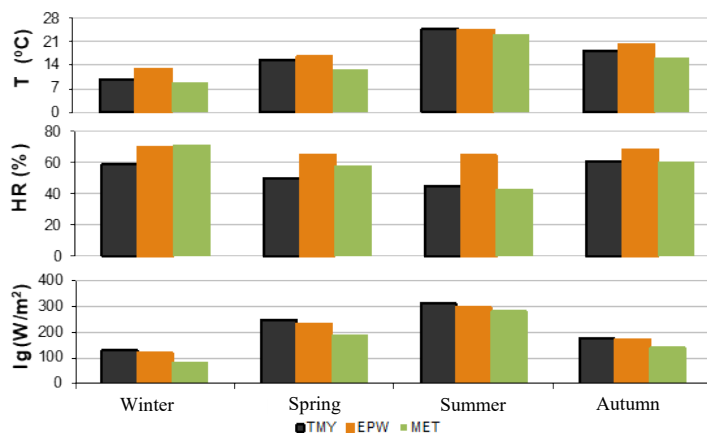


**Fig. 1.** Seasonal comparison of the average values of the three most representative climatic variables: temperature (T), relative humidity (RH) and global solar irradiance (Ig).

A series of climate surface plots have been made for each of the climatic files evaluated (Figures 2, 3 and 4). These figures highlight the daily distribution of environmental variables, indicating when and for how long the most extreme values occur. A typical

6

day has been calculated for each month of the year (and for each data file), and temperature, relative humidity and irradiance data for those days are selected in order to elaborate the surface plots.

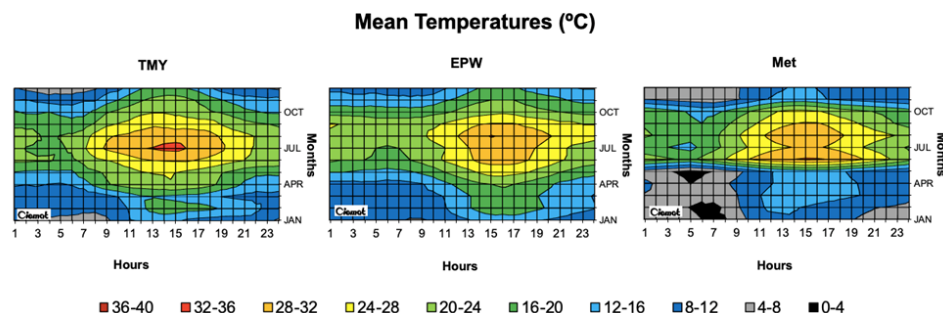


**Fig. 2.** Comparison of the mean temperatures for the three climate data files. a) TMY b) EPW and c) MET.

In the case of mean temperature (Fig. 2), it can be observed that TMY (a) presents higher temperatures throughout the year than EPW (b) and MET (c) files, reaching values of up to 36°C. EPW follows the temperature trend of TMY, but being less warm, in the same way as MET during the summer months. However, during the rest of the year there is a difference in the temperature pattern, presenting values well below the experimental data, with minimum temperatures around 0°C during the 4-8 h period in January and April.

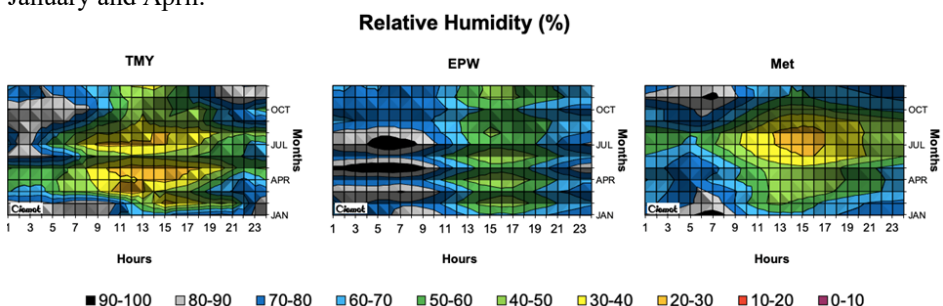


**Fig. 3.** Comparison of the relative humidity for the three climate data files. a) TMY b) EPW and c) MET.

Regarding relative humidity (Fig. 3), in the TMY (a) it can be seen that the central hours of the day are the ones showing much lower humidity (20-30%) than the rest of the day and the seasons with lower relative humidity are spring and summer. The EPW (b) shows that the relative humidity of this file is much higher, especially in the early hours of the day, which can reach 100% humidity. Finally, the MET (c) shows that the relative humidity is at its lowest during the central hours of the day and mid-afternoon during the summer months, corresponding to the hours of highest temperature.

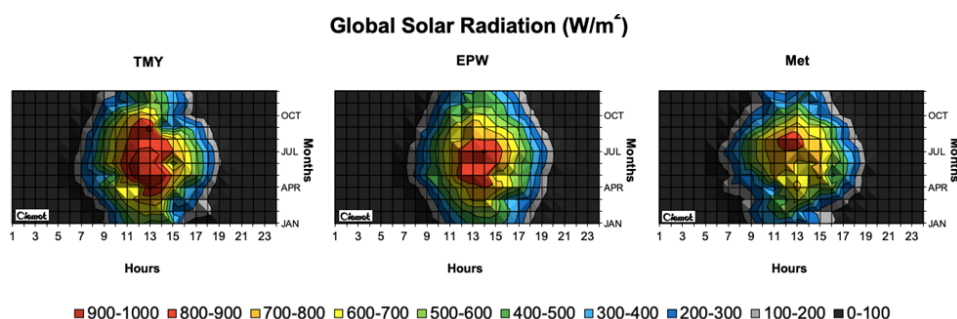


**Fig. 4.** Comparison of the global solar radiation for the three climate data files. a) TMY b) EPW and c) MET.

Finally, in Fig. 4, which presents the global irradiance values, it can be seen that the three data files show the same trend, with the central hours of the day in the summer months being those with the highest irradiance, reaching values of 900-1000 W/m<sup>2</sup>. In TMY (a) the values are higher than in the other two cases. In addition, EPW (b) presents the points with the highest irradiance in the months from April to July, corresponding to the end of spring and the beginning of summer, while in MET (c), the point of highest irradiance is at the end of the summer, in August.

### 3.3 Energy demand of the building: Degree-days methodology

An analysis regarding the influence of climate on the building's energy demand is carried out by calculating the heating and cooling degree days, and comparing the results from the three climate data files analyzed (TMY, EPW and MET). In this analysis, the needs for heating use in winter (HDD) and cooling use in summer (CDD) are calculated by applying the following equations:

$$HDD = (18 - T_{ext}) \cdot N \tag{1}$$

$$CDD = (T_{ext} - 24) \cdot N \tag{2}$$

where  $T_{ext}$  is the monthly average outdoor temperature at the site and  $N$  is the number of days in the corresponding month.

Table 1 shows the calculated degree days from the three climate data files. In the winter period, EPW data is 39.2% lower than the TMY whilst the MET data is 10.7% higher. In summer, both synthetic values are lower than TMY ones (17.1% lower for EPW and 81.4% lower for MET).

Therefore, the MET synthetic file presents an overestimation of the heating needs in the winter and spring months (42.3% higher than TMY) and on the contrary underestimates the cooling needs for summer by 81.4%. However, the EPW file data underestimates both heating (38% lower than TMY) and cooling needs (17.1% for CDD), being in this case slightly lower than the experimental data, but more similar to the MET file.

8

**Table 1.** Heating degree days (HDD) and cooling degree days (CDD) calculated for the standard days of each month for each of the climate databases.

	TMY		EPW		MET	
	HDD	CDD	HDD	CDD	HDD	CDD
January	278	0	172	0	304	0
February	236	0	140	0	243	0
March	152	0	113	0	223	0
April	81	0	56	0	74	0
May	0	0	0	0	0	0
June	0	0	0	0	0	0
July	0	65	0	45	0	9
August	0	64	0	62	0	15
September	0	0	0	0	0	0
October	0	0	0	0	59	0
November	112	0	54	0	201	0
December	236	0	144	0	283	0
Total	1095	129	679	109	1558	24

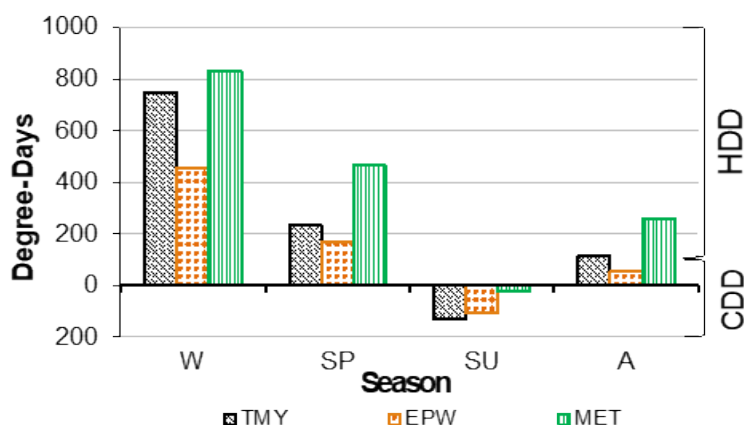


**Fig. 5.** Seasonal comparison of heating and cooling degree days for the three climate data files.

A comparative seasonal plot of the HDD and CDD from the three data files can be seen in Figure 5. In all the evaluated cases, the pattern of degree days is the same, with the building presenting cooling needs in the summer season and heating needs during the rest of the seasons of the year, being in all cases the heating needs much higher than the cooling needs (88.2% TMY case, 83.9% EPW case and 98.5% MET case). However, the quantitative values confirm what has been previously commented, that the EPW data presents lower values than the real data while the MET data presents higher values. In addition, it can be observed that during the spring and autumn seasons, the building

presents heating needs as well, although the calculated degree-days have much lower values than those required during the winter. Only in summer there is a need for cooling, and the required degree-days do not reach 200.

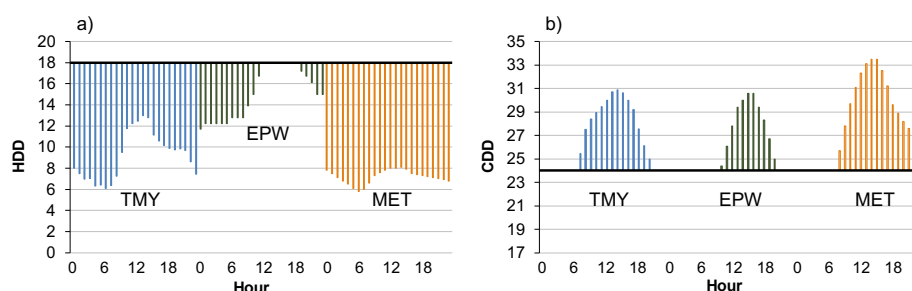


**Fig. 6.** Heating (a) and cooling (b) degree days for a typical winter and summer day throughout the 24 hours of the day for the three climate data files.

In Figure 6, the hourly evolution of heating degree days HDD (a) and cooling degree days CDD (b) is represented for a typical summer and winter day. In the case of HDD, the TMY (blue) predicts that heating will be needed throughout the day, since the outdoor temperature values are below 18°C, with the temperature difference being more pronounced in the hours when there is no solar irradiance. A typical winter day for EPW data (green) requires fewer heating hours since during the central hours of the day the outdoor temperature will be above 18°C. Finally, the MET data (orange) shows temperatures well below 18°C throughout the day, presenting the highest heating needs.

On the other hand, for the CDD, the temperatures during the hours of solar irradiance exceed 24°C. The EPW (green) and MET (orange) cases respectively need less and more cooling hours compared to the TMY case (blue). A variability in terms of HDD and CDD between the synthetic files and the experimental data is assessed. The EPW data underestimates the energy needs of the building with respect to those calculated based on the experimental data, whilst the MET data files overrate these needs.

### 3.4 Bioclimatic strategies

Finally, the passive and active bioclimatic strategies to be adopted in the design of the buildings located in arid regions are determined. A comparative psychometric analysis is carried out and used to identify strategies to reestablish comfort conditions inside the building. The comfort zone is defined as the range of climatic conditions in which most people do not feel discomfort, neither hot nor cold. In order to find out the comfort conditions of the site it is necessary to analyze the type of climate and evaluate the different climatic variables of the location. The bioclimatic Givoni diagram is divided into different zones in which the strategies necessary to achieve human comfort inside a building are identified [22]. Fourteen zones are defined as shown in Fig. 7. Accordingly, zones 1 and 2 are those in which comfort is achieved. Outside these, the different strategies used to achieve comfort are defined according to the hygrothermal conditions

10

of the air [23, 24]. In addition, the graph can be divided into two zones, separated by the comfort zones. The zone above and to the right of the comfort zone is the one corresponding to overheated periods, in which case solar protection and passive cooling strategies will be needed. On the other hand, the zone to the left of the comfort zone is the one that is under heated and will require solar heating techniques [25].

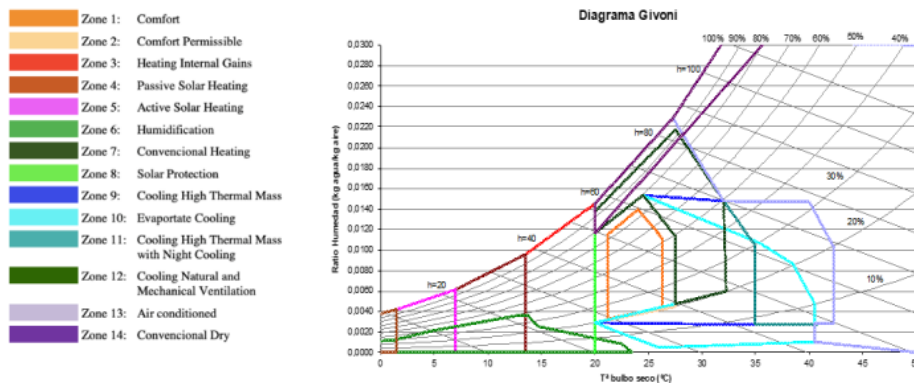


Fig. 7. Givoni zones: strategies to achieve thermal comfort inside the building.

In this study, the design strategies required in each of the climate scenarios evaluated will be determined globally for the summer and winter seasons, and specifically for a typical day of each month of the year, evaluating the hourly strategies.

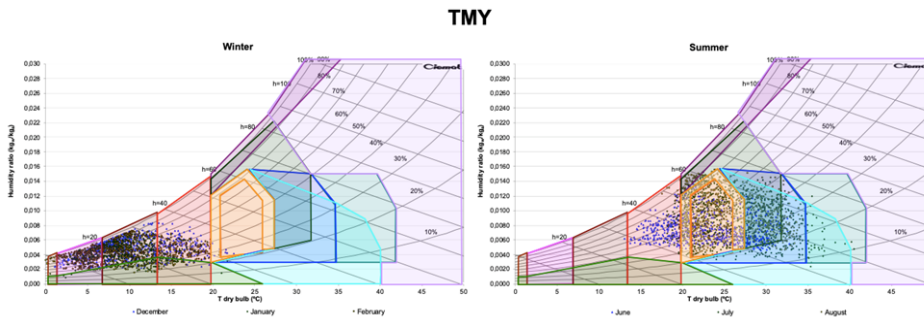


Fig. 8. Comparison of the Givoni diagram for the winter a) and summer b) months for the TMY.

Givoni diagrams (Fig. 8, 9 and 10) are created for summer (a) and winter (b) periods from the three climate databases under analysis. In the winter months, the points representing the outdoor air properties are located to the left of the comfort zone in all three cases, with the EPW data being the closest to comfort due to higher temperatures. The resulting strategies are heating by internal gains and by passive and active use of solar energy. In summer, however, the points are located in the comfort zone and to the right and above it (internal gain heating, solar shading, high thermal mass cooling, evaporative cooling, natural and mechanical ventilation cooling, and conventional dehumidification). At a quantitative level, the most representative strategies annually required for

TMY are heating by internal gains (30.48%) and by passive use of solar energy (26.16%). For EPW, required strategies are heating by internal gains (36.68%) and permissible comfort (26.82%). Identically, the most representative strategies for MET are heating by internal gains (33.04%) and permissible comfort (27.53%). Annually, heating strategies have greater weight and, even in the synthetic files, there are periods of permissible comfort during most of the hours of the year.

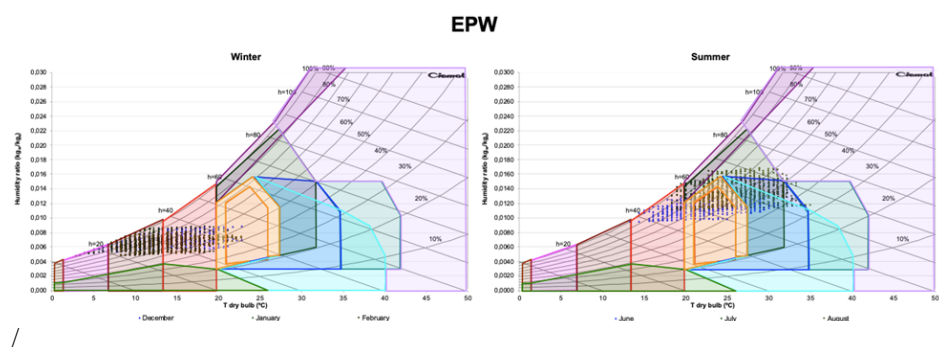


Fig. 9. Comparison of the Givoni diagram for the winter a) and summer b) months for the EPW.

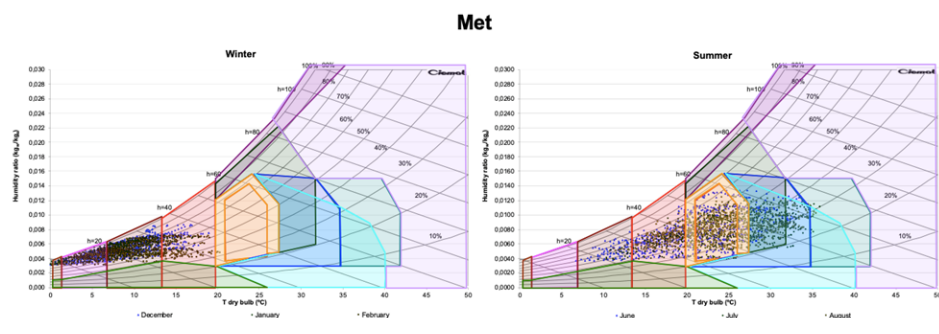


Fig. 10. Comparison of the Givoni diagram for the winter a) and summer b) months for the MET.

Table 2 shows a summary of the most important strategies required to achieve thermal comfort in each of the seasons for each of the three data files. Conventional dry strategy identified for EPW in summer period can be explained because it refers specifically to Almeria, a city at sea level close to Tabernas but with higher humidity.

Next, an hourly evaluation of the bioclimatic strategies required for a typical day is carried out, extending the previous seasonal analysis. Fig. 11 shows the required strategies for each hour of the day for TMY, EPW and MET. In winter TMY months (Fig. 11 a) it will be necessary to apply heating techniques by internal gain (34.7%) especially in the hours where there is no irradiance. Passive use of solar energy is the strategy of greater weight (58.3%) during solar radiation hours. In spring, heating strategies by internal gains (43.1%) and by passive use of solar energy (29.2%) will be needed in no solar radiation hours, the rest of the day presents comfort zones (22.2% and 27.8% for the comfort zone and permissible comfort zone, respectively) together with solar

protection techniques (23.6% of the total in spring). In the TMY summer period, cooling techniques by natural and mechanical ventilation (43.1%), solar protection (44.4%) and, as soon as the maximum point of solar radiation is reached, cooling techniques by high thermal mass and cooling by evaporation are necessary (each representing 37.5% of the total). Finally, in the autumn season, thermal comfort is reached (62.5% for both comfort zones in total) in the central hours of the day with solar protection techniques (23.6%) and internal gain heating techniques (44.4%) are necessary during the night.

**Table 2.** Summary of the most important bioclimatic strategies necessary to achieve thermal comfort for each of the seasons of the year and the data files analyzed

	TMY	EPW	MET
Winter	Passive Solar Heating Heating Internal Gains	Passive Solar Heating Heat- ing Internal Gains	Passive Solar Heating Active Solar Heating
Spring	Heating Internal Gains Passive Solar Heating Comfort Permissible	Heating Internal Gains Pas- sive Solar Heating	Passive Solar Heating Active Solar Heating
Summer	Comfort Permissible Solar Protection Cooling Natural & Mechanical Ventilation Cooling High Thermal Mass Evaporative Cooling	Solar Protection Cooling High Thermal Mass Comfort Permissible Conventional Dry	Comfort Permissible Solar Protection Cooling High Thermal Mass Evaporative Cooling
Fall	Heating Internal Gains Comfort Permissible	Heating Internal Gains Comfort Permissible	Heating Internal Gains Comfort Permissible

The EPW file (Fig. 11 b) follows the same trend as TMY. In winter, heating techniques by internal gains (27.8%) and by passive use of solar energy, which is the highest percentage at 72.2%, are required. In spring, the same heating techniques are still required, with a weight of 48.6% for heating by internal gains, and 36% for heating by passive solar energy use. During the summer, the most important techniques are cooling by natural and mechanical ventilation (62.5%), solar protection (41.7%) and cooling by high thermal mass (29.2%). As for the autumn months, the permissible comfort is reached to a large extent (41.7%) and heating techniques by internal gains (45.8%) are necessary especially at night.

Finally, the MET file (Fig. 11 c) shows some differences with the previous ones. In the winter months, the needs change as the active solar energy heating technique appears and accounts for 34.5% of the total, while 65.3% is for active solar energy use. During the spring months, both active (27.8%) and passive (57%) heating techniques are still needed. In the summer months, thermal comfort is achieved in 29.2% of the total and 48.6% for permissible comfort. In addition, solar protection techniques (41.7%), cooling by high thermal mass and evaporative cooling (32% each) and cooling by natural and mechanical ventilation (29.2%) are necessary. Finally, in the autumn months, thermal comfort is achieved for much of the time (20.8% for the comfort zone

and 29.2% for the permissible comfort zone) and the most needed strategy is internal gain heating, which accounts for 37.5% of the total.

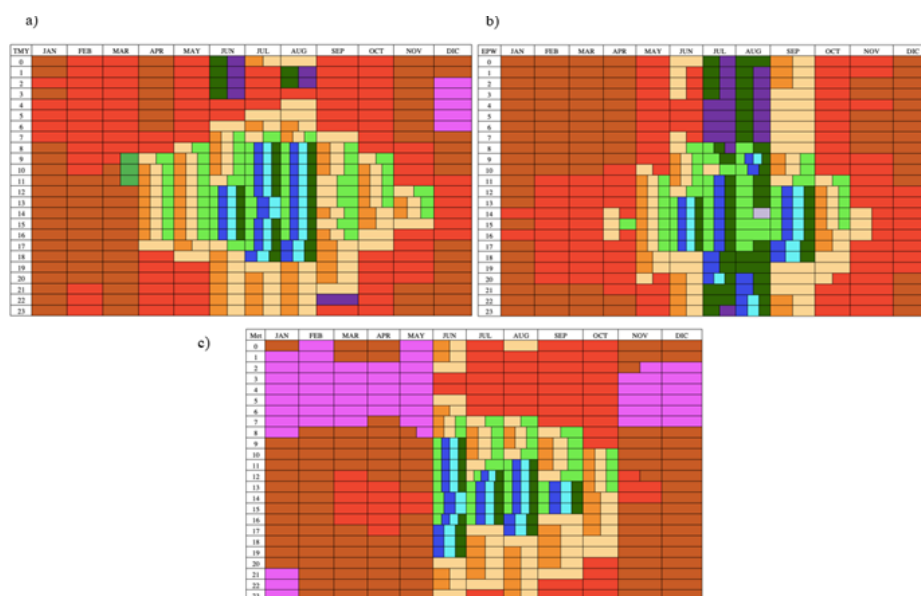


Fig. 11. Hourly bioclimatic strategies for the TMY a), EPW b) and MET c) file.

#### 4 Discussion and conclusions

The main conclusion is the importance of correctly determining the boundary conditions of the buildings, including the climate, since the local climatic conditions of the built-up areas have an impact on the thermal comfort and energy consumption of the cities. Consequently, having up-to-date climate data to perform a correct analysis of the energy needs of buildings is fundamental. In addition, this would help to reduce the difference between simulated and real values, and to implement urban regeneration strategies that mitigate adaptation to climate change.

The work develops a general methodology to quantify the impact of climate evolution on the energy performance of buildings based on long-term monitoring campaigns that record the values of the most representative climatic variables, such as temperature, relative humidity and solar radiation. Patterns of change and possible biases arising from the use of different climate databases have been identified in three scenarios: two based on synthetic reference climate files and one empirical meteorological year. Synthetic data files such as EPW and MET are frequently used in different building simulation programs when experimental files that characterize the local climatic conditions, such as the generated TMY, are not available. Normally this is due to the fact that it is not always possible to measure the climatic variables in all the locations where a building is to be constructed, in this case, Tabernas in Almeria.

Based on this, the results obtained in the comparison to the different climatic variables show, in temperature magnitude, a general tendency of the EPW synthetic data to overestimate the experimental data, while the MET file data underestimates the real data. The most significant differences in the EPW case correspond to the winter period while in the MET case, the largest differences are observed in spring. In the case of relative humidity and solar irradiance, the behavior patterns are opposite. TMY records the lowest values of relative humidity and the highest values of solar irradiance with respect to the two EPW and MET files. In accordance with the trend shown in the temperature patterns, the cooling demand of the building is overestimated in the MET case and underestimated in the EPW case. Conversely, the cooling demand is overestimated in the EPW case and underestimated in the MET case.

On the other hand, when performing the Givoni diagrams and evaluating the bioclimatic strategies needed to achieve thermal comfort inside the building, it can be seen that the greatest need is the heating demand, being heating techniques by internal gains and passive solar energy use the predominant strategies. In buildings with high internal gains, the comfort zone extends to the left of the diagram due to this passive heating. The bioclimatic chart indicates the potential to use the high internal gains characteristic of tertiary sector buildings to minimize conventional energy use.

When comparing the synthetic and experimental data, some differences are observed, since in EPW and in MET permissible comfort is achieved with a high percentage for a large part of the year. This means that the temperatures and relative humidity present values belong to the comfort zone, while for TMY these values are not in this zone, requiring heating techniques to achieve thermal comfort indoors.

Finally, it can be concluded, as previously mentioned, that climate data files showing reliable and current values are important in order to correctly analyze the needs of the building. This way we guarantee that we build promoting climate change resilient cities that minimize energy consumption in order to reduce GHG emissions from the building sector, since they account for a large percentage worldwide. In addition, the identification of optimized bioclimatic strategies in urban environments adapted to climate change allows better planning of more effective urban development and rehabilitation policies, taking into account the serious impacts of climate change in cities.

## **Acknowledgement**

This research was funded by the Spanish National Research Agency (Agencia Estatal de Investigación) through the In-Situ-BEPAMAS project, reference PID2019-105046RB-I00. The operation of the test facilities that supported this study was partially funded by the Spanish Ministry of Economy, Industry and Competitiveness through ERDF funds (SolarNOVA-II project Ref. ICTS-2017-03-CIEMAT-04). The authors wish to express their gratitude for all these funds.

## References

1. Wang, L., Liu, X., Brown, H.: Prediction of the impacts of climate change on energy consumption for a medium-size office building with two climate models. *Energy and buildings* 157, 218-226 (2017).
2. The Intergovernmental Panel on Climate Change (IPCC). Global Warming of 1.5 °C, <https://www.ipcc.ch/sr15/>, last accessed 21/09/2021.
3. Vasaturo, R., van Hooff, T., Kalkman, I., Blocken, B., van Wesemael, P.: Impact of passive climate adaptation measures and building orientation on the energy demand of a detached lightweight semi-portable building. *Build Simulation* 11(6), 1163-1177 (2018).
4. De Masi, R.F., Gigante, A., Ruggiero, S., Vanoli, G.P.: The impact of weather data sources on building energy retrofit design: case study in heating-dominated climate of Italian back-country. *Journal of building performance simulation* 13(3), 264-284 (2020).
5. Kočí, J., Kočí, V., Maděra, J., Černý, R.: Effect of applied weather data sets in simulation of building energy demands: Comparison of design years with recent weather data. *Renewable & sustainable energy reviews* 100, 22-32 (2019).
6. Erba, S., Causone, F., Armani, R.: The effect of weather datasets on building energy simulation outputs. *Energy procedia* 134, 545-554 (2017).
7. Cui, Y., Yan, D., Hong, T., Xiao, C., Luo, X., Zhang, Q.: Comparison of typical year and multiyear building simulations using a 55-year actual weather data set from China. *Applied energy* 195, 890-904 (2017).
8. Plataforma Tecnológica Española de Eficiencia Energética, <https://www.ptee.org/>, last accessed 21/09/2021.
9. Hosseini, M., Bigtashi, A., Lee, B.: A systematic approach in constructing typical meteorological year weather files using machine learning. *Energy and buildings* 226, 110375 (2020).
10. Skeiker, K., Ghani, B.A.: A software tool for the creation of a typical meteorological year. *Renewable energy* 34(3), 544-54 (2009).
11. Yang, L., Wan, K.K.W., Li, D.H.W., Lam, J.C.: A new method to develop typical weather years in different climates for building energy use studies. *Energy* 36(10), 6121-6129 (2011).
12. Huang, J., Gurney, K.R.: The variation of climate change impact on building energy consumption to building type and spatiotemporal scale. *Energy* 111, 137-153 (2016).
13. Pernigotto, G., Prada, A., Cóstola, D., Gasparella, A., Hensen, J.L.M.: Multi-year and reference year weather data for building energy labelling in north Italy climates. *Energy and buildings* 72, 62-72 (2014).
14. Ebrahimpour, A., Maerefat, M.: A method for generation of typical meteorological year. *Energy conversion and management* 51(3), 410-417 (2010).
15. Chen, D., Chen, H.W.: Using the Köppen classification to quantify climate variation and change: An example for 1901–2010. *Environmental development* 6, 69-79 (2013).
16. Sánchez, M.N., Soutullo, S., Olmedo, R., Bravo, D., Castaño, S., Jiménez, M.J.: An experimental methodology to assess the climate impact on the energy performance of buildings: A ten-year evaluation in temperate and cold desert areas. *Applied energy* 264, 114730 (2020).
17. Olmedo, R., Sánchez, M.N., Enríquez, R., Jiménez, M.J., Heras, M.R.: ARFRISOL Buildings-UIE3-CIEMAT. Chapter of " Report of Subtask 1a: Inventory of full scale test facilities for evaluation of building energy performances". IEA EBC Annex 58 Final Reports, Leuven (2016) ISBN: 9789460189906.

16

18. Castaño, S., Guzmán, J.D., Jiménez, M.J., Heras, M.R.: LECE-UiE3-CIEMAT. Chapter of "Report of Subtask 1a: Inventory of full scale test facilities for evaluation of building energy performances". IEA EBC Annex 58 Final Reports, Leuven (2016) ISBN: 9789460189906
19. Skeiker, K., Ghani, B.A.: A software tool for the creation of a typical meteorological year. *Renewable energy* 34(3), 544-54 (2009).
20. Climate final report. PASCOOL project. Joule II Programme of the European Commission. (JOU2-CT79-0013), Athens (1995).
21. Soutullo, S., Sánchez, M.N., Enríquez, R., Jiménez, M.J., Heras, M.R.: Empirical estimation of the climatic representativeness in two different areas: Desert and Mediterranean climates. *Energy Procedia* 122, 829–834 (2017).
22. Givoni, B.: Comfort, climate analysis and building design guidelines. *Energy and buildings* 18(1), 11-23 (1992).
23. Manzano-Agugliaro, F., Montoya, F.G., Sabio-Ortega, A., García-Cruz, A.: Review of bioclimatic architecture strategies for achieving thermal comfort. *Renewable & sustainable energy reviews* 49, 736-755 (2015).
24. Daemei, A.B., Eghbali, S.R., Khotbehsara, E.M.: Bioclimatic design strategies: A guideline to enhance human thermal comfort in Cfa climate zones. *Journal of Building Engineering* 25, 100758 (2019).
25. Soutullo, S., Sánchez, M.N., Enríquez, R., Olmedo, R., Jiménez, M.J.: Bioclimatic vs conventional building: experimental quantification of the thermal improvements. *Energy Procedia* 122, 823–828 (2017).

# Potential of biogas production in Waste Treatment Center Santa Rosa in Rio de Janeiro: A theoretical estimation

Gardênia Mendes de Assunção<sup>1</sup>[0000-0002-8015-0839]

gardeniassuncao@gmail.com

Ronney Arismel Mancebo Boloy<sup>1</sup>[0000-0002-4774-8310]

ronney.boloy@cefet-rj.br

<sup>1</sup> Group of Entrepreneurship, Energy, Environment and Technology - GEEMAT/CEFET-RJ.

<sup>1</sup> Federal Centre of Technological Education Celso Suckow da Fonseca, Rio de Janeiro, Brazil

**Abstract.** This article aims to analyze theoretically the potential for biogas production the Waste Treatment Center (WTC) Santa Rosa, located the city of Seropédica, in the state of Rio de Janeiro, based on two estimation models. The models used were the Intergovernmental Panel on Climate Change (IPCC) and LandGEM, developed by US Environmental Protection Agency (USEPA). The period analyzed was of (2011-2020), concerning methane generation, power, and energy available. The results indicate a variation between two models, in IPCC, the averages were higher, that presented by the LandGEM, that which may be related to the parameters that each model uses. In the IPCC the wastes are segregated by type and different percentages. In LandGEM there is not such segregation. Other factors can influence the results among with, the data, the climatic conditions to define the closest alternative to reality. The results also show that the potential of biogas as a renewable source in energy generation, can contribute to sustainable urban mobility.

**Keywords:** Landfill Gas; Renewable Energy; Estimation Models

## 1 Introduction

The economic model centered on large-scale production, with the intensive use of the natural resources, due to the accelerated industrialization process, has influence in consumption, waste produced, and its consequent increase over time [1]. Another point that relates to this issue is the growing urbanization. The report presented by the United Nations (UN), stated that in 2017, the world population was 7.6 billion people. The trend is that by 2030 this number should reach 8.6 billion people. As a result of this process, there is also an increase in waste production [2].

The growth trend in waste production in a study presented by the World Bank is that 2.01 billion tons of urban solid wastes produced annually and that the equivalent of least 33% are disposed of incorrectly and not managed environmentally friendly

mode. The average waste generated per person per day is 0.74 kg [3]. The large volume of waste generated originates mostly in high-income developed countries, representing only 16% of the world's population, generating around 34% or 683 million tons of global waste [3].

Although transformations in production processes have advanced in search of productive efficiency about the waste it is still a problem to be resolved [4; 5], there are still insufficient initiatives aimed at waste treatment, which implies the inadequate disposition of much of what could be used, having the correct destination, for example, the use to energy.

In the case of Brazil, a considerable amount of waste still goes to such as the dumps and controlled landfills, which results in many problems, arising from long-term negative effects on the environment and society. According to Solid Waste Panorama 2020, with data from 2019, the disposal for dumps and controlled landfills showed growth, from 25 million tons per year to another 29 million tons. However, the disposal in sanitary landfills increased by 10 million tons in a decade from 33 million tons per year to 43 million tons [6].

However, Brazil even faced with the increasing number of wastes disposed in dumps and controlled landfills, the increase in the volume of what was sent to sanitary landfills with the capacity to treat this waste through the recovery of biogas shows that the country is heading towards the treatment of its waste, such as the production of biogas. There are currently 638 plants in operation in the country with the capacity to operate 2.2 million m<sup>3</sup> biogas, with the use of different substrates such as agriculture, industry, landfill, and sewage treatment plants (USW and STP). Of this total 57 are USW and STP plants representing 9%, which are responsible for 73% of biogas production in the country [7].

In the international context, countries such as Austria, Germany, Sweden, Belgium, Denmark, Switzerland, the United Kingdom, Singapore, China, Japan, and others, stand out for investments in the reuse of a large part of the waste generated. These countries are moving towards solving the waste problem by developing recovery alternatives [8].

Europe is emerging as a global model in the search for alternatives to deal economically and environmentally with its waste. According to the Association of Energy Recovery Companies of Urban Waste- AEVERSU, in 2019, plants treated the equivalent of 2.504.443 tons of waste, generating 1.762.585 MWh of energy, sufficient to supply 500 residences [9], which results in environmental gains, with adequate destination, and economical energy production with low-cost material and high energy potential.

Given the above, the objective of this research is to theoretically analyze the energy potential of a landfill for biogas production based on forecasting models. The models used were the Intergovernmental Panel on Climate Change -IPCC and Landfill Air Emissions Estimation Model-LandGEM, the United States Environmental Protection Agency (USEPA). The study object selected was the Waste Treatment Center (WTC), Santa Rosa, located in the city of Seropédica, in the state of Rio de Janeiro. The information about the WTC were based on Caixa Econômica Federal project for solid waste management and carbon financing in partnership with United Nations, the United Nations Framework Convention on Climate Change (UNFCCC), the project proposes the

mitigation of greenhouse gases (GHG) from the promotion of renewable energies, including landfill biogas [10].

Several studies about theme were identified in the literature and focused on the reality of Brazilian sanitary landfills, among those highlighted are, [11; 12; 13; 14]. The study carried by [11] aimed to analyze the efficiency these models of application of first order decay in three sanitary landfills in Brazil, two in São Paulo and one in Rio de Janeiro, the landfill of Nova Iguaçu, which operate within the ambit of the Clean Development Mechanism (CDM).

In the study carried out by [12], the authors presented the application the IPCC and LandGEM models with the objective of estimating the biogas generation potential of the municipal landfill of Guarapuava (PR). In the study carried out by [13] aimed to study the technical aspects associated with the capture of biogas and its use from solid urban waste in landfills in northwestern São Paulo. The study carried out by [14] was analyzed the economic and environmental viability of using the biogas from the landfill of the municipality of Varginha (MG). These studies present the applications of models in landfill in the Brazil and the results indicate that models are important to analysis the potential de biogas generation the landfills, characterizing the relevance of the theme.

Thus, this research reinforces discussions on the subject from the proposal of comparative analysis of the two models for the WTC Santa Rosa, which justifies its relevance when focusing on waste treatment and its energy potential, and how this process can contribute to reduction of greenhouse gases and the consequent negative impacts that not treating waste can cause. And yet, as biogas is a source of bioenergy renewable source can contribute to sustainable urban mobility.

The research is structured into five parts, in the first the introduction. In the second part are presented the wastes and their energy potential; the biogas of landfills; the technologies of conversion of biogas into energy; the two estimation models used in the study. In the third part the methodology and in the fourth the discussions of the results and in the fifth part the conclusions, followed by the references.

## **2 The solid waste, its energy potential**

The issue of urban waste is not recent, it had its rise with the Industrial Revolution, with the intensive use of non-renewable natural resources and the consequent production of waste, reflecting the growth of the urban population and changes in consumption patterns, with the excessive increase of disposable products and that after used are disposed of inadequate form. This problem has been aggravated over time, mainly in underdeveloped or developing countries due to their technical or economic limitations to deal with the issue of the proper treatment of waste [5; 16].

The municipal solid wastes (MSW) are considered according to its origin and characteristics, such as household waste (originating from domestic activities in urban residences) and urban cleaning (originating from sweeping, cleaning of streets and public roads, and other urban cleaning services); industrial and agricultural. Physical characteristics may include inert materials: glass, metals, earth and ash, and inert waste; or

combustible materials: paper, cardboard, plastics, wood, gums, leather, food, among others [15].

In Brazil, the gravimetric composition of waste is mostly organic waste, which represents 43%, followed by plastics with 16.8% and rejects 14.1%, the remaining waste is composed of paper and cardboard 10.4%; textiles 5.6% and still glass, metals, multilayer packagings and other types not defined [6].

Given the diversity in the composition of the waste various are the alternatives or technological routes of final destination, that can be given for its utilization from an integrated solid waste management system in which waste is managed as a valuable resource and thus should be recovered, which are configured in four possible destinations: recycling, composting, energy recovery of energy waste and landfills final disposal of waste that cannot be used in an appropriate place [15].

A study conducted by Abiogás, in partnership with the Brazilian Association of Public Cleaning and Special Waste Companies (ABRELPE), focused on landfill sites, showed the generation of solid urban waste as its final destination, and the energy production potential wasted in Brazil.

Data show that Brazil allocated more than 42 million tons of solid waste to landfills in 2018. Abiogás and ABRELPE estimate that Brazil has captured 4.2 billion Nm<sup>3</sup> of biogas. However, only 9% of this potential was used for electricity generation (751 GWh) and less than 2% produced 35 million Nm<sup>3</sup> of biomethane. However, if all the organic matter generated in 2018 had been destined for landfills, the country's potential could supply 49 million homes [7].

## 2.2 The landfill biogas

The gas of landfill is composed of several other gases, in large quantities by methane (CH<sub>4</sub>), carbon dioxide (CO<sub>2</sub>), originating from the anaerobic decomposition of biodegradable compounds of organic waste. Other gases that appear in small amounts are, ammonia (NH<sub>3</sub>), hydrogen (H<sub>2</sub>), hydrogen gas (H<sub>2</sub>S), nitrogen (N<sub>2</sub>), and oxygen (O<sub>2</sub>) [1;17; 18;19].

The methane gas produced in landfills is 25 times more harmful than carbon dioxide in terms of greenhouse gases (GHG) emissions, but its simple conversion and burning in the form of biogas is an environmental benefit [8]. It is estimated that a Landfill Gas (LFG) energy project will capture about 60% to 90% of the methane emitted by the landfill, depending on the design and efficiency of the system [19; 20].

Another point to consider is the calorific value (CV) of biogas can be defined as the amount of energy (heat) released in the combustion of a unit amount of fuel. In the case of a gaseous fuel, the energy content is commonly defined in units of megajoules per cubic meter of fuel MJ / m<sup>3</sup>. The calorific value of biogas is approximately 21.600 kJ/m<sup>3</sup>, corresponding to 6,0 kWh / m<sup>3</sup> [21].

There are many environmental factors to consider when developing biogas energy sources including the potential impact on air quality. The concentrations of chemical and biological components in biogas differ from those found in other fuels. Some of these components may be toxic to human health and the environment, to form toxic

substances during the combustion process, or to form toxic substances after photochemical aging in the atmosphere [18].

### **2.3 The Biogas energy conversion technologies**

The technological alternatives for the energy use of waste are not recent, dating back to 1960 in Europe with the first thermoelectric plant and later in the 1980s in the United States and Japan [15]. The initiatives mark the beginning of waste treatment projects, which not only reduce the amount that ceases to be disposed of inappropriately impacting negatively on the environment but also on economic gains, as the use of waste in energy generation requires a large volume, equivalent to 150 tons / day [15].

The biogas of urban solid waste USW and its energy use can take place through two technologies: sanitary landfills, or specialized biodigesters. In the first case, the organic material of the cities, when deposited in the landfill in closed cells where an anaerobic environment is created, turns into biogas. It is then captured through a network of collecting pipes scattered over the landfill, treated, and eventually applied to electricity generation, usually in internal combustion engines [5].

The technologies for the treatment and energy valuation of USW can be heat treatment, chemical biological treatment, and physical-mechanical treatment [5]. The conversion of biogas into electricity is possible through gas engines and gas turbines [22]. Internal combustion engines are the most widely used technologies in the process of converting Biogas into energy [23]. The capacity of most landfill gas generators ranges from 0,3 to 4,5 MW and their power is defined by the work carried out in a time unit [24].

The engines with higher power such as microturbines have also been employed to produce electricity from biogas, with a minimum methane concentration of approximately 35%. Another advance in the energy recovery of waste is through a relatively recent process, Oxidation Gradual (GO), which can produce electricity from the LFG at lower methane concentrations, which is equivalent to 1.5%, which ensures better use [23].

### **2.4 The estimation models of biogas production in landfill sites**

#### **The LandGEM Model**

There are models for estimating biogas production from landfills, the first-order decay model is commonly used in practice assumes that the generation of methane, after reaching its peak, decreases exponentially over time-First Order Decay (FOD) - (IPCC, 2019). Examples of these models are the Landfill Gas Emissions Model (LandGEM) of the US Environmental Protection Agency (USEPA) and the IPCC model [5; 24].

The US Environmental Protection Agency (USEPA) Landfill Gas Emissions Model (LandGEM) is the most widely used model. The model equation consists of the following parameters [25]:

$$QCH4 = \sum_{i=1}^n \sum_{j=0,1}^1 KLo \left(\frac{Mt}{10}\right) e^{-ktij} \tag{Equation (1)}$$

Where:

- QCH4 = anual methane generation in the year of the calculation (m3/year);
- i = 1 year time incremente
- n = (year of the calculation) – (initial year of waste acceptance)
- j = 0.1 year time incremente
- k = methane geration rate (year -1)
- Lo = potential methane geration capacity (m3 / Mg)
- Mi = mass f waste accepted in the ith year (Mg)
- tij = age of the jth section of waste mass Mi accepted in the ith year (decimal year, eg 3.2 years).

**The IPCC Model**

The IPCC model implies determining the Lo (methane generation potential) from the degradable organic content (DOC) of municipal solid waste, which is estimated using the information on the different types of waste (food, paper, wood, textiles, etc.) in terms of emissions [26]. Emissions are calculated from the following equation:

$$= [ \sum_x CH4 \text{ generated } x,T - RT ] \cdot (1 - OXT) \tag{Equation (2)}$$

Where:

- CH4 Emissions = CH4 emitted in year T, Gg
- T = inventory year
- x = waste category or type/material
- RT = recovered CH4 in year T, Gg
- OXT = oxidation factor in year T, (fraction)

This method to estimate the potential of methane generation is based on a FOD (First Order Decay) model using a mass balance that requires determination of the degradable organic carbon fraction (DOC) in the residues. In waste, only part of the mass is decomposed into biogas (Ddocm) and can be calculated according to the following equation [26].

$$DDOCm = DOC \cdot DOCf \cdot W \tag{Equation (3)}$$

- DDOCm = mass of decomposable DOC deposited, Gg
- W = mass of waste deposited, Gg
- DOC = degradable organic carbon in the year of deposition, fraction, Gg C / Gg waste
- DOCf = fraction of DOC that can decompose (fraction)

MCF = CH<sub>4</sub> correction factor for aerobic decomposition in the year of deposition (fraction)

The methane generation potential (Lo) is given by equation below [26].

$$Lo = DDOCm.F.16/12 \quad \text{Equation (4)}$$

Where:

Lo = CH<sub>4</sub> generation potential, Gg CH<sub>4</sub>

DDOCm = mass of decomposable DOC, Gg

F = fraction of CH<sub>4</sub> in generated landfill gas (volume fraction=0,5)

16/12 = molecular weight ratio CH<sub>4</sub>/C (ratio)

Some data are already predefined based on previous analyses generally adopted as a hypothesis in the period of one year between the deposit of the waste in the landfill and the beginning of biogas generation. For variable k, the values can vary from 0.003 to 0.21 according to the internal characteristics of the landfill and local environmental conditions, the most important variable being the climate (the drier, the lower the value of k) [5].

The variable Lo represents the potential to generate methane per ton of waste. It can vary from 0 to 187 m<sup>3</sup> / ton, with values suggested between 47 and 140 m<sup>3</sup> / ton. Variable. The Lo variable is entirely dependent on the type of waste sent to the landfill. The higher the percentage of organic material in the RSU, the higher the value of Lo [5].

### 3 Methodology and data analysis

The objective of the research was to theoretically analyze the energy potential of a landfill site for biogas production, based on prediction models, with the object of a study at Waste Treatment Center (WTC) Santa Rosa, in city of Seropédica, in the state of Rio de Janeiro. To compare the power generation potential were used two models, the LandGEM V. 3.02, and the Intergovernmental Panel on Climate Change -IPCC (2006). Data the landfill were from the initial partnership project between UNFCCC-United Nations Framework Convention on Climate Change and Caixa Econômica Federal (CEF), Brazil [10]. For the energy analysis were used data of the population from four municipalities, Mangaratiba, Itaguaí, Seropédica, and Rio de Janeiro that target residues to the WTC.

The estimate of population growth was based on historical census data and estimated by Brazilian Institute of Geography and Statistics (IBGE), until 2020 [37]. For the gravimetric position of the waste, the data were from the municipality of Rio de Janeiro, available on the Datario website, the used percentages were food (47%); garden (1); paper (15%); wood (1%); textile (4%); nappies (8%); plastic and other inert (24%) [27].

For the power (P) and energy (E) estimates available at the landfill, were used the following equations:

$$P = Q \times PCI \times n / 860.000 \quad \text{Equation (5)}$$

$$E = P \times \text{Motor efficiency} \times \text{Operating Time} \quad \text{Equation (6)}$$

Where:

P = available power (MW); Q = annual methane generation (m<sup>3</sup> of CH<sub>4</sub> / year); PCI = Lower Calorific Power of Methane. If the landfill does not have the real PCI value of methane, 5,500 kcal / m<sup>3</sup> can be adopted CH<sub>4</sub> (value adopted for 50% of methane present in landfill biogas)

n = efficiency of motors (usually 28%, value adopted = 0,33%) [29].

860,000 = conversion from kcal to MW [28].

E = available energy (MWh / day)

Motor efficiency = efficiency of engines operating at full load (estimated at 87% = 0.87); Engine operating time = 24 hours / day, value adopted n° / year = 8.760.

Therefore, depending on the methane flow, the power (MW) and energy calculations can be performed (MWh/day) available at the landfill year by year [28].

### 3.1 The study area

The Waste Treatment Center (WTC) Santa Rosa, it's a private company of owned of the Ciclus Ambiental, went in operation in 2011, through a concession contract with Urban Cleaning Company (COMLURB), a public company from municipality of Rio de Janeiro. With an area of approximately 2 million m<sup>2</sup>, it was designed to operate with an estimated lifetime of 20 years with a daily demand of about 10,000 tons of waste, being from Rio de Janeiro (90%), Seropédica, Itaguaí, Mangaratiba (5%) and large-generators (5%). The landfill is considered one of the safest, most modern, and efficient waste treatment facilities in Latin America [31; 34].

Currently, in WTC is in operation a plant for the recovery of biogas. The biogas generated is composed of 50% methane, purified through complete removal of CO<sub>2</sub>, removal of sulfur and other contaminants, and nitrogen reduction. At the end of the biogas purification process, the methane level rises to 95% and only 5% of nitrogen, above the minimum of 90%, is considered biomethane fuel, renewable natural gas (NRG). The capacity for production is 200.000 m<sup>3</sup> / day of biomethane, the NRG initially destined for sale in beam trucks, to industrial customers and fuel distributors, [32]

## 4 Results and discussion

The data on the volume of waste were estimated for the period of the 10 years, starting in the 2011, year of opening the landfill. The volume of waste was 1,826,302 (tons / year). In the 2020 year, the volume estimated accumulated of the wastes was 16,844,377(tons / year). From these data is possible to observe that the amount of waste of the period is considered high, and the landfill has capacity of recovery the wastes in the energy generation, contributing to the energy matrix and in the reduce the negative impacts that untreated waste can cause.

#### 4.1 Estimated generation of biogas The LandGEM Model

For the analysis, the parameters used are determined by model and the values for conventional landfills, Methane Generation rate (k), 0.05; Potential Methane Generation capacity (Lo), 170; NMOC concentration, 4,000, and Methane content, 0.05 [29].

The Fig. 1 shows the estimates of biogas and methane generated in WTC, in m<sup>3</sup>/year, from the LandGEM model. It was observed that the growth reaches its maximum point in 2032, with 426,257,246 m<sup>3</sup> of biogas and 213,128,623 m<sup>3</sup> of methane, the year the landfill will be closed. Following the decay of the curve, since the landfill will not receive waste, however this process is considered normal, the generation of methane extends over the years [24; 29]. In this case, the process extends over 100 years.

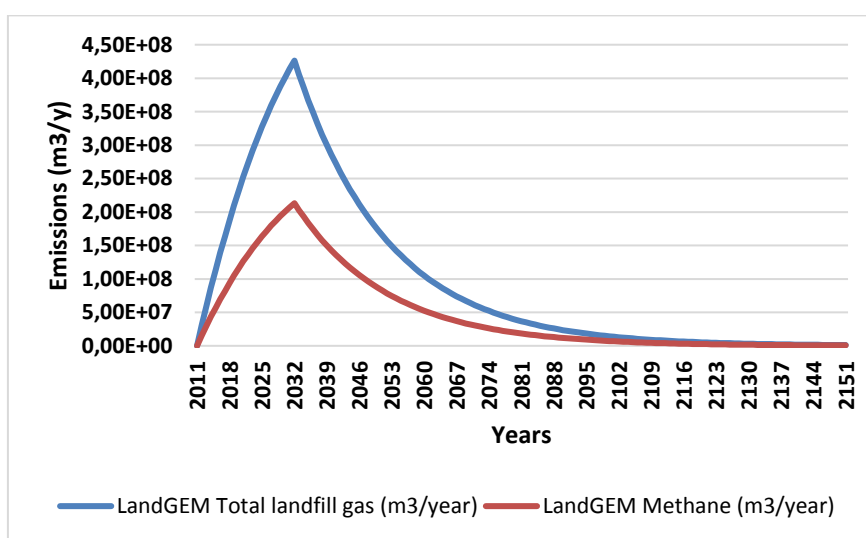


Fig. 1 Landfill gas and methane generation in WTC Santa Rosa estimated by LandGEM model

#### The IPCC Model

For the analysis, the parameters used are determined on the project do landfill that are: Fraction of methane (F) in developed gas (0,5); Conversion factor, C to CH<sub>4</sub> (1.33); Oxidation factor (OX) (1) [10]. The model IPCC considers a delay time of 6 months for biogas generation [33].

In the IPCC model, it was obtained the similar behavior about the methane generation presented by LandGEM in the analyzed period (2011-2020), and it is important to emphasize that the unit of methane generation potential (Lo), LandGEM is given in cubic meters of methane per ton of waste (m<sup>3</sup> CH<sub>4</sub>/t W) and in the IPCC model the values are given in gigagram (Gg), Lo is given in tons of methane per ton of waste (t CH<sub>4</sub>/t W) [37].

Considering the density of methane that is 0.657 kg/m<sup>3</sup> [24], for the analysis the data were calculated in m<sup>3</sup>/year according to Fig. 2, the methane volume was higher in 2021 in 65,763,482 m<sup>3</sup>/Gg. From this period already begins the decay. This difference in behavior may be related to the period considered by the model, being smaller about the LandGEM. In the IPCC the limit is up to 2030, so 19 years were considered.

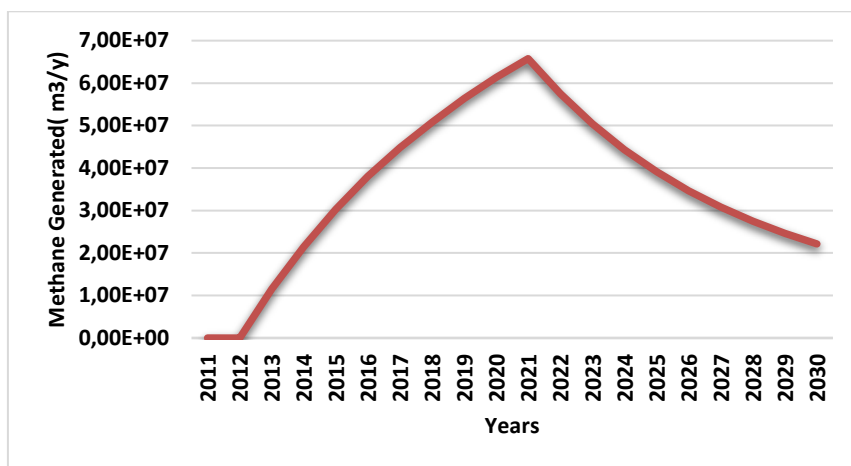


Fig. 2 Methane generation in WTC Santa Rosa estimated by IPCC model

The analysis between two models estimated the volume in m<sup>3</sup>/year of methane is presented in Fig 3.

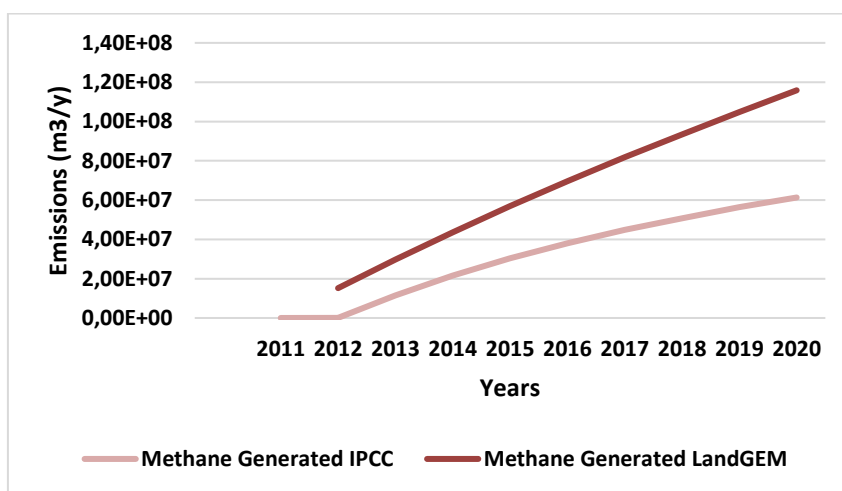


Fig. 3 Methane generated by IPCC and LandGEM models

The graphic indicates a similar growth in methane generation in the period by the two models. The variation presented is influenced for parameters of each model, the

LandGEM considers that the emission of methane will start only after the first year of disposal of the waste in the landfill. The model allows you to evaluate other gases, such as carbon dioxide that is equal to methane, however, the model not consider the gravimetric composition of the waste. For the IPCC, emissions start in the first year, is considered the gravimetric composition of the waste [12].

In the IPCC the apex appears in 2021 with 65,763,481 m<sup>3</sup>/Gg, however for the following years emissions ending in the year 2030 are registered with 22,124,630 m<sup>3</sup>Gg, the time limit of the model. The LandGEM presented emissions for period most long in 555,379 m<sup>3</sup>Gg in the 2151 year. The results indicates that methane flow depends directly the volume and quality of solid wastes deposited in the landfill.

Next, the comparative analysis of the two models and the energy analysis.

### Energy analysis

In the Table 1, are presented the results the two models IPCC and LandGEM concerning methane emissions, power, and available energy. The differences in the results obtained with the two models imply considering the different parameters since the IPCC analyzes the data segregating the wastes by gravimetric composition [12; 13; 24]. According to [36], in the LandGEM the generation of methane is integrated in more than ten (10) periods of 0.1 years. These results can be relevant and influence the results produced [24].

**Table 1:** Averages of methane generation, power and available energy generated from IPCC and LandGEM models (EPA) the WTC Santa Rosa – period (2011-2020)

Models	Methane Emissions (m <sup>3</sup> /year)	Power (kW/year)	available energy (kWh)
IPCC	31,460,993	66,397	506,027,325
LandGEM	61,105,531	128,961	982,838,279

To calculate the energy estimated, the reference was an internal combustion engine model brand GE Jenbacher model (JMS-BL), the same model cited in the WTC project. It has a capacity of 8.000h/year. This type of engine is suitable for landfills with a large volume of waste [34]. According to the manufacturer’s specifications, the model has the following characteristics: electric power, kW (1501); thermal power with heat exchanger, kW (1500); thermal power without heat exchanger, kW (911); electrical efficiency (42,7%); thermal efficiency with heat exchanger (42,8%); thermal efficiency without heat exchanger (25,7%); biogas consumption at (55%); methane (642) m<sup>3</sup>/h [35].

The results of these analyses are that the average energy generated in the landfill is equivalent to 337,052 kW by IPCC model and 655,226 kW by LandGEM model. Considering that the average energy consumption in Brazilian residences in which the value for 2019 was 162 kWh/month (EPE, 2019), the energy generated can supply 3,123,625

homes by the IPCC model and a more expressive number by LandGEM of 6,066,903 homes.

These results reflect the differences in which different models in the same analysis may present, which may be related to the parameters that each model uses [36]. These differences were identified in the studies of [11; 12; 36], in which the authors emphasize these issues that may still be related to other factors such as, composition and age of the wastes, among others, which may influence the quality and quantity of biogas [11].

Another aspect that can influence the differences in the results in the production of biogas is time that the waste is disposed on the landfill that are different in the two models [12]. The LandGEM is limited by not considering possible differences in the composition of waste deposited over time, as occurs in the IPCC model [36].

## Conclusion

The increase of waste production over time has been going widely debated in the literature and thus also the search for alternatives that aim at its energy use as one of the ways to reduce greenhouse gases (GHG). In this sense, this research aimed to theoretically analyze the energy potential of the WTC Santa Rosa located in the state of Rio de Janeiro, based on the forecast models of the IPCC and LandGEM.

The results indicate a significant variation presented by the models, which may be related to the parameters that each one uses. The averages of the analyzed period 2011-2020 generated by the IPCC were: methane 31,460,993 m<sup>3</sup>/year; power 66,397 kWh; available energy 506,027,325 kWh. By LandGEM, the averages were: methane 61.105,531 m<sup>3</sup>/year; power 128,961 kWh; available energy 982,838,279 kWh.

The LandGEM model presented better results than the IPCC in terms of methane generation, power and available energy, which is related to the parameters that each model uses. However, it is noteworthy that since these are theoretical estimates, the practical application of the models requires an analysis in order to identify the main aspects that can influence the results of biogas production.

These results show the importance of biogas as an alternative for energy generation, from a renewable source and that can contribute to the solid waste treatment, expanding the capacity of WTC for energy recovery processes, which consequently contributed to the reduction of greenhouse gases, and still provide economic benefits, in addition to the use, with the sale of energy by Waste Treatment Center.

## References

1. Piñas, J. A. V., Venturini, O. J., Lora, E. E. S.; Oliveira, M. A. de, Roalcaba, O. D. C. Landfill sites for electric power generation from biogas production in Brazil: comparison of LandGEM (EPA) and Biogas (Cetesb) models. *Rev. bras. estud. popul.* vol.33, n.1, pp.175-188. <https://doi.org/10.20947/S0102-309820160009>, (2016).
2. United Nations. *World Population Prospects The 2017 Revision: Key Findings and Advance Tables*. UNITED NATIONS, New York, (2017).

3. Kaza, S.; Yao, L., Bhada-Tata, P., Woerden, F. V. What a Waste 2.0: global snapshot of solid waste: management to 2050. World Bank (2018). <https://openknowledge.worldbank.org/handle/10986/30317>, last accessed 2021/04/20.
4. Oliveira, D. E. P. et al. Analysis of the potential of energy production from municipal solid waste incineration in the city of São Paulo. *Interciencia*, vol. 43, núm. 11. Asociación Interciencia, (2018). <https://www.redalyc.org/jatsRepo/339/33957918007/html/index.html>, last accessed 21/09/10.
5. Carvalho, R. Q., Tavares, A. N., Santos, G. V. dos, Bajay, S.V. Buried opportunities [electronic resource]: electricity generation from urban solid waste biogas /-Electronic data. Vitória : EDUFES, 320 p., (2019). last accessed 2021/04/09
6. Abrelpe. Panorama of solid waste in Brazil. (2020). <https://abrelpe.org.br/panorama/>, last accessed 2021/08/10.
7. ABiogás - Brazilian Association of Biogas and Biomethane. Proposal for a national biogas and biomethane programme, (2018). [https://abiogas.org.br/wp-content/uploads/2021/01/PNBB\\_Versao\\_Final.pdf](https://abiogas.org.br/wp-content/uploads/2021/01/PNBB_Versao_Final.pdf), last accessed 2021/08/22.
8. Abren. Brazilian Association for Energy Recovery of Waste. Institutional Plan. <https://abren.org.br/wp-content/uploads/2020/06/Plano-Institucional-ABREN-2020-mai2020.pdf>, (2020), last accessed 2021/05/10.
9. AEVERSU- Asociación de Empresas de Valorización Energética de Residuos Urbanos. ¿Qué es la valorización energética?, (2021). <https://aeversu.org/valorizacion-energetica/>, last accessed 2021/06/10.
10. UNFCCC- United Nations Framework Convention on Climate Change. CPA 6573-P1-0001-CP1 : CPA-1: Landfill gas recovery, energy generation and biogas distribution from CTR Santa Rosa. Caixa Econômica Federal Solid Waste Management and CarbonFinance Project. (2019) [https://cdm.unfccc.int/ProgrammeOfActivities/cpa\\_db/XQMN648JU5LVRA\\_C2OBFE3H1PW0KG79/view](https://cdm.unfccc.int/ProgrammeOfActivities/cpa_db/XQMN648JU5LVRA_C2OBFE3H1PW0KG79/view), (2019), last accessed 2021/07/15.
11. Santos, M. M., Romanel, C., Van Elk, A.G. H.P. Analysis of the efficiency of first-order decay models in forecasting greenhouse gas emission in Brazilian sanitary landfills. *Eng Sanit Ambient | v.22 n.6 | nov/dez 2017 | 1151-1162*. DOI: 10.1590/S1413-41522017156311. (2017)
12. Bianek, J. et al. Comparison between usepa and IPCC methodologies for theoretical estimation of biogas production in landfill. *BIOFIX Scientific Journal v. 3 n. 1 p. 34-40*. DOI: [dx.doi.org/10.5380/biofix.v3i1.56038](https://dx.doi.org/10.5380/biofix.v3i1.56038), (2018).
13. Silva, T. F. da, Freitas, I. R. Potential for biogas generation from urban solid waste in the north-west region of São Paulo by different technical forecasting models. *Bioenergia em revista: diálogos*, ano 9, n. 1, p. 87-100, jan./jun, (2019). <http://fatecpiracicaba.edu.br/revista/index.php/bioenergiaemrevista/article/view/299/PDF>, last accessed 2021/09/10.
14. Souza, A. R. de et al. Analysis of the potential use of landfill biogas energy and simulation of greenhouse gas emissions of different municipal solid waste management scenarios in Varginha, MG, Brazil. *Eng Sanit Ambient. v.24 n.5 set/out 2019; 887-896*. DOI: 10.1590/S1413-41522019187066, (2019).
15. EPE- Empresa de Pesquisa Energética . Technical Note DEA 18/14 - Energy Inventory of Solid Urban Waste (2014). <https://www.epe.gov.br/sites-pt/publicacoes-dados-abertos/publicacoes/PublicacoesArquivos/publicacao-251/topico-311/DEA%2018Abertos/publicacoes/PublicacoesArquivos/publicacao309/NT%20Biometano%20de%20Aterro%20v%2019%202019> 2018. pdf, last accessed, 2021/05/10.
16. Nascimento, V. F.. Modeling environmental susceptibility of municipal solid waste disposal sites in regional scale. Doctorate Thesis of the Graduate Course in Earth System Science. INPE (2017). [https://bdtd.ibict.br/vufind/Record/INPE\\_3\\_c909c\\_b56a1a\\_3f75a25ff5dc135801fd](https://bdtd.ibict.br/vufind/Record/INPE_3_c909c_b56a1a_3f75a25ff5dc135801fd), last accessed 2021/10/05.

17. Govindan, S.S., P Agamuthu, P. Quantification of landfill methane using modified Intergovernmental Panel on Climate Change's waste model and error function analysis. *Waste Management & Research* 32(10), 1005-1014. <https://doi.org/110.1177/0734242x14552551>, (2014).
18. Li, Y. et al. Composition and toxicity of biogas produced from different feedstocks in California, (2019). *Environ Sci Technol.* October 01; 53(19): 11569–11579. doi:10.1021/acs.est.9b0300, (2014).
19. USEPA-United States Environmental Protection Agency. LFG Energy Project Development Handbook.(2020). [https://www.epa.gov/sites/production/files/2016-11/documents/pdh\\_full.pdf](https://www.epa.gov/sites/production/files/2016-11/documents/pdh_full.pdf) , last accessed 2021/8/23.
20. USEPA-United States Environmental Protection Agency. Landfill Methane Outreach Program (LMOP), (2017). <https://www.epa.gov/lmop/benefits-landfill-gas-energy-projects>, last accessed 2021/8/23.
21. USEPA-United States Environmental Protection Agency. Management of Low Levels of Landfill Gas (2011). <https://www.epa.ie/pubs/advice/waste/waste/managementoflowlevelsoflandfillgas.html>, last accessed 2021/8/23.
22. Manasaki, V., et al. Techno-economic assessment of landfill gas (LFG) to electric energy selection of the optimal technology through field-study and model simulation. *Chemosphere* 269 (2021) 128688. <https://doi.org/10.1016/j.chemosphere.2020.128688>, (2021)
23. Sing, H. N., A. Layek, A. An exposition on the results of utilizing biogas as an alternative fuel on the attributes of internal combustion engines. *International Journal of Renewable Energy Research*, Vol.9, No.3, September, (2019). <https://www.ijrer.org/ijrer/index.php/ijrer/article/view/9472/pdf>, last accessed 2021/09/23.
24. Lambuazau, A. Q. G. Energy potential of urban solid waste in Luanda Province (ASM) by different technical forecasting models, (2021). [https://run.unl.pt/bitstream/10362/127211/1/Lambuazau\\_2021.pdf](https://run.unl.pt/bitstream/10362/127211/1/Lambuazau_2021.pdf), last accessed 2021/09/10.
25. USEPA-United States Environmental Protection Agency.(2005)Landfill Gas Emissions Model (Land GEM) Version 3.02 User's Guide<https://www3.epa.gov/ttnecat1/dir1/landgem-v302-guide.pdf>, last accessed 2021/08/10.
26. Intergovernmental Paineel on Climate Change (IPCC). 2019 Refinement to the 2006 IPCC Guidelines for National Greenhouse Gas Inventories. Volume 5.Waste (2006). <https://www.ipcc-nggip.iges.or.jp/public/2019rf/vol5.html>, last accessed 2021/08/10.
27. DATA.RIO. Main characteristics of household waste: percent gravimetric composition, specific weight and moisture content according to the Planning Areas (AP) of the Municipality of Rio de Janeiro between 1995-2019 (2021). <https://www.data.rio/documents/ccdc3c0946ff430db6ef479befe8a5a5/about>, last accessed 2021/09/14.
28. ICLEI - Brazil - Local Governments for Sustainability Manual for the use of biogas: volume one, landfills. ICLEI - Local Governments for Sustainability, Secretariat for Latin America and the Caribbean, Project Office at Brazil, São Paulo, 2009. [http://www.resol.com.br/cartilha12/manual\\_iclei\\_brazil.pdf](http://www.resol.com.br/cartilha12/manual_iclei_brazil.pdf), last accessed 2021/08/20.
29. Barrak, E. Analysis of the theoretical potential of energy generation from the biogas landfill in Varginha. *Brazilian Journal of Renewable Energy*, v.8, n.1, p. 61-75, 2019. DOI: <http://dx.doi.org/10.5380/rber.v8i1.53660>, (2019).
30. Guarieiro, A.L. N., Madeira, C.F.N.M., Costa, L. F. da, Oliveira, M.P.B.V. The environmental licensing of a waste treatment plant: the case of WTC Seropédica. *Revista Ineana*. v.5 n. 1 p. 42 - 57 jul- dez (2019). [http://www.inea.rj.gov.br/cs/groups/public/@inter\\_vpres\\_geiat/documents/document/zwew/mtq4/~edisp/inea0148993.pdf](http://www.inea.rj.gov.br/cs/groups/public/@inter_vpres_geiat/documents/document/zwew/mtq4/~edisp/inea0148993.pdf), last accessed 21/05/10.
31. Abegás- Green Gas opens biogas units in Rio (2019). <https://www.abegas.org.br/arquivos/73011>, last accessed 21/08/10.

32. ABiogás - Brazilian Association of Biogas and Biomethane. Technical Note: N° 001/2021 - Panorama of Biogas in Brazil 2020. Foz do Iguaçu, March (2021). [https://abiogas.org.br/wp-content/uploads/2021/06/PANORAMA-DO-BIOGAS-NO-BRASIL-2020-v.8.0-1\\_1.pdf](https://abiogas.org.br/wp-content/uploads/2021/06/PANORAMA-DO-BIOGAS-NO-BRASIL-2020-v.8.0-1_1.pdf), last accessed 21/09/13.
33. World Bank. Brazil: integrated solid waste management na carbon finance project. Independent Evaluation Group, Project performance assessment report 123798, Washington, DC: World Bank. (2018). <https://ieg.worldbankgroup.org/sites/default/files/Data/reports/ppar-brazilintsolidwastemgmt.pdf>, last accessed 21/08/14.
34. Nascimento, D. P. Energy analysis of landfill processes metropolitan sanitarium of João Pessoa/PB (2020). [http://www.cear.ufpb.br/ppger/contents/documentos/dissertacoes-apresentadas/dissertao\\_de\\_dayse\\_pereira\\_do\\_nascimento.pdf](http://www.cear.ufpb.br/ppger/contents/documentos/dissertacoes-apresentadas/dissertao_de_dayse_pereira_do_nascimento.pdf), last accessed 21/09/14.
35. Zorg-Biogas. Jenbacher JMS 420 GS-B.L. 1500 kW el biogas generator (2021). <https://zorg-biogas.com/equipment/generators/jenbacher-jms-420-gs-bl-1500-kw-el-biogas-generator-building>, last accessed 21/09/15.
36. Dornela, N. M. de O., Faria, B. P. Z., Kim, V. J. H., Paula, E. C. de. Comparison of methane generation forecast models in Brazilian sanitary landfills for your use Energy. 4° South Brazilian Congress on Solid Waste and Sustainability. <http://www.ibeas.org.br/conresol/conresol2021/XIV-001.pdf>. (2021), last accessed 2021/09/20.
37. Brazilian Institute of Geography and Statistics -IBGE. Population Estimates Table 6579 - Estimated resident population <https://sidra.ibge.gov.br/tabela/6579>, last accessed 21/08/10.

# A practical approach for sustainable Transit Oriented Development in Montevideo, Uruguay

Silvina Hipogrosso<sup>[0000-0003-2124-7267]</sup> and  
Sergio Nesmachnow<sup>[0000-0002-8146-4012]</sup>

Universidad de la República, Montevideo, Uruguay,  
{silvina.hipogrosso, sergion}@fing.edu.uy

**Abstract.** The need for a proper development of transportation systems in modern smart cities is motivated and driven by relevant factors, including conceiving territorial and transportation planning as part of an unified urban activity. In this line of work, this article presents an empirical analysis of sustainable mobility under the Transit Oriented Development paradigm, focuses on properly capturing the relationships between urban environment, activities, and mobility, by analyzing diverse indicators. As a relevant case study, the article analyzes the current situation regarding sustainable mobility and Transit Oriented Development in the area surrounding Engineering Faculty, in Parque Rodó Neighborhood, Montevideo, Uruguay. Specific recommendations are provided to improve sustainable mobility under the studied paradigm.

**Keywords:** sustainable mobility; Transit-Oriented Development; public transportation; smart cities

## 1 Introduction

Mobility is a crucial component of modern smart cities, allowing daily activities social participation of citizens on urban areas [21]. The relationship of mobility with sustainable development has been recognized as one of the main issues to achieve the 2030 Sustainable Development Goals (SDG), as defined by the United Nation, since mobility is part of the great environmental challenges existing nowadays. Several of the defined SDG are related to sustainable mobility, including relevant issues as health and road safety, affordable and clean energy, economic growth, resilient infrastructure for sustainable cities, access to transportation modes and expanded public transportation, and sustainable consumption and production. Thus, promoting sustainable mobility has been a major concern and one of the toughest environmental and social challenges.

The main concepts of sustainability and sustainable development have been applied to conceive new approaches and models to guarantee mobility with a reduced environmental impact. Sustainable mobility is defined as the ability to “meet the needs of society to move freely, gain access, communicate, trade and establish relationships without sacrificing other essential human or ecological values, today or in the future” [29]. Three main pillars support the sustainable

2 S. Hipogrosso and S. Nesmachnow

mobility paradigm: environmental, social, and economic [15]. These pillars must be properly respected to develop positive contributions, by collaborative efforts by public and private sectors, suitably considering citizens and their participation. Transit-Oriented Development (TOD) [7, 22] is a paradigm for urban planning and development that has revitalized city urbanization, by combining the renewal of suburban spaces and friendly walkable environments in neighborhoods. Although TOD has been successfully applied in USA, Europe, and Asia to ensure sustainable mobility and economic development, few proposals have applied the paradigm in Latin America.

In this line of work, this article presents a practical approach for analyzing and developing sustainable mobility initiatives under the TOD paradigm. The analysis is focused on properly capturing the relationships between urban environment, activities, and mobility. The main contributions of the research reported in this article are: the evaluation of the area surrounding Engineering Faculty, in Parque Rodó neighborhood using TOD indicators and the analysis of mobility demand through quantitative indicators and the formulation of several suggestions and recommendations to improve sustainable mobility in the studied zone, applying the TOD paradigm.

The article is organized as follows. Next section introduces the main concepts regarding sustainable mobility and TOD. A review of related works is presented in Section 3. The methodology applied for the analysis of the studied zone is reported in Section 4. Results and discussion of the analysis are presented in Section 5, and specific suggestions and recommendations to improve sustainable mobility under the TOD paradigm in the studied area are presented in Section 6. Finally, Section 7 presents the conclusions and the main lines for future work.

## 2 TOD approach

In the last thirty years, sustainability has been a major concern of modern society. The concept of sustainable development, i.e., development to fulfill important roles of nowadays without compromising the future, has been promoted to build a more equitable, environment friendly, and inclusive model of society.

The sustainable mobility paradigm integrates many relevant concepts, including those related with their impacts on environment and society [2]. Overall, the main idea is to consider mobility as a valued activity regarding environmental, social, and economic concerns [19]. One of the most studied aspects has been the impact of mobility on the environment, with the main idea of conceiving new transportation paradigms accounting for cleaner means, accessibility, and integration of people. Other important aspects have also been analyzed, including the impact on economy, and the overall quality of life (safety, health, etc.). Raising awareness and involving citizens are key aspects for sustainable mobility. In turn, technology has been identified as one of the most valuable tools to help developing environmental friendly sustainable mobility. Different methods and indicators have been proposed to analyze means of transportation [12] and other important issues related to sustainable mobility.

In turn, the TOD paradigm for urban planning is a trendy model for planning sustainable urban communities by creating dense, walkable communities that greatly reduce the need for driving and energy consumption. The goal TOD is ensuring sustainable mobility and economic development, while protecting global energy. TOD has become a great prominence for urban planning and transport since the first proposals by Calthorpe [7] and Newman and Kenworthy [22] in the 1990s. The approach was later supported by the empirical works of Bertolini et al. [3,4] and Cervero et al. [8,9], among other authors.

TOD is the key to more sustainable, efficient, and equitable communities because it works under the “3Cs” concepts (compact, coordinated, and connected). In turn, it is related to other five principles for decision makers and urban planners strengthen their communities according to the TOD standard:

1. *Compactness*: The closer the activities are located between each other in a compact city/district, the less time consuming and energy is required.
2. *Density*: Instead of building out to increase the urban sprawl, TOD supports building up to create dense cities in a more compact way.
3. *Transit-public transportation*: Public transportation connects and integrates many distant areas around the city. A good public transportation planning that contemplate all area of a city creates an equitable and accessible city.
4. *Connectivity*: Create dense networks of streets and paths for pedestrians and cyclists as well as public transportation.
5. *Mix*: Plan for mix use in order to create shorter trips and more lively neighborhoods.
6. *Cycling*: Prioritize non-motorized transport networks. Cycling provides people an efficient and convenient way to travel for short/medium distances, increase accessibility as well as coverage of transit.
7. *Shift (to sustainable transportation modes)*: Closer locations between activities and a good transportation network do not imply people shift to sustainable transportation modes. Other actions are needed, such as regulating car parking and road use, to discourage the use of non-sustainable means.
8. *Walk*: Develop neighborhoods that promote walking creating vibrant, active streets where people feel safe.

In the related literature, TOD is conceived to hold urban sprawl, prioritizing sustainable mobility as well as driving to environmentally and economically-balanced growth TOD is closely related to the *smart growth* and *new urbanist* approaches [6] conceiving walkable, compact, pedestrian-oriented, and mixed-use communities centered around high quality public transport systems [26] reducing, in this way, the utilization of automobiles.

Several articles have defined a buffer of 400 m as the walkable distance to get to a bus stop and a buffer of 800 m as the walkable distance to get to a rail station [23,24]. According to these radius, urban designers and planners design mixed used areas around bus stops and rail stations to promote sustainable mobility. Accessibility also plays an important role when designing a project based on TOD principles. The interaction between urban structure, accessibility, and travel behavior has been discussed for several authors [23].

4 S. Hipogrosso and S. Nesmachnow

Based on the TOD approach, this article presents an analysis of the zone surrounding Engineering Faculty in Parque Rodó neighborhood, describing the mixed uses of land (services, public spaces, open spaces, pedestrian paths and bike lanes, maintenance condition of the built environment and green places, bicycle parking facilities and transport nodes.) The data collected was examined by some factors to characterize the built environment.

Furthermore, an empirical approach is followed to consider subjective opinions, based on personal questionnaires to people traveling from/to the area. The resulting data are processed and analyzed following a urban data approach, in order to extract useful information and elaborate specific suggestions towards a sustainable mobility plan in the studied area.

### 3 Related work

Sustainable mobility has been an important concern for researchers in the last twenty years. Litman and Burwell [17] recognized that sustainable transportation initiatives must be developed considering a broad point of view, for properly capturing the interrelations between economic and social welfare, energy efficiency, ecological integrity, human health, and proper land use. The authors proposed a paradigm shift for rethinking transportation, considering different integrated solutions for sustainable transportation systems. Some of the proposed indicators for detecting trends, assessing and comparing activities, and evaluating policies related to sustainable transportation, are those considered in TOD principles.

The main concepts in TOD are strongly related to sustainability. On the one hand, successful examples of applying TOD in USA, Europe, and Asia, are commonly associated to mass rail systems. On the other hand, in Latin America, most of the TOD-related initiatives have been implemented on Bus Rapid Transit (BRT) or similar public transportation systems, which allow providing a cost-effective service more adapted to the economic reality of developing countries.

Hasibuana et al. [13] studied the applicability of TOD ideas for improving urban mobility in a case study in Jabodetabek, Indonesia, with more than 27 million population. The main results of the analysis showed that TOD concepts can definitely contribute to restructuring urban land use and growth, improving the modal share of public transportation and the quality of the urban environment. Loo and Verle [18] proposed a sustainable mobility approach oriented on people and places. Three lines were proposed for TOD planning: improving the built environment at both neighbourhood and city scales; improving walking and related urban planning/design related to public spaces; and encouraging non-uniform designs for different neighborhoods. A case study in Hong Kong, China, analyzed several indicators for five different neighborhood types. The authors recognized that further efforts are needed to quantify and fostering both direct and indirect benefits associated with TOD, benefits beyond traditional impacts on transportation. Tsigdinos et al. [27] studied surrounding zones of metro stations (line 4) in Athens, Greece, regarding several TOD features (density, walkability, public transportation, land uses, and public spaces).

Spatial analysis, indicators for categorizing TOD regions, multi-criteria analysis and geo-visualization were applied to identify differences between categories and contrast between central and suburban stations. The authors found important limitations of the studied areas and common weaknesses of more than a half of the studied stations, which hinders the implementation of integrated transportation and urban planning strategies. Specific suggestions for improving the identified weaknesses were also proposed.

Woo [28] evaluated TOD features in Seoul, Korea, to characterize subway station areas and their neighborhoods, for a urban rail transit. Accessibility analysis and clustering methods were applied to categorize TOD types using the targeted 246 subway station areas at the neighborhood level. The main results of the analysis grouped the studied zones in four categories: (1) high-density mixed-use areas for residential and retail purposes, which have good accessibility; (2) moderate-density, with average accessibility and high-mixed land use; (3) compact business, mainly offices and commerce, with high accessibility and a high transit demand; and (4) compact housing with high-rise buildings, mostly used for residences. The study concluded that the period of urban development significantly affects the main features of each identified category. and category (2) offers the best option for urban redesign under TOD concepts.

In Latin America, TOD-related developments have been scarce. The region mostly focused on building and developing infrastructures based on mass transit corridors and BRT systems. Some articles argued that BRT systems, even though applying a more restricted paradigm, are able to produce a similar impact on land utilization than TOD strategies [9]. However, Moscoso et al. [20] stated that Latinamerican cities have considered BRT as a mobility solution, without integrating key TOD concepts to promote compact, dense, and well-connected urban development. Nevertheless, the most well-known BRT development in Latin America (Curitiba, Brazil) is also a model of TOD, due to a long-term integration of transportation and land use planning, which was crucial for the success of the mobility model. The land development impacts of BRT have been also studied in other Latinamerican cities, such as Bogota and Quito [5,25].

Other analysis of sustainable transportation considering TOD-based indicators have been developed for specific cases, such as the study for universities in the Guadalajara metropolitan area, Mexico, by de Alba et al. [1].

The analysis of related works allows concluding that few articles have studied TOD analysis and characterization for specific cases in Latin America. This article contributes in this line of research, by proposing a TOD-based sustainable mobility analysis in a specific zone of Montevideo, Uruguay.

#### **4 TOD-based sustainable mobility analysis for Engineering Faculty, Montevideo, Uruguay**

This section describes the analysis of sustainable mobility and urban structure in the area surrounding Engineering Faculty, Montevideo, Uruguay, considering TOD-related indicators.

6 S. Hipogrosso and S. Nesmachnow

#### 4.1 Motivation and objectives of the study

The objective of the study is to analyze how the studied area can be transformed in a walkable, compact, pedestrian-oriented, and mixed-use community, where people want to live and work, built around sustainable public transportation.

Since global concern of environmental pollution appeared, only few initiatives have been proposed towards sustainable mobility in Montevideo. Most of the recent initiatives focused on public transportation, e.g., electric buses were introduced in the system, and a few private initiatives, e.g., a leasing plan to acquire electric vans for last mile distribution of people and goods.

The studied area (called *The Isle*) is located nearby Engineering Faculty, in Montevideo. It is an area of 0.25 km<sup>2</sup> surrounded by about 1 km<sup>2</sup> of green areas (Parque Rodó/Rodó Park). Although The Isle is a residential area, where more than 5.000 people live, it has high daily flow of people traveling to/from services, institutions, green and recreation areas, and other places located in the zone. In this regard, this area creates opportunities for multi-modal travel, sustainable mobility and urban planning development based in TOD approach.

The studied area includes four avenues: Herrera y Reissig, where Engineering Faculty is located, Sarmiento, Sosa, and Bulevar Artigas. In 2021, Engineering Faculty has more than 10 000 students, 1 000 professors, and 200 employees. In addition, students and professors of other faculties also assist to lectures in Aulario Massera, a large classroom building nearby Engineering Faculty.

#### 4.2 Methodology

The main details of the applied methodology are described next.

*Overall description.* The study is based on two methodological stages: i) applying urban data analysis to develop a spatial-functional definition of the study area; and ii) characterizing the current mobility in the studied area;

The proposed methodology combines different quantitative elements and analysis to identify the mixed uses of land in the area, transportation connectivity, and infrastructure for bikers and pedestrians, in order to improve accessibility and create opportunities for sustainable development in the area.

*Data collection.* Three main sources of data were considered in the study.

First, data from Google Maps (in JSON format) and from personal inspection (from photographs taken in the area) were collected to identify a spatial-functional definition in the studied area. The collected data include the following information about the environment: infrastructure for non-motorized traveling mode (pedestrian-only paths, bicycle paths, accessible ramps for sidewalks); land uses (commercial, residential, institutional); semi-public spaces (restaurants, education center, health center, sport centers); open spaces (green areas, parks, squares); the maintenance condition of the built environment and green spaces (bus stop shelters, sidewalks, bicycle paths); and parking facilities and transportation nodes (bicycle parking, and bus stops).

The study defines two areas for the analysis: The Isle, located within 400 m of Engineering Faculty, and an extended area delimited by a radius of 800 m from Engineering Faculty (mostly in directions North and East).

Second, the study gathered operational data (e.g., bus lines that operates in the zone, timetables, etc.) and also information about the available infrastructure (e.g., bus stops, bicycle lanes and bicycle parking facilities.) either from open data sources or by personal inspection.

Third, a survey was performed in-situ in the studied area, to gather data for the analysis and characterize sustainable public transportation in Montevideo [14]. Data from 617 persons were collected: 79 living in the area and 538 commuting from other zones of the city. The study identified four relevant groups of people: students of Engineering Faculty and attending Aulario Massera professors and employees of Engineering Faculty, people living in the neighborhood, and people working in the neighborhood. [14]

The survey focused on gathering mobility information for the four groups of people. The study reported in this article includes the most relevant information for the analysis: origin/destination of trips and relevant aspects of transportation mode(s) used for commuting. Interviews were performed in November–December 2019, from Monday to Friday, from 8:00 to 19:00. Weekend trips were not surveyed, as the mobility demand is significantly lower than working days trips.

*Indicators/metrics.* For the analysis of urban infrastructure, the study examined the surveyed area through different metrics, including:

- The existence and total distance of infrastructure for non-motorized traveling modes, including pedestrian paths and bicycle paths;
- The existence of different elements, such as ramps, on sidewalks that provide universal accessibility;
- To evaluate the land uses, the total area of commercial, residential, educational, recreation and green areas;
- The number of commercial areas in both areas, separated in public places (supermarkets, mini markets or food store) and semi-public places (restaurants, utility shops, health centers, and pharmacies);
- The number of bicycle parkings and bus shelters;
- The maintenance condition of the built environment (bus shelters condition, sidewalks, bicycle paths and green areas, evaluated in three qualitative categories (low, medium, and high). The analysis considers ‘The 8 principles of sidewalks’ [11] as reference for design and construction of sidewalks and the NACTO Urban Bikeway Design Guide as reference for bicycle paths.

For the mobility analysis in the studied area, two relevant (quantitative) sustainable mobility indicators proposed by the World Business Council for Sustainable Development were used:

- Distance between origin and destination of trips: the real distances that people travel, considering the zones that originate trips to the studied area and also the destination of trips that initiate in the studied area.

8 S. Hipogrosso and S. Nesmachnow

- Commuting travel time the average time spent by a person when traveling from/to the studied area. The average walking speed is assumed to be 5 km/h. For bus, the commuting travel time includes the time for a person to walk to the bus stop and the time waiting for the bus to arrive. For bicycles, the average speed is 13.5 km/h.

*Methodology for data analysis.* For the analysis of urban infrastructure, distances were computed using the Google Maps service, and both green and residential areas were computed using the Google Maps Area Calculator tool. The area of institutions and commercial buildings were measured by personal inspection, using a laser device. Furthermore, bus stops, bike roads, and bicycle parking were also identified by personal inspection to evaluate their maintenance conditions.

The overall characteristics of mobility demand in the area were studied in a previous article [14] using quantitative mobility indicators to evaluate the opportunities that the studied area offers for communication with other zones of Montevideo. According to Calthorpe [7], TOD is conceived to promote non-motorized transportation modes or public transportation instead. However, some studies [10,16] that travel behavior are more associated to human attitudes than to land use characteristics, influenced by certain factors as income, or household composition. On the other hand, Papa and Bertolini [23] stated that the travel behavior can change if other urban characteristics significantly change too (e.g., universal accessibility, good connectivity, safe neighborhoods and attractive streets that promote walking, etc).

## 5 Sustainable TOD analysis

The studied area was analyzed through TOD principles followed by decision makers and urban planners to strengthen their communities, and relevant indicators for sustainable development [24].

*Compactness and mix.* Citizens prefer traveling shorter distances to perform their activities, which implies the closer the activities are from each other, the less time required. The study identified that residents have first-needs stores only a few blocks away from home. Maps in Fig. 1 present accurate information about the location of different services, bus stops, bicycle parking, pedestrian only paths, and also identified land uses in the studied area. The upper map reports the information for the studied area (buffer area of 400 m), whereas the map at the bottom reports services in the extended area (buffer area of 800 m).

*Public spaces.* Public spaces contribute to enhance the beauty and environmental quality of neighborhoods, and also contribute to socialization and sustainability. The studied zone provides 0.217 km<sup>2</sup> of green areas, which corresponds to 40.6% of the overall land. The average distance for residents walk to a green area is 200 m. Regarding maintenance conditions, municipal workers are responsible for keeping green and public recreation areas clean and in proper conditions.

Practical approach for sustainable TOD in Montevideo, Uruguay

9

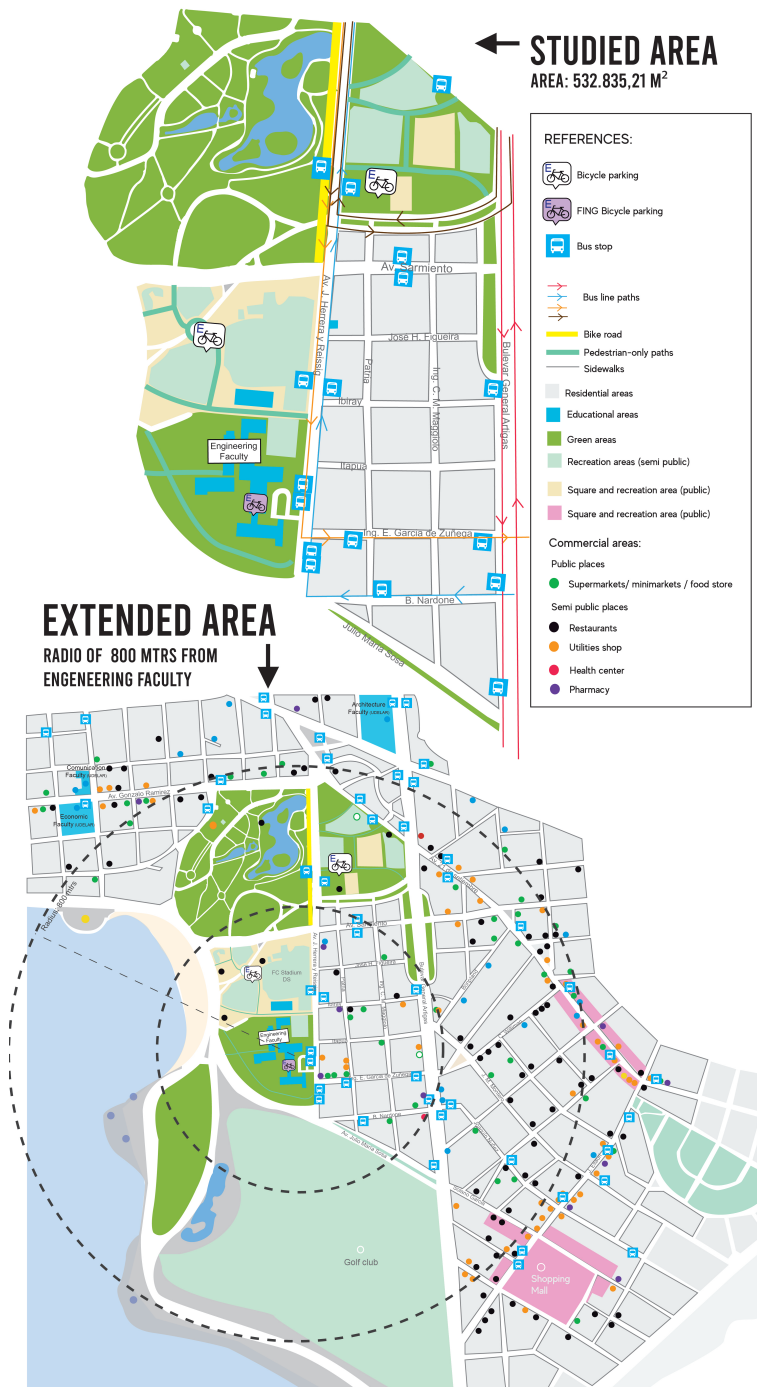


Fig. 1. Information for the studied area and the extended area

10 S. Hipogrosso and S. Nesmachnow

*Density.* Urban density is a fundamental principle of sustainable development. Dense development sustains public transportation, shortens travel distances and keeps travel cost affordable. For dense cities, the TOD paradigm supports building up instead of building out to avoid urban sprawl. In this regard, the study analyzed two criteria: residential density and commercial activities density. The residential density correspond to 13.18 residents/ha, and the commercial activities density (over total uses) is 0.1%. These figures confirm that the studied area is most a residential (rather than commercial) area of the city.

*Transit–public transportation.* A good public transportation service should connect many distant areas, creating a more accessible and equitable city. High bus frequencies and the existence of a bus stop in the proximity of residential areas is one of the principles of the TODs approach. The study identified 17 bus stops in the studied area, and residents can walk to them in less than 5 minutes from their homes. During working days, the bus service operates with a mean frequency of 12 to 17 minutes on peak hours (7:00 to 22:00), 25 to 35 minutes from 22:00 to 0:00, and low frequency between 0:00 and 5:00. On weekend days the demand is lower and so the frequency. In general, the maintenance conditions of bus shelters is low. The original design presents a sitting bench, a roof, a commercial panel, lighting, bus line signage and a trash bin. However, the majority of commercial panels, lightening and bus line signage are damaged; 7 out of 10 have the sitting bench, 15 out of 17 already have the roof, and the trash bin is missing in all of them. Moreover, 8 bus shelters are located closer the corner of the street, blocking the visibility for pedestrian that are crossing the street.

*Connectivity and cycling.* Safety and comfortable walking and cycling contribute to the TOD approach. Relevant indicators to evaluate those sustainable mobility means are the proportion of pedestrian and cycling routes, intersections density, and the network connectivity. The proportion of cycling and pedestrian routes over the total road network is just 0.2%, a very small proportion. The intersection density in the area is 0.2 and the gamma index connectivity is 0.3, which are reasonable values for a residential neighborhood.

*Infrastructure for pedestrians and walkability.* Regarding design and maintenance conditions of sidewalks, the study analyzed the area through guidelines provided by municipal technicians and city planners to facilitate the design and construction of sidewalks [11], to encourage people to walk more in their daily routine. Overall, sidewalks on the studied area present a proper width that provides pedestrians a comfort and safety walking. Also, the studied area offers universal accessibility with curb ramps in every corner and at the entrance of pedestrian-only paths, providing easy access for people with reduced mobility (e.g., elderly and wheelchair users), people with temporary limitations, pregnant women, or parents with baby strollers. Public lightening is located in all sidewalks in the area, increasing the sensation of security while walking. In turn, vegetation is plentiful in the studied area, motivating people to walk and occupy urban public spaces. However, the connections of sidewalks to other means of

transportation presents some issues, such as the lack of crosswalks, poor quality paving, crude design of urban furniture and vegetation, no tactile surfaces integrated into the sidewalks and few informative signage. Furthermore, the studied area present few initiatives to discourage the use of car in the area.

The bicycle path width in the studied area is 2.0 m (two-way bicycle lines with a yellow centerline), well below the minimum recommended of 2.5 m. For the intersection crossing markings, color pavement is used to increase visibility within conflict areas or across entire intersections. Elephant feet marks are also used as an alternative to dotted line extensions, to offer increased visibility. Relevant examples of bicycle path design in the studied area are shown in Fig. 2.



**Fig. 2.** Bicycle lane design in the studied area (Herrera y Reissig Avenue)

*Shift.* To promote sustainable mobility, parking and road use must be regulated to discourage the use of car. According to the guide by NACTO, the maximum recommended speed limits are 15 km/h for shared streets or alleys, 30 km/h for minor streets, and 60 km/h for major streets that have well-protected lines for pedestrians and bicycles. Car speed limit in the studied area is 45 km/h on streets and 60 km/h on avenues. There are no parking restrictions and no fee is charged for parking on the streets. Furthermore, there are three free car parking areas and many open places to park in. Overall, the studied area does not meet with the recommended speed limit and with other policies regulations in order to reduce the use of car and increase sustainable mobility.

*Travel distances and percentage of trips.* Regarding the number of trips from/to the studied zone, the main findings of the analysis is that many people travel from/to near locations: one third commute from/to less than 3 km away, and 60% from a maximum distance of 5 km). This tendency suggests that the impact of implementing sustainable mobility initiatives following the TOD approach, specially focused on accessibility to nearby locations, will be notable. Furthermore, the study also revealed that 95% of people make a round trip and more than 90% commute from/to the same location at least three times a week. These results demonstrate that mobility demands in the studied zone are regular and steady.

*Commuting travel time.* In line with the analysis of travel distances, Table 1 reports the average commuting travel times from/to the five most demanded origin/destination of trips to/from the studied zone, which are less than 4 km away from the studied zone. One neighborhood that is far away (Prado, 8 km from the studied zone) is also included to analyze the scalability to larger distances (no walking travels were registered for Prado).

**Table 1.** Commuting travel time to Engineering Faculty from the five most frequent neighborhoods as origin/destination of trips (in minutes).

<i>neighborhood (average distance)</i>	<i>bus</i>	<i>bicycle</i>	<i>walking</i>	<i>car</i>
Parque Rodó (~ 1.0 km)	-	4.4	12.0	5.7
Cordón (~ 2.5 km)	18.9	11.0	30.0	12.0
Tres Cruces (~ 3.0 km)	21.2	13.3	36.0	15.2
Pocitos (~ 3.5 km)	28.4	15.5	42.0	17.0
Centro (~ 3.7 km)	24.4	21.4	44.4	20.8
Prado (8.0 km)	44.4	35.5	n/a	28.8

For nearby neighborhoods (up to 3.5 km from Engineering Faculty) bicycle is the fastest transportation mode. This is a relevant result, since a large percentage of travels have origin/destination in closer neighborhoods. Up to 8.0 km, car has similar travel time than bicycle and both are faster than bus, suggesting that public transportation is not optimized to provide an appropriate travel time. Even though bicycle is the most convenient traveling mode, the length of bicycle-only lanes in the studied area is not appropriate, as previously commented.

## 6 Suggestions and recommendations to improve sustainable mobility under the TOD paradigm

From the obtained results, there is evidence to confirm that sustainable mobility in the studied area can be enhanced considering specific TOD-related actions.

*Extend the bicycle network.* The studied area offers a very short bicycle network. The analysis suggest it should be extended along main avenues. This way, the studied area would be connected with relevant places by extending bicycle lanes: seaside (through Sarmiento), other faculties (through Ramirez and Herrera y Reissig), shopping center (through Sosa) and other major neighborhoods and the Terminal Bus Station in Montevideo (through Bulevar Artigas).

*Signal locations for safe pedestrian crossing.* A proper signaling of crossings improves walkability, pedestrian safety, and also promotes a better pedestrian behavior. The study also recommend installing a pedestrian crosswalk in front of Engineering Faculty, to improves accessibility for students.

*Reallocate bus shelters for safe crossing.* The study recommend reallocating eight bus shelters that are installed closer to corners, in order to improve pedestrian visibility when crossing. Car parking should be prohibited or discouraged in those locations where it implies a risk to pedestrians and other vehicles.

*Re-pavement damaged sidewalks.* The study recommend re-pavementing low-quality sidewalks, especially those damaged by tree roots, which pose a serious risk for universal accessibility. Also, this issue must be considered for the selection of trees, to avoid them cracking and raising the sidewalks. Sidewalk surfaces must be firm and leveled, for a proper use of wheelchairs, the elder, or people with temporary or permanent walking limitations.

*Add tactile surfaces to guide blind or visually impaired people.* The area does not provide elements to allow safe walking of visually impaired people. Guides are also missing on bus stops and other relevant locations and they must be properly installed to provide and improve universal accessibility.

*Improve bus shelters.* Comfort on bus shelter improves the image of public transportation. The study recommends an appropriate design to prevent bus shelter being so vulnerable to vandalism, using concrete or other highly resistant materials. Also, the design must provide better protection for adverse climate conditions (e.g., strong wind and rainy days). Every bus shelter must provide a garbage bin and a proper bench for people wait for the bus to arrive.

*Promote walking and interaction with the environment.* The study demonstrated that sidewalks play an important role in encouraging the interaction between people and the urban environment. Several actions must be developed to provide a better and more pleasant experience: improve information to guide pedestrian to reach destination, provide better and more functional urban furniture and vegetation (planter boxes, garbage bins, benches, etc.), to make the environment more attractive and improve the walking experience.

## 7 Conclusions and future work

This article presented an empirical analyzing of sustainable mobility under the TOD paradigm in the area surrounding Engineering Faculty, Universidad de la República, Montevideo, Uruguay. Several relevant indicators were studied to determine the reality and relationships between territory, activities, and mobility.

The study applied urban data analysis to identify a spatial/functional definition of the studied area, using operational data, personal inspection, and a survey performed in/situ in the original and an extended area.

The main findings of the analysis are related on the characterization of several TOD concepts and metrics, related to sustainable mobility. Based on the results of the analysis, specific recommendations are provided to develop a TOD-based approach to improve sustainable mobility in the studied area. The main goals of the proposed suggestions are related to improve the walking experience, provide universal accessibility, promote walking and bicycle, and the interaction with public transportation. This is a direct contribution of the reported research, since no previous similar studies have been developed in Montevideo.

The main lines for future work are related to extend the analysis to consider other relevant TOD concepts and indicators to better characterize sustainable mobility and the impact of recommended actions in the studied zone.

14 S. Hipogrosso and S. Nesmachnow

## References

1. Alba, H., Grindlay, A., Ochoa, G.: (in)equitable accessibility to sustainable transport from universities in Guadalajara metropolitan area, México. *Sustainability* 13 (2020)
2. Banister, D.: The sustainable mobility paradigm. *Transport Policy* 15, 73–80 (2008)
3. Bertolini, L.: Nodes and places: complexities of railway station redevelopment. *European Planning Studies* 4.3, 331–45 (1996)
4. Bertolini, L., Curtis, C., Renne, J.: Station area projects in Europe and beyond: towards transitoriented development. *Built Environment* 38.1, 31–50 (2012)
5. Bocarejo, J., Portilla, I., Pérez, M.: Impact of transmilenio on density, land use, and land value in Bogotá. *Research in Transportation Economics* 40(1), 78–86 (2013)
6. Burchell, R., Listokin, D., Galley, C.: Smart growth: More than a ghost of urban policy past, less than a bold new horizon. *Housing Policy Debate* 11, 821–879 (2000)
7. Calthorpe, P.: *The Next American Metropolis: Ecology, Community and the American Dream*. Princeton Architectural Press (1993)
8. Cervero, R.: Transit-oriented development's ridership bonus: a product of self-selection and public policies. *Environment and Planning A: Economy and Space* 39.9, 2068–2085 (2007)
9. Cervero, R., Dai, D.: BRT TOD: Leveraging transit oriented development with bus rapid transit investments. *Transport Policy* 36, 127–138 (2014)
10. De Vos J., Van Acker V., W.F.: The influence of attitudes on transit oriented development: an explorative analysis. *Transport Policy* 35,5, 326–329 (2014)
11. Dos Santos, P., Caccia, L., Barbosa, A., Zoppaas, L.: *The 8 Principles of Sidewalks*. World Resources Institute (2019)
12. Gudmundsson, H., Hall, R., Marsden, G., Zietsman, J.: *Sustainable Transportation*. Springer Berlin Heidelberg (2016)
13. Hasibuan, H.S., Soemardi, T.P., Koestoer, R., Moersidik, S.: The role of Transit Oriented Development in constructing urban environment sustainability, the case of Jabodetabek, Indonesia. *Procedia Environmental Sciences* 20, 622–631 (2014)
14. Hipogrosso, S., Nesmachnow, S.: Analysis of Sustainable Public Transportation and Mobility Recommendations for Montevideo and Parque Rodó Neighborhood. *Smart Cities* 3(2), 479–510 (2020)
15. Jeon, C., Amekudzi, M.: Addressing sustainability in transportation systems: Definitions, indicators, and metrics. *Infrastructure Systems* 11(1), 31–50 (2005)
16. Kitamura, R., Mokhtarian, P.: A micro-analysis of land use and travel in five neighborhoods in the San Francisco Bay area. *Transportation* 24, 125–158 (1997)
17. Litman, T., Burwell, D.: Issues in sustainable transportation. *International Journal of Global Environmental Issues* 6(4), 331–347 (2006)
18. Loo, B., Du Verle, F.: Transit-oriented development in future cities: towards a two-level sustainable mobility strategy. *Urban Sciences* 21, 54–67 (2016)
19. Marshall, S.: The challenge of sustainable transport. In: Layard, A., Davoudi, S., Batty, S. (eds.) *Planning for a Sustainable Future*, pp. 131–147. Spon (2001)
20. Moscoso, M., van Laake, T., Quiñones, L. (eds.): *Sustainable Urban Mobility in Latin America: assessment and recommendations for mobility policies*. Despacio: Bogotá, Colombia (2019)
21. Neckermann, L.: *Smart Cities, Smart Mobility: Transforming the Way We Live and Work*. Troubador Publishing Ltd. (2017)
22. Newman, P., Kenworthy, J.: The land use–transport connection: an overview. *Land Use Policy* pp. 1–22 (1995)

## Practical approach for sustainable TOD in Montevideo, Uruguay 15

23. Papa, E., Bertolini, L.: Accessibility and Transit-Oriented Development in european metropolitan areas. *Journal of Transport Geography* pp. 70–83 (2015)
24. Renne, J.: From transit-adjacent to transit-oriented development. *Local Environment* 14:1, 1–15 (2009)
25. Rodriguez, D., Vergel, E.: Urban development around bus rapid transit stops in seven cities in latin-america. *Journal of Urbanism: International Research on Place-making and Urban Sustainability* 11(2), 175–201 (2017)
26. Sung, H., Oh, J.: Transit-oriented development in a high-density city: Identifying its association with transit ridership in Seoul. *Cities* 28, 70–82 (2011)
27. Tsigdinos, S., Paraskevopoulos, Y., Rallatou, N.: Transit Oriented Development (TOD). Challenges and Perspectives; The Case of Athens' Metro Line 4. In: *European Transport Conference* (2019)
28. Woo, J.: Classification of TOD typologies based on pedestrian behavior for sustainable and active urban growth in Seoul. *Sustainability* 13(6), 3047 (2021)
29. World Business Council for Sustainable Development: The sustainable mobility project (2002)

# Outdoor efficiency model for photovoltaic modules and its experimental validation

Luis Diego Murillo-Soto<sup>1</sup>  and Carlos Meza<sup>2</sup> 

<sup>1</sup> Electromechanical Eng. School, Costa Rica Institute of Technology, Cartago, Costa Rica, [lmurillo@tec.ac.cr](mailto:lmurillo@tec.ac.cr)

<sup>2</sup> M.Sc. Photovoltaic Engineering Science, Anhalt University of Applied Sciences, Anhalt, Germany, [carlos.meza@hs-anhalt.de](mailto:carlos.meza@hs-anhalt.de)

**Abstract.** The study of the efficiency of photovoltaic modules in outdoor conditions allows to determine their correct operation and to detect abnormal behavior. The efficiency models that are available in the literature use ad-hoc measurements that are few practical as they require specialized equipment and a long measurement time to identify or adjust the model parameters. In this article, we propose a linear equation that estimates the efficiency of photovoltaic modules using irradiance and back panel temperature measurements as input variables. The main contribution is that the parameters of the proposed model can be obtained directly from the reference information (IEC61853-1 power values) without any data regression. The proposed model was validated using experimental data obtained from three different climatic zones during a whole year.

**Keywords:** Photovoltaic efficiency model, Outdoor efficiency estimation, Experimental validation.

## 1 Introduction

The operation and maintenance activities in photovoltaic (PV) plants can be incredibly beneficial if an accurate model of the expected PV plant's power or efficiency is available. With an efficiency model, PV operators can identify underperformance due to failures or soiling. Even though a PV module datasheet provides information that can be used to get an idea of the electrical characteristics of a PV plant, that information has been obtained under laboratory conditions which, in several cases, are different from outdoor conditions. Hence, measured experimental efficiency differs considerably from the efficiency reported in the PV panel datasheet as it has been verified in [9] and [16]. The difference above is not suitable for the proper maintenance and operation of a PV plant.

During the years, there have been many efficiency models in the literature, i.e., Skoplaki [18] summarizes 53 models and Dubey [4] presents 23 different models. Several models are based on the model presented by Evans in [6] that defines the efficiency as a function of the temperature of the cell and the irradiance (see equation 11). Other types of models also incorporate the air mass

( $AM$ ), such as the one proposed by Durisch in [5]. The main disadvantage of the models mentioned above is that they require additional measurements and fitting algorithms to find the optimal values of the parameters.

It would be more appropriate to obtain an efficiency model that is accurate for outdoor conditions and calculated from reference points without any type of regression. In this regard, the present paper proposes an outdoor efficiency model that can be constructed with the standard data provided by the PV module datasheet or other efficiency points provided by norms, i.e., IEC 61853-1.

The proposed model is inspired by the fact that efficiency measures plotted in a temperature, irradiance, and efficiency space resemble a surface when low irradiance values are not considered. In this regard, we demonstrate in this paper that using classical regression techniques, it is possible to obtain a best-fit plane equation (BFPE) that estimates with reasonable accuracy the efficiency of a PV module using irradiance and temperature measurements. This paper also derives a simpler efficiency plane equation (PE) that can be obtained using the datasheet values of the PV module and that does not require the use of best-fitting techniques.

This article used several data sets obtained with different methodologies. The reference efficiencies obtained according to the IEC 61853-1 and the outdoor efficiencies were obtained by the National Renewable Energy Laboratory (NREL), which carried out all the data acquisition. In summary, we prove that a proposed PE model calculated from the power matrix is equivalent to the BFPE model calculated from a data set gathering during a whole year for several locations.

To prove that our model is as accurate as the BFPE model, the following general steps were applied: The first one was to calculate the BFPE model from outdoor efficiency measurements. For this task, we selected six locations and panel technology; then, we filtered the efficiency records in specific ranges of temperature and irradiance. The second step was to calculate our plane model, and this was calculated from an efficiency dataset obtained from the power matrix according to the IEC 61853-1. Then, a third model was used to compare our results with a well-known model, i.e., we selected the Evans' model given that it is widely referenced as indicated above. The fourth step consisted in study the fitting of the models and then hypothesized about the similarities between the PE and BFPE models. The process mentioned above is summarized in figure 1. The authors believe that the simplicity of the PE model, along with obtained accuracy, makes this model an appropriate tool for fault detection and/or PV power production estimation when there are not historical efficiency measures available.

The rest of this document is structured as follows: section 2 presents a small review of efficiency models and the proposed model, section 3 describes the used experimental data, and section 4 explains how calculate the coefficients for the model. The section 5 explains the methodology to prove if the proposed plane cuts the cloud of efficiency points, and the analysis and result are presented in section 6. The main conclusions of this work are presented in section 7.

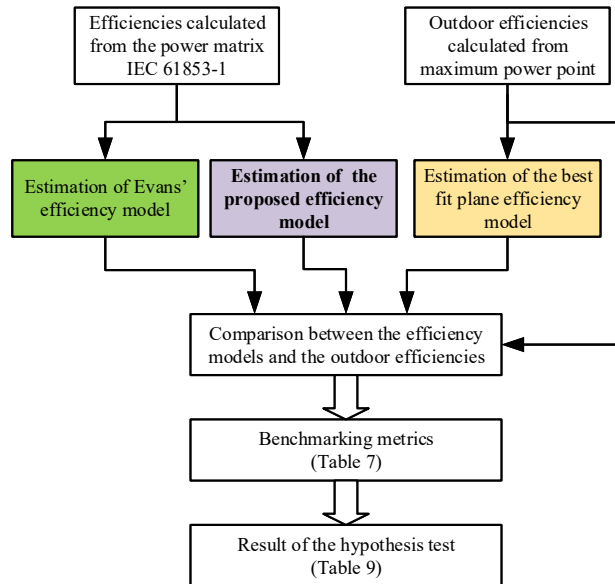


Fig. 1. Summary of the validation process

## 2 Efficiency models for PV modules

The efficiency of a PV module is the ratio between the output electrical power,  $P_{pv}$ , and the received solar irradiance on its surface panel,  $P_i$ , as indicated in equation (1).

$$\eta = \frac{P_{pv}}{P_i}. \tag{1}$$

The input power is  $P_i = G_i A$ , where  $G_i$  is the sum of direct, diffuse, and ground-reflected irradiance incident upon an inclined surface parallel to the plane of the PV module and  $A$  is the area of the PV module.

PV module datasheet provides rated efficiency values at given conditions, being the most common the efficiency at standard test conditions (STC),  $\eta_{STC}$ , as indicated in (2), where the considered output power,  $P_{mpp,STC}$ , is the maximum power that the PV module can produce at a temperature in the PV module of  $T_{STC} = 25 \text{ }^\circ\text{C}$  (298.15 °K), and incident irradiance of  $G_{STC} = 1000 \text{ W/m}^2$  and an air mass of 1.5.

$$\eta_{STC} = \frac{P_{mpp,STC}}{AG_{STC}} \tag{2}$$

The STC efficiency of 72-cell crystalline PV module ranges from 18 % to 22.8 % [8]. The efficiency of a PV module is not a constant value but depends on several variables and parameters as shown next.

To illustrate the PV module efficiency dependence on environmental variables consider the ideal three-parameter model for a PV model shown on equation (3), i.e.,

$$i_{pv}(T, G) = I_{ph}(T, G) - I_s(T) \left( \exp \left( \frac{qv_{pv}}{N_s k T a} \right) - 1 \right) \quad (3)$$

where the variables and parameters used are defined in Table 1. According to [19] and [17] the influence of the temperature ( $T$ ) and irradiance ( $G$ ) in (3) can be expressed as,

$$I_{ph}(T, G) = (I_{ph,n} + K_I \Delta T) \frac{G}{G_n} \quad (4)$$

$$I_s(T) = \frac{I_{ph,n} + K_I \Delta T}{\exp \left( \frac{q(V_{oc,n} + K_V \Delta T)}{a k T N_s} \right) - 1} \quad (5)$$

where  $\Delta T = T - T_n$  and  $v_m$  is the PV voltage at its maximum power point for a given irradiance,  $G$ , and temperature,  $T$ .

**Table 1.** Parameters for the PV model used. (Standard Test Conditions (STC): Irradiance of 1000 W/m<sup>2</sup>, a temperature 298.15 °K and an air mass of 1.5.)

Parameter	Description
$I$	Current generated by the PV module
$V$	Voltage drop across the PV module
$a$	Ideality factor
$N_s$	Number of cells in series in the PV module
$I_{ph}$	Photocurrent defined according to (4)
$I_s$	Diode saturation current defined according(5)
$k$	Boltzmann constant ( $1.38 \times 10^{-23}$ J/K)
$q$	Charge of the electron ( $1.6 \times 10^{-19}$ C)
$T$	Cell temperature
$T_n$	Temperature at Standard Test Conditions (STC) ( $T_n = 298.15$ °K)
$I_{ph,n}$	Photocurrent measured at STC
$K_I$	Short circuit current thermal coefficient
$G$	Plane of Array Global Irradiance
$G_n$	Irradiance at STC ( $G_n = 1000$ W/m <sup>2</sup> )
$K_V$	Thermal coefficient for the open circuit voltage
$V_{oc,n}$	Open circuit voltage measured at STC

Based on (2) and (3) it is possible to infer that the efficiency varies concerning the temperature. Even though the input power,  $P_i$ , of the efficiency expression (1) does not vary with  $T$ , according to the simplified model shown in (3) the PV generated power changes with respect to  $T$ .

In this regards, several authors (e.g. [21] and [4]) have proposed temperature-dependent efficiency models most of them derived from the seminal models presented by Evans in [6] and by Green in [7], where, in all cases, as the temperature

in the PV module increases the efficiency decreases reaching zero value at 270 °C as indicated in [18]. In this regard, it is important to highlight that the STC efficiency is an optimistic value given that a PV module temperature of 25 °C occurs at low ambient air temperature.

It has also been reported that a PV module efficiency is affected by changes in solar irradiance. As mentioned previously, the efficiency reported in a PV module datasheet is obtained from measurements with a constant air mass (AM) of 1.5. In photovoltaics, AM is used to approximate the effects of spectral responsivity in PV modules. Nevertheless, air mass changes according to the relative position of the sun and the molecules present in the atmosphere. According to [2] there is a 2% difference between the efficiency measured at AM 1.5 and AM 0. These other effects that take place in the PV module affect efficiency and they have been studied by some authors. For instance, Mavromatakis ([14]) proposes a third-order polynomial to model PV module efficiency that takes into account AM. Durisch in [5] proposes an efficiency expression as a function of the in-plane irradiance, PV module temperature, and air mass. In both of the aforementioned cases, it is necessary to perform specific measurements to the PV modules to obtain the required parameters.

In [16] a simple PV module efficiency expression that can be derived from values readily available in PV modules datasheets. Employing simulations, the authors were able to verify that the efficiency values obtained from the proposed model at different temperatures and irradiances had at most 2.6% difference with respect to more complex and validated models such as the Evans efficiency model, e.g. [6]. Nevertheless, in [16] no experimental analysis or validation was provided.

## 2.1 Efficiency expression to validate

A PV module efficiency,  $\eta$ , can be defined as a function in terms of the PV module temperature,  $T$ , and the in-plane irradiance,  $G$ , i.e.,  $\eta = f(T, G)$ . The simplest expression for  $f(T, G)$  is a linear function, i.e.,

$$\eta = K_1T + K_2G + K_3 \quad (6)$$

where  $K_1$ ,  $K_2$  and  $K_3$  are constants. The parameters  $K_1$ ,  $K_2$  and  $K_3$  can be obtained from at least three points from the efficiency space, i.e., each efficiency point is defined by three values which are  $\eta$ ,  $T$  and  $G$ . Assume that such three points in are named as:  $P = \langle T_p, G_p, \eta_p \rangle$ ,  $Q = \langle T_q, G_q, \eta_q \rangle$  and  $R = \langle T_r, G_r, \eta_r \rangle$ , then an efficiency expression can be derived from the following set of equations,

$$\begin{aligned} \mathbf{P} \cdot (\overrightarrow{PQ} \times \overrightarrow{PR}) &= 0 \\ \mathbf{P} &= \langle (T - T_p), (G - G_p), (\eta - \eta_p) \rangle \\ \overrightarrow{PQ} &= \langle (T_q - T_p), (G_q - G_p), (\eta_q - \eta_p) \rangle \\ \overrightarrow{PR} &= \langle (T_r - T_p), (G_r - G_p), (\eta_r - \eta_p) \rangle. \end{aligned} \quad (7)$$

The solution of eq (7) is obtained solving the following determinant

$$\det \begin{bmatrix} (T - T_p) & (G - G_p) & (\eta - \eta_p) \\ (T_q - T_p) & (G_q - G_p) & (\eta_q - \eta_p) \\ (T_r - T_p) & (G_r - G_p) & (\eta_r - \eta_p) \end{bmatrix} = 0 \quad (8)$$

however, choosing special points where  $T_r = T_p$  and  $G_q = G_p$  allow us to solve eq.(8) easier. Then, comparing (6) with (8) it can be seen that parameters  $K_i$  are equal to

$$\begin{aligned} K_1 &= (\eta_q - \eta_p)/(T_q - T_p) \\ K_2 &= (\eta_r - \eta_p)/(G_r - G_p) \\ K_3 &= \eta_p - K_1 T_p - K_2 G_p. \end{aligned} \quad (9)$$

The constants  $K_1$ ,  $K_2$ , and  $K_3$  can also be obtained from a set of experimental points using multivariate nonlinear regression techniques yielding a best-fit plane efficiency (BFPE) model.

### 3 Experimental data used for validation

The data set used for validation was obtained from measurements made on four multi-crystalline PV modules, all of them having a surface of 0.3429 m<sup>2</sup> and consisting of 36 cells connected in series. The data above was facilitated by the NREL [12] in the US, and it was taken in three different locations with distinct climates as indicated in Table 2. The data used for validation was taken with high-precision equipment as detailed in [12], and the measured variables were plane-of-array (POA) irradiance, PV module back-surface temperature, and the maximum power produced (MPP).

The outdoor data used in this analysis were limited to PV module back-surface temperatures greater than 298.125 °K and less than 338.125 °K, a POA irradiance greater than 200 W/m<sup>2</sup> but less or equal than 1000 W/m<sup>2</sup>, and a PV module soiling derate equal to one (clean panels). The cloud of points comprising the aforementioned range can be seen in Figure 2 for the case of a PV panel in Cocoa, Florida.

**Table 2.** Identification (ID) of the PV modules and the climate region from which the experimental data was obtained

ID	State	Climate Region	File
C-mSi0166	Florida	Subtropical	Cocoa_mSi0166.csv
C-mSi0188	Florida	Subtropical	Cocoa_mSi0188.csv
E-mSi0166	Oregon	Marine West Coast	Eugene_mSi0166.csv
E-mSi0188	Oregon	Marine West Coast	Eugene_mSi0188.csv
G-mSi0247	Colorado	Semi-arid	Golden_mSi0247.csv
G-mSi0251	Colorado	Semi-arid	Golden_mSi0251.csv

With the measurements of temperature and POA irradiance, an experimental efficiency ( $\eta$ ) has been calculated for each data point according to (1). In this way, a point located in a three-dimensional space  $(T, G, \eta)$  has been obtained for each PV panel and each geographical location. For instance, these efficiency values for the module  $C - mSi0166$  are shown as light-brown circles in Figure 3.

Moreover, the NREL database includes for every panel their power matrix following the IEC 61853-1: Irradiance and Temperature Performance Measurements and Power Rating [10], which describes requirements for evaluating PV module performance in terms of power rating over a range of irradiances and temperatures. These data are used later as references to calculate the PE and Evans' model and are represented as blue asterisks in Figure 3.

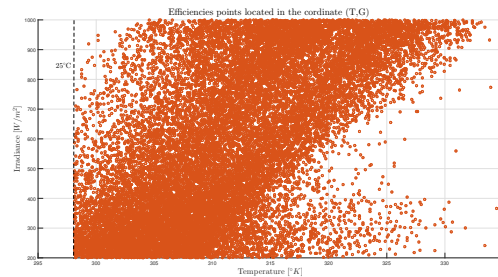


**Fig. 2.** Data cloud considered for the validation of the efficiency expression. Case of module ID  $C - mSi0166$  in Cocoa Florida.

## 4 Definition of the Efficiency Plane Coefficients

### 4.1 Best Fit Plane Equation

The best-fit plane efficiency (BFPE) model are obtained fitting the constants  $\{K_1, K_2, K_3\}$  to the outdoor efficiency data. This procedure was done with using the nonlinear least-squares with a trust-region (NLS-TR) algorithm of the Matlab Curve Fitting Toolbox [13]. The results are shown in table 3.

### 4.2 Proposed plane equation

The efficiency surface expression (6) is constructed using the following three points in the efficiency space:

- The point  $P$  would be the equivalent efficiency obtained at the Standard Test Conditions (STC) point. This efficiency data point,  $\eta_E@STC$ , has an incident irradiance of  $G_{STC} = 1000 \text{ W/m}^2$  and a back panel temperature of  $T_{STC} = 25 \text{ }^\circ\text{C}$ .

**Table 3.** Constants for the BFPE

Modules	$K_1$	$K_2$	$K_3$
C-mSi0166	-0.0557	0.0021	27.8336
C-mSi0188	-0.0557	0.0021	27.8336
E-mSi0166	-0.0652	0.0022	30.4959
E-mSi0188	-0.0650	0.0020	30.5986
G-mSi0247	-0.0425	0.0018	23.8447
G-mSi0251	-0.0431	0.0015	24.1377

- The point  $Q$  would be the efficiency obtained at the high temperature condition point and for this model we selected the efficiency obtained at the PV-USA Test Condition (PTC) equivalent point. This efficiency data point,  $\eta_E@PTC$ , has an incident irradiance of  $G_{PTC} = 1000 \text{ W/m}^2$  and a back panel temperature of  $T_{PTC} = 50^\circ\text{C}$ . This point has been selected due to the possibility of pairing it with the PV-USA Test Condition (PTC) point reported in some PV manufacturer data sheets, which is an US-standard that was developed in collaboration with the U.S Department of Energy [3].
- The point  $R$  would be the equivalent efficiency obtained at the Low Irradiance Condition (LIC) point. This efficiency data point,  $\eta_E@LIC$ , has an incident irradiance of  $G_{LIC} = 200 \text{ W/m}^2$  and a back panel temperature of  $T_{LIC}=25^\circ\text{C}$ .

These reference points are calculated from the matrix powers given by IEC 61853-1 in the NREL database. Table 4 shows the experimental efficiency values obtained for the aforementioned three points for the panels under study.

**Table 4.** Experimental efficiency measures  $\eta_E$  calculated with the IEC 61853-1 for the standard conditions

Module	$\eta_E@STC$ ( $\eta_p$ )	$\eta_E@PTC$ ( $\eta_q$ )	$\eta_E@LIC$ ( $\eta_r$ )
C-mSi0166	13.48%	12.06%	11.83%
C-mSi0188	13.39%	11.92%	11.90%
E-mSi0166	13.48%	12.06%	11.83%
E-mSi0188	13.39%	11.92%	11.90%
G-mSi0247	13.36%	12.04%	11.78%
G-mSi0251	13.32%	12.01%	11.68%

Using the efficiency measures in the table 4 and the expressions in (9), the constants of the table 5 are obtained. The following example shows the calculus for the module C-mSi0166,

$$\begin{aligned}
 K_1 &= (\eta_E@PTC - \eta_E@STC)/(T_{PTC} - T_{STC}) = -0.0568 \\
 K_2 &= (\eta_E@LIC - \eta_E@STC)/(G_{LIC} - G_{STC}) = 0.0021 \\
 K_3 &= \eta_E@STC - K_1T_{STC} - K_2G_{STC} = 28.3485
 \end{aligned}
 \tag{10}$$

**Table 5.** Constants for the proposed model

Modules	$K_1$	$K_2$	$K_3$
C-mSi0166	-0.0568	0.0021	28.3485
C-mSi0188	-0.0586	0.0019	28.9854
E-mSi0166	-0.0568	0.0021	28.3485
E-mSi0188	-0.0586	0.0019	28.9854
G-mSi0247	-0.0528	0.0020	27.1420
G-mSi0251	-0.0524	0.0020	26.8869

### 4.3 Definition of parameters for Evans efficiency model

The PE model is compared with the nonlinear efficiency model proposed by Evans in [6] and widely referenced in the literature. This model defines an expression for the efficiency as follows,

$$\eta = \eta_{STC} \cdot (1 - \beta \cdot \Delta_T + \gamma \cdot \log_{10}(G/G_{STC})), \tag{11}$$

$$\Delta_T = T - T_{STC}$$

where  $\eta$  and  $\eta_{STC}$  are the estimated efficiency and the efficiency at Standard Test Conditions (STC), and  $\beta$  and  $\gamma$  are the temperature and irradiance coefficients, respectively. However, this equation has been used with the equivalent efficiency point at Standard Test Condition ( $\eta_E@STC$ ) calculated from the power matrix (IEC 61853-1). For each PV panel, the coefficient  $\beta$  is taken from the NREL database reported as  $\delta Pm$ . The  $\gamma$  coefficient was calculated with the NLS-TR algorithm, the equation (11), and all the efficiency points derived from the power matrix. The constants used to estimate the efficiency measures are shown in table 6.

**Table 6.** Constants for the Evans' model

Modules	$\beta$	$\gamma$
C-mSi0166	0.0041	0.1706
C-mSi0188	0.0041	0.1477
E-mSi0166	0.0041	0.1706
E-mSi0188	0.0041	0.1477
G-mSi0247	0.0041	0.1556
G-mSi0251	0.0042	0.1527

As an illustrative example, the figure 3 shows the aforementioned representations for the module C-mSi0166. In the figure, the outdoor efficiency values are presented as light-brown circles; the experimental efficiency values obtained with the power matrix according to IEC 61853-1 are presented as blue asterisks; the surface that estimates the efficiency using the model (6), with the three reference points, is the purple mesh and here it looks like a line. The BFPE model that estimates the efficiency using (6), with the parameters obtained from the data

cloud (light-brown circles), is presented as a yellow mesh. Finally, the Evans' efficiency model adjusted to the efficiency values obtained according to IEC 61853-1 (blue asterisks) is presented as a green mesh.

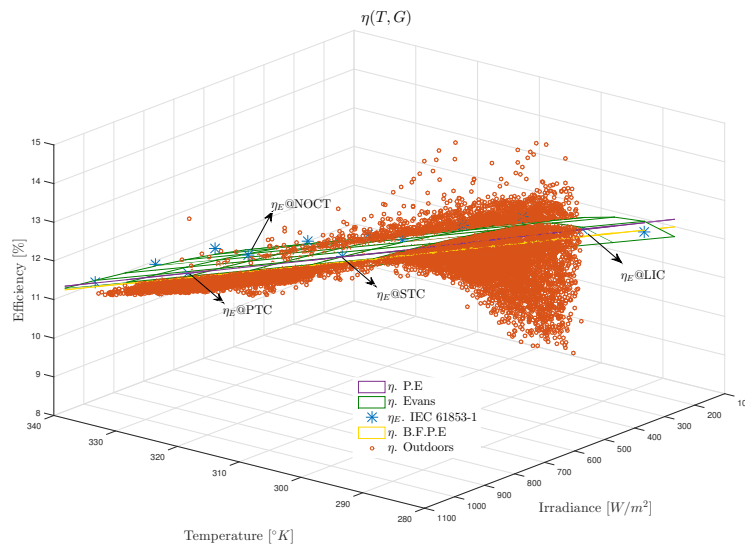


**Fig. 3.** Efficiency values obtained at outdoors conditions (light-brown circles) and with IEC 61853-1 procedures (blue asterisks) for the PV module *C-m.Si0166*. The presented efficiency models are: Evans efficiency expression (green surface), the proposed plane expression calculated from three references points (purple line) and the best-fit plane model (yellow line) calculated from the outdoor efficiency measures.

## 5 Validation methodology

In order to prove that the plane equation behaves as well as the best-fit plane equation, the following steps have been done:

1. For every data set selected, to calculate the metrics to compare the models.
2. For every data set selected, prove using hypothesis test if the efficiency plane models could have equivalent precision and if they could have equivalent accuracy.

### 5.1 Metrics for model analysis

The metrics to evaluate the accuracy and precision of the models are based on the analysis of the residues. We consider the residue  $r_i$  as the difference between

the  $i_{th}$  value of observed efficiency ( $\eta_i$ ) and the estimated result by the model  $\hat{\eta}$  for the outdoor conditions ( $T_i, G_i$ ) as follows,

$$r_i = \eta_i - \hat{\eta}(T_i, G_i) . \tag{12}$$

Notice that from (12) it is possible to obtain a relative error ( $r.e$ ), i.e.,

$$r.e_i = \frac{r_i}{\eta_i} \cdot 100 . \tag{13}$$

This metric explains how far are the efficiency point predicted by the model from the point of view of the experimental data.

Another metric that it is used to compare the models is the normalized root mean square deviation (nRMSD) which is the RMSE value divided by a nominal value [11], and it is defined as,

$$nRMSD = \frac{1}{\eta_p} \sqrt{\frac{\sum_{i=1}^n r_i^2}{n}} , \tag{14}$$

where  $n$  represent the number of elements to analyze.

Also, the coefficient of determination  $R^2$  is used to determine if the variability of the data is captured by the model [20], and it is calculated as follows,

$$R^2 = 1 - \frac{\sum_{i=1}^n r_i^2}{\sum_{i=1}^n (\eta_i - \bar{\eta})^2} \tag{15}$$

where  $\bar{\eta}$  is the average of the observed efficiency values  $\eta_i$ . The adjusted  $R^2$  ( $R_{adj}^2$ ) is also used and obtained as in [1],

$$R_{adj}^2 = 1 - \frac{(n - 1) \cdot \sum_{i=1}^n r_i^2}{(n - p) \cdot \sum_{i=1}^n (\eta_i - \bar{\eta})^2} \tag{16}$$

where  $p$  is the number of coefficients in the estimation model. Also, the mean of the relative error  $\bar{x}_r$ , a type of percentage bias is calculated as,

$$\bar{x}_r = \frac{\sum_{i=1}^n r.e_i}{n} \tag{17}$$

and the standard deviation of the relative error,  $\sigma_r$ , which is calculated as following,

$$\sigma_r = \sqrt{\frac{1}{n - 1} \sum_{i=1}^n (r.e_i - \bar{x}_r)^2} . \tag{18}$$

It should be noticed that the value of  $\bar{x}_r$  indicates on average how far are the data from the estimations of the model chosen, and this value can be associated with the accuracy of the models. The other metric, the value  $\sigma_r$  represents the dispersion of the relative error, and it can be associated with the precision. Table 7 shows the metrics mentioned for the three models: the proposed plane efficiency (PE) model, the best-fit plane efficiency (BFPE) model, and the Evans' models.

**Table 7.** Metrics of the efficiency models calculated with the outdoor efficiency values

Panel	Model	$n$	$nRMSD$	$R^2$	$R_{adj}^2$	$\bar{x}_r(\%)$	$\sigma_r(\%)$
C-mSi0166	P.E.	22427	0.0342	0.4669	0.4668	-1.3975	4.1689
	BFPE	22427	0.0324	0.5208	0.5207	-0.1553	4.0944
	Evans	22427	0.0408	0.2408	0.2408	-3.2483	4.0690
C-mSi0188	P.E.	18678	0.0372	0.4107	0.4106	-1.4229	4.6362
	BFPE	18678	0.0352	0.4725	0.4725	-0.1831	4.4648
	Evans	18678	0.0455	0.1189	0.1189	-3.5920	4.6404
E-mSi0166	P.E.	14726	0.0426	0.1978	0.1977	-3.1917	4.4908
	BFPE	14726	0.0333	0.5104	0.5103	-0.1689	4.3244
	Evans	14726	0.0524	-0.2104	-0.2104	-4.8944	4.4820
E-mSi0188	P.E.	7689	0.0399	0.3196	0.3194	-2.6817	4.3759
	BFPE	7689	0.0329	0.5376	0.5374	-0.1606	4.2319
	Evans	7689	0.0504	-0.0867	-0.0867	-4.5038	4.4685
G-mSi0247	P.E.	6179	0.0381	0.3047	0.3045	-1.7857	4.6315
	BFPE	6179	0.0348	0.4186	0.4184	-0.1807	4.4895
	Evans	6179	0.0445	0.0482	0.0482	-3.2290	4.7840
G-mSi0251	P.E.	3337	0.0374	0.2079	0.2074	-2.1379	4.1730
	BFPE	3337	0.0315	0.4372	0.4369	-0.1463	4.0295
	Evans	3337	0.0446	-0.1255	-0.1255	-3.6960	4.1982

### 5.2 Establishment of the hypothesis test

To quantify the similarity between the BFPE model and the PE model, 12 hypothesis tests are made with the data provided. The Minitab Software [15] was used to process the data. The hypothesis tests, formulated in equation (19) was analyzed with the Bonetts' method, and according to [15], this method is more rigorous than the Fisher or Levene methods. Another benefit is that Bonetts' method can be used with data that do not have a normal distribution, therefore the normality test is not required. The hypothesis test proves if the standard deviation of the relative errors of the studied models can be considered equivalent. Thus, the formalization of the hypothesis is presented as follows,

$$\begin{aligned}
 \forall \mathbf{p} \in \{ & \text{C - mSi0166, C - mSi0188, E - mSi0166,} \\
 & \text{E - mSi0188, G - mSi2047, G - mSi0251} \} \\
 \mathbf{H}_0^{\mathbf{p}} : & \sigma_r^{PE} / \sigma_r^{BFPE} = 1 \quad , \quad (19) \\
 \mathbf{H}_1^{\mathbf{p}} : & \sigma_r^{PE} / \sigma_r^{BFPE} \neq 1 \\
 & \alpha = 0.05
 \end{aligned}$$

where  $\sigma_r$  is the standard deviation of the relative errors. For the second hypothesis expressed in (20), the analysis method uses the two-sample t-test without the assumption of equal variances, which measure the distance between the two

planes as follows,

$$\begin{aligned}
 \forall \mathbf{p} \in \{ & \text{C - mSi0166, C - mSi0188, E - mSi0166,} \\
 & \text{E - mSi0188, G - mSi2047, G - mSi0251} \} \\
 \mathbf{H}_0^{\mathbf{p}} : & \bar{x}_r^{PE} - \bar{x}_r^{BFPE} = 0 \quad , \quad (20) \\
 \mathbf{H}_1^{\mathbf{p}} : & \bar{x}_r^{PE} - \bar{x}_r^{BFPE} \neq 0 \\
 & \alpha = 0.05
 \end{aligned}$$

where the mean of the relative errors is expressed as  $\bar{x}_r$ . In both hypothesis equations, the superscript  $^{PE}$  means plane equation, and  $^{BFPE}$  means best-fit plane-equation.

## 6 Analysis and results

It is clear for the authors that the adjusted Evans’ model is the best model to represent the behavior of the efficiency values calculated from the power matrix obtained according to the IEC 61863-1 [10]. Evans’ models present higher  $R_{adj}^2$  and lower  $nRMSD$  concerning the other models. For example, Table 8 shows the metrics for the panel C-mSi0166. It is seen that the efficiency values calculated from the IEC standard are better described by Evans’ model than the proposed PE model and the BFPE model. However, when thousand of outdoor efficiencies are used, the PE model performs much better than Evans’ model, as it is shown in table 7. Outdoor efficiency values are not taken at specific conditions (temperature, irradiance), as is when the IEC 61863-1 standard is used.

**Table 8.** Metrics of the models calculated from the efficiency values using IEC61853-1

Panel	Model	$n$	$nRMSD$	$R^2$	$R_{adj}^2$	$\bar{x}_r(\%)$	$\sigma_r(\%)$
C-mSi0166	P.E.	13	0.0249	0.8369	0.8043	1.9728	2.1142
	BFPE	13	0.0163	0.9297	0.9156	-0.0306	1.8851
	Evans	13	0.0087	0.9800	0.9800	0.2767	0.9716

In Table 7 the  $nRMSD$  column presents results in the range of [0.0315 – 0.0524] which represents how the outdoor efficiency values are scattered around the efficiency models. Notice that the plane-based models have the best-adjusted coefficient of determination,  $R_{adj}^2$ , i.e., the plane models capture much better the variability of the error than the Evans’ model calculated from IEC 61853-1. In summary, the efficiency prediction model based on a plane in which parameters were calculated using a best-fit algorithm (BFPE) performs better than the model-based which parameters have been calculated using only three points (PE) or the Evans’ model. Nevertheless, as stated before, the three-point plane-based model is more practical due to the possibility of constructing it just with three reference values which may be taken from IEC references or datasheets.

A relevant characteristic to consider is that the BFPE and PE models differ only by an offset value that is on average  $-1.94\%$  as it can be appreciated graphically in the figure 3. The displacement between the models is measured with the mean relative error ( $\bar{x}_r$ ) and for the plane models do not vary significantly in all the modules analyzed (see Table 7). The aforementioned information can be verified using the histogram of the relative errors; for example, Figure 4 shows the histogram of the  $C - miSi0166$  module. The results presented in this figure are confirmed in Table 7 where it can be seen that the average of the relative error ( $\bar{x}_r$ ) for the PE is  $-1.39\%$  while for the BFPE is  $-0.1533\%$ , i.e., the difference between these averages is only  $1.24\%$ . Therefore, the hypotheses established in (20) is rejected because those averages are not equals. On the other hand, the standard deviation of the  $r.e.$  ( $\sigma_r$ ) presents similar results for both models indicating that the hypothesis in eq. 19 may be accepted or rejected

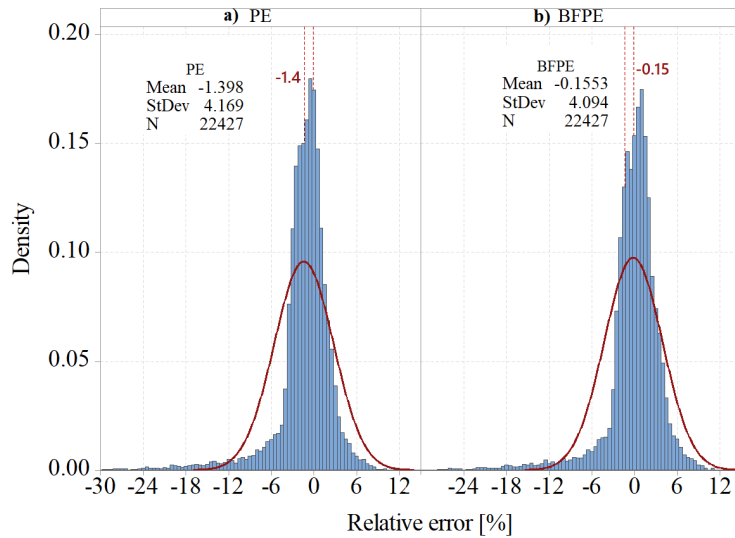


**Fig. 4.** Histograms of the R.E. for panel C-mSi0166. a)  $r.e.$  distribution for the proposed equation. b)  $r.e.$  distribution for the BFPE.

Based on observation of the previous results, we hypothesized that the three-point plane efficiency model could give the same prediction results as the best-fit plane model if the former is rewritten as,

$$\eta^{BFPE} \approx \eta^{APE} = \eta^{PE} \cdot (1 + f), \quad (21)$$

where  $f = \bar{x}_r^{PE} - \bar{x}_r^{BFPE}$ .

The previous model is called the adjusted plane equation (APE). Notice that according to Table 7  $\bar{x}_r^{BFPE}$  is at least one order of magnitude smaller than  $\bar{x}_r^{PE}$

**Table 9.** Results of the hypothesis test

Tag	Number $n$	Ratio $\sigma_r^{APE} / \sigma_r^{BFPE}$	P-value	Difference (%) $\bar{x}_r^{APE} - \bar{x}_r^{BFPE}$	P-value
C-mSi0166	22427	1.00556	0.745	0.0174	0.654
C-mSi0188	18678	1.02551	0.188	0.0176	0.706
E-mSi0166	14726	1.00709	0.758	0.0965	0.056
E-mSi0188	7689	1.00797	0.817	0.0676	0.324
G-mSi2047	6179	1.01508	0.656	0.0287	0.725
G-mSi0251	3337	1.01501	0.743	0.0426	0.668

and therefore  $f \approx \bar{x}_r^{PE}$ . This equation means that if we multiply one PE model by a constant  $(1 + f)$  it is possible to displace the plane equation and obtain an equivalent plane to BFPE.

Table 9 shows the results obtained when the hypothesis tests (19) and (20) are tested with the adjusted plane equation, where the P-Valued is the criteria used to accept or to reject the null hypothesis  $H_0$ . The results in table 9 are quite satisfactory. First of all, the standard deviation of the APE can be considered equivalent to the standard deviation generated by the BFPE. Second, both models generate an equivalent average of the relative error. It should be noticed that for all the tests made, the P-value is always higher than the acceptance value of 0.05; therefore, for all the six modules, it can be confirmed that both planes can be considered “parallel” and with equivalent error distributions.

## 7 Conclusions

This work has proposed a simple plane efficiency model to predict the efficiency value of PV modules using back-panel temperature and POA irradiance for outdoor conditions. The proposed PE model is calculated from three reference efficiency values obtained from the power matrix using the IEC 61853-1 standard. It was validated with outdoor efficiency values in three locations with data collected during one year. All the efficiency values data taken from the NREL database correspond to clean PV panels, with a temperature and irradiance in the ranges  $[25 - 65]^\circ C$  and  $[200 - 1000] W/m^2$ .

The proposed PE mode can be considered “parallel” to the best-fit-plane equation obtained from nonlinear regression of the efficiency data, and on average, the PE model is more optimistic with the predictions than the BFPE model. This means that the PE gives on average 1.94% higher efficiency predictions for all the modules ( $f = -0.0194$ ). However, when the PE is adjusted by the factor  $(1 + f)$ , the adjusted plane equation generates, statistically speaking, equivalent results than the BFPE as demonstrated with the hypothesis test.

The usefulness of the proposed efficiency plane expression hinges on the possibility to construct it with only three points. Even though a more accurate expression can be obtained by applying a best-fit algorithm to a set of measurements, these are not always available or desirable to obtain. A cloud of data,

such as the one used in this paper for validation, requires measuring each PV module for months with high precision equipment, which makes it impractical to determine the parameters of an efficiency model. Therefore, the main advantages of the proposed model are the simplicity of calculating the model constants and that the PE model describes the efficiency behavior also like the best-fit plane efficiency model for a cloud of efficiency points, this without experiments nor data regression.

## Acknowledgment

This project was supported thanks to the scholarship program of the Costa Rica Institute of Technology and the project number VIE 5402-1360-4201.

The authors thank Dr. William Marion from the National Renewable Energy Laboratory (NREL) for providing the experimental data used in this article.

## References

1. MATLAB help, Coefficient of Determination (R-Squared) (2021), <https://www.mathworks.com/help/stats/coefficient-of-determination-r-squared.html>, the MathWorks, Natick, MA, USA
2. Bailey, S., Raffaele, R.: Iiid-2 - operation of solar cells in a space environment. In: Markvart, T., ner, L.C. (eds.) Practical Handbook of Photovoltaics, pp. 705–721. Elsevier Science, Amsterdam (2003). <https://doi.org/https://doi.org/10.1016/B978-185617390-2/50030-1>, <https://www.sciencedirect.com/science/article/pii/B9781856173902500301>
3. Dows, R.N., Gough, E.J.: Pvusa procurement, acceptance, and rating practices for photovoltaic power plants (1995). <https://doi.org/10.2172/119944>, <https://www.osti.gov/biblio/119944>
4. Dubey, S., Sarvaiya, J.N., Seshadri, B.: Temperature dependent photovoltaic (PV) efficiency and its effect on PV production in the world - A review. Energy Procedia **33**, 311–321 (2013). <https://doi.org/10.1016/j.egypro.2013.05.072>, <http://dx.doi.org/10.1016/j.egypro.2013.05.072>
5. Durisch, W., Bitnar, B., Mayor, J.C., Kiess, H., hang Lam, K., Close, J.: Efficiency model for photovoltaic modules and demonstration of its application to energy yield estimation. Solar Energy Materials and Solar Cells **91**(1), 79–84 (2007). <https://doi.org/10.1016/j.solmat.2006.05.011>
6. Evans, D.: Simplified method for predicting photovoltaic array output. Solar Energy **27**(6), 555–560 (1981). [https://doi.org/10.1016/0038-092X\(81\)90051-7](https://doi.org/10.1016/0038-092X(81)90051-7), <http://www.sciencedirect.com/science/article/pii/0038092X81900517>
7. Green, M.A.: Accuracy of analytical expressions for solar cell fill factors. Solar Cells **7**(3), 337–340 (1982). [https://doi.org/10.1016/0379-6787\(82\)90057-6](https://doi.org/10.1016/0379-6787(82)90057-6)
8. Green, M.A., Dunlop, E.D., Hohl-Ebinger, J., Yoshita, M., Kopidakis, N., Ho-Baillie, A.W.: Solar cell efficiency tables (version 55). Progress in Photovoltaics: Research and Applications **28**(1), 3–15 (2020)
9. Gulkowski, S., Zdyb, A., Dragan, P.: Experimental Efficiency Analysis of a Photovoltaic System with Different Module Technologies under Temperate Climate Conditions. Applied Sciences **9**(1), 141 (2019). <https://doi.org/10.3390/app9010141>

10. IEC 61853-1: Photovoltaic (pv) module performance testing and energy rating—part 1: Irradiance and temperature performance measurements and power rating (2011)
11. Livera, A., Theristis, M., Makrides, G., Ransome, S., Sutterlueti, J., Georghiou, G.E.: Optimal development of location and technology independent machine learning photovoltaic performance predictive models. In: 2019 IEEE 46th Photovoltaic Specialists Conference (PVSC). pp. 1270–1275. IEEE (2019)
12. Marion, B., Anderberg, A., Deline, C., del Cueto, J., Muller, M., Perrin, G., Rodriguez, J., Rummel, S., Silverman, T.J., Vignola, F., et al.: New data set for validating pv module performance models. In: 2014 IEEE 40th Photovoltaic Specialist Conference (PVSC). pp. 1362–1366. IEEE (2014)
13. MATLAB, Curve Fitting Toolbox 3.5.1 (2015), the MathWorks, Natick, MA, USA
14. Mavromatakis, F., Vignola, F., Marion, B.: Low irradiance losses of photovoltaic modules. *Solar Energy* **157**(February), 496–506 (2017). <https://doi.org/10.1016/j.solener.2017.08.062>, <https://doi.org/10.1016/j.solener.2017.08.062>
15. Minitab 18 Statistical Software (2014), State College, PA: Minitab Inc
16. Murillo-Soto, L.D., Meza, C.: A simple temperature and irradiance-dependent expression for the efficiency of photovoltaic cells and modules. In: 2018 IEEE 38th Central America and Panama Convention (CONCAPAN XXXVIII). pp. 1–6 (2018)
17. Petrone, G., Ramos-Paja, C.A., Spagnuolo, G., Xiao, W.: Photovoltaic sources modeling. Wiley Online Library (2017)
18. Skoplaki, E., Palyvos, J.A.: On the temperature dependence of photovoltaic module electrical performance : A review of efficiency / power correlations. *Solar Energy* **83**(5), 614–624 (2009). <https://doi.org/10.1016/j.solener.2008.10.008>, <http://dx.doi.org/10.1016/j.solener.2008.10.008>
19. Villalva, M.G., Gazoli, J.R., Ruppert Filho, E.: Modeling and circuit-based simulation of photovoltaic arrays. In: 2009 Brazilian Power Electronics Conference. pp. 1244–1254. IEEE (2009)
20. Walpole, R.E., Myers, R.H., Myers, S.L., Ye, K.: Probability and statistics for engineers and scientists, vol. 5. Macmillan New York (1993)
21. Ye, Z., Nobre, A., Reindl, T., Luther, J., Reise, C.: On pv module temperatures in tropical regions. *Solar Energy* **88**, 80–87 (2013)

## Analysis about the hybridization of PV solar and low enthalpy geothermal energies by using green hydrogen as energy vector

Cristina Sáez Blázquez<sup>1,2</sup> [0000-0002-5333-0076], Ignacio Martín Nieto<sup>2</sup> [0000-0003-3984-7228], Arturo Farfán Martín<sup>2</sup> [0000-0002-1506-1207] and Diego González-Aguilera<sup>2</sup> [0000-0002-8949-4216]

<sup>1</sup>Department of Electric, System and Automatic Engineering, Universidad de León, León, Spain

<sup>2</sup>TIDOP Group, Department of Cartographic and Land Engineering, University of Salamanca, Higher Polytechnic School of Avila, Avila, Spain  
csaeb@unileon.es/u107596@usal.es

### Abstract.

In spite of the high number of promising advantages for a future sustainable scenario, renewable resources are not yet cost-competitive with fossil fuels in all locations and present serious limitations that need to be addressed. Worldwide, the integration of geothermal and solar energies is possible and advantageous for most applications. Unfortunately, when hybridization of shallow geothermal systems and PV solar plant is considered, the principal concern is the dependence on external energy supply of the geothermal heat pump when solar energy is not available. In order to propose a solution to this aspect, the present research considers the implementation of two different geothermal-solar systems including green hydrogen as energy vector (case 1 with electrical heat pump supplied with the electricity coming from the solar panels and from storage hydrogen; case 2 with gas engine heat pump aided by hydrogen gas). Results derived from the analysis of the projected assumptions on a real approach show that both cases could be possible in a near future as technological progress facilitates the inclusion of green hydrogen gas in common devices and applications. However, case 1 is considered the most appropriate schema from both the feasibility and economic point view. In this way, the solution presented here constitutes a significant starting point in the achievement of renewable and self-sufficient energy strategies within the domestic heating industry.

**Keywords:** sustainability, renewable resources, solar and geothermal hybridization, green hydrogen, self-sufficient energy systems.

## 1 Introduction

As global energy needs grow at an exponential rate, the development of alternative renewable solutions has become an essential concern, especially for developing countries. Despite having numerous promising advantages for environment and sustainability, some limitations associated to the use of the current renewable technologies are the main matters to solve. The most common renewables sources such as solar or wind energies have a fluctuated nature that forces them to have energy storage or a

hybrid system to balance the changes in their production. Other solutions, such as low enthalpy geothermal applications, are still subjected to the use of an external energy source (usually electricity) for the operation of the heat pumps. These limitations (and many others) lead to consider the use of multigeneration systems with the aim of guarantying a distributed energy production [1].

Focusing in this paper on the energy needs of a domestic building, solar and geothermal resources are the most implemented options. However, these energies are not yet cost-competitive with traditional fuels in all locations due to aspects related to the intermittency and instability. Despite this fact, the availability of both sources worldwide, makes its integration possible and recommended in numerous cases. In this sense, hybridization of both alternatives has been evaluated in many different scenarios. Solar is sometimes used to increase the temperature of geothermal fluids, to improve the efficiency of the geothermal power generation. Geothermal fluids can also serve as storage systems for solar energy, in the context of solving the problems of instability and weather dependence of solar systems [2].

In the field of low enthalpy geothermal installations, solar PV systems are integrated as a solution to cover the energy needs of the geothermal heat pump. But once again, the intermittency and climatic dependence of solar energy makes it necessary to have external electricity supply. With this limitation in mind, it is clear the need of an alternative solution to get an energy self-sufficiency system, without depending on the electricity coming from fossil sources. In this context, green hydrogen could be the perfect match for the objective of achieving efficient and completely renewable building systems.

### **1.1 Green hydrogen**

Hydrogen, the only zero-carbon energy carrier (other than electricity), can be produced from several feedstocks and energy pathways. When hydrogen meets some sustainability criteria, the term “green hydrogen” is usually established. Thus, green hydrogen arises as an alternative to fossil fuels, being produced entirely from renewables. The process consists of the water electrolysis by using an electric current that splits water into oxygen and hydrogen with no greenhouse gases emissions [3].

Nowadays, green hydrogen is used in numerous sectors as a chemical feedstock, used as a reagent for synthetic fuel generation, burned for heat, or converted back to electricity by the use of fuel cells. An additional advantage is the possibility of its storage in tanks or in underground structures that makes this technology the only green solution with energy storage across seasons [4].

The importance of green hydrogen in the energy global sector can be seen in the large number of scientific works carried out in recent times. Thus, different researchers have focused on investigating hydrogen production systems bases on renewable technologies or waste treatments [5-7]. Existing literature also addresses the effect of

green hydrogen production on the environment, considering different factors, such as land use, water discharge quality, temperature, or maintenance requirements [8-9].

The other main category under investigation is the integration of green hydrogen in currently available renewable technologies. The great potential of this gas has produced a fast development of hybridization renewable systems based in different sectors and applications [10]. This energy vector helps in decreasing the effect of fluctuations of renewable energies, also providing extra power during peak-time demands. A lot of research is focused on renewable energy based multigeneration systems to produce hydrogen [11-12], solar hydrogen production methods or geothermal-based hydrogen generation technologies [13-14].

Despite all the mentioned existing literature, there is still the need to advance in self-sufficient energy solutions at the household level that contribute to the future global decarbonization. For this reason, the present research aims to analyze the integration of a PV solar and low enthalpy geothermal plant and the implementation of green hydrogen following different supply patterns. The following sections include the description of the proposed system and the calculation on a real study case of the main parameters that define it.

## 2 Materials and method

### 2.1 Study case

The integrated system proposed in this work is planned to be located in the Spanish region of Ávila (center of Spain). The specific location expressed in geographical coordinates is shown in the following Table 1.

**Table 1.** Geographical coordinates of the area in which the study is set.

Latitude	Longitude
40°39'02.4"N	4°40'45.7"W

This area is characterized by short, hot, and mostly clear summers with numerous hours of solar radiation. Winters are very cold and dry, but radiation is also common during most part of the season. During the course of the year, the temperature generally ranges from -1 °C to 29 °C and rarely drops below -6 °C or rises above 33 °C.

Regarding the geological context, this region of the province is mainly constituted by an igneous rock environment, belonging to the Spanish Central System. The following rocky levels can be distinguished; (i) pre-Hercynian igneous rocks (glandular and banded biotitic ortho-gneiss, leucocratic ortho-gneiss and foliate pegmatites), (ii) Hercynian granitic rocks (tonalites and quartz diorites, biotitic medium-coarse grained adamellites, porphyritic coarse-grained leucogranites with biotite, biotitic fine-grained leucogranites, and two-mica fine-grained leucogranites), (iii) philonian rocks (granit-

ic-adamellite porphyries, fine-grained leucogranites and aplite, micro-diorites, quartz, syenite and lamprophyre dykes) [15].

## 2.2 System description

As mentioned in the introduction section, the particular limitations of renewable resources make it necessary to combine different available solutions. In this way, the system here presented is designed to cover the heating energy needs of a building placed in the study area (region of Ávila). Given the climatic and geological characteristics of the place, solar and shallow geothermal energies are considered especially appropriate for being included in the installation. Thus, the hybridization system proposed in this work is constituted by the following modules:

- Low enthalpy geothermal system  
Considering the granitic environment of the area, the geothermal plant is the main component of the heating system. The weakness of this technology is the dependence on electricity for supplying the heat pump, so this need will be considered in the present research.
- PV solar plant  
The high number of hours of solar radiation during the whole year in Ávila makes this alternative a suitable choice for the place. This module is thought to be the electricity supplier for the geothermal heat pump when available. However, the intermittency of this generation obliges to consider additional sources for those moments in which solar production is not possible. In this way, this PV solar plant will be also used for the generation of green hydrogen.
- Green hydrogen module  
Green hydrogen will be directly produced using the electricity coming from the PV solar plant. Providing water and through the process of electrolysis, hydrogen will be produced and stored in specific tanks. This green hydrogen will follow two different ways:
  - Case 1: hydrogen will be converted into electricity through the use of fuel cells to be then used in the Electrical Heat Pumps (EHP). In this case, electricity will be also used from the PV solar panels when available.
  - Case 2: hydrogen will be directly used for supplying specific Gas Engine Heat Pumps (GEHP), thus constituting the source of the geothermal installation.

The following Figure 1 shows the global description of both cases and each of the modules included on them.

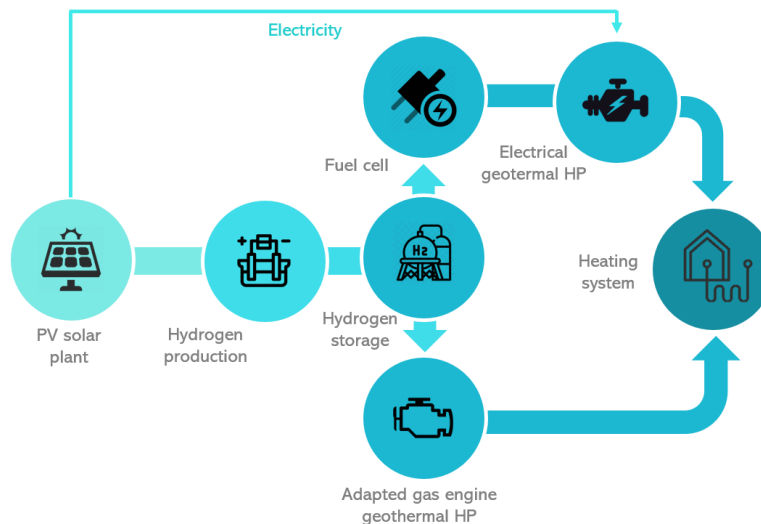


**Fig. 1.** Description of the energy solutions presented in this work.

### 2.3 Heat pump operation

Geothermal heat pumps are highly efficient renewable energy technologies that are gaining wide acceptance for residential buildings. These devices have undergone a very important evolution, which continues in progress. Despite the high operational efficiency of the geothermal heat pumps, they need a certain amount of electricity (depending on the Coefficient of Performance “COP”) that obliges to have an external energy supply. In the last years, gas engine heat pumps are also possible in this kind of installations, usually working with natural gas.

From the analysis of the conditions about the operation of geothermal heat pumps and their limitations, the present study suggests the following types of energy supply:

- Following the pattern of Case 1, this first assumption considers the operation of electrical heat pumps using the electricity directly derived from the solar module when possible. Considering the intermittency of the solar production, hydrogen will be produced and stored to be subsequently converted into electricity through fuel cells. This mechanism will ensure the constant electricity supply even when no solar radiation is available.
- As explained in Case 2, the geothermal heat pump will be working using the hydrogen gas produced by the solar plant. For this purpose, gas engine heat pump will be required. However, since the existing devices are designed for usually working with natural gas, this solution needs to incorporate the appropriate adaptations to operate with hydrogen. After produced in the PV solar module, hydrogen is stored in specific tanks so the geothermal heat pumps will use this gas when needed.

### 3 Results

Considering an isolated single-family house, of medium size, thermal needs are estimated for the sizing of the installation of 50 MWh per year. Limitations of available land or initial investment are not taken into account, just considering the experimental nature of the project.

#### 3.1 PV solar production

For the dimensioning of the photovoltaic collection field, which will be in principle the only source of energy in the facility, data on the energy that reaches the location in a year must be collected (Figure 2).

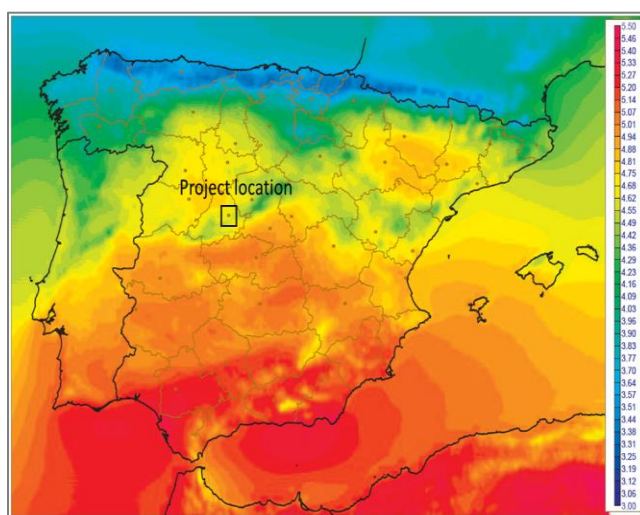


Fig. 2. Average global irradiance in the area under study ( $\text{kWh m}^{-2} \text{ day}^{-1}$ ) [16].

To establish the possibilities of capturing energy it is required to know its monthly distribution. In this way it is possible to estimate the energy that can be stored in the months where the heating installation is stopped (Table 2).

Table 2. Average direct irradiance (ADI) values per month ( $\text{kWh m}^{-2} \text{ day}^{-1}$ ) in Ávila. Source: Atlas of Solar Radiation in Spain. National Institute of Meteorology.

Month	ADI ( $\text{kWh m}^{-2} \text{ day}^{-1}$ )
January	1.26
February	1.87
March	2.79
April	3.37
May	3.75

June	5.08
July	5.77
August	4.75
September	3.60
October	2.08
November	1.33
December	1.01
<b>TOTAL</b>	<b>36.66</b>

It is also interesting to know the monthly distribution of the energy needs of the installation, to define how these can be coupled to the energy inputs and outputs of the system. Table 3 includes the mentioned information

**Table 3.** Thermal needs of the project, annual distribution.

Month	Fraction	Energy (MWh)
January	0.155	7.75
February	0.148	7.4
March	0.125	6.25
April	0.099	4.95
May	0.064	3.2
June	0	0
July	0	0
August	0	0
September	0.061	3.05
October	0.087	4.35
November	0.117	5.85
December	0.144	7.2

With the above data it is possible to estimate the necessary surface area of photovoltaic solar panels for the geothermal solutions here considered, electrical and gas engine (supplied by hydrogen) heat pumps.

- **Electrical heat pump**

It is necessary to establish an estimation of the energy losses in the different transformations and processes to design the photovoltaic field correctly. The following Equation 1 shows the overestimation considered for the electric driven heat pump.

$$E_{tot} = E_0 / (\rho_{pv} * \rho_{elect} * \rho_{fc} * \rho_{hp}) \tag{1}$$

Where:

- $E_{tot}$  Total energy needed from the solar panels to be captured.
- $E_0$  Energy needed for the thermal installation.
- $\rho_{pv}$  Performance of the solar panels.
- $\rho_{elect}$  Performance of the electrolyzer.
- $\rho_{fc}$  Performance of the fuel cell.
- $\rho_{hp}$  Performance of the heat pump (including the COP).

With all these data, the energy that must be captured is calculated from the previous Equation 1 and takes the value presented in Equation 2:

$$E_{tot} = 50 \text{ MWh} / (0.2 * 0.6 * 0.5 * 4.3) = 193.8 \text{ MWh} \quad (2)$$

The last value is the energy that the solar panels must contribute throughout the year to the system. To ensure this, it is necessary to dimension them so that the month where the highest percentage of total energy is captured (July), the dimensioning allows to accept that same percentage of cake needs. In this way, the energy captured in July must be 15.74% of the total necessary energy calculated before, **30.504 MWh**. That energy throughout the month, which implies that the daily intake must be: **0.984 MWh**.

Taking into account that the ADI in July is 5.77 kWh m<sup>-2</sup> day<sup>-1</sup>, **170.5** square meters of photovoltaic solar panels must be installed.

- **Gas engine heat pump**

For the gas engine heat pump Eq. (1) must be adapted, mainly to cope with the different performance in the geothermal system:

$$E_{tot} = 50 \text{ MWh} / (0.2 * 0.6 * 0.5 * 1.7) = 490.2 \text{ MWh} \quad (3)$$

Again, the energy captured in July must be 15.74% of the total necessary energy calculated in Eq. (3), **77.157 MWh**. The daily intake must be: **2.489 MWh**.

Considering again the ADI in July (5.77 kwh m<sup>-2</sup> day<sup>-1</sup>) and repeating the same calculus for this heat pump type it is necessary to install **431.4** square meters of photovoltaic solar panels.

The following Table 4 presents a summary of the data obtained for the photovoltaic solar installation in the two cases.

**Table 4.** Data obtained of each photovoltaic installation.

Heat pump type	PV energy caption (MWh)	PV surface (m <sup>2</sup> )
Electric	193.8	170.5
Thermal engine	490.2	431.4

### 3.2 Hydrogen generation and storage

The perspective adopted when sizing the hydrogen production and storage system has to do with being able to respond to the energy production of the months when there is no consumption. It has also been assumed that a water supply is available capable of feeding the electrolyzer without further limitation.

As a consequence of the difference in performance between the heat pumps, two different systems for the production and storage of hydrogen must be designed.

- *Electric heat pump*

It must have the capacity to store all the energy produced in the months of zero consumption of thermal energy. For reasons of security of supply, the months of May and September will also be taken into account for storage purposes (where production could still be higher than consumption). Table 5 presents the energy that will be received for its storage.

**Table 5.** Energy received for storage.

Month	ADI ( kwh m <sup>-2</sup> day <sup>-1</sup> )	Energy received (kWh)
May	3.8	19820.6
June	5.1	26850.3
July	5.8	30497.3
August	4.8	25106.1
September	3.6	19027.8
<b>TOTAL</b>		<b>121302.2</b>

There are, at the moment, two ways of hydrogen storage, gas under pressure or in liquid form at a very low temperature. Given the technical sophistication necessary for the handling and storage of gas in the liquid phase, for a domestic installation, the storage in the gas phase at 320 bar has been selected, which is currently common as handling pressure. In this way, the electrolyzer is also selected for that pressure. The following Table 6 shows the technical considerations for selecting the electrolyzer both in power and in daily operating time.

**Table 6.** Technical items to select the electrolyzer.

<b>H<sub>2</sub> E. density (MJ/l)</b>	<b>H<sub>2</sub> E. density (kWh/m<sup>3</sup>)</b>	<b>Energy received (kWh)</b>	<b>Energy to store (kWh)</b>
4.21	11944.46	121302.23	14556.31
<b>Elect. Production (m<sup>3</sup>/h)</b>	<b>Elect. Production (kW) project/max.</b>	<b>Working Hours (tot)</b>	<b>Working Hours (per day)</b>
30	126/150	962,72	6,42

With these data, the technical device of the following Figure 3 has been selected.



**Fig. 3.** Sinohy PEM electrolyzer (Dupont membrane technology), model HGPS-30, 150 kW. Certified ISO9001, ISO14001, OHSAS18001. Pressure 3.2 Mpa.

With the above data, the storage needs of **6.1 m<sup>3</sup>** are established in a conventional tank for hydrogen in this pressure regime.

- **Gas engine heat pump**

The different magnitude of the energy involved implies a new dimensioning of the hydrogen production and storage system necessary in the case of the geothermal energy with a gas heat pump (Table 7).

**Table 7. Energy received for storage**

Month	ADI ( kwh m <sup>-2</sup> day <sup>-1</sup> )	Energy received (kWh)
May	3.8	50150.3
June	5.1	67936.9
July	5.8	77164.5
August	4.8	63523.7
September	3.6	48144.2
<b>TOTAL</b>		<b>306919.5</b>

The below Table 8 presents an analogous description of the technical data for the selection of the electrolyzer of this case.

**Table 8.** Technical items to select the electrolyzer in the gas engine heat pump scenario.

H <sub>2</sub> E. density (MJ/l)	H <sub>2</sub> E. density (kWh/m <sup>3</sup> )	Energy received (kWh)	Energy to store (kWh)
4.21	11944.46	306919.52	36830.34
Elect. Production (m <sup>3</sup> /h)	Elect. Production (kW) project/max.	Working Hours (tot)	Working Hours (per day)

60	263/300	1167.2	6.51
----	---------	--------	------

The electrolyzer selected is similar to the previous one but a higher power model, specifically the Sinophy HGPS-60 with 300 kW and 60 m<sup>3</sup> hour of production.

Based on the above data we establish storage needs of **15.4 m<sup>3</sup>** in a conventional tank for hydrogen in this pressure regime.

### 3.3 Geothermal design

For energy needs in heating of 50 MWh/year, the geothermal well field is going to be designed. For this purpose software GES-CAL, the geothermal design program will be applied to the selected area [17]. The following table Table 9 shows the results obtained in the design of the geothermal installation for both the electric heat pump and the thermal engine one.

**Table 9.** Geothermal system design by GES-CAL.

Heat pump	COP	Total drilling length (m)	Number of boreholes
Electric	4.3	372.5	3
Thermal engine	1.7	218.4	2

Both systems have been designed with double 32 mm diameter pipes and PE-100 polyethylene. Standard geothermal filler of thermal conductivity 2.4 W/mk. The following Figure 4 shows the program screen in the initial data entry phase.

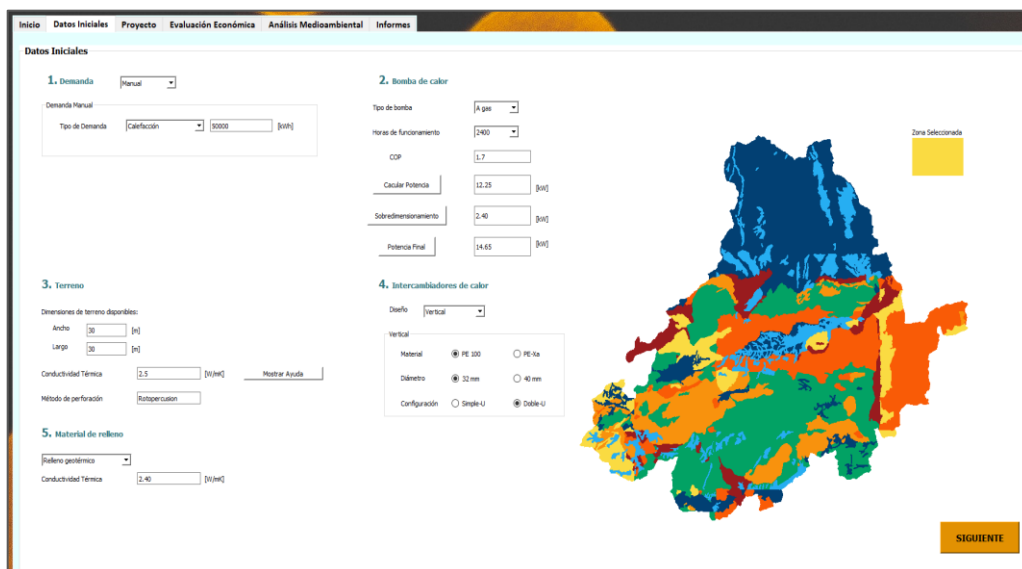


**Fig 4.** GES-CAL data acquisition module.

For the scenario with the electric heat pump, a fuel cell according to the power of the heat pump (6 kW) and capable of dealing with hydrogen of purity and conditions compatible with our stored gas is also required. Thus, the commercial fuel cell G-HFCS-6kW has been selected. Some additional data about the fuel cell can be found in Table 10.

**Table 10.** Information of the fuel cell selected for case 1, EHP.

Nominal Power	Efficiency	Hydrogen Purity	Hydrogen Pressure	Hydrogen Consumption
6000 W	≥ 50%	> 99.99% (CO<1 ppm)	0.04 - 0.06 MPa	70 L/min

With all the above, the self-sufficient energy chain for heating needs using geothermal energy is estimated to be complete.

## 4 Discussion

### 4.1 General evaluation of the suggested solutions

Observing the results presented in the previous section for each of the solutions included in this research, some important statements can be deduced:

- The first aspect to consider is the difference in the total energy that needs to be captured by the solar plant. In the case of the EHP (case 1) the higher COP of the system (4.3) significantly reduces this value in comparison to the one associated to the GEHP (case 2), in which the COP is comparatively lower (1.7). As a consequence of the above, the solar panel surface required in this last case with gas engine heat pump is higher (more than double) than in the electrical case.
- Regarding the design of the shallow geothermal well field, as Table 5 shows, the total drilling length of the system of case 1 (EHP) is relatively higher than the one required for case 2 (GEHP), due to the differences in the COP of both solutions. In the same context, the number of boreholes is also lower in this last assumption. However, the cost of the new GEHP aided by hydrogen will be probably higher than the EHP, which is highly extended in the energy industry.
- In relation to the green hydrogen module, one of the most negative aspects associated to case 2 (GEHP) is the requirements of generation and storage. The great difference in the needs of electrolyzer and store of this gas translates into an important increase of the costs of this case 2. It is also true that in the case of the electric heat pump, it is necessary to add the fuel cell, which could have a high cost, although it is more than compensated for the extra cost caused by the increase in power of the electrolyzer.

Taking into account the above aspects, despite both solutions seem to be technically feasible, the economic factor is an important limitation when implementing the system of case 2. In this way, the costs associated to each of the modules that constitute each solution have been calculated and included in the following Figure 5.

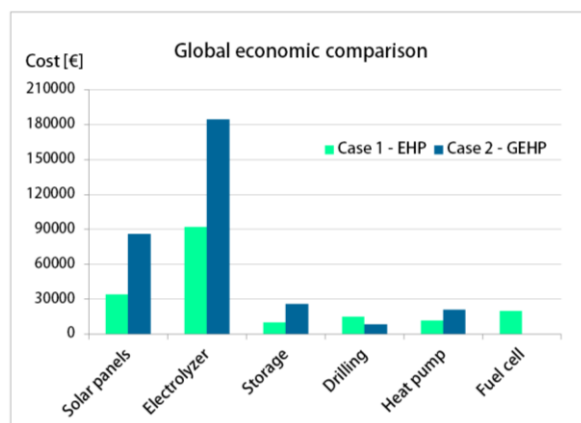


Fig 5. Economic comparison of cases 1 and 2 based on the current commercial costs of each module.

Based on the previous Figure, the initial investment of case 2 would be considerably higher considering the costs of the solar panels (with 431 m<sup>2</sup> of panels), the cost of the hydrogen production and storage system (much more demanding than case 1), and the cost of a gas engine heat pump especially designed for working with hydrogen. Despite drilling costs are lower in this system, the difference is not significant to suppose a change in the economic trend of this case 1. For all the mentioned reasons, case 1 is positioned as a technically and economically reasonable solution to constitute a self-sufficient and energetically renewable system (Figure 6).

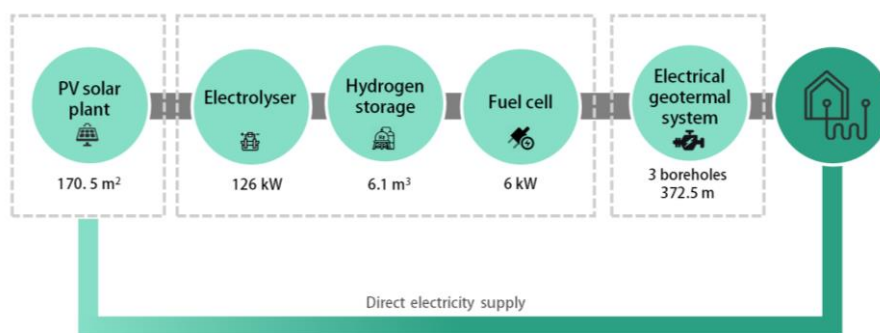


Fig 6. Characteristics of the most proper solution as a self-sufficient renewable system.

## 5 Conclusions

Numerous publications and works of hybrid solar-geothermal systems can be found in the existing literature. Both the drawbacks and benefits of the hybridization have been summarized, highlighting that the integration is possible and increase the performance of both systems in terms of economic profit and thermal efficiency. Although the hybrid of PV solar and shallow geothermal plants presents many advantages, the dependence on external energy input is still unresolved. For this reason, the solutions presented in this research lay the foundations for a self-sufficient and renewable energy concept within the heating sector. The inclusion of green hydrogen as energy vector in this kind of systems is key in achieving a zero-emission heating pattern.

According to the results of the suggested hybridization scenarios, the solution in which electrical geothermal heat pump is considered, constitutes the most recommended schema from both the feasibility and economic point of view. Although both cases are possible, the lack of information and specific equipment for the use of gas engine heat pumps aided by hydrogen is the main limitation of the system.

Based on all the calculations, the hybrid PV solar and EHP geothermal plant enhanced by the production and storage of hydrogen is seen as a promising option to offset the limitations of renewable technologies and, in turn, allow a better exploitation of both energy systems. However, there are still several technological challenges to get more efficient and affordable solutions, especially with regard to the management of green hydrogen, its production, storage and later use as gas, but also its subsequent conversion into electricity. The drawbacks associated with these types of integrations might be addressed with the further development and progress in solar, geothermal and green hydrogen industries with a view to an energy system not dependent on fossil fuels.

## References

1. Bicer, Y., & Dincer, I. Development of a new solar and geothermal based combined system for hydrogen production. *Solar Energy*, 127, 269-284 (2016).
2. Mahmoud, M., Ramadan, M., Naher, S., Pullen, K., Abdelkareem, M. A., & Olabi, A. G. A review of geothermal energy-driven hydrogen production systems. *Thermal Science and Engineering Progress*, 100854 (2021).
3. Abad, A. V., & Dodds, P. E. Green hydrogen characterisation initiatives: Definitions, standards, guarantees of origin, and challenges. *Energy Policy*, 138, 111300 (2020).
4. Tarkowski, R. Underground hydrogen storage: Characteristics and prospects. *Renewable and Sustainable Energy Reviews*, 105, 86-94 (2019).
5. Fragiaco, P., & Genovese, M. Technical-economic analysis of a hydrogen production facility for power-to-gas and hydrogen mobility under different renewable sources in Southern Italy. *Energy Conversion and Management*, 223, 113332 (2020).

6. Yuksel, Y. E., Ozturk, M., & Dincer, I. Energy and exergy analyses of an integrated system using waste material gasification for hydrogen production and liquefaction. *Energy Conversion and Management*, 185, 718-729 (2019).
7. Mahata, C., Ray, S., & Das, D. Optimization of dark fermentative hydrogen production from organic wastes using acidogenic mixed consortia. *Energy Conversion and Management*, 219, 113047 (2020).
8. Ganjehsarabi, H., Gungor, A., & Dincer, I. Exergetic performance analysis of Dora II geothermal power plant in Turkey. *Energy*, 46(1), 101-108 (2012).
9. Chen, J., Xu, W., Zuo, H., Wu, X., Jiaqiang, E., Wang, T., ... & Lu, N. System development and environmental performance analysis of a solar-driven supercritical water gasification pilot plant for hydrogen production using life cycle assessment approach. *Energy conversion and management*, 184, 60-73 (2019).
10. Peterseim, J. H., White, S., Tadros, A., & Hellwig, U. Concentrating solar power hybrid plants—Enabling cost effective synergies. *Renewable energy*, 67, 178-185 (2014).
11. Al-Sulaiman, F. A., Dincer, I., & Hamdullahpur, F. Exergy modeling of a new solar driven trigeneration system. *Solar Energy*, 85(9), 2228-2243 (2011).
12. Karellas, S., & Braimakis, K. Energy–exergy analysis and economic investigation of a cogeneration and trigeneration ORC–VCC hybrid system utilizing biomass fuel and solar power. *Energy conversion and management*, 107, 103-113 (2016).
13. Kalogirou, S. A., Karellas, S., Badescu, V., & Braimakis, K. Exergy analysis on solar thermal systems: a better understanding of their sustainability. *Renewable Energy*, 85, 1328-1333 (2016).
14. Balta, M. T., Dincer, I., & Hepbasli, A. Thermodynamic assessment of geothermal energy use in hydrogen production. *International Journal of hydrogen energy*, 34(7), 2925-2939 (2009).
15. López Ruiz, J., Aparicio, A., & García Cacho, L. El metamorfismo de la sierra de Guadarrama. *Sistema Central español*. Instituto Geológico y Minero de España (1975).
16. Sancho Ávila, J. M., Riesco Martín, J., Jiménez Alonso, C., Sánchez de Cos, M. D. C., Montero Cadalso, J., & López, M. *Solar Radiation Atlas for Spain based on Surface Irradiance Data from EUMETSAT Climate Monitoring-SAF* (2012).
17. Blázquez, C. S., Nieto, I. M., Mora, R., Martín, A. F., & González-Aguilera, D. GES-CAL: A new computer program for the design of closed-loop geothermal energy systems. *Geothermics*, 87, 101852 (2020).

## Off-grid photovoltaic system in an existing urban building. Case of the library at the ETSEIB

Roberto Villafafila-Robles<sup>1</sup>[0000-0003-4372-2575], Elena Alcázar Mateos, Oriol Boix-Aragonès<sup>1</sup>[0000-0003-3182-9703], Daniel Montesinos-Miracle<sup>1</sup>[0000-0003-3983-0514], Sara Barja-Martínez<sup>1</sup>[0000-0003-4126-8858]

<sup>1</sup> Centre d'Innovació Tecnològica en Convertidors Estàtics i Accionaments (CITCEA-UPC), Departament d'Enginyeria Elèctrica, Universitat Politècnica de Catalunya, ETS d'Enginyeria Industrial de Barcelona, Avinguda Diagonal, 647, 2nd Floor, 08028 Barcelona, Spain

roberto.villafafila@citcea.upc.edu

montesinos@citcea.upc.edu

boix@citcea.upc.edu

sara.barja@upc.edu

**Abstract.** Photovoltaic technology is being more and more installed. This technology permits obtaining electricity from a local energy resource. Then, it is also used to extend access to energy to people and facilities that lack it by off-grid systems. Nevertheless, such off-grid systems can be also used in existing buildings already connected to the grid for supplying a new demand. This paper presents this situation for the case of the library at the Escola Tècnica Superior d'Enginyeria Industrial de Barcelona (ETSEIB), Barcelona (Spain).

**Keywords:** off-grid, photovoltaic system, building integration.

### 1 Introduction

Renewable resources have arisen as the most convenient sources for sustainable energy future and reducing emissions from the energy sector. Among the different renewable technologies, wind turbines and photovoltaic systems are being widely installed for electricity generation. These renewable systems have been mainly connected to the grid. Nevertheless, where there is a lack of grid connection or even a lack of fossil fuel energy resources, off-grid renewable systems have been used for facilitating energy access to those places.

Off-grid renewable systems can provide power to remote households, schools, and hospitals, among other buildings. This has been a common solution for areas with a significant gap in energy access rate, like developing countries or rural areas. Literature has paid special attention to this intending to promote universal access to energy [1, 2]. In addition, stand-alone applications like remote telecommunications towers [3] and water pumping [4], which can be found in both developed and developing countries, usually require off-grid renewable systems to have energy supply.

However, off-grid renewable systems are not considered as a choice for providing electricity in existing buildings in urban areas with access to the grid. Nevertheless, these systems could be a potential solution for supplying new demand if, for example, the cost of such a system was lower than upgrading the existing facility, or administrative procedures are a cumbersome prerequisite for connecting on-site renewable generation. It could be also used for assuring that the supply of the new demand comes from renewable sources as a complement/alternative to Tradable Green Certificates.

The Universitat Politècnica de Catalunya (UPC) aims to become a low-energy and low carbon university, in addition to experiencing innovation on its different campuses towards an energy-sustainable society. Therefore, among other actions, it is promoting on-site renewable energy installations to move towards energy self-sufficiency. Within this framework, UPC has promoted photovoltaic systems in its buildings, counting around 234 kW at present in service, and has planned to install about 400 kW more during 2022. The photovoltaic facilities already in operation, all of them installed in the roofs of UPC's buildings, are 230 kW for self-consumption and 4 kW off-grid [5].

This paper deals with the 4kW off-grid photovoltaic system that is installed in an existing building. Firstly, the photovoltaic installation is described. Secondly, the performance of the systems is shown and analyzed. Finally, main conclusions and further work are depicted.

## 2 Off-grid photovoltaic installation

The origin of the off-grid photovoltaic installation was the aim of providing electricity to the study room for students placed in the library of the Escola Tècnica Superior d'Enginyeria Industrial de Barcelona (ETSEIB), the Industrial Engineering school, that belongs to the UPC.

The off-grid photovoltaic system consists of 16 polycrystalline photovoltaic modules of 250 W<sub>p</sub> installed on the roof of the library. These are mounted in four rows with four modules each one (see Fig. 1) with an inclination angle of 60°. The whole set of modules is connected in series.

The system uses a hybrid PV-inverter CirPower 4k-48, with an output power of 4 kW, configured in off-grid mode. This hybrid PV-inverter has an input for the photovoltaic modules, an input for the battery system, and two AC single-phase outputs: one for injecting its power into the power grid, and a second one for supplying critical loads as an uninterruptible power supply (UPS). The main technical features of this hybrid PV-inverter are listed in Table 1. In this facility, AC output to the power grid is not connected.

There is a battery system with a total capacity of 21.8 kWh consisting of 24 modules of 2 V OPzV battery type connected in series. As the installation is off-grid, the AC output of the hybrid PV-inverted is disconnected when its State-of-Charge (SOC) is lower than 40% to avoid to stress battery system.

The AC output of this off-grid photovoltaic installation provides electricity to a set of plugs placed in the room in the library of ETSEIB. This room has 66 individual sites for individual study, originally without any plug for charging handle devices like tablets

and smartphones. Due to the spread of such devices, it was decided to install plugs. But instead of connecting the new plugs to the existing electrical installation in the building, it was decided to deploy the mentioned off-grid photovoltaic system. After the commissioning of the photovoltaic installation, each of the sites has a single-phase 230 V plug. The single-phase AC output of the PV-inverter is divided into 3 single-phase circuits, counting each of the circuits with 22 plugs. Moreover, this facility is used as a campus lab for students of ETSEIB [7, 8, 9, 10].



**Fig. 1.** Off-grid PV system at the roof of the library of the ETSEIB building

**Table 1.** Electrical features of CirPower 4k-48 [6].

DC input	Maximum DC power	4250 W
	Minimum - Maximum voltage	170 – 550 V <sub>DC</sub>
	MPPT voltage range	170 to 500 V <sub>DC</sub>
	Maximum current	20 A
Battery input	Rated voltage	48 V
	Voltage range	36 to 60 V
	Maximum current charge/discharge	80/50 A
AC output	AC power (2 outputs)	4000 W
	Rated voltage – frequency	230 V – 50/60 Hz
	AC voltage range	180 to 270 V
	Frequency range	45 to 65 Hz

To supervise the features of the system, a monitoring system was also deployed (see Fig. 2). It consists of one EDS and 3 CVM-1D from Circutor. EDS device collects data from the webserver of the hybrid PV-inverter and from the 3 CVM-1 that are measuring the 3 single-phase AC output circuits.

The data are available through the webserver of the EDS, but its access is limited. To make available the current data to the ETSEIB community, a public website has been developed (see Fig. 3) which is shown on library information TV screens.

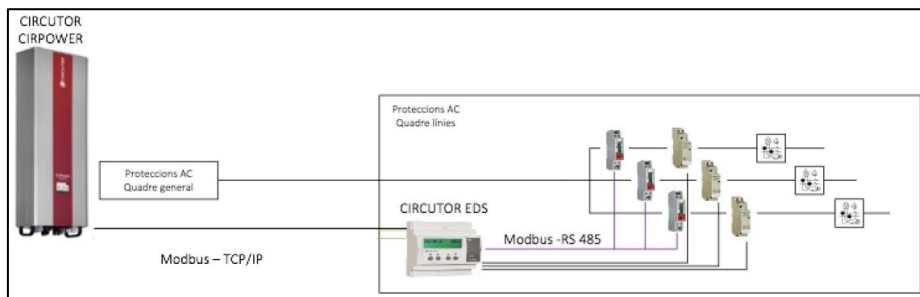


Fig. 2. Monitoring system of the off-grid PV system

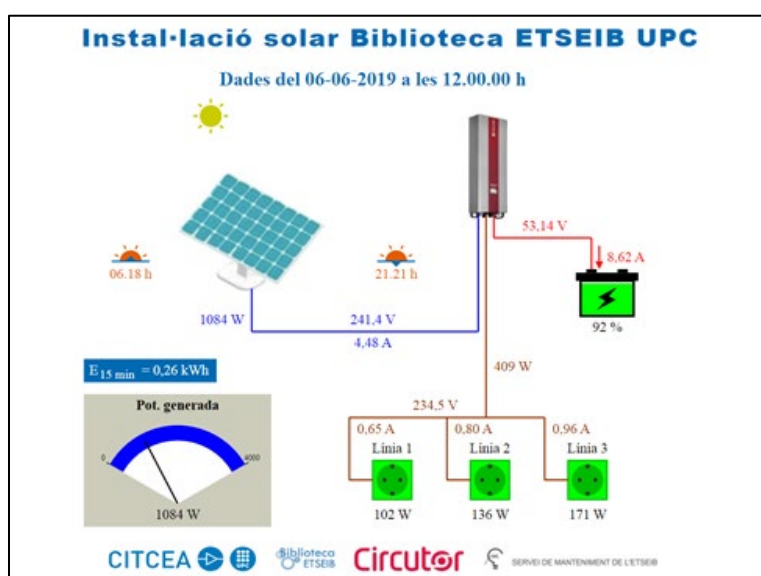


Fig. 3. Public website with current data from the off-grid PV system (available at <https://recursos.citcea.upc.edu/bisol/bisol.php>)

### 3 Performance analysis

The off-grid photovoltaic installation entered in service during 2017 and from March 2018 there are data available. Based on these data, the performance of this installation is described following. The description will be done based on the academic calendar, namely in the spring and fall semesters, as the use of this off-grid facility depends highly on it. The mid-term exams period (corresponding to red lines) for each semester is also indicated.

Unfortunately, the analysis has been limited to the years 2018 and 2019, because due to COVID-19 from March 2020 the use of the facility has changed as Fig. 4 shows, although the photovoltaic modules have been generating (Fig. 5).

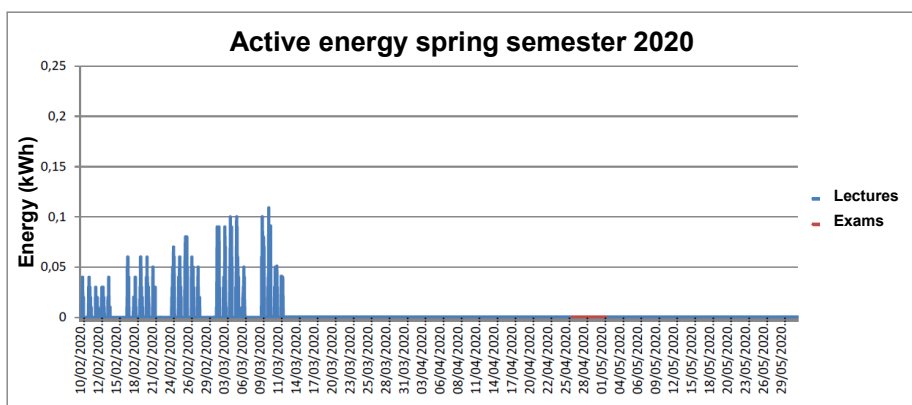


Fig. 4. Active energy consumption during spring semester 2020

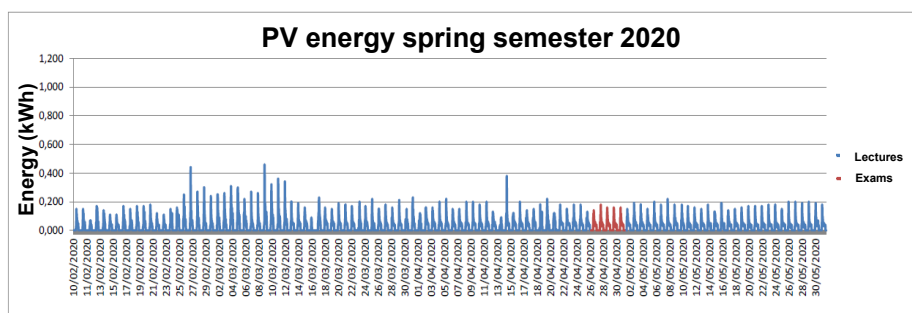


Fig. 5. Photovoltaic generation during spring semester 2020

As the aim of the off-grid photovoltaic installation is to provide electricity to a study room, active energy demand is presented first. Afterward, the energy generated by photovoltaic modules is also displayed. Finally, as the battery system is used for balancing demand and consumption, the evolution of its SOC is shown.

### 3.1 Energy demand

Active energy demands for the spring and fall semesters of 2018 and 2019 are presented in Fig. 6, Fig. 7, Fig. 8, Fig. 9, respectively. These figures show that when the week of mid-term exams (corresponding to red lines) approaches, demand increases confirming that students increase the use of the study room. After this examination period, the demand decreases a bit, but when the final of the semester is close, demand raises again due to the effect of final exams at the end of each semester.

The days without active demand correspond to weekends and public holidays (for example, Easter in the spring semester) when the library is usually closed as its opening timetable is during weekdays. However, the figures show active demand during the previous weekend to the week of mid-term exams because the library is open for students.

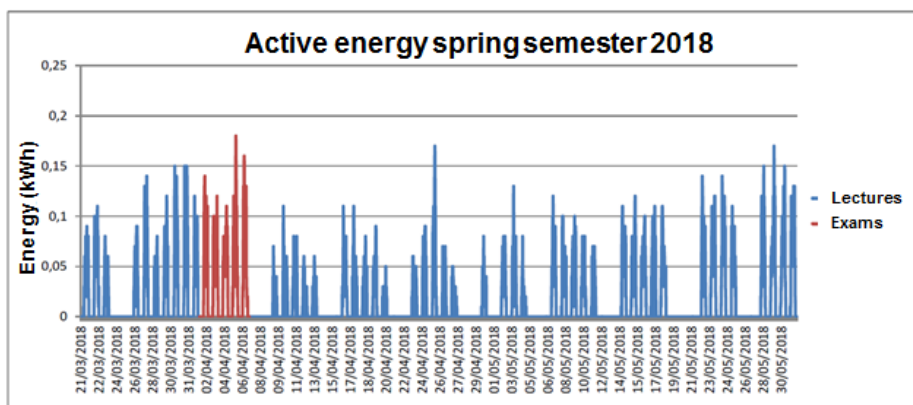


Fig. 6. Active energy consumption during spring semester 2018

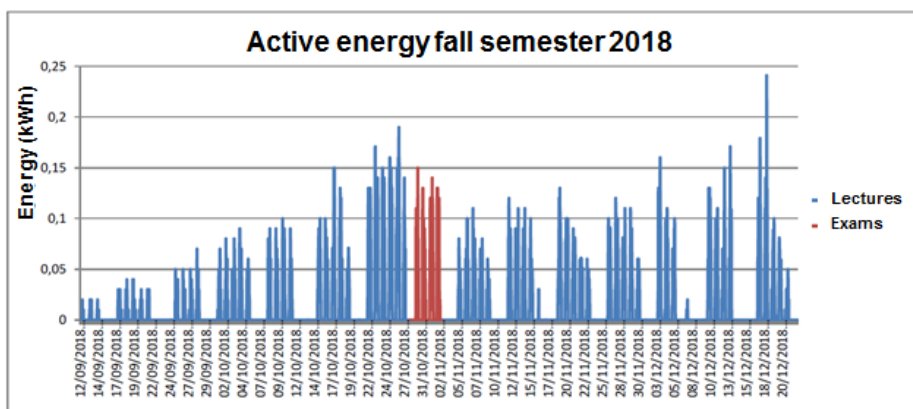


Fig. 7. Active energy consumption during fall semester 2018

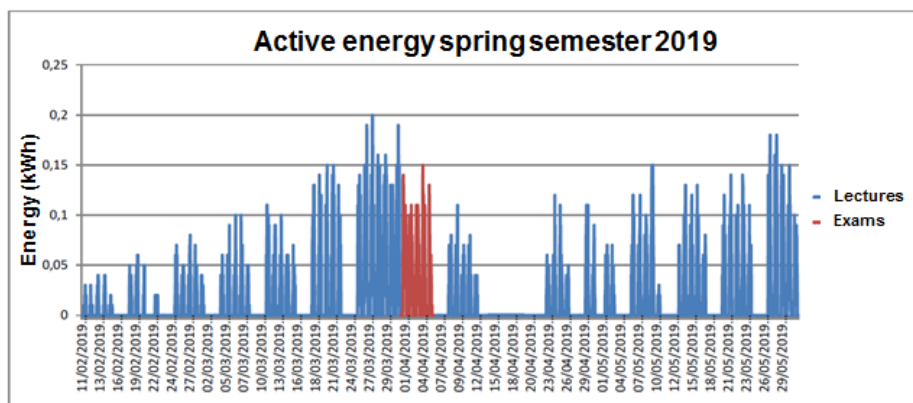


Fig. 8. Active energy consumption during spring semester 2019

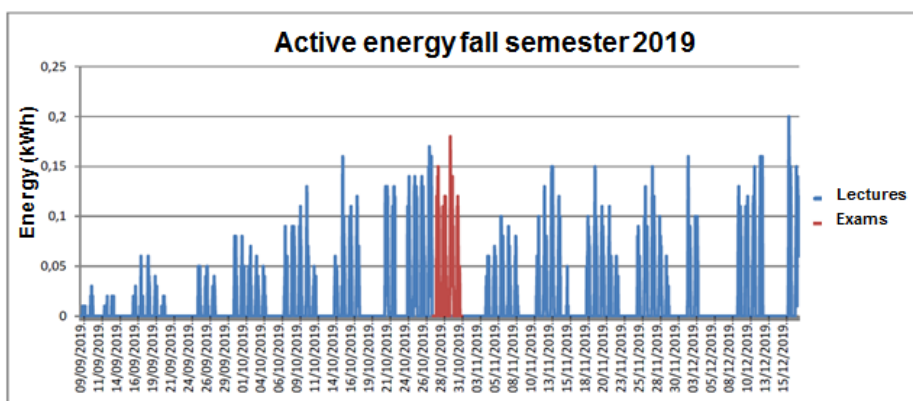


Fig. 9. Active energy consumption during fall semester 2019

To confirm the previous conclusion on the evolution of the active demand concerning the academic calendar, an analysis of the daily curves has been performed. Such analysis consists of obtaining the hourly average demand of the days for the following type of weeks:

- Weeks with just lectures, except the weeks before and after mid-term exams weeks (Fig. 10): the active demand is low because the examination period is far and the use of that room is few. It is also possible to identify the opening hours of the library, from 8:00 to 20:00 h.
- Week previous to the week of mid-term exams (Fig. 11): corresponds to the week with higher demand during the semester. The hourly active demand is around three times the demand of days from weeks with just lectures for the different hours. Moreover, the opening hours of the library are extended from 8:00 to 22:00 h.
- Week of mid-term exams (Fig. 12): the daily demand during this week is high, but not as much as it is in the previous week. However, the behavior of the demand

differs from the week previous to mid-term exams. Both afternoon and evening hours present higher demand than morning hours, opposed to the week previous to mid-term exams. Regarding opening hours, the schedule is the same as the week previous to the examination period.

- Week after the week of mid-term exams (Fig. 13): the demand decreases to around half of the week previous to mid-term exams keeping the maximum hourly demand during mornings. The opening hours of the library return to the usual schedule from 8:00 to 20:00 h.

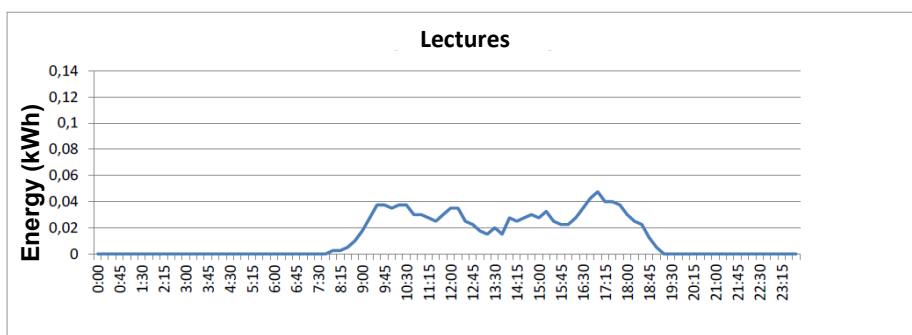


Fig. 10. Average energy demand for days of lectures time

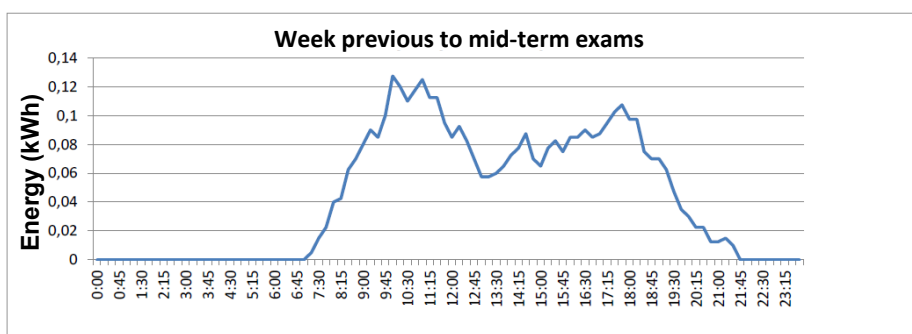


Fig. 11. Average energy demand for days of the week previous to mid-term exams

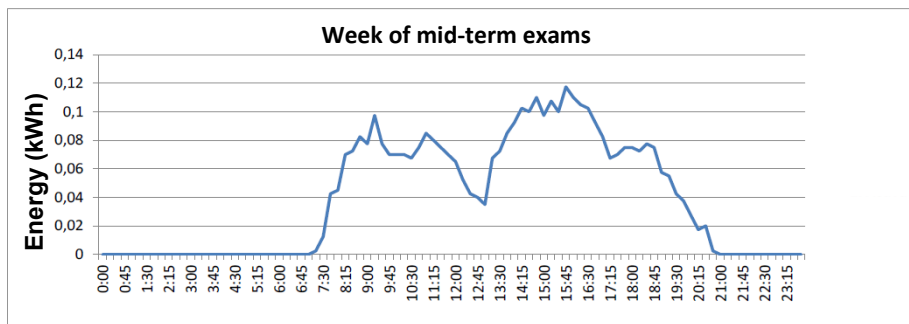


Fig. 12. Average energy demand for days of the week of mid-term exams

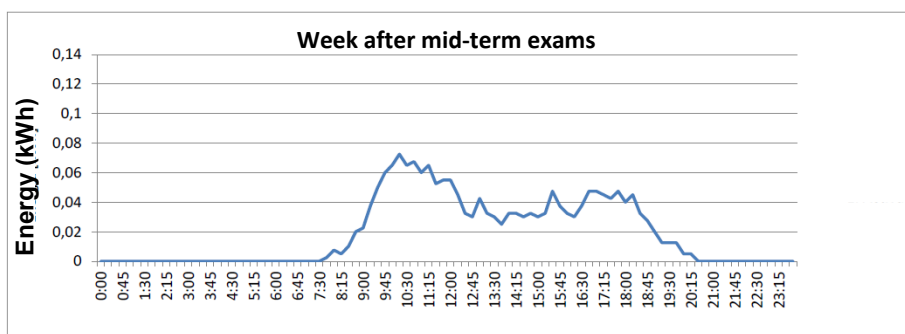


Fig. 13. Average energy demand for days of the week after mid-term exams

### 3.2 Photovoltaic generation

Energy generated by photovoltaic modules for spring and fall semesters of 2018 and 2019 is presented in Fig. 14, Fig. 15, Fig. 16, Fig. 17, respectively. As the system is isolated, the inclination of the photovoltaic modules was set according to the worse situation, that is, winter-time. This effect can be seen in the figures. Energy generation for the fall semester is higher at its end, which corresponds to December; and for the spring semester is higher at the beginning, which corresponds to February.

As an isolated system with storage, the behavior of the demand also influences the energy generated. From the previous section, it has been observed that the demand increases during the week previous to mid-term exams, during such examination week, and the week after. This provokes that more energy from the off-grid system is required, and therefore, more energy is converted by the hybrid PV-inverter from its DC input to the AC output. This can be seen in Fig. 14 to Fig 17.

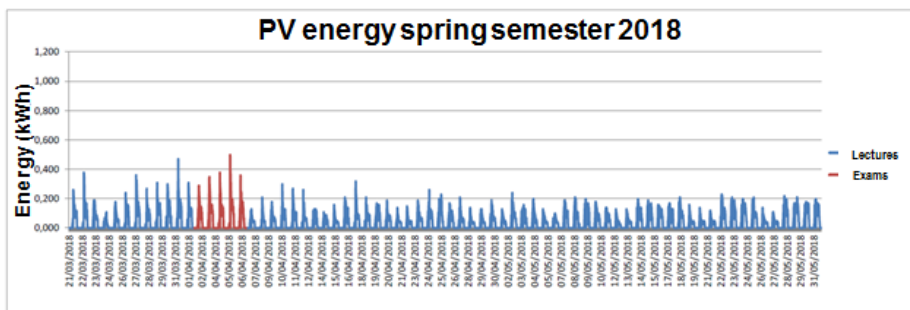


Fig. 14. Photovoltaic generation during spring semester 2018

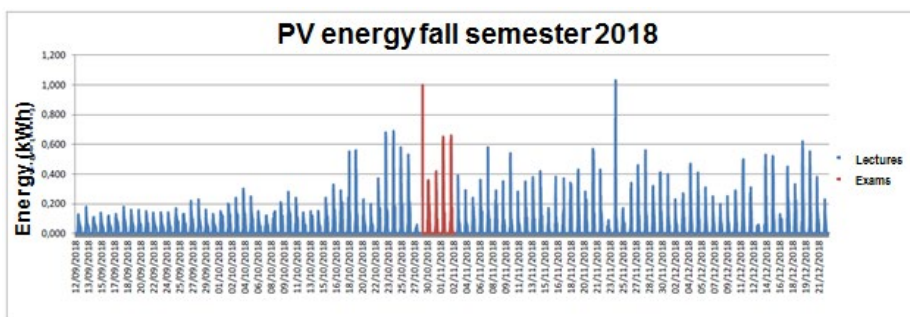


Fig. 15. Photovoltaic generation during fall semester 2018

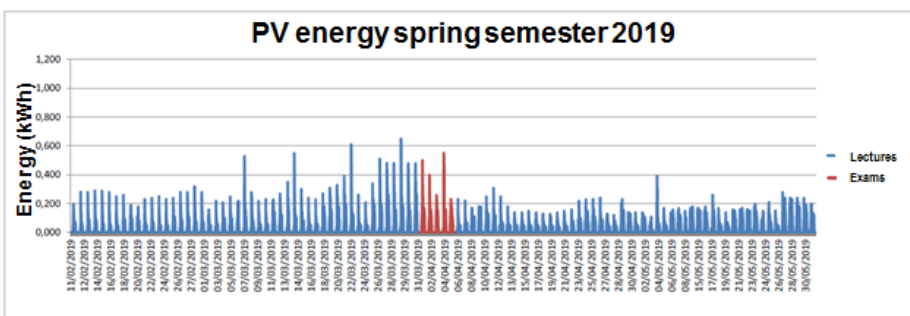


Fig. 16. Photovoltaic generation during spring semester 2019

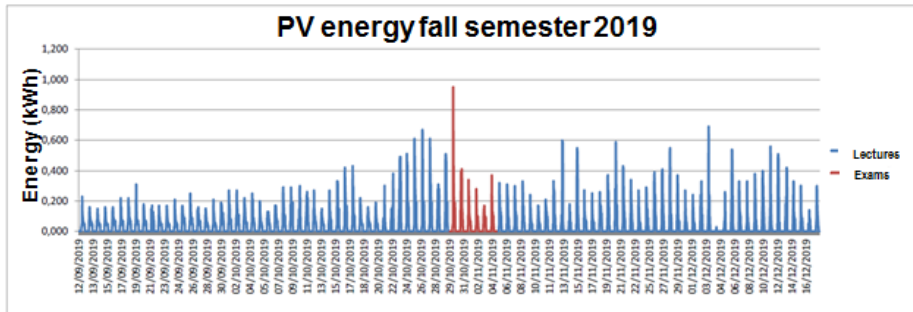


Fig. 17. Photovoltaic generation during fall semester 2019

### 3.3 Battery system

The battery system was sized considering one day of self-sufficiency, and the whole system was configured limiting to 40% SOC the availability of power supply from the off-grid installation. As Fig. 18 shows SOC usually evolves between 60% and 100%. However, at some moments 40% of SOC was achieved, and then, there was no power in the plugs. These situations were caused due to cloudy weather for several days, avoiding that the battery system recovered its SOC. This has happened six times during 2018 and 2019. Once cloudy weather disappeared, the battery system recovered its usual behavior, as Fig. 19 presents.

Fig. 18 and Fig. 19 show a repetitive charge-discharge cycle of the battery system. The reason for this is that batteries are charged when solar resource exceeds existing demand. If the solar resource is scarce for covering the demand, battery system supplies such a lack of energy. Moreover, monitoring devices are connected to the hybrid PV-inverter AC output, and then, they also consume from the off-grid system.

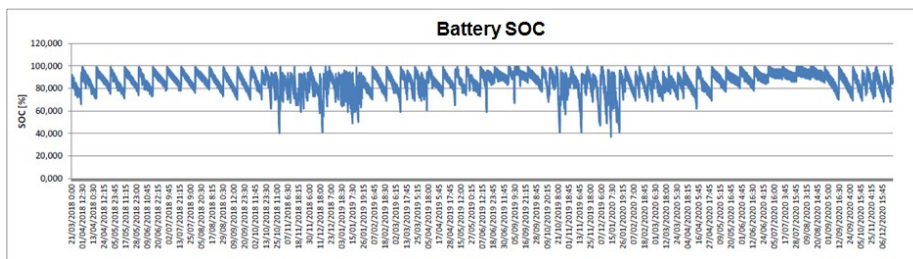


Fig. 18. Evolution of battery SOC

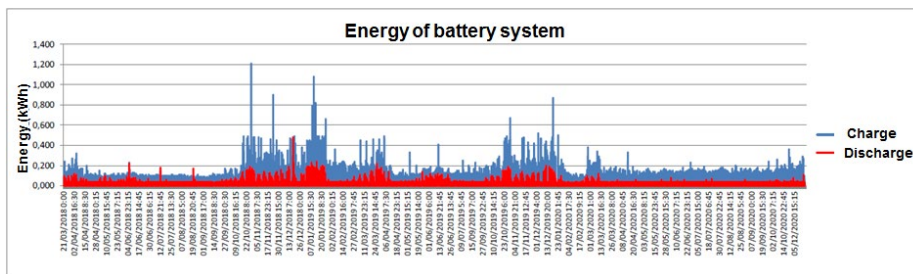


Fig. 19. Evolution of energy charged/discharged from the battery system

#### 4 Conclusions

Off-grid photovoltaic systems facilitate access to electricity in developing countries, rural areas, or isolated facilities. Nevertheless, it can be considered as an alternative for satisfying demand in existing buildings already connected to the grid.

This paper has presented the case of an off-grid photovoltaic system that supplies a room of the library at the ETSEIB, as an alternative solution to traditional upgrades of existing installations in buildings connected to the grid. It shows the dependency of such off-grid systems on the behavior of the demand and the SOC of the battery system due to the demand being highly correlated with the academic calendar. This has to be taken into account in further works as forecasting demand to inform the users of the room about the energy available.

#### Acknowledgments

The authors would like to thank the personnel from the *Maintenance* Area of the Escola Tècnica Superior d’Enginyeria Industrial de Barcelona (ETSEIB) and the *Infraestructure* Area of Universitat Politècnica de Catalunya (UPC) for funding and deploying this installation, and the company *Circuitor* for donating the hybrid PV-inverter. Moreover, the authors would also like to thank our colleagues from the *Centre d’Innovació Tecnològica en Convertidors Estàtics i Accionaments* (CITCEA) de la UPC and students from the ETSEIB that have participated in the deployment and analysis of this installation.

#### References

1. Mandelli, S., Barbieri, J., Mereu, R., Colombo, E.: Off-grid systems for rural electrification in developing countries: Definitions, classification and a comprehensive literature review. *Renewable and Sustainable Energy Reviews* 58 (2016), pp. 1621-1646, ISSN: 1364-0321. DOI: <https://doi.org/10.1016/j.rser.2015.12.338>.

2. Feron, S.: Sustainability of Off-Grid Photovoltaic Systems for Rural Electrification in Developing Countries: A Review. *Sustainability*. 8, 1326 (2016). DOI: <https://doi.org/10.3390/su8121326>.
3. Aris, A., Shabani, B.: Sustainable Power Supply Solutions for Off-Grid Base Stations. *Energies* 8 (2015), pp.10904-10941. DOI: <https://doi.org/10.3390/en81010904>.
4. Aliyu, M., et al.: A review of solar-powered water pumping systems. *Renewable and Sustainable Energy Reviews* 87 (2018), pp. 61-76, ISSN: 1364-0321. DOI: <https://doi.org/10.1016/j.rser.2018.02.010>.
5. UPC Energia Homepage, <https://www.upc.edu/energia2020/ca/renovables>, last accessed 2021/09/14.
6. Circutor CirPower homepage, <http://circutor.es/en/products/renewable-energies/self-consumption-with-storage/cirpower-detail#documentation>, last accessed 2021/09/14.
7. Pastor Torrens, MH.: Instal·lació solar fotovoltaica per a l'alimentació d'ordinadors portàtils i de telèfons mòbils dels usuaris d'una biblioteca. TFG (2016). URL: <https://upcommons.upc.edu/handle/2117/96860>.
8. Sanchez Massaneda, P.: Avaluació del funcionament d'un sistema fotovoltaic aïllat a l'ETSEIB. TFG (2019). URL: <http://hdl.handle.net/2117/128787>.
9. Morera Tonijuan, B.: Visualització sistema de generació fotovoltaic aïllat. TFG (2018). URL: <https://upcommons.upc.edu/handle/2117/118156>.
10. Alcázar Mateos, E.: Estudi del funcionament del sistema fotovoltaic aïllat a l'ETSEIB. TFG (2021). URL: <https://upcommons.upc.edu/handle/2117/339756>.

## Ahorro de Energía: Acoplamiento directo de sistemas de absorción para enfriamiento y calentamiento

V. Cano, J. A. Hernández, A. Huicochea

Centro de Investigación en Ingeniería y Ciencias Aplicadas (CIICAp), Universidad Autónoma de Estado de Morelos, Av. Universidad No. 1001, Col. Chamilpa, C. P. 62209, Cuernavaca, Morelos, México.

dlnacs@springer.com

**Resumen.** El uso eficiente de la energía reduce la huella del humano al medio ambiente, por lo cual los estudios de energía y exergía deben ser imperativos. Una alternativa es el acoplamiento directo de dos ciclos termodinámicos compartiendo procesos y la fuente de energía de activación. En este trabajo se presenta un análisis teórico de la integración de dos sistemas de absorción para calentamiento y enfriamiento usando  $LiBr-H_2O$ , y temperaturas de calentamiento en el generador desde 338.15 a 363.15K. Los procesos de desorción y condensación se llevan a cabo a las mismas condiciones para ambos sistemas térmicos en donde el refrigerante se divide a los evaporadores de alta y baja presión. El objetivo del estudio es determinar las mejores condiciones de operación para maximizar los rendimientos de operación de energía y exergía. Los resultados muestran que es posible alcanzar rendimientos de operación de energía en el sistema de calentamiento y enfriamiento de hasta 0.31 y 0.50 respectivamente, manteniendo una temperatura de activación a 363.15K, mientras, los rendimientos de operación de exergía en el sistema de calentamiento y enfriamiento son de 0.19 y 0.16 respectivamente. La presencia de irreversibilidades en el absorbedor y generador del sistema de calentamiento limita significativamente la eficiencia de exergía. Se ha demostrado que es posible llevar a cabo el acoplamiento, obteniendo los rendimientos de energía y exergía inferiores a los reportados para los sistemas de calentamiento y enfriamiento en forma individual debido a las condiciones de operación limitantes. Sin embargo, el rendimiento de energía global alcanza valores de hasta 1.31.

**Palabras clave:** Acoplamiento de sistemas de energía, ahorro de energía, rendimiento de energía y exergía, sistema enfriamiento y calentamiento, irreversibilidad

### 1. Introducción

En los últimos años, grandes cantidades de calor generadas por parte de diferentes sectores han sido rechazadas a la atmósfera como calor residual, generando un desperdicio de energía e incrementando la temperatura ambiental. A nivel mundial, la mayor cantidad de calor residual mundial proviene de la generación de electricidad con un 61%, sector de transporte con 18%, sector residencial e industrial cercano al 7%. El 63% del calor residual se disipa a temperaturas por debajo de los 373.15K como gases residuales y efluentes [1]. El aprovechamiento de la energía de desecho puede darse con los sistemas térmicos como bombas de calor por absorción para calentamiento y enfriamiento a través de un ciclo termodinámico y una solución de trabajo.

Para los sistemas de calentamiento, una cantidad de energía residual con niveles térmicos de 333.15 a 353.15K puede ser revalorizada a un nivel térmico hasta de 383.15K mediante un Transformador de Calor por Absorción (TCA). Mientras que, para los sistemas de enfriamiento, la conservación de alimentos y el acondicionamiento de espacios donde se requiera una temperatura por debajo de la temperatura ambiente puede ser alcanzarse con una Bomba de Calor por Absorción Convencional (BCAC).

### **1.1 Estudios de Transformadores Calor por Absorción**

Colorado et al. [2] realizaron el análisis de exergía en un TCA acoplado a un sistema purificación de agua de evaporación de simple efecto. El calor latente del sistema de purificación de agua se reusó: a) en la solución de trabajo fuerte que va al absorbedor, b) en el vapor del refrigerante entre el evaporador y el absorbedor, y c) para precalentar el refrigerante entre el evaporador y condensador. La irreversibilidad más alta se obtuvo en el generador y absorbedor para todas las configuraciones. El primer arreglo presentó los mejores resultados, alcanzando una eficiencia exergética en el generador de hasta 0.53. Hernández et al. [3] llevaron a cabo una comparación de un TCA simple y de doble absorción con un transformador de calor por resorción de una etapa (TCR) y dos etapas (TCDR), los cuales funcionan con la mezcla de nitrato de amoníaco y litio ( $NH_3-LiNO_3$ ). El ciclo TCR aumentó la temperatura del calor suministrado entre 303.15 y 323.15K con un coeficiente de operación de energía hasta 0.51, mientras tanto, en el ciclo TCDR la temperatura se incrementó hasta 333.13K con un coeficiente de operación de energía más bajo. Se demostró que la mezcla de trabajo  $LiBr-H_2O$  puede lograr mejores coeficientes de operación de energía e incremento bruto de temperatura, pero tiene problemas de corrosión y cristalización a altas temperaturas de funcionamiento. Heredia et al. [4] estudiaron teóricamente el ahorro de energía en un TCA usando de tubos calóricos entre el evaporador y el condensador. Este estudio demostró que se requieren siete tubos de calor comerciales para condensar 0.714kW y reutilizar 0.177kW a 333.15K en el evaporador, Por lo tanto, el rendimiento de operación del TCA se puede mejorar hasta en un 20%. Merkel et al. [5] realizaron un estudio experimental de un TCA usando como fluido de agua/líquido iónico (metanosulfonato de 1-etil-3-metilimidazolio). El rendimiento de operación de energía experimental más alto fue de 0.43 y un aumento de temperatura de 18.5K con un flujo de calor de 5.5kW en el absorbedor. El aumento de temperatura más alto fue de 47K con un rendimiento de operación de energía de 0.27 con un flujo de calor en el absorbedor de 1.7kW. Gao et al. [6] analizaron el acoplamiento térmico entre los sub-ciclos de compresión y absorción. El máximo rendimiento de operación de energía fue de 2.15, mientras tanto, un prototipo experimental fue establecido para la validación del rendimiento de operación de energía, donde el calor residual mejoró de 320.15-324.15K a 372.15– 375.15K con un coeficiente de operación de energía global de 1.81. Fangtiang et al. [7] propone un sistema de calefacción urbana basado en bombas de calor por compresión y un TCA con una capacidad de 152MW. Los resultados muestra que el coeficiente de rendimiento, la eficiencia energética anual del producto y el costo de calefacción del sistema propuesto resultó ser de 24.5, 61.4% y 55,62 ¥ / GJ respectivamente. Esto indica que a diferencia del sistema hidrotermal convencional, el coeficiente de rendimiento y la eficiencia energética anual del producto propuesto se pueden mejorar aproximadamente 4.34 y 7.4%

respectivamente. Kim et al. [8] realizaron un estudio experimental para analizar el coeficiente de transferencia de calor de tres tipos de absorbedores de diferente material de construcción (Cu, Cu-Ni, Cu-Ni floral), operando como película descendente dentro de un TCA. Los coeficientes globales de transferencia de calor del tubo de Cu, el Cu-Ni y el Cu-Ni floral fueron 1484, 1448 y 1299  $W/m^2K$  respectivamente.

### ***1.2 Estudios de Bombas de Calor por Absorción Convencional***

Soto et al. [9] evaluaron experimentalmente un sistema BCAC enfriado por aire usando amoníaco-nitrato de litio. El BCAC fue activado con temperaturas de generación entre 353.15 y 373K, y temperaturas de condensación de 293.15 a 305K. Las potencias de enfriamiento externas alcanzaron valores de hasta 3.4kW con un rendimiento de operación de energía de hasta 0.33 usando temperaturas de enfriamiento cercanas a 275.7K. Gogoi et al. [10] realizaron un estudio de exergía en un Ciclo Rankine Orgánico (OCR) accionado por energía solar y acoplado a una BCAC. El sistema BCAC alcanzó una temperatura de evaporación de 278.15K manteniendo las temperaturas de condensación y absorción constantes de 304.15K. A partir del análisis de exergía, se encontró que la máxima irreversibilidad ocurrió en el colector parabólico, seguido del ciclo OCR y del BCAC. Liu et al. [11] compararon el rendimiento de operación de energía de dos sistemas híbridos de absorción - compresión utilizando R1234yf/[HMIM][TfO], R1234yf/[HMIM][PF6] y R1234yf/[HMIM][BF4]. Ambos sistemas mejoraron su rendimiento de operación de energía para enfriamiento. El primero tuvo un hasta 1.68 reduciendo la carga térmica del condensador hasta un 18%. Jahin et al. [12] presentaron una estructura novedosa del sistema de refrigeración integrado de absorción-compresión de vapor transcrito (TVCAIRS). La integración del sistema de refrigeración por absorción de vapor (VARS) al sistema de refrigeración por compresión de vapor transcrito (TVCRS), proporciona un subenfriamiento de 278.15K en la configuración propuesta. Por lo tanto, el rendimiento de operación de energía y exergía del TVCAIRS fue de 28.6 y 26.9% respectivamente, la cual es más alta que el sistema TVCRS. Matjanov [13] realizaron un estudio para mejorar la eficiencia de una turbina de gas mediante un BCAC, usada para impulsar el proceso de enfriamiento. El enfriador de absorción utiliza tres tipos de fuente de calor: gases residuales de turbinas de gas, gases residuales del generador (HRSG), y energía solar. Los resultados obtenidos muestran que el uso de los gases residuales de la turbina de gas no podrían ser rentable desde el punto de vista económico debido a que la eficiencia se reduce del 81.4 al 74.4%. Sin embargo, el campo solar puede resultar económicamente rentable cuando los gases residuales HRSG no tienen suficiente calor, es decir, la temperatura es inferior a 393.15K. Boman et al. [14] estudiaron el rendimiento de un BCAC para purificar agua mediante humidificación-deshumidificación. Este ciclo supera los rendimientos de operación de energía dados por un sistema de ósmosis directa hasta en un 19% y destilación por membrana por un 12%.

### ***1.3 Estudios de acoplamientos de BCAC y TCA.***

Colorado et al. [15] compararon el rendimiento de operación de energía y exergía de un sistema de refrigeración por compresión de vapor convencional (VCR), un sistema

de absorción de un solo efecto (CASS) y sistema de absorción de doble efecto (CADS). El rendimiento de operación de energía en CADS fue mayor que el CASS, ya que aumentó de 0.58 a 0.91. La irreversibilidad total del ciclo que opera con  $R134a/LiBr-H_2O$  fue de 17% menos con respecto a  $CO_2/LiBr-H_2O$ . Eisavi et al. [16] estudiaron el acoplamiento de un CADS a un OCR accionado por energía solar para generar electricidad, calor y potencia. Con la misma cantidad de calor de entrada, el sistema CADS incrementó la potencia de refrigeración hasta 48.5% que un CASS. Al mismo tiempo, la potencia de calefacción mejoró un 20.5%, por lo cual el rendimiento de operación de energía incrementó hasta un 96%, mientras que la producción neta de energía eléctrica se redujo en un 27%. Mahalle et al. [17] analizaron el acoplamiento de un sistema VCR a un CADS para evaluar el rendimiento de operación global de energía y exergía. El primero mejoró hasta 2.4 con una temperatura enfriamiento de 271.15K, mientras tanto, el segundo alcanzó valores máximos de 0.88. Sin embargo, la instalación del sistema es aproximadamente 1.8-2 veces más grande en tamaño físico. Agarwal et al. [18] examinaron teóricamente un sistema de refrigeración en cascada de absorción-compresión (ACCRS) para evaluar los rendimientos de energía y exergía, así como el consumo de energía eléctrica. Demostraron que el ahorro de electricidad del sistema ACCRS fue de 45.8% en comparación con el ciclo de VCR, además, se tuvo un aumento del 85.3 y 85.8% en el coeficiente de operación de energía y exergía respectivamente. Acevedo et al. [19] estudiaron el acoplamiento de un TCA con  $LiBr-H_2O$  y un VCR usando R123. El calor recuperado por el VCR representó un ahorro de energía para el TCA entre 49.7 y 50.6%. El rendimiento de operación de energía y exergía para el sistema de calentamiento variaron de 0.40 a 0.48, y 0.37 a 0.35 respectivamente, mientras que para el sistema de enfriamiento de 0.85 a 0.69, y 0.16 a 0.12. Alcanzando un coeficiente de operación de energía global de hasta 0.93. Zhang et al. [20] experimentaron un sistema de cogeneración (de un ciclo orgánico Rankin y una BCAC) para recuperar el calor residual condensado del vapor de escape de una central eléctrica de carbón de 600MW. Se utilizó una turbina con refrigeración directa por aire para mejorar la utilización de la energía en la central eléctrica. La potencia generada aumento hasta 16.2 MW, así como la carga de calefacción hasta 78541.16 kW. La tasa de consumo de carbón estándar y la pérdida total de exergía disminuyeron en 48.98 g/kWh y 62.21 MW respectivamente. Mientras que la eficiencia energética y exergética mejoraron en 11.97 y 4.01% respectivamente.

Basado en la revisión bibliográfica indicada arriba, existen diversos trabajos reportados sobre sistemas de enfriamiento y calentamiento por absorción, los cuales se han estudiado en forma individual. También, existen estudios de acoplamientos de sistemas térmicos donde la energía residual de uno ha sido usada en forma indirecta para activar el otro. Sabiendo que los sistemas de absorción para enfriamiento y calentamiento usan el ciclo de Carnot (directo e inverso) para reducir y aumentar la temperatura con respecto al nivel térmico que posee el calor residual, y que poseen los mismos procesos físicos a diferentes temperaturas y presiones, se propone acoplar en forma directa ambos ciclos termodinámicos para alcanzar rendimientos de operación global de energía y exergía superiores a los individuales. Las temperaturas de activación variaron entre 338.15 a 363.15K para cuantificar los rendimientos de operación en forma individual e integral.

## 2. Descripción del sistema

La **figura 1** muestra el diagrama esquemático del acoplamiento de un TCA y BCAC usando tres niveles de presión y cuatro niveles de temperatura. En la sección de calentamiento, el evaporador y el absorbedor operan a una presión alta, los procesos de evaporación y absorción en la sección de enfriamiento se desarrollan a una presión baja, y los procesos de desorción y condensación se llevan a cabo a una presión intermedia para ambos sistemas térmicos.

### 2.1 Sistema de enfriamiento

Para la sección de enfriamiento, se suministra calor al generador ( $\dot{Q}_{gen}$ ) para evaporar una parte del refrigerante de la solución de trabajo y tener una solución concentrada, la cual va al absorbedor. El refrigerante en fase vapor llega al condensador para liberar calor ( $\dot{Q}_{con}$ ), y tener un refrigerante en fase líquida. El fluido de trabajo recibe una cantidad de calor ( $\dot{Q}_{eva,enf}$ ) a una temperatura en el evaporador para cambiar a vapor el refrigerante, el cual es absorbido en la solución de trabajo concentrada en el absorbedor, generando una reacción exotérmica ( $\dot{Q}_{abs,enf}$ ) y una disminución en la concentración de la solución de trabajo, la cual llega al generador para nuevamente repetir el ciclo.

### 2.2 Sistema de calentamiento

El principio de funcionamiento es similar al sistema de enfriamiento. En el condensador se tienen dos salidas de refrigerante, una de ellas suministra líquido condensado al evaporador a alta presión para obtener vapor saturado mediante un suministro de calor de desecho ( $\dot{Q}_{eva,cal}$ ). El vapor resultante ingresa en el absorbedor para ser absorbido en la solución de trabajo concentrada, produciéndose una reacción exotérmica, y como consecuencia un calor útil ( $\dot{Q}_{abs,cal}$ ) a una temperatura alta. La solución de trabajo diluida resultante va al generador para iniciar el proceso nuevamente.

## 3. Modelo matemático

El análisis de energía está basado en la primera ley de la termodinámica para estudiar las relaciones entre las diversas formas de interacción de energía (calor y trabajo). Para el acoplamiento de los sistemas de enfriamiento y calentamiento se utiliza la ecuación general para un sistema abierto como se indica en la ecuación 1, despreciando la energía cinética y potencial por ser mínimas:

$$\sum_E \left( h + \frac{v^2}{2} + zg \right) \dot{m}_E - \sum_S \left( h + \frac{v^2}{2} + zg \right) \dot{m}_S + \sum \dot{Q} + \sum \dot{W} = 0 \quad (1)$$

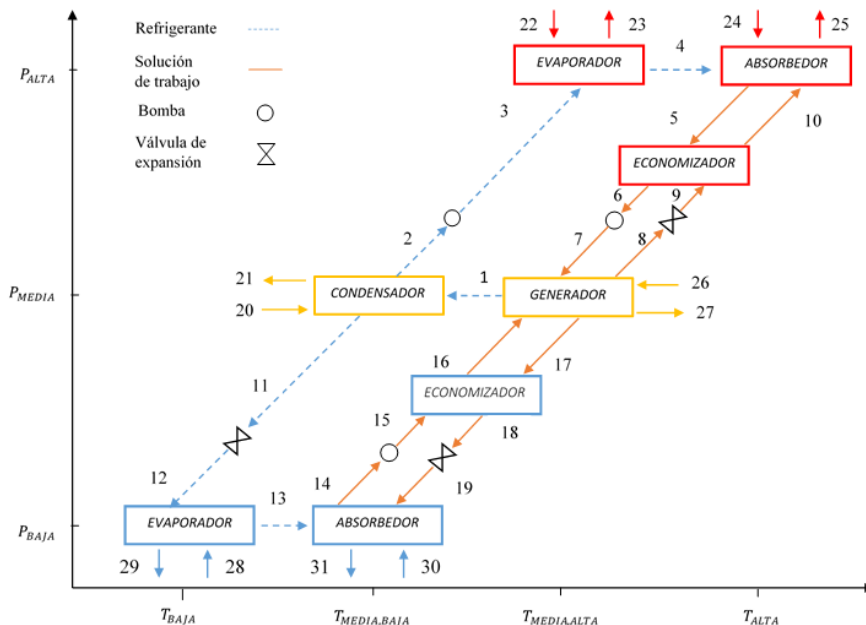


**Fig. 1.** Diagrama del acoplamiento entre el sistema de enfriamiento y calentamiento.

El flujo másico que entra y sale del sistema funciona como un mecanismo adicional de transferencia de energía. El principio de conservación de la masa para un intercambiador de calor que opera de forma estacionaria requiere que la suma de los flujos másicos de entrada sea igual a la suma de los flujos másicos que salen. Por lo tanto, el balance de masa para el sistema abierto se muestra en la ecuación 2.

$$\sum \dot{m}_E = \sum \dot{m}_S \tag{2}$$

Por otro lado, el balance de especies involucra el flujo másico y concentración de la solución para cada línea de entrada y salida donde se tenga una solución de trabajo, como se presenta en la ecuación 3:

$$\sum \dot{m}_E X_E = \sum \dot{m}_S X_S \tag{3}$$

La degradación de la energía durante un proceso se estudia a través de la segunda ley de la termodinámica para determinar el máximo trabajo cuando se alcanza el estado muerto. Un flujo de exergía se determina con referencia al medio ambiente, el cual no tiene cambios de temperatura y presión considerables con respecto al tiempo. Para este estudio, solo se considera la exergía física, donde el flujo de exergía para cada línea de entrada o salida se da en la ecuación 4.

$$\dot{E}x = \dot{m}[(h - h_0) - T_0(s - s_0)] \tag{4}$$

La irreversibilidad es equivalente a la exergía destruida y es el potencial de trabajo desperdiciado, el cual se determina a partir de la ecuación 5:

$$i = \sum \left(1 - \frac{T_0}{T_i}\right) \dot{Q}_j + (\sum \dot{E}x_i)_E - (\sum \dot{E}x_i)_S - \dot{W} \quad (5)$$

Para los balances energía y exergía de cada intercambiador de calor se toman en cuenta las entradas y salidas correspondientes a la **figura 1**:

**Componentes de presión baja:**

**Absorbedor**

$$\dot{m}_{13} + \dot{m}_{19} = \dot{m}_{14} \quad (6)$$

$$\dot{m}_{19} * X_{19} = \dot{m}_{14} * X_{14} \quad (7)$$

$$\dot{Q}_{abs,enf} = \dot{m}_{14}h_{14} - \dot{m}_{13}h_{13} - \dot{m}_{19}h_{19} \quad (8)$$

$$\dot{I}_{abs,enf} = \dot{E}x_{30} + \dot{E}x_{13} + \dot{E}x_{19} - \dot{E}x_{14} - \dot{E}x_{31} \quad (9)$$

**Evaporador**

$$\dot{m}_{12} = \dot{m}_{13} \quad (10)$$

$$\dot{Q}_{eva,enf} = \dot{m}_{13}(h_{13} - h_{12}) \quad (11)$$

$$\dot{I}_{eva,enf} = \dot{E}x_{12} + \dot{E}x_{28} - \dot{E}x_{13} - \dot{E}x_{29} \quad (12)$$

**Componentes de presión media:**

**Generador:**

$$\dot{m}_7 + \dot{m}_{16} = \dot{m}_1 + \dot{m}_8 + \dot{m}_{17} \quad (13)$$

$$\dot{m}_7X_7 + \dot{m}_{16}X_{16} = \dot{m}_8X_8 + \dot{m}_{17}X_{17} \quad (14)$$

$$\dot{Q}_{gen} = \dot{m}_{17}h_{17} + \dot{m}_1h_1 + \dot{m}_8h_8 - \dot{m}_7h_7 - \dot{m}_{16}h_{16} \quad (15)$$

$$\dot{I}_{gen} = \dot{E}x_7 + \dot{E}x_{16} + \dot{E}x_{26} - \dot{E}x_8 - \dot{E}x_1 - \dot{E}x_{17} - \dot{E}x_{27} \quad (16)$$

**Condensador:**

$$\dot{m}_1 = \dot{m}_2 + \dot{m}_{11} \quad (17)$$

$$\dot{Q}_{con} = \dot{m}_{11}h_{11} + \dot{m}_2h_2 - \dot{m}_1h_1 \quad (18)$$

$$\dot{I}_{con} = \dot{E}x_1 + \dot{E}x_{20} - \dot{E}x_{21} - \dot{E}x_{11} - \dot{E}x_2 \quad (19)$$

**Componentes de presión alta:**

**Absorbedor**

$$\dot{m}_{10} + \dot{m}_4 = \dot{m}_5 \tag{20}$$

$$\dot{m}_{10} * X_{10} = \dot{m}_5 * X_5 \tag{21}$$

$$\dot{Q}_{abs,cal} = \dot{m}_5 h_5 - \dot{m}_4 h_4 - \dot{m}_{10} h_{10} \tag{22}$$

$$\dot{I}_{abs,cal} = \dot{E}x_4 + \dot{E}x_{10} + \dot{E}x_{24} - \dot{E}x_5 - \dot{E}x_{25} \tag{23}$$

**Evaporador**

$$\dot{m}_3 = \dot{m}_4 \tag{24}$$

$$\dot{Q}_{eva,cal} = \dot{m}_4 (h_4 - h_3) \tag{25}$$

$$\dot{I}_{eva,cal} = \dot{E}x_3 + \dot{E}x_{22} - \dot{E}x_{23} - \dot{E}x_4 \tag{26}$$

Los parámetros más importantes para analizar el rendimiento del sistema acoplado utilizando la primera y segunda ley de la termodinámica son el incremento de temperatura bruto (*GTL*), el descenso bruto de temperatura (*GTD*), los rendimientos de operación de energía (*COP*) y exergía (*ECOP*).

El *GTL* representa la revalorización térmica del calor de desecho, y se obtiene con la diferencia entre las temperaturas del absorbedor y evaporador del sistema de calentamiento:

$$GTL = T_{abs,cal} - T_{eva,cal} \tag{27}$$

El *GTD* indica la disminución térmica del calor de desecho, y se representa como el delta de temperaturas entre el generador y el evaporador del sistema de enfriamiento:

$$GTD = T_{gen} - T_{eva,enf} \tag{28}$$

El *COP* para el sistema de calentamiento se define como la energía útil a alta temperatura con respecto a la energía suministrada. Para el sistema de enfriamiento, se relaciona la energía útil a baja temperatura a la energía suministrada:

$$COP_{cal} = \frac{\dot{Q}_{abs,cal}}{\dot{Q}_{eva,cal} + \dot{Q}_{gen} + \dot{W}_{con} + \dot{W}_{gen}} \tag{29}$$

$$COP_{enf} = \frac{\dot{Q}_{eva,enf}}{\dot{Q}_{gen} + \dot{W}_{abs}} \tag{30}$$

El *ECOP* se obtiene a partir de los flujos de exergía del absorbedor de calentamiento y evaporador de enfriamiento con respecto a la exergía suministrada para cada sistema independiente, como se indican:

$$ECOP_{cal} = \frac{(\dot{E}x_{25} - \dot{E}x_{24})}{(\dot{E}x_{26} - \dot{E}x_{27}) + (\dot{E}x_{22} - \dot{E}x_{23})} \tag{31}$$

$$ECOP_{enf} = \frac{(\dot{E}x_{29} - \dot{E}x_{28})}{(\dot{E}x_{26} - \dot{E}x_{27})} \tag{32}$$

Para el rendimiento de operación de energía global ( $COP_{glo}$ ) se considera la cantidad de energía útil a alta y baja temperatura de los sistemas de enfriamiento y calentamiento con respecto al suministro de energía para ambos sistemas:

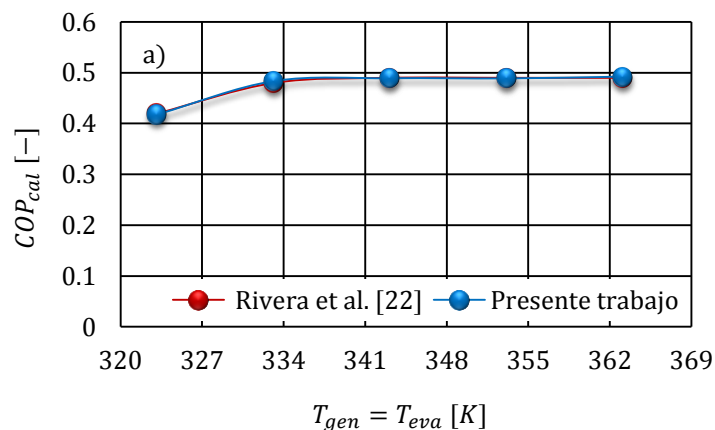
$$COP_{glo} = \frac{\dot{Q}_{abs,cal} + \dot{Q}_{eva,enf}}{\dot{Q}_{eva,cal} + \dot{Q}_{gen} + \dot{W}_{con} + \dot{W}_{gen} + \dot{W}_{abs,enf}} \tag{33}$$

#### 4. Resultados y discusión

El algoritmo usado en el acoplamiento térmico se desarrolla en el lenguaje de programación Engineering Equation Solver (EES), usando las propiedades termodinámicas de la solución de trabajo de  $LiBr-H_2O$  reportados por Patek et al. [21].

##### 4.1 Validación del sistema de calentamiento y enfriamiento

El sistema de calentamiento se valida con los resultados reportados por Rivera et al. [22], considerando una  $T_{con} = 303.15K$ ,  $T_{abs} = 343.15$  a  $393.15K$  y  $T_{gen} = T_{eva} = 323.15K$ . Los máximos errores obtenidos fueron de 0.12 a 0.79% como se aprecia en la **figura 2a**. Para el caso del sistema de enfriamiento, se usaron datos reportados por Kaynakli et al. [23] considerando una  $T_{eva} = 275.15K$  y  $T_{con} = T_{abs} = 303.15K$ . Los resultados obtenidos en este trabajo son similares a los reportados en la literatura con una variación máxima de 0.12% en un intervalo de  $T_{gen} = 336.15$  a  $358.15K$ , como se aprecia en la **figura 2b**.



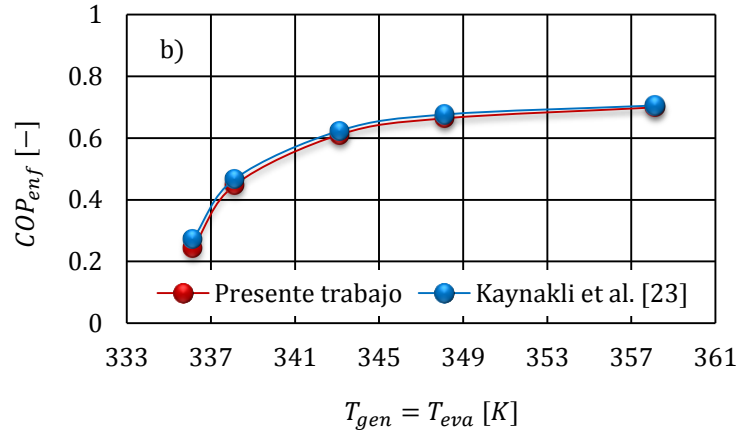


**Fig. 2.** Validación del simulador termodinámico a) sistema de calentamiento y b) sistema de enfriamiento.

La **figura 3** muestra los rendimientos de operación de energía para los sistemas térmicos acoplados usando  $T_{gen} = T_{eva} = 338.15$  a  $363.15K$  y  $T_{con} = 293.15K$ , manteniendo constante  $T_{abs} = 383.15K$  para el sistema de calentamiento, y  $T_{eva} = 283.15K$  para el sistema de enfriamiento. A medida que se incrementa la temperatura de activación se genera mayor vapor sobrecalentado y líquido saturado en el generador y condensador respectivamente para alimentar ambos sistemas térmicos, así como, una solución de trabajo con mayor concentración en la salida del generador, es decir de 0.61 a 0.71. La reacción exotérmica en el absorbedor a alta presión siempre es favorecida por la máxima absorción del refrigerante en la solución de trabajo concentrada, mejorando el  $COP_{cal}$  de 0.28 a 0.30. Sin embargo, el refrigerante líquido que va al sistema de enfriamiento es inferior al 50% que se genera en el proceso de desorción y condensación, por lo que el  $COP_{enf}$  disminuye de 0.50 a 0.46.

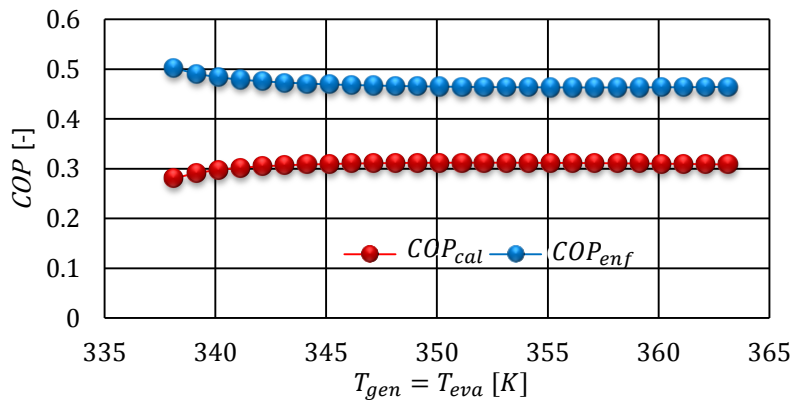


**Fig. 3.**  $COP_{cal}$  y  $COP_{enf}$  considerando diferentes temperaturas de activación de ambos sistemas térmicos.

En la **figura 4** se indica la revalorización y desvalorización de ambos sistemas a varias temperaturas de activación. Se tiene un  $GTL$  mayor a  $40K$  a una temperatura de activación de  $338.15K$  (**figura 4**) debido a que el masa del refrigerante a presión media es de  $3.882 \times 10^{-4}$  kg/s, sin embargo, cuando la temperatura de activación se aumenta, la masa del refrigerante y la concentración se incrementan a  $3.947 \times 10^{-4}$  kg/s limitando el  $GTL$ , y favoreciendo el  $COP_{cal}$  hasta 0.31. Se aprecia en la **figura 4b** que los  $GTD$  son mayores que los  $GTL$  debido a su definición por las ecuaciones 27 y 28. Cuando la temperatura de activación se incrementa el  $GTD$  aumenta de  $55$  a  $70K$ , debido a que el nivel térmico de enfriamiento se mantiene a  $T_{eva,enf} = 283.15K$ , es decir para mantener esta temperatura de refrigeración, se requiere que el absorbedor de baja presión se encuentre a  $T_{abs,enf} = 308.15K$  lo que limita que la concentración de trabajo sea de  $0.52$ , sin embargo un  $GTD$  mayor no representa el mejor rendimiento para el  $COP_{enf}$ , es decir, si se tiene un  $GTD$  de  $70$  podemos alcanzar un  $COP_{enf}$  de  $0.46$ , mientras con un  $GTD$  de  $55$ , se tiene un  $COP_{enf}$  de  $0.50$ .

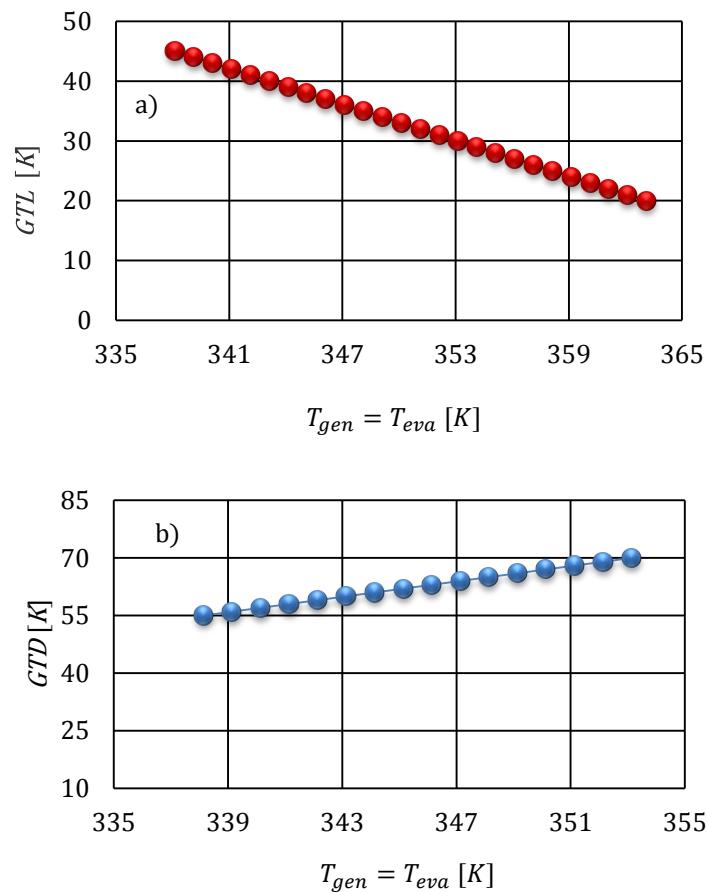


**Fig. 4.** Ascenso y descenso bruto de temperatura en función de la temperatura del generador para el TCA y BCAC.

Analizando los resultados obtenidos por la segunda ley de la termodinámica se muestra en la **figura 5**, el comportamiento de  $ECOP_{enf}$  y  $ECOP_{cal}$  a diferentes temperaturas del generador. Para ambos casos la presencia de alta irreversibilidad juega un rol importante para los  $ECOP$ . Cuando se tiene mayor temperatura de activación a 363.15K, la irreversibilidad general del ciclo acoplado se incrementa en 1.16kW, disminuyendo el  $ECOP_{cal}$  de 0.19 a 0.15, mientras que el  $ECOP_{enf}$  desciende de 0.16 a 0.12.

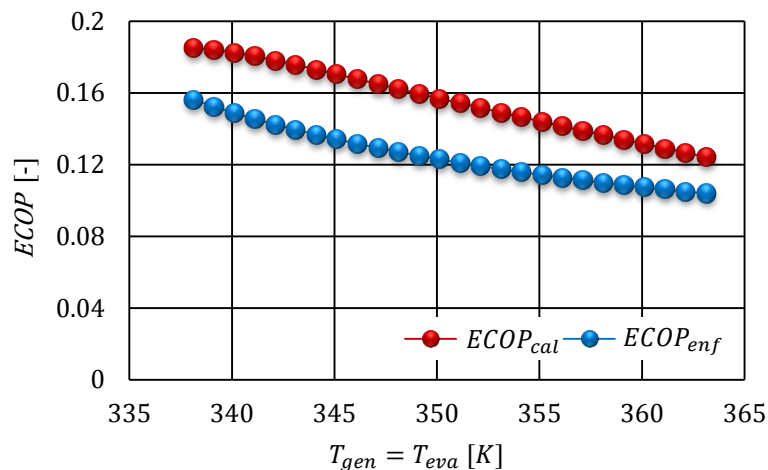


**Fig. 5.**  $ECOP_{cal}$  y  $ECOP_{enf}$  a diferentes temperaturas de activación.

La **figura 6** presenta el  $COP_{glo}$  cuando la  $T_{gen}$  varía de 338.15 a 363.15K y  $T_{con} = 293.15K$  para ambos sistemas térmicos. Es claro que la  $T_{gen}$  juega un rol importante para el proceso de desorción, y como consecuencia para los rendimientos de operación de energía y exergía. Cuando la  $T_{gen} = 338.15K$  es posible alcanzar valores de  $COP_{glo} = 1.28$ , el cual representa un 62.2% mayor que los obtenidos en la suma de ambos sistemas térmicos en forma individual a los mismos parámetros de operación. Tomando en cuenta las condiciones de operación analizadas, el mejor  $COP_{glo} = 1.31$  se alcanza cuando  $T_{gen} = 363.15K$ . A pesar de que los rendimientos de operación de energía individuales son menores en el acoplamiento, a los reportados de manera individual en la literatura (Rivera et al. [22] y Kaynakli et al. [23]) como se indica en la **figura 3**, se tiene un rendimiento de operación de energía global hasta de 1.31, el cual representa el uso de energía más eficiente.

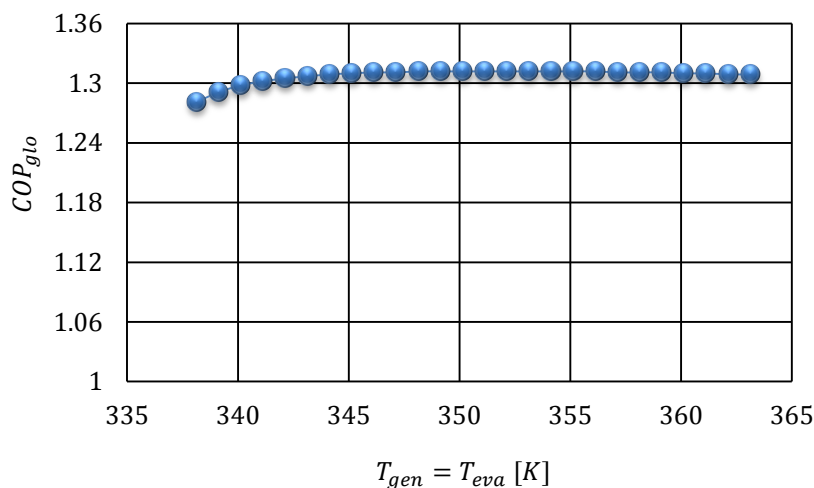


**Fig. 6.**  $COP_{glo}$  a diferentes temperaturas de activación.

## 5. Conclusiones

La recuperación del calor residual a temperatura menor a 373.15K se puede lograr a través de las bombas de calor por absorción para enfriamiento y calefacción. El estudio teórico demuestra la factibilidad de acoplar dos sistemas de absorción (enfriamiento y calentamiento) en forma directa para incrementar el rendimiento de operación de energía global. El análisis cuantitativo y cualitativo del uso energía es mediante la primera y segunda ley de la termodinámica considerando diferentes temperaturas de calentamiento. Los procesos de desorción y condensación son comunes para ambos sistemas térmicos a presión media, mientras que los procesos de evaporación y absorción para el sistema de enfriamiento y calentamiento, es a baja y alta presión respectivamente. Ambos sistemas térmicos son validados con datos reportados en la literatura, donde el sistema de calentamiento refleja un error máximo de 0.79%, y para el sistema de enfriamiento un valor máximo de 0.12%. A pesar de que el rendimiento de operación de energía para ambos sistemas térmicos es bajo en el acoplamiento con respecto los sistemas convencionales reportados en la literatura, el rendimiento de operación de energía global varía de 1.28 a 1.30, lo cual representa hasta un 62.2% mayor que los obtenidos en la suma de ambos sistemas térmicos en forma individual a los mismos parámetros de operación analizados en este artículo. Con respecto a la desvalorización (sistema de enfriamiento) y revalorización (sistema de calentamiento) de calor alcanzados en este estudio son similares a los reportados en la literatura. Alcanzando valores para el primero de hasta 70K, y para el segundo de hasta 45K. Es decir, se tiene mejor rendimiento de operación de energía global con similares niveles térmicos en el evaporador a baja presión y absorbedor a alta presión a los publicados.

## Referencias

1. Forman C., Muritala I, Pardemann R. and Meyer B. Estimating the Global Waste Heat Potential. *Renew Sustain Energy Reviews*; Vol. 57, (2016), pp. 1568–157. <https://doi.org/10.1016/j.rser.2015.12.192>.
2. Colorado D., Demesa N., Huicochea A., Hernández J. A., Irreversibility analysis of the absorption heat transformer coupled to a single effect evaporation process, *Applied Thermal Engineering*, Vol. 92, (2016). pp. 71. <https://doi.org/10.1016/j.aplthermaleng.2015.09.076>.
3. Hernández-Magallanes J. A., Rivera W., Coronas A., Comparison of single and double stage absorption and resorption heat transformers operating with the ammonia-lithium nitrate mixture, *Applied Thermal Engineering*, Vol. 125, (2017) pp. 53-68, <https://doi.org/10.1016/j.aplthermaleng.2017.06.130>.
4. Heredia I., Siqueiros J., Perez J.A., Juarez-Romero D., Gonzalez-Rodriguez, J. Energy saving into an absorption heat transformer by using heat pipes between evaporator and condenser. *Applied Thermal Engineering* (2017). doi.128. [10.1016/j.aplthermaleng.2017.09.017](https://doi.org/10.1016/j.aplthermaleng.2017.09.017).
5. Merkel N., Bucherl M., Zimmermann M., Wagner V., Schaber K. Operation of an absorption heat transformer using water/ionic liquid as working fluid, Vol.131, pp.370 (2018). <http://dx.doi.org/10.1016/j.aplthermaleng.2017.11.147>.
6. Gao J., Xu, Z., Wang, R.Z. Enlarged temperature lift of hybrid compression-absorption heat transformer via deep thermal coupling (2021). *Energy Conversion and Management*. [234, 113954. 10.1016/j.enconman.2021.113954](https://doi.org/10.1016/j.enconman.2021.113954).
7. Fangtian S., Baoru H., Lin Fu., Hongwei Wu., Yonghua X., Haifeng W. New medium-low temperature hydrothermal geothermal district heating system based on distributed electric compression heat pumps and a centralized absorption heat transformer (2021). *Energy*, Elsevier, Vol. 232. doi: [10.1016/j.energy.2021.120974](https://doi.org/10.1016/j.energy.2021.120974).
8. Kim J., Bae K. J., Kim Y. C., Kwon O. K. An experimental study on the heat transfer performance characteristics of horizontal tube falling film absorbers for single-stage absorption heat transformer, *Applied Thermal Engineering*, Vol. 198, (2021), <https://doi.org/10.1016/j.aplthermaleng.2021.117485>.
9. Soto P., Rivera W., Experimental assessment of an air-cooled absorption cooling system, *Applied Thermal Engineering*, Vol 155, pp. 147-156, (2019). <https://doi.org/10.1016/j.aplthermaleng.2019.03.104>.
10. Gogoi T.K., Saikia S., Performance analysis of a solar heat driven organic Rankine cycle and absorption cooling system, *Thermal Science and Engineering Progress*, Vol 13, (2019), <https://doi.org/10.1016/j.tsep.2019.100372>.
11. Liu X., Zheng Y., Lihang B., Maogang H., Performance comparison of two absorption-compression hybrid refrigeration systems using R1234yf/ionic liquid as working pair, *Energy Conversion and Management*, Vol. 181, pp. 319-330,(2019), <https://doi.org/10.1016/j.enconman.2018.12.030>.
12. Jain V., Colorado D. Thermoeconomic and feasibility analysis of novel transcritical vapor compression-absorption integrated refrigeration system, *Energy Conversion and Management*, Vol. 224, (2020), <https://doi.org/10.1016/j.enconman.2020.113344>.
13. Matjanov E., Gas turbine efficiency enhancement using absorption chiller. Case study for Tashkent CHP, *Energy*, Vol. 192, (2020), <https://doi.org/10.1016/j.energy.2019.116625>.
14. Boman D., Garimella S. Performance improvement of a water-purifying absorption cooler through humidification-dehumidification, *Applied Thermal Engineering*, Vol. 185, (2021), <https://doi.org/10.1016/j.aplthermaleng.2020.116327>.

15. Colorado D., Rivera W. Performance comparison between a conventional vapor compression and compression-absorption single-stage and double-stage systems used for refrigeration, *Applied Thermal Engineering*. (2015). [doi:10.1016/j.applthermaleng.2015.05.029](https://doi.org/10.1016/j.applthermaleng.2015.05.029)
16. Eisavi B., Khalilarya s., Chitsaz A., Rosen M. A. Thermodynamic analysis of a novel combined cooling. Heating and power system driven by solar energy, *Applied Thermal Engineering*. (2017). <https://doi.org/10.1016/j.applthermaleng.2017.10.132>
17. Mahalle, K., Parab, P., Bhagwat, S. Optimization of cooling load in the combined vapour absorption–vapour compression refrigeration cycle using exergy analysis. *Indian Chemical Engineer*, vol. 61, pp. 52–66. (2019). <https://doi.org/10.1080/00194506.2017.1418439>
18. Agarwal S., Arora A., Arora B. Energy and exergy analysis of vapor compression–triple effect absorption cascade refrigeration system. *Engineering Science and Technology, an International Journal*. (2019). <https://doi.org/10.1016/j.jestch.2019.08.001>
19. Acevedo A., Hernández J.A., Juárez D., Parrales A., Saravanan R., Huicochea A. Thermodynamic analysis of cooling and heating systems for energy recovery. *International Journal of Refrigeration*. (2020). <https://doi.org/10.1016/j.ijrefrig.2020.02.034>.
20. Zhang H., Zhang H., Liu X., Liu Y., Duan C., Dou Z., Qin, J. Energy and exergy analyses of a novel cogeneration system coupled with absorption heat pump and organic Rankine cycle based on a direct air cooling coal-fired power plant. *Energy*, Vol. 229, (2021).
21. Pátek J., Klomfar J. A computationally effective formulation of the thermodynamic properties of LiBr–H<sub>2</sub>O solutions from 273 to 500K over full composition range, *International Journal of Refrigeration*, Vol. 29, pp. 566-578, (2006).
22. Rivera W., Estudio teórico de transformadores de calor por absorción operando con la mezcla Bromuro de Litio-Agua, Thesis of Master, Instituto de Investigaciones en Materiales, Universidad Nacional Autónoma de México, México, (1991).
23. Kaynakli O., Kilic M., Theoretical study on the effect of operating conditions on performance of absorption refrigeration system. *Energy Conversion and Management* vol. 48 (2007) pp. 599–607\_ <https://doi.org/10.1016/j.enconman.2006.06.005>.

**Nomenclatura**

ACCRS	Sistema de refrigeración en cascada de absorción-compresión
BCAC	Bomba de calor por absorción
CADS	Sistema de absorción de doble efecto
CASS	Sistema de absorción de un solo efecto
COP	Coficiente de operación de energía [-]
ECOP	Coficiente de operación de exergía [-]
$\dot{E}_x$	Flujo de exergía [kW]
GTL	Ascenso bruto de temperatura [K]
GTD	Descenso bruto de temperatura [K]
$h$	Entalpía específica [kJ/kg]
$i$	Irreversibilidad [kW]
$\dot{m}$	Flujo másico [kg/s]
$\dot{Q}$	Flujo de calor [kW]
$s$	Entropía específica [kJ/K kg]
$T$	Temperatura [K]
TCA	Transformador de calor por absorción
VCR	Refrigeración por compresión de vapor
$\dot{W}$	Potencia [kW]
$X$	Concentración de la solución de trabajo [-]

**Subíndices**

$abs$	Absorbedor
$cal$	Calentamiento
$con$	Condensador
$E$	Entrada
$enf$	Enfriamiento
$eva$	Evaporador
$gen$	Generador
$glo$	global
$S$	Salida

## Upgrading urban services through BPL: practical applications for Smart Cities

Noelia Uribe-Pérez<sup>1</sup>[000-0001-6154-1087], Igor Fernández<sup>2</sup>[0000-0002-9312-5886] and David de la Vega<sup>2</sup>[0000-0003-4811-4173]

<sup>1</sup> TECNALIA, Basque Research and Technology Alliance (BRTA), Parque Científico y Tecnológico de Bizkaia. C/ Astondo Bidea, Edificio 700, E-48160 Derio-Bizkaia, Spain

<sup>2</sup> UPV/EHU, Dpt. Communications Engineering, University of the Basque Country (UPV/EHU), Pz. Torres Quevedo s/n, E-48013, Bilbao, Spain  
noelia.uribe@tecnalia.com, igor.fernandez@ehu.eus,  
david.delavega@tecnalia.com

**Abstract.** Current initiatives related to smart cities in LATAM reveal an increasing interest in the improvement of cities and the wellbeing of their citizens. In addition, specific working groups have been created for this purpose. In this sense, the communication technologies set the basis for gathering, transporting, and managing the large amount of data generated in cities to provide a wide range of services. Within the many alternatives available, BPL positions as a promising technology, since smart cities can greatly benefit of its higher data rates and low latency. In addition, since the medium is already deployed and most of the assets and sensors are connected to the same medium, the cost of the communication systems will be reduced in price and simplicity. The work presents four practical applications: smart buildings, urban lighting, energy assets management and broadband access, in which the possibilities and advantages of BPL are further addressed. Finally, some conclusions and key aspects relating BPL to the success of smart cities are identified.

**Keywords:** Smart city, Broadband Power Line Communications, urban services, communication technologies.

### 1 Introduction

Latin America is the region with the highest concentration relative to urban population, but it is also one of the most lagging behind in when it comes to Smart Cities. However, there is notably increase in related initiatives, which shows that there is a growing interest in this field. Medellín, Buenos Aires, Mexico and Santiago are at the top of the list of smart cities in Latin America. Other cities such as Bogotá, São Paulo and Rio de Janeiro are also deploying initiatives in the field of smart cities, showing that these trends have come to stay. In addition, specific groups in relevant international groups, such as the SG20 Regional Group for Latin America (SG20RG-LATAM) at the International Telecommunication Union (ITU), has been created and

is responsible for studies relating to Smart Cities and Communities and Internet of Things (IoT) and its applications [1].

When referring to technologies for Smart Cities, it is usual to associate them to wireless options. Recent trends related to IoT are usually conceived as wireless. But the reality is that there are still wired alternatives with very remarkable advantages that can play an interesting role in the Smart City context. One of them is the electric cable, nevertheless, the power wire, with more than 100.000 km deployed throughout Latin America, is an option to consider. Specially in those assets already connected to the grid (traffic lights, urban lighting, buildings, energy resources, ...) a communication system can be easily deployed through Power Line Communication (PLC) devices without relying on external batteries. Specifically, this work addresses the potential of the broadband version of PLC – Broadband Power Line Communications (BPL) for smart cities applications in LATAM region. BPL technology allow high transfer data rate, being able to offer rates of up to hundreds of Mbps and significantly shorter response times of less than 50 ms, while using a communication media already deployed as well as robust and secure, hence leading to less installation costs when establishing the communication system.

The remaining work in this documented is grouped as follows: Section 2 reviews the concept of smart city and particularly, within the LATAM region; Section 3 introduces the fundamentals of PLC and highlights the benefits of BPL; Section 4 describes the opportunities of BPL for the smart city and, finally, Section 5 summarizes the main conclusions of this work.

## 2 Smart Cities of XXI Century

Beyond the concept of “digitalization”, Smart Cities are conceived as enablers of better-living for their citizens as well as increasing sustainability through technology-driven initiatives. The Inter-American Development Bank (IDB) understands that smart cities *“use connectivity, sensors distributed in the environment and computerized intelligent management systems to solve immediate problems, organize complex urban scenarios and create innovative responses to meet the needs of their citizens... [using] technologies to integrate and analyses an immense amount of data generated and captured from different sources that anticipate, mitigate and even prevent crisis situations.* In this sense, the communication infrastructure of the city set the basis for a whole set of applications and services.

### 2.1 Needs of Smart Cities in terms of communications

Digital technology can indeed make a city better. Energy efficiency can be improved through the street lighting control and the management of the energy resources. Citizens can be connected using mobile applications with cameras while receiving alerts and useful information as well as send data to the government. Safety can be improved in the streets and buildings through cameras and sensors. Also, the traffic can be benefited from the installation of cameras combined with motion sensors installed

on the streets. Pollution can be controlled and effectively reduced with sensors and air quality monitoring systems. In the same line, smoke, toxic gases, and temperature sensors associated with ambient cameras and warning systems can prevent environmental disasters. At the core of these applications are a communication infrastructure, sensors, an integrated operation and control center and communication interfaces [2].

Focusing on the communication infrastructure, it is required that the smart city ensures not only the existence of broadband networks that can support digital applications, but also the availability of this connectivity throughout the city and to all citizens. This communication infrastructure can be a combination of different data network technologies using cable transmission, optical fiber, and wireless networks. In summary, communication technologies should allow the following [3]:

- Interconnection between very different devices.
- Hybrid communications systems, where wired and wireless systems must live together.
- Fast communications.
- Robustness in communications.
- Flexibility and scalability in infrastructure.
- Security in communications and devices

In addition, some important requirements that a city should consider when selecting a technology for their network foundation are listed as follows [4]:

- End-to-end solutions: the network should encompass wired and wireless indoor spaces and wireless outdoor and network backbone coverage and provide a service-delivery platform for functions such as identifying end users and the applications and resources they access.
- Standards-based: the network should support security standards, and consider the use of both licensed and unlicensed frequencies.
- Easy to deploy: the access points should be configured themselves for optimum performance, eliminating the need for personnel to configure each device manually.
- Highly reliable: the selected solution should be “self-healing” and automatically selects an alternate path through the network if a link fails and avoids congested areas.
- Unified, easy management: the communication system should enable the management of the wired and wireless outdoor networks and wireless indoor networks as one unified network.
- Scalable: the network should enable the city to build and expand outdoor coverage incrementally, without reconfiguring the installed base. Scalability of a mesh network is a function of the number of channels available, which is why the network should use different channels for access and backhaul
- Secure: the network should incorporate integrated security technologies to maintain the confidentiality of private information, protects against the spread of viruses, and provides different levels of access to municipal constituents.

## 2.2 Smart Cities in LATAM

According to [5], Latin America is the most urbanized region of the developing world. Two thirds of the Latin American population live in cities of 20,000 inhabitants or more and almost 80% in urban areas and is projected to increase up to 89% by 2050. However, it is also one of the most lagging regions when it comes to Smart Cities. Following the annually Smart City Index prepared by the Institute for Management Development, which ranks cities based on economic and technological data, the Latin American city that has advanced the most in this field is Medellin, which ranks 72nd in the world, followed by Buenos Aires (88th), Mexico (90th), Santiago (91st), Bogotá (92nd), São Paulo (100th) and Rio de Janeiro (102nd) from a list with a total of 109 cities listed and headed by Singapore [6].

Large cities such as Buenos Aires, Medellín or Rio de Janeiro are making budgetary efforts to modernize both their urban infrastructure and the services they provide to citizens, from smart traffic lights to improve mobility, and the installation of surveillance cameras to improve public safety [7]. Santiago is addressing air contamination and traffic congestion through different initiatives moving towards clean mobility (electric vehicles, bike sharing). Medellin has implemented an Intelligent Mobility System of Medellin (SIMM) that uses cameras, networked traffic lights and traffic lights with vehicle detection sensors to detect traffic violations and capture traffic information. Bogota has also moved towards sustainable mobility with the increase of the public transportation system while to connected horizontal and vertical signage, smart traffic lights, and monitoring cameras. Rio de Janeiro has implemented an integrated risk management system which includes connected weather radars and a rain gauge network installed in mobile phone towers. Itu has implemented a selective garbage collection system, able to identify need for repair or replacement of containers and the optimization of the routing of collection while reducing collection time and fuel expenses [6]. These are just a few examples of the initiatives which show a growing interest in the field of smart cities in Latin America.

## 3 Broadband Power Line Communications

### 3.1 Fundamentals of Power Line Communications

Power line communications (PLC) use the power lines typically employed for electricity transmission and distribution for the transmission of communication signals by adding a modulated carrier signal over the electricity signal at 50/60 Hz. According to the bandwidth of use, PLC can be classified into three main groups:

- Ultra-narrow band PLC (UNB-PLC): this technology operates in the frequency range from 30 Hz to 3 kHz. Its main drawback is that it provides low data rates (up to 100 bps) but for long distances (up to 150 km). Some typical and proprietary examples of this technology are ripple control systems and TWACS [8].

- **Narrow-band PLC (NB-PLC):** operates in the frequency range up to 500 kHz, depending on the region and it can provide high reliability of data transmission up to several hundreds of Kbps and can reach up to hundreds of km. NB-PLC had experienced a remarkable rise for smart metering due to their good overall performance and efficiency, setting an inflection point in the rise of smart grids. Most deployed standards of NB-PLC are: PRIME (ITU-TG.9904), G3-PLC (ITU-T G.9903), IEEE 1901.2 and ITU-T G.hnem.
- **Broadband PLC (BPL):** this technology operates in the frequency band from 1.8 to 250 MHz, reaching data rates up to hundreds of Mbps for relatively short distances - up to few km. Traditionally, BB-PLC has been used for internet access and but it is currently experiencing a wide presence in smart metering, substation automation and control, and related applications within the smart grids due to the high available data rate, the secure & cybersecure as well as the robust transmission media that it provides.

The biggest advantage of PLC is that there is no alternative with such as an extensive infrastructure already deployed, leading to reduction of deployment costs while guaranteeing a secure communication at rationale speeds. In addition, PLC systems are robust and secure. In contrast to wireless alternatives, PLC allows an immediate establishment of communication during the installation process, does not need antenna tuning or adjustment of antenna direction required and the communication is also possible in difficult environments (e.g., metal-shielded cases, deep underground installations, etc.), where no other access technology can provide a solution [9]

On one hand, PLC presents some valuable advantages for smart city applications, as it has a wide potential coverage due to the electricity wires, making every line-powered device a potential target of value-added services through PLC. Moreover, the installation is already deployed, easy to manage, and stable. On the other hand, the greatest disadvantages of PLC are mainly related to the medium, due to existing disturbances, noises, and attenuations, and consequently, the global capacity of PLC in terms of bandwidth is less than other technologies [10].

### **3.2 The role of BPL**

Since the beginning of the 21st century, BPL technologies have been widely used within homes for internet communications, as an alternative or complement to WiFi networks. Currently, these technologies offer speeds of one megabit per second (Mbps). The success of NB-PLC in smart metering suggest a technological evolution towards higher bandwidths and lower latencies, in line with stricter requirements regarding real time management and cybersecurity. This has made BPL increasingly considered in monitoring and control applications within the smart grid in the recent years.

Added to the benefits to the power grid system, other smart services, such as the management of electric vehicles (EVs), energy resources, building automation, traffic and lighting control, disposal management, among others, all of them typical systems

of smart cities, can be greatly improved with the higher data rates and low latency inherent to BPL, since they could be performed through BPL in real time while assuring cybersecurity and integrity of the data.

## **4 Opportunities of BPL for the Smart City**

### **4.1 Smart buildings**

Smart Buildings are buildings which integrate and account for intelligence, enterprise, control, and materials and construction as an entire building system, with adaptability, not reactivity, at the core, in order to meet the drivers for building progression: energy and efficiency, longevity and comfort [11]. By means of available data from different sources, smart buildings become adaptable and resilient.

Smart buildings use technologies with automated controls, networked sensors and meters, advanced building automation, energy management in conjunction with information systems and data analytics software. Among the different applications within a smart building, Figure 1 shows a visual summary of some of them [12]. The following can be highlighted:

- Building energy management: entails the management of loads as well as the generation sources, if included. Heating, ventilating, and air-conditioning (HVAC) systems, which represent a very notable percentage of the electricity consumption, specially in commercial buildings, shall be considered as energy assets as well. All the connected devices (computers, machinery, office appliances, lighting, etc.) are loads of the building, that define the load profile of the building. This load profile can be efficiently managed through an energy control center (CC) when combined with internal data from the building, generation, and storage systems, for instance; and with external data, such as the energy market. As generation sources, renewable energy, such as photovoltaics, and storage sources can be integrated into smart buildings to reduce retail electricity purchases, peak load demands in buildings while moving towards energy self-sufficiency [13]. EV charging stations can be included in the energy management, so that the energy control center of the building can identify the most appropriate time slot to recharge EV with the surplus renewable energy from the building.
- Building management system: this system can include applications such as building entrance control, capacity control, parking slots management and lighting control. These systems get the information from a network of sensors deployed all over the infrastructure: humidity, heat, and lighting sensors; presence detection; people counters, cameras, etc. These sensors get the information and send it through the proper transmission media towards the management control center. In advanced system, the communication can be bidirectional, and some orders can flow from the control center towards actuators installed in specific areas. For instance, if too many people are within the same area, the center station can decide to decrease the temperature or activate the ventilations system, if

necessary. Sometimes it is common to see a general building management system on which the rest of the subsystems/applications depend (energy, surveillance, ...) depending on the complexity of the system itself.

- Surveillance systems: the degree of sophistication of surveillance systems implies that it is getting increasingly common to see independent systems. Real time images in HD as well as video recording, including data processing (facial recognition) is becoming more and more common. Some government buildings and businesses with high security needs are including the systems, hence, high available bandwidth and secure communication networks are required.

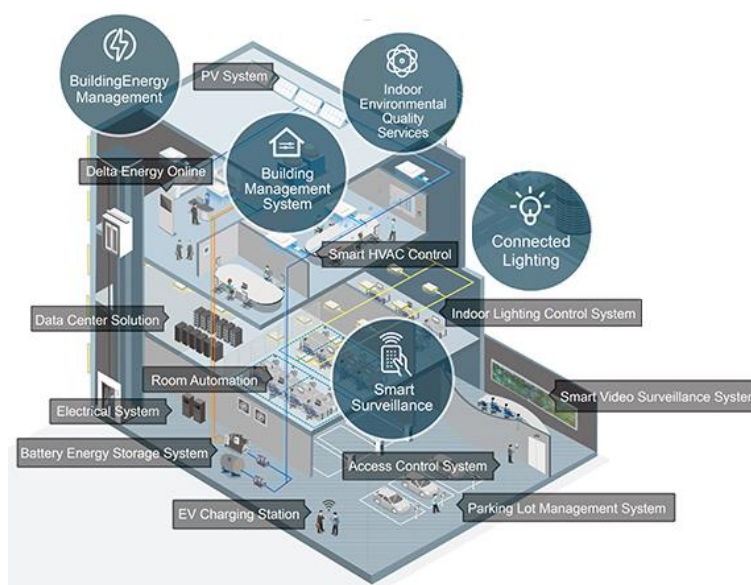


Figure 1. Overview of services and applications in a smart building.

The particularity of most of the services commented above is that they are connected somehow to the electricity wire of the building, either because they control energy resources (consumption, EV monitoring) or because they need electricity (lighting). In addition, secure communications and high bandwidth are also demanded (surveillance systems, control and monitoring). In these scenarios, BPL can serve as communication media with high bandwidth, robust and reliable, while providing an already installed infrastructure (the power wire of the building)

In line with the possibilities of BPL for smart buildings, there are some related initiatives: authors in [14] explore the efficacy of PLC as a sensor network backbone in a modern building by testing BPL modules. First results show a promising role for BPL as a viable physical and link layer for wired sensor networks. In the same line, in [15] two different BPL technologies are evaluated under different conditions of noise and

attenuation, the results show a sufficient throughput on the application layer (18 Mbps in the worst case) for smart building applications. Finally, authors in [16] present the design of a BPL module suitable for installation in an electrical outlet to increase energy efficiency and power management or in local networks as a possible alternative to existing technologies.

#### **4.2 Urban lighting**

Streetlights are one of the most important assets to maintain and control, providing safe roads, inviting public areas, and enhancing security in homes, businesses, and city centers. However, lighting is indeed very costly to operate, with a share of about 40% of the total amount of electricity spent in a city [17].

LED (Light Emitting Diode) has being an inflection point in the lighting field, specially regarding efficiency, improved options (color, intensity and direction of the light beam) and durability. When combined with a smart control on the lighting management system, new advantages emerge, such as the ability of the system for reducing energy consumption and decreasing costs with the possibility of being operated and monitored remotely.

In fact, outdoor lighting is projected to register approximately 20% growth rate through 2025 due to the increasing smart city development initiatives worldwide [18]. The smart lighting solutions are widely used across highways and roadways, bridges and tunnels, as well as public places to optimize the lighting, reduce energy consumption and provide safety. In addition, the need among the government authorities to optimize the use of energy is further increasing the adoption of smart lighting solutions.

Regarding technologies, wired technology captures the major share in the smart lighting market, accounting for more than 70% in 2018 [18], due to its robust nature coupled with high reliability and control, makes it an ideal solution for outdoor lighting applications. A further step in smart lighting can be seen in the infographic of Figure 2 where the street light set the basis of the smart city platform. This approach presents the streetlight as a multidisciplinary asset with basic and advanced light applications as well as the inclusion of several sensors (noise, traffic, air quality), cameras and assets (EV charging, digital signaling), which can provide additional services such as traffic monitoring; surveillance and safety; EV charging station; parking control; environmental quality;

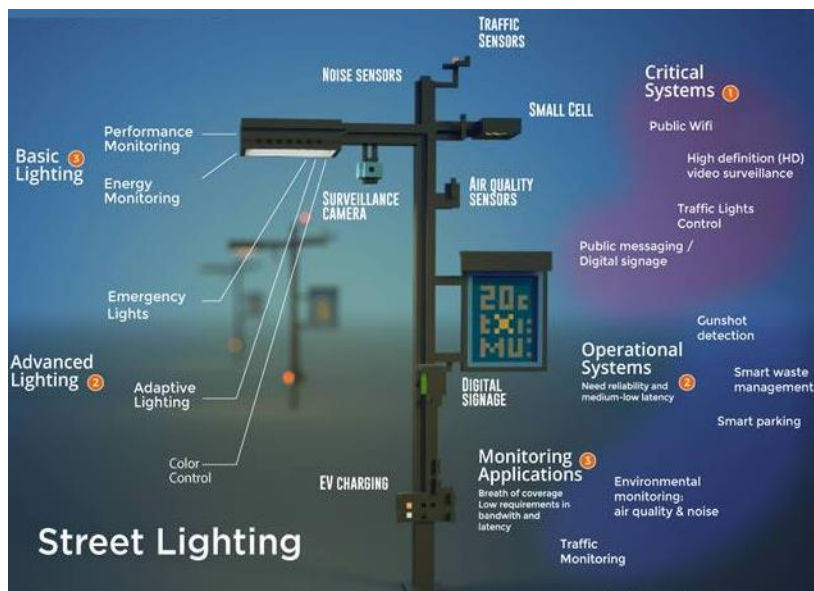


Figure 2. Smart Street Lighting as a Smart City Platform [19].

Related experiences taking advantage of BPL for lighting can be found in the literature. For instance, in [20] a lighting solution based on BPL for the smart city is described, aiming at transforming outdoor lighting networks into high speed data networks for additional smart city services.

### 4.3 Energy assets management

In a smart city, the optimal management of the energy resources within the city is gaining importance, especially considering the current concern for the environment and increasingly stricter energy efficiency regulations. In this sense, two considerations can be done: first, the management of resources in terms of production of the energy in the cities and secondly, the elaboration of a comprehensive plan for generation, storage and distribution of the energy [21].

In the coming future, each home and building might have the chance not only to generate their own energy, but also it can have the plan to sell the produced energy. In a smart city, there are, and there will be many assets related to energy somehow: starting with buildings and houses, through fleets of EVs to the city's own energy resources and prosumers. Hence, having a management system and a schedule for all these assets of the city could significantly cause a huge improvement in the context of the energy in the smart communities [22]. The data that should be collected from all the assets includes the generation capacity (from resources and prosumers), storage and a plan that determines how each source could distribute energy among all parts of the city. Therefore, an extensive, reliable, and robust communications network is required.

An example of a city smart energy management can be seen in Figure 3, where the pilot of the smart city of Yokohama is represented. In this envision, the comprehensive energy management system (EMS) is established integrating ICT, energy resources (e.g., solar panel and EVs), and other smart infrastructure. The hierarchical bundling of EMS enables energy management at the level of individual EMS and demand-side management at the level of the overall system. This involves introducing HEMS (EMS for house) for homes, BEMS (EMS for building) for offices and commercial buildings, FEMS for factories (EMS for factory), and EV and charging stations for the transport sector [23].

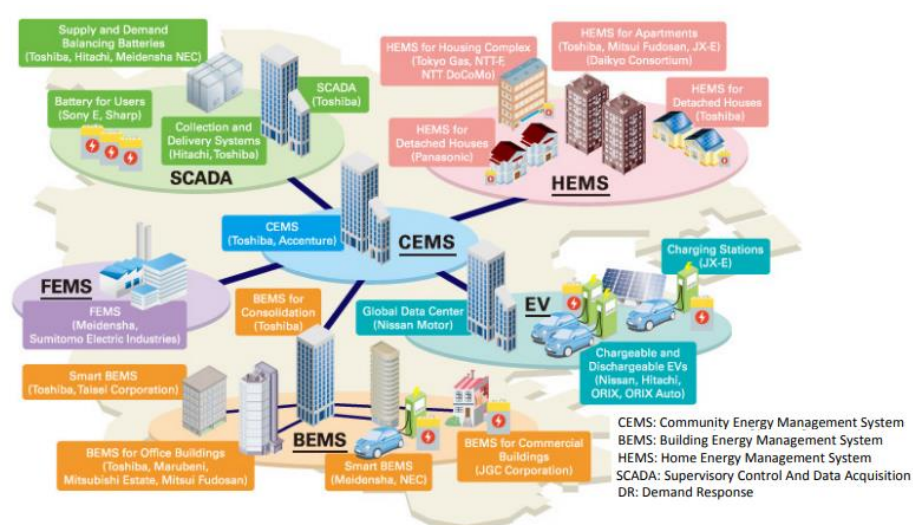


Figure 3. Overview of an energy management system for the smart city [23].

Considering that most of the energy assets will be connected to the power line, it seems natural to think of BPL as a powerful option for the management of resources. In this sense, related initiatives are taking advantage of the ubiquity of PLC in their cities. Smart City Mannheim, under the scope of the German government funded program ‘E-Energy’, was created to demonstrate how renewable energy can be optimally integrated into the grid as well as how the city can act as an energy store through the use of BPL [24].

#### 4.4 Broadband access

The Inter-American Development Bank (IDB) designed the Broadband Development Index (BDI), which allows to easily measure the current status and development of broadband in the region of Latin America and the Caribbean [25]. This index not only helps BDI to identify the barriers towards the development of the broadband access in member countries, but also is a measurement of the quality of life in a region. According to the IDB, the benefits of the broadband access can be broadly classified in two groups:

- Quantifiable benefits: those derived both from investment in infrastructure and from the creation of public policies to promote demand and the use of services made possible by broadband. Within these we find three types of benefits: benefits that users themselves would obtain from the service (e.g. tariff reduction); increased productivity of companies as a result of the adoption and use of the services that broadband enables; and improvement in activities during the working day (efficiency in tasks, remote work, ...)
- Intangible benefits: externalities resulting from the impact of broadband in various sectors. Among them, the IDB includes the government spending reduction; greater transparency in government processes; improved communications at the country level; knowledge sharing; increase in literacy rates and educational levels; reduction of crime and violence, enabling telemedicine services, creation of new companies and new ways of relating on a personal and commercial level; improved productivity of companies and reduced environmental pollution, among others.

Based on the latest version of the index, it can be derived that the gap between the IDB region and the OECD is on average decreasing slightly. However, there is a very important gap in the development of digital infrastructure, which continues to be the main obstacle to the development of the digital ecosystem in the countries of the region.

In this sense, BPL can play an interesting role towards the broadband access. It has been historically employed for in-home internet access and considering the power grid extension, its network can be considered as a massive internet provider. Since the power grid extends to both urban and rural areas (particular in the latest, where often broadband access is less present), this advantage of the technology will be not limited only the urban areas.

## 5 Conclusions

This work presents the advantages of BPL for the smart cities through the practical application of four examples: smart buildings, urban lighting, energy assets managements and broadband access. In addition, related initiatives of BPL within the urban context are also described.

Through these applications it has been shown that BPL is a promising technology for the enforcement of smart cities since it provides real-time communications with low latency and guaranteeing cybersecurity while providing a robust and reliable communication backbone for the city. In addition, since the communication medium is already deployed and most of the assets are connected to the power grid, the commissioning of the system is reduced in time, costs and complexity.

## 6 Acknowledgments

This work has been partially funded by the Basque Government (Ref. KK-2020/00095 “BB-Grid project”, and Ref. IT-1234-19).

## References

1. ITU-T Regional Group for Latin America, SG20RG-LATAM. Available online: <https://www.itu.int/en/ITU-T/studygroups/2017-2020/20/sg20rglatam/Pages/mandate.aspx>
2. IDB. The Road toward Smart Cities: Migrating from Traditional City Management to the Smart City. Available online: <https://publications.iadb.org/publications/english/document/The-Road-toward-Smart-Cities-Migrating-from-Traditional-City-Management-to-the-Smart-City.pdf>
3. Hamaguchi, K. et al. Telecommunications Systems in Smart Cities. *Hitachi Rev.*, 61, 152–58, (2012).
4. Villa, N. Wireless Cities: A Strategic Roadmap. CISCO Whitepaper (2007). Available online: [https://www.cisco.com/c/dam/en\\_us/about/ac79/docs/wp/Wireless\\_Roadmap\\_WP\\_0629a.pdf](https://www.cisco.com/c/dam/en_us/about/ac79/docs/wp/Wireless_Roadmap_WP_0629a.pdf)
5. Giannattasio, G. “America Latina, Ciudades Inteligentes” Available online: <https://www.itu.int/en/ITU-T/webinars/20210920/Documents/Presentations/Gustavo%20Giannattasio.pdf>
6. Institute for Management Development. “Smart City Index 2020”. Available online: <https://www.imd.org/smart-city-observatory/smart-city-index/>
7. Cacace, J. Digital Latam: Smart Cities - The Long Latin American Road. Available online: <https://www.accesspartnership.com/smart-cities-the-long-latin-american-road/>
8. Mak, Sioe Tho, Moore, Thomas G. TWACSTM, A New Viable Two-Way Automatic Communication System for Distribution Networks. Part II: Inbound Communication. In: Proceedings of the IEEE Transactions on Power Apparatus and Systems. vol. PAS-103, no. 8, pp. 2141–2147 (1984).
9. Landis+Gyr. Introducing the power of PLC. White paper. Available online: [http://eu.landisgyr.com/hs-fs/hub/358550/file-673231343-pdf/Resources/LG\\_White\\_Paper\\_PLC.pdf](http://eu.landisgyr.com/hs-fs/hub/358550/file-673231343-pdf/Resources/LG_White_Paper_PLC.pdf)
10. Uribe-Pérez, N.; Angulo, I.; De la Vega, D.; Arzuaga, T.; Fernández, I.; Arrinda, A. Smart Grid Applications for a Practical Implementation of IP over Narrowband Power Line Communications. *Energies* 2017, 10, 1782.
11. Buckman, A. H., Mayfield, M., & Beck, S. B. (2014). What is a smart building?. *Smart and Sustainable Built Environment*.
12. DELTA. Building Automation. Available online: <https://www.deltaww.com/en-US/products/23/ALL/>.
13. QI, Junjian, et al. Demand response and smart buildings: A survey of control, communication, and cyber-physical security. *ACM Transactions on Cyber-Physical Systems*, 2017, vol. 1, no 4, p. 1-25.
14. Pannuto, Pat & Dutta, Prabal. (2011). Exploring Powerline Networking for the Smart Building.
15. Mlýnek, P.; Rusz, M.; Beneš, L.; Sláček, J.; Musil, P. Possibilities of Broadband Power Line Communications for Smart Home and Smart Building Applications. *Sensors* 2021, 21, 240.

16. M. Rusz and P. Mlýnek, "Broadband Power Line Module Integrated into Power Plug for Smart Buildings," 2020 12th International Congress on Ultra Modern Telecommunications and Control Systems and Workshops (ICUMT), 2020, pp. 159-162
17. Catro, Miguel; Jara, Antonio J.; Skarmeta, Antonio FG. Smart lighting solutions for smart cities. En 2013 27th International Conference on Advanced Information Networking and Applications Workshops. IEEE, 2013. p. 1374-1379.
18. Global Market Insights. Smart Lighting Market Trends, 2018. Available online: <https://www.gminsights.com/industry-analysis/smart-lighting-market>.
19. Navigant Research. Smart Street Lighting as a Smart City Platform. Available online: <https://www.pdxeng.ch/wp-content/uploads/2018/10/Smart-Street-Lighting.jpg>
20. Martínez Vázquez, M. G. Technology for Industrial and Smart Grid Applications. ITU-T Roadmap and HomeGrid Forum Certification Update. IEEE International Symposium on Power Line Communications and its Applications (ISPLC), May 2020.
21. C. F. Calvillo, A. Sánchez-Miralles, and J. Villar, "Energy management and planning in smart cities," *Renew. Sustain. Energy Rev.*, vol. 55, pp. 273–287, 2016.
22. Azgomi, Hamid & Jamshidi, Mo. (2018). A Brief survey on Smart Community and Smart Transportation.
23. Li, Lichunhua & Dong, Liang. (2015). A Comparable Study on China and Japan's Energy Utilization and Efficiency Using Energy Flow Analysis.
24. Moma – Smart City Mannheim Research Project. Available online: <https://www.ppc-ag.com/projekte/moma-smart-city-mannheim/>
25. IDB. Informe Anual del Índice de Desarrollo de la Banda Ancha en América Latina y el Caribe, 2018. Available online: [https://publications.iadb.org/publications/spanish/document/Informe\\_anual\\_del\\_%C3%8Dndice\\_de\\_Desarrollo\\_de\\_la\\_Banda\\_Ancha\\_en\\_Am%C3%A9rica\\_Latina\\_y\\_el\\_Caribe\\_es.pdf](https://publications.iadb.org/publications/spanish/document/Informe_anual_del_%C3%8Dndice_de_Desarrollo_de_la_Banda_Ancha_en_Am%C3%A9rica_Latina_y_el_Caribe_es.pdf).

## Design and Installation of an IoT Electricity and Water Technological and Monitoring Solution

Ponciano J. Escamilla-Ambrosio<sup>[0000-0003-3772-3651]</sup>, Maria G. Pulido-Navarro<sup>[0000-0002-5496-7044]</sup>, Marco A. Ramírez-Salinas<sup>[0000-0002-9376-2893]</sup>, Marco A. Moreno-Ibarra<sup>[0000-0002-0349-5585]</sup>, J. Humberto Sossa-Azuela<sup>[0000-0002-0521-4898]</sup>

Instituto Politécnico Nacional, Centro de Investigación en Computación, Ciudad de México, México

{pescamilla, mars, marcomoreno, hsossa}@cic.ipn.mx,  
gpulidon@hotmail.com

**Abstract.** Nowadays, monitoring electricity and water usage is becoming very important to obtain consumption baselines towards establishing savings goals. Therefore, this work details the design and implementation of electricity and water monitoring networks installed to monitor electricity and water consumption inside three research and academic buildings of the Instituto Politécnico Nacional. Internet of Things is also implemented as it allows the systems to send the gathered information to the cloud in an Internet connection for analysis purposes. The main objective of this development is to have an electricity and water usage data repository and visualization tool to make users aware of these resources consumptions and then make changes in the infrastructure that will produce better usage and savings. This design included the installation of electricity and water consumption meters. Also, data concentrators are used to send the information obtained from the meters to monitoring software. A technical memory was recorded demonstrating the components and activities carried out in each of the monitoring points. Finally, the collected data served to estimate the electricity and water consumption baselines on the considered instances. As a major objective all the information gathered will serve to form a baseline on which improvement and political proposals will be generated for the implementation of saving actions on energy and water handling in these buildings.

**Keywords:** Water and electricity monitoring, Data concentration, IoT system.

### 1 Introduction

This paper presents the technical aspects that were considered in the design and installation of a monitoring network for electricity and water consumption at three facilities of Instituto Politécnico Nacional (IPN): Centro de Investigación en Computación (CIC), Centro de Innovación y Desarrollo Tecnológico en Cómputo (CIDETEC), and Escuela Superior de Cómputo (ESCOM). The information of the results generated from

the initial planning and corresponding monitoring of the project is presented. Additionally, the visualization of the data, generated through the activation of the Strategic System for the Evaluation and Performance for Sustainability (SEEDS) technological platform, is shown. All the information gathered has been used to determine the consumptions baseline to state new policies and rules that could be implemented in the future to make improvements and savings in energy and water usage. Internet of Things (IoT) is also implemented for the collecting of data and for their analysis. An IoT architecture is a system that allows the communication between smart devices that make use of wireless communication and Internet technologies [1]. In this way, devices can collect and transmit data efficiently.

In the IoT ecosystem, communication between devices is done in different ways. For example, by multihop short range communication (ZigBee, Bluetooth and RF) [2, 3]. In [4, 5] the authors worked on a home energy management system unit in a wireless sensor network using a ZigBee module to communicate with sensor nodes. Here the structure monitors energy consumption data and is able to send control signals to end nodes when detects peak loads. Another example on reducing energy expenses is presented in [6], in this article the authors propose a cost modeling scheme for an optimization based energy management. They take into account many scenarios such as local energy generation capacity, peak load hours, length of cycle of appliances, time of use, and also tariff have been taken into consideration. In [7], for example, the authors used ZigBee technology with mesh topology. They were able to construct a network for intercommunicating devices allowing maximum effectiveness when receiving and sending data. Another system for water monitoring [8] was built in a city based on the platform Bristol Is Open, here the authors used WiFi due to its long range (up to 100 m).

For this project, the activities carried out in the research and academic centers considered are shown from the initial planning of the requirements to the start-up of the electrical energy and water monitoring systems. An effective approach on how to persuade energy usage and to engage in sustainable practice is by providing people with information about their consumption habits [9]. As being said by [10] a study in developing countries, every year more than 16 billion cubic meters of treated water from urban supply systems are lost. That is why information on water usage brings along possible irregularities in water consumption such as leaks, meter failure, warning situations, peak water use, etc. All this data can be used as feedback for planning and policy implementation concerns. Similarly, according to [11], if consumers have a display that offers real-time feedback on their energy and water consumption it could help people on making better decisions about their usage behavior and might inspire them in using less water and electricity. According to [12-14] in some countries an automated accounting monitoring of electricity and water consumption have already shown efficacy.

The monitoring systems used in this work are tools that aim to facilitate the design of strategies for the efficient use of electricity and water. These systems have components such as: meters, data concentrators, single board computers, routers, modems, etc. Through monitoring systems, it is possible to have an alert system when energy and water consumption present atypical behaviors; equally, it is expected to incorporate

automation and control mechanisms to optimize the use and saving of resources. Considering the baseline of energy and water consumption, the following actions were carried out that made it possible to measure the consumption of electricity and water:

- Activation of the SEEDS technological platform.
- Installation of a monitoring network for electricity and water consumption.
- Quantification of energy, economic and environmental savings.
- Substitution of infrastructure and equipment for efficient consumption.
- Development of measurement systems (meter, data concentrator and transmission module).

Once the initial information was analyzed, some actions were taken for energy and water savings purposes. For instance, changes in certain guidelines such as turning off computing systems whenever they weren't in use as it was detected that, over time, they consume more energy than a microwave oven (which consumes lots of energy but only in a short period of time). Replacement of devices that had high consumption energy for devices that present energy savings such as replacement of lamps, replacement of hand dryers and the replacement of air conditioning units. Once these high consumption points were detected and some of them replaced, new policies were created. Moreover, once this consumption base is taken as a starting point, a photovoltaic system was installed in the parking lot and rooftop of the CIC, CIDETEC, and ESCOM, description of the analysis and installation of these systems can be found in [15].

The realization of the presented project is explained in the next sections as follows: Section 2 shows the network architecture, recording the energy and water consumption data that is sent to a data concentrator. Section 3 details the installation of the monitoring system for energy and water consumption for the three academic buildings. Results on the monitoring and quantification of energy and water consumption baselines at the three buildings are shown in Section 4. Finally, conclusions are presented in Section 5.

## 2 Network Architecture

The measurement systems installed in the IPN facilities has seven basic components [16]:

1. Energy meters
2. Water meters
3. Analog pulse transmitting antennas
4. System for data acquisition
5. Information processing systems
6. Components for sending data
7. Information display system

Fig. 1 shows the general architecture of the monitoring network. For the implementation, the first step consisted in the installation of the electricity and water meters in the general connections wherever was necessary. Transmitting and receiving antennas

were enabled to send the information to the data acquisition system. Then, these meters were connected to the data acquisition system to enable the reception and sending of records of electricity and water consumption. The fourth step consisted of sending the data according to the type of connection available (Ethernet, Wi-Fi or 3G). Finally, a screen was installed so that general users could monitor electricity and water consumption in real time.

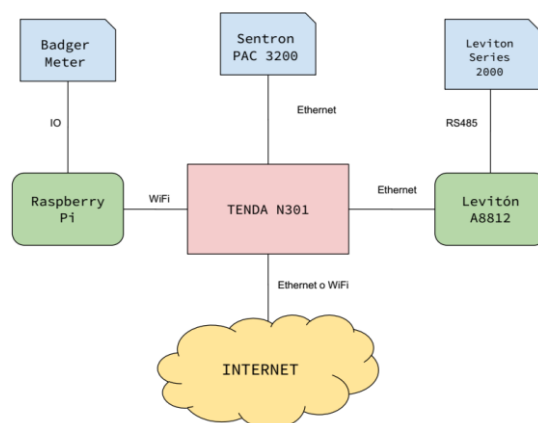


Fig. 1. Network architecture diagram.

### 2.1 Measurement of Electrical Energy Consumption

The electrical energy monitoring network has four types of meters. The most widely used meter in the project is the Siemens Sentron PAC3200 [17]. This meter permits obtaining measurements of energy consumption and energy quality parameters such as harmonic distortion, real, reactive and apparent powers, phase unbalance, frequency, etc. It has a digital display to show energy consumption and over 50 parameters. The meter has the ability to send electrical system’s current consumption information through a twisted pair cable that connects to a data concentrator. According to the scope that was established for this project, the installation of individual meters or a series of meters was considered. Such meters were located according to the requirements to have the general electricity consumption measurements of the buildings.

### 2.2 Measurement of Water Consumption

Measurement of water consumption is done with Badger Meter volumetric nutating disc or turbine meters [18]. These varied according to the characteristics of the facilities in the different buildings. The meters have an additional register type HR-LCD 4-20 (High Resolution 4-20 scaled / unscaled register), this device is completely electronic in solid state and unlike its predecessors it does not have moving parts. Solid state drives generate a scaled / unscaled output signal and a pulse in the 4-20 mA range over a Two wire / passive cable. The meters that were considered according to the project requirements are:

- Thermoplastic Disc Type Recordall Cold Water Meter Certified ANSI / NSF Standard 61 Size DN15mm (5/8 ")
- Recordall thermoplastic disc type cold water meter Size DN20mm (3/4 ") Certified ANSI / NSF Standard 61
- Thermoplastic Disc Type Recordall Cold Water Meter Size DN25mm (1 ") Certified ANSI / NSF Standard 61

These three meters work on the same principle. The water flows through the filter of the meter to reach the measurement chamber where it causes nutation of the disc. The disc moves freely, never on its own sphere, guided by a push roller. A magnetic coupling transmits the movement of the disc to a follower magnet that is located within the permanently sealed register. The follower magnet is connected to the register gear train. The gear train converts disk rotations to units of totalized volume displayed on the register panel.

### 2.3 Data Acquisition System

In order to export the information to a server it is necessary to use a data concentrator (see Fig. 2). This data concentrator can receive digital signals (ModBus, RS485 and RTU), and analog signals such as pulses, XYZ pulses, 0- 10 V, etc. The Data Hub (EMH) can connect metering equipment such as gas, water, electricity, etc. Up to 32 different devices can be connected by the RS485 communication ModBus and 8 resistive, analog and pulse output devices. This connection can be digital or analog; this will always depend on the manufacturer of the meter. In both cases, it is always important to consider the distance between the data concentrator and the meters, since one more good thing about the system is that the link can be made by wiring the equipment, or wirelessly with transceiver devices (Mod-Hopper).

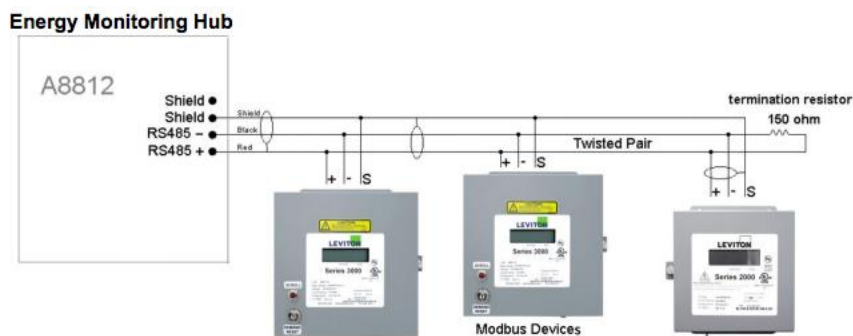


Fig. 2. Connecting the Leviton Series 2000 meter to the data concentrator.

Before connecting to the concentrator, each meter must be connected with a different configuration to the electric power transmission lines, which will be the object of study. For the Leviton meter, Series 2000 model, the following configuration is available. It

is necessary to assign a network node for each of the EMH Hubs. The system provides the necessary materials, but it is necessary that the administrators of the voice and data network provide the IP addresses and enable the network to send data.

### 3 Installation of Monitoring Systems

#### 3.1 Installation of Monitoring Systems at CIC

##### Electric power

The CIC has an electric power supply contract in conjunction with the ESCOM and the CIDETEC and therefore only one meter. The above is a main substation that receives electrical energy at 23,000 [V] in medium voltage and is in charge of distributing 120/220 [V] to the named institutions. Through the CIC substation located in the basement parking lot, it receives energy from the general substation. This energy goes through a 500 [kVA] transformer that is derived to the 1600 [A] capacity general panel which is in charge of distributing 120/220 [V] energy to all the spaces that make up the property. In this sense, the CIC's own electrical connection is the site where the real-time energy monitoring system was installed (see Fig. 3).



Fig. 3. Meter installation in the CIC substation.

##### Water

For the real-time water metering system, a 3" Badger Meter turbine meter was installed in the drinking water connection, located in the main cistern of the building. This meter is connected to the data concentrator through an antenna (Modhopper), see Fig.4.



Fig. 4. Water meter installed in the CIC.

### 3.2 Installation of Monitoring System at CIDETEC

#### Electric Power

The CIDETEC has an electricity supply contract in conjunction with the ESCOM and the CIC and therefore only one meter. The above has a main substation that receives electrical energy at 23,000 [V] in medium voltage and is in charge of distributing to said institutions at 120/220 [V]. However, the CIDETEC has its own substation located on one side of the building. It receives energy from the general substation, which through a 225 [kVA] transformer derives the 800 [A] capacity general panel. From this panel, the 120/220 [V] energy distribution gets to all the spaces that make up the property. The general panel is located at the back of the stairs in the main hall, where the real-time energy monitoring system was installed as shown in Fig. 5.



Fig. 5. General dashboard and energy monitoring system at CIDETEC.

#### Water

For the real-time water metering system, a 3"Badger Meter turbine meter was installed in the drinking water connection, located next to the CIC connection. This meter will be connected to the data concentrator through an antenna (Modhopper) see Fig. 6.



Fig. 6. Water meter installed at CIDETEC.

### 3.3 Installation of Monitoring Systems at ESCOM

#### Electric Power

The ESCOM has a contract for the supply of electricity in conjunction with the CIC and the CIDETEC, which means only one meter. Stated the above is a main substation that receives electrical energy at 23,000 [V] in medium voltage that is in charge of distributing 120/220 [V] to said institutions. However, ESCOM has its own substation located in building 5. It receives energy from the general substation, which by means of two 500 [kVA] transformers are derived two general panels with their own 1600 [A] capacity thermomagnetic switches. They are in charge of distributing energy in 120/220 [V] to all the spaces that make up the property. In this sense, ESCOM's own electrical connection is the site where the real-time energy monitoring system was installed (see Fig. 7).



Fig. 7. ESCOM general dashboard and energy monitoring system.

#### Water

For the real-time water metering system, a 3” Badger Meter turbine meter was installed in the drinking water connection. This meter was connected to the data concentrator through an antenna (Modhopper), as shown in Fig. 8.



Fig. 8. ESCOM water monitoring system.

## 4 Monitoring and Quantification of Electricity and Water Consumption Baselines

### 4.1 Consumption Baselines at CIC

#### Electricity

Derived from the analysis of the information collected by the monitoring systems, the CIC baseline consumption of electricity through the SEEDS Platform was obtained. Fig. 9 shows a view of the information that is recorded in the SEEDS system about the electricity consumption (KWh) of the CIC on a particular day, in this case 12/18/2018.

The electrical energy consumption (KWh) per day of the CIC, which have been obtained from the SEEDS platform, corresponding to the months of November 2018, December 2018, January 2019 and February 2019, are shown in Fig. 10.



Fig. 9. View of the information that is recorded in the SEEDS system on the electricity consumption (KWh) of the CIC on a particular day, in this case 12/18/2018.

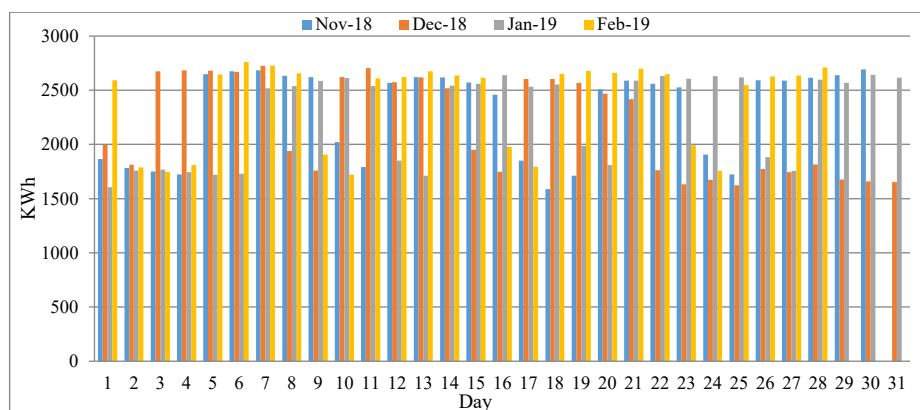


**Fig. 10.** Electric energy consumption per day (KWh) in the CIC in the months of November 2018, December 2018, January 2019 and February 2019.

Using the data collected from the monitoring network over the four months considered before, the average daily and monthly electricity consumption were obtained, and an estimate of the average annual consumption was made. The values obtained are shown in Table 1.

Table 1. Average daily, monthly, and annual electricity consumption in the CIC.

Concept	Value in KWh
Average daily consumption	2,285
Average monthly consumption	68,453
Average annual consumption (estimated)	821,436

#### 4.2 Consumption Baseline at CIDETEC

##### Electricity

From the analysis of the information collected by the monitoring systems, the CIDETEC baseline consumption of electricity through of the SEEDS Platform was obtained. From Fig 11 it can be observed the information recorded in the SEEDS system about the electricity consumption (KWh) of the CIDETEC on a particular day (for example 01/22/2019).

The electrical energy consumption (KWh) per day of the CIDETEC, which have been obtained from the SEEDS platform, corresponding to the months of November 2018, December 2018, January 2019 and February 2019, are shown in Fig. 12.



**Fig. 11.** View of the information that is recorded in the SEEDS system on the electricity consumption (KWh) of CIDETEC on a particular day, in this case 01/22/2019.

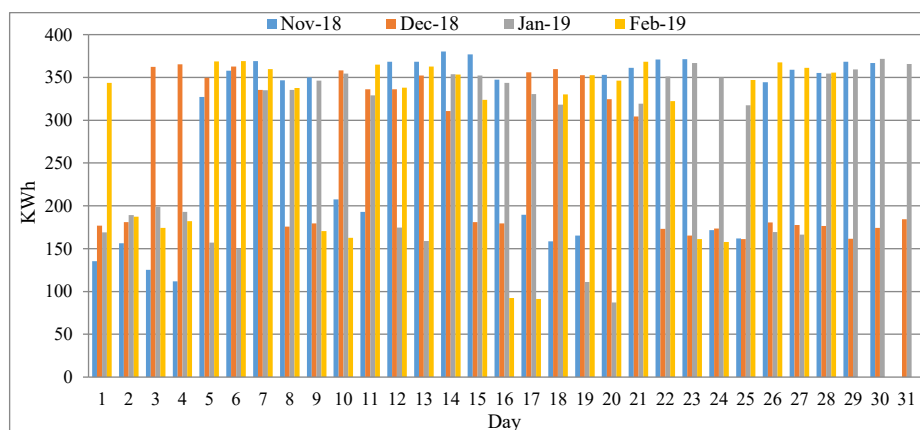


**Fig. 12.** Electric energy consumption per day (KWh) in CIDETEC in the months of November 2018, December 2018, January 2019 and February 2019.

Using the data collected from the monitoring network over the four months considered before, the average daily and monthly electricity consumption were obtained, and an estimate of the average annual consumption was made. The values obtained are shown in Table 2

**Table 2.** Average daily, monthly and annual electricity consumption in the CDETEC.

Concept	Value in KWh
Average daily consumption	276
Average monthly consumption	8,279
Average annual consumption (estimated)	99,348

### 4.3 Consumption Baselines at ESCOM

#### Electricity

From the analysis of the information collected by the monitoring systems, the ESCOM baseline consumption of electricity through the SEEDS Platform was obtained. Fig. 13 shows a view of the information that is recorded in the SEEDS system about the electricity consumption (KWh) of the ESCOM on a particular day (for example in this case the date 04/01/2019).

The electrical energy consumption (KWh) per day of the ESCOM, which have been obtained from the SEEDS platform, corresponding to the months of November 2018, December 2018, January 2019 and February 2019, are shown in Fig. 14.

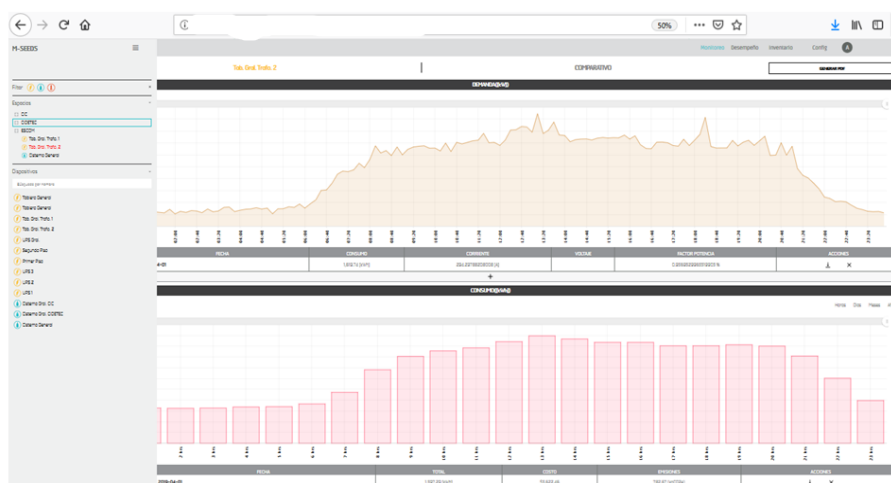


**Fig. 13.** View of the information that is recorded in the SEEDS system on the electrical energy consumption (KWh) of the ESCOM on a particular day, in this case 04/01/2019.

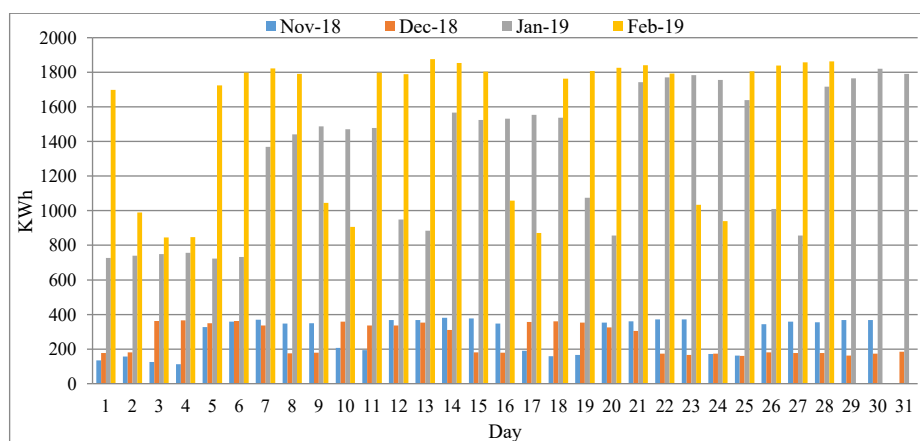


**Fig. 14.** Electric energy consumption per day (KWh) of the ESCOM in the months of November 2018, December 2018, January 2019 and February 2019.

Using the data collected from the monitoring network over the four months considered before, the average daily and monthly electricity consumption were obtained, and an estimate of the average annual consumption was made. The values obtained are shown in Table 3.

Table 3. Average daily, monthly and annual electricity consumption in the ESCOM.

Concept	Value in KWh
Average daily consumption	1,383
Average monthly consumption	41,341
Average annual consumption (estimated)	496,094

## 5 Conclusions

This work presented a whole project from planning to installation of an electrical and water monitoring network based on the SEEDS technological platform. For a remote monitoring, IoT was also implemented, which allowed the three systems to send the collected data to the cloud to be analyzed. The systems were implemented at three research and academic units of the Instituto Politécnico Nacional (IPN): CIC, CIDETEC, and ESCOM. The system included changes in the infrastructure such as the installation of electricity and water consumption meters, and the IoT implementation for the collection of data. All this data generated helped to estimate the electricity and water consumption baselines on the considered instances. For example, the baseline electricity consumption per year, estimated based on the collected data, are at CIC 821,436 KW, at CIDETEC 99,348 KW, and at ESCOM 496,094 KW. These baselines served as the basis for implementing saving actions in these research and academic units. Having the above information, it was possible to integrate data that allowed to know the consumption pattern of these resources, in real time, identifying possibilities for savings with the implementation of operational measures and/or technological substitutions that would lead to a lower environmental impact and being able to reduce the carbon footprint.

## References

1. Abedin, S., Alam, G., Haw, R., Hong, C.: A System Model for Energy Efficient Green-IoT Network. International Conference on Information Networking (ICOIN) IEEE 177-182 (2015).
2. Miorandi, D., Sicari, S., De Pellegrini, F., Chlamtac, I.: Internet of things: Vision, applications and research challenges. *Ad Hoc Networks* 10 1497–1516 (2012).
3. Gubbi, J., Buyya, R., Marusic, S., Palaniswami, M.: Internet of things (iot): A vision, architectural elements, and future directions. *Future Generation Computer Systems* 29 1645–1660 (2013).

4. Abo-Zahhad, M., Ahmed, S., Farrag, M., Ahmed M., Ali, A.: Design and implementation of building energy monitoring and management system based on wireless sensor networks. Tenth International Conference on Computer Engineering & Systems (ICCES) 230-233 (2015).
5. Nguyen, N., Tran, Q., Leger, J. Vuong, T.: A real-time control using wireless sensor network for intelligent energy management system in buildings. IEEE Workshop on Environmental Energy and Structural Monitoring Systems 87-92 (2010).
6. Erol-Kantarci, M., Mouftah, H.: Wireless Sensor Networks for Cost-Efficient Residential Energy Management in the Smart Grid. IEEE Transactions on Smart Grid 2 314-325 (2011).
7. Marais, J., Malekian, R., Ye, N., Wang, R.: A review of the topologies used in smart water meter networks: a wireless sensor network application. Hindawi LTD 9857568 1–12 (2016).
8. Chen, Y., Han, D.: Water quality monitoring in smart city: a pilot project. Elsevier Science BV 89 307–316. (2018).
9. Peterson, D., Steele, J., Wilkerson, J.: WattBot: A Residential Electricity Monitoring and Feedback System. ACM 978-1-60558-247 Student Design Competition (2009).
10. Kingdom, B., Liemberger, R., Marin, P.: The challenge of reducing nonrevenue water (NRW) in developing countries. How the private sector can help: A look at performance-based service contracting, World Bank Group 8 (2006).
11. Chetty, M., Tran, D., Grinter, R.: Getting to green: understanding resource consumption in the home. Proc. UbiComp (2008).
12. Ikramov, N., Majidov, T., Kan, E., Mukhammadjonov, A.: Monitoring system for electricity consumption at pumping stations. IOP Conf. Ser.: Mater. Sci. Eng. 883 012101 (2020).
13. Singh, P., Kansal, A.: Energy and GHG accounting for wastewater infrastructure. Resour Conser Recycl 128 499–507 (2018).
14. Bessa, J., Alves, M.: Data-driven predictive energy optimization in a wastewater pumping station. Appl Energ 252 (2019).
15. Escamilla-Ambrosio, P.J., Ramírez-Salinas, M. A., Espinosa-Sosa, O.: IPN Sustainability Program: Solar Photovoltaic Electricity Generation and Consumption Reduction. Springer Nature Switzerland CCIS 1152, 109–120 (2020).
16. Leviton Homepage, <https://www.leviton.com>. Accessed 1 Sept 2019.
17. PAC3200 Power Meter, Siemens, [https://www.downloads.siemens.com/download-center/Download.aspx?pos=download&fct=getasset&id1=BTLV\\_50409](https://www.downloads.siemens.com/download-center/Download.aspx?pos=download&fct=getasset&id1=BTLV_50409). Accessed 1 Sept 2019.
18. Badger Meter Home page, <https://www.badgermeter.com/es-us>. Accessed 1 Sept 2019.

## A review of the role of electric vehicles in carbon regulation policies related to the transport sector

Rayssa Paula Correia Lima<sup>1</sup> and Vanessa de Almeida Guimarães<sup>2</sup>[0000-0001-7662-3499]

<sup>1</sup> Centro Federal de Educação Tecnológica Celso Suckow da Fonseca, Angra dos Reis, Brazil

vanessa.guimaraes@cefet-rj.br

rayssa.lima@aluno.cefet-rj.br

**Abstract.** The increase in greenhouse gas emissions – GHGs and their concentration in the atmosphere cause a rise in the global average temperature of the atmosphere and the oceans, causing global warming. To change this scenario, many countries established emission reduction targets based on international protocols and conventions. The transport sector has been one of the main sources of GHGs emission from human activities, mainly carbon dioxide (CO<sub>2</sub>), in Brazil and in the world. In this context, the increase in the awareness of environmental preservation has encouraged the development of more efficient technologies that emit less GHG. Among them, there are electric vehicles that do not emit CO<sub>2</sub> during their use. Therefore, this paper aims to identify the role of electric vehicles in carbon regulation policies related to the transport sector. Thus, we carried out a survey of articles published in the Web of Science database until the year 2019. These articles were categorized and, subsequently, those with keywords related to electric vehicles were analyzed, as possible action of improvement for the decarbonization of the transport sector. It was found that, although there is a scarce literature dealing with both subjects, there are carbon policies and government subsidies that encourage technological projects to reduce emissions around the world. Furthermore, among the main topics of study of the articles are: models of Battery Electric Vehicle Battery and Plug-in Hybrid, battery autonomy, use of renewable energy sources and charging stations.

**Keywords:** Carbon Regulation, Transport, Electric Vehicle.

### 1 Introduction

With the growing use of automobiles, the transport sector has been one of the main emitters of greenhouse gases (GHGs) [1], since most vehicles are powered by fossil fuels and, in the process of burning these fuels, it is emitted carbon dioxide (CO<sub>2</sub>), one of the main GHGs [2]. Among the modes of transport, road (cargo and passengers) accounted for 72% of global emissions in 2018 [3]. Furthermore, according to the Annual Estimates of GHG Emissions in Brazil, the Fossil Fuel Burning sub-sector contributed 94.8% of the energy sector's emissions in 2016 [2]. Besides the greenhouse effect, the global warming and the climate change resulting from the increase in emissions of GHGs into the atmosphere, there is also a concern related to the dependence on fossil fuels in the transport sector and to the scarcity of natural resources [4].

In this context, governments and companies has been encouraged the development of alternative technologies more efficient and cleaner (emitting less GHGs). Among them are the electric vehicles, which are considered “greener technologies” because they use batteries and electricity, not emitting CO<sub>2</sub> during their use [5]. However, the electric vehicle has not necessarily zero CO<sub>2</sub> emissions if one considers its manufacturing process and the source the electric energy consumed (which might be fossil, as those from coal-fired plants). There are also other problems associated with its use, such as battery disposal. However, investments in research and technological innovation might resolve or mitigate these issues [5].

In addition to electric vehicles, regulatory policies (such as carbon cap-and-trade, carbon tax, carbon cap and personal carbon trading) associated with other instruments/policies for carbon mitigation (e.g. use of taxes to promote the development and use of alternative sources of energy, policies to encourage the adoption of electromobility, funding to develop new technologies) could encourage the search for solutions to problems related to emissions. In countries like Brazil, the use of electric vehicles might have a greater contribution to reducing emissions from conventional vehicle models (Internal Combustion Engine - ICE), as well as the electric vehicle does not emit CO<sub>2</sub> during its use and the electricity supply come, mostly, from a renewable source (manly from hydroelectric) [6]. The opposite happens in countries like China and India, where electricity comes mainly from thermoelectric plants, which might result in higher CO<sub>2</sub> emissions compared to Brazil [6]. Nevertheless, the fact that Brazil has a variety of renewable source available (as ethanol) must be considered since the policies related to biofuels and electric vehicles compete for funding and both might help to mitigate the emissions.

In this scenario, this paper aims to identify the role of electric vehicles in carbon regulation policies related to the transport sector. Therefore, a systematic review was performed from the data gathered in the Web of Science database until the year 2019. Previously papers had already carried out the evaluation of carbon regulation policies in the Brazilian transport sector [7,8]. However, this paper emphasis is on the role of the electric vehicle to reduce CO<sub>2</sub> emissions in the transport sector.

Based on this introduction, this paper was divided into four sections: the theoretical framework addressing the carbon regulation policies and electric vehicles; the methodological procedures; findings and final considerations. Finally, we have the acknowledgments and references.

## **2 Carbon Regulation Policies and Electric Vehicles**

Climate change might occur due to natural causes (such as changes in solar radiation and the in the earth's orbital movements) and by consequences of human activities (such as deforestation and industrialization). The increase of the GHGs emission levels cause an increase in the global average temperature, causing global warming [4]. To change this scenario, many countries set their own emission reduction targets based on international protocols and conventions. Following the Nationally Determined Contribution (NDC) of the Paris Agreement, Brazil has committed to promote a reduction of its GHG emissions to a value 37% below 2005 levels, by the year 2025. Furthermore, it has established a subsequent indicative contribution of 43% reduction below 2005 emission

levels by 2030 [8]. The concern with carbon emissions is evidenced by international commitments, such as the United Nations Framework Convention on Climate Change (UNFCCC) and the Conferences of the Parties (COPs), in which the countries search together for solutions to this issue.

Regulatory carbon policies are a set of actions aiming to promote emission reductions in the countries. They emerged as a way to attribute “cost” to the impacts caused by the increase of GHG emissions. The main policies are: carbon cap, carbon tax and carbon cap-and-trade. The carbon cap sets a limit on the level of emission (in tonnes of CO<sub>2</sub> or CO<sub>2</sub>-equivalent) that participants (countries, sectors, industries and so on) can emit during a certain period [9]. The carbon tax is a type of carbon pricing, where a fee is charged for each ton of CO<sub>2</sub> or CO<sub>2</sub>-equivalent emitted [10].

In the carbon cap-and-trade, a carbon credit certificate is issued with an established limit and these credits can be traded in a market (called Emissions Trading System - ETS). Therefore, companies could manage to reduce their GHG emissions (e.g. by investing in cleaner efficient technologies), so they can obtain these carbon credits from government and sell them on the financial market. Companies that emit above of the permitted amount (cap), by its turn, must purchase extra credits in order to increase their emission beyond of their limit. Another option for these companies is to reduce emissions by adopting technological projects and/or cleaner production processes, such as replacing them with more efficient equipment, investing in carbon offsetting projects, using carbon purifiers etc. [11]. According to [12], the mitigation policies might decrease the emissions levels by encouraging companies to develop new low-carbon technologies. Besides, according to [13], cap-and-trade policy generate government revenue that could be use to funding greener projects and to help the most vulnerable sectors. To a better understanding of the cap-and-trade policy, we suggest [13].

World Bank (2020) report summarize the carbon pricing instruments implemented or scheduled for implementation, by sectors. The use of one instrument or the combination of instruments depends on factors, such as: emissions profile, sector structure, institutional capacity, among others [1]. It is observed that, among the countries which have implemented or scheduled pricing instruments, there is a balance between the emission trading systems, carbon tax and both. In addition, most of the policies are targeted to industry, energy and fossil fuel sectors. Policies related to the transport sector were found only in New Zealand, Washington, Kazakhstan, California and China.

Historically, energy consumption by the transport sector has been dominated by fossil fuels (such as gasoline and diesel) [1]. It contributed to global economic growth, however, the transport sector has become one of the largest emitters of GHGs, contributing to the aggravation of climate change [14]. In this context, alternatives for the decarbonization of the transport sector should be sought. Among the alternatives, electric vehicles stand out. In this case, the electricity is used as an alternative (or complementary) fuel to gasoline and diesel. So, it might increase the use of renewable energy sources in transport, if the source of the electricity is green. Besides, with an increase demand for energy from the grid, there will be a need for new sources. In addition, electric vehicles also tend to be more energy efficient, has low noise and is vibration free [15].

The models of electric vehicles currently available on the market are: Hybrid Electric Vehicle (HEV), Plug-in Hybrid Electric Vehicle (PHEV), Battery Electric Vehicle (BEV) and Fuel Cell Electric Vehicle (FCEV).

HEVs have two propulsion systems: the internal combustion engine (using gasoline/alcohol or diesel) and an electric motor (in addition to having a bank of batteries to power the electric motor) [16]. This type of vehicle cannot be recharged through the electrical network; therefore, the batteries are charged by the combustion engine and by the regenerative brakes (part of the kinetic energy dissipated as heat is captured and transformed into electricity, which is stored in the battery) [17]. Some examples of these car models in Brazil are: Lexus CT200h, Toyota Prius, Ford Fusion Hybrid and Corolla Altis Hybrid.

PHEVs also work with two propulsion systems: the internal combustion engine, the electric motor and a battery bank. However, unlike conventional hybrids, PHEVs can recharge batteries in two ways: through regenerative braking (Kers) or by a cable powered by an external source [17]. As advantage, they can reach greater distances using only electricity as fuel and, when the battery runs out, the combustion engine works like a conventional vehicle. Furthermore, they do not emit GHGs when they are running only with the electric motor and, even in hybrid mode, there is an emission reduction. Some of these vehicle models in Brazil include: the Golf GTE, Panamera E-Hybrid, Volvo XC60 T8 Hybrid, BMW i8 and 530e.

BEVs have an electric-only propulsion system, using the energy stored in the battery to power the engine [16]. The battery is recharged using regenerative brakes and an external source of electrical energy. They are considered 100% electric as they are powered only by electricity. Examples in Brazil include Nissan Leaf, Renault Zoe, JAC iEV 40, Chery Arrizo 5e and Chevrolet Bolt.

Finally, FCEVs also have an electric-only propulsion system, however, their energy source are fuel cells, mainly from hydrogen (or another fuel such as bioethanol, when there are reformers) [20]. Electricity is produced by combining hydrogen with oxygen to power the electric motor: the conversion of this gas to electricity produces water and heat, and the cells store the energy used in the electric motor. Therefore, there is no GHGs emissions, only production of hydrogen gas. Pressurized hydrogen is sold at refueling stations and FCEV have regenerative brakes that help recharge the battery [14]. This type of electric vehicle is not yet available in Brazil, but some examples of models are: Toyota Mirai, Honda Clarity Fuel Cell, Hyundai Tucson FCEV and Hyundai Nexa.

Another important factor about electric vehicle is the recharge time: cars can take about eight hours to recharge in a household outlet, but when on public roads, the recharge must be done in minutes [18], which requires a greater and stable electric network grid. Therefore, both recharge time and the electric network must be carefully considered during the planning of increasing the electric vehicle fleet.

Europe has invested in the installation of charging points so that electric vehicles can circulate through cities without the risk of a shortage of supply. This advance has been led by electricity distribution companies such as IDC Energy Insights and Iberdrola, which have as an objective to reduce GHGs emissions, promote the transition to sustainable mobility and the electrification of transport [19,20]. In Brazil, the Protocol of

Intentions was signed between the government and private companies (Renault-Nissan, Petrobras Distribuidora, Light, Ampla and Rio Negócios) to produce electric vehicles and charging stations in Rio de Janeiro [21]. In addition, in São Paulo, in 2012, the first fast-recharge electric station was installed at the Institute of Electrotechnics and Energy (IEE) at USP, with an average price of 10 reais. The project was carried out in partnership with EDP, a Portuguese multinational. This electrical station will allow to gather data (such as consumption, efficiency and useful life of vehicle batteries) and estimate the impacts on electricity distribution networks [22].

Improvement in batteries is also sought by some studies. They search for lighter and smaller materials, with lower cost, a longer life cycle and that a better energy storage. In Brazil, an agreement between FINEP (Financiadora de Estudos e Projetos), FPTI (Fundação Parque Tecnológico Itaipu) and Itaipu Binacional has innovated with the use of a national sodium-based battery for electric cars [23].

From the context presented, one can note that electric vehicles may become more financially viable as technological advances and government incentives increase. The Electric Vehicle Program (EV), for example, is the result of a partnership initially signed between Itaipu and KWO – Kraftwerke Oberhasli AG (a Swiss energy supply company), with the objective of developing solutions in electromobility that are technical and economically viable. Besides, it analyzes of impacts on the electrical system, and propose new technologies to minimize environmental impacts in the transport sector [23]. In addition, according to [24], the increase in the fuel prices, the development of low-cost batteries and the implementation of carbon taxes (considering a low carbon electricity matrix) would make the electric vehicles more affordable.

### 3 Methodological Procedures

The proposed search was performed in the Web of Science (WoS) database, as detailed in Table 1. It is about the continuation of studies [7,8].

**Table 1.** Description of the search in the Web of Science database

Criterion	Description
Topic	“Transport*” AND (“carbon trade*” OR “carbon cap” OR “carbon tax*” OR “carbon regulation”)
Database	Web of Science (all areas)
Time	All years until 2019 (excluding 2020, as the year of the search)
Search date	March 2 <sup>nd</sup> , 2020 at 6:26 p.m.

This search found 426 articles published about the topic until the year 2019. From these, only articles published in journals were considered, resulting in 358 documents. After that, we select only the articles that have a direct relation with the carbon emission restriction policies and the transport sector, which resulted in 279 papers. Subsequently, we selected only the articles that have, at least, one keyword related to electric vehicles, since we aim at studying it as a decarbonization action in the transport

sector. Then, only 20 articles were found, which were systematically analyzed in Section 4.

## 4 Results

Related to this search, articles [7,8] presented how the scientific literature has been dealing with carbon regulation policies in the transport sector. Among the main findings, we highlight that several actions have been proposed to reduce CO<sub>2</sub> emissions in transport sector, such as: production and use of low carbon fuels (e.g. biofuels) to reduce the use of fossil fuels; use of electric vehicles; improvement in public transport system; improvement on the management of transport systems and logistics; development of new engines in order to improve the efficiency of the vehicles, among others. There are also actions related to the energy sector, such as the use of renewable energy sources (installation of photovoltaic panels to recharge electric vehicles) and project to increase the energy efficiency. Some of the articles [25, 26, 27, 28] also mention the concern that each person must have to collaborate in the mitigation of GHGs, actions such as using public transport more frequently and avoiding energy waste.

It was also found that Brazil has the potential to achieve its goals established by international treaties and it has already implemented projects of Clean Development Mechanism - CDM projects [7, 8]. Based on those previous studies, this present paper analyzes the role of the electric vehicle as a way to reduce the GHGs emissions in a context of carbon emissions restriction.

Figure 1 shows the temporal evolution of publications about the subject “transport and carbon regulation policies”. The number of articles that address the electric vehicles subject in this context are highlighted in green. The first record of studies about electric vehicles in the mentioned context was published in 1995 (three years after the first publication on carbon regulation in the transport sector made in 1992 [7,8]). From 1995 to the year 2007, there was an interval of 12 years without publications. In 2017 there was a small increase in the published articles, with 3 papers; and 2019 had the highest rate of articles published (6), twice the year of 2017.

From the 279 articles gathered in the database, only 20 deal specifically with the electric vehicle as an alternative for decarbonizing the transport sector. This scarcity might be related to the fact that the discussions about the main topic “carbon regulation in transport” are recent (as shown by [7,8]). Then, there are many studies and reports focusing in how to propose a carbon regulation policy. In addition, Paris Agreement was proposed in 2015, therefore, it is acceptable that the mitigation actions will become more investigated over the years, since the countries has specific targets to accomplish. Besides, it is expected that the tax generated by the carbon emission policies (auditions in carbon trade or taxes) can be used to funding innovation and mitigation actions.

Table 2 present a systematic review of the 20 articles surveyed. The articles are ordered by the number of citations at the time the search was made. Most of the papers were published at Energy Policy, with 6 records (4 of them are among the 10 most cited). Then, we have Journal of Cleaner Production, with 3 articles, Applied Energy and Transportation Research Part A-Policy and Practice with, 2 records each.

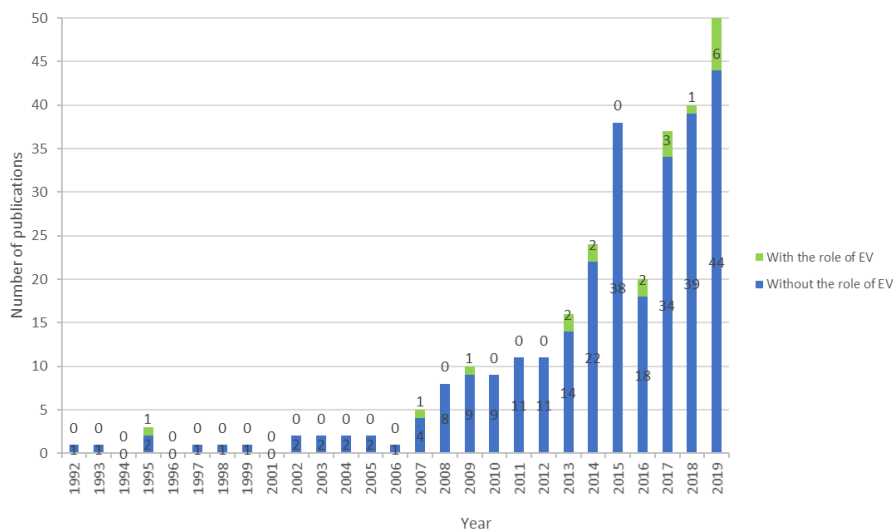


**Figure 1.** Evolution of publications per year (Source: Own elaboration, 2021)

It was found that the most analyzed types of vehicles are cars, trucks and electric vans. Furthermore, as shown in Table 3, all are related to passenger transport and 20% of also mention the freight transport, but none of them addresses intermodality.

Regarding the government subsidies, the Electric Vehicle program stands out, resulting from the partnership between Itaipu Binacional and Kraftwerke Oberhasli AG (Swiss company), which seeks solutions to introduce electromobility in cargo and passenger transport, where they developed the first electric truck in Latin America, in partnership with Iveco. Later, they created the first 100% electric and another hybrid bus in Brazil. In addition, there was the utility Agrale Marruá Eléctrico, in partnership with the companies Agrale and Stola do Brasil, where the vehicle was presented during the United Nations Conference on Sustainable Development, Rio+20, in Rio de Janeiro [23]. Vermeque, F. [29, 30] present some government subsidies in other countries as USA, China and Spain.

Furthermore, it was found that plug-in hybrid electric vehicle and battery electric vehicle are the models most discussed, being present in 11 of the 20 articles. The use of shared autonomous vehicles is also studied [30, 31], and shows that such vehicles they could reduce costs, GHGs emissions, congestion and waiting times.

Table 3 shows that most of the papers are mainly concerned with the battery, addressing some issues, such as: duration time, recharge time, weight, autonomy etc. Some papers are concerned with the use of renewable energy sources to recharge vehicles. Studies [14, 32, 33, 34] are dealing with electricity generated from photovoltaic panels, as a way to replace fossil fuels to meet the obligations stipulated of the carbon emission reduction targets.

Some articles [13, 33, 34, 35, 36, 37, 38, 39, 40, 41] addressed fuel cell electric vehicles (which use hydrogen gas as the main source of energy) and made a comparison between some fuels like: electricity and gasoline.

**Table 2.** Main features of the surveyed articles

<b>Papers</b>	<b>Country</b>	<b>Objective</b>	<b>Study Object</b>	<b>Type</b>
[24] (2013)	USA	Builds PHEV simulation models to account for the effects of additional batteries on fuel consumption, cost and GHG emissions at a variety of charging frequencies	Battery	P
[15] (2016)	USA	Analyzes a plug-in electric vehicle photovoltaic charging station, located in a work garage, for daytime charging	Parking charging station powered by photovoltaic panels	P
[35] (2014)	USA	Presents a comparative analysis based on simulation of the transition pathways from hydrogen and electricity to an almost carbon neutral transport sector in Iceland	Electricity / Hydrogen (H <sub>2</sub> ) / Mixed Hydrogen Electricity (EVH <sub>2</sub> )	P
[36] (2014)	Iceland / New Zealand	The impact of low emission vehicles is assessed using the AIM / Enduse model in 10 regions in Japan	Low carbon vehicles / Renewable Energy Source (solar photovoltaic and wind energy)	P, C
[32] (1995)	Japan	It presents a feasibility analysis of electric vehicles powered by photovoltaic energy, considering the technological and economic aspects involved	Photovoltaic Energy / Battery	P
[33] (2017)	China	Different strategies to reduce the emissions of nitrogen oxides and carbon dioxide from the Swedish transport sector are evaluated through scenarios for the year 2015, using a bottom-up approach.	Photovoltaic energy / Battery / Alternative fuels	P, C
[14] (2016)	Switzerland	Choice experiment in Jiangsu, China, to assess whether personal carbon trading influences individual decisions to adopt battery-powered electric vehicles	Battery / Vehicle Performance Attributes	P
[34] (2013)	Australia / China	Analysis of the perspective of a public authority on the various innovation policies for the deployment of electric vehicles powered by solar photovoltaic energy by 2030	Photovoltaic Energy / Battery	P
[45] (2007)	France	Evaluation of the use of electrically powered vehicles (EPV) instead of conventional vehicle systems for Istanbul.	Renewable Energy Source (Wind Energy)	P
[42] (2017)	Turkey	It addresses the technologies and energy policies that the next USA president should implement to slow global warming	Renewable Energy Source	P
[12] (2019)	USA	Investigates the diffusion of electric and hybrid commercial vans and their facilitating factors in the city's logistics contexts	Biofuels / Charging Stations	P, C

[30] (2017)	Italy	It makes a detailed estimate of the cost of the Autonomous Electric Vehicle fleet based on vehicle purchase prices, vehicle maintenance, batteries, electricity, charger construction, charger maintenance, insurance, registration and general administrative costs	Battery / Electricity / Charging Stations	P
[37] (2019)	USA	Assesses the financial feasibility and environmental impact of light electric vehicles (LD-EVs) and hydrogen fuel cell light vehicles (LD-HFCVs)	Comparison of Electric Fuel, Hydrogen and Gasoline	P
[31] (2019)	Canada	It develops an energy system optimization model that integrates the electricity and transport sectors, calculates the adoption of endogenous technology, and distinguishes autonomous vehicles (SAVs) from private vehicles (POVs) to explore contributions to climate change mitigation	Battery	P
[38] (2019)	USA	Compares alternative “paths” to decarbonize the electricity and heavy-service transport sector by 2060	Renewable Energy Source / Comparison of fossil, alternative and hydrogen fuels	P, C
[39] (2018)	Canada / USA	Examines the transition to low carbon vehicles such as battery electric vehicles, hydrogen fuel cell vehicles and natural gas vehicles to reduce GHG emissions in Japan	Charging Stations	P
[46] (2019)	Finland / Iceland / Japan / New Zealand	It presents a cost model of taxi systems for electric vehicles, based on the cost of taxi companies, charging stations or changing batteries, passenger time and emission costs	Battery / Charging Stations	P
[40] (2020)	China	Examines subsidies for electric vehicles, the conditions under which state and federal vehicle policies can have long-term positive social benefits	Battery / Charging Stations	P
[41] (2019)	USA	Evaluates political incentives to stimulate the electric vehicle market with the objective of reducing fossil fuel consumption	Battery / Charging Stations	P
[43] (2013)	Denmark / Greece	It uses the choice experiment method and the potential effects of policy schemes were explored and compared to encourage the adoption of BEVs	Battery / Charging Stations	P

Notes: P = passenger; C = Cargo

An interesting analysis was carried out in the article [14], which addresses the implementation of a photovoltaic charging station for an electric vehicle, during the day, located in a work garage. Its main proposal was to increase the penetration of renewable energy sources in the transport sector without strongly affecting the electricity grid. The results showed that a vehicle would save approximately 0.6 ton of CO<sub>2</sub> per year using solar charging at the workplace, which equates to a 55% savings in CO<sub>2</sub> emissions by charging the vehicle at home overnight.

Regarding the economic, environmental and social criteria (which composes the concept of sustainability) are presented in Table 3. It is verified that, in the economic dimension, the articles are mainly concerned with the purchase cost (considering that the value of electric vehicles is still high compared to conventional vehicles), with the cost of electricity for recharging, the cost of the battery and the cost of maintenance. It is noteworthy that, in some studies, it was found that the price of energy to recharge vehicles is lower than the cost of refueling with fuels such as gasoline [24, 35].

Regarding the environmental criteria, as expected due to the keywords used, the criteria analyzed the most was GHGs emissions and carbon neutral transport. For the social dimension, most articles addressed government subsidies and incentives, such as: government fleet purchases, support for public charging infrastructure, clear labeling of gasoline and electricity consumption, advances in infrastructure (such as automatic charging connections) etc. [12, 14, 24, 31, 33, 34, 40, 41, 42, 43].

In addition, some papers addressed education programs aiming at increasing people's knowledge about their consumption behavior and helping them make better choices to reduce emissions [14, 24, 35, 36, 43]. INEE (National Institute of Energy Efficiency) and ABVE (Brazilian Electric Vehicle Association) organized workshops related to environment and social responsibility, electric vehicles and Brazilian automakers, barriers to the development of EVs in Brazil, public policies for EVs, incentives and removal of fiscal barriers. [15]. Besides, there is a discount on the Motor Vehicle Property Tax as a tool to encourage the purchase of electric and hybrid cars in Brazil. Currently, the states of Alagoas, Maranhão, Paraná, Piauí, Pernambuco, Rio Grande do Norte and Rio Grande do Sul offer total IPVA exemption. Ceará has a discount tax rate of 0.5% on the value of the car, Mato Grosso do Sul has 50%, in Rio de Janeiro has 50% and in São Paulo it has 50% in the capital. The states of Bahia, Espírito Santo, Federal District, Goiás, Mato Grosso, Pará and Rondônia have ongoing projects to reduce IPVA [44].

Finally, regarding the GHG emission mitigation policies carbon tax was the most frequent among the articles surveyed, followed by carbon trade policy. From the analysis of the articles, other policies found were: Personal carbon trading (PCT) and Carbon offset. PCT is addressed as the main theme of two articles [13, 43]. Its implementation can influence the transportation choices of individuals as a method to reduce private carbon emissions. Through economic, psychological and social incentives, it generates changes in individual behavior and encourages decisions to adopt electric vehicles, reduce energy consumption and travel by private car, among others. So, people would achieve greater environmental awareness and be able to understand the importance of reducing GHG emissions.

**Table 3.** Analysis of the economic, environmental and social criteria of the 20 articles in the database (Source: Own elaboration, 2021)

Papers	Economic Criteria	Environmental Criteria	Social Criteria	Improvement Actions
[24] (2013)	Battery cost / Fuel price / Purchase price / Operating costs	GHG Emission	Government Incentives / Consumer Education	Battery improvement / Government incentives (financial incentives, government fleet purchases, public charging infrastructure) / Low carbon electricity generation / Increased price of fossil fuels / Infrastructure advances (automatic charging connections installed in garages or designated places of public parking)
[15] (2016)	Structure installation cost / Electricity price / Parking fee / Operation and maintenance cost	GHG Emission	Tax reduction and financial incentives	Renewable energy sources
[35] (2014)	Petroleum price / Purchase price / Complementary biogas price	Almost carbon neutral transport / Renewable fuels	Consumer behaviors	Energy efficiency / Alternative fuels / Improved vehicle technology
[36] (2014)	Energy price / GDP growth	GHG Emission / Seasonal Electricity Demand Characteristic	None	Energy efficiency / Use of public transport, cycling or walking
[32] (1995)	Energy cost / Battery cost / Photovoltaic panel price / Resale rate	GHG Emission	None	Renewable Energy (in photovoltaic electricity)
[33] (2017)	Methanol Usage Cost	GHG Emission	None	Energy Efficiency / Use of fuels from renewable sources / Better vehicle maintenance / Increased vehicle occupancy
[14] (2016)	Price of carbon permits on the market	GHG Emission	Psychological encouragement Gender, age and income	Government Subsidies / Actions to encourage BEVs (free parking, exemption from road tolls, vehicle taxes) / Energy efficiency
[34] (2013)	Purchase price	GHG Emission	Government subsidies	Subsidies / Fiscal policies (carbon tax, fuel tax) / Investments in R&D of low-carbon technologies (PV, EV and smart grid batteries)
[45] (2007)	Investment cost	GHG Emission	None	R&D Studies / Renewable Energy Sources
[42] (2017)	Investment cost / Energy cost	GHG Emission	None	Renewable Energy Source / Carbon Offset Projects / Using Carbon Purifiers / Energy Efficiency / Technological Innovation

[12] (2019)	Operating costs / Investment cost	GHG Emission	Public incentives	Use of biofuels / Transport management / Infrastructure investments, new vehicle technologies and alternative fuels / Government subsidies (purchase of vehicles, charging stations, operations and maintenance)
[30] (2017)	Vehicle purchase costs/ Cost of maintenance, batteries, electricity, construction of chargers (including land acquisition and paving)	GHG Emission	None	Energy Efficiency / Improved battery charging
[37] (2019)	Vehicle purchase price and operating cost / Maintenance cost / Recycling cost	GHG Emission	None	Low carbon hydrogen production / Adoption of alternative fuel vehicles / Energy Efficiency
[31] (2019)	Maintenance costs	GHG Emission	None	Changing individual behavior (Driving more efficiently by avoiding traffic congestion, accelerating the adoption of alternative fuel vehicles and charging for alignment with renewable electricity generation)
[38] (2019)	Fuel costs / Costs for electricity generators	GHG Emission	None	Renewable energy sources / Adoption of alternative fuel vehicles / Energy Efficiency
[39] (2018)	Purchase cost / Charging station cost / Fuel price / Maintenance cost / Battery replacement cost	GHG Emission	None	Renewable energy sources
[46] (2019)	Cost of electricity, battery and gasoline/ Vehicle purchase and maintenance/ Cost of recharging or battery exchange stations	GHG Emission	None	Energy Efficiency / Improved battery charging
[40] (2020)	Purchase cost	GHG Emission	Subsidies	Federal subsidies (tax credits for purchase and charging infrastructure) / R&D financing
[41] (2019)	Purchase, Operation, Maintenance and Taxes/ Recycling and Disposal Costs	GHG Emission	Subsidies / tax incentives	Promote electromobility / Energy Efficiency / Subsidies (purchase concessions, tax exemptions, free parking and access to restricted lanes and charging infrastructure)
[43] (2013)	Purchase cost	GHG Emission / Environmental Awareness	Subsidies / tax incentives / gender, age, education and income	Renewable energy sources / Adoption of alternative fuel vehicles / Energy Efficiency / Changing individual behavior

## 5 Final Considerations

This paper presented the role of the electric vehicles in carbon regulation policies related to the transport sector based on a survey of articles published in the Web of Science database until the year 2019. It was found that plug-in hybrid electric vehicle and battery electric vehicle were the models most discussed. In addition, the main topics of study are: vehicle battery autonomy, use of renewable energy sources, recharge stations and government subsidies. The articles also address consumer education aiming at increasing people's knowledge about their consumption behavior and helping them to make better choices to reduce emissions. A general concern is related to the cost (purchase, electricity, battery and maintenance).

Regarding GHGs emissions mitigation policies, carbon tax is the most studied, which can be explained by the fact that carbon trade policy is more complex. It is consonant with the World Bank (2020) report. However, there are several studies about carbon markets in Brazil and in the world [13] and it is expected to increase in the coming years due to the international targets and protocols.

Furthermore, we identified that mitigation policies would reduce emissions by encouraging companies to develop new low-carbon technologies. Besides it might generate government revenue. We also identified that the implementation of charging stations using electricity from photovoltaic panels can be an alternative to replace fossil fuel generation.

As a limitation of this research, we highlight that the results are related to keywords and the database. In addition, there is a lack of consolidated data, mainly for electric vehicles, as this is an area of recent interest. For future studies, it is suggested the evaluation of the transport sector emissions, the development of applied research considering the implementation of carbon policies (such as carbon trading), the evaluation of government subsidies in relation to electric vehicles in Brazil and in the world.

## Acknowledgments

The authors thank CNPq for the scientific initiation scholarship provided and to the CYTED Thematic Network “Ciudades Inteligentes Totalmente Integrales, Eficientes y Sostenibles (CITIES)” process number 518RT0558.

## References

- [1] EPE. Precificação de carbono: riscos e oportunidades para o Brasil. Relatório, 2020.
- [2] Ministério da Ciência, Tecnologia, Inovações e Comunicações. Estimativas anuais de emissões de gases de efeito estufa no Brasil. 5ª edição, 2020.
- [3] Observatório do Clima. Análises das emissões brasileiras de gases de efeito estufa e suas implicações para as metas do Brasil, 2019.
- [4] WWF-Brasil. As Mudanças Climáticas. Disponível em: <[https://www.wwf.org.br/natureza\\_brasileira/reducao\\_de\\_impactos2/clima/mudancas\\_climaticas2/](https://www.wwf.org.br/natureza_brasileira/reducao_de_impactos2/clima/mudancas_climaticas2/)>

- [5] Neocharge. O que são veículos elétricos. Disponível em: <<https://www.neocharge.com.br/tudo-sobre/carro-eletrico/veiculo-eletrico>>
- [6] EPE. Matriz Energética e Elétrica. Disponível em: <<https://www.epe.gov.br/pt/abcdenergia/matriz-energetica-e-eletrica>>
- [7] Guimarães, V., Lima, R., Ferreira, M., González, P. “Carbon regulation policies in transport: a review”, CITIES, 2020.
- [8] Lima, R., Ferreira, M., Boloy, R., Guimarães, V. “Avaliação das políticas de regulação de carbono no setor de transporte”, CIEEMAT 2020.
- [9] Carbon-Cap? Carbon emission mitigation by Consumption-based Accounting and Policy. Disponível em: <<https://www.carboncap.eu/what-is-carbon-cap>>
- [10] World Bank. Pricing Carbon. Disponível em: <<https://www.worldbank.org/en/programs/pricing-carbon>>
- [11] Bluevision. Como Funcionam Os Créditos De Carbono 2019. Available in: <<https://bluevisionbraskem.com/inteligencia/economia-florestal-como-funcionam-os-creditos-de-car-bono/>>
- [12] Cagliano, A.C., Carlin, A., Mangano, G., Rafele, C. “Analyzing the diffusion of eco-friendly vans for urban freight distribution”, International Journal of Logistics Management, 2017.
- [13] Gusmão, F., F.B. Carloni, W. B.A, Wills, M. Netto e C.E. Ludena. (2015). Estudos sobre Mercado de Carbono no Brasil: Análise da Alocação de Permissões. Banco Interamericano de Desenvolvimento, Monografia No. 309, Washington DC.
- [14] Chen, H., Geng, J.C., LI, W.B., Long, R.Y., Yang, M.Y., Yang, T. “Effects of personal carbon trading on the decision to adopt battery electric vehicles: Analysis based on a choice experiment in Jiangsu, China”, Applied Energy, v. 209, pp. 478–488, 2018.
- [15] Marano, V., Rizzoni, G., Tulpule, P.J., Yurkovich, S. “Economic and environmental impacts of a PV powered workplace parking garage charging station”, Applied Energy, v.108, pp. 323–332, 2013.
- [16] Instituto Nacional De Eficiência Energética. Sobre veículos elétricos. Disponível em: <[http://www.inee.org.br/veh\\_sobre.asp?Cat=veh](http://www.inee.org.br/veh_sobre.asp?Cat=veh)>
- [17] Neocharge. Tipos De Veículos Elétricos. Disponível em: <<https://www.neocharge.com.br/tudo-sobre/carro-eletrico/tipos-veiculos-eletricos>>
- [18] Calçado, T. “Estudo Preliminar de Implantação de Estações de Recarga de Veículos Elétricos no Centro de Tecnologia da UFRJ”, TCC, 2015.
- [19] IDC Corporate USA. Disponível em: <<https://www.idc.com/prodserv/insights#government>>
- [20] Iberdrola. Mobilidade Sustentável. Disponível em: <<https://www.iberdrola.com/sustentabilidade/mobilidade-sustentavel>>
- [21] Rodrigues, M.; Ferreira, C. Rio De Janeiro Lança Parceria Público-Privada Para Transporte Com Emissão Zero. UOL. Disponível em: <<https://economia.uol.com.br/noticias/pr-newswire/2013/06/19/rio-de-janeiro-lanca-parceria-publico-privada-para-transporte-com-emissao-zero.htm>>
- [22] Universidade De São Paulo. IEE inaugura primeiro eletroposto em São Paulo para veículos elétricos. Disponível em: <<https://www5.usp.br/noticias/tecnologia-2/iee-inaugura-primeiro-eletroposto-em-sao-paulo-para-veiculos-eletricos/>>
- [23] Itaipu Binacional. Veículos Elétricos. Disponível em: <<https://www.itaipu.gov.br/tecnologia/veiculos-eletricos>>
- [24] Hauffe, R., Michalek, J.J., Samaras, C., Shiau, Ching-Shin. “Impact of battery weight and charging patterns on the economic and environmental benefits of plug-in hybrid vehicles”, Energy Policy, v. 37, pp. 2653–2663, 2009.
- [25] Tulpule, P., Marano, V., Yurkovich, S., Rizzoni, G. “Economic and environmental impacts of a PV powered workplace parking garage charging station”. Applied Energy, v. 108, pp. 0306–2619, 2013.
- [26] Büchs, M., Schnepf, S. “Who emits most? Associations between socio-economic factors and UK households' home energy, transport, indirect and total CO2 emissions”. Ecological Economics, v. 90, pp.0921–8009, 2013.

- [27] Horne, M., Jaccard, M., Tiedemann, K. "Improving behavioral realism in hybrid energy-economy models using discrete choice studies of personal transportation decisions", *Energy Economics*, v. 27, pp. 0140-9883, 2005.
- [28] Cachon, G. "Retail Store Density and the Cost of Greenhouse Gas Emissions". *Management Science*, pp. 1–19, 2014.
- [29] Verneque, F. H. A.; Ferreira, M. A.; Guimarães, V. A. Otimização das estações de recarga de veículos elétricos: um estudo da literatura. CASI, 2021.
- [30] Li, J., Lu, Q., Tang, J., Wang, D., Ye, B. "Economic Analysis of Photovoltaic Electricity Supply for an Electric Vehicle Fleet in Shenzhen, China", *International Journal of Sustainable Transportation*, v. 8, pp. 202-224, 2014.
- [30] Kockelman, K.M., Loeb, B. "Fleet performance and cost evaluation of a shared autonomous electric vehicle (SAEV) fleet: A case study for Austin, Texas", *Transportation Research Part A*, v. 121, pp. 374–385, 2019.
- [31] Jones, E.C., Leibowicz, B.D. "Contributions of shared autonomous vehicles to climate change mitigation", *Transportation Research Part D*, v. 72, pp. 279–298, 2019.
- [32] Li, J., Lu, Q., Tang, J., Wang, D., Ye, B. "Economic Analysis of Photovoltaic Electricity Supply for an Electric Vehicle Fleet in Shenzhen, China", *International Journal of Sustainable Transportation*, v. 8, pp. 202-224, 2014.
- [33] Johansson, B. "Strategies for Reducing Emissions of Air-Pollutants from the Swedish Transportation Sector", *Transportation Research Part A*, v. 29, pp. 371-36199, 1995.
- [34] Popiolek, N., Thais, F. "Multi-criteria analysis of innovation policies in favour of solar mobility in France by 2030", *Energy Policy*, v. 97, pp. 202–219, 2016.
- [35] Asgerirsson, E.I., Davidsdottir, B., Leaver, J.D., Shafiei, E., Stefansson, H. "Energy, economic, and mitigation cost implications of transition toward a carbon-neutral transport sector: A simulation-based comparison between hydrogen and electricity", *Journal of Cleaner Production*, v. 141, pp.237-247, 2017.
- [36] Masui, T., Oshiro, K. "Diffusion of low emission vehicles and their impact on CO2 emission reduction in Japan", *Energy Policy*, v. 81, pp. 215–225, 2015.
- [37] Hewage, K., Perera, P., Sadiq, R. "Are we ready for alternative fuel transportation systems in Canada: A regional vignette", *Journal of Cleaner Production*, v.166, pp.717-731, 2017.
- [38] Donald, J., Fowler, M., Keller, V., Lyseng, B., Palmer-Wilson, K., Robertson, B., Rowe, A., Scholtysik, S., Wade, C., Wild, P. "Electricity system and emission impact of direct and indirect electrification of heavy-duty transportation", *Energy*, v. 172, pp. 740-751, 2019.
- [39] Ishida, H., Leaver, J.D., Shafiei, E., Watabe, A. "Impact of low emissions vehicles on reducing greenhouse gas emissions in Japan", *Energy Policy*, v. 130, pp. 227–242, 2019.
- [40] Linn, J., Mcconnell, V. "Interactions between federal and state policies for reducing vehicle emissions", *Energy Policy*, v. 126, pp. 507–517, 2019.
- [41] Kiarizis, S., Nanaki, E.A., Xydis, G.A. "Are only demand-based policy incentives enough to deploy electromobility?", *Policy Studies*, 2020.
- [42] Lokey, E. "How the next US president should slow global warming", *Energy Policy*, v. 35, pp. 5399–5402, 2007.
- [43] Chen, F.Y., Chen, H., Li, C.F., Li, W.B., Long, R.Y., Yang, M.Y., Zheng, X. "Would personal carbon trading enhance individual adopting intention of battery electric vehicles more effectively than a carbon tax?", *Resources Conservation and Recycling*, v. 149, pp. 638–645, 2019.
- [44] Associação Brasileira do Veículo Elétrico. IPVA para veículos elétricos, 2017. Disponível em:<<http://www.abve.org.br/ipva-para-veiculos-eletricos/>>
- [45] Erdinc, O., Karakas, A., Uzunoglu, M., Yagcitekin, B. "Assessment of electrically-driven vehicles in terms of emission impacts and energy requirements: a case study for Istanbul, Turkey", *Journal of Cleaner Production*, pp. 1-7, 20, 2014.
- [46] Dong, D.C., Liu, X., Wang, N. "A Cost-Oriented Optimal Model of Electric Vehicle Taxi Systems", *Sustainability*, 2018.

## Educación en eficiencia energética para el desarrollo de ciudades inteligentes: fortaleciendo la conciencia ambiental ciudadana.

José Gabriel Pérez Canencio<sup>1,2,3</sup>, Mary Luz Ojeda Solarte<sup>1,2,4</sup>, Andrés Rey Piedrahita<sup>1,2,5</sup>, Daniel Hernán Moreno Gutierrez<sup>1,2,6</sup>

<sup>1</sup> Unidad Central del Valle del Cauca, Tuluá. Colombia

<sup>2</sup> Grupo de Investigación Gigae3d, Facultad de ingeniería, Unidad Central del Valle del Cauca

<sup>3</sup> jperez@uceva.edu.co

<sup>4</sup> mojeda@uceva.edu.co

<sup>5</sup> arey@uceva.edu.co

<sup>6</sup> daniel.moreno01@uceva.edu.co

**Resumen.** Apostarle al desarrollo de las ciudades inteligentes a partir de conceptos como eficiencia energética, emisiones contaminantes y cambio climático es un reto interesante que conduce a pensar estrategias que permitan a la población conocer los problemas y crear soluciones asociadas a estos conceptos.

El crecimiento permanente de la población mundial y sus necesidades obliga a los Gobiernos a satisfacer la demanda en servicios esenciales y aumentar la generación de recursos energéticos.

La utilización administrada y racional de la energía eléctrica es vital para disminuir las emisiones de gases de efecto invernadero que se generan por el uso de este recurso esencial.

El problema que se aborda en este artículo es la necesidad de educar a la ciudadanía para que haga un uso eficiente del recurso energético para disminuir emisiones contaminantes. Se presenta un marco de trabajo con fundamento en los postulados para la educación ambiental contenidos en la carta de Belgrado y la incorporación de herramientas tecnológicas aplicables en ciudades inteligentes para alcanzar el propósito de Educar y aumentar la conciencia ambiental ciudadana

Como resultado se incluye un marco de trabajo que se ejecuta por medio de talleres por el cambio climático y en la discusión y conclusiones se muestran las fases del taller que conducen a la sensibilización de personas en el tema de calentamiento global, cambio climático y la forma como pueden aumentar su conciencia ambiental y aportar para disminuir los impactos de las emisiones sobre el planeta, lo cual representa una oportunidad para el desarrollo de ciudades inteligentes.

2

**Palabras clave:** Eficiencia energética, educación ambiental, Green It, cambio climático, talleres de sensibilización ambiental

## 1 Introducción.

No cabe duda que el consumo energético en la ciudad es un tema de gran interés para los Gobiernos, especialmente por el auge moderno de la ciudad como destino final de la población.

En la medida en que una ciudad antigua crece se vuelve más segura y con el tiempo se va convirtiendo en el centro del comercio y la economía fortaleciendo lugares de consumo tales como restaurantes, teatros, clubes, bares o grandes centros comerciales que terminan atrayendo a la población circundante y como consecuencia aumenta la demanda energética [1]; tal como lo afirma Glaeser

Al cambiar el verde de la naturaleza del campo por el gris de las ciudades, se encuentra con fenómenos muy particulares como la contaminación ambiental propia de las urbes donde la concentración de la población aumenta las emisiones de CO<sub>2</sub> y otros gases efecto invernadero que terminan afectando la salud humana. [2], razón por la cual se hace necesario trabajar en el desarrollo del concepto de ciudad sostenible.

Un efecto inmediato de las grandes concentraciones de población en las ciudades es el incremento de las necesidades básicas en una relación directamente proporcional, que deben ser atendidas por los Gobiernos mediante sus instituciones. Este hecho provoca de inmediato que los centros de atención de estos servicios esenciales incrementen el uso de las redes móviles a través de internet para la prestación de los servicios obligando al fortalecimiento de la infraestructura de comunicaciones que conlleva al aumento del consumo de energía eléctrica.

Otro aspecto a tener en cuenta es el uso de las tecnologías de la información y las comunicaciones TIC para el atender las necesidades básicas; en síntesis, las TIC se hacen presentes en la actividad normal de la ciudadanía y consumen recursos energéticos.

De igual forma, nos encontramos con el ecosistema económico que mueve a la ciudad, representado en las organizaciones y sus modelos de negocio que utilizan el potencial de las TIC para impulsar su actividad y creando la fuerza de trabajo necesaria para atender la demanda de productos y servicios de la población. [3]

La atención y la prestación de servicios como los mencionados y otros haciendo uso de las TIC ha conducido a autores como [4] a configurar una definición de ciudad inteligente a partir de conceptos como eficiencia energética, emisiones contaminantes, cambio climático, envejecimiento de la población, calidad de vida, competitividad o la transparencia en la toma de decisiones que en suma responde a las necesidades y los

retos que tienen planteadas las ciudades contemporáneas a partir de aspectos como complejidad, diversidad e incertidumbre.

De acuerdo con la Unidad de Planeación Minero Energética UPME [5], Colombia cuenta con una capacidad instalada aproximada de 14.4 GW de los cuales el 69.9% es por generación hidráulica, 24.8% térmicas a gas, 4.9% térmica a carbón, 0.3% cogeneraciones y 0.1% eólicos, tal como se muestra en la figura 1. Dependemos en gran medida de la generación por hidroeléctricas, por eso es importante que se aborde el tema de la eficiencia energética para crear conciencia ambiental en la ciudadanía a cerca de los beneficios de cuidar este recurso y administrarlo de la mejor manera posible y por consiguiente también se cuida el agua y las fuentes naturales.

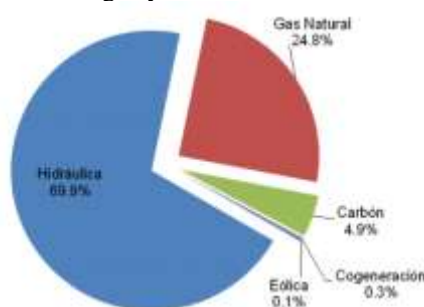


Fig. 1 Distribución del parque de generación eléctrica Colombiano según fuente: XM

Al revisar la literatura, hemos identificado un vacío conceptual relacionado con la necesidad de educar a la ciudadanía [6] en temas ambientales para que haga un uso eficiente del recurso energético y evitar despilfarros mitigando las emisiones de gases efecto invernadero GEI que se generan por el uso de la energía eléctrica proveniente de las fuentes hídricas.

Como aporte, este artículo presenta un marco de trabajo en el tema de la Educación ambiental y eficiencia energética en la ciudad inteligente, que se ha venido implementando mediante talleres sobre cambio climático con foco principal en los hábitos de consumo de los usuarios de las TIC.

Este artículo se estructura de la siguiente forma: en la sección 2, se presentan los fundamentos en relación a los objetivos de desarrollo sostenible, los objetivos de la educación ambiental y las iniciativas de la UPME en el tema de la demanda energética, el cambio climático y su relación con la energía eléctrica, el Green It como alternativa para reducir emisiones de GEI, en la sección 3, se abordan los aspectos metodológicos definidos para desarrollar el marco de trabajo en educación ambiental y eficiencia energética; en la sección 4, se presentan los resultados obtenidos con los talleres por el cambio climático; en la sección 5 y 6, la discusión y las conclusiones acerca de los logros alcanzados con los talleres y la sensibilización de la ciudadanía en estos temas.

4

## **2 Fundamentos.**

### **2.1 Legislación Colombiana en eficiencia energética.**

El Gobierno Colombiano por intermedio del Ministerio de Minas y Energía impulsa programas para el desarrollo y promoción de la gestión eficiente de la energía a partir de la ley 1715 de 2014 [7] y subsiguientes, esta ley contiene consideraciones especiales en el tema del fortalecimiento de la investigación y los requisitos ambientales para favorecer el consumo sostenible de energía en el país. Esta ley es fundamento para el marco de trabajo en educación ambiental y eficiencia energética que se ha implementado y divulgado en varios escenarios universitarios a nivel nacional e internacional.

### **2.2. Los Objetivos de desarrollo sostenible de referencia**

Indudablemente, los objetivos de desarrollo sostenible ODS, son una guía de gran importancia para el desarrollo de este trabajo porque constituyen un marco de referencia para abordar los temas de educación ambiental, especialmente cuando nos enfocamos en aquellos objetivos asociados con la energía y el cambio climático: [8]

ODS 7: Garantizar el acceso a una energía asequible, fiable, sostenible y moderna para todos

ODS 11: Lograr que las ciudades y los asentamientos humanos sean inclusivos, seguros, resilientes y sostenibles

ODS 13: Adoptar medidas urgentes para combatir el cambio climático y sus efectos

Consideramos que todos los esfuerzos que se hagan por cumplir estos objetivos aportan significativamente a disminuir las emisiones de gases de efecto invernadero, en especial las que se producen cuando se consume energía eléctrica proveniente de las hidroeléctricas.

### **2.3 La educación ambiental desde la mirada del seminario de Belgrado**

El Seminario Internacional fue celebrado en Belgrado en 1975, organizado por la UNESCO y el PNUMA como plataforma de lanzamiento del Programa Internacional de Educación Ambiental.

La Carta de Belgrado, un documento resultante del seminario que clarifica ampliamente las metas, objetivos y procedimientos de un movimiento en favor de la educación ambiental desde una perspectiva muy clara de los modelos económicos y de sus repercusiones ecológicas y sociales.

Tal como se menciona en [9] “Es absolutamente vital que los ciudadanos del mundo insistan en que se tomen medidas en apoyo de un tipo de crecimiento económico que no tenga repercusiones nocivas sobre la población, que no deteriore de ningún modo su medio ni sus condiciones de vida. Es necesario encontrar la forma de que ninguna

nación crezca o se desarrolle a expensas de otra, y de que ningún individuo aumente su consumo a costa de otros”

Esta afirmación hace referencia a la sostenibilidad ambiental, concepto que es fundamento importante de este trabajo.

En las Recomendaciones Finales de la Conferencia se confirma el vínculo entre la educación ambiental y los modelos y problemas del desarrollo. Estas son, textualmente, algunas de las recomendaciones:

“Ayudar a comprender claramente la existencia e importancia de la interdependencia económica, social, política y ecológica.

Considerar el medio ambiente en su totalidad, es decir, en sus aspectos naturales y creados por el hombre, tecnológicos y sociales (económico, político, técnico, histórico-cultural, moral y estético)

Considerar de manera explícita los aspectos ambientales en los planes de desarrollo y de crecimiento”.

Por lo anterior, este trabajo se ha diseñado desde las recomendaciones de la Carta y atiende los conceptos de los ODS mencionados.

## **2.4 Cambio climático y gases de efecto invernadero**

Los GEI absorben y emiten radiación en determinadas longitudes de ondas del espectro de radiación infrarroja emitido por la superficie de la Tierra, la atmósfera, y las nubes [10]. El dióxido de carbono(CO<sub>2</sub>) es uno de ellos.

Las emisiones de GEI impactan el balance climático global causando efectos adversos sobre las condiciones para la supervivencia de la vida en el planeta. [11]

La Huella de carbono, [10] es una forma de medir el impacto que deja una persona sobre el planeta, por actividades cotidianas o por la comercialización de un producto.

Se ha clasificado en tres alcances que definen las emisiones directas, indirectas y combinadas. Para este trabajo, se considera el alcance 2 que hace referencia a las emisiones indirectas originadas por las compras de electricidad y vapor que nos conduce a los conceptos de eficiencia energética en las ciudades.

## **2.5 La energía eléctrica y su relación con el cambio climático**

Al comprar electricidad generada en centrales hidro electricas, se contribuye a la emisión de gases de efecto invernadero, debido a que en el proceso de transformación de agua en electricidad. tanto en el recorrido que hace el agua cuando cae de la represa a la sala de máquinas como en el embalse, se libera CO<sub>2</sub>. Lo preocupante es que cuando

6

el agua sale de la central y sigue río abajo, se continúa el fenómeno por varios kilómetros.

Sin embargo, esta es una condición inmodificable y por eso las compañías productoras de energía eléctrica ejecutan planes de recuperación de ecosistemas afectados y de compensación de la huella de carbono.

El Ministerio de Minas y Energía, calcula la relación de la cantidad de toneladas de CO<sub>2</sub> en función de los megavatios de energía generada. [12]. Esta relación se llama Factor de Emisión.

La relación entre la cantidad de energía utilizada en una actividad y la prevista para su realización hace referencia a la eficiencia energética. De acuerdo con una publicación de [13] “La eficiencia energética es clave para que Colombia cumpla con reducción de la emisión de gases de efecto invernadero adquirida en la Cumbre por el Cambio Climático - COP21 realizado en París en el año 2015. Se ha identificado que un 40% de esta meta podría cumplirse solo con eficiencia energética”

De igual forma la inficiencia energética se refiere al desperdicio de energía que se produce cuando se hace mal uso de la misma. Por ejemplo usando más de la energía eléctrica necesaria para alguna actividad, usando luces más tiempo del requerido o simplemente cuando se deja un aparato eléctrico o electrónico apagado pero recibiendo una carga eléctrica. El presidente de Andesco, Camilo Sanchez afirmó que a “Colombia le cuesta 21 billones de pesos anuales el despilfarro de la energía” [13]

## **2.6 Factor de Emisión - Ministerio de minas y energía**

La unidad de planeación minero energética, UPME, [14] entidad adscrita al Ministerio de Minas y Energía publica anualmente la resolución que define el factor de emisión anual para efectos de cálculo de la huella de carbono corporativa y en hogares para el Sistema de Interconexión Nacional, SIN

A este dato del Factor de Emisión utilizado para los cálculos de la huella de carbono de alcance 2 se hace referencia en la sesión de resultados de este artículo

Como antecedente importante para este trabajo, cabe mencionar que entre los años 2018 y 2019, los autores de este artículo realizaron un proceso de aplicación de la norma ISO / IEC 33000 para validar un modelo de madurez en el cual se mencionan prácticas verdes responsables con el medio ambiente, utilizando como parte de la fórmula de cálculo el factor de emisión del año 2017 [15]

## **2.7 Cifras de la demanda energética en Colombia**

De acuerdo con cifras publicadas por la UPME, el comportamiento de la demanda energética en Colombia está muy relacionado con el crecimiento económico del país y

7

eventos como los racionamientos de 1992 o la recesión económica de 1999 y la desaceleración económica de 2009 que han provocado alguna discontinuidad en el porcentaje de crecimiento. La siguiente figura 2 ilustra este comportamiento y se estima que para la década de 2020 a 2030 el crecimiento esté por el orden del 2.9% [5]

Como se puede notar, la demanda energética mantiene un crecimiento permanente provocado por la creciente demanda energética de los colombianos y la venta de este recurso a otros países.

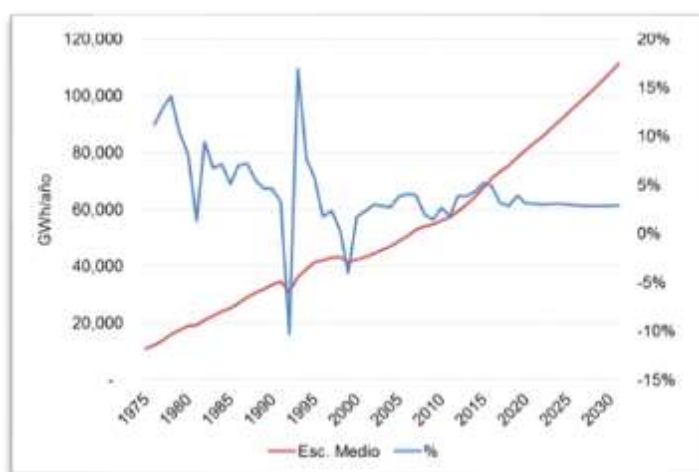


Fig. 2 Tasa de crecimiento anual y proyección de demanda de energía eléctrica. Fuente UPME. La demanda energética la representa la curva roja

## 2.8 Green IT. Tecnologías verdes

Para el área de las Tecnologías de la Información TI en la organización, han surgido diferentes prácticas sostenibles conocidas como prácticas de TI verde. Algunas de estas prácticas son aplicadas para gestionar el consumo energético en los dispositivos de TIC. [15]. Las prácticas verdes conocidas como Green It, se clasificado en:

**Green in IT:** cuando las propias TI tienen un impacto en el medioambiente, debido a su consumo energético y las emisiones que producen, y dicho impacto debe reducirse (es decir, las TI como productor). **Green by IT:** en el sentido de que las TI proporcionan las herramientas necesarias que permiten llevar a cabo tareas de diversa índole de una manera sostenible con el medioambiente (Las TI como habilitador o capacitador). Referenciado por [15]

## 3. Metodología

8

Abordamos una metodología desde las acciones que pueda hacer el hombre por la naturaleza y por sí mismo y que lo conduzcan a vivir en armonía con el planeta en ciudades sostenibles, sin embargo, estamos convencidos de que es una tarea difícil dadas las condiciones humanas que lo han impulsado a fabricar productos y/o a ofrecer servicios sin tener en cuenta que muchas de sus acciones generan gases de efecto invernadero que terminan haciendo el daño y provocando el calentamiento global.

Por eso, un punto de partida que nos ha impulsado a generar este trabajo es el concepto de educar en la sostenibilidad ambiental y la eficiencia energética desde los claustros universitarios para que el ciudadano fortalezca su relación con el medio ambiente de una manera natural y voluntaria

Con base en la metodología investigación- acción – participación que permita construir soluciones desde los O.D.S. en escenarios diversos por medio del diálogo constructivo con los actores mencionados el equipo definió un marco de trabajo -framework - basado en los Objetivos de la Educación Ambiental consagrados en la Carta de Belgrado y en acciones para administrar la eficiencia energética, que se incluye en la sección de resultados, como producto de la aplicación de una metodología propia de 3 fases, Figura 3.

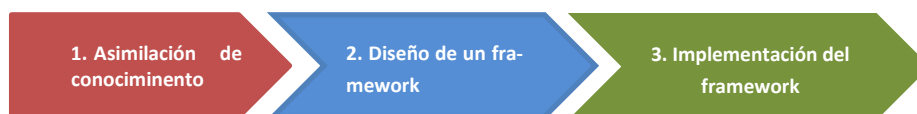


Fig. 3 Metodología de trabajo diseñada por los autores

1. Asimilación de conocimiento. En esta fase inicial se aborda el tema de la conciencia ambiental con el propósito de analizar y entender los hábitos de los ciudadanos en el uso de la tecnología que generan ineficiencia energética con las consecuencias negativas en la generación de gases efecto invernadero que afecta la convivencia en las ciudades inteligentes, teniendo en cuenta los saberes ancestrales y populares que con sus experiencias nos enriquecen el conocimiento.

2. Diseño de un framework. Diseñar un marco de trabajo a partir de los postulados de la educación ambiental que conduzca a la sensibilización del ciudadano en las temáticas relacionadas con el cambio climático y el cuidado del medio ambiente para el fortalecimiento de las ciudades inteligentes desde el uso de la tecnología.

3. Implementación del framework. En un formato de taller interactivo, aplicar el framework en comunidades universitarias y en otros grupos sociales para impulsar acciones de eficiencia energética que fortalezcan la sostenibilidad de las ciudades en el marco de la acción climática global impulsada por la ONU.

#### 4. Resultados.

Al aplicar la metodología diseñada desde el trabajo del grupo de investigación GIGAE3D de la facultad de ingeniería de la universidad a la cual están vinculados los autores, se construyó un marco de trabajo en educación ambiental y eficiencia energética—framework - que se ha llevado a varias instituciones de educación superior en la modalidad de talleres interactivos.

En el diseño del framework se incorporan como participantes a agentes, actores y diferentes grupos de interés de la sociedad para construir de manera colaborativa procesos de aprendizaje y práctica basados en los O.D.S.

Participantes del proyecto:

- La ciudadanía tanto individual como colectivamente
- La administración local de ciudades, instituciones y pequeños gobiernos
- Recursos técnicos y profesionales.

Aportes

- El saber ancestral y popular con sus experiencias y vivencias
- El saber político para la administración de recursos y las políticas públicas
- El saber científico de estudiantes y profesionales aportando métodos y técnicas de investigación de diferentes disciplinas desde las universidades.

El framework desarrollado tabla 1, se compone de: los objetivos de la educación ambiental según la carta de Belgrado, las acciones diseñadas para cada objetivo y la forma como se llevan a cabo las acciones implementando diversas actividades denominadas “Talleres por el cambio climático” que se desarrolla en tres momentos llamados fase 1, fase 2 y cierre.

Tabla 1 Framework desarrollado por los autores, para los talleres por el cambio climático

Objetivo de la Educación ambiental	Acción	Cómo
Conocimiento (Taller fase 1)	Transmitir conocimiento para facilitar la comprensión del ecosistema ambiental y sus relaciones con los actores de las ciudades inteligentes.	Conferencia con temas sobre: Cambio climático, calentamiento global, huella de carbono, consumo energético, eficiencia energética, cumbres mundiales por el clima y buenas prácticas tecnológicas Green It.
Actitudes	Impulsar al participante a trabajar por el mejoramiento del problema asociado con la generación de CO <sub>2</sub> como consecuencia del consumo energético.	Aplicación de un método de cálculo de la huella de carbono de alcance 2 para que el participante entienda el impacto que generan los consumos asociados a las acciones que realiza cotidianamente.

10

(Taller fase 1)	Los participantes consumen una aplicación móvil registrando sus consumos energéticos actuales. La aplicación calcula automáticamente el CO2 generado por los datos registrados.	
Sensibilización	Concientizar al ciudadano sobre los problemas y las consecuencias relacionadas con el cambio climático	Motivación sobre temas relacionados con el despilfarro de energía, el CO2 generado por el consumo energético y el impacto negativo que generan al medio ambiente
Aptitudes	Desarrollar habilidades para resolver problemas y luego transmitirlos a otros escenarios.	Impulsar al participante para que mediante su creatividad diseñe estrategias para disminuir el consumo energético aportando en la solución el problema del calentamiento global. Además aplique estas estrategias desde su hogar y luego las transfiera a las comunidades en las cuales está inmerso.
(Taller fase 2)	Los participantes usan la app para registrar sus nuevos consumos, aplicando estrategias para reducir los consumos anteriores. La aplicación calcula automáticamente el CO2 generado por los nuevos datos registrados.	
Capacidad de Evaluación	Desarrollar competencias y programas de educación ambiental	Enseñar al participante a que cree sus propios programas de educación ambiental en su comunidad. Práctica con los participantes para comprobar conocimientos mediante un test en una Aplicación móvil con componente lúdico.
(Taller fase 2)		
Participación	Desarrollar responsabilidad e involucrarse en la solución	Fomentar en los participantes al taller el compromiso con su planeta a partir de acciones propias y ajenas. Convertir al participante en un multiplicador de esta información en otras comunidades.
(Cierre del taller - conclusiones y compromisos)		

Con el fin de adquirir el conocimiento necesario que condujera a la construcción del framework, se hizo un trabajo con personas de algunas organizaciones y ciudadanos urbanos para conocer aquellos hábitos que generan despilfarros de energía, de igual forma se visitaron datacenters y oficinas para observar el comportamiento de los usuarios de las TIC y determinar en que actividades es recurrente la ineficiencia energética. Esta actividad se enriqueció con la lectura de artículos que se han publicado en revistas como Semana, XM y portales del gobierno en las cuales se mostraron cifras referentes al despilfarro de energía en el país. Posteriormente se calculó la generación de gases efecto invernadero que resultan del despilfarro energético para comprender la magnitud del problema ambiental.

Para implementar el framework, se han organizado talleres y se ha participado en eventos de instituciones universitarias, con el propósito de concientizar a los participantes para que comprendan la importancia de cuidar el recurso energético y de esa manera disminuir las emisiones de GEI y trabajar por una ciudad inteligente mas comprometida en los temas de eficiencia energética, emisiones contaminantes, cambio climático, envejecimiento de la población, entre otros.

Los talleres se desarrollan de la siguiente manera:

Mediante una aplicación web los participantes se inscriben y reciben un código de activación de la App que utilizará para el taller. Se inicia el taller con los participantes inscritos. En la figura 4 podemos ver algunos participantes durante la aplicación del taller, en la primera etapa se recibe la capacitación y posteriormente entran en contacto con la aplicación desarrollada.



Fig. 4 Imágenes de talleres realizados. Conferencia y utilización de la App

El taller inicia con la Fase 1. Mediante una conferencia se contextualiza a los participantes en el tema de calentamiento global, huella de carbono de alcance 2, crecimiento de la población mundial, ciudades sostenibles, causas y consecuencias de éstos fenómenos como resultado de la actividad antrópica, consumo energético, eficiencia energética, despilfarro de energía, CO<sub>2</sub> generado por el consumo energético y prácticas de Green It.

Los participantes descargan una aplicación móvil – app – y se les conduce a ejecutar los módulos de la misma iniciando por la calculadora para la huella de carbono de alcance 2. El propósito es que los participantes registren sus consumos energéticos actuales y comprendan mediante cifras sus propia generación de CO<sub>2</sub>. La app calcula automáticamente estas cifras. Los datos se envían automáticamente a una base de datos desplegada en un servidor en la nube.

12

La aplicación móvil desarrollada por el equipo cuenta con cuatro módulos interactivos los cuales juegan un importante papel durante el taller. En el primer módulo se encuentra una calculadora de CO<sub>2</sub> y mediante un menú se pueden escoger los diferentes dispositivos que tengan en casa e ingresarlos para calcular el consumo generado por ellos. En el segundo módulo se pone a prueba el conocimiento adquirido durante el taller a través de divertidas preguntas tipo juego lúdico. En el tercer módulo se despliega un ranking en donde se comparan los resultados obtenidos en el cuestionario enviado los participantes del taller. En el cuarto módulo se visualiza un bot que se encuentra en entrenamiento y puede responder cualquier pregunta relacionada con el tema del taller.

Para iniciar la Fase 2, los conferencistas intervienen de nuevo para explicar los problemas asociados con los consumos energéticos en la ciudad, la generación de CO<sub>2</sub> como resultado de estos consumos, los desperdicios de energía denominados consumo fantasma, buenas prácticas tecnológicas para reducir las emisiones de estos GEI mediante la aplicación de Green it tanto en el hogar como en las organizaciones; todo con datos reales de emisiones generadas por las TIC.

Se espera que en esta actividad se sensibilice a los participantes en estos temas y tomen conciencia acerca del daño que hacemos al planeta. Posteriormente se da a conocer el método de cálculo de la huella de carbono de alcance 2, así:

$HdC = DA * Fe * WGP$ ; donde: (ecuación 1)

HdC : huella de carbono de alcance2

DA : són los datos de actividad expresados en watios hora

Fe: es el factor de emisión publicado por la Upme.

WGP: es el potencial de calentamiento global publicado por GreenFacts [10]

Los participantes ingresan nueva información a la app esperando que voluntariamente reduzcan las cifras iniciales de tal manera que puedan comprender los beneficios de una administración eficiente de la energía y la disminución de GEI.

En la aplicación web, mediante un gráfico de barras, se despliegan los resultados de los cálculos de CO<sub>2</sub> realizados en ambas fases. Se espera que la segunda medición sea inferior a la primera.

Posteriormente, se termina la fase 2 con una práctica en otro módulo de la app para comprobar conocimientos mediante un cuestionario de preguntas sobre lo expuesto en el taller, incluyendo un componente lúdico que se visualiza en el módulo ranking que los participantes pueden ver para conocer sus puntajes y posiciones.

En la figura 5 se observan los diferentes módulos previamente descritos de la aplicación con los cuales los participantes interactúan en el taller.



Fig. 5 Interfaces gráficas de la app para el cálculo de la huella de carbono de alcance 2

En la figura 6 se muestran dos interfaces gráficas de la aplicación web que permite gestionar la información de cada taller y sus participantes.

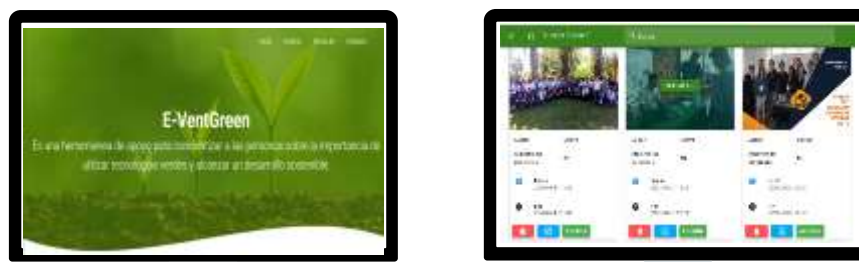


Fig. 6 Interface gráfica de la aplicación web para eventos e inscripciones

Se finaliza el taller con las conclusiones y compromisos. Para el cierre se invita a los participantes a que se comprometan con aportes a las soluciones a la problemática del cambio climático en las ciudades desde el concepto de la eficiencia energética y que divulguen esta información a sus comunidades para alcanzar ciudades inteligentes sostenibles.

Cada taller tiene una duración de 4 horas aproximadamente y se realizan con una frecuencia mensual. Cada organización en la cual se realiza el taller se convierte en un aliado estratégico para seguir con esta labor de concientizar a la población en general. Hasta ahora se ha logrado impactar a más de 500 personas a lo largo de los talleres realizados con diversas entidades entre las que se encuentran universidades y empresas del sector comercial e industrial y se calcula que cada una multiplique este conocimiento a diez personas de su círculo social.

### 5. *Discusión.*

Indudablemente, la eficiencia energética y la sostenibilidad están estrechamente relacionados con el desarrollo de las ciudades inteligentes. Este tema es abordado en los talleres por el cambio climático diseñado por los autores de éste artículo y representan

14

una oportunidad para que los participantes a estos eventos se concienticen sobre la importancia de cuidar el medio ambiente desde sus consumos energéticos.

Igualmente, se procura que se cierre el evento con compromisos que aporten soluciones a la problemática ambiental de las ciudades. El enfoque que se ha trazado en el framework diseñado desde la educación ambiental ha tenido una acogida importante en las instituciones que han recibido estos talleres.

La carta de Belgrado como fundamento para el marco de trabajo ha representado un eje fundamental para diseñar estrategias de solución a los problemas de sostenibilidad ambiental de las ciudades inteligentes desde la Educación en el tema de la eficiencia energética.

Consideramos importante que todo esfuerzo que se realice en favor del cambio climático será una nueva oportunidad para las generaciones futuras y un alivio para el planeta

La participación del grupo de investigación Gigae3d en eventos universitarios donde se ha tenido oportunidad de aplicar estos talleres por el cambio climático se muestran en la siguiente figura 7. En el año 2017 se inicia el proceso con un ciclo de conferencias en universidades de la región sur occidente y se continuaron de forma presencial hasta el 2019. En el año 2020 se han realizado de forma virtual debido a la emergencia nacional por la pandemia del Covid19.

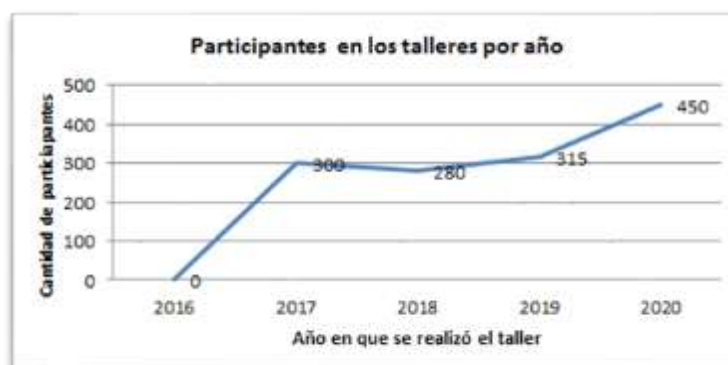


Fig. 7 Participantes en los talleres por año. Fuente: Grupo de investigación Gigae3d

Al finalizar los talleres se les solicita a los participantes que como compromiso divulguen la información recibida y logren concientizar como mínimo a otras 10 personas para que en conjunto aporten soluciones para reducir las emisiones de GEI desde la eficiencia energética y entre todos desarrollar una ciudad inteligente y sostenible.

## 6. Conclusiones

La educación ambiental es necesaria para contribuir al desarrollo de las ciudades inteligentes desde los conceptos de la sostenibilidad y el cuidado del ambiente para favorecer un planeta que hoy sufre los rigores de la acción antrópica indiscriminada por la generación continua de GEI.

El framework diseñado por los autores con fundamento en la educación ambiental y la eficiencia energética se convierte en una herramienta de gran valor para lograr los objetivos planteados por el grupo de investigación gigae3d, en el proyecto en favor del desarrollo de las ciudades inteligentes desde la concepción del cuidado del planeta

Este trabajo es una contribución a los compromisos del Gobierno nacional para atender los acuerdos pactados en la cumbre de las Naciones Unidas por el cambio climático celebrada en París en el año 2015 y en la cumbre de 2021

Las prácticas de Green It que se enseñan en los talleres por el cambio climático ayudan a reducir las emisiones de CO<sub>2</sub> desde el hogar, las comunidades y las organizaciones. Este hecho aporta significativamente un beneficio al planeta y al cambio climático, como sustento al desarrollo de las ciudades inteligentes

El trabajo que se está realizando mediante la aplicación de los talleres por el cambio climático favorece los siguientes aspectos de las ciudades: la eficiencia energética porque ayuda a sensibilizar a las personas sobre sus consumos y la forma de reducirlos; la reducción de las emisiones de GEI generadas por el consumo de energía eléctrica tanto en el hogar como en el comercio y la industria; retardo en el envejecimiento de la población por problemas de salud derivados de la contaminación del aire, puesto que se espera un ambiente más limpio; y mejora en la calidad de vida del ciudadano.

Es necesario despertar en las personas la conciencia ambiental ciudadana y mediante la educación que comprendan cómo desde las acciones diarias ponen en riesgo el planeta y sus generaciones, que entiendan que los recursos se deben utilizar de una manera racional.

Que las situaciones ambientales se conviertan en parte de su vida y en una preocupación constante para que adopten aptitudes, actitudes, compromisos y otros valores para luchar contra el cambio climático y también que si se unen con otros ciudadanos y trabajan sinérgicamente el planeta obtendrá mejores resultados hacia el futuro.

## Referencias

- [1] E. Glaeser, El triunfo de las ciudades: Cómo nuestra gran creación nos hace más ricos, más listos, más sostenibles, más. ., Barcelona: Taurus, 2018.

16

- [2] J. D. Pabón y R. S. Nicholls, «El cambio climático y la salud humana,» *Biomédica*, vol. 25, n° 1, pp. 5-8, 2005.
- [3] T. Zhiwei, K. Jayakar, X. Feng, H. Zhang y R. Peng, « Identifying smart city archetypes from the bottom up: A content analysis of municipal plans.,» *Telecommunications Policy*, vol. 43, n° 10, p. 101834, 2019.
- [4] J. M. Fernandez Guell, «Ciudades inteligentes: la mitificación de las nuevas tecnologías como respuesta a los retos de las ciudades contemporáneas,» *Economía industrial*, n° 395, pp. 17-28, 2015.
- [5] A. M. Macías Parra y J. Andrade, «Estudio de generación eléctrica bajo escenario de cambio climático,» Upme, Bogotá, 2012.
- [6] J. A. Cerrillo Vidal, «Medición de la conciencia ambiental: Una revisión crítica de la obra de Riley E Dunlap,» *Athenea digital*, vol. 1, n° 17, pp. 33-25, 2010.
- [7] Congreso de la República de Colombia, *Ley 1715 de 2014*, Bogotá, 2014.
- [8] FAO, «Objetivos de desarrollo sostenible,» de *El apoyo de la FAO para alcanzar los Objetivos de desarrollo sostenible en America del Sur*, Santiago de Chile, 2019.
- [9] Unesco, «Seminario Internacional de Educación Ambiental,» de *Environmental Education, a genuine education for sustainable development*, París, 1976.
- [10] GreenFacts, «Facts on health and the environment,» GreenFacts, 15 Agosto 2007. [En línea]. Available: <https://www.greenfacts.org/es/glosario/ghi/gas-efecto-invernadero.htm>. [Último acceso: 20 Agosto 2020].
- [11] WWF, «WWF - Glosario ambiental,» 03 Abril 2018. [En línea]. Available: <https://www.wwf.org.co/?uNewsID=325754>. [Último acceso: 15 Agosto 2020].
- [12] UPME, «UPME - Calculo d lfactor de emisión de CO2 del SIN,» UPME, 27 Diciembre 2019. [En línea]. Available: <https://www1.upme.gov.co/siame/Paginas/calculo-factor-de-emision-de-Co2-del-SIN.aspx>. [Último acceso: 12 Febrero 2020].
- [13] ANDESCO, «ANDESCO. Asociación Nacional de Empresas de servicios publicos y comunicaciones,» ANDESCO, 2 Mayo 2019. [En línea]. Available: <https://www.andesco.org.co/2019/05/07/la-ineficiencia-energetica-le-cuesta-a-colombia-21-billones-de-pesos-anuales/>. [Último acceso: 2 Abril 2020].
- [14] M. Madriñan Bonilla, H. H. Herrera Florez y J. D. Sanchez, «Factores de Emisión del Sistema Interconectado Nacional,» MinMinas, Santa Fé de Bogotá, 2017.
- [15] J. B. M. R. M. P. C. J. G. O. S. M. L. R. P. A. & P. V. M. Patón Romero, «Application of ISO/IEC 33000 to Green It: A case Study,» *IEEE Access*, vol. 7, pp. 116380 - 116389, 2019.
- [16] M. Novo, «La educación ambiental, una genuina educación para el desarrollo sostenible,» *Revista de educación*, pp. 195 - 217, 2009.
- [17] UPME, «UPME - SIAME,» 28 Diciembre 2019. [En línea]. Available: <https://www1.upme.gov.co/siame/Paginas/calculo-factor-de-emision-de-Co2-del-SIN.aspx>. [Último acceso: 16 Mayo 2020].

## Integration of PV technologies for rural sustainable tourism

M. Sánchez-Aparicio<sup>1</sup>[0000-0002-7931-9561], E. González-González<sup>1</sup>[0000-0002-8025-2464], J. Martín-Jiménez<sup>1</sup>[0000-0003-4383-9386], S. Del Pozo<sup>1</sup>[0000-0003-4869-3742], P. de Andrés<sup>1</sup>[0000-0001-7708-3260] and S. Lagüela<sup>1</sup>[0000-0002-9427-3864]

<sup>1</sup> University of Salamanca, Ávila 05003, Spain  
mar\_sanchez1410@usal.es

**Abstract.** Energy uses in rural and urban areas go from residential to industrial uses, including the services sector, which is the main activity in most cities and towns in countries such as Spain. The recent interest in nature and rural tourism by the citizens, especially increasing after the COVID-19 pandemics, has provoked a rise in the energy consumption by the assets related to tourism in rural areas. In order to comply with the objectives of the Agenda 2030 and the reduction in GreenHouse Gases emissions, the integration of renewable energies in the touristic uses in rural areas can be a solution. Solar PV technology is the most mature technology for the supply of electrical energy in self-consumption. Thus, this study evaluates the integration of solar PV panels in different rural tourism assets through a technological, environmental and economic analysis.

**Keywords:** Rural tourism; PV System; Solar energy; Sustainable development; Self-consumption

### 1 Introduction

In recent decades, tourism has been one of the fastest growing activities, becoming one of the main pillars of the economy of the countries [1]. Data from the World Travel Tourism Council (WTTC) indicate that in 2019, the tourism sector contributed 10.4% to World GDP [2]. Spain is one of the countries in which tourism is the main source of income. According to WTTC data, tourism in 2019 contributed 14.1% of GDP, with more than 2.8 million jobs [3]. This growth has the drawback of implying an increase in the energy demand of the tourism sector, with the consequent growth in GreenHouse Gases (GHG) emissions: the International Tourism Partnership (ITP) calculates that only the hotel industry should reduce its carbon emissions by 66% by 2030 and 90% by 2050 to meet the objectives established at COP25 [4]. According to [4], the carbon footprint of tourism involves 8% of global CO<sub>2</sub> emissions. In addition, tourism is indirectly involved in all Sustainable Development Goals, especially in SDG 8, SDG 11 and SDG 12, related to inclusive economic growth and decent work; sustainable cities and communities and responsible production and consumption [5].

With the pandemic caused by Covid-19 and the restrictions applied, many tourists have opted for national rural tourism [6]. But the focus of attention on rural areas has not only occurred after Covid-19. In recent times before the pandemics, rural areas in Spain have been object of preoccupation due to the rural depopulation commonly known as Empty Spain [7] where one of the possible solutions is to encourage rural tourism [8].

The increase in rural tourism entails an increase in energy needs, that requires an adaptation to the objectives of the 2030 Agenda, in order to be able to bear the seal of “Sustainable Tourism” [9]. In addition to contributing to reduce the inequalities within and between countries and to provide learning opportunities for both genders, the tourism sector should promote low carbon strategies for all stages: from the construction of touristic infrastructure to its use and operation. That is, the long-term sustainability of the tourism business is directly related to the correct management of the environment. In order to minimize the carbon footprint as much as possible, the main first solution is through the implementation of renewable resources [10]. Although there is a wide variety of renewable technologies, nowadays the photovoltaic solar technology is the most used not only due to the homogenization of the resource but also due to the cost, performance and level of integration of the technology [11–13]. Although Spain is not one of the countries with the highest installed power, it is one of the countries that receives the most solar radiation in Europe. The study [14] shows a clear example of the contribution of solar energy in the development of sustainable tourism.

One of the main advantages of solar energy is its versatility: the technology of solar panels has led to their adaptation to different positions, consequently allowing their installation for a variety of uses: from the most traditional uses in touristic villages [15], where the solar PV panels are combined with other renewable energies such as wind and biomass; to the energy supply in isolated areas such as the mountainous region of Annapurna [16] and the tropical area of Guapán hot springs in Ecuador [17]. Novel developments have allowed the solar exploitation in hotel windows, where solar film also works as shading element [18]; and in maritime vessels [19]. Awelewa et al. [20] show how solar energy in rural spaces can also be useful for lighting.

With this study, the aim is to carry out a technological, energy and economic analysis of the integration of solar technologies in one of the main rural tourism areas in Spain: protected natural areas. In this case, the implementation of solar PV installations is of special interest for several reasons: (i) reducing the carbon footprint in the tourism sector in the area; (ii) providing clean and sustainable electricity in isolated mountain locations otherwise dependent on fuel deposits; (iii) enabling the use of energy in isolated areas increasing their quality of use, by for example allowing the installation of public lighting.

## 2 Possibilities of self-consumption in rural spaces

Nowadays, the main use of solar energy is to produce electricity for self-consumption [21]. These installations, can be used connected to the electrical grid or not, and are usually used for defraying domestic consumption of energy. In rural areas, the isolated installations take on special relevance, since in many cases electricity is required at points that the electrical grid does not reach [22].

Within the rural environment, apart from domestic and accommodation buildings such as hotels or apartments, there are other types of buildings of special interest for the installation of solar panels: hostels and huts. Generally, these buildings are located in mountain areas and used by hikers. Although both allow the tourist to be housed and protected from inclement weather, there are some differences such as the size or the electrical connection. Hostels are large buildings that allow to accommodate a large number of people. The services available in these buildings vary a lot but there is usually a space to rest and cleaning and common areas mainly for food. Some of them also have air conditioning systems. Therefore, hostels are buildings with a large consumption of energy depending on the services. Hostels are usually next to urban areas and are accessible. Instead huts are small buildings for few hikers with complex access far from rural areas without connection to the electrical grid.

The energy consumption involved in mobility is another interesting point of use for solar energy [23]. With the rise of electric vehicles it is increasingly necessary to install points for their recharging. In urban zones, the recharging points that are being installed are individual and powered by the electrical grid. In areas with large surfaces, the installation of solar recharging points using canopies is a common alternative. In rural areas, especially in areas far from the urban center that the electrical grid does not reach, the installation of solar parkings is interesting. Thanks to this option, users or electric vehicles can go and enjoy rural tourism.

Another important aspect in mountain areas is the security of the tourist. This type of spaces usually has no illumination due to the lack of electrical grid. In this sense, the installation of different PV technologies such as streetlights [24] or traffic signals [25] are a good option for improving the safety of both pedestrians and drivers.

## 3 Solar technologies for energy use

Within the solar market, there is a wide variety of alternatives for the production of electricity for self-consumption. All of them are based on the integration of solar panels in different types of structures (Fig. 1).

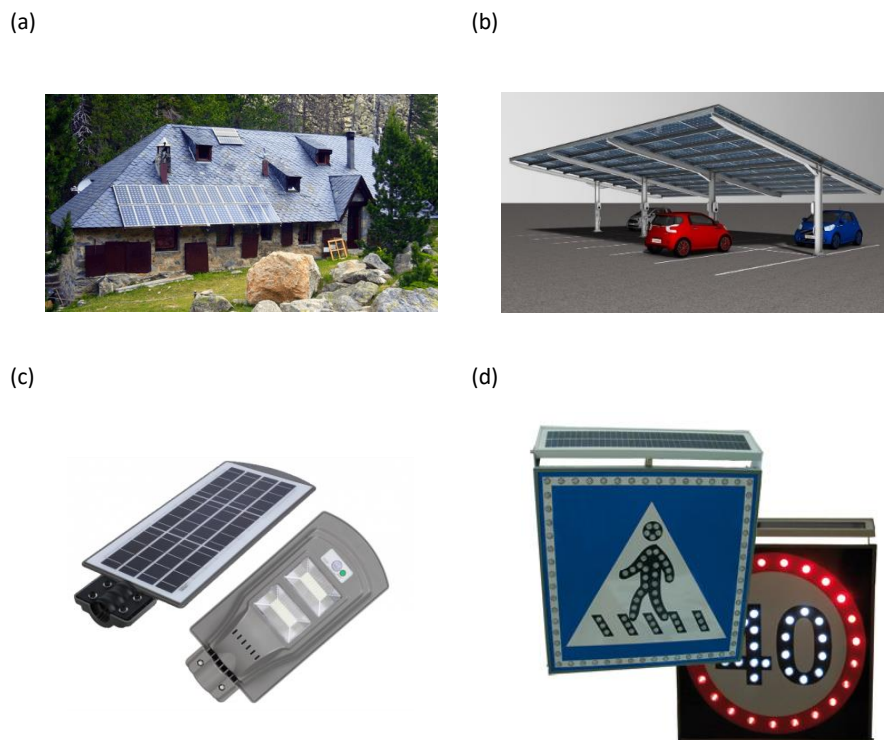


**Fig. 1.** Examples of integration of solar panels for the generation of electricity in: (a) buildings [26] (b) parking [27] (c) streetlights [28] (d) traffic signals [29].

### 3.1 Buildings

Solar panels installed in buildings are the most used PV technology for the production of clean energy for self-consumption. In this case, solar panels can be installed in an integrated way with the same orientation and slope of the rooftop or with different orientation or/and slope of the rooftop using a metal structure. The power of the solar installation is variable, depending on the needs.

### 3.2 Parking

Solar canopies are the main alternative to recharge electric vehicles though the integration of solar panels in the rooftop. This kind of structure has an enormous potential of integration in public spaces and has two important functions: (i) to be a covered parking area allowing to protect the vehicles from inclement weather (ii) to produce clean energy during the day. They are prefabricated modular structures that can be

expanded according to the needs. The slope of the rooftop has a low value, no more than 10 degrees.

### 3.3 Streetlights

LED streetlights are one of urban furniture most used for solar use. There is a wide variety of models of solar streetlights: from streetlights in which the solar panel allows any orientation and slope to streetlights that integrate the panel with a fixed orientation and slope. Nowadays, all the streetlight models are LED due to their low consumption and high lighting. In order to optimize energy consumption, these structures integrate a motion sensor and also a small battery inside for storing the generated energy.

### 3.4 Traffic signals

Although not as a direct way such as streetlights, LED traffic signals are other urban furniture that can help to improve the safety of the tourists. These elements are powered by small solar panels and integrate batteries into their structure. They usually have a twilight sensor that allows to adjust the light according to the darkness.

## 4 Energy and economy analysis

The evaluation from the economic and energetic perspective of the different technologies previously described is carried out through an example of the solar installation in a hostel, a hut and a parking area implementing lighting and traffic signals. Average dimension values and mean solar radiation in Spain are considered for the computations. A location in the North hemisphere is considered, in such a way that the South orientation of the panels is the optimal.

### 4.1 Hostel

For the energy and economic analysis of a hostel, a building with a rectangular shape of 300 m<sup>2</sup> with an average slope of 30 degrees is considered (Fig.2).

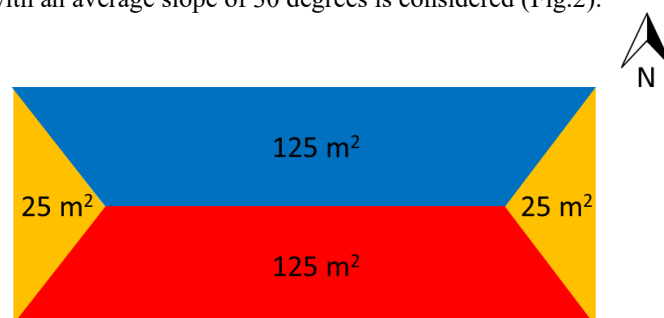


**Fig. 2.** Floor plan of the hostel considered for the analysis.

The design of a self-consumption installation requires the knowledge of the energy demand. In this case, it is considered that the hostel has lighting [30], air conditioning system [31], connection to recharge small devices and equipment for cleaning and for the users (Table 1).

**Table 1.** Estimated energy consumption in a hostel

Equipment	Power (Wh)	Use time (Hours)	Energy consumption (Wh/day)
Lighting	1200	4	4800
Fridge	74	24	1776
Washing machine	700	1	700
Drying machine	700	1	700
Ceramic hobs	1200	0.67	800
Microwave	800	0.25	200
Small devices	300	1	300
Air conditioning/heating system	10000	6	60000

Due to the geometry of the roof and discarding the rooftop oriented to the north, the self-consumption installation is designed in order to meet the energy demand with the following characteristics: peak power of 25 kWp with 76 panels of 330 W. Of the 76 panels that make up the installation, 55 are installed in the south facing rooftop, 10 in the east and 11 to the west. This installation allows to produce an annual daily average of 94 kWh/day (Table 2), allowing surplus energy to be discharged into the grid in those months in which there is a surplus.

**Table 2.** Annual daily average production through the solar installation in the hostel considering an air-conditioning system (kWh /day)

Jan.	Feb.	Mar.	Apr.	May	Jun.	Jul.	Aug.	Sept.	Oct.	Nov.	Dec.
51	62	83	97	115	133	148	138	108	83	57	54

Although it is an installation that generates large amounts of energy, hostels have a high energy consumption mainly due to the air conditioning system considered (60000W). If the installation is designed according to the energy demand without considering the air conditioning system (9276 W), the peak power of the installation would be 3630 kWp with a total of 11 panels of 330 W. This installation would allow to produce, an average of 14.50 kWh on a daily basis (Table 3) allowing the discharge of surplus energy to the grid in the corresponding months.

**Table 3.** Annual daily average production through the solar installation in the hostel without considering an air-conditioning system (kWh /day)

Jan.	Feb.	Mar.	Apr.	May	Jun.	Jul.	Aug.	Sept.	Oct.	Nov.	Dec.
8	10	13	15	17	20	22	21	17	13	9	9

From an economic perspective, the solar installation with an air conditioning system has a total cost of € 24,963 while without this cost it would drop to € 3,630. In both cases, based on the daily energy demand and the average daily solar production together with the sale of surpluses, the installation has a payback time of 8 years (Table 4).

**Table 4.** Average economic parameters in the hostel (kWh /day)

	Installation cost (€)	Daily saving of self-consumed energy (€)	Daily energy surplus savings (€)	Payback time (years)
With air-conditioning system	24963	4.16	4.40	8
Without air-conditioning system	3630	0.56	0.70	8

From an environmental point of view and taking [32] as reference, the implementation of the solar installation in a hostel with air-conditioning system would reduce the annual carbon footprint on average by 14.02 t CO<sub>2</sub>, while without it would reduce by 2.16 t CO<sub>2</sub>.

### 4.2 Mountain hut

Unlike the hostel, the mountain hut considered for this study has a very small surface (40 m<sup>2</sup>). It is a building with a regular geometric shape that has two rooftops oriented towards the north and towards the south with an average slope of 30 degrees (Fig. 3).

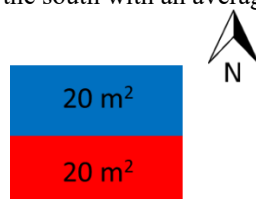


**Fig. 3.** Floor plan of the hut considered for the analysis.

As these are usually small buildings, their energy demand is much lower compared to the hostel considering that in this type of buildings the main need is lighting, the connection of portable equipment or recharging of small devices (Table 5).

**Table 5.** Estimated energy consumption for the mountain hut

Equipment	Power (Wh)	Use time (Hours)	Energy consumption (Wh/day)
Lighting	160	4	640
Portable fridge	8	24	192
Portable cooker	2000	0.67	1333
Small devices	30	1	30

Based on the above, the number of panels to be installed in order to meet the energy demand of the mountain hut, are 2 solar panels facing south. The proposed installation has a peak power of 0.66 kWp. Thanks to this installation, the average energy produced daily is 2.64 kWh (Table 6).

**Table 6.** Annual average daily production through the solar installation in the mountain hut (kWh /day)

Jan.	Feb.	Mar.	Apr.	May	Jun.	Jul.	Aug.	Sept.	Oct.	Nov.	Dec.
1.52	1.79	2.34	2.69	3.13	3.55	3.99	3.81	3.07	2.42	1.70	1.64

Due to the fact that mountain huts usually require isolated installations, due to the location far from the electricity network, the surplus energy cannot be discharged into the grid and the price of the installation is higher because a battery is required for its

storage. Specifically, the proposed installation would have a cost of 1,320 € with a payback time 8 years (Table 7).

**Table 7.** Average economic parameters in the hut (kWh /day)

Installation cost (€)	Daily saving of self-consumed energy (€)	Daily energy surplus savings (€)	Payback time (years)
1320	0.04	0.00	8

In this case, the annual carbon footprint would be reduced on average by 0.39 t CO<sub>2</sub>.

### 4.3 Parking area

Parking in rural areas are usually much smaller in size than car parks located in cities. In this case, the installation that is proposed is made up of a total of 5 canopies that allow the parking of 4 cars each facing south as the optimal orientation in facilities located in the northern hemisphere. The canopy model used has 30 panels with a power of 280 W with a slope of 10 degrees.

The average daily energy production for the five canopies is 159 kWh (Table 8), allowing the complete recharge of 3 cars with 40 kW of capacity. Analyzing the energy production for the east /west orientation, the production would decrease slightly around 10 kWh (Table 8), also allowing the complete recharging of 3 cars.

**Table 8.** Annual average daily production through the solar installation in the parking with south orientation and with east/west orientation (kWh /day)

Orient	Jan.	Feb.	Mar.	Apr.	May	Jun.	Jul.	Aug.	Sept.	Oct.	Nov.	Dec.
South	78	96	136	168	207	241	266	240	180	130	88	80
East/West	63	83	124	158	199	235	258	227	162	112	73	63

Regarding cost, this type of infrastructure costs 12,735 €, so the installation of the five canopies would have a cost of 63,675 €. Thanks to this type of infrastructure, an average daily energy saving of 30 € would be achieved, with a payback period of 5 years for south facing canopies and 6 years for east / west facing canopies (Table 9).

**Table 9.** Average economic parameters in the parking with south orientation (kWh /day)

Orientation	Installation cost (€)	Daily saving of self-consumed	Daily energy surplus savings	Payback time (years)
-------------	-----------------------	-------------------------------	------------------------------	----------------------

		energy (€)	(€)	
South	63675	31.84	0.00	5
East / West	63675	29.29	0.00	6

Apart from the canopies for recharging vehicles, the installation of 6 LED lighting points and 2 LED signs has been considered in the parking area. In both cases, the daily solar production (Table 10 and Table 11) is quite low with respect to the rest of the installations since each of the elements only has a small solar panel (28 W in the case of streetlights and 10 W in the case of traffic signals). Both in the case of LED streetlighting and LED signals, the solar energy generated is not enough to ensure self-consumption.

**Table 10.** Annual average daily production though the solar installation in streetlights (kWh /day)

Jan.	Feb.	Mar.	Apr.	May	Jun.	Jul.	Aug.	Sept.	Oct.	Nov.	Dec.
0.39	0.46	0.60	0.68	0.80	0.90	1.01	0.97	0.78	0.62	0.43	0.42

**Table 11.** Annual average daily production though the solar installation in traffic signals (kWh /day)

Jan.	Feb.	Mar.	Apr.	May	Jun.	Jul.	Aug.	Sept.	Oct.	Nov.	Dec.
0.05	0.05	0.07	0.08	0.09	0.11	0.12	0.12	0.09	0.07	0.05	0.05

From an economic perspective, this type of infrastructure has a high price compared to the energy generated, so the amortization years increase (Table 12).

**Table 12.** Average economic parameters in urban furniture (kWh /day)

Street furniture	Installation cost (€)	Daily saving of self-consumed energy (€)	Daily energy surplus savings (€)	Payback time (years)
Streetlights	2640	0.11	0.01	62
Traffic signals	700	0.02	0.00	120

Regarding the carbon footprint, among the three elements implemented, the greatest reduction is obtained in car parks with a total reduction of 23.71 t CO<sub>2</sub>. In the cases of the streetlights and signs is the reduction in the carbon footprint quite low, with a value of 0.10 t CO<sub>2</sub> and 0.01 t CO<sub>2</sub> respectively.

## 5 Conclusions

With this contribution, it is possible to demonstrate how the different solar technologies can be integrated in natural rural spaces not only to help to minimize the carbon footprint but also to develop different sustainable activities. This practice can be carried out for the implementation of solar PV installation both in different spaces in Spain and in the world with a high percentage of tourists such as the Pyrenees, Picos de Europa or the Alps.

This study presents a complete analysis for the main PV installations in rural spaces: buildings, parking and different urban security elements such as streetlights and traffic signals. With them, technological, energetic and economic aspects were studied.

The results of the technology analysis show a wide variety of PV alternatives that exists in the current market. Thanks to them, it is possible to generate clean energy with a reduced visual impact not only in rural spaces but also in cities. All of them are based on the integration of solar panels in different structures.

From an energetic point of view, solar installations in buildings are those with the greatest power generation capacity due to the large surface available at the rooftops. In this sense, geometry plays a role because not all rooftops have an optimal orientation. In self-consumption installations, the energy demand of buildings is the main factor of influence for the design of the installation, as demonstrated with the installation in the hostel.

From the perspective of public safety, LED lighting points allow great daily savings, although in the winter months this type of installation does not ensure total self-consumption. Solar traffic signs are another element that improves public safety, but their installation is not recommended in areas where there is no connection to the electricity grid since the energy balance is negative.

In the economic aspect, both solar installation in buildings and parking have a low payback time while in the case of the streetlights and traffic signal paybacks are too high due to the low energy production versus the inversion. The same conclusion can be reached from the study of the carbon footprint: its reduction in streetlights and traffic signals is negligible. As a consequence, these types of infrastructures are only interesting for urban areas where their installation is essential for the reduction of the energy cost

On the other hand, the impact of solar panels on the carbon footprint is higher in buildings (14.02 t CO<sub>2</sub>– 0.39 t CO<sub>2</sub>) and parking lots (23.71 t CO<sub>2</sub>). In both cases, the reduction of the carbon footprint is greater than that of the facility's own consumption due to the generation of surplus energy.

## References

1. Thommandru, A.; Espinoza-Maguiña, M.; Ramirez-Asis, E.; Ray, S.; Naved, M.; Guzman-Avalos, M. Role of tourism and hospitality business in economic development. *Mater. Today Proc.* 2021, doi:10.1016/J.MATPR.2021.07.059.
2. World Travel & Tourism Council Economic Impact Reports Available online: <https://wttc.org/Research/Economic-Impact> (accessed on Oct 4, 2021).
3. World Travel & Tourism Council *Spain. 2021 Annual Research: Key Highlights*; 2021;
4. BBVA ¿Cuánta energía eléctrica consume y puede ahorrar un hotel? Available online: <https://www.bbva.com/es/sostenibilidad/cuanta-energia-electrica-consume-y-puede-ahorrar-un-hotel/> (accessed on Oct 4, 2021).
5. World Tourism Organization (UNWTO) Tourism in the 2030 Agenda Available online: <https://www.unwto.org/tourism-in-2030-agenda> (accessed on Oct 4, 2021).
6. Duro, J.A.; Perez-Laborda, A.; Turrion-Prats, J.; Fernández-Fernández, M. Covid-19 and tourism vulnerability. *Tour. Manag. Perspect.* 2021, 38, 100819, doi:10.1016/J.TMP.2021.100819.
7. Redondo de Sa, M.; Postigo Mota, S. La España vaciada. *Rev. Rol Enfermería* 2021, 44, 21–32.
8. HOSTELTUR Cómo contribuye el turismo a dinamizar la España vaciada Available online: [https://www.hosteltur.com/143291\\_como-contribuye-el-turismo-a-que-la-espana-vaciada-sea-la-espana-visitada.html](https://www.hosteltur.com/143291_como-contribuye-el-turismo-a-que-la-espana-vaciada-sea-la-espana-visitada.html) (accessed on Oct 4, 2021).
9. Biosphere Tourism Carta Mundial de Turismo Sostenible +20 Available online: <https://www.biospheretourism.com/es/carta-mundialde-turismo-sostenible-20/25> (accessed on Oct 4, 2021).
10. Ali, Q.; Yaseen, M.R.; Anwar, S.; Makhdum, M.S.A.; Khan, M.T.I. The impact of tourism, renewable energy, and economic growth on ecological footprint and natural resources: A panel data analysis. *Resour. Policy* 2021, 74, 102365, doi:10.1016/J.RESOURPOL.2021.102365.
11. Singh, B.P.; Goyal, S.K.; Kumar, P. Solar PV cell materials and technologies: Analyzing the recent developments. *Mater. Today Proc.* 2021, 43, 2843–2849, doi:10.1016/J.MATPR.2021.01.003.
12. Chen, M.; Zhang, W.; Xie, L.; He, B.; Wang, W.; Li, J.; Li, Z. Improvement of the electricity performance of bifacial PV module applied on the building envelope. *Energy Build.* 2021, 238, 110849, doi:10.1016/J.ENBUILD.2021.110849.
13. Honrubia-Escribano, A.; Ramirez, F.J.; Gómez-Lázaro, E.; Garcia-Villaverde, P.M.; Ruiz-Ortega, M.J.; Parra-Requena, G. Influence of solar technology in the economic performance of PV power plants in Europe. A comprehensive analysis. *Renew. Sustain. Energy Rev.* 2018, 82, 488–501, doi:10.1016/J.RSER.2017.09.061.
14. Michalena, E.; Tripanagnostopoulos, Y. Contribution of the solar energy in the sustainable tourism development of the Mediterranean islands. *Renew.*

- Energy* 2010, *35*, 667–673, doi:10.1016/J.RENENE.2009.08.016.
15. Jahangiri, M.; Haghani, A.; Heidarian, S.; Alidadi Shamsabadi, A.; Pomares, L.M. Electrification of a Tourist Village Using Hybrid Renewable Energy Systems, Sarakhiyeh in Iran. *J. Sol. Energy Res.* 2018, *3*, 201–211.
  16. Nepal, S.K. Tourism-induced rural energy consumption in the Annapurna region of Nepal. *Tour. Manag.* 2008, *29*, 89–100, doi:10.1016/J.TOURMAN.2007.03.024.
  17. Gonzalez, V.G.; Icaza, D.; Posgrados, J. De; De Tesis, D. Design of Lighting Systems using Solar Energy Sources for Rural Outdoor use: Case Study of the Guapán Hot Springs Tourism Project. *9th Int. Conf. Renew. Energy Res. Appl. ICRERA 2020* 2020, 520–525, doi:10.1109/ICRERA49962.2020.9242856.
  18. Chan, W.W.; Mak, L.M.; Chen, Y.M.; Wang, Y.H.; Xie, H.R.; Hou, G.Q.; Li, D. Energy Saving and Tourism Sustainability: Solar Control Window Film in Hotel Rooms. *J. Sustain. Tour.* 2008, *16*, 563–574, doi:10.1080/09669580802159636.
  19. Shi, Y.; Luo, W. Application of solar photovoltaic power generation system in maritime vessels and development of maritime tourism. *Polish Marit. Res.* 2018, 176–181, doi:10.2478/POMR-2018-0090.
  20. Awelewa, A.A.; Okoma, C.; Popoola, O.M.; Olajube, A.A.; Samuel, I.A. Rural Household Space Cooling and Lighting through a Solar Power-based Electric Supply System. *IOP Conf. Ser. Mater. Sci. Eng.* 2021, *1107*, 012106, doi:10.1088/1757-899X/1107/1/012106.
  21. Chiaroni, D.; Chiesa, V.; Colasanti, L.; Cucchiella, F.; D’Adamo, I.; Frattini, F. Evaluating solar energy profitability: A focus on the role of self-consumption. *Energy Convers. Manag.* 2014, *88*, 317–331, doi:10.1016/J.ENCONMAN.2014.08.044.
  22. Blum, N.U.; Sryantoro Wakeling, R.; Schmidt, T.S. Rural electrification through village grids—Assessing the cost competitiveness of isolated renewable energy technologies in Indonesia. *Renew. Sustain. Energy Rev.* 2013, *22*, 482–496, doi:10.1016/J.RSER.2013.01.049.
  23. Huang, P.; Zhang, X.; Copertaro, B.; Saini, P.K.; Yan, D.; Wu, Y.; Chen, X. A Technical Review of Modeling Techniques for Urban Solar Mobility: Solar to Buildings, Vehicles, and Storage (S2BVS). *Sustainability* 2020, *12*, 7035, doi:10.3390/SU12177035.
  24. Mohammed, H.A.Z. Design and implementation of a photovoltaic system used for streetlights. *Proc. 2016 2nd Int. Conf. Control Sci. Syst. Eng. ICCSSE 2016* 2016, 169–175, doi:10.1109/CCSSE.2016.7784376.
  25. Manikandan, P.; Karthick, S.; Saravanan, S.; Divya, T. IRJET-Role of Solar Powered Automatic Traffic Light Controller for Energy Conservation Role of Solar Powered Automatic Traffic Light Controller for Energy Conservation. *Int. Res. J. Eng. Technol.* 2008, 989.
  26. Damian Solar El uso de la energía solar en refugios y casas de montaña Available online: [https://www.damiasolar.com/actualidad/blog/articulos-sobre-la-energia-solar-y-sus-componentes/uso-energia-solar-en-refugios-de-montana\\_1](https://www.damiasolar.com/actualidad/blog/articulos-sobre-la-energia-solar-y-sus-componentes/uso-energia-solar-en-refugios-de-montana_1) (accessed on Oct 4, 2021).

27. Sunpark Sunpark Available online: <https://sunpark.es/> (accessed on Oct 4, 2021).
28. Ilumax Farola Solar ILU100G Available online: <https://www.ilumax.es/es/farolas-solares/654-farola-solar-ilu100g-10w-4000k-8436540842657.html> (accessed on Oct 4, 2021).
29. Servi Ajustaments SENYALS DE TRÀNSIT SOLARS solar Available online: <http://www.serviajustaments.com/senyals-traffic-solar.htm> (accessed on Oct 4, 2021).
30. efectoLED.blog ¿Cómo Guía para planificar la iluminación de una estancia? Available online: <https://www.efectoled.com/blog/es/planificar-iluminacion/> (accessed on Oct 4, 2021).
31. Hitachi ¿Cómo calcular la potencia de aire acondicionado por m2? Available online: <https://www.hitachiaircon.es/noticias/descubre-como-calcular-la-potencia-de-aire-acondicionado-que-necesitas-para-tu-casa> (accessed on Oct 4, 2021).
32. ECODES Hogares Sostenibles: Calcula la Huella de Carbono de tu consumo eléctrico Available online: <https://ecodes.org/tiempo-de-actuar/hogares-sostenibles/ahorro-energetico/calculadora-electricidad> (accessed on Nov 25, 2021).

## El Hidrógeno Verde en Costa Rica: una revisión

Rhonmer Orlando Pérez-Cedeño<sup>1</sup>[0000-0003-4343-0935], Leonardo Suárez-Matarrita<sup>2</sup>[0000-0002-6835-8362], Carmen Luisa Vásquez-Stanescu<sup>1</sup>[0000-0002-0657-3470], Valeria Vargas-Torres<sup>2</sup>[0000-0003-3273-6701], Rodrigo Ramírez-Pisco<sup>3</sup>[0000-0001-8648-3805]

<sup>1</sup> Universidad Nacional Experimental Politécnica Antonio José de Sucre (UNEXPO), Barquisimeto, Venezuela

<sup>2</sup> Universidad Técnica Nacional y Universidad de Costa Rica, San José, Costa Rica

<sup>3</sup> Universitat Carlemany, Andorra, Andorra

rhonmerperez@gmail.com

cvasquez@unexpo.edu.ve

lsuarezm@utn.ac.cr

**Resumen.** La evolución energética ha logrado elaborar diversas alternativas para la generación de energía limpia empleando la tecnología eólica, solar, geotérmica, entre otras, con el objetivo de mitigar el impacto medioambiental provocado por la quema de combustibles de origen fósil. A pesar de las grandes ventajas que ofrece la generación de energía empleando tecnologías verdes, su recurso primario de generación la hace inestable. Por tal razón, para aprovechar con una mayor eficiencia y continuidad estas tecnologías renovables, éstas son empleadas para generar hidrógeno verde, catalogado así por su forma de producirlo, como medio de almacenamiento energético. Costa Rica aprovecha su ubicación geográfica y geología para generar electricidad con fuentes renovables, resaltando la hidroeléctrica como la más utilizada, sin embargo, más del 30 % de su capacidad instalada en la matriz eléctrica consta de la generación eólica y geotérmica lo cual es un excelente indicativo base para la producción del hidrógeno verde. En la actualidad Costa Rica se encuentra bajo discusión de un proyecto de Ley fundamentado en la Directriz 002 enmarcada por el Ministerio de Ambiente y Energía en 2018. En el panorama internacional, se muestra alto interés en utilizar el hidrógeno como el combustible del futuro con un plan a corto y mediano plazo de emplear el hidrógeno azul y, a largo plazo, el hidrógeno verde para el 2050.

**Palabras clave:** Costa Rica, Hidrógeno, Energía, Hidrógeno Verde

### 1 Introducción

El gran impacto económico generado por la emergencia mundial del COVID-19, acompañado de una década crítica para enfrentar el cambio climático, ha provocado en diversos países a la denominada recuperación verde. De esta forma contribuyendo a reconstruir parte de las problemáticas haciendo uso de cambios estructurales considerando el diseño en el impacto futuro que generen riesgos al cambio climático que afecta al planeta.

El hidrógeno verde ha recibido un impulso significativo como repuesta a la urgencia de la reducción de las emisiones de gases de efecto invernadero y a la caída al

2

costo de producir con energías renovables. Particularmente llegando a aquellos sectores que su proceso de descarbonización ha sido difícil, tales como las industrias de minería, petróleo y los sectores transporte sistemas masivos, vial de carga pesada aéreo e incluso el marítimo.

Costa Rica se posiciona como uno de los países más innovadores de América Latina y con la mayor capacidad de generación eléctrica con fuentes renovables para el año 2020 con más del 98 %. Esto es debido a su posición geográfica, que le favorece al utilizar en gran escala las diversas fuentes tales como la energía eólica, hídrica, solar y geotérmica. Sin embargo, la mayor contribución a las emisiones de CO<sub>2</sub> de este país corresponde al sector transporte, lo cual ha sido un punto relevante para considerar al hidrógeno como alternativa ante esta condición actual desfavorable.

El artículo está organizado de la siguiente manera. La siguiente sección muestra los conceptos relacionados con el hidrógeno como fuente energética, su producción y clasificación por colores, la matriz energética y sus recursos naturales, las oportunidades y economía del hidrógeno y el marco legal para la regulación y uso del hidrógeno en Costa Rica. Finalmente, se ofrece las visiones internacionales para el uso del hidrógeno verde. La metodología aplicada se describe en la Sección 3 y en las Secciones 4 a la 7 se relacionan con datos característicos del hidrógeno en Costa Rica. Finalmente, la Sección 8 corresponde a las conclusiones.

## 2 Desarrollo

### 2.1 El Hidrógeno como fuente energética

El hidrógeno (H<sub>2</sub>) es el primer elemento de la tabla periódica más básico que conocemos en su composición diatómica estable, siendo común en el universo, mostrando un 75 % de abundancia [1]. Este elemento es un combustible con aplicaciones en pilas electroquímicas o motores alcanzando generar electricidad a partir de esa reacción electroquímica e impulsar vehículos, respectivamente [2].

A pesar de su abundancia, el hidrógeno se encuentra combinado con otros elementos químicos en la naturaleza. Por ejemplo, al observar la composición de la fórmula del agua (H<sub>2</sub>O) o el gas metano (CH<sub>4</sub>). Por tanto, es un vector energético, es decir, no es un combustible que pueda tomarse directamente para su uso, lo que implica que se debe “procesar” para poder hacer uso del mismo [3].

La demanda que tiene el hidrógeno, reflejada en figura 1, ha mostrado un incremento gradual en el período de 1975 al año 2018, observándose una mayor participación de otros sectores (fronjas verdes) que lo utilizan en su estado puro.

Una comparación entre el potencial energético del H<sub>2</sub>, el diesel y el gas natural y, además, sus emisiones relacionadas por su uso es mostrado en la Tabla 1 donde es notorio los grandes beneficios del H<sub>2</sub> y las razones de ser el combustible prometedor para el futuro como energía limpia [1].

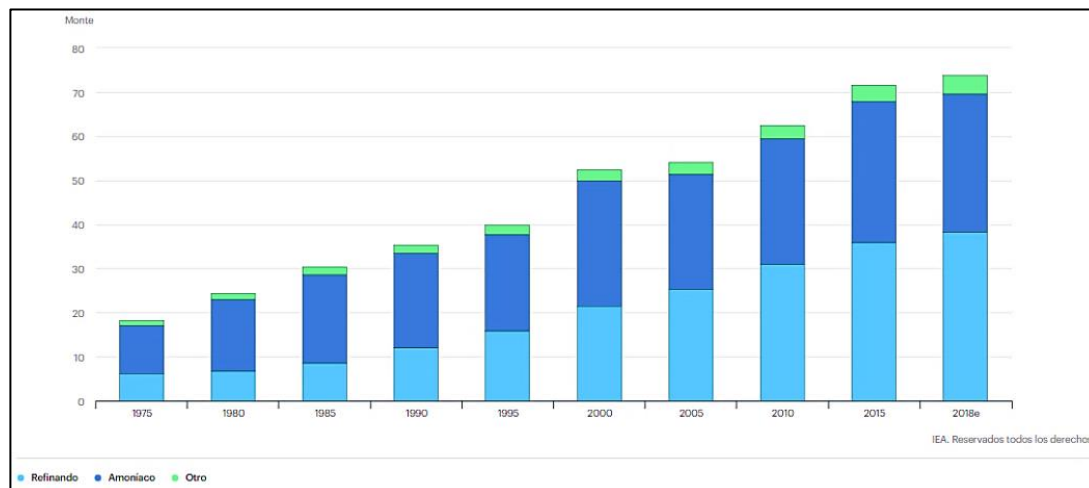


**Fig. 1.** Demanda mundial del hidrógeno puro, 1975-2018

Fuente: [4]

**Tabla 1.** Comparación del potencial energético y emisiones en algunos combustibles

Combustible (Unidad)	Poder Calorífico (kWh/unidad)	Equivalencia energética (kg H <sub>2</sub> /unidad)	Emisiones (kg CO <sub>2</sub> /unidad)
H <sub>2</sub> (kg)	33,3	1	0
Diésel (L)	10,2	3,3	3,18
Gas Natural (m <sup>3</sup> )	9,6	3,5	1,97

Fuente: Adaptado de [5]

## 2.2 Producción del hidrógeno y su clasificación por colores

Los distintos métodos para producir hidrógeno dependen de la materia prima y la fuente energética, clasificándolos en modelos renovables, fósiles e incluso híbridos en un porcentaje determinado [3] con una producción del 96 % para el año 2015 [1]. La figura 2 muestra el proceso de obtención de H<sub>2</sub> por los métodos de la termólisis, electrólisis, reformado y gasificación.

El hidrógeno promete ser un medio de transición energética [6]. Sin embargo, para indicar que el uso del H<sub>2</sub> está asociado a cero (0) emisiones necesariamente se debe obtener de fuentes renovables, sino seguirá anclado a emisiones indirectas de CO<sub>2</sub> en su ciclo de vida.

4

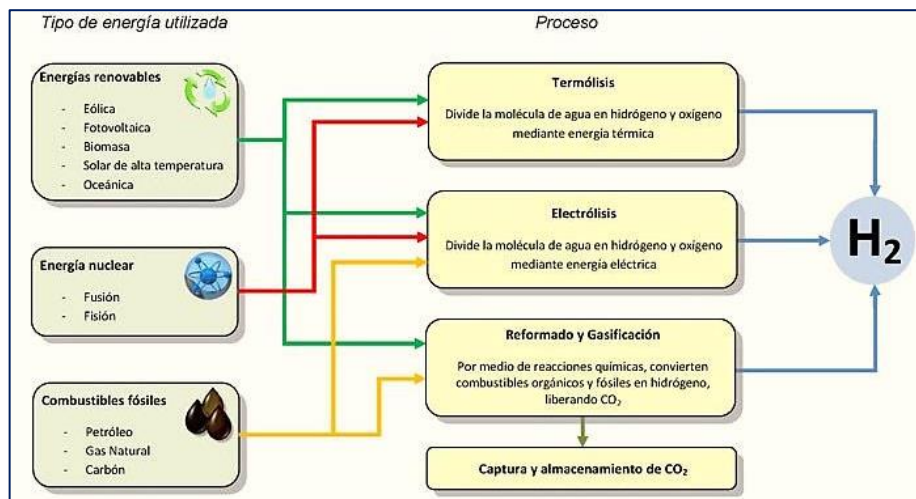


**Fig. 2.** Energía empleada y proceso de obtención de hidrógeno  
**Fuente:** [7]

El hidrógeno es un gas incoloro, sin embargo se ha propuesto asignarle un código de colores que guardan relación con su tipo de energía primaria para producirlo y sus emisiones asociadas, así se nombra al hidrógeno gris, azul y verde, como los más resaltantes, donde al primero se le acredita mayores emisiones de CO<sub>2</sub> y al último, el verde, es catalogado como el medio más limpio de obtenerlo con cero (0) emisiones, relacionado al desarrollo de electrolizadores dinámicos con energía renovable [8] [9]. Las características y usos de cada color de H<sub>2</sub> son mostrados en la Tabla 2 y en la figura 3 de forma resumida e ilustrativa.

Existen otras denominaciones para el hidrógeno que, al igual que el hidrógeno gris, azul y verde, guardan relación con sus emisiones y origen de producción. Así, el hidrógeno marrón proviene del carbón; el turquesa de la pirolisis; el amarillo haciendo uso de la energía solar; rosado empleando energía nuclear; el blanco de origen natural [8].

**Tabla 2.** Características de cada denominación del hidrógeno y sus usos particulares

Denominación del hidrógeno	Características	Usos
Gris y Marrón	Es ampliamente generado a nivel mundial y con origen fósil mediante la separación molecular del gas natural (hidrógeno gris) o del carbón (hidrógeno marrón).	<ul style="list-style-type: none"> <li>▪ En la industria petroquímica para la producción de metanol, amoníaco, resinas y polímeros.</li> <li>▪ La refinería de BP Oil España S.A.U. en Castellón emplea este tipo de hidrógeno en sus procesos para producir biocombustibles [10] y crudos más ligeros.</li> <li>▪ En la producción de vidrio y aplicaciones como la refrigeración de generadores eléctricos [11].</li> <li>▪ En industrias de metal; en la fabricación de semiconductores; como propulsor de combustibles para cohetes espaciales [12].</li> </ul>
Azul	Es obtenido a partir combustibles fósiles como el hidrógeno gris con la diferencia del empleo de tecnologías de captura y almacenamiento del dióxido de carbono (CO <sub>2</sub> ) para sus usos y ofertas en el mercado del carbono.	
Turquesa	Se emplea la pirólisis (descomposición química de materia orgánica en ausencia de oxígeno y cualquier halógeno) para su obtención utilizando como recurso primario el gas natural pero como es un combustible fósil, no es considerado libre de emisiones [13].	
Verde	Se obtiene del agua mediante electrólisis con electricidad completamente renovable como la eólica o solar [14]. Es posible obtenerlo de la biomasa o biogás.	<ul style="list-style-type: none"> <li>▪ En vehículos eléctricos con pilas de combustible.</li> <li>▪ Como medio energético de almacenamiento cuando la generación de electricidad renovable es excedente comparado con la demanda.</li> <li>▪ Cogeneración de electricidad y calor en edificios por medio de Pilas de Combustible [15].</li> <li>▪ En la obtención de energía eléctrica, es un combustible capaz de sustituir al uranio y los hidrocarburos actualmente utilizados [16].</li> </ul>

**Fuente:** Elaboración propia de los autores

6

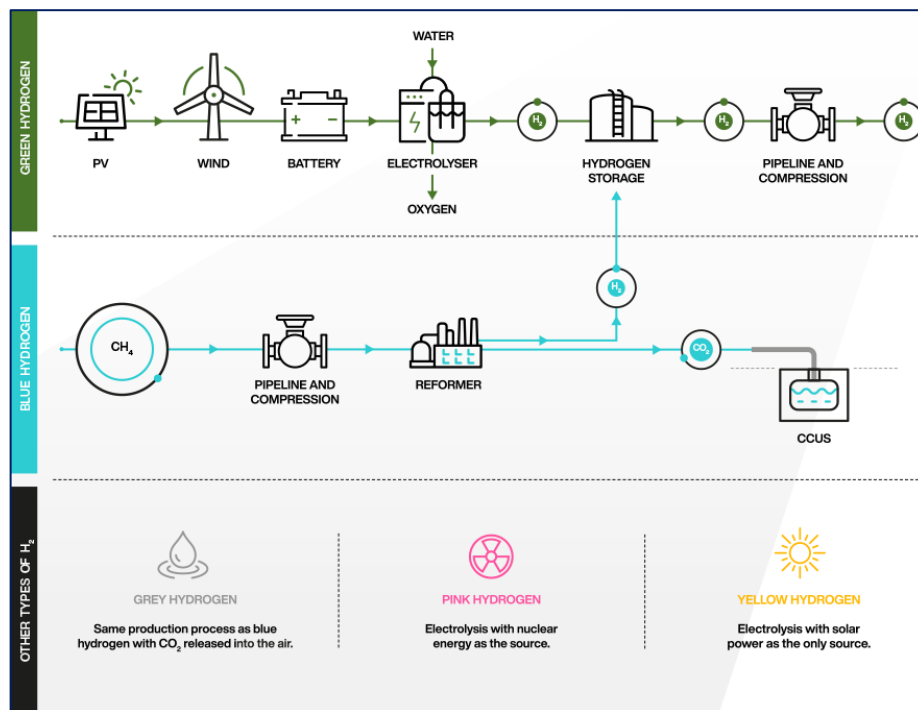


Fig. 3. Características del origen y tipo de color del hidrógeno  
Fuente: [8]

### 3 Metodología

En la precisión de los lineamientos metodológicos es oportuno indicar que el estudio es desarrollado bajo una metodología descriptiva, estando conformado por:

- Una revisión de la matriz energética de Costa Rica y sus recursos renovables, señalando los grandes beneficios de este país centroamericano en aprovechar su geología y ubicación geográfica.
- Las oportunidades y economía del hidrógeno en Costa Rica haciendo énfasis en sectores macro como la Matriz eléctrica nacional y las fuentes renovables, Transporte y Nuevas industrias.
- El marco legal para el manejo y uso del hidrógeno en Costa Rica donde se reflejan las normas vigentes del país referente al uso del hidrógeno bajo aplicaciones energéticas y su situación actual de este vector energético.
- La visión del hidrógeno verde a nivel internacional donde países latinoamericanos como Costa Rica, Paraguay y Uruguay, que poseen grandes oportunidades con la participación de fuentes renovable más altas del mundo y con posibilidad de inclusión de procesos de electrólisis haciendo uso de los excesos de energía generada.

#### 4 Matriz energética de Costa Rica y sus recursos renovables

Costa Rica aprovecha su geología y ubicación geográfica para generar electricidad con fuentes renovables, resaltando la hidroeléctrica como la más utilizada. Incluso, desde la electrificación del país ha sido la hidroelectricidad quien ha sustentado al Sistema Eléctrico Nacional [17]. La Tabla 3 reúne los tipos de tecnologías de generación eléctrica para el año 2019.

**Tabla 3.** Tecnología y porcentaje de participación en la matriz energética de Costa Rica para el año 2019

Tecnología	Capacidad Instalada (%)
Hidroeléctrica	67,5
Eólica	17,0
Geotérmica	13,5
Biomasa y Solar	0,84
Térmica	1,16

**Fuente:** Elaboración propia a partir de [17].

Cabe destacar que en Costa Rica el uso de la fuente termoeléctrica es solamente de respaldo cuando no se logra suplir la demanda energética del país. Como se detalla en la figura 4, las bajas emisiones dadas en el sector de electricidad y calor, señalan una oportunidad para utilizar la tecnología de vehículos eléctricos en este país. Además, es posible incluir al hidrógeno como combustibles para sus nuevas flotas vehiculares procurando la reducción a las emisiones del sector transporte.

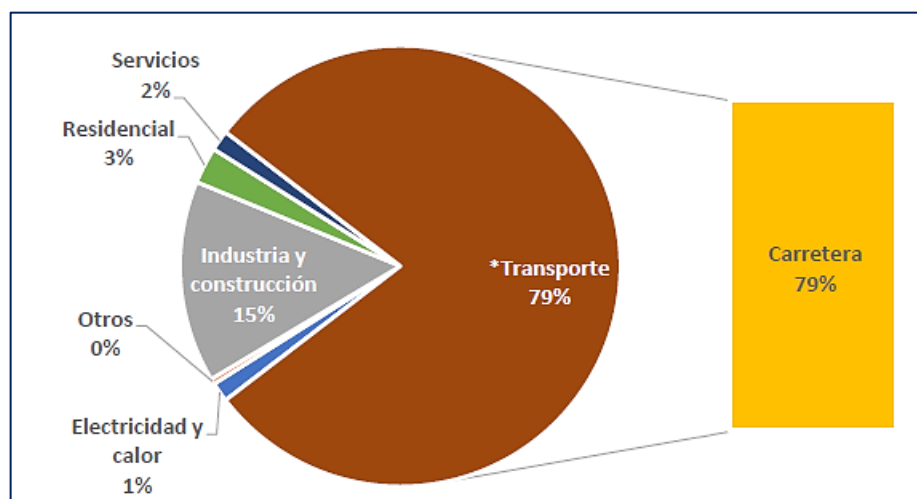


**Fig. 4.** Emisiones de CO<sub>2</sub> debido a la combustión de combustibles fósiles en Costa Rica

**Fuente:** [18] [19]

8

## 5 Oportunidades y economía del hidrógeno en Costa Rica

Costa Rica se destaca por su impulso para descarbonizar su economía y por su matriz eléctrica limpia, planteando una gran oportunidad para que el país desarrolle el mercado del hidrógeno verde [20]. Las oportunidades por sector macro en Costa Rica se muestran en la Tabla 4 siendo notoria la matriz energética de esta nación.

Para garantizar la seguridad energética del país es relevancia visualizar los siguientes ítems basados en el uso del hidrógeno [1]:

- La economía del hidrógeno a partir de sus recursos autóctonos.
- Estudios previos de factibilidad económica y ambiental.
- Impulsos para la mitigación del impacto ambiental en cuanto a la contaminación y el calentamiento global.
- El desplazamiento del uso de los recursos de origen fósil dependientes del petróleo.

**Tabla 4.** Sectores macro de Costa Rica y sus oportunidades en el empleo del hidrógeno

Sector	Oportunidad
Matriz eléctrica y fuentes renovables	Con las proyecciones mundiales en el incremento de la demanda del hidrógeno verde, Costa Rica puede considerar y evaluar su actual matriz energética y competir en el mercado como exportador, debido a que aproximadamente más del 98 % de su electricidad generada se hace con energía renovable que incluso en oportunidades la generación eléctrica es superior a la demanda del país y este excedente puede utilizarse para la generación del hidrógeno verde [21]. Todo esto sin incluir el potencial energético renovable del país que aún no ha sido explotado [22].
Transporte	En el año 2019, el consumo energético de Costa Rica fue distribuido en 21 % por el uso de electricidad y 65 % proveniente de los derivados del petróleo. Solamente el 61% de la energía secundaria consumida es atribuida al sector transporte, quien además representó el 69 % de las emisiones de gases de efecto invernadero (GEI) en este país para ese mismo año. Por tal motivo, uno de los ejes del Plan de Descarbonización de Costa Rica incluye al sector transporte abriendo paso al uso del hidrógeno que puede resultar particularmente útil en la mitigación de las poluciones generadas por el transporte pesado y de largas distancia [23].
Nuevas industrias	El hidrógeno como alternativa verde para el país le ofrece una oportunidad de posicionarse como uno de los pioneros mundiales en este tipo de vector energético, para la creación y desarrollo de infraestructuras y capital humano, nuevas aplicaciones así como ingresar en el mercado verde.

Fuente: Elaboración propia adaptado de [20]

## 6 Marco legal para el manejo y uso del hidrógeno en Costa Rica

En la actualidad, Costa Rica se encuentra bajo discusión de un proyecto de Ley que tiene como origen la normativa denominada Directriz 002 enmarcada por el Ministerio de Ambiente y Energía para el año 2018 [24] donde se establece acciones articuladas en las instituciones del sector energético y ambiental a efectos de desarrollar ac-

ciones que propicien la investigación, la producción y la comercialización del hidrógeno como combustible para este país. No obstante, el país cuenta con determinadas normas técnicas referentes al uso del hidrógeno en aplicaciones energéticas como se resalta en la Tabla 5.

**Tabla 5.** Normas técnicas referentes a las aplicaciones energéticas del hidrógeno

Código	Nombre	Descripción General
INTE/ISO 17268:2020	Dispositivos de conexión de reabastecimiento para vehículos terrestres a hidrógeno gaseoso.	Define las características de diseño, seguridad y operación de los conectores de reabastecimiento de vehículos terrestres a hidrógeno gaseoso que tienen presiones nominales de hidrógeno de hasta 70 MPa. No es aplicable a los conectores de reabastecimiento que dispensan mezclas de hidrógeno con gas natural.
INTE/ISO 22734:2020	Generadores de hidrógeno que utilizan electrólisis del agua. Aplicaciones industriales, comerciales y residenciales.	Define los requisitos de construcción, seguridad y desempeño de los equipos de generación de hidrógeno modulares o gaseosos construidos de fábrica que utilizan reacciones electroquímicas para electrolizar agua para producir hidrógeno, tales como: grupo de ácidos acuosos, materiales poliméricos sólidos con adiciones de grupos funcionales ácidos, grupo de bases acuosas. Aplicable a generadores destinados a usos residenciales, comerciales e industriales.
INTE/ISO 14687:2020	Calidad del hidrógeno para aplicaciones energéticas. Requisitos.	Especifica las características de calidad mínimas del hidrógeno y sus mezclas distribuidas para su utilización en aplicaciones estacionarias y vehiculares.
INTE/ISO 19880-1:2021	Hidrógeno gaseoso. Estaciones de abastecimiento. Parte 1: Requisitos generales.	Define los requisitos mínimos de diseño, instalación, puesta en marcha, operación, inspección y mantenimiento para la seguridad y el desempeño de estaciones de abastecimiento que dispensan hidrógeno gaseoso a vehículos livianos.
INTE/ISO 19880-3:2021	Hidrógeno gaseoso — Estaciones de abastecimiento — Parte 3: Válvulas	Establece los requisitos y métodos de prueba relativos al desempeño de seguridad de las válvulas de gas de alta presión que se utilizan en las estaciones de hidrógeno gaseoso de hasta la designación H70.

**Fuente:** Adaptado de [25]

## 7 Visión del hidrógeno verde a nivel internacional

La región de América Latina cuenta con una enorme potencial de recursos renovables en forma de solares, geotérmicos, eólicos e hidrológicos, permitiendo tener un 55 % de generación limpia en comparación con el promedio mundial del 35 %. El hidrógeno es una importante oportunidad para que las regiones de América Latina y el Caribe establezcan matrices energéticas domésticas más limpias, particularmente para ese 17 % de las emisiones que se originan en actividades industriales [26].

10

En esta nueva economía del hidrógeno, países como Paraguay, Uruguay y Costa Rica poseen importantes oportunidades, los cuales se posicionan en una de las cuotas de participación renovable más altas del mundo y con excedentes que podrían ser destinados a procesos de electrólisis.

Costa Rica ya publicó una directiva en 2018 con el propósito de promover el hidrógeno como parte de su estrategia de descarbonización y Chile para 2020 aprobó su Hoja de Ruta Nacional para el Desarrollo del Hidrógeno, incluso, países como El Salvador, Honduras, Panamá, Colombia, Perú, Brasil, Bolivia, Uruguay y Argentina están siendo auspiciados por el Banco Interamericano de Desarrollo (BID) a través de diálogos, asistencia técnica e inversión para acelerar el uso del hidrógeno como parte de la transición energética en estas naciones [26].

Australia, con su proyecto *Asian Renewable Energy Hub* generará 26.000 MW de energía renovable en Australia Occidental donde la mayor parte de esta energía se utilizará para la producción a gran escala de hidrógeno verde para los mercados nacionales y de exportación [27].

Por otra parte, la empresa petrolera Shell en los Países Bajos desarrolla un estudio de viabilidad que podría llevar a la generación de gigavatios (GW) de energía eólica marina de uso exclusivo para la fabricación de hidrógeno verde. Los planes prevén que para el 2030 ya sean instalados 4 GW de capacidad eólica marina en el Mar del Norte con capacidad de ampliación a 10 GW para 2040 y los electrolizadores tendrán su base en alta mar y también en *Eemshaven*, a lo largo de la costa norte de los Países Bajos [28].

En Alemania, el pionero mundial del hidrógeno verde procedente de la electrólisis eólica marina *AquaVentus* tiene como objetivo establecer señales en todo el mundo con tecnología de hidrógeno respetuosa con el clima. Este proyecto visionario para el año 2035 consta de 10 GW de capacidad de generación de hidrógeno verde a partir de energía eólica marina transportado por tierra.

Arabia Saudita, el país árabe con las mayores reservas de petróleo, también pretende incluir el hidrógeno verde en su matriz energética con un proyecto denominado *Helios Green Fuels*, ubicado en la ciudad inteligente de NEOM. Este proyecto prevé una capacidad de procesamiento de este hidrógeno de 4 GW de 4 electrolizadores para el año 2050 [29].

## 8 Conclusiones

La evolución energética ha logrado elaborar diversas alternativas para la generación de energía limpia empleando la tecnología eólica, solar, geotérmica, entre otras, con el objetivo de mitigar el impacto medioambiental provocado por la quema de combustibles de origen fósil. A pesar de las grandes ventajas que ofrece la generación de energía empleando tecnologías verdes, su dependencia a la fuente de obtención energética la hace inestable, es por esta razón que, para aprovechar con una mayor eficiencia y continuidad estas tecnologías, se utiliza como medio de obtención de hidrógeno verde, catalogado así por su forma de producirlo.

Costa Rica aprovecha su ubicación geográfica y geología para generar electricidad con fuentes renovables, resaltando la hidroeléctrica como la más utilizada, sin embargo, más del 30 % de su capacidad instalada en la matriz eléctrica consta de la genera-

ción eólica y geotérmica lo cual es un excelente indicativo base para la producción del hidrógeno verde para el cambio que esta nación se plantea como medida de transición energética para apuntar la reducción de emisiones de GEI atribuidas al sector transporte, principalmente.

En la actualidad Costa Rica se encuentra bajo discusión de un proyecto de Ley fundamentado en la Directriz 002 enmarcada por el Ministerio de Ambiente y Energía en 2018. No obstante, el hidrógeno verde como alternativa para el país centroamericano le ofrece una oportunidad de posicionarse como uno de los pioneros mundiales en este tipo de vector energético poco explotado, para la innovación y desarrollo de infraestructuras y capital humano, nuevas aplicaciones así como ingresar en el mercado verde a nivel mundial como exportador.

A nivel internacional, se muestra alto interés en utilizar el hidrógeno como el combustible del futuro con un plan a corto y mediano plazo de emplear el hidrógeno azul y a largo plazo el hidrógeno verde para el año 2050. Por esta razón, países de todo el mundo buscan la generación del hidrógeno verde para garantizar cero emisiones en aquellos sectores donde será aplicado este nuevo combustible, con especial interés en el sector transporte.

### **Agradecimiento**

Los autores de este artículo quieren agradecer al Programa Iberoamericano de Ciencia y Tecnología para el Desarrollo (CYTED), ya que el mismo fue elaborado en el marco del proyecto Red Iberoamericana de Transporte y Movilidad Urbana Sostenible (RITMUS, 718RT0566).

### **Referencias**

1. Bonilla Delgado, J.A.: Presentación de la Asociación Costarricense de Hidrógeno. , Costa Rica (2021).
2. Salinas López, F., Cantoral Ceballos, J.A., Funes Gallanzi, M.: GENERADOR DE ELECTRICIDAD MODULAR ALIMENTADO POR MÚLTIPLES ENERGÍAS RENOVABLES. In: Academia Journals, pp. 1619–1624. , México (2020).
3. Centro Nacional del Hidrógeno: El hidrógeno, <https://www.cnh2.es/el-hidrogeno/>, last accessed 2021/11/01.
4. IEA: Demanda global del hidrógeno puro, 1975-2018, <https://www.iea.org/reports/the-future-of-hydrogen>, last accessed 2021/10/01.
5. Jiménez Sáez, F.L.: EVALUACIÓN TÉCNICA Y ECONÓMICA DEL USO DE HIDRÓGENO VERDE EN APLICACIONES PARA LA INDUSTRIA Y DESPLAZAMIENTO DE COMBUSTIBLE FÓSIL, (2020).
6. Morales Ramos, A.C., Pérez Figueroa, M., Pérez Gallardo, J.R., Almaraz, S. de L.: Energías renovables y el hidrógeno: un par prometedor en la transición energética de México. *Investig. Cienc.* 25, 92–101 (2017).
7. Monzó Lacueva, N.: LOS COLORES DEL HIDRÓGENO: VERDE, AZUL Y GRIS, <https://plataformazeo.com/es/colores-hidrogeno-verde-azul-gris/>, last accessed 2021/10/20.
8. Petrofac: The difference between green hydrogen and blue hydrogen, <https://www.petrofac.com/media/stories-and-opinion/the-difference-between-green-hydrogen-and-blue-hydrogen/>, last accessed 2021/08/01.
9. Cisneros, P.: El Hidrógeno y su relación con energías renovables y sus excedentes,

12

- <https://www.caf.com/es/conocimiento/visiones/2021/02/el-hidrogeno-y-su-relacion-con-energias-renovables-y-sus-excedentes/>, last accessed 2021/10/15.
10. bp España: bp, Iberdrola y Enagás estudian el desarrollo del mayor proyecto de hidrógeno verde en la Comunidad Valenciana, [https://www.bp.com/es\\_es/spain/home/noticias/notas-de-prensa/bp--iberdrola-y-enagas-estudian-el-desarrollo-del-mayor-proyecto.html](https://www.bp.com/es_es/spain/home/noticias/notas-de-prensa/bp--iberdrola-y-enagas-estudian-el-desarrollo-del-mayor-proyecto.html), last accessed 2021/10/12.
  11. CertifHy: Overview of the market segmentation for hydrogen across potential customer groups, based on key application areas. , Europe (2015).
  12. Enérgya VM: Energía por hidrógeno, ¿en qué consiste?, <https://www.energyavm.es/energia-por-hidrogeno-en-que-consiste/>, last accessed 2021/10/01.
  13. Matute Sánchez, D.A., Ramos Jaramillo, R.F.: Análisis de las emisiones producidas en la quema de combustibles líquidos obtenidos en el proceso de pirólisis de caucho vulcanizado, <https://dspace.ups.edu.ec/handle/123456789/8873>, (2015).
  14. Asociación Española de Operadores de Productos Petrolíferos: Hidrógeno verde, azul, renovable, de bajas emisiones. Claves del papel del hidrógeno en la transición energética, <https://www.aop.es/blog/2020/09/22/claves-hidrogeno-transicion-energetica/>, last accessed 2021/10/23.
  15. Sánchez, J.B.: Aplicaciones y usos del hidrógeno, <https://www.enerclub.es/file/YPiYHxBJPpb6gqdnJquPKw;jsessionid=086B79F21BB1F8FC0BFAC3C6540225B>, last accessed 2021/11/01.
  16. Sánchez-Dirzo, R., Silva-Casarín, R., Mendoza-Baldwin, E., González-Huerta, R.: Hidrógeno del mar. TIP Revista Especializada en ciencias químico-biológicas. 15(1), 49–61 (2012).
  17. Instituto Costarricense de Electricidad: Somos electricidad renovable y solidaria, [https://www.grupoice.com/wps/wcm/connect/7a3172c0-b703-4bbf-9d61-b363e822f1c1/Fasciculo\\_Electricidad\\_2020\\_compressed.pdf?MOD=AJPERES&CVID=m.pLjj8](https://www.grupoice.com/wps/wcm/connect/7a3172c0-b703-4bbf-9d61-b363e822f1c1/Fasciculo_Electricidad_2020_compressed.pdf?MOD=AJPERES&CVID=m.pLjj8), last accessed 2021/10/15.
  18. IEA: Emissions by sector, <https://www.iea.org/reports/greenhouse-gas-emissions-from-energy-overview/emissions-by-sector#abstract>, last accessed 2021/08/14.
  19. Van Dijk, N.: Sistema de dispensado de hidrógeno para vehículos - hidrogeneras. , San José (2021).
  20. Larrea, S., Echeverría Fernández, E., Ernest Mondol, W.: Hidrógeno Verde: Oportunidad para liderar la descarbonización de Costa Rica, <https://blogs.iadb.org/energia/es/hidrogeno-verde-oportunidad-para-liderar-la-descarbonizacion-de-costa-rica/>, last accessed 2021/08/01.
  21. CENCE: Informes Anuales de Generación y Demanda Eléctrica 2015-2019, <https://apps.grupoice.com/CenceWeb/CenceDescargaArchivos.jsf?init=true&categoria=3&codigoTipoArchivo=3008>, last accessed 2021/08/01.
  22. Instituto Costarricense de Electricidad: Plan de expansión de la generación eléctrica 2018-2034, <https://www.grupoice.com/wps/wcm/connect/d91d6f4f-6619-4a2f-834f-6f5890eebb64/PLAN+DE+EXPANSION+DE+LA+GENERACION+2018-2034.pdf?MOD=AJPERES&CVID=mIeNZKV>, last accessed 2021/08/01.
  23. Secretaría de Planificación Subsector Energía: Balance Energético Nacional 2018, [https://sepse.go.cr/documentos/Balance\\_Energetico\\_2018.xlsx](https://sepse.go.cr/documentos/Balance_Energetico_2018.xlsx), last accessed 2021/08/01.
  24. Ministerio de Ambiente y Energía: Directriz 002 del 08/05/2018, [http://www.pgrweb.go.cr/scij/Busqueda/Normativa/Normas/nrm\\_texto\\_completo.aspx?param1=NRTC&param2=1&nValor1=1&nValor2=86729&nValor3=112681&strTipM=TC&lResultado=2&nValor4=1&strSelect=sel#up](http://www.pgrweb.go.cr/scij/Busqueda/Normativa/Normas/nrm_texto_completo.aspx?param1=NRTC&param2=1&nValor1=1&nValor2=86729&nValor3=112681&strTipM=TC&lResultado=2&nValor4=1&strSelect=sel#up), last accessed 2021/09/11.
  25. INTECO: Normas Técnicas, <https://www.inteco.org/shop?&search=hidrógeno>, last accessed 2021/09/10.
  26. García, J., Gischler, C., Hallack, M.: Cinco cosas que debe saber sobre el desarrollo del

- hidrógeno en América Latina, <https://blogs.iadb.org/energia/es/cinco-cosas-que-debe-saber-sobre-el-desarrollo-del-hidrogeno-en-america-latina/>, last accessed 2021/09/12.
27. The Asian Renewable Energy Hub: Low cost renewable energy for local and export markets, <https://asianrehub.com/>, last accessed 2021/09/10.
  28. EcoInventos: Proyecto North2, el proyecto de hidrógeno verde más grande del mundo, <https://ecoinventos.com/proyecto-north2/>, last accessed 2021/09/12.
  29. HELIOS INDUSTRY: Fomento De Una Energía Más Limpia Para Nuestro Planeta, <https://www.heliosindustry.com/Project/>, last accessed 2021/09/09.

## LTSpice Polynomial Modeling of Peltier-Seebeck Thermoelectric Module

Miguel Baldera Arvelo<sup>1</sup>[✉][0000-0001-9842-6402], Miguel Baldera Echavarría<sup>1</sup>[✉][0000-0001-6038-1894], Juan Castellanos<sup>1</sup>[0000-0001-5559-6612]

<sup>1</sup> Faculty of Engineering, Instituto Tecnológico de Santo Domingo, INTEC, Distrito Nacional, Dominican Republic  
miguel.balderae@intec.edu.do  
baldera\_arvelo@siemens.com

**Abstract.** The energy transformation and optimization in all aspects always will be a focus of interest and challenge for science and engineering. The thermoelectric module is widely used in power electronics applications such as heat dissipation of semiconductors. To achieve modeling and incorporation of thermoelectric modules of the Peltier (TEC) or Seebeck (TEG) type, some computational models have been made in software environments where the integration with power electronics applications models result difficult and strong computational process is required. The simulations realized in LTSpice software presented in this work are based on the TEC1-12706 thermoelectric module, according to the mathematical references for improved proposed with polynomial form model provided by FerroTEC Corporation. The modeling results have been compared with work by another author, who has also made a generalized analogy modeling for the electrical and thermal characteristics of a Peltier-Seebeck thermoelectric module.

**Keywords:** LTSpice, Thermoelectric Module, Peltier Effect, Seebeck Effect, Seebeck Coefficient, Thermal Conductance, Power Electronics, Electrical Vehicles, Heat Dissipation.

### 1 Introduction

The study of the behavior of elements and systems related to thermodynamics area represent a challenge and, in some circumstances, is necessary to work with high level of complexity to modeling and handling to incorporate the parameters related to the physical reality of a system. Today we have multiple options to perform computational modeling and investigations based on mathematical models or integrations in one system simulation.

To achieve modeling and incorporation of thermoelectric modules of the Peltier (TEC) or Seebeck (TEG) type in SPICE software is an interesting propose for integrate power electronics circuits and thermal dissipation in same system simulation. Some models of thermoelectric modules are difficult to simulate, others where behavior would not have

similarity to some scenarios of physical reality of the TEC and TEG modules. Some computational models have been made in environments where integration with power electronics applications is difficult and, in some cases, the computational processing is complex and some modeling require more hardware and machine capacity [1]. This is the reason why the experimental polynomial modeling has been realized in LTSpice software (Spice based lightweight software). Future integrations of the power electronics elements (MosFET, IGBT, SCR) could be simulated in the same system incorporating the proposed thermoelectric module.

The Peltier effect module or element, which convert electricity into heat transfer and another possibility, is convert the differential temperature between sides into electricity. In other point of view, each Peltier module can handle a heat dissipation controlled by voltage and electric current [2]. In this experiment and investigation, we make a validation functionality of the commercial thermoelectric module TEC1-12706, based in a polynomial equations and generalized parameters from FerroTEC Corporation, and compared with the modeling work by the authors Kubov, Dymyrov, based on circuit analogy modeling of the same module [3] [4].

In effect for multiple applications where the integration between a thermoelectric module with electronic components or power electronic circuits is required, could be useful to develop as lightweight simulations in SPICE software [5] [6], applied to most of requirements to modeling and design of electronic control stability for a Peltier module as parts of any colling systems. Some applications for automatic controlled heat transfer from TEC and TEG modules are difficult to integrate in one software environment, but the polynomial modeling of the thermoelectric module is very convenient tool [7]. For this experimental work, the absolute gap in temperature difference between sides of thermoelectric module is being considered, where the layer with the greatest possibility of deviation would be the hot side [8]. It is normal and today is acceptable in engineering design for commonly applications, in small portable colling, general heat dissipation, small and domestic colling devices, nano technologies portable colling applications, portable store vaccines, small colling in confined situations, confined battery colling in general or electric vehicles, confined dissipation for power semiconductors in mobility applications and or general applications within today's smart city.

## 2 Peltier-Thermoelectric Module Model

To realize the modeling of the Thermoelectric Peltier module, it is necessary first establish the three basic equations that define the behavior and operation of the physical thermoelectric effect. The behavior of the module will be basically defined by the Seebeck coefficient, the internal module resistance and the thermal conductance. In effect, other factory parameters of the TEC1-12706 module will be set as numerical values as input constants to the model developed in LTSpice software.

### 2.1 Seebeck Coefficient

The basic principle of the Seebeck coefficient is interpreted from the physical phenomenon of the detection of a voltage level at the electrical terminals, when a temperature difference occurs in both faces of the thermoelectric device. The magnitude of the resulting voltage, called the Seebeck EMF (electromotive force) and it is proportional to the magnitude of the temperature difference between both sides of module. The Seebeck coefficient for the module as a function of temperature  $S_M$ , is expressed as a third order polynomial expression in equation (1), for the condition of the differential temperature between cold and hot sides of module is equal to zero,  $DT = 0$ . For the condition of  $DT > 0$ , the model switch to equation (2), from where  $S_M$  is given in Volts/ $K$  and  $T$  in Kelvin degree  $K$ . The coefficient of Seebeck for hot side temperature is given by  $S_{MTh}$  in equation (3), and for the cold side temperature the coefficient is provided by  $S_{MTc}$  in the equation (4).

$$S_M = s_1 + s_2T + s_3T^2 + s_4T^3 \tag{1}$$

$$S_M = \frac{(S_{MTh} - S_{MTc})}{DT} \tag{2}$$

$$S_{MTh} = s_1T_h + \frac{s_2T_h^2}{2} + \frac{s_3T_h^3}{3} + \frac{s_4T_h^4}{4} \tag{3}$$

$$S_{MTc} = s_1T_c + \frac{s_2T_c^2}{2} + \frac{s_3T_c^3}{3} + \frac{s_4T_c^4}{4} \tag{4}$$

The input parameters  $s_1, s_2, s_3$  and  $s_4$ , are defined in Table 1 for the thermoelectric module, according to the references model by FerroTEC Corporation [9].

**Table 1.** Input parameters for Seebeck coefficient of thermoelectric module, by FerroTEC Corporation.

Seebeck Coefficient Parameters ( $s_n$ )			
$s_1$	$s_2$	$s_3$	$s_4$
$1.33450 \times 10^{-2}$	$-5.37574 \times 10^{-5}$	$7.42731 \times 10^{-7}$	$-1.27141 \times 10^{-9}$

The Seebeck coefficient is implemented in LTSpice as one part of model with all parameters declared from table 1. See in figure 1 the Seebeck coefficient sub-module in LTSpice with input parameter and the conditioning for  $DT = 0$  and  $DT > 0$ , dependent of differential temperature between sides in the module. The output result is declared as  $S_m$  variable in LTSpice.

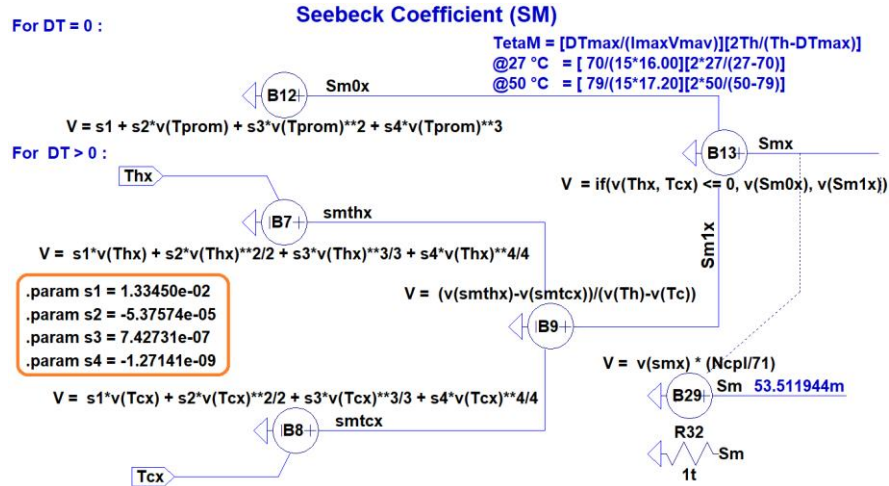


Fig. 1. Seebeck coefficient sub-module in LTSpice.

## 2.2 Module Resistance

For the modeling of the thermoelectric module, the equivalent electrical resistance  $R_M$  will be considered as a function of temperature, expressed in third order polynomial expression and it result in Ohm units [9]. The model compute as two specific conditions and choose the equations (5) or (6), depend of logic conditions of temperature between sides of module. For the condition of the differential temperature between sides is equal to zero  $DT = 0$ , will be use the equation (5), and for the condition of  $DT > 0$ , the model switch to equation (6). The electrical resistance of the module for hot side temperature is given by  $R_{MTh}$  in equation (7), and  $R_{MTc}$  is the electrical resistance for the cold side temperature, calculated as the equation (8).

$$R_M = r_1 + r_2 T + r_3 T^2 + r_4 T^3 \quad (5)$$

$$R_M = \frac{(R_{MTh} - R_{MTc})}{DT} \quad (6)$$

$$R_{MTh} = r_1 T_h + \frac{r_2 T_h^2}{2} + \frac{r_3 T_h^3}{3} + \frac{r_4 T_h^4}{4} \quad (7)$$

$$R_{MTc} = r_1 T_c + \frac{r_2 T_c^2}{2} + \frac{r_3 T_c^3}{3} + \frac{r_4 T_c^4}{4} \quad (8)$$

The input parameters  $r_1, r_2, r_3$  and  $r_4$ , are defined in Table 2 for the thermoelectric module, according to the references model by FerroTEC Corporation [9].

**Table 2.** Input parameters for electrical resistance of thermoelectric module by FerroTEC Corporation.

Electrical Resistance Parameters ( $r_n$ )			
$r_1$	$r_2$	$r_3$	$r_4$
2.08317	$-1.98763 \times 10^{-2}$	$8.53832 \times 10^{-5}$	$-9.03143 \times 10^{-8}$

The electrical resistance sub-module is integrated in LTSpice as another part of model with all parameters declared from table 2. See in figure 2 the electrical resistance sub-module in LTSpice with input parameter and the conditioning for  $DT = 0$  and  $DT > 0$ , dependent of differential temperature between sides in the module. The output result is declared as Rm variable in LTSpice.

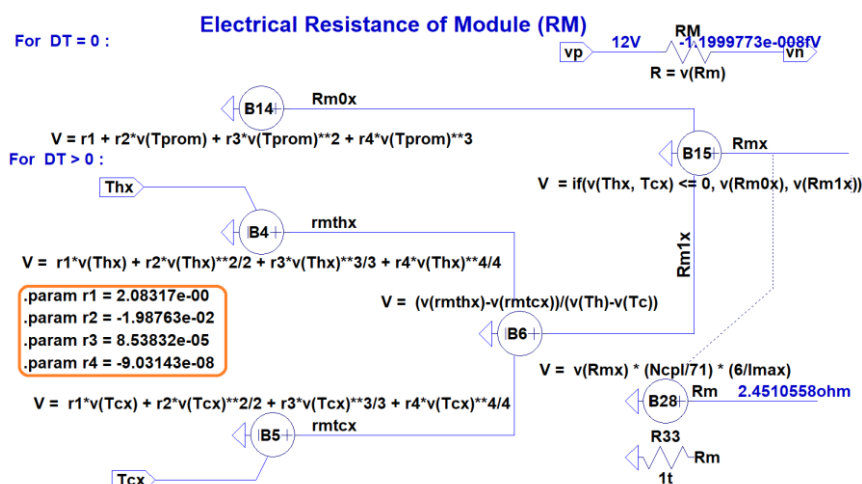


**Fig. 2.** Electrical resistance sub-model in LTSpice.

### 2.3 Thermal Conductance

The model of thermoelectric module needs an essential part of the thermal conductance as a function of the temperature. The thermal conductance  $K_M$  is based on third order polynomial expressed in the equation (9), in units of Watt/K, when the differential temperature between sides of module is zero,  $DT = 0$ . For the condition of  $DT > 0$ , the model switch to equation (10). The thermal conductance of the module for hot side temperature is given by  $K_{MTh}$  in equation (11), and  $K_{MTc}$  is the thermal conductance for the cold side temperature, calculated as the equation (12).

$$K_M = k_1 + k_2T + k_3T^2 + k_4T^3 \tag{9}$$

$$K_M = \frac{(k_{MTh} - k_{MTc})}{DT} \tag{10}$$

$$K_{MTh} = k_1 T_h + \frac{k_2 T_h^2}{2} + \frac{k_3 T_h^3}{3} + \frac{k_4 T_h^4}{4} \tag{11}$$

$$K_{MTc} = k_1 T_c + \frac{k_2 T_c^2}{2} + \frac{k_3 T_c^3}{3} + \frac{k_4 T_c^4}{4} \tag{12}$$

The input parameters  $k_1, k_2, k_3$  and  $k_4$ , are defined in Table 3 for the thermoelectric module, according to the references model by FerroTEC Corporation [9].

**Table 3.** Input parameters for thermal conductance of thermoelectric module by FerroTEC Corporation.

Thermal Conductance Parameters ( $k_n$ )			
$k_1$	$k_2$	$k_3$	$k_4$
$4.76218 \times 10^{-1}$	$-3.89821 \times 10^{-6}$	$-8.64864 \times 10^{-6}$	$2.20869 \times 10^{-8}$

The thermal conductance sub-module is integrated in LTSpice as another part of modelling the thermoelectrical module with all parameter declared from table 3. See in figure 3 the thermal conductance calculation sub-module in LTSpice, with input parameter and also the conditioning for  $DT = 0$  and  $DT > 0$ , dependent of differential temperature between sides in the module. The output result is declared as  $K_m$  variable in LTSpice.

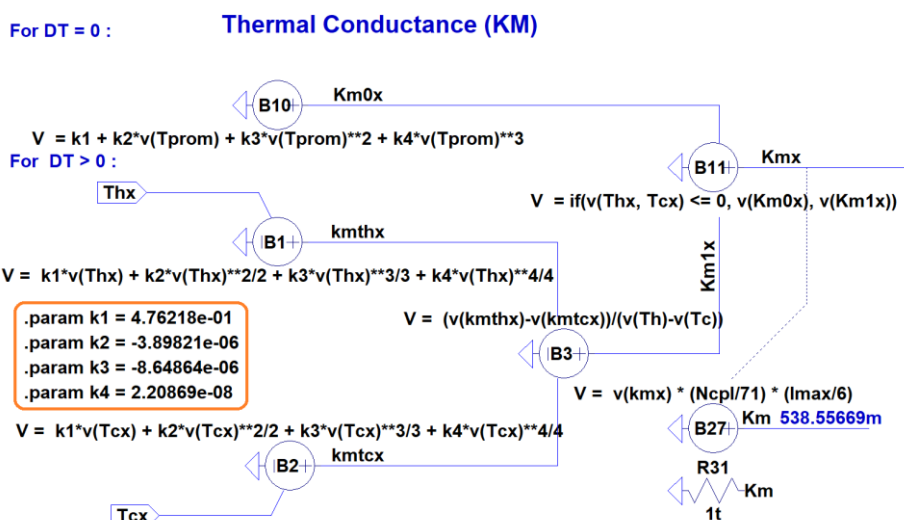


**Fig. 3.** Thermal conductance sub-model in LTSpice.

### 2.4 Normalized Parameter Conversions for Generic Module Configuration

To convert and adjust the model for our case of TEC1-12706 thermoelectric module simulations, is necessary to convert and adjust to 127 couples module. Starting from the basic and standard parameters normalized by FerroTec for one module of 71 couples and 6 Ampere [9], those new parameters, Seebeck coefficient  $S_{Mnew}$ , module resistance  $R_{Mnew}$  and thermal conductance  $K_{Mnew}$ , are adjusted by conversion factors from Table 4, for example, number of couples from any model as input constant declared in LTSpice, in our case  $N_{cpl} = 127$ , the maximum current for the model  $I_{max} = 6$  Ampere and for amount of modules  $N_m = 1$ .

To convert the parameters for TEC1-12706 proposed model, the equations (13), (14) and (15) of Table 4 are implemented in LTSpice and the model is open normalized to incorporate others Peltier thermoelectric modules with different number of couples and electric current parameters [9].

**Table 4.** Conversion factor parameters for normalized Seebeck coefficient, module resistance and thermal conductance of any thermoelectric module, by FerroTEC Corporation.

Conversion Factor Parameter for Peltier Thermoelectric Module		
$S_{Mnew} = S_M \times \frac{N_{cpl}}{71}$ (13)	$R_{Mnew} = R_M \times \frac{6}{I_{max}} \times \frac{N_{cpl}}{71}$ (14)	$K_{Mnew} = K_M \times \frac{I_{max}}{6} \times \frac{N_{cpl}}{71}$ (15)

### 2.5 Integration of TEC1-12706 Peltier Module in LTSpice

For obtain all integration sub-models in LTSpice to make the general model for TEC1-12706, is very similar to work with electronic circuit and simulation software based in SPICE for electronics modeling.

For the modeling of the thermoelectric module in LTSpice, is necessary to established the unit equivalences analogy according to the German standard DIN-66201.

The Table 5, shows the units equivalences used for the model. In effect the standard analogy, for example show the voltage parameter, and it is represented the temperature measurement, according to analogy equivalences in Table 5.

**Table 5.** Unit equivalences for modeling of TEC1-12706 module in LTSpice.

Unit Equivalences (DIN-66201)		
Electrical Side		Thermal Side
Potential	Volt	(K) or (°C) <sup>[1]</sup>
Flow	Ampere	(W/m <sup>2</sup> )
Charge	Coulomb	(J)
Resistance	Ohm	(W/K · m)
Conductance	Siemens	(J/m · s · K)
Capacity	Farad	(J/K) or (cal/°C) <sup>[2]</sup>

Notes: [1] You can use either of the two, only which once you have chosen one, everything else must continue with the same unit.  
 [2] If degrees Kelvin has been chosen, then Joule (J) must be used, to choose. For used all in degrees centigrade, then calories must be used.

The proposed model for TEC1-12706 is integrated in LTSpice Software with two external electrical connections to the variable DC power supply (from -8 to 15 Volts), from where, (vp) is the positive terminal of thermoelectric module and (vn) is the negative terminal. In the modeling, both thermal sides have two independent input connections, one is for hot temperature (Th) and the other for the cold temperature (Tc).

In additional, electrical resistance (RM), thermal conductance (KM) and the Seebeck coefficient (SM) have been computed by their corresponding sub-models. The Figure 4 shows the proposed model for TEC1-12706 in LTSpice. For internal setting parameters and LTSpice simulations, the ambience temperature is established to 30 degrees in Celsius, and the others parameters are incorporated from datasheet of TEC1-12706 [10], as number of couples Ncpl=127, maximum current I<sub>max</sub>= 6 Ampere and amount of modules Nm = 1. In this first test the cold side is consider to keep without thermal load, the Tc terminal is connected with a big value of resistor RTc1 (RTc1 = 1TOhms) between ambience temperature and it terminal (thermal isolated).

For the first experiment, the hot side terminal (Th) is connected to the ambience temperature by resistor RTh1, selected by heat sink temperature ratio, equivalent to 0.250 Ohm [3] [4]. The cold side terminal (Tc) is not connected or is thermal isolated, for the reason to obtain the result more dependent from the input voltage changing values, it is convenient for observe the complete plot span of temperature conduct between both sides at different input voltages tested.

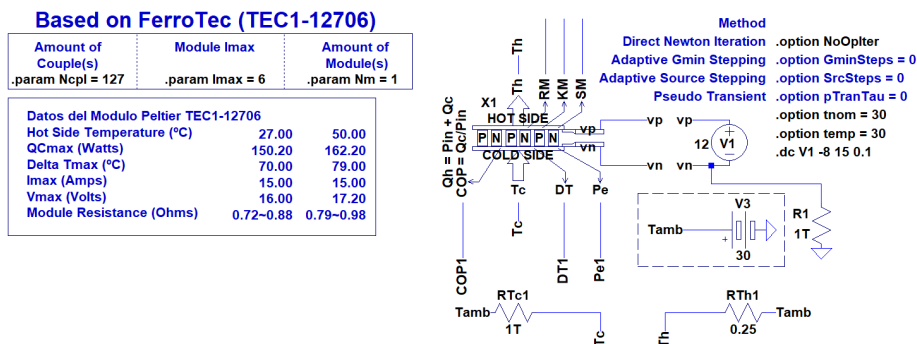


**Fig. 4.** Proposed model of TEC1-12706 with basic connections in LTSpice.

The figure 5 shows the resulting plot from modeling in LTSpice. The first simulation test behavior is the same as standard thermoelectric modules. When de input voltage is increased the cold side trend to get more lower values of temperatures and the difference between hot and cold sides is increased ( $DT$ ).

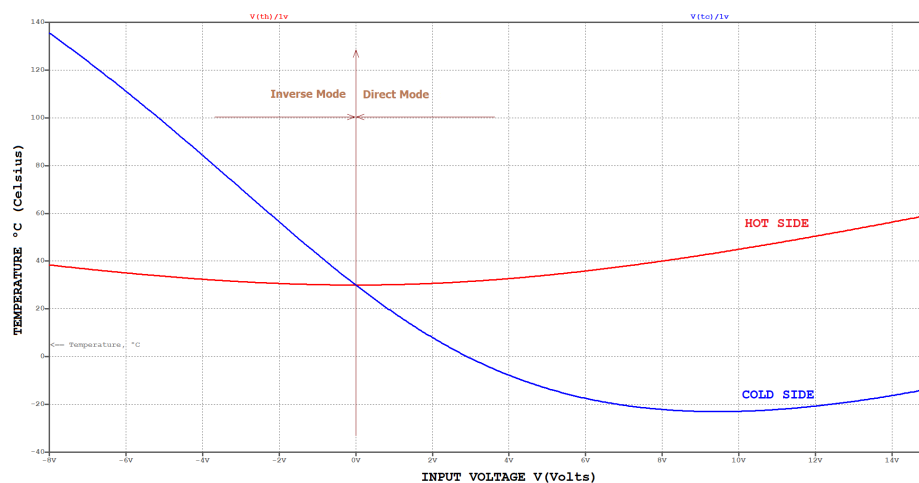


**Fig. 5.** Temperature behavior of TEC1-12706 module at variable input voltage (from -8 to +15 Volts) simulated in LTSpice.

### 3 Comparative Simulations of TEC1-12706 Models

The comparative experiment part between the proposed polynomial model and the module by Kubov & Dymyrov, is based in to the same thermoelectrical module of TEC1-12706, and both are simulated in parallel at same scenarios, ambience temperature ( $T_{amb} = 30$  Celsius) and input voltage variable from -8 to 15 Volts at the same time.

For the experiment the cold side and hot side of both modules are in the condition of  $DT = 0$  (very closed values of  $T_c = T_h$ ), because is the point of maximum thermal dissipation and transference between sides of module [4] [9] [10]. This procedure is necessary to observe differences in temperature behaviors between models, closed as possible, to the maximum thermodynamic transfer point. Figure 6 shows both models integrated in LTSpice for the comparative and parallel simulation.

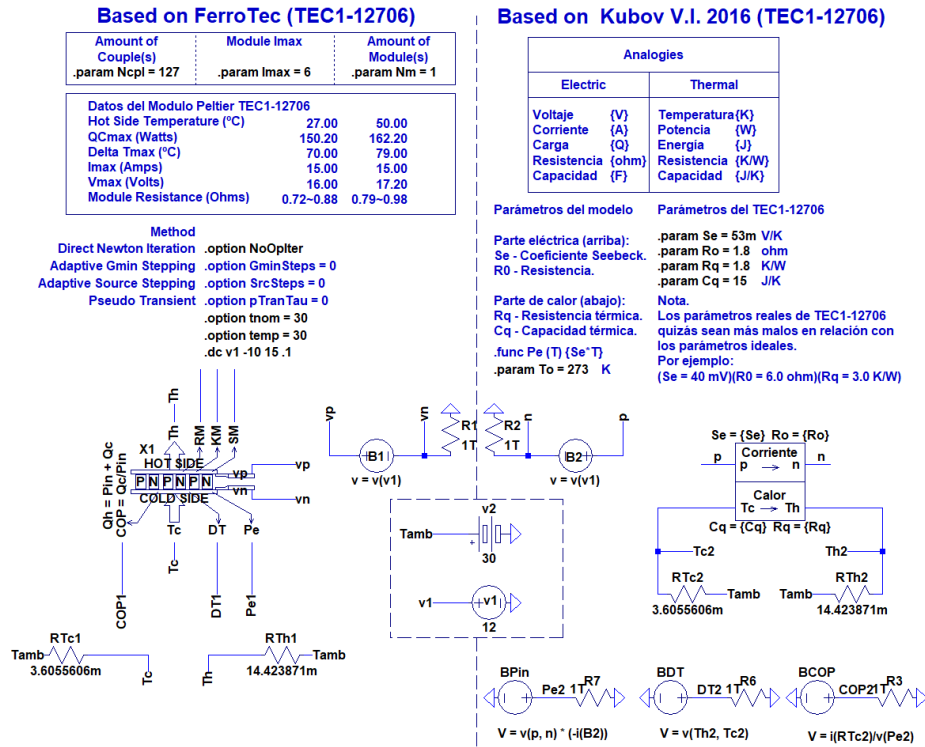


Fig. 6. LTSpice parallel modeling of both thermoelectric modules, TEC1-12706 for  $DT = 0$ , closed to the maximum thermodynamic transfer point ( $T_c = T_h = T_{amb}$ ).

The figure 7 is the simulation plot result of temperature for hot side and cold side of both modules simulated in parallel in LTSpice model of figure 6.

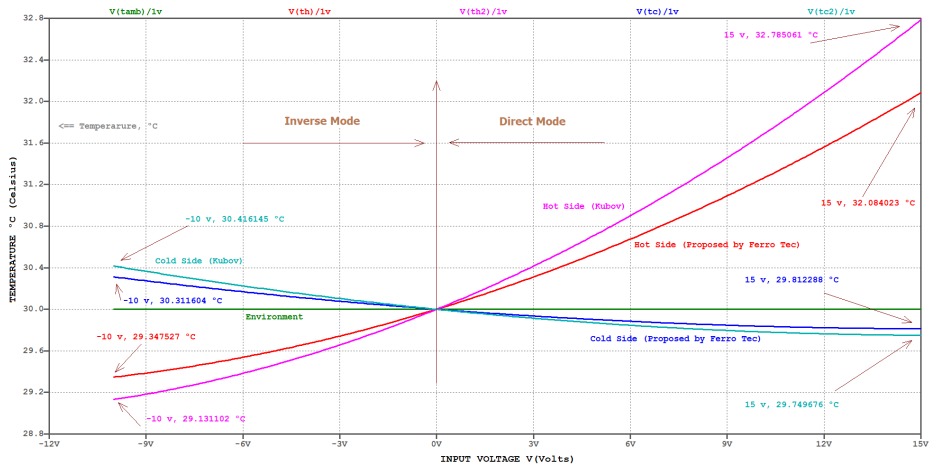


Fig. 7. LTSpice Simulation result for cold side and hot side between both thermoelectric modules TEC1-12706.

#### 4 Analysis of the results and discussion.

The experiment were realized and completed according to the objective of validating a simple polynomial proposed model of Peltier module TEC1-12706. The acquiring data is shown in Table 6, for each value of input voltage the resulting temperature is obtained from both models simulated in parallel, established in the methodology for it evaluation.

According to the data resulting from the experiment, both models show a very closed differences between hot and cold sides comparison and absolute differences. In exceptional case, at the input voltages greater than 6 volts, the values have more deviation and the differences in the hot side temperature is increased. But for practical applications the maximum voltage applied is closed to 12 Volts, it is representing only 0.52 degree in Celsius of difference between models.

**Table 6.** Comparative data result of parallel simulation in LTSpice between the proposed polynomial model and Kubov & Dymyrov model for Peltier module TEC-12706.

Input voltage (Volts)	Proposed Polynomial Model of TEC1-12706		Kubov & Dymyrov Model of TEC1-12706		Absolute Differences Between Cold Sides (Celsius)	Absolute Differences Between Hot Sides (Celsius)
	Cold Side Temperature (Tc in Celsius)	Hot Side Temperature (Th in Celsius)	Cold Side Temperature (Tc in Celsius)	Hot Side Temperature (Th in Celsius)		
-10	30.31	29.34	30.41	29.13	0.1	0.21
-6	30.16	29.53	30.22	29.38	0.06	0.15
-3	30.07	29.74	30.10	29.65	0.03	0.09
0	29.99	30.00	30.00	29.99	0.01	0.01
3	29.93	30.31	29.91	30.41	0.02	0.1
6	29.88	30.67	29.84	30.9	0.04	0.23
10	29.83	31.24	29.78	31.66	0.05	0.42
12	29.82	31.56	29.76	32.08	0.06	0.52
15	29.81	32.08	29.74	32.78	0.07	0.7

5

## 5 Conclusions & Future Works

The results obtained in the tests between each model in parallel simulations are acceptable. The lightweight polynomial model of module TEC1-12706, no require high and complex computational process in LTSpice, and represent an acceptable proposal for use in posterior simulations integrated with power electronics systems built in same LTSpice software.

From the result of this work is possible to start to new testing possibilities and integrations for future investigations. For new future simulation from the point of view of efficiency of thermoelectric conversion effect in power and energy terms, should be interesting to work with relative coefficient of performance (COP) in heat dissipation mode from Peltier-Seebeck modules. From another approach, it would also be interesting to work in modeling for optimization point of operability as possible optimum point of current and voltage control of the thermoelectric module.

This could represent a tool to obtain improvements for heat dissipation in difficult and complex circumstances such as battery storage array in electric cars with confined spaces.

From the point of view of develop applications and modeling in power electronics area, and dynamic controlled power dissipation for semiconductors, the simple polynomial model in LTSpice, represent an interesting simplified module solution. The dynamic and controlled power dissipation modeling it is an area with a lot of field and infinite applications for now and next few years.

## 6 References

- [1] Fang, E., et al. (2017). "Numerical Modeling of the Thermoelectric Cooler with a Complementary equation for heat circulation in air gaps." 15(1): 27-34.
- [2] Ferro Tec (2016). Mathematical Modeling of TEC Modules (Seebeck Coefficient). Thermoelectric Technical Reference. F. s. T. T. R. Guide, Ferro Tec.
- [3] Kubov, V., et al. (2016). LTSpice-Model of Thermoelectric Peltier-Seebeck Element. Electronics and Nanotechnology (ELNANO), 2016 IEEE 36th International Conference on, IEEE.
- [4] Kubov, V. (2016). Peltier-Seebeck Thermoelectric Element TEC1-12706. Electronics and Nanotechnology (ELNANO), 2016 IEEE 36th International Conference on, IEEE.
- [5] Teffah, K., et al. (2018). "Modeling and Experimentation of New Thermoelectric Cooler–Thermoelectric Generator Module." 11(3): 576
- [6] J. A. Chavez, J. A. Ortega, J. Salazar, A. Tury, M. J. Garcia , "SPICE model of thermoelectric elements including thermal effects", Conference Record - IEEE Instrumentation and Measurement Technology Conference, vol. 2, 2000, pp. 1019-1023.

- [7] S. Lineykin, S. Ben-Yaakov, "PSPICE-compatible equivalent circuit of thermoelectric coolers", IEEE Power Electronics Specialists Conference, PESC'05, Recife, Brazil, 2005, pp. 608-612.
- [8] Y. Moumouni, R. Jacob Baker, "Improved SPICE Modeling and Analysis of a Thermoelectric Module", IEEE 58th International Midwest Symposium on Circuits and Systems (MWSCAS), Fort Collins, USA, 2015, pp. 600-603.
- [9] <https://thermal.ferrotec.com/technology/thermoelectric-reference-guide/thermalref11/>
- [10] M. Hebei I.T. Co., "Peltier Thermoelectric Cooling Modules", TEC1-12706 Datasheet.

# Effectiveness of PV string current measurements to detect fault in PV systems

Bryan Rodriguez<sup>1</sup>, Leonardo Cardinale-Villalobos<sup>1</sup>, Carlos Meza<sup>1,2</sup>, Luis Diego Murillo-Soto<sup>1</sup>, and Hugo Sanchez<sup>1</sup>

<sup>1</sup> Costa Rica Institute of Technology,  
30101 Cartago, Costa Rica

<sup>2</sup> Anhalt University of Applied Sciences  
06366 Köthen, Germany

**Abstract.** Low-cost solutions for detecting suboptimal conditions in photovoltaics are essential to maximizing the lifetime and the energy produced by this technology. In this work, we experimentally analyze a PV system using a cost-effective solution to evaluate the behavior of current measurements for detection of suboptimal conditions, more specifically, shadowing and partial covering of the PV array. First, a grid-connected PV array was subjected to shadowing, producing a power loss greater than 10 %. Then we evaluated which cases it is possible to detect this condition when only string current is measured. The study found that when the global solar incident irradiance is lower than  $300 \text{ W/m}^2$ , it is possible to shadows in a PV string.

**Keywords:** Shadowing, Fault detection, IoT, PV systems

## 1 Introduction

The utilization of photovoltaic (PV) technology in cities has increased in the last year due to the cost reduction of the associated technology and its modularity, [1]. The latter characteristic is quite relevant in cities given that it allows PV plants to be installed in many different places and configurations in a town.

Commercially available photovoltaic technology exhibits low power density when compared to other power generation technologies. Therefore, PV plants require a large surface and the interconnection of several PV modules. These characteristics make it challenging to maintain the PV plant operating in optimal conditions. It is necessary that the whole solar radiation collecting area is clean and free from any shadow or obstruction; if not, a reduction in the incident solar radiation will occur, causing a loss in the PV energy production, [2].

Several efforts deal with the identification and correction of the partial covering of a PV array, [3], [4], [5]. For instance, Mekki in [6] proposes an artificial intelligence technique to identify partial shadowing in a PV array. In [7] the authors propose to mitigate energy losses caused by the partial covering of soiling by smart heating and night tilting of the PV modules. A IoT device has been proposed and tested in [8] to detect suboptimal conditions in PV installation for

2 Bryan Rodriguez, et. al

Household-Prosumers. Drones with specialized cameras have also been used for detecting faults in PV arrays, [9], [10], [11].

The simplest, most effective, and extensively used method to correct partial shadowing is a bypass-diode that creates an alternative path for the current in a PV module [12]. In this way, the negative effect of irradiance mismatch in the PV submodule is avoided. Therefore, the bypass diode takes out electrically the shadowed or covered PV submodule. Power losses will occur with bypass diodes where the affectation depends on the configuration of the diodes, the distribution of the panels, and the electrical configuration of the array. Several configurations of bypass diodes have been studied ([4], [13]); however, the three non-overlapping diodes per channel are the most used. The vast majority of commercially available PV modules have integrated this bypass diode configuration.

When bypass diodes conduct, they alter the shape of the i-v curve of the PV array. I-V curve-based fault-identification techniques use this effect to detect partial shadowing and partial covering in the PV array [14], [15]. Even though these methods are effective, they require moving the operating point of the PV array from its optimal position.

If there is no sufficient voltage and PV power, the bypass diode will not conduct, and the shaded or partially covered PV module will affect the string current. This condition gives an interesting opportunity to detect partial shadows or partial covering in the PV array by measuring the string current.

This paper analyzes the effectiveness of PV string current measurements to detect partial shading or partial covering of PV array. In addition, the authors evaluate the difference in the string current between non-shadowed and shadowed strings at low-irradiance conditions, i.e., when the bypass diodes are not conducting. To achieve the aforementioned, an experiment was designed in which the methodology is described in section 2. Section 3 describes and discusses the obtained. And Section 4 presents the main conclusions and future work.

## 2 Methodology

The PV plant under study corresponds to a PV installation in Santa Clara city, located in the northern part of Costa Rica, 10°32' latitude and -84°31' longitude. According to the Köppen-Geiger system, the climate in this location is classified as tropical rainforest climate (Af). The installation comprising 72 PV modules is grouped as shown in Figure 1. Only three groups of strings identified with the numbers 2, 4 and 6 were used. These strings are named as S2, S4, and S6 from now on. Each string consists of 12 monocrystalline modules.

An experiment was developed to perform a quantitative analysis of the effect of partial shadowing on the string current; for this purpose, the experiment performed by [11] was taken as a reference.

One PV module from one string was shadowed. The PV modules for the rest of the strings were left unshadowed. All the PV modules have been cleaned before the set of experiments. The shadow has been done in such a way that there is a power difference of at least 10% at a 800 W/m<sup>2</sup> between the unshadowed PV



Fig. 1: PV strings used for this research and the location of the irradiation sensor of the system.

array and the shadowed PV array, as can be seen in Table 1. Figure 2 shows the appearance of the shadows. The PV modules used have three bypass diodes and the imposed shadows are meant to activate them.

Table 1: Output power losses due to shadowing

Treatment	Power difference(%)
Shadow SP1	12,935
Shadow SP2	10,139



Fig. 2: Images of the shadows used. a) Shadow SP1 b) Shadow SP2

### 2.1 Materials

The instrumentation used to obtain the measurements were:

- A monocrystalline silicon-based sensor for measuring the solar irradiance, model Spektron 210, with an accuracy of  $\pm 5\%$  annual mean and a measurement range from 0 to 1500 W/m<sup>2</sup>.

4 Bryan Rodriguez, et. al

- A shunt-based current measurement circuit to obtain the PV-array current.

### 2.2 Current measurement circuit

The current measurement circuit used consists of the following elements:

- 15 A shunt resistors of 75 mV class 0.5 according to IE-62053-11, i.e., a 0.5% accuracy at full scale for a unity power factor.
- Galvanic isolation amplifier (AMC1200).
- A 16-bits analog to digital converter (ADS1115).

Figure 3 shows the schematic diagram of the current measurement unit and Fig. 4 the printed circuit board used in the experiment.

The current measurements are processed by an embedded system on a Raspberry Pi 4 that takes measurements of the currents of the three PV arrays approximately every 5 seconds and stores them in a text file for further analysis.

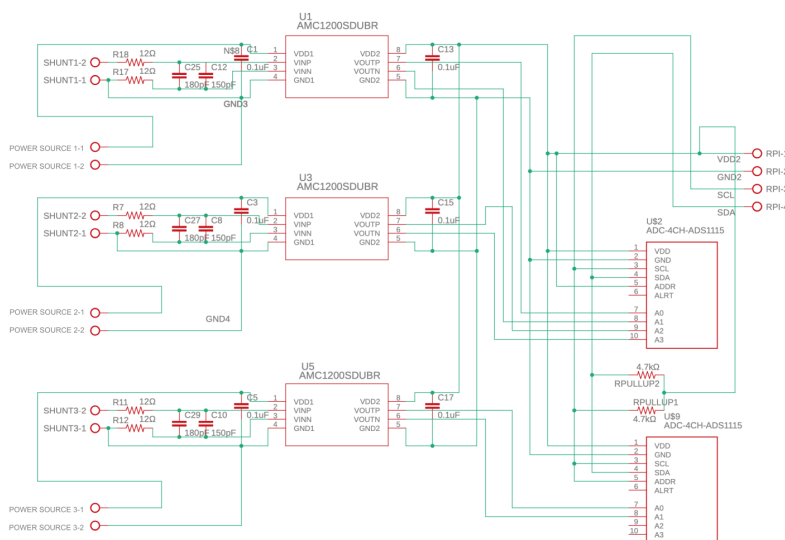


Fig. 3: Schematic of the current measuring stage.

## 3 Experimental results and discussion

The currents of the three PV arrays have been registered and compared among each other. Recall that there is always one PV string with one PV module partially shadowed in each test while the other PV strings are free of shadows and obstructions.

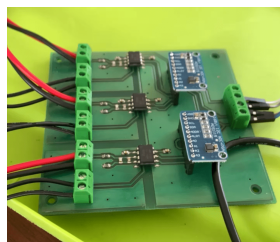


Fig. 4: PCB for the current measurement. On the left side, the voltage of the shunt resistors is input and on the right side, the digital signal that goes to the processing unit is obtained.

Table 2: Data sets selected for the analysis

Data set ID	A	B	C	D
Start time	09:21:38	09:25:31	08:58:08	09:01:32
End time	09:24:32	09:28:22	09:00:57	09:04:25
Average Irradiance (W/m <sup>2</sup> )	137.18	149.11	652.20	759.42
Number of samples	24	24	26	26
Array shadowed	S6	S6	S4	S4
Type of shadow applied	SP1	SP1	SP2	SP2

Based on the obtained string current measurements, we observed a clear difference between low-irradiance and high-irradiance conditions. Therefore, we selected the set of data that met one of the two following conditions:

- Low irradiation data: At all times during the particular experiment the irradiance is less than 300 W/m<sup>2</sup>.
- Medium/High irradiation data set: At all time during the particular experiment the irradiance is above 500 W/m<sup>2</sup>.

The main characteristics of data sets that met the aforementioned requirements are shown in Table 2. Figures 5 and 6 show the string currents obtain for the experiments. In the cases of lower irradiance, there is a notable difference between the currents of the strings.

We can quantify the difference between the current measurements in a shadowed string and an unshadowed string with inferential statistics. More specifically, we use the statistical test t-test, [16], between strings S4 and S2 for shadow SP-1 and S6 and S2 for shadow SP-2. The results are shown in tables 3 and 3. In the applied t-test, the null hypothesis assumes equal population means, i.e, the string current are the same. Therefore, if we assume a alpha of 0.05, the null hypothesis can be reject if the p-value is smaller than 0.05. Table 3 shows the p-value of the statistical tests. Notice that the hypothesis of equal currents can be rejected for data sets A and B, i.e., we obtain p-values of 0.00 in both cases. This is because data sets A and B were taken under low irradiance.

6 Bryan Rodriguez, et. al

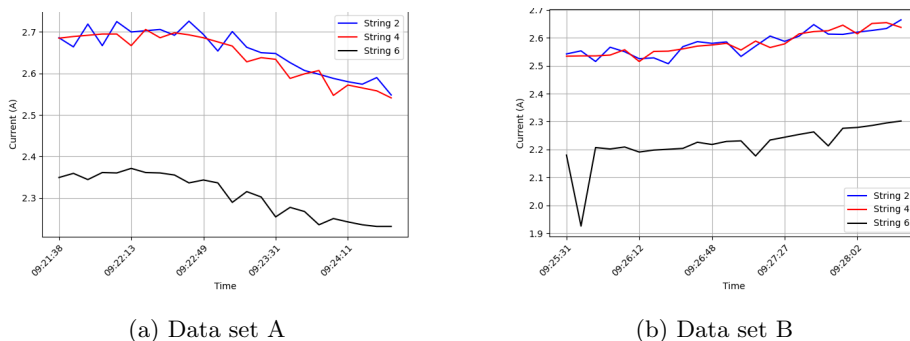


Fig. 5: String current for low irradiance

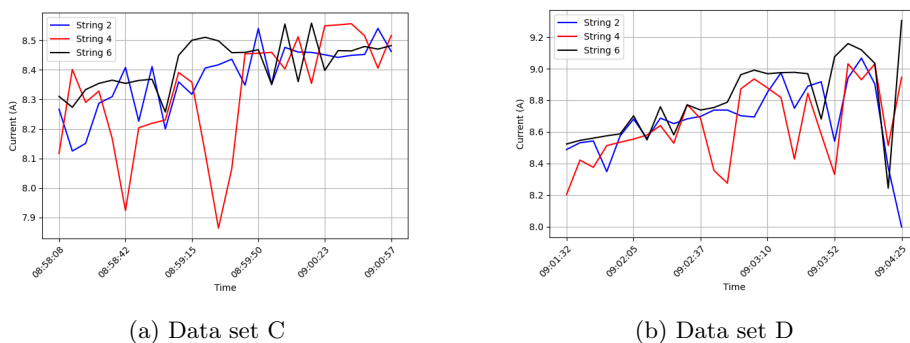


Fig. 6: String current for high irradiance

Table 3: P-value with alpha of 0.05 for the T-test results between string S2 and S4 and S2 and S6

Data set ID	A	B	C	D
S2 and S4	0.436	0.924	0.244	0.582
S2 and S6	0.000	0.000	0.110	0.055

The current curves shown in Fig.5 and the results summarized in Table 3 attest that for the low-irradiance ( $< 300 \text{ W/m}^2$ ) case, it is possible to detect shadowing conditions only by measuring string current. On the other hand, it is not possible to determine if a module is shadowed using only string current measurements under medium/high irradiance conditions (see Fig. 6 and Tables 3). The situation above is probably due to the activation of the bypass diodes on the shadowed module in cases of higher irradiance. Therefore, it seems plausible to infer that the bypass diodes do not conduct in low irradiance conditions and considerably reduce the string current during partial shadow conditions. Additionally, the variations in the measured PV string current (Figs. 5, 6) may be attributed to the maximum power point tracker of the inverter. Notice that, when bypass diodes activate, multiple power points will emerge, making it possible that the PV array operating point changes from one local maximum to another for fast irradiance changes.

#### 4 Conclusion and future work

The present paper dealt with the possibility of detecting faults and suboptimal conditions using only string current measurements. Such a strategy is helpful to implement within PV inverters. An experimental setup was designed to produce shadows conditions on PV modules. The obtained results and performed analysis allow us to conclude that, for the experiment done, it is possible to identify a shadow of 2.5% of the PV array surface using only PV string current when the incident irradiance is below  $300 \text{ W/m}^2$ . Nevertheless, when the irradiance is higher than  $500 \text{ W/m}^2$  there is no statistical difference between the mean values of a shadowed string module and a non-shadowed one. We believe that this situation may also occur in the case of heavy soiling and will be part of further investigation. It is necessary to analyze other electrical variables and the current to detect faults under conditions in which the bypass diodes are activated. The aforementioned will be the subject of future research.

#### Acknowledgment

This paper is part of a project entitled: Fault Identification in Photovoltaic Systems, ID 5402-1360-4201, financed by the Costa Rica Institute of Technology.

## Bibliography

- [1] Atasoy T, Akinc HE, Ercin O (2015) An analysis on smart grid applications and grid integration of renewable energy systems in smart cities. In: 2015 International Conference on Renewable Energy Research and Applications (ICRERA), IEEE, pp 547–550, DOI 10.1109/ICRERA.2015.7418473
- [2] Mellit A, Tina G, Kalogirou S (2018) Fault detection and diagnosis methods for photovoltaic systems: A review. *Renewable and Sustainable Energy Reviews* 91:1–17
- [3] Orozco-Gutierrez M, Ramirez-Scarpetta J, Spagnuolo G, Ramos-Paja C (2013) A technique for mismatched pv array simulation. *Renewable Energy* 55:417–427, DOI <https://doi.org/10.1016/j.renene.2013.01.009>
- [4] Diaz-Dorado E, Suarez-Garcia A, Carrillo C, Cidras J (2010) Influence of the shadows in photovoltaic systems with different configurations of bypass diodes. In: SPEEDAM 2010, IEEE, pp 134–139, DOI 10.1109/SPEEDAM.2010.5542226
- [5] Appiah AY, Zhang X, Ayawli BBK, Kyeremeh F (2019) Review and performance evaluation of photovoltaic array fault detection and diagnosis techniques. *International Journal of Photoenergy* 2019:1–19
- [6] Mekki H, Mellit A, Salhi H (2016) Artificial neural network-based modelling and fault detection of partial shaded photovoltaic modules. *Simulation Modelling Practice and Theory* 67:1–13, DOI 10.1016/j.simpat.2016.05.005
- [7] Khan MZ, Naumann V, Hagedorf C, Gottschalg R, Ilse K (2021) Mitigation of soiling losses by smart heating and night tilting for asc and standard pv module glass. In: 2021 IEEE 48th Photovoltaic Specialists Conference (PVSC), pp 0399–0402, DOI 10.1109/PVSC43889.2021.9518557
- [8] Corrales D, Cardinale-Villalobos L, Meza C, Murillo-Soto LD (2022) Detection of Suboptimal Conditions in Photovoltaic Installations for Household-Prosumers. pp 26–36, DOI 10.1007/978-3-030-78901-5\_3
- [9] Cardinale-Villalobos L, Rimolo-Donadio R, Meza C (2020) Solar panel failure detection by infrared uas digital photogrammetry: A case study. *International Journal of Renewable Energy Research (IJRER)* 10(3):1154–1164
- [10] Alfaro-Mejía E, Loaiza-Correa H, Franco-Mejía E, Hernández-Callejo L (2019) Segmentation of thermography image of solar cells and panels. In: Ibero-American Congress of Smart Cities, Springer, pp 1–8
- [11] Cardinale-Villalobos L, Meza C, Murillo-Soto LD (2021) Experimental Comparison of Visual Inspection and Infrared Thermography for the Detection of Soling and Partial Shading in Photovoltaic Arrays. pp 302–321, DOI 10.1007/978-3-030-69136-3\_21
- [12] Zhao Y (2015) Fault Detection, Classification and Protection in Solar Photovoltaic Arrays. Tech. Rep. August, Massachusetts
- [13] Silvestre S, Boronat A, Chouder A (2009) Study of bypass diodes configuration on PV modules. *Applied Energy* 86(9):1632–1640, DOI 10.1016/j.apenergy.2009.01.020

- [14] Bressan M, El Basri Y, Galeano A, Alonso C (2016) A shadow fault detection method based on the standard error analysis of i-v curves. *Renewable Energy* 99:1181–1190, DOI <https://doi.org/10.1016/j.renene.2016.08.028>
- [15] Liu H, Arora M, Jian K, Zhao L (2021) Automatic iv curve diagnosis with deep learning. In: 2021 IEEE 48th Photovoltaic Specialists Conference (PVSC), pp 2242–2246, DOI 10.1109/PVSC43889.2021.9519033
- [16] Semenick D (1990) Tests and measurements: The t-test. *Strength & Conditioning Journal* 12(1):36–37

## Hybrid AC/DC Architecture in CEDER-CIEMAT Microgrid: a case study

Paula Peña-Carro<sup>1</sup>, Óscar Izquierdo-Monge<sup>1</sup>, Siro Soria Franco<sup>1</sup>, Mariano Martín Martínez<sup>1</sup>, Gonzalo Martín Jimenez<sup>1</sup>

<sup>1</sup> CEDER-CIEMAT, Autovía de Navarra A15 salida 56, 422290 Lubia (Soria), Spain, P.P.C.: paula.pena@ciemat.es; O.I.M.: oscar.izquierdo@ciemat.es; S.S.F.: siro.soria@ciemat.es; M.M.M.: mariano.martin@ciemat.es; G.M.J.: gonzalomj96@gmail.com;

**Abstract.** TIGON demonstration project at the CEDER centre of a microgrid with DC-based smart grid architecture and integrated into the current energy system, in which it is proposed as a future solution to reduce energy losses caused by DC-AC conversions, increasing overall performance and profitability of hybrid grids. In addition, it seeks to ensure the supply, stability and reliability of the system, as is the case with the microgrids known and used to date.

**Keywords:** DC microgrid, direct current (DC), hybrid architecture, DC/AC conversion.

### 1 Introduction

Microgrids are characterised by being a network with clearly defined limits managed as a single system, in which we find different sources of distributed generation, storage and consumption systems. One of the benefits associated with this way of operating is the use of local resources, managing to reduce energy transport distances and thus the losses related to them, improving the generation-consumption energy efficiency.

These distributed generation sources are mostly of renewable origin, the best known and most widely used being wind and photovoltaic systems. These types of technologies generate direct current (DC), either directly or through a power converter. Another element that operates in DC, highlighting its importance within the microgrid due to the intermittency associated with renewable energy sources, is the storage systems, which play a significant role in balancing load and power within the DC microgrid [1]. Thus, we observe that the predominant operation within a microgrid is in DC versus alternating current (AC) operation.

Modern electrical equipment, computers, mobile phones, ventilation systems, electric vehicles, etc. [2], are also used in this mode of operation, direct current. In contrast, we find that most of the infrastructure of the electricity grid is centralised and is operated in AC. The reason for its use in this type of current is the reduction of electricity losses at high voltages during transport compared to direct current. Due to

this disparity in the type of current, between the generation mode and consumption mode, it is necessary to convert from DC to AC by using a DC/AC converter in order to be able to use the equipment that is plugged into the mains. This conversion produces energy losses, both in the converter, producing a total energy loss of approximately 10-25% [1], [3], [4], and in the transport from the point of generation to the point of consumption. In turn, they reduce the efficiency of electrical systems.

These disadvantages associated with alternating current consumption make direct current grids attractive in the energy sector [5], [6]. This is largely due to the increase in DC loads, such as LED lighting, electric vehicle charging stations, energy storage, etc. It is also due to the increasing growth of distributed generation sources, where the transport of electricity is significantly reduced.

The main factors driving this electricity paradigm shift are related to the improved efficiency, flexibility, safety and reliability that DC grids can provide, thus increasing the sustainability of the power distribution system.

This TIGON project (Towards Intelligent DC-based hybrid Grids Optimizing the Network performance) is framed within the European Union, financed by Horizon 2020. Fifteen entities from eight European Union countries are participating. Among them is the CEDER centre, which is one of the demonstrators of the project.

TIGON was created to demonstrate the possibilities offered by microgrids with DC architectures. The advantages/disadvantages over their AC counterparts and to consolidate all the control systems, topologies and applications. With the aim that these solutions can go from being a promising solution for future smart grids to a commercially available technological option.

The DC microgrid proposes a four-level approach aimed at improving reliability, resilience, performance and cost-efficiency through the development of power electronics solutions, systems and software tools focused on the efficient monitoring, control and management of DC grids.

The document is developed in sections as follows: Section 2 presents the CEDER centre where the hybrid architecture microgrid is located. Section 3 details the monitoring implemented in the centre for the follow-up of the different equipment. Finally, section 4 describes the future work planned with this project.

## **2 Scenario: CEDER - CIEMAT**

One of the project's demonstrators is the Renewable Energy Development Centre (CEDER) in Lobia (Soria - Spain). This public research organisation is part of the Centre for Energy, Environmental and Technological Research (CIEMAT) and is attached to the Department of Energy. The centre specialises in the development and promotion of renewable energies. It has extensive facilities for scientific and technological demonstrations. For these reasons, it is an ideal environment for the installation and study of the microgrid project with a DC grid.

The centre can be considered a microgrid, with different generation systems, such as photovoltaic panels, wind turbines, biomass, mini-hydro, storage systems (LFP batteries and Pb-acid batteries) and different loads. All of this is operated and man-

aged in real-time through an interface with the capacity to switch on, switch off and vary the power of all the equipment instantaneously.

The general microgrid of the CEDER has a medium voltage grid (15kV) in which eight transformer substations can be identified that adjust the voltage from 15 kV to 400 V three-phase low voltage. For the TIGON demonstration, we will focus on an area within the centre's facilities called PEPA II. It will host the microgrid with DC-based grid architecture connected via a solid-state transformer (SST). The SST is developed exclusively for this project by one of the consortium members. It will have the function of connecting the main grid of the centre with the DC microgrid. Through this point of common coupling (PPC), which connects LVAC - MVDC, the microgrid will be able to operate in isolation or connected to the distribution network.

We are currently in the second year of the project. Different equipment is being developed simultaneously, such as the solid-state transformer. The SiC medium voltage DC/DC power converters. And the energy management system, WAMPAC, together with the development of a cybersecurity system.

At the same time, the project demonstrators, in this case, our CEDER centre, are adapting their facilities to host all the equipment.

Figure 1 shows the organisation and composition of all the elements that configure the hybrid AC/DC microgrid in Pepa II.

Apart from the devices under development, the centre has generation and storage systems that are currently installed and in operation.

We are collecting data on their operation for subsequent analysis. This will serve as a comparison between production and consumption in an alternating current network and, later, in a direct current network.

Thanks to these records with the same equipment but in different operating scenarios, referring to direct current/alternating current, we will be able to carry out different studies. Studies of production yields, costs, etc., thus eliminating factors such as, for example, the difference in equipment or different locations with different productions influenced by local resources.

Following are the details of all the installed components that make up the project.

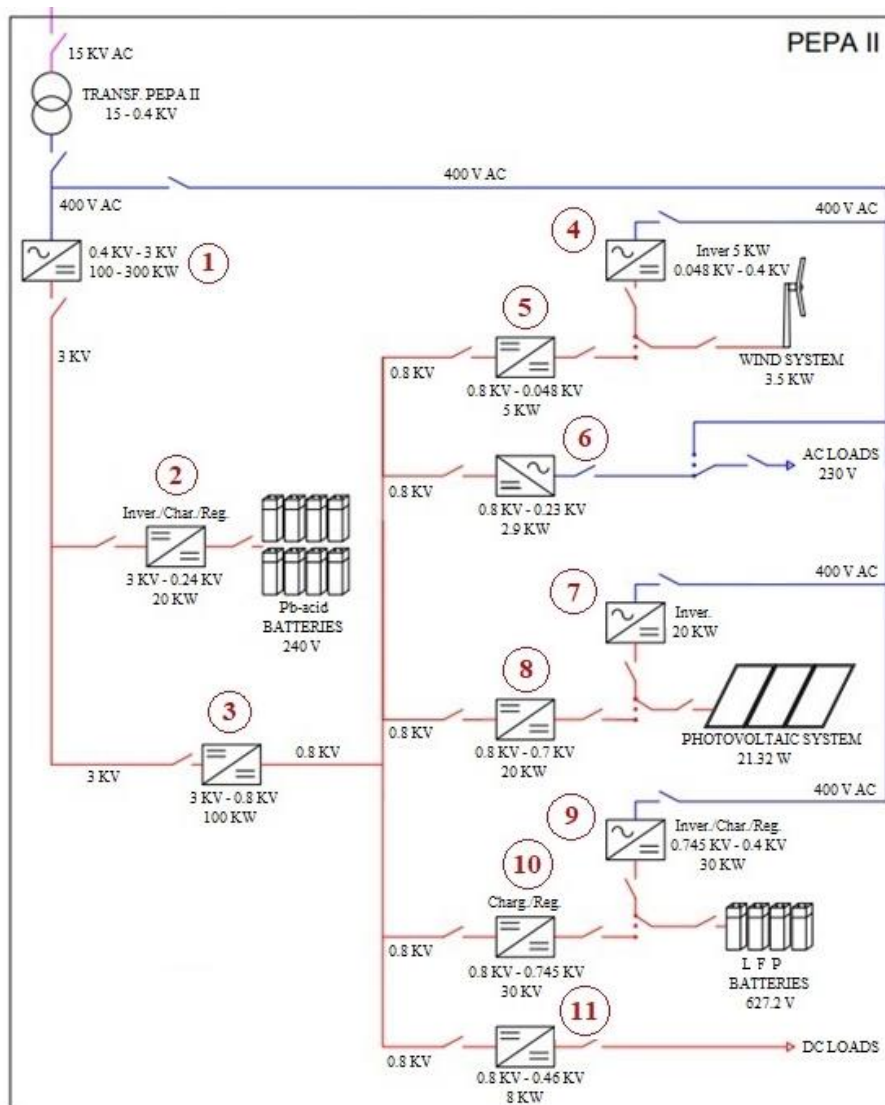


**Fig. 1.** Schematic diagram of AC/DC hybrid microgrid architecture.

If we look at the DC part (red line) we find a medium voltage grid containing the Pb-acid batteries. And a low voltage grid housing the photovoltaic system, wind turbine, LFP batteries, and loads.

On the AC side (blue line), there are the AC loads of the centre, such as offices, laboratories, computers, etc.

## 2.1 Generation elements

Two technologies have been installed in the low-voltage part of the project, a wind and a photovoltaic system.

- Figure 2 shows the wind system. Ryse Energy E5 three-bladed, wind turbine with a rated output of 3.5 kW windward horizontal axis.



**Fig. 2.** Ryse Energy E5 wind turbine.

- Figure 3 presents the photovoltaic panel system: consisting of 52 panels of 410 W monocrystalline silicon in a series-parallel arrangement. Connected to an Ingecon Sun 3 Play inverter with a nominal power of 20 kW.



**Fig. 3.** Photovoltaic system.

## 2.2 Storage systems

The centre has two electrochemical storage systems. The first is a bank of Pb-acid batteries located in the medium voltage grid (MVDC). The other system is a bank of LFP batteries on the low-voltage grid (LVDC).

- Figure 4 shows the Pb-acid battery system: battery bank consisting of 120 cells of 2 V each, with a capacity of 1080 Ah ( $C_{120}$ ) and a total voltage of 240 Vdc.



**Fig. 4.** Pb-acid battery bank.

- Figure 5 shows the LFP battery bank: made up of 14 modules, with 14 cells of 3.2 V each, achieving a total voltage of 627.2 Vdc and a nominal capacity of 50 Ah. Managed via a BMS and an Ingecon Sun 30 inverter adapted for this function.



**Fig. 5.** LFP battery bank.

### **2.3 Loads**

We distinguish three loads. The first of these is the microgrid of the CEDER in AC (lights, computers, machinery, laboratory processes, etc.), located upstream of the transformer substation, which is the largest load in terms of power.

The remaining two loads are programmable, one located on the AC grid and the other on the DC grid.

As for the AC programmable loads, Figure 6 shows three AC2928 programmable loads whose working mode is master-slave with a power of 2.9 kW. We have one master, two slaves. Thanks to their programmability (daily and hourly), they allow us to set operating periods coinciding with different desired consumption patterns.



**Fig. 6.** AC2928 programmable AC loads.

With regard to the continuous loads, there are two 4 kW Enelec resistive loads installed (see Figure 7), which allow the possibility of working in both three-phase and continuous, depending on the required needs. In our case, we will opt for DC consumption, which can be manually applied to different percentages of variation of the total power of the loads, thereby achieving the application of different consumptions and seeing how the microgrid responds.



**Fig. 7.** Enelec programmable DC loads.

## 2.4 Power converters

Within the proposed hybrid architecture microgrid, we identified seven converters. All of them are being developed in parallel by members of the consortium and professors from the University of Valladolid (UVA).

The members of the consortium are responsible for the converters of the Pb-acid batteries and the DC low voltage grid input. The UVA is in charge of the converters located in each of the generation equipment, LFP batteries, and loads.

The development is being carried out under several premises, the material used is silicon carbide (SiC), a medium voltage which aims to develop several power electronics building blocks (PEBB) that can be joined in series/parallel to achieve the desired nominal voltage and power levels in the final application, being flexible configurations that have the simplest possible replicability.

The function of each of the converters will be to adapt the voltage and power of the DC grid to that of the downstream equipment (generation systems, storage, and loads) for its correct operation.

### **3 Microgrid monitoring**

Efficient management of the microgrid is essential for the correct operation of all the equipment that compose it. For this reason, it is necessary to know the instantaneous generation and consumption values. Therefore, it is essential to develop a control system that allows real-time monitoring of the power consumed by the loads, the power produced by the generation sources and the power consumed or produced by the storage systems.

In most cases, the management system communicates directly with the converters of each of the units using the Modbus communication protocol. If it is not possible to communicate directly with a converter, it is necessary to install an intelligent measurement system (network analysers). With the installation of this equipment, the aim is to measure the necessary parameters and communicate with the control system using a communication protocol.

This monitoring makes it possible to see what is happening in the microgrid in real-time and also to take instant decisions to improve its performance, such as starting batteries, stopping loads, regulating the power generated by photovoltaic systems by giving instructions to the inverter, etc.

The main objective of the WAMPAC system is to detect, prevent and mitigate possible problems that may occur in the microgrid in as short a time as possible without the occurrence of high impact effects such as power outages, failure to supply critical loads, etc.

To develop the microgrid monitoring and control system, we will use the Home Assistant software installed on a Raspberry Pi 4. This will allow the power data of each element of the microgrid to be monitoring in real-time [7].

At present, we have a record of the systems already installed in the microgrid. As the project progresses and the rest of the equipment is developed and installed, it will be incorporated into the management system in order to act on them as well.

To connect all the elements, it is necessary to have a data network that connects each of the elements, as well as the equipment where the control system is developed. In our case as shown in Figure 8, an Ethernet data network has been deployed to connect all of them.

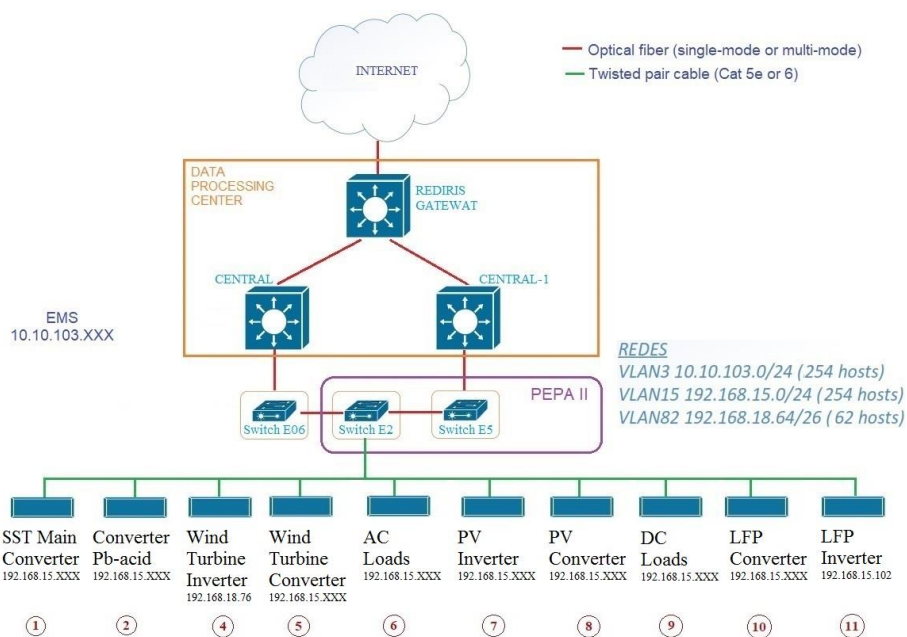


**Fig. 8.** Microgrid communications network.

The control software was developed with Home Assistant and accessible in a decentralised manner from any point in the CEDER-CIEMAT communications network, which can be accessed remotely via its mobile application.

In addition to real-time monitoring data for instant decision making, it is of great interest to store data for later analysis to establish medium and long-term management strategies.

The data is stored every second, but it is better to use fortnightly averages for the study, as this is the minimum time scale used by the electricity distribution company. Home Assistant allows data to be stored using SQL alchemy, saving only the value changes in each of the stored variables, which makes it difficult to analyse later.

Therefore, instead of using Home Assistant for data storage, we will use a Maria DB database management system, that is a relational database that allows to store the Home Assistant data in real time per second using scheduled events and to calculate the fortnightly averages through the corresponding queries.

A topic closely related to the management and control software of the microgrid is cyber security. Due to the number of devices, the number of entry points to the network and, the protocols used, the potential online attack surface increased.

The current cybersecurity market cannot yet coherently handle the deployment of the entire electricity system. For this reason, the project is developing a security framework that will provide a set of defence measures in grid attack scenarios.

This means that the way the cyber security system works and is prepared is based on an assessment of vulnerabilities and attack scenarios to design a malware-smart grid architecture. In turn, security behaviour will be analysed to reduce the impact due to human error and spear-phishing campaigns.

## **4 Conclusions and future work**

The CEDER centre is a demonstration centre for the TIGON project, which houses a microgrid with hybrid AC/DC architecture within its facilities.

Currently, in the second active year of the project, all generation, storage, and consumption systems are installed and connected as a microgrid as we know them today, in alternating current.

The current operation of the electrical microgrid, data recording, and instantaneous action on the equipment. This will allow us to carry out studies, comparisons, analysis of the variations in behaviour, costs, benefits, energy losses at the equipment level, at a global level, all of this compared to the hybrid microgrid registers.

All these studies and analyses are part of future work. To get there, we are researching and developing, as discussed in this document; SST, power converters, management systems, and cybersecurity.

Once all the components are installed and systems are created. We will then be able to start setting up the hybrid microgrid. With its operation and recording of values of; energy generated at equipment and global level, energy consumed at global level, energy recorded before and after the converters and equipment performance. We will be able to complete the proposed studies.

The conclusions of the project are intended to support the decision-making of grid operators and to steer actions towards decentralised hybrid microgrids. At present, the lack of DC microgrids prevents them from being a promising solution for future distribution grids to become a commonly used technology.

In this way, a positive impact is achieved with the demonstration of the project in our facilities. Ease of replicability with the technologies developed, the management system, and the cybersecurity system implemented, both for operators and consumers. To be the basis for establishing microgrids based on DC and to see it as an optimal solution and future horizon to be addressed. To improve generation efficiency and facilitate the energy transition following the decarbonisation targets set by the European Union.

## **Acknowledgments**

The authors thank the possibility to participate as a demonstration centre in the TIGON (Towards Intelligent DC-based hybrid Grids Optimizing the Network

performance) project. This work has been supported by European Union's Horizon 2020 research and innovation programme under grant agreement No 957769.

## References

- [1] M. Gunasekaran, H. Mohamed Ismail, B. Chokkalingam, L. Mihet-Popa, and S. Padmanaban, "Energy Management Strategy for Rural Communities' DC Micro Grid Power System Structure with Maximum Penetration of Renewable Energy Sources," *Appl. Sci.*, vol. 8, no. 4, 2018, doi: 10.3390/app8040585.
- [2] M. Fotopoulou, D. Rakopoulos, D. Trigkas, F. Stergiopoulos, O. Blanas, and S. Voutetakis, "State of the Art of Low and Medium Voltage Direct Current (DC) Microgrids," *Energies*, vol. 14, no. 18, 2021, doi: 10.3390/en14185595.
- [3] L. Gao, Y. Liu, H. Ren, and J. M. Guerrero, "A DC Microgrid Coordinated Control Strategy Based on Integrator Current-Sharing," *Energies*, vol. 10, no. 8, 2017, doi: 10.3390/en10081116.
- [4] B. T. Patterson, "DC, Come Home: DC Microgrids and the Birth of the 'Enernet,'" *IEEE Power Energy Mag.*, vol. 10, no. 6, pp. 60–69, 2012, doi: 10.1109/MPE.2012.2212610.
- [5] D. Bosich, A. Vicenzutti, S. Grillo, and G. Sulligoi, "A Stability Preserving Criterion for the Management of DC Microgrids Supplied by a Floating Bus," *Appl. Sci.*, vol. 8, no. 11, 2018, doi: 10.3390/app8112102.
- [6] S. Saponara, R. Saletti, and L. Mihet-Popa, "Recent Trends in DC and Hybrid Microgrids: Opportunities from Renewables Sources, Battery Energy Storages and Bi-Directional Converters," *Appl. Sci.*, vol. 10, no. 12, 2020, doi: 10.3390/app10124388.
- [7] O. Izquierdo-Monge, P. Peña-Carro, R. Villafafila-Robles, O. Duque-Perez, A. Zorita-Lamadrid, and L. Hernandez-Callejo, "Conversion of a Network Section with Loads, Storage Systems and Renewable Generation Sources into a Smart Microgrid," *Appl. Sci.*, vol. 11, no. 11, 2021, doi: 10.3390/app11115012.

# Alocação Ótima de Sistemas de Armazenamento de Energia Visando o Despacho Econômico

Raphael van der Linden<sup>1</sup>, Lucas Carlos da Silva<sup>2</sup>, Yuri Percy Molina Rodriguez<sup>3</sup>

Departamento de Engenharia Elétrica, Universidade Federal da Paraíba, Brasil.  
(raphael.linden<sup>1</sup>, lucascarlos.silva<sup>2</sup>, molina.rodriguez<sup>3</sup>)@cear.ufpb.br

**Resumo.** A demanda energética do Brasil viveu um crescimento significativo nos últimos anos. Simultaneamente, questões ambientais relacionadas a preservação ambiental e redução da emissão de poluentes vem ganhando destaque. Neste contexto, torna-se de grande importância o estudo e desenvolvimento de novas formas e tecnologias que permitam uma maior eficiência energética, melhor aproveitamento das fontes renováveis de natureza intermitente e a diminuição dos efeitos oscilatórios indesejados na rede resultantes desta intermitência. Este trabalho busca colaborar com esta discussão a partir do estudo e desenvolvimento de um modelo de otimização para solucionar o problema de alocação ótima de Sistemas de Armazenamento de Energia (SAEs) em Sistemas de Distribuição de Energia Elétrica (SDEEs). Os SAEs apresentam-se como dispositivos capazes de proporcionar um melhor aproveitamento das fontes renováveis, armazenando sua energia quando há excedente e despachando quando há aumento da demanda. Os resultados obtidos permitem a observação do comportamento dos SAEs além da economia proporcionada.

**Palavras-chave:** SAE, Despacho Econômico, Alocação Ótima, SDEE

## 1 Introdução

A demanda energética do Brasil viveu uma expansão e crescimento significativo ao longo dos últimos anos, simultaneamente com a discussão e preocupação acerca do meio ambiente, tópico que detêm urgência nos dias atuais. A reestruturação do setor elétrico das duas últimas décadas introduziu mudanças consideráveis na forma de produção, com uma maior inserção de fontes renováveis, como eólica, hídrica e solar [1]. Com políticas de incentivos governamentais, o percentual de energia renovável da matriz energética mundial foi aumentado com o objetivo de atingir metas relacionadas à redução de emissões de CO<sub>2</sub> e independência energética através da geração distribuída [2]. Com este novo cenário de desafios, a preocupação no despacho de energia elétrica para atender à demanda de uma forma mais econômica e eficaz tornou-se constante, levando em consideração a natureza intermitente e custo das novas fontes de produção de energia que podem ter diversos efeitos negativos em todo o sistema de distribuição [3]. Os sistemas de armazenamento de energia (SAE) se mostraram nesse cenário

2 Linden, R. v. d.; Silva, L.C.; Rodriguez, Y.P.M.

uma solução viável, tendo por objetivo atenuar as flutuações na geração e no suprimento de energia, pois possibilitam que a energia seja armazenada e liberada em diferentes momentos [4]. Porém, o custo de aquisição e manutenção desses dispositivos é ainda bastante elevado, por se tratar de uma tecnologia ainda em estágio bastante inicial, afetando diretamente a sua implementação quando se tem o objetivo de ter um despacho energético econômico.

Com o crescimento contínuo da demanda de energia elétrica, aumentou também a necessidade do uso de novas tecnologias que buscam solucionar problemas de expansão e planejamento da operação de Sistema de Distribuição de Energia Elétrica (SDEE) [4]. A busca pela modernização e automatização do sistema elétrico é antiga e tem sido acelerada ao longo dos últimos anos, produzindo modificações substanciais nesse processo, ocasionando mudanças na estruturação dos sistemas elétrico atreladas também ao aumento da importância dos fatores sócio-ambientais. No presente, as concessionárias de energia elétrica já dispõem de softwares que permitem a gerência de suas atividades, com foco na otimização dos resultados em variados setores, como planejamento, operação e comercial [1]. A criação e desenvolvimento de modelos matemáticos de otimização para resolução de problemas de planejamento se tornou também uma ferramenta importante na transformação do SDEE, promovendo de forma direta a redução substancial nos custos de expansão e operação [4].

Como dito anteriormente, uma grande problemática atual de planejamento do SDEE é o desenvolvimento de SAEs abrangem toda a cadeia de fornecimento de energia elétrica, da geração ao uso final, de maneira inteligente [5]. Dentro da concepção desses sistemas diversos pontos devem ser analisados, mas os pontos de destaque são a alocação e a operação, que buscam proporcionar uma melhor distribuição da energia armazenada na rede de uma forma que provoquem um saldo positivo na análise econômica, além da maximização dos ganhos oriundos desta tecnologia com a menor quantidade possível de recursos utilizados [6] [7]. Sob este aspecto, justifica-se o desenvolvimento de novos modelos matemáticos de otimização, tal como, um algoritmo para alocação ótima de SAEs visando o despacho econômico no sistema de distribuição que abranja os novos desafios de alocação dos dispositivos e operação do SDEE, criados pela integração da geração distribuída.

Em [8], é visto que as equações de fluxo de carga são não lineares e a geração das fontes renováveis é estocástica, dificultando a obtenção das decisões de controle do algoritmo [8]. As variáveis de decisões de controle na literatura relacionadas à alocação e operação dos SAEs são a potência (kW), capacidade de armazenamento (kWh) e a localização no sistema [9]. [10] nos apresenta um algoritmo genérico híbrido para resolver o problema de alocação e dimensionamento da geração distribuída, sistemas de armazenamento de energia e bancos de capacitores, porém, que não garante uma solução ótima global [11]. Portanto, visando a solução desses obstáculos e uma melhoria nas soluções apresentadas, este artigo propõe e evidencia um modelo matemático de programação não-linear inteira misto (PNLIM), com o objetivo de determinar a quantidade e localização de SAEs em um SDEE, a minimização do custo de compra de en-

ergia em sistemas de distribuição com presença de geração através de fontes renováveis e intermitentes. Foi usado como base o modelo apresentado por [12], com custo da energia comprada pela subestação como função objetivo e baterias de chumbo-ácido como dispositivos de armazenamentos de energia escolhidos. Foram colocadas algumas restrições matemáticas visando maximizar a vida útil das baterias, simular as perdas no carregamento e descarregamento dos SAEs e respeitar as restrições da rede elétrica. De forma a demonstrar a aplicação do modelo matemático desenvolvido e a eficiência do algoritmo, foi utilizado o sistema IEEE-24 barras modificado apresentado por [4] para um período de 24 horas.

As principais contribuições deste trabalho podem ser resumidos a seguir:

- Desenvolvimento de um algoritmo de otimização para alocação de SAEs em SDEEs;
- Análise do comportamento dos SAEs quando inseridos em SDEEs;
- Simular o comportamento do SDEE quando são inseridos SAEs;
- Análise da economia que pode ser obtida a partir da alocação de SAEs em SDEEs.

Este trabalho é organizado da seguinte maneira: Seção 2: descrição da modelagem dos componentes do sistema e das funções objetivos utilizados; Seção 3: resultados; Seção 4: considerações finais do trabalho.

## 2 Método Proposto

### 2.1 O Software GAMS

O GAMS, *General Algebraic Modeling System*, foi desenvolvido em 1980 inicialmente para o Banco Mundial. Trata-se de um *software* com linguagem de programação de alto nível voltado para formulação de problemas de otimização, que permite a descrição compacta de modelos de otimização complexos. Para solucionar estes problemas, o GAMS faz uso de *solvers*, que são diferentes métodos de solução voltados para diferentes tipos de problemas de otimização [12].

Este *software* foi escolhido para implantação do presente modelo, visto sua facilidade e agilidade para elaboração e manipulação de modelos de otimização, permitindo escrita e alterações desses sem obstáculos. Uma das facilidades apresentadas pelo GAMS que contribuiu para sua escolha foi a possibilidade de utilização de diversos algoritmos na resolução de um mesmo problema.

Apesar de não ser uma ferramenta voltada a sistemas elétricos, o GAMS é uma poderosa ferramenta de otimização em que pode ser modelado qualquer sistema descrito por equações matemáticas. No desenvolvimento deste trabalho foi utilizada programação não-linear inteira mista utilizando o solver *BONMIN*, como ferramenta de modelagem da otimização do sistema de distribuição proposto.

Para esta modelagem no GAMS, é necessário que se descreva todas as características elétricas do sistema. A seguir são descritas as principais características e que foram consideradas neste trabalho.

4 Linden, R. v. d; Silva, L.C.; Rodriguez, Y.P.M.

## 2.2 Equações de Fluxo de Carga

As equações de fluxo de carga são obtidas satisfazendo as leis de Kirchhoff em cada uma das barras. Em outras palavras, a potência que entra em cada barra deve ser igual a potência que sai da barra [13]. Sendo assim, o fluxo de carga pode ser formulado a partir das seguintes equações:

$$\sum_{j \in \Omega_i} P_{ij,t} = -P_{i,t}^d + P_{i,t}^s \quad (1)$$

$$\sum_{j \in \Omega_i} Q_{ij,t} = -Q_{i,t}^d + Q_{i,t}^s \quad (2)$$

$$P_{ij,t} = \frac{V_{i,t}^2}{z_{ij}} \cos(\theta_{ij}) - \frac{v_{i,t}v_{j,t}}{z_{i,j}} \cos(\delta_{i,t} - \delta_{j,t} + \theta_{ij}) \quad (3)$$

$$Q_{ij,t} = \frac{V_{i,t}^2}{z_{ij}} \text{sen}(\theta_{ij}) - \frac{v_{i,t}v_{j,t}}{z_{i,j}} \text{sen}(\delta_{i,t} - \delta_{j,t} + \theta_{ij}) \quad (4)$$

Onde:

- $j \in \Omega_i$ : entende-se como  $j$  pertence a vizinhança de  $i$ ;
- $P_{ij,t}$ : Fluxo de Potência Ativa da barra  $i$  para a barra  $j$ , no instante  $t$ ;
- $Q_{ij,t}$ : Fluxo de Potência Reativa da barra  $i$  para a barra  $j$ , no instante  $t$ ;
- $P_{i,t}^d$ : Demanda de Potência Ativa da barra  $i$ , no instante  $t$ ;
- $P_{i,t}^s$ : Potência Ativa fornecida na barra  $i$ , no instante  $t$ ;
- $Q_{i,t}^d$ : Demanda de Potência Reativa da barra  $i$ , no instante  $t$ ;
- $Q_{i,t}^s$ : Potência Reativa fornecida na barra  $i$ , no instante  $t$ ;
- $V_{i,t}$ : Módulo da Tensão na barra  $i$ , no instante  $t$ ;
- $V_{j,t}$ : Módulo da Tensão na barra  $j$ , no instante  $t$ ;
- $z_{ij}$ : Módulo da Impedância da linha entre as barras  $i$  e  $j$ ;
- $\theta_{ij}$ : Fase da Impedância da linha entre as barras  $i$  e  $j$ ;
- $\delta_{i,t}$ : Fase da Tensão na barra  $i$ ;
- $\delta_{j,t}$ : Fase da Tensão na barra  $j$

Além das equações que descrevem o fluxo de carga, devem ser considerados as restrições do sistema. São elas: limites de potência nas linhas e limites de tensão nas barras normalizado pelos órgãos reguladores. Além disso, é limitado os ângulos das barras entre  $-\pi/2$  e  $\pi/2$  para evitar instabilidades no sistema.

$$S_i^{min} \leq S_{i,t} \leq S_i^{max} \quad \forall i \in \Omega_s, \forall t \in \Omega_t \quad (5)$$

$$P_{ij}^{min} \leq P_{ij,t} \leq P_{ij}^{max} \quad \forall j \in \Omega_i, \forall t \in \Omega_t \quad (6)$$

$$Q_{ij}^{min} \leq Q_{ij,t} \leq Q_{ij}^{max} \quad \forall j \in \Omega_i, \forall t \in \Omega_t \quad (7)$$

$$V_i^{min} \leq V_{i,t} \leq V_i^{max} \quad \forall i \in \Omega_i, \forall t \in \Omega_t \quad (8)$$

Onde:

- $S_{i,t}$ : Potência fornecida pela subestação  $i$ , no instante  $t$ ;
- $\Omega_g$ : Conjunto Subestações;
- $\Omega_t$ : Conjunto dos períodos;
- $\Omega_i$ : Conjunto dos barramentos;

### 2.3 Características dos SAEs

O objetivo da utilização dos SAEs é armazenar energia em duas situações, são elas: excedente de geração de fontes renováveis e baixo custo de compra de energia da subestação. Posteriormente esta energia armazenada nos SAEs será despachada quando houver pico de demanda no sistema, evitando efeitos indesejados como oscilações.

Os sistemas de armazenamento são alocadas em barras e em quantidade que otimizem a função objetivo. Dessa forma, a alocação dos sistemas devem seguir as seguintes restrições, que restringem o estado de carga de cada SAE, a quantidade de dispositivos de armazenamento totais no sistema e a carga mínima de cada um deles [12]:

$$SOC_i^{min} * N_i^{SAE} \leq SOC_{i,t} \leq SOC_i^{max} * N_i^{SAE} \quad \forall i \in \Omega_{SAE}, \forall t \in \Omega_t \quad (9)$$

$$\sum_i N_i^{DAE} \leq N_{max}^{SAE} \quad \forall i \in \Omega_{SAE} \quad (10)$$

$$SOC_{i,0} = \alpha_0^{SAE} * SOC_{i,max} \quad (11)$$

$$N_i^{SAE} \in \{0, 1\} \quad (12)$$

Onde:

- $SOC_{i,t}$ : Estado de Carga do SAE alocado na barra  $i$ , no instante  $t$ ;
- $N_i^{SAE}$ : Quantidade de SAEs alocados na barra  $i$ ;
- $N_{max}^{SAE}$ : Quantidade máxima de SAEs alocados no sistema;
- $\Omega_{SAE}$ : Conjunto dos SAEs alocados;

Os SAEs têm capacidade de armazenamento limitada. Uma variável muito importante no uso desses dispositivos é o SOC (*State of charge* ou Estado de Carga), uma medida da energia armazenada em relação a capacidade do SAE.

A potência do SAE pode se apresentar de duas formas: valores positivos indicam que o SAE está carregando absorvendo potência do sistema e valores negativos indicam que o SAE está descarregando injetando potência no sistema.

As equações que regem o comportamento de carga e descarga dos dispositivos são descritas a seguir [12]:

$$SOC_{i,t} = SOC_{i,t-1} + \left( P_{i,t}^{carga} * n_{carga} - \frac{P_{i,t}^{descarga}}{n_{descarga}} \right) \Delta t \quad (13)$$

6 Linden, R. v. d; Silva, L.C.; Rodriguez, Y.P.M.

$$\forall i \in \Omega_{SAE}, \forall t \in \Omega_t$$

$$P_{i,min}^{carga} * N_i^{SAE} \leq P_{i,t}^{carga} \leq P_{i,max}^{carga} * N_i^{DAE} \quad (14)$$

$$P_{i,min}^{descarga} * N_i^{SAE} \leq P_{i,t}^{descarga} \leq P_{i,max}^{descarga} * N_i^{SAE} \quad (15)$$

Onde:

- $P_{i,t}^{carga}$ : Potência de carga do SAE alocado na barra  $i$ , no instante  $t$ ;
- $P_{i,t}^{descarga}$ : Potência de descarga do SAE alocado na barra  $i$ , no instante  $t$ ;
- $n_{carga}$ : Eficiência de carga do SAE;
- $n_{descarga}$ : Eficiência de descarga do SAE;

## 2.4 Função Objetivo

Um problema de otimização tem por propósito a minimização ou maximização de uma função, onde se deve levar em conta as condições e restrições de cada uma das variáveis contidas nesse. Esse projeto tem por intuito resolver o problema de alocação e operação ótima de SAEs com foco em baterias, propondo a determinação da quantidade e os locais em que os dispositivos devem ser instalados, bem como seu ciclo ótimo de carga e descarga dos dispositivos, visando o despacho econômico e considerando os custos de operação destes dispositivos. Desta forma, a função objetivo adotada é apresentada na Equação 16, onde o primeiro produto corresponde ao custo de compra de energia da subestação e o segundo corresponde ao custo de operação do SAE. A fim de comparação e futura validação dos resultados, foi utilizada também a Equação 17, voltada apenas para minimização dos custos da energia comprada da subestação e sem restrições que visam à extensão de vida útil dos SAEs.

$$OF1 = \sum_t c_t^s * P_t^s + c^{SAE} * P_{it}^{descarga} \quad \forall t \in \Omega_t \quad (16)$$

$$OF2 = \sum_t c_t^s * P_t^s \quad \forall t \in \Omega_t \quad (17)$$

- $c_t^s$ : Custo da energia comprada da subestação, no instante  $t$ ;
- $P_t^s$ : Potência Ativa despachada pela subestação, no instante  $t$ ;
- $c^{SAE}$ : Custo de uso da energia do SAE;
- $P_{it}^{descarga}$ : Potência de descarregamento do SAE, na barra  $i$ , no instante  $t$ ;
- $\alpha_0^{SAE}$ : Fator de proporcionalidade de armazenamento;

## 3 Resultados

Neste tópico serão analisados os resultados das simulações em um sistema de distribuição de vinte e quatro barras, alimentado por uma subestação e por quatro unidades geradoras intermitentes, sendo uma solar e três eólicas. O objetivo

do estudo é diminuir os custos de compra de energia para abastecer o SDEE, obtendo de forma otimizada o número de SAEs que poderiam ser utilizadas no sistema, o impacto dessas na curva de custo da energia da subestação, a preferência de alocação otimizada e a maximização da vida útil dos SAEs. O algoritmo desenvolvido retorna como resultados o valor da função objetivo, as barras de alocação dos SAEs, descarga diária de cada SAE e gráficos ilustrativos da potência gerada por fonte e comportamento de carga/descarga dos SAEs.

### 3.1 Sistema teste 24 barras

Na Figura 1 é ilustrado o sistema IEEE 24-Barras modificado, apresentado por [4]. Este sistema é alimentado por uma subestação conectada a barra b15, com potência nominal de 1,5MVA e tarifação horosazonal, com tarifas por kWh de R\$0,53 no horário fora-ponta e R\$0,93 no horário de ponta, das 18h às 21h, e por quatro fontes renováveis de natureza intermitente, sendo três eólicas nas barras b7, b8 e b18 e outra solar na barra b13.

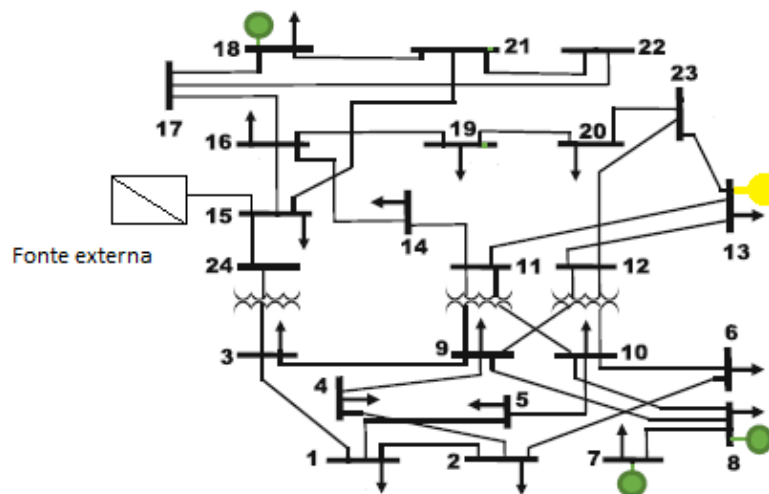


Figura 1: Modelo IEEE 24 barras modificado  
Fonte: [4]

As potências fornecidas por estas fontes ao longo do dia são descritas na Tabela 1, as demandas de potência ativa e reativa do sistema ao longo do dia são descritas na Tabela 2 e as características das linhas entre as barras são descritas na Tabela 3.

8 Linden, R. v. d; Silva, L.C.; Rodriguez, Y.P.M.

Geração das Fontes Renováveis Intermitentes (kW)									
	Eólica b7	Eólica b8	Solar b13	Eólica b18		Eólica b7	Eólica b8	Solar b13	Eólica b18
t1	340	340	0	340	t13	510	510	600	510
t2	350	350	0	350	t14	560	560	600	560
t3	305	305	0	305	t15	580	580	410	580
t4	320	320	0	320	t16	600	600	300	600
t5	290	290	0	290	t17	515	515	0	515
t6	295	295	0	295	t18	400	400	0	400
t7	395	395	0	395	t19	395	395	0	395
t8	350	350	300	350	t20	330	330	0	330
t9	300	300	380	300	t21	330	330	0	330
t10	315	315	410	315	t22	325	325	0	325
t11	450	450	485	450	t23	425	425	0	425
t12	415	415	600	415	t24	500	500	0	500

Tabela 1: Geração das fontes renováveis intermitentes

Fonte: [4]

	P (kW)	Q (kVAr)		P (kW)	Q (kVAr)
t1	1950,86	397,02	t13	2481,33	504,97
t2	1835,75	373,59	t14	2377,62	483,87
t3	1747,25	355,58	t15	2327,13	473,59
t4	1709,24	347,85	t16	2335,27	475,25
t5	1678,29	341,55	t17	2491,10	506,96
t6	1704,35	346,85	t18	2850,00	580,00
t7	1786,34	363,54	t19	2803,31	570,50
t8	1857,47	378,01	t20	2668,65	543,09
t9	2012,21	409,50	t21	2529,65	514,81
t10	2242,97	456,46	t22	2306,50	469,39
t11	2391,20	486,63	t23	2125,69	432,60
t12	2430,29	494,59	t24	2090,40	425,41

Tabela 2: Demandas de Potência Ativa e Reativa do SDEE ao longo do dia

Fonte: [4]

### 3.2 Características dos SAEs Adotados

Existem diferentes metodologias para descrever o comportamento dos SAEs disponíveis na literatura, visto que o funcionamento das baterias é comumente dessemelhante ao previsto pelo fabricante. Aspirando estimar de forma assertiva a vida útil dos SAEs, utilizou-se neste trabalho a sistemática apresentada por [15] que autentica uma forma de previsão de vida útil e dimensionamento de baterias de chumbo-ácido para aplicações de armazenamento de microgeração.

Seguindo o método apresentado por [15] que indica que um tamanho de bateria de Q amperes-horas fornece  $(390 \cdot Q)$  horas de amperes efetivas ao longo de sua vida útil, as Equações 18 e 19 apresentam a formulação utilizada para estimar a vida útil das baterias de chumbo-ácido:

Alocação Ótima de SAEs visando Despacho Econômico 9

De	Para	R (pu)	X (pu)	B (pu)	Limite (kVA)	De	Para	R (pu)	X (pu)	B (pu)	Limite (kVA)
b1	b2	0,0026	0,0139	0,4611	175	b11	b13	0,0061	0,0476	0,0999	500
b1	b3	0,0546	0,2112	0,0572	175	b11	b14	0,0054	0,0418	0,0879	500
b1	b5	0,0218	0,0845	0,0229	175	b12	b13	0,0061	0,0476	0,0999	500
b2	b4	0,0328	0,1267	0,0343	175	b12	b23	0,0124	0,0966	0,2030	500
b2	b6	0,0497	0,1920	0,0520	175	b13	b23	0,0111	0,0865	0,1818	500
b3	b9	0,0308	0,1190	0,0322	175	b14	b16	0,0050	0,0389	0,0818	500
b3	b24	0,0023	0,0839	0,0000	400	b15	b16	0,0022	0,0173	0,0364	1000
b4	b9	0,0268	0,1037	0,0281	175	b15	b21	0,0032	0,0245	0,2060	1000
b5	b10	0,0228	0,0883	0,0239	175	b15	b24	0,0067	0,0519	0,1091	500
b6	b10	0,0139	0,0605	2,4590	175	b16	b17	0,0033	0,0259	0,0545	500
b7	b8	0,0159	0,0614	0,0166	175	b16	b19	0,0030	0,0231	0,0485	500
b8	b9	0,0427	0,1651	0,0447	175	b17	b18	0,0018	0,0144	0,0303	500
b8	b10	0,0427	0,1651	0,0447	175	b17	b22	0,0135	0,1053	0,2212	500
b9	b11	0,0023	0,0839	0,0000	400	b18	b21	0,0017	0,0130	0,1090	1000
b9	b12	0,0023	0,0839	0,0000	400	b19	b20	0,0026	0,0198	0,1666	1000
b10	b11	0,0023	0,0839	0,0000	400	b20	b23	0,0014	0,0108	0,0910	1000
b10	b12	0,0023	0,0839	0,0000	400	b21	b22	0,0087	0,0678	0,1424	500

Tabela 3: Características das Linhas - Impedâncias e Limites

Fonte: [4]

$$I \cdot tempo = \frac{Energia (kWh)}{\sqrt{3} \times V} (A \cdot h) \tag{18}$$

$$Vida \text{ útil} = \frac{390 \times Q (A \cdot h)}{I \cdot tempo (A \cdot h)} [anos] \tag{19}$$

Além disso, os SAEs adotados tem o  $c^{DAE} = 250\$/kWh$  e eficiência de descarga fixada em 0.85, dados descritos no modelo apresentado por [14] para baterias de chumbo-acido de alta capacidade.

### 3.3 Alocação dos SAEs

Foram simulados quatro cenários como forma de validar o algoritmo proposto. São eles:

- Caso 1: neste caso foi utilizado a Função Objetivo 1. Foram consideradas as seguintes variáveis  $SOC_{max} = 1000kWh$ ,  $SOC_{min} = 20\%$  do  $SOC_{max}$ ,  $\alpha_0^{ESS} = 0.2$  e  $N_{max}^{DAE} = 5$ .
- Caso 2: para esse caso também foi utilizado a Função Objetivo 1, com os parâmetros de  $SOC_{max} = 1000kWh$ ,  $SOC_{min} = 50\%$  do  $SOC_{max}$ ,  $\alpha_0^{ESS} = 0.2$  e  $N_{max}^{DAE} = 5$  visando garantir uma maior durabilidade do equipamento.
- Caso 3: já neste caso foi utilizado a Função Objetivo 2, com os parâmetros de  $SOC_{max} = 1000kWh$ ,  $SOC_{min} = 20\%$  do  $SOC_{max}$ ,  $\alpha_0^{ESS} = 0.2$  e  $N_{max}^{DAE} = 5$ .

10 Linden, R. v. d.; Silva, L.C.; Rodriguez, Y.P.M.

- Caso 4: neste caso também foi utilizado a Função Objetivo 2, com os parâmetros de  $SOC_{max} = 1000kWh$ ,  $SOC_{min} = 50\%$  do  $SOC_{max}$ ,  $\alpha_0^{ESS} = 0.2$  e  $N_{max}^{DAE} = 5$ .

Dentro deste contexto, o fator  $\alpha_0^{ESS}$  é a característica que limita a carga e descarga dos SAEs. Ou seja, nos casos apresentados a carga e descarga máxima das baterias é fixada em 20% do  $SOC_{max}$ .

Para uma melhor validação dos resultados, as análises apresentadas terão foco nas variações de funções objetivos, ou seja, o Caso 1 será comparado ao caso Caso 3 assim como o Caso 2 será comparado ao Caso 4, visto que os parâmetros utilizados na construção desses casos foram iguais.

A Tabela 4 apresenta os resultados de alocação e a Tabela 5 os custos operacionais da subestação para cada caso:

Casos	N° de SAEs alocados	Barras de Alocação
Caso 1 - F01	3/5	b2, b5, b6
Caso 2 - F01	5/5	b1, b2, b4, b5, b6
Caso 3 - F02	3/5	b4, b6, b13
Caso 4 - F02	5/5	b2, b4, b6, b10, b13

Tabela 4: Alocação de SAEs no Sistema

Casos	Compra de energia da subestação (\$)
Caso 1 - F01	17018.4
Caso 2 - F01	16961.88
Caso 3 - F02	16786.47
Caso 4 - F02	16751.01

Tabela 5: Custos de Compra de Energia da Subestação

### 3.4 Análise da alocação ótima dos SAEs

Ao analisarmos a Tabela 4 para os diferentes casos, nota-se um otimização diferente de alocação dos SAEs nas barras. Nos quatro casos, existiam cinco SAEs disponíveis para serem alocados, entretanto, a solução ótima alocou somente três SAEs no primeiro caso e terceiro caso e cinco SAEs no segundo caso e quarto caso. Existiu apenas uma barra em comum de alocação entre os casos, a b6.

O número de SAEs alocados nas barras demonstrou ser diretamente ligado a variação do parâmetro de  $SOC$  na modelagem, ou seja, nos casos onde o  $SOC_{min}$  era de 20% do  $SOC_{max}$  foram alocados 3 SAEs, o que significa que a potência alocadas nas baterias durante o dia foi suficiente para suprir a demanda

## Alocação Ótima de SAEs visando Despacho Econômico 11

de energia nos horários de picos, logo não havendo uma necessidade de alocar um número maior de baterias disponíveis. Já nos casos onde o  $SOC_{min}$  era de 50% do  $SOC_{max}$ , foi necessário alocar o número máximo de SAEs disponíveis, 5, para garantir a otimização das funções objetivos. Além disso, a diferença de número de baterias alocadas também sofre interferência atrelada ao objetivo de cada função, sendo o propósito da F01 não apenas alocar otimamente os SAEs, mas sim maximizar a vida útil desses.

É possível perceber pequenas variações nos custos da subestação (Tabela 5), sendo os casos com maior número de SAEs alocados os que tem os menores custos. Esse fato confirma a afirmação apresentada em [16], de que uma maior quantidade de dispositivos instalados em diferentes barras do SDEE podem proporcionar melhor distribuição da capacidade de armazenamento no sistema e acarretar em um menor custo de compra de energia da subestação.

Na Tabela 6 observa-se a comparação entre os quatro diferentes casos, onde nos casos com a F02 foi considerada somente a minimização do custo de energia da subestação e já nos casos com a F01 era visado a minimização do custo de energia da subestação e a maximização da vida útil das baterias. No que se trata da estimativa do ciclo de vida dos SAEs, os casos com a F01 obtiveram resultados inegavelmente superiores, minimizando o uso dos dispositivos e consequentemente prolongando a expectativa de vida útil dos mesmos se comparados aos casos similares que utilizaram a F02.

	Caso 1 - F01	Caso 2 - F01	Caso 3 - F02	Caso 4 - F02
Custo diário de uso SAE 1 (\$)	3934.71	2228.09	3934.71	2533.31
Custo diário de uso SAE 2 (\$)	3852.74	2465.75	3934.71	2465.75
Custo diário de uso SAE 3 (\$)	1320.94	1403.65	3934.71	2326.18
Custo diário de uso SAE 4 (\$)	-	1813.05	-	2465.75
Custo diário de uso SAE 5 (\$)	-	1065.89	-	2465.75
Custo total de uso dos SAEs (\$)	393428.54	386980.94	510000.0	528567.16
Função Objetivo (\$)	410446.94	403942.82	16786.47	16751.01
Vida útil do DAE 1 (anos)	1.88	3.32	1.88	2.92
Vida útil do DAE 2 (anos)	1.92	3.0	1.88	3.0
Vida útil do DAE 3 (anos)	5.6	5.27	1.88	3.18
Vida útil do DAE 4 (anos)	-	4.08	-	3.0
Vida útil do DAE 5 (anos)	-	6.94	-	3.0

Tabela 6: Resultados dos Custos de Operação e Estimativa de Vida Útil dos SAEs

Casos 1-3 (A): A média entre a vida útil das baterias é 40% maior no caso 1 comparada a vida útil dos SAEs no caso 3. É possível visualizar também que o caso 3 tem um custo total de uso dos SAEs 22,8% maior que no caso 1, comprovando assim uma deterioração da vida útil mais rápida e um maior custo de operação ao não restringir o uso do dispositivo visando a maximização do seu ciclo de vida.

12 Linden, R. v. d; Silva, L.C.; Rodriguez, Y.P.M.

Casos 2-4 (B): Já para esses casos, onde foram alocados 5 SAEs, a média do ciclo de vidas das baterias é 33,22% maior no caso 2 em comparação ao caso 4. Além disso, o custo total de uso dos SAEs é 26,79% maior no caso 4 quando analisado em relação ao caso 2, comprovando a tendência já apresentada nas comparações do casos 1-3 e ainda tenho um aumento de 3,93% em relação a mesma estatística apresenta nos casos anteriores.

Numa análise integral, é possível confirmar que a utilização da F01 é eficaz na extensão de sua vida útil dos SAEs em ambos os casos onde foi utilizada, independente do conjunto de parâmetros utilizados. Além disso, promove um menor custo de operação dos SAEs que é uma das variáveis mais importantes quando o assunto abordado é o despacho econômico em SDEEs que utilizam SAEs em sua estrutura.

### 3.5 Análise da operação ótima dos SAEs

O algoritmo utilizou três SAEs nos casos 1-3 (A) para respeitar a restrição da subestação nos horários de pico e utilizou cinco SAEs nos casos 2-4 (B).

A Figura 2 (Casos A) representa a operação das baterias em um planejamento horizontal de 24 horas. É possível observar que nos dois casos (1-3) os SAEs estão operando em estado de carregamento nos horários fora de ponta e descarregamento apenas na hora de ponta, fazendo com que as restrições da subestação nos horários de pico fossem respeitadas. Para os dois casos não há nenhum momento em que existe um carregamento em horário de ponta. Porém, ao analisarmos a Figura 3 (Casos B), que apresenta a visualização apresentada anteriormente agora para os Casos 2-4, é possível observar que existe no Caso 4 um único momento onde ocorre um carregamento em horário de ponta, ato indesejoso no sistema, dado que para um melhor despacho econômico é visado apenas o descarregamento das baterias nesses horários para gerar uma economia na compra de energia da subestação que está funcionando a custos mais elevados.

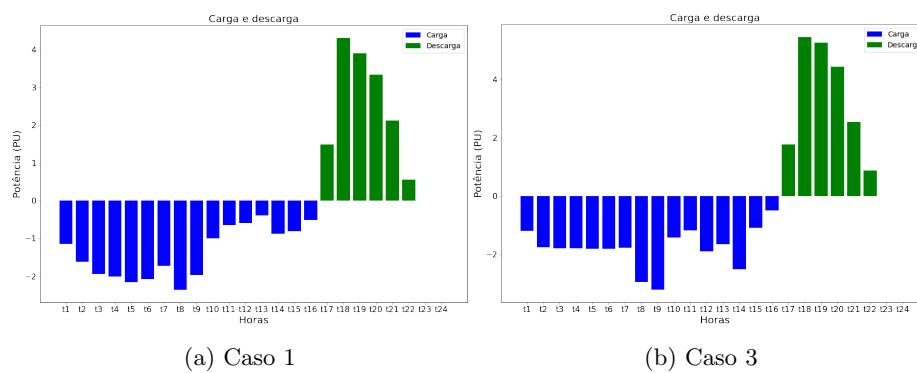


Figura 2: Carga e Descarga dos SAEs no sistema (Casos A)

Alocação Ótima de SAEs visando Despacho Econômico 13

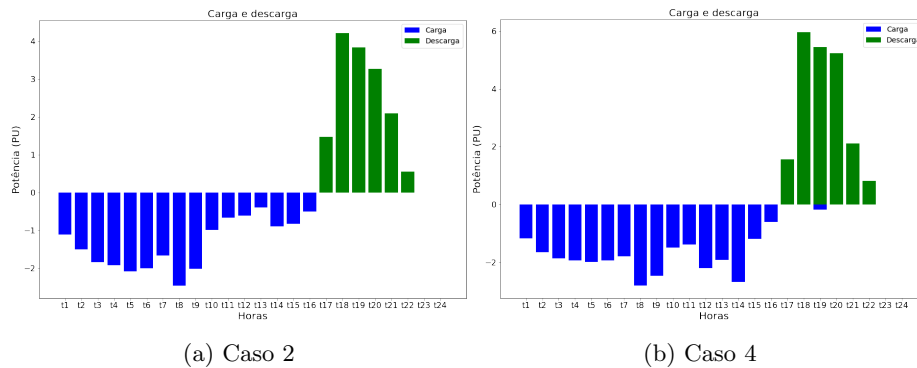


Figura 3: Carga e Descarga dos SAEs no sistema (Casos B)

Analisando as Figuras 4 e Figuras 5 para todo o período dos diferentes casos, foi observado que não houve existência de descarga profunda, ou seja, um pico de descarga maior que 50% da capacidade armazenada, ato que prejudica a vida útil da bateria e implica diretamente um menor número de ciclos de vida existentes do equipamento. Apesar da F02 não impor restrições relacionadas ao prolongamento de vida útil dos SAEs, a adoção do fator  $\alpha_0^{ESS}$  garantiu uma proporcionalidade saudável na carga e descarga das baterias, acarretando em uma maior vida útil dos sistemas.

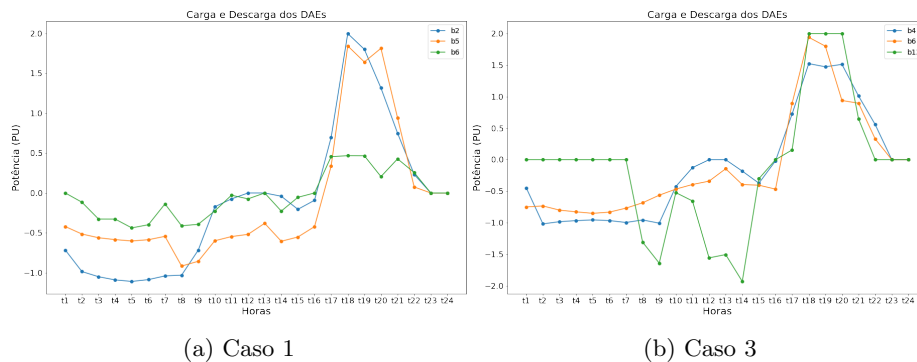


Figura 4: Carga e Descarga de cada SAE no sistema (Caso A)

A Tabela 7 apresenta a descarga diária em kWh por SAE para cada barramento e assim é possível observar que nos casos A, o caso 3 tem uma descarga média diária 30% maior do que o caso 1. Esse fator é diretamente correlacionado a diferença de restrições impostas em cada função objetivo, tendo assim o caso 1 - que utiliza a FO1 - uma descarga mais equilibrada e menos prejudicial a vida útil da bateria. Esse mesmo fato se repete quando são comparados os casos B,

14 Linden, R. v. d; Silva, L.C.; Rodriguez, Y.P.M.

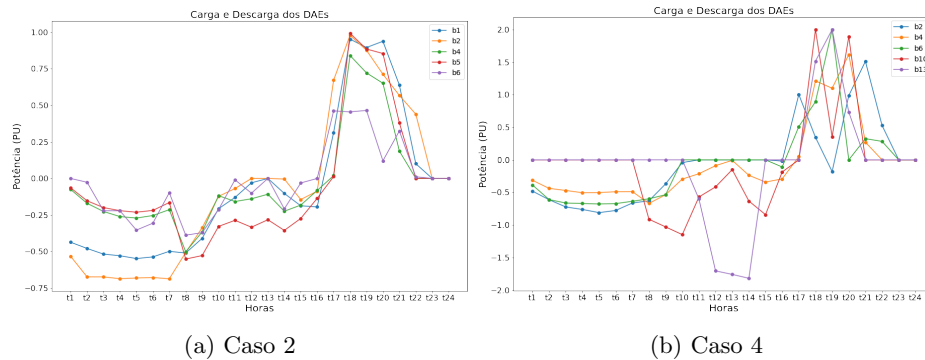


Figura 5: Carga e Descarga de cada SAE no sistema (Caso B)

onde temos o caso 4 apresentando uma descarga 37% maior que o caso 2, que também utiliza a FO1, que visa além do despacho econômico o prolongamento da vida útil dos SAEs.

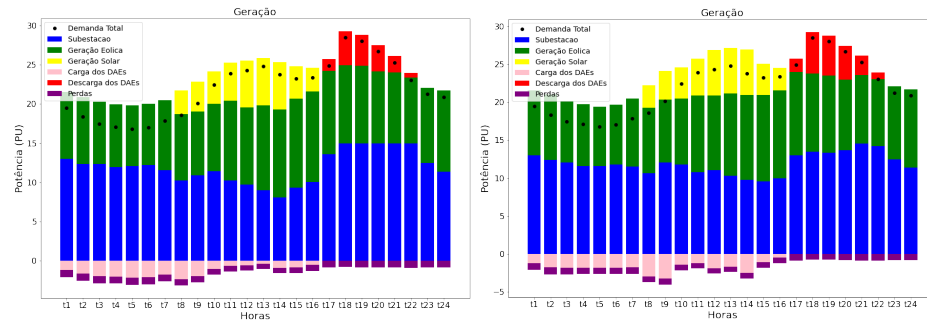
Caso 1 - F01		Caso 3 - F02	
Barramento	Descarga por SAE (kWh/dia)	Barramento	Descarga por SAE (kWh/dia)
b2	680.0	b4	680.0
b5	665.62	b6	679.99
b6	228.08	b13	680.0
Caso 2 - F01		Caso 4 - F02	
Barramento	Descarga por SAE (kWh/dia)	Barramento	Descarga por SAE (kWh/dia)
b1	384.11	b2	437.98
b2	425.0	b4	425.0
b4	242.09	b6	401.3
b5	312.68	b10	425.0
b6	184.04	b13	425.0

Tabela 7: Descarga por dia de cada DAE (kWh/dia)

As Figuras 6 e 7 demonstram as potências fornecidas pelos componentes do sistema e a demanda de carga total em cada período para os casos A e B. Ao analisar os casos B, especificamente o caso 4, é possível perceber que houve as 19 horas uma injeção de potência na rede por parte do SAE apesar da demanda já estar suprida, o que resultou em um movimento de carga e descarga nos SAEs no mesmo horário. A utilização dos dispositivos de armazenamento de energia em momentos não necessários é um dos principais fatores a serem prevenidos para a maximização de vida útil de um equipamento. Entretanto, nos casos restantes houve injeção de potência na rede apenas quando a demanda de energia do sistema foi maior que a ofertada, tanto pela subestação quanto pelas fontes

Alocação Ótima de SAEs visando Despacho Econômico 15

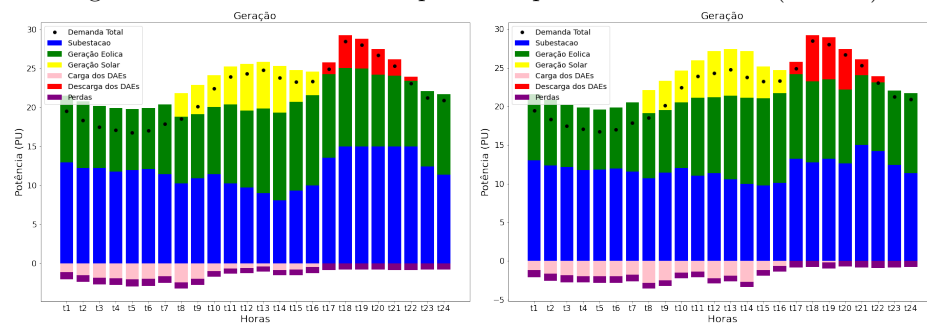
intermitentes, fazendo valer assim o objetivo de maximização da vida útil de todo sistema nos casos que utilizaram a FO1.



(a) Caso 1

(b) Caso 3

Figura 6: Potências fornecidas pelos componentes do sistema (Caso A)



(a) Caso 2

(b) Caso 4

Figura 7: Potências fornecidas pelos componentes do sistema (Caso B)

Em uma comparação generalista das FO1 e FO2, é possível concluir que a parcela de potência injetada pela bateria é extremamente importante para um correto gerenciamento de operação dos dispositivos e quando bem administrado gera aumento no tempo de vida destes. Com isso, é apropriado afirmar a eficácia do algoritmo criado para o despacho econômico focado na maximização da vida útil dos SAEs e da predileção da FO2 para alocação e operação das baterias no sistema.

#### 4 Conclusão

Este trabalho propôs um algoritmo que objetiva encontrar a solução ótima do problema de alocação de SAEs em sistemas de distribuição de energia elétrica

16 Linden, R. v. d.; Silva, L.C.; Rodriguez, Y.P.M.

com despacho de fontes renováveis intermitentes, tendo como objetivo o despacho econômico considerando a vida útil dos dispositivos. Os resultados obtidos propuseram soluções para um sistema teste de 24 barras considerando diferentes casos e mostram que o algoritmo cumpre sua proposta, retornando como resultados o valor do custo de compra de energia da subestação, as barras de alocação dos SAEs, descarga diária e vida útil estimada de cada SAE, gráficos ilustrativos da potência gerada por fonte e o ciclo ótimo de carga/descarga dos SAEs que resultam no despacho econômico do sistema.

Diante dos resultados obtidos, fica evidente a que alocação e operação de SAEs nos SDEE devem ocorrer para promover auxílio as subestações, porém injetando potência no sistema apenas em horários de ponta, quando o custo da energia da subestação é maior, e quando a demanda de carga é superior ao limite da subestação e das fontes intermitentes, dando ao sistema uma confiabilidade e estabilidade.

As simulações foram agrupadas e analisadas em dois casos: Caso A, agrupando os dois cenários com SOCmin de 20% e Caso B, agrupando os dois cenários com SOCmin de 50%. Para o Caso A ocorreu a alocação de 3 SAEs e para o Caso B 5 SAEs.

Comparando as duas funções objetivo adotadas, observou-se que a adoção da função objetivo FO1, que visa o prolongamento da vida útil dos dispositivos, resultou em uma vida útil em média 40% maior para o Caso A e 33,22% para o Caso B. Em termos de custos operacionais dos SAEs, a economia obtida foi de 22,8% para o Caso A e 26,79% para o Caso B.

Analisando a operação dos SAEs para os diferentes casos, observa-se uma descarga média 30% menor para o Caso A e 37% para o Caso B quando adotada a FO1, de forma que os dispositivos operam com ciclos mais equilibrados e menos prejudiciais a sua vida útil.

## Referências

1. Falcão, D. M.: Smart Grids e Microredes: o futuro já é presente. In: Simpósio de Automação de Sistemas Elétricos. vol. 8, (2009).
2. da Costa, Ernani Rodrigues and Halmenschlager, Viniciu. Energias Renováveis, Desempenho Econômico e Emissões de CO<sub>2</sub> no Mundo: Uma Análise Via Dados em Painel. Universidade Federal do Rio Grande (2019)
3. Maffei, A., Meola, D., Marafioti, G., Palmieri, G., Iannelli, L., Mathisen, G., ... Glielmo, L. (2014). Optimal Power Flow model with energy storage, an extension towards large integration of renewable energy sources. IFAC Proceedings Volumes, 47(3), 9456–9461. doi:10.3182/20140824-6-za-1003.01983
4. Pontes, L. R. B. and Rodriguez, Y. P. M.: Alocação e operação ótimas de dispositivos de armazenamento de energia visando a operação econômica em sistemas de energia com fontes intermitentes. Universidade Federal da Paraíba (2019).
5. Braz Pontes, L. R., Percy Molina Rodriguez, Y., Luyo Kuong, J., and Rojas Espinoza, H. (2021). Optimal Allocation of Energy Storage System in Distribution Systems with Intermittent Renewable Energy. IEEE Latin America Transactions, 19(02), 288–296. doi:10.1109/tla.2021.9443071

6. OLIVEIRA, T. T.; ARAUJO, D. R. R. P.; ARAUJO, L. R. d.: Método para alocação e operação ótima de baterias em sistemas de distribuição com restrições de tensão e redução das perdas. Universidade Federal de Juiz de Fora (2018)
7. dos Santos, A. L., Oliveira, L. W., Dias, B. H., and de Oliveira, J. G. Otimização da Operação de Baterias em Sistemas de Distribuição de Energia Elétrica. XII Latin-American congress on electricity generation and transmission (2017)
8. Macedo, L. H., Franco, J. F., Rider, M. J., and Romero, R. (2015). Optimal Operation of Distribution Networks Considering Energy Storage Devices. *IEEE Transactions on Smart Grid*, 6(6), 2825–2836. doi:10.1109/tsg.2015.2419134
9. Zidar, M., Georgilakis, P. S., Hatziargyriou, N. D., Capuder, T., and Škrlec, D. (2016). Review of energy storage allocation in power distribution networks: applications, methods and future research. *IET Generation, Transmission & Distribution*, 10(3), 645–652. doi:10.1049/iet-gtd.2015.0447
10. Carpinelli, G., Mottola, F., Proto, D., and Russo, A. (2010). Optimal allocation of dispersed generators, capacitors and distributed energy storage systems in distribution networks. In *2010 Modern Electric Power Systems* (pp. 1-6). IEEE.
11. Glover, F. W., and Kochenberger, G. A. (Eds.). (2006). *Handbook of metaheuristics* (Vol. 57). Springer Science & Business Media.
12. Soroudi, A. (2017). *Power System Optimization Modeling in GAMS*. doi:10.1007/978-3-319-62350-4
13. Monticelli, A. J. (1983). Fluxo de carga em redes de energia elétrica. E. Blucher.
14. Schoenung, S. (2001). Characteristics and Technologies for Long- vs. Short-Term Energy Storage: A Study by the DOE Energy Storage Systems Program. doi:10.2172/780306
15. Jenkins, D. P., Fletcher, J., & Kane, D. (2008). Lifetime prediction and sizing of lead–acid batteries for microgeneration storage applications. *IET Renewable Power Generation*, 2(3), 191–200. doi:10.1049/iet-rpg:20080021
16. Ribeiro, Érica Tatiane Almeida. (2013). Modelos de programação inteira mista para a alocação ótima de bancos de capacitores em sistemas de distribuição de energia elétrica radiais. Universidade Estadual Paulista (UNESP).

# A Multi-Lens Approach to Smart City Planning: Philadelphia

Jennifer Kim<sup>1</sup>, Sésil Koutra<sup>2</sup>, Zacharie De Grève<sup>2</sup>

Université de Mons, 7000, Mons, Belgium  
jenskim@alumni.princeton.edu

**Abstract.** Smart city planning has become a popular concept in a time of increasing urbanization and its accompanying challenges, particularly in the face of climate change. Critiques say it is too generic to prove more useful beyond utilization as a buzzword in political discourse. Smart planning requires a cross-disciplinary and adaptable effort that combines and optimizes the range of quantitative and qualitative methodologies available to identify opportunities and actionable solutions while acknowledging the challenges and shortcomings of a given approach. In this paper, this theory of smart planning is applied to the case of Philadelphia, where a multi-perspective lens – specifically, from the viewpoints of mobility and quality of life – is used to develop an integrated and adaptive evaluation of the needs of the city along with practical solutions for implementation. We show that integrating interdisciplinary resources and perspectives can uncover alternative solutions which enrich planning development.

**Keywords:** Mobility, Philadelphia, Quality of life, Smart cities, Urban planning.

## 1 Introduction

The idea of Smart Cities has rapidly grown since the start of the 21<sup>st</sup> century, first appearing in the early 2000s and being utilized in many papers and debates especially since 2013 [1]. The definition of what constitutes a smart city is still unresolved given that different stakeholders such as Giffinger [2], Caragliu [3], and Angelidou [4], have divergent ideas regarding what makes a city “smart.” However, there are general characteristics which hold consistent, these being: 1) the role of technology, 2) the planning for sustainability, and 3) the role of governance in managing these for a policy that is beneficial to people [1–4]. The Centre of Regional Science at the Vienna University of Technology (CRS) identified six main areas which have become widely accepted as background for the framework upon which a city can be assessed for smartness: smart economy, mobility, environment, people, living, and governance [2]. One popular definition based on these axes says a city is smart “when investments in human and social capital and traditional (transport) and modern (ICT) communication infrastructure fuel sustainable economic growth and a high quality of life, with a wise management of natural resources, through participatory governance.” [3]

This paper seeks to assess the opportunities and challenges for contributing to a “ideal plan” for a city and to develop proposals tackling these opportunities in an innovative manner using a multi-perspective, integrated, and adaptive approach. The City of Philadelphia is evaluated as a case study using this methodology to assess the needs of the city and to develop solutions that could be proposed for practical implementation. The methodology used may at first seem self-evident but is important to revise with an open mind that seeks opportunities for adaptations and syntheses for an ideal solution. Thus, the main contributions of this work are to show the value obtained by 1) synthesizing and finding relationships between seemingly disparate variables, data sources, and disciplines, 2) using a flexible and adaptive approach to optimize solution alternatives, and 3) applying this methodology to offer new perspectives on some urban planning challenges faced by Philadelphia.

The article is organized as follows: in the following section, the methodology adopted for approaching the planning project is discussed. Sect. 3 through Sect. 5 present the case study of Philadelphia through the phases described in Sect. 2. Sect. 6 discusses weaknesses of the methodology, and Sect. 7 presents the conclusions with some remarks and recommendations for future works.

## **2 Methodology and Materials**

### **2.1 Methodology**

The methodology adapted for a time-constrained evaluation of a city can be divided into three phases. First is selection of a research focus for the case study, exploring the motivation and background information for determining a location and the smart city pillars for comprehensive study. Given the smart city characteristics identified by the CRS [2], it is useful to select more than one to evaluate individually and also in relation to each other. Once these pillars are chosen, an extensive review is performed of the city’s history and current situation with respect to the selected pillars of study, including recent statistics and planning documents developed by the city administration. This establishes a baseline from which challenges can be identified for further investigation. Case study constraints should also be defined in this phase.

Next, the identified challenges are evaluated to develop broad solutions for an “ideal city” from the lens of the selected perspectives. The proposals should be assessed both quantitatively and qualitatively for their impacts.

Following that is a refinement process to reevaluate the proposed solutions and process them into strategies and actions for implementation. Alternative scenarios are studied, and a “best approach” selected using varying methodologies of evaluation.

### **2.2 Materials**

There are a plethora of tools and materials available for developing solutions for an “ideal city,” to be selected depending on the area of interest and researcher’s expertise. For this case study, the resources used include academic literature, open geospatial and survey-based data, articles and institutional reports, and planning documents.

### **3 Case Study Introduction: Philadelphia**

#### **3.1 Motivation and Research Focus**

Given the long-term nature of infrastructure, planning a city by default requires consideration for sustainability from social, economic, and – increasingly – environmental perspectives. Following a preliminary review of the city’s background, two issues of interest are selected for development using a multi-perspective approach.

The first is based on the phenomenon of the decrease in the city’s population following publication of its first comprehensive city plan in 1960, from a peak of 2.1 million inhabitants in 1950 to 1.5 in 2010 [5]. Decline in population and neglected properties have become prominent characteristics of “unsavory” neighborhoods, giving rise to the question of whether these areas are thus due to the inherent qualities of their inhabitants or due to a systemic issue exacerbated by the built environment. Given that Philadelphia is still considered one of the most unsafe cities in the United States [6], it is of interest to explore how smart city solutions can improve safety and hence quality of life in the city. This assumes a correlation between safety and quality of life, which also bears further investigation.

The second issue centers upon transportation in Philadelphia. In 2020, Philadelphia was the second-most congested city in the United States, and the fifth most congested city in the world [7]. Although the city recently produced an extensive transit improvement plan and has been subject to discussions regarding new mobility solutions, there is a question of whether transportation issues can be cured just by improving transit, or whether there are more nuanced issues to examine in solution proposals.

The following two-pronged approach is adopted: examining how to plan a city smartly through the perspectives of quality of life and mobility. These two pillars may seem disparate and utilize different methodologies for analysis but are linked if only in the purest sense by the city resident for whose benefit the solutions are devised.

#### **3.2 Case Study Constraints**

Constraints must be identified at the beginning of the work which should be borne in mind throughout solution development, evaluation, and proposal:

- Data: Availability, relevance, and quality of data may be limited.
- Scope: given a city’s magnitude, the study scope should be limited to devise an applicable solution; thus, it is useful to focus on a single district or neighborhood.

#### **3.3 Review of Extant Information**

To develop a solution proposal, it is first necessary to understand the existing situation. This diagnosis can be performed by investigating the city history, contemporary facts and figures, reference plans, and literature review of the areas of interest. Integrating this information helps guide the development of a preliminary proposal.

The history of the selected location's urban development provides context leading to present-day characteristics. Recent plans present the planning efforts of the city while helping contemporize research efforts to actual developments in progress. This avoids redundancy in proposals developed through the study. Studying the academic information concerning the areas of interest related to the city helps the researcher better understand the complexities of the situation and contextualizes the interaction of the selected issues with social implications along with scientific investigations.

**Historical Review.** The City of Philadelphia was chartered in 1701 and became a key location for culture, science, and education. Until 1800, Philadelphia was the largest city in the United States and the second-largest English-speaking city worldwide [8].

By the early 20th century, Philadelphia was a railroad hub experiencing great transit growth in addition to the manufacturing, industrial, and financial growth from the century prior [9]. However, political corruption, disease, and violence caused waste and stagnation in infrastructure expenditures. This was exacerbated by the Great Depression, which hit the city hard, followed by suburbanization, as residences and businesses moved out from the city center to the Greater Philadelphia region [9].

In 1960, the first comprehensive plan for the city was developed by the Philadelphia City Planning Commission, which laid out a 20-year plan for the physical development of the city. At the time, the city plan had a population estimate of around 2.5 million residents by 1980, since between 1890 and 1950, the population had doubled in size from one million to two million inhabitants. However, instead of continuing the trend, Philadelphia's population would instead decline to 1.5 million by 2010 [5].

Entering the 21st century, Philadelphia's population has experienced some growth (+0.6%) between 2000 and 2010, according to the 2010 census [5]. However, as of 2013, the city still had the highest unemployment rate in the region, also 1.9% higher than the national rate of 6.5% [10]. Even though the population is no longer declining, Philadelphia has yet to return to the economic prowess it was known for in its past.

**City Plans.** The principal city plans examined are the comprehensive development plan [5] and transportation plan [11]. Other documents contributing information regarding Philadelphia's visions and goals include the city's plans for smart city planning [12], sustainability [13], road safety [14], and transit [15].

**Academic Literature Review.** The study undertaken ranges from exploring the design philosophies involved behind the 1960 Comprehensive Plan [16] to assessing the impact of urban revitalization plans through programs such as historic preservation and anchor institutions [17, 18]. Other literature also critiques the sustainability and smart planning efforts previously undertaken by the city, discussing strengths and drawbacks to Philadelphia's previous proposals for becoming "smart" [10, 19].

When measuring quality of life in a city, the determinant factors are difficult to identify, and usually only validated through subjective surveys and estimated correlations between select indicators and the mental/physical satisfaction of citizens. While some authors such as Cohen argue that incidents of crime do not have as strong of an

impact upon quality of life as other factors [20], others find that exposure to high rates of crime can adversely impact short- and long-term health, which are associated with quality of life [21]. From an alternative lens, studies of crime and resulting costs to society find that programs designed to prevent crime reduce costs incurred by stakeholders on individual and systemic scales, impacting overall quality of life [22].

Publications on mobility in Philadelphia provide historical and social contexts for the present-day transportation system and current conditions. They emphasize the importance of the role that mobility plays in society with social, economic, and environmental impacts on both Philadelphia's residents and its physical setting. These papers range from explaining relationships between urban spatial form and mobility with the role of social issues such as racial segregation and discrimination in historic policies [23, 24] to recommendations for context-sensitive transport design [25] and strategies for reducing greenhouse gas emissions from transport [26].

### 3.4 Challenges and Areas for Development

**Challenges.** From the background research, several challenges can be identified. Predominantly, Philadelphia's physical infrastructure has been deteriorating in hand with its declining economy since the previous century. Its neighborhoods are also home to high rates of crime: 139% more violent crimes and 41% more property crimes compared to the national averages [27]. High crime rates also deter investors, both commercial and residential, creating a feedback loop resulting in locations left to degrade into conditions that may facilitate the occurrence of crime.

Deteriorating infrastructure is also a challenge for Philadelphia's transportation system. Lack of space and funding for new transportation infrastructure has resulted in reduced reliability of transit options and a declining public transport ridership [15]. The impact upon reliability is both a reason for and a result of growing congestion on the city's roadways with the corresponding increase in the number of single-occupancy vehicles. This negatively impacts economy, environment, and health.

**Opportunities.** Addressing the challenges of each pillar separately allows brainstorming of multiple opportunities. For example, to tackle the challenge of high crime rates, the authors select an urban planning lens, as design is not often considered as relevant to crime prevention yet is a potent tool for creating safer environments that deter crime occurrence [28]. Rather than examining individual motivation, environmental factors are assessed for correlations with crime occurrences including issues such as access for intervention, likelihood of passerby, and the likes.

From the mobility perspective, the authors choose to focus on congestion, which has social, environmental, and economic implications making it an ideal study in sustainability. Socially, relieving congestion has a safety impact and would also improve accessibility of transit for carless travelers. Reducing congestion decreases greenhouse gas emissions from vehicles that spend less time idling in traffic and through the increased use of transit. Economically, congestion management could add a revenue source for the city, and partnerships may boost economic growth.

## 4 Analysis and Initial Proposals

### 4.1 Quality of Life

**Analysis.** The analysis is primarily based on the census block groups defined by the U.S. Census Bureau. The data used is sourced from ESRI Living Atlas and from Philadelphia’s open data portal, OpenDataPhilly. Population and economic data have been obtained from the U.S. Census Bureau and ESRI Living Atlas.

First, Incidents and Shootings from 2020 have been mapped in ArcGIS Pro [29] and Optimized Hot Spot Analysis performed over the data sets, using a fishnet grid data aggregation method over the census blocks. **Fig. 1** shows two main areas identified through this analysis, as indicated by the red zones.

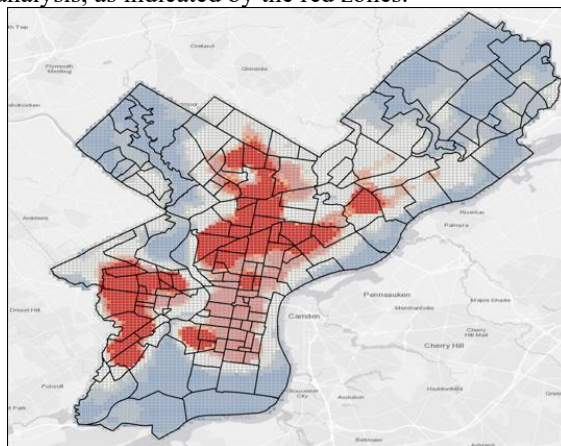


**Fig. 1.** Hotspot analysis of 2020 incidents. Data source: opendataphilly.org/dataset. Shapefiles downloaded April 14, 2021

Incidents are classified into Violent/Non-Violent and Opportunistic/Non-Opportunistic sets to determine whether patterns exist in motivations and/or nature of the crime. Hotspot analyses are performed over these and mapped against factors such as land use and demographic indicators. Positive correlations exist between crime and factors like vacant spaces, low household income, and high population density.

Google Earth Pro Street View [30] is used to examine neighborhoods of high crime rates; we observe that these areas are characterized by large, empty lots. These unused spaces are in disarray and may thus attract undesirable characters and their misdeeds.

**Solutions.** Defining a solution to address the problem of high crime rates in Philadelphia is complex due to the observed feedback cycle: neighborhoods with higher rates of crime are correlated to high poverty, low education, and low employment, but it is unclear which causes which.

Two possible solution approaches are considered: addressing crime motivations and addressing crime enablers. Looking at crime motivations evaluates which incidents are crimes of opportunity compared to personal grievances and helps understand

which crimes might be addressable before the deed, and which are arbitrarily motivated by the human factor. Reducing crime enablers requires searching for specific scenarios or environments that are more conducive to crime occurrence, and how to suppress them. The practical implications of both approaches may be manifested in two ways: through environmental design, and through on-the-ground actions.

When evaluating the built environment, Crime Prevention Through Environmental Design (CPTED) is considered, which targets “designing safety and security into the environment of a specific area” [31]. This methodology first emerged in the 1960s following Jane Jacobs’ theorization of concepts such as “eyes on the streets,” the idea that urban design should locate people on public streets, thereby increasing the number of public witnesses which could deter potential offenders from committing crimes [32]. These implications are valuable not only for new developments but also for revitalization of an existing area. Studies investigating the relationship between safety and neighborhood vibrancy show that making more use of spaces in a neighborhood could significantly reduce the probability that a crime occurs in that location [33, 34].

To implement this concept in solution, one approach lies in enabling community ownership through a communal lens promoting actions such as 1) increasing community initiatives, 2) fostering formation of local-level leadership, 3) enabling community ownership via participatory actions like townhalls, surveys, etc., 4) developing “block properties” to be collectively used and maintained (such as gardens, playgrounds, and gathering areas), and 5) organizing communal activities like a cleanup day or “block party” cookouts. These actions are meant to foster sense of community and camaraderie and encourage communal upkeep of public and private properties.

A second approach uses an operational lens focusing on technical solutions, through services such as monitoring platforms or surveillance technologies which analyze locations of crime occurrences to optimize resource deployment to prevent or mitigate crime. Some actions promoted through this include 1) coordination and collaboration with neighboring municipal police divisions, 2) optimization of response routes, 3) predictive analysis using historic incidents to optimize patrols, 4) streetlight maintenance and surveillance camera installation in crime-prone areas, and 5) installation of smart cameras to detect weapons, incidents, flagged license plates, etc.

## 4.2 Mobility

**Analysis.** The analysis draws upon on traffic and congestion resources such as Texas A&M Transportation Institute, Google Maps, and the ESRI Living Atlas Portal. Neighborhood boundaries defined using PhillyOpenData’s Philadelphia Neighborhood Boundary shapefile have been mapped with ESRI’s World Traffic Service layer to identify areas of high congestion. The benefits of a congestion management solution are then analyzed using data from Texas A&M Transportation Institute.

First, congestion patterns can be identified by examining traffic patterns and average daily traffic within the city. The intent is to identify where and when congestion is most experienced to select an area best suited for implementing a pilot program with the proposed solution. This area is in and around the Center City neighborhood, a central location for many firms and a key commuter destination.

**Solutions.** Multiple strategies are studied for alleviating congestion: congestion pricing, lowering speed limits, restricting certain zones and times to public transit access, adding park & ride stations near key intersections and entry points to the city, and implementing electric shuttles between transit access locations and points of interest.

Since the part of the city experiencing the highest amount of congestion is the downtown, central area, downtown congestion pricing (DCP) is first explored for development. DCP is a strategy for reducing congestion by charging a payment for vehicles entering a city’s downtown area.

A full in-depth analysis of the costs and benefits of implementing such a program is beyond the scope of this project; however, it is beneficial to identify the cost variables needed to be considered in an extensive feasibility analysis, as well as to develop high-level quantifications of the possible benefits.

The main costs include study and design, physical and systems infrastructure capital and integration, commercial costs, and operations and maintenance. The primary benefit of a DCP program is congestion reduction. The pricing mechanism should be designed to encourage drivers to take alternative modes of transportation or to enter the downtown part of the city during less crowded times of the day, thereby smoothing out traffic peaks and reducing the overall traffic delay resulting from congestion. The knock-on impact is a shift to modes of transport that have lower greenhouse gas emissions compared to a single occupancy vehicle.

Because crashes are more likely occur with higher speed variability [35], reducing congestion will also reduce stop-and-go motion with high variations of speed, thus effecting a decrease in car crashes. This not only increases safety, but also increases the total time that roads are clear, since accidents cause congestion when cars and emergency responders are blocking one or more lanes.

Reducing congestion should also improve trip times for travelers on all roadway transport modes. This produces cost savings in time and fuel, since time is money, in addition to the monetary cost per gallon of fuel. Based on studies in other cities where congestion pricing has been implemented, we estimate a 10% reduction in trips and 30% decrease in travel delays [36, 37]. Cost savings according to the value of time and from conservation of fuel wasted when idling in traffic are an estimated \$1.1 billion annually. The reduction in travel delay will also have an environment impact of approximately 0.6 million-tons of annual CO<sub>2</sub>-equivalent reduction in greenhouse gas emissions. These values are calculated using the assumptions in **Table 1**. In addition to these benefits, the program could also potentially procure revenues for investment in other initiatives like cycling, walking, and public transport.

**Table 1.** Congestion pricing benefits assumptions and sources

<b>Indicator</b>	<b>Quantity</b>	<b>Source</b>
Philadelphia annual VMT	11,132,500,000	Streetlight Data (2021)
Average fuel economy of passenger vehicle, miles/gallon	22	U.S. Environmental Protection Agency (EPA) (2018)
Average CO <sub>2</sub> emission rate for passenger vehicles, g CO <sub>2</sub> /mile	404	EPA (2018)
Average tailpipe CO <sub>2</sub> emitted, g CO <sub>2</sub> /gallon	8,887	EPA (2018)

Average price of gasoline, \$/gallon	2.57	Texas A&M Transportation Institute (TTI) (2019)
Annual total delay, hours	194,655,000	TTI (2019)
Value of time, \$/hour	18.12	TTI (2019)
Idling fuel use, gallons/hour	0.39	Calculated from U.S. Department of Energy (2015)

## 5 Revisions and Recommendations for Action

**Quality of Life.** The advantages and disadvantages of the two alternative scenarios previously proposed are evaluated in **Table 2** below. “The Vibrant Block” refers to the communal approach; “The Policed State” refers to the technological method.

**Table 2.** Pros and cons of “The Vibrant Block” vs “The Policed State”

	The Policed State	The Vibrant Block
<b>Pros</b>	<ul style="list-style-type: none"> <li>- More sensors allow quicker detection and deployment of resources to prevent or mitigate a situation</li> <li>- Data aids prediction of incident location and time of occurrence</li> </ul>	<ul style="list-style-type: none"> <li>- Fosters ownership behavior</li> <li>- Fosters relationships between community members, reducing likelihood of anonymous or unattended incidents</li> <li>- Supports economic development in underutilized spaces</li> </ul>
<b>Cons</b>	<ul style="list-style-type: none"> <li>- Unclear if increase in police force guarantees lower crime rates</li> <li>- Difficult to implement surveillance and responsive monitoring solutions on local scale</li> <li>- Subjective human factor complicates incident prediction</li> </ul>	<ul style="list-style-type: none"> <li>- Soft approach makes it difficult to quantify immediate impact</li> <li>- Difficult to assess scale of implementation</li> <li>- Requires community buy-in</li> </ul>

“The Vibrant Block” is selected upon which to develop an action plan and strategy due to an interest in addressing design elements particularly following observation of the correlation between land use (or disuse) and crime occurrence shown in **Fig. 2**.

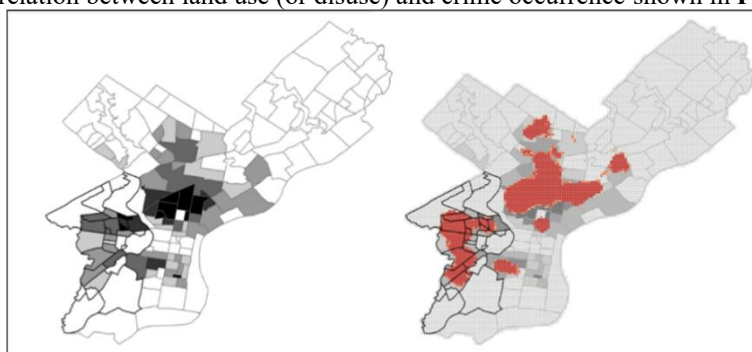


**Fig. 2.** Vacant lots per square mile (left), vacant lots per square mile overlaid with 2020 shootings hotspot analysis (right). Data source: OpenDataPhilly, US Census. Shapefiles downloaded April 14, 2021. Census data accessed May 14, 2021.

**Actions and Strategies.** The proposed action plan adapts the more recently developed Second Generation Crime Prevention Through Environmental Design (2<sup>nd</sup> Gen CPTED), which uses urban design to influence a potential offender's decision to commit a crime in a given space [32]. This approach centers on four main pillars: social cohesion, community culture, connectivity, and threshold capacity.

*Social cohesion* is the belief that communities form bonds by addressing problems together: proposed action elements associated with this pillar include 1) developing a local leadership committee, 2) organizing townhalls, listservs, etc., and 3) forming neighborhood watch groups. *Community culture* is the concept of creating a sense of ownership through interactions between residents as well as the built space. This can be fostered through 1) organization of neighborhood events like cleanup days or barbecues, and 2) cultivating shared spaces such as community gardens or art installations. *Connectivity* is important in and between neighborhoods due to the “permeability” of connected spaces, in which enacting measures in one space sometimes results in the criminal activities simply moving one street over, not actually mitigating the overall perpetration of crimes [38]. To address this, 1) neighborhood cluster leadership committees should be formed, and 2) inter-neighborhood activities will help improve network bonds. Lastly, *threshold capacity* is the concept of maximizing use of open spaces to reduce the physio-temporal opportunities for a crime to be committed. Some practical applications include 1) cleaning and transforming abandoned lots and buildings into communal spaces, and 2) diversifying uses for common public spaces. For example, vacant lots can be reimagined into a multi-functional space used for community-building, economy-boosting, health-improving initiatives.

A community-centric approach with design element considerations for the built environment creates an environment that is not only designed for, but also by, the community. To ensure this, community surveys would help determine which initiatives to prioritize. One major aspect of cultivating a sense of ownership and responsibility over a space is to motivate upkeep and order of the neighborhood. Areas with greater physical disorder tend to embolden criminals while (and perhaps because) residents are less protective of the common space and are hence less willing or able to intervene and prevent crime. An act as simple as “greening” a vacant lot can result in reduction of gun assaults and petty crimes, while also decreasing resident stress and improving health [34]. Proposed uses include spaces for picnic tables and playgrounds, an open space for multi-modal use, such as community activities, and spaces for mobile vendors like food trucks on various days throughout the week.

**Mobility.** Although downtown congestion pricing was initially the focus of the proposed solutions for resolving the issue of congestion in Philadelphia, other solutions should also be evaluated. Those programs already implemented or planned by the city are left out of the diagnosis to avoid redundancy, although it is helpful to keep them in mind for possible syntheses. The alternatives considered previously are assessed in comparison with the initial congestion pricing proposal and summarized in **Fig. 3**.

1. *Changing downtown speed limits:* Implement lower speed and/or variable speed limits near intersections downtown. Contrary to intuitive expectation that lowering

speed limits results in slower trips (and more congestion), studies show that congestion causes slow speeds but slow speeds do not necessarily cause congestion, and in some cases actually improve traffic flow [39].

2. *Transit-only geo-temporal zones*: Define lanes along key transit routes dedicated exclusively for bus/transit use during peak travel periods. Implementing dedicated bus lanes during peak hours should improve travel times for buses and reliability of public transit options [40] while motivating drivers to shift to public transit.
3. *Expansion of Park & Rides*: Expand park-&-ride lots to key locations in suburbs and in the city with express routes to downtown. There is a dearth of parking lots providing good connections to the transit network. Designing lots as commercial centers may also help foster economic growth in areas near these access points.
4. *Micro-transit services*: Establish on-demand flexible or fixed route electric shuttle service between key transit stops and destinations of interest. Micro-transit services can help reduce traffic by 15%-30% [41] and can be implemented as a standalone solution or integrated with existing transit fleets running during off-schedule hours.

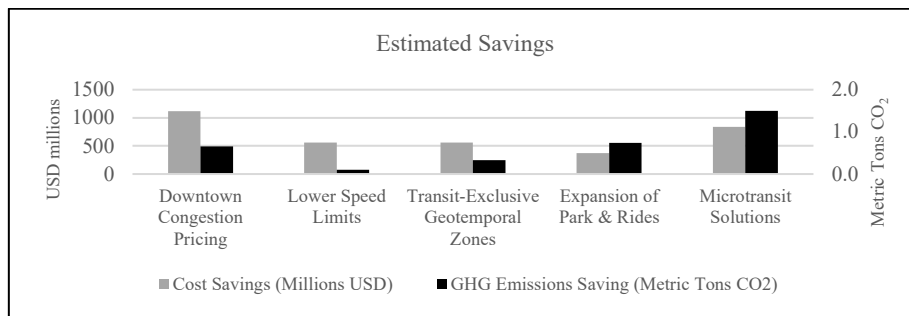


Fig. 3. Estimated benefits of time/fuel costs savings and GHG emissions.

To select the optimal solution, B-Box Software [42] is used to perform an analytic hierarchy process which evaluates the five alternatives discussed above, ranking them against and with respect to six different criteria. The criteria are defined and ranked using Saaty’s scale [43] to assign intensities of importance and develop pairwise comparisons between alternatives with respect to the criteria, followed by establishing priorities of the criteria with respect to the objective as shown in Fig. 4 and Table 3. Based on the given inputs, micro-transit emerges as the alternative of choice.

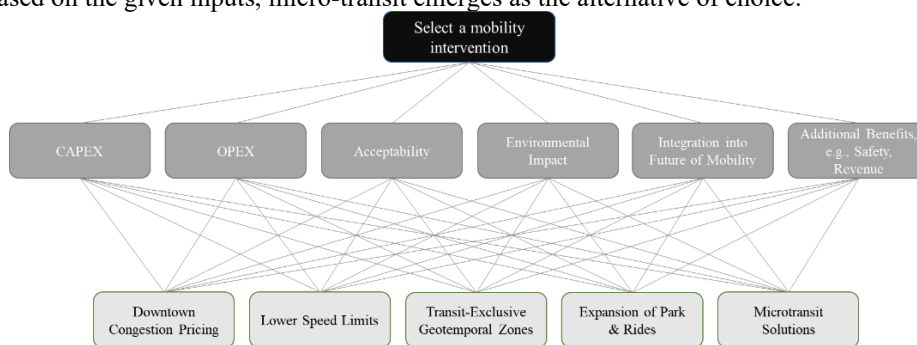


Fig. 4. Analytic Hierarchy Process for selecting a mobility intervention.

**Table 3.** AHP computation of final priorities and conclusion

	CAP-EX	OP-EX	Acceptability	Environmental Impact	Future of Mobility	Additional Benefits	Total
<b>Downtown Congestion Pricing</b>	0.078	0.064	0.038	0.198	0.377	0.314	<b>0.150</b>
<b>Lower Speed Limits</b>	0.260	0.294	0.147	0.048	0.037	0.342	<b>0.183</b>
<b>Transit-Exclusive Zones</b>	0.481	0.409	0.075	0.325	0.104	0.047	<b>0.231</b>
<b>Electric Micro-transit</b>	0.128	0.157	0.370	0.325	0.393	0.086	<b>0.252</b>
<b>Weight(s)</b>	0.136	0.109	0.273	0.273	0.031	0.179	

**Actions and Strategies.** The proposed action plan is divided into three phases: planning, implementation, and follow-up. In the first phase, travel routes are assessed to determine which corridors would most benefit from micro-transit solutions. From these, one or two which run through the downtown area will be selected for an initial pilot. This phase will also consider on-demand options for non-fixed route services, i.e., if shuttles can deviate from usual routes to deliver passengers to alternative stops. Next, several options are assessed for implementing the solution: 1) form a public-private partnership with a micro-transit provider; 2) select an existing transit fleet to repurpose; 3) purchase new (ideally electric) vehicles for on-demand services. In addition, the platform for accessing the service must be developed and ideally integrated with existing services like that of the local transit operator. To follow-up, a marketing campaign will increase familiarity with the new service. Ridership and usage over the pilot period will be monitored and evaluated for continuity and scaling.

## 6 Weaknesses

The following are the most salient limitations identified in the case study.

First, **the city is a dynamic entity that changes continuously.** Even with limitations in accessibility, data collection continues to improve; however, it is critical to maintain organized, reliable, and updated information to ensure accuracy and relevancy of analyses. Philadelphia is a clear case demonstrating that a city is always changing and that it is crucial to remain up to date on information that serves as the foundation for planning. Philadelphia did not follow the growth trajectory expected in its 1960 plan; as a result, trends from recent years are not representative of the long term.

Second, **studies are restricted in time and expertise.** Researching, analyzing, developing, and evaluating an “ideal solution” for a city is a daunting endeavor. Even with restriction to just two of the six smart city pillars in this case study, it was difficult to narrow the scope to meet the time constraints of the project. Lack of expertise in the field also costs more time and effort spent collecting background information as well as limiting access to certain sector-specific resources.

Lastly, **robust quantitative data is necessary to support proposals.** The analyses of the demonstrated case study were highly simplified. Applying advanced statistical

analyses and simulations would provide validation for the impact of proposed solutions. Proposals could be further strengthened with firsthand evidence like community surveys, which could be analyzed to assess scenarios and priorities of stakeholders.

## 7 Conclusions and Future Work

A key problem with traditional city planning is that most decisions are made in silos without accounting for the nuanced interactions between supposedly disparate variables. This work offers an integrated methodology to address this challenge, emphasizing the benefits of using a multi-perspective approach. The open-ended approach offers an innovative perspective that places seemingly disparate issues in the same room, enabling a more comprehensive evaluation of the city's needs.

It is seen through the evolution of hypotheses and solutions ultimately selected that the optimal solution is not always the first. For example, the initial expectation for addressing quality of life was to find a technological solution to mitigate crime, but additional research led to the conclusion that a human-centric approach is paramount. In the mobility case, while the study initially began with one value-adding solution, evaluating other criteria led to a different optimal solution. This demonstrates the importance of remaining open to new inputs which may influence initial hypotheses.

Future research lines include further exploration of the mathematical correlations between the different socio-economic and environmental factors and occurrences of crime, along with sensitivity analyses. Statistical analyses verifying the qualitative observations made in initial studies would further serve to support solution proposals.

## References

1. Trindade, E.P., Hinnig, M.P.F., da Costa, E.M., Marques, J.S., Bastos, R.C., Yigitcanlar, T.: Sustainable development of smart cities: a systematic review of the literature. *J. Open Innov. Technol. Mark. Complex.* 3, 11 (2017). <https://doi.org/10.1186/s40852-017-0063-2>
2. Giffinger, R., Fertner, C., Kramar, H., Kalasek, R., Pichler-Milanović, N., Meijers, E.: Smart cities: Ranking of European medium-sized cities. Centre of Regional Science (SRF), Vienna University of Technology (2007)
3. Caragliu, A., Del Bo, C., Nijkamp, P.: Smart Cities in Europe. *J. Urban Technol.* 18, 65–82 (2011). <https://doi.org/10.1080/10630732.2011.601117>
4. Angelidou, M.: Smart cities: A conjuncture of four forces. *Cities.* 47, 95–106 (2015). <https://doi.org/10.1016/j.cities.2015.05.004>
5. City of Philadelphia: Philadelphia2035: Citywide Vision, [https://drive.google.com/file/d/1gGEqfOR\\_WUWD3pgkc7TVyBHxzpvm4HLj/view](https://drive.google.com/file/d/1gGEqfOR_WUWD3pgkc7TVyBHxzpvm4HLj/view), (2011)
6. Samantha, D.: Philadelphia ranks among the least safe cities in the country, [www.thedp.com/article/2019/12/philadelphia-safety-report-wallet-hub](http://www.thedp.com/article/2019/12/philadelphia-safety-report-wallet-hub), (2019)
7. Pishue, B.: 2020 Global Traffic Scorecard. INRIX (2021)
8. Hein, C., Schubert, D.: Resilience and Path Dependence: A Comparative Study of the Port Cities of London, Hamburg, and Philadelphia. *J. Urban Hist.* 47, 389

- 419 (2021). <https://doi.org/10.1177/0096144220925098>
9. Weigley, R.F., Wainwright, N.B., Wolf, E. eds: Philadelphia: a 300 year history . W.W. Norton, New York (1982)
  10. Wiig, A.: The empty rhetoric of the smart city: from digital inclusion to economic promotion in Philadelphia. *Urban Geogr.* 37, 535–553 (2016). <https://doi.org/10.1080/02723638.2015.1065686>
  11. City of Philadelphia: CONNECT: Philadelphia’s Strategic Transportation Plan, [http://www.phillyotis.com/wp-content/uploads/2018/11/Connect\\_9.8\\_11-09-18\\_sm.pdf](http://www.phillyotis.com/wp-content/uploads/2018/11/Connect_9.8_11-09-18_sm.pdf), (2018)
  12. City of Philadelphia: SmartCityPHL Roadmap, <https://www.phila.gov/media/20190204121858/SmartCityPHL-Roadmap.pdf>, (2019)
  13. City of Philadelphia: Greenworks: A Vision for a Sustainable Philadelphia, [http://www.phila.gov/media/20161101174249/2016-Greenworks-Vision\\_Office-of-Sustainability.pdf](http://www.phila.gov/media/20161101174249/2016-Greenworks-Vision_Office-of-Sustainability.pdf), (2016)
  14. City of Philadelphia: Vision Zero Action Plan 2025, <https://visionzerophl.com/uploads/attachments/ckhnt3jvf042cx4d6x9nperbc-visionzeroactionplan2025-2020-11-17-print-compressed.pdf>, (2020)
  15. City of Philadelphia: The Philadelphia Transit Plan: A Vision for 2045, [www.phila.gov/media/20210222110702/OTIS-Philadelphia-Transit-Plan.pdf](http://www.phila.gov/media/20210222110702/OTIS-Philadelphia-Transit-Plan.pdf), (2021)
  16. Arkaraprasertkul, N.: Toward Modernist Urban Design: Louis Kahn’s Plan for Central Philadelphia. *J. Urban Des.* 13, 177–194 (2008). <https://doi.org/10.1080/13574800801965676>
  17. Ryberg, S.R.: Historic Preservation’s Urban Renewal Roots: Preservation and Planning in Midcentury Philadelphia. *J. Urban Hist.* 39, 193–213 (2013). <https://doi.org/10.1177/0096144212440177>
  18. Ehlenz, M.M.: Neighborhood Revitalization and the Anchor Institution: Assessing the Impact of the University of Pennsylvania’s West Philadelphia Initiatives on University City. *Urban Aff. Rev.* 52, 714–750 (2016). <https://doi.org/10.1177/1078087415601220>
  19. Moscovici, D., Dilworth, R., Mead, J., Zhao, S.: Can sustainability plans make sustainable cities?. *Sustain. Sci. Pract. Policy.* 11, 32–43 (2015). <https://doi.org/10.1080/15487733.2015.11908137>
  20. Cohen, M.A.: The Effect of Crime on Life Satisfaction. *J. Leg. Stud.* 37, S325–S353 (2008). <https://doi.org/10.1086/588220>
  21. Office of Disease Prevention and Health Promotion: Crime and Violence, <https://www.healthypeople.gov/2020/topics-objectives/topic/social-determinants-health/interventions-resources/crime-and-violence>
  22. McCollister, K.E., French, M.T., Fang, H.: The cost of crime to society: New crime-specific estimates for policy and program evaluation. *Drug Alcohol Depend.* 108, 98–109 (2010). <https://doi.org/10.1016/j.drugalcdep.2009.12.002>
  23. Sheller, M.: Racialized Mobility Transitions in Philadelphia: Connecting Urban Sustainability and Transport Justice: Racialized Mobility Transitions in Philadelphia. *City Soc.* 27, 70–91 (2015). <https://doi.org/10.1111/ciso.12049>
  24. Korb, A.B.: NOTE: SEPTA, Philadelphia, and Transportation Equity in America. *Georget. J. Law Mod. Crit. Race Perspect.* 3, (2011)

25. Casello, J.M., Wright, R.M., Vuchic, V.R.: Context-Sensitive Urban Transportation Design in West Philadelphia, Pennsylvania. *Transp. Res. Rec. J. Transp. Res. Board.* 1956, 165–174 (2006). doi.org/10.1177/0361198106195600121
26. Al-Rijleh, M.-K., Alam, A., Foti, R., Gurian, P.L., Spatari, S., Hatzopoulou, M.: Strategies to achieve deep reductions in metropolitan transportation GHG emissions: the case of Philadelphia. *Transp. Plan. Technol.* 41, 797–815 (2018). <https://doi.org/10.1080/03081060.2018.1526879>
27. CityRating.com: Philadelphia Crime Rate Report (Pennsylvania), <https://www.cityrating.com/crime-statistics/pennsylvania/philadelphia.html>
28. Gaur, P.: How is urban planning an essential tool in crime prevention?, <https://www.re-thinkingthefuture.com/city-and-architecture/a3485-how-is-urban-planning-an-essential-tool-in-crime-prevention/>, (2019)
29. ArcGIS Pro. ESRI (2020)
30. Google Earth Pro. Google LLC (2021)
31. U.S. Department of Transportation: “Built Environment Strategies to Deter Crime.,” <https://www.transportation.gov/mission/health/built-environment-strategies-to-deter-crime>
32. ICA: Primer in CPTED - What is CPTED?, <https://cpted.net/Primer-in-CPTED>
33. Humphrey, C., Jensen, S.T., Small, D.S., Thurston, R.: Urban vibrancy and safety in Philadelphia. *Environ. Plan. B Urban Anal. City Sci.* 47, 1573–1587 (2020). <https://doi.org/10.1177/2399808319830403>
34. Branas, C.C., Cheney, R.A., MacDonald, J.M., Tam, V.W., Jackson, T.D., Ten Have, T.R.: A Difference-in-Differences Analysis of Health, Safety, and Greening Vacant Urban Space. *Am. J. Epidemiol.* 174, 1296–1306 (2011). <https://doi.org/10.1093/aje/kwr273>
35. Marchesini, P., Weijermars, W.: The relationship between road safety and congestion on motorways. SWOV Institute for Road Safety Research (2010)
36. Peach, J.: 5 Cities with Congestion Pricing, <https://www.smartcitiesdive.com/ex/sustainablecitiescollective/five-cities-congestion-pricing/28437/>
37. Parks, H.: Investigating the Impact of Congestion Pricing Around the World, <https://climate-xchange.org/2019/05/29/investigating-the-impact-of-congestion-pricing-around-the-world/>
38. Metropolitan Area Planning Council: Crime Prevention through Environmental Design, <http://cpted.mapc.org/index.html>
39. Soriguera, F., Martínez, I., Sala, M., Menéndez, M.: Effects of low speed limits on freeway traffic flow. *Transp. Res. Part C Emerg. Technol.* 77, 257–274 (2017). <https://doi.org/10.1016/j.trc.2017.01.024>
40. National Association of City Transportation Officials: Dedicated Curbside/Offset Bus Lanes, <https://nacto.org/publication/urban-street-design-guide/street-design-elements/transit-streets/dedicated-curbside-offset-bus-lanes>
41. Hazan, J., Lang, N., Wegscheider, A.K., Fassenot, B.: ON-DEMAND TRANSIT CAN UNLOCK URBAN MOBILITY. BCG Henderson Institute (2019)
42. B-Box. CalebABC Co., LTD (2009)
43. Forman, E.H., Gass, S.I.: The Analytic Hierarchy Process—An Exposition. *Oper. Res.* 49, 469–486 (2001). <https://doi.org/10.1287/opre.49.4.469.11231>

## **Análisis de la evolución del uso del transporte urbano público en ciudades de Latinoamérica, Europa y Asia durante la pandemia del COVID-19**

Melva Inés Gómez-Caicedo<sup>1</sup>[0000-0002-9020-0051], Anderson Quintero<sup>2</sup>, Rodrigo Ramírez-Pisco<sup>3</sup> [0000-0001-8648-3805], Mercedes Gaitan-Angulo<sup>2</sup>[0000-0002-8248-8788], Renato Andara<sup>4</sup> [0000-0002-6706-1567], Jesús Ortego<sup>5</sup>[0000-0001-6173-2940], Luis Manuel Navas<sup>5</sup> [0000-0020-7895-925X], Carmen Luisa Vásquez<sup>4</sup>[0000-0002-0657-3470],

<sup>1</sup> Fundación Universitaria Los Libertadores, Bogotá, Colombia

<sup>2</sup> Fundación Universitaria Konrad Lorenz, Bogotá, Colombia

<sup>3</sup> Universitat Carlemany, Andorra, Andorra

<sup>4</sup> Universidad Nacional Experimental Politécnica Antonio José de Sucre, Barquisimeto, Venezuela

<sup>5</sup> Universidad de Valladolid, Valladolid, España

cvasquez@unexpo.edu.ve

**Abstract.** Actualmente, existe aún bastante desconocimiento sobre la efectividad de las medidas implementadas para adaptar la prestación del servicio de transporte urbano público durante la pandemia del COVID-19, entre las que se encuentra la reducción de la ocupación de las unidades de transporte y las restricciones de circulación, entre otras. El presente estudio se realiza con el propósito de este artículo es analizar de la evolución del uso del transporte urbano público en ciudades de Latinoamérica, Europa y Asia durante la pandemia del COVID-19. Las ciudades seleccionadas, en base a criterios de disponibilidad y accesibilidad de datos de movilidad, son Bogotá (Colombia), Lima (Perú), Brasilia (Brasil), Madrid (España), París (Francia), Lisboa (Portugal), Auckland (New Zealand), Hong Kong (China) y Singapur (Singapur). Para ello se correlacionaron los datos del número de contagios diarios ocasionados por COVID-19 en cada país, publicados por *Johns Hopkins Hospital University*, con los de pasajeros del transporte urbano público obtenidos de la plataforma *Moovit insights*, que muestra de forma pública las estadísticas por país y ciudad. Para el estudio se utilizaron los datos publicados en el periodo desde el 15 de enero de 2020 hasta el 30 de junio de 2021. Las ciudades se han agrupado en tres (3) grupos (A, B y C) en función de la velocidad de recuperación del número de pasajeros y, en este sentido, del uso del transporte en relación al de contagios, correspondientes a velocidades de recuperación rápida, media y lenta. Se obtiene modelos matemáticos como funciones diferenciales que aplica el método de minimización de error, programados con el lenguaje de Python. Entre las principales conclusiones destaca que la recuperación del número de pasajeros en las ciudades de Auckland y Madrid, pertenecientes al Grupo B, no poseen una aproximación favorable como el resto de las ciudades.

**Keywords:** Contagios de COVID-19, pandemia COVID-19, transporte urbano público.

2

## 1 Introducción

Las actividades que permiten el relacionamiento social y económico se han visto afectadas debido al impacto generado por la pandemia por el coronavirus COVID-19, identificado como SARS-CoV-2 [1] [2]. Inicialmente, la necesidad de disminuir el número de contagios genera la implementación de una serie de medidas por parte del Estado y de la población de distanciamiento social, reducción en la movilidad [3] y del uso del transporte urbano [4], entre otros [5]. Considerando que la movilidad es una de las actividades que mayores cambios ha registrado [6] [7] se hace importante conocer la dinámica establecida y las políticas derivadas del control del transporte público urbano por parte de las naciones [8].

La pandemia de la COVID – 19 es catalogada por la Organización Mundial de la salud (OMS) como un virus que se transmite cuando una persona enferma tose, estornuda o entra en contacto con otras. La posibilidad su transmisión ha ocasionado efectos negativos en el uso del transporte urbano [9], el cual representa un papel importante del diario vivir de diversas personas [10]. Desde su comienzo, los operadores de los sistemas de transporte urbano han aplicado diferentes medidas para enfrentar y ofrecer bioseguridad a los pasajeros, con el objetivo de garantizar medidas que aseguren la salud pública y lograr que sea una opción utilizada y atractiva para los diferentes usuarios [11], [12]

La mayoría de las ciudades del mundo han establecido políticas con relación al uso del transporte público, con el fin de frenar la propagación del virus y mitigar con ello los efectos que se puedan presentar. En este marco, al analizar las medidas adoptadas para controlar la propagación de la pandemia COVID-19 se pueden clasificar en medidas de bioseguridad y distanciamiento para los usuarios, de mantenimiento y limpieza de las unidades y, finalmente, las destinadas al uso del transporte urbano que se muestra en la Tabla 1, para algunos países.

**Table 1.** Restricciones en el porcentaje de uso del transporte urbano en algunos países [13].

País	Medidas
Colombia	Restricciones en el uso del transporte público
Perú	Aislamiento preventivo y obligatorio, con restricciones de libre circulación en el país. No permite circular los vehículos particulares
Brasil	A nivel federal no hay medidas de confinamiento. Rio de Janeiro y Sao Paulo, declaradas en emergencia, suspendieron el uso del transporte público, entre otras medidas.
Francia	Se restringe el uso del transporte público sólo para ir a trabajar
Portugal	La ocupación del transporte público y privado no puede pasar de un tercio de su capacidad
China	Suspensión del transporte público y restricciones de circulación de los vehículos privados.
Singapur	Confinamiento de las personas lo que impacta en una reducción del uso del transporte público y personal.

A pesar de la diversidad de medidas aplicadas, existe aún un desconocimiento en la implementación de modelos para mejorar la prestación del servicio de transporte público, que permitan su transformación y se comiencen a generar medidas dirigidas al desarrollo de procesos sostenibles [14]. Con base en esto, el objetivo de este artículo analizar de la evolución del uso del transporte urbano público en ciudades de Latinoamérica, Europa y Asia durante la pandemia del COVID-19.

Para los casos de contagio diarios del país ocasionados por COVID-19 se han utilizado los publicados por *Coronavirus Reserch Center del Johns Hopkins Hospital University* [15] y los datos del transporte público los de la plataforma *Moovit insights* [16] que muestra de forma pública las estadísticas por país y ciudad. Para el estudio se utiliza los datos publicados en el Bogotá (Colombia), Lima (Perú), Brasilia (Brasil), Madrid (España), París (Francia), Lisboa (Portugal), Auckland (New Zelanda), Hong Kong (China) y Singapur (Singapur) durante 15 de enero de 2020 hasta el 30 de junio de 2021.

## 2 Metodología

Se seleccionaron un total de nueve (9) ciudades de Latinoamérica, Europa y Asia, en base a la disponibilidad y accesibilidad de datos de movilidad publicados por *Moovit insights* [16], bajo los siguientes tres (3) criterio:

- Grupo A: Ciudades que han tenido una evolución rápida de la normalización de los niveles de tráfico en función a la recuperación del impacto de la pandemia. Por ejemplo Brasilia, que pasa de un  $-40,4$  (07/07/2020) a  $2\%$  (15/01/2021) con una afectación del  $8,8\%$ .
- Grupo B: Ciudades que han tenido una evolución media de la normalización de los niveles de tráfico en función a la recuperación del impacto de la pandemia. Por ejemplo, Madrid, que pasa de un  $-89$  (12/04/2020) a  $6\%$  (15/01/2021) con una afectación media de  $25\%$
- Grupo C: Ciudades que han tenido una evolución lenta. Por ejemplo, Lima  $93,5$  (16/04/2020) a  $-51,5\%$  (30/06/2021), con una media de  $58,5\%$  de pérdida

Tabla 2. Grupos y ciudades que lo integran.

Grupo	Ciudad
A	Brasilia
	Singapore
	Hong Kong
B	Madrid
	Lisboa
	Auckland
C	Paris
	Bogota
	Lima

4

Las políticas y medidas implementadas las ciudades son el producto de las necesidades de sus residentes y de sus características socio económicas. Debido a ello, los fenómenos endógenos a los que son expuestos sus habitantes generan dinámicas evolutivas totalmente ajenas entre naciones. Con el fin de analizar de la evolución del uso del transporte urbano público en ciudades de Latinoamérica, Europa y Asia durante la pandemia del COVID-19 y su progresiva recuperación se estudia un modelo teórico que haga explícita la relación entre los dos (2) fenómenos y como este es ajustado a contextos territoriales usando datos reales que evidencien la efectividad del modelo.

Inspirados por el patrón mundial recurrente durante los años 2019-2021 debido a las medidas durante la pandemia del COVID-19, las limitaciones en la movilidad y las características epidemiológicas de los virus en sus etapas tempranas de desarrollo y gestación, se generaron patrones equivalentes de acción y reacción a lo largo del mundo. Sin embargo, pese a la aparente relación social y cultural entre los fenómenos, se desea establecer una interacción matemática formal entre la disponibilidad del transporte público y la evolución de la población infectada por la enfermedad.

De tal manera, en este estudio se realizará un análisis de un modelo matemático que se ajusta a los datos de nueve (9) ciudades. Los datos obtenidos se distribuyeron en dos grupos (2): el primero referido a los datos del transporte público, donde cada dato representa un porcentaje de la proporción de unidades de transporte disponibles enviados por la ciudad en base al primer día considerado. En otras palabras, son los errores relativos calculados en base a la cantidad de los disponibles el 15 de enero de 2020. El segundo, posee la cantidad de personas infectadas por la COVID-19. Ambos grupos, poseen la información diaria desde el 15 de enero de 2020 hasta el 30 de junio de 2021 en las ciudades del estudio. En estos se encuentran infectados diarios y acumulados. Para el desarrollo de este documento sólo se utiliza las cifras de contagio acumuladas

Este estudio se divide en tres (3) partes. La primera parte será analizar los datos individuales de las ciudades, identificar las múltiples tendencias y sus características. Además, evaluar los infectados en relación del porcentaje del transporte; con el fin de establecer la hipótesis para la modelación del fenómeno. La segunda, consta de interpretar las hipótesis corroboradas para los datos, lo cual permitirá realizar la descripción y construcción del modelo, así como su estructuración matemática.

La tercera parte consiste en ajustar el modelo a los datos de cada ciudad a partir de un método de minimización de error local. El resultado final del estudio genera un conjunto de parámetros acoplados a cada ciudad que permitirán identificar el comportamiento de cada una ante el crecimiento de infectados y las políticas implementadas para el desarrollo de la movilidad, así como una posible herramienta que permita predecir o identificar tendencias del transporte bajo las mismas condiciones de vulnerabilidad.

### 3 Resultados

Como se puede observar en la Fig. 1, el comportamiento general de los contagios es distante entre cada ciudad del grupo en estudio. Sin embargo, las características inherentes al territorio son el crecimiento progresivo en los primeros días de contagio y un leve estancamiento en los días finales de la recolección de datos. La Fig. 2 representa la inestabilidad altamente volátil en el número de pasajeros abordados del transporte

público disponible para este período. Sin embargo, el estatus general para la época por efectos de las medidas de confinamiento por parte de los gobiernos es generar una tendencia monótona progresiva al crecimiento con algunos cambios de concavidad.

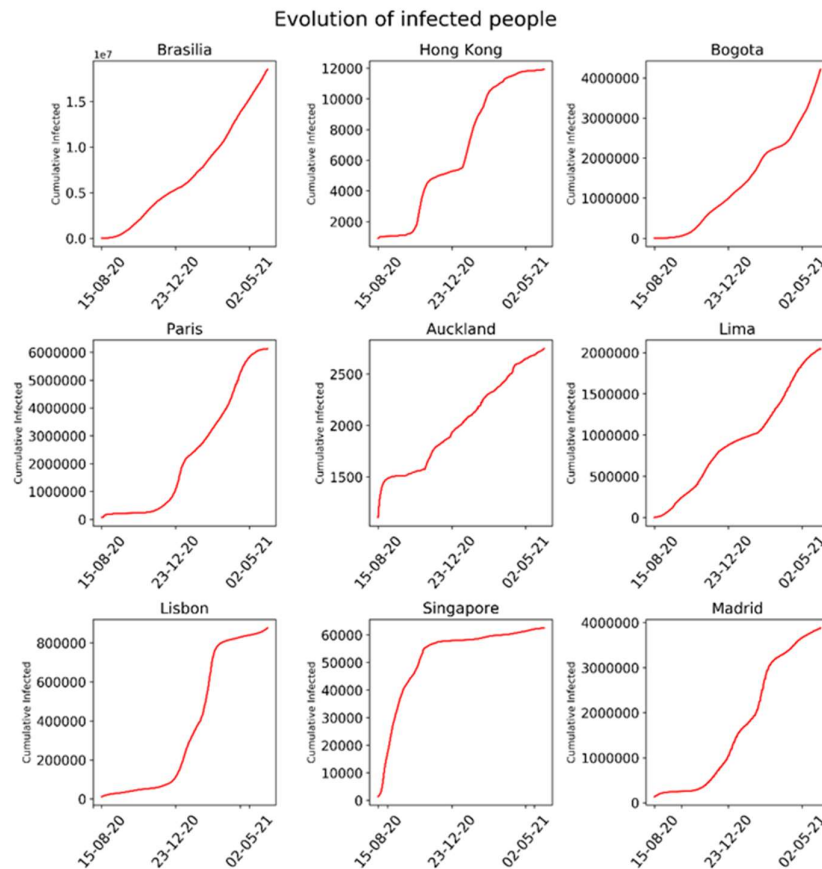


**Fig. 1.** Evolución de la población contagiada.

Existen ciertas características análogas entre el número de pasajeros de transporte disponible y de pasajeros mostrado en las Fig. 1 y 2. El efecto más relevante es visto en Singapore, ya que prevalece una tendencia constante entre ambos después de un punto determinado de tiempo. Por otro lado, ciudades como Bogotá, Lima y Brasilia, generan tendencias al crecimiento y estabilidad. Finalmente, Hong Kong y Auckland son ajenos a las características relacionadas entre ambos, ya que no aparentan un comportamiento específico relacionado entre las variables.

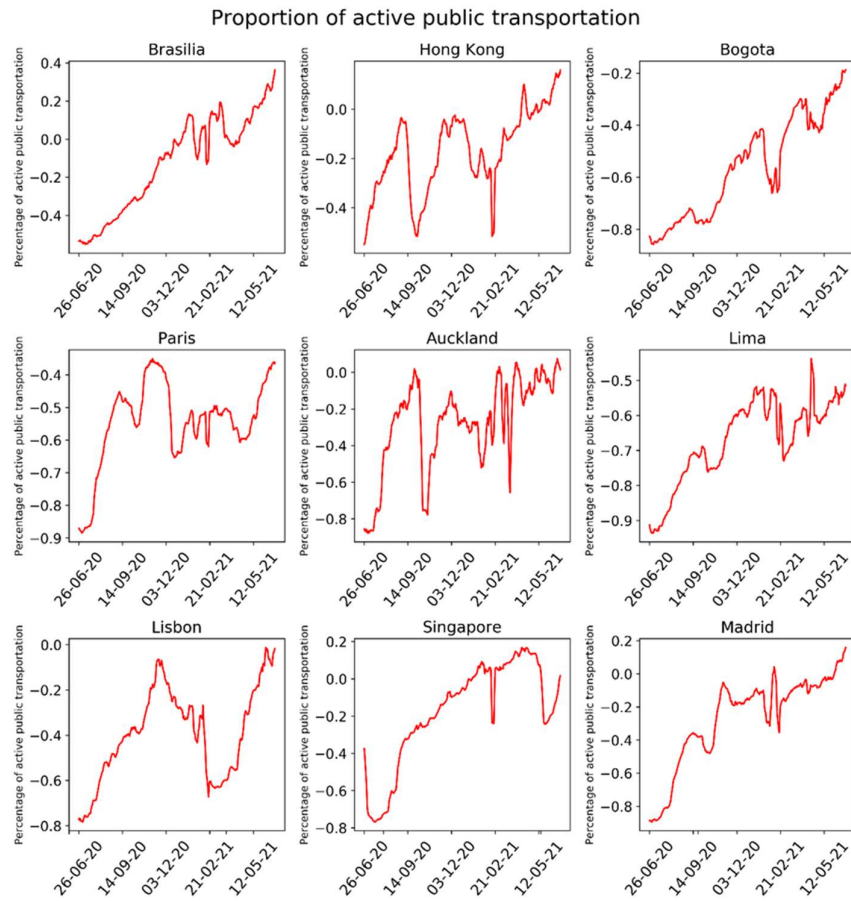


**Fig. 2.** Evolución de la proporción del transporte público respecto al 15 de enero de 2020.

Según lo observado hasta ahora de las Fig 1 y 2, la supuesta existencia de una relación matemática entre el crecimiento de número de pasajeros de transporte disponible y de pasajeros mostrado se mantiene en ciertas ciudades, la cual puede ser vista en la Fig.3. En ella se ilustra el efecto de relacionar los fenómenos, existen comportamientos fácilmente identificables como el de Bogotá y Brasilia que presenta una tendencia pseudolineal, mientras en ciudades como Madrid y Paris hay una tendencia a mantener un número de pasajeros constante. Otro de los efectos visualmente perceptibles en la Fig. 3, es que la dependencia del transporte es afectada por el crecimiento de los contagios en ese período, como se observa en Singapur, Lisbon, Madrid, Bogotá, Brasilia y Lima. A medida que los crecimientos de infectados son más prolongados, el cambio en el número de pasajeros es menos perceptible y posee saltos menos abruptos.

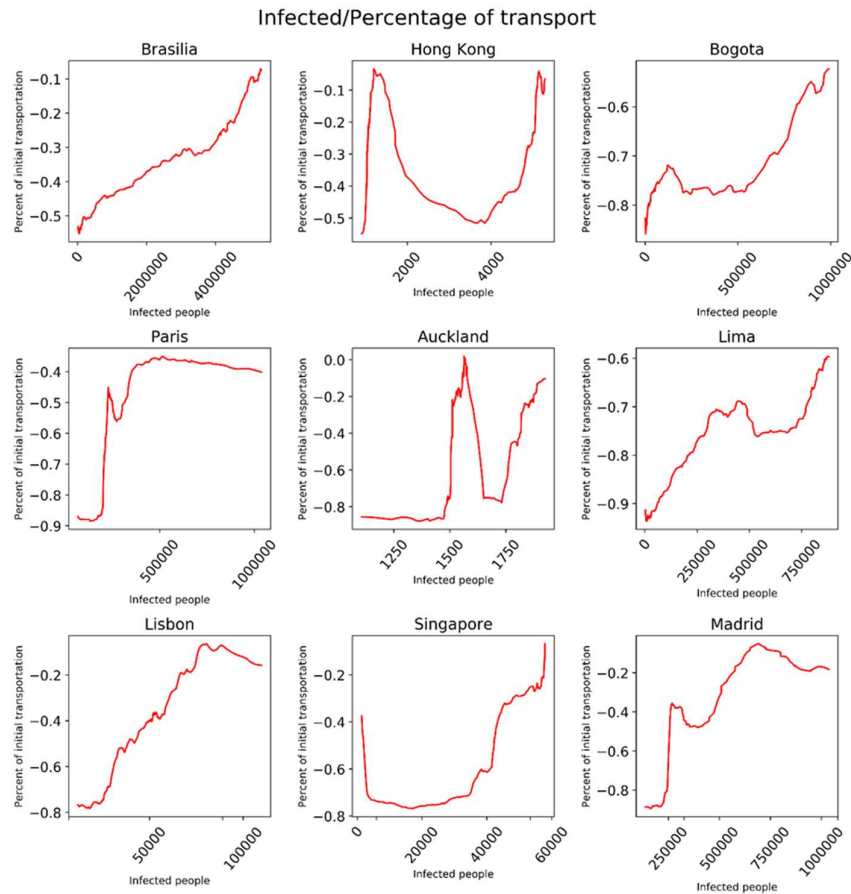


**Fig. 3.** Porcentaje de transporte graficado respecto a la cantidad de contagios graficada.

Inicialmente para que un estudio teórico basado en ecuaciones diferenciales tenga sentido, es necesario que la variable independiente sea monótona creciente, de aquí la justificación de utilizar el acumulado de contagios por día, ya que presenta un crecimiento suave y continuo. Para la evolución de contagios se deben realizar las siguientes suposiciones:

- La cantidad de contagios por día es real y no está alterada por errores de medición.
- No hay población inmune a la enfermedad.
- La población infectada en el transporte público se distribuye uniformemente en el territorio.
- No hay eventos determinantes que modifiquen drásticamente el contagio.
- La cantidad de contagios siempre aumenta.

Estas suposiciones garantizan la evolución monótona y progresiva de los contagios, además de garantizar la continuidad y la confiabilidad de las políticas generales en el

8

territorio. De la misma forma, se considerarán las siguientes suposiciones con respecto al porcentaje:

- La proporción necesitada por el territorio siempre puede ser cubierta.
- El transporte público ramifica sus rutas por todo el territorio.
- No hay otras restricciones vehiculares más que un confinamiento.
- La cantidad mínima de unidades de transporte público disponibles por día es una cantidad fija.
- Antes de que ocurriera el fenómeno, la proporción de vehículos estimados a enviar cubría totalmente las necesidades públicas.

Así mismo, estas suposiciones garantizan que la proporción del transporte no discrimine a la población portadora del virus que no estén infectados, asintomáticos e infectados. De tal manera, si consideramos que el porcentaje del transporte ( $T$ ) depende de la cantidad de infectados ( $I$ ), el cambio inmediato del porcentaje disponible por infectado depende de la proporción esperada por infectado ( $P_E$ ) y de la proporción que debe ingresar para cubrir la necesidad pública faltante o sobrante ( $P_I$ ), en otras palabras, como muestra la Ec. 1.

$$\frac{dT}{dI} = P_E + P_I \quad (\text{Ec. 1})$$

Para determinar la proporción esperada por infectado ( $P_E$ ), por las suposiciones efectuadas, la cantidad de transporte a enviar es una cantidad fija, por ende ( $P_E$ ) es proporcional a la cantidad de infectados, como se muestra en la Ec. 2.

$$P_E = k \times I \quad (\text{Ec. 2})$$

Siendo el coeficiente de proporcionalidad ( $k$ ) el porcentaje promedio de vehículos públicos enviados por unidad de infectados, medida en (%Transporte/infectados). Con respecto a la necesidad pública faltante o sobrante ( $P_I$ ) es un excedente o faltante de la cantidad usual anterior al fenómeno, de tal manera, entre más recuperados e inmunes haya en el territorio menos excedente o faltante existirá, lo que indica que este término converge progresivamente a cero conforme la ciudad se recupera.

Si consideramos la cantidad de personas infectadas totales con un indicador de adaptación progresivo, entonces la tecnología territorial, las estructuras sanitarias y la adaptación poblacional se encargarán de subsistir con estos comportamientos hasta recuperar la normalidad de la movilidad usual.

Entonces el ( $P_I$ ) sería inversamente proporcional a la cantidad total de infectados. Así mismo, entre mayor sea el porcentaje actual enviado indica que mayor cantidad de gente está saliendo a las calles, de tal manera ( $P_I$ ) es directamente proporcional al porcentaje actual por infectado, como se muestra en la Ec. 3.

$$P_I = \alpha \frac{(T - \beta)}{I} \quad (\text{Ec. 3})$$

Donde  $\alpha$  es la población infectada que progresivamente regresa al transporte público, el cual es un indicador de población que retoma actividades (recuperados) y  $\beta$  es el porcentaje del transporte esperado que se requiere para cubrir las necesidades de movilidad urbana.

En este marco referencial, al incrementar el número de infectados, el término  $P_I$  converge a cero (0), un comportamiento esperado por parte de una ciudad que estructura su estrategia a partir de una época de crisis sanitaria. En resumen, el modelo final se muestra en la Ec. 4.

$$\frac{dT}{dt} = kI + \alpha \frac{(T - \beta)}{I} \quad (\text{Ec. 4})$$

Donde:

$k$  el porcentaje promedio de vehículos enviados por unidad de infectados.

$\alpha$  la población infectada que progresivamente regresa al transporte público.

$\beta$  el porcentaje del transporte esperado que se requiere para cubrir la necesidad de movilidad.

Para ajustar los parámetros de la ecuación diferencial se aplica un método de minimización de error en el lenguaje de programación Python. El problema consiste en hallar por cada ciudad el conjunto de parámetros  $k$ ,  $\alpha$ ,  $\beta$  y el valor de la condición inicial  $I_0$  que minimiza la distancia entre los datos generados por la solución de la ecuación diferencial y los datos reales. Para su implementación se aplica usando la librería `scipy` específicamente con la función `curve fit`. Este procedimiento se hace por cada una de las ciudades en los intervalos en los que sus datos generen un incremento o decremento de concavidad durante más de 50 días consecutivos.

El resultado de esta investigación además de presentar un modelo diferencial teórico enfocado en la evolución del transporte público que se puso a disposición en periodos de pandemias y confinamientos, también se implementa para ajustar datos reales, un ejemplo de ello es visualizado en la Fig. 4, que tiene en cuenta desde el día 83 del estudio (6 de abril del 2020) hasta el día 283 (23 de octubre de 2020).

La Fig. 4 muestra la efectividad de la aproximación generada en el intervalo de tiempo seleccionado, pese a la simpleza del modelo. Si bien ciudades como Auckland y Madrid no poseen una aproximación favorable como el resto de las ciudades, si parece describir adecuadamente una tendencia similar. Por otro lado, la Tabla 3 muestra los coeficientes para este periodo de tiempo es.

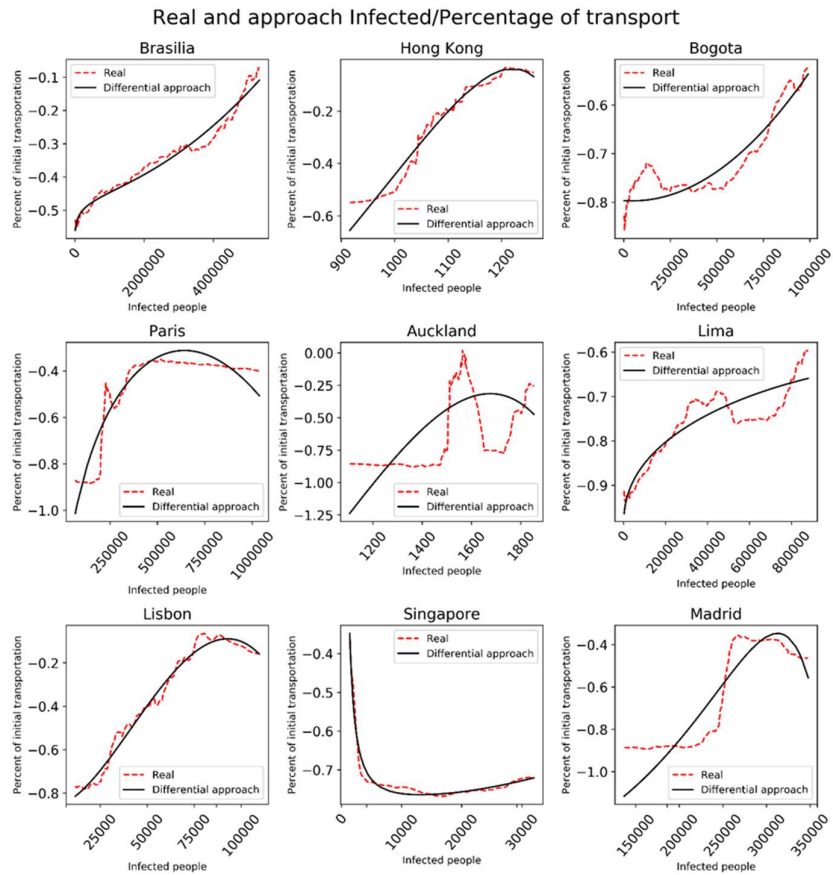


Tabla 3. Parámetros obtenidos para el primer periodo de tiempo.

Ciudad	k	$\alpha$	$\beta$	$I_0$
Brasilia	1,85E-14	0,160433	-0,661564	-0,560632
Hong Kong	-1,68E-05	14,0146	-1,82253	-0,655407
Bogota	2,77E-13	1,06175	-0,796576	-0,796606
Paris	-1,37E-12	0,396605	-1,73257	-1,01317
Auckland	-4,48E-06	4,75E+00	-2,96332	-1,2376
Lima	-4,95E-14	0,42072	-0,994055	-0,963246
Lisbon	-2,24E-10	2,51036	-0,857721	-0,81404
Singapore	2,25E-10	1,51E+00	-0,790042	-0,347545
Madrid	-1,15E-10	11,1873	-1,34923	-1,1159

Según el modelo y los parámetros vistos en la Tabla 3, el coeficiente de  $k$  indica el porcentaje promedio de transporte enviados por cantidad de infectados, lo indica que la demanda fue mayor en Singapore, indicando un leve incremento de unidades de transporte con respecto a los infectados totales. Lo que demuestra que esta ciudad generó políticas de movilidad que repercutían directamente en el transporte.

Por otro lado, ciudades como Brasilia y Bogotá generaron unas políticas similares en cuanto a la movilidad por unidad de infectados. Sin embargo, pese a las características inestables en la evolución del contagio, estas medidas no fueron suficientes para contener el contagio progresivo. Con respecto al resto de las ciudades, se determina un decremento importante en el transporte, lo que indica que en estos países las políticas de movilidad no se centraron en incrementar su flujo sino en alternativas como trabajar desde casa o utilizar vehículos particulares.

La existencia de una relación matemática entre el crecimiento de número de pasajeros de transporte disponible y de pasajeros en ciertas ciudades. Hay un efecto relacionar los fenómenos, existen comportamientos fácilmente identificables como el de Bogotá y Brasilia que presenta una tendencia pseudolineal, mientras en ciudades como Madrid y París hay una tendencia a mantener un número de pasajeros constante. Otro de los efectos visualmente perceptibles es que la dependencia del transporte es afectada por el crecimiento de los contagios en ese período, como se observa en Singapur, Lisbon, Madrid, Bogotá, Brasilia y Lima. A medida que los crecimientos de infectados son más prolongados, el cambio en el número de pasajeros es menos perceptible y posee saltos menos abruptos.

Así mismo, el coeficiente  $\alpha$  determina la población infectada que progresivamente regresa al transporte público, la cual está directamente relacionada con el índice de recuperación diaria. En este marco Hong Kong procede con mayor participación teniendo un índice de recuperación de 14 personas, seguido por Auckland y Lisbon.

Finalmente, el parámetro  $\beta$  indica el porcentaje del transporte esperado que se requiere para cubrir la necesidad de movilidad, de la cual se obtiene que el mayor porcentaje esperado es del -0,661564%, siendo una cantidad coherente con la obtenida por el parámetro  $k$ , ya que fue una de las ciudades que más unidades de transporte público requerido.

## Conclusiones

El desconocimiento sobre la efectividad de las medidas implementadas para adaptar la prestación del servicio de transporte urbano público durante la pandemia del COVID-19. En el presente estudio se analiza de la evolución del uso del transporte urbano público en ciudades de Bogotá (Colombia), Lima (Perú), Brasilia (Brasil), Madrid (España), París (Francia), Lisboa (Portugal), Auckland (New Zelanda), Hong Kong (China) y Singapur (Singapur), durante la pandemia del COVID-19. En este se correlacionaron los datos del número de contagios diarios, publicados por *Johns Hopkins Hospi-*

12

tal University, y los de pasajeros del transporte urbano público obtenidos de la plataforma *Moovit insights* para el periodo desde el 15 de enero de 2020 hasta el 30 de junio de 2021.

Se obtiene modelos matemáticos sobre el comportamiento general de los contagios, el cual muestra que son distantes entre cada ciudad. Sin embargo, son de crecimiento progresivo en los primeros días de contagio y un leve estancamiento en los días finales de la recolección de datos.

Existe una inestabilidad altamente volátil en el número de pasajeros abordados del transporte público disponible para este período. Sin embargo, el estatus general para la época por efectos de las medidas de confinamiento por parte de los gobiernos es generar una tendencia monótona progresiva al crecimiento con algunos cambios de concavidad.

La Ec.4 es el resultado del estudio teórico basado en ecuaciones diferenciales, donde la variable independiente sea monótona creciente, y de utilizar el acumulado de contagios por día, ya que presenta un crecimiento suave y continuo. Para ajustar los parámetros de la ecuación diferencial se aplica un método de minimización de error en el lenguaje de programación Python. Se encuentra para cada ciudad el conjunto de parámetros  $k$ ,  $\alpha$ ,  $\beta$  y el valor de la condición inicial que minimiza la distancia entre los datos generados por la solución de la ecuación diferencial y los datos reales.

El resultado presenta un modelo diferencial teórico enfocado en la evolución del transporte público que se puso a disposición en periodos de confinamientos. Además, este se implementa para ajustar datos reales.

## References

1. S. Verma y A. Gustfsson, «Investigating the Emerging COVID-19 Research Trends in the Field of Bussnes and Managamente: A bibliometric Analysis Aproach,» *Journal of Business Resarch*, vol. 118, pp. 253-261, 9 2020.
2. S. Saadat, D. Rawtani y C. Hussain, «Environmental perspective of COVID-19,» *Science of The Total Enviorenment*, vol. 728, 01 08 2020.
3. A. Dingil y D. Esztergár-Kiss, «The Influence of the COVID-19 Pandemic on Mobility Patterns: The First Wave's Results,» *Transportation Letters*, pp. 434-446 , 17 04 2021.
4. J. Ortego-Osa, R. Andara, L. Navas-Gracia, C. Vásquez y R. Ramírez-Pisco, «Impact of the Covid-19 Pandemic on Traffic Congestion in Latin American Cities: An Updated Five-Month Study,» *Ibero-American Congress of Smart Cities ICSC-CITIES 2020*, pp. 216-229, 07 02 2021.
5. C. Musselwhite, E. Avineri y Y. Susilo, «The Coronavirus Disease COVID-19 and implications for transport and health,» *Journal of Transport & Health*, vol. 16, 2020.
6. F. Benita, «Humana mobility behacior in COVID-19: A systematic literature review and bibliometric analysis,» *Sustainable Cities and Society*, vol. 70, p. 102916, 07 2021.
7. M. Háncean, M. Slavinec y M. Perc, «The impact of human mobility networks on the global spread of COVID-19,» *Journal of complex Network*, vol. 70, pp. 1-14, 07 03 2021.

8. S. Lai, F. Leone y C. Zoppi, «COVID-19 and spatial planning. A few issues concerning public policy,» *TeMA-Journal of Land Use, Mobility and Environment*, pp. 231-246, 19 06 2020.
9. A. Calatayud, M. Monsreal, J. Mangan y V. J., «Benefits of Technology Adoption for Enhanced Integration of Port-Hinterland Operations,» *Transportation Research Record*, pp. 606-6015, 10 09 2020.
10. W. Maloney y T. Taskin, «Determinants of social distancing and economic activity during COVID-19: A global view,» *The World Bank*, nº 942, 2020.
11. A. Guitierrez, D. Miravet y A. Doménech, «COVID-19 and urban public transport services: emerging challenges and a research agenda,» *Cities & Health*, pp. 1-4, 20 08 2020.
12. A. Przybylowski, S. Stelmak y M. Suchanek, «Mobility Behaviour in View of the Impact of the COVID-19 Pandemic-Public Transport User in Gdansk Case Study,» *Sustainability*, p. 364, 03 01 2021.
13. MITMA, «Seguimiento de las medidas en el sector transporte por COVID-19,» Madrid, 2020.
14. K. Gkiotsalitis y O. Cats, «Public transport planning adaption under the COVID-19 pandemic crisis: literature review of research needs and directions,» *Transport Reviews*, vol. 41, nº 3, pp. 374-392, 2021.
15. JHU, «Johns Hopkins Hospital University & Medicine,» 2021. [En línea]. Available: <https://coronavirus.jhu.edu/map.html>.
16. Moovit, «Moovit Insights,» 2021. [En línea]. Available: [https://moovitapp.com/insights/es/Moovit\\_Insights\\_%C3%8Dndice\\_de\\_Transporte\\_P%C3%BAblico-countries](https://moovitapp.com/insights/es/Moovit_Insights_%C3%8Dndice_de_Transporte_P%C3%BAblico-countries).
17. A. R., J. Ortego-Osa, M. Gómez-Caceido, R. Ramírez-Pisco, L. Navas-Gracia, C. Vásquez y M. Gaitan-Angulo, «Behavior of traffic congestion and public transport in eight large cities in Latin America during the COVID-19 pandemic,» *Applied Science*, vol. 11, nº 4703, pp. 1-13, 20 05 2021.
18. MinTransporteCo, «MinTransporteCo,» 24 12 2020. [En línea]. Available: <https://www.mintransporte.gov.co/publicaciones/9303/gobierno-nacional-amplia-la-capacidad-de-ocupacion-de-los-vehiculos-de-transporte-publico-hasta-el-70/>.
19. SUTRAN, «Protocolo sanitario sectorial para la prevención del COVID-19, en el transporte terrestre y ferroviario de cargas y mercancías y actividades conexas en el territorio nacional,» Lima, 2020.

## Análisis Multiobjetivo de la Degradación del Acetaminofén usando TiO<sub>2</sub> Degussa P25

Alfredo Cristóbal-Salas<sup>1</sup>[0000-0003-2297-6031], Bardo Santiago-Vicente<sup>1</sup>[0000-0002-9096-9311], Neiel-Israel Leyva-Santes<sup>2</sup>[0000-0003-0287-3318], Raúl-Alejandro Luna-Sánchez<sup>3</sup>[0000-0003-2932-882X], Carolina Solis-Maldonado<sup>3</sup>[0000-0002-9419-2001]

<sup>1</sup>Facultad de Ingeniería en Electrónica y Comunicaciones, Universidad Veracruzana, Poza Rica – México. [acristobal@uv.mx](mailto:acristobal@uv.mx), [bardosantiago.v@gmail.com](mailto:bardosantiago.v@gmail.com)

<sup>2</sup>Centro de Supercomputación de Barcelona, España. [neiel.leyva@bsc.es](mailto:neiel.leyva@bsc.es)

<sup>3</sup>Facultad de Ciencias Químicas, Universidad Veracruzana, Poza Rica - México. [raluna@uv.mx](mailto:raluna@uv.mx), [casolis@uv.mx](mailto:casolis@uv.mx)

**Resumen.** Este trabajo presenta una propuesta química-computacional para mejorar el tratamiento de agua contaminada con acetaminofén. Este fármaco es conocido por sus propiedades analgésicas en el tratamiento de fiebre y dolor moderados. Cuando el acetaminofén se concentra en el agua para beber es considerado como un micro-contaminante emergente. Este fármaco puede afectar la salud de la población sensible en los hospitales, clínicas y casas de retiro. Reducir la concentración del acetaminofén en el agua implica un incremento en el costo del tratamiento por lo que es necesario un equilibrio entre los objetivos en conflicto: cantidad de catalizador utilizado, tiempo de tratamiento y costo del tratamiento. Los resultados obtenidos muestran que es posible planificar la producción de hasta 300 litros de agua para beber cada 24 horas con concentraciones entre 5 y 15 partículas por millón de acetaminofén considerando costos mínimos de operación.

**Palabras clave:** Contaminante Emergente, Algoritmo Genético, Acetaminofén, Agua Limpia, Saneamiento.

### 1 Introducción

Los sistemas de tratamiento de agua convencionales incluyen procesos físicos, químicos y biológicos para eliminar materiales, sustancias y moléculas que contaminan el agua. Sin embargo, algunas moléculas químicas no pueden ser detenidas o degradadas por lo que es posible encontrarlas aún después de los tratamientos como se hace referencia en [18].

Los contaminantes emergentes son moléculas que están presentes en cuerpos de agua en muy bajas concentraciones (en el orden  $\mu\text{g/L}$  o  $\text{ng/L}$ ). A pesar de ser muy baja la concentración, estos contaminantes representan un riesgo importante ya que generan un gran impacto en la salud de los seres vivos y al medio ambiente [1, 2, 17, 21, 26].

Por esta razón, estos contaminantes se han convertido en un problema de interés mundial. Estos contaminantes provienen de diversos productos como: agentes tensoactivos, aditivos industriales, plastificantes, artículos de limpieza para el hogar y de cuidado personal, pesticidas y productos farmacéuticos.

Se ha reportado que los procesos avanzados de oxidación son tecnologías que logran degradar estos contaminantes hasta lograr la mineralización de las moléculas orgánicas y formar  $\text{CO}_2$  y  $\text{H}_2\text{O}$ . Entre estos procesos se destacan los no fotoquímicos: Oxidación electroquímica [12], Ozonización [3, 15, 16], Procesos Fenton [19], y Plasma no térmico [23], entre otros; y los fotoquímicos: fotólisis, Procesos Foto-Fenton y la Fotocatálisis [10]. Los procesos de fotocatalisis han demostrado ser una tecnología prometedora por ser sencilla y amigable con el medio ambiente. Por ello, esta investigación propone el tratamiento de contaminantes emergentes diluidos en agua con procesos fotocatalíticos como se sugiere en [6].

Esta investigación considera el tratamiento de agua contaminada con 20 ppm de acetaminofén, esto es, 20  $\mu\text{g}$  del fármaco por litro de agua. Además, se utiliza un reactor químico de flujo continuo PFR con cuatro lámparas de luz ultravioleta con capacidad de procesar hasta 2 litros de agua por carga como se presenta en [25].

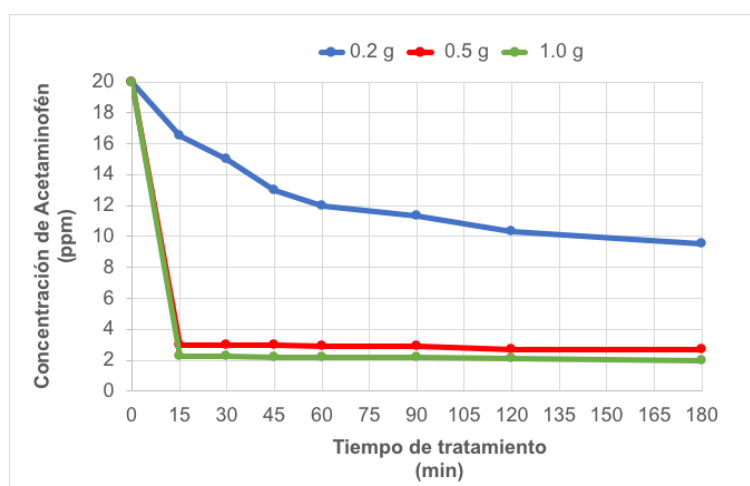


**Fig. 1.** Concentración de acetaminofén diluido en agua medida en partículas por millón (ppm) usando 0.2, 0.5 y 1.0 gramos de  $\text{TiO}_2$  Degussa P25 a lo largo de 180 minutos de tiempo de reacción en un reactor químico de flujo continuo PFR con iluminación UV. Fuente: [25].

La Fig. 1 presenta las curvas de reducción de la concentración del acetaminofén cuando se utilizan 0.2, 0.5 y 1.0 gramos de  $\text{TiO}_2$  Degussa P25 como parte de tratamiento del agua en el reactor químico. En todo momento, el tratamiento presentado en [25] se considera posterior al tratamiento convencional físico, químico o biológico que se lleva a cabo en una planta tratadora de aguas residuales [5, 7, 8, 9, 14, 20].

## 1.1 Problemática

Esta investigación busca apoyar a hogares, hospitales, casas de ancianos, centros de emergencia médica, albergues en caso de desastres u otros sitios donde se consuman medicamentos. En este tipo de lugares, existe la posibilidad que el acetaminofén se combine con otras sustancias, y esta combinación, pueda afectar la salud de la población. En investigaciones previas, como la presentada por [25], demostró que es posible degradar el acetaminofén diluido en agua usando  $\text{TiO}_2$  Degussa P25 en un reactor fotocatalítico PFR que expone la reacción química a luz ultravioleta. En dicha investigación se encontraron las curvas de degradación que se muestran en la Fig.1.

Ahora, la presente investigación se centra en garantizar la entrega de agua con bajas concentraciones de acetaminofén dentro de los rangos de consumo de la población objetivo. La pregunta ahora es: ¿existe una forma de tratar el agua que cumpla con los rangos permitidos de concentración de contaminantes emergentes, con el presupuesto disponible para el tratamiento del agua y a la vez que cumpla con los patrones de consumo de la población?

La investigación tiene las siguientes restricciones: (1) el tiempo máximo para el tratamiento del agua (24 horas). (2) una cantidad limitada de  $\text{TiO}_2$  Degussa P25 para utilizar durante el proceso de tratamiento del agua (10kg). (3) presupuesto diario destinado para el tratamiento del agua (\$350 pesos mexicanos). (4) concentración del acetaminofén en el agua (entre 5 y 15 ppm).

Para esta investigación se tiene un reactor fotocatalítico descrito en [25] el cual puede dar tratamiento a dos litros de agua por carga. Además, se tiene una cantidad de agua contaminada con 20 partículas por millón de acetaminofén y sin presencia de otros contaminantes.

A continuación, se describen algunas de las variables consideradas para resolver la problemática presentada. Las variables controladas de la investigación son:

Consumo de agua ( $v$ ). Esta variable se refiere a la cantidad de agua que la población destino consume por unidad de tiempo. Para esta investigación se considera el consumo de 200 y 300 litros de agua cada 24 horas.

Catalizador por ciclo ( $m$ ). Esta variable se refiere a la cantidad de gramos de  $\text{TiO}_2$  Degussa P25 usado para el tratamiento de agua contaminada. Un ciclo de tratamiento se refiere a la reducción de la concentración de acetaminofén en dos litros de agua.  $m = \{0.2, 0.5, 1.0\}$  gramos.

Tiempo por ciclo ( $t$ ). Esta variable se refiere al tiempo de tratamiento del agua en el reactor fotocatalítico PFR.  $0 \leq t \leq 1440$  minutos.

Las variables no controladas son:

Concentración objetivo ( $k_f$ ). Esta variable se refiere a la cantidad de partículas por millón de acetaminofén aún presentes en el agua después del proceso de tratamiento.

Costo del sistema ( $c$ ). Esta variable considera el costo en dinero del catalizador más el costo de consumo energético producido por el reactor fotocatalítico PFR.

## 2 Metodología

Esta investigación tiene como objetivo encontrar una combinación  $(m, t)$  que resuelva los objetivos:  $\text{Min}(k_f)$ ,  $\text{Min}(c)$ . Es conocido que este tipo de problemas requiere de una heurística que permita encontrar una combinación viable en tiempos razonables cuando los valores de las variables involucradas en el problema combinatorio crecen de manera significativa. Los algoritmos genéticos son una herramienta heurística muy conocida para resolver este tipo de problemas [4]. Estos algoritmos están inspirados en el proceso genético de los organismos vivos cuyos elementos básicos (genes) están organizados en estructuras llamadas cromosomas. Cada cromosoma representa la información esencial del organismo vivo y de acuerdo con los principios de selección natural y supervivencia, los cromosomas que mejor se adaptan al entorno pueden sobrevivir. Algunos ejemplos del uso de los algoritmos se describen a continuación.

En [13], se usaron en el sistema de transporte público para transportar a la máxima cantidad de personas de un punto a otro de la ciudad usando la menor cantidad de unidades de transporte público y utilizando la menor cantidad de combustible. En [11], los algoritmos genéticos han sido utilizados para mejorar el servicio de recolección de basura reduciendo la cantidad de unidades de recolección, así como la cantidad de combustible y recolectando la máxima cantidad de basura. En [22], los algoritmos genéticos han sido usados para ejecutar la máxima cantidad de procesos computacionales, pero con el menor costo energético. Finalmente, en [24], se describe un modelo de programación matemática para identificar redes de uso y tratamiento de agua con menor consumo y con rentabilidad óptima. Como puede notarse en los ejemplos anteriores los algoritmos genéticos se utilizan para resolver objetivos en conflicto en problemas combinatorios.

### 2.1 Definición de un algoritmo genético

En esta sección se presenta la interpretación del problema presentado en la sección anterior en términos de los algoritmos genéticos, esto es, en términos de cromosomas. Cada población de cromosomas debe ser evaluada de acuerdo con la función de ajuste para revisar cuales de los cromosomas sobrevivirán para la siguiente generación y cuales de ellos serán eliminados. Esta evaluación se concibe como la adaptación de los cromosomas al entorno en el cual deben sobrevivir. Una vez seleccionados los cromosomas ganadores se procede a crear variantes aleatorias de cada uno de los cromosomas mediante las operaciones mutación y cruzamiento. A continuación, se presentan detalles de la representación del problema en términos de algoritmos genéticos.

## 2.2 Diseño del cromosoma.

En la teoría de los algoritmos genéticos, un cromosoma está compuesto por una secuencia de valores que representan una combinación válida dentro del problema que se requiere representar. En esta investigación, un cromosoma representa una combinación válida  $(m, t)$  donde  $m$  tiene la siguiente codificación de la cantidad de catalizador utilizado en cada reacción química por litro de agua.

$m=1$  significa 0.2g de catalizador

$m=2$  significa 0.5g de catalizador

$m=3$  significa 1.0g de catalizador

Por otro lado,  $t$  es un valor en el rango 0 a 180 minutos que representa el máximo tiempo de experimentación en laboratorio de acuerdo con la información presentada en la Fig. 1.

Con la anterior información, un cromosoma válido del problema donde  $m=2$  y  $t=100$  es el par ordenado  $(2, 100)$ . La representación binaria del par ordenado es:  $(10, 01100100)$ . Con esta representación, un cromosoma válido del problema tiene la forma "1001100100".

## 2.3 Diseño de la función de ajuste

La función de ajuste o fitness evalúa que tan adaptado está un cromosoma a su entorno. De acuerdo con el modelo evolutivo solo los cromosomas que mejor se ajusten al contexto donde habitan pueden sobrevivir. En términos matemáticos la función de ajuste evalúa a cada cromosoma en el cumplimiento de los objetivos del problema.

Un cromosoma bien adaptado al contexto es uno que mejor cumple los objetivos. Los objetivos de un problema pueden ser encontrar el mínimo o el máximo de los valores. Cuando hay más de un objetivo por cumplir de manera simultánea se dice que el algoritmo es multiobjetivo.

Para esta investigación se tiene la siguiente función de ajuste para la concentración objetivo  $(k_f)$  del contaminante en el agua.

$$k_f = -0.20 * t + 20; \text{ si y solo si } (m = 1) \wedge (0 \leq t < 15) \tag{1}$$

$$k_f = 32.42 * t^{-0.2357}; \text{ si y solo si } (m = 1) \wedge (t \geq 15) \tag{2}$$

$$k_f = -1.1333 * t + 20; \text{ si y solo si } (m = 2) \wedge (0 \leq t < 15) \tag{3}$$

$$k_f = 2.0; \text{ si y solo si } (m = 2) \wedge (t \geq 15) \tag{4}$$

$$k_f = -1.2 * t + 20; \text{ si y solo si } (m = 3) \wedge (0 \leq t < 15) \tag{5}$$

$$k_f = 3.0; \text{ si y solo si } (m = 3) \wedge (t \geq 15) \tag{6}$$

6

De igual forma, se tiene una función para calcular el ‘costo del sistema’ ( $c$ ) representado de la siguiente manera.

$$c = (X * Y) + Z \quad (7)$$

donde  $X$  es el costo de la energía tomada de la página oficial de la de dependencia del gobierno federal llamada Comisión Federal de Electricidad la cual es una empresa del estado mexicano responsable de fijar el precio de la electricidad.  $Y$  son las horas necesarias para terminar el ciclo de tratamiento del agua contaminada.  $Z$  es el costo de adquisición del catalizador. Para esta investigación, se consideran los siguientes datos constantes: (1) El reactor químico consume 385 W/h. (2) El costo de la energía eléctrica de 0.956 pesos/kWh. (3) 1kg de catalizador cuesta \$2000 pesos mexicanos.

#### 2.4 Operaciones del algoritmo genético

A continuación, se definen los operadores genéticos de “reproducción”, “cruzamiento”, y “mutación” con la finalidad de producir la siguiente generación de cromosomas.

##### Operador reproducción.

Este operador genera nuevos pares  $(m, t)$  de manera aleatoria, esto es, se generan nuevas soluciones posibles al problema modelado. Se busca la aleatoriedad de los nuevos cromosomas para evitar que el algoritmo genético se quede estacionado en una solución local a la problemática en lugar de una solución global.

##### Operador cruzamiento.

Este operador genera un nuevo elemento de la población a partir de las características de cada uno de los padres. Por ejemplo, teniendo un padre  $(3, 37)$  representado en forma binaria por  $(11, 00100101)$  generando la cadena  $C_1 = "1100100101"$  y un padre  $(2, 56)$  representado en binario por  $(10, 00111000)$  generando la cadena  $C_2 = "1000111000"$ . Para los siguientes ejemplos se cuentan los bits de derecha a izquierda.

Una vez generadas las cadenas se selecciona un bit para hacer el cruzamiento, para este ejemplo, el cruzamiento se lleva a cabo en el bit 4 por lo que las cadenas de 10 bits se separan en dos cadenas: una de 6 bits y otra de 4 bits. Con lo anterior, se genera lo siguiente: para la cadena  $C_1 = "1100100101"$  se generan las cadenas  $C_{1A} = "110010"$  y  $C_{1B} = "0101"$ . Para la cadena  $C_2 = "1000111000"$  se generan las cadenas:  $C_{2A} = "100011"$  y  $C_{2B} = "1000"$ . Una vez divididas las cadenas  $C_1$  y  $C_2$  se procede a hacer el cruzamiento de las soluciones juntado la cadena  $C_{1A}$  con la cadena  $C_{2B}$  y la cadena  $C_{2A}$  con la cadena  $C_{1B}$ . Con lo anterior, se tendrían las nuevas cadenas  $C_3 = "1100101000"$  y  $C_4 = "1000110101"$ . Una vez generadas las cadenas se representan en forma de par ordenado de la siguiente manera:  $C_3 = (11, 00101000)$  y  $C_4 = (10, 00110101)$ . Traducidos a su forma decimal se tienen los siguientes pares ordenados  $C_3 = (3, 40)$  y  $C_4 = (2, 53)$ .

**Operador mutación.**

Con este operador es posible generar una solución nueva a partir de una solución existente cambiando solamente un bit de la cadena que representa a la solución. Por ejemplo, tomando la cadena  $C_3 = "1100101000"$  y mutando la cadena en la posición 7 es posible tener la siguiente cadena "1101101000" que representa al par ordenado (11, 01101000) en decimal se tiene el par ordenado (3, 104).

A continuación, se presenta el diseño general del pseudo-código que implementa un algoritmo genético.

**Generar población inicial con soluciones aleatorias.****hacer**

**Calcular** valores de la función objetivo.

**Seleccionar** dos soluciones para reproducirlos y generar la siguiente población.

**Cruzar** las soluciones seleccionadas para generar nuevas soluciones.

**Hacer** mutaciones aleatorias a las nuevas soluciones.

**Elegir** una nueva población de las soluciones principales o de la población inicial y las nuevas soluciones en función de los valores de aptitud (cercanía al cumplimiento de los objetivos).

**Mientras** no se cumpla el criterio de detención (Número de iteraciones u otro).

**3 Implementación del algoritmo**

La implementación del algoritmo se realizó en el Lenguaje R usando la interfaz RStudio. Al algoritmo se le incluyó la librería "mco" el cual contiene una colección de funciones para resolver problemas de optimización con múltiples criterios. En esta librería se encuentra una función llamada 'nsga2'. Esta librería minimiza las funciones objetivo para aproximar las probables soluciones a la una que logre un mejor balance de los objetivos. A continuación, se describen los parámetros utilizados durante la implementación del algoritmo.

```
nsga2(fn, idim=3, odim=10,
      constraints = NULL, cdim = 0,
      lower.bounds = (0,0,0,0,0,0,0,0,0,0),
      upper.bounds = (1,1,1,1,1,1,1,1,1,1),
      popsize = 20, generations = 1000,
      cprob = 0.8, cdist = 3,
      mprob = 0.9, mdist = 9,
      vectorized=FALSE)
```

8

donde los parámetros tienen la siguiente interpretación.

<code>fn</code>	función de ajuste para la evaluación de los objetivos.
<code>idim</code>	dimensión de entrada
<code>odim</code>	dimensión de salida
<code>constrains</code>	función que aplica restricciones al cálculo de la evaluación <code>fn</code> .
<code>cdim</code>	dimensión de la función de restricciones
<code>lower.bowns</code>	parámetros de límite inferior. El vector es de longitud 10.
<code>upper.bowns</code>	parámetros de límite superior. El vector es de longitud 10.
<code>popsize</code>	tamaño de la población
<code>generations</code>	número de generaciones
<code>cprob</code>	probabilidad de cruzamiento
<code>cdist</code>	índice de distribución de cruzamiento
<code>mprob</code>	probabilidad de mutación
<code>mdist</code>	índice de distribución de mutación

#### 4 Análisis de resultados

En esta sección, se presentan los resultados obtenidos en la ejecución del algoritmo genético. Para esta investigación se tomaron los siguientes objetivos:

- Análisis de concentración-costo:  $\text{Min}(k_f), \text{Min}(c)$
- Análisis de concentración-tiempo:  $\text{Min}(k_f), \text{Min}(t)$
- Análisis de concentración-tiempo-costo:  $\text{Min}(k_f), \text{Min}(t), \text{Min}(c)$

##### 4.1 Análisis de concentración-costo

La idea detrás del análisis de los objetivos:  $\text{Min}(k_f), \text{Min}(c)$  está en tratar agua cuya concentración de acetaminofén se encuentre en el rango de  $5 \leq k_f \leq 15$  ppm mientras que los costos de producción del agua se encuentren en el rango de  $\$0.00 \leq c \leq \$175.00$ . Los resultados obtenidos por el algoritmo se muestran en la Tabla 1 para el tratamiento de 200 litros de agua mientras que los resultados para el tratamiento de 300 litros de agua se muestran en la Tabla 2. La presentación visual de las soluciones sugeridas para 200 y 300 litros se muestra en la Fig. 2 y Fig. 3 respectivamente. Para el caso del tratamiento de 200 litros de agua se tienen cinco combinaciones  $(m, t)$  que minimizan ambos objetivos mientras que para el tratamiento de 300 litros de agua se tienen seis combinaciones posibles.

**Tabla 1.** Tratamiento de 200 litros de agua considerando  $\text{Min}(k_f), \text{Min}(c)$ .

$m$ (g)	$t$ (min)	$k_f$ (ppm)	$c$ (\$)
0.5	1300	5.27	120.71
0.5	1100	7.54	117.53
0.5	800	10.94	112.75
0.5	600	13.20	109.56
0.5	500	14.34	107.97

**Table 2.** Tratamiento de 300 litros de agua considerando  $\text{Min}(k_f)$ ,  $\text{Min}(c)$ .

$m$ (g)	$t$ (min)	$k_f$ (ppm)	$c$ (\$)
0.5	1500	8.67	173.90
0.5	1350	9.80	171.51
0.5	1200	10.93	169.12
0.5	1050	12.07	166.73
0.5	900	13.20	164.34
0.5	750	14.33	161.95

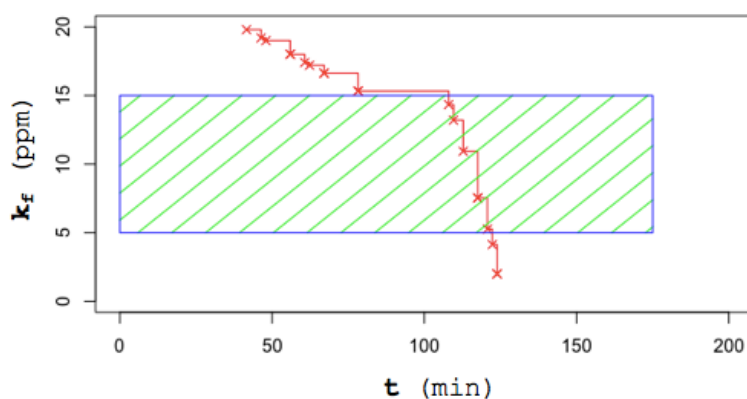


**Fig. 2.** Frente de Pareto obtenido por el algoritmo durante el tratamiento de 200 litros de agua con los objetivos simultáneos  $\text{Min}(k_f)$ ,  $\text{Min}(c)$ .

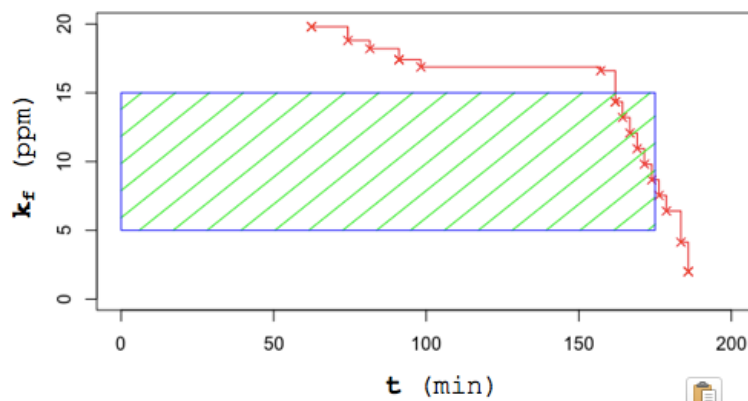


**Fig. 3.** Frente de Pareto obtenido por el algoritmo durante el tratamiento de 300 litros de agua con los objetivos simultáneos  $\text{Min}(k_f)$ ,  $\text{Min}(c)$ .

10

En la Fig. 2 y la Fig. 3 se puede observar que todos los valores encontrados por el algoritmo en el tratamiento de 200 litros y 300 litros de agua consideran el uso de 0.5 gramos de TiO<sub>2</sub> Degussa P25. Este comportamiento resulta interesante puesto que para  $m = 0.2$  gramos no se logra alcanzar un rango de valores ( $k_f$ ) para el rango de tiempo medido por el algoritmo. Esto mismo sucede cuando  $m = 1.0$  gramos, el algoritmo no logra alcanzar un valor aceptable de ( $c$ ). Este comportamiento nos alerta a considerar el tiempo del tratamiento junto con el costo del tratamiento del agua (Ver Tabla 3 y Tabla 4).

**Tabla 3.** Rangos de valores encontrados por el algoritmo genético durante el tratamiento de 200 litros de agua con 0.2, 0.5 y 1.0 g de TiO<sub>2</sub> Degussa P25 como catalizador y considerando los objetivos  $\text{Min}(k_f)$ ,  $\text{Min}(c)$ .

$m$ (g)	$t$ (min)	$k_f$ (ppm)	$c$ (\$)
0.2	$100 \leq t \leq 2400$	$15.33 \leq k_f \leq 19.8^{(*)}$	$41.59 \leq c \leq 78.24$
0.5	$100 \leq t \leq 1500$	$2 \leq k_f \leq 18.87$	$101.59 \leq c \leq 123.9$
1.0	$100 \leq t \leq 1500$	$3 \leq k_f \leq 18.8$	$201.59 \leq c \leq 233.9^{(**)}$

(\*) Valores fuera de rango  $5 \leq k_f \leq 15$

(\*\*) Valores fuera de rango  $0 \leq c \leq 175$

**Tabla 4.** Rangos de valores encontrados por el algoritmo genético durante el tratamiento de 300 litros de agua con 0.2, 0.5 y 1.0 g de TiO<sub>2</sub> Degussa P25 como catalizador y considerando los objetivos  $\text{Min}(k_f)$ ,  $\text{Min}(c)$ .

$m$ (g)	$t$ (min)	$k_f$ (ppm)	$c$ (\$)
0.2	$150 \leq t \leq 2400$	$16.87 \leq k_f \leq 19.8^{(*)}$	$62.39 \leq c \leq 98.24$
0.5	$150 \leq t \leq 2400$	$2 \leq k_f \leq 18.87$	$152.39 \leq c \leq 188.24$
1.0	$150 \leq t \leq 2400$	$3 \leq k_f \leq 18.8$	$302.39 \leq c \leq 338.24^{(**)}$

(\*) Valores fuera de rango  $5 \leq k_f \leq 15$

(\*\*) Valores fuera de rango  $0 \leq c \leq 175$

## 4.2 Análisis de concentración-tiempo

Un punto de interés en el análisis de la degradación del contaminante es revisar el tiempo requerido para alcanzar un nivel de concentración. Para hacer este análisis, se establecen los objetivos:  $\text{Min}(k_f)$ ,  $\text{Min}(t)$ . Esto significa que se busca minimizar de manera simultánea la concentración del contaminante y el tiempo requerido para alcanzar dicha concentración (Ver Tabla 5 y Tabla 6). En la Fig.4 y Fig. 5 se muestran los resultados obtenidos de ejecutar el algoritmo para tratar 200 y 300 litros. El algoritmo muestra ocho combinaciones ( $m, t$ ) posibles en el caso del tratamiento de 200 litros mientras que para el tratamiento de 300 litros solo obtiene cuatro combinaciones. Como es de esperar, el algoritmo recomienda usar 1.0 gramos de TiO<sub>2</sub> Degussa P25 puesto que es la concentración que más rápidamente reduce la concentración del acetaminofén.

**Tabla 5.** Tratamiento de 200 litros de agua considerando  $\text{Min}(k_f)$ ,  $\text{Min}(t)$ .

$m$ (g)	$t$ (min)	$k_f$ (ppm)	$c$ (\$)
1.0	1200	5.6	219.12
1.0	1100	6.8	217.53
1.0	1000	8	215.93
1.0	900	9.2	214.34
1.0	800	10.4	212.75
1.0	700	11.6	211.15
1.0	600	12.8	209.56
1.0	500	14	207.97

**Tabla 6.** Tratamiento de 300 litros de agua considerando  $\text{Min}(k_f)$ ,  $\text{Min}(t)$ .

$m$ (g)	$t$ (min)	$k_f$ (ppm)	$c$ (\$)
1.0	1350	9.2	321.51
1.0	1050	11.6	316.73
1.0	900	12.8	314.34
1.0	750	14	311.95

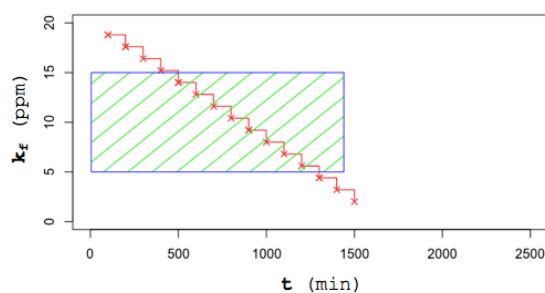


**Fig. 4.** Fronte de Pareto obtenido por el algoritmo durante el tratamiento de 200 litros de agua con los objetivos simultáneos  $\text{Min}(k_f)$ ,  $\text{Min}(t)$ .

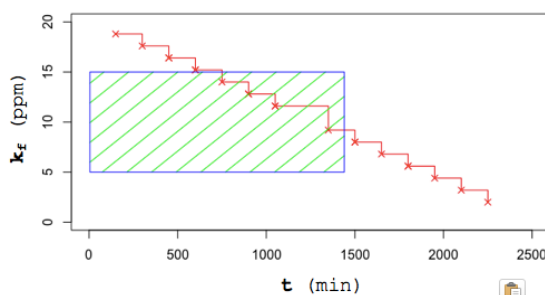


**Fig. 5.** Fronte de Pareto obtenido por el algoritmo durante el tratamiento de 300 litros de agua con los objetivos simultáneos  $\text{Min}(k_f)$ ,  $\text{Min}(t)$ .

Sin embargo, como se puede observar en la Tabla 7 y Tabla 8, los valores de concentración y costo están fuera del rango definido ( $5 \leq k_f \leq 15$ ,  $0 \leq c \leq 175$ ) cuando se aplican 0.2 y 1.0 gramos de TiO<sub>2</sub> Degussa P25. Para este caso, el algoritmo no pudo considerar las restricciones de costo por lo que encontró combinaciones ( $m, t$ ) que no serían recomendadas. Por esta razón, no es posible considerar combinaciones con análisis de dos objetivos y en la siguiente sección se presenta un análisis para minimizar las tres variables.

**Tabla 7.** Rangos de valores encontrados por el algoritmo genético durante el tratamiento de 200 litros de agua con 0.2, 0.5 y 1.0 gramos de TiO<sub>2</sub> Degussa P25 como catalizador.

$m$ (g)	$t$ (min)	$k_f$ (ppm)	$c$ (\$)
0.2	$100 \leq t \leq 2400$	$15.33 \leq k_f \leq 19.8^{(*)}$	$41.59 \leq c \leq 78.24$
0.5	$100 \leq t \leq 2400$	$2 \leq k_f \leq 18.87$	$101.59 \leq c \leq 138.24$
1.0	$100 \leq t \leq 2400$	$3 \leq k_f \leq 18.8$	$201.59 \leq c \leq 238.24^{(**)}$

(\*) Valores fuera de rango  $5 \leq k_f \leq 15$

(\*\*) Valores fuera de rango  $0 \leq c \leq 175$

**Tabla 8.** Rangos de valores encontrados por el algoritmo genético durante el tratamiento de 300 litros de agua 0.2, 0.5 y 1.0 gramos de TiO<sub>2</sub> Degussa P25 como catalizador.

$m$ (g)	$t$ (min)	$k_f$ (ppm)	$c$ (\$)
0.2	$150 \leq t \leq 2400$	$16.87 \leq k_f \leq 19.8^{(*)}$	$62.39 \leq c \leq 98.24$
0.5	$150 \leq t \leq 2400$	$2 \leq k_f \leq 18.87$	$152.39 \leq c \leq 188.24$
1.0	$90 \leq t \leq 150$	$12.8 \leq k_f \leq 18.8$	$302.39 \leq c \leq 314.34^{(**)}$

(\*) Valores fuera de rango  $5 \leq k_f \leq 15$

(\*\*) Valores fuera de rango  $0 \leq c \leq 175$

### 4.3 Análisis de concentración-tiempo-costo

En esta sección, se presentan los resultados del algoritmo para encontrar combinaciones ( $m, t$ ) para cumplir los objetivos  $\text{Min}(k_f)$ ,  $\text{Min}(t)$ ,  $\text{Min}(c)$  simultáneamente. Los resultados se muestran en la Tabla 9 y Tabla 10. Los resultados presentados permiten tomar mejores decisiones dependiendo de la prioridad del tratamiento del agua. Por ejemplo, en caso de requerir tratar 200 litros de agua en menos de 1000 minutos se puede garantizar una concentración de 8.0 ppm del contaminante con un costo de \$215.93 pesos mexicanos. Sin embargo, si se requiere de tratar agua en menos de 1440 minutos se puede obtener 200 litros con concentración de 3.20 ppm o 300 litros con concentración de 9.20 ppm.

**Tabla 9.** Valores obtenidos del algoritmo considerando 3 objetivos simultáneos  $\text{Min}(k_f)$ ,  $\text{Min}(t)$ ,  $\text{Min}(c)$  en el tratamiento de 200 litros de agua contaminada con acetaminofén.

$m$ (g)	$t$ (min)	$k_f$ (ppm)	$c$ (\$)
1.0	1400	3.20	222.31
0.5	1400	4.13	122.31
1.0	1300	4.40	220.71
1.0	1200	5.60	219.12
0.5	1200	6.40	119.12
1.0	1100	6.80	217.53
1.0	1000	8.00	215.93
1.0	900	9.20	214.34
0.5	800	10.93	112.75
1.0	700	11.60	211.15

**Tabla 10.** Valores obtenidos del algoritmo considerando 3 objetivos simultáneos  $\text{Min}(k_f)$ ,  $\text{Min}(t)$ ,  $\text{Min}(c)$  en el tratamiento de 300 litros de agua contaminada con acetaminofén.

$m$ (g)	$t$ (min)	$k_f$ (ppm)	$c$ (\$)
1.0	1350	9.20	321.51
0.5	1350	9.80	171.51
1.0	1200	10.40	319.12
0.5	1200	10.93	169.12
1.0	1050	11.60	316.73
0.5	1050	12.07	166.73
1.0	900	12.80	314.34
0.5	900	13.20	164.34
1.0	750	14.00	311.95
0.5	750	14.33	161.95

## 5 Conclusiones

En este trabajo de investigación se presenta un algoritmo genético para equilibrar, de manera simultánea, varios objetivos dentro de un sistema de purificación de agua contaminada con acetaminofén. El algoritmo encuentra un conjunto de combinaciones de cantidad de catalizador y tiempo de reacción química de los componentes necesarios para el tratamiento de 200 o 300 litros de agua. Este algoritmo minimiza la concentración del contaminante, el costo del tratamiento del agua y el tiempo requerido para producir la cantidad de agua deseada. Este algoritmo permite producir agua con presencia de acetaminofén en las porciones mínimas recomendadas asegurando la calidad del producto y reducir la afectación a personas sensibles al fármaco.

El algoritmo obtuvo los siguientes resultados tomando en consideración como: concentraciones entre 5-15 ppm, tiempo de reacción química entre 0-1440 minutos y costos por tratamiento del agua entre \$0.00-\$175.00 pesos mexicanos.

Considerando minimizar la concentración del contaminante y el costo del tratamiento se obtuvieron cinco soluciones para demandas de 200 litros por día y seis soluciones de

14

300 litros por día. Minimizando la concentración del contaminante y el tiempo de la reacción química se obtuvieron ocho y cuatro soluciones para demandas de 200 y 300 litros por día, respectivamente. Finalmente, considerando tres objetivos: mínima concentración del contaminante, mínimo costo, mínimo tiempo de reacción química se tuvieron 3 y 5 posibles soluciones para demandas de consumo de 200 y 300 litros por día. Aunque los resultados encontrados en esta investigación resultan prometedores, es necesario mayor experimentación para aumentar las curvas de degradación y aumentar el espacio de soluciones que al momento se reduce a tres curvas de degradación de las moléculas del acetaminofén. Además, se requiere experimentar con la interacción entre los catalizadores para el tratamiento de múltiples contaminantes y su afectación combinada a las personas sensibles a los contaminantes.

## 6 Referencias

1. Álvarez-Ruiz, R., Picó, Y: Analysis of emerging and related pollutants en Aquatic Biota. Trends in Environmental Analytical Chemistry 25, (2020).
2. Barceló, D., López, M.J.: Contaminación y calidad química del agua: el problema de los contaminantes emergentes. En Panel Científico-Técnico de seguimiento de la política de aguas, pp. 1-24, Sevilla, España (2007).
3. Beltrán, F. J.: Ozone Reaction Kinetics for Water and Wastewater Systems. 1st edn. Lewis Publishers, (2003).
4. Coello, C.C., Lamount, G.B., Veldhuizen, D.A.: Evolutionary Algorithms for Solving Multi-Objective Problems. 2nd edn. Springer US, (2007).
5. De Luna-Escamilla, J.M., Hernández-Soto, J.C.: Sistema computacional para facilitar la documentación de experimentos fotocatalíticos realizados en un reactor químico de flujo-continuo. Facultad de Ingeniería en Electrónica y Comunicaciones, (2021).
6. Giraldo-Garcés, L.F., Mejía-Franco, E.A., Santamaría-Arango, J.J.: La fotocatalisis como alternativa para el tratamiento de aguas residuales. En Revista Lasallista de Investigación 1(1), pp. 83-92 (2004).
7. Hitachi Ltd. Sistema para el Tratamiento del Agua. En Registro de Patente IMPI, <https://vidoc.impi.gob.mx/visor?usr=SIGA&texp=SI&tdoc=E&id=MX/a/2010/001965>. Último acceso: 2021/11/27.
8. Klemola, Martti.: Método para purificar agua. En Registro de Patente IMPI, Registro de patente disponible en: <https://vidoc.impi.gob.mx/visor?usr=SIGA&texp=SI&tdoc=E&id=MX/a/2019/008405>. Último acceso: 2021/11/27.  
Meano, B.: Sistema y método para purificar agua de una masa de agua. Registro de Patente. In ViDoc Mexican System, Disponible en: <https://vidoc.impi.gob.mx/visor?usr=SIGA&texp=SI&tdoc=E&id=MX/a/2017/009097>. Último acceso: 2021/11/27.
9. Monge, S.B., Silva, A.M.T., Bengoa, C.: Manual técnico sobre procesos de oxidación avanzada aplicados al tratamiento de aguas residuales industriales. Programa Iberoamericano de Ciencia y Tecnología para el Desarrollo, España (2018).
10. Nesmachnow, S., Rossit, D., Toutouh, J.: Comparison of Multiobjective Evolutionary Algorithms for Prioritized Urban Waste Collection in Montevideo, Uruguay. Electronic Notes in Discrete Mathematics 69, pp. 93-100 (2018).
11. Patiño, K.V., Arroyava, S.M., Marín, J.M.: Oxidación Electroquímica y Ozonización Aplicadas al Tratamiento de Aguas de Lavado de la Producción de Biodiesel. Información Tecnológica 23(2), pp. 41-52 (2012).

12. Peña-Morales, D., Ruiz, P., Tchernykh, A., Dorronsoro, B.: Multi-Objective Optimization Model for Sustainable Urban Transportation Ensuring the Quality of Service. En International Conference in Optimization and Learning, Catania, Sicilia, Italy (2021).
13. Ramírez-Vargas, A.: Sistema de purificación de agua y unidad de destilación. Registro de Patente. In ViDocMexican System, Disponible en: <https://vidoc.impi.gob.mx/visor?usr=SIGA&texp=SI&tdoc=E&id=MX/a/2019/009140>
14. Rakness, K.L., Corsaro, K.M., Hale, G., Blanck, B.D.: Wastewater Disinfection with Ozone: Process Control and Operating Results. *Ozone: Science and Engineering* 15(6), pp.497-514 (1993).
15. Rakness, K.L., Renner, R.C., Vornehm, D.B., Thaxton, J.R.: Start-Up and Operation of the Indianapolis Ozone Disinfection Wastewater Systems. *Ozone: Science and Engineering* 10(3), pp. 125-240 (1988).
16. Robledo, Z.V., Velázquez, M.M., Montañez, S.j., Pimentel, E.J., Vallejo, C.A., López, C.M., Venegas, G.J.: Hidroquímica y contaminantes emergentes en aguas residuales urbano-industriales de Morelia, Michoacán, México. *Revista Internacional de Contaminación Ambiental* 33(2), pp. 221-235 (2017).
17. Sanabria-Pérez, F.J., Alanís-Méndez, J.L., Pech-Canché, J.M. Solís-Maldonado, C.: Principales residuos de medicamentos generados en los hogares y su potencial ecotóxico en Tuxpan, Veracruz. *Acta Universitaria* vol. 29, pp. 1-12 (2019).
18. Schrank, S.G. José, H.J., Moreira, R.F.P.M, Schröder, H.Fr.: Applicability of Fenton and H<sub>2</sub> O<sub>2</sub>/UV Reactions in the Treatment of Tannery Wastewaters. *Chemosph* vol. 60, pp. 644-655 (2005).
19. Sítou, D., Mazet, N., Mauran, S.: Sistema y metodo de purificacion de liquidos mediante osmosis inversa. En Registro de Patente IMPI, <https://vidoc.impi.gob.mx/visor?usr=SIGA&texp=SI&tdoc=E&id=MX/a/2019/005985>. Último acceso 2021/11/27
20. Tadeo, J.L., Sánchez, C., Albero, B., García A.I., Pérez R.A.: Analysis of emerging organic contaminants in environmental solid samples. *Central European Journal of Chemistry* 10 (3), pp. 480-520 (2012).
21. Tchernykh, A., Lozano, L., Schwiegelshohn, U., Bouvry, P., Pecero, J.E., Nesmachnow, S., Drozdov, A.Y.: Online Bi-Objective Scheduling for IaaS Clouds Ensuring Quality of Service. *Journal of Grid Computing*. Springer-Verlag 14(1), pp. 5-22 (2016).
22. Torres-Andrade, G.F.: Tratamiento de aguas residuales mediante la combinación de técnicas avanzadas de oxidación y biofiltros. Universidad de las Palmas de Gran Canaria (2014).
23. Tsai, M.J., Chang, C.T.: Water Usage and Treatment Network Design Using Genetic Algorithms. *Industrial & Engineering Chemistry Research* 40(22), pp. 4874-4888 (2001).
24. Uribe-García, J.A. Diseño y construcción de un reactor fotocatalíticotipo pfr para el tratamiento de microcontaminantes emergentes en el agua. Facultad de Ciencias Químicas, Universidad Veracruzana (2018).
25. Vargas-Borrones, K., Bernal-Jácome, L., Díaz-De León, L., Flores-Ramírez, R. Emerging pollutants (EPs) in Latin América: A critical review of under-studied EPs, case of study – Nonylphenol. *Science of The Total Environment* vol. 726, (2020).

# Energy-aware smart home planning: a real case study in Montevideo, Uruguay

Diego G. Rossit<sup>1,2</sup> and Sergio Nesmachnow<sup>3</sup>

<sup>1</sup> Department of Engineering, Universidad Nacional del Sur, Argentina

<sup>2</sup> INMABB UNS-CONICET, Argentina

<sup>3</sup> Universidad de la República, Uruguay

**Abstract.** This article presents an approach for energy-aware smart home planning via direct control and planning of residential electric appliances for smart cities. Energy-aware planning is a crucial concept for achieving a better utilization of resources and improving the quality of life in modern cities. In this line of work, this article proposes a stochastic optimization approach to plan the utilization of domestic appliances considering stochastic user preferences. A specific case study is addressed, considering residential households in Montevideo, Uruguay. The case study is modeled using built using real data from existing appliances and a data analysis approach for modeling user preferences. The proposed approach is able to compute accurate plannings in the experimental evaluation performed. The developed approach contributes to energy efficiency and sustainability in modern smart cities.

**Keywords:** energy efficiency, smart planning, smart cities

## 1 Introduction

Energy utilization has largely increased in modern cities, and it is expected to continue growing for years to come [9]. For instance, in 2019, the residential sector accounted for more than 27% of the total energy consumption in the European Union [4] and more than 21% in the USA [27]. The share of energy consumption was even larger for households in 2020, due to the COVID-19 pandemic. Thus, energy-aware planning is a crucial concept for achieving a better utilization of resources and improving the quality of life in modern smart cities.

An effective planning of residential energy consumption certainly contributes towards sustainability and the highly demanding environmental standards required by sustainable development approaches, to reduce both the incurred monetary costs and the carbon footprint of electric grid systems [7]. A crucial feature of smart residential energy planning is the ability of re-shaping the energy demand by users to provide cost-effective and rational energy consumption. In this regard, demand response strategies are one of the most important components of the modern smart grid paradigm for electric systems [15]. These mechanisms are highly regarded as valuable strategies in the transition process of energy utilization towards a decarbonized economy, highlighting the importance of users as relevant agents in the energy market.

2 D. Rossit, S. Nesmachnow

Effective energy management strategies must be complemented with easy-to-understand and easy-to-use computer-assisted applications, to properly involve citizens and organizations, and encourage them to be part of the improved energy utilization model. On the one hand, electricity companies should be able to implement effective demand response actions, properly evaluated in advance to reduce the negative impacts on users comfort [22]. On the other hand, citizens should have available useful applications for monitoring, managing, and evaluating the energy consumption at household level [16]. Smart computer-aid tools that help to take better decisions in energy planning are an important component of the smart electric grid, facilitating citizen engagement towards environment preservation and a better use of the energy resources in smart cities [20].

In this line of work, this article presents an energy-aware smart home planning strategy to determine proper schedules for the use of deferrable electrical appliances, i.e., those appliances that can be controlled by the user and deferred to be switched on in different time-slots on the scheduling horizon without a critical result in the comfort of users, in residential buildings. The planning strategy, which is based on a stochastic optimization model, simultaneously considers the cost of the electricity bill and the Quality of Service (QoS) offered to the users and is specially tailored for addressing this problem in the Uruguayan households. For this aim, the novel dataset ECD-UY [1] about the consumption of different households in Uruguay is used for retrieving information related to Uruguayans electric consumption patterns. The stochastic optimization model considers uncertainty on the users preferences by performing simulations of many probable scenarios based on historical data of the households and the computational experimentation is performed over scenarios of both individual households and community buildings. The obtained results demonstrate that the proposed planning strategy is able to compute accurate schedules, accounting for different trade-offs between the cost of the electricity bill and the Quality of Service (QoS) offered to the users. This way, the proposed approach is able to provide users different suggestions for planning the utilization of domestic appliances.

Thus, the main contributions of the research reported in this article are a planning strategy for scheduling deferrable appliances considering the electricity cost and the QoS provided to users which comprehends a mixed-integer programming formulation and a stochastic resolution algorithm and a computational experimentation based on case studies built using real data from residential electricity consumption for several appliances in the city of Montevideo, Uruguay.

The article is organized as follows. Next section introduces the energy-aware planning problem considered in the article, its mathematical formulation and a review of relevant related works. The proposed optimization model for the planning strategy is described in Section 3. The computational experimentation of the proposed approach performed over case studies in Montevideo, Uruguay, is reported in Section 5. Finally, Section 6 presents the conclusions and the main lines for future work.

## 2 Problem description and related work

This section presents an overview of the household energy planning problem that is addressed in this work and reviews the most relevant related works.

### 2.1 Problem description

The household energy planning problem addressed in this article is modeled considering the following elements:

Sets:

- a set of users  $U = (u_1 \dots u_{|U|})$ , each user represents a household;
- a set of time slots  $T = (t_1 \dots t_{|T|})$  in the planning period;
- sets of domestic appliances  $L^u = (l_1^u \dots l_{|L^u|}^u)$  for each user  $u$ ;

Parameters:

- a parameter  $D_l^u$  that indicates the average time of utilization for user  $u$  of appliance  $l \in L^u$ ;
- a parameter  $C_t$  that indicates the cost of the power in time slot  $t$  in the ToU pricing system;
- a parameter  $P_l^u$  that indicates the power consumed by appliance  $l$ ;
- a parameter  $n_l^u$  that indicates the number of times per day that each appliance is used by each user;
- a binary parameter  $UP_{tt}^u$  that is 1 if user  $u$  prefers to use the appliance  $l \in L^u$  at time slot  $t$ , 0 in other case;
- a parameter  $E^u$  that indicates the maximum power contracted by user  $u$ ;
- a parameter  $E^{joint}$  that indicates the maximum power that the (whole) set of users  $U$  are allowed to consume, which is used in building-like instances;
- a penalty cost  $\rho$  applied when surpass the maximum (electric) power contracted in building-like instances;

Variables:

- a binary variable  $x_{tt}^u$  that is 1 if user  $u$  has appliance  $l \in L^u$  turn on at time slot  $t$  and 0 if the appliance is turn off;
- a binary variable  $\delta_{tt}^u$  that indicates if the appliance  $l \in L^u$  of user  $u$  is turn on from time slot  $t$  up to a period of time that its at least equal to  $D_l^u$ ;
- a binary variable  $\psi_t$  that indicates if users are using more power than the maximum power contracted  $E^{joint}$  in building-like instances.
- a binary variable  $\Psi_t$  that indicates if users are using more power than 130% of the maximum power contracted  $E^{joint}$  in building-like instances.
- a non-negative continuous variable  $e_t$  that measures the excess of power used over the contracted power in building-like instances.

The problem aims at scheduling the usage of household appliances considering the maximization of users satisfaction and the minimization of the total cost of the power consumed, at the same time.

4 D. Rossit, S. Nesmachnow

Two different situations in the electric market of Uruguay are analyzed: i) when users are considered standalone units for the electric system, and ii) when users conform a unique building -and, thus, represent a large consumer for the electric system-. In the case of buildings, the overall power usage by the building can surpass the contracted power but a penalization cost is applied. In the case of standalone users, each user has to strictly respect the individual contracted power. If the power used by the user is larger than the contracted power, the user is disconnected from the supply by the electric protections. This variation affects the corresponding mathematical model. The model for buildings is outlined in Eqs. (1)-(6).

$$\max F = \sum_{u \in U} \sum_{l \in L^u} \sum_{\substack{t_1 \in T \\ t \leq |T| - D_l^u}} \left( \delta_{lt_1}^u \left( \sum_{\substack{t_2 \in T \\ t_1 \leq t_2 < t_1 + D_l^u}} U P_{lt_2}^u \right) \right) \quad (1)$$

$$\min G = \sum_{t \in T} \left( \sum_{u \in U} \sum_{l \in L^u} x_{lt}^u P_l^u C_t + e_t \rho (2\psi_t + 2\Psi_t) \right) \quad (2)$$

subject to

$$\delta_{lt}^u \leq 1 - \frac{D_l^u - \left( \sum_{\substack{t_2 \in T \\ t \leq t_1 < t + D_l^u}} x_{lt_1}^u \right)}{D_l^u}, \quad \forall u \in U, l \in L^u, t \in T \quad (3)$$

$$\sum_{t \in T} \delta_{lt}^u = n_l^u, \quad \forall u \in U, l \in L^u \quad (4)$$

$$\psi_t \geq \frac{\sum_{\substack{u \in U \\ l \in L^u}} P_l^u x_{lt}^u - E^{joint}}{\sum_{\substack{u \in U \\ l \in L^u}} P_l^u}, \quad \forall t \in T \quad (5)$$

$$\Psi_t \geq \frac{\sum_{\substack{u \in U \\ l \in L^u}} P_l^u x_{lt}^u - 1.3E^{joint}}{\sum_{\substack{u \in U \\ l \in L^u}} P_l^u}, \quad \forall t \in T \quad (6)$$

$$e_t \geq \sum_{\substack{u \in U \\ l \in L^u}} P_l^u x_{lt}^u - E_{joint}, \quad \forall t \in T \quad (7)$$

$$e \geq 0; \psi, \Psi, \delta, x \in \mathbb{B}$$

Regarding the objective functions of the problem, Eq. (1) maximizes the users satisfaction according to the time in which each appliance is used and their preferences. In turn, Eq. (2) aims at minimizing the energy expense budget, which include the charge for power consumption and the penalization for exceeding the maximum power contracted.

Several constraints are specified in the proposed model. Eq. (3) enforces  $\delta_{lt}^u$  to be one when the length of time an appliance will be on is equal or larger than the required by the user. Eq. (4) enforces that each appliance is turn on the number of times per day required by the user. Eq. (5) enforces  $\psi_t$  to be one if the users exceed the maximum power contracted. Eq. (6) enforces  $\Psi_t$  to be one if the users exceed the maximum power contracted for more than 30%. Eq. (7) measures the excess power used at each time interval.

The mathematical model for a set of standalone users replaces Eqs. (5)–(7) by Eq. (8), which establishes that each user cannot surpass the maximum power contracted.

$$\sum_{l \in L^u} P_l^u x_{lt}^u \leq E^u, \forall u \in U, t \in T \quad (8)$$

## 2.2 An smart home energy planning strategy for the Uruguayan households

The proposed problem model was conceived to capture the reality of the Uruguayan residential electricity market, by including specific constraints to model different aggregations of users and contracted power. In turn, specific details of real scenarios and real electricity tariffs are considered, taking into account the relevance of modeling real scenarios for smart home energy planning. The main motivation lays in the fact that different countries have different characteristics of electricity consumption and users behavior.

In addition, the cost of the electricity for the residential sector has a large dispersion through all countries around the world. According to the statistics provided by the U.S. Energy Information Administration, the average value in the world is 0.137 USD per kWh, but in December 2020 German households were charged 0.37 USD per kWh. In South America, electricity cost values have an average of 0.18 USD per kWh, but Uruguay has the most expensive prices, 0.204 USD per kWh. These different prices generate different user behaviors, according to the economic realities of each household. Cost is one of the major factors that influence energy consumption in households, significantly larger than non-financial benefits offered to users [23].

Furthermore, the type of tariffs also influences on the users behavior. Historically, almost all residential users have been subject to fixed (i.e., time-invariant) electricity prices, e.g., 95% in the US [27]. But the emergence of the modern smart grid paradigm has provided users a different alternative for managing electric devices, and more households have chosen to participate in time-varying pricing programs. The behavior of these users is changing for adapting to the new tariffs. All these matters must be taken into account when studying smart home planning strategies, which also must fulfill the regulations of each country.

Finally, the type of domestic appliances must match those most used in the country. In Uruguay, heating and air conditioning account for a significant share of electricity consumption (around 40%), following a global trend in developed countries. In Uruguay however, water heater is the appliance with the largest

6 D. Rossit, S. Nesmachnow

electricity consumption overall (almost 45% of the total consumption in households). A specific characteristic of the aforementioned appliances is that they have a seasonal electricity-intensive use, with a larger consumption in winter. Other appliances like fridge, washing machine, electric oven, electronic devices, etc., have a similar year-round electricity consumption.

All the aforementioned considerations have been taken into account in this research to build real scenarios, using real data gathered from Uruguayan homes in a pilot plan developed using smart meters. After processing the collected information, real instances of the problem were defined by properly defining the appliances, electricity prices, contracted power, and computing the user preference function based on statistical analysis of real data. The created scenarios and problem instances are specific contributions of the reported research.

### 2.3 Related work

The household energy planning problem has been addressed in several works of the related literature [14]. Considered a NP-hard optimization problem already in its deterministic version [12], this work focuses on the complex stochastic version of the household energy planning problem [13].

Some other works have addressed stochastic version of this problem, by including uncertainty in different parameters. Chen *et al.* [2] considered uncertainties in the power consumed by the appliances and the renewable solar energy gathered by a photovoltaic array. A three-stages resolution process was proposed: i) a deterministic linear programming optimization model considering mean values for the appliances consumption and maximum solar power generation is solved, ii) they improved the obtained solution with Monte Carlo simulation considering different energy consumption rates of appliances, and iii) an online adjustment system is implemented to adapt the previous (offline) solution to the actual reality. Hemmati and Saboori [6] proposed a particle swarm optimization algorithm to deal with uncertainty of photovoltaic panels in a similar problem. Assuming that the energy generated in the panels has a Gaussian probabilistic distribution, a Monte Carlo simulation was used to evaluate the stochastic function and obtain a sample of the generation values. Our previous work [25] considered a stochastic approach based on Monte Carlo simulation and discrete optimization to maximize the user preferences and minimize the cost of energy in households. Different instances were considered using REDD dataset [11]. Imanloozadeh *et al.* [8] proposed a model for scheduling appliances in a household located in an extreme desert environment while considering uncertainties in usage of deferrable appliances, electric vehicles discharge, illumination system and hot water heating. Different heuristics were applied to solve the problem and the best results were obtained by a grey wolf optimization algorithm. Waseem *et al.* [28] proposed a complex model that includes households appliances scheduling incorporating uncertainty in sudden absence of distributed energy resources and power failures. The problem model aimed at optimizing electricity cost, end-users comfort, and peak to average consumption ratio.

### 3 The proposed optimization approach for the stochastic household energy planning problem

This section describes the proposed resolution approach.

**Stochastic approach.** The Sample Average Approximation (SAA) method is applied to deal with stochastic users preferences. In a stochastic optimization problem, the expected value of the objective function is optimized. For considering stochastic UP, Eq. (1) is replaced by the expected value of the function  $F$  as it is expressed in Eq. (9), in which  $\mathbf{UP}$  is the random vector of the stochastic users preferences and  $\mathbf{\Delta}$  is the vector of decision variables  $\delta$ .

$$e = \mathbb{E}_{\mathbf{P}} [F(\mathbf{\Delta}, \mathbf{UP})]. \quad (9)$$

Optimizing Eq. (9) requires computing all the possible realizations of vector  $\mathbf{UP}$  with its corresponding probability of occurrence. Considering that there are  $|\mathcal{T}|^{\sum_{u \in \mathcal{U}} |L^u|}$  realizations of this vector, simpler approaches have been proposed in the literature, such as the SAA [26] which is applied in this work. In this approach the expected value (Eq. (9)), is approximated with an independently and identically distributed (i.i.d.) random sample. Thus, Eq. (10) is an estimator of the expected value of Eq. (9), in which the set of values  $UP^1, \dots, UP^N$ , is an i.i.d. random sample of  $N$  realizations of the stochastic vector parameter  $\mathbf{UP}$ .

$$\hat{e} = \frac{1}{N} \sum_{j=1}^N F(\mathbf{\Delta}, \mathbf{UP}^j) \quad (10)$$

The optimization problem obtained when Eq. (10) is used instead of Eq. (9), is the sample average approximation optimization problem (hereafter SAA) and can be solved deterministically with commercial solvers. Since the solution of the SAA problem depends on the realizations  $\mathbf{UP}$  that are included in the random sample, the larger the size of the sample ( $N$ ), the smaller is the difference between Eq. (9) and its estimator Eq. (10). Particularly, when  $N \rightarrow \infty$ ,  $\hat{e} \rightarrow e$ . An important feature of this approach is that different samples of size  $N$  (i.e., different set of realizations of the stochastic vector parameter  $\mathbf{UP}$ ) allow shaping different forms of Eq. (10). Therefore, all algorithms based on sample average usually solve the SAA problem several times with different samples and after that select the most promising solution as the final solution. In this case, to select the final solution we use the procedure proposed by Norkin *et al.* [19]. Let  $\hat{s}_N^1, \hat{s}_N^2, \dots, \hat{s}_N^M$  be the solutions (values of decision values) when solving  $M$  SAA optimization problems each one with a different sample of size  $N$ . Then, an independent sample of size  $N'$  with  $N' \gg N$  is built to evaluate the  $M$  solutions using this sample and the solution with the best value problem is selected. This method takes advantage from the fact that although using the large sample size  $N'$  for the optimization phase is very time consuming (specially in NP-hard problems as the one addressed in this paper), using it for just for evaluation of the objective function is achievable in reasonable computing time [10].

8 D. Rossit, S. Nesmachnow

**Biobjective optimization.** A weighted sum is applied to simultaneously optimize the objectives of user satisfaction and electricity cost. This approach has been successfully applied to related household energy planning problems[3].

A joint function is optimized, in which the two objectives are normalized by the ideal and nadir values of the objectives, and weighted by the parameters  $\alpha$  and  $\beta$ , in the unique expression reported in Eq. (11).

$$\max H = \alpha \frac{F - F^{ideal}}{F^{ideal} - F^{nadir}} - \beta \frac{G - G^{ideal}}{G^{nadir} - G^{ideal}} \quad (11)$$

The ideal and nadir values are approximated by single-objective optimization of each objective, i.e., the payoff table. Since the nadir value can be underestimated [24], the ideal and nadir values of the payoff table are used in the weighted sum formula along with a biased combination of weights. Two different problems are solved, using  $\alpha \gg \beta > 0$  and using  $\beta \gg \alpha > 0$ . Finally, the ideal and nadir values are obtained from the solutions of the last two multiobjective problems.

## 4 Real scenarios for smart home planning: case studies in Montevideo, Uruguay

This section describes the methodology for designing real scenarios of the household energy planning problem addressed in this article.

### 4.1 Motivation and overall description

The evaluation of effective smart home planning strategies must be performed on realistic problem scenarios and instances.

Many related works have evaluated previously proposed methods over synthetic or non-realistic problem instances, in which several assumptions were formulated for users behavior, disaggregated energy consumption, or even energy prices and tariff schemes. This practice hinders a proper evaluation of the applicability of the proposed strategies in practice.

The specific methodology applied in this article for the evaluation of smart home planning strategies is directly focused on considering real information from residential users, disaggregated energy consumption, and energy rate/tariff plans, as described in the next subsection.

### 4.2 Data sources

Data for the generated scenarios were gathered in a previous research effort (project ‘Computational intelligence for detecting residential energy consumption patterns’) that built the ECD-UY dataset [1]. The considered data include:

- *Residential users.* The ECD-UY dataset includes information about electricity consumption records of nine different households, recorded during a period of three weeks in 2019 in Montevideo, Uruguay. Five of those households were considered for the evaluation. Relevant information for those households includes the total electricity consumption, the contracted power, and the disaggregated energy consumption (described on the next item).

- *Dissagregated energy consumption.* For each household, real electricity consumption of relevant domestic appliances were considered, including fridge, air conditioner, dehumidifier, electric air heater, electric oven, electric water heater, microwave, tumble dryer, and washing machine. Overall, water heater is the appliance that demands the largest energy consumption in Uruguayan households. The considered set of appliances accounts for more than 80% (in average) of the total electricity consumption in the considered households. Other minor electric devices were not considered in the analysis since they do not contribute significantly to energy consumption.
- *Energy tariffs.* Real energy tariffs and plans from the Uruguayan Electricity Company (UTE) are considered. The company provides two smart plans that are based on Time-of-Use pricing systems to encourage users to displace appliances usage from peak hours to relatively cheaper off-peak hours ([www.ute.com.uy](http://www.ute.com.uy)).

### 4.3 Modeling user preferences

A specific model was proposed based on data analysis for modeling user preferences and defining the stochastic vector parameter **UP**.

Noticeable differences in the electricity consumption of appliances are observed in weekends, mainly because the different lifestyle of users in weekends, which tend to stay at home more hours than in working weekdays [21], and the different ToU tariff that the electricity companies applies. Therefore, instances were divided among weekdays and weekends [18, 17, 25]

Historical information retrieved from the dataset about the power consumption of the selected appliances on each household was analyzed. This task involved cleaning the data from comparatively very small power consumption that are related to stand-by operation mode of each appliance, for example, small screen leds. After this, for each combination of user and appliance, a probability of usage for each time slot was estimated ( $p_{it}^u$ ). With this probability,  $M$  instances were constructed for each sample size  $N$  as is described in Section ??.

The parameter of the power consumption  $P_t^u$  was calculated as the median of all the values of power that were consumed by the appliance. Before calculating the median, a filter to discard outlier values of power consumption that can be due to atypical conditions or malfunctioning was applied. The filter discards the values that were outside of the range  $[median - 8MAD; median + 8MAD]$  where MAD is the median absolute deviation used a robust measure of dispersion. A similar procedure was applied to calculate the duration of time of utilization of each appliance ( $D_t^u$ ) as the median of all the durations and the times per day that each appliance is turn on ( $n_t^u$ ).

## 5 Computational experimentation

This section reports the validation of the proposed optimization approach for smart home electricity planning.

10 D. Rossit, S. Nesmachnow

### 5.1 Validation scenarios

The validation of the proposed approach is based of real data of the city of Montevideo. Five households of the ECD-UY dataset [1] were retrieved. Table 1 reports the electric appliances considered in the five households.

Table 1: Electric appliances considered in each household.

<i>household</i>	<i>appliances</i>
170001	electric air heater, electric oven, electric water heater, fridge, microwave, and washing machine.
170004	electric water heater, fridge, microwave, tumble dryer and washing machine.
170005	electric water heater, fridge, microwave, and washing machine.
170006	air conditioner 1, air conditioner 2, and electric water heater.
170007	electric air heater, and washing machine.

The ToU tariff systems that are used in this work were retrieved from UTE. As aforementioned, the company offers two ToU tariff systems: the Double Hour Residential Rate (hereafter double tariff system) and the Triple Hour Residential Rate (hereafter triple tariff system). The Double Hour Residential Rate tariff considers two categories of hours: the peak hours and the off-peak hours. For better customizing the system, UTE allows that each user selects the peak hours. These hours must be a four-hours consecutive hours between 5pm and 11pm. The Triple Hour Residential Rate considers three categories of hours. These are, from the most expensive to the cheapest, the peak hours, the plain hours and the valley hours. Similarly to the double tariff system, the peak hours can be selected by the user regarding they are four consecutive hours between 5 PM and 11 PM. The valley hours are between midnight and 7am and the rest of the hours are considered valley hours.

The five households were considered in four different scenarios: using the double tariff system, using the triple tariff system, and, finally, using a mix of both systems in a building-like fashion. Thus, considering weekdays and weekends profiles the instances are:

- the five households using double tariff system in weekdays (d.wd) and weekends (d.we).
- the five households using triple tariff system in weekdays (t.wd) and weekends (t.we).
- three households using double tariff system and two homes using triple tariff system in a building-like fashion in weekdays (b.wd) and weekends (b.we).

### 5.2 Methodology

After preliminary calibration experiments, three sample sizes were chosen  $N = 1000$ ,  $10000$ , and  $100000$ . The number of independent samples of each size ( $M$ ) was set to 100. The evaluation sample size ( $N'$ ) was set to  $10000000$ . Five weight vectors  $(\alpha, \beta)$  were used for exploring different trade-off combinations between

the problem objectives: (0.909,0.01), (0.25, 0.75), (0.5, 0.5), (0.75, 0.25), and (0.01, 0.909). The SAA problems were solved with ILOG CPLEX Optimization Studio version 20.1 through Pyomo as modelling language [5].

Experimentation was divided in two parts: computation of random realizations of vector **UP** and optimization considering the generated samples. The separation aims at studying the impact of the random samples of vector **UP** in the overall efficiency of SAA. Then, for each instance and size  $N$ , a set of 100 ( $M$ ) independent realizations of vector **UP** were generated.

### 5.3 Experimental results

Table 2 reports the execution times of the generation of independent samples of the scenario. The execution times indicate that the average time increases

Table 2: Computing times for generating the realizations of vector **UP**.

instance	N	time (s)		instance	N	time (s)	
		avg.	std.			avg.	std.
d.wd	1000	8.0847	0.1381	d.we	1000	8.0678	0.1097
	10000	81.9886	0.0870		10000	82.4326	0.1279
	100000	821.8834	1.1814		100000	821.8033	1.6480

linearly with the sample size  $N$  e.g., as shown for instances with double tariff system. This result is connected to the trade-off between having a large sample size  $N$ , which is computationally expensive but provides a better estimation of the real expected value, or a smaller sample size  $N$ , which is less time-consuming but provides a worse approximation of the real expected value.

Table 3 reports the experimental results of SAA in validation experiments. For each instance, the sample size  $N$ , the combination of weights  $(\alpha, \beta)$ , and five relevant metrics are reported:

- the average and standard deviation of the execution time;
- the average and standard deviation of the users satisfaction function  $F$  evaluated over  $N'$ ;
- the average and standard deviation of the cost function  $G$  evaluated over  $N'$ ;
- the values of  $F$  and  $G$  of the best solution, i.e., the solution that has the minimal value of function  $H$ , as defined in Eq. (11);
- the deviation of the solution to the ideal vector  $\Sigma$ , computed using the  $L^2$  distance norm, according to Eq. (12).

$$\Sigma = \sqrt{\sum_{o \in O} \left( \frac{value - best_o}{best_o} \cdot 100\% \right)^2} \tag{12}$$

Table 3: Results of the SAA.

N	( $\alpha, \beta$ )	time (s)	$F(H_{best}^{N'})$	$G(H_{best}^{N'})$	$\Sigma$	time (s)	$F(H_{best}^{N'})$	$G(H_{best}^{N'})$	$\Sigma$
<i>Double tariff system instances</i>									
		<i>weekday (d.wd)</i>				<i>weekend (d.wd)</i>			
	(0.99,0.01)	0.1131	5.4423	17351.2209	34.63%	0.1069	5.0784	12145.3422	5.67%

1000

12 D. Rossit, S. Nesmachnow

	(0.01,0.99)	11.1970	5.2366	12888.6759	4.46%	10.2117	5.0783	11494.3428	0.19%	
	(0.50,0.50)	0.6365	5.2760	13454.9187	5.77%	0.5805	5.0785	11907.8682	3.60%	
	(0.75,0.25)	0.2705	5.4520	15449.8332	19.88%	0.2702	5.0786	12131.9154	5.55%	
	(0.25,0.75)	2.6556	5.2363	12983.3649	4.52%	2.6105	5.0785	11781.4158	2.51%	
10000	(0.99,0.01)	0.1255	5.4824	16497.0978	28.00%	0.1200	5.0706	11949.2508	3.96%	
	(0.01,0.99)	12.8881	5.2662	12888.6759	3.92%	12.6046	5.0680	11513.7816	0.17%	
	(0.50,0.50)	0.9855	5.4807	14922.8241	15.78%	1.0742	5.0702	11785.3236	2.53%	
	(0.75,0.25)	0.3444	5.4823	15003.9861	16.41%	0.3120	5.0704	11846.0448	3.06%	
	(0.25,0.75)	3.6069	5.3246	13147.1661	3.49%	3.4554	5.0702	11741.1354	2.15%	
100000	(0.99,0.01)	0.1524	5.4824	16695.0423	29.53%	0.1411	5.0705	11824.5018	2.87%	
	(0.01,0.99)	14.0165	5.2663	12888.6759	3.92%	14.4370	5.0710	11494.3428	0.05%	
	(0.50,0.50)	2.7312	5.4812	14882.2431	15.47%	2.6138	5.0710	11682.6186	1.64%	
	(0.75,0.25)	0.5974	5.4824	14963.4051	16.10%	0.6177	5.0713	11922.2970	3.72%	
	(0.25,0.75)	4.9002	5.3243	13120.1121	3.38%	5.2922	5.0698	11594.3424	0.87%	
<i>Triple tariff system instances</i>										
		<i>weekday (t.wd)</i>					<i>weekend (t.wd)</i>			
1000	(0.99,0.01)	0.1176	5.4408	14653.6178	116.99%	0.0983	7.2459	12562.4901	108.45%	
	(0.01,0.99)	6.7751	4.8329	6753.0488	11.73%	5.7147	5.7662	6028.7598	20.45%	
	(0.50,0.50)	0.6827	5.2832	9488.7445	40.66%	0.7872	6.9618	6921.9294	15.37%	
	(0.75,0.25)	0.2820	5.4507	12749.1934	88.79%	0.2853	7.0990	8742.6267	45.11%	
	(0.25,0.75)	1.3912	5.0483	7116.8405	9.48%	1.8756	6.9028	6701.5782	12.17%	
10000	(0.99,0.01)	0.1324	5.4820	15957.4220	136.30%	0.1120	7.2677	12687.4428	110.52%	
	(0.01,0.99)	7.1755	4.8433	6753.0488	11.54%	5.9961	5.8158	6030.3285	19.77%	
	(0.50,0.50)	1.2873	5.3228	9268.1675	37.35%	1.5423	6.9630	6741.1074	12.49%	
	(0.75,0.25)	0.4755	5.4812	12302.0264	82.17%	0.7575	7.2271	9192.6075	52.53%	
	(0.25,0.75)	2.5086	5.0592	7032.9137	8.66%	2.7973	6.9623	6724.3662	12.23%	
100000	(0.99,0.01)	0.1624	5.4819	15154.8956	124.42%	0.1428	7.2679	12465.7851	106.84%	
	(0.01,0.99)	7.9994	4.8437	6753.0487	11.54%	6.0057	5.8164	6030.3285	19.76%	
	(0.50,0.50)	2.1318	5.3236	9158.1686	35.72%	2.7583	6.9631	6731.4012	12.34%	
	(0.75,0.25)	0.8098	5.4805	11825.5112	75.11%	1.5354	7.2673	9236.5179	53.26%	
	(0.25,0.75)	4.0831	5.0592	7011.6512	8.51%	3.6560	6.9536	6708.0816	12.02%	
<i>Building-like instances</i>										
		<i>weekday (b.wd)</i>					<i>weekend (b.wd)</i>			
1000	(0.99,0.01)	0.1852	5.4415	15573.6492	57.17%	0.1691	7.2166	11231.0796	34.28%	
	(0.01,0.99)	23.0971	5.2353	9908.8092	4.35%	25.1296	5.9513	8364.0303	18.05%	
	(0.50,0.50)	6.3228	5.3736	12506.7870	26.28%	6.3418	6.2954	8367.1677	13.31%	
	(0.75,0.25)	1.6910	5.4423	14981.6673	51.20%	1.5304	6.9626	8751.6237	6.20%	
	(0.25,0.75)	16.7783	5.2561	10395.6621	6.32%	16.3588	6.3058	8367.1677	13.17%	
10000	(0.99,0.01)	0.2602	5.4820	16280.9307	64.31%	0.2573	7.2662	10839.6924	29.60%	
	(0.01,0.99)	28.7164	5.2663	9908.8092	3.79%	29.2907	5.9532	8364.0303	18.02%	
	(0.50,0.50)	9.6899	5.4813	12686.0631	28.03%	9.6318	6.5224	8445.7521	10.23%	
	(0.75,0.25)	2.0274	5.4827	14050.4841	41.80%	1.9017	7.0697	8819.7003	6.06%	
	(0.25,0.75)	16.3678	5.3246	10242.3396	4.33%	15.2221	6.3064	8367.1677	13.16%	
100000	(0.99,0.01)	0.3001	5.4822	16385.9607	65.37%	0.2743	7.2676	10516.6188	25.74%	
	(0.01,0.99)	28.3730	5.2660	9908.8092	3.79%	30.8415	5.9529	8364.0303	18.03%	
	(0.50,0.50)	12.2024	5.4812	12533.7021	26.49%	13.2396	6.5221	8445.7521	10.24%	
	(0.75,0.25)	4.2573	5.4811	12727.4946	28.45%	4.1211	7.0715	8819.7003	6.05%	
	(0.25,0.75)	17.4095	5.3246	10235.2521	4.27%	19.0460	6.3065	8367.1677	13.16%	

Results in Table 3 indicate that the proposed approach is able to solve the instances in relatively short computing times. The instances that prioritize the cost over the user satisfaction, i.e., with a combination of weights (0.01,0.99) and (0.25,0.75), are more difficult to solve and require larger computing times. Additionally, the average resolution time for building-like instances is significantly larger than for the other instances, since more integer variables are integrated in the MIP formulation with the penalization variables.

Results show that the triple tariff system allows reducing the cost of the energy consumed for similar level of preferences. For example, in Fig. 1, the solutions of the triple tariff system dominates in terms of cost and/or user satisfaction the solutions of the double tariff system, specially in the weekend.

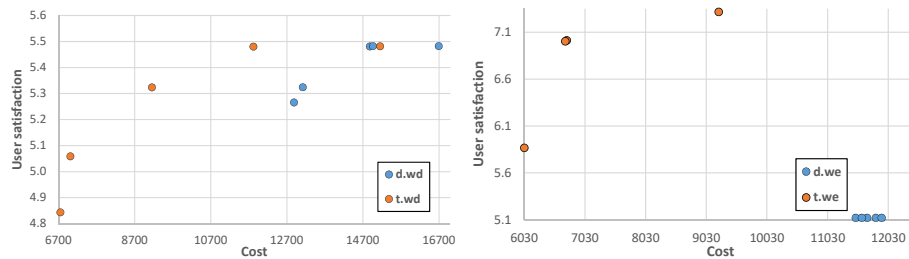


Fig. 1: Comparison of the best solutions for instances with double and triple tariff system with sample size  $N = 10000$ .

Table 4 compares the results of representative SAA solutions with a business as usual (BaU) strategy. The BaU strategy proposes assigning ON times to each appliance without planning considering only user satisfaction. These plannings have good user preference values, but inefficient costs. The SAA representative solutions that are compared are the best compromising solution of SAA, i.e., the one with the smallest  $\Sigma$ , and the solution biased to the user satisfaction, i.e., with a weight vector (0.99,0.01). Table 4 reports the percentage relative improvement of the SAA solution over the BaU solution for each objective.

Table 4: Comparison of SAA with BaU solutions.

	<i>d.wd</i>		<i>t.wd</i>		<i>b.wd</i>	
	<i>F</i>	<i>G</i>	<i>F</i>	<i>G</i>	<i>F</i>	<i>G</i>
<i>compromising</i>	-2.89%	35.35%	-7.72%	62.84%	-3.95%	48.16%
<i>best preferences</i>	0.00%	18.71%	-0.01%	15.44%	-0.01%	14.27%
	<i>d.we</i>		<i>t.we</i>		<i>b.we</i>	
	<i>F</i>	<i>G</i>	<i>F</i>	<i>G</i>	<i>F</i>	<i>G</i>
<i>compromising</i>	-30.25%	18.91%	-4.33%	59.20%	-2.69%	40.65%
<i>best preferences</i>	-30.11%	14.47%	0.00%	24.17%	0.00%	29.23%

Results indicate that, except for instance *d.we*, the compromising solution of the SAA are only slightly worse in terms of user satisfaction than the BaU solutions, less than 5% in all cases (Table 4). Regarding *d.we*, BaU solutions are about 30% better than SAA solution. In terms of cost, as expected, compromising solutions are substantially better than BaU solutions (up to 62%). In the case of the solutions of SAA biased to user satisfaction, i.e., those that have a large value of  $\alpha$ , BaU solutions are almost equally competitive in terms of respecting user preferences but with higher electricity costs (up to 29%). The exception is *d.we* in which the SAA solution is around 30% worse than BaU in terms of user satisfaction.

14 D. Rossit, S. Nesmachnow

## 6 Conclusions and future work

This article addressed the problem of scheduling deferrable appliances in smart homes considering stochastic user preferences for appliances, focused on a specific case study on Uruguayan households. For solving the problem, a new MIP mathematical formulation of is presented, and a resolution approach based on exact solver and Monte Carlo simulation is proposed.

Results obtained in the computational experimentation on a set of real-world instances show that the proposed method is competitive to address the household planning problem, computing solutions that are similar in terms of user satisfaction to the business as usual strategy, but with smaller electricity costs.

The main lines for future work are related to the enlargement of the computational experimentation taking further advantage of the extensive database that has been published about households of Montevideo, including the use of electricity for water heating, and the application of other resolution approaches that explicitly consider the multiobjective nature of the problem, such as evolutionary algorithms.

## References

1. Chavat, J., Nesmachnow, S., Graneri, J., Alvez, G.: ECD-UY: Detailed household electricity consumption dataset of Uruguay. *Scientific Data* (2021), in press
2. Chen, X., Wei, T., Hu, S.: Uncertainty-aware household appliance scheduling considering dynamic electricity pricing in smart home. *IEEE Transactions on Smart Grid* 4(2), 932–941 (2013)
3. Colacurcio, G., Nesmachnow, S., Toutouh, J., Luna, F., Rossit, D.: Multiobjective household energy planning using evolutionary algorithms. In: *Smart Cities, Communications in Computer and Information Science*, vol. 1152, pp. 269–284. Springer (2019)
4. Eurostat: Energy consumption in households 2021, <https://ec.europa.eu/eurostat>, accessed September 2021
5. Hart, W., Laird, C., Watson, J., Woodruff, D., Hackebeil, G., Nicholson, B., Sirola, J.: *Pyomo—optimization modeling in Python*, vol. 67. Springer (2017)
6. Hemmati, R., Saboori, H.: Stochastic optimal battery storage sizing and scheduling in home energy management systems equipped with solar photovoltaic panels. *Energy and Buildings* 152, 290–300 (2017)
7. Hu, Z., Li, C., Cao, Y., Fang, B., He, L., Zhang, M.: How smart grid contributes to energy sustainability. *Energy Procedia* 61, 858–861 (2014)
8. Imanloozadeh, A., Naziffard, M., Sadat, S.: A new stochastic optimal smart residential energy hub management system for desert environment. *International Journal of Energy Research* (2021)
9. International Energy Agency: World energy outlook 2021, [www.iea.org/topics/world-energy-outlook](http://www.iea.org/topics/world-energy-outlook), accessed September 2021
10. Kleywegt, A., Shapiro, A., Homem-de Mello, T.: The sample average approximation method for stochastic discrete optimization. *SIAM Journal on Optimization* 12(2), 479–502 (2002)

11. Kolter, J., Johnson, M.: REDD: A public data set for energy disaggregation research. In: Workshop on data mining applications in sustainability. San Diego, USA (2011)
12. Koutsopoulos, I., Tassiulas, L.: Control and optimization meet the smart power grid: Scheduling of power demands for optimal energy management. In: Proceedings of the 2nd International Conference on Energy-efficient Computing and Networking, pp. 41–50 (2011)
13. Liang, H., Zhuang, W.: Stochastic modeling and optimization in a microgrid: A survey. *Energies* 7(4), 2027–2050 (2014)
14. Lu, X., Zhou, K., Zhang, X., Yang, S.: A systematic review of supply and demand side optimal load scheduling in a smart grid environment. *Journal of Cleaner Production* 203, 757–768 (2018)
15. Momoh, J.: *Smart Grid: Fundamentals of Design and Analysis*. Wiley (2012)
16. Nesmachnow, S., Baña, S., Massobrio, R.: A distributed platform for big data analysis in smart cities: combining intelligent transportation systems and socioeconomic data for Montevideo, Uruguay. *EAI Endorsed Transactions on Smart Cities* 2(5), 153478 (2017)
17. Nesmachnow, S., Colacurcio, G., Rossit, D., Toutouh, J., Luna, F.: Optimizing household energy planning in smart cities: A multiobjective approach. *Revista Facultad de Ingeniería Universidad de Antioquia* 101, 8–19 (2021)
18. Nesmachnow, S., Rossit, D., Toutouh, J., Luna, F.: An explicit evolutionary approach for multiobjective energy consumption planning considering user preferences in smart homes. *International Journal of Industrial Engineering Computations* 12(4), 365–380 (2021)
19. Norkin, V., Pflug, G., Ruszczyński, A.: A branch and bound method for stochastic global optimization. *Mathematical Programming* 83, 425–450 (1998)
20. Orsi, E., Nesmachnow, S.: Smart home energy planning using IoT and the cloud. In: *IEEE URUCON* (2017)
21. Paatero, J., Lund, P.: A model for generating household electricity load profiles. *International Journal of Energy Research* 30(5), 273–290 (2006)
22. Porteiro, R., Chavat, J., Nesmachnow, S.: A thermal discomfort index for demand response control in residential water heaters. *Applied Sciences* (2021)
23. Rademaekers, K., Smith, M., Yearwood, J., Saheb, Y., Moerenhout, J., Pollier, K., Debrosses, N., Badouard, T., Peffen, A., Pollitt, H., Heald, S., Altman, M.: Study on energy prices, costs and subsidies and their impact on industry and households. Tech. Rep. Final report, EU publications (2018)
24. Rossit, D., Toutouh, J., Nesmachnow, S.: Exact and heuristic approaches for multiobjective garbage accumulation points location in real scenarios. *Waste Management* 105, 467–481 (2020)
25. Rossit, D., Nesmachnow, S., Toutouh, J., Luna, F.: A simulation-optimization approach for the household energy planning problem considering uncertainty in users preferences. In: *International Conference of Production Research–Americas*. pp. 253–267. Springer (2020)
26. Shapiro, A.: Monte Carlo simulation approach to stochastic programming. In: *Proceeding of the 2001 Winter Simulation Conference*. IEEE, Arlington, USA (2001)
27. U.S. Energy Information Administration: Annual energy outlook 2021, <https://www.eia.gov/aeo>, accessed September 2021
28. Waseem, M., Lin, Z., Liu, S., Zhang, Z., Aziz, T., Khan, D.: Fuzzy compromised solution-based novel home appliances scheduling and demand response with optimal dispatch of distributed energy resources. *Applied Energy* 290, 116761 (2021)

# A Covid-19 Vaccination Tracking and Control Platform in Santiago de Cali

Andres Felipe Fuentes<sup>1</sup>[0000-0003-4687-9316], Diego Fernando Botero<sup>2</sup>[0000-0003-1922-9078], Cristhian Torres Ramirez<sup>3</sup>[0000-0002-6885-8703],  
and

<sup>1</sup> Pontificia Universidad Javeriana Cali, Colombia

[affuentesv@javerianacali.edu.co](mailto:affuentesv@javerianacali.edu.co)

<sup>2</sup> GRIEPIS - Universidad Libre Cali, Colombia

[diego.botero@unilibre.edu.co](mailto:diego.botero@unilibre.edu.co)

<sup>3</sup> Universidad Santiago de Cali Cali, Colombia

[cristhian.torres00@usc.edu.co](mailto:cristhian.torres00@usc.edu.co)

**Abstract.** The monitoring and control of epidemics is one of the most relevant topics in the field of smart health within smart cities. Smart health take advantage of a new generation of information technologies, such as big data, mobile internet, cloud computing and artificial intelligence, in order to transform the traditional medical system in a comprehensive way, making healthcare more efficient and personalized. From electronic Health records (EHR), diverse information about the epidemiological situation in institutions that provide health services can be extracted. This document describes the development of a platform to carry out the control and monitoring of vaccination process against Covid-19, which is based on cloud data storage technologies and make use of a existing platform designed for the registration of EHR emphasizing on data collection for structuring of epidemiological control strategies. The main goal is to identify and characterize patients who meet the prioritization criteria for Covid-19 vaccination according to stages defined by the Colombia Ministry of Health, execute the geocoding processes and identification of health conditions according to their previous EHR records, in order to accomplish an efficient and intelligent execution, monitoring and control of vaccination that impacts the epidemiological risk mitigation process. At the end of the document is described the use of the developed platform for the monitoring and control of the Covid-19 vaccination process in a Basic Health Services Unit called Medicips, which provides health services to approximately 90,000 people in the city of Santiago de Cali, Colombia.

**Keywords:** Smart Health Services · Electronic Health Records (EHRs) · Covid-19 · Epidemic control · BigData · Geocoding

## 1 Introduction

New trends in information and communication technologies (ICT) are used by smart city models to mitigate problems that affect the quality of life in the

2 A.F. Fuentes et al.

population such as pollution, traffic, climate change, public health, epidemics, among others [1] [2]. In regard to public health problems and epidemiology the use of ICTs provide the structural basis for the development of smart health services.

Smart health services, as part of the development of citizen-centered smart city services, must seek to offer efficiency, effectiveness, opportunity and availability in order to improve the quality of life of citizens. To achieve this objective is necessary to understand the interactions that arise between the different aspects of a population, analyzing the social determinants of health in which people lives, works, studies and interacts with the community [3]. It is here where technologies such as big data, mobile internet, cloud computing and artificial intelligence begin to be incorporated, through which data can be collected and transformed into useful information for resource planning, efficient provision of services, making of decisions adjusted to the needs in real time [4].

Within the framework of public health, vaccination schemes focus on breaking the chain of transmission of a virus, vaccinating as many people as possible, but these people should be prioritized in such a way that brings effectiveness interruption of the chain of transmission of the disease, taking into account the limitation of resources and availability of doses [5]. At this point, smart health services are used to support the vaccine supply model to a specific population within a territory, taking into account the quantities of doses, the dispersion of the population and the prevalent risk of this population determined for the EHR records analysis.

Applications like the previous one demand a technological platform that allows the interconnection of different data sources, as well as the identification and characterization of the population. This paper analyzes briefly some of the main components of smart health services applied to public health for a better understanding, including assisting diagnosis and treatment, health management, disease prevention and risk monitoring, epidemic Control [6].

Once the different components of smart health services have been analyzed, a platform based on some open source components and cloud services is proposed, which contains various of the functionalities that smart health systems must provide for the monitoring and control, in this case, applied to the Covid-19 vaccination process.

The presented platform works in real time and takes data from a previous EHR system implemented in a Big Data as a Service (BDaaS) [7] known as BigQuery which is a fully-managed, serverless data warehouse that enables scalable analysis over petabytes of data and is used for storage of EHR records. The presented platform uses BigQuery as well for data analysis. In addition, the platform includes in its development open source software such as javascript, Nodejs environments and MySQL database as well as cellular communications for mobile access to the platform and Google Maps API for the geocoding system.

At the end of the document, the results obtained through the developed platform are presented. To obtain the results, the platform was tested in a basic unit for the provision of health services called Medicips, located in Cali, Colombia,

which was selected by the Colombian Ministry of Health as one of the entities in charge of the process of Covid-19 vaccination in the city of Cali and from which the previous EHRs were obtained. These results show an approach to the use of new ICT technologies applied to health platforms that involve an epidemiological control component, providing mechanisms for planning, monitoring and control of public health processes, within the framework of smart cities.

## 2 Related Work

Through different perspectives, several researchers have presented formal definitions of a smart city. In [8], it is defined as the need for a connection between the physical, social, business and information and communication technology (ICT) infrastructure to improve the intelligence of the urban area. In [9], it is defined as a modern city, which must get advance from ICT to improve the life quality and the condition of urban services for citizens. These two definitions shows that a smart city deals with a smart urban environment enhanced with ICT technologies in order to improve the daily life in communities. [10].

In [6], the concept of smart healthcare is introduced in which a new generation of information technologies are used, such as the Internet of Things (IoT), big data, cloud computing and artificial intelligence, transforming the traditional healthcare delivery systems in a comprehensive way, making medical care more efficient, convenient and personalized.

In [11], an overview of smart health is provided where the use of mobile technologies and ICT brings opportunities for existing information health systems taking advantage of the ubiquity of mobile devices which provides immediacy, availability and capabilities of monitoring in dispersed territories.

Already in the application of the smart healthcare concept, in [12] a framework is proposed whereby enables various smart health services aimed at epidemic control and ways of implementing them, using EHR records.

On the other hand, works such as [13] exposes an overview of how the smart city infrastructure supports strategic healthcare through the use of mobile and environmental sensors combined with machine learning, considering the challenges that will be faced as that healthcare providers take advantage of these opportunities.

In the reviewed papers, definitions of smart cities are introduced which incorporates different aspects such as smart people, smart government, smart transport, smart health, etc, with a focus on taking advantage of data management technologies (that is, IoT, Big Data and Cloud Computing, etc.) to establish a deep connection between each component and each aspect of a city [14].

## 3 Smart Health Services

Smart Health Services are applicable to different branches of health such the clinical treatment, clinical research, family health, studying of social determinants of health among others. For the purpose of this work, services that are

4 A.F. Fuentes et al.

considered directly related to the monitoring and control of public health diseases are analyzed, without pretending that they are the only ones. This analysis identifies the importance of incorporating key technologies such as IoT, cloud computing, big data, Machine Learning, 5G, and artificial intelligence, as well as the participation of all entities involved in the provision of both private and public health services as well as the community itself.

In order to understand an Smart Health Services, it can be expressed in several applications such as (1) Assisting diagnosis and treatment, (2) Health management, (3) Disease prevention and risk monitoring and (4) Epidemic control component [15].

**Assisting Diagnosis and Treatment.** Medical diagnostic and treatment processes can take great advantage of technologies that apply intelligent algorithms to reduce diagnostic errors and personalize disease treatments. It is possible to use data from the EHR system to feed intelligent systems that previously trained can provide the healthcare professionals with guidance for making decisions about the patient and issue alerts about possible treatments and diagnoses.

**Health Management.** The health management of the disease becomes important with the increase of chronic diseases since it allows the decentralization of health services through smartphones, portable smart devices, smart homes and technologies such as 4G and 5G networks [16]. This empower a more precise monitoring of patients with chronic diseases by analyzing individual behavior facing their illnesses, performing preventive health maintenance and providing more economical solutions for the monitoring of chronic diseases [17].

**Disease Prevention and Risk Monitoring.** Customarily, the patient disease risk prediction is based on the collection of patient data according to the clinical guidelines defined by the health authorities, comparing these data with the guidelines and issuing a concept. This mechanism takes time and does not provide an accurate diagnosis to the patient. Predicting disease risk with smart healthcare is dynamic and personalized. The new disease risk prediction model collects data through mobile devices and smart applications, uploads it to the cloud using a network, and analyzes the results hinge on machine learning based algorithms witch feed back predicted results to users in real time [6].

**Epidemic Control.** A special area within smart health is dedicated to epidemic control. The existence of electronic data about health status claims of people, as well as knowledge of the social determinants of health on a specific territory improve the processes of detection and control of epidemics. Data about locations and activities of people can be introduced to machine learning algorithms and the results could be used to anticipate potentially new cases during an epidemic, effectively identify high-risk sites, and successfully manage an epidemic [12]. These methods are also useful for the identification and monitoring of other public health risks such as environmental pollution. [11].

### 4 Architecture of the Platform.

Thus, considering the different models used by the applications previously exposed as service components in smart health and the way in which information and communication technologies (ICT) are incorporated, in Figure 1 is depicted a basic architecture used for the development of a Covid-19 Vaccination Tracking and Control platform, the main objective of this work. The architecture is based on two layers, a *Backend Layer* with access to a EHR data warehouse and a *Frontend Layer* for access and data visualization by end users.

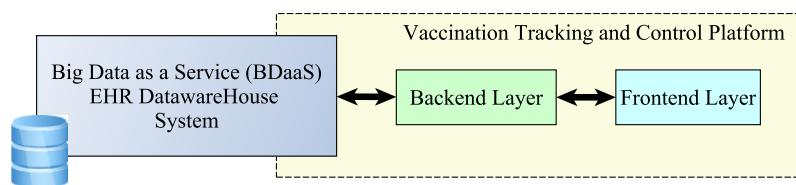


**Fig. 1.** Layered architecture used for the development of a Covid-19 Vaccination Tracking and Control platform

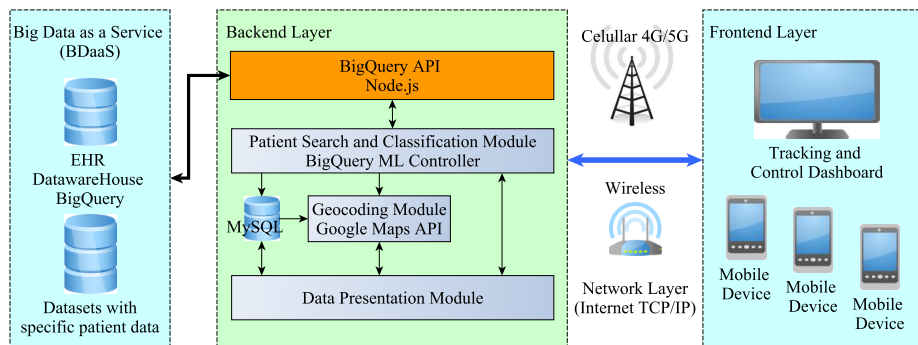


**Fig. 2.** Covid-19 Vaccination Tracking and Control platform including used technologies

Figure 2 depicts a diagram with a more detailed view of the components of the Covid-19 Vaccination Tracking and Control platform. The proposed architecture starts from an EHR data warehouse based on a BDaaS platform (previously developed) which provides the electronic health record data of a set of patients. From this information a new dataset with specific patient data is created selecting the necessary information for segmentation and classification of each patient

6 A.F. Fuentes et al.

according to Covid-19 vaccination phases [18]. The new dataset is set on the BDaaS BigQuery which provides the ability to interactively store, process and query massive datasets recorded [19].

In order the Covid-19 Vaccination Tracking and Control platform interacts with the EHR data warehouse an API was designed using the Google BigQuery API [20]. The API developed is part of the *Backend Layer* of the system. Similarly, a module for controlling the extraction, transformation and load process from BigQuery is developed, this module send to BigQuery the queries for the search and classification of patients according to the prioritization characteristics for vaccination defined by the health authorities.

Once the queries are executed on Bigquery, the results are stored on a Bigquery dataset, then through the API developed a summarie of the results are extracted to the backlayer and the data is processed according to the *Frontend Layer* requirements in the data presentation module which is part of the backlayer. The data presentation module generate the views used in the tracking and control dashboard shown in the *Frontend Layer* where health professionals who make up the coordinating team of the vaccination process located in the health center, can follow and make decisions about the vaccination process.

The tracking and control dashboard presents the indicators defined for the process, additionally in the dashboard the geolocation of the prioritized patients is presented whose information is obtained from the geocoding module which performs the addresses conversion of each patient into geographic coordinates and then carry out the geolocation on the map of the territory. The geocoding module is developed on the backlayer and is based on the Google Maps API [21]

In addition, the vaccination process requires a team of health professionals who commute to the homes of prioritized patients that will be vaccinated. Taking into account the above, the geolocation of each patient together with their prioritization allows establishing a route for the team commuting, who using mobile devices connected to a 4G network for access the frontlayer which display a responsive interface adapted for small screens devices, where they can follow the location of each patient on a map and record each visit made. The information registered by each team can be followed in real time by the coordinating team of the process located in the health center.

The description of the technologies chosen for the development of the architecture proposed in Figure 2 are described below, indicating the advantages they offer regarding to smart health.

**Big Data as a Service (BDaaS).** Big data impose significant challenges to the traditional infrastructure, due to the characteristics of volume, velocity and variety of data. One of the challenges of designing big data infrastructure is the requirement to support many different data types. Currently, Big Data as a Service includes Storage-as-a-Service and Computing-as-a-Service, to store and process the massive data [7].

There are different BDaaS such as Google BigQuery, Amazon RedShift, Apache Drill among others. In this work BigQuery was used, since it started from an EHR data warehouse developed previously.

BigQuery is a Google Cloud product that can be used as a data warehouse, also offering support for interactive SQL queries through a graphical interface. This product implements the main features of Dremel technology, used internally by Google for tasks such as spam analysis or bug reporting for various Google products. Big Query shares with Dremel the performance, the internal structure, composed of data ordered by columns (column-oriented storage) and the division of queries on servers through a tree-shaped structure [22].

BigQuery includes BigQuery ML which lets create and execute machine learning models in BigQuery using standard SQL queries. BigQuery ML increases development speed by eliminating the need to export data to another schema to apply Machine Learning algorithms [23] [24]. BigQuery ML supports the following types of models: Linear regression for forecasting, Binary logistic regression for classification, Multiclass logistic regression for classification, k-means clustering for data segmentation, Matrix Factorization for creating product recommendation systems, Time series for performing time-series forecasts, and others

Access to Big Query can be done through a web client, an API or a third-party software. This work uses the API for Node.js framework.

Google BigQuery offers storage for up to 10GB and 1TB of data processed per query for free.

**Geocoding System.** Geocoding is a process for converting a text address into geographic coordinates. This process includes access the text address database, processing the text address and returning geographic coordinates along with described data back to the user [25].

There is geocoding services like TAPDM geocoder, ArcGIS Online, Google Maps API, Bing Maps API, MapQuest Maps.

This work uses The Google Maps API. This API allows using the Google Maps Platform service, which offer various services which can be included in web or mobile applications. For the proposed platform, the Google Maps API for javascript was used, which allows access to:

1. Geocoding, convert coordinates into addresses and addresses into coordinates.
2. Maps SDKs, Allow use of maps for the web and mobile and is possible add marks in order to show position into a geographic area shown in the map (Geolocation).
3. Directions, provide directions for multiple transportation modes, featuring real-time traffic information.

**BackEnd Technologies.** Additionally, for the development of the proposed *Backend Layer*, an integration of different technologies was carried out.

8 A.F. Fuentes et al.

These technologies include the development of Representational State Transfer (REST) services, which is an interface between systems that uses the HTTP protocol to obtain data or generate operations on that data in various possible formats, such as XML and JSON [26]. REST services are useful for consuming subroutines, functions and procedures of systems exposed through an API.

The algorithms and programming logic were developed in Node.js which is an open source, cross-platform runtime environment for the server layer based on the JavaScript programming language. Node.js is oriented to the development of dynamic applications with access to information stored in databases. In Node.js, REST services can be developed by establishing subscription mechanisms to receive data from external applications and store it in a database, using its capabilities to connect with database engines such as MongoDB or MySQL [27]. Node.js in conjunction with HTML, Javascript and CSS can also be useful for the development of web pages in order to display data and information to the end user, as well as the design of forms to collect information.

#### 4.1 Smart Health Service for Covid-19 Vaccination Tracking and Control System Development.

According to the design of Figure 2, both the *Backend Layer* and the *Frontend Layer* compose the architecture for the development of the Covid-19 Vaccination Tracking and Control Platform in Santiago de Cali, which is developed by integrating technologies previously exposed, bringing the design of the platform closer to the concepts analyzed in the smart health services section.

**Backend Layer** The *Backend Layer* integrates the patient search and classification module, the EHR Datawarehouse API connection, a geocoding module, as well as the data presentation module.

*Patient Search and Classification Module.* This module is developed in Nodejs, mainly contains functions that execute the extraction, transformation and loading processes from BigQuery datasets. This module controls the data extraction queries from the EHR data warehouse creating datasets with specific patient data to be used by the BigQuery feature called BigQuery ML used to execute machine learning models such k-means clustering [23]. Additionally, this module records summaries of the results of the queries executed in BigQuery in a relational database (MySQL) where they are available to the other modules of the *Backend Layer* such as the geocoding module and the data presentation module. Additionally, this module controls the updating of the data of the vaccinated patients registered by the vaccination teams from the *Frontend layer*.

*API Connection.* For the API developed for the connection with the EHR Datawarehouse, a REST service was developed in Nodejs, which sends the requests from the patient search and classification controller module to the EHR Datawarehouse in BigQuery. Once the clustering models are executed in the

EHR Datawarehouse, the results contain patient sets which are registered in a new dataset in BigQuery. These datasets are processed by machine learning algorithms and the results are interpreted and exposed to be consumed by the *Backend Layer* to make it available for the geocoding and data presentation modules.

*Geocoding Module.* The geocoding module processes the addresses of each patient through Google geocoding API. The API returns geocoding information represented in latitude and longitude corresponding to the location of each patient [21]. This data is stored in the MySQL database in order to be available to the other layers. Google Geocoding API allows the processing of 25,000 requests per user per day at no cost.

*Presentation Module.* Based on the information of the clustering, classification and prioritization of patients obtained from BigQuery process and the geocoding of each address, information is available to be sent to the monitoring and control dashboard. For this, the data presentation module managed the data for visualization in the dashboard in the *Frontend Layer*.

**Frontend Layer** The *Frontend Layer* is developed using the HTML, CSS and Javascript languages and is composed of two basic modules, the dashboard module and the vaccination process registration module.

*Dashboard Module.* This module presents the summary data of the vaccination process. In this module is depicted the geolocation of prioritized patients using the Google Maps API which allows to locate marks on a interactive map of a territory that indicate the location of patients. Additionally, the lists of prioritized and classified patients can be seen, as well as performance indicators and compliance with vaccination goals and vaccination team tracking. This module can be accessed by the user through a web browser.

*Registration Module.* Is used by the vaccination teams to visualize the patients prioritized for vaccination, locate them in a interactive map in order to be able to commute to the place where they are and thus vaccinate the patient. This module can be used as an app from a mobile device connected to a cellular network (4G/5G) and allows to view the geolocation of each patient and allows to register the status of the vaccine application process of each patient (application of first dose, second dose, not vaccinated, the patient was not found), via the completion of a form. These records can be observed in real time in the dashboard module.

## 5 Platform Implementation

In order to test the Covid-19 Vaccination Tracking and Control Platform in Santiago de Cali, the platform was implemented in the Medicips Basic Health

10 A.F. Fuentes et al.

Services Unit, which is an institution that provides basic health services to approximately 90,000 people and has the authorization of the Ministry of Health of Colombia to carry out vaccination processes for Covid-19 in the population assigned for the provision of health services. The EHR information for the Medicaps population is located in the BigQuery-based EHR data warehouse. The implementation was developed in several steps:

First step, the classification of the population is carried out according to the stages of the vaccination plan of the Ministry of Health of Colombia [18], for which the following characteristics of the first three stages were taken.

1. Stage 1 (Population 80 years of age or older)
2. Stage 2 (Population between 60 and 79 years of age)
3. Stage 3 (Population between 50 and 59 years old and people between 16 and 59 years old with comorbidities or hypertensive diseases: Diabetes, Renal insufficiency, HIV, Cancer, Tuberculosis, COPD, ASMA, Obesity, on the waiting list for transplantation of vital organs or Post-transplantation vital organs)

In Table 1 the basic classification by age and the number of users by classification are shown.

**Table 1.** Population classification by age ranges

Age Ranges	Population quantity
Population 80 years of age or older	3,003
Population between 60 and 79 years of age	14,046
Population between 50 and 59 years old	11,675

In order to approximate the distribution of the population and its relationship with the diagnoses of chronic diseases, necessary for the classification of stage 3, the BigQuery ML k-means Clustering model was used, identifying diagnoses associated with the patients, grouping the population by: age, age group, gender and ICD-10 group [28]. The grouping was performed on a set of 219,540 EHR records, belonging to Medicaps patients older than 16 years.

**Table 2.** Population clustering in relation to age ranges and diagnoses

Cluster	EHR Count	Age Avg.	I10 Group Hypertension	E10 Group Mellitus diabetes
1	59,282	60	16.26%	1.49%
2	40,346	27	0%	0%
3	55,351	72	39.74%	1.52%
4	64,561	45	2.96%	0.1%

Covid-19 Vaccination Tracking and Control Platform 11

Table 2 shows the clustering results with k-means, using four (4) clusters and Euclidean distance. It is observed that cluster # 3 has an average of 72 years and contains patients with diagnoses of Hypertension and Diabetes, as well as cluster #1, whose average age is 60 years. Cluster #2, which has an average age of 27, does not contain patients with chronic diseases. With the previous results, the population can be prioritized, taking into account that vaccinating patients between 60 and 79 years old covers a high percentage of patients with chronic diseases related to hypertension and diabetes, allowing optimization of costs and logistical resources.

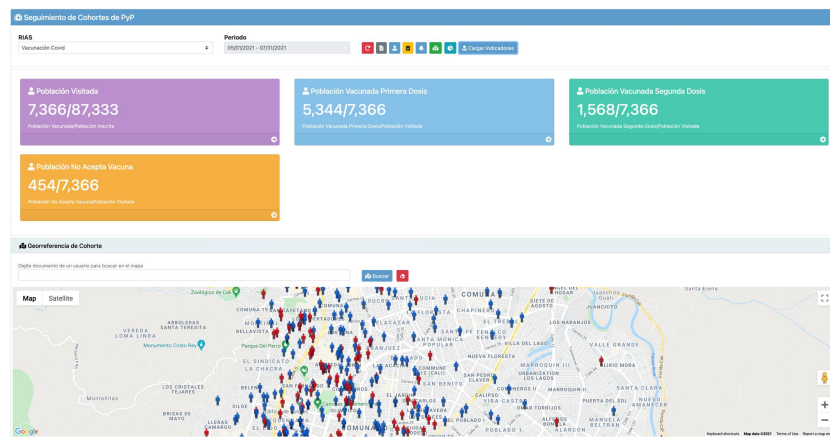


**Fig. 3.** Dashboard for Covid-19 Vaccination Tracking and Control Platform in Santiago de Cali

Previously defined the clusters, proceed with a second step, where the lists of the patients that belong to each of the clusters are obtained. These lists are processed through the geocoding module, obtaining the geolocation of each one.

further, in a third step the clustered patient lists are taken to build basic indicators which are deployed in the *Frontend Layer* and displayed in the control and tracking dashboard and in the app-type interface accessed by the vaccination teams.

Figure 3 shows dashboard for Covid-19 Vaccination Tracking and Control in Santiago de Cali which is deployed through the implemented platform. Figure 4 shows the access to the app from a mobile device. Across this interface, prioritized patients and their location can be accessed using geolocation on Google Maps. Additionally, the interface includes a functionality to calculate the route from a specific location to the position of a patient, which allows finding an optimal commuting route for the vaccination teams. Moreover, through the app interface the status of the vaccination process of each patient can be recorded, which will be showed in the indicators and data displayed on the monitoring and control dashboard.

12 A.F. Fuentes et al.

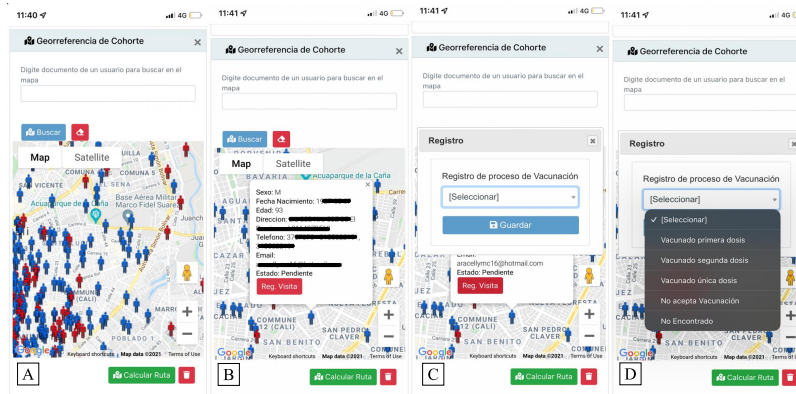


**Fig. 4.** *Frontend Layer.* user interface used by vaccination teams in a mobile device to record the individual vaccination process of each patient. (A) Map, (B) Patient information, (C)(D) Register of vaccination process.

## 6 Concluding Remarks

This paper proposes a platform for the Monitoring and Control of Covid-19 Vaccination in Santiago de Cali, which was implemented in order to support the vaccination process of the population of a basic health unit. As a result, this allowed the application of smart health features, making possible the classification and prioritization of the population providing a better understanding of the inherent attributes of health from the application of Machine Learning algorithms in an EHR data warehouse.

The proposed platform shows the usage of information and communication technologies applied to health services, including smart characteristics, providing elements in decision-making adjusted to the real demands of a population, helping to improve health services, reduce inequity and enhance prevention strategies that impact the life quality.

Furthermore, from the proposed platform, it is possible to develop the implementation of the monitoring and control for other types of health services such as chronic diseases, social determinants of health, disease transmission, among others. Including sources of information from other areas of smart cities such as pollution data analysis, air quality, solar radiation, waste management, public security, public transport and alternative mobility among others, which can be used to feed the epidemiological data of a territory and its population, generating impact mechanisms about the smart management of public health, including the participation of private entities, the government of cities and his population.

**Acknowledgement.** The authors would like to acknowledge the cooperation of the research group *GrIEpiS: Grupo de Investigación en Epidemiología y Servicios* and the basic unit of healthcare *Medicips Cali*.

## References

1. Andres Felipe Fuentes and Eugenio Tamura. Lora-based iot data monitoring and collecting platform. In *Ibero-American Congress of Smart Cities*, pages 80–92. Springer, 2019.
2. Andres Felipe Fuentes Vasquez and Eugenio Tamura. From sdl modeling to wsn simulation for iot solutions. In *Workshop on Engineering Applications*, pages 147–160. Springer, 2018.
3. Carlos E Jiménez, Francisco Falcone, Agusti Solanas, Héctor Puyosa, Saleem Zoughbi, and Federico González. Smart government: Opportunities and challenges in smart cities development. *Civil and Environmental Engineering: Concepts, Methodologies, Tools, and Applications*, pages 1454–1472, 2016.
4. Luis Fernando Cruz Gómez, Ángela María Cruz Libreros, Rodrigo Alberto Alzate Sánchez, Diego Fernando Botero Henao, Andrés Felipe Fuentes Vásquez, and Jhon Housseman Bolaños Ramos. *Epidemiología y servicios en salud*. Ediciones de la U, 2021.
5. Mohammad Mohsen Jadidi, Pegah Moslemi, Saeed Jamshidiha, Iman Masroori, Abbas Mohammadi, and Vahid Pourahmadi. Targeted vaccination for covid-19 using mobile communication networks. In *2020 11th International Conference on Information and Knowledge Technology (IKT)*, pages 93–97. IEEE, 2020.
6. Shuo Tian, Wenbo Yang, Jehane Michael Le Grange, Peng Wang, Wei Huang, and Zhewei Ye. Smart healthcare: making medical care more intelligent. *Global Health Journal*, 3(3):62–65, 2019.
7. Zibin Zheng, Jieming Zhu, and Michael R Lyu. Service-generated big data and big data-as-a-service: an overview. In *2013 IEEE international congress on Big Data*, pages 403–410. IEEE, 2013.
8. Colin Harrison, Barbara Eckman, Rick Hamilton, Perry Hartswick, Jayant Kalagnanam, Jurij Paraszczak, and Peter Williams. Foundations for smarter cities. *IBM Journal of research and development*, 54(4):1–16, 2010.
9. SN Kondepudi, V Ramanarayanan, A Jain, GN Singh, NK Nitin Agarwal, R Kumar, R Singh, P Bergmark, T Hashitani, P Gemma, et al. Smart sustainable cities analysis of definitions. *The ITU-T focus group for smart sustainable cities*, 2014.
10. Bhagya Nathali Silva, Murad Khan, and Kijun Han. Towards sustainable smart cities: A review of trends, architectures, components, and open challenges in smart cities. *Sustainable Cities and Society*, 38:697–713, 2018.
11. M Al-Azzam and Malik Bader Alazzam. Smart city and smart-health framework, challenges and opportunities. *Int. J. Adv. Comput. Sci. Appl*, 10(2):171–176, 2019.
12. Aldina R Avdić, Ulfeta M Marovac, and Dragan S Janković. Smart health services for epidemic control. In *2020 55th International Scientific Conference on Information, Communication and Energy Systems and Technologies (ICEST)*, pages 46–49. IEEE, 2020.
13. Diane J Cook, Glen Duncan, Gina Sprint, and Roschelle L Fritz. Using smart city technology to make healthcare smarter. *Proceedings of the IEEE*, 106(4):708–722, 2018.
14. Ayca Kirimtut, Ondrej Krejcar, Attila Kertesz, and M Fatih Tasgetiren. Future trends and current state of smart city concepts: A survey. *IEEE Access*, 8:86448–86467, 2020.
15. Hamdan Hejazi, Husam Rajab, Tibor Cinkler, and László Lengyel. Survey of platforms for massive iot. In *2018 IEEE International Conference on Future IoT Technologies (Future IoT)*, pages 1–8. IEEE, 2018.

- 14 A.F. Fuentes et al.
16. Javier Andreu-Perez, Daniel R. Leff, H. M. D. Ip, and Guang-Zhong Yang. From wearable sensors to smart implants—toward pervasive and personalized healthcare. *IEEE Transactions on Biomedical Engineering*, 62(12):2750–2762, 2015.
  17. Lili Liu, Eleni Stroulia, Ioanis Nikolaidis, Antonio Miguel-Cruz, and Adriana Rios Rincon. Smart homes and home health monitoring technologies for older adults: A systematic review. *International journal of medical informatics*, 91:44–59, 2016.
  18. Ministerio de Salud de Colombia. [www.minsalud.gov.co/salud/publica/vacunacion/paginas/mivacuna.aspx](http://www.minsalud.gov.co/salud/publica/vacunacion/paginas/mivacuna.aspx).
  19. Sérgio Fernandes and Jorge Bernardino. What is bigquery? In *Proceedings of the 19th International Database Engineering & Applications Symposium*, pages 202–203, 2015.
  20. Caio Ribeiro Pereira. *Building APIs with Node.js*. Springer, 2016.
  21. Ying Zhu. Introducing google chart tools and google maps api in data visualization courses. *IEEE computer graphics and applications*, 32(6):6–9, 2012.
  22. Kazunori Sato. An inside look at google bigquery. *White paper*, URL: <https://cloud.google.com/files/BigQueryTechnicalWP.pdf>, 2012.
  23. Mark Mucchetti. Bigquery ml. In *BigQuery for Data Warehousing*, pages 419–468. Springer, 2020.
  24. Jordan Tigani and Siddhartha Naidu. *Google BigQuery Analytics*. John Wiley & Sons, 2014.
  25. Daniel W Goldberg, John P Wilson, and Craig A Knoblock. From text to geographic coordinates: the current state of geocoding. *URISA journal*, 19(1):33–46, 2007.
  26. Bo Cheng, Shuai Zhao, Junyan Qian, Zhongyi Zhai, and Junliang Chen. Lightweight service mashup middleware with rest style architecture for iot applications. *IEEE Transactions on Network and Service Management*, 15(3):1063–1075, 2018.
  27. Dany Laksono. Testing spatial data deliverance in sql and nosql database using nodejs fullstack web app. In *2018 4th International Conference on Science and Technology (ICST)*, pages 1–5. IEEE, 2018.
  28. AR Martín-Vegue, JL Vázquez-Barquero, and S Herrera Castanedo. Cie-10 (i): Introducción, historia y estructura general. *Papeles medicos*, 11(1):24–35, 2002.

## Smart Mobility in Cities: Solar E-bikes share system design in the city of Ávila

E. González-González<sup>1</sup>[0000-0002-8025-2464], M. Sánchez-Aparicio<sup>1</sup>[0000-0002-7931-9561], S. La-güela<sup>1</sup>[0000-0002-9427-3864], J. Martín-Jiménez<sup>1</sup>[0000-0003-4383-9386], S. Del Pozo<sup>1</sup>[0000-0003-4869-3742] and P. de Andrés<sup>1</sup>[0000-0001-7708-3260]

<sup>1</sup> University of Salamanca, Ávila 05003, Spain  
sulaguela@usal.es

**Abstract.** Electric bicycles (e-bikes) are considered a sustainable alternative to fuel vehicles because of their capacity to reduce pollutant emissions in cities. In spite of all the benefits offered by conventional bicycles offer, e-bikes are more accepted by users thanks to being faster, more comfortable and allowing longer trips with the same effort by the user. If, solar power is used for battery recharging, the CO<sub>2</sub> emissions of e-bikes are the same as those from conventional bikes. This research is based on the city of Ávila, where previous BIPV (Building Integrated PhotoVoltaics) studies in urban furniture allowed to determine the capacity of a net of recharge points for e-bikes thanks to the surplus energy of the bus shelters. Data showed that the maximum capacity of the system proposed is 810 solar kilometers, considering the maximum consumption for an e-bike (20Wh per Km) in the city of Ávila. This capacity could cover the demand for 160 users per day considering displacements of 5 km each.

**Keywords:** solar energy, e-bikes, BIPV bus shelters, municipal self-consumption.

### 1 Introduction

Most air pollutant emissions in urban environments are caused by transport [1]. For years, government authorities have been promoting the development of emission-free mobility and supporting sustainable strategies to change the current mobility model, which is based on fossil fuels and private vehicles, to a mobility model using cycling as one of the main alternatives [2].

Comparing the bicycle as a means of urban transport with other alternatives (public buses, vehicles, motorbikes), it is the most efficient means of transport for distances under 5 km [3]. In recent years, the promotion of e-bikes has led to a significant increase in their use in urban environments, also increasing the average distance of journeys [4]. Combining the use of renewable energies with the recharging of public e-bike share systems increases the benefits of this means of transport by further reducing its carbon footprint [5].

The implementation of self-consumption strategies associated with the use of renewable energies presupposes a reduction in municipal economic expenditure [1]. Furthermore, this possibility improved the penetration of renewable energies in the urban area, as well as the transport supply. The consequent reduction of greenhouse gas emissions would lead to an improvement in the liveability of municipalities through improved air quality.

At the urban level, the Sustainable Development Goal of “sustainable cities and communities” requires the promotion of the use of alternative individual transport, such as bicycles and scooters, which allow for faster mobility and can be managed in a way that is accessible to all users and integrated with other means of public transport [6].

The use of e-bikes allows users to reach speeds similar to cars in urban environments, which homogenises the range of possibilities, increasing the perception of safety for cyclists and reducing the risk of accidents, as well as attracting users who are discouraged from cycling by the city's orography and their physical fitness [7].

Planning the distribution and sizing the different solar installations to supply the energy demand of municipal services requires prior knowledge of the particular needs of each component of this demand [8]. The optimal location of solar-powered recharging points for all the types of transport considered requires a detailed study of the autonomy of the most used batteries, as well as the influence that both the orography and the climatic conditions of the municipality have on them.

## **2 Integration of e-bike in cities**

The evolution of the use of e-bikes in urban environments has grown considerably in recent years. Nowadays, an increasing number of cities around the world have adopted public bicycle sharing systems as a transport option. According to the Bike Sharing World Map [9], there are 1892 bike-share programs in operation worldwide and 254 being planned or under construction. Cities such as Beijing, Shanghai or London [10, 11] have implemented public e-bike share systems that have led to significant reductions in energy consumption and pollutant gas emissions [1]. The combination of these systems with other means of public transport considerably reduces the dependency on private vehicles [2] and therefore reduces traffic congestion in urban environments.

A public e-bike share system needs an individual monitoring system that allows the traceability of each e-bike in order to optimise and monitor their use [9], increase the security of the e-bikes against possible acts of vandalism, and calculate autonomy and distances in real time, as well as monetise their use if necessary. This real-time control of the system allows information to be displayed to the users immediately, allowing them to know the status and availability of the network, improving user experience and acceptance [12]. Diverse technologies can be used for communication, but the casuistic of this case requires the properties of networks with low energy consumption and large coverage area. Low Power Wide Area Networks (LPWAN), such as LoRaWAN, are the best solution for monitoring public e-bike share systems [13], also improving the management and optimizing the system [14, 15].

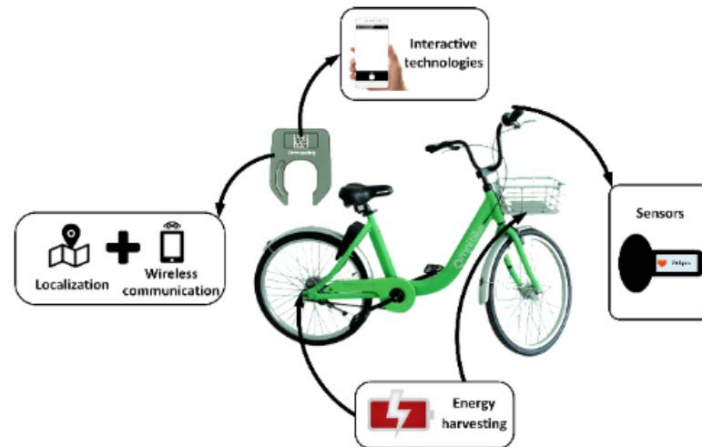


Fig. 1. E-Bike IoT monitoring. Source: [15]

## 2.1 Charging points for e-bikes.

The sizing of the e-bike fleet and the location of the charging points is a strategic decision that directly affects the achievement of the system objectives. The design of the network of services is based on an optimisation model, called the facility location model, based on decision variables such as location, capacity, coverage area and other types of properties [16, 17].

In addition, other factors can be considered, such as minimising costs and satisfying user demand as much as possible. For the case of e-bike share systems, [18] proposes a method that considers the interest of users and investors to determine the number and location of charging points, including the stock of e-bikes at the charging points in [19].

Considering the maximization of the revenue, the method presented in [16] optimizes the location of shared e-bike stations assuming a fleet size and bicycle relocation calculation for a regular operating day.

Other methods consider an optimization method that relates public bikes to private cars [20]. The methodology is essentially a bi-level mathematical programming model that optimizes the location of public bicycle stations.

GIS methodologies are also considered to estimate the potential trip demand and its spatial distribution, the location of the stations, the station capacity and demand profiling for stations [21].

Bike share system in the city of Hangzhou [22], the program Vélib in Paris (France) [23], or Bicimad in Madrid (Spain) [24], located their stations every 200 – 300 m. In small cities such as Drama (Greece) with a population close to 60K residents, a bike-sharing scheme has been introduced with 50-60 bikes in 3-5 docking stations [25].

## **2.2 Solar e-bikes integration with urban furniture.**

Considering the strategic location of the urban furniture of public transport, such as bus stops or metro stations, within the urban core, the location of e-bike charging points next to this type of furniture is the most appropriate. This type of furniture, such as bus shelters, also allows the integration of photovoltaic energy installations [8], generating its own energy and discharging surpluses into the grid when possible. These surpluses could be used to recharge e-bikes by integrating the charging points with the urban furniture.

## **2.3 E-bikes power assistant regulation**

Regulation (EU) No 168/2013 [26] on the approval and market surveillance of two- or three-wheel vehicles and quadricycles provides that all electric bicycles except those with a maximum speed of 25 km/h and a continuous rated motor output of 250 W are subject to type approval. These levels, therefore, are the maximum power levels for electric bicycles in the EU.

Other jurisdictions, such as the United States in the H.R.727 [27], consider that ‘low-speed electric bicycles’ are those with a motor output lower than 750 W and a maximum speed of 20 mph or 32 km/h. These are, therefore, not considered to be motor vehicles.

Considering EU regulations, a typical e-bike can travel up to 25 km/h, with motor power up to 250Watts, a battery of 24 V, 36 V or 48 V, and capacity depending of the manufacturer and model (Fiido D11 - 11.6 Ah [28], Fiido D2S – 7.8 Ah [29], Elops 120 – 8.7 Ah [30], Elops 920 – 11.6 Ah [31]).

The power assistance is commonly provided through either a hub motor (front or rear) or through direct drive to the chain near the crank. There can be a torque sensor built into the cranks which results in higher power assistance being provided when the rider is working the hardest (e.g. standing up or riding uphill). The controls on some models allow the user to completely turn off assistance or to vary the power assistance level. Some models include a regenerative energy feature to put power back into the battery either under braking or when traveling downhill. They can also add to the drag in the motor (compared to models with no regenerative function) which can have the advantage of moderating the speed on downhills but the disadvantage of harder pedaling once the battery is flat. [32]

# **3 Analysis of solar e-bikes integration in Ávila**

## **3.1 Solar energy in bus shelters in Ávila**

Taking into account that one of the criteria followed when selecting the locations of the charging points throughout the city of Ávila was the proximity to bus shelters with the possibility of installing solar panels on their roofs in order to use part of the energy produced at the charging points, this section aims to analyse in more detail the energy that could be used by the charging points.

Considering the results obtained in the study of installing solar panels on bus shelters in the city of Avila [8], the following table shows the surplus energy for the case of flexible panels in the different months of the year.

**Table 1.** Energy surplus for flexible panels installed on bus shelters in Ávila

Month	Energy surplus [Wh/day]
Jan.	0
Feb.	0
Mar.	445
Apr.	799
May	1208
Jun.	1493
Jul.	1625
Aug.	1333
Sep.	839
Oct.	25
Nov.	0
Dec.	0

### 3.2 Consumption of e-bikes in Ávila.

To determine the consumption of an e-bike in the city of Avila, different energy consumption studies have been performed considering the influence of real conditions such as the city orography, which is quite steep. These studies were carried out with the Fido D1 e-bike model [33], with a fully charged battery (36v, 10.7Ah, 385Ah), with a cyclist weight of 90 kg travelling along different routes throughout the city. The theoretical consumption indicated by manufacturer is about 10Wh per km. Nevertheless, the results obtained offer different consumptions, from 20Wh per km in steeper routes to 15Wh in normal routes.

Therefore, considering a consumption of 20Wh per kilometre (the most unfavourable data obtained) for an electric bicycle in the city of Ávila, the autonomy estimated would be 17.5 km, which is enough to travel from one point to another in the city of Ávila. It should be noted that the model of e-bike used does not have gear shift, which reduces the force delivered by the cyclist's pedalling in the most unfavourable conditions (start-up and slope). This consumption value can be reduced by improving this aspect of the e-bike.

### 3.3 Location of charging points for e-bikes in Ávila.

The success of the bicycle share system as a public transport alternative depends on the use that people make of bicycles to make their journeys within a city. Therefore, it is necessary to know the flow of people and their movements, in order to choose the optimal locations where there may be more demand from users to place the delivery and return systems of the bicycles.

For this study, 10 charging points have been proposed for the city of Ávila, analysing the journeys made by its inhabitants using public transport (urban buses). The following table shows the use of the different urban bus routes in the city of Avila on a working day.

**Table 2.** Daily bus users for a working day.

Bus route	Total daily users	Ratio %
Line 1	1739	27%
Line 2	472	7%
Line 3	1186	18%
Line 4	581	9%
Line 5	947	15%
Line 6	1594	24%

Taking into account the routes and uses of each line, being lines 1 and 6 the most popular, with more than 50% of total daily passengers between them, and urban points of interest such as hospitals, shopping centres and universities, we can propose the following locations for the e-bike charging points (Fig. 2).

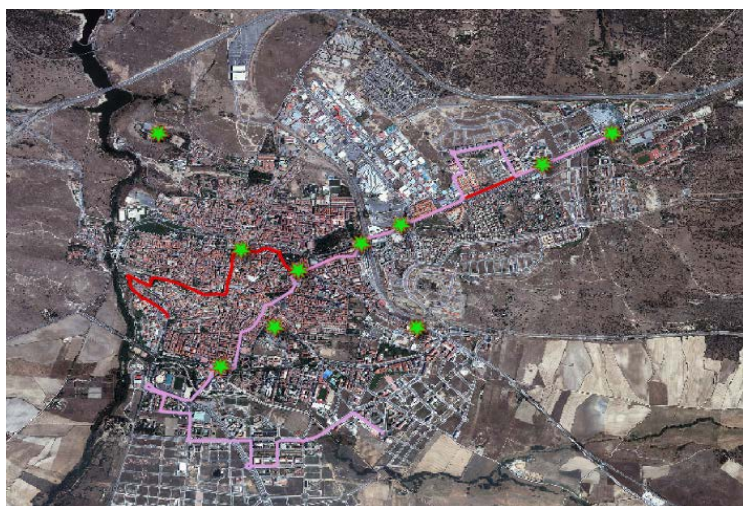


**Fig. 2.** Urban map of Ávila with the charging points proposed. Red line (Route 1) and Pink line (Route 6) show the bus routes most used.

Analysing the number of passengers throughout the day (working day), an average of 10 users is observed, with two peaks of increase, at the beginning of the working day (8:30h) and at midday (15:00h), as well as a small rise in the evening (19:30h - 20:00h). This data gives an idea of the total number of bicycles in the fleet of the municipal bicycle loan system, as well as helping in the management of the recharging process.

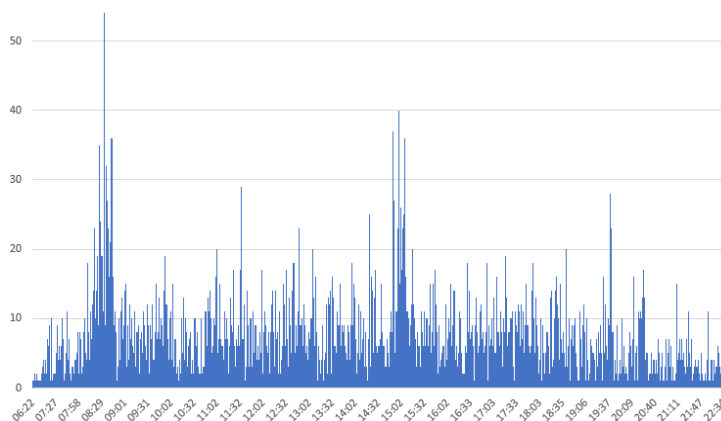


Fig. 3. Daily bus users in a working day by hours

#### 4 Discussion

Considering the most conservative case of consumption obtained from the studies carried out (20Wh) and taking into account the surplus energy coming from the photovoltaic installations integrated in the bus shelters, the following graph has been made showing the number of km per day available, for each month of the year.

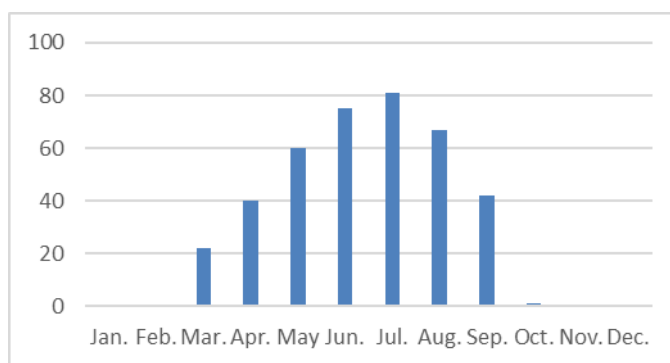
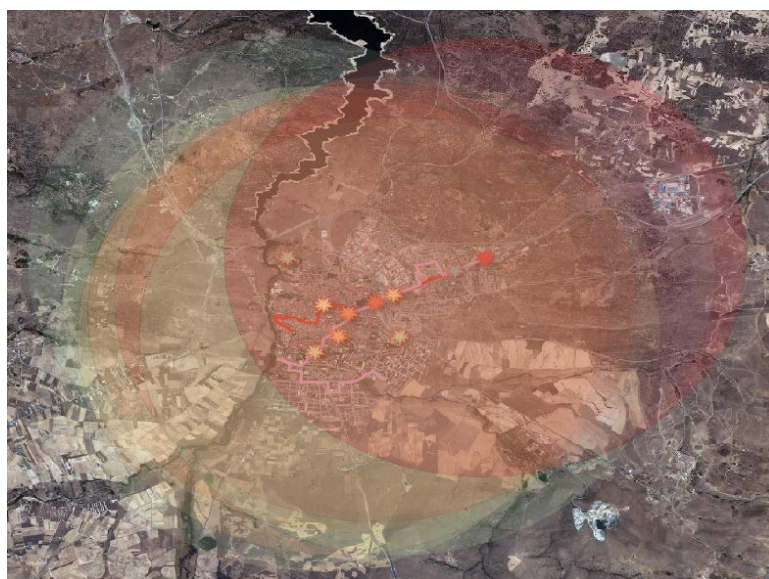


Fig. 4. Surplus energy kilometres per bus shelter by month.

The 10 charging points proposed for the city of Avila would obtain a maximum charging capacity in the most favourable month (July) of 81 km each, so that the total capacity would mean a range of 810 km per day for the fleet of e-bikes.

Analysing the travel distances for the different routes in the city of Ávila, considering any proposed charging point as a starting point, it is possible to cover the entire area of the city and part of the surrounding municipalities with a radius of 5 km. The following figure shows the 5 km buffer areas of influence for the proposed charging points.



**Fig. 5.** Buffer areas (5 km) for the charging points proposed.

The full capacity of the system proposed (810 km per day) is able to reduce 99 kg of CO<sub>2</sub> emissions regarding the use of a private car, with an average emission of 122.3 g CO<sub>2</sub> per kilometer for new cars released in 2019 [34].

## 5 Conclusions

Considering an average trip of 5 km per e-bike user per day, with the solar charging capacity of flexible solar PV panels installed on bus shelters (810 km), we can estimate a capacity of 160 users per day for the most favourable month. For the most unfavourable months (Nov., Dec., Jan and Feb.) in which there is no surplus to allow e-bike charging, the demand for e-bikes is also estimated to be lower due to the possibility of low temperatures and the snow precipitations [35]. For this reason, the production of solar energy can be considered directly related to the demand for e-bikes, which increases the benefit and advantages of the proposed system.

The city size plays an important role in affecting cycling safety (small cities are safer than bigger ones) and the very marginal cost compared to other transport investments

for a city similar to Avila regarding size and economy. This study concludes with a robust recommendation of implementing e-bikes share system in the city of Ávila.

Further research will deal with energy consumption from different models of e-bikes, with gear shift that would reduce the power demand during start-up and slope routes, because the force delivered by the cyclist's pedalling increases. This kind of improvements must be analysed in order to optimize the performance of the e-bike share system proposed.

## References

1. 'Air quality in Europe - 2020 report — European Environment Agency'. <https://www.eea.europa.eu/publications/air-quality-in-europe-2020-report> (accessed Sep. 30, 2021).
2. K. Martens, 'The bicycle as a feeding mode: Experiences from three European countries', *Transportation Research Part D: Transport and Environment*, vol. 9, pp. 281–294, Jul. 2004, doi: 10.1016/j.trd.2004.02.005.
3. 'La bicicleta como medio de transporte - Diputación Foral de Bizkaia, 2002'. Accessed: Sep. 23, 2021. [Online]. Available: <https://www.bizkaia.eus/home2/Archivos/DPTO6/Temas/Pdf/La%20bicicleta.pdf?hash=a3e7a49e7ed01243f5632d0c35dfd2c2>
4. A. Fyhri and N. Fearnley, 'Effects of e-bikes on bicycle use and mode share', *Transportation Research Part D: Transport and Environment*, vol. 36, pp. 45–52, May 2015, doi: 10.1016/j.trd.2015.02.005.
5. G. Apostolou, A. Reinders, and K. Geurs, 'An Overview of Existing Experiences with Solar-Powered E-Bikes', *Energies*, vol. 11, no. 8, Art. no. 8, Aug. 2018, doi: 10.3390/en11082129.
6. L. Böcker, E. Anderson, T. P. Uteng, and T. Throndsen, 'Bike sharing use in conjunction to public transport: Exploring spatiotemporal, age and gender dimensions in Oslo, Norway', *Transportation Research Part A: Policy and Practice*, vol. 138, pp. 389–401, Aug. 2020, doi: 10.1016/j.tra.2020.06.009.
7. B. Muñoz, A. Monzon, and D. Lois, 'Cycling Habits and Other Psychological Variables Affecting Commuting by Bicycle in Madrid, Spain', *Transportation Research Record*, vol. 2382, no. 1, pp. 1–9, Jan. 2013, doi: 10.3141/2382-01.
8. M. Sánchez-Aparicio, S. Lagüela, J. Martín-Jiménez, S. Del Pozo, E. González-González, and P. Andrés-Anaya, 'Smart Mobility in Cities: GIS Analysis of Solar PV Potential for Lighting in Bus Shelters in the City of Ávila', in *Smart Cities*, Cham, 2021, pp. 154–166. doi: 10.1007/978-3-030-69136-3\_11.
9. 'The Meddin Bike-sharing World Map'. <https://bikesharingworldmap.com/> (accessed Oct. 02, 2021).
10. Y. Tang, H. Pan, and Q. Shen, 'Bike-sharing systems in Beijing, Shanghai, and Hangzhou and their impact on travel behavior (No. 11-3862).', vol. 11, Jan. 2011.

11. H. Li, Y. Zhang, H. Ding, and G. Ren, 'Effects of dockless bike-sharing systems on the usage of the London Cycle Hire', *Transportation Research Part A: Policy and Practice*, vol. 130, pp. 398–411, Dec. 2019, doi: 10.1016/j.tra.2019.09.050.
12. 'Bike Share Map', *Bike Share Map*. <http://bikesharemap.com/> (accessed Oct. 02, 2021).
13. D. Ibrahim and D. Hussein, *Internet of Things Technology based on LoRaWAN Revolution*. 2019. doi: 10.1109/IACS.2019.8809176.
14. A. R. Al-Ali *et al.*, 'IoT-Based Shared Community Transportation System Using e-Bikes', in *2021 5th International Conference on Smart Grid and Smart Cities (ICSGSC)*, Jun. 2021, pp. 61–65. doi: 10.1109/ICSGSC52434.2021.9490509.
15. S. Shen, Z.-Q. Wei, L.-J. Sun, Y.-Q. Su, R.-C. Wang, and H.-M. Jiang, 'The Shared Bicycle and Its Network—Internet of Shared Bicycle (IoSB): A Review and Survey', *Sensors*, vol. 18, p. 2581, Aug. 2018, doi: 10.3390/s18082581.
16. I. Frade and A. Ribeiro, 'Bike-sharing stations: A maximal covering location approach', *Transportation Research Part A: Policy and Practice*, vol. 82, pp. 216–227, Dec. 2015, doi: 10.1016/j.tra.2015.09.014.
17. C. S. Revelle and H. A. Eiselt, 'Location analysis: A synthesis and survey', *European Journal of Operational Research*, vol. 165, no. 1, pp. 1–19, 2005, doi: 10.1016/j.ejor.2003.11.032.
18. J.-R. Lin and T.-H. Yang Ta-Hui, 'Strategic design of public bicycle sharing systems with service level constraints', *Transportation Research Part E: Logistics and Transportation Review*, vol. 47, no. 2, pp. 284–294, 2011, doi: 10.1016/j.tre.2010.09.004.
19. J.-R. Lin, T.-H. Yang, and Y.-C. Chang, 'A hub location inventory model for bicycle sharing system design: Formulation and solution', *Computers & Industrial Engineering*, vol. 65, no. 1, pp. 77–86, May 2013, doi: 10.1016/j.cie.2011.12.006.
20. J. P. Romero, A. Ibeas, J. L. Moura, J. Benavente, and B. Alonso, 'A Simulation-optimization Approach to Design Efficient Systems of Bike-sharing', *Procedia - Social and Behavioral Sciences*, vol. 54, pp. 646–655, Oct. 2012, doi: 10.1016/j.sbspro.2012.09.782.
21. J. C. García-Palomares, J. Gutiérrez, and M. Latorre, 'Optimizing the location of stations in bike-sharing programs: A GIS approach', *Applied Geography*, vol. 35, no. 1, pp. 235–246, Nov. 2012, doi: 10.1016/j.apgeog.2012.07.002.
22. S. Shaheen, S. Guzman, and H. Zhang, 'Bikesharing in Europe, the Americas, and Asia', *Transportation Research Record*, no. 2143, pp. 159–167, 2010, doi: 10.3141/2143-20.
23. 'Vélib' Métropole - Location de vélos en libre-service'. <https://www.velib-metropole.fr/> (accessed Oct. 02, 2021).
24. 'BiciMAD'. <https://www.bicimad.com/index.php?s=que> (accessed Oct. 02, 2021).
25. A. Nikitas, 'Understanding bike-sharing acceptability and expected usage patterns in the context of a small city novel to the concept: A story of "Greek Drama"', *Transportation Research Part F: Traffic Psychology and Behaviour*, vol. 56, pp. 306–321, Jul. 2018, doi: 10.1016/j.trf.2018.04.022.
26. 'Regulation (EU) No 168/2013 of the European Parliament and of the Council of 15 January 2013 on the approval and market surveillance of two- or three-wheel vehicles and quadricyclesText with EEA relevance', p. 77.
27. C. Stearns, 'Text - H.R.727 - 107th Congress (2001-2002): To amend the Consumer Product Safety Act to provide that low-speed electric bicycles are consumer products subject to such

- Act.’, Apr. 12, 2002. <https://www.congress.gov/bill/107th-congress/house-bill/727/text> (accessed Oct. 03, 2021).
28. ‘FIIDO D11 Folding Sport Electric Bike’, *Fiido*. <https://www.fiido.com/products/fiido-d11> (accessed Oct. 03, 2021).
  29. ‘Fiido D2S Folding Sport Electric Bike’, *Fiido*. <https://www.fiido.com/products/fiido-d2s> (accessed Oct. 03, 2021).
  30. ‘BICICLETA URBANA ELECTRICA ELOPS EBIKE 120 CUADRO BAJO NEGRO’. [https://www.decathlon.es/es/p/bicicleta-urbana-electrica-elops-ebike-120-cuadro-bajo-negro/\\_/R-p-305582](https://www.decathlon.es/es/p/bicicleta-urbana-electrica-elops-ebike-120-cuadro-bajo-negro/_/R-p-305582) (accessed Oct. 03, 2021).
  31. ‘BICICLETA URBANA ELÉCTRICA ELOPS EBIKE 920 CUADRO BAJO BLANCO’. [https://www.decathlon.es/es/p/bicicleta-urbana-electrica-elops-ebike-920-cuadro-bajo-blanco/\\_/R-p-300604](https://www.decathlon.es/es/p/bicicleta-urbana-electrica-elops-ebike-920-cuadro-bajo-blanco/_/R-p-300604) (accessed Oct. 03, 2021).
  32. G. Rose, ‘E-bikes and urban transportation: emerging issues and unresolved questions’, *Transportation*, vol. 39, no. 1, pp. 81–96, Jan. 2012, doi: 10.1007/s11116-011-9328-y.
  33. ‘Fiido Electric Bike, E-Scooter, Sea-Scooter | Fiido E-Power Sports’, *Fiido*. <https://www.fiido.com/> (accessed Oct. 03, 2021).
  34. ‘CO2 performance of new passenger cars in Europe’. <https://www.eea.europa.eu/ims/co2-performance-of-new-passenger> (accessed Nov. 22, 2021).
  35. A. E. de Meteorología, ‘Datos climatológicos - Agencia Estatal de Meteorología - AEMET. Gobierno de España’. <http://www.aemet.es/es/serviciosclimaticos/datosclimatologicos> (accessed Nov. 22, 2021).

# Smart technologies for monitoring older adults with dementia

Jessica Beltrán<sup>1</sup>, Omar A. Montoya-Valdivia<sup>2</sup> Ricardo Bañuelos-De La Torre<sup>2</sup>,  
Leonardo Melendez-Lineros<sup>2</sup>, Gabriel Parada-Picos<sup>2</sup>, Cynthia B. Pérez<sup>3</sup>, and  
Ciro Martínez-García-Moreno<sup>1</sup>

<sup>1</sup> Instituto Politécnico Nacional, México

jbeltranm@ipn.mx, cmarting@ipn.mx

<sup>2</sup> Universidad Autónoma de Baja California, México

montoya.omar@uabc.edu.mx, ricardo.banuelos@uabc.edu.mx,  
leonardo.melendez@uabc.edu.mx, gabriel.parada@uabc.edu.mx

<sup>3</sup> Instituto Tecnológico de Sonora

cynthia.perez@itson.edu.mx

**Abstract.** Nowadays, the elderly population has increased considerably as well as health problems related to old age, such as dementia. Consequently, there is a need for constant monitoring, assistance and support provided by caregivers in people's home causing high economic costs and a shortage of healthcare professionals. Informal caregivers, usually relatives, provide many caregiving services although they might suffer of stress and burden for being aware 24/7. This has motivated the development of systems based in new technologies such as Internet of Things, Cloud Services and Machine learning. In this work, we propose a system architecture based on these new technologies along with a dashboard prototype for monitoring older adults with dementia through a video, sound and map visualization. Hence, we obtained GPS, audio and video data for future behavior analysis in order to provide as well, notification services to caregivers to inform them about the status of people with dementia.

**Keywords:** internet of things, aging in place, smart monitoring, dementia, dashboard

## 1 Introduction

In cities, and generally worldwide, older adults population is on the rise since life expectancy has increased during the last decades. However, age-related health problems also have shown an increase, for instance, the number of people with dementia is expected to grow from 55 million to 139 million in 2050 [10].

People living with dementia (PwD) suffer a cognitive and a functional decline and are incrementally dependent on caregivers support. However, people with early dementia, like most older adults, choose aging in place as much as possible [7], which means they rather live in their own homes being independent instead

2 Jessica Beltrán et al.

of living in geriatric residences [19]. Indeed, public policy makers encourage new smart cities technologies for healthy aging [4] due to shortage in healthcare professionals and health services costs [16].

However, there are various risks associated with PwD aging in place, such as wandering, being engaged in hazardous activities, insufficient food and fluid intake and many others as shown in [15]. Although people in early stages of dementia might not require 24/7 attendance, their caregivers, usually a relative, can leverage their stress and burden [3] with new technologies that allow the development of systems to aid aging in place [18]. These systems can be designed to support PwD and their caregivers, for instance, by detecting when a PwD is engaged in a potentially risky situation, and notify the carer if the person has fallen, missed food or medication or any other action towards delaying geriatric residence or hospital admissions [13].

An example of these technologies is Internet of Things (IoT) that makes it possible to use wearable or fixed sensing devices in PwD houses to capture relevant data from their context. These devices can be interconnected either for sharing or for data processing purposes. Additionally, recent advances in cloud services technologies, such as those provided by Amazon Web Services (AWS) or Google Cloud, allow gathering incoming data from heterogeneous sources. These data can be transformed, processed, stored and rules can be defined to enact actions to provide services to caregivers, such as to notify them when an event has occurred. Moreover, machine learning techniques can be applied over the collected data, weather within IoT devices or within the cloud services. These techniques could be used for detecting PwD's activities, behaviors and surrounding events.

While urgent situations can be notified via messaging, dynamic dashboards allow caregivers to visualize real time information about PwD. For example, the PwD's location to know if they are wandering, the activities performed by the PwD and even a tool to see inside PwD home [17]. All of these information is gathered with sensors such as GPS devices, microphones and cameras.

In this paper, we present a system architecture base on smart technologies along with a dashboard in an scenario to support caregivers of people with early dementia. This dashboard depicts information collected and processed with IoT devices and AWS. Moreover, machine learning techniques are applied to detect relevant sounds from the environment.

In the next section, we present related work, followed by the description of the architecture, the dashboard and conclusions.

## 2 Related work

Since the availability of IoT devices, different approaches have been developed towards supporting PwD and their caregivers. Literature reviews summarize the trends, challenges and advances in this field. These reviews show that the growth of this approach started in 2000 showing a big increase from 2016 to nowadays [9]. Also, describe the emerging areas, such as robotic technology and

integrated applications [14] and recommendations to design new approaches, such as using geo-fencing services, i.e. services triggered depending on a defined location, emergency support and the incorporation of user experience [12].

Apart from data collection and transmission, processing is important when developing systems to support PwD and their caregivers. It's possible for instance, to infer behaviors or behavior changes by analyzing sensor data provided by doors sensors [11] or smart glasses [5]. The prediction of behaviors or activities can be used to generate daily reports or to alert in case of emergencies. Moreover, visualizations have been proposed to display relevant information of PwD using dashboards. For example, to inform to caregivers about sleep patterns of PwDs [8] or other activities such as dietary consumption and step counting [20].

Among the different types of sensors that can be used, we are interested in analyzing audio since it can provide relevant information from PwD context; while providing user's privacy. With audio analysis it's possible to infer activities, disruptive behaviors [2], emotions, and to identify keywords and even have interaction with users through speech recognition [6]. Moreover, it has been found that levels or quality of audio can affect the mood or emotions of PwD and that we can even relate audio levels with socialization, which is also important for their mental health [1].

In this work, we describe the development of a prototype cloud architecture and a dashboard to support PwDs and their caregivers. We are interested in provide geo-fencing services to alert in case of wandering, since it has been found to be relevant for caregivers [12]. We are also interested in performing audio processing and display sound levels in a PwD's house, to know the audio quality and because it serves as a proxy to know what the PwD doing, for instance if sound levels are bigger than a threshold are found in the kitchen it can be inferred that the person is performing an activity there. With machine learning techniques it's also possible to identify audio events and inform emergency situations to caregivers or store the events for later reports. We also display the content of a camera in PwD's homes to provide caregivers with an extra tool in case they can't communicate or know the status of PwD, for instance if they suspect PwD fell. We also provide caregivers the ability to control the camera from distance using the dashboard to move it as they find convenient. Moreover, we storage the GPS locations and events detected for further behavior analysis that can be used to monitor the deterioration or to understand more about PwD. The cloud service used has the advantage of being elastic so more sensors could be easily added.

### 3 Proposed system architecture

To collect data from PwD, we propose using the devices shown in Figure 1. The cloud architecture is based in AWS and is composed by three modules: the GPS, the sound and the camera modules, see Figure 2. The devices send data using the Message Queuing Telemetry Transport (MQTT), that is a publish-subscribe lightweight protocol commonly used in IoT.

4 Jessica Beltrán et al.

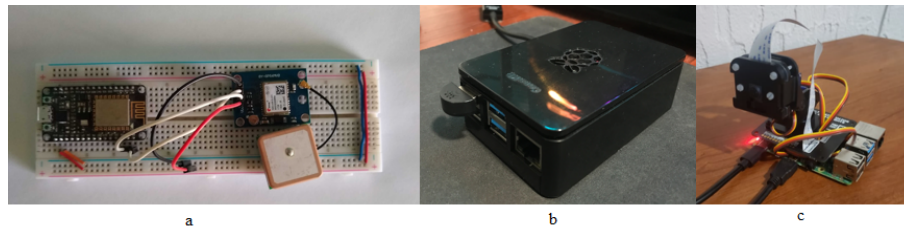


**Fig. 1.** IoT devices. a) GPS Module in NodeMCU. b) RaspberryPi 4 with mini USB microphone. c) Raspberry Pi 4 camera module, with Sony Exmor IMX219 sensor mounted over a pan-tilt hat.

### 3.1 GPS Module

The purpose of the GPS Module is to gather location information from PwD and to inform the caregiver in case the PwD has exited a predefined area over a map, i.e provide a geo-fencing service. All data is stored to be used in future work for behavior analysis. To capture location, we are using a basic GPS module in NodeMCU (see Figure 1), set to send data every minute using the MQTT protocol. Additionally, the GPS current location of the PwD is displayed in the map section of the dashboard shown in Figure 3.

The detailed description of the components of the GPS module of Figure 2 are the following:

**PwD** represents the PwD GPS tracker device.

- A0 MQTT protocol, the GPS tracker sends data with the location using this protocol. The device publishes payloads to the topic 'aws/gpsDevices'.
- A1 Broker where A0's payloads arrive. From there, they are distributed to all AWS services subscribed to the 'aws/gpsDevices' topic. Since the Dashboard is subscribed to this topic it also receives the payload for visualization.
- A2 IoT rule where the messages are distributed to both IoT Analytics and a Lambda function.
- A3 Lambda function that computes if the PwD is inside or outside a predefined virtual area. If it detects that the PwD is exiting the area, an email to notify the caregiver is sent.
- A4 Amazon Simple Email Service (SES) used to send notifications to caregivers.
- A5 IoT Analytics where the data is processed, cleaned and stored.
- A6 A Channel to pass the data to be analyzed.
- A7 A Pipeline where the data is transformed.
- A8 Lambda function that adds the timestamp to arriving payloads.
- A9 A Datastore where all the messages from the IoT Analytics channel are stored.
- A10 The Dataset where all the payloads from the GPS are stored. This can be used to query the Datastore (A9) to get historical information from the PwD
- A11 A Bucket where the Dataset is stored to allow client-applications to get the historical information.

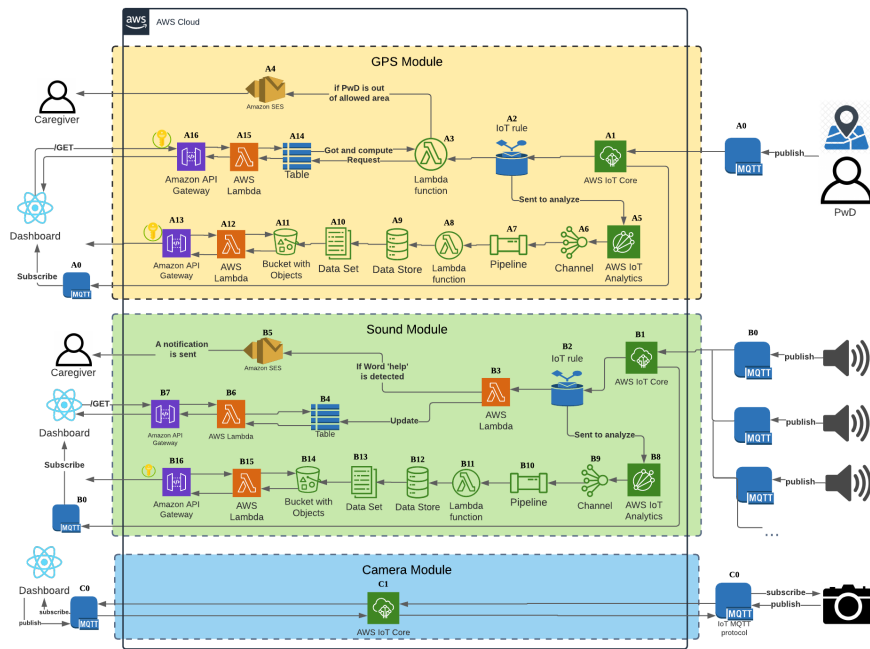


Fig. 2. Proposed system architecture. We used Lucidchart to create this figure <sup>4</sup>.

- A12 Lambda function that access the A11 Bucket to retrieve data for the Api Gateway.
- A13 Endpoint where client-applications can request the historical information.
- A14 DynamoDB table containing information about the PwD. This information comprises the location of the PwD, the caregiver email and the allowed area (described with a polygon).
- A15 Lambda function that queries the DynamoDB table A14.
- A16 Endpoint where the dashboard request the information to be displayed.

**Caregiver** is the person that will visualize the dashboard and receive notifications.

The flow of information in the GPS module is the following. First, from right to left according to the Figure 2, the GPS device from the PwD publishes to the topic “aws/GpsDevices” through MQTT protocol a message with a Json payload including the *deviceId*, *latitude*, *longitude*. The message is received by the AWS IoT Core broker.

Afterwards, two Iot Rules are defined to distribute the message. In one rule, the message is sent to a lambda function (A3) that uses the library *robust-point-in-polygon* <sup>5</sup> and a function used to classify if the PwD is inside our outside the

<sup>4</sup> <https://www.lucidchart.com/pages/es>

<sup>5</sup> <https://www.npmjs.com/package/@types/robust-point-in-polygon>

6 Jessica Beltrán et al.

polygon area. This lambda function queries the DynamoDB Table (A14) that already includes the information of a polygon defining a virtual geo-fencing. This polygon is defined previously by the caregiver. If the PwD exits the polygon area, the Lambda function (A3) invokes Amazon SES to send an email to the caregiver. Afterwards, the lambda function updates the current location stored in the DynamoDB table of the PwD with the GPS data.

The other rule is to send the payload to IoT Analytics (A5) in order to create a Dataset with the PwD's GPS historical data. The pipeline to store the data goes from A6 to A11 and the services A12-A13 will be used in case we require to query the stored data. For instance, to apply machine learning algorithms.

In the other hand, from left to right we can see that the dashboard requests the data through an endpoint (A16) to get the current location of the PwD stored in the DynamoDB table to display it as a map as seen in Figure 3.

### 3.2 Sound module

This module is in charge of managing the information coming from microphones located in the PwD's house. In this case, we process the audio information before sending it to AWS which helps maintain user privacy. The results of audio processing are stored for further behavior analysis and also displayed to the caregiver. The dashboard shows in the upper right (see Figure 3) the intensity of sounds in decibels of different rooms from the PwD house. A color map is used to show different decibels (dB) intensities (see Figure 4). These sound intensities inform to caregiver in which room are activities been performed, for example, from the Figure 3 the caregiver would interpret that the PwD is in the living room. Since the raw audio data is not sent, neither the current activities are informed, this setup allows to maintain PwD' privacy.

We used mini USB microphones (see Figure 1) to capture audio with 16kHz, 16-bits and a single channel. The microphones are connected to a RaspberryPi 4 module where we compute the root mean square (rms) and then apply the next formula to compute the decibels:  $dB = 20 \log_{10}(\text{rms}) \pm \text{ref}$ .

We trained Hidden Markov Models (HMM) using the *hmmlearn* library<sup>6</sup> over Mel Frequency Cepstral Coefficients (MFCC) obtained from the sounds using the *Python Speech Features* library<sup>7</sup> as mentioned in our previous work [6]. Since we are developing a prototype we tested only with few classes, but we planned to include more classes and to improve the F1Score results. Also, a reason to use in this case HMM is because it does not require large processing, compared to deep learning approaches, and it can be deployed within the Raspberry Pi devices. For future work, we will use Nvidia Nano devices to allow more processing. In any case, the AWS cloud architecture does not change since the payload would be the same.

If the sound intensity is larger than 20dB, we use previously trained models to classify four different types of sound events, the words "ayuda" and "help"

<sup>6</sup> <https://hmmlearn.readthedocs.io/en/latest/index.html>

<sup>7</sup> <https://python-speech-features.readthedocs.io/en/latest/>

and the sounds of "coughing" and "unknown" (keyboard, yawn, singing, etc.). Each HMM model was trained using 10 recordings and tested with 5 different recordings, giving a 90% of F1Score. The purpose of classifying these keywords is to identify if the PwD is trying to ask for help, for example if he/she fell. Predefined keywords would send a notification to caregivers. In general, the detection of all sound events will be stored for future behavior analysis.

We formed a json payload to send it to AWS using *Paho MQTT client*<sup>8</sup>. This payload includes the *dB* and the *class* with the type of sound detected. The detailed description of the components of sound module of Figure 2 are the following:

- B0 MQTT protocol. The sound devices send information about their sound intensity and the event detected using this protocol, the device publishes to the topic 'aws/soundDevices.
- B1 Is the broker where B0's payloads arrive and are distributed to all the devices that are subscribed to a 'aws/soundDevices topic. Since the dashboard is subscribed to this topic, it also receives the payload for visualization.
- B2 Iot rule where the message is distributed to IoT Analytics and to a Lambda function.
- B3 Lambda function that checks if the payload from B0 has an attribute 'tag' with the value 'help'. If it has it, it sends a notification to the caregiver using Amazon SES.
- B4 DynamoDB table where data about the sound devices attached to the cloud are stored
- B5 Amazon SES to send email notifications to the Caregiver.
- B6 Lambda function that gets the data from the DynamoDB table B4
- B7 An Endpoint where the dashboard requests the data from the sound devices stored in a DynamoDB table B4 using a lambda function B6.
- B8 IoT Analytics where the data is processed, cleaned and stored.
- B9 A Channel where the data passes through in order to get analyzed.
- B10 A Pipeline where the data is transformed using activities.
- B11 A Lambda function that adds the current time to the new payload from a device.
- B12 A Datastore where all the messages from an IoT Analytics channel are stored.
- B13 Dataset where all the payloads from the sound devices devices are stored. This Dataset queries the Datastore B12 to retrieve data. In this case the historical data is stored in order to do machine learning with it.
- B14 A Bucket where the data of the Dataset is stored so that client-applications can get the historical data of any sound devices .
- B15 Lambda function that access the B14 bucket to retrieve the data for the Api Gateway
- B16 An endpoint where the dashboard requests the required information about the sound devices.

The Dashboard is the same in all modules.

<sup>8</sup> <https://www.eclipse.org/paho/index.php?page=clients/python/index.php>

8 Jessica Beltrán et al.

The flow from the sound module is similar to the GPS module. The difference is that in this module a notification is sent in case that a keyword suggesting help has been detected and instead of location, the sound intensity levels are sent to the dashboard. The three dots in the sound module indicate that more sound devices could be added without changing the cloud's architecture.

### 3.3 Camera module

The purpose of this module is to display the content of a camera inside the PwD's home. This camera is mainly turned off, due to privacy constraints, however, if the caregivers considers important to visualize video from within the PwD's house it can be turned on. Moreover, the caregiver can move the camera using the dashboard to explore different parts of a room. We used a Raspberry Pi 4 camera module, with Sony Exmor IMX219 Sensorlens to broadcast images of 640x480 pixels to the main dashboard every second (although the camera can reach over 4k resolution at 60fps). We encode the image using the standard python library *base64* to send it to AWS using MQTT. The camera was mounted in a two degrees of freedom structure (pan-tilt HAT) that uses two servo motors to move it from -90 to 90 degrees (see Figure 1). These signals can be controlled with a python library called *pantiltthat*<sup>9</sup>. To control the camera-movement we made a 5 button control on the main dashboard that sends (via MQTT) two variables that moves the structure with a 5 degrees resolution.

The description of the Camera module from Figure 2 is the following.

- C0 MQTT protocol, the camera device sends an image every second, the device publishes to the topic 'aws/cameraView'. The Dashboard publishes to the 'aws/cameraControls' topic using MQTT to remotely control the camera.
- C1 Is the broker where C0's payloads arrive and are distributed to the Dashboard, that is subscribed to a 'aws/cameraView' topic and to the camera that is suscribed to the 'aws/cameraControls' topic.

## 4 Dashboard

The proposed dashboard consists of multiple panels that show visualizations of the data being generated by heterogeneous sensors, see Figure 3. Data queried from AWS Tables A14 and B4 is processed within the dashboard platform to provide updated and accurate visualizations of the PwD's current state. The dashboard shows the location of the PwD in case that wandering is suspected, sound levels in their home serve as a proxy of the activities that the PwD is performing and to monitor the sound quality and video coming from a camera located in the PwD's home in case the caregivers needs to see if she/he suspects risks or that the PwD fell. For the later case, the dashboard is interactive providing buttons to the caregiver to move the camera.

<sup>9</sup> <https://github.com/pimoroni/pantilt-hat>

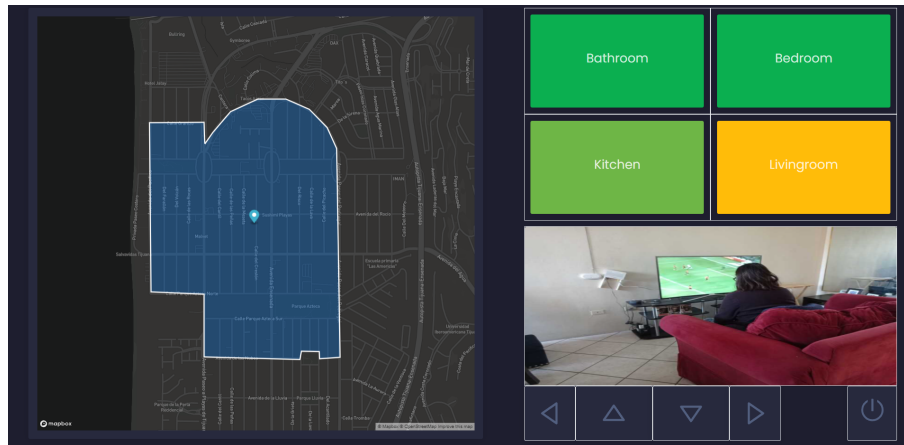


**Fig. 3.** Example of a visualization of the Dashboard. In the left, the map is shown along with a predefined area. In the upper right, the sound levels are shown and in the lower right, the video along with the camera controls are shown.

The dashboard is designed with simplicity in mind, and to provide to users important information without having to navigate menus. A dark scheme with contrasting colors is used, where the elements can be easily distinguished from each other. The dashboard is based on the React project, since it provides useful tools for bootstrapping a web app. The widespread support React also provides advantages in terms of the implementation of useful libraries and tools, such as Mapbox and MaterialUI. Considering the cases of a monitoring application, the dashboard has to be accessible from different devices, while being simple to use.

#### 4.1 Map visualization

We decided to implement the map visualization using *Mapbox GL JS*<sup>10</sup>, a JavaScript library useful for rendering custom maps. The map panel focuses on the PwD's home location and the surrounding area, with indicators that show the current position of the GPS sensor, as well as a blue outline of the area geofenced. The caregiver can move, zoom in or out, and drag the map as needed.

The geolocation data from the sensors is rendered through the use of layers, which define the way data is represented on the map. This data is obtained from multiple types of sources. Given that we are working with JSON, we can format the data obtained from the endpoint into a *GeoJSON*<sup>11</sup> data type, since Mapbox supports it nicely. The GPS coordinates of the sensor are used to create a marker object that the user can click on to obtain additional information.

Currently, the GPS coordinates defining the geofenced polygon are predefined within a DynamoDB table inside the cloud architecture (A14 from Figure

<sup>10</sup> <https://docs.mapbox.com/mapbox-gl-js/api/>

<sup>11</sup> <https://geojson.org/>

10 Jessica Beltrán et al.

2). However, in a future work, we will allow the caregiver to changes it. We chose polygons instead of squares since allow delimitate better on map streets, as shown in the defined area in Figure 3.

#### 4.2 Sound visualization

Sound levels in each of the rooms can be monitored through the corresponding panel, showing the decibels reported by each sensor, with the intensity of the background color changing according to a predefined threshold (see Figure 4) . The number of panels can be adjusted depending on the amount of sensors used.



Fig. 4. Sound intensity levels colors

#### 4.3 Video visualization

A component containing the camera feed is used to observe a particular room. The React app uses the *aws-iot-device-sdk*<sup>12</sup> to subscribe to a IoT Core topic where the device that operates the camera continuously publishes images encoded using the base64 Python library. The use of the MQTT protocol allows for a streamlined flow of data from our distributed devices all the way to the dashboard application. Accounting for possible image quality fluctuations, the image component takes up a relatively small space. There are several buttons located below the camera feed. The user can turn the camera on or off by pressing the power button. A yellow icon indicates that the camera is powered on. The user can also control the camera angle with the arrow buttons.

## 5 Conclusions and future work

Our main contribution in this work is the implementation of a system oriented to support PwD and their caregivers. The adoption of this systems within smart cities brings social benefits since allows to reduce stress and burden of people with caregiving activities, it also provides them the opportunity to work and perform other activities besides caregiving. This system takes advantage of several available benefits from current technologies. For example, the ability to deploy a complete infrastructure to manage and process data using AWS. This infrastructure can be easily modified and scaled if new services or devices are added and it can manage data from heterogeneous sources. We implemented

<sup>12</sup> <https://github.com/aws/aws-iot-device-sdk-js>

audio processing and machine learning algorithms over inexpensive computing devices, such as the Raspberry Pi module, to detect sound events that can be used to infer PwD's activities, this can be used for future behavior analysis and to provide monitoring elements to caregivers. We also implemented a geo-fencing notification services to inform caregivers if a PwD could be wandering and to notify if a help scream has been detected. Future directions include sessions with older adults with mild dementia and their primary caregivers to conduct a user-centered design approach and further evaluation of the user experience and effectiveness of the system. Another work in progress is to develop a wearable device for GPS data gathering. Additionally, we will work in including the detection of more sound classes and automatic image analysis to detect falls or other relevant events. Another future direction includes to develop a communication channel between the PwD and the caregiver, for example using voice assistant devices. Finally, we can take advantage of having stored data to analyze and find patterns and predictions about the PwD's behavior.

## 6 Acknowledgments

This work was partially supported by project 20210010 from the Secretaría de Investigación y Posgrado of the Instituto Politécnico Nacional in Mexico.

## References

1. Aletta, F., Botteldooren, D., Thomas, P., Vander Mynsbrugge, T., De Vriendt, P., Van de Velde, D., Devos, P.: Monitoring sound levels and soundscape quality in the living rooms of nursing homes: a case study in flanders (belgium). *Applied Sciences* **7**(9) (2017) 874
2. Beltrán, J., Navarro, R., Chávez, E., Favela, J., Soto-Mendoza, V., Ibarra, C.: Recognition of audible disruptive behavior from people with dementia. *Personal and Ubiquitous Computing* **23**(1) (2019) 145–157
3. Bossen, A.L., Kim, H., Williams, K.N., Steinhoff, A.E., Strieker, M.: Emerging roles for telemedicine and smart technologies in dementia care. *Smart homecare technology and telehealth* **3** (2015) 49
4. Bryant, N., Spencer, N., King, A., Crooks, P., Deakin, J., Young, S.: Iot and smart city services to support independence and wellbeing of older people. In: 2017 25th International Conference on Software, Telecommunications and Computer Networks (SoftCOM), IEEE (2017) 1–6
5. Chen, W.L., Chen, L.B., Chang, W.J., Tang, J.J.: An iot-based elderly behavioral difference warning system. In: 2018 IEEE International Conference on Applied System Invention (ICASI), IEEE (2018) 308–309
6. Cruz-Sandoval, D., Beltran-Marquez, J., Garcia-Constantino, M., Gonzalez-Jasso, L.A., Favela, J., Lopez-Nava, I.H., Cleland, I., Ennis, A., Hernandez-Cruz, N., Rafferty, J., Synnott, J., Nugent, C.: Semi-automated data labeling for activity recognition in pervasive healthcare. *Sensors* **19**(14) (2019)
7. Grave, A., Robben, S., Oey, M., Ben Allouch, S., Mohammadi, M.: Requirement elicitation and prototype development of an intelligent environment to support people with early dementia. In: 2021 17th International Conference on Intelligent Environments (IE). (2021) 1–8

12 Jessica Beltrán et al.

8. Hu, X., Abdulghani, A.M., Imran, M., Abbasi, Q.H.: Internet of things (iot) for healthcare application: Wearable sleep body position monitoring system using iot platform. In: Proceedings of the 2020 International Conference on Computing, Networks and Internet of Things. (2020) 76–81
9. Morato, J., Sanchez-Cuadrado, S., Iglesias, A., Campillo, A., Fernández-Panadero, C.: Sustainable technologies for older adults. *Sustainability* **13**(15) (2021)
10. Organization, W.H.: Dementia. <https://www.who.int/news-room/fact-sheets/detail/dementia> (2021) Accessed: 2021-09-30.
11. Pandey, P., Litoriya, R.: An iot assisted system for generating emergency alerts using routine analysis. *Wireless Personal Communications* (2020) 1–24
12. Ray, P.P., Dash, D., De, D.: A systematic review and implementation of iot-based pervasive sensor-enabled tracking system for dementia patients. *Journal of medical systems* **43**(9) (2019) 1–21
13. Rostill, H., Nilforooshan, R., Morgan, A., Barnaghi, P., Ream, E., Chrysanthaki, T.: Technology integrated health management for dementia. *British journal of community nursing* **23**(10) (2018) 502–508
14. Stavropoulos, T.G., Papastergiou, A., Mpaltadoros, L., Nikolopoulos, S., Kompatsiaris, I.: Iot wearable sensors and devices in elderly care: A literature review. *Sensors* **20**(10) (2020)
15. Thoma-Lürken, T., Bleijlevens, M.H., Lexis, M.A., de Witte, L.P., Hamers, J.P.: Facilitating aging in place: A qualitative study of practical problems preventing people with dementia from living at home. *Geriatric Nursing* **39**(1) (2018) 29–38
16. van Boekel, L.C., Wouters, E.J., Grimberg, B.M., van der Meer, N.J., Luijkx, K.G.: Perspectives of stakeholders on technology use in the care of community-living older adults with dementia: A systematic literature review. *Healthcare* **7**(2) (2019)
17. VandeWeerd, C., Yalcin, A., Aden-Buie, G., Wang, Y., Roberts, M., Mahser, N., Fnu, C., Fabiano, D.: Homesense: Design of an ambient home health and wellness monitoring platform for older adults. *Health and Technology* **10**(5) (2020) 1291–1309
18. Wang, S., Bolling, K., Mao, W., Reichstadt, J., Jeste, D., Kim, H.C., Nebeker, C.: Technology to support aging in place: Older adults’ perspectives. *Healthcare* **7**(2) (2019)
19. Wiles, J.L., Leibing, A., Guberman, N., Reeve, J., Allen, R.E.S.: The Meaning of “Aging in Place” to Older People. *The Gerontologist* **52**(3) (10 2011) 357–366
20. Yoo, B., Muralidharan, S., Lee, C., Lee, J., Ko, H.: Klog-home: A holistic approach of in-situ monitoring in elderly-care home. In: 2019 IEEE International Conference on Computational Science and Engineering (CSE) and IEEE International Conference on Embedded and Ubiquitous Computing (EUC), IEEE (2019) 390–396

## **Análisis inteligente de oferta de estacionamientos de bicicletas potenciales aplicando diagrama de Voronoi y densidad Kernel: Caso Centro Histórico de Arequipa**

Edith Gabriela Manchego Huaquipaco<sup>1</sup>, Belen Arlett Flores Chambi<sup>1</sup>, Ernesto Mauro Suarez Lopez<sup>1</sup>, Cinthya Lady Butrón Revilla<sup>1</sup> and Ursula Estefany Pinto Enriquez<sup>1</sup>

<sup>1</sup> Universidad Nacional de San Agustín de Arequipa, Perú  
emanchegoh@unsa.edu.pe  
bfloresc@unsa.edu.pe  
cbutronr@unsa.edu.pe  
esuarezl@unsa.edu.pe  
upintoe@unsa.edu.pe

**Abstract.** Las ciudades presentan condicionantes físicas o geográficas para la elección de desplazamientos, los cuales se miden de forma objetiva. Sin embargo, existen condicionantes subjetivas intrínsecas a cada usuario que se presentan como un desafío para la toma de decisiones en planificación urbana. En este sentido, este estudio se enfoca en el desarrollo de una metodología que evalúe de forma inteligente los desplazamientos de los ciclistas y la oferta de estacionamientos públicos y privados para el cálculo de la demanda de servicio de aparcamientos para usuarios ciclistas y la relación entre la densidad de estacionamientos y el flujo de ciclistas. El estudio de caso elegido fue el Centro Histórico de Arequipa, la muestra seleccionada fueron 50 ciclistas y 79 rutas registradas en el app Strava, que se clasificaron por intensidad de flujo alta, media y baja y Así también, se realizó el levantamiento de la oferta de estacionamientos existentes en el área de estudio. Con los datos obtenidos, se empleó el diagrama de Voronoi para determinar el estacionamiento más cercano al que puede acceder un ciclista y densidad Kernel evaluar el área de cobertura del servicio de estacionamientos. Los resultados obtenidos permiten identificar la demanda de servicios ciclistas a partir del análisis inteligente de oferta disponible y del comportamiento ciclista, brindado un aporte para la planificación de ciudades empleando fuentes de datos disponibles. evaluar adecuadamente cuando las áreas de cobertura de dos o más estacionamientos que se intersecan.

**Keywords:** Comportamiento Ciclista, Estacionamientos, Movilidad Inteligente, Planificación del Transporte.

## 1 Introducción

La movilidad urbana ha tenido una mayor evolución hacia una movilidad inteligente con el desarrollo de conceptos como el internet de las cosas. Además, uno de los desafíos en la movilidad urbana sostenible es determinar servicios de movilidad activa que incrementen los desplazamientos en modos de transporte no motorizados. Por otro lado, las ciudades latinoamericanas presentan centros históricos con características peculiares como la estructura urbana, manzaneo cuadrangular y calles ortogonales y estrechas, edificios históricos tanto civiles como religiosos. Además, la conservación patrimonial y la perdurabilidad como centro habitado de la ciudad exigen la realización de actuaciones para la promoción de estrategias inclusivas que mejoren la calidad de vida de sus habitantes.

Al estudiar el territorio bajo el nuevo paradigma de la movilidad urbana sostenible, se requiere una aproximación a entender el comportamiento de los desplazamientos comprendidos en el concepto de micro movilidad. En este contexto, como parte de las políticas y planes de promoción de modos activos en ciudades emergente, la implementación de estacionamientos de bicicleta ha cobrado un reciente interés por parte de las autoridades y planificadores, teniendo en cuenta el comportamiento del usuario ciclista, sus preferencias y su influencia. Por lo tanto, los escasos de datos libres en la gestión pública y los escasos presupuestos, obligan a los técnicos a experimentar con nuevas herramientas de análisis del territorio, como el Diagrama de Voronoi y Densidad de Kernel que aportan en el análisis de la oferta y demanda de servicios ciclistas.

Esta investigación, se enfoca en analizar el comportamiento del ciclista y su influencia en los potenciales espacios de estacionamientos para bicicletas en un sector de la ciudad de Arequipa. Para ello, el uso de software de procesamiento de datos geoposicionados han sido aplicados en otras investigaciones para contribuir con los estudios de movilidad compartida, movilidad activa y micro movilidad. El documento está organizado de la siguiente manera: presentación de la aborda la literatura académica, luego el desarrollo de la metodología explicando el estudio de caso, que dará paso a los resultados y finalmente las conclusiones del trabajo.

## 2 Marco Teórico

### 2.1 La planificación de movilidad urbana sostenible

El concepto de movilidad se refiere a una serie de variables que incorpora condiciones sociales, políticas, económicas y culturales de quienes se movilizan a diferencia del transporte que sólo considera los desplazamientos [1]. Entonces el concepto de movilidad urbana sostenible debe ser entendido como el resultado de un conjunto de políticas de transporte y circulación que buscan proporcionar el acceso amplio y democrático al espacio urbano, a través de la priorización de los modos no motorizados y colectivos

de transportes, de forma efectiva, socialmente inclusiva y ecológicamente sostenible, basado en las personas y no en los vehículos [2]. Entonces, al añadirse al concepto de movilidad urbana el calificativo de sostenible se aspira a una planificación que restablezca el equilibrio entre todos los medios de desplazamiento [3]. Por tanto, la planificación de la movilidad urbana sostenible prioriza la promoción de viajes para el transporte no motorizado.

## **2.2 Toma de decisiones basada en datos libres para la planificación**

Las primeras civilizaciones recolectaban datos para gestionar su territorio. Como afirma Scott [4], el acto mismo de recolectar datos y medir diferentes aspectos de la sociedad se estableció a favor de la clase dominante, ya sea mediante la recaudación de impuestos o el establecimiento de derechos territoriales. Por otro lado, hoy en día los sistemas digitales producen inmensos flujos de datos que pueden emplear para el bien público y para ayudar a informar cómo gestionar y planificar ciudades [5]. Además, la recolección de datos puede realizarse con la participación de personas interesadas y seleccionadas en los lugares de estudio. También es importante reconocer la necesidad de la objetividad en el manejo, análisis e interpretación de datos para la toma de decisiones en particular en la planificación de las ciudades.

Las ciudades requieren de planes de promoción del transporte no motorizado, TNM, siendo este cualquier forma de transporte que no se basa en mecanismos impulsados por baterías y/o combustión de combustible [6]. En este sentido los planificadores de transporte se encuentran desarrollando planes de movilidad alternativa, promoviendo el uso del TNM. Sin embargo, los limitados recursos económicos de los gobiernos locales y la falta de estudios en ciudades en vías de desarrollo condicionan la toma de decisiones a la experiencia del planificador [7]. En los últimos años, los gobiernos locales vienen impulsando la implementación de infraestructura ciclista e instalaciones como estacionamientos para bicicletas, a través de planes de movilidad urbana sostenible, redes de infraestructura ciclista, sistemas de bicicleta compartida, entre otros. En la planificación del transporte no motorizado, los datos libres deben integrarse en los procesos de formulación de planes y proyectos. Los datos permiten ofrecer una amplia gama de perspectivas y comunicación directa de planificadores, usuarios y público en general. Además, los datos libres proporcionan un medio rápido y económico de recopilar información de un grupo disperso de personas [8].

## **2.3 Servicio de bici estacionamiento y el comportamiento de su uso**

La promoción del transporte no motorizado, como la bicicleta, requiere no solo de infraestructura vial sino de servicios complementarios. Existen estudios vinculados al servicio de estacionamiento de bicicletas, que se han abordado desde una perspectiva transversal con resultados limitados y específicos, generando la necesidad de realizar investigaciones de manera integral para una mejor comprensión a nivel ciudad [9]. Se ha identificado que los servicios relevantes para promover el uso de la bicicleta son la disponibilidad de estacionamientos sea público o privado, presencia de una red óptima

de ciclovías, su acondicionamiento para distancias cortas y el costo de alquiler en el caso de tener bicicletas públicas [10], [11]. En este sentido, Heinen and Buehler [9], mencionan que el nivel de servicio de estacionamiento para bicicletas se evalúa por 3 aspectos: (i) la protección y seguridad garantiza el nivel de calidad, (ii) el cobro por estacionamiento reduce las posibilidades de usar la instalación y (iii) la necesidad de estacionamientos frente a la oferta se evidencia con bicicletas ancladas a mobiliario urbano al que no está destinado con esa función. Si se garantizan estas condiciones, puede alentar a ciclistas y ciclistas potenciales a movilizarse con mayor facilidad.

Los datos obtenidos desde los dispositivos móviles de los ciudadanos pueden utilizarse como base para las herramientas de planificación urbana. Este tipo de datos puede facilitar tareas de análisis, como la extracción de patrones de movilidad humana [12], o la determinación de la dinámica urbana de las ciudades. Además, los datos obtenidos desde diferentes usuarios se pueden visualizar simultáneamente en una sola vista, de esta forma es posible identificar trayectorias o agrupaciones de desplazamiento. Además, se puede analizar la similitud entre trayectorias, similitud entre puntos dentro de una misma agrupación, encontrar desplazamientos anómalos [13]. En este sentido, el análisis de datos para la movilidad urbana se puede utilizar para comprender el comportamiento de los ciudadanos y mejorar los servicios, el transporte y el uso de las zonas urbanas [14].

#### **2.4 Evaluación inteligente de servicios potencial de estacionamientos en base al comportamiento de viajes ciclistas**

La aplicación del paradigma del internet de las cosas en la planificación de la movilidad urbana sostenible permite la mejora de los servicios y experiencia del usuario por medio del desarrollo de aplicaciones, el uso del teléfono inteligente o dispositivos portátiles [15]. El uso de estas herramientas digitales basadas en la web permiten recopilar, analizar y compartir información espacial puede ser ofrecida voluntariamente por individuos [16]. Hoy en día existen diversas aplicaciones de rastreo, que muestran los desplazamientos de diversos usuarios con información georreferenciada que permiten analizar el comportamiento [17]. Los datos de las aplicaciones de rastreo tienen el potencial de proporcionar un seguimiento en tiempo real de los ciclistas en el tiempo y el espacio [18], [19]. El seguimiento de las actividades en bicicleta en el espacio y el tiempo es esencial para los planificadores de transporte activos, ya que pueden asignar recursos limitados donde más se necesitan [20]. Se ha demostrado que los datos de VGI proporcionan información útil sobre los comportamientos de elección de ruta de los ciclistas y el origen - destino de los viajes en bicicleta [16].

El comportamiento de los viajes está influenciado por factores como actitudes y preferencias, como hábitos e influencias impulsivas [21]. Por ejemplo, se ha observado que los datos de Strava representan de manera desproporcionada a ciclistas hombres y de mediana edad [18]. Además, tomar decisiones de transporte basadas únicamente en datos de fuentes colaborativas puede favorecer a las personas privilegiadas que tienen

acceso a la tecnología y excluir automáticamente las opiniones de los usuarios vulnerables de la carretera, como niños, adultos mayores y personas de bajos ingresos [16]. Una de las formas propuestas para compensar este sesgo es fusionar los diferentes conjuntos de datos de fuentes colaborativas o fusionar datos de fuentes colaborativas con otras fuentes de datos [22]. El 66% de los ciclistas encuestados informaron que no usaban ninguna aplicación de seguimiento de actividad física, aproximadamente el 16% de los ciclistas informaron usar la aplicación Strava para monitorear sus actividades de ciclismo y el 18% informó usar otras aplicaciones de seguimiento de actividad física.

Entonces, el análisis inteligente de servicios para el transporte no motorizado se fundamenta en sus actores y los datos existentes que permiten a los planificadores tomar decisiones, identificar comportamientos de los usuarios, reconocer niveles de oferta para los no usuarios (Ver Figura 1)

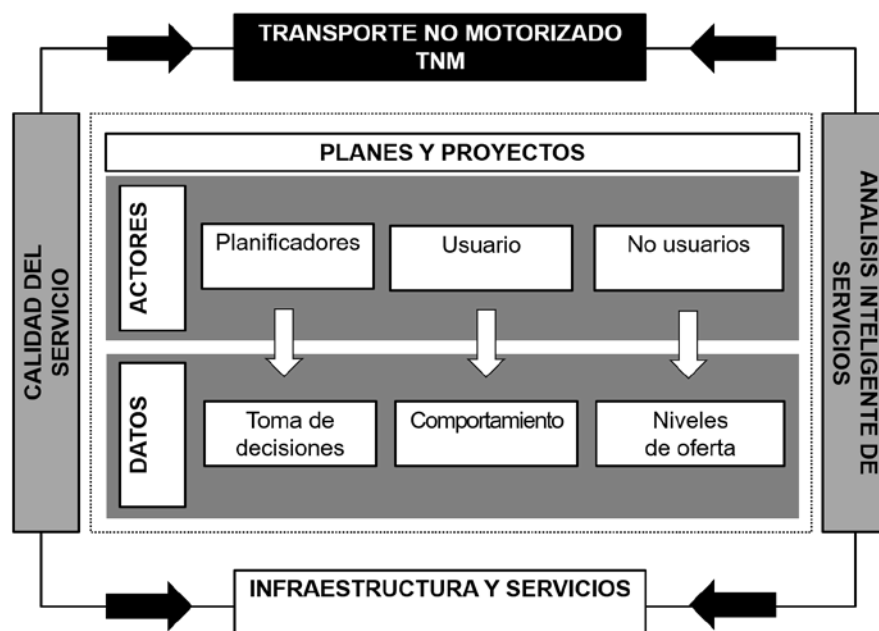


Figura 1. Análisis Inteligente de Servicios para el transporte no motorizado. Fuente: Elaboración propia.

### 3 Metodología

#### 3.1 Caso de estudio

La ciudad de Arequipa ubicada en el sur de Perú, localizada a una altitud 2.328 msnm. El emplazamiento de la ciudad es sobre el valle de Arequipa, protegido al norte y al este por la faja cordillerana andina y hacia el sur y oeste por las cadenas bajas de cerros. Desde la ciudad se observan una serie de conos volcánicos que forman nevados como el Misti, Chachani y Pichu Pichu. Según el Instituto Nacional de Estadística e Informática (INEI) tiene 1 millón 316 mil habitantes al 2017; siendo el 24,0% menores de 15 años, el 64,3% posee de 15 a 59 años y el 11,7% son adultos mayores.

Además, posee un centro histórico de más de 332 hectáreas y declarado Patrimonio Cultural de la Humanidad por la UNESCO en el año 2000. El patrimonio histórico y monumental que alberga y sus diversos espacios escénicos y culturales la convierten en una ciudad receptora de turismo nacional e internacional. Su centro histórico está configurado por dos polígonos de gestión, el primero conformado por el damero español con 49 manzanas, cada una de 200 m de lado aproximadamente (polígono rojo); el segundo polígono denominado zona de amortiguamiento con una configuración urbana diversa (línea gris), como se observa en la figura 2:

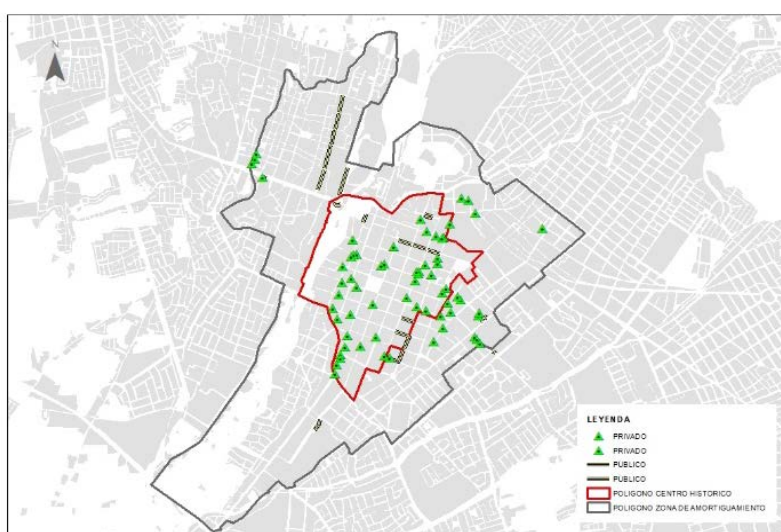


**Figura 2.** Distribución de estacionamientos en el Centro Histórico. Fuente: Elaboración propia.

El centro histórico de Arequipa concentra la mayoría de servicios públicos como salud, educación a distintos niveles y equipamientos administrativos. En consecuencia, es el punto de destino de la mayoría de viajes obligados de los ciudadanos.

### 3.2 Recolección de los datos

La recolección de los datos se ha desarrollado en base a fuentes primarias y secundarias. Respecto a las fuentes primarias, se realizó el relevamiento de campo de los estacionamientos existentes en centro histórico de Arequipa. Dicho conjunto de datos corresponde a estacionamientos privados y zonas de estacionamientos públicos (zonas azules). El servicio de estacionamientos oferta espacios para autos particulares, taxi, motocicletas y bicicletas; siendo el auto privado y el taxi los vehículos que mas usan este servicio.

El levantamiento de información se ha realizado en el centro histórico de la ciudad de Arequipa, la cual evidencia dos coronas la denominada centro histórico y la zona de amortiguamiento. Respecto al número de estacionamientos dispuestos en cada corona, se tienen 52 estacionamientos privados y 15 zonas de estacionamientos públicos (zonas azules) en corona correspondiente al polígono del centro histórico; y 11 estacionamientos privados y 4 zonas de estacionamientos públicos (zonas azules) en la corona correspondiente al polígono de la zona de amortiguamiento (Ver Figura 2). Además, de cada estacionamiento se obtuvo información relacionada con: ubicación, aforo, tarifa y horario (Ver tabla 1 y tabla 2).

**Tabla 1.** Tabla de estacionamientos dentro del polígono de la zona del centro histórico.

Tipo	N.º de Estacionamientos	Capacidad	Costo Promedio
Público	15	399 autos	S/.1.00 x 1h
Privado	52	1 005 autos	S/.2.50 x 1h

**Tabla 2.** Tabla de estacionamientos dentro del polígono de la zona de amortiguamiento.

Tipo	N.º de Estacionamientos	Capacidad	Costo Promedio
Público	4	120 autos	S/.1.00 x 1h
Privado	11	248 autos	S/.3.00 x 1h

De las fuentes secundarias se utilizaron datos del aplicativo Strava, utilizado con regularidad por ciclistas urbanos. La ciudad de Arequipa presenta diversos grupos de ciclista urbanos organizados; desde grupos de mujeres ciclistas, ciclistas recreativos, ciclistas de montaña, entre otros. El principal colectivo con más de diez mil seguidores en redes sociales es Enbiciados Aqp registrando actividades desde el mes octubre del año 2013. En el marco de la elaboración del plan de ciclovías de emergencia por la pandemia del COVID 19, el colectivo convoco por redes sociales a voluntarios para registrar sus rutas más frecuentes en el aplicativo Strava. Se registraron alrededor de 100 ciclistas en el aplicativo, Es así que se obtuvieron 50 voluntarios, de los cuales se seleccionaron 79 recorridos urbanos con motivo de viaje obligado.

### 3.3 Procesamiento de dato

La trayectoria realizada por un ciclista está representada por una serie de puntos. Cuando se presentan todas las trayectorias en el mapa se observa que varias de ellas son similares. Por tanto, para simplificar la trayectoria se toman puntos representativos. El algoritmo consiste en tomar un punto (p) inicial aleatorio, sobre ese punto se genera una circunferencia de 40 metros de radio (r), debido a la longitud de la manzana del estudio de caso. Luego, se identifican los puntos que están dentro de la circunferencia, y luego se calcula el centroide el cual será el punto representativo. Los puntos que se utilizaron en el cálculo no se consideran para calcular el siguiente punto representativo. Para el cálculo del siguiente punto se toma un siguiente punto aleatorio, y se repite todo el proceso anterior. (Ver Figura 3)

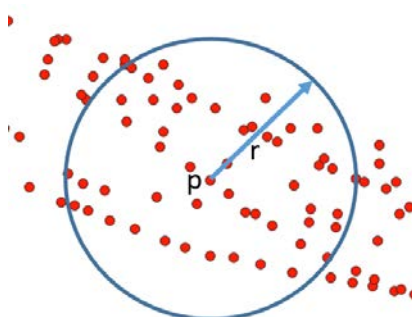


**Figura 3.** Simplificación de las trayectorias de los ciclistas. Fuente: Elaboración propia.

### 3.4 Determinación estacionamiento aplicando voronoi

Se empleó el diagrama de Voronoi para determinar el estacionamiento más cercano al que puede acceder un ciclista que se ubica dentro del centro histórico. El diagrama de Voronoi establece regiones sobre un plano. Cada región contiene un único elemento de interés que es el más cercano para todos los demás elementos de la región. En el presente estudio los límites del plano para el diagrama de Voronoi son acotados por los límites del centro histórico. Los puntos de interés sobre los cuales se crean las regiones son los estacionamientos.

La generación de las regiones de Voronoi se realizó empleando la herramienta postgis. El proceso consiste en los siguientes pasos:

- Generación de regiones de Voronoi: se aplicó la función `ST_VoronoiPolygons` sobre las coordenadas de los estacionamientos.
- Generación de regiones de Voronoi dentro de los límites del centro histórico: para la generación de estas regiones se aplicó la función `ST_Intersection` sobre las regiones de Voronoi y el polígono que representa el centro histórico de Arequipa.

- Cálculo del flujo de ciclistas por cada región de Voronoi. Se aplicó la función ST\_Contains sobre los puntos de las trayectorias y regiones de Voronoi.

### 3.5 Determinación de la densidad de estacionamientos

La densidad de estacionamientos es proporcional al número de estacionamientos por superficie de alcance, y la densidad decrece si esta superficie se incrementa. Entonces, la densidad depende de la superficie de alcance. De otro lado, tenemos que el método de Estimación de Densidad de Kernel (KDE en inglés) establece la densidad total como la suma de las funciones de distribución de densidades individuales. En la figura 4 se muestra la curva Cd que representa la función densidad. La curva Cd es la suma de las funciones Kernel Gaussianas c1, c2, y c3 las cuales se construyeron sobre los puntos 3, 4, y 7 del eje horizontal. Por tanto, si consideramos que los puntos 3, 4, y 7 son estacionamientos, podemos ver que a medida que nos acercamos o alejamos de esos puntos la densidad se incrementa o disminuye.

En el análisis se empleó la herramienta QGis y la función Quartic como Kernel con un valor 200 metros para el parámetro h de ancho de banda. Este valor se determinó en función de la longitud que tienen en promedio las cuadras (bloque) de la ciudad. Además, se considera factible el desplazamiento de 200 metros desde el estacionamiento hacia un destino de viaje o punto de interés por parte de una persona.

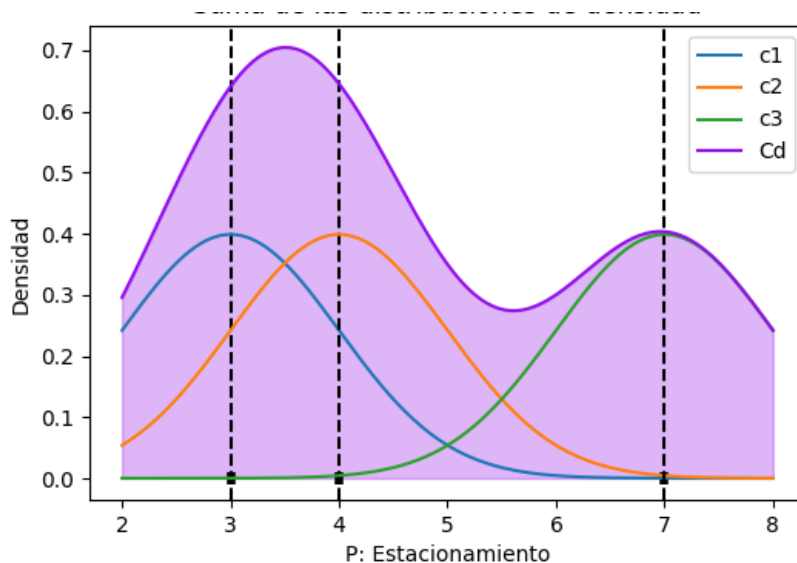


**Figura 4.** Suma de las distribuciones de densidad individuales c1, c2, y c3. Fuente: Elaboración propia.

## 4 Resultados

Los resultados de la investigación se establecen bajo dos criterios de análisis. En el primer criterio se entrecruzan los datos para estimar la proximidad entre los estacionamientos y las rutas ciclistas utilizando el diagrama de Voronoi. Los resultados evidencian el cálculo de demanda del servicio de estacionamiento respondiendo al comportamiento del flujo ciclista dentro del polígono determinado por Voronoi. Los polígonos se clasifican en escalas de 3 colores, siendo el color rojo los sectores con alta flujo de recorridos ciclistas, el color amarillo los sectores con flujo medio y el verde con flujo bajo de desplazamientos ciclistas. Así también, se muestra que la zona central concentra la mayor oferta de estacionamientos en los polígonos amarillos y verdes, sin embargo, el flujo de ciclistas evidencia una demanda de estacionamientos necesaria en los polígonos rojos. (Ver Figura 5)

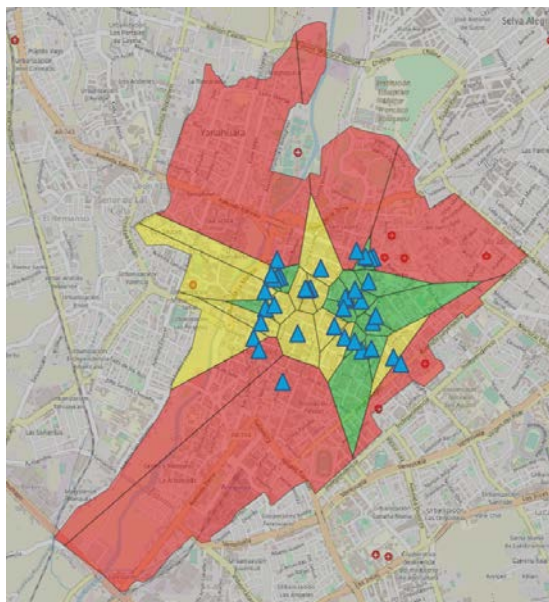


**Figura 5.** Cálculo de la Demanda de Estacionamientos Ciclistas según Polígonos de Voronoi. Fuente: Elaboración propia.

En el segundo criterio de evaluación se superpone densidad de estacionamientos y flujo ciclista. Los flujos ciclistas se clasifican en alto (color rojo), medio (color amarillo) y bajo (color verde); evidenciando las preferencias por los bordes del centro histórico. Luego la densidad de estacionamientos se concentra en 2 sectores del caso de estudio, en torno a 8 calles. Sin embargo, ninguna de ellas presenta un alto o medio flujo de desplazamientos ciclistas (Ver Figura 6).



**Figura 6.** Relación entre la densidad de estacionamientos y flujo ciclista. Fuente: Elaboración propia.

## 5 Conclusiones

Los gobiernos locales vienen impulsando la implementación de infraestructura ciclista e instalaciones complementarias como estacionamientos para bicicletas. En este sentido, es relevante el uso de los datos libres en los procesos de formulación de planes y proyectos. Este estudio muestra que los datos ofrecen una amplia gama de perspectivas y aportan en el análisis inteligente de la oferta de bici estacionamientos potenciales. Además de contribuir en la toma de decisiones de planificadores, basado en las necesidades de usuarios y público en general y fomentando la planificación participativa.

Constantemente, los planificadores de transporte de modos activos requieren priorizar la asignación de recursos económicos. Para realizar esta toma de decisiones, es fundamental reconocer el comportamiento del usuario, sus rutas de preferencias y sus itinerarios en el entorno urbano. Cada ciudad presenta condicionantes o limitaciones para los desplazamientos, que se pueden medir de forma objetiva; sin embargo, existen condicionantes subjetivas propias de cada usuario que se evidencian en sus desplazamientos. Por lo tanto, el seguimiento de las actividades en bicicleta en el espacio y el tiempo es esencial para proporcionar información útil sobre los comportamientos. Este estudio muestra el método de Voronoi y el método de Kernel, empleando software de información geográfica para el análisis inteligente de datos.

A partir de los resultados obtenidos del estudio de oferta de servicios ciclistas; se puede extender la metodología para otros servicios avituallamiento como bebederos, cajas de herramientas, entre otros; necesarios para una promoción integral de modos activos de movilidad. Así también, aplicando la herramienta de Voronoi se pueden

establecer áreas de priorización de infraestructura ciclistas para así descentralizar servicios, comprendiendo la relación del territorio y el comportamiento del usuario. No obstante, la metodología se puede aplicar para determinar la demanda de servicios o mobiliarios urbanos en otros modos de desplazamientos como transporte público y taxi, importantes para el desarrollo de una movilidad urbana sostenible e inteligente.

## 6 Discusión

Actualmente, existen diversas aplicaciones de rastreo utilizadas en estudios de comportamiento, que muestran los desplazamientos de diversos usuarios con información georeferenciada que permiten recopilar, analizar y compartir información espacial ofrecida voluntariamente por individuos; sin embargo, es importante recopilar información de dichas fuentes con el consentimiento y compromiso de los involucrados, para obtener información de mayor calidad y precisión.

Los datos obtenidos desde los dispositivos móviles de los ciudadanos pueden utilizarse como base para las herramientas de planificación urbana. Este tipo de datos facilita y disminuye el tiempo en la extracción y reconocimiento de patrones de movilidad humana, sin embargo, es relevante considerar el tiempo correspondiente a la toma de decisiones relacionadas con la etapa de preprocesamiento de los datos, para determinar la dinámica urbana de las ciudades.

## 7 Agradecimientos

Al proyecto de investigación “Smart city: Diseño de un Modelo conceptual para integración de sistemas sectoriales en ámbitos inteligentes. Al Grupo de Investigación Movilidad Urbana de la Facultad de Arquitectura y Urbanismo de la Universidad Nacional de San Agustín de Arequipa y al colectivo de ciclistas urbanos Enbiciados Aqp.

## 8 Referencias

- [1] I. Martínez-Arrúe, P. García-Escalle, and V. Casares-Giner, “Mobile User Location Management under a Random Directional Mobility Pattern for PCS Networks,” *Gestión la Movil. y Calid. Serv. para redes heterogéneas*, vol. 3, 55., pp. 3–55, 2009.
- [2] J. C. Xavier and R. Boareto, “The Implementation of Brazil Sustainable Urban Mobility Policy 1- The City Mobility Crisis,” pp. 1–12, 2005.
- [3] E. Poole Fuller, “¿ Hacia una movilidad sustentable ? Desafíos de las políticas de reordenamiento del transporte público en Latinoamérica . El caso de Lima Towards Sustainable Mobility ? Challenges of the public transportation reorganization policies in Latin America . The,” *Let. Verdes. Rev. Latinoam. Estud. Socioambientales*, vol. 21, pp.

- 4–31, 2017.
- [4] J. C. Scott, *Seeing Like a State*. 1998.
- [5] S. Williams, *Data Action: Using Data for Public Good*. 2020.
- [6] M. R. Mat Yazid, R. Ismail, and R. Atiq, “The use of non-motorized for sustainable transportation in Malaysia,” *Procedia Eng.*, vol. 20, pp. 125–134, 2011.
- [7] W. Hussein Ali Hussein, “A Sustainable Planning Approach to Resolving Transportation Hub Problems in Egyptian Cities ‘Proposed Measurement Matrix,’” *Am. J. Environ. Prot.*, vol. 4, no. 1, p. 1, 2015.
- [8] A. Misra, A. Gooze, K. Watkins, M. Asad, and C. Le Dantec, “Crowdsourcing and its application to transportation data collection and management,” *Transp. Res. Rec.*, no. 2414, pp. 1–8, 2014.
- [9] E. Heinen and R. Buehler, “Bicycle parking: a systematic review of scientific literature on parking behaviour, parking preferences, and their influence on cycling and travel behaviour,” *Transp. Rev.*, vol. 39, no. 5, pp. 630–656, 2019.
- [10] L. dell’Olio, A. Ibeas, M. Bordagaray, and J. de D. Ortúzar, “Modeling the Effects of Pro Bicycle Infrastructure and Policies Toward Sustainable Urban Mobility,” *J. Urban Plan. Dev.*, vol. 140, no. 2, p. 04014001, 2014.
- [11] C. L. B. Revilla, E. G. M. Huaquipaco, L. S. V. Caballero, G. M. Postigo, and L. Y. S. Mamani, “Smart tools to assessment the livability of commercial streets,” *2021 2nd Sustain. Cities Lat. Am. Conf.*, pp. 1–5, 2021.
- [12] Q. Wang, N. E. Phillips, M. L. Small, and R. J. Sampson, “Urban mobility and neighborhood isolation in America’s 50 largest cities,” *Proc. Natl. Acad. Sci. U. S. A.*, vol. 115, no. 30, pp. 7735–7740, 2018.
- [13] H. Senaratne *et al.*, “Urban Mobility Analysis with Mobile Network Data: A Visual Analytics Approach,” *IEEE Trans. Intell. Transp. Syst.*, vol. 19, no. 5, pp. 1537–1546, 2018.
- [14] D. Ahlers, A. Kristoffer Gebuhr, E. Jeppe, and J. Krogstie, “Visualizing a City Within a City – Mapping Mobility Within a University Campus,” *Smart City 360°*, vol. 166, pp. 492–503, 2016.
- [15] F. Oliveira, D. Nery, D. G. Costa, I. Silva, and L. Lima, “A survey of technologies and recent developments for sustainable smart cycling,” *Sustain.*, vol. 13, no. 6, pp. 1–28, 2021.
- [16] T. Nelson, C. Ferster, K. Laberee, D. Fuller, and M. Winters, “Crowdsourced data for bicycling research and practice,” *Transp. Rev.*, vol. 41, no. 1, pp. 97–114, 2021.
- [17] E. Suarez-Lopez, C. Butron-Revilla, and L. Laura-Ochoa, “An Analysis of Students’ Urban Mobility using Arequipa Smart Mobility Application,” *2019 IEEE Ist Sustain. Cities Lat. Am. Conf.*, pp. 1–6, 2019.
- [18] B. Jestico, T. Nelson, and M. Winters, “Mapping ridership using crowdsourced cycling data,” *J. Transp. Geogr.*, vol. 52, pp. 90–97, 2016.
- [19] M. K. Selala and W. Musakwa, “The potential of strava data to contribute in non-motorised transport (NMT) planning in johannesburg,” *Int. Arch. Photogramm. Remote Sens. Spat. Inf. Sci. - ISPRS Arch.*, vol. 41, no. June, pp. 587–594, 2016.
- [20] K. M. Kwayu, S. M. Lyimo, and V. Kwigizile, “Characteristics of cyclists using fitness tracker apps and its implications for planning of bicycle transport systems,” *Case Stud. Transp. Policy*, vol. 9, no. 3, pp. 1160–1166, 2021.

- [21] C. Butron-Revilla, E. Suarez-Lopez, and L. Laura-Ochoa, "Discovering Urban Mobility Patterns and Demand for Uses of Urban Spaces from Mobile Phone Data," *2021 2nd Sustain. Cities Lat. Am. Conf.*, pp. 1–6, 2021.
- [22] M. Lesiv *et al.*, "Comparison of Data Fusion Methods Using Crowdsourced Data in Creating a Hybrid Forest Cover Map," *Remote Sens.*, vol. 8, no. 3, p. 261, Mar. 2016.

## Análisis histórico de la movilidad individual ECOBICI en la Ciudad de México

Gilberto Loreno Martínez Luna<sup>1</sup>[0000-0002-8236-0469], Adolfo Guzmán Arenas<sup>1</sup>[0000-0002-0105-1112] y Eduardo Vargas Reyes<sup>2</sup>[0000-0002-8092-1437]

<sup>1</sup> Centro de Investigación en Computación, Avenida Juan de Dios Bátiz S/N, 07738 Ciudad de México, México.

<sup>2</sup> Instituto Politécnico Nacional, Avenida Té 950, 08400 Ciudad de México, México.  
lncs@springer.com

**Abstract.** El sistema de bicicletas públicas de la Ciudad de México, ECOBICI, al igual que muchos sistemas internacionales de movilidad en bicicletas, comparte los datos de los viajes que realizan sus usuarios en las bicicletas.

En el Centro de Investigación en Computación del I.P.N., haciendo uso de estos datos, se desarrolló un sistema de análisis histórico de movilidad individual, llamado SAHMI [1] compuesto de visualizaciones, que permitan describir la movilidad y el crecimiento de este sistema.

Las visualizaciones se comparten en una página web, visualizaciones que permiten identificar algunos patrones relacionados: a los meses de mayor uso en los once años de servicio; al género de los usuarios; a su edad; entre otros patrones. También se busca, si el enunciado de Pareto se cumple, que en este caso, debería estar en relación con la frecuencia de los viajes, tanto en estaciones y bicicletas, dándose una explicación del porqué no se cumple. En la mayoría de las visualizaciones se mantiene la presencia de líneas con los valores del máximo, mínimo, promedio, mediana, cuartil inferior y cuartil superior, por ser esenciales en la descripción de los datos, valores relacionados a la frecuencia de viajes.

La herramienta, es un ejemplo que ayuda a entender la importancia del análisis exploratorio de los datos, actividad previa a la Minería de Datos y en la Ciencia de Datos.

**Keywords:** Análisis Exploratorio de Datos, Minería de Datos, Visualización.

### 1 Introducción

ECOBICI inició sus operaciones en febrero de 2010. Está conformado por bicicletas, cicloestaciones, usuarios, organización y otros recursos necesarios para su funcionamiento. Publica mensualmente sus datos abiertos, ver Figura 1, sobre el servicio y comparte cuatro gráficas estadísticas [2]: usos, usuarios registrados, usos acumulados y registros acumulados.



Fig. 1. Gráficas de ECOBICI.

Existen otros sistemas involucrados a ECOBICI, ver Figura 2:

- Bike Share Map [3]. Se muestran muchos sistemas de bicicletas del mundo, entre ellos a ECOBICI y la ubicación geográfica de cada cicloestación y el número de bicicletas que tienen. Es un sistema en tiempo real.
- The Meddin Bike-sharing World Map [4]. Indica los distintos sistemas de bicicletas que hay en el mundo, entre ellos a ECOBICI y muestra información relacionada a los cambios que ha tenido con el paso del tiempo como el incremento de cicloestaciones y bicicletas.
- PLANBIKE [5]. Muestra visualizaciones sobre el comportamiento de los viajes entre cicloestaciones, disponibilidad de bicicletas y movilidad entre colonias de la ciudad de México, por hora, día o semana. Fue desarrollado por el Laboratorio de Ciencia de Datos y Tecnología de Software del CIC-IPN.



a) Bike Share Map

b) The Meddin Map

c) PLANBIKE

Fig. 2. Software con información de ECOBICI.

Sin embargo, no es posible describir el comportamiento histórico de ECOBICI con esos sistemas. Parte de esta descripción se puede hacer con PLANBIKE, pero su análisis es por semana a mayor detalle y entre estaciones, que por análisis de modularidad queda fuera de SAHMI.

Los datos abiertos que publica ECOBICI, en su página, recogen un conjunto de hechos y en ellos existen patrones que describen el conjunto total o un subconjunto de los datos [6, 7, 8].

Los patrones, que pueden ser de interés (p. ej. por temporada), describen la movilidad o dinámica en ECOBICI, patrones relacionados el número de viajes por: mes, año, género, intervalos de edad, el número de cicloestaciones o de bicicletas. También puede existir relación entre el número de bicicletas, cicloestaciones y de viajes.

SAHMI se desarrolló con visualizaciones interactivas que permitan describir el comportamiento de ECOBICI, para que los investigadores de Ciencia de Datos, estudiantes de diversas carreras o maestrías, usuarios de ECOBICI y en general interesados en la Ciencia de Datos lo revisen como un ejemplo del análisis exploratorio de datos de un fenómeno de interés, como la movilidad en la Ciudad de México. La utilidad de este sistema está en mostrar que el análisis exploratorio de datos permite detectar, corroborar, plantear o destruir hipótesis de patrones, también de interés.

## 2 Métodos

Para comprender el comportamiento de la movilidad en ECOBICI y la elaboración de SAHMI se realizaron las actividades de la Figura 3:

- Preparación de los datos. Se aplicaron filtros para eliminar datos nulos que existían en algunos atributos. También se transformaron algunos datos, p. ej. las letras “F” y “M” se cambiaron por “Femenino” y “Masculino”, respectivamente.
- Exploración de los datos. Se crearon visualizaciones de los tres grupos en los que se divide SAHMI utilizando el software Tableau con una licencia académica.
- Resultados. Se creó la página web y se compartieron las visualizaciones, las cuales se actualizan conforme se actualiza la base de datos con los datos abiertos.



Fig. 3. Proceso de elaboración de SAHMI.

Se dividió SAHMI en tres grupos, ver Figura 4.



Fig. 4. Estructura de SAHMI.

El grupo “Histórico”, ver Figura 5, está dividido en seis categorías (nivel verde) para visualizar los datos con un enfoque distinto, cada uno tiene diferentes gráficas (nivel azul) y subgráficas (nivel naranja).



Fig. 5. Categorías del grupo “Histórico”.

Tanto “Gráficos de Pareto” y “Comparaciones” tienen cinco gráficas, ver Figura 6.



a) Gráficos de Pareto

b) Comparaciones

Fig. 6. Estructura de los otros grupos de SAHMI.

Se diseñó una página web para presentar las visualizaciones, ver Figura 7.

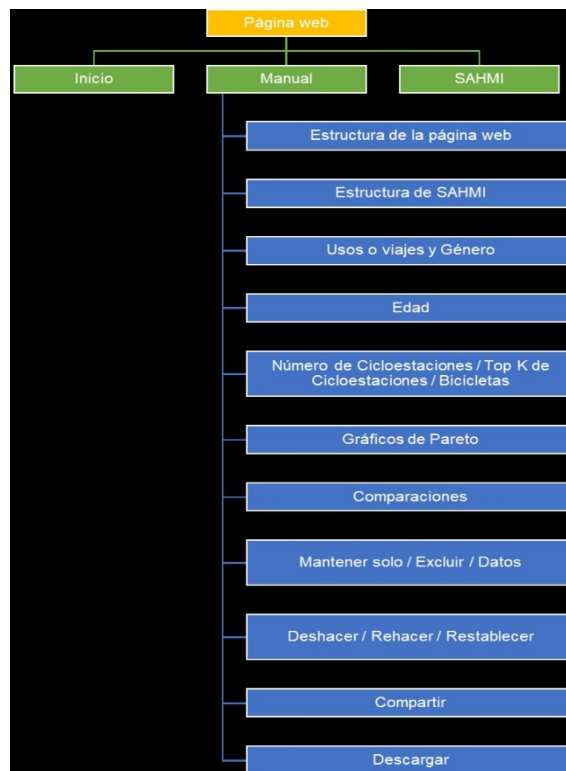


Fig. 7. Estructura de la página web de SAHMI.

### 3 Resultados.

SAHMI es un sistema que presenta diversas visualizaciones interactivas de su base de datos. Esta comparte lo siguiente:

- El número de registros con los que cuenta la base de datos del LCDyTS y que son analizados por SAHMI.
- El grupo “Histórico”.
- El grupo “Gráficos de Pareto”.
- El grupo “Comparaciones”.

#### 3.1 Grupo “Histórico”.

La mayoría de las visualizaciones de este grupo incluyen líneas de medida del máximo, mínimo, promedio, mediana, cuartil inferior y cuartil superior [9]. Las visualizaciones están agrupadas en seis categorías:

**Categoría “Usos o viajes”, ver Figura 8.**

1. Viajes realizados por año: se muestra el número de viajes realizados (eje vertical) por año (eje horizontal), cada columna tiene un color diferente. Es la gráfica principal de esta categoría, permite filtrar las otras dos gráficas, dependiendo del año o los años seleccionados.
2. Viajes realizados por mes del año “Ninguno” (la palabra “Ninguno” se cambiará por el mes seleccionado): se muestra el número de viajes realizados (eje vertical) por mes (eje horizontal), cada columna tiene un color diferente. Aparece por predeterminado la suma de los viajes de todos los años por mes, es decir, para el mes de enero se suman los viajes de todos los años correspondientes a dicho mes y pasa lo mismo para los otros meses. Cambiará de acuerdo con los años seleccionados en la gráfica principal de esta categoría.
3. Tendencia de los viajes realizados: se muestra el número de viajes realizados (eje vertical) por año y mes (eje horizontal), la curva cambia de color de acuerdo con el año y su color corresponderá al de las columnas del gráfico principal de esta categoría. Aparecerá por predeterminado todos los años y meses, es por esto por lo que no podrá distinguirse el nombre de todos los meses en el eje horizontal. Cambiará de acuerdo con lo seleccionado en la gráfica principal de esta categoría.

El primer patrón observado, es que en años en que se mantiene estable el número de estaciones y de bicicletas, los meses con mayor frecuencia es en - marzo o abril - y - septiembre u octubre, ver gráfica, en la parte baja de la Figura 8.



**Fig. 8.** Categoría “Usos o viajes”.

**Categoría “Género”, ver Figura 9.**

4. Viajes realizados por año y género: se muestra el número de viajes realizados (eje vertical) por año y género (eje horizontal), el color de la columna será rosa para el género femenino y azul para el masculino. Es la gráfica principal de esta categoría, permite filtrar las otras dos gráficas, dependiendo del año, años, columna o columnas seleccionadas.
5. Viajes realizados por mes: se muestra el número de viajes realizados (eje vertical) por mes (eje horizontal), cada columna tiene un color diferente. Aparece por prede-

terminado la suma de los viajes de todos los años y géneros por mes. Cambiará de acuerdo con lo seleccionado en la gráfica principal de esta categoría.

6. Tendencia de los viajes realizados por género: muestra el número de viajes realizados (eje vertical) por año y mes (eje horizontal). La curva color rosa corresponde al género femenino y la azul al masculino. Aparecerá por predeterminado todos los años y meses, es por esto por lo que no podrá distinguirse el nombre de todos ellos en el eje horizontal. Cambiará de acuerdo con lo seleccionado en la gráfica principal de esta categoría.

Se identificó que los viajes del género femenino crecieron más lento que los del masculino y representan solo el 26% de los viajes históricos totales. El patrón observado, es que se mantiene casi siempre una razón de tres veces más los viajes de hombres que los viajes que realizan las mujeres.



Fig. 9. Categoría “Género”.

**Categoría “Edad”, ver Figura 10.**

7. Viajes realizados por edad: se muestra el número de viajes realizados (eje vertical) por intervalos de edad de diez años (eje horizontal), cada curva corresponde a un año y color diferente. Tiene un filtro en la parte superior derecha, para seleccionar uno o varios años. También tiene una sección para indicar el color de la curva que le corresponde a cada año, en la parte inferior derecha.

El tercer patrón observado, es que la mayoría de los viajes se alterna entre los grupos de 20-29 o 30-39, cabe aquí mencionar, no se sabe si se actualiza la edad de los usuarios que renuevan su membresía.

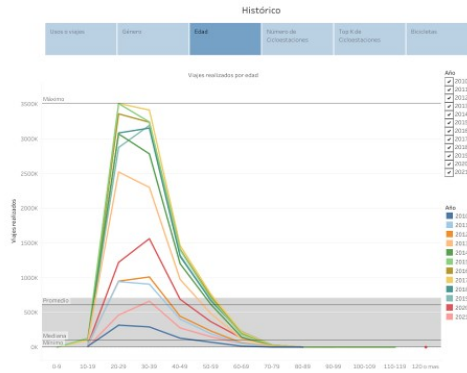
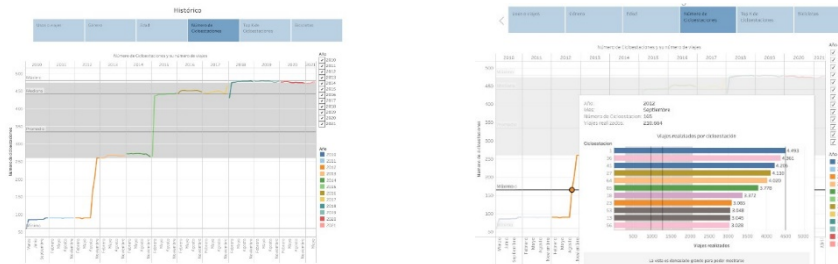


Fig. 10. Categoría “Edad”.

**Categoría “Número de Cicloestaciones”, ver Figura 11.**

8. Número de cicloestaciones y el número de viajes que se originan en la estación referenciada: se muestra el número de cicloestaciones en función o disponibles (eje vertical) por año y mes (eje horizontal), la curva cambia de color de acuerdo con el año. Tiene un filtro en la parte superior derecha, para seleccionar uno o varios años. También tiene una sección para indicar el color de la curva que le corresponde a cada año, en la parte inferior derecha.
9. Viajes realizados por cicloestación: aparecen como mensaje emergente al poner el cursor sobre cualquier punto de la gráfica “Número de cicloestaciones y su número de viajes”. Esta subgráfica muestra las cicloestaciones en función, en orden descendente (eje vertical), del año y mes en el que se coloque el cursor, de acuerdo con el número de viajes realizados en cada una (eje horizontal), cada cicloestación tiene un color diferente.

Un cuarto patrón de interés, que se observa, al cambiar de posición el cursor en los años, es que las primeras 10 estaciones con mayor frecuencia de viaje permanecen mientras permanezca estable el número de estaciones.



a) Gráfica de la categoría

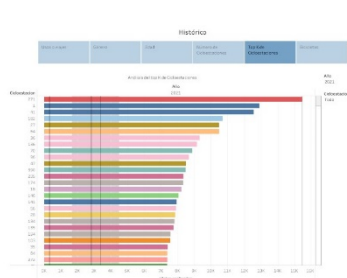
b) Subgráfica de la categoría

Fig. 11. Categoría “Número de cicloestaciones”.

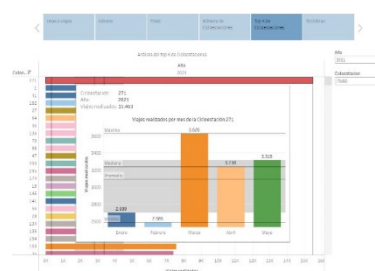
**Categoría “Top K de cicloestaciones por año”, ver Figura 12.**

10. Análisis del Top K de cicloestaciones: se muestran cicloestaciones en orden descendente (eje vertical), de acuerdo con el número de viajes realizados en ellas por año (eje horizontal), cada cicloestación tiene un color diferente. Tiene dos filtros en la parte superior derecha, para seleccionar uno o varios años o para seleccionar una o varias cicloestaciones. Aparece 2021 y todas las cicloestaciones por predeterminado.
11. Viajes realizados por mes de la cicloestación “X” (donde “X” será el número de cicloestación de la barra donde se pone el cursor): aparece como mensaje emergente al poner el cursor sobre cualquier barra de la gráfica “Análisis del Top K de cicloestaciones”. Esta subgráfica muestra los viajes realizados (eje vertical) por mes (eje horizontal), de la cicloestación en la que se ponga el cursor, cada columna tiene un color diferente.

El cuarto patrón observado en la visualización anterior aquí se aprecia mejor, pero año con año. La cicloestación 27 (barra color verde olivo, ver Figura 13) es la que más viajes tiene y la cicloestación 271 (barra color rojo) entró en funcionamiento en enero de 2014 y es la octava con más viajes, esto puede indicar que ambas están en una ubicación muy estratégica y se corrobora al ver los últimos tres años, ya que es la que más viajes tiene.



a) Gráfica de la categoría

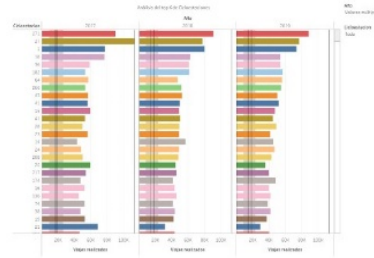


b) Subgráfica de la categoría

**Fig. 12.** Categoría “Top K de cicloestaciones por año”.



a) Históricamente



b) De 2017 a 2019

Fig. 13. Cicloestaciones con más viajes.

**Categoría “Bicicletas”, ver Figura 14.**

- 12. Número de bicicletas y su número de viajes: se muestra el número de bicicletas en funcionamiento o disponibles (eje vertical) por año y mes (eje horizontal), la curva cambia de color de acuerdo con el año. Tiene un filtro en la parte superior derecha, para seleccionar uno o varios años. También tiene una sección para indicar el color de la curva que le corresponde a cada año, en la parte inferior derecha.
- 13. Viajes realizados por bicicleta: aparece como mensaje emergente al poner el cursor sobre cualquier punto de la gráfica “Número de bicicletas y su número de viajes”. Esta subgráfica, muestra las bicicletas en función, del año/mes en el que se coloque el cursor, en orden descendente (eje vertical) por el número de viajes realizados en cada una (eje horizontal). Cada bicicleta tiene un color diferente.

El sexto patrón, que pudiese ser observado es, el número bicicletas en uso, es irregular en todos los años. Debido tal vez la antigüedad o apariencia de ellas que no se usen o que no se cambian cuando se requiere por una nueva o no se repara si está dañada.



a) Gráfica de categoría



b) Subgráfica de categoría

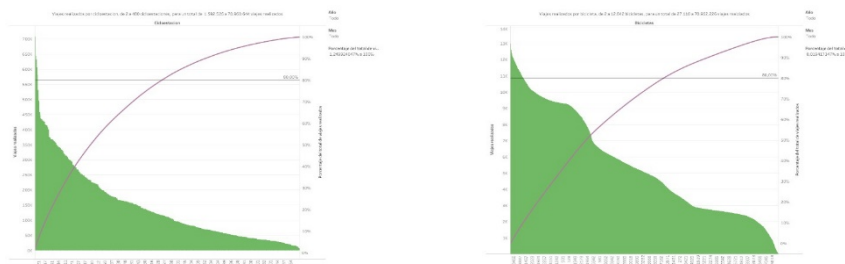
Fig. 14. Categoría “Número de bicicletas”.

### 3.2 Grupo “Gráficos de Pareto”.

Son dos gráficas y cada una tiene dos ejes verticales y una curva morada que indica el porcentaje del total acumulado de viajes realizados (eje vertical derecho). Cuentan con tres filtros en la parte superior derecha: año, mes y porcentaje acumulado del total de los viajes realizados. Ver Figura 15:

- 14. Viajes realizados por cicloestación: se muestra el número de viajes realizados (eje vertical izquierdo) por cicloestación (eje horizontal), en orden descendente, de acuerdo con el número de viajes.
- 15. Viajes realizados por bicicleta: se muestra el número de viajes realizados (eje vertical izquierdo) por bicicleta (eje horizontal), en orden descendente, de acuerdo con el número de viajes.

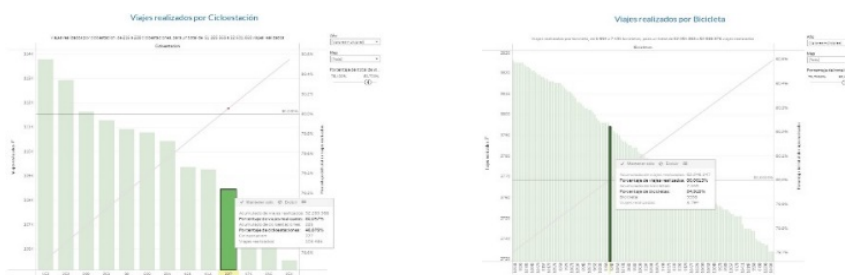
En ambas gráficas no se observa el séptimo patrón deseado de la relación 80-20, ya sea viajes contra estaciones o viajes contra bicicletas. El 80% de los viajes realizados por los usuarios de ECOBICI, los realizan en el 46% de las cicloestaciones y el 54% de las bicicletas, ver Figura 16.



a) Por cicloestación

b) Por bicicleta

Fig. 15. Grupo “Gráficas de Pareto”.



a) Por cicloestación

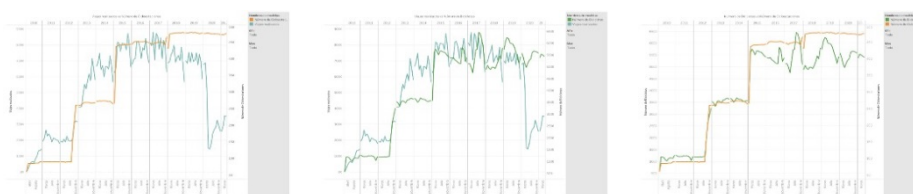
b) Por bicicleta

Fig. 16. Principio de Pareto de los viajes realizados.

### 3.3 Grupo “Comparaciones”.

Son tres gráficas que tienen dos ejes verticales, uno por variable a comparar. En la parte superior derecha hay una sección para indicar el color del nombre de la variable a comparar: la curva de los viajes realizados es de color azul, el número de cicloestaciones es color naranja y el número de bicicletas es color verde. También tienen dos filtros: año y mes. Ver Figura 17.

16. Viajes realizados vs número de cicloestaciones: se muestra el número de viajes realizados (eje vertical izquierdo) y el número de cicloestaciones en funcionamiento o disponibles (eje vertical derecho) por año y mes (eje horizontal). El octavo patrón de viajes contra estaciones es irregular, se mantienen las estaciones, pero la frecuencia de viajes no se mantiene.
17. Viajes realizados vs número de bicicletas: se muestra el número de viajes realizados (eje vertical izquierdo) y el número de bicicletas en funcionamiento o disponibles (eje vertical derecho) por año y mes (eje horizontal). De igual forma el noveno patrón, viajes contra bicicletas no se mantiene dada la irregularidad del número de bicicletas y también el número de viajes.
18. Número de bicicletas vs número de cicloestaciones: se muestra el número de bicicletas en funcionamiento o disponibles (eje vertical izquierdo) y el número de cicloestaciones en funcionamiento o disponibles (eje vertical derecho) por año y mes (eje horizontal). También de igual forma el décimo patrón, bicicletas contra estaciones no se mantiene dada la irregularidad del número de bicicletas, aunque permanece constante en años el número de estaciones.



a) Viajes vs cicloestaciones

b) Viajes vs bicicletas

c) Bicicletas vs cicloestaciones

**Fig. 17.** Grupo “Comparaciones”.

## 4 Discusión.

Se analizaron las visualizaciones de SAHMI, correspondientes a los años 2010 a 2019 (diez años), de los años 2020 y 2021, no se dan conclusiones por ser afectados por la pandemia con COVID-19, con la reducción de viajes. Los primeros seis patrones son una regularidad, salvo los restantes cuatro patrones.

## 5 Conclusiones.

Con las visualizaciones se logró identificar varios patrones que permiten describir la movilidad en ECOBICI.

SAHMI es un ejemplo para interesados en el área de Ciencia de Datos, una forma de desarrollar un análisis exploratorio de datos a un fenómeno de interés, tanto para investigadores y estudiantes y posiblemente a la administración de ECOBICI. Los investigadores y estudiantes de Ciencia de Datos y otras áreas pueden utilizar como fuente de datos, los datos de ECOBICI, probar y aplicar técnicas de ciencia de datos (Machine Learning, Data Mining, entre otras) [10, 11, 12] y localizar más patrones de interés y confrontar sus resultados con las visualizaciones de SAHMI.

## References

1. SAHMI, <https://sites.google.com/view/sahmi/inicio?authuser=0>, ultimo acceso 04/10/21.
2. Estadísticas de ECOBICI, <https://www.ecobici.cdmx.gob.mx/es/estadisticas>, ultimo acceso 04/10/21.
3. Bike Share Map, <https://bikesharemap.com/mexicocity/#/13/-99.1736/19.3996/>, ultimo acceso 04/10/21.
4. The Meddin Bike-sharing World Map, <https://world.bikesharemap.com/#/all/10/-99.15/19.44/>, ultimo acceso 04/10/21.
5. PLANBIKE, <http://148.204.66.79/neoecobiciweb/index.php>, ultimo acceso 04/10/21.
6. García, J., Molina, J., Berlanga, A., Patricio, M., Bustamante, A., Padilla, W.: Ciencia de datos: técnicas analíticas y aprendizaje estadístico en un enfoque práctico. 1ra Edición. Editorial Alfaomega. Bogotá, Colombia (2018).
7. Jones, H: Ciencia de Los Datos: La Guía Definitiva Sobre Análisis de Datos, Minería de Datos, Almacenamiento de Datos, Visualización de Datos, Big Data Para Empresas Y Aprendizaje Automático Para Principiantes. Editorial Independiente. USA (2019).
8. Jones, H: Ciencia de los datos: Lo que saben los mejores científicos de datos sobre el análisis de datos, minería de datos, estadísticas, aprendizaje automático y Big Data - que usted desconoce. Editorial Independiente. USA (2019).
9. Gutiérrez, E., Vladimirovna, O.: Probabilidad y estadística, aplicaciones a la ingeniería y las ciencias. Primera Edición. Grupo Editorial Patria. México (2014).
10. Witten, I., Frank, E., Hall, M.: Data Mining: Practical Machine Learning Tools and Techniques. 3ra Edición. Editorial Morgan Kaufmann, USA (2011).
11. Clarke, B., Fokoue, E., Zhang, H.: Principles and Theory for Data Mining and Machine Learning. Springer. USA (2011).
12. Clark, J.: Artificial Intelligence: Teaching Machines to Think Like People. Primera Edición. O'Reilly Media. USA (2017).

# Travel time estimation in public transportation using bus location data

Renzo Massobrio and Sergio Nesmachnow

Universidad de la República  
renzom@fing.edu.uy, sergion@fing.edu.uy

**Abstract.** The user experience of passengers using public transportation is highly sensitive to travel time. In this regard, travel time is a key input to assess the quality of service offered by a public transportation system and to compute performance and service-level metrics. Moreover, travel time is needed to evaluate the accessibility to different opportunities in the city (e.g., employment, commercial activities, education) that can be reached using public transportation. This article presents a data analysis approach to estimate in-vehicle travel time in public transportation systems. Vehicle location data, bus stops locations, bus lines routes, and timetables from the public transportation system in Montevideo, Uruguay, are considered in the case study used to evaluate the proposed approach. Results are compared against scheduled timetables and are used to compute several performance indicators of the public transportation system of the city.

**Keywords:** travel time, public transportation, data analysis, GPS data

## 1 Introduction

In urban scenarios, citizens are required to travel in order to engage in the social and economic activities of their city [3]. In this context, public transportation plays a major role, since it is the most efficient and socially-fair mean of transportation [7]. Understanding the accessibility of citizens to the public transportation service of a city is paramount in order to identify inequalities among the population and implement policies that aim at improving the quality of service offered to passengers. Several indicators may be considered to measure the accessibility offered by a transportation system, among them, travel time strikes as the most intuitive one, since it is tightly related to the perception of passengers of the quality of service of a transportation system [17].

Public transportation systems operate on predefined routes and depend on schedules that vary throughout the day. Additionally, travel speeds vary greatly due to traffic congestion, passenger demand, and road infrastructure. Thus, assuming constant speed of vehicles along routes usually results in significant travel time differences between the estimations of the model and the actual reality. A comprehensive model for travel time estimation in public transportation networks needs to account for all these factors.

2 Massobrio and Nesmachnow

This article presents a model to estimate in-vehicle travel times in public transportation systems. The proposed model applies a data analysis approach [12] incorporating real vehicle location data from on-board GPS units as well as open data regarding the public transportation lines and bus stops. The public transportation system in Montevideo, Uruguay, is used as a case study. For the studied scenario, the difference between the estimated travel times and those available in the public timetables are reported. Furthermore, relevant metrics to assess the quality of service of public transportation systems are computed. Results indicate that the proposed approach is suitable to accurately estimate in-vehicle travel times in the city. The applied methodology is also useful to detect situations that prevent users from having a good quality of experience when using the public transportation system, which should be the focus of further studies by the city administration.

The remainder of the paper is organized as follows. Section 2 gives an overview of the topic and the context for this study. Section 3 reviews works in the related literature. Section 4 outlines the proposed methodology for travel time estimation. The application to the case study is presented in Section 5 and the conclusions and future work are presented in Section 6.

## 2 Characterizing travel times of the public transportation system

In the context of the research project that studies the territorial, universal, and sustainable accessibility in Montevideo, Uruguay, one of the most relevant tasks is the characterization and analysis of the public transportation system. In this regard, accessibility and quality of service provided by the public transportation system is a very important issue that can significantly affect vulnerable groups in society. A proper analysis of public transportation allows conceiving and applying sustainable mobility strategies (e.g., including electric mobility options and other alternatives for non-polluting means of transportation).

For studying accessibility, it is crucial to compute relevant indicators that allow determining the impact and availability of different means of transportation. Travel time using the public transportation system is a relevant indicator that assess how long it takes [a citizen] to make a trip using the public transportation system, and it is also considered as an indicator of mobility, defined as “the ease of traveling between locations within a community” [2]. The travel time metric is not only valuable as a subjective indicator, i.e., related to the user-experience of passengers of the public transportation system, but is also meaningful to determine the quality of service of any given bus route or the system as a whole. Furthermore, travel time also allows computing comparative indicators, such as the additional travel time required over an automobile making the same trip, as defined by the Transportation Research Board [1], and other metrics of route directness. Travel time is also useful to determine the reliability of the public transportation system, defined as “the ability of the transit system to adhere to schedule or maintain regular headways and consistent travel times” [18].

In order to quantify the provision of the public transportation system, the problem studied in this article consists in estimating in-vehicle travel times at each stop along the routes of the bus lines in the system. Travel times can be estimated from the (fixed) schedules established by the city administration for the different bus lines in the city, providing a static view of mobility and accessibility. Complementing this approach, this article proposes using real GPS data of the buses from the Metropolitan Transport System of Montevideo and open data providing information about the existing infrastructure for public transportation in the city (e.g., bus stops, bus lines). These sources of data allow characterizing the mobility offered by the transportation system and its accessibility, to complement the use of fixed information that may not accurately reflect reality.

### 3 Related works

Lei and Church presented a short review on measuring the accessibility in public transportation systems [11]. The survey showed that several authors focus on the physical aspects of a system (e.g., distance to a bus stop) instead of focusing on the travel time between pairs of locations. Furthermore, previous works which do focus on travel times usually make assumptions which significantly impact the accuracy of their estimations, e.g., constant transfer and waiting times, average speed of vehicles, or not considering bus schedules at all. The authors propose an extended GIS data structure to account for the temporal dimension of public transportation systems which is applied to the public transportation system in Santa Barbara, California.

Salonen and Toivonen presented a comparison of different travel time measures [17]. The work covers both travel times using private vehicles and public transportation. Regarding the latter, three models are outlined and applied to a case study in the capital region of Finland: a simple model which does not include vehicle schedule information at all, an intermediate model which uses schedules only to estimate the average waiting time, and an advanced model which queries a government API with up-to-date schedules and uses its routing engine as a black-box to compute travel times. The proposed models identified travel time disparities across modes (i.e., private vs. public transportation), with a lower effect in areas near the city center.

Previous works have addressed the public transportation system in Montevideo, Uruguay, which is used as a case study in this article. Massobrio and Nesmachnow proposed an urban data analysis approach to understand mobility in the city using different sources of urban data [12]. Origin-destination matrices, which describe mobility, were built using ticket sales data. Other studies have measured the quality of service offered by the public transportation service in Montevideo, by analyzing punctuality based on GPS bus location data [13, 14].

Hernández et al. studied accessibility to employment opportunities in Montevideo, Uruguay [8]. For this purpose, the authors built a travel time matrix using the scheduled timetables for bus lines in the city. The methodology pro-

4 Massobrio and Nesmachnow

posed by the authors models the public transport network as a graph, to compute travel times between different zones in the city. This model allows configuring the maximum walkable distance and the maximum number of transfers within the route. The computed travel time matrix was validated against a government web application and the results from a household mobility survey.

According to the review, few previous works have applied a systematic procedure to estimate travel times of public transportation in Montevideo, Uruguay. The model proposed in this article combines several sources of information including bus location data from on-board GPS units. Thus, the proposed approach extends the static approaches that only consider fixed timetables data when computing in-vehicle travel time by incorporating real data that reflect the reality of the buses operating throughout the network.

## 4 Methodology

This section outlines the methodology applied for data processing and analysis.

### 4.1 Data sources

One week of bus GPS location data were obtained, corresponding to buses operating from Monday 5<sup>th</sup> to Sunday 11<sup>th</sup> of August 2019. Records in the bus location dataset correspond to measures registered with the on-board GPS unit in each bus, which are sampled every 20-30 seconds. Each record in the dataset includes a bus line identifier, a unique trip identifier (to discriminate different trips of the same bus line), the scheduled departure time for the trip, GPS coordinates, and a timestamp. For this study, we aimed to compute travel times during the morning peak, so we considered only trips with scheduled departures on working days between 7.00 am and 9.00 am (inclusive) as reported in [12]. Some trips had corrupted records, with timestamps spreading for very long periods. For this purpose, we discarded all trips that lasted more than four hours, as they are not representative of bus line lengths in the city and they are very likely outliers. After this filtering, the bus location dataset held more than 2.8 million records, corresponding to 8224 trips of 258 different bus lines.

Bus stop location data were also used for the analysis. Open data from the local government were processed to obtain, for each bus line, the ordered set of bus stops it visits, with their locations. Another source of open data used for the analysis were the timetables for each bus line. Records hold the scheduled departure of each trip and the expected arrival time at each bus stop. The same filter was applied to consider only trips within the morning peak. Open data were obtained in July 2021, thus, some discrepancies appear when combining it with bus location data from 2019. For instance, some bus lines and bus stops were modified, schedules were updated, etc. We deal with these issues throughout the data analysis process described next.

## 4.2 Data processing

Each trip in the dataset is processed independently to compute in-vehicle travel times. The result of this processing is an ordered list of the time it takes from the first bus stop in the journey to each of the bus stops corresponding to the bus line of the trip. Vehicle location using GPS is prone to errors from a variety of sources, so several methodologies have been proposed to cope with this phenomena [10]. To address this issue we created a buffer on bus stops of 25 meters in all directions and discarded all measures falling outside these buffers. When processing the records of a given trip, the timestamp assigned to each bus stop is set as the timestamp of the earliest record that falls within the bus stop buffer. This applies to all bus stops except the first one in the journey, where the latest timestamp is selected, as buses usually turn on their GPS device before departing, thus multiple records fall within the first stop. In some cases, drivers forget to update the on-board machine at the end of the trip. As a consequence, the trip identification is kept for more than one trip (e.g., inbound and outbound consecutive trips of the same line). This issue was mitigated by adding a validity check ensuring that the time between consecutive measures assigned to stops needs to be smaller than 30 minutes. Additionally, integrity checks are made to ensure that timestamps and bus stop identifiers are increasing monotonically and the bus line and trip identifier is unchanged. If any assertion does not hold, the process of that trip is interrupted.

As a result of the previous processing, the proposed method computes travel times (measured from the first stop of the bus line) for each of the bus stops with a valid nearby GPS record. However, some of the bus stops of the bus line being processed may still have no travel time information. For bus stops located between other bus stops that already have assigned travel times, we interpolate the values based on the distance between the stops along the bus route. For bus stops at the start or end of the bus line with no travel time assigned, we extrapolate using the travel times offered in the timetable for that bus line.

## 4.3 Metrics

After computing the travel times between bus stops for every line in the public transportation system, a set of relevant metrics are considered in the analysis. These metrics focus on evaluating different features of the public transportation system. The studied metrics include:

- *Difference between scheduled and real travel time*: This metric evaluates the gap between the scheduled time and the actual travel time computed from GPS records. It is a very relevant metric to assess the punctuality of buses when arriving at each stop. The ideal value for this metric is zero, for a perfectly synchronized bus system.
- *Operational speed (OS)*: This metric evaluates the average speed of buses when operating a route. Operational speed is defined as the length of a bus route divided by the average travel time required to perform a trip from the

6 Massobrio and Nesmachnow

beginning to the end of the route. Larger values of the operational speed indicate a more efficient transportation system. Related to this metric, in a recent article, Deng and Yang [4] introduced an holistic metric to evaluate the dispersion of the operational times for all bus lines in a public transportation system, i.e., dispersion OS (dOS). This metric is defined by  $dOS = \max(OS_i) - OS_i$ .

- *On-time arrival rate* (OTAR): This metric evaluates the number of trips performed without a significant delay, considering a predefined delay threshold (the *buffer time*). OTAR is defined as the ratio of buses arriving on time at the final stop over the total number of bus trips performed. The buffer time coefficient accounts for any unexpected delay during the trip. It is computed as the ratio of the difference between the 95<sup>th</sup> percentile travel time and the average travel time, and the average travel time [6].
- *Additional travel time over automobile* (ATToA): This metric evaluates the directness of a bus route, by comparing the travel time required for performing a trip on the public transportation system over the time required using private transportation (automobile) that makes the same trip. Smaller values of this metric means a more direct route; thus, a most efficient transportation system [1].

## 5 Results and discussion

This section reports and discusses the main results and finding of the proposed analysis of the public transportation system in Montevideo, Uruguay.

### 5.1 Analysis of GPS records

Fig. 1 shows an example of the data processing methodology to assign GPS records to bus stops to compute in-vehicle travel times. The example corresponds to the final stops of bus line 306 from Parque Roosevelt (located in the east side of the city, in the border with Canelones department) to Casabó (a neighborhood in the west of Montevideo). Blue dots correspond to GPS measures and gray circles correspond to the buffered stops for the bus line. Bus stops with at least one GPS measure in their vicinity (i.e., at least one blue dot within the gray area) are assigned the timestamp of the earliest of those GPS measures. Bus stops with no GPS measures in their vicinity are assigned a timestamp by interpolating the timestamps of the previous and next bus stops with matching GPS records and taking into account the distance between those stops along the route of the bus. This case is shown in yellow in the figure. Finally, the last four stops (shown in orange in the figure) have no matching GPS records. This happens on some trips when the driver turns off the on-board GPS unit prematurely, thus the end of the trip is not recorded. In this case, the travel time to reach each bus stop is extrapolated using the information available in the timetable for the bus line and the latest GPS timestamp assigned to a bus stop of the line.

Travel time estimation in public transportation using bus location data 7

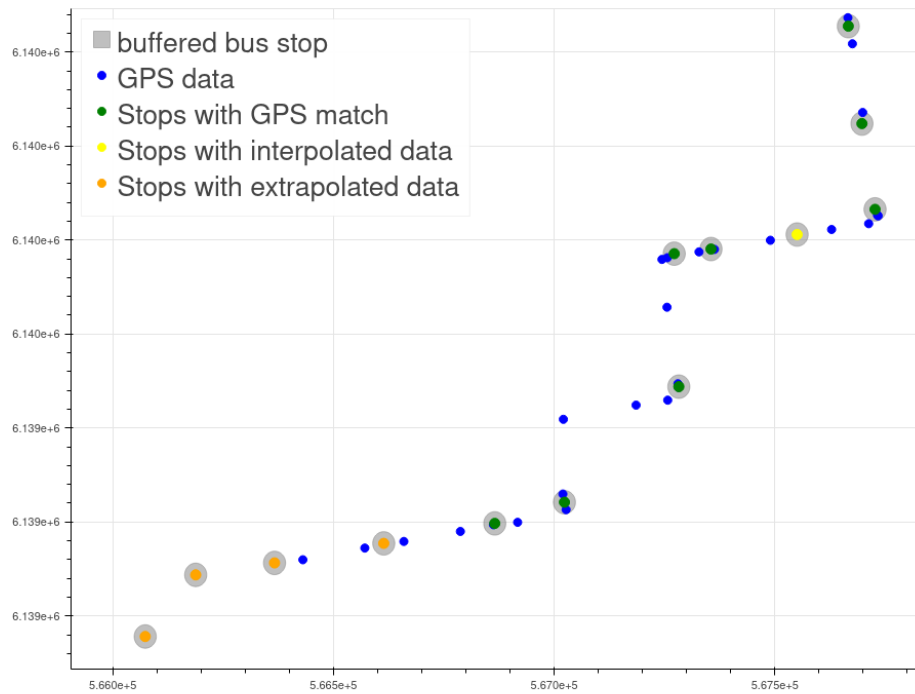


Fig. 1: Example of travel time assignment to bus stops at the end of line 306 from Parque Roosevelt to Casabó

As a result of the data processing, travel time estimations for 8 195 trips corresponding to 257 different bus lines were obtained. Overall, travel times of trips at each bus stop were estimated directly in 67.9% of the cases, when there was a matching GPS measure of the trip at the bus stop. In turn, 21.6% of travel times were interpolated based on nearby GPS measures and 10.5% were extrapolated using data from the available timetables.

**5.2 Differences between scheduled and real travel times**

The in-vehicle travel times estimated using bus location data can be compared against the scheduled timetables of the corresponding bus lines, to assess deviations from the scheduled times that may exist due to passenger demand, traffic congestion, and other external factors.

Fig. 2 presents histograms of the difference between the (estimated) real travel time and the scheduled travel time that appears on the timetable. Histogram in Fig. 2a corresponds to each independent trip in the studied dataset, whereas results in Fig. 2b correspond to the median difference in travel time of each bus line. Values greater than zero correspond to trips/lines where the total travel time was larger than the scheduled time whereas negative values indicate that the travel time was shorter than that indicated by the schedule.

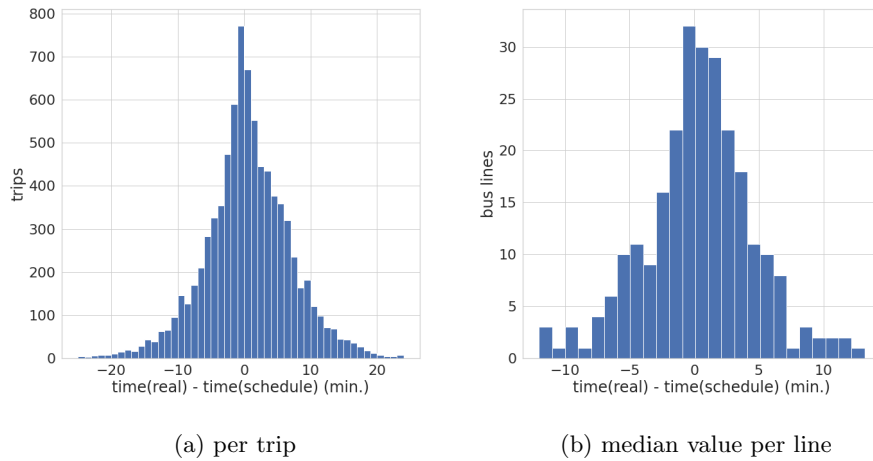


Fig. 2: Histogram of difference between (estimated) real travel times and scheduled travel times

Results show that most trips adhere to their scheduled total travel time, with an average difference of half a minute with regards to the timetable. When looking at the 25<sup>th</sup> and 75<sup>th</sup> percentiles, the differences are of 3 and 4.4 minutes, respectively. These differences, while small, might affect passengers that may miss the bus and need to wait for a full headway for the next bus of the line and is specially significant for travelers transferring between different bus lines. Extreme values of trips arriving 30 minutes before the scheduled time and 37 minutes after the scheduled time were found, which might be useful to detect special events taking place along the route of those bus lines. When looking at the median differences of trips grouped by bus lines (Fig. 2b) it can be observed that, while most lines are consistent to their scheduled total travel time, some bus lines have significant differences with their schedules. On one extreme, line 137 from Paso de la Arena arrives to its destination in Plaza de los Treinta y Tres 12 minutes (in median) before its scheduled time. In contrast, line L1, a short local line that connects Paso de la Arena with Pajas Blancas arrives (in median) 13 minutes after its scheduled time.

Besides looking at overall differences in travel times among the trips and bus lines in the system, travel times of specific trips can be analyzed. Fig. 3 shows the difference between the estimated travel time and the scheduled travel time at each bus stop of a trip of bus line 185, a bus line that travels through several neighborhoods of Montevideo going from Casabó to Pocitos. The same information is displayed in Fig. 4 using the bus stop location and the street map of the city. Each bus stop in the figure is colored according to the absolute difference between the estimated travel time to reach the bus stop and the scheduled time.

Travel time estimation in public transportation using bus location data 9

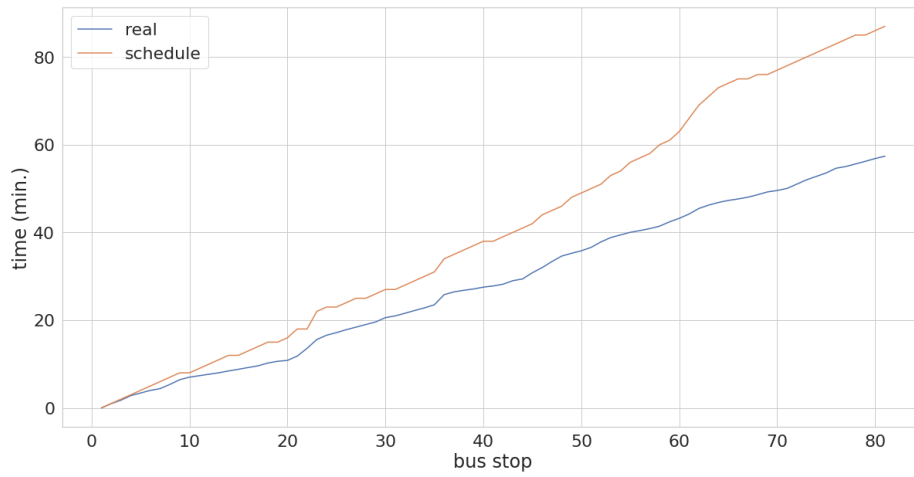


Fig. 3: Real (estimated) vs. scheduled travel time of a trip of bus line 185 from Casabó to Pocitos

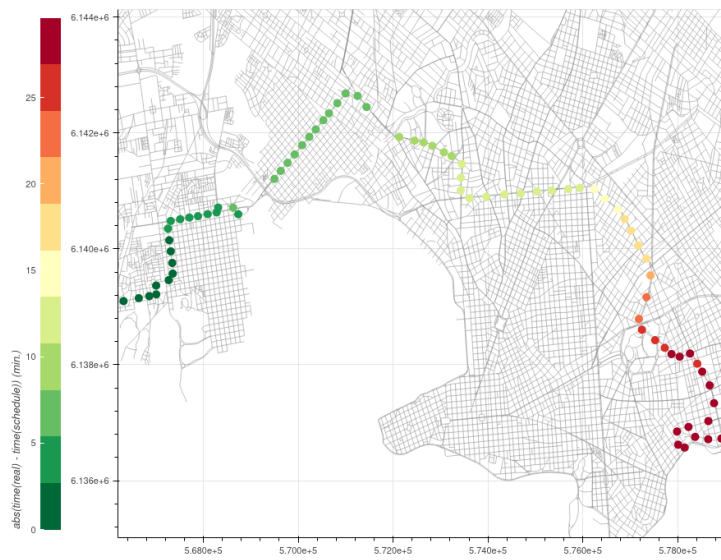


Fig. 4: Absolute difference of estimated and scheduled travel times of a trip of bus line 185 from Casabó to Pocitos

In the studied example, the trip of line 185 is, on average over all stops, 12 minutes ahead of its schedule. The difference increases along the route, reaching its maximum at the last stop, where the bus arrives nearly 30 minutes ahead of its schedule. The average headway of this bus line for the morning peak considered is 5 minutes. Thus, in this case, a severe case of bus bunching occurs, which is detrimental to the quality of service and reliability offered to citizens.

### 5.3 Operational speed

Several indicators can be computed using the estimated travel times as input. Among these, the operational speed is very useful to transport operators and authorities. Fig. 5 outlines the results of computing the operational speed for all trips in the studied dataset. Descriptive statistics are outlined in Fig. 5(a) and a boxplot of the operational speed is presented in Fig. 5(b). Results are expressed in km/h.

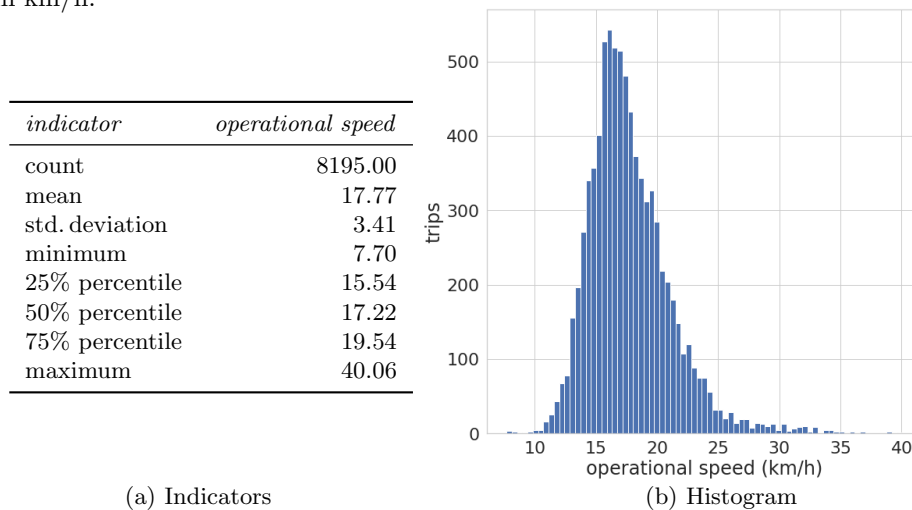


Fig. 5: Descriptive statistics of operational speed

Results in Fig. 5 show that the average operational speed for all trips in the studied dataset is 17.77 km/h. This result is consistent with performance indicators published by local authorities corresponding to the year 2018 ([www.montevideo.gub.uy/observatorio-de-movilidad](http://www.montevideo.gub.uy/observatorio-de-movilidad), October 2021). The largest operational speed (40 km/h) is achieved by a trip of line L13, which operates on the outskirts of the city. The slowest operational speed (7.7 km/h) corresponds to a trip of line L31, a short local line. This particular trip took almost 17 minutes to complete the nearly 2 km of the bus line. Short local lines have the higher dispersion regarding operational speed. The median of operational speed (17.22 km/h) corresponds to a trip of line 105 from Parque Roosevelt (in the east of the city) to Plaza Independencia in the city center. This is a very long bus line, with a total route length of over 21 kms. In this specific trip, the total length of the route was covered in nearly one hour and fifteen minutes.

In turn, the dispersion of the operational speed (dOS) is outlined in Fig. 6. Descriptive statistics are reported in Fig. 6(a) and the distribution of results is shown in the histogram of Fig. 6(b).

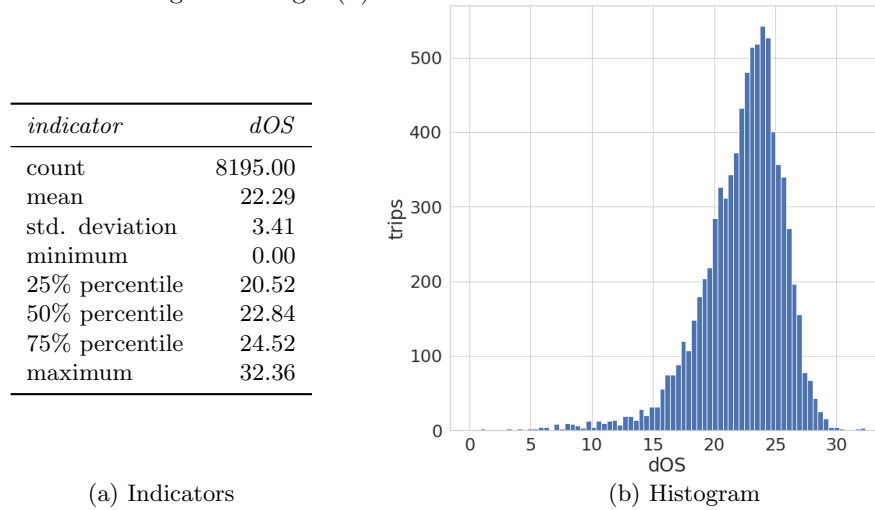


Fig. 6: Descriptive statistics of OS dispersion

The dOS metric results indicate that most lines have a large dispersion of OS values, with a mean of 22.29 km/h. This result is mainly conditioned by the extreme values of the OS metric for short local lines, which account for both the maximum and minimum values of OS, as reported in the previous analysis.

#### 5.4 On-time arrival rate

The calculation of the OTAR metric requires computing the buffer time, i.e. the coefficient that defines the acceptable delay threshold for completing a trip, with respect to the scheduled time. Table 1 outlines descriptive statistics for the buffer coefficients of the bus lines of the studied scenario. According to the computed results, the average value for acceptable delay is 11%.

<i>indicator</i>	<i>buffer coefficient</i>
count	257.00
mean	0.11
std. deviation	0.06
minimum	0.00
25% percentile	0.08
50% percentile	0.11
75% percentile	0.15
maximum	0.38

Table 1: Descriptive statistics of buffer coefficients for on-time arrival rate

After determining the buffer coefficients, the OTAR metric was computed for each of the bus lines in the considered scenario. Results are shown in the histogram in Fig. 7.

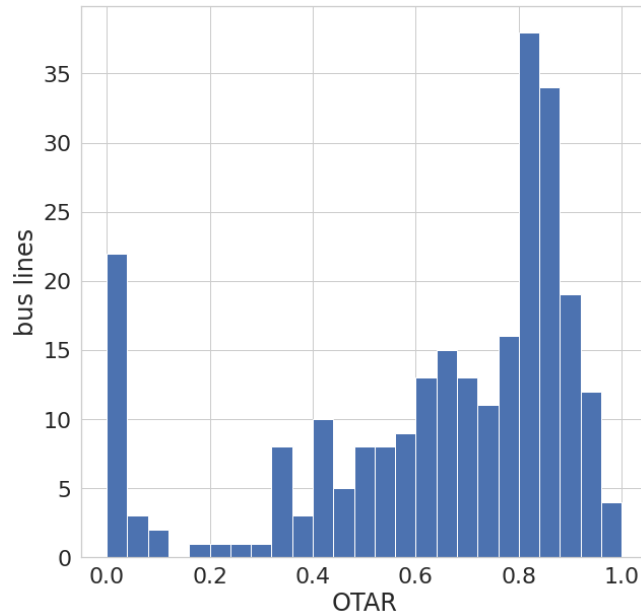


Fig. 7: Histogram of on-time arrival rate for bus lines

Results in Fig. 7 indicate that the average OTAR among all bus lines in the studied scenario is 0.64, with a standard deviation of 0.27. The histogram allows identifying a large number of bus lines with an OTAR value of 0.0. In these cases, none of the trips of a given bus line completed their journey within their scheduled time (even considering the time tolerance). In these extreme cases, authorities should review the predefined schedules and modify them to reflect the real operation times. These results confirm the usefulness of the proposed approach to detect anomalous situations in the public transportation system.

**5.5 Additional travel time over automobile (ATToA)**

The heatmap in Fig. 8 reports the values of the ATToA metric for bus line 185. Bus line 185 has a higher-than-average operational speed, considering all bus lines in the city. The analysis is representative of those performed for other ‘fast’ bus lines in the city. Results correspond to the ATToA values computed from/to 17 (regularly spaced) stops along the route. Travel times in automobile were computed using the API provided by Google Maps.

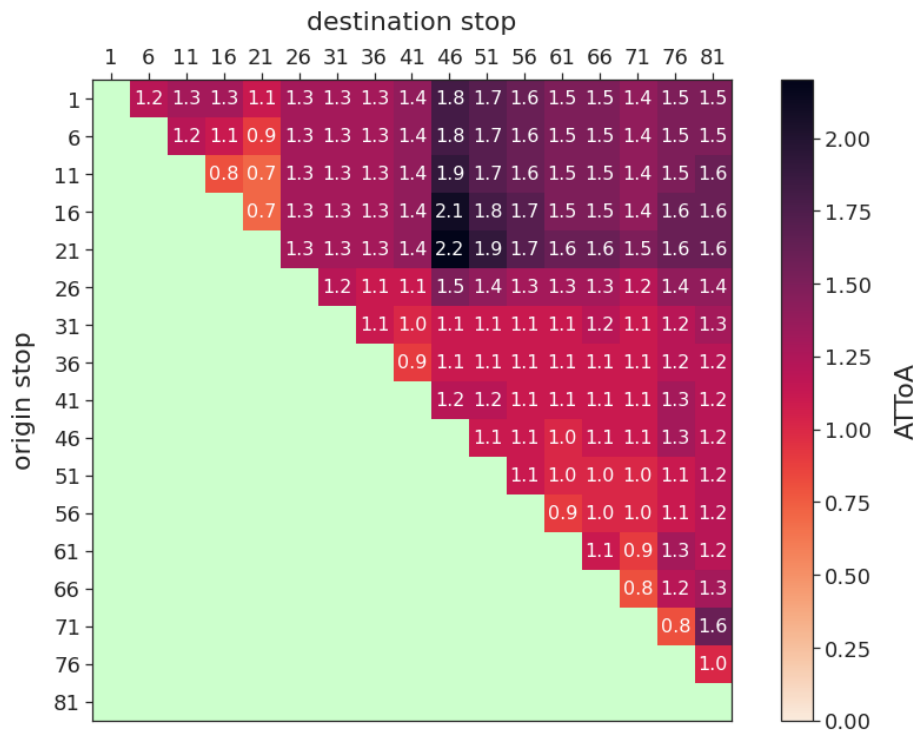


Fig. 8: Additional travel time over automobile (ATToA) of a trip of bus line 185 from Casabó to Pocitos

Results in Fig. 8 allow observing an almost regular pattern: the bus is very (time-wise) efficient for traveling between nearby stops, as demonstrated by ATToA values lower than 1.0, meaning that bus is faster than automobile in those cases. Values slightly increase for longer trips, up to reasonable 1.5× to 1.6× additional time factors. The only exceptions are for bus stop #46, for which the ATToA values are closer to 2.0 (and a worst value of 2.2 was computed for a trip with origin on stop #21). Two main reasons explain this result: between stops #21 and #46 the bus route has a big detour, which impacts on route directness, whereas the fastest way is traveling using automobile via a direct avenue (Bv. Artigas). Furthermore, bus stop #46 is located after a long red light that allows buses to turn left towards Bv. Artigas. Despite the reported delay, the bus line manages to recover a normal operational speed, as ATToA values after bus stop #46 reduce to a reasonable 1.6× additional time factor.

Overall, reported ATToA values are similar to the ones reported for other bus networks in similar cities (e.g., Stockholm, Sweden and Amsterdam, the Netherlands), and lower than values reported for larger cities such as São Paulo, Brazil and Sydney, Australia, for which average values up to 2.6× longer than driving a car have been reported [17].

## 6 Conclusions and future work

This article presented a data analysis approach to estimate in-vehicle travel time in public transportation systems, using GPS bus location data and several other sources of open data regarding the system infrastructure. The public transportation system in Montevideo, Uruguay, was used as a case study. A specific data analysis methodology is presented and then applied to one week of GPS bus location data comprised of over 2.8 million records corresponding to the morning peak hours. Estimated travel times were obtained for over 8 000 trips, corresponding to 257 different bus lines. These travel times were used as input to compute several relevant metrics, focused on evaluating different features of the public transportation system, including: i) differences against scheduled timetables, ii) operational speed, iii) on-time arrival rate, and iv) additional travel time over automobile. Computed metrics are a useful input for operators to evaluate the reliability of the transportation system and are relevant to policy-makers aiming to improve the quality of service offered to citizens.

The main lines of future work focus on improving the analysis and applying the computed results to solve relevant problems regarding public transportation in the case study considered. Regarding the first line, the data analysis process could be further improved by considering data from different peak and non-peak hours, as well as weekends, and by processing larger amounts of historical data. For the latter, parallel computing strategies should be devised to deal with the increased computational burden. Regarding the application of the computed travel times and indicators, several relevant lines are planned for future work, including bus timetable synchronization [15, 16], bus network redesign [5], sustainable mobility plans [9], and assessing accessibility using public transportation to different opportunities in the city. For this last application, a specific line of work is to extend the model presented in our previous work [8], which only used scheduled timetables, and incorporate the estimated (real) in-vehicle travel times to further refine the accessibility metric.

## Acknowledgments

The research was partly funded by ANII (Uruguay), under grant ANILFSDA\_1.2018.1.154502 “Territorial, universal, and sustainable accessibility: characterization of the intermodal transportation system of Montevideo”. The work of R. Massobrio and S. Nesmachnow was partly funded by ANII and PEDECIBA, Uruguay.

## References

1. Benn, H.: Bus route evaluation standards a synthesis of transit practice. Tech. Rep. TCRP Synthesis 10, Transportation Research Board (1995)
2. Bhat, C., Guo, J., Sen, S., Weston, L.: Measuring access to public transportation services: Review of customer-oriented transit performance measures and methods

## Travel time estimation in public transportation using bus location data 15

- of transit submarket identification. Tech. Rep. 0-5178-1, Center for Transportation Research, The University of Texas at Austin (2005)
3. Cardozo, O.D., Rey, C.E.: La vulnerabilidad en la movilidad urbana: aportes teóricos y metodológicos. In: Foschiatti, A. (ed.) *Aportes conceptuales y empíricos de la vulnerabilidad global*, pp. 398–423. Editorial Universitaria de la Universidad Nacional del Nordeste (2007)
  4. Deng, Y., Yan, Y.: Evaluating route and frequency design of bus lines based on data envelopment analysis with network epsilon-based measures. *Journal of Advanced Transportation* 2019, 1–12 (2019)
  5. Fabbiani, E., Neschachnow, S., Toutouh, J., Tchernykh, A., Avetisyan, A., Radchenko, G.I.: Analysis of mobility patterns for public transportation and bus stops relocation. *Programming and Computer Software* 44(6), 508–525 (2018)
  6. Federal Highway Administration: Travel time reliability: Making it there on time, all the time. Tech. Rep. HOP-06-070, U.S. Department of Transportation (2005)
  7. Grava, S.: *Urban Transportation Systems*. McGraw-Hill Professional (2000)
  8. Hernández, D., Hansz, M., Massobrio, R.: Job accessibility through public transport and unemployment in Latin America: The case of Montevideo (Uruguay). *Journal of Transport Geography* 85, 102742 (2020)
  9. Hipogrosso, S., Neschachnow, S.: Analysis of Sustainable Public Transportation and Mobility Recommendations for Montevideo and Parque Rodó Neighborhood. *Smart Cities* 3(2), 479–510 (2020)
  10. Jagadeesh, G.R., Srikanthan, T., Zhang, X.D.: A map matching method for gps based real-time vehicle location. *Journal of Navigation* 57(3), 429–440 (2004)
  11. Lei, T.L., Church, R.L.: Mapping transit-based access: integrating GIS, routes and schedules. *Int. Journal of Geographical Information Science* 24(2), 283–304 (2010)
  12. Massobrio, R., Neschachnow, S.: Urban Mobility Data Analysis for Public Transportation Systems: A Case Study in Montevideo, Uruguay. *Applied Sciences* 10(16), 1–20 (2020)
  13. Massobrio, R., Neschachnow, S., Tchernykh, A., Avetisyan, A., Radchenko, G.: Towards a cloud computing paradigm for big data analysis in smart cities 44(3), 181–189 (2018)
  14. Massobrio, R., Pías, A., Vázquez, N., Neschachnow, S.: Map-Reduce for Processing GPS Data from Public Transport in Montevideo, Uruguay. In: *Simposio Argentino de Grandes Datos, 45 Jornadas Argentinas de Informática*. pp. 41–54 (2016)
  15. Neschachnow, S., Muraña, J., Goñi, G., Massobrio, R., Tchernykh, A.: Evolutionary approach for bus synchronization. In: *High Performance Computing*, pp. 320–336. Springer International Publishing (2020)
  16. Neschachnow, S., Risso, C.: Exact and evolutionary algorithms for synchronization of public transportation timetables considering extended transfer zones. *Applied Sciences* 11(15), 7138 (2021)
  17. Salonen, M., Toivonen, T.: Modelling travel time in urban networks: comparable measures for private car and public transport. *Journal of Transport Geography* 31, 143–153 (2013)
  18. Turnquist, M., Blume, S.: Evaluating potential effectiveness of headway control strategies for transit systems. *Transportation Research Record* 746, 25–29 (1980)

## Methodology for inspection of defects in photovoltaic plants by drone and electroluminescence

Hernández-Callejo, Luis<sup>1[0000-0002-8822-2948]</sup>, Gallardo-Saavedra, Sara<sup>1[0000-0002-2834-5591]</sup>, Morales-Aragonés, José Ignacio<sup>1[0000-0002-9163-9357]</sup>, Alonso-Gómez, Víctor<sup>1[0000-0001-5107-4892]</sup>, Redondo Plaza, Alberto<sup>1[0000-0002-2109-5614]</sup> and Fernández Martínez, Diego<sup>1[0000-0003-1468-9083]</sup>

<sup>1</sup> University of Valladolid, Campus Universitario Duques de Soria 42004 Soria, Spain  
luis.hernandez.callejo@uva.es (L.H-C.)  
s.gallardosaavedra@gmail.com (S.G-S.)  
ziguratt@coit.es (J.I.M-A.)  
victor.alonso.gomez@uva.es (V.A-G.)  
alberredon@gmail.com (A.R.P.)  
diego-brivi@hotmail.com (D.F.M.)

**Abstract.** The integration of photovoltaic systems is increasing in cities. Advanced maintenance methods should provide interesting results for maintenance companies. Of the inspection techniques, one of the most promising is that based on electroluminescence, although it has its drawbacks, such as the need to disconnect the string and photovoltaic modules. In this work, a new methodology for capturing electroluminescence images is presented for the detection of defects in photovoltaic modules, using a drone and a bidirectional inverter. The method is validated in an existing plant, and the results are satisfactory.

**Keywords:** electroluminescence, dron, bidirectional inverter.

### 1 Introduction

In the 21st century, the integration of renewable generation sources is a reality. Within renewable technologies, wind and photovoltaic systems are the most installed, and specifically in the last five years photovoltaic plants are the most interesting [1].

This increase in the installation of renewable plants will require changes in the electrical infrastructure. However, there are other areas that are going to change, and many of them will be in cities. These cities of the future (Smart Cities, SC) will need different control and management strategies from the current ones, and this will mean a paradigm shift in their design [2–4]. SC needs to integrate generation sources (mainly renewable) in order to meet its energy needs, and in this sense, photovoltaic technology is easily installable in its infrastructures [5,6].

Regardless of the size of the photovoltaic plant (small and integrated in SC or large photovoltaic plant), photovoltaic systems need novel inspection techniques to keep their productive performance high [7]. Numerous techniques are used for this purpose, but the most important are those that detect failures in photovoltaic modules, and this

is because this type of failure is the most common and the one that produces greater production losses [8].

Of the failure inspection techniques in photovoltaic modules, there are two of them above the others. Specifically, the inspection techniques with thermography [9–11] and electroluminescence [12–14] are the most used and promising.

The use of the drone for maintenance in photovoltaic plants is being used. The drone can do thermographic inspection with good results [15,16], and the electroluminescence sensor is also shipped on drone [17]. Electroluminescence is very interesting, since many defects are detected, but it has a disadvantage, this technique is invasive, since it requires the disconnection of the photovoltaic module and its connection to an external source. However, lately work is being done on inspection techniques with electroluminescence, but without the need for disconnection, for which a bidirectional inverter is used [9,14].

Therefore, it is clear that photovoltaic plants need maintenance. The photovoltaic systems integrated into the SC infrastructures will require advanced maintenance. The use of drones together with techniques such as electroluminescence are very interesting combinations. As already seen, electroluminescence has the disadvantage of the need to disconnect the photovoltaic modules for current injection. With all these conditions, this work presents a methodology for the inspection of defects in photovoltaic plants by drone and electroluminescence, for which a bidirectional inverter will be used (avoiding the disconnection of photovoltaic modules) together with the drone and an InGaAs camera. The document is as follows: section 2 shows materials and methods; section 3 shows the results; and section 4 presents the conclusions.

## 2 Materials and methods

In this section the materials that have been used for the investigation will be presented, and later the methods used to carry it out.

### 2.1 Materials

The experiments have been carried out in the facilities of the Duques de Soria University Campus of the University of Valladolid, in Soria (Spain). The experience has been performed in 11 PV modules connected in series (string) to a bidirectional inverter. The nominal characteristics of the modules are shown in **¡Error! No se encuentra el origen de la referencia.**, and **¡Error! No se encuentra el origen de la referencia.** shows a real photograph of the installation previously described

**Table 1.** Main nominal data of photovoltaic (PV) modules.

Module	Model	Power (W)	Voc (V)	Vmpp (V)	Isc (A)	Impp (A)
1	Eoplly	175	44.35	36.26	5.45	4.83
2	Eoplly	175	44.35	36.26	5.45	4.83

Module	Model	Power (W)	Voc (V)	Vmpp (V)	Isc (A)	Impp (A)
3	Eopllly	175	44.35	36.26	5.45	4.83
4	Eopllly	175	44.35	36.26	5.45	4.83
5	Eopllly	175	44.35	36.26	5.45	4.83
6	Eopllly	175	44.35	36.26	5.45	4.83
7	Eopllly	175	44.35	36.26	5.45	4.83
8	Eopllly	175	44.35	36.26	5.45	4.83
9	Eopllly	175	44.35	36.26	5.45	4.83
10	EGNG	180	44.40	35.40	5.35	5.08
11	SKY Global	175	42.60	35.50	5.20	4.93



Fig. 1. Experimental installation, Campus of the University of Valladolid, in Soria (Spain).

A specific power inverter with bidirectional power flow capability was placed in the pilot-site for this study. The power inverter is a neutral point clamped (NPC I-type) that has been recently developed to help in the maintenance of photovoltaic plants by means of electroluminescence image processing [14]. Fig. 2 shows a classical converter control block scheme, electroluminescence control action is performed inside the high level controller layer (highlights in blue the blocks concerning EL functionality). Solar cells convert solar energy into electricity, however they also have the characteristic of being able to emit light if they are connected to an electrical current. This process, let's say inverse, is called electroluminescence.

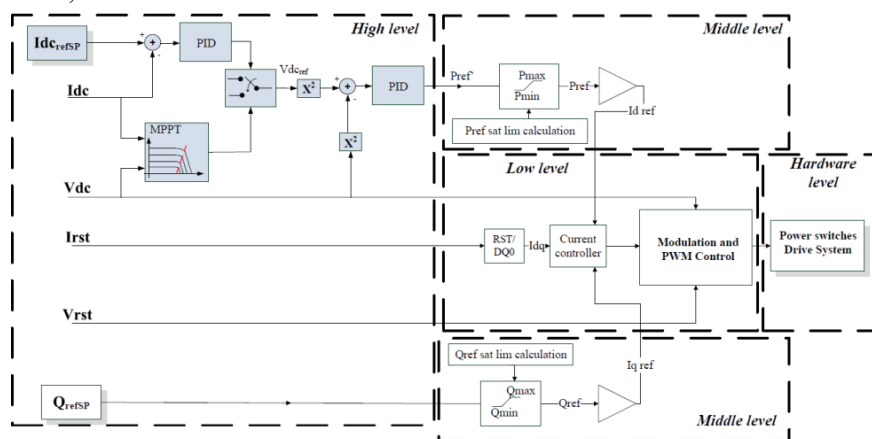


**Fig. 2.** Main control diagram of a photovoltaic inverter controller: in blue are marked the high-level control blocks related to the maximum power point tracking (MPPT) and electroluminescence (evaluation working modes. Experimental installation installed in Campus of the University of Valladolid, in Soria (Spain).

Finally, Fig. 3 shows the drone and the electroluminescence camera used. The camera is special, it is an InGaAs camera (Hamamatsu brand and C12741-03 model), specially designed to capture the light emission of the photovoltaic module when it is electrically excited. The drone used is a hexacopter drone.



**Fig. 3.** Drone and InGaAs camera installed on gimbal.

**2.2 Methods**

The elements described in section 2.1. must be integrated with each other. All the elements described are shown in Fig. 4, in order to later comment on their operation.

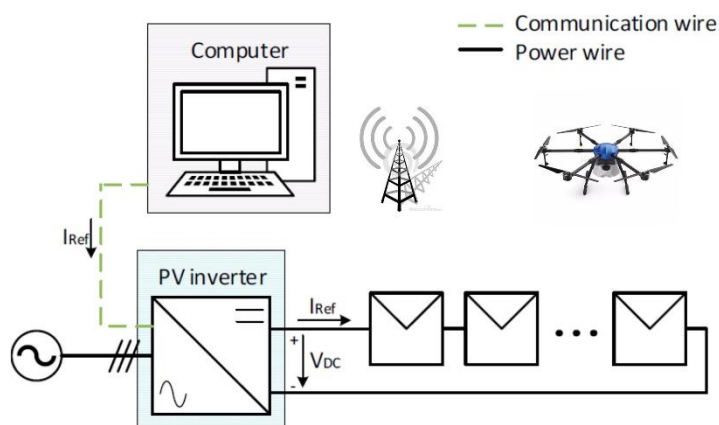


**Fig. 4.** Inspection process diagram.

Fig. 5 shows the sequence of the process, which is related to the elements of Fig. 4, to later comment on the five steps that compose it.

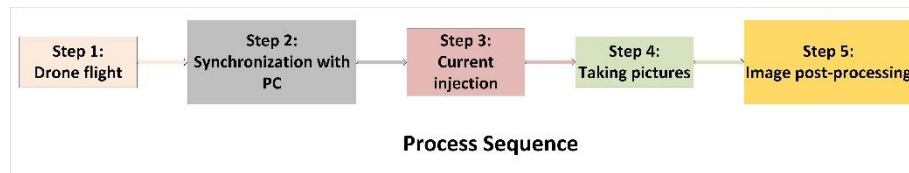


**Fig. 5.** Sequence process of electroluminescence measurements performed.

Next, the five steps of the process will be described:

- **Step 1:** the drone with the camera (InGaAs) installed will be put into flight. The drone will have the flight prerecorded. In this case, the drone pilot will need to control the camera angle, but this process can be automated in another test.
- **Step 2:** with the drone in position to capture images (video in this case), the drone will send a signal to the PC in the field. The mission of this PC is to control the current ( $I_{ref}$ ) to be injected into the string of the photovoltaic generator.
- **Step 3:** once the current reference is set in the bidirectional inverter control script, the converter changes its mode, and this device begins to inject the setpoint current into the string bus of the photovoltaic generator. This reference can be varied, and the value of the injected current will influence the luminosity emitted by the photovoltaic modules.
- **Step 4:** once the current injection is established, the PC sends a control command to the drone. At this time, and with the camera activated and in recording mode, the drone makes the programmed route, capturing the images of all the photovoltaic modules emitting light.
- **Step 5:** this step is the only one done with the drone on the ground. The images taken are recorded in the memory installed in the drone, so the post-processing must be carried out once the flight is finished. When performing the night flight, it is not necessary to apply a lock-in technique on the images, since these are of sufficient definition to identify the defects. Post-processing will consist of identifying the contour of the panels and correcting the angle of the image. The actual camera lens is not ideal and introduces some distortion to the image. To account for these non-idealities, it is necessary to add a distortion model to the perspective projection equation. Therefore, it is necessary to use a correction algorithm, and python or matlab has some optimized algorithms implemented.

### 3 Results and analysis of results

In this section the results of the experience will be presented, and an analysis of them will be made.

#### 3.1 Results

As already mentioned, the bidirectional inverter is a fundamental element in this experiment. In addition, the possibility of regulating the current to be injected into the string

of the photovoltaic generator has been discussed. This will allow this experiment to be carried out at different injected currents, and therefore at different light emissions from the photovoltaic modules. Fig. 6 shows the transition from 5 A to 0.5 A in the injected current, as well as the voltage ( $V_{DC}$ ) of the string. It is possible to see a good response stabilization of the bidirectional inverter. As is logical, a decrease in the injected current causes a decrease in the voltage in the string, since the current cuts the I-V curve of the photovoltaic module at a lower voltage.

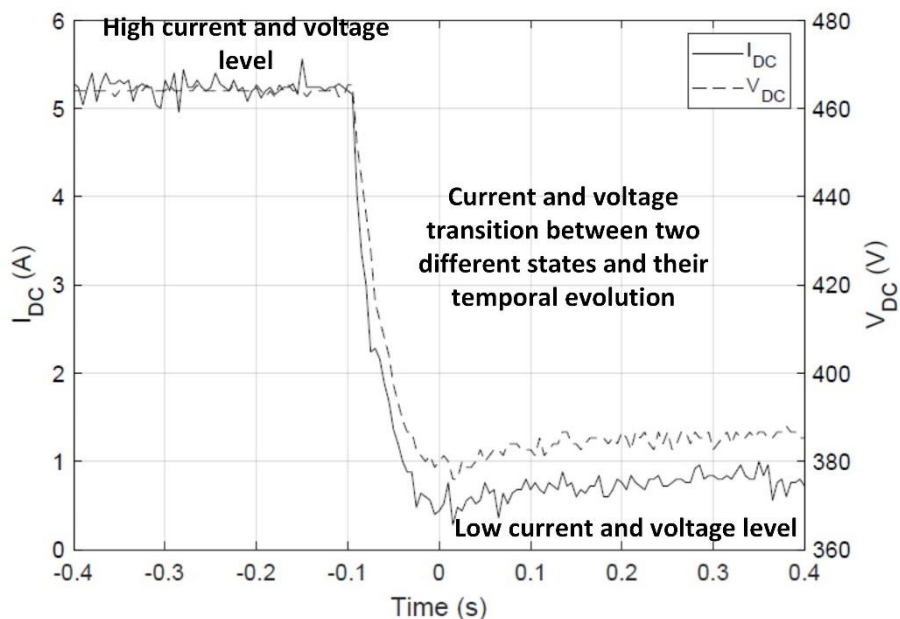
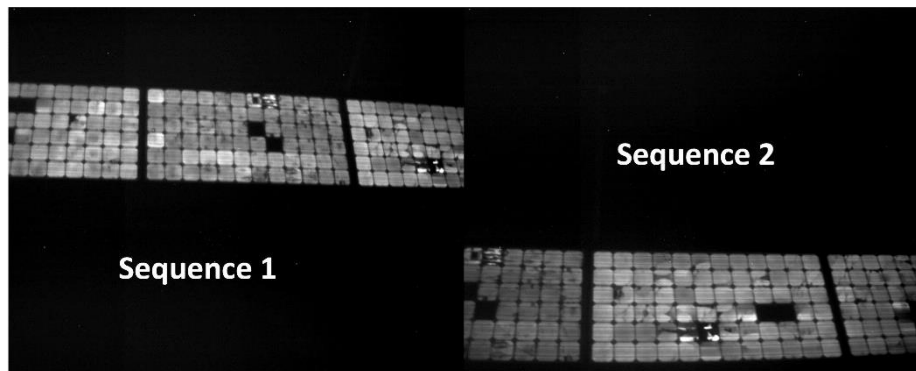


Fig. 5. Current set-point changed from 5 A to 0.5 A.

The flight data were: distance from the drone to the photovoltaic modules of 5m, the flight in low light, wind speed 0.5 m/s. Below, in Fig. 6 several non-post-processed images obtained in flight are shown. As can be seen, the images are of high quality, and this test has been carried out by injecting 5 A into the string of the photovoltaic generator. The figure represents two different image sequences, with different photovoltaic modules.



**Fig. 6.** Two different sequences of the flight of the InGaAs camera drone. Photovoltaic modules emitting light from 5 A of injected current.

As discussed above, in step 5 the contours of the photovoltaic modules are identified. In this way, it is possible to cut the contour of the photovoltaic module, and obtain a more optimal image than the views in Fig. 6. Fig. 7 shows all the photovoltaic modules already cut, with interesting information.

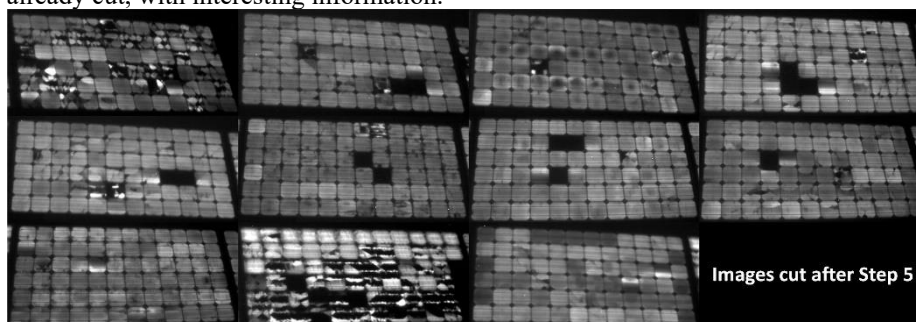


**Fig. 6.** Electroluminescence images of the 11 photovoltaic modules. Images taken with a drone, and with 5 A of injected current.

Another action in step 5 is the geometric correction of the images, mainly as a consequence of the fisheye in the image. Fig. 7 shows the sequence of the geometric correction. The image shows the image enhancement, showing a rectangular image, without loss of information.

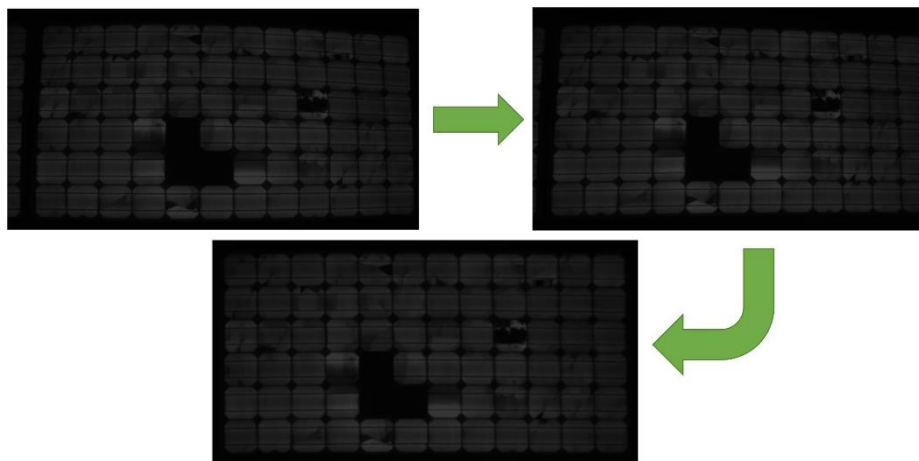


**Fig. 7.** Geometry correction process. Electroluminescence image taken by drone.

Once the image has been corrected, it is possible to increase or decrease the quality of the information by acting on the image histogram. In Fig. 8 the effect of acting on the histograms of the images is shown.

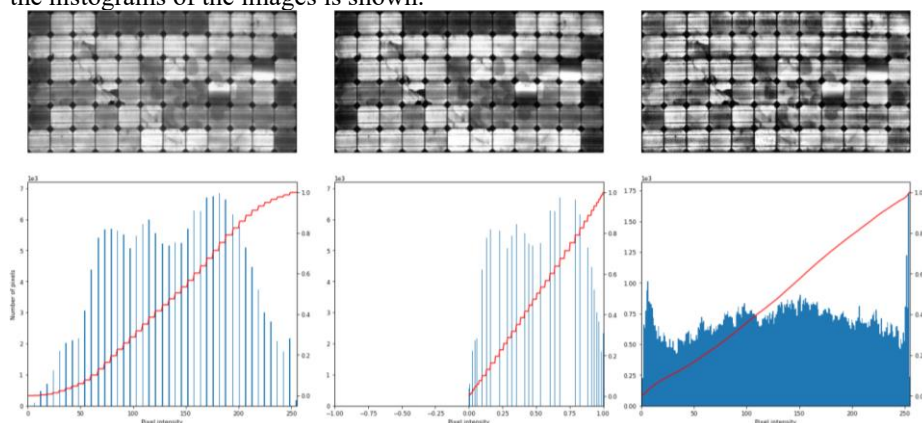


**Fig. 8.** Modification of the information displayed through the image histogram.

Finally, a last detection of the edges of the photovoltaic module is performed. With the geometrically corrected image, the edge detection algorithm is executed, and the results can be seen in Fig. 9. A projective transformation called homography has been used.

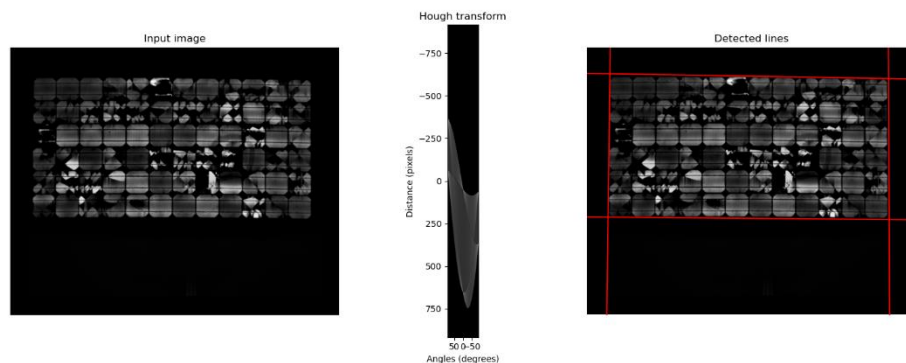


Fig. 9. Result of the edge detection algorithm.

### 3.2 Analysis of results

As shown in the previous section, the bidirectional inverter is a critical element for electroluminescence imaging. This device has some interesting characteristics to be able to carry out the electroluminescence technique. The device presents a very interesting current control, allowing images to be made at different currents injected into the string, and thus being able to have images with different lighting. This device is essential for the electroluminescence technique, since the device avoids having to disconnect the string (or each photovoltaic module), and it is possible to take the images without disconnecting the photovoltaic modules.

Once the current is injected into the string, and synchronized with the drone, the drone can perform the scheduled flight, and capture all the images of the photovoltaic modules. These photovoltaic modules will be emitting light, which will depend on the amount of current injected. In the test carried out, the capture of electroluminescence images was carried out with a current injection of 5 A. On this occasion, as it is a night flight, the images obtained are of excellent quality, as can be seen in Fig. 6, so it is not necessary to apply lock-in techniques.

However, the amount of current injected is very important, as it is related to the amount of light emitted. The defects detected are related to the emissivity of the photovoltaic module. In this experience, electroluminescence imaging has been carried out at different injected currents, as can be seen in Fig. 10, where the electroluminescence image taken from the drone on the same photovoltaic modules, but at different injected currents, can be seen. Fig. 10 a) shows a photovoltaic module illuminated with different currents injected into the string (0.0 A, 0.5 A, 1.5 A, 3.5 A and 5.0 A). It is possible to appreciate the clear differences between them, and it is possible to affirm that the higher the injected current (in this case the  $I_{sc}$ ) the electroluminescence image obtained is of higher quality. Fig. 10 b) shows the same images as in Fig. 10 a) but once processed, and it can be seen that the images obtained with a current injection of 3.5 A and 5.0 A are very similar.

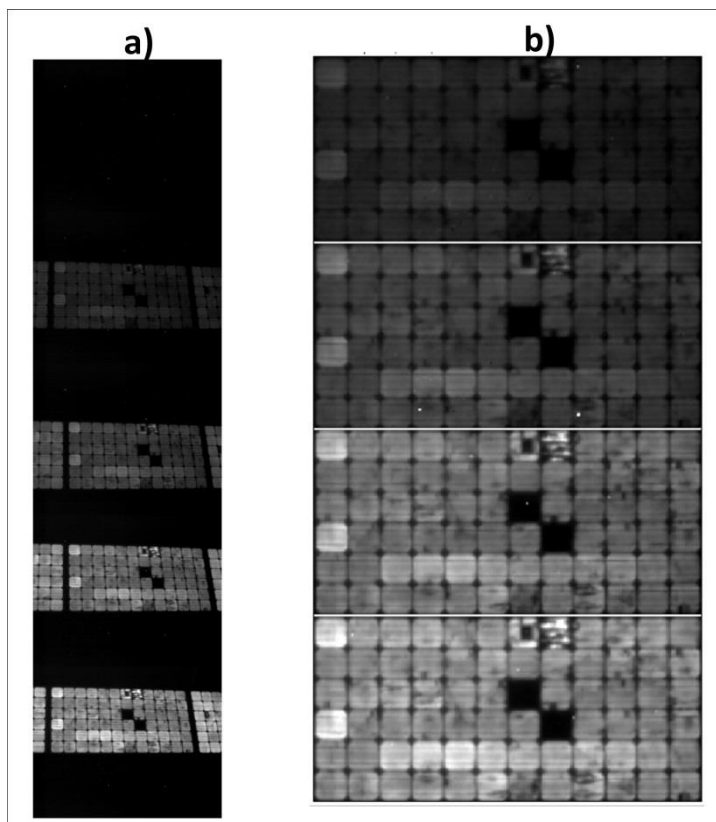


**Fig. 10.** Electroluminescence image taken by drone of the same photovoltaic module with different injected currents (0.0 A, 0.5 A, 1.5 A, 3.5 A and 5.0 A). a) uncorrected images; b) Corrected images.

Once the images are corrected, it is easy to detect the main defects of the measured photovoltaic modules. In the images shown in the results section, it is possible to see totally inactive cells (black cells in the image), or cells with a very high illumination density as a consequence of the inactivity of part of it.

Electroluminescence images by themselves serve to draw conclusions about the state of the photovoltaic module. And to corroborate this statement, Fig. 11 shows the electroluminescence images of the photovoltaic modules 4, 9 and 11, completed with the I-V curves of said photovoltaic modules. It is possible to observe in the I-V curves the clear deterioration of the photovoltaic module, from the point of view of its performance. All the photovoltaic modules shown present a clear degradation in their I-V curve, and this deterioration can be inferred from the electroluminescence images.

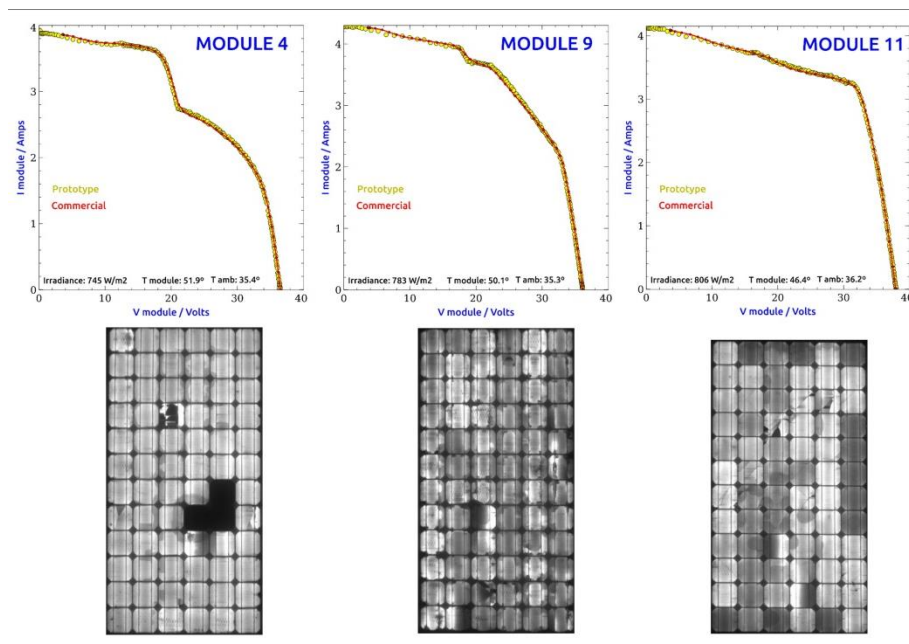


Fig. 10. Electroluminescence image and I-V curve of photovoltaic modules 4, 9 and 11.

#### 4 Conclusions and future work

This work presents a new methodology for capturing electroluminescence images of photovoltaic modules, using drone, InGaAs camera and bidirectional inverter. The method has been validated in the photovoltaic plant located in Duques de Soria University Campus of the University of Valladolid, in Soria (Spain).

To begin with, the work has made clear the need for a bidirectional inverter. This new functionality (bidirectionality) allows taking electroluminescence images without the need to disconnect the string or the photovoltaic modules. It is possible to affirm that this device allows the technique to be non-invasive, and that it does not require human intervention to disconnect devices. In addition, this inverter gives the method a lot of versatility, since it allows electroluminescence to be made by injecting different amounts of current. In this work, images have been taken with 5 A current, but electroluminescence images have also been taken at lower currents.

The synchronization between the bidirectional inverter and the drone is essential. In this work, the results of electroluminescence images have been shown taking into account this synchronization.

Once the images have been taken, they have been found to be of sufficient quality to detect failures in the photovoltaic modules. However, the images have been subjected to classical algorithms to correct the effect of geometry. The results of this correction have been good, and there is no loss of quality in the image.

The results obtained from the electroluminescence images have been compared with the I-V curves obtained from the photovoltaic modules. It is possible to affirm that the images alone are used to make a decision regarding the state of the photovoltaic module.

These researchers will continue to work on new bi-directional inverters with complementary benefits. In addition, it is possible to investigate the possibility of locking in this method, but it will require greater rigor in synchronization. In addition, and from these electroluminescence images, the researchers will work on defect classification techniques based on artificial intelligence, and on photovoltaic module performance estimators.

The use of other drone models (for example DJI) is an interesting topic to address. The decision will depend on several issues, on the one hand, the drone must be able to raise and keep a camera stable (in this work a special and weighted camera has been used), and on the other hand, the flight time of the drone will also be critical, and this will depend on the size of the plant to be measured.

## Acknowledgements

We would like to thank the CEDER by providing information for the development of this work. The authors thank the CYTED Thematic Network “CIUDADES INTELIGENTES TOTALMENTE INTEGRALES, EFICIENTES Y SOSTENIBLES (CITIES)” no518RT0558.

This research was funded by the “Ministerio de Industria, Economía y Competitividad” grant number “RTC-2017-6712-3” with name “Desarrollo de herramientas Optimizadas de operación y mantenimiento Predictivo de Plantas fotovoltaicas—DOCTOR-PV”.

## References

- [1] Korkeakoski M. Towards 100% Renewables by 2030: Transition Alternatives for a Sustainable Electricity Sector in Isla de la Juventud, Cuba. *Energies* 2021, Vol 14, Page 2862 2021;14:2862. <https://doi.org/10.3390/EN14102862>.
- [2] Tanwar S, Popat A, Bhattacharya P, Gupta R, Kumar N. A taxonomy of energy optimization techniques for smart cities: Architecture and future directions. *Expert Syst* 2021:e12703. <https://doi.org/10.1111/EXSY.12703>.
- [3] Elberzhager F, Mennig P, Polst S, Scherr S, Stüpfert P. Towards a Digital Ecosystem for a Smart City District: Procedure, Results, and Lessons Learned. *Smart Cities* 2021, Vol 4, Pages 686-716 2021;4:686–716. <https://doi.org/10.3390/SMARTCITIES4020035>.
- [4] James P, Astoria R, Castor T, Hudspeth C, Olstinske D, Ward J. *Smart Cities: Fundamental Concepts 1* 2021. [https://doi.org/10.1007/978-3-030-69698-6\\_2](https://doi.org/10.1007/978-3-030-69698-6_2).
- [5] Dai Y, Bai Y. Performance Improvement for Building Integrated Photovoltaics in Practice: A Review. *Energies* 2021, Vol 14, Page 178 2020;14:178. <https://doi.org/10.3390/EN14010178>.

- [6] Mahian O, Ghafarian S, Sarrafha H, Kasaeian A, Yousefi H, Yan W-M. Phase change materials in solar photovoltaics applied in buildings: An overview. *Sol Energy* 2021;224:569–92. <https://doi.org/10.1016/J.SOLENER.2021.06.010>.
- [7] Hernández-Callejo L, Gallardo-Saavedra S, Alonso-Gómez V. A review of photovoltaic systems: Design, operation and maintenance. *Sol Energy* 2019;188:426–40. <https://doi.org/10.1016/J.SOLENER.2019.06.017>.
- [8] Gallardo-Saavedra S, Hernández-Callejo L, Duque-Pérez O. Quantitative failure rates and modes analysis in photovoltaic plants. *Energy* 2019;183:825–36. <https://doi.org/10.1016/J.ENERGY.2019.06.185>.
- [9] Gallardo-Saavedra S, Hernández-Callejo L, Alonso-García M del C, Muñoz-Cruzado-Alba J, Ballestín-Fuertes J. Infrared Thermography for the Detection and Characterization of Photovoltaic Defects: Comparison between Illumination and Dark Conditions. *Sensors* 2020, Vol 20, Page 4395 2020;20:4395. <https://doi.org/10.3390/S20164395>.
- [10] Alfaro-Mejía E, Loaiza-Correa H, Franco-Mejía E, Hernández-Callejo L. Segmentation of Thermography Image of Solar Cells and Panels. *Commun Comput Inf Sci* 2019;1152 CCIS:1–8. [https://doi.org/10.1007/978-3-030-38889-8\\_1](https://doi.org/10.1007/978-3-030-38889-8_1).
- [11] Dávila-Sacoto M, Hernández-Callejo L, Alonso-Gómez V, Gallardo-Saavedra S, González LG. Detecting Hot Spots in Photovoltaic Panels Using Low-Cost Thermal Cameras. *Commun Comput Inf Sci* 2020;1152 CCIS:38–53. [https://doi.org/10.1007/978-3-030-38889-8\\_4](https://doi.org/10.1007/978-3-030-38889-8_4).
- [12] Pratt L, Govender D, Klein R. Defect detection and quantification in electroluminescence images of solar PV modules using U-net semantic segmentation. *Renew Energy* 2021;178:1211–22. <https://doi.org/10.1016/J.RENENE.2021.06.086>.
- [13] Otamendi U, Martínez I, Quartulli M, Olaizola IG, Viles E, Cambarau W. Segmentation of cell-level anomalies in electroluminescence images of photovoltaic modules. *Sol Energy* 2021;220:914–26. <https://doi.org/10.1016/J.SOLENER.2021.03.058>.
- [14] Ballestín-Fuertes J, Muñoz-Cruzado-Alba J, Sanz-Osorio JF, Hernández-Callejo L, Alonso-Gómez V, Morales-Aragones JI, et al. Novel Utility-Scale Photovoltaic Plant Electroluminescence Maintenance Technique by Means of Bidirectional Power Inverter Controller. *Appl Sci* 2020, Vol 10, Page 3084 2020;10:3084. <https://doi.org/10.3390/APP10093084>.
- [15] Gallardo-Saavedra S, Hernández-Callejo L, Duque-Pérez Ó. Analysis and characterization of PV module defects by thermographic inspection. *Rev Fac Ing* 2019;92–104. <https://doi.org/10.17533/UDEA.REDIN.20190517>.
- [16] Gallardo-Saavedra S, Hernandez-Callejo L, Duque-Perez O. Image resolution influence in aerial thermographic inspections of photovoltaic plants. *IEEE Trans Ind Informatics* 2018;14:5678–86. <https://doi.org/10.1109/TII.2018.2865403>.
- [17] Dhimish M, d'Alessandro V, Daliento S. Investigating the Impact of Cracks on Solar Cells Performance: Analysis based on Nonuniform and Uniform Crack Distributions. *IEEE Trans Ind Informatics* 2021:1–1. <https://doi.org/10.1109/TII.2021.3088721>.

## Second life for LiFePo4 batteries as energy storage system in a smart microgrid

Óscar Izquierdo Monge<sup>1</sup>, Nicolás Alonso Gonzalez<sup>1</sup>, Paula Peña Carro<sup>1</sup>, Gonzalo Martín Jimenez<sup>1</sup>, Víctor Alonso-Gomez, Oscar Duque-Perez<sup>3</sup>; Angel Zorita-Lamadrid<sup>3</sup>

<sup>1</sup> CEDER-CIEMAT, Autovía de Navarra A15 salida 56, 422290 Lubia (Soria), Spain, O.I.M.: oscar.izquierdo@ciemat.es; N.A.G.: agnico23@hotmail.com; P.P.C.: paula.pena@ciemat.es; G.M.J.: gonzalomj96@gmail.com;

<sup>2</sup> University of Valladolid, Campus Universitario Duques de Soria, 42004 Soria, Spain, victor.alonso.gomez@uva.es

<sup>3</sup> University of Valladolid, Paseo del Cauce 59, 47011 Valladolid, Spain. O.D.P.: oscar.duque@eii.uva.es; A.Z.L.: zorita@eii.uva.es

**Abstract.** Faced with the increase in the consumption and production of batteries for different uses in recent years and the problem of reuse and recycling methods, the purpose of this paper is to develop a study on the recovery of a storage system based on LiFePo4 batteries for a second life through their integration into the intelligent microgrid of the CEDER-CIEMAT. During the study, a series of charging and discharging processes have been carried out on four individual cells at different values of voltage to determinate state of health and capability and characterize them calculating voltage-time curves. In addition, a software for monitoring and control of the storage system (SCADA) has been developed in Home Assistant with Python programming language for its integration in the management system of the CEDER's microgrid. This will allow to store the energy surplus from CEDER's distributed generation sources (mainly wind turbines and photovoltaics systems) and manage the microgrid more efficiently.

**Keywords:** Smart microgrid, LiFePo4 batteries, second life.

### 1 Introduction

In the last 30 years, society has faced on many problems related to the development of energy systems, the exhaustion of sources all around the world, economic recessions, climate change, carbon emissions and many other toxic substances[1].

To make society capable of confronting these problems, experts around the world have been working on investigations and developing new alternatives related to renewable energy sources and innovative energy storage systems

The alternatives to the conventional energy generation and storage methods have become one of the priorities of governments in most countries around the world. One

of the essential aims of them is to break up with the harmful effect of fossil fuels along their life, since they are produced until its final uses [2].

One of the most important developing fields is the automotive sector, in particular electric vehicles (EV). Related to economy and living conditions, merchandise this type of vehicles is suffering and exponential increase reaching numbers of more than 20 million since 2015, with China as the main powerful country in technology development and sales.

Beside this, the European Union is providing solutions related to the electrification in the sector of transport, promoting the use of lithium batteries [3], an alternative that emerged from the high carbon emissions responsible for greenhouse effect and the increase of consume of fossil fuels that are related to this type of vehicles.

All this confirms the increase in energy storage systems based on batteries for many different applications. However, after a cert period of time using them (first period of life), they lose their initial capacity and work conditions and consequently, their capacity to supply the necessary power in the applications for which they were created for. Despite of this, they can be used for other applications. Currently, LiFePO4 batteries retired from many different applications can be obtained for a very low cost and involve them in recycle or second life applications [4]. Its principal attractiveness comes from the relation between cost, efficiency, and density of energy storage.

Possible second life applications of this type of batteries are non-interrupt energy storage systems or renewable energy sources. All these systems are characterised for been stationary and need smaller amounts of energy in longer periods of time than in their first life uses, where the necessity of energy involves more powerful systems with bigger volumes of energy during shorter periods of time [5].

Among the most promising future applications for second life uses is the integration in microgrids, for which are generally involved packs of serie/parallel battery systems, previously involved in other first life applications. It is necessary to examine the state of those cells involved using analytical methods as “impedance spectroscopy” or “hybrid-pulse power characterisation” under a range of different conditions (voltage and current density) with the aim of aging and estimating the capacities of those batteries involved in second life applications [6].

Figure 1 shows the possible application uses during life of batteries.

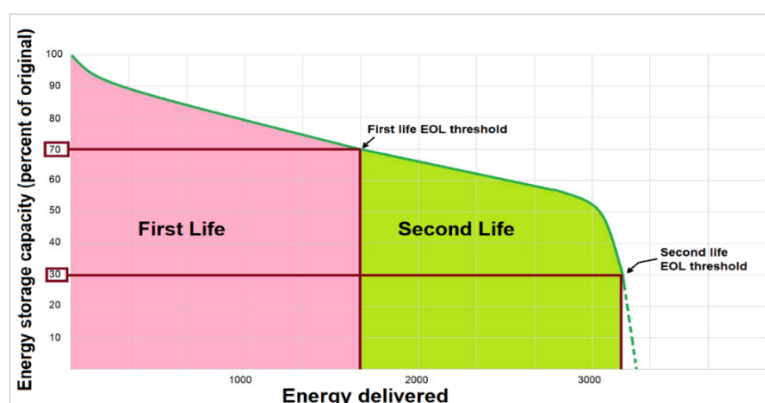


Fig. 1. First - Second Life for batteries [5].

Those batteries known as “retired” after its first life uses still maintains nearly an 80% of its initial capacity. Despite of this, they are considered as “out of service” as they cannot fully satisfy the demand established for the systems in which they were initially designed for. This aspect leads to the application of the concept of “second life”, “reuse” or “recycle” into other different fields with demands of fewer current values involved or uninterruptable energy storage systems [7].

Concretely, LiFePo<sub>4</sub> batteries have a useful period between 500 and 3500 cycles. When cells reach 80% of charge from its initial capacity its considered out of the range of the storage systems for which were designed (currently EV) [5]. However, after the initial 2000 cycles of these batteries, its residual capacity can be 4 or 5 times higher than in case of any acid battery (lead, sulfuric acid...).

It is estimated that still can have around 2000 more cycles in second life applications until their capacity is reduced until 60% and the loses of voltage are enough to consider the end of this second period of life [5].

From an economic aspect, these applications are attractive giving the fact that its cost is reduced to minimum values if we consider the price of a new battery, apart from the increase of a double useful period of time.

The first step on investigation of LiFePo<sub>4</sub> batteries and its life cycles is aging them and know its capacity and its behaviour against changes on charging and discharging processes, which bring the answer of if they are valid or not for different energy storage systems and why. This represents the principal aim of this document.

These applications are directly related with those energy sources they are connected with, what has a strong influence with charge and discharge conditions. Deeply charging and discharging processes exhaust very quickly the useful period of time in batteries, while those partial charging and discharging processes extend this period.

Particularly, this document presents a study for second life application LiFePo<sub>4</sub> batteries and the checking of the state of the cells involved on the storage system. The rest of the article is divided in the different sections: section 2 represents the description of the storage system, section 3 involves the jobs carried out for the recovery of the system and section 4 explains in detail the integration of the battery system on a smart microgrid for a second application, Finally the conclusions obtained are presented and the bibliography is cited.

## **2 Material and methods**

CEDER has an electrochemical storage system based on LiFePo<sub>4</sub> batteries, made up of 2 racks with 14 modules and 14 cells in each module, what suppose a total quantity of 392 cells. Each rack can work independently. Figure 2 shows a cell, a module, the complete system formed by both racks and grid inverter.



**Fig. 2.** Storage system, module, cell and grid inverter.

Table 1 shows cell specifications and Table 2 shows racks specifications.

**Table 1.** Cell specifications.

Cell technology	Lithium Iron Phosphate (LFP)
Nominal Voltage	3.2V
Min. Voltage	2.0 V
Max. Voltage	3.8 V
Capacity	50 Ah
Nominal Energy	160 Wh
Nominal Energy (discharging C2)	167 Wh
Nominal Energy (discharging C3)	176 Wh
Nominal Power	160 W
Max. Power	640 W

**Table 2.** Rack specifications.

Cells Number	196
Modules Number	14
Nominal Voltage	627.2V
Min. Voltage	529.2 V
Max. Voltage	729.1 V
Capacity	50 Ah
Nominal Energy	31360 Wh
Nominal Power	31360 W
Max. Power	125400 W

The system is connected to the grid by a three-phase inverter Ingecon Sun 30 (30 kW at 400V AC and 50Hz) showed in figure 2.

This storage system was installed in 2012, involved with an investigation project in CEDER with the aim of making it able to supply high power energy during short periods of time (less than 1 hour).

Once the Project was finished and after some years of no use of it, those cells were involved into a second life application, integrating them in the smart microgrid of CEDER, as a storage energy system. All this was run out with a completely different purpose than the initial, for which those cell were created for, considering that instead of working with high power energy supplies in short periods of time, (30 kW during as max. 1 hour), the main current objective is to work with less power energy supplies during longer periods of time (4-8 kW during some hours).

To make able the use of those batteries as storage energy system for the microgrid is necessary working on two different fields. On one hand, the recovery of the damaged cells or those that have suffered a decrease on their efficiency as a consequence of the passage of time and their first use application. On the other hand, it is necessary to work on the communication system and its integration on the CEDER microgrid.

### 3 Cells recovery

The first sept in the process of reuse the storage system is to check the capacity of each cell that compounds it. It is necessary to dismantle each module from its rack, open it and take notes of the voltage level of each cell, making it possible to know its state of charge (SOC).

The 392 cells that compounds the system can be classified on 5 different groups, depending on their voltage levels:

- 31 Cells with a voltage higher than 3.3 V.
- 86 Cells with a voltage between 3 y 3.3 V.
- 107 Cells with a voltage between 2 y 3 V.
- 121 Cells with a voltage between 0.5 y 2 V.
- 47 Cells with a voltage of 0.0 V.

The BMS of the system does not detects those cells with a voltage lower than 2V, as that corresponds to the minimum level stablished and it is considered that cells with a lower level are damaged and not useful for this purpose. For this reason, it is necessary to raise the voltage of those cells with other methods to make the BMS able to recognise them.

In the process of charging the cells and increase its voltage is necessary a charger, which in our case was used the model Revoelectrix (GT-500) that allow us to charge LiFePo4 batteries until 20 A and discharge them until 8 A. However, generally chargers (as in this case) are not able to recognise voltage levels lower than 2 V in LiFePo batteries. That is which is necessary to connect these cells to a power supply to achieve the voltage until a recognising level and after that, charging them until a voltage close to the nominal level. By way of this method, we make those cells that initially had a voltage of between 0.6 and 2V convert this level until the nominal voltage (3.2 V). On

the other hand, the 47 cells with a level of 0.0 V could not be recovered and were thrown out from the experiment.

Cells with a voltage higher than 2.0 V can be detected by the BMS. Those cells between 2.0V and 3.0V are charged with GT-500 until its nominal voltage, while those with a charge higher than 3.0V are not manipulated.

After a few days of rest, it is observed that in many of those cells with voltages of between 0.6 and 2.0V its voltage level falls again until levels under 2.0V. This means that they were not going to be recognised by the BMS and they are thrown out as well. The rest of cells that initially were between 0.6- 2.0 V and 2.0-3.0V also lost some of their voltage level but without reaching a level lower than 2.0V.

To know the functioning of cells in each group they are subjected to process of charge and discharge with charger GT-500 to study their behaviour. The process is showed on figure 3.



**Fig. 3.** Charging process with GT-500.

### 3.1 Cells charging process

To study the current state of charge on the different cells, is selected one of each group, a new cell (cell 1), a cell with a charge between 3.0-3.3 V (cell 2), a cell between 2-3V (cell 3) and another with a voltage less than 2V (cell 4).

The first step is a fully discharge of the four cells, to make them been in an initially similar state of charge, and after that subject them into a process of charge at 8A (with a limited voltage of 3.6 V for the four cells). The results are the following:

**Cell 1:** This is the case of a new cell that represents the correct operational behaviour of a LiFePo4 battery and works as a reference to compare the state with the rest of cells. Its voltage starting point is 3.05V and least 380 minutes in achieving the 3.6V scheduled in the charger as maximum voltage.

In approximately 15 minutes, the cell has converted the initially 3.05V until 3.26V. In the following 280 minutes, close to 5 hours later, it is produced a constant increase

in its voltage until achieving 3.4V. The next 30 minutes the cell suffers again a quickly increase of the voltage until 3.6V.

Finally, the cell maintains its level (3.6V) for a while. After stopping the process of charge, the voltage starts to decrease its level until it stabilizes itself at 3.34V.

**Cell 2:** At the beginning of the study this cell had a voltage level of between 3-3.3V. This level is considered right for the charge. In the process it is observed 3 phases as in cell 1, but with some differences.

The starting point is similar to cell 1 (3.06V). In this case, the first phase of charge is shorter than in case 1 (13 minutes) and rapidly achieves a voltage slightly higher than the case before (3.27V).

In the second phase, where the increase is slow and progressive, the time involved was 250 minutes approximately, until achieving 3.52V. Finally, the last phase least 20 minutes and the voltage is rapidly increased again, until achieving the 3.6V scheduled in the charger.

The time involved in achieving 3.6V is 280 minutes, a notable difference if we compare it with the 380 minutes with cell 1.

When the charge is finished, as in cell 1, the voltage level starts to decrease until been stabilized after a couple of hours in a value close to the nominal (3.3V).

**Cell 3:** At the beginning of this study, cell 3 had a voltage level of between 2 and 3 V. This range of voltage is a bit low. However, is considered inside the limits defined by the fabricant and understandable considering that the system has been with no use since a long time ago. Its behaviour is similar to cell 2, as can be observed on figure 4.

**Cell 4:** This cell had a starting point at the beginning of the study lower than 2 V, at the limit on the voltage established by the fabricant. This is a sign that cell can maybe could not be recovery for a second life application.

As the starting voltage point is lower than 2 V (concretely 0.6 V) the charger cannot recognise it, so it is necessary to rise the voltage using the power supply until more than 2 V to make the charger able to recognise the cell and start the charge.

During the first phase of charge, the voltage quickly arise 3.24 V in 30 minutes. From this moment, its behaviour is similar to cell 1. Phase 2 last 240 minutes and reaches 3.4 V. Finally, in phase 3 the voltage level increases again in a quickly way until 3.6 V. The total time involved in the charge process is slightly lower than in cell 1 (330 minutes).

This could lead us into the conclusion that, in contrast to what initially seemed, these cells could be reused in second life applications. However, when the charge is stopped, the voltage levels decrease until values lower than 2 V. This makes the systems unable to recognise them.

The summary of the results obtained are shown on figure 4.

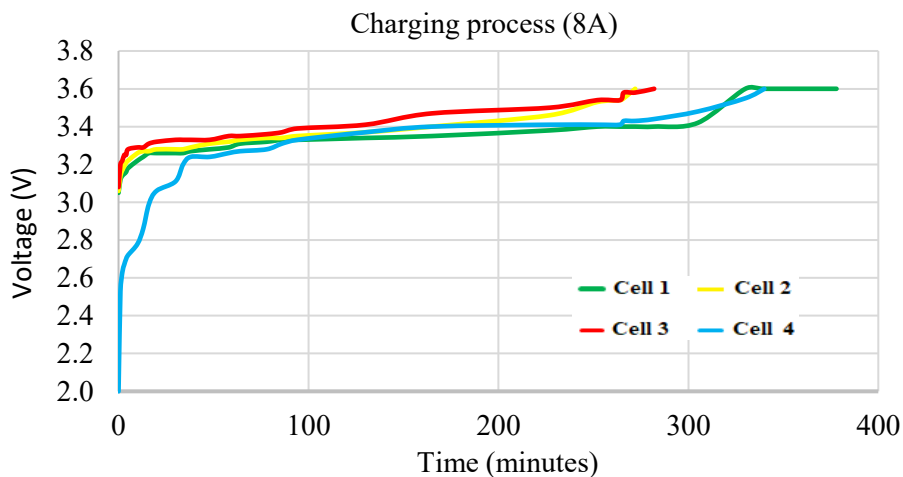


Fig. 4. Cells charging process with GT-500 at 8 A

In this process the charge is repeated with the same cells at different current levels to check if there are any differences. The results obtained lead to the conclusion that the behaviour is similar in all cases. Figure 5 shows the results obtained in a charging process with 16A.

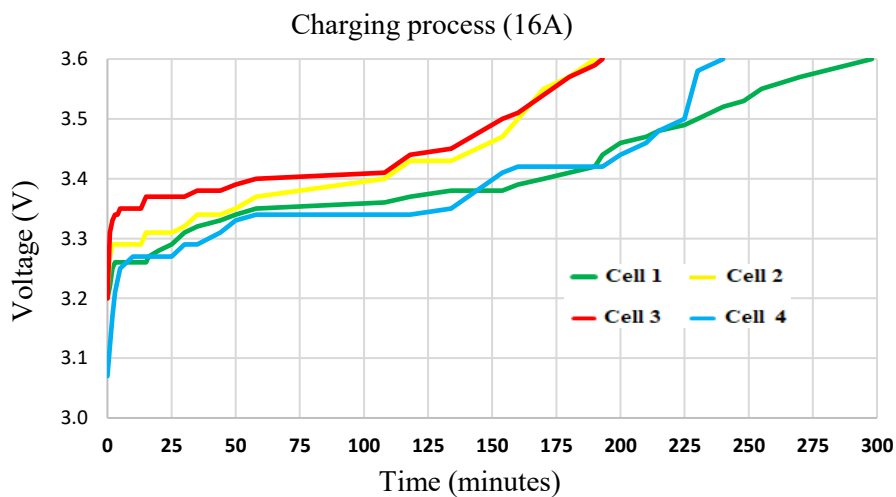


Fig.5. Cells charging process with GT-500 at 16 A

### 3.2 Cells discharging process

After charging the cells, they were subjected into discharging processes, limiting the voltage in the charger until 3 V, to compare the results. The initial current value of the discharging processes is 8 A.

The results obtained for the four cells are shown on figure 6.

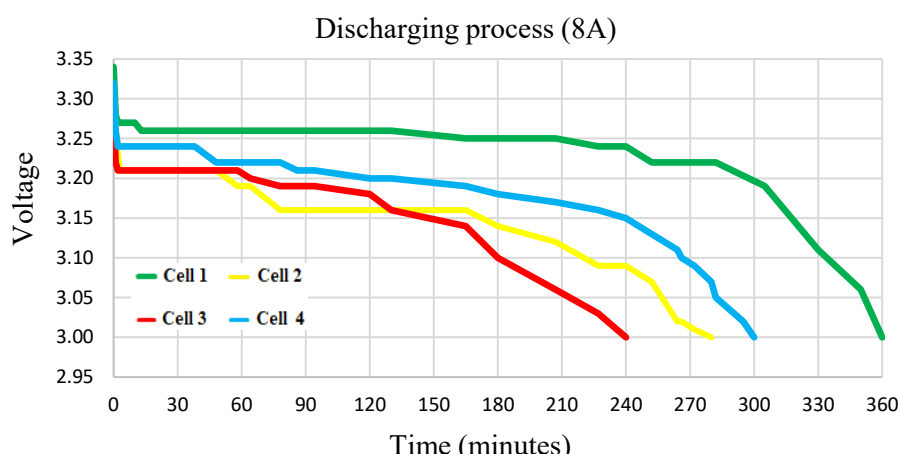


Fig.6. Cells discharging process with GT-500 at 8 A

**Cell 1:** Discharging process starts with 3.34 V. In about 10 minutes this level is decreased until 3.26 V, maintaining this value until almost 3 hours later. After this moment, the voltage decreases again but much more quickly, until achieve the 3 V scheduled in the charger.

The total time involved in the discharging process of this cell from the initially 3.34V until 3V was 360 minutes. When the discharge was stopped and after a period of time, the cell increase lightly the voltage until 3.2 V.

**Cell 2:** Initially, this cell had a voltage of 3.32 V. This level is a bit lower than cell 1. The voltage was decreased in a few minutes until 3.21 V and maintained on that value during almost 1 hour. After that, it goes down to 3.16 V staying on that value for more than 1 hour. From that moment starts to decrease the voltage quickly until 3 V.

In this case, the total time involved were 280 minutes approximately. When the discharge was finished, as occurred in cell 1, the voltage value of the cell achieves its nominal value.

**Cell 3:** As in the charging process, the discharge of cell 3 is like cell 2. However, there are some differences related to his bad conditions. A clear example of this is the time involved in the process, 240 minutes.

**Cell 4:** The total time involved in this cell were 300 minutes, less than cell 1 but higher than cells 2 and 3.

In phase 1, its voltage changes since the initial 3.32 V until 3.24 V in less than 5 minutes. This value is maintained during almost 2 hours and after that, it starts to decrease more quickly until 3 V.

In this case, as occurred during the charging process, the most evidence signs that the cell is not in good conditions are the nominal value that achieves after a time without been connected to the charger. This value increases until 3.1 V and instead of stabilizing, it starts to fall as time goes on.

Discharging process is repeated with the same cells at different current levels to check if there are any differences. The behaviour is similar in all cases. Figure 7 shows discharging process at 4 A.

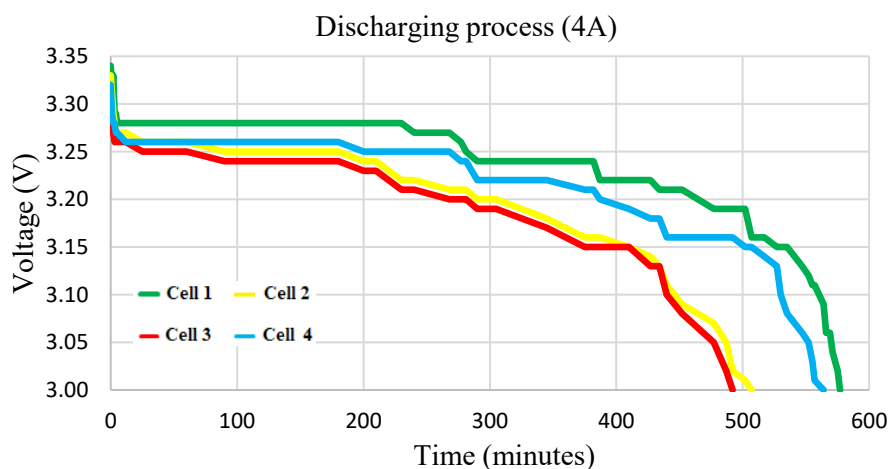


Fig.7. Cells discharging process with GT-500 at 4 A

### 3.3 Cells selection

Considering the results obtained in the sections of this document, it is demonstrated that the best option to select for second life applications are those cells whose behaviour is like 2 and 3, otherwise, 4 is not.

Apparently, cells like 4 have a better capacity and could be used during long and continuous processes of charge, giving the fact that if there are not long periods of time were the voltage falls, the cells work correctly. However, when they are in long periods of time without the charger connected to them, the voltage falls significantly. This can lead to a voltage lower than 2 V, which means that they are not going to be recognised by the system anymore.

On one hand, cells 2 and 3 have a worst charge capacity, but on the other hand they can keep constant voltage levels without been connected to the system, what means that from a functional point of view, they can work in a better way in this case. That is the reason by which they are selected to take part in the system.

Once the best cells were chosen to take part in the energy storage system formed by the 196 batteries necessities in each rack, next step is the integration of them in the system of the microgrid.

## **4 Second life. Integration of the energy storage system in the microgrid**

To make able the integration of the energy storage system with LiFePo4 in the microgrid of CEDER it is necessary to run out the next tasks:

- Establish the communication between the management app of the smart grid at CEDER (developed with Home Assistant) and the control system of batteries (BMS-Battery Management System) to know the information about cells and regulate the power supply of charges and discharges with the converter.
- Once established the communication, it is necessary to develop a SCADA inside the software of the management app to control the operation of the batteries, in the way of they could be managed manually with the microgrid operator.
- Finally, it is necessary to establish the automations in order to the strategies of energy administration, which defines the microgrid gestor, to make it able working automatically without necessity of an operator.

### **4.1 Communication with the management system and batteries control system**

The control system is formed by many different elements:

- BMS of each module: each one of the 14 modules of a rack has a BMS that allows keep under observation the voltage and temperature of each one of the 14 cells that are composed of. This BMS carry out a calibration of cells during its charge and controls the fan to keep cool the system. The communication between the BMS of the rack is carried through by means of CAN bus.
- BMS of each rack: keeps under observation the voltage and temperature of the 14 modules that take part in each rack, calculates the state of charge and their health conditions (SOH-State of Health) of each module. It establishes the communication with BMS of the system by means of CAN bus.
- BMS of the system: keeps under observation the voltage and temperature of the two racks that the system is composed by. It also calculates the SOC and SOH of the system. It leads the Modbus-RTU communicate with a computer where is installed the software for the control of the storage system.

The management app for the microgrid can communicate with BMS of the system using the protocol of Modbus communication by two different ways:

- Connecting a computer/raspberry/arduino etc. to the cable RS485 of the BMS of the storage system with a SCADA, what allows monitoring the information by way of a protocol of communication Modbus RTU, and after that, the management app of the microgrid must communicate with the SCADA to receive that information.
- Using a Modbus RTU-TCP/IP converter. It is connected to the entrance of the converter to the cable RS485 of the exit of the storage system and with the exit of the converter (RJ45-Ethernet) to the data of the microgrid. In this way, the software can communicate directly with it. The SCADA allows monitories the

information and it's been developed with the same managing app of the microgrid.

The first option presents some disadvantages that makes second option much more interesting. On one hand, using Modbus RTU it is only allowed one communication, while using Modbus TCP/IP allows more than one communication at the same time. On the other hand, it is more expensive and complex connecting the RS485 of the BMS to an equipment (pc, Raspberry or Arduino) that a converter TU-TCP/IP as would be necessary to have two different SCADAs. One of them for the monitoring of the BMS and other for the development of the control system of the microgrid to receive that information.

Also, apart from the communication with BMS of them energy storage system, the control system of the microgrid has to communicate with the converter to make able the transmission of the data of charging and discharging processes, as the BMS only produces the information about the batteries state, but does not allow its charge and discharge.

The converter allows the communication by means of Modbus TCP/IP, so it could be connected to the data grid Ethernet of the microgrid. Apart from that, the software of control can directly communicate with it once the parameters are defined.

Figure 8 shows a diagram of communications of the control system in the microgrid with the energy storage system and the converter [8].

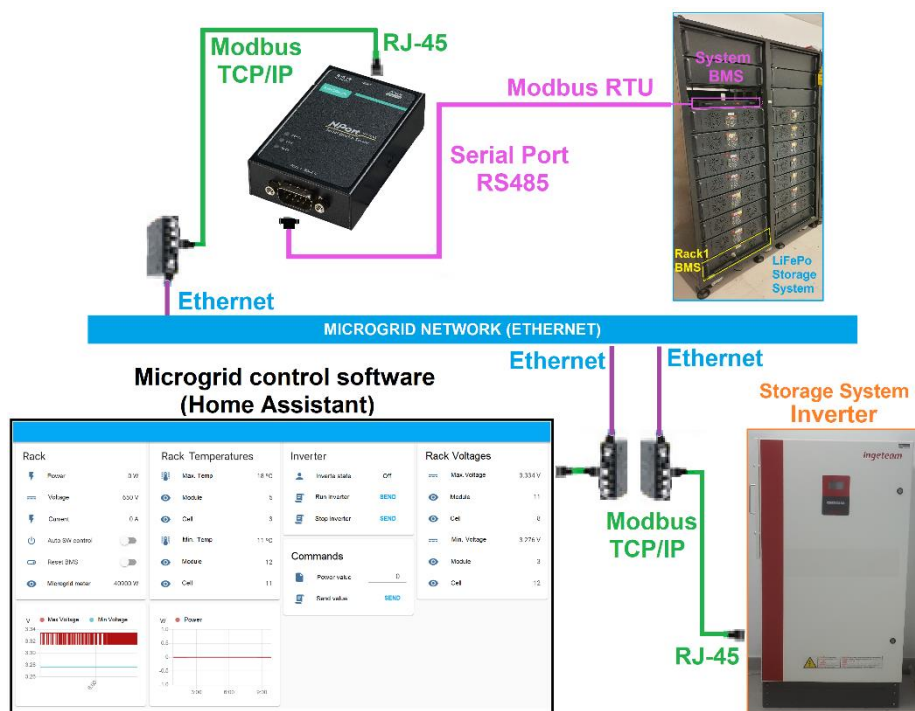


Fig.8. Communications diagram.

Once Modbus is established as way of communication with the BMS of the system as with the converter of the grid, it is necessary to define the equipment in the configuration of the software used for the management of the system. In this case, the managing software is carried out with Home Assistant, a software developed in Python. Despite it is used generally for home automation, it is a good solution for monitoring and control of the microgrid in real time

To establish the communication is necessary to define both elements. On one side the BMS of the system and on the other side, the converter to grid in the configuration file. For this is necessary to know the communication protocol (Modbus TCP), IP direction of each element and the connection link (which generally is 502 for Modbus TCP).

```

- name: BMS_sistema_LiFePo      # name (BMS)
  type: tcp                      # type of Modbus (RTU o TCP)
  host: 192.168.15.102          # BMS IP address
  port: 502                     # communication port

- name: inversor_red_LiFePo     # name (Inverter)
  type: tcp                      # type of Modbus (RTU o TCP)
  host: 192.168.15.90          # Inverter IP address
  port: 502                     # communication port
    
```

Once the elements of the configuration file are defined, it is necessary to read the Modbus directions desired and it is needed to know the plot of each Modbus equipment. In case of BMS, it only provides information about the state of the system, it is not possible to send him codes, so is only necessary to read the direction to monitor. An example of this are the temperatures and the voltage of cells. All this is defined with configuration file of Home Assistant in the following way:

```

- platform: Modbus              # Modbus
  scan_interval: 1              # monitoring interval
  registers:
    - name: Tensión_maxima_célula # variable to monitoring
      hub: BMS_sistema_LiFePo     # hub previously defined
      register_type: input         # type of register (input, holding, etc.)
      unit_of_measurement: W       # unit_of_measurement
      slave: 1                     # identification number
      register: 44                 # Modbus address
      count: 1                     # number of address
      scale: 1                     # scale (x1, x10, etc.)
    
```

For the inverter, apart from reading the parameters like voltage, current values and power supply for its monitoring (defining them in the configuration file) it is also necessary to send codes to carry out the charging and discharging processes in the specific conditions (previously defined). This is done by means of a script:

```

potencia_inversor_litio:      # script name
mode: single
sequence:                    # sequence of commands
- data:
  address: '1000'            # Modbus address
  hub: inversor_red_LiFePo  # hub previously defined
  unit: '1'                 # identification number
  value:
  - 8                       # Defined value to battery charge/discharge
  - sensor.consigna_potencia # charge/discharge power
service: modbus.write_register
    
```

The last step in the integration of the storage system is the creation of a control panel (interface) with Home Assistant that allows visualising in real time the parameters, monitoring the BMS of the system and the converter, sending codes for charging and discharging the batteries intuitively.

Using Home Assistant is very easy to develop this interface. The starting point is a frame that allows to insert the cards with many different functions. It is possible to add cards with all the values registered in the configuration files. This can be numerically or a historic graphic. Figure 9 shows the control panel of the storage system during a process of charge of the batteries.

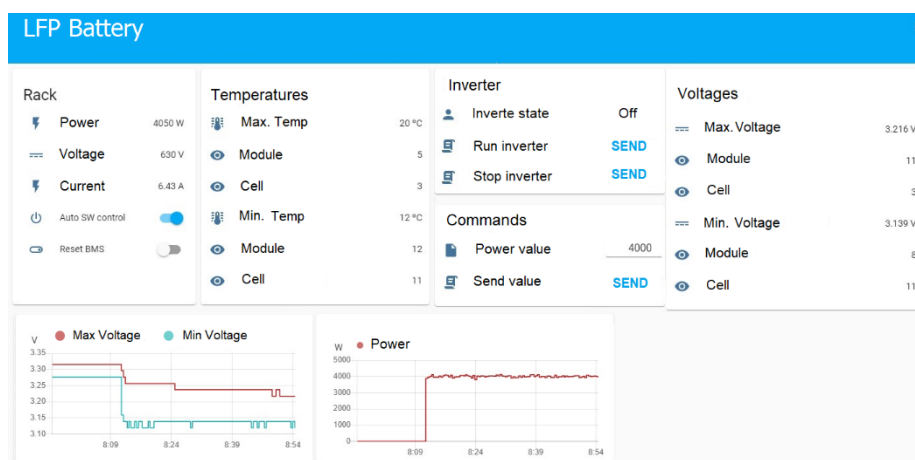


**Fig.9.** Control panel in Home Assistant.

Figure 9 shows a 4 kW discharge process. Voltage of the system is 630 V and the batteries are providing 4050 W to the grid (current value 6.43 A). The average of voltage at the rack is 3.198 V; with the cell 3 of the module 11 as the maximum (3.216 V) and cell 1 of module 8 as the minimum (3.139 V). The average of the rack temperature is 20 °C. Also, can be graphically observed that at the beginning of the discharge the

voltage of cells (the maximum and the minimum) lightly falls until achieving a value that is maintained for a long time during discharging process.

Figure 10 show the interface with those error than can occur in batteries. In that moment, discharging process, there are neither alarms (Warnings) nor errors (Faults). The system informs when the minimum voltage of the cell falls under the minimum working parameters.

LFP Battery			
Alarm-Warning Status		Error-Fault Status	
▲ Under temperature (UT < 0°C)	OK	▲ Under temperature	OK
▲ Over temperature (OT > 35°C)	OK	▲ Over temperature	OK
▲ Under voltage protection (UVP; V < 2.6V - 2.8V)	OK	▲ Under voltage protection (< 2.1V)	OK
▲ Over voltage protection (OVP; V > 3.8 V)	OK	▲ Over voltage protection (> 4V)	OK
▲ Fan failure	OK	▲ Over current protection	OK
▲ Voltage Dif. (Dif > 1 V)	OK	▲ Voltage Dif. (> 1.2v)	OK
▲ Temperature Dif. (dif > 40°C)	OK	▲ Temperature Dif.	OK
▲ Under voltage protection Rack (< 66% nominal)	OK	▲ Under voltage protection Rack	OK
▲ Over current protection Rack (> 112% nominal)	OK	▲ Over current protection Rack	OK
▲ Communication	OK	▲ Communication	OK
▲ Sensor SW fail	OK	▲ Auto SW Fail	OK
		▲ Sensor SW fail	OK

**Fig.10.** Battery errors.

Once the system is integrated in the LiFePo4 batteries system in the management app of the microgrid, it can be used as storage system for a second life application. This second life is under lower voltages than those that the system was initially created for.

Figures 11 and 12 show graphically the entire charging and discharging processes with a power value of 4 kW (the charging power supply is -4000 W and the discharging 4000 W). Figure 11 shows the power supply of the system and figure 12 the maximum and minimum of the cells.

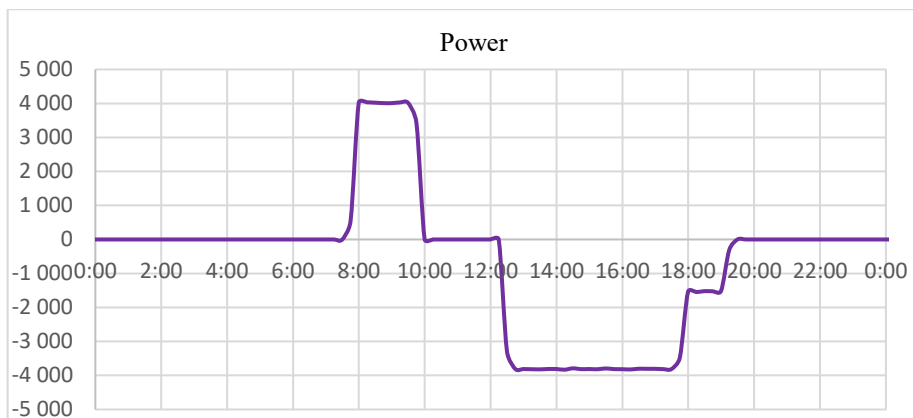


**Fig.11.** Charging and discharging process at 4 kW. Power.

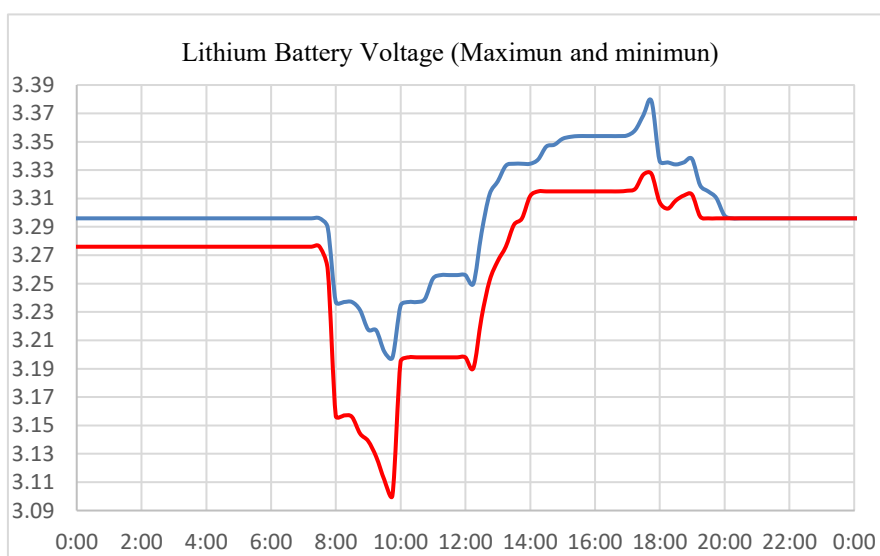


**Fig.12.** Charging and discharging process at 4 kW. Maximum and minimum voltage.

## 5 Conclusions

This paper explains the steps followed in CEDER to give a second life to LiFePo4 batteries as an energy storage system in a smart microgrid, after been a long time unused for its initial purpose.

After checking the initial state of health of each cell and study their charging and discharging curves (V-t), those that performed the best were selected to make operational one of the racks. There were not enough cells to recover both racks because many of them were damaged.

Once one of the racks has been completed with the best-performance cells, the battery management system (BMS) and the inverter to grid were integrated in the control system of CEDER's microgrid to allow it use (second life) as energy storage system of the microgrid.

In its second life, this battery system cannot put up with fast processes of charge and discharge with high power supplies, close to 30 kW (just a few minutes). However, it can work with lower power supplies (around 5 kW) for several hours, which is very useful in the energy management of the microgrid. This allows the storage of energy surplus from distributed generation systems (wind turbines and photovoltaic systems) and use that energy when needed, improving microgrids efficiency.

A future work would be trying to recover the second rack by using the remaining cells and buying new ones to complete the 196. This would double the storage capacity, in addition to improving the performance of the entire system by introducing new cells.

## References

1. M. H. Lee and D.-S. Chang, "Allocative efficiency of high-power Li-ion batteries from automotive mode (AM) to storage mode (SM)," *Renew. Sustain. Energy Rev.*, vol. 64, pp. 60–67, 2016, doi: <https://doi.org/10.1016/j.rser.2016.06.002>.
2. R. T. Jacob and R. Liyanapathirana, "Technical Feasibility in Reaching Renewable Energy Targets; Case Study on Australia," in 2018 4th International Conference on Electrical Energy Systems (ICEES), 2018, pp. 630–634, doi: 10.1109/ICEES.2018.8443251.
3. L. C. Casals, B. A. García, F. Aguesse, and A. Iturrondobeitia, "Second life of electric vehicle batteries: relation between materials degradation and environmental impact," *Int. J. Life Cycle Assess.*, vol. 22, no. 1, pp. 82–93, 2017, doi: 10.1007/s11367-015-0918-3.
4. M. Swierczynski, D.-I. Stroe, and S. Kar, "Calendar ageing of LiFePO<sub>4</sub>/C batteries in the second life applications," 2017, p. P.1-P.8, doi: 10.23919/EPE17ECCEEurope.2017.8099173.
5. P. Cicconi, D. Landi, A. Morbidoni, and M. Germani, "Feasibility analysis of second life applications for Li-Ion cells used in electric powertrain using environmental indicators," in 2012 IEEE International Energy Conference and Exhibition (ENERGYCON), 2012, pp. 985–990, doi: 10.1109/EnergyCon.2012.6348293.
6. P. J. Hart, P. J. Kollmeyer, L. W. Juang, R. H. Lasseter, and T. M. Jahns, "Modeling of second-life batteries for use in a CERTS microgrid," in 2014 Power and Energy Conference at Illinois (PECI), 2014, pp. 1–8, doi: 10.1109/PECI.2014.6804554.
7. H. C. Hesse, M. Schimpe, D. Kucevic, and A. Jossen, "Lithium-Ion Battery Storage for the Grid—A Review of Stationary Battery Storage System Design Tailored for Applications in Modern Power Grids," *Energies*, vol. 10, no. 12, 2017, doi: 10.3390/en10122107.
8. O. Izquierdo-Monge, P. Peña-Carro, R. Villafafila-Robles, O. Duque-Perez, A. Zorita-Lamadrid, and L. Hernandez-Callejo, "Conversion of a Network Section with Loads, Storage Systems and Renewable Generation Sources into a Smart Microgrid," *Applied Sciences*, vol. 11, no. 11, 2021, doi: 10.3390/app11115012.

## Renewable potential in urban environments: case study of the solar potential in municipal buildings in the city of Soria (Spain)

Sara Gallardo-Saavedra<sup>1</sup>[0000-0002-2834-5591], Alberto Redondo-Plaza<sup>1</sup>[0000-0002-2109-5614], Diego Fernández-Martínez<sup>1</sup>[0000-0003-1468-9083], Víctor Alonso-Gómez<sup>1</sup>[0000-0001-5107-4892], José Ignacio Morales-Aragón<sup>1</sup>[0000-0002-9163-9357] and Luis Hernández-Callejo<sup>1</sup>[0000-0002-8822-2948]

<sup>1</sup> Escuela de Ingeniería de la Industria Forestal, Agronómica y de la Bioenergía de Soria-(Ei-FAB), Campus Universitario Duques de Soria, Universidad de Valladolid, 42004 Soria, Spain; sara.gallardo@uva.es (S.G.-S.); alberredon@gmail.com (A.R.-P.); diego-brivi@hotmail.com (D.F.-M.); victor.alonso.gomez@uva.es (V.A.-G.); ziguratt@coit.es (J.I.M.-A.); luis.hernandez.callejo@uva.es (L.H.-C.)

\* Correspondence: sara.gallardo@uva.es (S.G.-S.); Tel.: +34-975129418

**Abstract.** This paper studies and analyzes the implementation of different types of clean and renewable solar energy in municipal buildings of Soria (Spain). Two different scenarios are analyzed. Firstly the implementation of photovoltaic (PV) solar energy on the roof of municipal buildings, secondly the implementation of hybrid solar energy (including thermal and PV solar energy) in buildings with significant thermal consumption, which corresponds to the buildings with a hemmed pool. The aim is to satisfy the electricity and/or thermal demand of the municipal buildings, as well as promoting self-consumption with renewable distributed generation in cities. This last aim is included within the Sustainable and Integrated Urban Development Strategies of the region, which encourages the improved energy efficiency and increased use of renewable energy in urban areas.

**Keywords:** Solar energy, building integration, smart cities.

### 1 Introduction

Transformation into a prosperous smart city has become an aspiration for many local governments across the globe [1]. The Spanish Urban Agenda (AUE) is a strategic document, non-normative, and therefore of voluntary adherence, which, in accordance with the criteria established by the 2030 Agenda, the new United Nations Urban Agenda and the Urban Agenda for The European Union pursues the achievement of sustainability in urban development policies. It also constitutes a working method and a process for all parties involved, public and private, who intervene in cities and who seek equitable,

fair and sustainable development from their different fields of action. This Agenda includes a total of 30 specific objectives, and 291 lines of action, which rest on more specific aspects and which contribute to the achievement of the ten main objectives. Among the ten main objectives, there is Strategic objective 3, which consists of preventing and reducing the impacts of climate change and improving resilience, which in turn includes the following specific objectives: (1) adapt the territorial and urban model to the effects of climate change and advance its prevention, (2) reduce greenhouse gas emissions and (3) improve resilience to climate change.

The increasing population growth as well as the quest for better quality of life are mainly responsible for growing demand for electricity generation. In the past, electricity generation from fossil fuels has been continuously exploited without any consequences, today climate change is a reality and had raised several questions about the exploration of fossil fuels for electricity generation [2]. Within the Sustainable and Integrated Urban Development Strategies, the Specific objective O.E.4.5.3 is included: Improved energy efficiency and increased use of renewable energy in urban areas. Therefore, the implementation of Renewable Energies in the urban environment contributes to the Energy Transition, that is already underway and that aims to guarantee the achievement of Spain's commitments to the European Union in terms of energy and climate, within the framework of the Agreement on Paris against global warming.

In addition, with the aim of promoting self-consumption with renewable distributed generation, recent legislation regulates the administrative, technical and economic conditions for self-consumption of electrical energy, the modes of self-consumption of electrical energy defined. Additionally, current normative establishes that self-consumed energy of renewable origin, cogeneration or waste, will be exempt from all types of charges and tolls in some areas [3].

In the mode of self-consumption with surplus and compensation the consumer uses the energy from the self-consumption installation when he needs it, being able to buy electricity from the grid at times when the produced energy is not enough to satisfy his electricity consumption. When not all of the energy from the self-consumption installation is consumed, it can be injected into the grid and, in each billing period (maximum one month), the invoice issued by the marketer will offset the cost of the energy purchased from the grid, with the surplus energy poured into the grid. In recent years, benefiting from the advancement of technology, the reduction of material costs, and the government's support for electricity production from renewable energy, solar photovoltaic (PV) technology has been increasingly developed [4].

This paper studies and analyzes the implementation of various types of clean and renewable energy in buildings and municipal areas of the city of Soria (Spain). Two different scenarios are analyzed, firstly the implementation of PV solar energy on the roof of all municipal buildings and secondly the implementation of hybrid solar energy (including thermal and photovoltaic solar energy) in buildings where there is significant thermal consumption, which corresponds to the buildings that have a heated pool. The aim is to satisfy the electricity and or thermal demand of the municipal buildings, as well as promoting self-consumption with renewable distributed generation in cities. The paper is structured in four sections. In the first section, an introduction to the study developed is included. Section two details firstly the municipal buildings included in

the study and secondly the software used for the different scenarios simulations. In section three it is included the main results obtained in the study, as well as the discussion of the results. Finally, the main conclusions of the study are detailed in section four.

## **2 Material and method**

This section details, firstly, the municipal buildings included in the study and secondly the software used for the different scenarios simulations.

### **2.1 Municipal buildings analyzed**

The energy analysis developed focuses on the study of municipal buildings in the city of Soria. Below is a list that includes the 22 municipal buildings for which information has been obtained from the Soria City Council and their location, Fig. 1.

1. Town hall
2. Social services
3. Registry
4. Audience Palace
5. Cinema
6. Presentation Building
7. Market
8. Fuente del Rey Sports Center
9. Band
10. Juventud Sports Center
11. San Andrés Sports Center
12. Asperón Pool
13. Becquer Civic Center
14. Youth Center
15. San Saturio Hermitage
16. Rosa de León Nursery
17. Los Pajaritos Sports Center
18. Bullring
19. Gloria Fuertes Nursery
20. Firefighters building
21. Local Police building
22. Municipal warehouse

To analyze the energy possibilities of each of the buildings, three face-to-face visits have been made to all of them. In each of these visits, the roof of the buildings has been analyzed, accessed (in cases where the roof was accessible) and the general electrical panel has been reviewed to check its maximum amperage. With this information, the

maximum three-phase power of the general switch can be calculated. This data allows to know the maximum allowable power for the current electrical installation, which will be taken into account for the design of PV and hybrids systems.

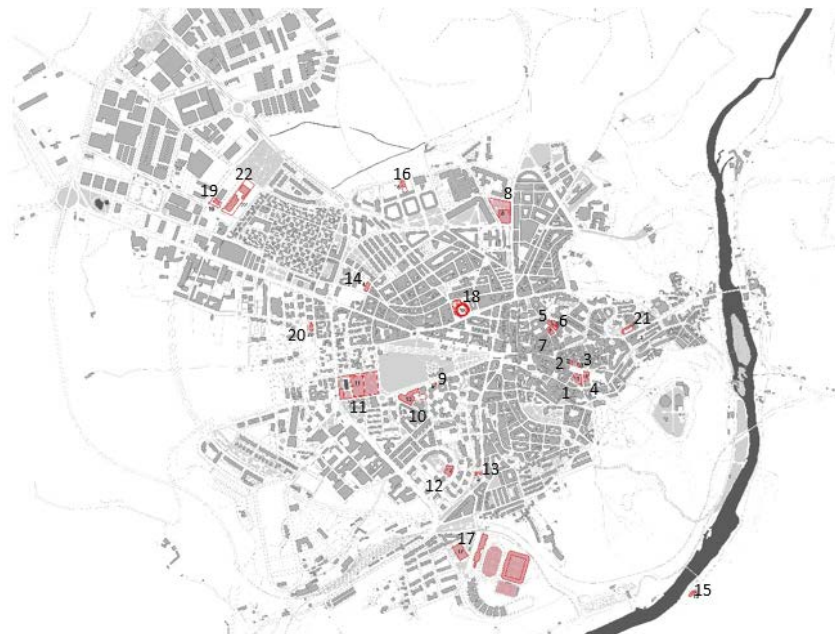


**Fig. 1.** Location of municipal buildings, in the city of Soria (Spain).

Once the visits have been made and the initial documentation provided has been analyzed, the buildings on which it is feasible to install photovoltaic and / or hybrid solar energy have been decided, as indicated below:

- In the case of PV solar energy, all but five buildings will be analyzed: the Town Hall and the band building, because they have a mostly north and not homogeneous roof, the Youth Center because it belongs to a neighbor’s community outside Soria City Council, the Hermitage of San Saturio for being heritage and the Bullring for having little cover and being surrounded by tall buildings that generate important shadows in the area. Therefore, the potential of other seventeen buildings have been analyzed, as they have been considered to be suitable for PV installation because of their orientation, previous electric installation, neighbor skyline, constructive and occupational patterns, among other reasons.
- In the case of hybrid solar energy, it will be analyzed for buildings where there is significant thermal consumption, which corresponds to buildings that have a heated pool: the Asperón, Fuente del Rey and Juventud sports centers.

## 2.2 Energy consumption

### 2.2.1 Electricity

The Soria City Council has provided the electricity consumption for each of the buildings. For the study, we have the consumption information, in terms of active energy (kWh), reactive energy (kVArh) and demanded power (kW) from October 2019 to July 2020 of each building.

To characterize the electricity demand in each of the proposals, these data had to be processed and corrected. In the first place, due to a change in the electricity marketing company in the buildings in October 2019, there were only consumption data from October 2019 to February 2020, which does not mean a full year. Likewise, several of the months coincide with the confinement due to the pandemic derived from Covid-19. Therefore, the data has been treated in such a way that it has been determined which buildings have not changed their activity due to the pandemic, and therefore the consumption data are reliable, such as the local Police or Firefighters. For the rest of the buildings, an extrapolation has been made from the complete data available. The final electricity demand data processed, which are used in the sizing of the PV and hybrid installation, are presented in Table 1.

**Table 1.** Annual electricity consumption of the municipal buildings analyzed.

Building	Annual energy consumption (MWh)
Social services	25.6
Registry	109.6
Audience Palace	135.2
Presentation Building	24.1
Market + Cinema	163.6
Fuente del Rey Sports Center	223.9
Juventud Sports Center	301.8
San Andrés Sports Center	245.0
Asperón Pool	288.3
Becquer Civic Center	52.4
Rosa de León Nursery	11.2
Los Pajaritos Sports Center	72.3
Gloria Fuertes Nursery	40.3
Firefighters building	37.4
Local Police building	40.0
Municipal warehouse	59.5

Additionally, it has been necessary to estimate the daily energy load curves in order to be able to perform the energy simulations. It is fundamental to be able to determine the self-consumed energy and the energy injected into the grid by a PV system. The

shape of the daily load curves will be estimated based on the characteristics of the building. In this way we have congregated the buildings into six groups. Each group will have those buildings whose consumption patterns are similar. This grouping is shown in Table 2. Likewise, the different daily load curves are represented in Fig. 2.

**Table 2.** Grouping of the municipal buildings analyzed according to their load curve.

Group	Building	Description
1	Fuente del Rey Sports Center	Sports centers identified as sports centers with an indoor pool.
	Juventud Sports Center	
	Asperón Pool	
2	San Andrés Sports Center	Sports centers identified as sports centers without swimming pools
	Los Pajaritos Sports Center	
3	Audience Palace	Recreational, courses etc. that present a higher consumption during morning and afternoon.
	Cinema	
	Becquer Civic Center	
	Presentation Building	
4	Social services	Offices, nurseries etc. that present a higher consumption during the mornings.
	Registry	
	Municipal warehouse	
	Rosa de León Nursery	
	Gloria Fuertes Nursery	
5	Market	The market consumption pattern has been considered different from the rest of the buildings.
6	Firefighters building	They present a more continuous consumption due to the fact that they are buildings used 24 hours a day
	Local Police building	

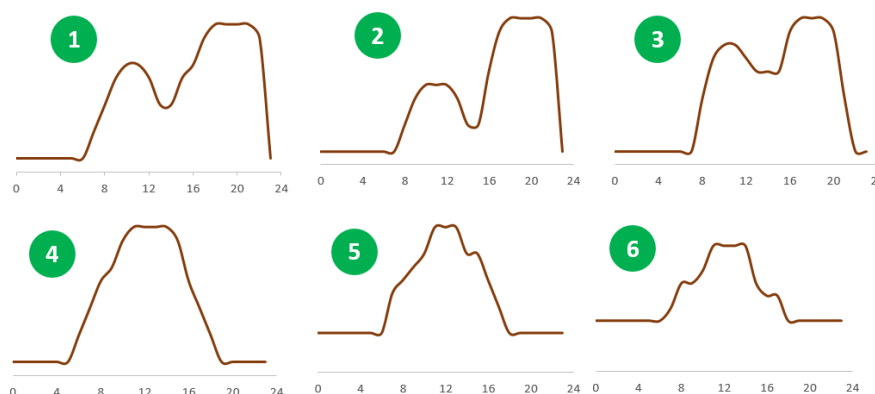


**Fig. 2.** Daily load curves estimated for each of the six groups

### 2.2.2 Thermal consumption

The annual thermal demand (kWh/year) given for the main thermal consumers is:

- Asperón Pool: 1,862,623.2 kWh / year
- Juventud Sports Center: 1,500,373.7 kWh / year
- Fuente del Rey Sports Center: 1,307,168.6 kWh / year

To obtain the monthly demand from the annual one, a percentage of consumption associated with the heating of the swimming pool and the constant domestic hot water has been estimated throughout all the months of 65% of the total demand, and a consumption of heating between the months of October to March, which corresponds to 35% of the total demand. The final results of the monthly thermal demand of the sports centers with heated swimming pools are presented in Table 3, and they have been used in the dimensioning of the solar hybrid installations.

**Table 3.** Monthly thermal demand of the sports centers with heated swimming pools.

Month	Monthly thermal energy consumption (MWh)		
	Asperón	Fuente del Rey	Juventud
January	209.5	147.1	168.8
February	209.5	147.1	168.8
March	209.5	147.1	168.8
April	100.9	70.8	81.3
May	100.9	70.8	81.3
June	100.9	70.8	81.3
July	100.9	70.8	81.3
August	100.9	70.8	81.3
September	100.9	70.8	81.3
October	209.5	147.1	168.8
November	209.5	147.1	168.8
December	209.5	147.1	168.8
TOTAL	1,862.6	1,307.2	1,500.4

## 2.3 Simulation software

### 2.3.1 PV simulations – PVSyst software

The different municipal buildings present a considerable electricity demand. Next, different alternatives for the installation of PV modules on the roofs of buildings are exposed. Said installations will make it possible to reduce the cost of the electricity bill and the savings will allow the installation to be amortized as quickly as possible. The simulations have been carried out with the PVSyst software [5].

In order to qualify for the Energy compensation rate, according to Royal Decree 244/2019, of April 5, the installed power cannot exceed 100 kWp [3]. According to this, the maximum PV power proposed in the different buildings does not exceed these 100kWp. The optimization process followed in the different simulations is as follows:

- First, the installation of the maximum possible PV power has been simulated according to the available roof area in each building, without exceeding 100 kWp.
- In the economic analysis, it has been detected that in some buildings, it is advisable to reduce the installed PV power, in order to adjust the sale price of the energy injected into the grid with the purchase price of the energy consumed.
- Therefore, in these buildings a lower PV power has been simulated, until the maximum benefit (the minimum payback time) has been obtained, improving their economic profitability

In PVSyst, the following information has been created for the simulations:

- Geographical data: Latitude: 41.755 °, Longitude: -2.471 °, Altitude: 1050 m above sea level, Time zone: + 1.
- Solar trajectories: The solar trajectories for the different months of the year are calculated for the aforementioned coordinates, using the PVSyst software. These trajectories can be seen in Fig. 3.

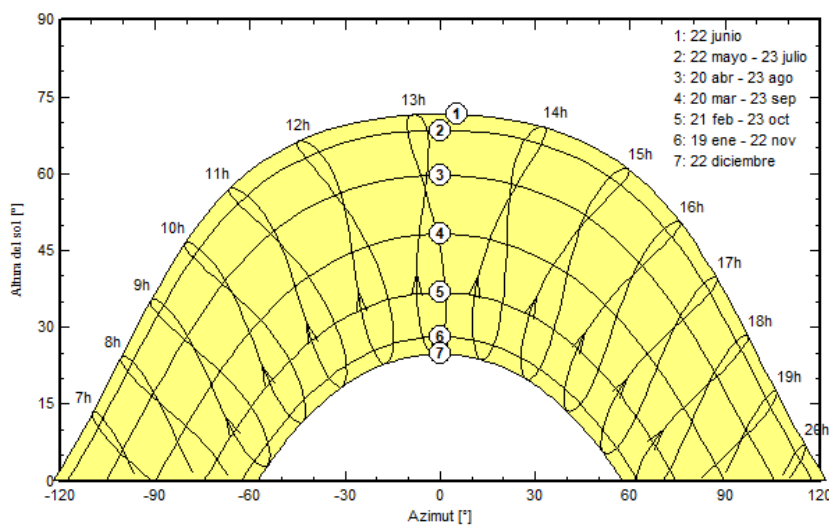


Fig. 3. Solar trajectory in the location of the municipal buildings analyzed

- Climate data: To determine the climatic data, fundamental for estimating the energy produced, the Meteonorm 7.3 (2000-2009) database will be used. Because all the facilities to be simulated are located in the town of Soria, the simulations of the different buildings will use the same data. This information is shown in Table 4.

**Table 4.** Climatic data on the location of the municipal buildings analyzed

	Horizontal global irradiation	Horizontal diffuse irradiation	Temperature	Wind speed	RH
	kWh/(m <sup>2</sup> · month)	kWh/(m <sup>2</sup> · month)	°C	m/s	%
January	59.5	27.6	3.2	3.70	82.1
February	78.1	31.1	4.9	3.91	73.2
March	124.1	49.1	8.2	4.39	66.1
April	152.5	67.0	10.0	4.40	66.5
May	191.5	78.1	14.6	3.89	63.3
June	217.2	61.3	19.8	4.00	55.1
July	228.5	64.4	22.2	3.99	47.4
August	201.0	55.6	21.7	4.00	51.1
September	147.9	45.8	17.4	3.70	58.3
October	100.2	40.7	12.8	3.90	69.7
November	61.2	27.3	6.6	4.10	79.3
December	51.3	21.5	3.8	3.70	80.6
<b>YEAR</b>	<b>1,613.0</b>	<b>569.5</b>	<b>12.1</b>	<b>4.0</b>	<b>66.1</b>

- Skyline Shadows: Distant mountains, hills, etc., can cause shading in the installation, especially in the early and late hours of the day. Therefore, taking into account the horizon profile of the area will help to quantify these losses and therefore the energy produced. The horizon profile has been obtained thanks to the PVGIS database. Due to the proximity of the facilities to be evaluated, a single profile is used for all of them, and it can be seen in Fig. 4.

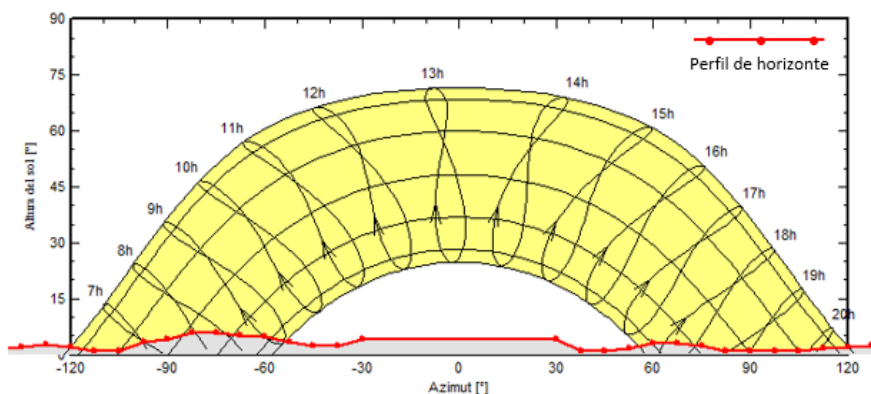


**Fig. 4.** Distant shadows in the location of the municipal buildings analyzed

- Neighboring shadows: this shadows are produced by near elements. For each of the municipal buildings analyzed, the near neighboring shadows have been analyzed in

PV-Syst by means of simulating them in perspective. An example can be seen in Fig. 5, in which the simulation of neighboring shadows for the Market building are shown. The iso-shadings diagram obtained with PV-Syst for the Market building from the perspective of neighboring shadows defined is presented in Fig. 6. This analysis makes it possible to quantify the real potential of solar radiation on the roof taking into account the near sky view factor that each building has.

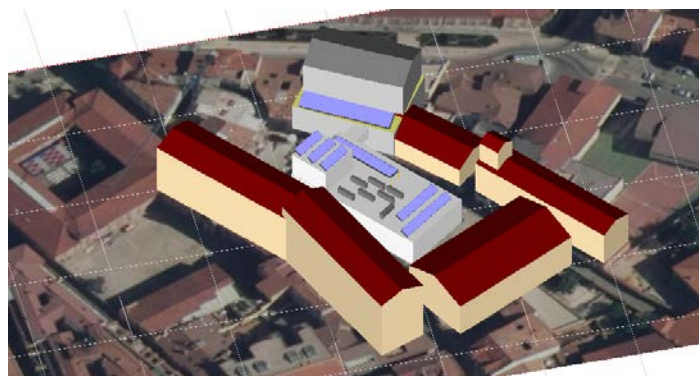


**Fig. 5.** Perspective of neighboring shadows defined for the Market building in PV-Syst software

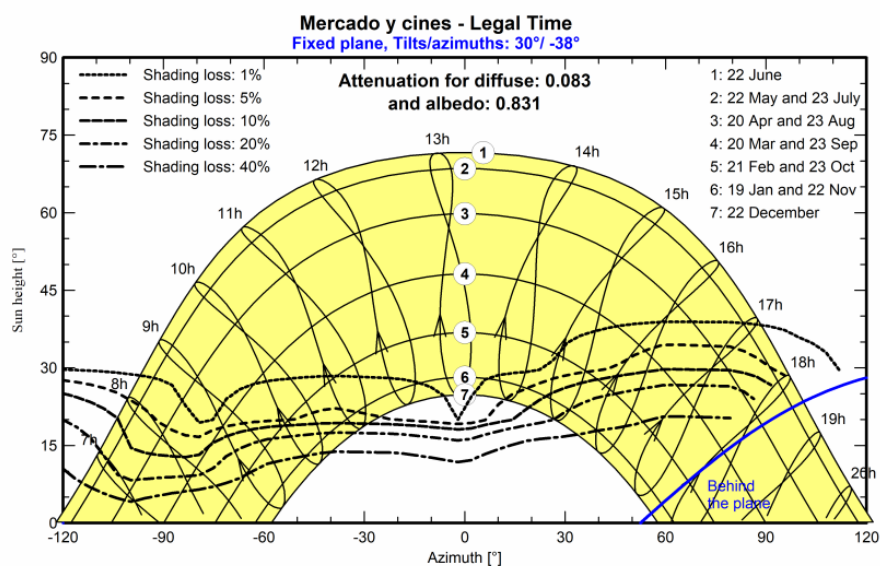


**Fig. 6.** Iso-shadings diagram obtained with PV-Syst for the Market building from the perspective of neighboring shadows defined in Fig. 5.

The PV module used in the simulations is the model BYD-385-M6K-36 of 385Wp. It is a monocrystalline PV panel manufactured by BYD Company Limited, with

19.78% efficiency, Voc 49.95V, Isc 9.83A, Vmpp 41.36V and Impp 9.32A. The maximum system voltage is 1,500V. The cell size is 156×156 mm and it counts with 72 cells (6\*12). Its exterior dimensions are 992mm \* 1962mm. For the economic calculations, an electricity price of 0.10€/kWh in tariff 3.0A and 0.14€/kWh in tariff 2.1 DHA has been considered. An annual increase of 6% in the cost of electricity has also been taken into account. In addition, it has been considered an installation cost of 1,000€/kWp and a fixed maintenance cost of 300€/year in each building plus 10€/kWp/year. The sell cost has been considered to be 0.05€/kWh.

### 2.3.2 Hybrid simulations – Abora Solar software

The modules used in all the simulations are the hybrid panel model aH72SK from the manufacturer Abora, with a total surface area of 1.96 m<sup>2</sup> and an electrical power of 350Wp. Its exterior dimensions are 995mm \* 1970mm. The PV module of the hybrid panel has 72 monocrystalline cells (6\*12), and the cell size is 156×156 mm, with 17.8% efficiency, Voc 48.82V, Isc 9.73A, Vmpp 39.18V and Impp 8.98A. The maximum system voltage is 1,000V.

The thermal and electricity demand data provided by the city council and previously defined have been used. For each sports center, two scenarios have been simulated; firstly, the option of installing 100 hybrid panels (35 kWp) and secondly, installing 285, which correspond to 100 kWp, the maximum amount of electrical power that allows self-consumption in Spain. For the first scenario, a 5,000-liter tank has been used, while for the second, a 10,000-liter tank.

For the economic calculations, an electricity price of 0.12€/kWh and a price of thermal energy (supplied by Rebi's heat network in Soria) of 0.055€/KWh have been considered. An annual increase of 5% in the cost of thermal energy and 6% in the case of electricity has also been taken into account. In addition, a maintenance of 700€/year has been considered for each hybrid installations.

## 3 Results and discussion

This section includes the main results obtained in the study, as well as the discussion of the results. It is structured in the subsections, each of them related to the two different scenarios analyzed; the first section correspond with the implementation of PV solar energy on the roof of municipal buildings and the second one with the implementation of hybrid solar energy (including thermal and photovoltaic solar energy) in buildings where there is significant thermal consumption, which corresponds to the buildings that have a hemmed pool.

### 3.1 PV solar energy

This section shows the energy and economical results obtained for the different alternatives proposed for each of the municipal buildings analyzed.

For each building, different alternatives according to the optimization process defined in the methodology have been developed. As an example, the following Fig. 7 includes five PV installation alternatives analyzed for “Los Pajaritos Sports Center”. Alternatives 1 to 4 includes a total power installed of 98.2 KWp, with different orientations and inclinations of the modules.

In the economic analysis, it has been detected that in this building, it is advisable to reduce the installed PV power. It can be seen in alternative 5, which includes 46.2 KWp. It is made up of modules with the same inclination and orientation as the roof, located on the west roof of the sports center.

- Alternative 1: Power 98.2 kWp. It is made up of modules with the same inclination and orientation as the roof, located on the west roof of the sports center. The installation has 255 modules (model BYD-385-M6K-36) of 385 Wp, with 15 strings, where each one has 17 modules in series; and a central inverter (model Sunny Highpower Peak 3 - SHP100-20) of 100 KW of nominal power.
- Alternative 2: Power of 98.2 kWp. It is made up of modules with an inclination of 30° and located on both roofs, with the orientation of the roofs respectively. The distance between rows is the maximum possible that allows the installation of the proposed power. The installation consists of 255 modules (model BYD-385-M6K-36) of 385 Wp, with 15 strings, where each one has 17 modules in series; and a central inverter (model Sunny Highpower Peak 3 - SHP100-20) of 100 KW of nominal power.
- Alternative 3: Power of 98.2 KWp. It is composed of 30° inclined modules with a 0° orientation (south) and located on the west side. The distance between rows is the maximum that allows the installed power to be installed on the indicated roof. The installation consists of 255 modules (model BYD-385-M6K-36) of 385 Wp, with 15 strings, where each one has 17 modules in series; and a central inverter (model Sunny Highpower Peak 3 - SHP100-20) of 100 KW of nominal power.
- Alternative 4: Power of 98.2 KWp. It is made up of modules inclined 30° with a 0° orientation (south) and located on both sides. The distance between rows is the maximum that allows installing the power set on both decks. The installation consists of 255 modules (model BYD-385-M6K-36) of 385 Wp, with 15 strings, where each one has 17 modules in series; and a central inverter (model Sunny Highpower Peak 3 - SHP100-20) of 100 KW of nominal power.
- Alternative 5: Power of 46.2 KWp. It is made up of modules with the same inclination and orientation as the roof, located on the west roof of the sports center. The installation consists of 120 modules (model BYD-385-M6K-36) of 385 Wp, with 6 strings, where each one has 20 modules in series; and a central inverter (model SUN2000\_50KTL\_C1) with a nominal power of 47.5 KW.

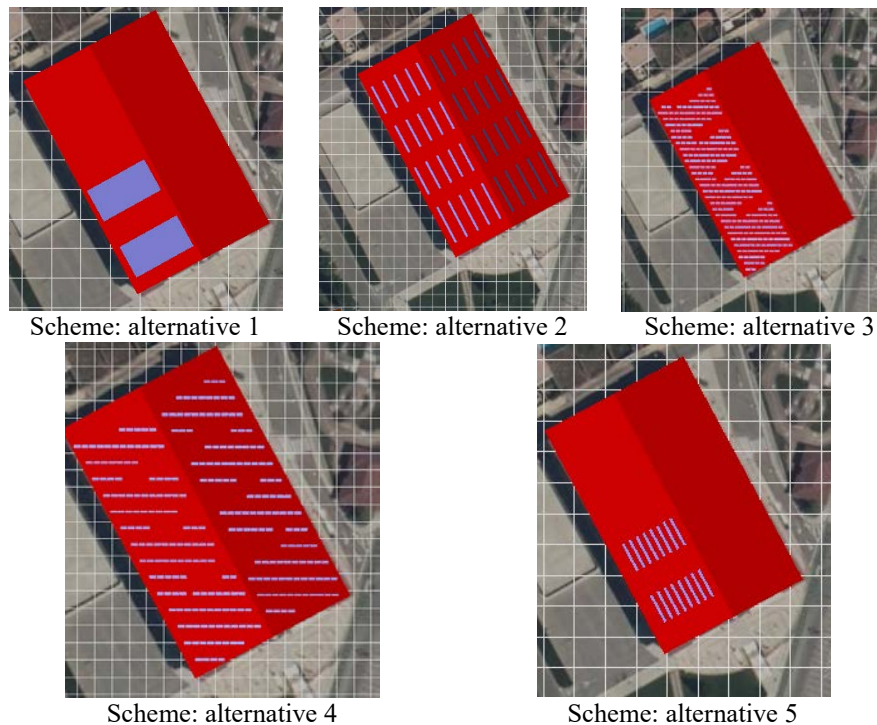


**Fig. 7.** Schemes in PVSyst of the different alternatives analyzed in “Los Pajaritos Sports Center”.

After simulating all the buildings in PVSyst for obtaining the optimized results, the final economic analysis can be seen in Table 5. The analysis includes the calculation of the Net Present Value (NPV) and Internal Rate of Return (IRR) of each investment. To calculate the NPV, an annual discount rate of 0.25% has been considered. As it can be seen in Table 5, the payback varies from approximately 8.6 years in the most unfavorable case to 4.3 years in the most favorable. Taking into account the most favorable PV simulation variant for each building, a global scenario or balance is proposed:

- The global installation would involve an initial investment of 640,870€.
- This investment would cause an average annual saving of 185,600€ per year.

**Table 5.** Economic results of the optimal PV installation in each building.

Building and simulation alternative number	Demand covered (%)	Initial investment (€)	Average annual savings (€ / year)	NPV	IRR	Payback (years)
Social services 1	67.2%	20,000	4,411.03	85,907.29	14.0%	8.6
Registry 1	19.6%	15,000	5,521.10	117,606.37	21.6%	5.5
Audience Palace 1	20.8%	20,000	7,339.71	156,307.03	21.7%	5.4
Presentation Building 1	50.5%	16,000	3,440.36	66,687.85	14.5%	8.0
Market + Cinema 2	39.3%	51,500	16,972.02	356,218.23	20.1%	5.8
Fuente del Rey Sports Center 2	36.8%	97,000	24,193.20	484,515.87	16.5%	7.1
Juventud Sports Center 2	34.2%	96,000	29,216.21	606,217.95	19.4%	6.0
San Andrés Sports Center 1	32.2%	102,000	24,371.52	484,117.12	16.4%	6.9
Asperón Pool 2	34.4%	98,200	25,151.50	505,823.24	16.1%	7.5
Becquer Civic Center 3	44.6%	23,100	11,793.72	260,042.19	27.1%	4.3
Rosa de León Nursery 2	57.5%	6,000	1,756.35	36,157.97	17.3%	7.1
Los Pajaritos Sports Center 5	34.8%	30,800	7,441.03	148,093.10	16.2%	7.2
Gloria Fuertes Nursery 2	54.2%	17,000	6,115.32	129,936.89	21.8%	5.3
Firefighters building 3	45.1%	20,790	8,395.23	180,752.22	22.5%	5.3
Local Police building 1	30.9%	9,000	3,061.67	64,513.93	19.9%	6.1
Municipal warehouse 4	43.1%	18,480	6,419.62	135,674.60	20.3%	5.8

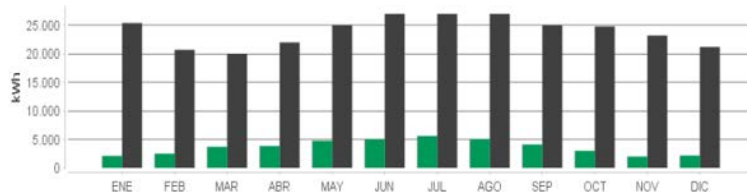
### 3.2 Hybrid solar energy

This section shows the energy and economical results obtained for the different alternatives proposed for the three municipal buildings (pools) analyzed.

For each building, two different alternatives according to the optimization process defined in the methodology have been developed. As an example, the following Fig. 8 and Fig. 9 includes the energetic results of the two hybrid installation alternatives analyzed for “Asperón Pool”: 100 hybrid panels (35 kWp) and 285 hybrid panels (100 kWp), respectively. Energetic results for both “Asperón Pool” alternatives are summarized in Table 6.



(a) Monthly thermal energy production (green) vs demanded (black) in kWh.



(b) Monthly electrical energy production (green) vs demanded (black) in kWh.

**Fig. 8.** Energetic results in “Asperón Pool” for the installation of 100 hybrid panels (35 kWp).



(a) Monthly thermal energy production (green) vs demanded (black) in kWh.



(b) Monthly electrical energy production (green) vs demanded (black) in kWh.

**Fig. 9.** Energetic results in “Asperón Pool” for the installation of 285 hybrid panels (100 kWp).

**Table 6.** Energetic results in “Asperón Pool” for the installation of 100 hybrid panels (35 kWp) and 285 hybrid panels (100 kWp).

ALTERNATIVES	Thermal production (MWh/year)	Thermal demand covered	Electrical production (MWh/year)	Electrical demand covered
100 panels (35 kWp)	183.23	9.84 %	43.82	15.22%
285 panels (100 kWp).	458.87	24.64 %	120.81	41.9%

The thermal and electrical demand covered in “Fuente del Rey Sports Center” and “Juventud Sports Center” are:

- Fuente del Rey Sports Center:
  - 100 panels: thermal 13.87% and electrical 19.73%.
  - 285 panels: thermal 34.81% and electrical 56.24%.
- Juventud Sports Center:
  - 100 panels: thermal 12.23% and electrical 14.22%.
  - 285 panels: thermal 30.46% and electrical 39.73%.

Once analyzed the energetic results, in the following Fig. 10 it can be seen the cash flow for each alternative.

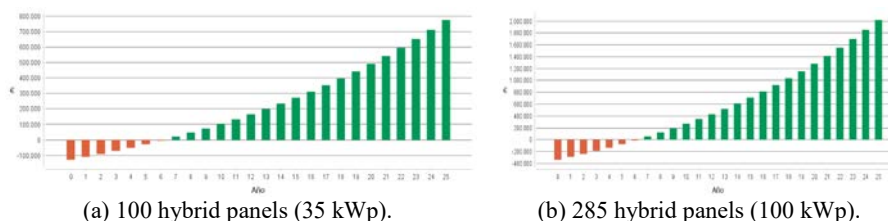


**Fig. 10.** Energetic results in “Asperón Pool” for the installation of (a) 100 panels and (b) 285 hybrid panels.

After simulating the three buildings in Abora Solar software, the final economic analysis can be seen in Table 7. To calculate the NPV, an annual discount rate of 0.25% has been considered.

**Table 7.** Economic results for the hybrid installation in each of the three building.

ALTERNATIVES	Initial investment (€)	Annual thermal savings (€/year)	Annual electrical savings (€/year)	Total annual savings (€/year)	NPV (€)	IRR (%)	Pay-back (years)
<b>Asperón Pool</b>							
100 panels	127.907	16.901	6.855	23.756	318.647	18,73	6
285 panels	336.488	42.325	18.872	61.197	830.615	18,68	6
<b>Fuente del Rey Sports Center</b>							
100 panels	127.907	16.721	6.902	23.622	316.167	18,64	6
285 panels.	336.488	41.969	19.669	61.638	839.756	18,80	6
<b>Juventud Sports Center</b>							
100 panels	127.907	16.931	6.926	26.857	320.632	18,80	6
285 panels	336.488	42.160	19.352	61.512	837.055	18,76	6

As it can be seen in Table 7, the payback is approximately 6 years in all hybrid alternatives analyzed.

#### 4 Conclusions

This paper studies the implementation of two different types of clean and renewable solar energy in municipal buildings of the city of Soria, in Spain: firstly the implementation of PV solar energy and secondly the implementation of hybrid solar energy (including thermal and PV solar energy) in buildings with indoor pool. The aim is to satisfy the electricity and or thermal demand of the municipal buildings, as well as promoting self-consumption with renewable distributed generation in cities.

Regarding the PV installation, it has been seen that the best alternative analyzed for each building would involve an initial investment of 640,870€ which creates an average annual saving of 185,600€ per year. The payback varies from approximately 8.6 years in the most unfavorable building to 4.3 years in the most favorable one.

On the other hand, according to the hybrid study, it has been seen that the payback is 6 years, approximately, in all the installations analyzed.

All the economic analysis carried out have not considered any type of subsidy for the installation of renewable systems. However, nowadays, the use of renewables is increasingly supported as part of the commitment of different institutions with climate change. Therefore, any type of subsidy of this type would reduce the payback of the proposed facilities.

## Acknowledgement

The authors thank the CYTED Thematic Network “CIUDADES INTELIGENTES TOTALMENTE INTEGRALES, EFICIENTES Y SOSTENIBLES (CITIES)” no518RT0558 and to the UVa and City Council of Soria Cátedra “AGENDA URBANA ESPAÑOLA 2030 PARA EL DESARROLLO LOCAL”.

Authors would also like to thank the City Council of Soria, for the opportunity given through the University of Valladolid, to carry out this energy study in the City of Soria.

Likewise, the authors thank the Spanish Ministry of Education and Professional Training, for the Department Collaboration Scholarship granted to Alberto Redondo Plaza in the course 2020/2021 and to the University of Valladolid for the postdoctoral research contract from the budget application 2018 180113-541A.2.01e691.

## References

1. Yigitcanlar, T., Degirmenci, K., Butler, L., Desouza, K.C.: What are the key factors affecting smart city transformation readiness? Evidence from Australian cities. *Cities*. 103434 (2021). <https://doi.org/10.1016/J.CITIES.2021.103434>.
2. Ayodele, T.R., Ogunjuyigbe, A.S.O., Nwakanma, K.C.: Solar energy harvesting on building's rooftops: A case of a Nigeria cosmopolitan city. *Renew. Energy Focus*. 38, 57–70 (2021). <https://doi.org/10.1016/J.REF.2021.06.001>.
3. Real Decreto 244/2019, de 5 de abril, por el que se regulan las condiciones administrativas, técnicas y económicas del autoconsumo de energía eléctrica. (2019).
4. Zhong, T., Zhang, Z., Chen, M., Zhang, K., Zhou, Z., Zhu, R., Wang, Y., Lü, G., Yan, J.: A city-scale estimation of rooftop solar photovoltaic potential based on deep learning. *Appl. Energy*. 298, 117132 (2021). <https://doi.org/10.1016/J.APENERGY.2021.117132>.
5. PVsyst, <https://www.pvsyst.com/>, last accessed 2021/08/27.

# Overshot waterwheel based grid-connected pico-hydro system

Vicente Leite

Research Centre in Digitalization and Intelligent Robotics (CeDRI)  
Instituto Politécnico de Bragança, Campus Santa Apolónia, Bragança, Portugal,  
avtl@ipb.pt,  
<http://cedri.ipb.pt>

**Abstract.** Recently, there has been growing interest in small-scale hydropower generation. It is a promising renewable energy source, generating power 24 hours a day, from a few watts to several kilowatts. Even for low head sites, it has become attractive, not only for remote areas where the utility grid is not available, but also for grid connection. These pico-hydro systems do not require expensive civil works and are environmentally friendly. Recent studies have shown they can be connected to the grid using competitive technology and widely available on the market. Waterwheels are emerging with enormous potential in this context. This paper presents an innovative approach for the grid connection of a pico-hydro system based on an overshot waterwheel, using a permanent magnet synchronous generator and a photovoltaic inverter. The waterwheel is operating in an aquaculture centre taking advantage of the water fall in one of its tanks.

**Keywords:** waterwheel, pico-hydro, grid-connected, PV inverter.

## 1 Introduction

Energy is a critical economic and environmental development challenge that the world continues to face today [1]. Hydropower gives a significant contribution for the world energy demand with 4,370 *TWh* electricity generated in 2020 [2]. Historically, it is associated with centralised generation based on big power plants [3]. Nowadays, energy generation is increasingly distributed [4] with great advantages mainly when associated with microgrids [5, 6]. Small-scale hydropower generation can be a fundamental foundation for sustainable development, public service delivery, as well as poverty alleviation. Despite the appeal and benefits of small-scale plants, 66% of their potential around the world remains untapped [2].

In the new paradigm of distributed generation and of self-consumption, the integration of small and very-small hydro systems in the local context, through the optimized use of water resources, can create positive impacts on the local ecosystem [3, 7]. These small systems, up to 5 *kW* [8] or 10 *kW* [3], are mentioned in the literature as pico-hydro systems. When integrated into existing infrastructures, the impact is twofold: renewable electricity generation and spread

2 Vicente Leite

of small-scale hydro systems. In such applications, where electricity generation is not the main priority, those systems are designated as multipurpose schemes [7]. Thus, the existing infrastructures continue to guarantee their main function and, at the same time, generate energy. Water supply systems, irrigation canals and wastewater treatment systems are just a few examples [3, 9]. Under this purpose, this paper presents a pico-hydro system suitably integrated in the existing infrastructure, which consists of using the water discharge for a tank at the Centro Aquícola de Castrelos (Castrelos' Aquaculture Centre), in Bragança, Portugal. This is one of several tanks into which the water collected from the river is brought, by gravity, through a channel. The tanks are used in the process of raising trout to repopulate the region's rivers. This work was carried out under the project BIOURB-NATUR - Bio constructive diversity, bioclimatic building, sustainable rehabilitation and application in natural parks, funded by European Commission - POCTEP.

During the last decades, small-scale water turbines have been used in off-grid pico-hydro systems in rural areas [10] and some works present new developments for improved quality [11]. Recently, the development of these systems has gained new impetus through its use in new applications, such as: in hybrid systems with pumped-hydro energy storage [12], in microgrids for energy storage [13], or as a cost effective and well-established way to generate electricity [5]. In fact, there is a wide use of pico-hydro systems, especially in off-grid systems, which are very popular in developing countries [3, 14, 15]. However, despite the trigger of emerging applications, there is still a lack of information on the most efficient and flexible solutions for connecting them to the grid.

Recently, studies have been published based on two distinct approaches. The first consists of the development of specific control for the power electronics responsible for the generator operating point and grid interface [4, 6]. The second uses a more practical and flexible solution. This later approach is based on the "plug and play" principle, with integration of technology widely available on the market and at very competitive prices [16, 17]. This work follows this second strategy. It is based on the proper integration of a permanent magnet synchronous generator (PMSG), widely used in small wind turbines [18], and photovoltaic (PV) string inverters. In general, an overvoltage protection circuit is additionally required [19].

Water turbines used to generate electricity are a mature and widely spread technology, even for small hydropower plants [6, 14, 15]. In ancient times, more than 2000 years ago, waterwheels were an important discovery as hydraulic machines used to convert water energy into mechanical energy. They were extensively used during many centuries, in many applications, until they were replaced by the electric motor in the middle of the last century [20, 21]. They were considered as a relic from the beginning of the industrial revolution [20]. During the last decades, due to new societal challenges related to the environmental sustainability, the need to explore low head hydroelectric power sources to generate electricity became greater than ever [20].

Nowadays, waterwheels are becoming again attractive as water turbines for power generation. This happens not only where large distances usually require decentralized electricity production and off-grid power plants but also as a grid-connected system [6, 13, 16]. Waterwheels are environmentally friendly and can help to preserve cultural heritage [21] such as in the Silk House museum, where a waterwheel was installed in the place there was a former mill [22]. Moreover, they can contribute to the promotion of eco-tourism and social activities [21, 22] as in the present case of the BIOUB NATUR project. However, most of the knowledge about waterwheels is very old with lack of information and uncertainty [23]. Therefore, several recent studies have been carried out to evaluate their performance and efficiency improvements [21, 23, 24], even for power ranges of just a few hundred watts [9].

Despite this recent interest in very small-scale turbines, including waterwheels, there is still another challenge: how to make the connection to the grid in a cost-effective, robust and flexible way. This paper is a contribution to this challenge: first, with the design of a waterwheel using a free available tool [25, 26]; second, through the detailed presentation of a grid connection approach based on standard components; third, discussing the analysis of the experimental results regarding the compatibility between the PMSG and PV inverter; and fourth, contributes to the promotion of eco-tourism activities and to the development and dissemination of grid-connected pico-hydro systems based on existing infrastructures - a tank of an aquaculture centre.

## 2 Overshot waterwheel

Among all kind of waterwheels, the overshot one presents the highest efficiency (up to 85-90%) over a wide range of water flows [24]. The site conditions for the implementation of an overshot waterwheel at the Castrelos Aquaculture Centre do not completely satisfy the ideal site parameters. Indeed, the overshot waterwheel is generally used for head differences of 2.5 – 10 *m*, and flow rates of 100 – 200 *l/s* per metre width [20]. The main channel that captures the water from the river has a flow of approximately 100 *l/s*.

After interviewing the people working at the Aquaculture Centre, and in order to suitably integrate the waterwheel into the existing infrastructures, it was designed to take advantage of the water falling into a tank. Therefore, the highest head available was 2.5 *m* and the flow rate was about 15 *l/s* by the time of the data survey. Considering that the efficiency these waterwheels is approximately constant over a wide range of flow rates [20, 24] it was decided to design a wheel for 25 *l/s* with a diameter of 2 *m*.

There are some recent works related to the design of waterwheels, namely the overshot type [23, 24, 26]. In this work, the platform available online [25] and the master's thesis [26] were used. Figure 1 shows a draw of the designed overshot waterwheel and an implantation scheme in the fish breeding tank. The waterwheel was built in stainless steel with 4 radial arms, 26 *cm* width and a total of 20 buckets 26 *cm* length, 20 *cm* depth and 31.4 *cm* width and spacing.

The estimated rotational speed at maximum power is 6.8 *rpm*. The estimated hydraulic power depends on the design water flow (25 *l/s*) and head available (2 *m*) on the site. The generated mechanical power  $P$  (*W*) at the turbine shaft is estimated by Equation 1, as follows [27]:

$$P = \eta \times g \times Q \times H \tag{1}$$

where  $\eta$  is the turbine hydraulic efficiency,  $g$  is the acceleration due to gravity ( $\simeq 9.8 \text{ m/s}^2$ ),  $Q$  is the water flow in the turbine (*l/s*), and  $H$  is the gross head (*m*). Assuming an overall efficiency (including waterwheel, gearbox, generator, cable, rectifier and inverter) of 50%, the power injected into the grid will be 245 *W*.

### 3 Grid-connection approach

Nowadays, the grid connection of small wind turbines and PV modules is a mature technology and spread worldwide. Therefore, PMSGs and PV inverters are widely available and at competitive prices. On the contrary, grid-connected pico-hydro systems are not widespread enough, as the level of standardization is low. In effect, for these systems, each solution is designed for the specific site requirements. Anyway, PMSGs based small-scale hydro turbines are emerging as grid-connected energy sources.

The strategy of connecting the waterwheel to the grid is shown in Fig. 2. It consists of a suitable integration of a PMSG and a PV inverter. This approach has been investigated over the last few years [16, 17], including for very small-scale hydro systems [16, 17, 19]. It is a viable alternative to the conventional way of connecting hydro generators to the grid [4, 27]. In fact, with this approach the PMSG does not need to operate at constant speed, close to the rated speed, and its operating point can vary within a wide range of operation. In this way, the use of complex mechanical devices to control the generator speed is avoided.

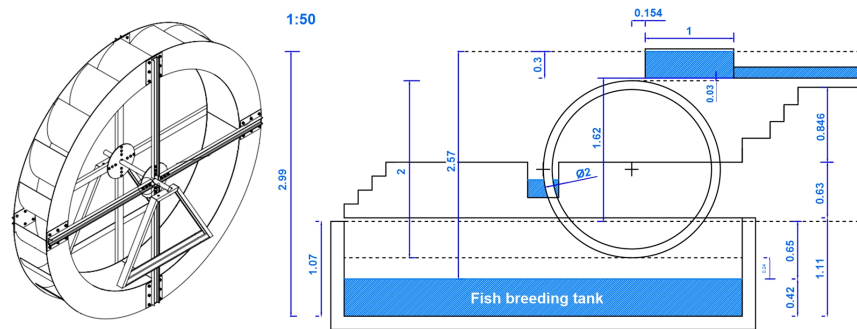


**Fig. 1.** Draw of the designed overshot waterwheel (on the left, by Luís Queijo) and implantation scheme in the fish breeding tank (on the right, by Rui Oliveira).

## Overshot waterwheel based grid-connected pico-hydro system 5

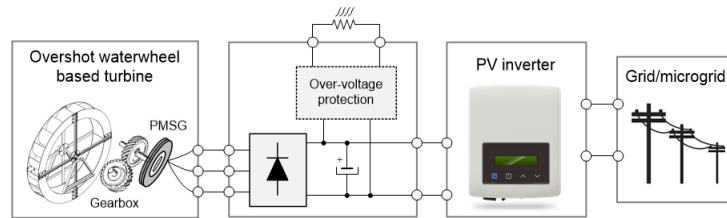


**Fig. 2.** General grid-connection scheme.

The first stage of power conversion in Fig. 2 is from hydraulic (Equation 1) to mechanical, given by  $\omega \times T$ , where  $T$  is the torque (Nm) and  $\omega$  is the waterwheel rotational speed ( $rad/s$ ). Unfortunately, this speed is very low ( $\leq 20rpm$ ) and operating speeds less than  $10 rpm$  are expected [23, 27]. Because of this drawback, a second mechanical power conversion stage is necessary, from low speed to higher speed (and lower torque). This is achieved through a high ratio gearbox as illustrated in Fig. 2. Even so, it may be necessary to use a low speed PMSG, commonly used in small wind turbines. Indeed, from calculator [25], the rotation speed of the waterwheel ( $6.8 rpm$ ). This is very low, even for PMSGs used in low speed wind turbines, where the speed is in the range of some hundreds of  $rpm$ . Because of this constraint, and to achieve a rotational speed of not less than  $300 rpm$ , a gearbox available on the market, with a gear ratio of 1:45 was selected. The generator performs the third conversion stage, converting the shaft's mechanical power ( $\omega \times T$ ) into AC electrical power, characterized by a three-phase voltage system. Next, a full-bridge rectifier converts these voltages into a DC voltage and current. After this fourth stage, the power ( $W$ ) is given by  $P = V_d \times I_d$ , being  $V_d$  and  $I_d$  the average values of voltage and current, respectively, at the output of the rectifier bridge.

Last but not least, a fifth conversion stage (DC to AC) is needed to perform the interface with the grid. For this purpose, there are available 3 approaches: developing specific power converters [4, 16], using wind turbine inverters, or using PV inverters [17]. The first requires a lot of development time and several legal requirements must be accomplished. Even so, as with the second option, using wind inverters, the solution requires knowledge of the turbine's power curve and the consequent parameterization of the inverter. The third approach is the most "plug and play" of all and is based on widely available PV string inverters [16] or microinverters [17].

Whichever the approach, an overvoltage protection circuit is most likely required [19], as illustrated in Fig. 2. Unfortunately, the third approach is not completely universal. The compatibility of the PV inverter with a pico-hydro turbine depends on the maximum power point tracking (MPPT) algorithm and mainly on the way it is initialized [28]. For the PV inverters compatible with a water turbine, it is still necessary to make compatible the operating point range of both: generator ( $\omega, T$ ) and inverter ( $V_{dc}, I_{dc}$ ).

6 Vicente Leite

In the literature, there are published works which, under certain assumptions, show that the voltage and current at the output of the rectifier bridge are proportional, respectively, to the rotational speed and torque of the generator [18]. In this way, the PV inverter controls the operating point of the waterwheel (turbine), i.e. the rotational speed and torque, by controlling, respectively, the voltage  $V_d$  and current  $I_d$  at the output of the rectifier bridge.

## 4 Implementation and experimental results

This section describes the implementation of the constructed overshoot waterwheel and the solution adopted for its connection to the grid. Figure 3 shows the overshoot waterwheel installed in the fish tank. The flow rate was measured indirectly by averaging several counts of the time it took a colored spot to travel through the inlet pipe. The flow rate obtained was about 13 l/s.

During the tests carried out over the first 6 months of 2021, at different times, the no-load rotational speed of the wheel varied between 22.5 and 25.5 rpm. The speed under load, around the maximum power, and for the flow available at each moment, varied between 7.8 and 12 rpm. For the initial design requirements, the expected operating speed was 6.8 rpm (with 25 l/s).

Taking into account the 1:45 speed ratio of the selected gearbox, the shaft speed of the generator is in the range 351 – 540 rpm. At no-load conditions, this speed reaches 1148 rpm. On the one hand, this speed must be higher enough to generate a DC voltage at the rectifier output higher than the start operating voltage of the PV inverter. On the other hand, the rectifier's output voltage should be sufficiently lower than the maximum value of the DC input voltage of the PV inverter. Otherwise, the grid connection will not be completely “plug and play”, being necessary to use an overvoltage protection circuit [19]. Furthermore, the DC operating voltage, around the MPP of the turbine, must be within the MPPT voltage range of the PV inverter. Therefore, a suitable rated voltage of the generator, or speed constant  $V/rpm$ , must be selected for a given PV inverter or, for a given inverter, the rated speed of the generator must be conveniently selected, together with the gearbox ratio.



**Fig. 3.** Stainless steel overshoot waterwheel installed in the fish tank.

In practice, the solution design is an iterative process, and takes into account the equipment available on the market and its cost. Fortunately, for the power in question, new inverters are being launched on the market with a wide MPPT range, where the lower limit is getting smaller. For instance, from the datasheets of the Solax X1-0.6 and Solis-mini-700-4G PV inverters, it can be seen that the lower limit of the MPPT range is, respectively, 45 and 50 V. On the other hand, the maximum voltage of input is high enough, respectively 450 and 600 V, to make the overvoltage protection circuit unnecessary. For this project, the Solax X1-0.7-S-D(L) inverter was purchased with maximum  $DC$  input power 840 W, maximum  $DC$  input voltage 400 V, MPPT voltage range 55-380  $V_{DC}$  and start operating voltage 50  $V_{DC}$ .

Tests were carried out with 3 different generators connected to the gearbox and waterwheel. The first was a low speed axial flux permanent magnet generator, AFPMG260, designed for small wind turbines. The rated output power, speed,  $DC$  voltage and  $DC$  current are, respectively, 300 W, 300 rpm, 28  $V_{DC}$ , 10.71  $A_{DC}$ . The stator is star connected and the  $DC$  values refer to the output of the three-phase rectifier. The second generator was a higher voltage PMSG, PGS 100R-WB 488, with the following rated characteristics: 800 W, 1500 rpm, 385  $V_{AC}$ , 1.25  $A_{AC}$ . This is a 100 Hz, 8 pole axial PMSG and these nameplate values are for star connection. In this work, the stator connections were reconfigured from star to delta to reduce the voltage. The third generator is based on a three-phase BLDC (Brushless  $DC$ ) electrical machine working as a permanent magnet alternator [29]. This is a lower cost solution for small power applications. To operate as a generator, like the previous two, it is connected to a three-phase rectifier and the  $DC$  output voltage constant is 0.199  $V/rpm$  (under no-load). It is based on a delta connected 80-7s-2p stator with 42 poles and a rotor type 2 (0.75  $W/rpm$ ). According to [29], the rated output power, speed,  $DC$  voltage and  $DC$  current are, respectively, 1200 W, 1600 rpm, 180 V and 6.7 A. The tests with generators AFPMG260, PGS 100R and 80-7s-2p were performed on site, respectively, on 21 December 2020, 23 February 2021 and 9 June 2021.

To identify the point of maximum power, for the available flow rate, the curves  $P_{DC}$  versus  $V_{DC}$  were obtained, through the variation of a load resistance. The results are presented in Fig. 4. This figure also presents the values of  $DC$  voltage and  $DC$  current for a power variation less than 5%, around the MPP. The values of the voltages and currents presented in Fig. 4, and used to calculate the  $DC$  power, correspond to the average of 3 to 5 readings.

The waterwheel was connected to the grid using the PV inverter Solax X1-0.7, either with generator 80-7s-2p or generator PGS 100R. Unfortunately, the inverter was not yet available when the AFPMG260 generator was attached to the waterwheel.

Figure 5 shows the first 4 minutes of the waterwheel connection to the grid. The maximum  $AC$  power obtained with the 80-7s-2p generator was 137 W and 130 W with generator PGS 100R. The average  $AC$  power, during the last minute, was 125.8 W and 119.6 W, respectively. The waterwheel speed under no-load

8 Vicente Leite

was 25 rpm and under load operation it was 9 rpm with generator 80-7s-2p and 11 rpm with generator PGS 100R.

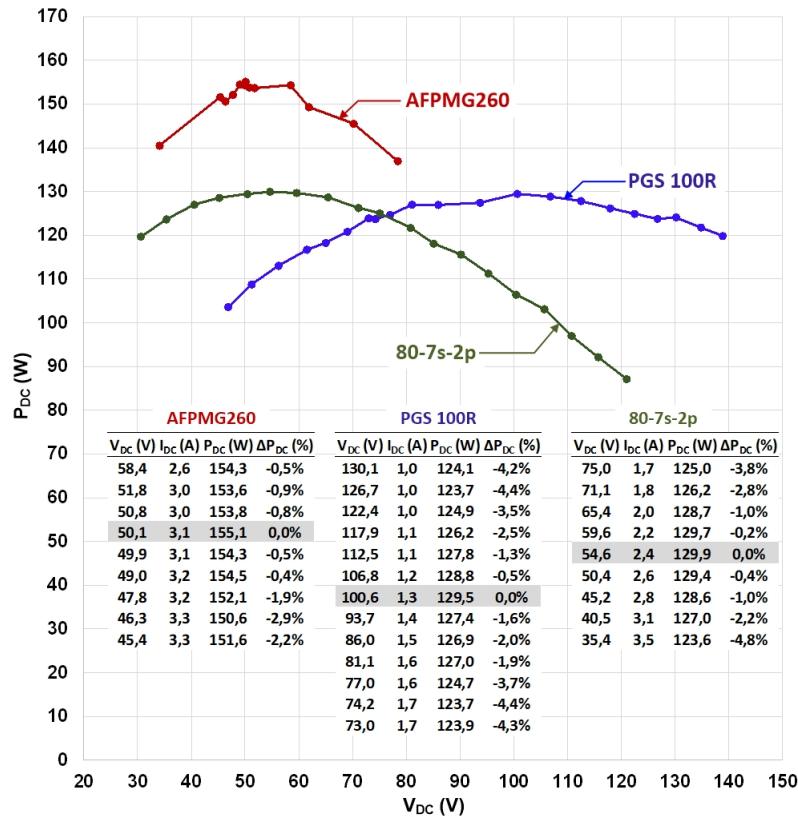


Fig. 4. P-V curves of the waterwheel with 3 different generators.

## 5 Discussion

Tests with the different generators were carried out at different times of the year and, most likely, with different flow rates. For practical reasons, it was not possible to measure the flow rate with acceptable accuracy. Thus, it is not possible to accurately compare the DC power values obtained with the 3 generators shown in Fig. 4. This work is focused on the analysis of the compatibility between the waterwheel, generator and PV inverter (Fig. 2). In this context, it is particularly relevant to observe the compatibility between the operating speed of the generator (and the waterwheel) with the corresponding DC voltage at the output of the rectifier bridge. This voltage must be within the MPPT range of the PV

Overshot waterwheel based grid-connected pico-hydro system

9

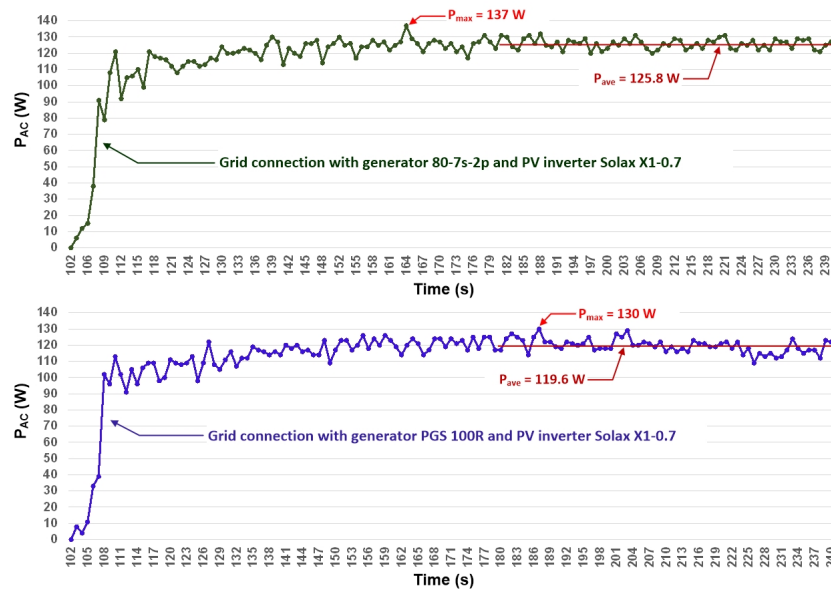


**Fig. 5.** Grid connection of the waterwheel using PV inverter Solax X1-0.7 and generators 80-7s-2p (above) and PGS 100 (below).

inverter, so that it can be adjusted by the MPPT algorithm and thus extract the maximum power.

By analysing Fig. 4 and considering a variation less than 5% around the MPP, it can be seen that the voltage range is 45.4 – 58.4 V, 73 – 130.1 V and 35.4 – 75 V for generators AFPMG260, PGS 100R and 80-7s-2p, respectively. On the other hand, although the MPPT range on the nameplate of the PV inverter is 55 – 380 V, in practice the lower limit is around 50 V. Thus, the inverter works close to the lower limit of its MPPT range with generators AFPMG260 and 80-7s-2p and inside the first quarter of the MPPT range with the generator PGS 100R.

After the gearbox has been selected (with a high transmission ratio, 1:45 in this case), a generator with a suitable voltage constant ( $V/rpm$ ) must be selected. In practice, there is a compromise: on the one hand, this constant must be large enough so that the voltage around the MPP is within the MPPT range of the inverter and, on the other hand, it must be small enough so that in case of no-load operation, the voltage does not exceed the upper limit of the inverter’s input voltage (400 V in this case). Otherwise, an overvoltage protection circuit is required. It must be taken into account that the voltage constant ( $V/rpm$ ) of the generator on load can be significantly lower than its value under no-load operation. For example, for the 80-7s-2p generator, the value at maximum output power was expected to be in the range 55-60% of the value under no-load [29]. However, according to the tests carried out it was about 31%.

Figure 5 shows the evolution of the  $AC$  power injected into the grid (at the inverter output) during a start-up with generators 80-7s-2p and PGS 100R. The Solax X1-0.7 inverter took about 100 seconds to start injecting power into the grid after switching ON the switch on the  $DC$  side. About 40  $s$  later it reached the steady-state operation. After that, it continued to extract power, oscillating around the MPP due to the voltage perturbation introduced by the MPPT algorithm of the inverter. Before switch ON the input breaker of the PV inverter, the  $DC$  open circuit voltage was approximately 186  $V$  and 252  $V$  with generators 80-7s-2p and PGS 100R, respectively. This means that an overvoltage protection circuit is not needed since the maximum input  $DC$  voltage of the PV inverter is 400  $V$ .

## 6 Conclusions

This paper described the design of a grid-connected pico-hydro system based on an overshot waterwheel. A practical and innovative grid-connection approach was used which is based on the integration of a permanent magnet synchronous generator and a photovoltaic inverter. Three generators and a conventional string inverter were used for this purpose. This waterwheel is operating in an aquaculture centre, taking advantage of the water fall in one of its tanks, with a head of 2  $m$  and a flow rate of only about 13  $l/s$ . This pico-hydro system injects 126  $W$  into the grid, with a global efficiency of about 50%.

This work demonstrates, on the one hand, how hydroelectric energy can be generated on a very small-scale, properly integrated into existing infrastructures and, therefore, without the need for any civil construction works. On the other hand, it shows how the generated energy can be injected into the grid, in a simple and effective way, using only equipment widely available on the market. In short, the generator's three-phase voltage system is converted to a  $DC$  voltage. Then, a conventional photovoltaic inverter (through its MPPT algorithm) controls the operating point of the waterwheel, i.e. the rotational speed and torque, by controlling, respectively, the voltage and current at the output of the rectifier bridge. This work also demonstrates that an additional overvoltage protection circuit can be dispensed by suitably selecting the generator's ratios  $W/rpm$  e  $V/rpm$ .

**Acknowledgments:** The author would like to thank: the CYTED Thematic Network 518RT0558 - Ciudades Inteligentes Totalmente Integrales, Eficientes y Sostenibles; Project BIOURB-NATUR supported by European Union; and IPB-ICNF partnership in this project. The author would also like to thank to students Victor Polidório and Marina Pietrobelli for their collaboration. Many thanks to colleagues Luís Queijo, Rui Oliveira and also to Vitor Gomes, José Batista, and Jorge Paulo for their technical support.

## References

1. United Nations: World Small Hydropower Development Report 2019. [https://www.unido.org/sites/default/files/files/2020-08/Global\\_overview.pdf](https://www.unido.org/sites/default/files/files/2020-08/Global_overview.pdf)

## Overshot waterwheel based grid-connected pico-hydro system 11

2. International Hydropower Association: Status Report Sector, trends and insights, 2021. [https://assets-global.website-files.com/5f749e4b9399c80b5e421384/60c37321987070812596e26a\\_IHA20212405-status-report-02\\_LR.pdf](https://assets-global.website-files.com/5f749e4b9399c80b5e421384/60c37321987070812596e26a_IHA20212405-status-report-02_LR.pdf)
3. Pérez-Sánchez, M., Sánchez-Romero, F., Ramos, H., López-Jiménez, P.: Energy Recovery in Existing Water Networks: Towards Greater Sustainability. In: MDPI Special Issue Water Systems towards New Future Challenges, Vol. 9, No. 2 (2017). doi:10.3390/w9020097
4. Molina, M., Pacas, M.: Improved power conditioning system of microhydro power plant for distributed generation applications. In: International Conference on Industrial Technology (ICIT), pp. 1733–1738 (2010). doi:10.1109/ICIT.2010.5472461
5. Sharma, K R., Kewat, S., and Singh, B.: Robust 3IMPL Control Algorithm for Power Management of SyRG/PV/BES-Based Distributed Islanded Microgrid. In: IEEE Transactions on Industrial Electronics, Vol. 66, no. 10, October 2019. doi: 10.1109/TIE.2018.2880673
6. Kerdtuad, P., Simma, T., Chaiamarit, K., Visawaphatradhanadhorn, S.: Establishment of a Pico Hydro Power Plant Using Permanent Magnet Synchronous Generator Supplied for AC Microgrid. In: 44th Annual Conference of the IEEE Industrial Electronics Society (IECON) (2018). doi:10.1109/IEECON.2018.8712214
7. Project Shapes (work package 5- WP5): Energy recovery in existing infrastructures with small hydropower plants, multipurpose schemes - Overview and examples. [http://www.infrawatt.ch/sites/default/files/2010\\_06\\_07\\_Mhyllab&ESHA\\_Energyrecoveryinexistinginfrastructureswithsmallhydropowerplants.pdf](http://www.infrawatt.ch/sites/default/files/2010_06_07_Mhyllab&ESHA_Energyrecoveryinexistinginfrastructureswithsmallhydropowerplants.pdf)
8. Sopian, K. and Razak, J.: Pico hydro: Clean power from small streams. In: 3rd WSEAS Int. Conf. on Renewable Energy Sources, pp. 414-419 (2009). doi:10.1016/j.renene.2008.12.011
9. Titus, J., Ayalur, B.: Design and Fabrication of In-line Turbine for Pico Hydro Energy Recovery in Treated Sewage Water Distribution Line. In: Elsevier Energy Procedia, 156, pp. 133–138 (2019). doi:10.1016/j.egypro.2018.11.117
10. Koirala, N., Dhakal, R., Lubitz, D., Bhandari, S., Dev, G.P., Dhakal, Y., Uttam Niraula, U.: Review of Low Head Turbines System of Nepal for Rural Electrification. In: 6th International Conference on Renewable Energy Research and Applications (ICRERA), pp. 861–869 (2017). doi:10.1109/ICRERA.2017.8191182
11. Chandran, V. P., Murshid, S., Singh, B.: Voltage and Frequency Controller with Power Quality Improvement for PMSG Based Pico-Hydro System. IN: IETE Journal of Research (2019). doi:10.1080/03772063.2019.1571953
12. Pali, B.S., Vadhera, S.: An Innovative Continuous Power Generation System Comprising of Wind Energy along with Pumped-Hydro Storage and Open Well. IEEE Transactions on Sustainable Energy, Vol. 11, no. 1, pp. 145–153 (2020). doi:10.1109/TSTE.2018.2886705
13. Vasudevan, K.R., Ramachandaramurthy, V.K., Gomathi, V., Ekanayake, J.B., Tiong, S.K.: Modelling and simulation of variable speed pico hydel energy storage system for microgrid applications. In: Elsevier Journal of Energy Storage, Vol. 24, pp. 1–14 (2019). doi:10.1016/j.est.2019.100808
14. Yah, N. F., Oumer, A. N. and Idris, M. S.: Small scale hydro-power as a source of renewable energy in Malaysia: A review. In: Elsevier Renewable and Sustainable Energy Reviews, Vol. 72, May 2017, pp. 228–239. doi:10.1016/j.rser.2017.01.068
15. Okot, D. K.: Review of small hydropower technology. In: Elsevier Renewable and Sustainable Energy Reviews, 26, pp. 515–520 (2013). doi:10.1016/j.rser.2013.05.006
16. Leite, V., Couto, J., Ferreira, A., Batista, J.: A practical approach for grid-connected pico-hydro systems using conventional photovoltaic inverters. In: In-

12 Vicente Leite

- ternational Energy Conference (ENERGYCON), p.p. 1–6 (2016). doi:10.1109/ENERGYCON.2016.7513911
17. Ribeiro, G., Silva, W., Leite, V., Ferreira, Â: Grid Connection Approach for Very Small-Scale Pico-Hydro Systems Using PV Microinverters. In: 45th Annual Conference of the IEEE Industrial Electronics Society (IECON), Lisbon, Portugal (2019). doi:10.1109/IECON.2019.8926691
  18. Rahimi, M.: Modeling, control and stability analysis of grid-connected PMSG based wind turbine assisted with diode rectifier and boost converter. In: Elsevier International Journal of Electrical Power & Energy Systems, Vol. 93, pp. 84–96 (2017). doi:10.1016/j.ijepes.2017.05.019
  19. Scotta, I., Silva, W., Leite, V.: Overvoltage protection for grid-connected pico-hydro generation using photovoltaic inverters. In: Revista Facultad de Ingeniería, No 99 (2021). doi:<https://doi.org/10.17533/udea.redin.20200581>
  20. Müller, G. & Kauppert, K.: Performance characteristics of water wheels. In: Journal of Hydraulic Research, Vol. 42, no 5, pp. 451–460 (2004). doi:10.1080/00221686.2004.9641215
  21. Quaranta, E., Revelli, R.: Hydraulic Behavior and Performance of Breastshot Water Wheels for Different Numbers of Blades. In: Journal of Hydraulic Engineering, Vol. 143, Issue 1 (January 2017). doi:10.1061/(ASCE)HY.1943-7900.0001229
  22. Figueiredo, L.G., Maidana, W., Leite, V.: Implementation of a smart microgrid in a small museum: the Silk House. In: Springer Communications in Computer and Information Science, Vol. 1152 (2020). doi:10.1007/978-3-030-38889-8\_10
  23. Quaranta, E.: Investigation and optimization of the performance of gravity water wheels. Ph.D Thesis, Politecnico di Torino (2017). <https://core.ac.uk/download/pdf/84252843.pdf>
  24. Quaranta, E., Revelli, R.: Performance characteristics, power losses and mechanical power estimation for a breastshot waterwheel. Elsevier Energy, Vol. 87, No. 1, pp. 315–325 (2015). doi:10.1016/j.energy.2015.04.079
  25. Borst Engineering & Construction LLC: Overshot Water Wheel Design Calculator. [https://www.borstengineeringconstruction.com/Overshot\\_Water\\_Wheel\\_Design\\_Calculator.html](https://www.borstengineeringconstruction.com/Overshot_Water_Wheel_Design_Calculator.html)
  26. Polidorio, V.: Design and Analysis of an Overshot Water Wheel for a Grid-Connected Pico-Hydro System. MSc Thesis, Polytechnic Institute of Bragança (2020). <http://hdl.handle.net/10198/23880>
  27. Laghari, J.A., Mokhlis, H., Bakar, A.H.A. and Mohammad, H.: A comprehensive overview of new designs in the hydraulic, electrical equipments and controllers of mini hydropower plants making it cost effective technology. In: Elsevier Renewable and Sustainable Energy Reviews, Vol. 20, pp. 279–293 (2013). doi:10.1016/j.rser.2012.12.002
  28. Guimarães, T. F., Leite, V.: Analyses of MPPT Algorithms in Real Test Conditions. In: 9th International Conference on Renewable Energy Research and Application (ICRERA), Glasgow, UK (2020). doi:10.1109/ICRERA49962.2020.9242873
  29. EcoInnovation: Smart Drive Applications for DIY projects, Applications Manual (2016). [https://drive.google.com/file/d/0BzVDBix3S\\_qbNnZvbDByQUhIcjA/view?resourcekey=0-\\_MFILhtc\\_rqvP55ZBEDtoA](https://drive.google.com/file/d/0BzVDBix3S_qbNnZvbDByQUhIcjA/view?resourcekey=0-_MFILhtc_rqvP55ZBEDtoA)

## Photovoltaic cells defects classification by means of Artificial Intelligence and electroluminescence images

Héctor Felipe Mateo-Romero<sup>1</sup>[0000-0002-5569-3532], Álvaro Pérez-Romero<sup>2</sup>[0000-0002-4292-6640], Luis Hernández-Callejo<sup>1</sup>[0000-0002-8822-2948], Sara Gallardo-Saavedra<sup>1</sup>[0000-0002-2834-5591], Víctor Alonso-Gómez<sup>1</sup>[0000-0001-5107-4892], José Ignacio Morales-Aragonés<sup>1</sup>[0000-0002-9163-9357], Alberto Redondo Plaza<sup>1</sup>[0000-0002-2109-5614] and Diego Fernández Martínez<sup>1</sup>[0000-0003-1468-9083]

<sup>1</sup> Universidad de Valladolid, Campus Universitario Duques de Soria, Soria 42004, Spain

<sup>2</sup> Universidad de Cantabria, Av. de los Castros, s/n, Santander 39005, Spain

thehfmr2011@gmail.com: H.F.M-R.; alvaro.pr470@gmail.com: A.P-R.;  
luis.hernandez.callejo@uva.es: L.H-C.; sara.gallardo@uva.es:  
S.G-S.; victor.alonso.gomez@uva.es: V.A-G.; ziguratt@coit.es:  
J.I.M-A.; alberredon@gmail.com: A.R.P.; diego-brivi@hotmail.com:  
D.F.M.

**Abstract.** More than half of the total renewable additions correspond to solar photovoltaic (PV) energy. In a context with such an important impact of this resource, being able to produce reliable and safety energy is extremely important and operation and maintenance (O&M) of PV sites must be increasingly intelligent and advanced. The use of Artificial Intelligence (AI) for the defects identification, location and classification is very interesting, as PV plants are increasing in size and quantity. Inspection techniques in PV systems are diverse, and within them, electroluminescence (EL) inspection and current-voltage (I-V) curves are one of the most important. In this sense, this work presents a classifier of defects at the PV cell level, based on AI, EL images and cell I-V curves. To achieve this, it has been necessary to develop an instrument to measure the I-V curve at the cell level, used to label each of the PV cells. In order to determine the classification of cell defects, CNNs will be used. Results obtained have been satisfactory, and improvement is expected from a greater number of samples taken.

**Keywords:** photovoltaic cell defect, classifier, artificial intelligence, electroluminescence.

### 1 Introduction

During the last years, global installation of renewable generation installations has significantly increased. In 2019, the last analyzed year in the Global Status Report [1], 201 GW of renewable power capacity were installed in the World, being 115 GW of Solar Photovoltaic (PV) capacity, which corresponds with more than 57% of the total renewable additions.

In this context in which solar PV energy has such an important impact, being able to produce reliable and safety energy is extremely important. Ensuring energy production is a key factor in warranting plant profitability, and this has forced the design of increasingly intelligent and advanced Operation and Maintenance (O&M) strategies. Traditionally, different inspection techniques have been used in PV sites with the objective of detecting anomalies that reduce the system efficiency and can generate safety issues, as Infrared thermography inspections (IRT) [2], electroluminescence (EL) [3–5] or current-voltage (I-V) curves capturing [5, 6]. The development of new equipment and methodologies for its application in PV plants are necessary, and in this sense, research and industry are evolving rapidly [7]. The increased plant size has promoted the use of drones for the image capturing [8, 9], however the amount of data to process is unapproachable, requiring important human efforts and being very expensive and time-consuming.

The use of Artificial Intelligence (AI) for the defects identification, location and classification is very interesting. AI is already being applied in PV solar plants. However, its main application has being long focused on energy production forecasting issues. Authors in [10] develop a solution that provides the electricity production based on historical and current available solar radiation data in real-time. Some authors present a taxonomy study, which is a process to divide and classify the different forecasting methods, and the authors also present the trends in AI applied to generation forecasting in solar PV plants [11]. The use of artificial neural networks (ANN) has been successful in the last decade, some authors use ANN together with climatic variables to forecast generation in PV solar plants [12], while others use Support Vector Machine (SVM) together with an optimization of the internal parameters of the model [13]. ANN have also been used for other tasks, such as for the detection of problems in energy production, as is the case of work [14], where the authors use radial basis function (RBF) to detect this type of failure in production. A similar goal is sought in [15], where this time an SVM-based model is employed for describing a failure diagnosis method that uses a linear relation between the solar radiation and the power generation graphs. This research studies the following failure types: inverter failures, communication errors, sensor failures, junction box errors and junction box fire. The model classifies string and inverter failures. However, in actual PV plants each inverter can cover thousands of modules, and therefore important failures information can be lost in the classification [16].

In general, the application of AI technologies based on data-driven mechanisms helps to construct automatic fault classifiers and improves the efficiency and accuracy of faulty diagnoses [17]. A convolutional network, based on the analysis of the difference in the I-V curves of PV arrays under different failure states, capable of identifying not only a single failure (e.g., short circuit, partial shading, and abnormal aging) but also hybrid failures [17]. Authors in [18], authors investigate the effect of data augmentation techniques to increase the performance of our proposed convolutional neural network (CNNs) to classify anomalies between up to eleven different classes, in PV modules through thermographic images in an unbalanced dataset. This work is performed at the PV module level.

This work presents a classifier of defects at the PV cell level, based on AI, EL images and cell I-V curves. To achieve this, it has been necessary to make an instrument to measure the I-V curve at the cell level, used to label each of the PV cells. In order to determine the classification of cell defects, CNNs will be used. The document is structured as follows: section 2 presents the materials and methodology used, section 3 shows the results and discussion and section 4 deals the conclusions and future work.

## 2 Materials and methodology

This section is intended to explain the materials used, as well as the followed methodology to validate the classifier.

### 2.1 Materials

For this work, it has been necessary to develop special equipment and material. Firstly, regarding the PV devices, individual PV cells have been used. In this case, researchers have made the necessary welds to connect the required equipment, as it can be seen in Figure 1. One hundred PV cells have been used, which have subsequently been reused with artificial shadows, to have a greater number of measurements. Table 1 shows the basic electrical information of the PV cells used.

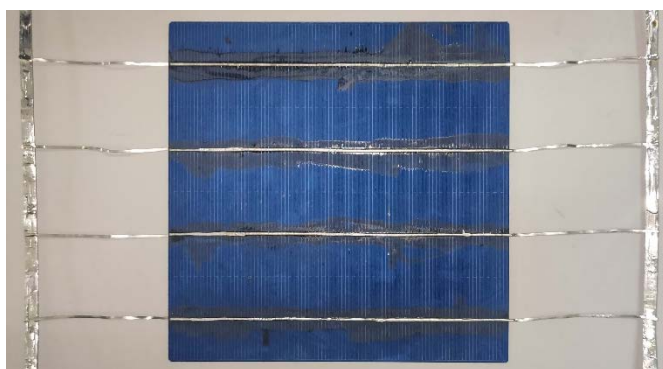


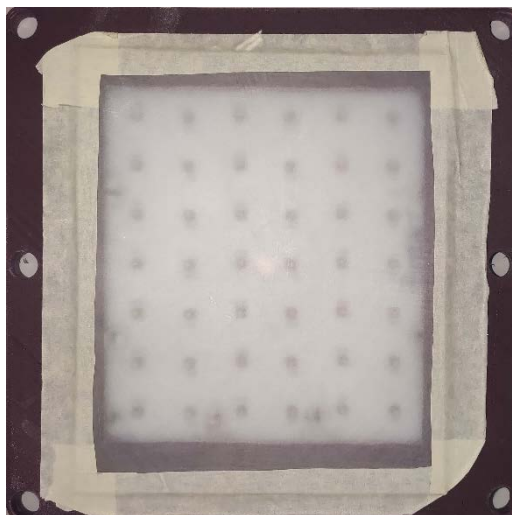
Figure 1. PV cell sample with welds already made.

Table 1. Information of PV cells.

PV cell parameter	PV cell parameter value
I <sub>sc</sub> (A)	7.5
V <sub>oc</sub> (V)	0.6
P <sub>MP</sub> (W)	4.67

Once the PV cells were prepared as detailed before, it is necessary to obtain their individual I-V curves. To do this, it has been required to excite the PV cells, for which a LED board composed of 42 LEDs has been used with the following characteristics: OSRAM brand, 850 nm, 1 A forward current, 630 mW of radiant flux at 1 A and 100

microseconds, with a maximum temperature of 145 °C. Figure 2 shows an image of the LED board. It has a diffuser screen to be able to homogenize the flow of light.



**Figure 2.** LED plate with diffuser mounted on support to take measurements.

Once the PV cells are illuminated with the LED board, the I-V curves are taken from an ingenious device developed by the authors, based on the charging and discharging of capacitors, and controlling the sweep by means of a simple microprocessor. This device is very versatile, since it allows to make the I-V curve from the second quadrant to the fourth quadrant through the first quadrant. However, for the presented research, the interest is only focused in the first quadrant.

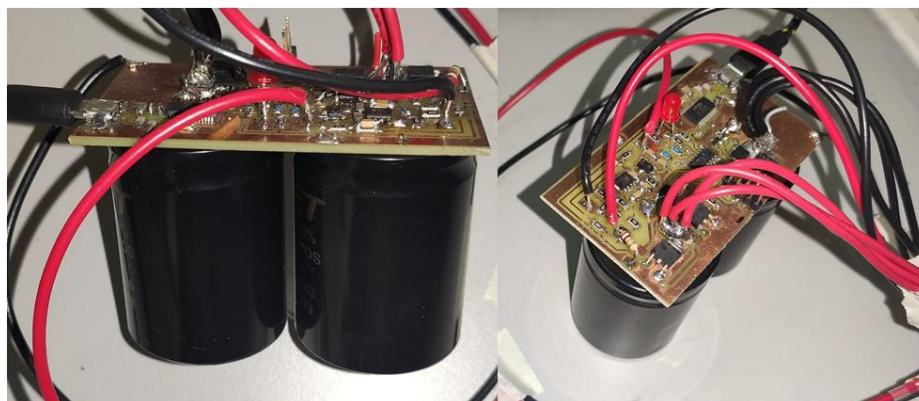


**Figure 3.** Device for drawing I-V curves at the PV cell level.

On the other hand, to be able to do EL, it is necessary to connect the PV cell to an external power source and to obtain the corresponding image. In this case, it is not needed to illuminate the PV cell (by means of an LED board). To be able to make the

capture, a special camera is necessary, specifically, it has been used an InGaAs camera, Hamamatsu brand and C12741-11 model.



**Figure 4.** InGaAs camera, Hamamatsu brand and C12741-11 model, for EL imaging.

Figure 5 a) shows a PV cell exposed to artificial irradiance to obtain its I-V curve, and Figure 5 b) shows the same PV cell subjected to inverse voltage to obtain its EL image.

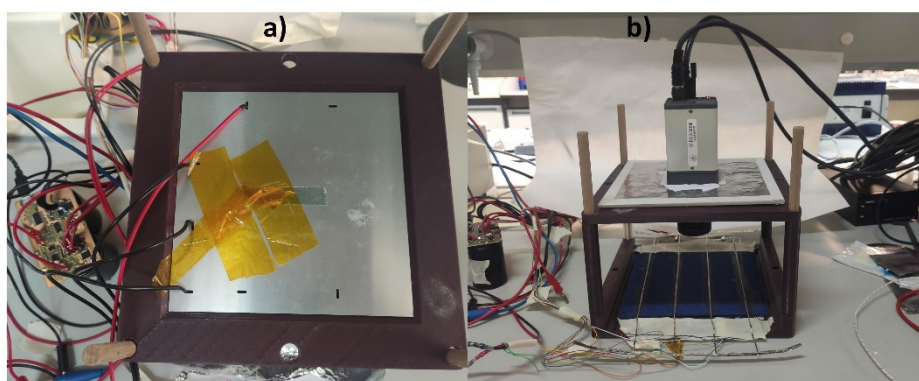


**Figure 5.** a) Obtaining I-V curve of PV cell; b) Obtaining EL image of PV cell.

## 2.2 Methodology

As already mentioned, the data was obtained manually, since the I-V curve of each of the cells of the data set was required, as well as their EL images. Therefore, none of the datasets that were in free repositories could be used. To carry out the EL images, an EL camera has been used, using different shades and irradiances to increase the amount of

data available in the final set. To obtain the I-V curve, the device built by the research team and previously presented has been used.

All images have had histogram adjustment done, making details and differences easier to see for the human eye, as well as for AI models. In order to be able to use the data of the I-V curve, the power values have been computed. Of all the values, only the highest value of each of the measurements will be taken into account. The power values will depend on the irradiance at which the measurement has been made, therefore, all measurements taken at the same irradiance will be processed. For this, the 5 highest power values will be chosen and the average will be made. In this way, authors will obtain a value that will represent the maximum power of a cell in good state. By choosing only the highest powers, the false information that the defective or shaded cells would provide will be ignored.

In order to have a greater number of samples, each of the measured cells has been subjected to partial shading, in order to repeat the measurements.

With the measurement of the absolute maximum power, authors will compute the relative power, calculating the proportion between the maximum power of each of the panels and the calculated power. This will give a continuous variable that will need to be divided into intervals if the problem is posed as a classification. The intervals should be decided in such a way that they allow the training to be carried out correctly and also the classes have a meaning in the context, that they are useful.

In Figure 6 it can be seen the histogram of the random variable and of the chosen classes. Class 0: PV cells in good condition (relative power  $\geq 0.825$ ); Class 1: PV cells in questionable condition (relative power  $< 0.825$  and  $\geq 0.725$ ); Class 2: PV cells in poor condition (relative power  $< 0.725$ ).

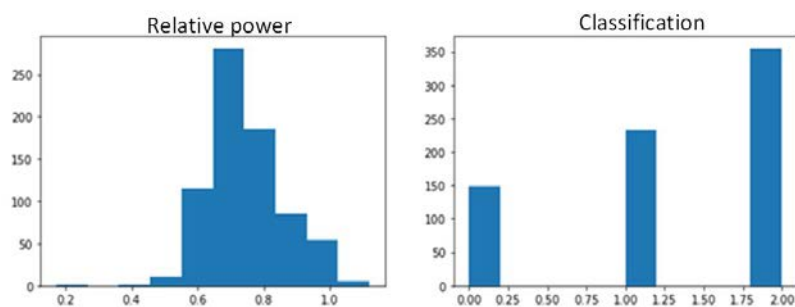


**Figure 6.** Relative power and classification of PV cells once the I-V curves have been made.

Once the information is available (I-V curves and EL images), it is necessary to use AI-based models to be able to train these models and to make the classifier. To resolve the classifier issue, it was decided to use an ANN-based architecture, specifically a CNNs, since it is a network that works very well with images. This is evident in the scientific literature. Figure 7 shows the architecture used and the relevant hyper-parameters.

CONV 64	<table border="1"> <thead> <tr> <th>Hyper-parameters</th> <th>Value</th> </tr> </thead> <tbody> <tr> <td>Learning rate</td> <td>0.00005</td> </tr> <tr> <td>Epochs</td> <td>200</td> </tr> <tr> <td>Batch size</td> <td>16</td> </tr> <tr> <td>Trigger function</td> <td>ReLU</td> </tr> <tr> <td>Output function</td> <td>softmax</td> </tr> <tr> <td>Dropout</td> <td>Si</td> </tr> <tr> <td>Optimizer</td> <td>Adam</td> </tr> <tr> <td>Función loss</td> <td>Sparse categorical crossentropy</td> </tr> <tr> <td>Metrics</td> <td>accuracy</td> </tr> </tbody> </table>	Hyper-parameters	Value	Learning rate	0.00005	Epochs	200	Batch size	16	Trigger function	ReLU	Output function	softmax	Dropout	Si	Optimizer	Adam	Función loss	Sparse categorical crossentropy	Metrics	accuracy
Hyper-parameters		Value																			
Learning rate		0.00005																			
Epochs		200																			
Batch size		16																			
Trigger function		ReLU																			
Output function		softmax																			
Dropout		Si																			
Optimizer		Adam																			
Función loss		Sparse categorical crossentropy																			
Metrics		accuracy																			
MAX POOL																					
CONV 128																					
CONV 128																					
MAX POOL																					
CONV 256																					
CONV 256																					
MAX POOL																					
DENSE 256																					
DROPOUT 0.6																					
DENSE SOFTMAX																					

Figure 7. Optimized architecture and hyper-parameters.

The structure was chosen following a systematic procedure of trial and error. Different configurations were tried until the best results were found, a deeper network only resulted on over-fitting and shallow networks performed worse.

The hyperparameters were optimized following a similar approach. Different learning rates (0.05, 0.005, 0.0005, 0.00005, 0.000005) were compared. The one which the best performance was found to be 0.00005. This same principle was followed when setting the activation function: Relu was compared with Elu, Selu and Leaky Relu. The optimizer was chosen after comparing Adam with Nadam.

Other important feature of the system was the use of Data-Augmentation. An online data generation was used in the network training in other to improve its performance. The images went through limited rotations of less than 5 degrees and vertical or horizontal flips. The reason is that more intrusive modifications would not be real. Cells with big distortions would have a different IV curve. In each epoch new instances were generated choosing a new angle and flip.

Figure 8 shows the evolution of the accuracy and loss during the training and validation phases. In the accuracy graph, it can be seen how there is no difference between the train and validation sets, which implies that the network hardly experiences over fit. In the loss graph, an increase in over fit is observed from iteration 100, but at no point does it become considerable. The final network chosen will be that of iteration 195, which has a 90% in the validation set and a 0.5 in loss.

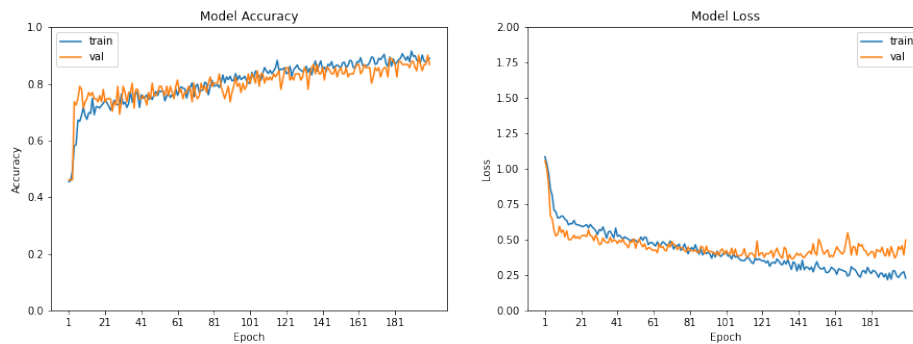
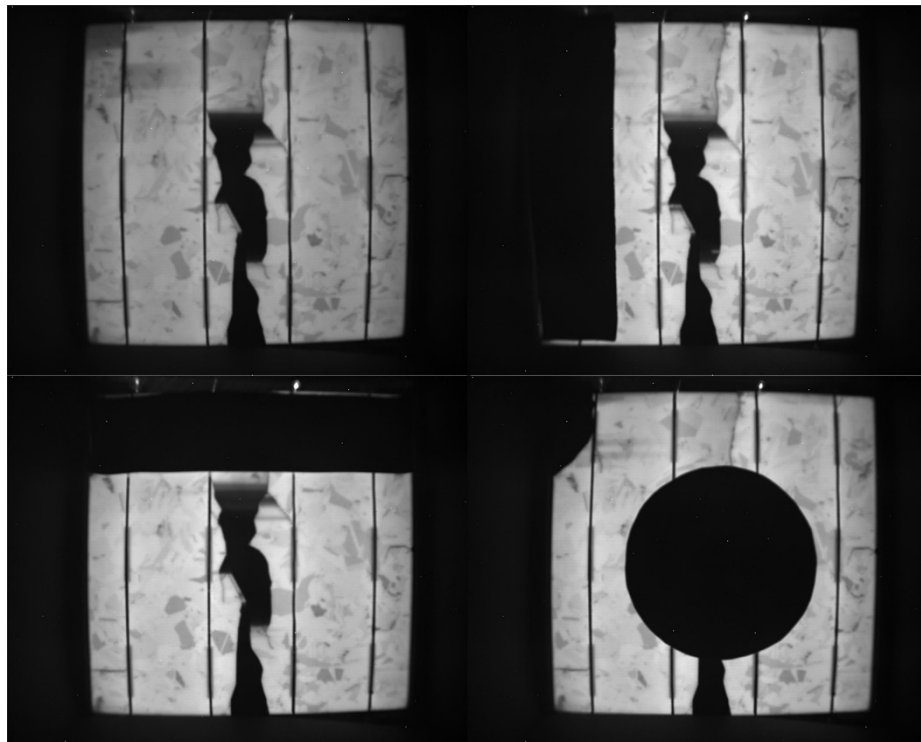


**Figure 8.** Evolution of accuracy and loss, for the training and validation phases.

### 3 Results and discussion

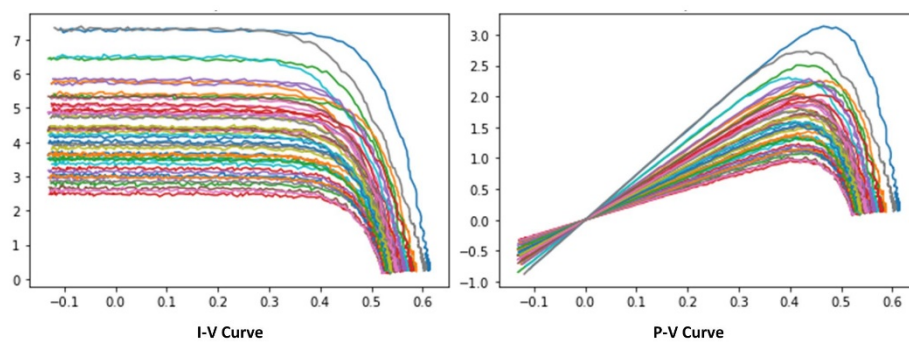
#### 3.1 EL imaging and I-V curves

Figure 9 shows some EL images measured for this work. The images in the figure show the same PV cell, but with a different shade. The figure at the top left shows a PV cell without a shadow, but with a failure defect in the middle of it. The rest EL images, show the same PV cell with different added artificial shadows.



**Figure 9.** EL images of a PV cell with different artificial shadows.

Figure 10 shows the measurements of the I-V curves of a specific PV cell. The different curves represent the I-V curve at different irradiances levels and/or with artificial shadows. The figure also shows the P-V curves of the PV cell.



**Figure 10.** I-V curves of a specific PV cell and P-V curves.

### 3.2 CNNs

With the available data, the CNNs has been trained and its results have been obtained, after the validation phase.

In Figure 11, it can be seen how the behavior in the non-training data set is similar to the validation one, reaching 87% precision, a very high behavior and very similar to that obtained in the validation during the training phase. It can be seen how the CNNs perfectly distinguishes classes 0 and 2, with only one instance in which an error occurs, which indicates that the model differentiates PV cells in good condition from PV cells in poor condition. For class 1, its behavior can be improved, since it has more difficulties to classify this class well, although it still gives good results. The inclusion of data augmentation improved the performance of the model.

Validation set					Final set				
<b>Confusion matrix</b>					<b>Confusion matrix</b>				
[[20 0 0] [ 1 24 4] [ 0 4 38]]					[[18 1 0] [ 1 26 1] [ 1 7 31]]				
<b>Classification report</b>					<b>Classification report</b>				
	precision	recall	f1-score	support		precision	recall	f1-score	support
0	0.95	1.00	0.98	20	0	0.90	0.95	0.92	19
1	0.86	0.83	0.84	29	1	0.76	0.93	0.84	28
2	0.90	0.90	0.90	42	2	0.97	0.79	0.87	39
accuracy			0.90	91	accuracy			0.87	86
macro avg	0.90	0.91	0.91	91	macro avg	0.88	0.89	0.88	86
weighted avg	0.90	0.90	0.90	91	weighted avg	0.89	0.87	0.87	86

Figure 11. Results of the CNNs.

#### 4 Conclusions and future work

The work has presented a classifier of defects in PV cells, based on AI and from EL images. For the perfect classification, it was necessary to use the I-V curve of each of the PV cells. For this, it has been necessary to make an instrument to measure the I-V curve at the cell level, which has served to label each of the PV cells. A CNNs has been used, and the results obtained have been satisfactory, and improvement is expected from a greater number of samples taken.

The researchers will expand the data set manually and using techniques to generate synthetic data as Generative Adversative Neural Networks (GANN), and will try another type of PV cell. In addition, the intention is to classify the defects of complete PV modules.

#### Acknowledgments

The authors thank the CYTED Thematic Network “INTELLIGENT CITIES FULLY INTEGRAL, EFFICIENT AND SUSTAINABLE (CITIES)” n° 518RT0558.

## References

1. REN21 Secretariat: Renewables 2020 Global Status Report. (2020).
2. Jordan, D.C., Silverman, T.J., Wohlgemuth, J.H., Kurtz, S.R., VanSant, K.T.: Photovoltaic failure and degradation modes. *Prog. Photovoltaics Res. Appl.* 25, 318–326 (2017). <https://doi.org/10.1002/pip.2866>.
3. Kendig, D., Alers, G.B., Shakouri, A.: Characterization of defects in photovoltaics using thermoreflectance and electroluminescence imaging. *Conf. Rec. IEEE Photovolt. Spec. Conf.* 1733–1736 (2010). <https://doi.org/10.1109/PVSC.2010.5616126>.
4. Fuyuki, T., Kitiyanan, A.: Photographic diagnosis of crystalline silicon solar cells utilizing electroluminescence. *Appl. Phys. A Mater. Sci. Process.* 96, 189–196 (2009). <https://doi.org/10.1007/s00339-008-4986-0>.
5. Gallardo-Saavedra, S., Hernández-Callejo, L., Alonso-García, M. del C., Santos, J.D., Morales-Aragón, J.I., Alonso-Gómez, V., Moretón-Fernández, Á., González-Rebollo, M.Á., Martínez-Sacristán, O.: Nondestructive characterization of solar PV cells defects by means of electroluminescence, infrared thermography, I-V curves and visual tests: experimental study and comparison. *Energy*. 205, 1–13 (2020). <https://doi.org/https://doi.org/10.1016/j.energy.2020.117930>.
6. Blakesley, J.C., Castro, F.A., Koutsourakis, G., Laudani, A., Lozito, G.M., Riganti Fulginei, F.: Towards non-destructive individual cell I-V characteristic curve extraction from photovoltaic module measurements. *Sol. Energy*. 202, 342–357 (2020). <https://doi.org/10.1016/j.solener.2020.03.082>.
7. Hernández-Callejo, L., Gallardo-Saavedra, S., Alonso-Gómez, V.: A review of photovoltaic systems: Design, operation and maintenance. *Sol. Energy*. 188, 426–440 (2019). <https://doi.org/10.1016/j.solener.2019.06.017>.
8. Gallardo-Saavedra, S., Hernández-Callejo, L., Duque-Perez, O.: Technological review of the instrumentation used in aerial thermographic inspection of photovoltaic plants. *Renew. Sustain. Energy Rev.* 93, 566–579 (2018). <https://doi.org/10.1016/j.rser.2018.05.027>.
9. Gallardo-Saavedra, S., Hernandez-Callejo, L., Duque-Perez, O.: Image Resolution Influence in Aerial Thermographic Inspections of Photovoltaic Plants. *IEEE Trans. Ind. Informatics*. 14, 5678–5686 (2018). <https://doi.org/10.1109/TII.2018.2865403>.
10. Gligor, A., Dumitru, C.D., Grif, H.S.: Artificial intelligence solution for managing a photovoltaic energy production unit. *Procedia Manuf.* 22, 626–633 (2018). <https://doi.org/10.1016/j.promfg.2018.03.091>.
11. Wang, H., Liu, Y., Zhou, B., Li, C., Cao, G., Voropai, N., Barakhtenko, E.: Taxonomy research of artificial intelligence for deterministic solar power forecasting. *Energy Convers. Manag.* 214, 112909 (2020). <https://doi.org/10.1016/j.enconman.2020.112909>.
12. Kayri, I., Gencoglu, M.T.: Predicting power production from a photovoltaic panel through artificial neural networks using atmospheric indicators. *Neural Comput. Appl.* 31, 3573–3586 (2019). <https://doi.org/10.1007/s00521-017-3271-6>.
13. Li, L.L., Wen, S.Y., Tseng, M.L., Chiu, A.S.F.: Photovoltaic array prediction on short-term output power method in Centralized power generation system. *Ann. Oper. Res.* 290, 243–263 (2020). <https://doi.org/10.1007/s10479-018-2879-y>.

14. Hussain, M., Dhimish, M., Titarenko, S., Mather, P.: Artificial neural network based photovoltaic fault detection algorithm integrating two bi-directional input parameters. *Renew. Energy*. 155, 1272–1292 (2020). <https://doi.org/10.1016/j.renene.2020.04.023>.
15. Cho, K.H., Jo, H.C., Kim, E. sang, Park, H.A., Park, J.H.: Failure Diagnosis Method of Photovoltaic Generator Using Support Vector Machine. *J. Electr. Eng. Technol.* 15, 1669–1680 (2020). <https://doi.org/10.1007/s42835-020-00430-9>.
16. Pérez-Romero, Á., Mateo-Romero, H.F., Gallardo-Saavedra, S., Alonso-Gómez, V., Alonso-García, M. del C., Hernández-Callejo, L.: Evaluation of Artificial Intelligence-Based Models for Classifying Defective Photovoltaic Cells. *Appl. Sci.* 11, 4226 (2021). <https://doi.org/10.3390/app11094226>.
17. Gao, W., Wai, R.J.: A Novel Fault Identification Method for Photovoltaic Array via Convolutional Neural Network and Residual Gated Recurrent Unit. *IEEE Access*. 8, 159493–159510 (2020). <https://doi.org/10.1109/ACCESS.2020.3020296>.
18. Fonseca Alves, R.H., Deus Júnior, G.A. de, Marra, E.G., Lemos, R.P.: Automatic fault classification in photovoltaic modules using Convolutional Neural Networks. *Renew. Energy*. 179, 502–516 (2021). <https://doi.org/10.1016/j.renene.2021.07.070>.

## Dependence on solar activity as a factor in the energy consumption of supermarkets

López-Meraz R. A. <sup>1</sup>[0000-0002-3236-3709], Hernández-Callejo L. <sup>2</sup>[0000-0002-8822-2948], Del Ángel-Ramos J. A. <sup>1</sup>, Jamed-Boza L. O. <sup>1</sup>[0000-0002-6378-758X], Marín-Hernández J. J. <sup>1</sup>, Arenas-Del Ángel J. L. <sup>1</sup> and Alonso-Gómez V. <sup>2</sup>[0000-0001-5107-4892]

<sup>1</sup> Universidad Veracruzana, Circuito Universitario Gonzalo Aguirre Beltrán s/n, 91000, Mexico

<sup>2</sup> Universidad de Valladolid, Campus universitario Duques de Soria s/n, 42004, Spain  
 raullopez03@uv.mx: R.L-M.; luis.hernandez.callejo@uva.es: L.H-C.; jdelangel@uv.mx: J.D-R.; lojb33@gmail.com: L.J-B.; jmarin@uv.mx: J.M-H.; jorarenas@uv.mx: J.A-D.; victor.alonso.gomez@uva.es: V.A-G.

**Abstract.** Possibly the biggest problem electric power consumers face is the need to reduce and understand this cost. In this sense, there are strategies such as installing more efficient equipment and controlling demand at various operating hours. However, the commercial sector, particularly the one referring to supermarkets, does not consider environmental factors or occupation to make projections of consumption or their influence on it. The present work proposes models based on monthly averages of four factors, namely: influence of solar radiation through sunspots, temperature, humidity, and store occupancy. The case study is seven self-service stores, with different environmental conditions, of a recognized chain in Mexico. The analysis period runs from September 2012 to December 2015. The results indicate that the four factors are essential in the behavior of electricity consumption, achieving models with correlation coefficients with good predictive quality.

**Keywords:** Electricity Consumption Behavior, Regressive Model, Sunspots.

### 1 Introduction

Knowing the solar activity will bring us closer to predicting with greater certainty its repercussions in different areas of society. Briefly, it can be said that the Sun has been studied in very long time series, finding that it has several cycles, the best known is the so-called undecenal. The most widely observed manifestation of the Sun is sunspots (*Ms*) and according to [1] making its historical monitoring a reliable approach to solar activity is possible.

On the other hand, perhaps the most well-known consequence of solar activity are geomagnetic storms that produce geomagnetically induced currents (GIC's) mainly affecting power transformers and hence the power grid [2]. However, there are several studies that associate *Ms*, which are an indirect measure of solar activity, with topics as different as earthquakes, particularly in Chile [3], the dependence of climate behavior

2

with variations in the Sun [4], the incidence of solar cycles in economic areas such as unemployment and recessions [5] and in commercial cycles [6], the relationship between social and solar activity, mainly in war events [7], even in the sector of health in [8, 9] the relationship between  $Ms$  and influenza pandemics has been studied.

This paper proposes the insertion of the factor  $Ms$ , together with temperature ( $T$ ), relative humidity ( $H$ ) and the occupation of the shops ( $O$ ), in the behavior and prediction of the electricity consumption of seven supermarkets in Mexico, providing an innovative line of research in this area. The interest lies in the prediction made by the Ministry of Energy (SENER) for the period 2020-2034 where it estimates that final consumption in the commercial, agricultural and services sectors will be 12.4% [10]; that is, our problem represents an important area of opportunity to improve this area. The objective is to provide reliable models that allow this commercial group to have a greater capacity to control these parameters. Statistical analyzes were developed with the statistical application software JMP [11]. The text is structured as follows: section two describes the characteristics of the case study, then the justification for the use of sunspots is presented, finding the relationship with the total solar irradiance, the third aspect refers to obtaining the proposed model and, finally, the participation of factors in consumption is considered; the next section checks the approach of the adjusted irradiance model, the validity and justification of the complete cubic model with four factors in each store is presented, in addition to its prediction profiles and its participation; finally, the most relevant conclusions are presented.

## 2 Materials and methods

### 2.1 Case of study

Of the population of shops located in the southeastern region of Mexico with which it was counted, three different climatic conditions were observed taking as reference the temperature, for the above was considered a sample of seven stores with, at least two per climate achieving variability in them. The proposed climates were determined by considering climate 1:  $T \leq 20^{\circ}C$ ; climate 2:  $20^{\circ}C < T \leq 25.7^{\circ}C$ ; and climate 3:  $T > 25.7^{\circ}C$ . Table 1 shows the cities in the corresponding climate. The cities in which they are located are Xalapa, Orizaba, Veracruz, Tuxtla Gutiérrez, Cancun, Chetumal and Mérida, respectively. Table 2 presents the main characteristics of these spaces. The reporting period runs from September 2012 to December 2015. The  $T$  and  $H$  data were taken from weather stations located in each of the cities and are the monthly averages; the  $O$  factor corresponds to the number of total tickets issued per box in each month.

**Table 1.** Classification of climates.

City	$T$ (°C)	$H$ (%)	Climate by temperature
Xalapa	18.66	80.38	Climate 1
Orizaba	19.66	75.92	
Veracruz	24.87	76.10	Climate 2
Tuxtla G.	25.66	67.81	
Cancún	25.97	80.47	Climate 3
Mérida	27.62	72.97	
Chetumal	27.85	74.09	

**Table 2.** Supermarkets analyzed

City	Supermarket key	Average consumption (kWh)	Occupation	Sale floor (m <sup>2</sup> )
Xalapa	Txal1	104,832.2	97,216.375	2,200
Veracruz	Tver1	231,954	181,966.75	6,738
Cancún	Tcan1	244,747.9	142,024.51	6,027
Orizaba	Tori1	194,148.3	154,054	5,522
Tuxtla G.	Ttux1	203,458	116,082.02	5,423
Chetumal	Tche1	235,157.2	81,151.51	7,527
Mérida	Tmer1	323,477.7	130,477.54	8,157

**2.2 Variations in total solar irradiance**

The solar constant contains variations in the distance of the Earth-Moon system with respect to the Sun, on average, it is an astronomical unit (AU) and is a reference in the theory of the black body. Furthermore, the emissivity property  $\epsilon = 1$  is supported by the same theory applied to the Sun. The radiation is obtained with the Stefan-Boltzmann relation (1) considering the temperature  $T_1$  in the Sun's photosphere. Where  $q$  is the emissive power,  $A$  is the area and  $\sigma$  is the Stefan-Boltzmann constant.

$$q' = \frac{q}{A} = \sigma\epsilon(T_1^4 - T_0^4) \tag{1}$$

To obtain the solar constant in (1) the temperature  $T_0$  is considered at the absolute thermodynamic zero and  $\epsilon = 1$ , in addition, the solar radius ( $R_{sol}$ ) is taken into account and the radius of the sphere of the mean Earth-Moon distance, (2) describes the above.

$$K = \sigma T_1^4 \left(\frac{R_{sol}}{AU}\right)^2 = 1361.645166 \frac{w}{m^2} \tag{2}$$

The value obtained coincides with that reported in [12], giving validity to our calculation. To estimate the values of the estimated total solar irradiation ( $ISTe$ ), the distance of the Earth-Moon system was obtained exactly in the middle of each month considering  $K = 1362 \frac{w}{m^2}$ ,  $T_1 = 5773.308^\circ K$  and  $\sigma = 5.670373 * 10^{-8} \frac{w}{m^2 * K^4}$ . The model

4

used to obtain the variations of the *IST* according to the orbital distance is presented in equation (3).

$$y = b + e(a - b)[1 + \sin(c[x - d])] + \xi \tag{3}$$

Where *a* is maximum *ISTe* (January), *b* is minimum *ISTe* (July), *c* is frequency in  $\frac{rad}{month}$ , *d* is shift in month, *e* is attenuation (dimensionless), *x* is the number of month, and  $\xi$  is the residual.

### 2.3 Sunspots

The number of sunspots has been correlated with the *IST* measured with the satellite network around the Earth, which has been useful to have a basis for indirect use of the energy behavior of the sun in its influence with the Earth's climate. The foregoing has given the possibility of forecasting its average monthly number to integrate said information as an influencing factor in energy consumption. In Fig. 1 the follow-up of the correlation between the *IST* and the number of monthly averages *Ms* is visualized [13].

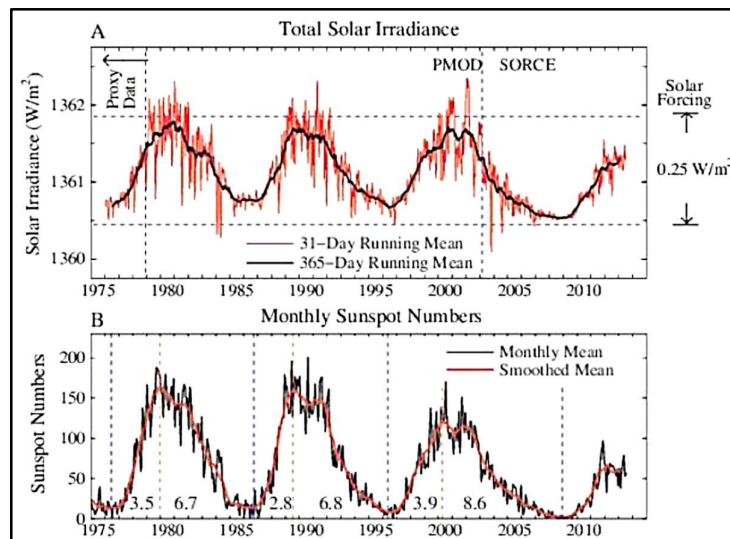


Fig. 1. *IST* Association and *Ms*.

### 2.4 Complete cubic model with four factors

The regression technique allows handling polynomials of any degree such that their effects are significant, this facilitates the study of curvature changes in fitted models. Regression uses least squares methods leaving the degree of the polynomial free. The theoretical support for this technique is based on the linear statistical model shown in equation 4.

5

$$y_i = \beta_0 + \beta_1 x_{i1} + \beta_2 x_{i2} + \dots + \beta_p x_{ip} + \varepsilon_i \tag{4}$$

The previous model is expressed in a matrix in equation 5:

$$\mathbf{y} = \mathbf{X}\mathbf{b} + \boldsymbol{\varepsilon} \tag{5}$$

The elements of the model (5) are the matrix and vectors that are represented by the set of equations (6).

$$\mathbf{X} = \begin{bmatrix} 1 & x_{11} & \dots & x_{1p} \\ 1 & x_{21} & \dots & x_{2p} \\ \vdots & \vdots & \ddots & \vdots \\ 1 & x_{n1} & \dots & x_{np} \end{bmatrix}, \quad \mathbf{y} = \begin{bmatrix} y_1 \\ y_2 \\ \vdots \\ y_n \end{bmatrix}, \quad \mathbf{b} = \begin{bmatrix} \beta_0 \\ \beta_1 \\ \vdots \\ \beta_p \end{bmatrix}, \quad \boldsymbol{\varepsilon} = \begin{bmatrix} \varepsilon_1 \\ \varepsilon_2 \\ \vdots \\ \varepsilon_n \end{bmatrix} \tag{6}$$

The matrix  $\mathbf{X}$  is of size  $n \times (p + 1)$  where  $n \geq p + 1$ , vector  $\mathbf{y}$  is  $n \times 1$ , vector  $\mathbf{b}$  is  $(p + 1) \times 1$  and vector  $\boldsymbol{\varepsilon}$  is  $n \times 1$ . Where  $n$  represents the total number of experimental points,  $p$  represents the number of parameters  $\beta_j$  of the regressor variables  $x_{i1}, x_{i2}, \dots, x_{ip}$ ,  $\beta_0$  represents an additive constant that, since there are no effects caused by the regressor variables, usually represents the mean of the response variable  $\mathbf{y}$ . The estimator of vector  $\mathbf{b}$  in expression (5) where  $\mathbf{X}'\mathbf{X}$  is the variance-covariance matrix is defined, according to [14] by equation (7).

$$\hat{\mathbf{b}} = (\mathbf{X}'\mathbf{X})^{-1}\mathbf{X}'\mathbf{y} \tag{7}$$

The answer of our regressive analysis is the monthly electricity consumption in kWh ( $Y_1$ ). The model can be simplified in (8).

$$Y_1 = \beta_0 + \beta_1 x_1 + \dots + \beta_{111} x_1^3 + \dots + \beta_{444} x_4^3 + \beta_{12} x_1 x_2 + \dots + \beta_{34} x_3 x_4 + \dots + \beta_{112} x_1^2 x_2 + \dots + \beta_{344} x_3 x_4^2 + \varepsilon_i \tag{8}$$

The model handles four factors with 34 effects combined to create a cubic polynomial model with its full double and triple interactions. The factors are:  $x_1 \rightarrow Ms$ ;  $x_2 \rightarrow T$ ;  $x_3 \rightarrow H$ ;  $x_4 \rightarrow O$ ; double interactions are:  $x_1 x_2$  until  $x_3 x_4$ ; triple interactions include the linear and quadratic effects of each factor:  $x_1^2 x_2, x_1 x_2^2$  until  $x_3 x_4^2$ . Creating 12 individual effects of each factor up to the cubic, 6 double interaction effects, and 16 triple interaction effects. Each effect is equally weighted.

### 2.5 Contribution of factors involved

With the intention of knowing the participation of the factors in the electricity consumption of the supermarkets was obtained its presence, in the form of percentage, in the seven adjusted models. In addition, this same characteristic was quantified by reference to the type of climate in which these shops are located. On the other hand, the symbolic analysis of the behavior (growth and/or reduction) of the factors in the estimated conditions of the average and maximum response is made. From the average condition of each store their highs were obtained. It was thus decided to consider that the most frequent behavior is found in the average.

6

### 3 Results

#### 3.1 Adjusted model for total monthly irradiation

The theoretical values of the parameters were located under the assumption of a circular orbit to be modified to an elliptical orbit; the theoretical values are:

$$c_{teo} = \frac{2\pi}{12} = \frac{\pi}{6}; d_{teo} = 0; e_{teo} = 0.5$$

Where  $c_{teo}$  is the theoretical frequency,  $d_{teo}$  is the theoretical shift,  $e_{teo}$  is theoretical attenuation. The initial values for minimization are in Table 3, and Table 4 indicates the variability of the estimate with the theoretical parameters. The *ISTe* column was obtained from the solar constant by measuring exactly (half a month and half hours) the Earth-Sun orbital distance, the column *y* is the result of the adjusted model taking the theoretical values above. The difference in the comparison of both curves is observed, as seen in Fig. 2.

**Table 3.** Theoretical parameters

Parameter	Value
<i>a</i>	1407.1332
<i>b</i>	1318.2192
<i>c</i>	0.5235988
<i>d</i>	0
<i>e</i>	0.5
<i>SS<sub>dif</sub></i>	16772.76
<i>StdDev<sub>e</sub></i>	33.596805
<i>StdError<sub>e</sub></i>	9.6985622
<i>StdDev<sub>y</sub></i>	32.833685
<i>StdError<sub>y</sub></i>	9.4782683

**Table 3.** General monthly behavior of radiation and PV power.

Month	<i>ISTe</i> ( $\frac{W}{m^2}$ )	<i>y</i>	<i>Difference</i>	<i>Square</i>
1	1407.13321	1384.9047	22.2285095	494.106634
2	1395.56813	1401.1771	-5.6089733	31.4605815
3	1375.87057	1407.13321	-31.2626444	977.352935
4	1351.70355	1401.1771	-49.4735537	2447.63252
5	1331.56761	1384.9047	-53.3370894	2844.84511
6	1319.2602	1362.67619	-43.4159909	1884.94827
7	1318.21918	1340.44769	-22.2285095	494.106634
8	1328.36941	1324.17529	4.19412768	17.590707
9	1347.17767	1318.21918	28.9584929	838.594313
10	1370.80905	1324.17529	46.6337613	2174.7077
11	1392.29672	1340.44769	51.8490391	2688.32286
12	1406.02469	1362.67619	43.3484908	1879.09166
		<i>SS<sub>dif</sub></i>		16772.7599

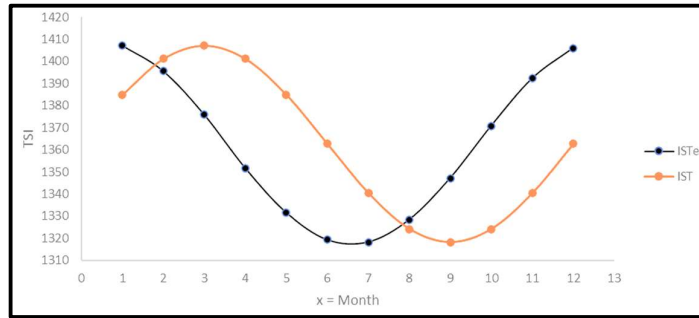


**Fig. 2.** Behavior of the model with the theoretical parameters before minimization.

With the above values it is minimized using the Solver Excel plugin by applying the Generalized Reduced Gradient method. The results obtained are presented in Table 5 and in Table 6, for its part in Fig. 3 we can see the approach obtained. By changing the parameters  $c$ ,  $d$  and  $e$  corresponding to the elliptical orbit, it is noticeable the approach in the two curves ( $ISTe$  and  $IST$ ), this can be seen in the sum of squares of the difference for each month which is initially  $SS_{dif}$  of 16772.76 and was reduced to 5.23 given by the correction for the elliptical orbit.

**Table 5.** Minimized parameters for fitted model

Parameter	Value
$a$	1407.1332
$b$	1318.2192
$c$	0.5040001
$d$	-2.749782
$e$	0.5160452
$SS_{dif}$	5.2274033
$StdDev_e$	33.596805
$StdError_e$	9.6985622
$StdDev_y$	33.149505
$StdError_y$	9.5694378

**Table 6.** Matching values between *ISTe* and *y* (*IST*).

Month	$ISTe \left( \frac{W}{m^2} \right)$	<i>y</i>	<i>Difference</i>	<i>Square</i>
1	1407.13321	1407.6703	-0.53708656	0.28846197
2	1395.56813	1395.3017	0.26642637	0.07098301
3	1375.87057	1375.17444	0.69613294	0.48460107
4	1351.70355	1352.29384	-0.59028842	0.34844042
5	1331.56761	1332.34995	-0.78233796	0.61205268
6	1319.2602	1320.30252	-1.04231128	1.0864128
7	1318.21918	1319.14753	-0.9283579	0.86184839
8	1328.36941	1329.17223	-0.80281967	0.64451942
9	1347.17767	1347.88363	-0.70596196	0.49838228
10	1370.80905	1370.62849	0.18055719	0.0326009
11	1392.29672	1391.75052	0.54620002	0.29833446
12	1406.02469	1405.99701	0.02767442	0.00076587
<i>SS<sub>dif</sub></i>				5.22740329

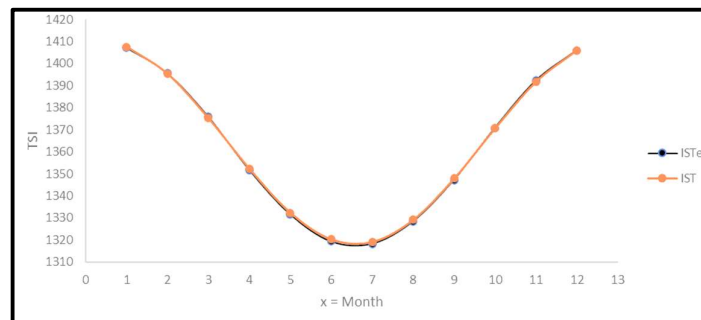


**Fig. 3.** Behavior of the fitted model after minimization.

It is evident that the adjusted model does comply with a total approach to the *ISTe*, the results being significant.

### 3.2 Fitted Models

By applying the proposed model (8) to the particular characteristics of each store, high determination factors ( $R^2$ ) and adjusted determination factors ( $R_{adj}^2$ ) are achieved. Table 7 shows them. These coefficients of determination show good predictive correlations. In this sense, all store models are above 0.85 and most exceed the value of 0.90. Table 8 presents the values of the estimated parameters of the adjusted models where each of them fulfills a 5% significance. In addition, the analysis of variance (ANOVA) of the seven stores was significant, representing the existence of regression in the models obtained.

**Table 7.** Determination coefficients

Supermarket	$R^2$	$R^2_{adj}$
Txal1	0.968002	0.948003
Tori1	0.99001	0.97565
Tver1	0.954375	0.915269
Ttux1	0.973734	0.948781
Tcan1	0.94107	0.908331
Tchel1	0.88628	0.866211
Tmer1	0.988514	0.98582

**Table 8.** Contribution of studied effects

Effect	Climate 1		Climate 2		Climate 3		
	Txal1	Tori1	Tver1	Ttux1	Tcan1	Tchel1	Tmer1
Intercept	4294680.46	-6655993.2	5111110.86	22833421.9	-41916897	681460.753	11592389.1
$Ms$	0	0	261097.237	-195930.9	0	0	-202534.02
$Ms^2$	0	169.771237	0	221.04121	0	0	702.277341
$Ms^3$	-0.103105	-0.2471456	0.61870018	0	0	0	-0.3131223
$T$	-246851.44	1142134	0	-2755265	1955446.71	0	-1534729.8
$T^2$	0	-46592.57	-69489.749	93511.7409	0	-2520.3026	27887.1657
$T^3$	-130.44831	0	0	-740.75088	-145.6544	0	0
$H$	-69621.134	317412.29	0	0	775044.952	-14618.595	-783404.3
$H^2$	0	0	-795.58014	0	-4333.2742	0	3606.00788
$H^3$	-0.8775686	13.6263305	0	-0.7206512	0	0	0
$O$	-33.509226	-192.62316	-207.87705	136.979265	112.328926	0	634.771907
$O^2$	0	0.00214053	0	-0.0010901	0	0	-0.0066048
$O^3$	0	-4.219E-09	0	0	7.3361E-10	0	1.7248E-08
$MsT$	1072.18726	-4503.0684	-10089.814	9749.06927	0	0	0
$MsH$	-245.49191	0	-3285.3597	1197.80547	0	0	0
$MsO$	0	0.4320961	0	0.18954125	-0.033171	0	2.14791528
$TH$	4943.91555	0	15935.0797	0	-34638.793	0	18597.0348
$TO$	0	0	16.8670891	0	-8.4938353	0	0
$HO$	0.88329379	-3.8917918	0	-0.5314927	0	0.35753206	4.06639766
$MsTH$	0	21.5747348	120.097326	-36.076967	0.72286731	0	0
$MsTO$	0	0.01768508	0	0	0	0	-0.0022426
$MsHO$	0	-0.0085725	0	-0.0023728	0	0	0
$THO$	-0.0492528	0.08252312	-0.2074079	0.02426226	0.04920956	-0.0211677	0.01805092
$Ms^2T$	0	0	6.77103979	-8.3786839	0	0	0
$T^2Ms$	-28.775303	0	0	-116.63147	0	0	0
$Ms^2H$	0.35830524	0	0	0	0	0	-1.9004692
$H^2Ms$	1.11884962	5.65054973	0	0	0	0	2.11962266
$Ms^2O$	0	-0.0007418	-0.0019962	0	0	0	-0.0036944
$O^2Ms$	0	0	9.5543E-07	0	1.7148E-07	0	-5.123E-06
$T^2H$	0	0	911.291144	0	0	44.7533733	-369.00775
$H^2T$	0	-96.671599	-216.00178	0	174.137235	0	0
$T^2O$	0.1035894	0.30170841	0	-0.2352579	0.08816598	0.02232877	0
$O^2T$	0	-6.416E-05	-3.236E-06	4.4305E-05	0	0	0
$H^2O$	0	-0.0108144	0.03394939	0	0	0	-0.0304498
$O^2H$	0	1.4322E-05	0	0	-4.361E-06	0	0

10

As can be observed, in no case are the 34 effects significant and the only one that is present in all is the triple *THO* interaction. On the other hand, the crosses with the lowest appearance are *TO, MsTO, MsHO, Ms<sup>2</sup>T, T<sup>2</sup>Ms, Ms<sup>2</sup>H* and *O<sup>2</sup>H* with 28.571%.

### 3.3 Prediction profiles

The models provide estimated average values of consumption with their respective uncertainty. When comparing the averages of the measured consumptions and those granted by the model, it is observed that they are very close. Figs. 4-6 show the average behavior of the four factors of the analyzed stores located by climate.

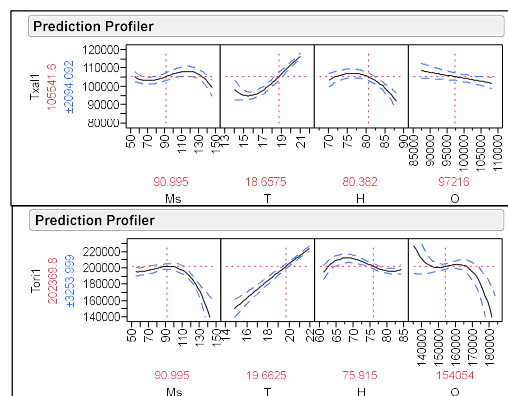


Fig. 4. Behavior of the factors in the estimated average in the climate 1.

The biggest difference in consumption between these stores is the occupancy factor because Tor11 has more than double the sales floor area. It is observable that the proposed model allows the studied factors to change curvature. It is also noticeable that the uncertainty (blue vertical data) in the estimated consumption has close intervals between the two supermarkets.

In climate 2 stores the main difference is present in relative humidity, but consumption in both is close. On the other hand, they are the stores where the number of significant effects is almost the same (18 and 19) and their models coincide in 9 effects and in 5 of these the *Ms* factor is present.

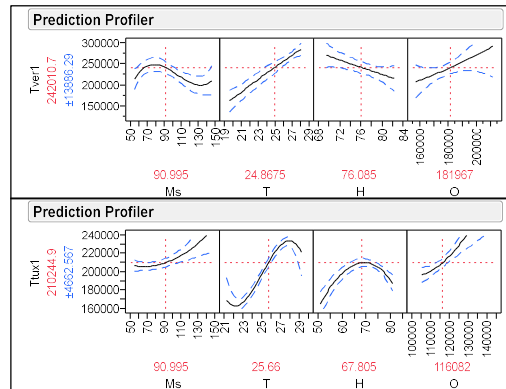


Fig. 5. Behavior of the factors in the estimated average in the climate 2.

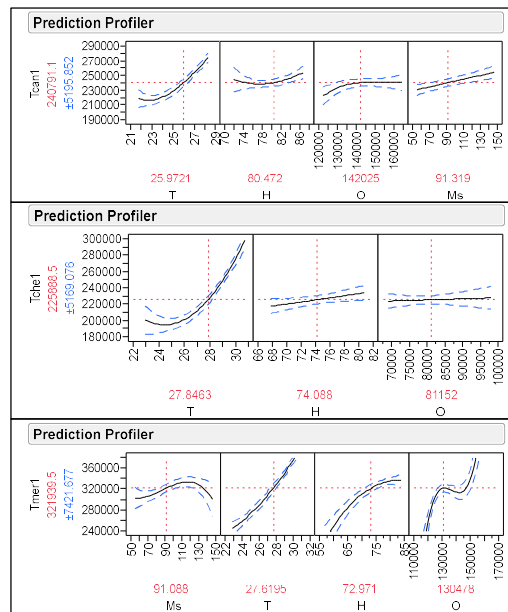


Fig. 6. Behavior of the factors in the estimated average in the climate 6.

Tmer1 is the store analyzed with the greatest number of m<sup>2</sup> and that leads to that on average is the most consumed. It can be observed that the behavior of the occupancy factor is very similar in the Tcan1 and Tche1 stores, tending to a stability (horizontal), on the other hand Tmer1 presents a tendency of increase. Another characteristic of climate 3 stores is the large difference in the number of significant effects (15, 6, 26). It is also noticeable the difference in the behavior of Ms, even in Tche1 this factor was not significant or any of its interactions. The average value of Ms is different in climate

12

3 by having a greater number of observations, this is the reason why three stores were studied instead of two.

### 3.4 Presence of effects

With the intention of observing the influence of each factor in the total sample, Table 9 is presented.

**Table 9.** Factor participation in stores

Factor	Porcentaje
<i>Ms</i>	19.16
<i>T</i>	28.07
<i>H</i>	26.95
<i>O</i>	25.82

It can be seen that the dominant factor in the set is T, however its difference with respect to the others does not exceed 9%. The contribution of the factors in the three climates was also obtained, as observed in Table 10.

The greatest differences between the factors are present in climate 3, this was observed in the prediction profiles; However, none exceeds an influence greater than one third, that is, the factors studied are important in the models that describe the consumption of the study case, distributing their influence. However, the foregoing only indicates the presence of significant factors, not their magnitude. The trends of the factors are also obtained in two consumption conditions, the average and the maximum, taking the average condition as a reference. Tables 11 and 12 detail the above. Where *M* means maximum, *I* is an inflection point, ↑ means that the factor increases and ↓ indicates that the factor decreases.

**Table 10.** Participation of factors by climate

Factor	Percentage	Climate
<i>Ms</i>	22.94	Climate 1
<i>T</i>	24.87	
<i>H</i>	28.07	
<i>O</i>	24.12	
<i>Ms</i>	25.72	Climate 2
<i>T</i>	30.30	
<i>H</i>	21.29	
<i>O</i>	22.69	
<i>Ms</i>	12.12	Climate 3
<i>T</i>	28.65	
<i>H</i>	30.12	
<i>O</i>	29.11	

**Table 11.** Behavior of the factors in the average condition of consumption.

Supermarket	Factors				
	$Ms$	$T$	$H$	$O$	$Y_1$
Txal1	↑	↑	↓	↓	↑
Tori1	$M$	↑	↓	$I$	↑
Tver1	↓	↑	↓	↑	↑
Ttux1	↑	↑	$M$	↑	↑
Tcan1	↑	↑	↑	↑	↑
Tchel	—	↑	↑	↑	↑
Tmer1	↑	↑	↑	$I$	↑

**Table 12.** Behavior of the factors in the condition of maximum consumption.

Supermarket	Factors				
	$Ms$	$T$	$H$	$O$	$Y_1$
Txal1	↓	↑	$M$	↓	↑
Tori1	↓	↑	$M$	↓	↑
Tver1	↑	↑	↑	↓	↑
Ttux1	↑	$M$	↓	↑	↑
Tcan1	↑	↑	↑	↑	↑
Tchel	—	↑	↑	↓	↑
Tmer1	$M$	↑	$M$	↑	↑

Considering fixed the characteristic of the increase in consumption, the behavior of the stores is different in the average condition, however, the temperature factor invariably increases. The reason that each store has a different general behavior comes from its own individual operating conditions, since each store serves a different type of market and consequently maintains in its stock (warehouse) varieties of products that require different amounts of energy to preserve them.

In climate 1 under the condition of maximum consumption, it can be observed that Txal1 and Tori1 have the same behavior, since their environmental conditions ( $T$  and  $H$ ) are very close. In conditions of maximum consumption, climate 1 differs from 2 and 3 in the behavior of  $Ms$  since in the first one, when these decrease, consumption increases, while in the remaining ones, when  $Ms$  increases, consumption increases. Factor  $O$  generates different behaviors characteristic of each store, however, it is observed that in climate 2 and 3 clearly an increase in it increases consumption, in contrast to climate 1, which increases consumption when decreasing. Regarding  $H$  in climate 1, when decreasing consumption increases, unlike climate 3 where increasing consumption increases in both conditions (average and maximum).

#### 4 Conclusions

The energy consumption of supermarket stores contains levels of magnitude of 6 digits measured in kWh that allows to visualize differences attributable to solar behavior and

14

it is verified that  $Ms$  is a reliable measure of the  $IST$ . The research grants a tool that can be used for the approximate prediction of the consumption of each store. Of the four consumption-related factors,  $T$  and  $H$  are measurable in situ and have some degree of modification within each store, the  $Ms$  factor is not modifiable, but there are reliable predictions that must be taken into account. In addition, it is important to consider that each store by its position in the city, by its geographical location, and by the type of customers it serves, produces differences in consumption. As a future work, the sample will be expanded to verify what is described in this work.

## 5 Acknowledgments

We want to thank Chedraui group for providing information for the development of this work.

## References

1. Usoskin, I.: A History of Solar Activity over Millennia. *Living Reviews in Solar Physics*, 10(1) (2013).
2. González, A., González, J.: Clima espacial y su efecto en la red eléctrica nacional. Reunión internacional de verano, RVP-AI (2017).
3. Mabel, V. y Larocca, P.: Estadística de manchas solares y terremotos en Chile. *Geoacta* 39 (2), 44-53 (2014).
4. Useros, J.: El cambio climático: sus causas y efectos medioambientales. *Anales de la Real Academia de medicina y cirugía de Valladolid*, 50, 71-98 (2012).
5. Gorbanev, M.: Can solar activity influence the occurrence of economic recessions? MPRA, No. 65502 (2015).
6. Luege, M.; Sistematización de índices de precios y ciclos comerciales: contribución de William Stanley Jevons. *Revista Digital Universitaria del Colegio Militar de la Nación*, No. 1 (2003).
7. Rodkin, M. and Kharin, E.: On the statical relationship between solar activity and spontaneous social processes. *Izvestiya, Atmospheric and Oceanic Physics*, 50 (7), 669-677 (2014).
8. Towers, S. and Levin, S.: Sunspot activity and influenza pandemics: a statical assessment of the purported association. Cambridge University Press, *Epidemiol. Infect.* 145, 2640-2655 (2017).
9. Karim, L. and Abbas, M.: The relation between influenza pandemics and solar activity. *Iraqi Journal of Science*, 55 (2A), 556-560 (2014).
10. Centro Nacional de Control de Energía (CENACE): Programa de ampliación y modernización de la red nacional de transmisión y redes generales de distribución del mercado eléctrico mayorista. (2020).
11. JMP 8.0.2 SAS Institute Inc. © 2009.
12. Kopp, G. and Lean, J.: A new, lower value of total solar irradiance: evidence and climate significance. *Geophysical research letters*, 38 (2011).
13. Hansen, J., Kharecha, P. and Sato, M.: Assessing “Dangerous climate change”: Required reduction of carbon emissions to protect young people , future generations and nature. *Plos one*, 8 (12) (2013).

15

14. Montgomery, D. : Diseño y análisis de experimentos, 2nd ed. México: Limusa Wiley, pp. 393-395 (2004).

# The current and future role of hydrogen in the EU Energy Transition

M. Pons, V. Canals, D. M. Bär, E. Isern, M. Roca, J. L. Rosselló and V. Martínez

Department of Industrial Engineering and Construction  
University of the Balearic Islands, Palma, Ctra. Valldemossa km 7.5,  
Campus UIB, Balearic Islands E-07122, Spain  
marta.pons@uib.es, v.canals@uib.es

**Abstract.** Hydrogen is an essential element in the European Union (EU) Energy Transition, i.e. the transition to a carbon-free economy, and can account for 24% of EU final energy demand by 2050. Since Hydrogen can address the several EU energy transition challenges ahead. Given the progressive electrification of the economy and the large-scale integration of intermittent renewable energy sources require large-scale energy storage, enabling seasonal storage and the efficient transport of clean energy across regions at low cost. In turn, the decarbonization of key segments such as the gas grid, transport, industrial processes requires the use of Hydrogen in large quantities. This work analyzes the different types of Hydrogen according to their origin and the technologies for the exploitation of Green Hydrogen. Finally, the main Green Hydrogen projects to deploy in the EU in the next years are analyzed.

**Keywords:** Hydrogen production, Green Hydrogen, Energy Transition, Decarbonization.

## 1 Introduction

Manmade global warming is the main source of Greenhouse Gases (GHG) emissions and the main cause of Climate Change. Fossil fuel extraction, transport, conversion, and particularly their combustion, have several negative impacts on the environment and directly influence the global economy and society [1, 2]. The energy sector was responsible for 73.2% of the global GHG emissions in 2016 [3] and nowadays accounts for 75% of EU emissions.

The climate crisis has become an undeniable global fact, as highlighted by the increase in the frequency of heatwaves and forest fire events [4] and the melting of polar and glaciers. The most ambitious climate change mitigation target was set under the 2015 Paris Agreement [5], where the United Nations agreed the objectives of holding an increase in the global average temperature to well below 2°C above pre-industrial levels. Since then, governments around the world have aligned their strategies for the future with these sustainability objectives.

In December 2019, the European Union announced the ‘European Green Deal’ to be at the forefront of global action against climate change and achieve EU climate neutrality by 2050 [6]. This roadmap has three main targets: a 55% reduction in GHG emissions compared to pre-industrial levels, an increase in the share of renewable energy to produce 40% of European energy from renewable sources, and a 36% improvement in energy efficiency in final energy consumption by 2030 [7]. This European strategy is focused on four foundations: carbon pricing [8], sustainable investment (e.g., the long-term budget for 2021-2027 with more than €800 billion for the Next Generation EU [9]), industrial policy, and a fair transition supported with the Just Transition Mechanism [10].

Power supply systems, buildings energy consumption, and transportation are the major sources of greenhouse gasses emissions. Thereby, the energy transition has become a critical global need to succeed in the transformation of the energy market into a cleaner, more affordable, and reliable sector. Despite the need for this socioeconomic reshaping, the energy transition cannot be implemented abruptly as there are still some challenges to be solved.

The world energy consumption levels increased by 49% in the developed countries between 1984 and 2004 [11] and it has been increasing proportionally according to industrial progress and population growth [12]. Currently, most of the demand is covered by fossil fuel resources [1]. Unlike renewable energy resources, fossil fuels have advantageous physical-chemical properties such as high-power densities, are storable and inert at standard ambient conditions, and are independent of the weather conditions such as wind speed or solar irradiance [13]. These conditions have positioned fossil fuels (coal, natural gas, petroleum, etc.) as one of the most cost-competitive, reliable, and abundant energy sources.

Moreover, the replacement of fossil fuel power generation with renewable energy sources, such as wind or solar, will require the introduction of electrical energy storage systems in the grid to avoid variability and intermittency in generation [14]. Recently, many electrical energy storage technologies have appeared in order to solve the grid balancing problem related to the high percentages of renewable energy deployment [15].

This work introduces the capabilities of Hydrogen as an energy carrier to later focus on the main Green Hydrogen technologies and the main devices involved from generation to consumption. Finally, the future trends of Green Hydrogen in the EU are analyzed through the projects announced for the period 2000-2030.

The paper is organized as follows: Section 2 briefly introduces the characteristics of Hydrogen as an energy carrier. Section 3 presents Green Hydrogen energy system configurations. Section 4 analyzes and discusses the UE Green Hydrogen future trends in the period 2000-2030. Finally, the conclusions are presented in section 5.

## 2 Characteristics of Hydrogen as an energy carrier

Hydrogen is the first and lightest chemical element and the most abundant element in the Universe. On Earth Hydrogen only can be found in molecular forms, basically integrated in form of water and organic compounds, but not as a pure element. Hydrogen is not a primary energy source; it is an energy vector [16] because it can be produced from other sources [17].

In the market exists several processes for Hydrogen production, but today's Hydrogen demand is mainly covered by processes based on fossil fuels, due to it is low cost, such as steam methane reforming (SMR), autothermal reforming (ATR), and coal gasification.

According to International Energy Agency, those processes generate around 830 million tons of CO<sub>2</sub> emissions annually. The Hydrogen Council named these pathways 'Gray Hydrogen' [18]. Additionally, the classification includes two new production processes that are considered promising in the energy transition context: the 'Blue Hydrogen' and 'Green Hydrogen'. 'Blue Hydrogen' is produced by combining SMR and Carbon Capture and Storage (CCS) technologies. With the addition of this final phase of steam carbon sequestration, the referring method is carbon neutral [19] but not strictly renewable. Instead, 'Green Hydrogen' is produced through the electrolysis of water powered by renewable energy, which generally means wind or solar power. The different pathways characteristics to produce Hydrogen are summarized in **Table 1**.

**Table 1.** Characteristics of Hydrogen production pathways.

Process	Color code	Primary Energy Source	GWP <sup>1</sup> [Kg CO <sub>2</sub> eq. / Kg H <sub>2</sub> ] [20, 21]	Cost in 2019 [USD/Kg H <sub>2</sub> ] [22]	Efficiency [23–25]
Water electrolysis with RES	Green	Water, Wind & PV	0,97 – 2,4	3,2 – 7,7	50 – 70%
Electrolysis + Nuclear <sup>2</sup>	Blue	Water + Cu-Cl cycle	2,1 – 12	2,17 – 7,00	45%
Autothermal Methane Reforming (ATR) CCS	Blue	Biomass / biomethane	4,9	1,2 – 2,1	60 – 75%
Steam methane reforming (SMR)	Gray	Natural Gas	12	0,7 – 1,6	70 – 85%
Gasification of coal (GC)	Gray	Coal	11,3	1,9 – 2,5	34 – 41%

<sup>1</sup> Global Warming Potential (GWP) is an index of global warming impacts of different gases. It represents the quantity of energy absorbed by any greenhouse gas in the atmosphere.

<sup>2</sup> The Hydrogen Council does not include the nuclear thermochemical water-splitting methodology in its classification. In the literature, such as in [37], some authors define this methodology as 'yellow Hydrogen'. In this work, we had classified as 'Blue Hydrogen' because can be low-carbon pathway to produce Hydrogen.

Therefore, Green Hydrogen is the most promising Hydrogen production pathway in terms of sustainability and overall efficiency. In turn, this production method is the most expensive of all and should evolve to become an economically competitive solution [26].

On the other hand, Hydrogen gas has the highest specific energy on a mass compared to other conventional fuels. Approximately, the energy density of Hydrogen is three times that of fuel oil [27]. Fig 1. presents the higher heating values and the associated specific CO<sub>2</sub> combustion emissions of most common fuel types compared to Hydrogen (which composition is carbon-free). Pure Hydrogen combustion (described in Equation 1) is a highly exothermic reaction that produces pure water as a by-product of the exhaust gases. This is the main advantage of Hydrogen compared to other conventional fuels since it does not produce CO<sub>2</sub> and has a high associated energy per unit mass.

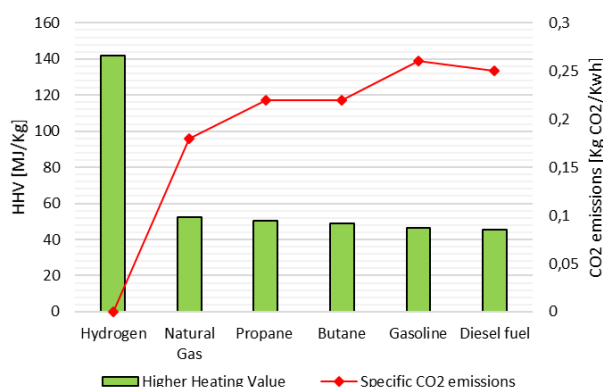


**Fig. 1.** Specific energy on the mass basis: HHV [MJ/Kg] and specific CO<sub>2</sub> emissions of common fossil fuels and Hydrogen. Source: own elaboration based on data from [28].

Reversely, Hydrogen gas has the lowest volumetric energy density. Therefore, Hydrogen needs three times more volume than gasoline, natural gas, and diesel fuel and two times more than propane and butane, to store the same energy [28]. The gravimetric density of Hydrogen can be considered an important disadvantage or technical challenge in some applications. For example, in the literature, many research works pointed out that the volume storage required to provide a common driving range in onboard vehicles may lead Hydrogen to be the fuel just in heavy-duty vehicles (trucks, ships, trains, etc.) [17, 29].

Furthermore, according to the 'Statistical Review of World Energy 2020' [30], proven fossil fuel reserves will be depleted in a maximum of 50,7 years for oil, 52,8 years for natural gas, and 114 years for coal. On the other hand, Hydrogen can be a renewable fuel if it is produced through water electrolysis based on renewable energy

sources [31], making it possible for an early transformation to a carbon-neutral economy.

This transformation requires the replacement of energy generation with fossil fuels by renewable energy sources, which in turn will require the introduction of energy storage systems to avoid variability and intermittency in generation [14]. In this framework, energy storage [32, 33] can be carried out by various technologies, such as batteries, flywheels, and supercapacitors, but all of them have the disadvantage of a long storage time and a short discharge time. Recently, a work [34] suggested that the candidate technologies for adjusting the multiday periods of power supply intermittency of RES, are pumped hydro storage (PHS) and compressed air energy storage (CAES). In turn, other work has analyzed various storage technologies, including Hydrogen, from an economic point of view [35] evaluating cost, storage duration, and efficiency. In this work, it is concluded that in an electrical network with high penetration of RES, the Hydrogen-based storage strategy presents relevant advantages. Furthermore, the authors estimated in a RES scenario for the period 2050-2070, that the only cost-effective solution for long-term electricity storage was Hydrogen due to its lower cost per energy capacity. Thus, Hydrogen has the potential to become a versatile energy storage technology that can mediate between energy supply and demand.

### 3 Green Hydrogen energy system configurations

In this Section, the elements of the Green Hydrogen Pathway components and the main configurations will be discussed, Fig. 2. The Green Hydrogen production would be performed through a water electrolyzer powered by dedicated renewable energy sources (normally wind or solar energy). The H<sub>2</sub> flow rate is then distributed for the following main purposes: Seasonal Energy Storage (SES), H<sub>2</sub> industry consumption, blending H<sub>2</sub> into natural gas pipelines, and its conversion to electricity to inject into the power grid.

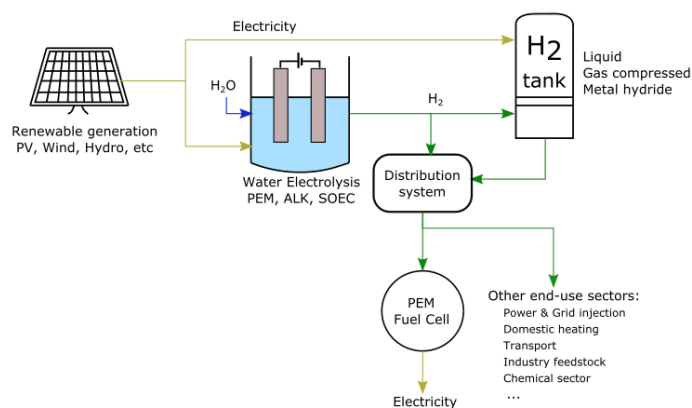


Fig. 2. Elements of the Green Hydrogen Pathway.

### 3.1 Water Electrolysis for Hydrogen production

The electrolysis of water consists of the decomposition of water molecules into Hydrogen and oxygen gases through a continuous electrical current [36]. The chemical reaction associated with electrolysis is described by:



Among the different existent methods for water electrolysis, nowadays only alkaline and proton exchange membrane (PEM) electrolysis are considered mature technologies, whereas the solid oxide electrolysis cell (SOEC) is still at the laboratory scale [37]. This can be seen in Fig. 3, the evolution of Hydrogen generation projects by electrolysis is represented, related to the different types of technologies.

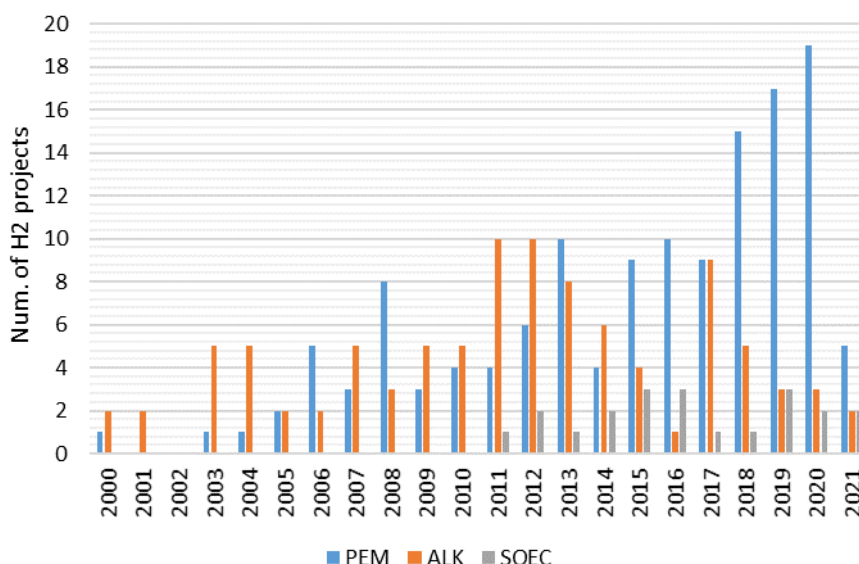


Fig. 3. Evolution of H<sub>2</sub> electrolyzers projects. Source: own elaboration based on data from [38].

Even so, SOEC can have an important role in the energy transition because, unlike PEM and Alkaline, it allows to operate in reverse mode, converting Hydrogen to electricity which could perform balancing services to the grid efficiently and more cheaply.

The basic operation principle is the same for all methodologies, the differences between them rely on constructive properties such as the material of the electrolyte or inner connection of cathode and anode. Their main technical and economic characteristics are summarized in Table 2.

### 3.2 Hydrogen storage technologies

The gravimetric density of Hydrogen represents a technical challenge for its storage. Fortunately, Hydrogen can be compressed, liquefied, or stored as metal hydrides in a solid phase. Hydrogen in a liquid phase (20°K at 1 atm) has a density of 71 Kg/m<sup>3</sup>, while its gaseous density is only of 0,09 Kg/m<sup>3</sup> at normal conditions, so it can be stored in insulated vessels.

The liquefying process requires between 8-12 kWh/Kg, converting Hydrogen liquid storage in the most expensive storage methodology, about 2,8-4,5\$/Kg of Levelized cost in front of 0,23-1,9 \$/Kg of the gaseous storage [39]. Even so, nowadays Hydrogen is usually sorted as a liquid due to the maturity of this technology [33]. The most economical option for storing Hydrogen in a limited volume consists in increasing the pressure, normally in the range of 300-700 bar, reaching densities of 20-42 Kg/m<sup>3</sup>. In this case, the benchmark Levelized Cost is about 0,19 \$/Kg but working with such high pressures levels implies hazardous conditions. Another solution, such as the storage of metal hydrides, as an ammonia compound, is currently under development and is considered an immature technology. The main advantage of this solution is to avoid high pressures and very low temperatures. On the other hand, it can be potentially more inefficient for many end-uses because the metal as a solid phase should be re-converted to gas or liquid Hydrogen to be used [33].

**Table 2.** Technical and economic characteristics of the most relevant existent water electrolyzer types. Source: own elaboration based on data from [40].

Process	Electrolyte	Operating Temp [°C]	Efficiency	Commercial Electrolyzer example	H <sub>2</sub> rate [Nm <sup>3</sup> /h]	2020 CAPEX <sup>3</sup> [\$/kW]	2030 in-stalled capacity
Proton Exchange Membrane (PEM)	Solid polymeric (Nafion)	60 - 80	65 - 82%	EL600N from H2B2 <sup>4</sup> (600 Nm <sup>3</sup> /h)	5 - 1400	1100-1800	15.500 MW <sub>el</sub>
	Liquid Potassium hydroxide (KOH)	50 - 80	59 - 70%	HYLINK from Sunfire <sup>5</sup>	1 - 400	500 - 1400	951 MW <sub>el</sub>
Oxide Electrolysis Cell (SOEC)	Solid ceramic	650 - 1.000	Up to 100%	(demonstration stage)	-	2800-5600	48 MW <sub>el</sub>

<sup>3</sup> Capital expenditure (CAPEX) includes system costs, power electronics, gas conditioning, and balance of plant.

<sup>4</sup> More information can be found in reference [48].

<sup>5</sup> The specifications of this product can be found in reference [49].

### 3.3 Hydrogen conversion to electricity technologies

In some end-use sectors, stored Hydrogen requires further conversion to generate electricity again, as in residential and industrial combined heat (CHP) scenarios [37]. The conversion of chemical energy into electricity can be done using fuel cell systems. The most relevant advantages of fuel cells are related to their low operating temperature, easy maintenance, and simplicity [41].

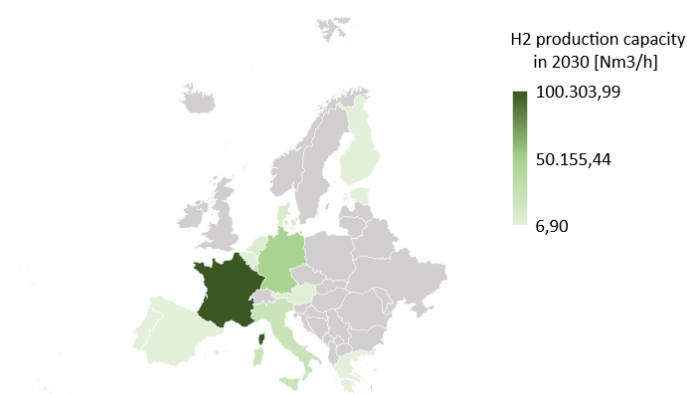


Fig. 4. Estimation of EU's H<sub>2</sub> production capacity by 2030. Source: own elaboration based on data from [38].

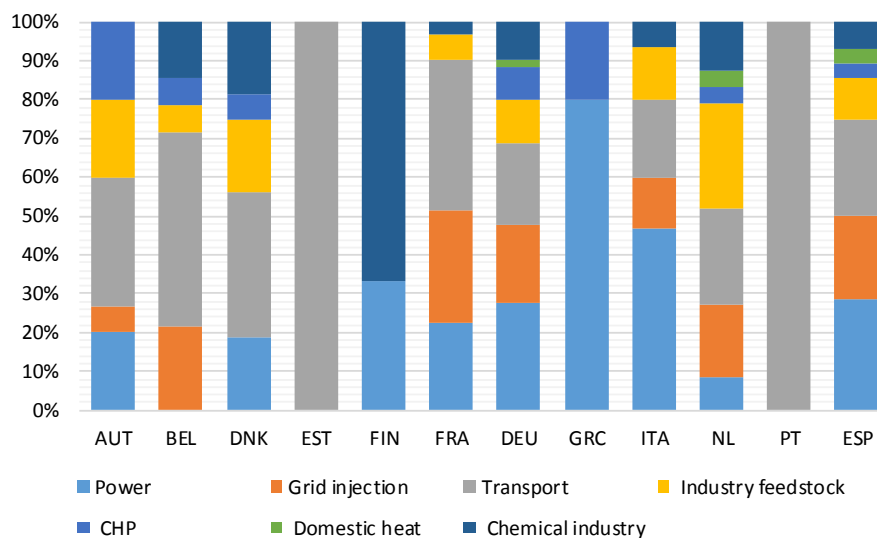


Fig. 5. Areas of interest by country. Source: own elaboration based on data from [38].

## 4 Hydrogen: current EU deployment

In reviewing the EU's long-term strategies, up to 2050, Hydrogen solutions will potentially be useful for the transition to a carbon-neutral economy. Specifically, if we analyze the evolution of the projects related to Hydrogen in the EU countries [38], for the period 2000-2030. Analysis of this information will allow us to estimate the EU's H<sub>2</sub> production capacity by 2030, Fig.4. The information available about Hydrogen projects demonstrates significant differences between EU members countries. According to this, the European countries that will be the principal producers of Hydrogen will be France, Germany, and Italy. All these countries have announced their strategic plans to achieve the Ecological transition. For example, Germany plans to shut down all nuclear reactors by 2022. Therefore, the country will need to produce a large amount of sustainable energy to deal with this transformation. Within this framework, the different EU countries are proposing different end uses of Hydrogen depending on their productive structure, Fig. 5. From this figure it can be appreciated how the different countries are focused mainly on three specific applications: power generation, blending Hydrogen into (CNG) pipelines, and sustainable mobility.

After a detailed analysis of Hydrogen projects in EU countries, we will present the five most relevant demonstration projects to chart the paths of the future EU Hydrogen roadmap. The projects have been chosen following three main criteria:

- The project must be currently operational. Most of them are in the initial stage.
- The project must seek a relevant impact in reducing Greenhouse Gases emissions.
- A maximum of one project per country has been allowed to achieve a complete European picture.

The main characteristics of these projects are described below:

- ***H-Vision (Netherlands)***

H-Vision is a Dutch project in which sixteen private companies, such as Air Liquide or BP, have joined forces to produce blue Hydrogen in Rotterdam before 2030 [42]. This project aims to generate and consume low-carbon Hydrogen for small-scale industry and, ultimately, to supply the system with electricity from renewable energy sources so that the Netherlands' emissions are significantly reduced. According to the feasibility project, 16% of the total national climate targets are related to the Rotterdam industrial sector. The main goal of the H-Vision project is to reduce CO<sub>2</sub> emissions up to 4.3 Mt CO<sub>2</sub>/year in 2030, which represents the 30% industry GHG emissions reduction national target. The Hydrogen production method chosen is methane reforming (ATR) combined with carbon capture and storage (CCS). Rotterdam is also carrying out the Porthos project [43] focused on developing a CCS system in the North Sea floor with a capacity of 2.5 Mt CO<sub>2</sub> /year so the synergies between projects will probably be inevitable.

- ***Hybridge (Germany)***

Hybridge is a German project that proposes to combine the electrolysis of water and the conversion of Hydrogen to methane to develop the first large-scale gas power plant in the country. The water electrolysis powered by RES will be responsible for generating Green Hydrogen.

The partners of this project are still considering the best electrolyzer technology to implement (PEM or alkaline methodologies) in the project, the expected power of the plant to be planned must be up to 100MW of plant and a maximum Hydrogen generation capacity of up to 22.000 nm<sup>3</sup> H<sub>2</sub>/h [44]. Once the Hydrogen is produced, it will be used to generate methane through the exhausted CO<sub>2</sub> gases precedent from industrial activities. Therefore, they will achieve the reduction of GHG emissions and will reduce the carbon footprint of industrial activities.

- ***H2V Normandy (France)***

H2V is a French project that proposes to deploy, in 2022, an entire Green Hydrogen energy system in the town of Saint-Jan-de-Folleville, France [45]. The partners aim to deploy a 100MW Alkaline electrolyzer, as indicated in the project, to be able to produce 28000 tons H<sub>2</sub>/year. Specifically, the project aims to recycle wastewater from the surrounding industries to feed the Alkaline electrolyzer. Moreover, the strategic plan of the project also includes the deployment of 11 fuel cell CHP systems for several end-use applications: industry, transport, and domestic heat.

- ***UpHy (Austria)***

UpHy is an Austrian project that proposes to produce Green Hydrogen through electrolysis at an industrial scale for use it in industry and mobility. The Hydrogen produced is planned to be used as fuel for public buses in the Vienna region, and for uses such as the hydrogenation of CO<sub>2</sub> from waste gas flows to produce sustainable fuels. One of the largest photovoltaic parks planned with 11.4MW will be implemented by the partner companies OMV and VERBUND [46]. The renewable electricity generated, will contribute to the Green Hydrogen production objective.

The UpHy project foresees the construction of a large electrolysis plant of up to 10 MW and 1.300 nm<sup>3</sup> H<sub>2</sub>/h based on a PEM electrolyzer, and the design of the complementary infrastructure for the supply of Hydrogen to the transport and industrial sectors. Furthermore, the goal of the project is to build a complete Hydrogen value chain, including H<sub>2</sub> purification, H<sub>2</sub> trailer loading, trailering, and a highly available, energy-optimized bus service station. The main goal of this project is to reduce up to 15.000 tons CO<sub>2</sub>/year.

- ***Green Hysland (Spain)***

Green Hysland is a Spanish project that proposes the deployment of a Green Hydrogen production plant on the island of Mallorca, Spain [47]. Hydrogen generation will be performed through a 7.5 MW PEM-based electrolysis plant fed with energy from PV parks. The partners of this project aim to produce up to 300 tons H<sub>2</sub>/year and reduce

GHG emissions up to 20.700 tons CO<sub>2</sub>/year. The complete Hydrogen ecosystem will also include 6 fuel cells used in the transport sector (mainly for buses and rental cars), two FC-based CHPs for commercial heating applications, an FCH power system for a ferry terminal, and pipelines, to inject H<sub>2</sub> into the local gas distribution grid. The expected duration of the project will be of four years and the construction of the Hydrogen generation plant will start at the beginning of 2022.

## 5 Conclusions

Climate change requires a global human response and the Green Transition represents a necessary action to slow down and avoid the effects of global warming. Within this framework, the EU aims to become the world's first carbon-neutral zone by 2050. In this context, Hydrogen has valuable characteristics that can help to achieve net-zero climate targets, but in scaling up to a Hydrogen economy, some challenges remain [39] that the EU is currently tackling in demonstration projects. Innovation work related to the world of Hydrogen is being considered as an opportunity to increase the productivity of the economy of European countries, in a perspective of recovery after the COVID-19 pandemic [37] thanks to policies and incentives implemented by the European Commission.

Different Hydrogen production technologies have been studied in this work. The review of the most relevant EU Hydrogen projects shows a real interest in this topic in many economic sectors and countries.

In turn, countries like France, Germany, and Italy will play a relevant role in the new Hydrogen economy as main producers, and having focused part of their national transport and energy decarbonization strategies on Hydrogen-based technologies, these countries will develop a leading industry in this area that will allow them to export services and products to the rest of the EU and the world.

Once the main demonstration projects have been analyzed, the EU shows a clear trend towards Green Hydrogen production from water electrolysis powered by renewable sources. Since, from a sustainability point of view, this option does not have any type of carbon emission associated. Regarding electrolysis technology, the trend is greater use of PEM solutions over alkaline, but this point is yet to be discerned in the coming years. Instead, today these technologies are not yet cost-competitive, so this is one barrier to overcome. Fortunately, the amount of research programs has increased in the last five years, especially focused-on PEM-type electrolyzers development. In addition, a greater presence of renewable energy sources in the grid is expected to reduce the cost of H<sub>2</sub> generation.

Once produced, multiple end uses are within the reach of Green Hydrogen. The use of this element as an energy storage method, based on the liquefaction or compression of H<sub>2</sub>, has potential benefits in fields such as the decarbonization of transport or for the stabilization of the electrical network. Conversely, significant efforts must be made to adapt and deploy new infrastructures, such as H<sub>2</sub> service stations or H<sub>2</sub> production plants.

## Acknowledge

This work has been funded in part by a research grant from *Cátedra Endesa-Red de Innovación Energética* of the University of the Balearic and by the Spanish Ministry of Economy and competitiveness and the EU with Regional European Development Funds under Grant PID2020-120075RB-I00.

## References

1. Veziroğlu TN, Şahin S (2008) 21st Century's energy: Hydrogen energy system. *Energy Conversion and Management* 49:1820–1831. <https://doi.org/10.1016/j.enconman.2007.08.015>
2. Tol RSJ (2009) The economic effects of climate change. *Journal of Economic Perspectives* 23:29–51. <https://doi.org/10.1257/jep.23.2.29>
3. Ritchie H, Rosr M (2020) CO<sub>2</sub> and Greenhouse Gas Emissions. In: Our-WorldInData.org. <https://ourworldindata.org/co2-and-other-greenhouse-gas-emissions>
4. Jones MW, Smith A, Betts R, et al (2020) Climate Change increases the risk of wildfires. *ScienceBrief Review* 116:117
5. Horowitz CA (2016) Paris Agreement. *International Legal Materials* 55:. <https://doi.org/10.1017/s0020782900004253>
6. Siddi M (2020) The European Green Deal: Assessing its current state and future implementation. FIIA Working Paper 14
7. European Commission Delivering the European Green Deal. [https://ec.europa.eu/info/strategy/priorities-2019-2024/european-green-deal/delivering-european-green-deal\\_en](https://ec.europa.eu/info/strategy/priorities-2019-2024/european-green-deal/delivering-european-green-deal_en). Accessed 1 Oct 2021
8. European Commission (2021) Study on the possibility to set up a carbon border adjustment mechanism on selected sectors. Final report.
9. de La Porte C, Jensen Dagnis M (2021) The next generation EU: An analysis of the dimensions of conflict behind the deal. *Soc Policy Adm* 55. <https://doi.org/10.1111/spol.12709>
10. McCauley D, Heffron R (2018) Just transition: Integrating climate, energy and environmental justice. *Energy Policy* 119:1–7. <https://doi.org/10.1016/j.enpol.2018.04.014>
11. Pérez-Lombard L, Ortiz J, Pout C (2008) A review on buildings energy consumption information. *Energy and Buildings* 40:394–398. <https://doi.org/10.1016/j.enbuild.2007.03.007>
12. Nicoletti G, Arcuri N, Nicoletti G, Bruno R (2015) A technical and environmental comparison between hydrogen and some fossil fuels. *Energy Conversion and Management* 89:205–213. <https://doi.org/10.1016/j.enconman.2014.09.057>
13. Capellán-Pérez I, Campos-Celador Á, Terés-Zubiaga J (2018) Renewable Energy Cooperatives as an instrument towards the energy transition in Spain. *Energy Policy* 123:215–229. <https://doi.org/10.1016/j.enpol.2018.08.064>

14. Ziegler MS, Mueller JM, Pereira GD, et al (2019) Storage Requirements and Costs of Shaping Renewable Energy Toward Grid Decarbonization. *Joule* 3:2134–2153. <https://doi.org/10.1016/j.joule.2019.06.012>
15. Aneke M, Wang M (2016) Energy storage technologies and real life applications – A state of the art review. *Applied Energy* 179:350–377
16. Abdin Z, Zafaranloo A, Rafiee A, et al (2020) Hydrogen as an energy vector. *Renewable and Sustainable Energy Reviews* 120:109620. <https://doi.org/10.1016/J.RSER.2019.109620>
17. Edwards PP, Kuznetsov VL, David WIF (2007) Hydrogen energy. *Philosophical Transactions of the Royal Society A: Mathematical, Physical and Engineering Sciences* 365:1043–1056. <https://doi.org/10.1098/rsta.2006.1965>
18. Hydrogen Council (2021) Hydrogen decarbonization pathways: Potential supply scenarios.
19. International Energy Agency (2020) Energy Technology Perspectives. Special Report on Carbon Capture Utilisation and Storage: CCUS in clean energy transitions.
20. Cetinkaya E, Dincer I, Naterer GF (2012) Life cycle assessment of various hydrogen production methods. *International Journal of Hydrogen Energy* 37:2071–2080. <https://doi.org/10.1016/j.ijhydene.2011.10.064>
21. Hajjaji N, Pons M-N, Renaudin V, Houas A (2012) Comparative life cycle assessment of eight alternatives for hydrogen production from renewable and fossil feedstock. <https://doi.org/10.1016/j.jclepro.2012.11.043>
22. Kayfeci M, Keçebaş A, Bayat M (2019) Hydrogen production. *Solar Hydrogen Production: Processes, Systems and Technologies* 45–83. <https://doi.org/10.1016/B978-0-12-814853-2.00003-5>
23. Hosseini SE, Wahid MA (2016) Hydrogen production from renewable and sustainable energy resources: Promising green energy carrier for clean development. *Renewable and Sustainable Energy Reviews* 57:850–866
24. Nikolaidis P, Poullikkas A (2017) A comparative overview of hydrogen production processes. *Renewable and Sustainable Energy Reviews* 67:597–611
25. Seyitoglu SS, Dincer I, Kilicarslan A (2017) Energy and exergy analyses of hydrogen production by coal gasification. *International Journal of Hydrogen Energy* 42:2592–2600. <https://doi.org/10.1016/j.ijhydene.2016.08.228>
26. Howarth RW, Jacobson MZ (2021) How green is blue hydrogen? *Energy Science and Engineering*. <https://doi.org/10.1002/ese3.956>
27. Midilli A, Ay M, Dincer I, Rosen MA (2005) On hydrogen and hydrogen energy strategies I : Current status and needs. *Renewable and Sustainable Energy Reviews* 9:255–271
28. The Engineer Toolbox Fuels - Higher and Lower Calorific Values. [https://www.engineeringtoolbox.com/fuels-higher-calorific-values-d\\_169.html](https://www.engineeringtoolbox.com/fuels-higher-calorific-values-d_169.html). Accessed 2 Oct 2021
29. Singh S, Jain S, Ps V, et al (2015) Hydrogen: A sustainable fuel for future of the transport sector. *Renewable and Sustainable Energy Reviews* 51:623–633
30. BP Full report – Statistical Review of World Energy 2021

31. Züttel A, Remhof A, Borgschulte A, Friedrichs O (2010) Hydrogen: the future energy carrier. *Trans R Soc A* 368:3329–3342. <https://doi.org/10.1098/rsta.2010.0113>
32. US Department of Energy, Office Of Electricity Delivery & Energy Reliability (2011) Energy Storage: Program Planning Document
33. Stetson N, Wieliczko M (2020) Hydrogen technologies for energy storage: A perspective. *MRS Energy & Sustainability* 7:41. <https://doi.org/10.1557/mre.2020.43>
34. Albertus P, Manser JS, Litzelman S (2020) Long-Duration Electricity Storage Applications, Economics, and Technologies. *Joule* 4:21–32. <https://doi.org/10.1016/J.JOULE.2019.11.009>
35. Guerra OJ, Zhang J, Eichman J, et al (2020) The value of seasonal energy storage technologies for the integration of wind and solar power. *Energy and Environmental Science* 13:1909–1922. <https://doi.org/10.1039/d0ee00771d>
36. Bessarabov D, Wang H, Li H, Zhao N (2015) PEM Electrolysis for Hydrogen Production: Principles and Applications. CRC Press
37. Noussan M, Raimondi PP, Scita R, Hafner M (2021) The role of green and blue hydrogen in the energy transition: a technological and geopolitical perspective. *Sustainability (Switzerland)* 13:1–26. <https://doi.org/10.3390/su13010298>
38. IEA (2020) Hydrogen Projects Database. <https://www.iea.org/reports/hydrogen-projects-database>. Accessed 8 Oct 2021
39. Bloomberg NEF, Bhavnagri K, Henbest S, Izadi-Najafabadi A (2020) Hydrogen Economy Outlook. Key messages
40. International Energy Agency (2019) The Future of Hydrogen: Seizing today's opportunities. Japan
41. Barbir F (2012) PEM Fuel Cells: Theory and Practice, Academic press
42. (2019) H-vision. <https://www.deltalinqs.nl/h-vision-en>. Accessed 5 Oct 2021
43. Port of Rotterdam (2020) 102 million euros in funding on the horizon for Porthos carbon storage project. <https://www.portofrotterdam.com/en/news-and-press-releases/102-million-euros-funding-horizon-porthos-carbon-storage-project>. Accessed 5 Oct 2021
44. Ampiron GmbH Hybridge: a project of Amprion and Open Grid Europe. <https://www.hybridge.net/index-2.html>. Accessed 5 Oct 2021
45. H2V Normandy project. <http://h2vnormandy-concertation.net/comprendre-projet/>. Accessed 5 Oct 2021
46. UpHy I&II: Upscaling of green hydrogen for industry and mobility. In: Energy innovation Austria. <https://www.energy-innovation-austria.at/article/uphy-iii-2/?lang=en>. Accessed 5 Oct 2021
47. European Commission (2021) GREEN HYSLAND: Deployment of a H2 Ecosystem on the Island of Mallorca. In: Fact sheet H2020 - CORDIS. <https://cordis.europa.eu/project/id/101007201>. Accessed 5 Oct 2021
48. H2B2 EL600N Datasheet. [https://www.h2b2.es/wp-content/uploads/2021/06/210504\\_H2B2-EL600N-Datasheet.pdf](https://www.h2b2.es/wp-content/uploads/2021/06/210504_H2B2-EL600N-Datasheet.pdf). Accessed 4 Oct 2021

49. Sunfire-Hylink Alkaline datasheet. [https://www.sunfire.de/files/sunfire/images/content/Sunfire.de%20\(neu\)/Sunfire-Factsheet-HyLink-Alkaline-20210111.pdf](https://www.sunfire.de/files/sunfire/images/content/Sunfire.de%20(neu)/Sunfire-Factsheet-HyLink-Alkaline-20210111.pdf). Accessed 4 Oct 2021

# Redes descentralizadas em sistemas conjugados de chaminés solares e trocadores de calor terra-ar

Erick Sabino de Oliveira<sup>1</sup>, Daduí Cordeiro Guerrieri<sup>1</sup>, José Luiz Zanon Zotin<sup>2</sup>,  
and Igor Leão dos Santos<sup>1</sup>

<sup>1</sup> Centro Federal de Educação Tecnológica Celso Suckow da Fonseca, Rua General  
Canabarro, 485 – Maracanã Rio de Janeiro – RJ CEP 20271-204,  
erick.sabino@aluno.cefet-rj.br,  
dadui.guerrieri@cefet-rj.br,  
igor.santos@cefet-rj.br,

<sup>2</sup> Centro Federal de Educação tecnológica Celso Suckow da Fonseca - UNED  
Itaguaí, Rodovia Mário Covas, lote J2, quadra J, Distrito Industrial de Itaguaí,  
Itaguaí/RJ - CEP: 23812-101,  
jose.zotin@cefet-rj.br,

**Resumo** A sociedade demanda por processos cada vez mais sustentáveis e econômicos. Na área de ventilação e refrigeração, as técnicas de ventilação, seja por efeito chaminé ou refrigeração por ação da temperatura do solo, apresentam bons resultados para se tornarem uma alternativa aos tradicionais equipamentos disponibilizados no mercado. Para que se possa aumentar a performance destes sistemas é indicado o uso de sensores modernos, que permitem monitorar e calcular os melhores parâmetros de funcionamento. Nos últimos anos, os tipos de rede para automação evoluíram e as redes *wireless* descentralizadas destacam-se em relação as habituais redes centralizadas e construídas com cabeamento físico. Este trabalho apresenta um modelo introdutório de uma rede *wireless* descentralizada para um sistema de ventilação e refrigeração passivo e o objetivo principal é apontar as possibilidades de ganho na eficiência do sistema.

**Keywords:** sustentabilidade, automação, chaminé solar, EAHE

## 1 Introdução

As cidades estão se tornando inteligentes. Não somente em termos da forma de automatizar a rotina das pessoas, dos edifícios e do sistema de trânsito, mas também nas formas que nos permitem monitorar, compreender, analisar e planejar a cidade com o intuito de melhorar a eficiência, a equidade e a qualidade de vida dos seus cidadãos. Isso muda a forma de se fazer o planejamento em diferentes escalas de tempo, fazendo com que a capacidade de evoluir no longo prazo seja aumentada pela reflexão no curto prazo[1].

2 E. Oliveira, D. Guerrieri, I. Santos e J. Zotin

A indústria 4.0, nascida na década de 2010 com Henning et al.[2] é um movimento de indústrias conectadas, mais eficientes e com a capacidade de tomar decisões baseadas em previsões e estimativas de forma antecipada [3]. Com relação ao meio ambiente, os governos e a sociedade demandam que as novas tecnologias, produto final ou fabricação, sejam sustentáveis. Por sustentabilidade entende-se que é o ato de satisfazer as necessidades do presente sem comprometer a capacidade das gerações futuras satisfazerem as suas próprias necessidades[4].

É uma tarefa desafiadora tornar a sociedade sustentável ao mesmo tempo em que as empresas e o Estado precisam ser rentáveis para serem duráveis e por muitos anos se debateu sobre este paradigma. Considerando que uma boa parcela do consumo de energia residencial e industrial ocorrem devidos aos processos de climatização[5,6], diminuí-lo implica num processo mais sustentável e também econômico. Um conceito de cidade sustentável promissor na Europa e em algumas localidades dos Estados Unidos, segundo Werner[7] é o *district heating*. São locais que utilizam recursos de calor que seriam desperdiçados para o meio ambiente e distribuem esta energia térmica para novos clientes, funcionando como um market place. Para que possam ser rentáveis, a captação deste recurso deve ter um custo de aquisição baixo, como por exemplo a utilização de energia do solo ou do calor desperdiçado por indústrias, etc.[7].

No Brasil, o fornecimento deste tipo de serviço seria vantajoso, principalmente pelo fato de algumas cidades já possuem o incentivo de clusterização da indústria, nos chamados distritos industriais. Em países frios, o *district heating* fornece ar e água aquecidos para indústrias, comércios e também residências, que precisam ser aquecidas. Já em países quentes, indústrias e comércios teriam maior aproveitamento da água/vapor aquecidos que são despreendidos de outras indústrias. No âmbito residencial, alguns estudos como por exemplo [8,9,10], indicam que o solo apresenta um bom potencial para refrigeração de fluidos e este poderia ser aproveitado como uma central de distribuição de ar frio para bairros ou então de forma individual, com cada residência tendo seu próprio trocador de calor que refrigera o ar no interior do solo.

O objetivo deste trabalho é atentar para a introdução de técnicas modernas de monitoramento, presentes neste novo momento da indústria, em um processo de ventilação e refrigeração passiva, que é sustentável e com boa possibilidade de redução do consumo de energia elétrica. Para isso, será abordado a forma de funcionamento do sistema proposto e demonstrado um conceito inicial sobre o uso de sensores *wireless* para operação do sistema.

### 1.1 Chaminé solar e trocador de calor terra-ar

A chaminé solar é uma alternativa viável para a geração de fluxo de ar em edificações, baseada no uso da energia solar como fonte de energia térmica. Seu funcionamento é similar ao processo natural de criação das correntes de vento: formam-se uma zona de alta pressão e outra de baixa pressão, onde o ar é forçado a fluir da zona de alta para baixa pressão[11].

A chaminé solar nada mais é do que um duto de ar que conecta o interior de uma edificação ao seu exterior. Possui as extremidades abertas para que o

ar possa entrar e sair e sua parte externa possui algum mecanismo para aquecimento do ar. Normalmente é utilizado um coletor solar composto por um face de material transparente e outra de material absorvente de calor, de forma a reter o máximo possível de calor nesta parte da tubulação e gerar a diferença de pressão entre a parte interna e externa.

O solo é composto de diversas subcamadas e quanto maior for a profundidade, menor a interação com os fatores climáticos da superfície[12]. Define-se, portanto, um limite de profundidade UGT, também conhecido como *undisturbed ground temperature* a partir do qual a temperatura se torna estável. Quanto mais próximo da superfície, mais influência do clima terá a temperatura do solo. Kurevija e Vulin [13], por exemplo, investigaram o gradiente de temperatura para uma estação meteorológica localizada na Croácia e chegaram a conclusão que a partir de 10m de profundidade a temperatura do solo era constante em 13°C e a 3m de profundidade a temperatura variou entre 8°C e 16°C ao longo do ano.

Dentre algumas possibilidades para aproveitamento desta energia, existem os sistemas denominados *Earth to Air Heat Exchanger* (EAHE), também conhecidos como trocadores de calor terra-ar, que são trocadores de calor de circuito aberto onde o ar é resfriado, ou aquecido, ao ser conduzido para o interior do solo. Os custos envolvidos para implementação de um trocador deste tipo ainda são altos, porém, a nível de sustentabilidade, apresenta resultados promissores. Agrawal e Misra[14], realizaram experimentos com este tipo de trocador de calor em solo úmido e seco e verificaram que em ambos os casos, uma tubulação com 30m de comprimento foi capaz de reduzir a temperatura do ar em aproximadamente 11.8°C.

Para que o ar circule pelo EAHE é necessário que ele seja forçado a passar pela tubulação e, como proposta altamente sustentável, pode-se utilizar a chaminé solar. Dentre as vantagens desta aplicação, se destacam o livre consumo de energia para redução da temperatura do ar. No entanto, a vazão de ar será dependente do quanto a radiação solar aquecerá a chaminé. Em algumas aplicações pode ser necessário introduzir um soprador de ar na entrada do EAHE para atingir a vazão de ar necessária. A ideia geral deste projeto é alcançar a vazão mássica de ar requisitada pelo trocador apenas com a chaminé, porém, caso se verifique sua impossibilidade, a chaminé solar possui um painel solar na sua face de absorção de calor, para alimentação do soprador de ar.

O objetivo principal deste sistema é fazer com que o ar entre para o cômodo com uma temperatura menor em localidades quentes e com uma temperatura maior em localidades frias. Ou seja, trata-se de um sistema de condicionamento do ar com um gasto mínimo de energia e que obviamente não será capaz de substituir por completo a necessidade de um ar condicionado, mas que pode ser um auxiliar e ajudar na redução dos custos com energia e etc.

O sistema proposto é apresentado na Fig. 1, onde os parâmetros climáticos são S1, que representa a incidência de energia solar, P1 a pressão atmosférica, T1 a temperatura externa e H1 a umidade externa do ar. Q1 apresenta a vazão de ar na entrada do EAHE e V representam válvulas para controle do fluxo, com seus

4 E. Oliveira, D. Guerrieri , I. Santos e J. Zotin

respectivos índices para as posições de instalação. O cliente, aqui representado por um ambiente fechado, apresenta medidores de temperatura (T3 a T7) e de umidade (H3 a H8) em diferentes pontos do ambiente. Por final, a chaminé solar possui também um medidor de vazão Q2, de temperatura T8 e umidade H8.

O EAHE é composto de 3 tubulações enterradas no solo, que podem ser controladas pelas válvulas V1,V2 e V3 para aumentar ou reduzir a vazão e, conseqüentemente, a troca térmica do ar. Da mesma forma, as válvulas V4 à V7 controlam o ar para o local com maior demanda, a partir das variáveis de temperatura e umidade. A chaminé solar possui uma articulação A1 para controle de sua inclinação e assim consegue ajustar o recebimento de energia solar e controlar a vazão de ar por ela.

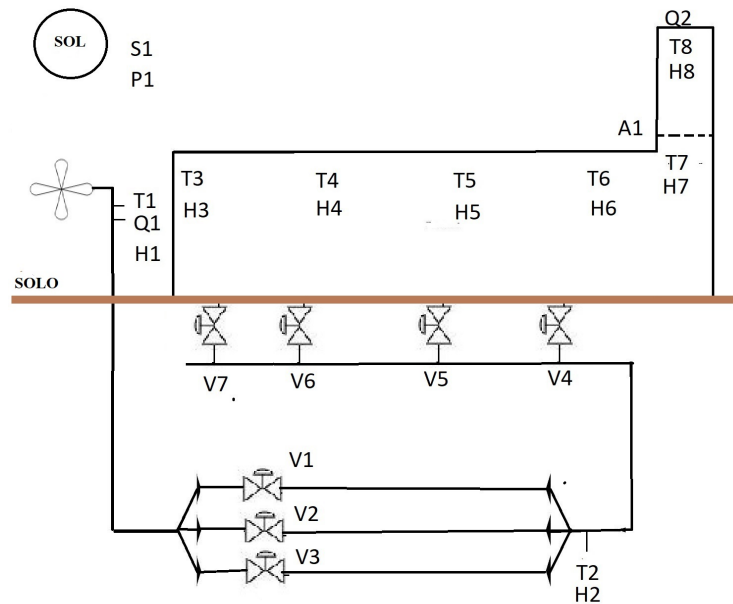


Figura 1. Desenho esquemático do sistema chaminé solar e EAHE

## 2 Desempenho da chaminé solar e do EAHE

As principais variáveis que afetam a eficiência da chaminé solar são o recebimento de energia solar e sua geometria. A incidência da energia solar é afetada por fatores incontroláveis, como a presença de nuvens e gases presentes na atmosfera ([15]). Na face do coletor solar, a inclinação da chaminé solar altera os valores de energia recebida. Devido as características do movimento rotacional do planeta, a máxima eficiência da chaminé é alterada de acordo com o mês de medição e

latitude do local de instalação. Por este motivo, não há consenso na literatura sobre o melhor ângulo de inclinação. Alguns autores calculam ângulos que variam entre 45° e 75° ([16,17]), já Seralgedin *et. al.*[18] calcularam entre 30° e 35°.

Para a cidade do Rio de Janeiro e Seropédica, Oliveira e Zotin [19] calcularam a eficiência térmica da chaminé solar com base na média dos dados climáticos entre Julho/2018 e Julho/2019 simulando 9 inclinações diferentes, conforme mostra a Fig. 2. É possível visualizar que em determinado mês a posição da chaminé se torna mais ou menos eficiente e, por este motivo, torna-se necessário uma rede de automatizada para calcular e controlar a vazão de ar na chaminé.

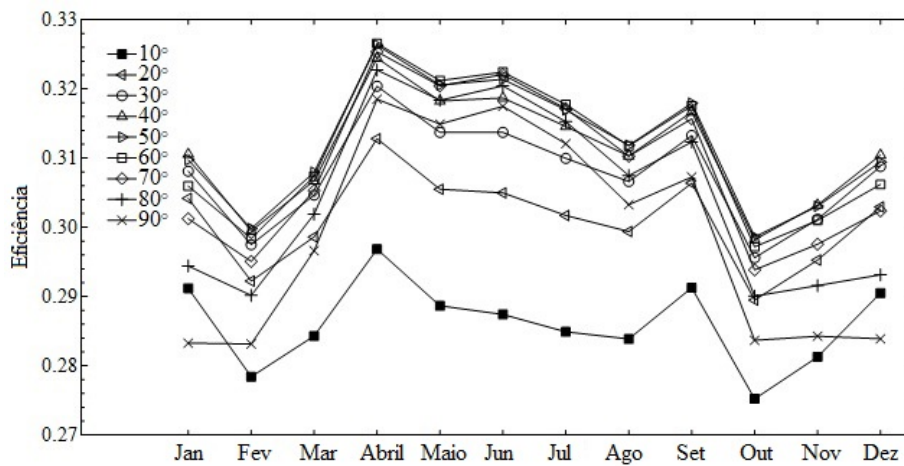


**Figura 2.** Variação da eficiência em relação a mês e à inclinação da chaminé, adaptado de [19].

Com relação ao EAHE, sua eficiência é correlacionada com a capacidade de transferência de calor do material utilizado, seu comprimento e sua profundidade. A troca térmica realizada pode ser representada pela Eq. (1),

$$\frac{T_e - T_r}{T_e - T_a} = e^{\frac{-U_e A_e}{\dot{m} c_p}} \tag{1}$$

onde  $T_e$  é a temperatura do solo,  $T_r$  a temperatura na saída do trocador,  $T_a$  é a temperatura de entrada,  $\dot{m}$  é a vazão mássica de ar,  $c_p$  é o calor específico a pressão constante do ar,  $A_e$  é a área do tubo e, por fim,  $U_e$  são as perdas associadas ao sistema. A escalabilidade deste sistema está associada no controle do ar por diversas tubulações de modo que se possa controlar a vazão ou a temperatura de saída do trocador de calor.

6 E. Oliveira, D. Guerrieri , I. Santos e J. Zotin

### 3 Monitoramento da desempenho do sistema para aumento da eficiência

Apesar de ser uma estratégia passiva para ventilação e refrigeração, o monitoramento dos parâmetros climáticos, da chaminé e do EAHE é fundamental para o aumento do desempenho do sistema. Grande parte dos sistemas de automação ainda são centralizados. Uma rede centralizada para chaminé e o EAHE pode ser representada pela Fig. 3 e é caracterizada pela monopolização das decisões em um ponto central. Neste tipo de rede, todos os nós (sensores) se conectam à um único controlador, com o uso de cabos, por onde flui o envio e recebimento de informações. Neste caso, o controlador é responsável por monitorar a rede e evitar a colisão de informações.

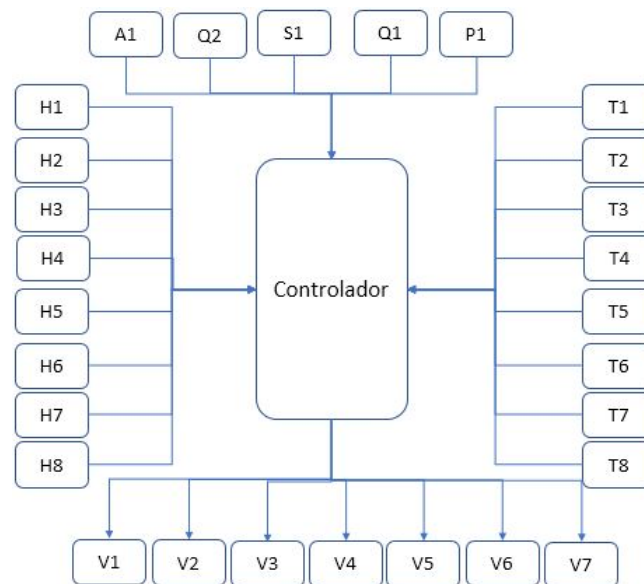


**Figura 3.** Sistema centralizado

A cada nova informação que um sensor fornecer, todo o sistema deverá ser recalculado pelo controlador central e este será responsável por distribuir as informações para as válvulas. No caso de falha em um sensor específico, a rede poderá entrar em falha e caso o problema ocorra no controlador central, é certo que o sistema deixará de funcionar corretamente. Essa é uma limitação comum em redes centralizadas, que sofrem também com a questão dos próprios acessos. No caso de uma grande quantidade de requisições ao mesmo tempo, o sistema pode não suportar devido a limitações em sua capacidade de processamento.

Segundo Moreno[20], o protocolo que mais se destacou nos últimos anos foi o CAN (*Controller Area Network*). Lançado em 1987, este protocolo foi desenvol-

vido pela Bosch<sup>®</sup> tendo em vista a sua aplicação nos automóveis, como forma de interligar os vários componentes eletrônicos neles presentes. Entretanto, devido ao baixo custo dos seus controladores e, principalmente, por ser um protocolo intrinsecamente seguro, o CAN tem vindo a ser progressivamente usado em aplicações médicas e industriais, nestas últimas como protocolo *fieldbus*. Talvez o ponto mais crucial para este tipo de rede seja os custos com infra-estrutura. Dependendo do local onde o controlador principal for posicionado, teremos uma grande quantidade de cabos a serem colocados. Cabos que ficam expostos ao meio ambiente podem vir a falhar, seja por rompimentos, envelhecimento e outros. Pode-se afirmar que a escalabilidade de uma rede física e centralizada é limitada devido a necessidade de recursos físicos para instalação.

### 3.1 Proposta de descentralização em rede híbrida

A proposta de descentralização para o sistema chaminé solar e EAHE é apresentada na Figura 4. A rede será composta de uma rede híbrida, onde os sensores são conectados em um determinado controlador por cabos e os controladores estão em rede *mesh*, que é uma rede descentralizada, onde não existem quaisquer unidades que concentrem a informação enquanto esta circula entre as unidades transmissoras e as receptoras. Esse formato é interessante pois, em caso de falha de um dos controladores, a forma de transmissão e recepção do sinal é adaptada e reformulada. Cada ponto da rede *mesh* contará com sub redes do tipo árvore. Neste tipo de rede, a unidade principal se comunica com uma ou mais unidades do nível hierárquico inferior, às quais, por sua vez, serão conectadas outras unidades hierarquicamente inferiores[20].

Esta configuração foi selecionada pelo fato do EAHE possuir sensores enterrados no solo e um sinal *wireless* poderia apresentar interferências, conforme se aumenta a profundidade do EAHE. Nessa configuração haverão 4 controladores principais. O Controlador 1 será responsável por operar a chaminé solar. Ele recebe as informações de inclinação da chaminé (A1), umidade e temperatura de entrada e saída do ar (T7, T8, H7, H8) e da vazão de ar (Q2). Para realizar os cálculos de melhor vazão e inclinação, o controlador 1 dependerá de receber as informações de energia solar, pressão atmosférica e temperatura do ar do controlador dos parâmetros climáticos.

Essas informações são requisitadas, mas na impossibilidade de recebê-las, o controle também pode ser efetuado usando apenas a medição de vazão de seu próprio módulo. Seu resultado será principalmente indicar a inclinação que a chaminé deve ficar para igualar à vazão de saída da chaminé com a vazão de entrada no trocador de calor.

O controlador 2 é responsável pelo trocador de calor. Ele atua sobre as válvulas do EAHE (V1, V2, V3) controlando a abertura e fechamento para ajuste da vazão (Q1) e temperatura e umidade do ar (T2, H2). O dado de entrada é a temperatura do ar e a umidade, que são fornecidos por módulo de parâmetros climáticos. Como alternativa no caso de falhas do módulo fornecedor, o controlador 1 pode fornecer as medições de vazão na saída para ajustar a vazão de entrada da chaminé.

8 E. Oliveira, D. Guerrieri, I. Santos e J. Zotin

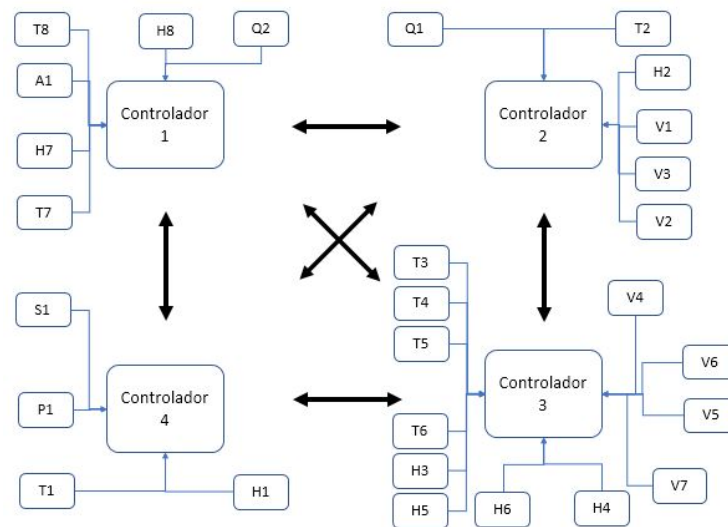


**Figura 4.** Sistema descentralizado

O controlador 3 é responsável por fazer a interface entre o trocador de calor e a chaminé. Ele fará o cálculo da sensação térmica em cada cômodo, baseado na temperatura e umidade (T3, T4, T5, T6, H3, H4, H5, H6) e fará o direcionamento do ar através das válvulas V4, V5, V6, V7. Suas medidas de temperatura são os *inputs* para a chaminé solar, ao enviar estes dados para o controlador 1.

O controlador 4 funciona como uma estação meteorológica, realizando as medições da energia solar (S1), temperatura externa do ar (T1), da umidade relativa do ar (H1) e pressão atmosférica (P1). Em sua ausência, os outros módulos podem continuar a funcionar, mas sua importância está na escalabilidade de compartilhamento de suas informações. O controlador 4 pode, por exemplo, ser uma estação meteorológica da cidade e novas chaminés e EAHE podem utilizar as informações deste controlador mesmo que à grandes distâncias, pois os sinais podem ser enviados e recebidos pela rede descentralizada.

Uma das formas mais práticas e com bom custo benefício para viabilizar esta rede são os módulos que utilizam os protocolos o IEEE 802.11 e o IEEE 802.15.4. O protocolo IEEE 802.11 é utilizado em residências e comércios, popularmente conhecido como wi-fi<sup>®</sup>. Já o protocolo IEEE 802.15.4 é um protocolo orientado para comunicações a curta distância, com velocidades máximas de cerca de 250 Kb/s, onde os consumos energéticos dos dispositivos envolvidos na troca de informação não ultrapassam as poucas dezenas de miliamperes[20].

As principais vantagens deste tipo de rede estão na economia de custos de instalação com o cabeamento, a possibilidade de escalar a transmissão de informações, maior flexibilidade, dentre outros[21]. É possível utilizar a rede *mesh* com componentes de baixo custo, como por exemplo, placas de Arduino<sup>®</sup>. Wang *et. al.*[22] testaram este tipo de rede para medição de parâmetros climáticos com

chaminés solares e trocadores de calor terra-ar 9

protocolo LoRa (*Long Range*) em mais de 40 casas e a adaptação dos transmissores e receptores apresentaram bom comportamento.

Da mesma forma que a flexibilidade de redes *mesh* facilitam em manter a comunicação, elas também dificultam encontrar pontos de acesso defeituosos, principalmente em larga escala. Mas isso pode ser facilmente resolvido com a introdução de relatórios de erro [23].

### 3.2 Proposta de implementação e avaliação do sistema

Nos tópicos anteriores foi apresentado uma modelagem genérica de um sistema de distribuição de ar gelado via chaminés solares e trocadores de calor do tipo EAHE. Foram apresentados os benefícios da automatização deste sistema de refrigeração passiva e também automatização por uma rede de sensores sem fio híbrida, com as topologias em *mesh* e árvore.

Para validar esta proposta de rede, existem alguns softwares disponíveis no mercado que realizam simulações de redes sem fio. Dentre as opções disponíveis, destaca-se o Contiki<sup>®</sup>[24], um sistema operacional voltado para simulação de dispositivos IOT e o programa CupCarbon<sup>®</sup>[25], software de código aberto que permite um design prático de redes de sensores sem fio e que aborda especialmente a modelagem e avaliação de desempenho de camadas físicas de rádio. Além disso, sua principal vantagem sobre outros ambientes de simulação de código aberto é seu foco na modelagem de propagação do rádio em ambientes urbanos, levando em consideração mapas 2D e 3D[26].

Uma proposta de área implementada com a rede é apresentada na Fig. 5. O bairro Gamboa e Santo Cristo são localidades que participam do centro empresarial do Rio de Janeiro. Neste local encontram-se muitos prédios que necessitam de climatização e por este motivo foi escolhido este local para representação, tendo em vista que uma estação de distribuição de ar gelado poderia possuir muitos clientes nesta área e por isso foram selecionados pontos aleatoriamente para instalação dos controladores.

Cada ponto da Fig. 5 representa o cliente que demanda ar refrigerado e possui um controlador do tipo 3 ou 4. Este controlador também servirá como ponto de transmissão e recepção de outros controladores. Os sensores foram configurados para protocolo LoRa e com isso já são identificadas as possíveis conexões que cada sensor pode ser atribuída caso esteja dentro de seu raio de alcance. Como métrica para validação e comparação da rede híbrida criada, pode-se escolher os parâmetros de tempo de vida da rede e pacotes enviados e recebidos.

A comparação do tempo de vida leva em consideração o tempo de início de funcionamento da rede até o momento em que o primeiro controlador é descarregado. Este parâmetro está diretamente associado ao consumo energético de cada nó da rede. Já a medição de pacotes enviados e recebidos irá determinar se a rede está se adaptando da melhor forma possível na ausência de um determinado controlador, ou seja, o quanto de informação está sendo entregue.

10 E. Oliveira, D. Guerrieri , I. Santos e J. Zotin

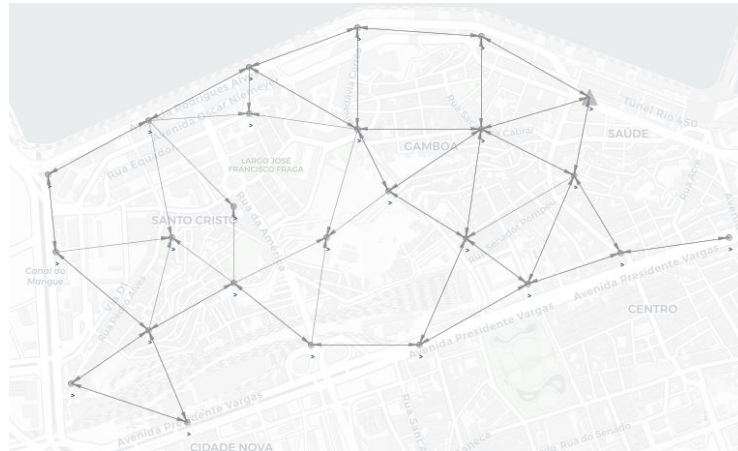


**Figura 5.** Distribuição esquemática dos controladores usando o CupCarbon

## 4 Conclusões

A descentralização de redes é um tópico com exponencial crescimento e que tende a trazer grandes benefícios para a transformação dos processos em termos de sustentabilidade. A implementação desta rede na ventilação e refrigeração sustentável, por chaminés solares e trocadores de calor terra-ar (EAHE), pode vir a apresentar uma boa otimização da eficiência destes sistemas, bem como poder contribuir para a escalabilidade desta solução. A automatização permite calcular o melhor grau de inclinação da chaminé solar, bem como a vazão ideal de ar para que possa suprir totalmente ou na maior quantidade possível o ar refrigerado e, com isso, diminuir o uso de condicionares de ar. Este trabalho procurou apresentar uma solução para automatização dos sistemas de chaminé solar acoplados aos trocadores de calor terra-ar. Trata-se de uma visão inicial, que deve ser aprimorada e validada. Para futuros trabalhos recomenda-se um detalhamento maior dos componentes utilizados e a realização da simulação da rede propriamente dita.

## Referências

1. M. Batty, K. W. Axhausen, F. Giannotti, A. Pozdnoukhov, A. Bazzani, M. Wachowicz, G. Ouzounis, and Y. Portugali, “Smart cities of the future,” *The European Physical Journal Special Topics*, vol. 214, no. 1, pp. 481–518, 2012.
2. K. Henning, W. Wolfgang, and H. Johannes, “Recommendations for implementing the strategic initiative industrie 4.0,” *Final report of the Industrie*, vol. 4, p. 82, 2013.
3. F. Almada-Lobo, “The industry 4.0 revolution and the future of manufacturing execution systems (mes),” *Journal of innovation management*, vol. 3, no. 4, pp. 16–21, 2015.
4. G. H. Brundtland and N. F. Comum, “Relatório brundtland,” *Our Common Future: United Nations*, 1987.
5. IEA, *The Future of Cooling*, IEA. 2018.
6. I. G. R. Outlook, “Energy transformation 2050,” *IRENA: Abu Dhabi, UAE*, 2020.
7. S. Werner, “District heating and cooling,” 2013.
8. K. K. Agrawal, R. Misra, G. D. Agrawal, M. Bhardwaj, and D. K. Jamuwa, “The state of art on the applications, technology integration, and latest research trends of earth-air-heat exchanger system,” *Geothermics*, vol. 82, pp. 34–50, 2019.
9. L. Moosavi, M. Zandi, M. Bidi, E. Behroozizade, and I. Kazemi, “New design for solar chimney with integrated windcatcher for space cooling and ventilation,” *Building and Environment*, vol. 181, p. 106785, 2020.
10. R. Misra, V. Bansal, G. D. Agarwal, J. Mathur, and T. Aseri, “Thermal performance investigation of hybrid earth air tunnel heat exchanger,” *Energy and Buildings*, vol. 49, pp. 531–535, 2012.
11. E. S. de Oliveira and J. L. Z. Zotin, “Thermodynamic analysis of a solar chimney using meteorological data from rio de janeiro and seropédica cities,” in *ENCIT 2020*, 2020.
12. M. Gwadera, B. Larwa, and K. Kupiec, “Undisturbed ground temperature—different methods of determination,” *Sustainability*, vol. 9, no. 11, p. 2055, 2017.
13. T. Kurevija and D. Vulin, “Determining undisturbed ground temperature as part of shallow geothermal resources assessment/odredvanje staticke temperature tla kao dijela vrjednovanja plitkih,” *Rudarsko-geolosko-naftni zbornik*, vol. 22, no. 1, p. 27, 2010.
14. K. K. Agrawal, R. Misra, and G. D. Agrawal, “To study the effect of different parameters on the thermal performance of ground-air heat exchanger system: In situ measurement,” *Renewable Energy*, vol. 146, pp. 2070–2083, 2020.
15. J. A. Duffie and W. A. Beckman, *Solar engineering of thermal processes*. John Wiley & Sons, 2013.
16. X.-H. Ren, L. Wang, R.-Z. Liu, L. Wang, and F.-Y. Zhao, “Thermal stack airflows inside the solar chimney with discrete heat sources: Reversal flow regime defined by chimney inclination and thermal rayleigh number,” *Renewable Energy*, vol. 163, pp. 342–356, 2021.
17. R. Bassiouny and N. S. Korah, “Effect of solar chimney inclination angle on space flow pattern and ventilation rate,” *Energy and Buildings*, vol. 41, no. 2, pp. 190–196, 2009.
18. A. A. Serageldin, A. K. Abdelrahman, and S. Ookawara, “Parametric study and optimization of a solar chimney passive ventilation system coupled with an earth-to-air heat exchanger,” *Sustainable Energy Technologies and Assessments*, vol. 30, pp. 263–278, 2018.

- 12 E. Oliveira, D. Guerrieri , I. Santos e J. Zotin
19. E. Oliveira and J. Zotin, “Thermodynamic analysis of a solar chimney using meteorological data from rio de janeiro and seropédica cities.,” 01 2020.
  20. I. D. G. Moreno, *Rede de sensores inteligentes sem fios para a supervisão de parques de reservatórios industriais*. PhD thesis, 2009.
  21. I. F. Akyildiz, W. Su, Y. Sankarasubramaniam, and E. Cayirci, “Wireless sensor networks: a survey,” *Computer networks*, vol. 38, no. 4, pp. 393–422, 2002.
  22. X.-L. Wang, B. Ha, F. A. Manongi, W.-K. Jung, Y. A. C. Jande, and S.-H. Ahn, “Arduino-based low-cost electrical load tracking system with a long-range mesh network,” *Advances in Manufacturing*, vol. 9, no. 1, pp. 47–63, 2021.
  23. Y. Liu, K.-F. Tong, X. Qiu, Y. Liu, and X. Ding, “Wireless mesh networks in iot networks,” in *2017 International workshop on electromagnetics: applications and student innovation competition*, pp. 183–185, IEEE, 2017.
  24. A. Dunkels, B. Gronvall, and T. Voigt, “Contiki-a lightweight and flexible operating system for tiny networked sensors,” in *29th annual IEEE international conference on local computer networks*, pp. 455–462, IEEE, 2004.
  25. K. Mehdi, M. Lounis, A. Bounceur, and T. Kechadi, “Cupcarbon: A multi-agent and discrete event wireless sensor network design and simulation tool,” in *7th International ICST Conference on Simulation Tools and Techniques, Lisbon, Portugal, 17-19 March 2014*, pp. 126–131, Institute for Computer Science, Social Informatics and Telecommunications . . . , 2014.
  26. C. Pham, A. Bounceur, L. Clavier, U. Noreen, and M. Ehsan, “Radio channel access challenges in lora low-power wide-area networks,” in *LPWAN Technologies for IoT and M2M Applications*, pp. 65–102, Elsevier, 2020.

# Prescriptive Analytics in Rescue Operations: A Combinatorial Optimization approach

Igor Morais [0000-0003-2006-5250]  
Vanessa de Almeida Guimarães [0000-0001-7662-3499]  
Eduardo Bezerra da Silva [0000-0001-9177-5503]  
Pedro Henrique González [0000-0003-0057-7670]

Federal Center for Technological Education of Rio de Janeiro, Rio de Janeiro, Brazil  
{igor.morais,pegonzalez}@eic.cefet-rj.br,  
{vanessa.guimaraes,eduardo.silva}@cefet-rj.br

**Abstract.** Rio de Janeiro has two of the biggest urban forests in Brazil. They receive many tourists every year and as they have such an extensive area, some people get lost. Rescue tasks have to mobilize firefighters, helicopters and many public resources. Seeking to reduce the public sector's cost, this paper presents an applied approach for monitoring visitors to reduce the time for these rescue tasks. In order to do that, sensors are displayed in a grid, taking into consideration limits of the technology and the area of the urban forest. Besides, an Unmanned Aerial Vehicle (UAV) is used to collect the data generated by the sensors and the UAV battery is also considered for making feasible solutions closer to the real scenario, as the urban forests usually have big areas. A metaheuristic framework is used for finding solutions for the proposed optimization problem. Experiments show that the methodology is feasible of implementation and solutions are obtained in, at most, 20 seconds. This approach could be used as public policies to improve urban management in the context of smart and digital cities.

**Keywords:** Rescue Operation · UAV · Combinatorial Optimization.

## 1 Introduction

The concept of smart cities is based on three pillars: urban management of governance, energy and transportation [6], having as main objective to enhance the quality of life in urban spaces [11]. This concept has arisen with the challenge of improving the cities' liveability and citizens' wellness [4]. Therefore, it involves agendas and policies dedicated to dealing with natural resources and energy, transport and mobility, buildings, living, government, economy and people [11].

In this sense, the design of smart cities must deal with [2]: (i) the understanding of urban problems, identifying the critical issues and uncertainty related to cities, transport and energy; (ii) the coordination of urban technologies; (iii) the development of models and methods for using urban data across spatial and temporal scales; (iv) developing and dissemination of new technologies for communication; and, (v) proposition of new forms of urban governance.

2 I. Morais et al.

Therefore, this paper presents a new application for the data mule routing problem, which consists of collecting data produced in sensors, that can monitor people in urban forests and reduce the time spent searching for missing people. Many searches are conducted every year for missing people in the National Park of Tijuca, one of Brazil's biggest Atlantic Forest parks. Another important urban forest in Rio de Janeiro is the Pedra Branca State Park, the most extensive urban forest in Brazil. Both of them are studied in this paper.

National Park of Tijuca receives approximately 2.5 million visitors every year, representing 3.5% of Rio de Janeiro's territory [7]. In such a vast area with that many visitors, many of them usually go missing (approximately 0.01%). Thanks to that, public resources such as firefighters and helicopters must be assigned to a rescue task force to rescue them. Such type of operation can have a high cost for the public sector. As a possible solution, wireless sensor networks can be used to monitor park users and reduce the cost of rescue task forces, although many sensors are necessary to cover the park's total area. To reduce the task force cost, an Unmanned Aerial Vehicle (UAV) can be used to collect data from sensors and return them to a base station, which the firefighters can analyze before the search starts. This problem can be viewed from the perspective of smart cities, considering that parks are part of the quality of life in urban areas. Besides, the application proposed could help the government to manage the public resources which is directly related to governance in smart cities.

Many papers have used Wireless Sensor Networks (WSN) for disaster, military and environmental monitoring [3, 10]. This type of network has been used due to its low cost, easy deployment and maintenance. In a multi-hop network, the sensors can communicate between themselves due to the communication range of the network sensors. Whenever networks are sparse, this kind of connection is impossible [13] to be made. One way of gathering the data in a Sparse WSN is using an Unmanned Aerial Vehicle (UAV), for this problem called data mule, due to its improved storage and computational capabilities.

UAVs are used for problems like delivery in big cities and other routing applications. Many papers present the concept of data mules [13], and some of them show ways of using it to collect data at the intersection of these sensors, while other papers use data mules to improve the reach of *ad-hoc* networks. Sugihara [13] shows an approach for the use of wireless sensor networks, the multi-hop. Those networks depend on all sensors having intersections for the communication to be made in a peer-to-peer way.

In Munhoz et al. [10], two meta-heuristics are used to solve the Data Mule Scheduling Problem: the GRASP with Random Variable Neighborhood Descent (RVND) and the General Variable Neighborhood Search (GVNS). In Munhoz et al. [10], the problem analyzed was the time spent to collect data from all sensors. Finally, in Munhoz et al. [9], the authors proposed an integer programming formulation and a distributed heuristic to solve the Data Mule Routing Problem (DMRP). Also, they proved that DMRP belongs to the NP-Hard class.

Considering the described problem, in this paper, we proposed the construction of an applied scenario to collect data on the position of urban forest visitors.

The data mule is responsible for gathering data of urban forest visitors' last position and guide the firefighters in the rescue process. A mathematical definition and metaheuristic are proposed for finding high-quality routes to collect all data in the sensors.

Following this Introduction, Section 2 describes the problem. For finding a solution, a GRASP metaheuristic is presented with its components in Section 3.5. In sequence, for the final part, Section 4.2 presents the description of the used instances and the computational experiments done. At last, Section 5 presents out conclusions and future work.

## 2 Data Mule Routing Problem with Limited Autonomy

An instance of Data Mule Routing Problem with Limited Autonomy (DMRP-wLA) can be mathematically represented as a complete graph  $G(V \cup \{b\}, E)$ , where  $V$  represents the set of sensors,  $b$  represents the base node from where the data mule leaves and where it returns and  $E$  are the set of edges that represent the possible paths between pairs of  $v \in V' = V \cup \{b\}$ . In addition, each  $v \in V$  sensor has a radius attribute that represents the range of its communication. Let us define that two sensors can communicate if there is an intersection between the areas covered by their communication rays. For each edge  $(i, j) \in E$ , a distance  $d_{ij}$  is used to calculate the cost of the displacement between  $i$  and  $j$  and, consequently, the cost of the final route that the mule will take to go through. Also, one must define that the data mule has limited autonomy and, thanks to that, it can not collect the data from all sensors without recharging. Knowing the characteristics of a DMRP-wLA instance, considering the set of cycles  $C$  as the set of all cycles that have cost inferior to a battery limit. A  $C_i$  is a subset of cycles of  $C$  that passes through all sensors contained in  $c_i \cup \{b\}$ , where  $c_i$ , is one of the subcycles, you can define the DMRP-wLA mathematically as Equation 1.

$$\text{DMRP-wLA} = \{C_i \subseteq C \mid \sum_{(i,j)} c_i d_{ij} \leq \sum_{(i,j)} c_j d_{ij}; \forall C_j \subset C, \text{ such that } C_i \cap C_j = b; \} \quad (1)$$

Once defined the problem, it is possible to verify that the DMRP-wLA can be reduced to the Traveling Salesman Problem (TSP), implying that the DMRP-wLA is an NP-Hard problem. Considering its complexity and the size of real-world-based instances, it is suitable to use a meta-heuristics approach to find high-quality solutions in an acceptable computational time. For finding solutions to the problem, the proposed approach divides the problem into two core sub-problems: (i) determine which sensors to visit; (ii) and, then, in what order they are visited. In the next section, the details of the methodology used are presented.

4 I. Morais et al.

### 3 Methodology

In this section, we present the components of the proposed method for obtaining a high-quality solution. The constructive approach consists of constructing a feasible solution. Then the local search procedure searches in a neighborhood of solution space for a local optima that improve the constructive solution. The two are combined using a Greedy Randomized Adaptive Search Procedure meta-heuristics.

#### 3.1 Semi Greedy Adaptive Constructive

The DMRP-wLA consists of finding a set of cycles that minimizes the total cost and collects all data produced by the sensors, while respecting the UAV autonomy. The data from a sensor is collected by visiting it or by visiting some other sensor in its communication ray. One way of solving this problem could be dividing it into two sub-problems, first finding the minimum number of sensors that have to be visited and, then, finding the route that reduces the cost of visiting them. These two problems are defined as the Minimum Dominating Set and the Vehicle Routing Problem (VRP), as each of the multiple vehicles could be viewed as one exiting many times from a base station.

To generate diverse solutions, the two heuristics procedures used were semi greed. This means that in each heuristic, a candidate is chosen at random in a window of proximity to the greedy candidate [5]. These two procedures will be explained in the following two subsections.

#### 3.2 Minimum Dominating Set

Given a graph  $G(V,E)$ , the Minimum Dominating Set(MDS) is defined as finding the subset of vertices " $\bar{V}$ "  $\subset V$  with the minimum cardinality that has a subset of edges  $\bar{E}$ , that connects every vertex of  $V$ . For solving this problem, a heuristic procedure was developed. At first, the eigenvector centrality [8] was used and it consists in finding the biggest Eigenvalue of an adjacency matrix and its associated eigenvector, this one has a property that every value in it is bigger than 0 and it measures connectivity between the vertices. This one was chosen because, as shown in [8], it is the most stable centrality measure between other centralities explored.

For the constructive heuristic, a candidate list is generated containing the centrality measure for each vertex, following Equation 2. This candidate list generates a window of possible candidates to be chosen at random. The maximization version of the Restricted Candidate List (RCL) ensures that each candidate visited has a reasonable amount of data from the other sensors.

$$RCL^{max} = \{i \in \mathcal{CL}_{m_{ds}} \setminus \mathcal{S} | h_{max} \geq h_i \geq h_{min} + \alpha(h_{max} - h_{min})\} \quad (2)$$

Title Suppressed Due to Excessive Length 5

The cost function  $h$  used for this problem is represented by the eigenvector centrality measure, the  $\mathcal{S}$  is the solution that is being constructed,  $i$  is the candidate to be chosen from the candidate list  $CL$ . Also,  $\alpha$  is a real number between zero and one, defining how greedy the choice will be. Algorithm 1 presents in detail how this whole process works.

---

**Algorithm 1:** Minimum Dominating Set
 

---

```

1 Data:  $G, \alpha$ 
2 begin
3    $\mathcal{S} \leftarrow \emptyset$ ;
4    $\bar{V} \leftarrow \emptyset$ ;
5    $CL_{mds} \leftarrow \text{EigenVectorCentrality}(G)$ ;
6   for  $v \in |\mathcal{V}|$  do
7     if  $|v_{neighbors}| = 0$  then
8        $\mathcal{S} \leftarrow \mathcal{S} \cup v$ ;
9        $\bar{V} \leftarrow \bar{V} \cup v$ ;
10    end
11  end
12  while  $|\bar{V}| < |\mathcal{V}|$  do
13     $RCL^{max} \leftarrow \text{GenerateRCL}(CL_{mds}, \alpha)$ ;
14     $v \leftarrow \text{rand}(RCL^{max})$ ;
15     $\mathcal{S} \leftarrow \mathcal{S} \cup v$ ;
16     $\text{UpdateCandidateList}(v)$ ;
17     $\text{UpdateVisited}(\bar{V}, v)$ ;
18  end
19  return  $\mathcal{S}$ ;
20 end
21 f

```

---

The functions “UpdateCandidateList” and “UpdateVisited” are responsible respectively for removing from the  $CL$  the values visited in the neighborhood of the selected vertex and updates the vector  $\bar{V}$ , that contains the sensors visited in the neighborhood of the chosen candidate. The parameter  $G$  that the constructive receives is the graph that represents the network. This method generates the set that has to be visited to ensure that all data were collected. With this, the first phase for finding a solution is complete. Now it is necessary to find an order to visit the chosen sensor with the heuristics of the VRP.

### 3.3 Vehicle Routing Problem (VRP)

This phase can be viewed as a VRP, as the necessity to visit all sensors is defined as a dominating set without consuming more than the capacity for the battery. This constructive uses the nearest neighborhood constructive defined as one heuristic for collecting that gets the sensor with the minimum distance to a node and then calculates if it is possible to visit the next chosen candidate and return to the base. For this approach, the cost function  $h$  is defined as the distance to visit a node.

6 I. Morais et al.

For this problem, an approach similar to the presented in Section 3.2, but the version used here is the minimization version because it is necessary to find a way of reducing the cost for the UAV travel. The differences are presented in Equation 3.

$$RCL^{min} = \{i \in \mathcal{CL}_{vrp} \setminus \mathcal{S} \mid h_{min} \geq h_i \geq h_{max} - \alpha(h_{max} - h_{min})\} \quad (3)$$

In Equation 3, the cost function  $h$  concerns the distance of adding one sensor in a trip, while the other elements are the same as the ones presented in Equation 2.

Using the defined equation to diversify solutions generated for the VRP and maintaining the battery restriction, a path is chosen using Algorithm 2.

---

**Algorithm 2:** Vehicle Routing Problem

---

```

1 Data:  $S, \alpha, max_{capacity}$ 
2 begin
3    $\mathcal{NS} \leftarrow \emptyset;$ 
4    $\mathcal{NS} \cup \mathcal{B};$ 
5    $CL_{vrp} \leftarrow \text{CreateCandidateList}(S);$ 
6    $capacity = 0;$ 
7    $cost = 0;$ 
8   while  $CL_{vrp}$  not  $\emptyset$  do
9      $RCL^{min} \leftarrow \text{GenerateRCLVRP}(CL_{vrp}, \alpha);$ 
10     $v \leftarrow \text{rand}(RCL^{min});$ 
11     $o \leftarrow$  last  $\mathcal{NS}$  value ;
12    if  $capacity + \text{get\_distance}(o, v) + \text{get\_distance}(v, \mathcal{B}) \leq max_{capacity}$ 
13      then
14         $\mathcal{NS} \cup v;$ 
15         $capacity \leftarrow \text{get\_distance}(o, v);$ 
16         $CL_{vrp} \leftarrow CL_{vrp} \setminus v;$ 
17         $cost \leftarrow cost + \text{get\_distance}(o, v);$ 
18      end
19    else
20       $\mathcal{NS} \cup \mathcal{B};$ 
21       $cost \leftarrow cost + \text{get\_distance}(o, \mathcal{B});$ 
22       $capacity \leftarrow 0;$ 
23    end
24  end
25  return  $\mathcal{NS}, cost;$ 
26 end
    
```

---

The set  $\mathcal{NS}$  represents the new solution created for the DMRP-wLA with its cost. The function GenerateRCLVRP calculates the distance between every candidate possible to visit. With the two constructive procedures executed, a complete solution is returned with its cost. For improving the solution quality, a local search procedure is defined in Subsection 3.4.

### 3.4 Random Variable Neighborhood Descent (RVND)

Local search is a heuristic procedure that changes components from the candidate solution, searching in the solution space for improving a solution’s quality based on a previously found solution. It consists of searching in the neighborhood definition for a change in a solution for improving the quality, guiding it to a local optimum. In this paper, two traditional neighborhoods were defined, using only existing neighborhoods for the VRP problem. In this paper, the used neighborhoods are the 2-Opt and the shift inter-trips (inter-trips are defined as a trip before returning to the base). The local search is the uses best improvement policy that tests every solution in the neighborhood then executes the best movement.

The 2-Opt, Figure 1, neighborhood structure consists of exploring the candidate solution, selecting two vertices and switching their position. As an example, the path for the trip on the left is using the arcs (2,3),(3,4),(4,5) and (5,6), and vertices 3 and 5 were chosen. The right trip represents the movement that uses the arcs (2,5),(5,4),(4,3) and (3,6) and explains the reversion made by the 2-Opt neighborhood.

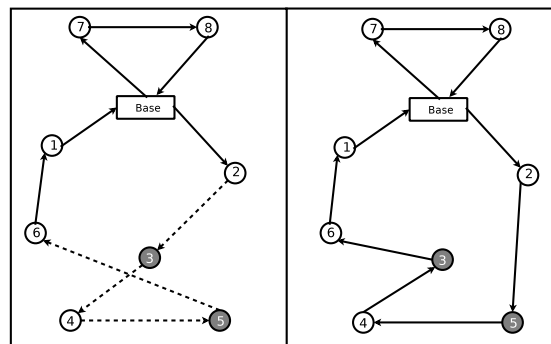


Fig. 1: Neighborhood structure 2opt

Neighborhood structure Shift, Figure 2, consists of exploring the search space by selecting a vertex and search for a new position, testing its insertion between every two vertices in a cycle, in the same route, and placing it in the position that best improves the solution. For example, the selected vertex is 4, connected by the arcs (5,4) and (4,3). The vertex is reinserted between the arc (3,6), generating a new solution that contains arcs (5,3),(3,4) and (4,6).

Random Variable Neighborhood Descent [12] is a local search process that combines more than one neighborhood structure, using the idea that it is hard to determine which order for the exploration of a neighborhood structure is better to explore. Having said that the order of exploration of the neighborhood is shuffled at the beginning of the local search phase, detailed in Algorithm 3.

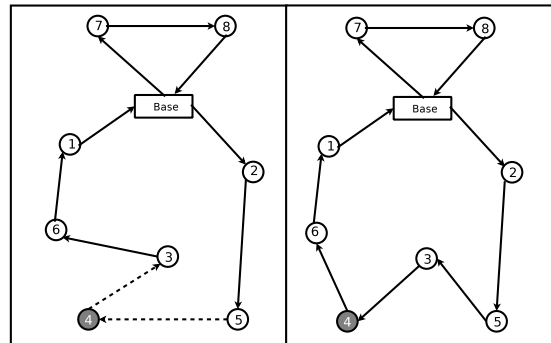


Fig. 2: Neighborhood structure Shift

---

**Algorithm 3: RVND for the DMRP-wLA**

---

```

1 Data: S
2 begin
3   Shuffle( $N^{2-opt(1)}, N^{Shift(2)}$ );
4    $k \leftarrow 1, S^* \leftarrow S$ ;
5   while  $k \leq 2$  do
6     Find best  $s' \in N^k(s)$ ;
7     if  $f(s') < f(s^*)$  then
8        $s^* \leftarrow s'$ ;
9        $k \leftarrow 1$ ;
10    else
11       $k \leftarrow k + 1$ 
12    end
13  return  $s^*, cost$ 
14 end

```

---

This procedure first randomizes the two neighborhood structures and then explores the neighborhoods in the pre-defined order to improve the solution received as a parameter. The function  $f$  evaluates the cost of a solution. After this component, the constructive and the local search procedure are united in a metaheuristic described in the next section.

### 3.5 Greedy Randomized Adaptive Search Procedure (GRASP)

In search of high-quality solutions, a Greedy Randomized Adaptive Search Procedure (GRASP) is used. The proposed GRASP combines the constructive heuristics and local search procedure [5]. This proposed GRASP generates a solution with the semi-greedy adaptive constructive that unites the heuristic for the minimum dominating set and the VRP with the RVND local search procedure. The best solution found is chosen as the solution for the problem. Algorithm 4 describes in detail the proposed method.

---

**Algorithm 4: GRASP-RVND**

---

```

1 Data:  $\alpha, max_{iter}$ 
2 begin
3    $bestcost \leftarrow \infty;$ 
4   for  $i$  from 1 to  $max_{iter}$  do
5      $s' \leftarrow \text{MinimumDominatingSet}(\alpha);$ 
6      $s', cost \leftarrow \text{VehicleRoutingProblem}(s', \alpha, max_{capacity});$ 
7      $s', cost \leftarrow \text{RVND}(s');$ 
8     if  $cost < bestcost$  then
9        $s^* \leftarrow s';$ 
10       $k \leftarrow 1;$ 
11    end
12  end
13 end

```

---

## 4 Computational Experiments

This section is divided into two sub-sections that present more from the applied scenario and explore the proposed methodology results. The case instances are based on the two urban forests from Brazil: Tijuca's National Park and Pedra Branca State Park.

### 4.1 Instances Generation

The applied context consists of using sensors and a smartphone application that captures the last active location of the person while in the urban forest to reduce the rescue time whenever someone gets lost. This data would only be used when people are lost and firefighters need it to rescue the missing person.

For the applied scenario, five instances were created based on the limits defined on two urban forests from Rio de Janeiro. The first four instances are defined based on the Tijuca's National Park. The others consider the Pedra Branca State Park. Sensors placements are defined as a grid that intersects the polygon of the urban forest limits. All points are approximately 200 meters of distance between each other, so they can intercept each other and communicate data. The distance between sensors is structured based on a real sensor distance radius of 110 meters to connect sensors. Figure 3 presents the park limits.

Instances were created using the urban forests' delimitation available at the National Register of Public Forests, which is used to manage and publicize the data about Forests in Brazil [1]. As one could notice, Tijuca's National Park is divided into four parts and was used to construct Tijuca instances. To cover all the area the possible positions would be like described in Figures 4a,4b,4c,4d, which show in more details the divisions and the sensors positioning. It is possible to notice that the urban forest has these divisions because some roads cross its area.

10 I. Morais et al.

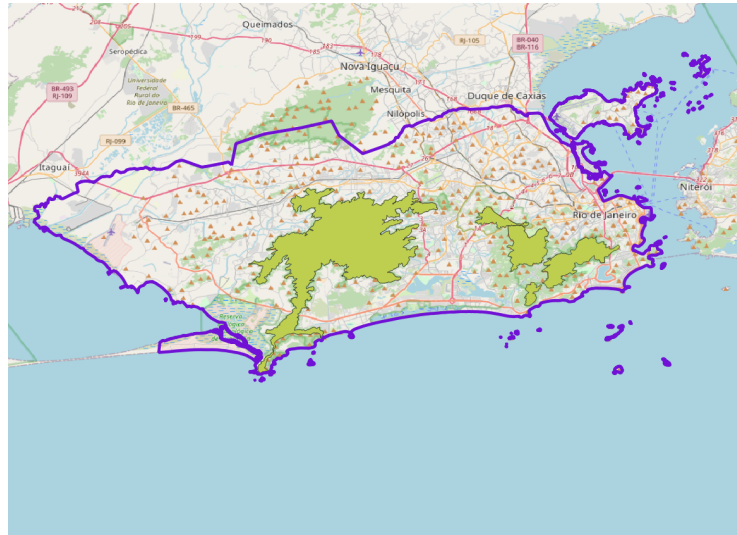


Fig. 3: Urban forest and city limits, the one in left is the Pedra Branca State Park and in the right is National park of Tijuca

The operation base is set to be in the entry of the urban forest areas. There are four different bases for Tijuca's National Park, while for Pedra Branca State Park, there is only one. Three densities were used to build the instances (60%, 70% and 90%) considering the percentage of the urban forest's area covered by the sensors. To define this, a sensor list with all sensor's degree of centrality was used and, after sorted, the sensors with the lowest degree were removed. Figures 5a, 5b, 5c, 5d show an example of the removed sensors. One may notice that the sensors near the limits of the urban forest are removed since they have fewer connections.

To create the instances, we considered that every sensor can multi-hop with its first neighbors and three levels of its neighborhood. To evaluate these neighborhoods, a Breadth-First Search (BFS) was used to create the neighborhood access and reduce the sensors that have to be visited.

From a practical point of view, the necessary infrastructure cost concerns to acquire the sensors, installing the sensors in the designated positions in the urban forest and the UAV. Sensors could be made using low-cost technologies like Arduino with a Wi-Fi shield, a data storage shield, and a battery shield that accepts two 18650 batteries, which can be associated in series in order to have a higher autonomy. Considering these specifications, the sensors would cost, at most, 70 US dollars. This data survey for the costs was done in August 2021 at Amazon.com. Deploying the sensor for all possible established positions would cost 338,660 US dollars. The studied scenarios considered covering 60%, 70%, 90% of the possible positions in the urban forest. However, to perform an economic analysis, the UAV price has to be taken into account. As the prices

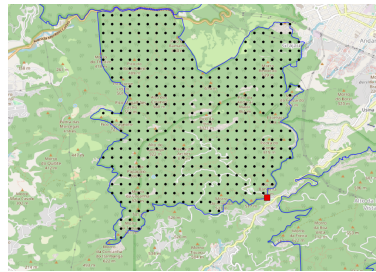
Title Suppressed Due to Excessive Length 11



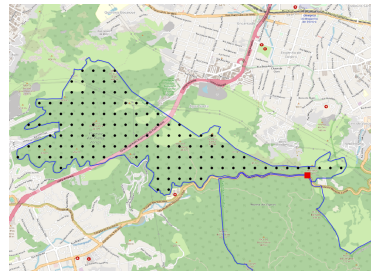
(a) Tijuca's National Park - Part 1



(b) Tijuca's National Park - Part 2



(c) Tijuca's National Park - Part 3



(d) Tijuca's National Park - Part 4

Fig. 4: Images with the total of sensors. (Black represent sensors and red the base)

depend on ranges and autonomy, it would be necessary to evaluate with more detailed specifications, which was not the focus of this project. The computational experiments are executed considering these instances.

## 4.2 Computational Results

The experiments were performed in a Intel Core i5 2.3 GHz with 16 GB of RAM machine and were implemented in C++. The main results are presented in Table 1, which details: (i) the best cost (BST), which is the sum of the distances covered in each trip of the best solution; (ii) the average cost (AVG), which is the average of the distances of the ten best solutions found; (iii) standard deviation for the solution (STD), related to the distance; (iv) average time to find the best solution (AVG.TIME); (v) standard deviation for time (STD.TIME); (vi) number of trips of the best solution (TRIPS); (vii) average number of trips (AVG.TRIPS); and (viii) standard deviation (STD.TRIPS).

The costs of solutions are presented in kilometers, the time to obtain solutions in seconds and trips are defined as collecting sensors and returning to the base with collected data. The instance names are defined as the name of the urban forest and the proportion of area covered. The UAV autonomy is defined as twice the distance between the base and the farthest sensor to be visited for the experiments. So, by adopting this autonomy, it guarantees that every instance

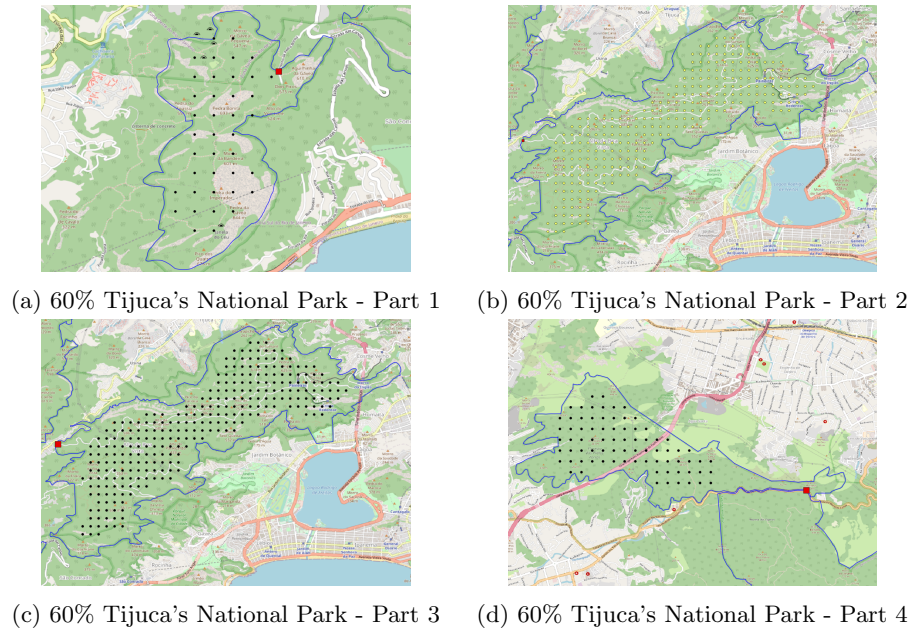


Fig. 5: Images of the reduction by 60% of sensors.(Black represent sensors and red the base)

has at least one feasible solution. Considering a 100% coverage, Pedra Branca State Park would have 3,448 sensors, while each of the four divisions of Tijuca's National Park would have, respectively, 68, 464, 401, 131 sensors.

As shown in Table 1 one may notice that the biggest time to obtain a solution is approximately 20 seconds which is not a problem as the routes are only used in the necessity of a rescue operation. Besides, the value is almost insignificant compared to the time a rescue operation team would take to search the whole area covered by the sensors.

Note that the number of sensors is not the only factor influencing solution costs: considering 60% of coverage, the Tijuca 3 has twice as many sensors as Tijuca 1, but the cost of the best solutions is almost ten times bigger. So, if someone intends to work with this problem, it has to have in mind that the solution cost does not increase linearly considering the growth in the number of sensors.

Regarding the number of trips, Pedra Branca State Park is the most challenging urban forest to be monitored. It would be necessary to cover the area defined in the proposed scenarios from 68 trips (in the smaller instance) to 81 trips. As for Tijuca's National Park, the maximum number of required trips is 16. Besides, less than ten trips would be necessary for seven of the twelve instances related to Tijuca's National Park. However, the proposed approach would still be valuable in supporting the rescue tasks considering the size of the monitored areas and

Title Suppressed Due to Excessive Length 13

Table 1: Computational Results

Instance	BST(KM)	AVG	STD	AVG.TIME	STD.TIME	TRIPS	AVG.TRIPS	STD.TRIPS
PedraBranca_0.6	1,522.64	1,556.72	17.40	10.709	1.009	68	69.90	10.90
PedraBranca_0.7	1,717.16	1,743.37	18.17	18.372	2.028	77	78.10	14.90
PedraBranca_0.9	2,008.55	2,069.09	30.75	20.125	1.258	81	83.60	26.40
Tijuca_1.0.6	3.77	4.39	350.24	0.005	0.001	1	1.80	1.60
Tijuca_1.0.7	5.37	5.58	140.98	0.006	0.000	2	2.00	0.00
Tijuca_1.0.9	6.36	6.66	343.81	0.007	0.000	2	2.10	0.90
Tijuca_2.0.6	103.68	114.77	5.35	0.072	0.004	11	11.90	2.90
Tijuca_2.0.7	122.06	130.71	3.54	0.099	0.008	13	13.70	2.10
Tijuca_2.0.9	158.75	166.46	4.25	0.197	0.014	16	16.70	2.10
Tijuca_3.0.6	57.21	65.94	3.90	0.060	0.002	9	10.10	2.90
Tijuca_3.0.7	75.21	79.97	2.49	0.079	0.005	11	12.00	2.00
Tijuca_3.0.9	96.94	103.87	3.83	0.122	0.009	14	14.70	2.10
Tijuca_4.0.6	33.64	34.93	1.63	0.012	0.001	5	5.10	0.90
Tijuca_4.0.7	34.77	38.77	2.51	0.016	0.002	5	5.60	2.40
Tijuca_4.0.9	44.00	50.32	2.85	0.026	0.005	6	7.00	2.00

the difficult of access (due to its forests features). It is important to emphasize that, even in the instances with smaller coverage (as 60%), the proposed approach would help rescue tasks, giving insight into missing people instead of searching in the whole urban forest. In this case, the rescue team would consider the last information collected in the monitored part to reduce the search area. Therefore, it would only be necessary to perform the rescue search in the area near the last information collected.

From the operational point of view, considering a UAV that travels at a speed of 40 km/h, collecting all the data from sensors would take on average 10 hours. However, each concluded trip gives insights about the person's location. If the last timestamp registered by the sensors are, for example, in the first trip, the UAV search could be interrupted. So, the time to identify the person's location might be inferior to 4 hours. Therefore, this governance knowledge could be joined to the heuristics procedure to improve efficiency.

Besides, in a real case, the decision-maker would know the critical areas for people to get lost, and the order of the trips could be modified to attend first these critical areas. Thus, the search process would be improved. In addition, other types of drones with higher speeds could be used instead of a UAV, reducing, even more, the rescue operation time.

In the end, we emphasize that the proposed decision-making tool needs interaction with the public agent to propose better solutions. Therefore, it would be helpful in the smart cities design since it deals with two issues pointed by [2]: the coordination of urban technologies and the development of models and methods for using urban data across spatial and temporal scales.

## 5 Conclusions and Future Works

This paper proposed a method that could be used as a decision-making tool to support the rescue search in urban forests. This support system would pro-

vide the last known person's location or, at least, restrict the search area in a reasonable computational time.

The method obtained solutions within 20 seconds. In these solutions, the time to collect the data was lesser than 4 hours. Besides, using data sensors to get information about missing people in urban forests would improve the efficiency (less public resource would be consumed in these hard rescue tasks) and the effectiveness of the rescues (the person would wait less time to be rescued). The proposed approach could also obtain information regarding areas that have to be closed or noticed as risk areas, generating more knowledge to be used in public policies and minimizing the risk of someone or some group getting lost.

We identified that the number of sensors is not the only factor that influences in the results. Therefore, it should be performed experiments with different base positions in order to evaluate this change in costs. The financial analysis of implementing this system could also be evaluated.

As future works, one may search for more insights of solution quality. Exact methods can be used to find how close the obtained solutions of the proposed method are to the optimal solution. With this would be possible to propose other heuristics procedures to find better solutions for instances of different structures and types. That would reduce the costs associated with creating this infrastructure and the rescue task for the public sector.

## 6 Acknowledgement

The authors thank the CYTED Thematic Network "Ciudades Inteligentes Totalmente Integrales, Eficientes y Sostenibles (CITIES)" no 518RT0558.

## References

1. of Agriculture, M.: Cadastro Nacional de Florestas Públicas - Atualização 2019 (2019 (accessed September 10, 2020)), <http://www.florestal.gov.br/cadastro-nacional-de-florestas-publicas/127-informacoes-florestais/cadastro-nacional-de-florestas-publicas-cnfp/1894-cadastro-nacional-de-florestas-publicas-atualizacao-2019>
2. Batty, M., Axhausen, K.W., Giannotti, F., Pozdnoukhov, A., Bazzani, A., Wachowicz, M., Ouzounis, G., Portugali, Y.: Smart cities of the future. *European Physical Journal: Special Topics* **214**(1), 481–518 (2012). <https://doi.org/10.1140/epjst/e2012-01703-3>
3. Erdelj, M., Król, M., Natalizio, E.: Wireless sensor networks and multi-uav systems for natural disaster management. *Computer Networks* **124**, 72–86 (2017)
4. Ferraris, A., Santoro, G., Papa, A.: The cities of the future: Hybrid alliances for open innovation projects. *Futures* **103**, 51–60 (2018). <https://doi.org/10.1016/j.futures.2018.03.012>, <https://doi.org/10.1016/j.futures.2018.03.012>
5. Gendreau, M., Potvin, J.Y.: *Handbook of Metaheuristics*. Springer Publishing Company, Incorporated, 2nd edn. (2010)

Title Suppressed Due to Excessive Length 15

6. Hammad, A.W., Akbarnezhad, A., Haddad, A., Vazquez, E.G.: Sustainable zoning, land-use allocation and facility location optimisation in smart cities. *Energies* **12**(7) (2019). <https://doi.org/10.3390/en12071318>
7. Institute, C.M.: Relatório Anual Tijuca, 2017 (2019 (accessed September 10, 2020)), [http://parquenacionaldatijuca.rio/files/report\\_anual\\_2017.pdf](http://parquenacionaldatijuca.rio/files/report_anual_2017.pdf)
8. Meghanathan, N.: On the use of centrality measures to determine connected dominating sets for mobile ad hoc networks. *Int. J. Ad Hoc Ubiquitous Comput.* **26**(4), 205–221 (Jan 2017). <https://doi.org/10.1504/IJAHUC.2017.087886>, <https://doi.org/10.1504/IJAHUC.2017.087886>
9. Munhoz, P.L., do Carmo, F.P., Souza, U.S., Drummond, L.M., González, P.H., Ochi, L.S., Michelon, P.: Locality sensitive algorithms for data mule routing problem. In: *International Conference on Algorithmic Applications in Management*. pp. 236–248. Springer (2019)
10. Munhoz, P.L.A., González, P.H., dos Santos Souza, U., Ochi, L.S., Michelon, P., Drummond, L.M.d.A.: General variable neighborhood search for the data mule scheduling problem. *Electronic Notes in Discrete Mathematics* **66**, 71–78 (2018)
11. Neirotti, P., De Marco, A., Cagliano, A.C., Mangano, G., Scorrano, F.: Current trends in smart city initiatives: Some stylised facts. *Cities* **38**, 25 – 36 (2014). <https://doi.org/https://doi.org/10.1016/j.cities.2013.12.010>, <http://www.sciencedirect.com/science/article/pii/S0264275113001935>
12. Silva, M.M., Subramanian, A., Ochi, L.S.: An iterated local search heuristic for the split delivery vehicle routing problem. *Computers & Operations Research* **53**, 234 – 249 (2015). <https://doi.org/https://doi.org/10.1016/j.cor.2014.08.005>, <http://www.sciencedirect.com/science/article/pii/S0305054814002159>
13. Sugihara, R., Gupta, R.K.: Path planning of data mules in sensor networks. *ACM Transactions on Sensor Networks* **8**(1), 1:1–1:27 (Aug 2011)

## Clasificación de perfiles de comportamiento para clientes no-residenciales considerando variable de consumo de energía eléctrica con/sin presencia de sistema de generación distribuida.

Jerson Olegario San Martín Ayala<sup>1</sup>, Luis García-Santander<sup>2</sup>[0000-0002-6474-6528],  
Dante Carrizo<sup>3</sup>[0000-0002-3011-9358] and Fernando Ulloa-Vásquez<sup>4</sup>[0000-0003-2897-2867]

<sup>1</sup> Universidad de Concepción, Concepción. E. Larenas 219, CHILE

<sup>2</sup> Universidad de Concepción, Concepción. E. Larenas 219, CHILE

<sup>3</sup> Universidad de Atacama, Copiapó. Av. Copayapu 485, CHILE

<sup>4</sup> Universidad Tecnológica Metropolitana, Santiago. Virginio Arias 1360, CHILE  
jesanmartin@udec.cl luis.garcia@udec.cl dante.carrizo@uda.cl  
fulloa@utem.cl

**Abstract.** El presente trabajo permite caracterizar y clasificar los perfiles de consumo de clientes no residenciales en función de las curvas de consumo obtenidas a partir de los registros reportados por 934 medidores inteligentes en el periodo de enero a diciembre del 2019 y que pertenecen a una empresa distribuidora de energía eléctrica en Chile.

Para lograr la caracterización y clasificación de los perfiles de consumo, se determinaron 3 días típicos a analizar, los cuales corresponden a día laboral, día sábado, y día domingo o festivo. Estos 3 días típicos fueron analizados para cada trimestre del año 2019. El procesamiento de los datos se realizó en las plataformas *Power Bi* y *Matlab*. En la primera se trabajaron los datos entregados por la empresa eléctrica, obteniendo las curvas de consumo promedio para cada cliente en cada periodo de estudio considerado, mientras que en la segunda se realizó la visualización, y clasificación de las curvas mediante el algoritmo *k-means*, para finalmente obtener los resultados y conclusiones.

Los resultados evidencian la existencia de 7 perfiles típicos representativos del comportamiento de los clientes no residenciales, los cuales, en algunos casos, muestran comportamientos similares o compartidos, a pesar de ser de categorías distintas.

**Keywords:** clustering, cliente no residencial, k-means, perfil de carga, medidores inteligentes.

### 1 Introducción

Los perfiles de consumo en un cliente, describen el comportamiento de estos, siendo fundamentales para las empresas proveedoras del suministro eléctrico, ya que con esto

pueden conocer cuándo y en qué momento sus clientes requieren la energía eléctrica. Esta información es útil tanto para la planificación como la operación de las redes eléctricas, optimizando así los sistemas eléctricos. Con la llegada de los medidores inteligentes o Smart Meters (SM) las empresas eléctricas obtienen mayor información del consumo de sus clientes, lo cual significa una ventaja en comparación a los años anteriores. A partir de la información que proveen los SM es posible caracterizar las curvas de consumo de los clientes para cada día en específico, teniendo mediciones de energía cada 15 minutos, lo que implica un total de 96 mediciones por día para cada cliente. La presencia de Generación Distribuida (GD) en algunos de los clientes del sistema en estudio, impacta en el comportamiento de los perfiles de carga y por lo tanto será un aspecto a considerar en este estudio.

Este trabajo tuvo por finalidad analizar perfiles de carga de clientes, agruparlos, clasificarlos e identificar los perfiles típicos para los diferentes tipos de clientes no residenciales considerados en el estudio. Los resultados obtenidos son importantes para la empresa asociada ya que le permite conocer los perfiles de consumo de sus clientes, actualizarlos, y considerar nuevos perfiles característicos de consumo, los cuales se relacionan estrechamente con las actuales demandas de energía de los clientes.

## 2 Perfil de carga

Un perfil de carga se define como una curva que representa el consumo de potencia de un cliente en particular en función del tiempo, pudiendo ser este diario, semanal, mensual o incluso anual. Las empresas de distribución de energía eléctrica consideran distintas categorías de clientes en función de su curva de consumo, los más típicos son residenciales, comerciales, industriales y retail. Cada uno de los clientes especificados anteriormente tienen distintos comportamientos, puesto que estos dependen específicamente de sus ciclos de operación en las actividades y requerimientos de potencia. El perfil de consumo, depende de diversos factores entre los cuales podemos mencionar por ejemplo, hábitos de consumo de los usuarios, niveles socioeconómicos, aspectos socioculturales, clima de la región, sector productivo, tamaño de la empresa, entre otras [1]. El importante crecimiento que ha tenido la incorporación de las fuentes de energía cercana los centros de consumo o Generación Distribuida (GD), la penetración del Vehículo Eléctrico (VE), los equipos de almacenamiento (baterías), los sistemas de climatización, electrodomésticos inteligentes, han provocado cambios los patrones de consumo en prácticamente en todos los clientes conectados a las redes de distribución [2]. Este nuevo escenario energético, que se ha vuelto más dinámico conlleva a que las empresas de distribución de energía eléctrica deban tener un sistema que les permita conocer con mayor certeza los perfiles de consumo de sus clientes de modo de alcanzar una optimización de la operación y planificación de su infraestructura eléctrica y evaluar la posibilidad de disponer nuevas tarifas finales hacia los clientes, acordes a la demanda requerida por cada uno de ellos.

### 3 Perfiles actuales de la empresa de distribución

Los datos de consumos aportados por la empresa distribuidora para los 934 clientes para el periodo enero-diciembre 2019, permitirán en primer lugar identificar y clasificar los actuales perfiles de consumo que poseen los clientes que están conectados a sus redes de distribución. Posteriormente estos serán comparados con los perfiles que la empresa ha trabajado históricamente para sus planificaciones y operaciones de la red eléctrica. En Fig. 1 y Fig. 2 se representan los perfiles de consumo actuales que la empresa considera para los clientes industriales y comerciales, respectivamente. Se destaca el hecho de que solo existe un perfil característico para cada cliente, para todo el año, a diferencia de lo presentado en esta metodología, la cual presentan más de un perfil característico, para distintos días típicos del año.

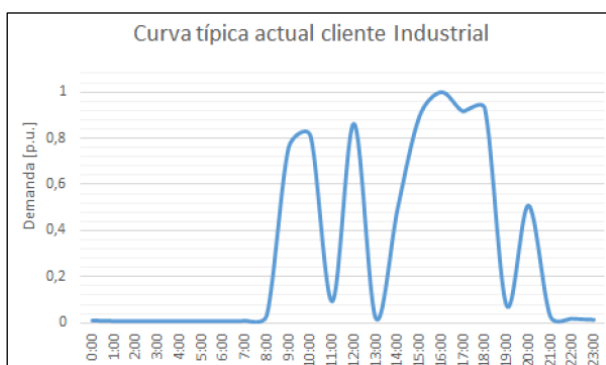


Fig. 1. : Perfil de consumo característico normalizado de cliente industrial, de acuerdo a los registros de la empresa. [Elaboración propia]

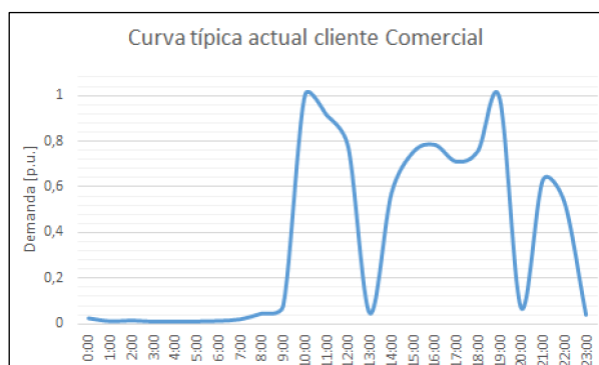


Fig. 2. Perfil de consumo característico normalizado de cliente comercial, de acuerdo a los registros de la empresa. [Elaboración propia]

## 4 Base de datos disponible

Los datos a utilizar para este trabajo fueron los proporcionados por una empresa distribuidora de energía de Chile. Esta empresa tiene alrededor de 6.700 clientes con medidores inteligentes instalados, entre los cuales se encuentran también clientes que presentan instalaciones de GD. La información que recogen los medidores inteligentes corresponden a mediciones en intervalos de 15 minutos de energía activa y reactiva, estas mediciones de energía consideran las inyecciones y los consumos del cliente. Además, se dispone de información complementaria tales como comuna, tarifa contratada, potencia conectada, actividad económica y constante de amplificación.

## 5 Metodología utilizada

La minería de datos tiene como objetivo preparar, sondear, y explorar los datos para obtener información útil de ellos [3]. En esta sección se describe la metodología de la minería de datos aplicada a cada etapa al caso en estudio con el fin de obtener resultados que permitan un análisis y las respectivas conclusiones del estudio. Las etapas de la minería de datos a aplicar son las siguientes:

### 5.1 Notación de la información

Para simplificar la notación de cada cliente y periodo en cada situación se utilizó la siguiente notación:

#### Tipo de cliente

- I1 : Cliente industrial con potencia instalada  $\leq 10$  kW.
- I2 : Cliente industrial con potencia instalada  $> 10$  kW.
- C1 : Cliente comercial con potencia instalada  $\leq 10$  kW.
- C2 : Cliente comercial con potencia instalada  $>10$  kW.

#### Trimestre a considerar

- T1 : Trimestre 1 (enero a marzo); T2 : Trimestre 2 (abril a junio)
- T3 : Trimestre 3 (julio a septiembre); T4 : Trimestre 4 (octubre a diciembre)

#### Tipo de día a considerar

- D : Día domingo o festivo; L : Día laboral; S : Día sábado

## 5.2 Selección de clientes

Los clientes seleccionados para este análisis serán los catalogados como no residenciales, siendo estos del tipo comercial e industrial. Como primer criterio para determinar cuáles se considerarán en el análisis, se estableció un mínimo del 80% de pulsos válidos para cada periodo en estudio, quedando una totalidad de 960 clientes a analizar, los cuales se desglosan en 853 clientes comerciales y 107 clientes industriales. Posteriormente, se eliminaron del análisis a aquellos clientes que tenían mediciones con curvas promedio nulas, es decir, valor cero para todo el rango de medición [3], mediciones con valores negativos, y también a aquellos que tenían menos de 20 valores diferentes en los intervalos de medición para cada día típico a considerar [4]. Finalmente, se consideraron como clientes válidos a aquellos que tenían al menos un perfil de día típico para cada trimestre en estudio [2].

Se determinó no considerar a todos aquellos clientes que poseen tarifas especiales. Dado que en la base de datos existen clientes con potencia instalada menor a 10 kW, y lo esperado para un cliente no residencial es que su potencia instalada sea mayor a 10 kW, se determinó dividir este análisis de acuerdo a la potencia instalada, siendo 10 kW el umbral que determina cada grupo. Esto se realizó con el fin de encontrar diferencias entre el comportamiento de los clientes bajo este criterio de diferenciación. La Tabla 1 resume los clientes considerados bajo este razonamiento.

**Tabla 1. Cantidad de clientes considerados en el estudio, según el criterio de los 10 kW.**

<b>Categoría</b>	<b>Clientes con potencia instalada menor o igual a 10 kW</b>	<b>Clientes con potencia instalada mayor a 10 kW</b>
Industrial	58	42
Comercial	399	435
<b>Total</b>	<b>457</b>	<b>477</b>

## 5.3 Selección de variable en estudio

Considerando que los datos entregados correspondían a mediciones de energía (activa), se utilizó la ecuación (1) para obtener las potencias activas en cada bloque de 15 minutos, representando este valor la demanda de cada cliente en el periodo obtenido:

$$P_a [\text{kW}] = (E_d [\text{kWh}] - E_r [\text{kWh}]) * 4 * cte \quad (1)$$

En donde  $P_a$  corresponde a la demanda activa en el intervalo de 15 minutos requerida por el cliente en kW,  $E_d$  es la energía activa que consume el cliente en kWh,  $E_r$  es la energía activa que inyecta el cliente hacia la red en kWh, y  $cte$  es la constante de amplificación para cada medición de acuerdo al medidor utilizado. Todas las transformaciones y cálculos se realizaron mediante la plataforma *Power Bi*.

#### 5.4 Días típicos considerados

Se definieron días típicos para el periodo en estudio, considerando una ventana de datos de un año para las mediciones inteligentes. Tomando como referencia lo propuesto por [2] se decide dividir el año en 4 periodos, esto es, verano, otoño, invierno y primavera, considerando 3 días típicos para cada temporada, siendo estos: día laboral, sábado y domingo o festivo. En resumen, para este estudio se analizaron 12 días típicos, los cuales se detallan en la Tabla 2.

**Tabla 2.** Días típicos considerados para el análisis

<b>Temporada o Periodo</b>	<b>Día típico a estudiar</b>
Verano (trimestre 1)	Día laboral, sábado, domingo o festivo
Otoño (trimestre 2)	Día laboral, sábado, domingo o festivo
Invierno (trimestre 3)	Día laboral, sábado, domingo o festivo
Primavera (trimestre 4)	Día laboral, sábado, domingo o festivo

Para la obtención de las curvas típicas de cada cliente, se utilizó nuevamente la plataforma *Power Bi*. En esta plataforma se pueden unir todas las bases de datos provenientes de las mediciones de los clientes, visualizar, y generar las curvas promedio para cada cliente de acuerdo al día típico en estudio.

#### 5.5 Normalización de curvas promedio

Para el análisis de los perfiles de carga, y su posterior clasificación, fue necesario que todas las curvas de los clientes estuviesen normalizadas con el fin de lograr un conjunto de curvas comparables. Considerando que la característica relevante del análisis es la forma de la curva, no se prestará atención a la magnitud de dicha curva, por lo tanto, se opta por normalizar los datos con el fin de obtener mediciones en el intervalo entre 0 y 1 [5]. Para lograr esta transformación matemática se utilizará la transformación Min-Max, mediante el uso de un algoritmo en Matlab®.

#### 5.6 Modelación de las curvas de consumo promedio

En esta etapa se generaron y visualizaron los perfiles de demanda promedio de los clientes, los cuales se obtuvieron al promediar las curvas de mediciones en tiempo real, para cada día típico considerado.

A continuación, a modo de ejemplo, en Fig. 3 y Fig. 4 se muestran el conjunto de perfiles representativos de los clientes comerciales con potencia instalada mayor a 10 kW considerados en este trabajo. Estos perfiles corresponden a un día laboral del cuarto trimestre del año 2019, siendo la demanda real y la demanda normalizada, respectivamente.

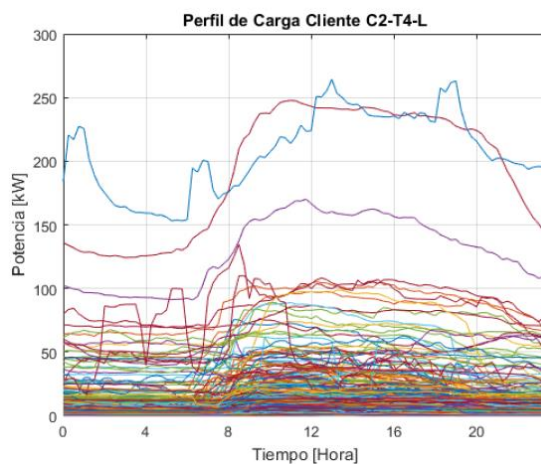


**Fig. 3. Perfiles de carga de clientes comerciales (sin agrupar).**

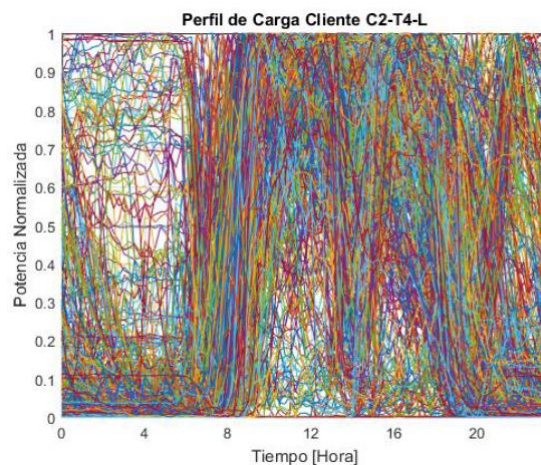


**Fig. 4. Perfiles de carga normalizados de clientes comerciales (sin agrupar).**

### 5.7 Determinación de la cantidad de grupos para el clustering

Para determinar la cantidad de grupos a utilizar en cada clustering se utilizaron índices de validación usados típicamente en trabajos de clustering con el fin de determinar el número de grupos que mejor resultado entregue. Los índices empleados en esta etapa fueron: *Índice de Silueta*, *Índice Davies-Bouldin*, *Índice Calinski-Harabasz*, y *Root Mean Square Error (RMSE)* [6]. El rango de  $k$  se fijó en el intervalo entre 1 y 5.

En Tabla 3 y Tabla 4 se resumen los valores obtenidos para  $k$ , para los clientes industriales y comerciales respectivamente.

**Tabla 3.** Número de grupos ( $k$ ) óptimos para días típicos por trimestre, en clientes industriales.

Tipo de Día	Clientes con potencia instalada menor o igual a 10 kW				Clientes con potencia instalada mayor a 10 kW			
	Trimestre				Trimestre			
	1	2	3	4	1	2	3	4
Domingo o festivo	3	3	3	3	2	3	2	2
Laboral	2	2	2	2	3	3	3	3
Sábado	2	2	2	2	3	3	3	3

**Tabla 4.** Número de grupos ( $k$ ) óptimos para días típicos por trimestre, en clientes comerciales.

Tipo de Día	Clientes con potencia instalada menor o igual a 10 kW				Clientes con potencia instalada mayor a 10 kW			
	Trimestre				Trimestre			
	1	2	3	4	1	2	3	4
Domingo o festivo	2	2	2	2	3	3	3	3
Laboral	2	2	2	2	3	3	3	3
Sábado	3	3	3	3	3	3	3	3

### 5.8 Agrupamiento de curvas mediante *K-means*

Los perfiles de consumo promedio para cada cliente, considerando los días típicos a estudiar, se agruparon mediante el algoritmo *K-means* [7], utilizando la distancia *cityblock* como medida de similitud. La Figura 5 muestra los resultados de clustering de clientes mencionado anteriormente, los tres grupos obtenidos, y el centroide característico de cada grupo. Los centroides de cada grupo se muestran marcados en azul en cada figura de agrupación.

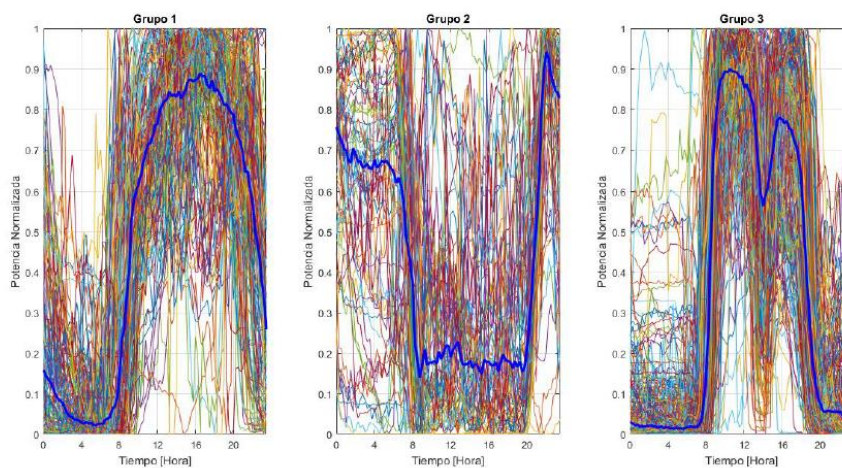


**Fig. 5. Grupos obtenidos a través del clustering mediante *K-means* para clientes comerciales con potencia instalada mayor a 10 kW, día laboral del trimestre 1.**

## 6 Resultados

De acuerdo a los resultados obtenidos, mediante la utilización *K-means*, se obtuvieron seis perfiles para los clientes no residenciales. Si bien el estudio se centró en clientes no residenciales con potencia instalada mayor a 10 kW, en esta sección se incluirán los resultados de los clientes con potencia instalada menor o igual a 10 kW debido a las similitudes encontradas. Para facilitar la comparación de las curvas, en el lado izquierdo estará la figura correspondiente al cliente industrial, mientras que en el lado derecho el correspondiente al cliente comercial.

El perfil *Tipo M* (Fig. 6) representa una jornada laboral bien definida, con dos momentos de alta demanda, separados por el horario de almuerzo, momento en que la demanda disminuye. Durante las horas en que no hay procesos o trabajo la demanda disminuye un 33% en clientes comerciales y un 50% en clientes industriales.

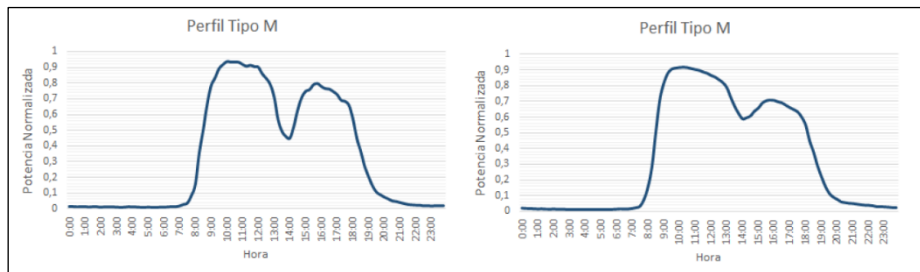


**Fig. 6. : Perfil "Tipo M" obtenido en clientes industriales I1 e I2 (L) y comerciales C1 y C2 (L), respectivamente.**

El perfil tipo Monte y/o Simple (Fig. 7) representa una jornada laboral con un comportamiento más constante durante gran parte del día, empezando a las 08:00 horas para tener peaks de demanda durante el mediodía. A diferencia del perfil tipo M, este perfil no sufre disminución de demanda en el mediodía, lo cual implique que sean industrias o comercios que tienen procesos activos durante toda la jornada laboral.

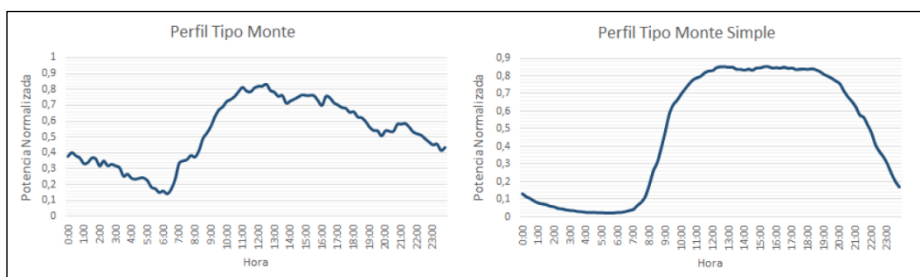


**Fig. 7. Perfil "Tipo Monte" obtenido en clientes industriales I2 (L) y comerciales C1 y C2 (L-S-D), respectivamente.**

El perfil Tipo U (Fig. 8) representa un comportamiento poco usual, más parecido al perfil de consumo del alumbrado público, debido a que evidencia altos consumos durante la noche y bajos consumos durante la jornada laboral típica. Este perfil representa evidencia altos niveles de demanda nocturna debido a la iluminación y/o sistemas de seguridad.

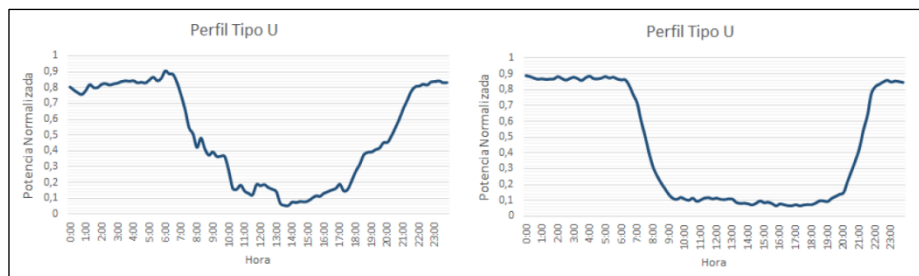


**Fig. 8. Perfil "Tipo U" obtenido en clientes industriales I1 e I2 (L-S-D) y comerciales C1 y C2 (L-S-D), respectivamente.**

El perfil Tipo Residencial (Fig. 9) muestra un comportamiento poco esperable en clientes no residenciales ya que la forma del consumo tiene semejanza a la esperable en un cliente residencial, por lo que se podría sugerir como hipótesis, que estos clientes en realidad son netamente residenciales, pero que están catalogados como industriales o comerciales por algún motivo específico o errores en la base de datos.

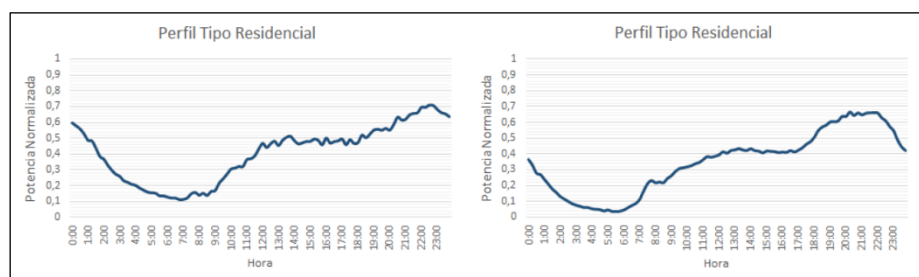


**Fig. 9. Perfil "Tipo Residencial" obtenido en clientes industriales I1 (L-S-D) y comerciales C1 (L-S-D), respectivamente.**

El perfil Tipo Monte Delgado (Fig. 10) representa un comportamiento esperable en clientes no residenciales, en donde se observa una jornada de trabajo de medio día, alcanzando su peak aproximadamente a las 12:00 horas, para luego ir disminuyendo su demanda hasta el fin del horario de trabajo (16:00 horas en clientes industriales, y 18:00 horas en clientes comerciales).

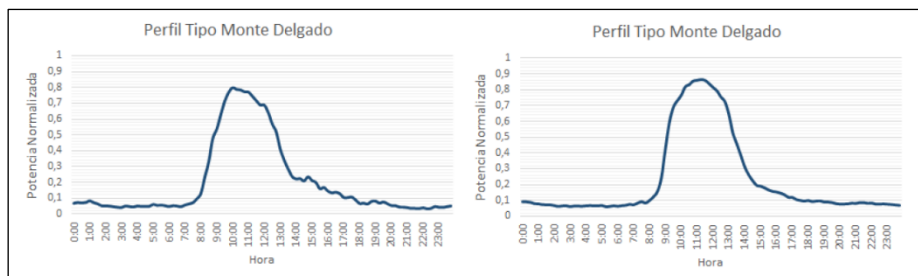


**Fig. 10. Perfil "Tipo Monte Delgado" obtenido en clientes industriales I1 e I2 (S) y en clientes comerciales C2 (S), respectivamente.**

El perfil Tipo W (Fig. 11) representa una demanda con valores similares durante el día, lo cual no evidencia un cambio notorio en la demanda de los clientes. Posiblemente este perfil agrupa a clientes con comportamientos distintos e irregulares, los cuales son representados por la curva obtenida.

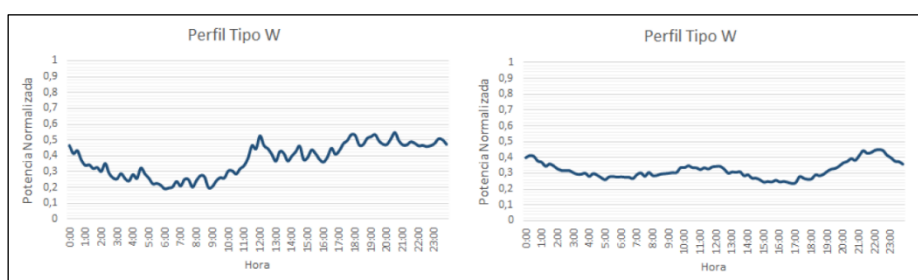


**Fig. 11. Perfil "Tipo W" obtenido en clientes industriales I1 (D) y en clientes comerciales C2 (D), respectivamente.**

## 7 Comentarios y conclusiones

La contribución de este trabajo fue la de encontrar nuevos perfiles de consume para los clientes no residenciales considerados en este estudio. Se puede afirmar que existe más de un perfil que representa a los clientes industriales y comerciales durante los distintos días típicos considerados.

Los perfiles muestran además que existe una correlación en la demanda de los clientes en función de las estaciones del año, evidenciando una similitud en los perfiles obtenidos en primavera-verano y otoño-invierno, respectivamente. Esto se evidencia de manera notoria en los perfiles tipo U.

Se aprecia que en algunos perfiles identificado existe una similitud tanto en los en clientes comerciales como industriales.

De acuerdo a los resultados se observan comportamientos similares a los de un cliente residencial, en clientes no residenciales con potencia instalada menor o igual a 10 kW, lo anterior permite deducir que estos clientes estén mal asignados en esta categoría y sean realmente clientes residenciales.

El perfil tipo M, obtenido para el día laboral, es el perfil que tiene una mayor representatividad en los clientes analizados, alcanzando un 71,44% en clientes industriales y un 51,6% en clientes comerciales. También se destaca que estos perfiles presentan siempre una menor varianza en comparación al resto de los perfiles obtenidos, teniendo un valor de 0,0304 y 0,0307 respectivamente.

Separar el análisis de los perfiles de los clientes en días típicos (domingos y festivos, día laboral, y sábado) es relevante ya que, a partir de los resultados, se demostró que los perfiles varían considerablemente entre cada día en estudio. En consecuencia, hacer esta segmentación es necesario ya que permite a las empresas distribuidoras conocer distintos comportamientos de un cliente durante la semana.

Finalmente, podemos decir que el comportamiento de los clientes es variado, lo cual implican que un único perfil no puede representar de manera correcta a una categoría de clientes no residenciales.

## **8 Trabajo futuro**

Considerar el efecto de la pandemia Covid-19 en los perfiles de carga durante los años 2020 y 2021, dado que, producto de las medidas sanitarias, tanto el sector comercial como el Industrial han visto alterados sus horarios de operación y sus requerimientos energéticos. Lo anterior significaría una modificación en los perfiles de carga de estos clientes.

Otra propuesta sería de le aplicar la misma metodología segmentando a los clientes únicamente de acuerdo a las tarifas contratadas, y no de acuerdo a la etiqueta comercial-industrial.

Y, por último, analizar y elaborar nuevos perfiles de comportamiento de los clientes considerando a aquellos que tienen generación distribuida, debido a que la base de datos disponible para este trabajo no poseía mediciones para este tipo de clientes. Es de esperar que la presencia de esta modalidad implique un cambio en la forma de los perfiles de consumo.

## References

1. D. Sánchez Ochoa, E. Pérez González y R. Cruz Rodríguez , «Characterization of the demand for electric energy considering the integration of distributed energy resources,» de 2019 FISE-IEEE/CIGRE Conference - Living the energy Transition (FISE/CIGRE), Medellín, 2019. Author, F., Author, S.: Title of a proceedings paper. In: Editor, F., Editor, S. (eds.) CONFERENCE 2016, LNCS, vol. 9999, pp. 1–13. Springer, Heidelberg (2016).
2. F. Pilo, G. Pisano y M. Troncia, «Update typical daily load profiles for LV distribution networks customers, » de 1 st International Conference on Energy Transition in the Mediterranean Area SyNERGY MED 2019, 2019.
3. Y. Belinchón Monjas, «Minería de Datos,» de Ingeniería de Telecomunicación, Universidad Carlos III de Madrid, Madrid.
4. S. Davarzani, I. Pisica y G. A. Taylor, «Study of missing meter data impact on domestic load profiles clustering and characterization, » de 51st International Universities Power Engineering Conference (UPEC), Coimbra, 2016.
5. W. J. Gil González, J. J. Mora Flórez y S. M. Pérez Londoño, «Análisis del procesamiento de los datos de entrada para un localizador de fallas en sistemas de distribución,» *Tecnura*, vol. 18, nº 41, pp. 64-75, 2014.
6. A. K. Zarabie, S. Lashkarbolooki , S. Das , K. Jhala y A. Pahwa , «Load Profile Based Electricity Consumer Clustering Using Affinity Propagation,» de 2019 IEEE International Conference on Electro Information Technology (EIT), Brookings, SD, 2019.
7. L. Marrero, D. Carrizo, L. García Santander y F. Ulloa Vásquez, «Uso de algoritmo K-means para clasificar perfiles de clientes con datos de medidores inteligentes de consumo eléctrico: Un caso de estudio,» de XI Conferencia Internacional de Computación e Informática del Norte de Chile (INFONOR 2020), Copiapó, 2020.

# Open-source big data platform for real-time geolocation in smart cities

Pedro Moreno-Bernal<sup>1</sup>[0000-0002-2811-5331], Carlos Alan Cervantes-Salazar<sup>1</sup>,  
Sergio Nesmachnow<sup>2</sup>[0000-0002-8146-4012], Juan Manuel  
Hurtado-Ramírez<sup>3</sup>[0000-0003-1710-7886], and José Alberto  
Hernández-Aguilar<sup>1</sup>[0000-0002-5184-0005]

<sup>1</sup> Universidad Autónoma del Estado de Morelos, Cuernavaca, Morelos, México  
{pmoreno, jose.hernandez}@uaem.mx, alan.cervantes19@gmail.com

<sup>2</sup> Universidad de la República, Uruguay  
sergion@fing.edu.uy

<sup>3</sup> Instituto de Biotecnología, Universidad Nacional Autónoma de México,  
Cuernavaca, Morelos, México  
jmanuel@ibt.unam.mx

**Abstract.** Nowadays, big data analytic tools and Internet of Things applications boost productivity in Intelligent Transportation Systems in the context of smart cities. Each day, location mobility data are generated continuously from Global Positioning System devices in a high temporal granularity. This article introduces a framework for public transportation mobility analysis. The proposed big data platform uses open source components for real-time geolocation tracking processing. The platform collects location information over Message Queue Telemetry Transport protocol to Apache Kafka, and then information is processed using Apache Storm, which guarantees fault tolerance, horizontal scalability, and low latency. Experimental evaluation is performed for a case study considering 10357 taxi tours (17 million GPS timestamps) using problem instances of different sizes. Results demonstrate that the proposed open-source big data platform is capable of processing a significantly large number of GPS timestamps of tested instances in reasonable execution times.

**Keywords:** Big Data · Internet of Things · real-time geolocation tracking

## 1 Introduction

Today, the Big Data revolution is advancing, and the Internet of Things (IoT) is driving it as an essential part of a transformative era of technology changes under the paradigm of smart cities [11]. As part of technological changes, urban mobility needs to provide intelligent mobility services that anticipate future changes and participate in decision-making. Mobility in high-density cities is complex for traffic, the different transportation modes, and the multiple origins

2 P. Moreno, C. Cervantes, S. Nesmachnow, J. Hurtado, J. Hernández

and destinations [19]. In recent years, traffic congestion and pollution have become a severe problem for the most significant cities. Cities are complex and dynamic and have associated problems related to high densities and mobility activities [13]. Traffic congestion is a severe problem that causes significant economic losses and impacts the quality of life of citizens. Hence, it is necessary to build intelligent traffic management systems by urban mobility tracking for achieving urban transportation efficiency and safety. For this reason, transportation systems require effective mobility techniques to reduce traffic incidents and congestion. In addition, transportation systems must ensure travel safety and efficiency, avoid negative impacts on the local economy, reduce environmental pollution, movement tracking, and impact the quality of people's lives, converging into Intelligent Transportation Systems (ITS). ITS are mobility systems that use technological advances, methods, and applications of the Information and Communication Technologies (ICT) field, with high technology and mobility data. ICT gather a wide range of data from sensors, infrastructure, and geolocation of mobility devices to operate and manage scientifically [1]. Also, ICT efficiently transfer the collected data to a data center to share and exchange information between connected devices [21]. Geolocation data are generated continuously from IoT devices, and these data streams are of high temporal granularity [13]. Every day, the amount of mobility data grows at an exponential rate.

Big data integrate high technologies and large amounts of data from ICT to develop new digital systems and applications in real-time to analyze, simulate, and process mobility data. Big data techniques require effective analytics, storage technologies, and distributed processing computer tools for exploiting large amounts of data on the cloud. Analyzing and processing large amounts of data has led organizations to develop distributed solution platforms to maximize the benefits of the value of large volumes data. Big data must be able to process data from Terabytes to Zettabytes at a high-velocity rate and near-real-time to explore and exploit the power of big data [20]. In real-time analytics, large volumes of data are continuously sending by mobile devices, and they are receiving on the cloud by online services for its process, analysis, and storage. Big data tools use models of batch, stream, and iterative methods for processing large-scale data. The model selected depends on the kind of problem to solve.

This article proposes a framework for gathering and processing large volumes of real-time geolocation data in the context of ITS. The proposed framework applies distributed computing and big data processing for real-time analysis by open source tools such as Message Queue Telemetry Transport (MQTT), Apache Kafka, and Apache Storm. Furthermore, a specific application of the proposed framework is presented for real-time vehicle tracking using geolocation data. The proposed framework provides fault tolerance, horizontal scalability, and low latency through the open-source tools used. Experimental evaluation is performed using three different size problem instances of tour trajectories of 10357 taxis, including 17 million GPS timestamps. Results demonstrate that the proposed big data platform can process a significantly large number of GPS timestamps in the considered scenarios in reasonable execution times.

The rest of the article is structured as follows. Section 2 describes the urban mobility problem in the smart cities context. Section 3 describes the proposed platform for real-time processing big data approach, including a brief description of the big data technologies used. Section 4 provides details of the experimental evaluation of the proposed platform, including describing different size problem instances of tour trajectories of 10357 taxis and the discussion of the results. Finally, Section 5 presents the conclusions and formulate the main lines for future work.

## 2 Transportation geolocation problem

This section describes the importance of geolocation data and how real-time vehicle tracking is essential in the context of smart cities and ITS. Also, the section reviews the related works about big data processing problems for geolocation mobility systems applying computational intelligence and distributed computing.

### 2.1 Transport geolocation

Transport services companies such as taxis and delivery companies need to track their assets to ensure their vehicles are using appropriately. Vehicle tracking is essential to locate any asset if it is stolen or if it needs to relocate the original path. Therefore, geospatial interaction is an essential element for transportation mobility. Real-time geospatial data help to track vehicle movements to provide information about the infrastructure environment [13]. Therefore, an intelligent transportation application based on geolocation information becomes essential for efficient and safe urban transportation.

In addition, ITS must provide reliable information for drivers about their driving environment. Information of vehicles and roads help to improve driving conditions for safety, efficiency, comfortable and cleaner urban mobility. Therefore, reliable information must be collected about vehicles, location, infrastructure, road conditions, among others. Data collected allows optimized routes for safe mobility considering the capacity of the road network infrastructure. This information helps to attend to incidents and hazards by a better mobility response. Also, ITS provide better services for the different transport modes decreasing any negative economic impact. ITS interoperability require large amounts of mobility data, particularly geographical locations about vehicle mobility, to ensure the ITS functionality for public and private decision-making. Other benefits to tracking a vehicle are maintenance schedule control by kilometers, quick location of the vehicle, data collection for estimate future operational cost, improved up-time, and vehicle utilization [19].

### 2.2 Real-time geolocation data processing

ICT, sensor technologies, and digital devices use wireless sensor networks to collect real-time geospatial data automatically [2]. Wireless sensor networks pro-

4 P. Moreno, C. Cervantes, S. Nesmachnow, J. Hurtado, J. Hernández

duce large amounts of real-time geolocation data. In addition, real-time traffic monitoring uses sensors mounted on road lampposts, under pavement, on vehicles (geolocation by GPS), bridges, toll booths, traffic light poles, among others, to collect location, speed, moving directions, and weather data to estimate traffic-flow conditions in an urban mobility context. Urban mobility data in the context of smart cities provide the creation of new rules, regulations, and methods to control the traffic vehicle density growth. Also, urban mobility data permit the expansion and construction of new routes, roads, and mobility infrastructure to solve existing problems impacting significantly on the local economy.

ITS integrate big data technologies, computational intelligence techniques, and transport systems engineering to improve transportation mobility services. ITS must gather large volumes of data in real-time by IoT devices and mobile sensor networks in vehicles and road network infrastructure [15]. Also, Big data tools for ITS require adequate analysis data, storage techniques, and parallel/distributed processing tools for efficient and accurate data processing (real-time or offline). These technologies provide tools to address issues to be tackled in the context of storage technologies, batch-processing/analysis, or real-time processing/analysis [3]. Specific frameworks for real-time data analysis in Teradata scale and parallel/distributed processing in big data are Apache Storm [9] and Apache Kafka [10]. Both frameworks are characterized by fault tolerance and scalability for real-time streaming data processing. Also, these frameworks support different streaming stages such as collection, transportation, and process. Other frameworks related with similar capabilities with a functional development approach are Apache Spark and Apache Hive. Data processing is the main goal to compute relevant metrics for efficient transportation services [15].

This work focuses on distributed big data processing platforms using open source tools for real-time geolocation tracking. The goal is to track vehicles based on urban mobility for ITS in the smart cities paradigm.

### 2.3 Related works

Research in smart cities uses big data technologies and IoT to support ITS for planning urban mobility. Many ITS applications use big data analytics tools for real-time data processing. Current works are proposing different architectures and platforms to collect, process, store, and analyze urban mobility data in the context of smart cities. A brief review of related works is presented next.

Wang et al. [22] proposed a real-time streaming data processing system using Apache Storm for road traffic monitoring. The system was evaluated on problem instances built with data of one-day trajectories of 7648 taxis. Every taxi sends a GPS timestamp at intervals of 3 to 5 minutes. The taxi trajectories represent a data set of 18 million GPS locations. The experimental analysis was made in a cluster with five PCs with processor 2-core 2.4Ghz, 1 GB of RAM, and Ubuntu operating system. Experimental results showed that the proposed system guaranteed correctness and low latency. Also, the article demonstrated a practical traffic estimation in cases where traffic trajectory data streams exhibit non-homogeneous sparseness in real-time.

## Open-source big data platform for real-time geolocation in smart cities 5

Ding et al. [4] proposed a collaborative approach for the travel-time calculation of vehicles in typical business transportation problems. The approach combines spatio-temporal parallelism for real-time data and Bayes prior rules for historical data mining. The performance was evaluated on Apache Storm and Hadoop MapReduce. Apache Storm cluster was implemented on five computers with 4-Cores, 4GB of RAM, 1.2 TB storage, and Centos 6 operating system. Also, the Hadoop cluster was implemented on five computers with the same characteristics. The system was evaluated considering real-data of vehicles collected from October 2012 to January 2013, about of 100 GB of data generated from 1000 monitors on the trunk roads at Beijing. The proposed approach maintained milliseconds latencies on a high streaming processing, showing nearly linear scalability with a predictive accuracy above 80%.

Zhou et al. [26] developed an efficient streaming mass spatio-temporal data access based on Apache Storm (ESDAS) for achieving real-time streaming vehicle data. Problems instances were made using Taiyuan BD bus network data. Experimental results showed that ESDAS speed insertion is approximately three times higher than the MongoDB platform.

Nesmachnow et al. [15] described a platform for Big Data analysis using a Map-Reduce approach in Hadoop in the context of smart cities. The problem instance data included different time intervals and GPS locations from buses of the transport system of Montevideo, Uruguay. The file sizes of the evaluated datasets are 10GB, 20GB, 30GB, and 60GB. The experimental analysis focused on evaluating the computational efficiency of the parallel/distributed Map-Reduce model and the correctness of the system over several scenarios using accurate GPS data collected in 2015 in Montevideo. The experimental evaluation was performed over the cloud infrastructure of Cluster FING, the high-performance computing facility at Universidad de la República, Uruguay [16]. The experimental results indicated that the solution approach scales appropriately when processing a large volume of data with a speedup of 22.16 times and computational efficiency of 0.92 using 24 computing resources compared to its sequential version.

Laska et al. [12] proposed a scalable architecture for real-time spatio-temporal stream data processing. The integration of IoT stream data used GeoMQTT to publish timestamp messages in Apache Kafka. The stream processing was made by Apache Storm. A dynamic amount of vehicle data were performed by the map matching algorithm on the proposed architecture. The dataset evaluated consists of 10357 taxi trajectories collected from 2 February to 8 February 2008. The dataset points were about 17 million, representing a distance of nine million kilometers. Experimental evaluation was performed using nine virtual machines with 2GB of RAM on a Hypervisor with 64 cores. The experimental results showed a stable latency in milliseconds for instances that do not exceed a ratio of 100 trajectory points per second.

Fan-Hsun et al. [6] proposed a real-time traffic prediction model by analyzing large-scale streams data of road density, traffic events, and rainfall volume. The proposed approach applied the Support Vector Machine and fuzzy theory to evaluate the traffic level on-road sections. The big data platform for the col-

6 P. Moreno, C. Cervantes, S. Nesmachnow, J. Hurtado, J. Hernández

lection, analysis, and processing was Apache Storm. The problem instances were created using open data from Police Broadcasting Service social media, Taiwan Area National Freeway Bureaus, and the Central Weather Bureau in Taiwan. Experimental evaluation was performed on virtual machines on a computer with an AMD Opteron processor, 16GB of RAM, a GigaByte Ethernet Controller, and a Xen Server 6.2 operating system. Experimental results showed that the proposed model improves the prediction accuracy by 25.6% than the prediction method based on the weighted exponential moving average method.

Massobrio and Nesmachnow [14] proposed an urban data analysis study for the public transportation system in Montevideo in ITS and smart cities. The study analyzed the GPS bus location dataset and smart card ticket sales. Several insights were obtained from data analysis, like the number of passengers traveling by the same smart card, frequency of use of the smart cards, and the number of bus transfers. Also, the ticket sales analysis revealed three peak hours during working days. Besides, the work proposed a methodology for built origin-destination matrices by trip changing to estimate the destinations. The implemented algorithm correctly estimated the destination for 81.62% of urban mobility trips of the studied dataset from 2016 with a Spearman correlation coefficient of 0.895.

The related works allow identifying several proposals using big data platforms for ITS applications processing and analysis in the context of smart cities. This work contributes with a real-time processing platform for distributed big data frameworks on vehicle tracking applications. The proposed platform considers gathering data by an IoT GPS device for real-time processing until its storage. The benefits of the proposed platform for real-time GPS data include: providing helpful information about geolocation on a specific time interval and storing distances information processed for future purposes. Next, big data platforms and IoT protocols to provide mobility services in real-time are described.

### 3 The proposed distributed big data platform

This section describes the proposed open-source big data platform for real-time geolocation tracking. In addition, the frameworks, protocols, design, and distributed architecture are described.

#### 3.1 Data gathering

MQTT is a client/server broker-based transport protocol for publishing and subscribes messages over the Transmission Control Protocol/Internet Protocol (TCP/IP). It is lightweight, open, simple, and it supports IoT Machine-to-Machine (M2M) communication. Recent MQTT specification has been standardized by the OASIS consortium and ISO/IEC 20922. Many IoT applications, such as autonomous/connected cars, smart cities, and cloud-connected industrial machines use MQTT to connect with cloud computing. The implementation of MQTT brokers supports different scenarios, including distributed computing, to

achieve high scalability and to provide high availability. MQTT by IoT technologies allows gathering data from smart-city devices. IoT acquires data through technologies such as RFID, WIFI, WSN, 5G, and satellite communication [13]. Generally, sensing technologies are used to gathering mobility information. Sensor technologies are classified into two categories: On-site and On-board. On-site technologies are sensors installed directly in the road infrastructure. On-board (or off-roadway) technologies collect information from vehicles/passengers to send it to a road device or the cloud for analysis [3].

### 3.2 Data collection

Real-time mobility information is collected by streaming, using physical sensing or mobile devices from remote technologies. Mobility information is generated from different sources such as GPS devices, mobile devices, IoT sensors, and social networks. Many collected mobility data have low spatial precision due to the acquisition device. Also, many applications require data in periods (time) for mobility tracking. However, mobility collected data can be sparse and noisy in the location accurate [23]. Therefore, the information must be classified and organized according to the application requirements; for example, ITS need to collect data in time intervals on different dates for route planning or scheduling [15]. For these reasons, considerable information must be stored using structured and unstructured data to be processed by computational intelligence algorithms. Streaming platforms, such as Apache Kafka, have been proposed for collecting large volumes of data by high-throughput message brokers. Kafka is an open-source platform for distributed event streaming, high-performance data pipelines, streaming analytics, data integration, and mission-critical applications.

### 3.3 Data processing

Processing of large volume of data on a single computer usually has limitations due to the computer resources, such as memory and CPU [13]. Nevertheless, the analysis of vast volumes of data in real-time requires many processing elements. Therefore, parallel and distributed systems are necessary to process large volumes of data. Parallel/distributed systems include a high-speed communication network and a distributed storage system as a part of the system.

Big data processing operates over data by applying batch or real-time stream data entry depending on the scenario. The batch processing work with collected data over some time, while the real-time processing work with collected data in a short time. Therefore, the real-time big data analysis must provide fault tolerance and scalability with a functional development approach, such as Apache Storm provides. Storm is a general propose parallel/distributed platform that provides flexibility, scalability, and real-time stream processing.

8 P. Moreno, C. Cervantes, S. Nesmachnow, J. Hurtado, J. Hernández

### 3.4 Data storing

Real-time mobility services in the context of the smart city need to handle and store a huge amount of data for analysis [26]. Structured (SQL) and unstructured (NoSQL) solutions provide scalability and data acquisition capabilities in an easier programming way. High availability is needed to dispose of information at any time. Cloud computing storage provides high availability, data replication, and load balancing on demand.

### 3.5 The proposed platform for real-time geolocation data processing

The design and architecture are divided into four stages. The first stage uses a GPS timestamp corresponding to location coordinates of a vehicle in movement. The timestamp contains four data: vehicle ID, date and time, latitude and longitude coordinates. Data are gathered from an IoT device that sends timestamps every time interval to an MQTT server. The IoT device components used in the platform design are an Arduino MEGA board and a GSM/SIM808 module. The second stage classifies information by topics using Kafka. The third stage computes the timestamps using a Storm topology. In this stage, timestamp strings are split by commas. Each part of the timestamp is sent to another process for processing. In the last stage, data persistence storing GPS timestamps directly on a database for future analysis. Fig. 1 shows the architecture of the proposed open-source big data platform for real-time geolocation tracking.

The proposed open-source big data platform for real-time geolocation tracking is implemented using MQTT, Kafka, Storm, and MySQL. An IoT device makes data gathering through an Arduino MEGA board and a GSM/SIM808 module. MQTT broker is available by a Mosquitto server on a cloud host with a public IP. The broker filters incoming messages from the IoT device client into the topic `gpsmqtt`. In addition, a Zookeeper server is installed to coordinate the process communication between the cluster nodes. The communication between Mosquitto and Kafka uses the Kafka connect plugin of Confluent for sending and receiving data from the MQTT broker. Then, a Kafka partition with a replication factor one is created on the Kafka broker to collect data in the topic `mqttgps`. Once MQTT and Kafka brokers are working, Storm topology is deployed on the Storm cluster.

Storm works on local mode and a cluster mode (i.e., master-slave model). Storm processes are coordinated through the Zookeeper service. Storm cluster has a master node called Nimbus and at least one worker node (Supervisor). Input data is sent by the Spout element that transforms the data into tuples (data streams). The Bolt element execute operators or functions over the tuples. The topology defines the data streams flow between Spouts and Bolts by a directed acyclic graph. The topology is used to deploy the computational parallel model on the Storm cluster.

Fig. 2 shows the spout/bolt workflow in the proposed topology. Blue arrows represent the spout phase, and green arrows represent the bolt phase. Each GPS timestamp is gathering by `kafkaSpout` component from a Kafka topic, and the

Open-source big data platform for real-time geolocation in smart cities 9

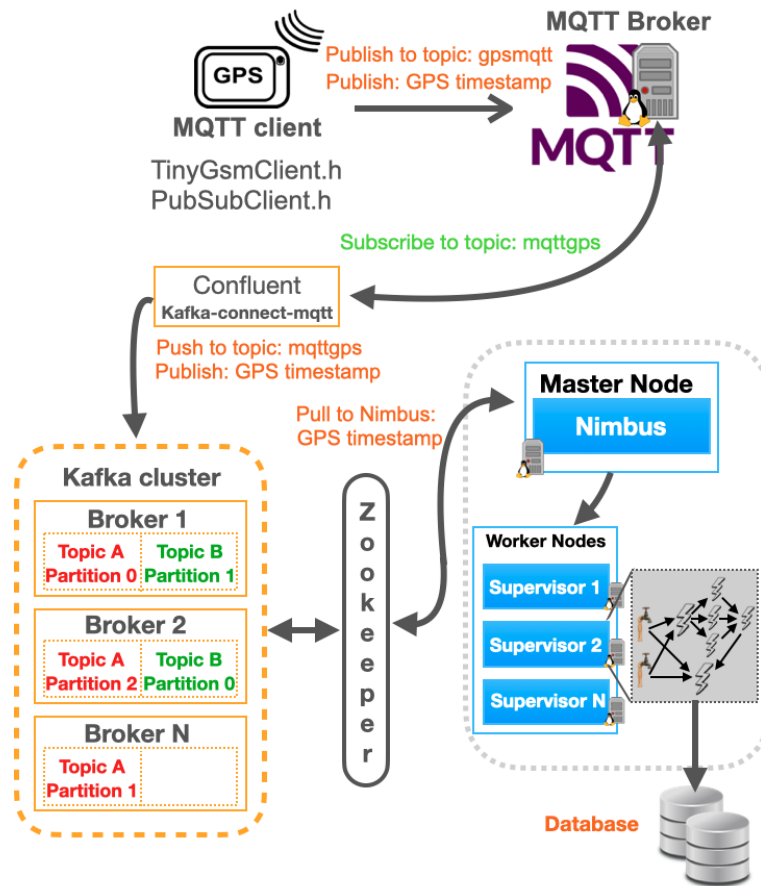


Fig. 1: Scheme of the platform for big data processing in real-time

data stream (tuple) is sending to different bolts (SplitBolt and MySQLBolt). Thus, each bolt performs a different task. First, SplitBolt receives a tuple that stores it on a string variable. After that, the string is split by commas, and two new tuples are sent to the CountBolt. Then, CountBolt classifies incoming tuples to accumulate the trajectories distances. Once the counting operation finishes, a new tuple with a distance value is sent by a new tuple to the ReportBolt and it stores processed distances on memory to show them on a final report. On the other hand, MySQLBolt performs the data persistence, storing the GPS timestamp directly on a MySQL database.

The proposed open-source big data platform collects, processes, and stores mobility location data every  $n$  seconds. Besides, Kafka and Storm setup guarantee fault tolerance, scalability, and low latency. The following section analyzes the experimental results of the proposed platform for three case studies.

10 P. Moreno, C. Cervantes, S. Nesmachnow, J. Hurtado, J. Hernández

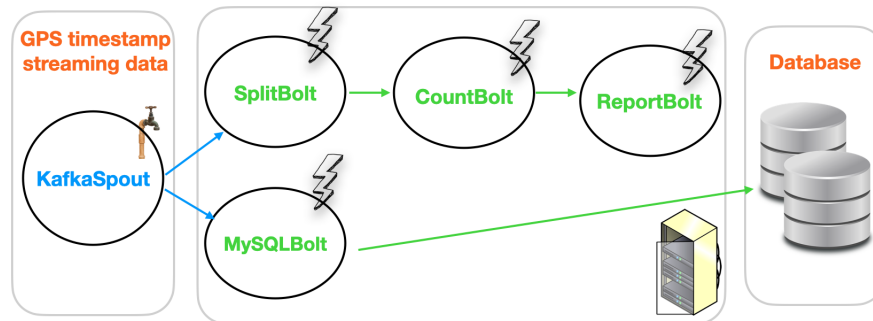


Fig. 2: Spout/bolt Storm topology for real-time geolocation tracking

## 4 Experimental validation and discussion

This section describes the experimental evaluation of the proposed platform and the problem instances are described. Finally, the computational efficiency results are reported and discussed.

### 4.1 Development and execution platform

The Storm topology was implemented in the Java programming language, and the distribution of jobs works independently depending on the topology distribution (Fig. 2). Every spout/bolt component was assigned at least one executor (thread), and each executor was assigned one task (spout/bolt instance).

The experimental evaluation was performed using an Intel i7-8700 (6 cores, 12 threads) processor at 3.2 GHz, 32 GB of RAM, and the Ubuntu 20.04 Linux operating system.

### 4.2 Problem instances and data

The problem instances considered in each case of study are described next. GPS timestamps from the T-Drive trajectories benchmark [25] are used to define different scenarios. Three scenarios were defined with 3500, 7500, and 10357 GPS trajectories of 10357 taxi routes collected during February 2 to 8, 2008, within Beijing. The data format in a file contains many lines with the following fields, separated by a comma: idTaxi, date-time, latitude, longitude.

The interval of time between two consecutive GPS timestamps is 10 minutes. Each file name in the dataset corresponds to the taxi ID, and contains the trajectory of the taxi. GPS timestamp data are sent from the file to the Mosquitto topic through a bash script to perform the experimental evaluation of big data processing. Problem instance #1 includes 3500 trajectory files. Problem instance #2 includes 7500 trajectory files containing, and problem instance #3 includes the whole 10357 trajectory files containing.

### 4.3 Computational efficiency metrics

The experimental evaluation focuses on evaluating the performance of the platform topology, composed of Kafka spout, split bolt, count bolt, report bolt, and persistent database bolt.

Two relevant metrics are considered for the evaluation: *latency* and *throughput*. Latency evaluates the (intra-worker) communication time within a worker process associated with an executor thread on the same Storm machine/node. Also, when an external service (Kafka broker) interacts with a spout component, the latency evaluates the inter-topology communication time of the response from a Storm node to a Kafka node across the network. Lower latency values mean a better execution time overall. In turn, the throughput evaluates the number of tuples successfully processed, regarding the number of GPS timestamps included in each problem instance. A higher value of throughput represents a better efficiency. Related counters are retrieved from the Storm user interface and used for computing throughput.

### 4.4 Experimental results

This subsection presents and discusses the results of the efficiency analysis for the three considered case studies, involving GPS timestamps of 10357 taxi trajectories in Beijing.

Table 1 reports the number of GPS timestamps on each problem instance, the number of tuples successfully processed (*acked*) by the topology, the throughput, the average latency, and the uptime of the system, i.e., the time from the beginning of the experiment until the topology stops emitting tuples. Latency times are reported in milliseconds.

Table 1: Efficiency counters, throughput, latency, and uptime of the topology for the three problem instances studied

<i>instance</i>	<i>#timestamps</i>	<i>acked</i>	<i>throughput</i>	<i>latency (ms)</i>	<i>uptime</i>
#1	5742560	5112220	89.02%	325.95	6h 8m
#2	12871223	12149800	94.39%	332.12	13h 35m
#3	17662984	17490880	99.02%	373.43	19h 4m

Results in Table 1 indicate that the topology is capable of processing a significantly large number of the GPS timestamps in each instance in reasonable execution times (considering the low-end computational platform used). Throughput values between 89% and 99% were achieved. The processing of the whole set of GPS timestamps was not attained, mainly because Storm uses three internal queues on a worker node, which generates additional latency. The developed implementation showed good scalability, as demonstrated by the latency values, which did not increase from instance #1 to #2, even though the number of processed GPS increased in a factor of  $2.25\times$ . Furthermore, latency only increased a mere 14%, when the problem dimension increased more than three times.

12 P. Moreno, C. Cervantes, S. Nesmachnow, J. Hurtado, J. Hernández

Table 2 reports the number of tuples transferred by a bolt component to the next component in the topology, the throughput, and the latency for each bolt component. The most relevant components are SplitBolt and MySQLBolt because they receive data directly from the spout. Hence, the number of transferred tuples on those bolt components is equal to or lower than the number of GPS timestamps stored on the Kafka topic for each instance. Throughput values for the CountBolt component are not reported because the number of transferred tuples are duplicated by the SplitBolt component, as reported in the transferred column on the table. In turn, throughput values for the ReportBolt component are not reported because the tuples it process and transfer correspond to distance values, not to GPS timestamps.

Table 2: Throughput and latency associated with bolt components

<i>instance</i>	<i>bolt</i>	<i>transferred</i>	<i>throughput</i>	<i>latency (ms)</i>
#1	SplitBolt	5402163	94.07%	0.009
	CountBolt	11545907	–	0.003
	ReportBolt	5540620	–	0.003
	MySQLBolt	5363354	93.39%	2.484
#2	SplitBolt	12343030	95.89%	0.012
	CountBolt	25545907	–	0.005
	ReportBolt	12650720	–	0.003
	MySQLBolt	12303074	95.58%	2.662
#3	SplitBolt	17345268	98.20%	0.017
	CountBolt	35280140	–	0.006
	ReportBolt	17139500	–	0.003
	MySQLBolt	17147527	97.08%	2.828

Results in Table 2 indicate that the bolt components of interest (SplitBolt and MySQLBolt) are able to process a significantly large number of timestamps for each instance in a reasonable execution time, using an executor for each task assigned to each bolt component. Throughput values between 93% and 98% were achieved. Ideal throughput values were not obtained due to lost tuples during the processing. The main reason for this loss is that the chosen level of reliability for bolt components does not guarantee complete message processing; it was set focused on efficiency instead. Finally, the bolt component that demanded the larger execution time was the persistent MySQLBolt, mainly due to the response time of network communication with the external database service.

Fig. 3 graphically summarizes the latency results. Latency values for the fully completed tuple processed through the topology are reported in Fig. 3a. In turn, Fig. 3b compares the latency values for each bolt component of the applied Storm topology.

Open-source big data platform for real-time geolocation in smart cities 13

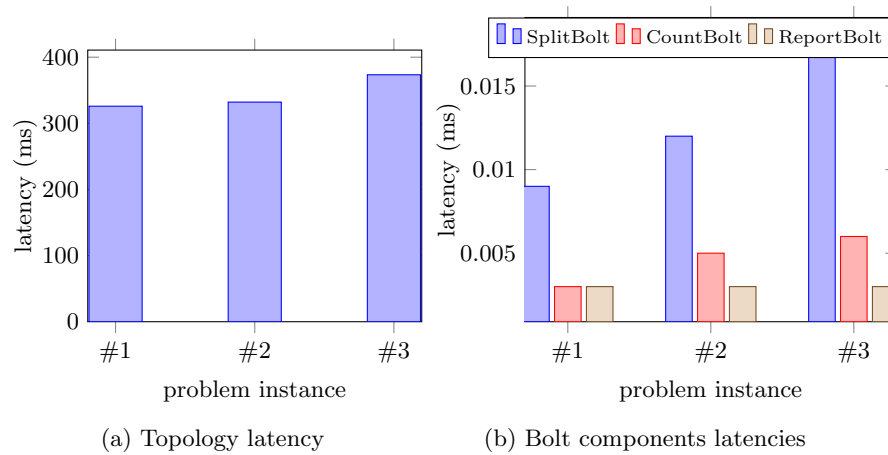


Fig. 3: Latency of the Storm topology and bolt components

Results in Fig. 3a clearly shows the slightly increasing latency behavior when solving problem instances with different sizes. In turn, Fig. 3b shows that the latency of bolt components increases with the number of transferred tuples for the considered problem instances. SplitBolt increases the latency mainly due to the timestamps split task transferred to the next bolt component. The CountBolt component has a slight latency increment between different instances sizes in relation to the number of transferred tuples from SplitBolt, mainly because it performs a low-demanding CPU computation (i.e., distance computation). Finally, the latency of ReportBolt had the same value from all problem instances.

Summarizing, results of the experimental evaluation demonstrate that the Storm topology deployed in the proposed open-source big-data platform is capable of processing a significantly large number of the GPS timestamps for each instance in reasonable execution times. Furthermore, the system showed good scalability properties, as latency values slightly increased when processing a significantly large number of GPS timestamps.

## 5 Conclusions and future work

This article presented a distributed open-source big data platform for real-time geolocation data processing in the context of smart cities, particularly for ITS applications.

The proposed platform combines parallel and distributed computing and geolocation to process real-time data for relevant analysis in smart cities. First, the platform collects location GPS timestamps from an IoT device over the MQTT protocol to Mosquitto broker; after that, the MQTT broker publishes the messages into an Apache Kafka topic by using a Confluent connector. Then, a particular Kafka consumer pushes the data into a Storm spout (KafkaSpout), to be processed by bolt components in a parallel topology.

14 P. Moreno, C. Cervantes, S. Nesmachnow, J. Hurtado, J. Hernández

The experimental validation focused on evaluating the efficiency of the proposed big data platform through two relevant metrics of the Storm components (latency and throughput) using real GPS timestamps from 10357 taxi trajectories from Beijing including more than 17 million GPS timestamps.

The main results indicate that the proposed Storm topology is effective for processing problem instances involving a large number of GPS timestamps in reasonable execution times. Accurate throughput values were achieved, between 93% to 98% for the bolt components and between 89% and 99% for the whole topology. A good scalability behavior was also shown, since latency values did not increase significantly when processing more GPS timestamps.

The main lines for future work are oriented to extend the proposed system to compute other essential indicators and statistics of ITS applications, such as public transportation systems from Mexico and Uruguay. Those analysis would certainly be valuable for relevant research such as bus timetable synchronization [17,18], bus network redesign [5], sustainable mobility plans [8], and also private transportation analysis [7,24].

Also, the proposed approach must be compared with other frameworks such as Apache Flink and distributed databases, like Apache Cassandra, to address the analysis in real-time for geolocation transportation tracking in smart cities. In turn, the data collected by the big data platform can be used for analysis through computational intelligence techniques to improve the quality of service of transportation systems.

## References

1. Alam, M., Ferreira, J., Fonseca, J.: Introduction to intelligent transportation systems. In: *Intelligent Transportation Systems*, pp. 1–17. Springer (2016)
2. Batty, M., Axhausen, K., Giannotti, F., Pozdnoukhov, A., Bazzani, A., Wachowicz, M., Ouzounis, G., Portugali, Y.: Smart cities of the future. *The European Physical Journal Special Topics* **214**, 481–518 (2012)
3. Campos, S., del Ser, J., Laña, I., Olabarrieta, I., Sánchez-Cubillo, J., Sánchez-Medina, J., Torre, A.: Big data in road transport and mobility research. In: *Intelligent Vehicles*, pp. 175–205. Butterworth-Heinemann (2018)
4. Ding, W., Zhang, S., Zhao, Z.: A collaborative calculation on real-time stream in smart cities. *Simulation Modelling Practice and Theory* **73**, 72–82 (2017)
5. Fabbiani, E., Nesmachnow, S., Toutouh, J., Tchernykh, A., Avetisyan, A., Radchenko, G.: Analysis of mobility patterns for public transportation and bus stops relocation. *Programming and Computer Software* **44**(6), 508–525 (2018)
6. Fan, T., Jen, H., Chia, T., Yao, Y., Han, C., Li, C.: Congestion prediction with big data for real-time highway traffic. *IEEE Access* **6**, 57311–57323 (2018)
7. Gabrielli, G., Ferreira, I., Dalchiele, P., Tchernykh, A., Nesmachnow, S.: Computational intelligence for analysis of traffic data. In: *Smart Cities*, pp. 167–182 (2021)
8. Hipogrosso, S., Nesmachnow, S.: Analysis of sustainable public transportation and mobility recommendations for Montevideo and Parque Rodó neighborhood. *Smart Cities* **3**(2), 479–510 (2020)
9. Jain, A.: *Mastering Apache Storm: Processing big data streams in real time*. Packt Publishing, Birmingham, UK (2017)

10. Kumar, M., Singh, C.: Building Data Streaming Applications with Apache Kafka. Packt Publishing, Birmingham, UK (2017)
11. Kumar, S., Tiwari, P., Zymbler, M.: Internet of things is a revolutionary approach for future technology enhancement: a review. *Journal of Big Data* **6**(1) (2019)
12. Laska, M., Herle, S., Klamma, R., Blankenbach, J.: A scalable architecture for real-time stream processing of spatiotemporal iot stream data-performance analysis on the example of map matching. *ISPRS International Journal of Geo-Information* **7**(7) (2018)
13. Li, W., Batty, M., Goodchild, M.: Real-time gis for smart cities. *International Journal of Geographical Information Science* **34**(2), 311–324 (2020)
14. Massobrio, R., Nesmachnow, S.: Urban mobility data analysis for public transportation systems: A case study in montevideo, uruguay. *Applied Sciences* **10**(16), 5400 (2020)
15. Nesmachnow, S., Baña, S., Massobrio, R.: A distributed platform for big data analysis in smart cities: combining Intelligent Transportation Systems and socio-economic data for Montevideo, Uruguay. *EAI Endorsed Transactions on Smart Cities* **2**(5), 320–347 (2017)
16. Nesmachnow, S., Iturriaga, S.: Cluster-UY: Collaborative Scientific High Performance Computing in Uruguay. In: *Supercomputing, Communications in Computer and Information Science*, vol. 1151, pp. 188–202. Springer (2019)
17. Nesmachnow, S., Muraña, J., Goñi, G., Massobrio, R., Tchernykh, A.: Evolutionary approach for bus synchronization. In: *High Performance Computing*, pp. 320–336. Springer International Publishing (2020)
18. Nesmachnow, S., Risso, C.: Exact and evolutionary algorithms for synchronization of public transportation timetables considering extended transfer zones. *Applied Sciences* **11**(15), 7138 (2021)
19. Rodrigue, J.: *The Geography of Transport Systems*. Routledge (2020)
20. Sharma, N., Shamkuwar, M.: Big data analysis in cloud and machine learning. In: *Big Data Processing Using Spark in Cloud*, pp. 51–85. Springer (2019)
21. Targio, I., Chang, V., Anuar, N., Adewole, K., Yaqoob, I., Gani, A., Ahmed, E., Chiroma, H.: The role of big data in smart city. *International Journal of Information Management* **36**(5), 748–758 (2016)
22. Wang, F., Hu, L., Zhou, D., Sun, R., Hu, J., Zhao, K.: Estimating online vacancies in real-time road traffic monitoring with traffic sensor data stream. *Ad Hoc Networks* **35**, 3–13 (2015)
23. Widhalm, P., Yang, Y., Ulm, M., Athavale, S., González, M.: Discovering urban activity patterns in cell phone data. *Transportation* **42**(4), 597–623 (2015)
24. Winter, H., Serra, J., Nesmachnow, S., Tchernykh, A., Shepelev, V.: Computational intelligence for analysis of traffic data. In: *Smart Cities*, pp. 167–182 (2021)
25. Yuan, J., Zheng, Y., Xie, X., Sun, G.: Driving with knowledge from the physical world. In: *Proceedings of the 17th ACM SIGKDD International Conference on Knowledge Discovery and Data Mining*. p. 316–324. KDD’11, Association for Computing Machinery, New York, NY, USA (2011)
26. Zhou, L., Chen, N., Chen, Z.: Efficient streaming mass spatio-temporal vehicle data access in urban sensor networks based on apache storm. *Sensors* **17**(4), 815 (2017)

# Techno-Economic Dimensioning Methodology for Battery Energy Storage Systems: Electricity Access Fee Reduction in Industrial Consumptions

Jorge Nájera<sup>1\*</sup>[0000-0002-3396-0062], Miguel Santos-Herran<sup>1</sup>[0000-0002-5338-6336],  
Marcos Blanco<sup>1</sup>[0000-0003-3641-1867], Gustavo Navarro<sup>1</sup>[0000-0002-5169-9080],  
Jorge Torres<sup>1</sup>[0000-0001-7524-9925], and Marcos Lafoz<sup>1</sup>[0000-0001-9613-1280]

<sup>1</sup>Centro de Investigaciones Energéticas, Medioambientales y Tecnológicas (CIEMAT),  
Government of Spain, 28040 Madrid, Spain  
jorge.najera@ciemat.es  
<http://rdgroups.ciemat.es/web/usep/>

**Abstract.** Industrial buildings account for few high peaks of power demand, which forces them to contract a high fixed electricity term to cover it. A more intelligent use of the energy in industrial buildings, together with an improved efficiency of the transmission and distribution of the energy along the electric power grid, can be achieved by reducing this industrial peak consumption. Lithium ion (Li-ion) batteries are one of the most promising technologies among energy storage systems for this task. However, selecting a proper Li-ion battery requires a techno-economic dimensioning process which is not straightforward. This paper proposes a dimensioning methodology that takes into consideration technical and economic implications (fixed and variable access fee), and applies it to a case example with real industrial consumption data and a commercial battery. Different charging strategies are implemented, depending on the Time-of-Use tariff. Results indicate that implementing Li-ion batteries for reducing this peak consumption can lead to a cost-benefit improvement, which can be fostered by selecting the most beneficial charging strategy.

**Keywords:** dimensioning methodology, battery energy storage system, industrial consumption, charging strategy, annualized cost

## 1 Introduction

The fee that electric energy consumers pay for using it, commonly known as electricity access rate, is split into a variable term and a fixed term in the majority of European countries [1]. The variable term is associated with the energy consumed by the user (kWh), while the fixed term corresponds to the contracted power (kW), defined as the maximum power that the user can consume before the power-limit switch is triggered.

2

Commonly, the fixed term is over-dimensioned, i.e. the usual consumption along a day is considerably lower than the power consumption limit, the latter being reached only during a few short periods per day. This behaviour is specially representative of industrial consumption, forcing them to contract a high fixed electricity term due to very few consumption peaks [2].

This electrical consumption pattern can be modified, leading to a more intelligent use of the energy in industrial buildings and fostering the "prosumer" behaviour among industrial consumers. Hence, the efficiency of transmission and distribution of the electricity across the power grid can be improved.

Among the different solutions proposed in the literature for achieving a reduction in industrial peak consumption, the inclusion of photovoltaic panels is presented as a feasible solution in [3,4]. However, the vast majority of studies opt for implementing an energy storage system (ESS), as in [5,6,7] among other studies.

Battery energy storage systems (BESSs) arise a promising ESSs for their connection in buildings and infrastructures, both industrial and residential [8]. The benefits of including BESSs encompass the majority of the electricity value chain, including peak shaving, continuity of supply for customers, ancillary services for transmission and distribution system operators, and flexibility and curtailment minimization for renewable generation [9].

However, selecting a BESS for its connection to an industrial consumption and reducing the peak power consumption is not a straightforward issue. Multiple solutions are offered by battery manufacturers and, given that BESSs are costly equipments, a dimensioning process based on a techno-economic assessment is mandatory in order to help decision makers. This techno-economic assessment should incorporate the load characteristics (power consumption profile), the BESS technical and economic features (power, energy, and cost), and the electricity access fee (fixed and variable term).

In this regard, BESS dimensioning for reducing the electricity access fee in industrial buildings has been studied together with photovoltaic in [10,11]. In those papers a dimensioning process is proposed for a BESS and photovoltaic installation, but using a brute force methodology, and applied to peak shaving and "prosumer" purposes, and for working isolated from the grid. In addition, the authors in [12] analyse the economic viability of BESS integration under different tariff structures and systems configurations, although a generalized and simplified ageing for the Li-ion BESS has been assumed for the yearly cost calculations. Hence, the importance of the BESS charge/discharge profile has not been taken into account properly, since it highly affects the ageing. A similar approach is proposed in [13,14] for residential consumption, assessing the economic viability of integrating BESS at a residential level with and without subsidies. Nevertheless, these studies lack a detailed analysis of the BESS lifespan, neglecting its influence in the overall yearly costs. Further studies, such as [15], also analyse the peak shaving of decentralised residential BESS, proposing a BESS model which includes the battery efficiency and SoC estimation, but an

over-simplified battery ageing assumption is made as well, where the payback period of the battery varies linearly with the battery size.

Alternative dimensioning methodologies have also been proposed in the literature, such as stochastic models for improving the decision making ([16]). The developed methodologies are applied to reach the optimal BESS investment for industrial buildings but, as identified previously, there is no detailed battery ageing analysis, being the influence of this variable is underestimated.

The BESS dimensioning studies mentioned above employ different selection criteria that are based on technical issues, or on techno-economic issues but using generic ageing data to calculate the BESS lifespan. Furthermore, they analyse the complete compensation of technical issues under study, e.g., feed an isolated load with a combination of a BESS together with photovoltaic or eliminate the consumption peaks via smart charging of electric vehicles, which may not be the most feasible scenario faced by residential or industrial consumers. As a main contribution, this paper proposes a BESS dimensioning methodology for diminishing the electricity access rate (fixed and variable) in real industrial consumption, employing a techno-economic criterion for selecting the optimum solution. Different BESS charging strategies are applied, depending on the Time-of-Use (ToU) tariff so the variable electricity term is minimized. Moreover, the proposed methodology includes a detailed evaluation of the BESS ageing, which is included in the cost-benefit analysis as a key component. This improved BESS ageing assessment highly influences the time for a BESS replacement and, hence, the annualized cost.

Regarding the variable term of the fee, it is expected to be fairly similar between installing and not installing a BESS. At the end, in the first case the energy is directly consumed by the load, and in the second case the energy is consumed by both the load and the BESS (charging process), but the total energy remains almost constant, being the BESS losses the only difference in energy. Hence, the variable economic term associated to this energy consumption could potentially be removed from the techno-economic analysis. However, given that the variable fee is charged based on (ToU) tariffs in the majority of European countries, it is worth considering the variable term in the techno-economic decision [17]. In this sense, a further cost-benefit improvement can be expected with a proper BESS charging/discharging control, since the BESS can be charged during the most favourable ToU period and discharge when during the most disadvantageous one.

Hence, the applicability of this methodology could be useful for industrial consumers, as well as BESS manufacturers aiming for specific developments for industrial consumption. The applicability of the developed methodology is exemplified in this paper for an existing industrial consumption and on a typical day, considering a commercial battery and standard fixed and variable prices for the economic analysis.

The paper is organized as follows: the BESS dimensioning methodology is described in Section 2. The different simulation models used along the different steps of the methodology are detailed in Section 3, including a power grid model,

4

an industrial consumption model, a power converter model, and a battery model. The annualized cost computation including the BESS cost, electricity access fee prices, and electricity variable prices is described in Section 4. A case example with real industrial consumption data, commercial BESS and standard prices is presented in Section 5, while conclusions are drawn in Section 6.

## 2 BESS dimensioning methodology

The BESS dimensioning methodology described in this section aims at reducing the electricity access fee by introducing a BESS that deals with the peaks of the industrial consumption. A few assumptions are made by the authors in the development of the BESS dimensioning methodology, which are presented at follows.

At first, the BESS ( $P_{BESS}$ ) and the electrical grid ( $P_{GRID}$ ) must cover the customers' demand ( $P_{LOAD}$ ) and the losses ( $P_{LOSS}$ ):

$$P_{BESS} + P_{GRID} = P_{LOAD} + P_{LOSS} \quad (1)$$

Besides, the BESS must account for enough energy to fulfill the extra energy demand not supplied/covered by the grid. Besides, a BESS must be able to recharge the same amount of energy as dispatched along one day. If not, the mean SoC will be decaying as the scenario repeats over time, being eventually unable to fulfil the load power demand.

The methodology comprises a set of steps, as seen in Figure 1.

1. Step 1: Models parameterizations. The different models, which are mathematical representations of physical systems, include variables (inputs and outputs) and parameters. In order to particularize the models to a specific system, those parameters must be adjusted.
2. Step 2: Define test cases. The variable that defines the test cases is the maximum fixed power that the grid delivers ( $P_{LIMIT}$ ). Reducing this power limit implies adding a greater contribution from the BESS, which yields to different scenarios. In each scenario, different BESS configurations are needed, and different BESS ageing is obtained.
3. Step 3: Simulate test case, calculate BESS requirements, and BESS configuration. Once the scenarios have been defined, a simulation is performed for the different scenarios. Each scenario implies different necessities from the BESS, regarding power and energy, resulting in different BESS configurations (number of cells in series and in parallel). The charge/discharge profile for the BESS is also obtained from the simulation, being the charge profile selected as a function of the ToU tariff. If the energy available for charging is unable to match the amount of energy dispatched by a BESS in a specific scenario, that scenario will not be considered for the dimensioning process, since this situation will force the BESS to not being able to feed the load when the scenario repeats over time.

4. Step 4: Calculate BESS ageing. Once the minimum BESS configuration that satisfies the power and energy requirements is selected for each scenario, a BESS ageing analysis is performed, considering also the different charging strategies. As a result of this step, the number of days until the BESS loses a 20% of capacity retention is obtained.
5. Step 5: Cost–benefit analysis. Prices and fees for both a BESS (as a function of the kW and kWh of the system) and the fixed and variable electricity tariff are needed for their incorporation into a cost function. BESS standard prices as well as Spanish electricity rates are provided in Section 5, with a case example. The cost can be computed yearly, taking into account the net present cost, and the capital recovery factor. The base scenario, i.e., when there is no BESS, is then compared to the rest of scenarios in terms of cost.

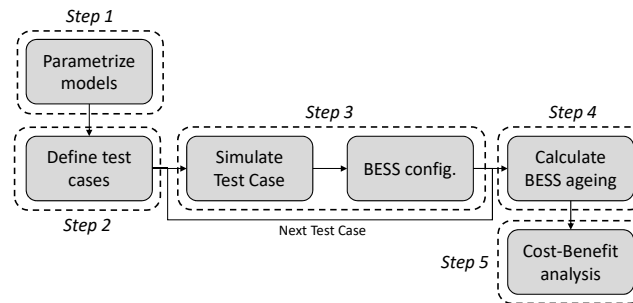


Fig. 1: Flow chart of the proposed BESS dimensioning methodology.

### 3 Industrial consumption, BESS, and grid modelling

The mathematical and simulation models used in Section 5 for performing a case example are described here. Three main models are considered: an industrial consumption, a BESS, and a power grid. The BESS is connected to the same point as the industrial consumption, the point of common coupling (PCC), and both of them are connected to the grid, as it can be seen in the general model diagram displayed in Figure 2. The complete model outputs several time series variables (P, Q, V, and I) for the three main models. Additional electrical variables (frequency or harmonic distortion) are also evaluated and calculated by the model, but they have not been considered in this paper since they are not relevant for the objective of this work.

The models are developed with MATLAB Simulink, under the Simscape Electrical environment. When developing simulation models, a higher complexity commonly implies a higher accuracy [25,26]. Nevertheless, complex models

6

tend to require a substantial computational effort, and a considerable amount of information to parameterize them. Besides, they are commonly valid only for a specific device, i.e. non-generalizable [27,28].

On the other hand, simplified models, usually composed by resistors, inductors, and capacitors, are easily parameterized, require low computational effort, and are generalizable for devices with similar characteristics. Moreover, even though

Hen  
was to  
ized.

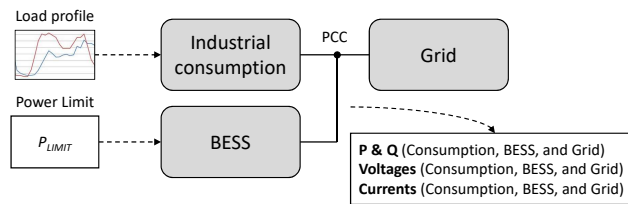


Fig. 2: General model diagram.

### 3.1 Industrial Consumption Model

The industrial consumption is modelled as a PQ load, consuming a predefined active and reactive power independently of the voltage at the PCC. Thus, it has to be modelled as a controlled current source. The inputs of the model (P and Q) correspond to the 24-h active and reactive power profile on a 1 second basis.

From those, together with the measured voltage ( $V_{abc}$ ), the complex values of the phase currents are calculated, and then redirected to the corresponding current controlled source. A resistor with a very high value is connected in parallel, acting as a snubber. Finally, the model is linked to the complete model via connectors A, B, C, and N.

### 3.2 BESS Model

The BESS model includes a battery model and a power electronic converter model. The power converter is necessary to manage the battery charge/discharge and to connect the battery to the AC grid.

**Electronic Converter Model** For the purpose of this work, there is no need to model the power electronic converter in detail, since neither efficiency nor power converter ageing are incorporated into the economic evaluation. Thus,

an ideal voltage source converter (VSC) has been selected, with no conduction or switching losses and no power limitations. Hence, the VSC is modelled as a controlled three-phase voltage source whose reference voltage is given by the converter control. This control manages the power that flows in and out of the battery.

The control of a VSC can be modelled as explained in [31], consisting of a high-level and a low-level control. The high-level control is in charge of selecting the power dispatched or consumed by the battery. Several strategies have been proposed in the literature([32,33,34]). For this paper, a simple strategy based on rules has been selected, which sets the reference power for the battery ( $P_{BATT}$ ) based on the maximum power that the industrial consumption can absorb from the grid ( $P_{LIMIT}$ ), the actual power that the industrial load is demanding ( $P_{LOAD}$ ), and the battery state of charge ( $SoC_{BATT}$ ). The flow diagram for this high-level control is shown in Figure 3.

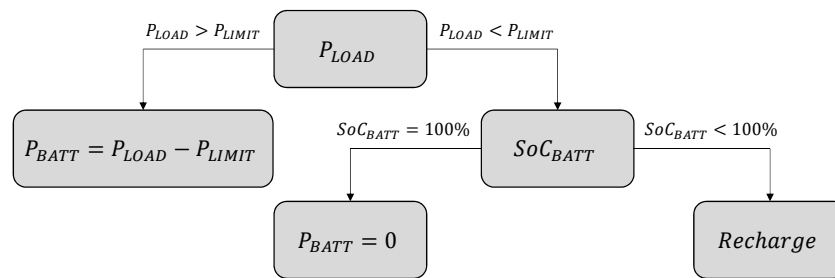


Fig. 3: Flow diagram for the VSC high-level control.

The low-level control is in charge of setting the voltage at the VSC terminals so that the power management commanded by the high-level control is set. Detailed explanation about the implemented control can be found in [31,35].

**Battery Model** The battery model is represented as an equivalent circuit model which sacrifices accuracy in favour of generality. Nevertheless, the equivalent circuit model account for errors lower than 5% [36], sufficient for obtaining general conclusions. The battery equivalent circuit is shown in Figure 4, where  $u$  is the instantaneous battery voltage [V],  $i$  is the battery current [A] ( $i > 0$  discharging;  $i < 0$  charging),  $I_{SELF}$  is the self-discharge current,  $R_{OHM}$  is the ohmic internal resistance [ $\Omega$ ],  $R_{POL}$  is the polarization internal resistance [ $\Omega$ ], and  $C_{POL}$  is the polarization capacitor [F].

The implemented battery model has been developed and validated in [26] and by the authors in [41,37]. The model comprises a voltage/runtime model, a thermal model, and an ageing model. Due to the limitation in the maximum

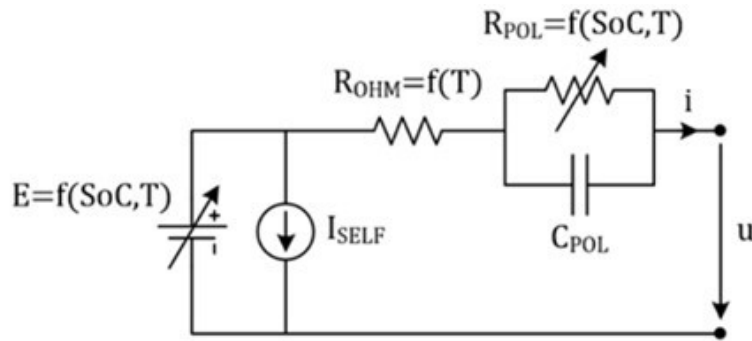


Fig. 4: Battery equivalent circuit model.

number of pages of the paper, the authors refer to [41] for detailed information about the battery model.

As a summary, the lithium-ion battery model used in this paper is a modification of the MATLAB Simulink model in [38]. The battery equivalent circuit is based on the Shepherd equation [39,40]. The heat generation model is modelled as [42], while the ageing model is published in [41], based on [46] and [47].

### 3.3 Grid Model

The grid is modelled as an infinite power grid, i.e. the frequency and voltage at the PCC are constant. A Three-Phase Source model has been selected with a swing generator type, high short-circuit power, and low X/R ratio.

## 4 Annualized cost computation

Electricity access fees for industrial consumption for the regulated market in Spain can be found in [21,22]. The regulation considers six ToU periods (P1 to P6). Regulated prices are shown in Table 1.

The cost equation must consider the following:

$$Cost\left(\frac{euro}{year}\right) = Fixed - fee + Variable - fee + BESS_{project-cost} \quad (2)$$

The contracted power ( $P_{LIMIT}$ ) is considered constant for the six ToU periods (as is requested to industrial consumption), and the variable term depends on the BESS charging strategy. The ToU periods by day and hour are shown in Fig. 5. Hence, three different charging strategies have been proposed. The first charging strategy forces the battery to be fully recharged during ToU period P6, the second strategy forces to charge it during P6 and the next cheapest ToU period, and the third strategy allows the battery to charge with a constant power when it is not delivering power. Thus, the BESS will be more stressed with the first strategy (higher C rate), and less with the last strategy.

Table 1: Electricity access fee costs [21,22].

ToU period [-]	Fixed term cost [€/kW year]	Variable term cost [€/kWh]
P1	30.5357	0.05089
P2	25.8947	0.03922
P3	14.9091	0.02193
P4	12.0944	0.01219
P5	3.9386	0.00443
P6	2.1086	0.00289

Hour	January & February	March	April & May	June	July	August & September	October	November	December
00:00 - 01:00	P6	P6	P6	P6	P6	P6	P6	P6	P6
01:00 - 02:00	P6	P6	P6	P6	P6	P6	P6	P6	P6
02:00 - 03:00	P6	P6	P6	P6	P6	P6	P6	P6	P6
03:00 - 04:00	P6	P6	P6	P6	P6	P6	P6	P6	P6
04:00 - 05:00	P6	P6	P6	P6	P6	P6	P6	P6	P6
05:00 - 06:00	P6	P6	P6	P6	P6	P6	P6	P6	P6
06:00 - 07:00	P6	P6	P6	P6	P6	P6	P6	P6	P6
07:00 - 08:00	P6	P6	P6	P6	P6	P6	P6	P6	P6
08:00 - 09:00	P2	P3	P5	P4	P2	P4	P5	P3	P2
09:00 - 10:00	P1	P2	P4	P3	P1	P3	P4	P2	P1
10:00 - 11:00	P1	P2	P4	P3	P1	P3	P4	P2	P1
11:00 - 12:00	P1	P2	P4	P3	P1	P3	P4	P2	P1
12:00 - 13:00	P1	P2	P4	P3	P1	P3	P4	P2	P1
13:00 - 14:00	P1	P2	P4	P3	P1	P3	P4	P2	P1
14:00 - 15:00	P2	P3	P5	P4	P2	P4	P5	P3	P2
15:00 - 16:00	P2	P3	P5	P4	P2	P4	P5	P3	P2
16:00 - 17:00	P2	P3	P5	P4	P2	P4	P5	P3	P2
17:00 - 18:00	P2	P3	P5	P4	P2	P4	P5	P3	P2
18:00 - 19:00	P1	P2	P4	P3	P1	P3	P4	P2	P1
19:00 - 20:00	P1	P2	P4	P3	P1	P3	P4	P2	P1
20:00 - 21:00	P1	P2	P4	P3	P1	P3	P4	P2	P1
21:00 - 22:00	P1	P2	P4	P3	P1	P3	P4	P2	P1
22:00 - 23:00	P2	P3	P5	P4	P2	P4	P5	P3	P2
23:00 - 00:00	P2	P3	P5	P4	P2	P4	P5	P3	P2

Fig. 5: ToU periods in Spain for tariff 6.1. Based on [18].

The yearly BESS project cost has been calculated based on [24,48,50], and has been defined as:

$$C_{ann} = CRF(i, R_{proj}) \cdot C_{NPC} \tag{3}$$

where  $C_{ann}$  is the annualized cost,  $C_{NPC}$  is the net present cost, and  $CRF$  is the capital recovery factor, which depends on the annual real discount rate ( $i$ ) and on the project lifetime ( $R_{proj}$ ).  $C_{NPC}$  is calculated as the present value of all the costs of installing and operating the battery over the project lifetime, minus the present value of all the revenues earned over the project lifetime.

Hence, the total yearly cost is calculated as follows:

$$Cost\left(\frac{euro}{year}\right) = (P1 + \dots + P6) \cdot P_{LIMIT} + 365 \cdot (P_{E-grid} + P_{E-charge}) + C_{ann} \tag{4}$$

10

being  $P_{E-grid}$  the cost of the energy consumed from the grid during the selected day (based on the ToU period), and  $P_{E-charge}$  the cost of the energy used for recharging the battery, which varies depending on the selected charging strategy.

## 5 Case example

A case example is analysed in order to illustrate how the described methodology could be implemented. The models developed in Section 3 are used for performing the simulations, and the same structure of steps defined in Section 2 is applied:

### 5.1 Step 1. Parameterize Models

At first, the simulations models need to be parameterized. For the grid model, an almost infinite power grid is implemented (Table 2).

Table 2: Grid model parameters.

Parameter	Value
Reference voltage	400 V
Short-circuit ratio	25
X/R ratio	20

The battery model can be parameterized following the methodology defined in [41]. A commercial lithium polymer battery cell from Kokam, model SLPB100255255HR2, has been selected for this case study [19]. The experimental data for calculating the ageing model parameters have been obtained from [19] and [41], where the complete theoretical and experimental validation for the selected battery cell has been performed. The battery ageing model performs with an error below 5%, as detailed in [41], and the selected battery cell main parameters are shown in Table 3.

The load needs a power consumption profile as input, with a format of 24-h profile on a 1 second basis, corresponding to a typical day in summer for an industrial building. The selected building is the CEDEX facility in Madrid, located at Julián Camarillo 30, 28037 Madrid (Spain). For the analysis performed in this paper, the load corresponds to a three-phase load with no unbalance between phases, whose active power profile is shown in Figure 6.

### 5.2 Step 2. Define Test Cases

Test cases are defined by the BESS control parameter ( $P_{LIMIT}$ ). Thus, as  $P_{LIMIT}$  decreases, the battery will increase its contribution. Steps of 5 kW have been selected, so the different scenarios are defined in Table 4.

Table 3: Battery model data and parameters [19,41].

Data	Value
Reference capacity	55 Ah
Impedance	0.60 m $\Omega$
Average voltage	3.7 V
Lower limited voltage	2.7 V
Upper limited voltage	4.2 V

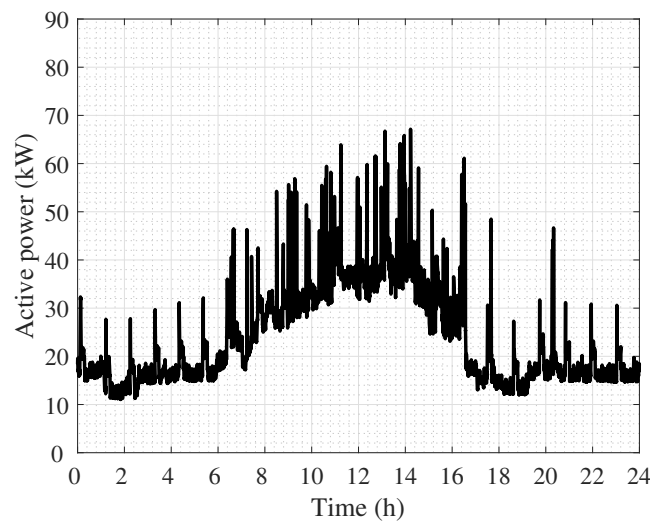


Fig. 6: Industrial consumption profile for a typical day in July.

### 5.3 Step 3. Simulate Scenarios and Obtain BESS Requirements and Configuration

As previously explained, BESSs that are not able to recharge as much energy as they have delivered along the day are considered as not valid. Once the simulations are performed, BESS power profiles for the valid configurations are obtained, and those valid BESS power profiles are shown in Figure 7. The displayed BESS profile also considers the three charging strategies defined in Section 4 based on the ToU periods. As aforementioned, the first strategy is more demanding during the charging process for the battery, although the energy prices during that period are lower (P6).

The power and energy requirements ( $P_{BESS-req}$  and  $E_{BESS-req}$ ) for the valid scenarios are shown in Table 5. Then, the most suitable BESS configuration must be selected (number of cells connected in series and in parallel). Commercial three-phase inverters for 400 V grids demand 48 V in the DC side. Hence, based

Table 4: Scenarios defined for the case example.

Scenario	$P_{LIM}$
SB	70 kW
S65	65 kW
S60	60 kW
...	...
S10	10 kW
S5	5 kW

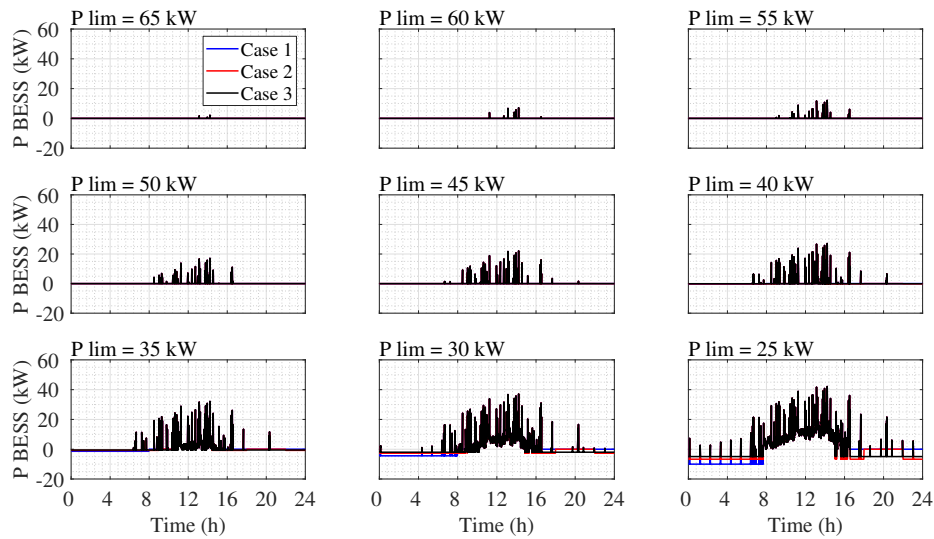


Fig. 7: BESS power profile for different values of  $P_{LIM}$ .

on the standard cell parameters, the number of cells in series so the DC side voltage reaches 48 V equals:

$$\frac{48V_{DC-side-voltage}}{3.7V_{Nominal-cell-voltage}} \approx 13 \tag{5}$$

The number of cells in parallel depends on the BESS energy requirements, taking into account that the energy stored in one branch of 13 cells equals 2.64 kWh.

#### 5.4 Step 4. Calculate BESS Ageing

BESS ageing is closely related to its C rate and temperature (among other factors). The higher the C rate, the higher the temperature augmentation in the

Table 5: BESS requirements for the different scenarios.

Scenario	$P_{BESS-req}$	$E_{BESS-req}$	Min. BESS	$E_{BESS}$
[-]	[kW]	[kWh]	config. [-]	[kWh]
SB	-	-	-	-
S65	2.13	0.0019	13s1p	2.6455
S60	7.13	0.0149	13s1p	2.6455
S55	12.13	0.0475	13s1p	2.6455
S50	17.13	0.1242	13s1p	2.6455
S45	22.13	0.3746	13s1p	2.6455
S40	27.13	2.0736	13s1p	2.6455
S35	32.13	10.9798	13s5p	13.2275
S30	37.13	34.7906	13s14p	37.0370
S25	42.13	74.1046	13s29p	76.7195

battery, the control strategy have a huge influence on the BESS ageing, since depending on the control strategy the BESS is forced to charge with higher or lower C rates. Fig. 8 shows the ageing associated to the different scenarios, and to the different charging strategies.

Commonly, a BESS is considered as aged when it loses 20% of its capacity retention.

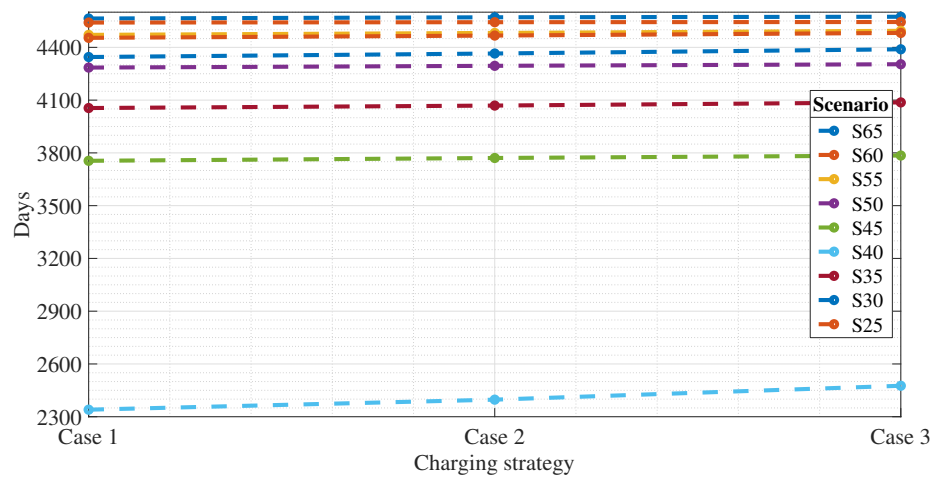


Fig. 8: Days until  $\nabla Q = 20\%$  as a function of the BESS charging strategy.

The relative relation between the capacity fade depending on the charging strategy is kept almost constant between scenarios. Moreover, there are mini-

14

imum differences between charging with the first charging strategy or the third, although ageing is always more severe for the charging strategy that forces the battery to charge during ToU period P6. The scenario with the highest ageing corresponds to S40, since is the one that is less overdimensioned, i.e. the BESS energy is close to the scenario energy requirements.

### 5.5 Step 5. Cost–Benefit Analysis

Electricity fixed and variable prices for the different ToU periods can be seen in Table 1, while the prices for the BESS project have been obtained from [23,24], and are listed in Table 6.

Table 6: Summarized costs for the BESS project [23,24].

Item	Value
BESS cost (power)	1876 €/kW
BESS cost (energy)	469 €/kWh
$C_{OM}$	10 €/kW year
$i$	3.41%
$N_{proj}$	25 years

where  $C_{OM}$  is the operation and maintenance cost, and  $N_{proj}$  is the number of years over which the cost is annualized. The total cost for each scenario is shown in Table 7.

Table 7 indicates that, for the selected scenario, reducing the fixed term to 65 kW and selecting a charging strategy that forces the BESS to charge during the ToU period P6 is the most favourable solution for the industrial consumer. It is noticeable that, given that there is no much difference among a specific scenario in the BESS ageing when the BESS is charged with different strategies, the yearly cost of the BESS project remains constant within each scenario.

## 6 Conclusions

This paper presents a BESS dimensioning methodology for reducing the electricity access fee for industrial consumption, considering battery ageing and the cost of the BESS and electricity access fees. By connecting a BESS together with a consumption, and selecting a proper BESS charging strategy, the yearly cost and the power demand peaks can be reduced.

Results drawn from the last section show that implementing a small battery to limit the consumption peaks together with a favourable charging strategy can lead to considerable cost reduction for the industrial consumer. In fact, the

Table 7: Yearly cost for the different scenarios.

Scenario	Charging case. [-]	Fixed fee [€/year]	Variable fee [€/year]	BESS project [€/year]	Total cost [€/year]
SB	-	6263.7	7063.2	-	13326.9
	Case 1		6543.7		12621.8
S65	Case 2	5816.3	6543.8	261.8	12621.9
	Case 3		6543.8		12621.9
	Case 1		6543.5		12737.8
S60	Case 2	5368.9	6543.6	825.4	12737.9
	Case 3		6543.7		12738.0
	Case 1		6543.0		12853.5
S55	Case 2	4921.5	6543.2	1389.0	12853.7
	Case 3		6543.4		12853.9
	Case 1		6541.7		12968.4
S50	Case 2	4474.1	6542.3	1952.6	12969.0
	Case 3		6542.9		12969.6
	Case 1		6537.7		13080.5
S45	Case 2	4026.6	6539.3	2516.2	13082.1
	Case 3		6541.1		13083.9
	Case 1		6509.4		13186.6
S40	Case 2	3579.2	6518.1	3080.0	13177.3
	Case 3		6528.0		13187.2
	Case 1		6363.0		13207.5
S35	Case 2	3131.8	6405.5	3712.7	13250.0
	Case 3		6452.3		13296.8
	Case 1		5973.9		13090.6
S30	Case 2	2684.4	6078.8	4432.3	13195.5
	Case 3		6207.1		13323.8
	Case 1		5368.5		12861.3
S25	Case 2	2237.0	5502.5	5255.8	12995.3
	Case 3		5809.7		13302.5

best techno-economical solution corresponds to a small BESS that limits the peak consumption, and for the charging strategy that forces the BESS to charge during the lowest ToU period. The low C rate, DoD, and steady temperature experienced by a BESS that only limits the top part of the peak consumption, guarantees a long lifespan that highly reduces the overall yearly costs. Given that BESS are over-dimensioned in energy in several scenarios, a higher contribution from the BESS could be imposed in order to reduce the fixed power contracted from the grid, achieving a higher peak reduction. However, this leads to an increased ageing (higher C rate, DoD, and temperature profile) that has an impact on the techno-economical decision, even with a beneficial charging strategy, turning those solutions into non-optimum. Considering all, the effect of reducing the variable term with a proper BESS charging strategy is crucial for increasing the user benefit.

One important conclusion drawn from the case example is that the optimum BESS is over-dimensioned in both power and energy. This may indicate that other energy storage technologies different than Li-ion batteries could be more beneficial from the techno-economic point of view, such as supercapacitors.

Further works derived from this article include the implementation of different charging controls in the methodology, based on different criteria than the ToU tariff, the application of the methodology to other consumptions such as commercial or residential buildings, and the inclusion of different energy storage technologies in the methodology, so the decision-making process is not only focused on li-ion batteries, but on a wider spectra of energy storage technologies.

## References

1. Eurostat, S.E.–Electricity prices for non-households consumers. [https://ec.europa.eu/eurostat/statistics-explained/index.php?title=Electricity\\_price\\_statistics#Electricity\\_prices\\_for\\_non-household\\_consumers](https://ec.europa.eu/eurostat/statistics-explained/index.php?title=Electricity_price_statistics#Electricity_prices_for_non-household_consumers)
2. Jardini, J.A.; Tahan, C.M.; Gouvea, M.R.; Ahn, S.U.; Figueiredo, F.: Daily load profiles for residential, commercial and industrial low voltage consumers. *IEEE Trans. Power Deliv.* 15, 375–380 (2000).
3. Svetozarevic, B.; Begle, M.; Jayathissa, P.; Caranovic, S.; Shepherd, R.F.; Nagy, Z.; Hischer, I.; Hofer, J.; Schlueter, A.: Dynamic photovoltaic building envelopes for adaptive energy and comfort management. *Nat. Energy.* 4, 671–682 (2019).
4. Biyik, E.; Araz, M.; Hepbasli, A.; Shahrestani, M.; Yao, R.; Shao, L.; Essah, E.; Oliveira, A.C.; Del Cano, T.; Rico, E.; et al.: A key review of building integrated photovoltaic (BIPV) systems. *Eng. Sci. Technol. Int. J.* 20, 833–858 (2017).
5. Niu, J.; Tian, Z.; Lu, Y.; Zhao, H.: Flexible dispatch of a building energy system using building thermal storage and battery energy storage. *Appl. Energy.* 243, 274–287 (2019).
6. Lizana, J.; Chacartegui, R.; Barrios-Padura, A.; Ortiz, C.: Advanced low-carbon energy measures based on thermal energy storage in buildings: A review. *Renew. Sustain. Energy Rev.* 82, 3705–3749 (2018).
7. e Silva, G.d.O.; Hendrick, P.: Pumped hydro energy storage in buildings. *Appl. Energy.* 179, 1242–1250 (2016).

8. Durand, J.M.; Duarte, M.J.; Clerens, P.: European energy storage technology development roadmap towards 2030. *Int. Energy Storage Policy Regul Work.* 108, 1–128 (2017).
9. EASE–Storage Applications. <http://ease-storage.eu/energy-storage/applications/>.
10. Yassin, M.A.; Kolhe, M.; Sharma, A.; Garud, S.: Battery capacity estimation for building integrated photovoltaic system: Design study for different geographical locations. *Energy Procedia.* 142, 3433–3439 (2017).
11. Salpakari, J.; Lund, P.: Optimal and rule-based control strategies for energy flexibility in buildings with PV. *Appl. Energy.* 161, 425–436 (2016).
12. Milis, K.; Peremans, H.; Van Passel, S.: Steering the adoption of battery storage through electricity tariff design. *Renew. Sustain. Energy Rev.* 98, 125–139 (2018).
13. Davis, M.; Hiralal, P.: Batteries as a service: A new look at electricity peak demand management for houses in the UK. *Procedia Eng.* 145, 1448–1455 (2016).
14. Mulder, G.; Six, D.; Claessens, B.; Broes, T.; Omar, N.; Van Mierlo, J.: The dimensioning of PV-battery systems depending on the incentive and selling price conditions. *Appl. Energy.* 111, 1126–1135 (2013).
15. Jankowiak, C.; Zacharopoulos, A.; Brandoni, C.; Keatley, P.; MacArtain, P.; Hewitt, N.: Assessing the benefits of decentralised residential batteries for load peak shaving. *J. Energy Storage.* 32, 101779 (2020).
16. Pandžić, H.: Optimal battery energy storage investment in buildings. *Energy Build.* 175, 189–198 (2018).
17. Oualmakran, Y.; Espeche, J.M.; Sisinni, M.; Messerve, T.; Lennard, Z.: Residential electricity tariffs in Europe: Current situation, evolution and impact on residential flexibility markets. *MDPI Proc.* 1, 1104 (2017).
18. CNMC–La nueva factura de la luz. <https://www.cnmc.es/la-nueva-factura-de-la-luz>.
19. Kokam: SLBP 55Ah High Power Superior Lithium Polymer Battery. Kokam (2015)
20. Nájera, J.: Study and Analysis of the Behavior of LFP and NMC Electric Vehicle Batteries Concerning Their Ageing and Their Integration into the Power Grid. Universidad Politécnica de Madrid, Madrid, Spain (2021).
21. Resolución de 18 de marzo de 2021, de la Comisión Nacional de los Mercados y la Competencia, por la que se establecen los valores de los peajes de acceso a las redes de transporte y distribución de electricidad de aplicación a partir del 1 de junio de 2021. [https://www.boe.es/diario\\_boe/txt.php?id=BOE-A-2021-4565](https://www.boe.es/diario_boe/txt.php?id=BOE-A-2021-4565)
22. Orden TED/371/2021, de 19 de abril, por la que se establecen los precios de los cargos del sistema eléctrico y de los pagos por capacidad que resultan de aplicación a partir del 1 de junio de 2021. [https://www.boe.es/diario\\_boe/txt.php?id=BOE-A-2021-6390](https://www.boe.es/diario_boe/txt.php?id=BOE-A-2021-6390)
23. Mongird, K.; Viswanathan, V.V.; Balducci, P.J.; Alam, M.J.E.; Fotedar, V.; Koritarov, V.S.; Hadjerioua, B.: Energy Storage Technology and Cost Characterization Report. Technical report, Pacific Northwest National Lab (PNNL) (2019).
24. Mongird, K.; Viswanathan, V.; Balducci, P.; Alam, J.; Fotedar, V.; Koritarov, V.; Hadjerioua, B.: An evaluation of energy storage cost and performance characteristics. *Energies.* 13, 3307 (2020).
25. Fotouhi, A.; Auger, D.J.; Propp, K.; Longo, S.; Wild, M.: A review on electric vehicle battery modelling: From Lithium-ion toward Lithium–Sulphur. *Renew. Sustain. Energy Rev.* 56, 1008–1021 (2016).
26. Zhang, L.; Hu, X.; Wang, Z.; Sun, F.; Dorrell, D.G.: A review of supercapacitor modeling, estimation, and applications: A control/management perspective. *Renew. Sustain. Energy Rev.* 81, 1868–1878 (2018).

27. Amiribavandpour, P.; Shen, W.; Kapoor, A.: Development of thermal-electrochemical model for lithium ion 18650 battery packs in electric vehicles. In: 2013 IEEE Vehicle Power and Propulsion Conference (VPPC), pp. 1–5. IEEE Press, Beijing, China (2013).
28. Rao, V.; Singhal, G.; Kumar, A.; Navet, N.: Battery model for embedded systems. In: 18th International Conference on VLSI Design held jointly with 4th International Conference on Embedded Systems Design, pp. 105–110. Kolkata, India (2005).
29. Lam, L.; Bauer, P.; Kelder, E.: A practical circuit-based model for Li-ion battery cells in electric vehicle applications. In: 2011 IEEE 33rd International Telecommunications Energy Conference (INTELEC), pp. 1–9. IEEE Press, Amsterdam, The Netherlands (2011).
30. Tremblay, O.; Dessaint, L.A.; Dekkiche, A.I.: A generic battery model for the dynamic simulation of hybrid electric vehicles. In: 2007 IEEE Vehicle Power and Propulsion Conference, pp. 284–289. IEEE Press, Arlington, TX, USA (2007).
31. Fan, L.: Control and Dynamics in Power Systems and Microgrids. CRC Press, Boca Raton, FL, USA (2017)
32. Allègre, A.L.; Trigui, R.: Different energy management strategies of Hybrid Energy Storage System (HESS) using batteries and supercapacitors for vehicular applications. In: 2010 IEEE Vehicle Power and Propulsion Conference, pp. 1–6. IEEE Press, Lille, France (2010).
33. Laldin, O.; Moshirvaziri, M.; Trescases, O.: Predictive algorithm for optimizing power flow in hybrid ultracapacitor/battery storage systems for light electric vehicles. *IEEE Trans. Power Electron.* 28, 3882–3895 (2012).
34. Zhou, F.; Xiao, F.; Chang, C.; Shao, Y.; Song, C.: Adaptive model predictive control-based energy management for semi-active hybrid energy storage systems on electric vehicles. *Energies*. 10, 1063 (2017).
35. Yazdani, A.; Iravani, R.: Voltage-Sourced Converters in Power Systems. Wiley Online Library, Hoboken, NJ, USA (2010).
36. Concha, P.M.T.: Analysis and Design Considerations of an Electric Vehicle Powertrain regarding Energy Efficiency and Magnetic Field Exposure. Ph.D. Thesis, ETSI Industriales (UPM), Madrid, Spain (2016).
37. Nájera, J.; Moreno-Torres, P.; Lafoz, M.; De Castro, R.M.; R Arribas, J.: Approach to hybrid energy storage systems dimensioning for urban electric buses regarding efficiency and battery aging. *Energies*. 10, 1708 (2017).
38. Omar, N.; Monem, M.A.; Firouz, Y.; Salminen, J.; Smekens, J.; Hegazy, O.: Lithium iron phosphate based battery—Assessment of the aging parameters and development of cycle life model. *Appl. Energy*. 113, 1575–1585 (2014).
39. Shepherd, C.M.: Design of primary and secondary cells: II. An equation describing battery discharge. *J. Electrochem. Soc.* 112, 657 (1965).
40. Tremblay, O.; Dessaint, L.A.: Experimental validation of a battery dynamic model for EV applications. *World Electr. Veh. J.* 3, 289–298 (2009).
41. Nájera, J.: Study and Analysis of the Behavior of LFP and NMC Electric Vehicle Batteries Concerning Their Ageing and Their Integration into the Power Grid. Ph.D. Thesis, ETSI Industriales (UPM), Madrid, Spain (2021).
42. Saw, L.; Somasundaram, K.; Ye, Y.; Tay, A.: Electro-thermal analysis of Lithium Iron Phosphate battery for electric vehicles. *J. Power Sources*. 249, 231–238 (2014).
43. Chen, Y.; Evans, J.W.: Three-dimensional thermal modeling of lithium-polymer batteries under galvanostatic discharge and dynamic power profile. *J. Electrochem. Soc.* 141, 2947 (1994).
44. Rao, L.; Newman, J.: Heat-generation rate and general energy balance for insertion battery systems. *J. Electrochem. Soc.* 144, 2697 (1997).

45. Redondo-Iglesias, E.; Venet, P.; Pelissier, S.: Calendar and cycling ageing combination of batteries in electric vehicles. *Microelectron. Reliab.* 88, 1212–1215 (2018).
46. Wang, J.; Purewal, J.; Liu, P.; Hicks-Garner, J.; Soukazian, S.; Sherman, E.; Sorenson, A.; Vu, L.; Tatara, H.; Verbrugge, M.W.: Degradation of lithium ion batteries employing graphite negatives and nickel–cobalt–manganese oxide+ spinel manganese oxide positives: Part 1, aging mechanisms and life estimation. *J. Power Sources.* 269, 937–948 (2014).
47. Iglesias, E.R.: Étude du vieillissement des batteries lithium-ion dans les applications “véhicule électrique”: Combinaison des effets de vieillissement calendaire et de cyclage. Ph.D. Thesis, Université de Lyon, Lyon, France (2017).
48. Budes, F.B.; Ochoa, G.V.; Escorcía, Y.C.: An Economic Evaluation of Renewable and Conventional Electricity Generation Systems in a Shopping Center Using HOMER Pro. *Contemp. Eng. Sci.* 10, 1287–1295 (2017).
49. Mehta, S.; Basak, P.: A case study on pv assisted microgrid using homer pro for variation of solar irradiance affecting cost of energy. *Contemp. Eng. Sci.* 10, 1287–1295 (2017).
50. Mehta, S.; Basak, P.: A case study on pv assisted microgrid using homer pro for variation of solar irradiance affecting cost of energy. In: 2020 IEEE 9th Power India International Conference (PIICON), pp. 1–6. IEEE Press, Sonapat, India (2020).

## **Methodology to design a polygeneration system (CCHP) in a hotel complex in Xalapa City, Veracruz**

Del Ángel-Ramos J. A. <sup>1</sup>, López-Meraz R. A. <sup>1</sup>[0000-0002-3236-3709], Camacho Ceballos, M.A<sup>1</sup>, Rivera-Peña J.<sup>1</sup>, Arenas-Del Ángel J.L. <sup>1</sup>, Marín-Hernández J.J.<sup>1</sup>

<sup>1</sup> Universidad Veracruzana, Circuito Universitario Gonzalo Aguirre Beltrán s/n, 91000, Mexico

jdelangel@uv.mx: J.D-R; raullopez03@uv.mx: R.L-M.;  
yarivera@uv.mx: Y.R-P.; jorarenas@uv.mx: J.A-D.; jmarin@uv.mx:  
J.M-H.

**Abstract.** In the present work developed as part of the professional intervention of the master's degree in energy engineering, shows the use of exergetic skills, including some thermal software, and shows how, together, could demonstrate which alternative could be allows the modeling of a wide range of thermal systems such as combined gas turbine cycles, steam plants, power generation systems, cogeneration and a wide range of power plant system. A) The thermal and electrical consumptions of the hotel complex were determined. B) The selection of the possible components and the probabilities of accommodation in an energy staggering were made. C) The system was shown in a Thermal software. D).- Border and environmental conditions were established for the derate adjustment and the initial exergetic conditions. E) Thermodynamic modeling was performed. .F) Each step was validated by direct calculation, First Law Analysis of Thermodynamics, Second Law of Thermodynamics and Exergetic Analysis to determinate wich component has the higher exergetic destruction. Thermoeconomically when implementing the trigeneration system in the hotel complex and through a cash flow, it is necessary understood ,that the joint trigeneration project of the two hotels is economically viable where the return on investment is 6.51 years and from that year will begin To generate savings, the internal rate of return of 18% higher than the 12% that was taken as reference and the net present value of \$ 6, 271,739.30.

**Keywords:** CCHP, Microturbine, Exergetic, Trigeneration component.

### **1 Introduction**

The applications of trigeneration systems could be use alternative engines, gas micro-turbines (MGTs) and fuel cells [1]. Although gas microturbines are less electrical generated efficient compared to reciprocating engines, but, their advantage is that turbines produce less Nitrogen Oxides emissions [2] and operate at lower cost compared to fuel cells and, by producing higher temperatures At 200 ° C are a good option when using natural gas [3]. A relatively common trigeneration system first uses high temperature

2

heat to power the gas turbine, and the low temperature residual heat (the heat of the exhaust gas) is recovered for steam, hot water and / or to produce refrigeration [4].

However, when sizing a trigeneration system, it is necessary to combine several variables that, combined, allow to select the components of the system, as well as their location in the process, this implies the development of simulation that if it were developed from others ways, would require surely, time and effort. In the present work developed as part of the professional intervention of the master's degree in energy engineering, shows the use of thermal software with energetic and exergetic simulation ranges, developed to visualize the thermal performance in the equipment used for the generation of Electrical energy, heating and air conditioning in a hotel complex in the Xalapa City.

The applications of trigeneration systems are usually directed at the use of alternative engines, with gas microturbines (MGTs) and fuel cells [3]. Although gas microturbines are less efficient compared to reciprocating engines, their advantage is that they produce less Nitrogen Oxides emissions [4] and operate at a lower cost compared to fuel cells and, on the other hand, Producing temperatures above 200 ° C is a better option for the use of natural gas [5]. A relatively common trigeneration system first uses high temperature heat to drive the gas or steam turbine, and low temperature residual heat (which may be exhaust heat) is recovered for heating and / or cooling [6,1].

Gas Turbine Plants (GT) are widely used worldwide for the generation of electricity, distributed energy and for cogeneration and trigeneration schemes [7, 8]. In most of these GT plants, natural gas is often used as fuel in such plants [6]. Today, many utilities strive to increase the efficiency (or heat rate) of thermoelectric power stations, many of which are over 25 years old [9]. A sustainable solution is often sought to address the problems of excessive use of fossil fuels through improved energy efficiency, reducing costs compared to conventional options. [5]

For the thermal study of the processes involved in the trigeneration projects, specialized programs are available for the dimensioning of these systems, such as the Thermoflow software, which has different subprograms such as the GT PRO & GT MASTER which Are used for simulations of combined cycle plants; As well as the STEAM PRO & STEAM MASTER used for the design of conventional steam plants. It has the PEACE (Plant Engineering And Construction Estimator) that is used for the design of equipment and estimation of labor costs and the heat balances they produce. This article will show the use of THERMOFLEX which allows the modeling of a wide range of thermal systems such as combined gas turbine cycles, steam plants, power generation systems, cogeneration and a wide range of power plant systems [10].

## **2 Materials and methods**

### **2.1 Case of study**

#### **The thermal and electrical consumptions of the hotel complex**

The hotel complex needs to cover an annual electricity demand of 879,892 kW, of which a hotel for adequate air conditioning needs 120 tons of refrigeration (TR); To supply the consumption of domestic hot water (DHW) at both hotels a water flow of 0.9 kg/s is required at a temperature of 60 °C.

#### **The selection of the possible components and the probabilities of accommodation in an energy staggering**

A mass flow of 5.08 kg / s of hot water at 95 ° C is required for the operation of the 75 TR absorption chiller [12]; To provide this increase in energy it is necessary to have 1.47 kg / s of flue gases, this mass flow would come from three 65kW gas microturbines connected in parallel.

Exhaust gases from the three gas microturbine systems still have sufficient energy for their use, which is why heat recovery devices are used for the use of waste heat for the generation of hot water for services (ACS) with the conditions required by the hotel complex. Once the components of the trigeneration system have been selected, a model is created in the Thermal software.

#### **The model was build in a Thermal software**

In the Thermal program for the construction of the model must be placed the necessary components of the system and interconnecting them. The software validates the interconnections since it has a wide variety of diagnostic messages; Once the switching is done you can move between the menus to specify the performance parameters of each component of the system.

Although Thermal software contains more than 100 components including boilers, condensers, cooling towers, feed water heaters, desalination plants, gasifiers, heat exchangers, absorption or adsorption chiller or more than 350 different models of gas turbines And reciprocating engines; For the case of the gas turbine of lower power round in the 400 kW, for which it was necessary to design a special commercial gas microturbine with the characteristics of Capstone C-65.

#### **Border and environmental conditions for the derate adjustment and the initial exergetic conditions**

Knowing the derating losses suffered by the microturbines in their performance is important when modeling the systems as it approaches a more accurate analysis in the modeling. Fig. 1 shows the performance diagram of a gas microturbine, where the main

4

losses will be found in the air intake under ambient conditions and the height above sea level where the microturbine will be installed

The city of Xalapa, Ver. Is at an altitude of 1460 msn (4790 ft) at an average annual temperature of 18 ° C (64.4 ° F); The gas microturbine delivered according to these conditions a maximum electrical capacity of 54 kW delivering a mass flow of 0.49 kg / sec, a temperature of 318.4 ° C and enthalpy of 309.4 kJ / kg calculated with the Thermoflex software.

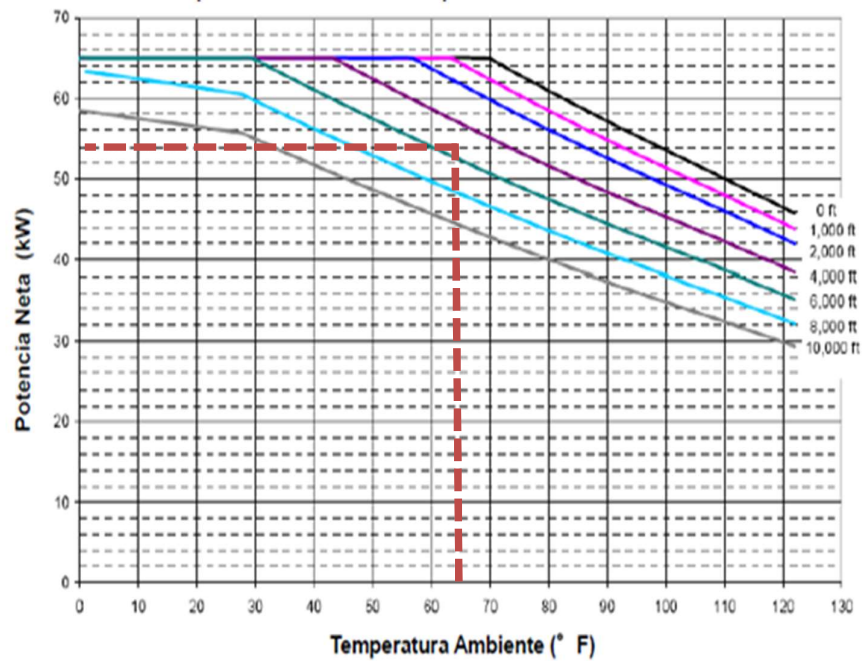


Fig. 1. Performance of a Capstone 65kW gas microturbine depending on the ambient temperature in which the system is located and height above sea level [11].

**Thermodynamic modeling**

For the thermodynamic modeling, several assumptions are made that simplify the analysis of second law, to make it manageable, but retaining the precision required to ensure a greater accuracy in the results, which are:

- 1) All processes are considered to be operating in steady state.
- 2) The air data and combustion products will be taken from the simulation results in the Thermoflex software
- 3) The fuel injected into the Combustion Chamber is considered natural gas.

4) The heat loss of DC is 2% of the energy of the fuel entering the DC, based on the lower calorific value (LHV), and all other components are considered adiabatic [13]

5) The dead state is  $P_o = 1.01385$  bar and  $T_o = 298.15$  K. (refers to the condition of a gas in any thermodynamic process, particularly its volume)

6) Once obtained the first law analysis will determine the specific exergies and exergies depending on the mass flow; The air the dead state  $T = 298.15$  K, a pressure of 1.0132 bar an enthalpy of 0 kJ/kg and entropy of 0.1883 kJ/kg K and for the water of  $T = 298.15$  K, a pressure of 1.0132 bar an enthalpy Of 104.93 kJ/ kg and entropy of 0.367 kJ / kg K.

It is understood as exergy to the maximum useful work that can be obtained from the system in a state for specific environment [13, 14]; This aid in the optimization of complex thermodynamic systems as well as in devices used in engineering [15 14.] Performing an exergetic analysis helps localization of the causes of system inefficiency and thus provide a clear insight into the factors that can not be found in a first law analysis [1].

## 2.2 Modeling of the trigeneration system for the hotel complex

In the simulation developed will be able to visualize the performance of the each element proposed in the trigeneration study for a hotel complex in the City of Xalapa, with even exergetic simulation scopes.

According to the needs that the hotels requires a trigeneration system was designed which consists of 3 gas microturbines model Capstone C65 in according to the environmental conditions of the city of Xalapa will each provide 54 kW obtaining a total of generation Net Power of 162 kW, the outgoing gases of the microturbines have sufficient energy to be recovered in a heat exchanger circulating hot water from a temperature of 80 ° C to 95 ° C in a closed system which is occupied to operate An absorption cooling system that will heat half of the air conditioning necessary for a hotel (the rest will be supplied by an electric air-conditioning system); The first heat exchanger emits sufficient energy to be used in another heat exchanger and to obtain an optimal sanitary water temperature for the distribution of services in the hotel complex. The results of the analysis for each microturbine component were obtained, in particular, because the exergetics losses occurring in the CCHP system were found in the gas turbine, this is due to the irreversibilities that exist between the compressor and the Turbine. As shown in the following: Fig. 2.

6

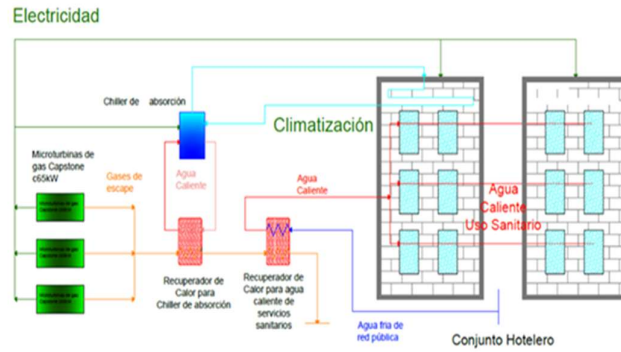


**Fig. 2.** Diagram of the trigeneration system for the hotel complex in the city of Xalapa, Ver.

On the other hand, the model obtained with the thermal software of the trigeneration system is represented in Fig. 3.

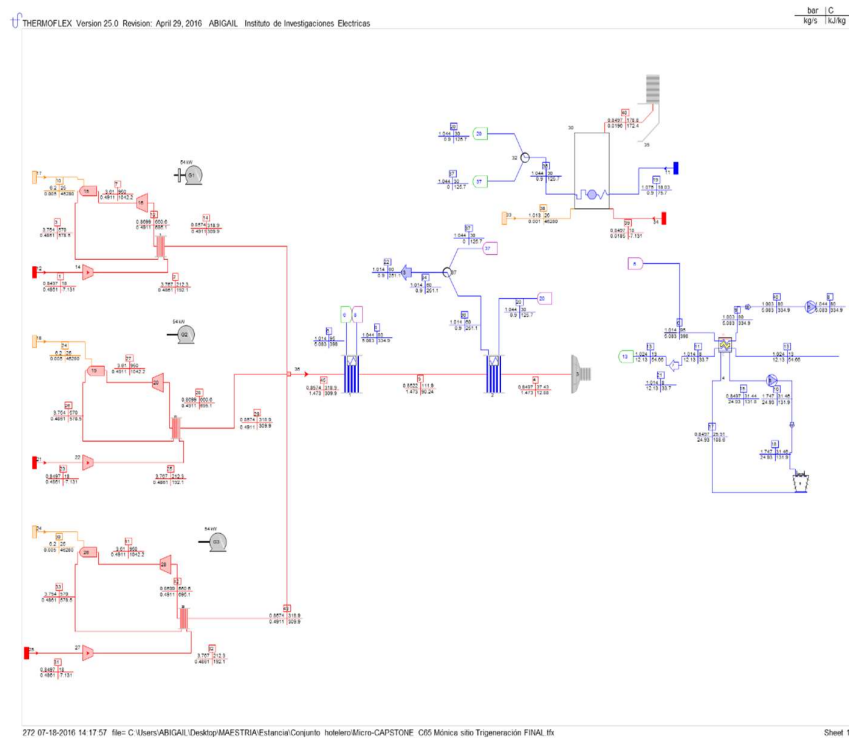


**Fig. 3.** Trigeneration System Model developed in Thermal Software.

### 3 Results

Table 1 shows the results and comparisons between the thermal calculations of first law and the calculations elaborated by the exergetic analysis for one of the microturbines proposed in the trigeneration system, where it is observed that in the first law analysis the highest efficiency Energy is given in the combustion chamber, for the air preheater regeneration efficiency is obtained while the largest exergene losses occurring in the system are in the gas turbine, this is due to the irreversibilities that exist between the compressor And the turbine. For the 3 gas microturbines they have a total destroyed exergy of 770.47 kW.

1) Air compressor. To calculate the volume and mass of air at the intake of the software turbine, it is obtained that the LHV of natural gas is 46280. If it is known from the manufacturer, that the output of the exhaust gas flow is equal at 0.49 kg / s, the fuel flow will have a value of 0.005329 kg / s and the mass flow of the air entering each microturbine will be 0.48.51 kg / s. The isentropic efficiency of the compressor will be 78.32% and the isentropic state ( $h_{2s}$ ) will be 148.94 kJ / kg. It is obtained that the real compressor input work is 199.27 kJ / kg or 96.87 kW if the mass flow is considered

2) Air preheater. With the thermodynamic states obtained and substituting the values in equation 3.5, an efficiency in the air preheater of 99% is obtained, the heat emitted by the exhaust gases is 189.20 kW and the heat absorbed by the air is 187.79 kW

3) Combustion Chamber. Describing the energy balance shown in equation 3.8 and solving for the efficiency, an efficiency of 99% will be obtained.

4) Gas turbine. From the simulation, the thermodynamic states and the isentropic efficiency of the turbine are obtained, which is 80.92%. The output work of the gas turbine has a result of 347.041 KJ / kg or 170.43 kW. According to equation 3.10, the backward relationship between the compressor and the turbine is 57.52%, this means that the compressor consumes 57.42% of the work produced by the turbine, this is due to the irreversibilities that occur within the compressor and the turbine. .

The net work is equal to 73.56 kW with a thermal efficiency of 31.87%

5) Heat exchanger for the generation of hot water for the operation of an absorption cooler, once the exhaust gases, has an energy efficiency delivered by the software of 99% where the heat absorbed by the exhaust gases is 323.61 kW and the heat absorbed by the air is 320. 45 kW

6) Heat exchanger for the generation of hot water for services has an energy efficiency of 99% with a heat emitted by the exhaust gases of 113.97 kW and by the water of 112. 85 kW

8

**Table 1.** Results and comparisons of the first law analysis and exergetic analysis of gas micro-turbines.

Equipo	Potencia	Eficiencia energética/eficacia	Exergía destruida considerando el flujo másico	Eficiencia exergética	Pérdidas por exergía
	<b>KW</b>	<b>%</b>	<b>KW</b>	<b>%</b>	<b>%</b>
Compresor	95.22	78.32%	11.83	87.57%	4.61%
Pre calentador		78.64%	13.23	88.47%	5.15%
Cámara de combustión		99.67%	76.68	81.25%	29.86%
Turbina de gas	64.94	80.92%	118.82	35.34%	46.27%
Trabajo útil	36.27		36.27		14.12%
Total			256.82		100.00%

Table 2 shows the energy efficiency obtained with the energy balance of the first law heat recuperators are those that contain higher energy efficiency, while the absorption chiller by the exergetic efficiency the largest component was the absorption chiller. The component with the greatest exergetic losses was found it in the three microturbines scenarios.

- 1) Air compressor. Considering a compressor power of 95.22 W, the exergy destroyed for the air compressor is 11.83 kW with an exergetic efficiency of 88%
- 2) Air preheater. The exergy destroyed by solving it from equation developed has a value of 13.23 kW with an exergy efficiency of 88%.
- 3) Combustion Chamber. For this component, the exergy destroyed is solved with a value of 76.68kW and an exergetic efficiency of 81.25%
- 4) Gas turbine. In this component, the shaft power is taken, which is 64.94 kW taken directly from the Thermoflex software and solving the destroyed exergy, a value of 118.82 kW and an exergetic efficiency of 35% are obtained.
- 5) Heat exchanger for the generation of hot water for the operation of an absorption cooler a destroyed exergy of 68.92 kW is obtained with an exergy efficiency of 44.48%.
- 6) Heat exchanger for the generation of hot water for services has an exergy efficiency of 43% and an exergy destroyed from equation 27 of 9.26 kW.
- 7) Chiller by absorption. From equation developed and solving for the destroyed exergy, a value of 249.43 kW is obtained with an exergetic efficiency of 75%

**Table 2.** Results and comparisons of the first law analysis and exergy analyzes of the proposed trigeneration system.

Equipo	Potencia	Eficiencia energética	Exergía destruida considerando el flujo másico	Eficiencia exérgica	Perdidas por exergía
	kW	%	kW	%	%
Microturbina de gas	64.7		770.470	49.30%	63.84%
Econormizador chiller		99.01%	68.919	44.48%	5.71%
Econormizador servicios		99.01%	9.263	43.11%	0.77%
Chiller	214	68.75%	249.427	75.02%	20.67%
Trabajo util	108.805		108.805		9.02%
Sisterra			1206.884		100.00%

#### 4 Conclusions

The Thermal software used here is a specialized software for the use of engineering with a graphical interface that allows to link thermodynamic models by means of icons that represent the components of the proposed systems and together with its package allows the design and simulation of power plants as is The case of this work where a proposal of trigeneration for a hotel complex was simulated in order to reduce operating expenses in a hotel complex in the city of Xalapa Veracruz and to have an idea with a short approximation.

However, the software still has small errors in the operation of the same components that are easy to locate as in the case of this work the energy efficiencies of some of the components, that is why it is used to a more detailed study of the Components of the systems by exegetic methods that once having the data of the thermodynamic states of the system is easy to calculate. With the software it is observed that the hotel suite currently presents a proportional consumption of both electricity and gas, when implementing the trigeneration system will have total electrical energy savings where the hotel suite will cover the thermal demand they will need for the operation of the System of trigeneration.

Economically when implementing the trigeneration system in the hotel complex and through a cash flow, it is necessary that the joint trigeneration project of the two hotels is economically viable where the return on investment is 6.51 years and from that year will begin To generate savings, the internal rate of return of 18% higher than the 12% that was taken as reference and the net present value of \$ 6, 271,739.30.

Economically when implementing the CCHP System in the hotel suite and through a cash flow, the project of CCHP in conjunction of the two hotels is economically viable where the return on investment is close to 5 years and from that year, would start to generate savings. The internal rate of return was higher than the reference rate and the positive net present value.

#### References

1. Anvari, S., Khoshbakhti, R. and Bahlouli, K.: Employing a new optimization strategy based on advanced exergy concept for improvement of a trigeneration system, Applied Thermal Engineering, vol. 113, pp. 1452-1463, 25 (2017).

10

2. Sibilio, S., Rosato, A., Ciampi, G., Scorpio, M. and Akisawa, A.: Building-integrated trigeneration system: Energy, environmental and economic dynamic performance assessment for Italian residential applications, *Renewable and Sustainable Energy Reviews*, 68, (2), 920-933 (2017).
3. Ünal, A., Ersöz, İ. and Kayakutlu, G.: Operational optimization in simple trigeneration systems, *Applied Thermal Engineering*, 107, 175-183 (2016).
4. Baghernejad, A., Yaghoubi, M. and Jafarpur, K.: Exergoeconomic comparison of three novel trigeneration systems using SOFC, biomass and solar energies, *Applied Thermal Engineering*, 104, 534-555 (2016).
5. Basrawi, F., Ibrahim, T., Habib, K. and Yamada, T.: Effect of operation strategies on the economic and environmental performance of a micro gas turbine trigeneration system in a tropical region, *Energy*, 97, 262-272 (2016).
6. Popli, S., Rodgers, P. and Eveloy, V.: Trigeneration scheme for energy efficiency enhancement in a natural gas processing plant through turbine exhaust gas waste heat utilization, *Applied Energy*, 93, 624-636 (2012).
7. Fallah, M., Siyahi, H., Akbarpour Ghiasi, Mahmoudi, Yari, R. and Rosen, M.: Comparison of different gas turbine cycles and advanced exergy analysis of the most effective, *ELSEVIER*, 116, 701-715 (2016).
8. Hatami, M., Ganji, D. and Gorji-Bandpy, M.: A review of different heat exchangers designs for increasing the diesel exhaust waste heat recovery, *Renewable and Sustainable Energy Reviews*, 37, 168-181 (2014).
9. Moussawi, H., Fardoun, F. and Louahlia-Gualous, H.: Review of tri-generation technologies: Design evaluation, optimization, decision-making, and selection approach, *Energy Conversion and Management*, 120, 157-196 (2016).
10. ThermoFlow company.: ThermoFlow, 2002. [on line]. Available: <https://www.thermoflow.com/images/ThermoFlowBrochure2002.pdf>. (2016)
11. Capstone Turbine Corporation.: Capstone Turbine Corporation All rights reserved, [on line]. Available: <https://www.capstoneturbine.com/products/c65>.
12. World Energy Co., Ltd.: World Energy, [on line]. Available: <http://www.worldenergy.mx/descargar>. (2016).
13. Thu, K., Saha, B., Chua, K. and Bui, T.: Thermodynamic analysis on the part-load performance of a microturbine system for micro/mini-CHP applications, *Applied Energy*, 178, 600-608 (2016).
14. Sadighi Dizaji, H., Jafarmadar, S. and Hashemian, M.: The effect of flow, thermodynamic and geometrical characteristics on exergy loss in shell and coiled tube heat exchangers, *Energy*, 91, 678-684 (2015).
15. Alimoradi, A.: Investigation of exergy efficiency in shell and helically coiled tube heat exchangers, *Case Studies in Thermal Engineering*, 10, 1-8 (2017).
16. Mahesh, N., Bagade, S. and Kilkarni, G.: Energy and Exergy analysis of diesel engine powered trigeneration systems, *Energy Procedia*, 90, 27-37 (2016).

## A low-cost device for measuring the complete $I$ - $V$ curve of solar cells integrated into a modular platform suitable for other techniques such as electroluminescence.

Víctor Alonso-Gómez<sup>1</sup>[0000-0001-5107-4892], José Ignacio Morales-Aragoneses<sup>1</sup>[0000-0002-9163-9357], Sara Gallardo-Saavedra<sup>1</sup>[0000-0002-2834-5591], Alberto Redondo Plaza<sup>1</sup>[0000-0002-2109-5614], Diego Fernández Martínez<sup>1</sup>[0000-0003-1468-9083] and Luis Hernández-Callejo<sup>1</sup>[0000-0002-8822-2948]

<sup>1</sup> University of Valladolid, Campus Universitario Duques de Soria, 42004, Spain

victor.alonso.gomez@uva.es (V.A-G.)

zigurat@coit.es (J.I.M-A.)

s.gallardosaavedra@gmail.com (S.G-S.)

alberredon@gmail.com (A.R.P.)

diego-brivi@hotmail.com (D.F.M.)

luis.hernandez.callejo@uva.es (L.H-C.)

**Abstract.**  $I$ - $V$  curves is one of the most important techniques available for characterizing photovoltaic cells. Measure an  $I$ - $V$  curve at single cell level has a lot of technical difficulties because of the low voltages and high current implied. In this paper, authors propose a low-cost device for measure  $I$ - $V$  curves of single cells and small amounts of cell in series using two capacitors as fundamental pieces. As an additional advantage, the strategy of measurement can obtain the second and fourth quadrant of the  $I$ - $V$  curve, as well as the usual first quadrant of the curve. A device has been constructed for demonstrating that is possible and good measurements of the  $I$ - $V$  curve has been obtained. For using the device in a laboratory without depending on the solar irradiation, a board with infrared LEDs has been designed and constructed. A modular platform has also been 3D printed for placing the photovoltaic cell, the LED board, and a camera for doing electroluminescence injecting current to the cell. The result is a very useful pack for doing  $I$ - $V$  curves and tacking electroluminescence images at cell or mini module level, that has been demonstrated to work as expected.

**Keywords:**  $I$ - $V$  curve, electroluminescence, photovoltaic, solar cell.

### 1 Introduction

There are a lot of different techniques for characterizing photovoltaic (PV) solar cells in many different aspects. Ones are focused on the microscopical composition of the cell and the influence over its macroscopical behaviour and others directly in this macroscopical aspect [1–5]. From the practical point of view, the cell is used to produce electricity, and this may be the most important aspect. Of course, it is very important to know why a cell is not performing as well as it should or what problems it is currently

experiencing and how they may evolve over time. However, we first need to be able to inspect them in a fast way and discover if it is working as expected or not. For this purpose, there are some techniques as electroluminescence (EL) imaging [6–8], thermal imaging [9,10] or the  $I$ - $V$  curve. The latter is the only one which directly can tell the output power of the PV cell with certainty, because measures the variation of the current leaving the cell when the voltage across its terminals is forced to change (that is, when the load resistance connected at its output is changed). It is not possible to do the  $I$ - $V$  curve of a single cell in a commercial PV module, just the full module  $I$ - $V$  curve. Nonetheless, it is possible to do it at the laboratory using single cells instead of complete modules. This information at cell level is used for manufacturers to detect bad cells and discard them before the integration into a module or to classify them and put similar cells into a module to avoid mismatching [11].

There are a various topologies used to measure the  $I$ - $V$  curve, based on different ways of varying the load seen by the PV cell or module [12]. Most of the commercial devices use a variable electronic load or the charge of a capacitor for tracing the  $I$ - $V$  curve. However, most of them are designed for standard modules (usually over 60 cells in series) or for an array of modules (usually about 30 modules). The main difficulty for measuring correctly the  $I$ - $V$  curve of a single cell is the fact that the voltages implied are very low (less than 1 V) while the currents can be high enough (in the order of 10 A). With these numbers, applying the Ohm's Law, it yields a resistance of 0.1  $\Omega$  or less (because these high currents must be output by the cell at near 0 V, as we will see later).

Determination of voltages can be done easily nowadays with an analog to digital converter (ADC), but noise in the order of microvolts to millivolts is produced by near electromagnetic fields, other components of a circuit, noise in the supply voltage of the converter, etc. Usually this is not a problem because the value measured is big enough compared to this noise, but this is not the case (a lot of precision measures below 0.4 V are needed here).

Regarding the current, if 10 A at 0.1 V is desired, an equivalent resistance in the total circuit lower than 10 m $\Omega$  is needed for it to flow. Most of the contact resistances of normal probes (like the ones in a regular multimeter), cable connectors, etc., are higher than this value. Many strategies can be used to solve this: high section cables, soldered connections, wide copper tracks at printed circuit boards (PCBs), short electric paths, gold plated connectors, etc.

As will be shown in next section, these problems are solved with the device proposed in this paper, with the added benefits of being very cheap (compared to professional commercial devices) and the possibility to get the complete  $I$ - $V$  curve (first, second and fourth quadrant) of the PV cell measured. Also, the electronics can be adjusted easily to measure a small number of cells in series a association (small module) by modifying only the value of a pair of resistors on the PCB.

## 2 Methods

### 2.1 Principles of operation

As shown in Fig. 1, the proposed *I-V* tracer is based just in the charge and discharge of two capacitors across a solar cell. The strategy of measurement could also be carried on small associations of solar cells in series (small modules) and even regular photovoltaic modules (PV modules). For this reason, we designate it as Device Under Test (DUT).

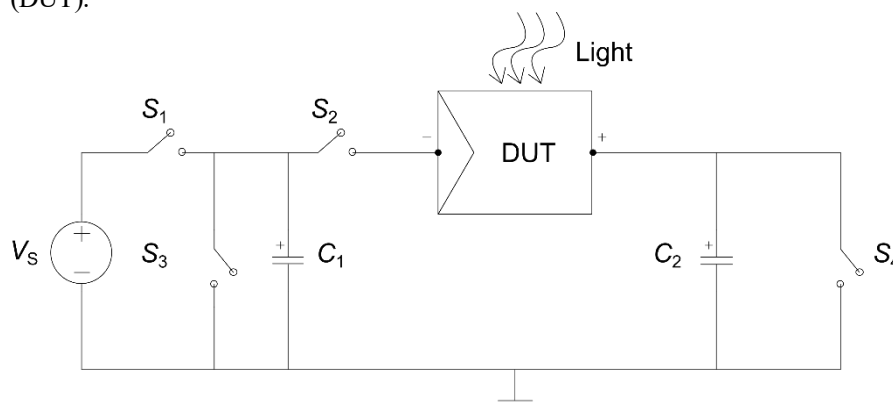


Fig. 1. Schematic topology for the proposed I-V tracer.

#### Measure process.

The process, controlled by opening or closing the needed switches at each step, is done as follows:

1. Firstly, both capacitors ( $C_1$  and  $C_2$ ) are discharged —  $V(C_1) = V(C_2) = 0$  — and all switches ( $S_1, S_2, S_3$  and  $S_4$ ) are opened.
2. Then, by closing  $S_1$ ,  $C_1$  is charged to the source voltage ( $V_s$ ).
3.  $S_1$  is then opened again.  $C_1$  and  $C_2$  negative sides are then at 0 V,  $C_1$  positive side is at  $V_s$  while  $C_2$  positive side is also at 0 V. So,  $V(C_1) = V_s$  and  $V(C_2) = 0$  V.
4.  $S_2$  is then closed so current flows through the DUT, charging  $C_2$  while discharging  $C_1$ . Note that the voltage at the DUT terminals is always the differential voltage between the positive plate of  $C_2$  and the positive plate of  $C_1$  (that is,  $V(DUT) = V(C_2) - V(C_1)$ , because both negative plates are always at ground level). Wrongly, one could think that the current will stop when  $C_1$  and  $C_2$  arrives to the same voltage level. That is not true because the DUT is a PV device under illumination, so it will raise the voltage between its terminals until its open circuit voltage,  $V(DUT)_{OC}$ , is reached. **Second and first quadrant of the *I-V* curve is then traveled by the DUT, inevitably, at this step**, as will be explained later.
5.  $S_2$  is then opened and, immediately,  $S_3$  is closed. This discharges  $C_1$ , so  $V(C_1) = 0$  now.

6.  $S_2$  is closed a gain while maintaining  $S_3$  also closed. Now, the negative side of the DUT will remains at ground level while its positive side is at  $V(C_2)$ . In this case,  $V(DUT) = V(C_2) - 0$ , which is far higher than the  $V(DUT)_{OC}$ . The current flows in this case from  $C_2$  to ground until  $V(DUT)_{OC}$  is reached going down from higher voltages. Consequently, **the DUT is forced to travel the first quadrant of its  $I-V$  curve at this step**, as will be also explained later.
7. Once the process ends and the current stop flowing,  $S_4$  is closed to discharge completely  $C_2$  to let the apparatus prepared to start a new measurement from step 1 ( $S_4$  is opened again after discharge).

**One diode model for a photovoltaic cell.**

For the sake of simplicity, diagram showed in Fig. 1 omits all the components needed to measure the current and voltage at the DUT, control switches, limit currents to reasonable values, etc. To better understand how the  $I-V$  curve of the DUT works, it is also important to remember the simplest electrical model of a PV cell: the one diode model (see Fig. 2). In this model, a current source ( $I_p$ ) is used to consider the photogenerated current of the solar cell; a diode ( $D$ ) to model the fact that a cell is, in essence, a P-N junction between two semiconductors. Finally, a parallel resistor ( $R_p$ ) and a series resistor ( $R_s$ ) model that the diode and the source are not ideals (contact resistances, impurities, annihilation between conduction electrons and holes, scattering and collisions with the crystalline net, etc.).

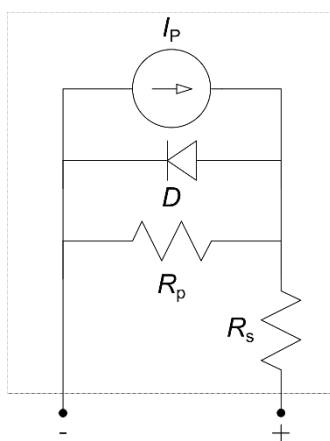


Fig. 2. One diode model for a photovoltaic cell.

The  $I-V$  curve of a single ideal diode is shown in the Fig. 3-a). A perfect diode won't let any current flow through it until the forward conduction voltage is reached. Once overpassed this voltage (also known as diode voltage or umbral voltage), the current increases exponentially so fast that the current goes to infinite in very low increment of voltage. At inverse voltage applied over its terminals (negative at the anode and positive at the cathode), the diode perfectly blocks the current flow, no matter how much negative voltage you applied. This is, obviously, incorrect at a real diode for some reasons

exposed at Fig. 3-b). Firstly, you cannot apply as much reverse voltage as you want because, at some point, the electric field felt by the charges separated by the PN junction will be so high that they will pass through the depletion zone. This effect is so abrupt in voltage changes that the current could go to very high currents as fast that will destroy the diode due to the heat generated (but is used in a calculated way sometimes, for example, in Zener diodes or other avalanche diodes). In addition, a very small current (in the order of  $\mu\text{A}$ ) is allowed to flow in the reverse voltage zone and in the forward zone, below the conduction voltage (this effect is greatly exaggerated in the drawing for being visible). After overpassing the conduction voltage (which depends on the semiconductors used), the current rapidly raises exponentially but not so fast as in the ideal case because of the limiting resistance associated to the real diode. This current will produce losses by heating itself. If the diode overpasses the power it can dissipate in terms of heat, it will also break. For this reason, a forward current and voltage exists and depends on the physical characteristics of the diode (composition but, especially, size in surface and volume terms, because of the heat dissipation it provides).

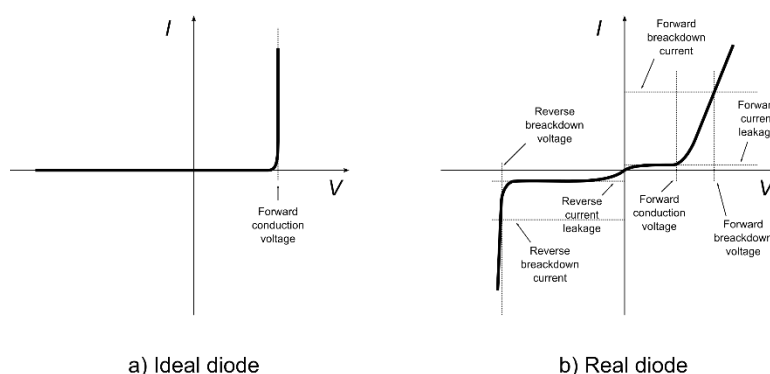
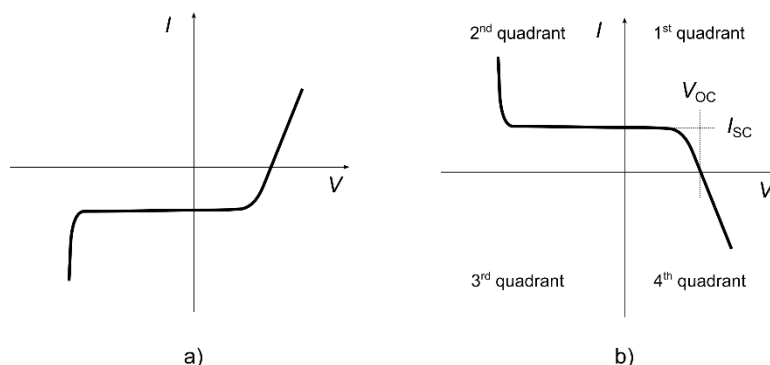


Fig. 3. *I-V* curve of a diode.

When the current source is added to the real diode model to take the photogenerated current into account, the curve lowers by the value of this current, as shown in Fig. 4-a). It goes down because, as can be seen in Fig. 2, this current flow opposed to the diode forward mode. Seen as a power production device (a PV cell), the zone when the current is generated by the cell will be at the fourth quadrant in this diagram. This will give positive voltage but negative current, so the power will be negative. For making this power positive, the criterion of the current is inverted, which makes sense in this case (consider positive when the cell gives you useful current and consider it negative when you inject more current to the cell than the current it gives to you). The effect over the graph is just a symmetry over the voltage axis (a flip), which is shown at Fig. 4-b). This is the *I-V* curve which most people are used to, where the first quadrant corresponds to the power generated by the PV cell and whose cuts with the axes define the short-circuit current ( $I_{sc}$ ) and open circuit voltage ( $V_{oc}$ ).



**Fig. 4.** *I-V* curve of a photovoltaic cell. a) Maintaining the current and voltage criterion from the diode. b) Inverting the current criterion from the diode.

**Tracing the *I-V* curve of a photovoltaic cell.**

Now it is easy to understand that in the step 4 of the described process, with the capacitor  $C_1$  charged to the source voltage ( $V_s$ ) and the capacitor  $C_2$  totally discharged, we are applying a positive voltage at the negative terminal of the PV cell and zero to the positive terminal, that is, we are applying a negative voltage in the diagram of Fig 4-b). In this case, the current will flow inside the cell mostly through the current source since the diode is reverse biased and the parallel resistance should ideally be very high (see Fig. 5-a). Consequently, the current value is determined by the PV cell short-circuit current ( $I_{sc}$ ). The discharge of  $C_1$  due to this current will produce the charge of  $C_2$  or, equivalently, moving to the right along the *I-V* curve (see Fig. 5-b). When the voltage of both capacitors is equalized, the difference across the terminals of the cell will be 0 V, so in the *I-V* curve it will be at the crossing point with the current axis ( $I_{sc}$ ). The cell will continue through its normal *I-V* curve until it reaches  $V_{oc}$ , where it cannot push more electrons outside itself (so,  $V(C_2) - V(C_1) = V_{oc}$ ). It could be demonstrated that these assumptions and graph are applicable also to a PV module. Indeed, a PV module is just a series association of single cells (sometimes there are also parallel associations) and some bypass diodes, so the effect over the *I-V* curve is just raise multiply the  $V_{oc}$  by the number of cells in series and the  $I_{sc}$  by the parallel lines (in case parallel association exist). Of course, these assumptions are only valid if all the cells are equals and are in good state. If there are bad cells, a lot of deformations over the *I-V* curve occurs, but the study of these cases is beyond the scope of this paper.

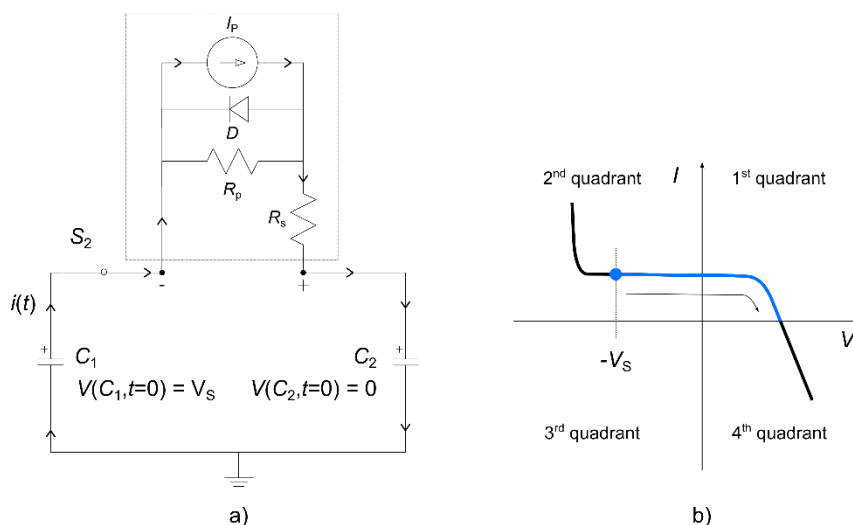


Fig. 5. Step 4 of the process of measurement. a) Equivalent circuit. b) Path on the  $I$ - $V$  curve.

After discharging the remaining charge in  $C_1$  at step 5, the capacitor  $C_2$  is positively charged so when the switch  $S_2$  is closed at step 6, the PV cell is forced to jump to a state where a positive voltage higher than its  $V_{OC}$  is applied to its terminals (the fourth quadrant of its  $I$ - $V$  curve). Then, as can be seen on Fig. 6-a), the current will flow mostly across the diode (now polarized in forward bias), because the photogenerated current goes on the opposite direction and the parallel resistance should be ideally very high. The current will flow until the difference of potential at the ends of the diode reaches its forward conduction voltage. The  $V_{OC}$  of the PV cell has now a clear meaning: the voltage needed to put its own diode in conduction, when all the generated photo-charges flow across the P-N junction and annihilates. For this reason, it is impossible to overpass this point just by illuminating the cell and it must be forced with an external source. On the  $I$ - $V$  curve, the path followed will be to the left until  $V_{OC}$  (see Fig. 6-b). This is also the zone when electroluminescence is easier to observe, will be explained later. The same reasons exposed before can be applied here, so the DUT can be a PV module and not just a PV cell and the process will be similar but with the voltages or currents raised.

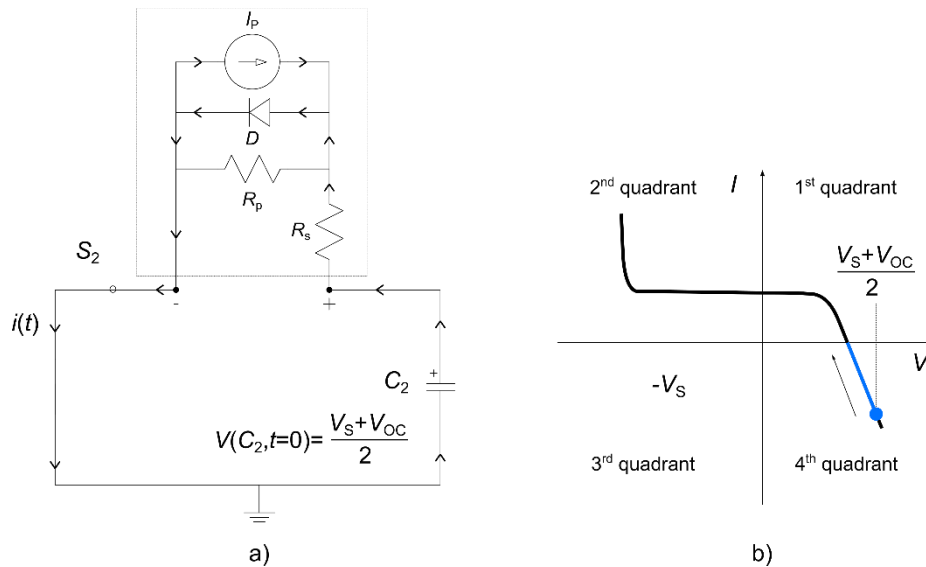


Fig. 6. Step 6 of the process of measurement. a) Equivalent circuit. b) Path on the  $I$ - $V$  curve.

## 2.2 Device implementation

### Time of the process and capacitance calculation.

The time of partial discharge of  $C_1$  and charge of  $C_2$  is given by the total charge moved across them. Of course, the higher the capacitance of both capacitors, the higher the time. Also, the maximum current given by the PV cell ( $I_{SC}$ ), determines this time. This current depends on the technology fabrication of the PV cell and its efficiency but, specially, of its surface area. For silicon technology (mono or polycrystalline) cells of common sizes today (around 160 mm by 160 mm)  $I_{SC}$  goes from 7 A to 12 A, more or less (but bigger sizes are coming next years). Current ( $I$ ) is related to charge ( $Q$ ) and time ( $t$ ) by its definition, and we also know the total charge accumulated in a capacitor by its capacitance ( $C$ ) and its voltage ( $V$ ). That is:

$$\begin{aligned} I &= Q/t \\ Q &= C \cdot V \\ t &= \frac{C \cdot V}{I} \end{aligned} \quad (1)$$

In reality, (2) will give the time of a capacitor charging or discharging at constant rate  $I$ . We know that is not true, even for a simple RC circuit (a resistor in series limiting que maximum current entering or leaving the capacitor). In this case, moreover, the DUT is not a linear device as a resistor but a more complex one. However, we can use this equation to determine the order of magnitude of the time for some chosen capacitance and voltage at source. For a more precise estimation of the real time, we simulate the circuit in LTSpice with the one diode model for the DUT (see Fig. 7).

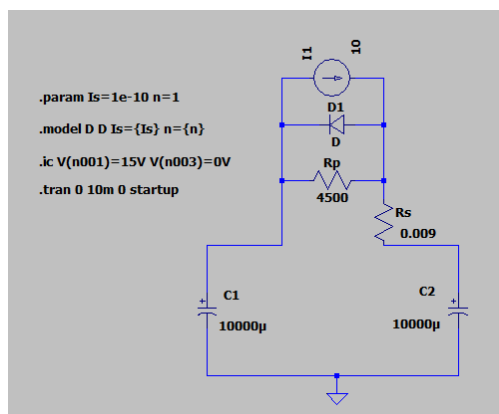


**Fig. 7.** Circuit simulated in LTSpice for estimating the necessary capacitance for C1 and C2.

As an example, for the circuit simulated in Fig. 7, with an initial  $V(C1) = 15\text{ V}$ ,  $I(\text{DUT})_{\text{SC}} = 10\text{ A}$  and  $C1 = C2 = 10000\ \mu\text{F}$  (with reasonable values for the diode characteristics, the parallel resistance and the series resistance), the current flow and voltages at capacitors are shown in Fig. 8. The usual I-V curve of the PV device (first quadrant) occurs here since the capacitors equalize their voltage, that is,  $V(\text{DUT}) = 0$  and after. We can appreciate better in Fig. 9 how, effectively, the final voltage of both capacitors is not equal and none of them stay at the middle of the initial voltage of C1 and the time since the zero voltage crossing time at the DUT (around 7.4 ms) and the end of current flow (around 9.4 ms), is about 2 ms. Of course, we can simulate capacitors as big as we want, but 10000 μF for one able of work safely at 15 V is a very big and not so cheap one at the real world. As low cost was one of the key parameters in this design, we chose a value of 22000 μF rated up to 40 V. This added to the use of PV cells with  $\text{ISC} = 7.5\text{ A}$ , give us a little more time for doing the measurements.

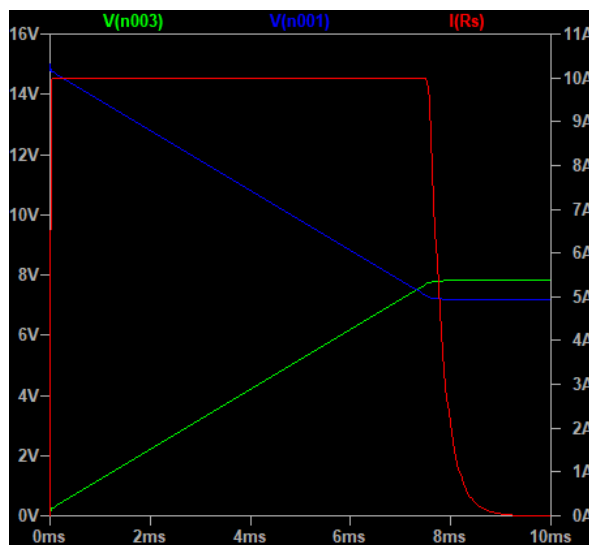


**Fig. 8.** Time simulation for the discharge of  $C_1$  and the charge of  $C_2$  across the DUT. Current flow (red line), voltage of  $C_1$  (blue line) and voltage of  $C_2$  (green line) over time.

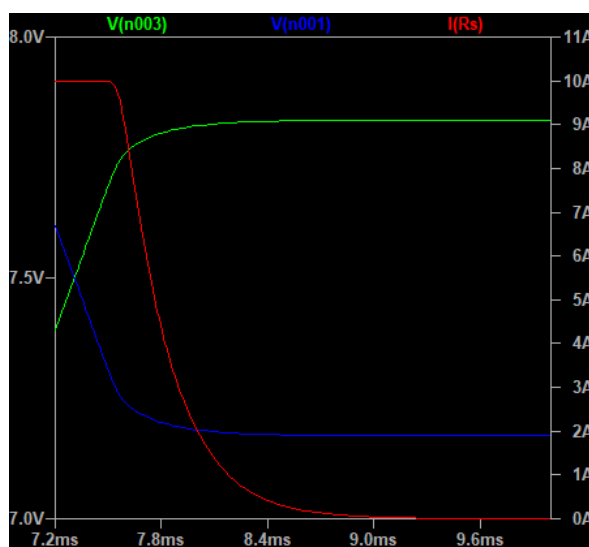


**Fig. 9.** Zoomed graph of the most interesting zone of the discharge of  $C_1$  and the charge of  $C_2$  across the DUT. Current flow (red line), voltage of  $C_1$  (blue line) and voltage of  $C_2$  (green line) over time.

Once simulated the time, we need fast, affordable, and low resistance switches. For this reason, we chose MOSFET (Metal Oxide Semiconductor Field Effect Transistor) devices controlled by a microcontroller (IC, Integrated Circuit) programmed adequately. The same IC (a PIC16F1615) is capable of measure the voltage and current

signal using two ADCs of 10 bits. DUT voltage is conditioned to the IC levels (0 to 5 volts) by using an operational amplifier (Op-amp). DUT current is converted to a voltage signal by using a Hall Effect sensor and then, conditioned to the IC levels through another Op-amp.

The internal memory of the IC is capable of store up to 248 pairs of values I-V at the precision used. As the IC used has no COM port, and additional chip is used for exporting the internal data to a computer via RS232 emulated over USB. However, the needed sampling rate is so fast (about 40  $\mu\text{s}$ /sample if we measure the complete curve showed at Fig. 8 or less than 10  $\mu\text{s}$ /sample if we just want the Fig. 9 zone) that it is impossible to do the measures continuously and send the data to the computer at real time (with this cheap hardware). Consequently, we are obliged to use the internal memory of the IC in terms of total samples at once, which are then send to the computer after the next measurement. As the first and second quadrant part of the I-V curve happens naturally and inevitably as soon as S2 is closed, this part must be sampled at once. Then, it is possible to download data from the internal memory to the computer and do the third quadrant of the measure with another 248 points of voltage and current after turning on S3. Actually, we have a little more time between as mentioned previously because of the bigger capacitance and lower short-circuit current.

If we simulate in LTSpice this second measure for the step 6 of the process, we also obtain a time of around 2 ms (see Fig. 11). But this is not very realistic because the current flowing across the PV cells is, theoretically, of hundreds of amperes for 0.2 ms or 0.3 ms. This is due to the low series resistance considered and the very ideal diode modelled (see Fig. 10). Something more realistic could be increase the series resistance of the PV cell or, alternately, put a low resistance of tenths of ohms which will reflect the effect of cables, solder joints, etc. The effect of changing this 0  $\Omega$  resistor for 0.3  $\Omega$  is shown in Fig. 12, where more realistic currents occurs and the time span to 20 ms.

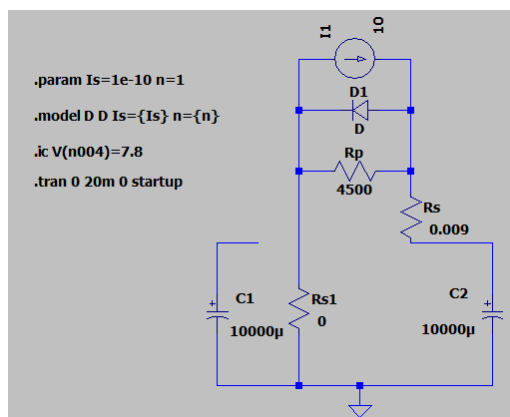


**Fig. 10.** Circuit simulated in LTSpice for estimating the duration of step 6 of the process with the chosen capacitors and voltages.

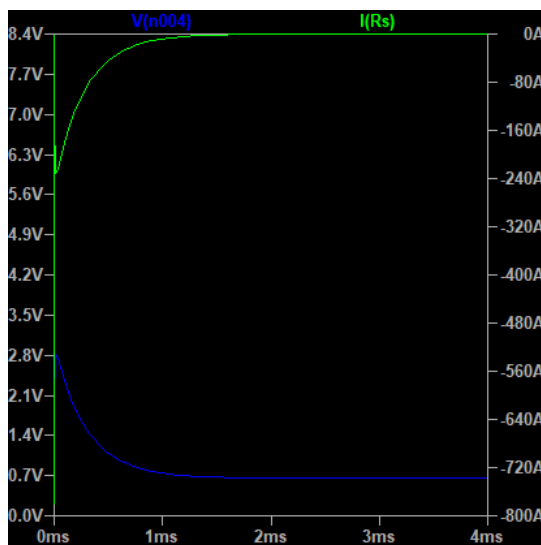


**Fig. 11.** Time simulation for the discharge of  $C_2$  across the DUT without additional resistance. Current flow (green line), voltage of  $C_2$  (blue line) over time.

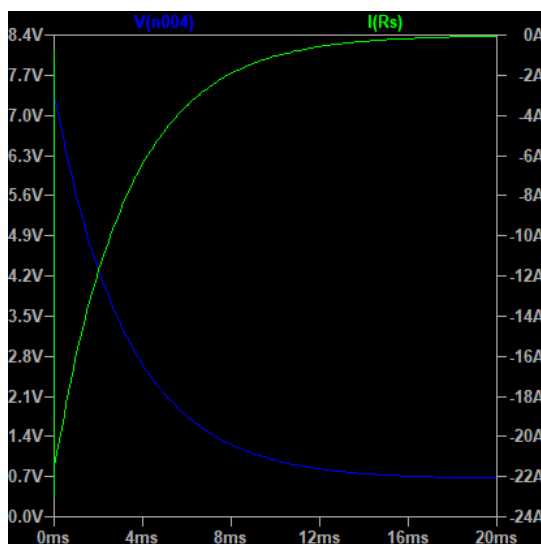


**Fig. 12.** Time simulation for the discharge of  $C_2$  across the DUT with additional resistance of  $0.3 \Omega$ . Current flow (green line), voltage of  $C_2$  (blue line) over time.

**Voltage and current measurement.**

The scheme used to measure of voltage and current is shown in Fig. 13. A four-terminal sensing is used to determine with enough precision both magnitudes. This concept must be then transferred to the PCB design and to the cables soldered to the DUT (using independent wires for the current and for the voltage to ensure a correct Kelvin sensing).

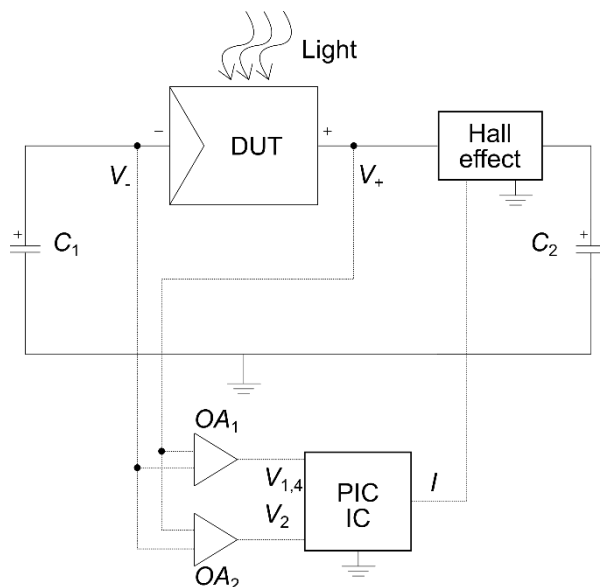


Fig. 13. Voltage and current measure schematic for the I-V tracer.

As has been mentioned, the current measurement is based in a hall effect IC (TMCS1100) which can output a voltage signal proportional to the current crossing it. The device is configured to give values of voltage in the range  $[0, 2.5)$  V for negative values of the current and in the range  $[2.5, 5]$  V for positive currents (including 0 A). The IC is available in different maximum currents (or, equivalently, in different sensibilities). Our device has a sensibility of 200 mV/A, covering a range from -1.5A to 1.5A. The voltage could be adapted to maximize the  $[0, 5]$  V range of main IC ADC if needed by using another Op-amp with the correct feedback, but if much lower or higher currents are needed to measure, probably it will be better to take another model with another sensibility. This is because it has its own Op-amp internally with, probably, less noise problems.

Voltage necessarily requires a conditioning stage of the signal, not only because it goes from positive to negative values but, in addition, for its low values in the (usually) most interesting zone of the curve: the first quadrant. For this reason, the negative zone of voltages (second quadrant,  $V_2$ ) is span to  $[0, 5]$  V by using an instrumentation Op-amp ( $OA_1$ ). The positive voltage zone (first and fourth quadrants,  $V_{1,4}$ ) is adapted to  $[0, 5]$  V through another instrumentation Op-amp ( $OA_2$ ). Each amplifier has its output in saturation when is in the zone where it has not to measure, so do not interfere the output from the other.

### 3 Results

#### 3.1 Prototype made

The real implementation of the proposed *I-V* tracer is displayed in Fig. 14. Capacitors are placed behind the PCB, while the rest of components are placed in the top layer. In addition to the components needed, can be seen the USB communication cable, the wires used to power the device and charge the capacitor, and the wires used to measure independently current and voltage. Its technical characteristics are shown in Table 1.

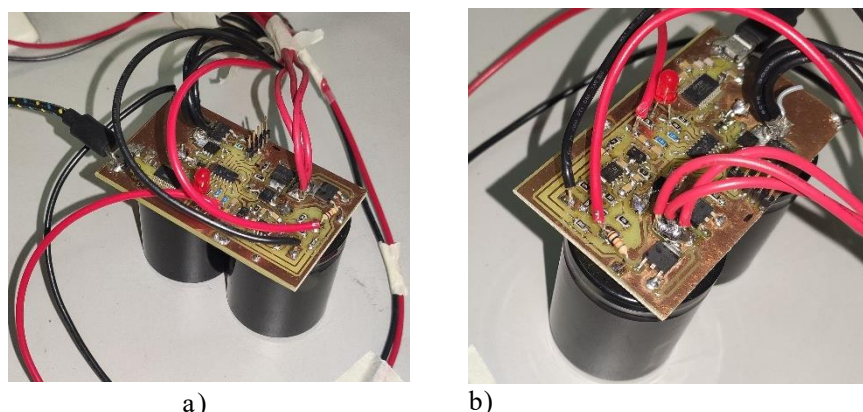


Fig. 14. Prototype implementation of the proposed device.

Table 1. Technical characteristics of the device produced.

Characteristic	Value
Power voltage	15 V
Capacitance of $C_1$ and $C_2$	22000 $\mu$ F
Current measure max ratings	$\pm 11.5$ A
Voltage measure max ratings	-15 V, +8.5 V
Number of points measured	248
Current resolution	25 mA
Voltage resolution	1 mV

#### 3.2 Modular platform used

A modular platform was designed and used to help placing the cell, the illumination used LED board and other techniques. For example, a support for the electroluminescence camera or another for the thermal camera. Design was made using Autodesk Fusion 360 and then 3D printed using FFF (fused filament fabrication) technology. In Fig 15 can be seen two configurations of the platform: just the base with the adapters for

the (156 x 156) mm cells and the supporting rods, in a); and with the adapter for the LED illumination board used, in b). Bigger cells up to M6 — (166 x 166) mm— are possible with this design. For future trend sizes as M8 — (182 x 182) mm— or M10 — (210 x 210) mm—, a redesign of the platform will be needed. The real result can be seen in Fig. 16 along with the *I-V* tracer device.

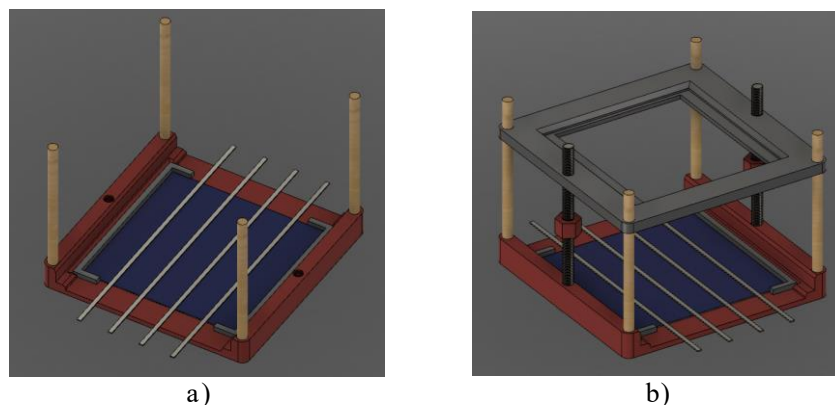


**Fig. 15.** Modular platform designed for the measurement of *I-V* curves, electroluminescence, thermography, and other techniques. a) Base with cell and adapters. b) With the addon for supporting the LED illumination board.

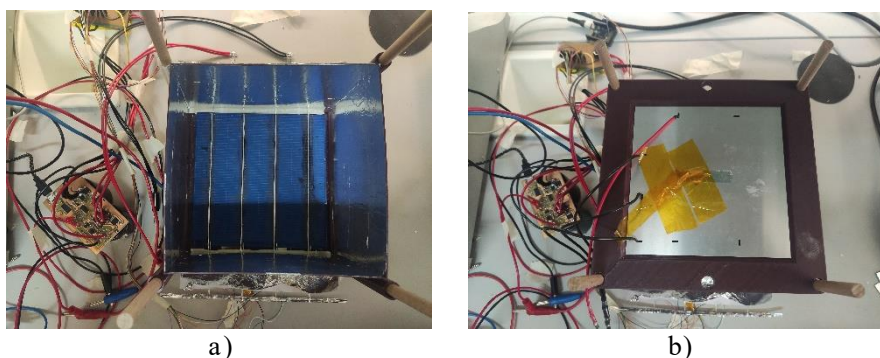


**Fig. 16.** Modular platform mounted in *I-V* tracer mode. a) Assembled except for the LED board. b) Fully assembled with the LED board in place.

**PV cells and LED illumination.**

The characteristics of the PV cells used for testing are in Table 2. Busbars were hand soldered to the cells using a soldering iron with the help of flux and hot air at 150 °C (see Fig. 18-a). The four busbars were then connected using a wider bar, which offers a low resistance path for the current and an easy zone to solder the voltage and current cables. Three cables were soldered at different points of each side (positive and negative)

from the cell to the device to ensure the current flow with the lower resistance possible. Another cable was solder in each side for the voltage measurement.

**Table 2.** Technical characteristics of the PV cells used at nominal conditions (1000 W/m<sup>2</sup> of solar spectrum and 25 °C).

Characteristic	Value
Max Power (MPPT)	4.67 W
V <sub>oc</sub>	0.64 V
I <sub>sc</sub>	9 A
Efficiency	19%
Number of busbars	4
Size	(156 x 156) mm
Thickness	200 μm
Technology	Polycrystalline

The illumination system consists of an aluminum PCB with 42 infrared (IR, 850nm) LEDs (see Fig. 18-b). This wavelength is chosen because the photon absorption curve for a silicon PV cell has its maximum of efficiency in the near infrared (NIR) zone, as is shown in Fig. 17. These photons illuminating the cell are at the peak wavelength it can absorb better, so less energy is needed to obtain a state at the cell similar to the nominal conditions (1000 W/m<sup>2</sup> with the spectral composition of the Sun irradiance at Earth surface). Under these conditions of irradiation, the PV cell can generate the free charges needed to reach its saturation current and, consequently, walk around its own I-V curve. The calibration of the current needed on the LEDs for getting the right density of photons has been done with a calibrated irradiation cell to get on it the same signal that it has exposed to Sun at nominal conditions.

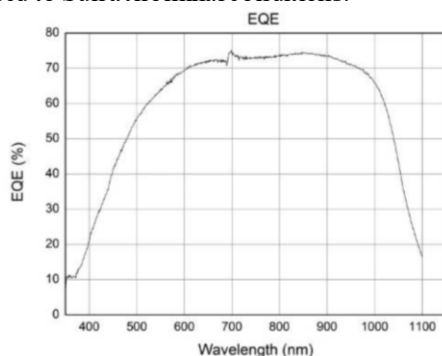


**Fig. 17.** External quantum efficiency of a silicon photovoltaic cell. Extracted from [13].

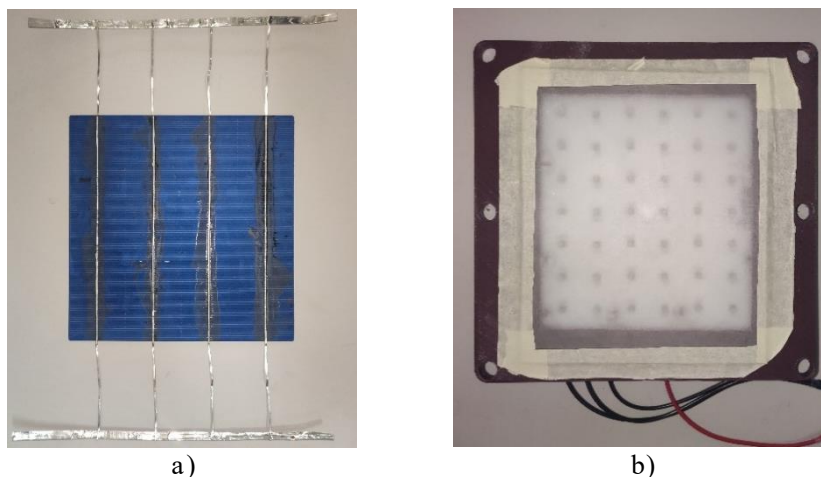


Fig. 18. a) Photovoltaic cell used. b) LED illumination system used.

### 3.3 I-V curves obtained

In Fig. 19 is the graphical representation of the dataset acquired for a measure of a single PV cell as the shown in Fig. 18-a), using our device for  $I$ - $V$  tracing and the platform with the LED board for illuminating. It can be seen just the first quadrant (positive voltages) and some of the second quadrant (negative voltages). The curve is the typical curve of a good cell, with a first zone at low voltages almost horizontal, that is, without changes in the current (almost  $I_{SC}$ ) and then a “neck” zone ending in a straight zone up to the open circuit ( $V_{OC}$ ). From these values at the begin and at the end could be possible to extract the values of  $R_p$  and  $R_s$ , respectively. Second quadrant of the curve is not traced because the firmware of the main IC is configured, in this case, for obtaining the curve with the maximum number of points at the first quadrant zone. To achieve this, the IC is measuring constantly the current and the voltage constantly from the moment it closes the switch  $S_2$  (the fourth step of the process) and calculates the time interval between measures that needs to span most of the 248 points over the first quadrant. All the measures from the second quadrant are discarded until the voltage is near the 0 V level, when it starts to save them at memory. That is why there are some points at negative values.

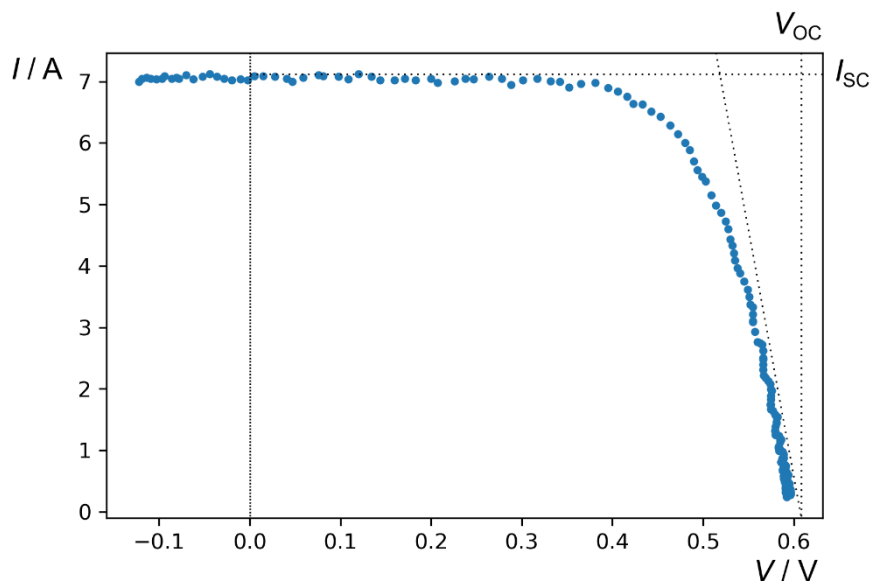
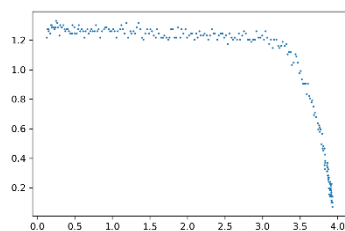
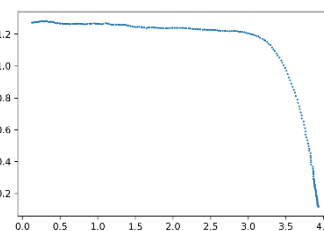


Fig. 19.  $I$ - $V$  curve of a real cell with the device and the platform proposed.

As said, it is possible to obtain also an  $I$ - $V$  curve of a small number of PV cells in series by simply changing the feedback loop of the voltage measure Op-amps. For this purpose, we have fabricated a mini-PV module with six cells that are sixths of a cell of the size used. Therefore, the mini module can be mounted in a size just slightly bigger than the single cell, so it fits in the modular platform and can also be illuminated with the same LED system. The corresponding  $I$ - $V$  curve can be seen in Fig. 20-a). As expected, the noise in the current measure is more notorious in this case, because the values of the current are lower (the current depends mostly on the cell surface for the same cell technology). For this reason, a software Savitzky-Golay filter has been used over the raw data. The filtered data is showed at Fig. 20-b) and shows a much better curve.



a)



b)

**Fig. 20.** *I-V* curve of the mini-PV module of six single cells fabricated. a) Raw data. b) Filtered data.

## 4 Discussion

We have demonstrated that the theoretical strategy that we thought is possible to implement and use to trace the *I-V* curve of a single cell and of a small number of cells. We solved the technical difficulties encountered for the correct measurement of the voltage and current of the cell and all the electronics needed to ensure it. We calibrated the Op-amps ranges and measured it against an oscilloscope to get the correct values to convert from the ADC values to the voltage values. All these conversions are done by software at the computer program that download the data from the device, save the files and plot them. We have not talk of this program, written by us in python, because it can be done in many ways and is now very simple (without interface, just in command line mode).

The device has been used to measure curves in more than 20 different single cells by the time (plus two mini-PV modules). All these cells were of the same manufacturer and same type as described in Table 2. The purpose of these measures, as well as serving to demonstrate the validity of the apparatus, has been used to train an artificial intelligence (AI) algorithm along with its correspondence EL images, to classify cells in some groups, according to their output power. This kind of data is very difficult to obtain for the same cell, so a device like this enables to do anyone with very low cost.

*I-V* tracers capable of take good measures at cell level are at the price range of a thousand dollar or above (1000 \$). Some laboratories make them manually with two good multimeters and a programmable electronic load or by the one capacitor charging method. One of this bank multimeters are also in the range of a thousand dollars or above, so the full equipment for an *I-V* curve could cost around 3000 \$ or more. The components used in our device cost around fifty dollars (50 \$). Obviously, we have not charged the cost of design, making, mounting, programming, calibrating, testing, etc. The LED illumination board components cost less than a hundred dollars (100 \$) and the 3D printed platform cost is derisory (10 \$ in filament or less plus the electricity consumption).

There is clearly a noise in the current measure that seems like a kind of ripple. This is clearly not a 50 Hz (electric network frequency in Spain) noise because, as it was explained, the process is so fast that it last less than 10 ms. With times of acquisition between points of around 10  $\mu$ s, it must have another origin. We have some ideas and will try to solve in future evolutions of the device.

It would be good to have a comparison between our device and a commercial device, but we have not such device capable of do the measurement at cell level, just at module or array level. This was the main motivation for making this low-cost device, but we are trying to buy a commercial and tested device. Nevertheless, the shape of the curve and the current and voltage values obtained are completely in line with what is to be expected, so we are confident that the device is measuring correctly. The comparison, however, would allow us to know the level of accuracy achieved by the device.

**Room for improvement and future works.**

We got a very promising result but, as in all processes from theory to reality, some problems arose. First of them was expected and related with the illumination. It is not exactly the same to illuminate a cell with the sun spectrum that just with single wavelength. However, the biggest problem of the LED board is that we need to put it relatively close to the cell (about 10 cm to 15 cm) to get the adequate signal. At this distance, it is difficult to get a homogeneous irradiance at the full cell area. Each LED is as a big spot with a spatial irradiation cone. To minimize this problem, a diffuser was placed below the LEDs, but is not a perfect solution.

Another problem derived from the proximity of the LEDs is the heat generated by them. It is well known that the  $I$ - $V$  curve of a PV cell depends not only on the irradiance but also a lot on the temperature it has. The cell raises its own temperature due to the absorption of the photons. Part of the energy of these photons is evacuated from cell due to the electrons current output, but not all. To this temperature raising we have to add the temperature increment due to the self-heating of the LED board, which heats the air gap trapped in the platform used. This is not a problem for the temperature across an individual  $I$ - $V$  curve, because as has been said, is so fast. But it is a problem between measures, as it can be seen on Fig. 21. For taking this problem into account, six very small temperature sensors based on thermistors have been added to the platform, which are measured by using another Arduino-like board. These sensors can be placed whenever we want: for example, across a single cell in different positions to check its temperature distribution or one in each cell of a six cells mini module. The problem can be converted into a feature: from these curves at different temperatures, the dependence of  $V_{OC}$ ,  $I_{SC}$  and the maximum power output can be calculated. Effect over the total power output of the mini module is showed in Fig. 22, which corresponds to the power calculated from data showed in Fig. 21.

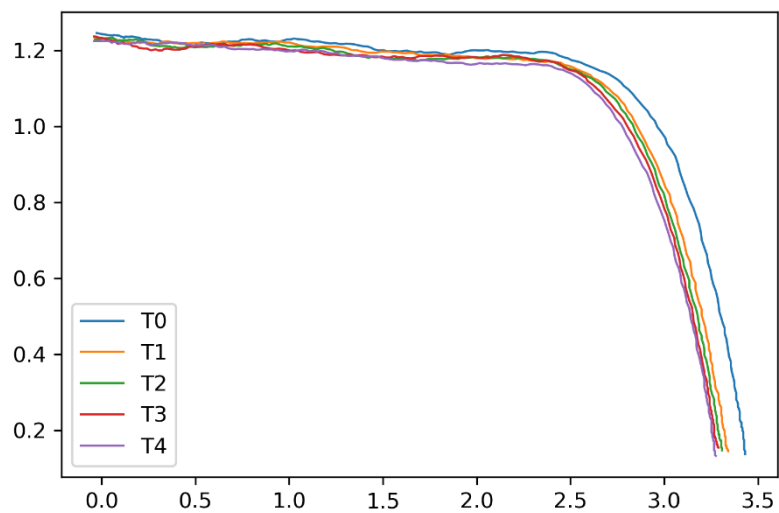


**Fig. 21.** *I-V* curves of a mini-PV module of six cells at different temperatures.

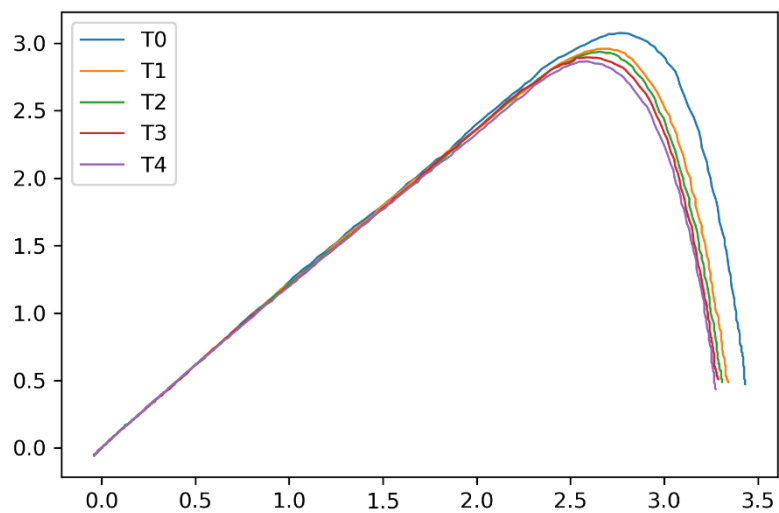


**Fig. 22.** *P-V* curves of a mini-PV module of six cells at different temperatures.

With the idea of incorporating all of these ideas and improvements, a new device is being designed using a most powerful main IC, with a higher clock, 12-bit ADC and

much more internal memory and processing power, which should be able of getting better precision measures, fastest times between them and up to 5000 points at once, while also sensing the temperature without the use of another board. In addition, this IC integrates the communication over USB with the computer, so the chip added for this purpose on current PCB will not be needed.

## 5 Conclusion

A new strategy of measurement for an I-V curve at single PV cell level, based on the charge and discharge of two capacitors, has been exposed. This strategy has been successfully implemented in a low-cost device capable of doing these difficult measures correctly. An illumination based on NIR LEDs has been designed and used too, demonstrating that can be a good replacement, for this purpose, of more complex and expensive systems.

All these equipment has been integrated into a modular platform designed and 3D printed, which proves to be useful for quickly interchanges between the I-V curve mode and the EL mode. This makes it possible to obtain easily and quickly a lot of I-V curves and EL images for different conditions of illumination and/or shading. Data of this kind can be very helpful for training AI algorithms but are very difficult to get at cell level. With this device and modular platform, we solve that problem in an easy and cheap way.

Future works will include a revised device, improving the quality of the measurement reducing noise in the I-V trace and some new planned functionalities as scale changing without soldering needed or simultaneous measurement of temperature of the cells.

## Acknowledgements

We would like to thank the CEDER by providing information for the development of this work. The authors thank the CYTED Thematic Network “CIUDADES INTELIGENTES TOTALMENTE INTEGRALES, EFICIENTES Y SOSTENIBLES (CITIES)” no518RT0558.

This research was funded by the “Ministerio de Industria, Economía y Competitividad” grant number “RTC-2017-6712-3” with name “Desarrollo de herramientas Optimizadas de operación y mantenimiento predictivo de Plantas fotovoltaicas — DOCTOR-PV”.

## References

1. N. Kwarikunda, E. E. Van Dyk, F. J. Vorster, W. Okullo, y M. K. Munji, *Phys. B Condens. Matter* **439**, 122 (2014).
2. J. Walter, D. Eberlein, J. Haunschild, M. Tranzitz, y U. Eitner, *Energy Procedia* **27**, 652 (2012).

3. R. A. Sinton, A. Cuevas, y M. Stuckings, *Conf. Rec. IEEE Photovolt. Spec. Conf.* **457** (1996).
4. O. Breitenstein, F. Frühauf, y J. Bauer, *Phys. status solidi* **214**, 1700611 (2017).
5. S. Fischer, J. C. Goldschmidt, P. Löper, G. H. Bauer, R. Brüggemann, K. Krämer, D. Biner, M. Hermle, y S. W. Glunz, *J. Appl. Phys.* **108**, 044912 (2010).
6. K. Bothe, P.-O. Logerais, E. Belaidi, J. Amina, P. Pohl, J. Schmidt, T. Weber, P. Altermatt, B. Fischer, y R. Brendel, en *21st Eur. Photovolt. Sol. Energy Conf.* (Dresden, Germany, s. f.), p. 2006.
7. T. Fuyuki y A. Kitiyanan, *Appl. Phys. A* **96**, 189 (2008).
8. S. Gallardo-Saavedra, L. Hernández-Callejo, M. D. C. Alonso-García, J. D. Santos, J. I. Morales-Aragón, V. Alonso-Gómez, Á. Moretón-Fernández, M. Á. González-Rebollo, y O. Martínez-Sacristán, *Energy* **205**, (2020).
9. E. D. Dunlop y D. Halton, *Sol. Energy Mater. Sol. Cells* **82**, 467 (2004).
10. S. W. Johnston, N. J. Call, B. Phan, y R. K. Ahrenkiel, en *Conf. Rec. IEEE Photovolt. Spec. Conf.* (Philadelphia, PA, USA, 2009), pp. 000276-000281.
11. A. Abete, E. Barbisio, F. Cane, y P. Demartini, *Conf. Rec. IEEE Photovolt. Spec. Conf.* **2**, 1005 (1990).
12. Y. Zhu y W. Xiao, *Sol. Energy* **196**, 346 (2020).
13. W. Ananda, *QiR 2017 - 2017 15th Int. Conf. Qual. Res. Int. Symp. Electr. Comput. Eng.* **2017-December**, 450 (2017).

## Charge Management of Electric Vehicles from Undesired Dynamics in Solar Photovoltaic Generation

Ivania Aguirre<sup>1</sup>[0000-0002-0651-2088], L.G. González<sup>1</sup>[0000-0001-9992-3494], Miguel Dávila-Sacoto<sup>1,2</sup>[0000-0001-6318-2137], Luis Hernández-Callejo<sup>2</sup>[0000-0002-8822-2948], and J.L. Espinoza<sup>1</sup>[0000-0002-7450-2084]

<sup>1</sup> University of Cuenca, Cuenca, Ecuador

<sup>2</sup> University of Valladolid, Valladolid, Spain  
miguelalberto.davila@alumnos.uva.es

**Abstract.** The power generation from photovoltaic solar systems contributes to mitigating the climate change issue. However, the intermittent nature of solar radiation affects the energy quality and causes instability in electrical networks connected to these systems. This paper assesses the dynamic behavior of solar radiation in an Andean city, which presents rapid power variations that can reach an average of 7.20 kW/min and a variability coefficient of 32.09%. The study applies the ramp-rate control technique to reduce the power fluctuations at the point of common coupling (PCC), with the incorporation of an energy storage system. The batteries of the electric vehicles were used as the storage system due to their high storage capacity and their contribution to power system flexibility. The application of the control strategy shows that with a minimum of five electric vehicles charging stations at PCC, the rate of change of the photovoltaic can be reduced by 14%.

**Keywords:** Photovoltaic solar system; power fluctuations; electric vehicle batteries; ramp-control.

### 1 Introduction

The use of energy is essential for the development and deployment of societies worldwide. At a global level, in the last five years, an average growth of more than 8% per year in renewable energy generation capacity has been evidenced. Among the energy sources with the highest installed capacity in 2019, photovoltaic solar energy (PV) and wind energy are the widest used, with a total of 115 GW and 60 GW respectively. These sources are increasingly cost competitive in relation to fossil fuel power plants [1]. However, its use is limited by the discontinuity of production, due to non-deterministic and complexly predictable seasonal variations since these depend mainly on climatic conditions.

Despite the benefits of PV systems, their high level of penetration into distribution networks can negatively affect the quality and reliability of electrical power service. Problems such as voltage variation and instability in the Point of Common Connection (PCC) affect the network, as a consequence of the lack of inertia of PV systems, typical of the electromechanical generators of conventional generation plants, which makes it

difficult to control active power and frequency [2], [3]. On the other hand, there are also problems such as the reversal of power flows, overvoltage along the distribution feeders, phase unbalance, greater wear of the voltage regulating equipment [2], [4], [5].

These problems of PV systems are due to the highly variable nature of the solar resource, which can change in periods of hours, minutes, and even in the order of seconds. Instantaneous changes in solar irradiance cause fluctuations in the power output of PV systems. Power fluctuations can be analyzed from various perspectives, such as a regulatory framework that defines the requirements for connecting PV plants to the electricity grid, and the incorporation of energy storage systems in the PCC, which help reduce the VA- relationships at this node [3].

From a regulatory point of view, several countries have established policies that limit the technical aspects of the use of these systems. These regulations define a limit for the range of variation of the active power of the PV generation [6]. This variation range, also called ramp rate, can be defined as a percentage of the nominal capacity of the PV plant, in time intervals of minutes or seconds. For instance, the German Association of Energy and Water Industries (BDEW) establishes a ramp of 1% of the nominal power per minute, while the Romanian Energy Regulatory Agency (ANRE), the Federal Regulatory Commission of United States Energy (FERC) and the Puerto Rico Electric Power Authority (PREPA) consider a ramp equal to 10% / min of the nominal power of the PV plant [7].

Energy storage systems also play a fundamental role in the management and control of the dynamic behavior of PV generation. With the large-scale implementation of photovoltaic systems in distribution networks, large-capacity storage systems temporarily connected to the PCC will be necessary. The battery bank of electric vehicles can be used for this purpose. As indicated by the study developed by [8], in which the impact of the introduction of PV systems in conjunction with electric vehicles in the Portuguese electricity grid is analyzed. The results indicate a notable decrease in the surplus energy generated, thanks to the good correspondence between the charging process and PV production. Therefore, to ensure the stability of the network and the large-scale diffusion of PV systems, a significant penetration of electric vehicles is necessary.

This study evaluates the dynamic behavior of photovoltaic solar energy generation under conditions of high variability of solar irradiation caused by the characteristic cloudiness of the mountainous region of the Andes. For which, the application of a control strategy to reduce power fluctuations in the PCC is presented, together with the incorporation of the energy storage system of the battery bank of electric vehicles. Thus, an analysis of the dynamic behavior of solar irradiation is carried out in an Andean city, with which an energy management system is developed to reduce the variations at the output of the photovoltaic system, applying the algorithm proposed for the case study determining the dynamics of variation of the power of the charging system of an electric vehicle, under instructions of the energy management system.

## 2 Power Photovoltaic Fluctuations

The photovoltaic (PV) systems use solar radiation as the prime resource for electricity production. The amount of energy these systems can produce is conditioned by the variability of the incident radiation on the surface of the solar panels. In this sense, energy produced can reach values above or below the required power demand [9]. The fluctuating behavior of the output power is related to the climate conditions, especially the density of the cloudiness in between the panel surface and the sun [10].

Therefore, to optimize the energy extracted from a PV solar system is necessary to use maximum power point tracking (MPPT) techniques [3]. There are various MPPT algorithms, such as perturb and observe (P&O), incremental conductance (IC), fuzzy logic control (FLC), fractional short circuit current (FSC), among others [11]. Regardless of the variations of climate conditions, these methods seek to extract the maximum of the energy of the PV array (PV module + DC/AC converter) [3].

The dynamic behavior of the solar radiation in the area of measurement shows wide ranges of fluctuations with periods in the order of hours, minutes, or seconds. These variations depend primarily on the density of cloudiness, with atypical behavior as the one shown in figure 1. The data of the figure comes from the meteorological station available in the microgrid laboratory of the University of Cuenca (Campus Balzay) [12], which is located in the city of Cuenca-Ecuador, belonging to the mountain region of the Andes in the coordinates (2°53'31.0"S 79°02'18.7"W).

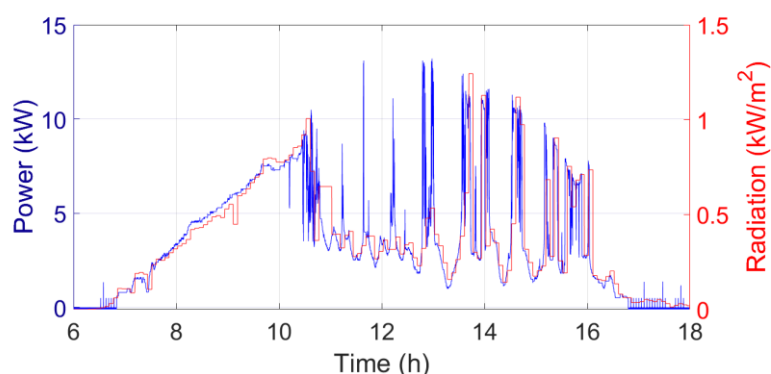


**Fig. 1.** Typical behavior of solar radiation. September 2020. Campus Balzay, Cuenca-Ecuador.

The city of Cuenca has the typical meteorological behavior of the Andean Mountain regions, which is characterized for having two different seasons. Between the months of March-April, and October-November is the rainy season, and in June and July is the dry season. These particularly conditions influence the behavior of irradiation and temperature [3].

For this same Andean city, a study evaluates the dynamic behavior of solar radiation [3]. According to this study, the PV power ramp rate can reach between 50% and 70% of the nominal power of the system in intervals near 15s. In this sense, it is assessed the use of electric-type storage systems with supercapacitors in the point of common coupling (PCC) to reduce the variations in power output in the PV system. The results show

a diminishment in the power ramp rate of nearly 6.66 times. Among other technologies of energy storage that can be used are batteries, fuel cells, and recently, electric vehicles (EVs) batteries [6], [13].

The energy storage system (ESS) of EV batteries contributes to the flexibility of the power system. The batteries help to store excess electricity and to provide ancillary services to the grid, such as frequency regulation, shaving peak demand, and the enhancement of operation and reserve capacity to secure the grid [14]. From a technical point of view, the massive insertion of EVs plays an important role in the integration of PV solar power generation systems into current distribution grids, and it constitutes a feasible solution for the control and diminution of PV power fluctuations in the PCC. For instance, an assessment determined that the good process correspondence between EV charging and PV generation makes it possible to manage the energy surplus produced by this source [14].

Despite the benefits of the high share of EVs in controlling PV power fluctuations, this can affect the power quality and reliability of the grid. The EV charging process brings about the increase of load profile during peak hours, overloading of power system components, voltage deviations, harmonics, and system stability issues [15].

### **3 Methodology**

The research takes as a base the modeling and simulation of a PV energy generation system and the EV battery bank, and it incorporates an algorithm for the PV output power fluctuations reduction. Following the approach made in [3], the study applies the control technique to the power inverter of the storage system to keep the power variations within a pre-established range. The technique mentioned corresponds to the ramp-rate control. Figure 2 shows the energy management system diagram used for the present study.

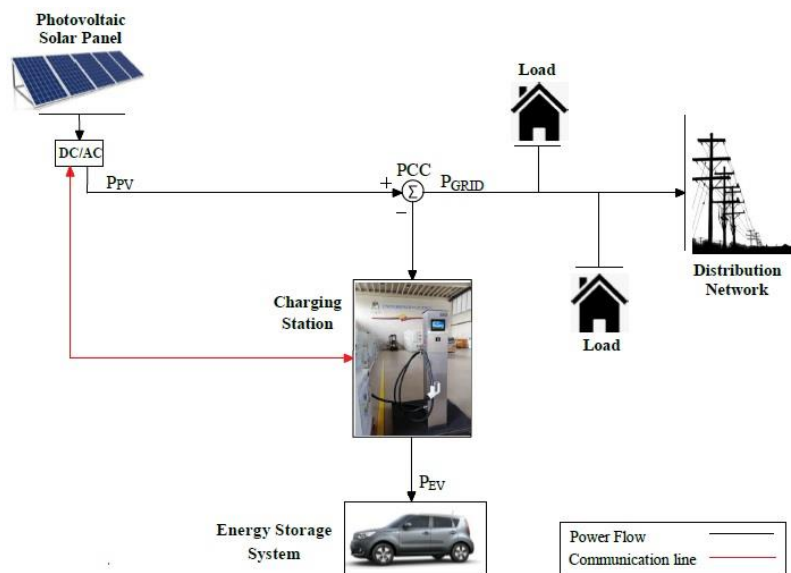


Fig. 2. Energy management system.

For the PV solar generation system, the study considers the one available at the micro grid laboratory of the University of Cuenca [12]. This system has 4 strings of 15 panels of the poly-Si type connected in series. Each panel has a nominal power of 250 Wp, model A250P from Artesa manufacturer, to reach a power of 15kWp for the system. The array is managed by a tri-phase, two-level DC/AC converter with Pulse Wide Modulation [3].

The PV generation system is connected directly to the electric grid and is operated through an MPPT algorithm. The dynamic behavior of these types of systems presents a wide range of power fluctuations. Then, with an increasing level of penetration, some instability issues could occur on the grid [1].

Concerning the ESS to be used, the study applies the control technique of ramp-rate power to reduce the PV power variations at the PCC simultaneously with the battery bank of the EV. According to figure 2, the charging system of the EV is responsible for modifying the supply power to the batteries depending on the dynamic behavior of PV generation, assuring the charging power ( $P_{EV}$ ) variation within the determinate limits.

The variation range for the charging system is defined in function of the electrical features of the vehicle model and what is stated on the SAE J1772 norm [16]. The maximum variation is delimited according to the standard monophasic slow  $P_{EV}$  from some EV models. The minimum limit considers the lowest level of current needed to initiate the charging process. The variation range is then  $7.2 \text{ kW} < P_{EV} < 1.32 \text{ kW}$ . Lastly, a reference level is set as 50% of the admissible variation range.

For the battery bank system, the response to charging power changes is not instantaneous. For instance, a study developed several tests with two different models of EVs to assess their response time [17]. With a variation from 30% to 50% of the duty cycle,

the EVs showed a rapid response of nearly 2 and 0.68 seconds. The analysis of the response time is important to obtain the battery system model. The present study varies this parameter to observe the reaction of the energy management system.

The algorithm of ramp-rate control applied for the study is presented in figure 3. It has been adapted so that the power fluctuations do not surpass the required limits and maintain the condition of avoiding the variation of active power above 10% of the nominal power per minute. This consideration was made according to the regulations accepted by PREPA since the Republic of Ecuador has no regulations in this regard.

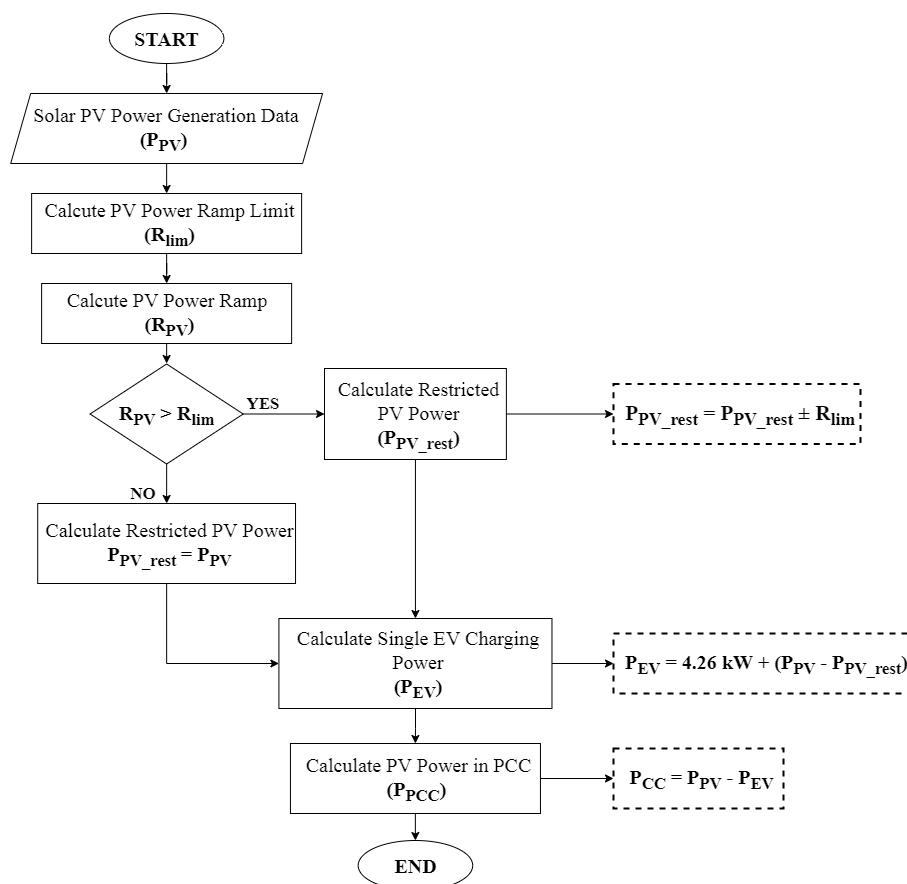


Fig. 3. Algorithm of PV power ramp-rate control.

Following the operation process of the ramp-rate (RR) algorithm shown in figure 3, it starts by reading the PV output power; then the PV power ramp limit ( $R_{lim}$ ) is settled. With a solar generation capacity of 15 kW<sub>p</sub>, the maximum rate of change admitted in this study reaches  $|RR| < 1.5$  kW/min. To estimate the dynamic power fluctuations in the PCC, the algorithm evaluates whether the PV power ramp ( $R_{PV}$ ) is greater or smaller than the desired limit. This evaluation defines the initial point for the charging system

to modify its power. If the condition  $R_{PV} > R_{lim}$  is accomplished, the power varies according to the instantaneous behavior of the slope of the PV output. Conversely, if the condition is not satisfied, the charging power is not needed to vary. In the end, the PV power in the PCC comes from the difference between the PV output power and the EV charging power.

### 4 Results

A probabilistic analysis of the PV maximum power fluctuations for September 2020 is presented in figure 4. The analysis aims to evaluate the dynamic behavior of PV generation in the zone under study. The information indicates a high level of variability along the 30 days, with a mean variation of 7.20 kW/min, a standard deviation of 2.32 kW/min, and a coefficient of variation of 32.09%. The highest average fluctuations were found on the 28th of September. This day presents a maximum and a mean rate of 8.95 kW/min and 67 W/min, respectively.

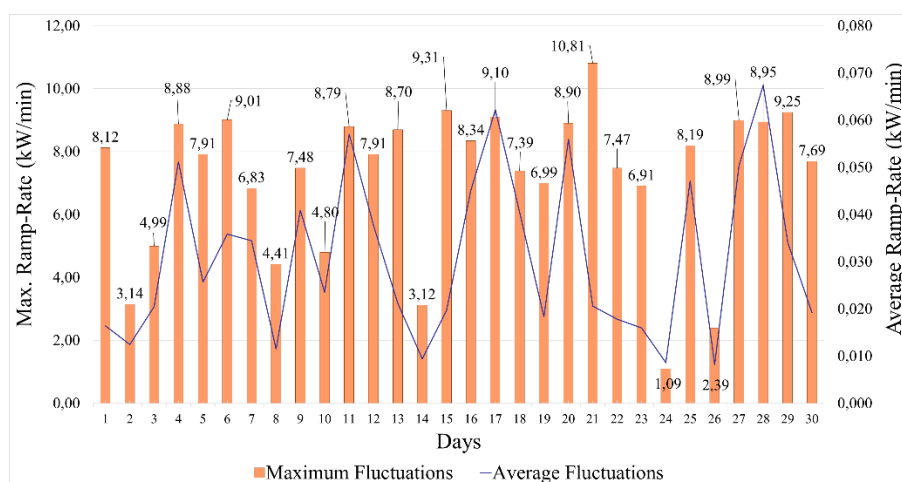


Fig. 4. Daily maximum and average fluctuations, September 2020.

The day with the highest average fluctuations registers a mean variation of 4.81 kW/min, a standard deviation of 3.13 kW/min, and a coefficient of variation of 65.4%. Besides, in the analysis is determined that the dynamic behavior of PV generation has more variability between 11:00 and 15:00, which corresponds to the instants when the sun is at its highest elevation. In this time interval, the ramp rate reaches values over 8 kW/min. Figure 5 shows the behavior for this day.

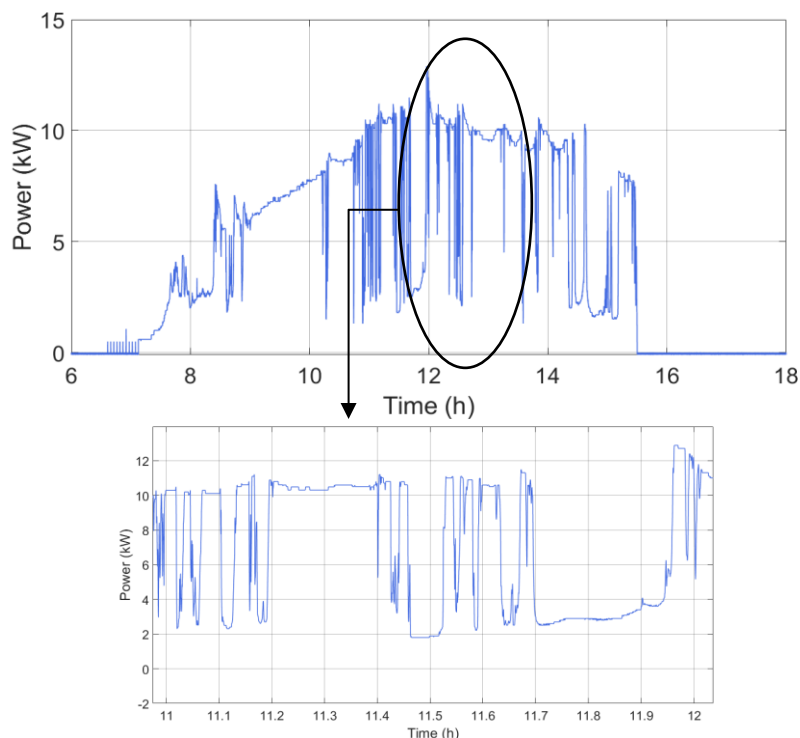


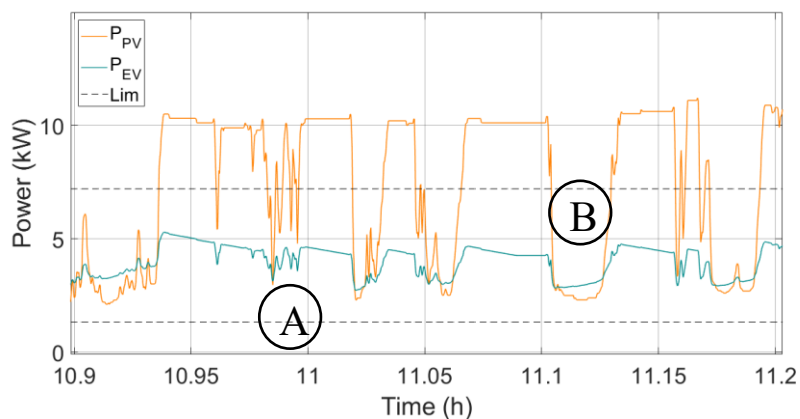
Fig. 5. Photovoltaic power output - most critical day.

An assessment of the required number of EVs connected in the PCC to reduce the instantaneous PV variations, found that is necessary a total of 5 charging stations nearby this node. For this condition, the algorithm designates the same level of charging power for each charging system.

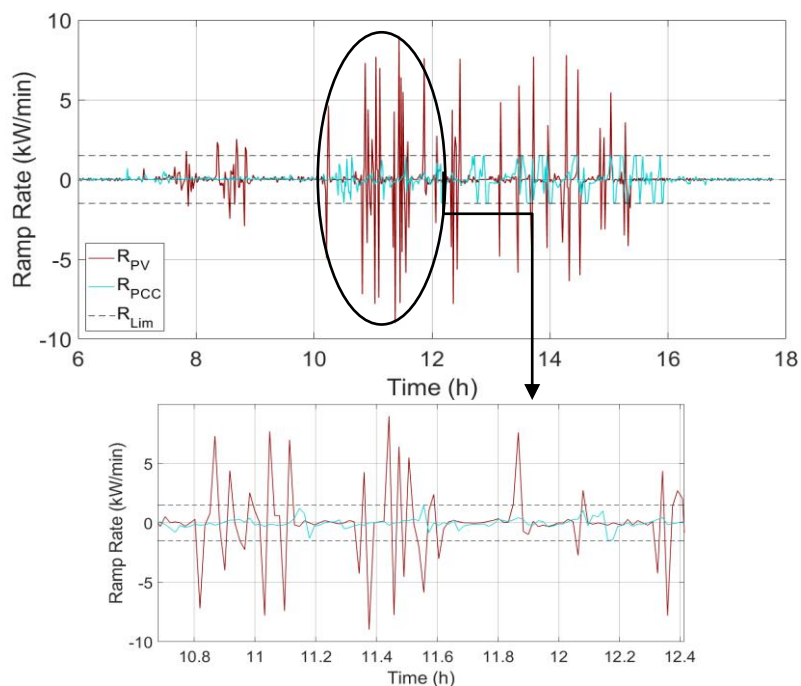
The response of one single EV charging system to the dynamic behavior of the PV power generation is shown in figure 6. It is observed that the charging profile stays within the desired range. Two areas are marked in figure 6 to highlight the performance of the ramp rate algorithm. In section A, the charging system detects rapid changes in the PV output power over the desired limit. Hence it starts to vary its charging power. In contrast, in section B, it is observed that the variation of PV generation grows slowly, and it's almost constant; therefore, the change in the charging system power is small. For both scenarios, the charging power varies following the same direction of the power PV rate of change. In addition, the  $P_{EV}$  tends to return to the charging reference point after any control action. The variation of the  $P_{EV}$  allows the energy management system to assure a PV power ramp rate of 25 W/s in the PCC.

To quantify the performance of the algorithm under study, figure 7 presents the rate of change of the generated power of the PV system. The PV fluctuations exceed the desired limit nearby 10.3%, reaching a maximum of 8.98 kW/min. However, after applying the control technique and considering the time response of the EV charging sys-

tem to be the same as the sampling time of the PV system, the power fluctuations diminish 8.8%, reaching a maximum ramp of 1.53 kW/min. This result shows that exists a favorable response of the energy management system to the dynamic behavior of PV generation, thanks to the restriction imposed by the power ramp-rate control technique.

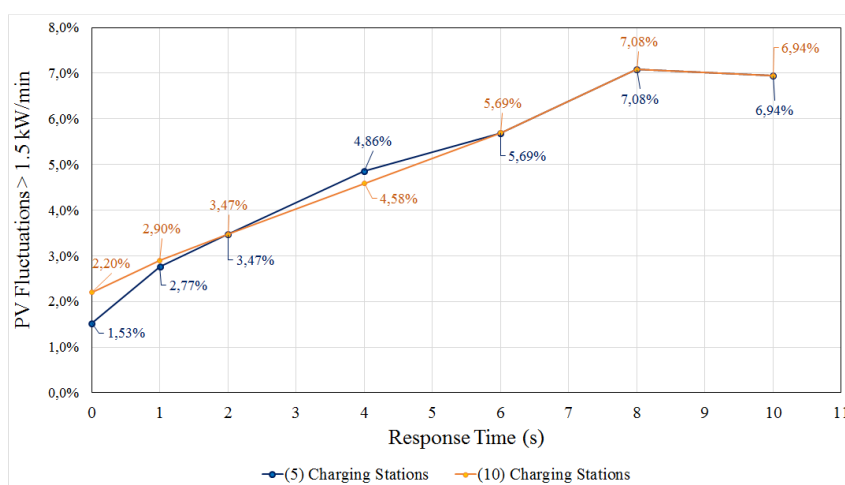


**Fig. 6.** Photovoltaic power and charging power of an EV.



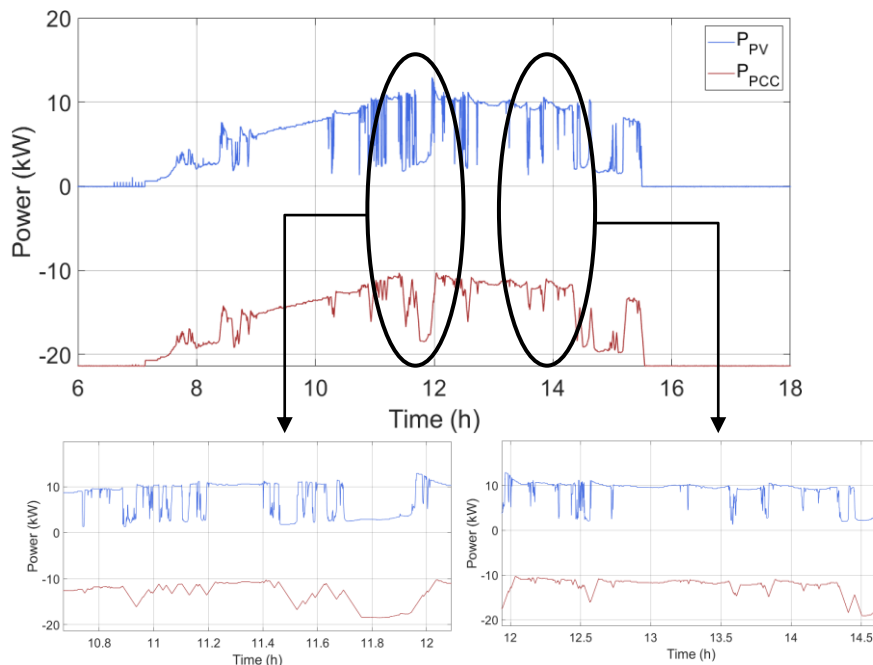
**Fig. 7.** Rate of change of photovoltaic power and injected power – most critical day.

The relationship between the response time of the charging system, the reduction of PV fluctuations, and the number of EVs connected in the PCC are presented in figure 8. According to the tendency observed in the graphic, when the response time increase, the proportion of the PV fluctuations greater than the ramp rate limit also increases; but, it is noticed that the addition of charging stations in the PCC doesn't show a significant effect on the softness of these fluctuations. Therefore, for a response time of 1 and 2 seconds, the group of 5 charging stations reached 97.23% and 96.53% of reduction in the rate of change, respectively. The group of 10 charging stations reached 97.1% and 96.53%.



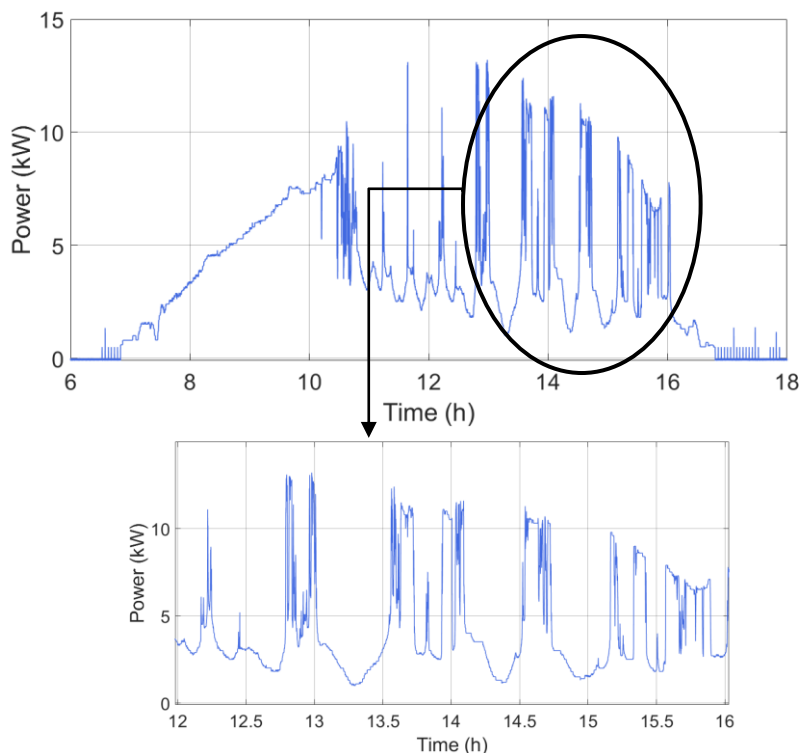
**Fig. 8.** Response time, photovoltaic power fluctuations, and number of charging stations.

Figure 9 presents the final result of the mitigated PV fluctuations that are injected directly into the grid. The power measured in the PCC demonstrates a significant reduction of the fluctuant dynamic of the PV generation. In figure 9, two different areas are enlarged in which the softening effect of the ramp rate control strategy can be better appreciated. It can be seen in this figure negative values of the power injected in the PCC, which indicate that the power flow in this node has inverted. Due to the PV generation isn't enough to supply the charging demand of the group of EVs, the missing power comes from the external sources of energy connected to the PCC.



**Fig. 9.** Photovoltaic power and injected power applying the control strategy under study.

Similar behavior is observed in the study of a day with an average profile of solar radiation. From the information presented in figure 4, September 6 is considered for the analysis. This day registers an average variation level of 36 W/min, with a maximum rate of 9 kW/min. Figure 10 shows the output power of the PV system for this day. According to its analysis, the PV fluctuations reach the highest values between 12:00 and 16:00.



**Fig. 10.** Photovoltaic output power - average day.

Figure 11 indicates the rate of change of PV output power. The dynamic behavior of PV generation shows a low level of power variations with 6.8% of fluctuations over the limit ramp. The maximum rate reaches 9.34 kW/min between 10:00 and 12:00. Therefore, this day will require less charge management from the energy storage system of the group of EVs. Figure 11 also presents the proportion of the rate of change that diminishes with the use of the control strategy under study. The power variations reduce 4.8%, reaching a maximum ramp of 1.52 kW/min. This mitigation effect is better to appreciate in figure 12.

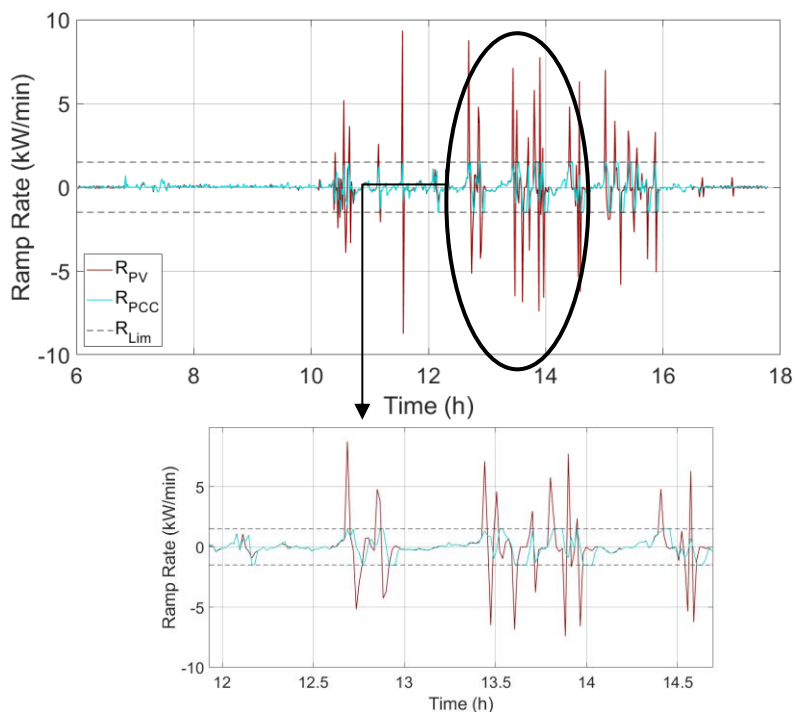


Fig. 11. Rate of change of photovoltaic power and injected power –average day.

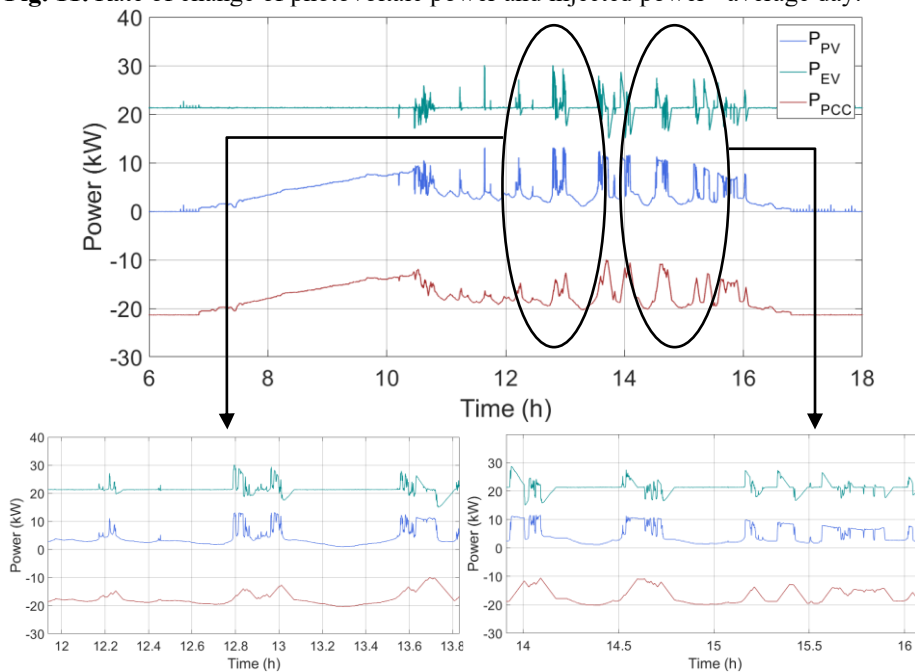


Fig. 12. Photovoltaic output power, power injected, and EV charging power.

## 5 Conclusion

The study shows the typical behavior of solar radiation in an Andean city, which presents a wide range of variations in time frames of seconds. This high variability of solar radiation conditions the power production capacity of the PV solar system. The average of the maximum fluctuations registered in the month of September, reached 48% of the nominal power per minute. The energy management system used in the study includes the application of the ramp rate control strategy and the incorporation of the charging system of a group of five EVs. The model developed allows handling the charging process following the dynamic behavior of the PV generation. Therefore, according to the capacity and characteristics of the radiation in the area under study, the storage system can increase and decrease its power by 99% without saturating itself. In the study is possible to reduce the rate of change of the power in the PCC by around 14%, with the use of an energy storage system based on the batteries of EVs.

## Acknowledgments

The authors thank the CYTED Thematic Network “INTELLIGENT CITIES FULLY INTEGRAL, EFFICIENT AND SUSTAINABLE (CITIES)” n° 518RT0558. This work has been supported by Spanish national project [RTC-2017-6712-3] of the Spanish Ministry of Science.

## References

- [1] “RENEWABLES 2020 GLOBAL STATUS REPORT,” 2020. <https://www.ren21.net/gsr-2020/>.
- [2] N. Mansouri, A. Lashab, D. Sera, J. Guerrero, and A. Cherif, “Large Photovoltaic Power Plants Integration: A Review of Challenges and Solutions,” *Energies*, vol. 12, no. 19, p. 3798, 2019, doi: 10.3390/en12193798.
- [3] L. G. González, R. Chacon, B. Delgado, D. Benavides, and J. Espinoza, “Study of Energy Compensation Techniques in Photovoltaic Solar Systems with the Use of Supercapacitors in Low-Voltage Networks,” *Energies*, vol. 13, no. 15, p. 3755, 2020, doi: 10.3390/en13153755.
- [4] J. Martins, S. Spataru, D. Sera, D.-I. Stroe, and A. Lashab, “Comparative Study of Ramp-Rate Control Algorithms for PV with Energy Storage Systems,” *Energies*, vol. 12, no. 7, p. 1342, 2019, doi: 10.3390/en12071342.
- [5] J. Traube *et al.*, “Mitigation of solar irradiance intermittency in photovoltaic power systems with integrated electric-vehicle charging functionality,” *IEEE Trans. Power Electron.*, vol. 28, no. 6, pp. 3058–3067, 2013, doi: 10.1109/TPEL.2012.2217354.
- [6] I. de la Parra, J. Marcos, M. García, and L. Marroyo, “Control strategies to use

- the minimum energy storage requirement for PV power ramp-rate control,” *Sol. Energy*, vol. 111, pp. 332–343, 2015, doi: 10.1016/j.solener.2014.10.038.
- [7] A. Cabrera-Tobar, E. Bullich-Massagué, M. Aragüés-Peñalba, and O. Gomis-Bellmunt, “Review of advanced grid requirements for the integration of large scale photovoltaic power plants in the transmission system,” *Renewable and Sustainable Energy Reviews*, vol. 62. Elsevier Ltd, pp. 971–987, 2016, doi: 10.1016/j.rser.2016.05.044.
- [8] T. Donato, F. Ingrosso, F. Licci, and D. Laforgia, “A method to estimate the environmental impact of an electric city car during six months of testing in an Italian city,” *J. Power Sources*, vol. 270, pp. 487–498, Dec. 2014, doi: 10.1016/j.jpowsour.2014.07.124.
- [9] F. Mwasilu, J. J. Justo, E. K. Kim, T. D. Do, and J. W. Jung, “Electric vehicles and smart grid interaction: A review on vehicle to grid and renewable energy sources integration,” *Renewable and Sustainable Energy Reviews*, vol. 34. Elsevier Ltd, pp. 501–516, Jun. 01, 2014, doi: 10.1016/j.rser.2014.03.031.
- [10] W. A. Omran, M. Kazerani, and M. M. A. Salama, “A study of the impacts of power fluctuations generated from large PV systems,” 2009, doi: 10.1109/SAE.2009.5534823.
- [11] K. Ishaque and Z. Salam, “A review of maximum power point tracking techniques of PV system for uniform insolation and partial shading condition,” *Renewable and Sustainable Energy Reviews*, vol. 19. pp. 475–488, 2013, doi: 10.1016/j.rser.2012.11.032.
- [12] J. L. Espinoza, L. G. Gonzalez, and R. Sempertegui, “Micro grid laboratory as a tool for research on non-conventional energy sources in Ecuador,” in *2017 IEEE International Autumn Meeting on Power, Electronics and Computing, ROPEC 2017*, Jan. 2018, vol. 2018-Janua, pp. 1–7, doi: 10.1109/ROPEC.2017.8261615.
- [13] N. B. G. Brinkel *et al.*, “Impact of rapid PV fluctuations on power quality in the low-voltage grid and mitigation strategies using electric vehicles,” *Int. J. Electr. Power Energy Syst.*, vol. 118, p. 105741, 2020, doi: 10.1016/j.ijepes.2019.105741.
- [14] IRENA, “Electric Vehicles: technology brief,” 2017.
- [15] S. Habib, M. M. Khan, F. Abbas, and H. Tang, “Assessment of electric vehicles concerning impacts, charging infrastructure with unidirectional and bidirectional chargers, and power flow comparisons,” *Int. J. Energy Res.*, vol. 42, no. 11, pp. 3416–3441, 2018, doi: 10.1002/er.4033.
- [16] “TIDA-010071 SAE J1772-compliant electric vehicle service equipment reference design for level 1 and 2 EV charger | TI.com.” <https://www.ti.com/tool/TIDA-010071>.
- [17] E. L. Maldonado Pineda, “Control de frecuencia mediante gestión de demanda durante el proceso de carga lenta en vehículos eléctricos,” Jun. 2020, Accessed: Mar. 16, 2021. [Online]. Available: <http://dspace.ucuenca.edu.ec/handle/123456789/34513>.

# Charging control of electric vehicles in microgrids with high penetration of photovoltaic generation: an integrated simulation method with Python and OpenDSS

Miguel Dávila-Sacoto<sup>1,2</sup>[0000-0001-6318-2137], Óscar Duque-Perez<sup>1</sup>[0000-0003-2994-2520], Luis Hernández-Callejo<sup>1</sup>[0000-0002-8822-2948], L.G. González<sup>2</sup>[0000-0001-9992-3494], Ángel L. Zorita-Lamadrid<sup>1</sup>[0000-0001-7593-691X] and J.L. Espinoza<sup>2</sup>[0000-0002-7450-2084]

<sup>1</sup> University of Valladolid, Valladolid, Spain

<sup>2</sup> University of Cuenca, Cuenca, Ecuador

M.D.S.: miguelalberto.davila@alumnos.uva.es

O.D.P.: oscar.duque@eii.uva.es

L.H.C.: luis.hernandez.callejo@uva.es

L.G.G.: luis.gonzalez@ucuenca.edu.ec

A.Z.L.: zorita@eii.uva.es

J.L.E.: juan.espinoza@ucuenca.edu.ec

**Abstract.** The simulation of microgrids with high penetration of electric vehicles and photovoltaic solar energy is a complex task that must consider realistic parameters of the agents that intervene in the generation of energy and in the control of the loads of the distribution system. In this study, an integrated simulation method with Python and OpenDSS is implemented for its application in microgrids with high penetration of photovoltaic generation and charging control of electric vehicles. For this, a simulation package is designed that incorporates parameters such as penetration of electric vehicles and photovoltaic systems, communication delay times between the system aggregator and charging stations, and connection event probability curves. The simulation system shows the effect of communication delay times and charging setpoint changes on the voltages of the connection bars of the clients, showing that due to high delay times in the communication between the vehicle and the aggregator there is a considerable impact on the load bars voltages..

**Keywords:** Microgrids, Electric Vehicle, high photovoltaic penetration, OpenDSS.

## 1 Introduction

The growing adoption of electric vehicles (EVs) and microgrids with distributed generation (DG) constitutes new challenges for the integration of these technologies within the classic paradigm of the electric power distribution grid. Thus, for its analysis it is necessary to have simulation tools that realistically integrate all the operating parameters of the agents that intervene in the grid, such as photovoltaic (PV) panels installed

by residential users, EVs, residential loads and the communication elements involved in the control of the system.

The simulation of grids with distributed renewable generation sources (DGS) and EVs is a complex task that requires simulation platforms that consider both electrical parameters of the system and specific models to determine the behavior of the load considering the human factor. Regarding the traditional simulation of distribution grids, the simulation is carried out with tools that allow the analysis of power flows, short circuits, load variations, distributed generation elements, unbalanced systems, among others, generally considering particular conditions of operation and power delivery at a defined point in time, however, there are few tools or software packages that can perform simulations in daily, weekly, monthly or annual periods of time [1].

The software packages usually used for the simulation of electrical grids are usually based on the integration of generation in high or medium voltage ranges, while the low voltage distribution grid is usually not important or is modeled in a simple way to obtain information on important elements for the control centers of energy distribution companies. On the other hand, the integration of generation in the low voltage grid, specifically at the customer's connection points, is increasingly common, so simulation programs must consider the parameters of the low voltage grid, the transformers, loads and additional generation that makes it a bidirectional network. In the same way, the adoption of EVs as a mobility alternative gives more importance to their analysis within distribution systems, since it is a load that not only increases considerably in the system due to the popularity of the technology, but it is difficult to predict, because it depends on many human factors such as driving style, vehicle battery capacity, characteristics of cities and terrain, knowledge of technology, etc. The response of the scientific community to these limitations in the simulation of DGS and EVs has resulted in the design and use of specialized tools, many of which are open-source to facilitate both the development of the tool and reduce licensing costs of software packages, most of which are designed for operation within a larger simulation system integrated with other tools. Thus, studies such as [2], [3] integrate geographic information systems (GIS) with open source simulators such as OpenDSS for the analysis of distribution grids, in [4] a tool is designed to create time series that describe EV mobility considering aspects of regenerative brakes and the availability of charging stations. In the same way as regards DGS, the use of open-source packages is used in simulation, for example in [5] the authors present a co-simulation option for distribution grids with PV generation with the goal of decreasing processing time.

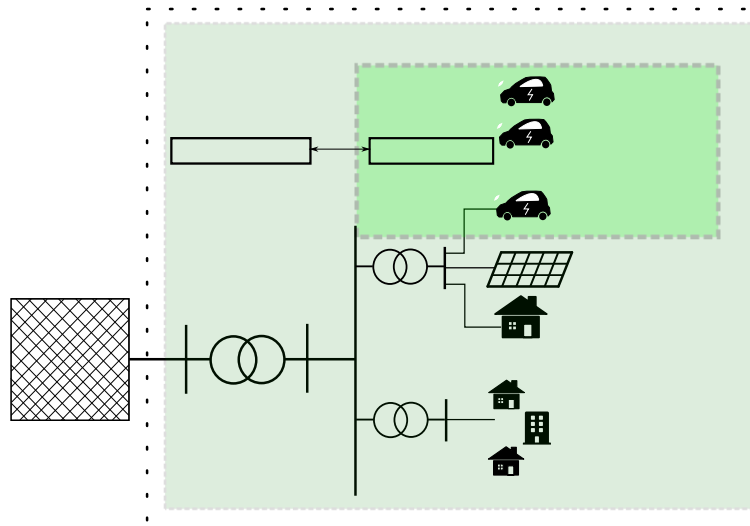
On the other hand, due to the challenges presented by the inclusion of EVs in a microgrid with high penetration of PV and wind under conditions of high variability of solar or wind resources, several studies have been carried out on the control of the charging process of EVs with the aim of reducing the negative effects on the grid or to counteract inherent drawbacks of DGS such as voltage and frequency variation [6], grid impact [7], PV output fluctuation suppression [8], among others. This type of control can be centralized in the power system operator, decentralized through agents within the distribution system, or automatic using EV charging stations as controllers without external communication [9]. In this way, studies such as [10] propose structures for the

use of PV systems and the charging of EVs through the use of integrated control systems within the home that allow the delivery of energy from the EV to the grid. These grid control systems must implement a control strategy to reduce the power variations caused by the variability of the PV systems [11]. The interaction between EVs and the grid in a unidirectional (V1G) or bidirectional (V2G) way allows this energy exchange for the administration of the grid [12], using the EV as an energy storage that can deliver a service to the grid in contingencies, for which the idle time is generally used to avoid a considerable impact on the EV's state of charge (SOC) [13]. The DGS simulation including the charging control allows to know the response of the grid to the variation of the charging setpoint of the EVs to specific states of the grid such as the variation of the power of the PV systems, for which the simulation platforms are limited, and it is required that they contemplate real behavior of the analyzed load.

In this work, a proposal for the integration of different criteria for the simulation of DGS with high PV and EV penetration is presented to achieve an approximate model to real operating conditions, focusing on the delays caused by the communication between the agents that intervene in the grid and in the charging setpoint command in the EV. The simulation is done using OpenDSS and Python controlled through a web interface.

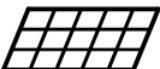
## **2 Design of an integrated simulation platform with Python and OpenDSS**

The effective simulation of a DGS with EVs is proposed by using the OpenDSS software package which is a simulator of electrical power distribution systems, controlled by Python, one of the most popular scripting languages in recent years [14]. To adjust to realistic parameters of the grid and of the EVs in the design of the proposed platform, the use of the system aggregator is adopted as the main agent of charging control of the EVs, which communicates with the operator of the system in charge of the control of PV systems and the residential and generic loads of the distribution system. The aggregator can carry out the charging control based on variables of the electricity market [15] and in the proposed scenario the control of the charging setpoint via V2G or V1G plus a control signal (see Fig. 1).



**Fig. 1.** Control areas of the system operator and the electric vehicle aggregator used in the simulation platform.

For the design of the platform, aspects that can be modified by the end user are considered that allow the analysis of the effect of penetration of both PV systems and EVs, parameters for the enablement of the systems (for an initial analysis), and communication and operation of each element (see Fig. 2).

 Aggregator Communication and control	Charging control strategies Number of communication nodes Transmission delay Propagation delay Queuing delay Processing delay
 Electric Vehicles	Setpoint change delay EV penetration Enable or disable EVs Charge event probability distribution function -User defined -Generated with peak hours
 PV systems	PV penetration Enable or disable PV systems Irradiation profile Efficiency profile P-T profile Temperature profile
 Residential loads	Load profile

**Fig. 2.** User modifiable parameters implemented in the proposed simulation platform.

Considering these parameters, the platform was designed as a co-simulation environment, where OpenDSS solves the electrical parameters of the system based on the inputs provided by the Python scripts. OpenDSS works in time-iteration mode for 24 hours, where the time-step is defined by the user. On the other hand, Python scripts generate or allow to load the profiles of the residential loads and irradiation, and by means of probability analysis it allows the generation of the charge/discharge control of the EVs, passing the connection or disconnection events to OpenDSS (see Fig. 3). The control is carried out at each time-step, modifying the characteristics of the main definitions that were introduced in the model in OpenDSS, and can be configured through a graphical interface encoded in HTML.

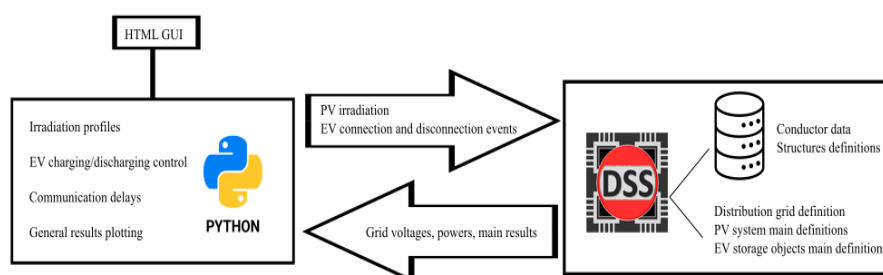


Fig. 3. Integrated simulation platform design using Python and OpenDSS.

### 2.1 Distribution grid modeling in OpenDSS

The proposed simulation paradigm is based on the definition of the distribution grid in OpenDSS in a way that allows the modification and control of the objects through the Python script. For this, the microgrid is defined modularly, redirecting the line files (see Fig. 4a), transformers, curves, PV systems and EVs, among others. Furthermore, elements such as PV systems and EVs are required to be connected to all system buses and then be activated or deactivated in the Python script (see Fig. 4b).

```
clear
new circuit.FEL basekV=230 pu=1.0 angle=0 frequency=60
phases=3
set defaultBaseFrequency=60
set EarthModel=Carson

redirect LinesMV.dss
redirect Transformers.dss
redirect LinesLV.dss
redirect Loadshapes.dss
redirect Loadshapes_PV.dss
redirect LoadsLV.dss
redirect Curves.dss
redirect EV_Storage.dss
```

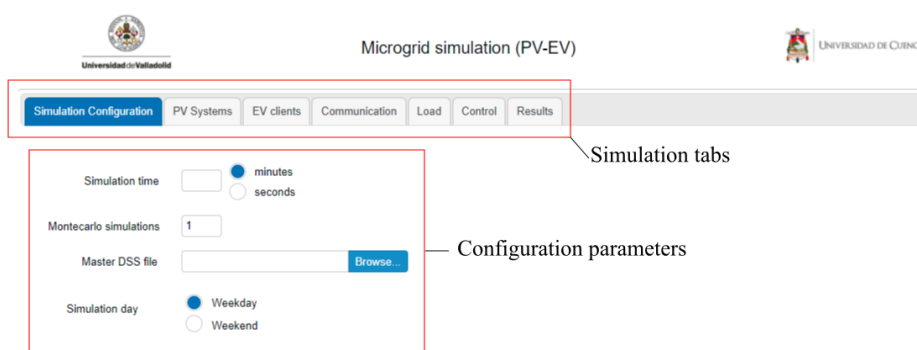
(a)

```

new PVSystem.pv_cliente_1 bus1=buscarga_cliente_1.1.2
kv=0.24 phases=1 kVA=3.00 pf=1 conn=wye irrad=1 Pmpp=3.00
temperature=14 effcurve=EffvsP P-TCurve=PvsT Daily=Radi-
acion TDaily=Temperatura %cutin=0

new storage.EV_1 bus1=buscarga_cliente_1.1.2 phases=2
model=1 kW=7.2 kV=0.24 pf=1 kWrated=7.2 kWhrated=24 %re-
serve=0 %stored=0 %EffCharge=100 %IdlingkW=0 Chargetrig-
ger=0 dischargetrigger=0 enabled=yes state=idling
    
```

(b)



(c)

**Fig. 4.** Definition of the microgrid in OpenDSS a) Redirection of libraries b) Definition of PV and EV systems c) configurable parameters by the user in the Html interface.

## 2.2 Electric Vehicles

The model for EVs shown in Fig. 4b is controlled by the Python script, where the power penetration of the EVs can be configured in relation to the total power of the system (equation 1).

$$EV_{penetration} = \frac{\sum P_{EV}}{\sum P_{Loads}} \tag{1}$$

To determine the EV connection event, a bimodal probability curve is used as determined in [16], being able to automatically generate the connection probability indicating two peaks based on the connection habits of EV users (see Fig. 5). In addition, the EV load command change delay time is considered as shown in [17].

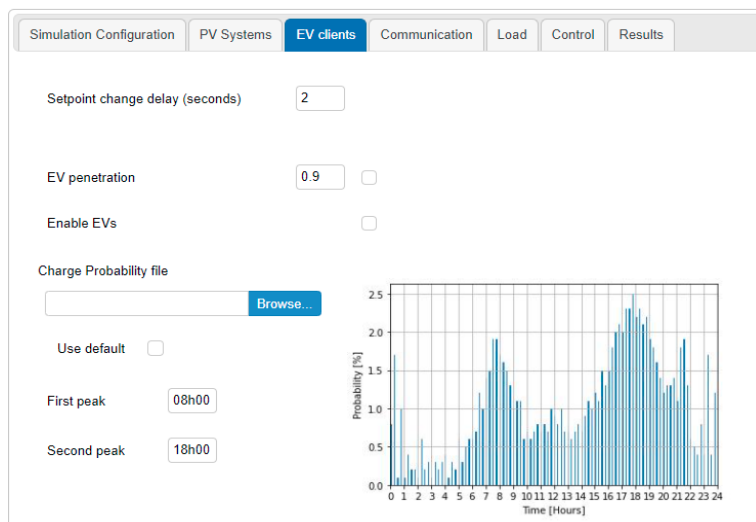


Fig. 5. User configurable parameters for electric vehicles.

### 2.3 Photovoltaic systems

The PV systems modeled in OpenDSS allow the modification of penetration parameters, system enablement, irradiation, efficiency, Power-Temperature, and cell-temperature curves (see Fig. 6).

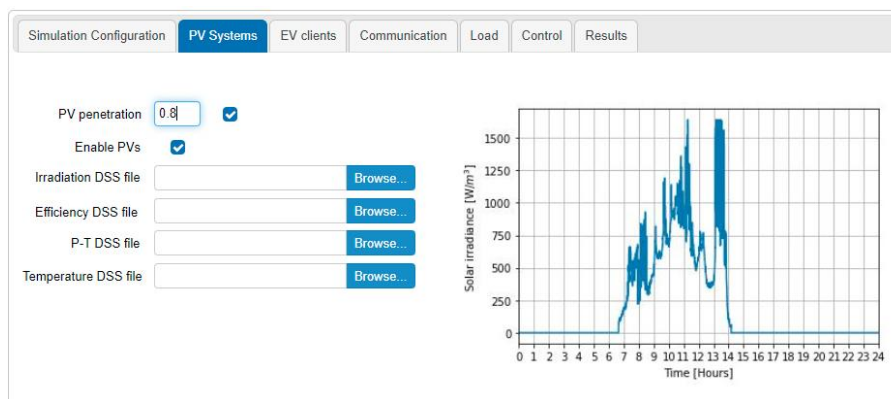


Fig. 6. User configurable parameters for photovoltaic systems.

### 2.4 Residential loads

The power of the loads connected to the distribution system modeled in OpenDSS can be modified by using a load curve in per unit that can be entered into the simulation by the end user (see Fig. 7).

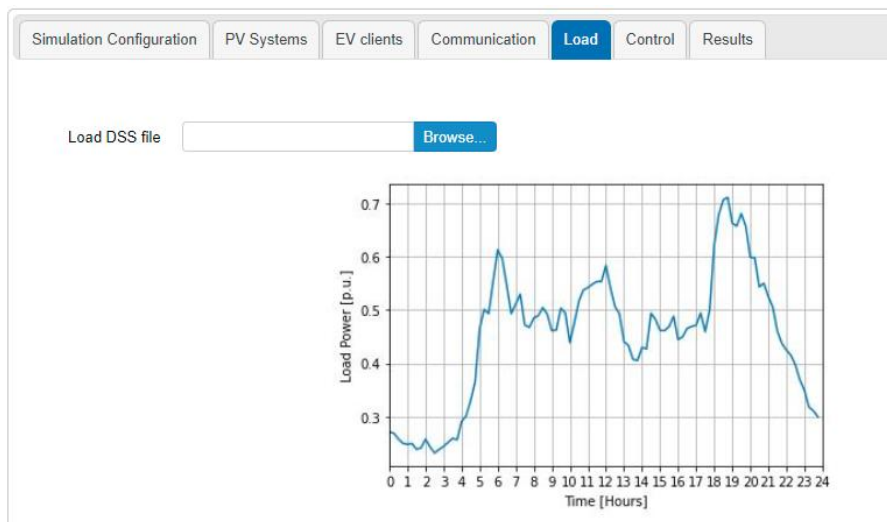


Fig. 7. User configurable parameters for residential loads.

### 2.5 Communication with the aggregator

One of the least considered parameters in the simulations with EVs in DGS is the communication delay between the aggregator and the charging stations because currently the communication equipment used have very low delay times, however, when it is considered that the variations of the PV resource is high, these times have a direct impact on the voltage and power values. Within communication parameters, the platform considers the existing delay times between the aggregator and the EV charging station. Transmission and propagation delays are calculated, and queuing and processing delays are considered (see Fig. 8). These delay times are mainly given by the characteristics of the transmission medium, the number of existing communication nodes, which must be considered in grids with high penetration of EVs, since requests to change the charging setpoint can lead to high processing and queue times.

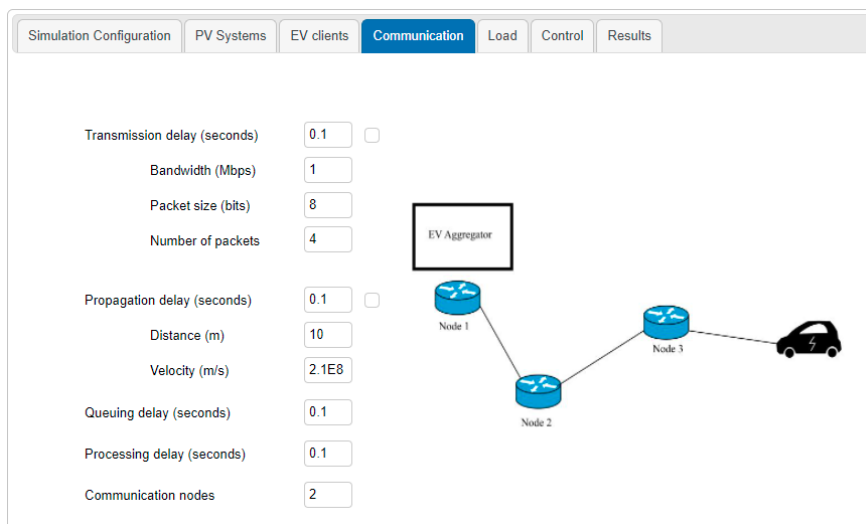


Fig. 8. User configurable parameters for communication delays.

### 2.6 Charging control

In a similar way to [17] where it is observed that a charging control algorithm based on the variations of the PV resource can be executed using a binomial Tustin transform, in this case a charging control based on in a Savitzky-Golay filter is used. This algorithm smooths the variations in PV irradiation and applies the variations to the charging command of all the EVs connected to the system (see Fig. 9). This command is applied to each vehicle during each simulation time as a function of connection time. The charge control is based on reducing the power consumed for charging the EV when the PV resource decreases, which causes less impact on the distribution system. This is important for grids with high penetration of PV generation because these systems provide very low inertia [18].

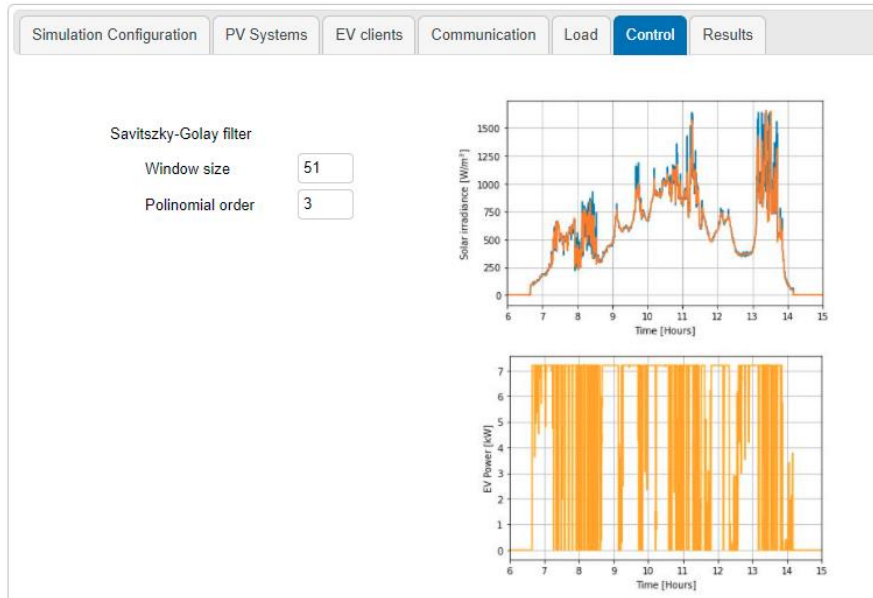
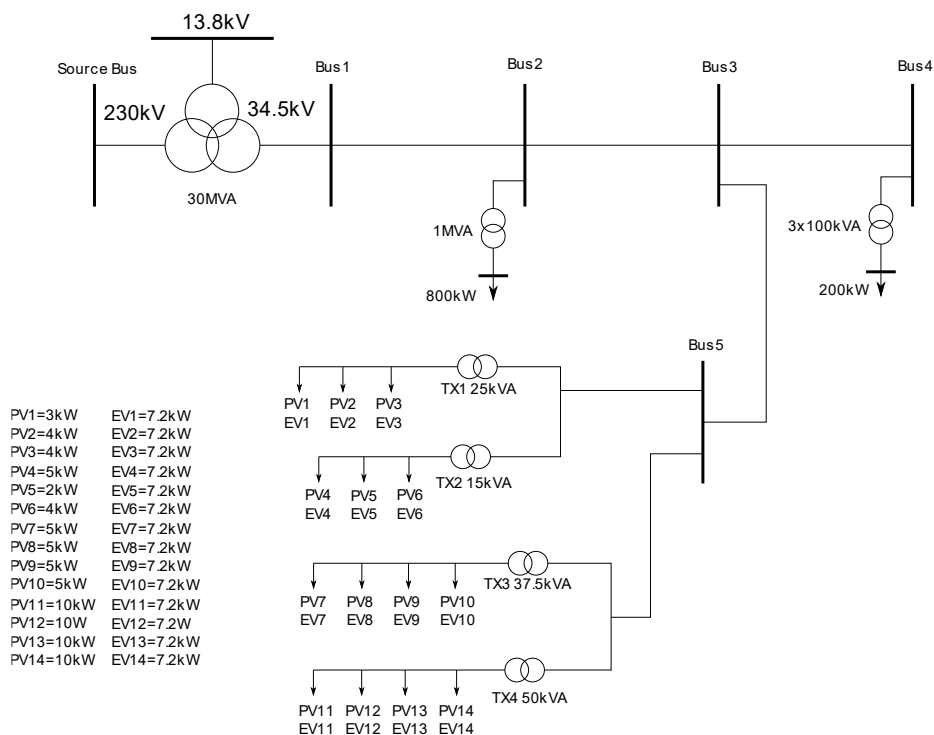


Fig. 9. User configurable parameters for charging control.

### 3 Simulation of electric vehicle charging and penetration of photovoltaic generation

As a case study, the distribution system shown in Fig. 10 was used. The system has PV generation systems and EVs at all the load points of the TX1, TX2, TX3 and TX4 transformers.



**Fig. 10.** Simulated distribution system.

The application of an integrated simulation platform that is focused on electrical grids with PV generation and EVs allows the execution of proofs of concept quickly. Thus, continuing with the difference between the delay times before a change in the charging setpoint of different manufacturers expressed in [17], simulations were run considering different values of this delay time (see Fig. 11), where it is observed that with high irradiation variations and controlling the charging setpoint in a VIG system using a Savitzky-Golay filter, the decrease in the response time of the EVs connected to the system causes the minimum voltages observed from the load buses to be lower in comparison with higher response times.

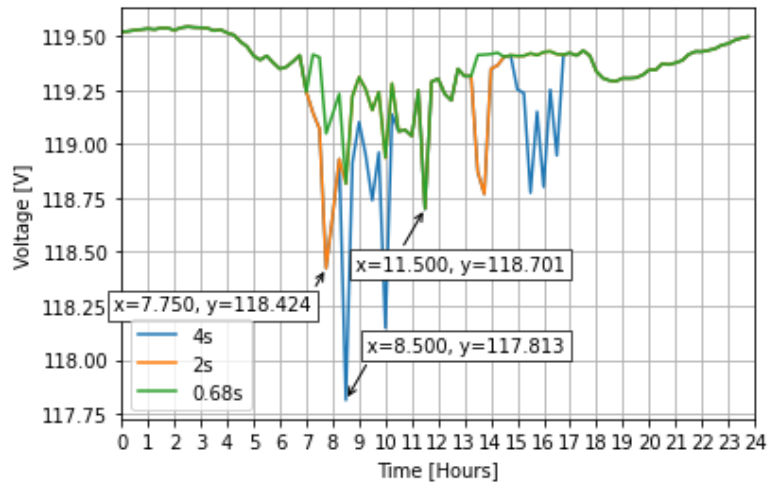


Fig. 11. Voltage in the load connection bar for different EV charging setpoint delay times.

Fig. 12 shows the charging setpoint and the SOC of an EV in the grid. It is observed that the charging control executes a variation in the power consumed by the EV by slightly varying the increase in the SOC.

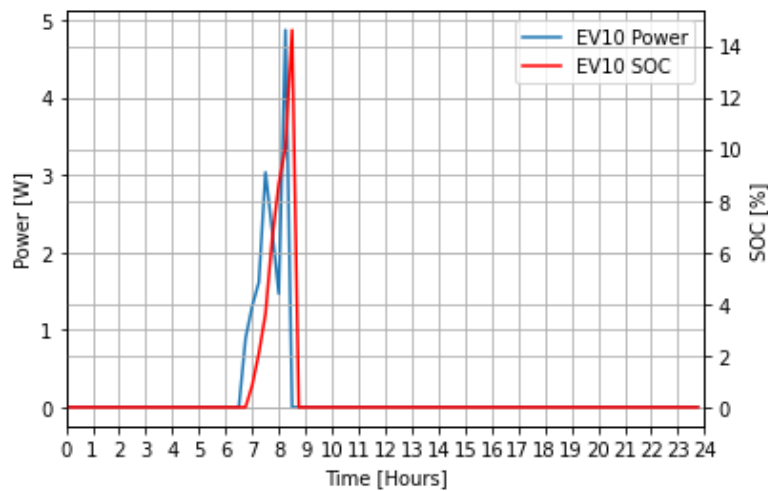


Fig. 12. Power and state of charge of an electric vehicle when applying charging control.

Executing the variation of the PV systems penetration, figure 13 shows the power in phase A of the substation transformer. It is observed that as the penetration of PV systems increases, the power of the transformer decreases. This visualization has the advantage of being able to run an analysis in 24 hours, observing the behavior of the power based on the profiles of the loads and the EVs connected to the system.

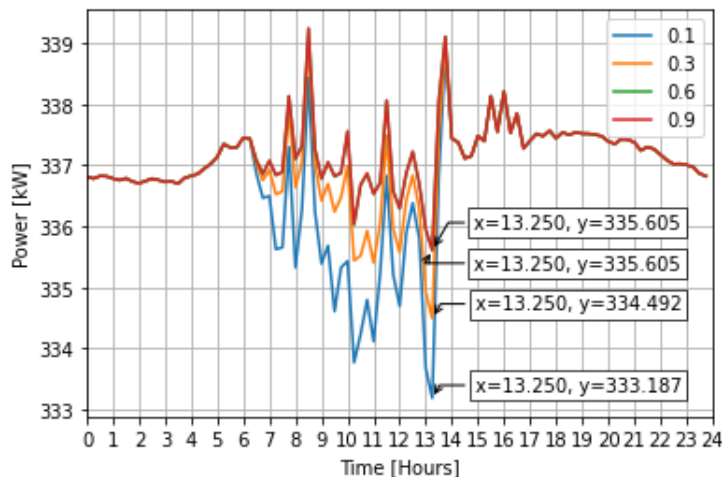


Fig. 13. Power of the feeder transformer at different levels of photovoltaic generation penetration.

#### 4 Conclusions

The simulation of the EV charging control involves the consideration of multiple parameters to ensure a realistic behavior of the agents that intervene in the distribution system. This study shows an approximation to consider important parameters within the control carried out by the aggregator considering significant variations in the PV resource by applying filters to change the charging setpoint as a function of the available PV irradiation.

It was observed that the time in which the charging command is effectively reflected in the EV has considerable effects within the voltage of the distribution system busbars, so a simulation package must consider these delays to evaluate the performance of the use of EVs to mitigate the effect of power variations on the grid.

The use of packages such as OpenDSS and Python for the simulation of distribution systems allows to integrate parameters that could not otherwise be easily integrated into a single simulation package or in traditional simulators of electrical systems. This reduces the time and effort of the users and researchers to run proofs of concept and evaluate case studies.

#### Acknowledgments

The authors acknowledge the CYTED Thematic Network “INTELLIGENT CITIES FULLY INTEGRAL, EFFICIENT AND SUSTAINABLE (CITIES)” 58RT0558. This work has been supported by Spanish national project [RTC-2017-6712-3] of the Spanish Ministry of Science.

## References

- [1] R. F. Arritt and R. C. Dugan, "Distribution system analysis and the future Smart Grid," in *2011 Rural Electric Power Conference*, Apr. 2011, pp. B2-1-B2-8, doi: 10.1109/REPCON.2011.5756725.
- [2] G. Valverde, A. Arguello, R. González, and J. Quirós-Tortós, "Integration of open source tools for studying large-scale distribution networks," *IET Gener. Transm. Distrib.*, vol. 11, no. 12, pp. 3106–3114, Aug. 2017, doi: 10.1049/iet-gtd.2016.1560.
- [3] R. Gonzalez, A. Arguello, G. Valverde, and J. Quiros-Tortos, "OpenDSS-based distribution network analyzer in open source GIS environment," in *2016 IEEE PES Transmission & Distribution Conference and Exposition-Latin America (PES T&D-LA)*, Sep. 2016, pp. 1–6, doi: 10.1109/TDC-LA.2016.7805643.
- [4] C. Gaete-Morales, H. Kramer, W. Schill, and A. Zerrahn, "An open tool for creating battery-electric vehicle time series from empirical data, emobpy," *Sci. Data*, vol. 8, no. 1, p. 152, Dec. 2021, doi: 10.1038/s41597-021-00932-9.
- [5] T. S. Theodoro, P. G. Barbosa, M. A. Tomim, A. C. S. de Lima, and M. T. C. de Barros, "MatLab-OpenDSS co-simulation environment: An alternative tool to investigate DSG connection," in *2018 Simposio Brasileiro de Sistemas Eletricos (SBSE)*, May 2018, pp. 1–7, doi: 10.1109/SBSE.2018.8395643.
- [6] A. Ali, D. Raisz, and K. Mahmoud, "Voltage fluctuation smoothing in distribution systems with RES considering degradation and charging plan of EV batteries," *Electr. Power Syst. Res.*, vol. 176, no. April, p. 105933, Nov. 2019, doi: 10.1016/j.epsr.2019.105933.
- [7] C. B. Jones, M. Lave, W. Vining, and B. M. Garcia, "Uncontrolled electric vehicle charging impacts on distribution electric power systems with primarily residential, commercial or industrial loads," *Energies*, vol. 14, no. 6, 2021, doi: 10.3390/en14061688.
- [8] K. Yukita, Y. Kobayashi, N. Duy-Dinh, T. Matsumura, and Y. Goto, "Suppression of PV output fluctuation using EV in a electric power system," *IFAC-PapersOnLine*, vol. 52, no. 4, pp. 93–98, 2019, doi: 10.1016/j.ifacol.2019.08.161.
- [9] S. Faddel, A. T. Al-Awami, and O. A. Mohammed, "Charge control and operation of electric vehicles in power grids: A review," *Energies*, vol. 11, no. 4, 2018, doi: 10.3390/en11040701.
- [10] H. Kikusato *et al.*, "Electric Vehicle Charge–Discharge Management for Utilization of Photovoltaic by Coordination Between Home and Grid Energy Management Systems," *IEEE Trans. Smart Grid*, vol. 10, no. 3, pp. 3186–3197, May 2019, doi: 10.1109/TSG.2018.2820026.
- [11] W. Ma, W. Wang, X. Wu, R. Hu, F. Tang, and W. Zhang, "Control Strategy of a Hybrid Energy Storage System to Smooth Photovoltaic Power Fluctuations Considering Photovoltaic Output Power Curtailment," *Sustainability*, vol. 11, no. 5, p. 1324, Mar. 2019, doi: 10.3390/su11051324.
- [12] A. Alsharif, C. W. Tan, R. Ayop, A. Dobi, and K. Y. Lau, "A comprehensive review of energy management strategy in Vehicle-to-Grid technology

- integrated with renewable energy sources,” *Sustain. Energy Technol. Assessments*, vol. 47, no. June, p. 101439, 2021, doi: 10.1016/j.seta.2021.101439.
- [13] A. Lucas, R. Barranco, and N. Refa, “EV Idle Time Estimation on Charging Infrastructure, Comparing Supervised Machine Learning Regressions,” *Energies*, vol. 12, no. 2, p. 269, Jan. 2019, doi: 10.3390/en12020269.
- [14] Berkeley University of California, “11 Most In-Demand Programming Languages in 2021 - Berkeley Boot Camps,” 2021. <https://bootcamp.berkeley.edu/blog/most-in-demand-programming-languages/> (accessed Aug. 09, 2021).
- [15] H. S. Das, M. M. Rahman, S. Li, and C. W. Tan, “Electric vehicles standards, charging infrastructure, and impact on grid integration: A technological review,” *Renew. Sustain. Energy Rev.*, vol. 120, no. November, 2020, doi: 10.1016/j.rser.2019.109618.
- [16] J. Quiros-Tortos, L. Ochoa, and T. Butler, “How Electric Vehicles and the Grid Work Together: Lessons Learned from One of the Largest Electric Vehicle Trials in the World,” *IEEE Power Energy Mag.*, vol. 16, no. 6, pp. 64–76, Nov. 2018, doi: 10.1109/MPE.2018.2863060.
- [17] M. Dávila-Sacoto, L. G. González, J. L. Espinoza, and L. Hernandez-Callejo, “Benefits of the integration of photovoltaic solar energy and electric mobility,” in *III Ibero-American Conference on Smart Cities (ICSC-2020)*, 2020.
- [18] J. Khazaei, Z. Tu, and W. Liu, “Small-Signal Modeling and Analysis of Virtual Inertia-Based PV Systems,” *IEEE Trans. Energy Convers.*, vol. 35, no. 2, pp. 1129–1138, Jun. 2020, doi: 10.1109/TEC.2020.2973102.

# P2P Energy Trading Model for a Local Electricity Community Considering Technical Constraints

Fernando García-Muñoz<sup>1</sup> and Francisco Díaz-González<sup>2</sup> Cristina Corchero<sup>1</sup>

<sup>1</sup> IREC Catalonia Institute for Energy Research, C. Jardins de les Dones de Negre, 1, Pl. 2a, 08930 Sant Adrià del Besòs, Spain

<sup>2</sup> Departament d'Enginyeria Elèctrica, Universitat Politècnica de Catalunya ETS d'Enginyeria Industrial de Barcelona, Avinguda Diagonal, 647, Pl. 2, 08028 Barcelona, Spain

**Abstract.** This article proposes a new formulation to model the energy traded among peers into a distribution network (DN) with high distributed energy resources (DERs) penetration, considering a centralized market design. The goal is to minimize the energy purchased to the grid and quantify the savings when exchanging energy among prosumers and consumers. The technical constraints are based on DC power flow equations, while the graph theory is used to model the local energy market (LEM). The proposed formulation is tested under two modified IEEE 5 and 33 bus systems, reporting savings in both study cases.

**Keywords:** Peer-to-peer energy trading, Distributed energy resources, Local energy markets, Smart grids

## 1 Introduction

Newmarket structures have emerged as an alternative to face an increasing penetration of distributed energy resources (DERs) in low voltage distribution networks (LVDN), where some more empowered, aware and active consumers have opted for self-consumption and to include storage energy systems to reduce the electricity bill and their dependence from the grid [14]. Peer-to-peer energy trading belongs to this new structure that seeks to increase self-generated energy efficiency by selling and buying its surplus within of small-scale smart-grid community. The residential areas composed of prosumers and consumers willing to exchange surplus energy are the baseline of this local energy market (LEM) [13]. However, the design of a platform that allows this new paradigm's correct operation is still under research, becoming the focus of many works over the last years [1–9].

The work done by [5] establishes a framework for local energy trading, presenting definitions and classification of market players and the different market-clearing approaches in the literature. Likewise, a state-of-the-art and perspective are presented in [6], discussing the critical aspect for a proper P2P energy

II Fernando García-Muñoz and Francisco Díaz-González Cristina Corchero

trading, which are: trading platforms, physical infrastructure, policy, market design, information and communication technology (ICT) infrastructure. Under the market design aspect (the focus of the model proposed in this article), there are three subcategories: centralized, decentralized or distributed markets. The first one could maximize the community's social welfare because a coordinator decides the energy amount exchange. In the decentralized market, the users have complete control over their devices, and they decide when selling or buying; however, the total community efficiency is affected. The distributed market design is between the two above, where a coordinator provides accurate information about pricing and the community requirement, and the peer decides when sell/buy, generating better coordination between them than decentralized design [6].

Two approaches are presented in [2] to compare the community-based and decentralized market based on optimal power flow (OPF) and continuous double auction (CDA), respectively. The work in [3] presents a bidding-based Hierarchical P2P energy transaction optimization model, which considers the prosumer's objective in terms of standard and green energy preference. The authors in [4] propose a bi-level optimization model for the decentralized P2P energy market without considering technical constraints; however, the proposed method in [4] achieves proper peers coordination without sacrificing privacy. A multi-class energy management concept is used in [9] to presents a P2P energy platform that allows coordinate trading among peers with preferences beyond the typical financial criteria, minimizing losses and battery depreciation. A game-theoretic approach is applied by [7] and [1] for P2P energy trading using the cooperative and the noncooperative game, respectively. However, both studies are not based on the power flow equations, and therefore, they do not include technical constraints in their formulation. The work done by [8] proposes a decentralized market clearing mechanism for the P2P energy trading considering the agents' privacy, power losses, and the utilization fees for using the third-party-owned network, where the fees are proportional to the electrical distance between producers and consumers.

The article's major contribution is a scalable and new P2P energy trading model, based on graph theory and the power flow equations, for a small-scale community local energy market with a centralized market design, considering high DERs penetration and flexible demand.

The rest of the paper is organized as follows. Section 2 describes the mixed-linear programming problem. Section 3 presents the computational results under two cases of study. Finally, the following steps to expand the model are discussed in Section 4.

## 2 Peer-to-Peer Energy Trading model

The formulation presented in this article pretends to model a small local community market with penetration of rooftop PV systems, batteries and flexible demand. Through the purchase and sale of energy exchanged among peers, the

## P2P Energy Trading Model for a Local Electricity Community III

community minimize the electricity purchased to the grid and maximize the use of the DERs, considering the following assumptions:

- The information related to the power loaded, generated and stored by peers is known.
- There is a safety mechanism to buy and sell energy within the small local market.
- The community is connected to an external grid which provides the remaining energy.
- The community buy and sell energy under a global internal market price and not an individual price.
- The peers seek to minimize their cost and maximize their benefits.
- The energy bought/sold to the grid is connected to the respective bus (not to slack bus), such that the power flow within the lines is only the energy exchanged among peers and not the energy from/to the grid.
- The power flow equations have been considered in their linear form (DC).

The last two assumptions aim to simplify the formulation, at least in this first approach, to improve the model's explanation, operation and results. Specifically, when the energy bought/sold to the grid is considered in the bus and does not in the slack-bus, all energy flows in the system belongs to the local market. Thus, the mixed-linear programming problem (MILP) is the following :

$$\begin{aligned} \text{minimize } z = & \sum_{i \in \mathbb{B}} \sum_{t \in \mathbb{T}} \lambda_t^{bg} p_{i,t}^{bg} - \lambda^{sg} p_{i,t}^{sg} + \lambda_t^{bm} p_{i,t}^{bm} \\ & - \lambda_t^{sm} p_{i,t}^{sm} + \sum_{(i,j) \in \mathbb{L}} \sum_{t \in \mathbb{T}} p_{i,j,t}. \end{aligned} \quad (1)$$

The objective function in (1) comprises, from left to right: the energy bought ( $p^{bg}$ ) and sold ( $p^{sm}$ ) to the grid, the energy traded within the local market ( $p^{bm}, p^{sm}$ ) (where the Lambdas indicates the respective trading prices), and the energy flow among peers ( $p_{i,j,t}$ ). Thus, (1) is subject to the following constraints:

Nodes constraints;  $\forall i \in \mathbb{B}, \forall t \in \mathbb{T}$

$$\sum_{(i,j) \in \mathbb{L}} p_{i,j,t} = pg_{i,t} - pl_{i,t} + p_{i,t}^{bg} - p_{i,t}^{sg} + (ds_{i,t} - ch_{i,t}). \quad (2)$$

Under the assumption of the DC version of the OPF, the constraints of the lines possess the following structure;  $\forall (i,j) \in \mathbb{L}, \forall t \in \mathbb{T}$

$$p_{i,j,t} = \frac{\theta_{i,t} - \theta_{j,t}}{x_{i,j}}. \quad (3)$$

Eq. (2) represents, from left to right, the power injected by the PV systems ( $pg$ ), the load ( $pl$ ), power bought/sold to the grid, and the power injected ( $ds$ ) or absorbed ( $ch$ ) by the storage system. Eq. (3) is the classic DC-OPF for the branches, and it does not present any variation.

IV Fernando García-Muñoz and Francisco Díaz-González Cristina Corchero

The power injected limits by the rooftop system, the voltages, and the flow between nodes are explained as follows:

Power injected by the PV system;  $\forall i \in \mathbb{B}$

$$0 \leq pg_{i,t} \leq I_i^{pg} \beta_i^p PG_t^{max}. \quad (4)$$

Voltage limits;  $\forall i \in \mathbb{B}, \forall t \in \mathbb{T}$

$$V^{min} \leq v_{i,t} \leq V^{max}. \quad (5)$$

Energy flow among peers;  $\forall (i, j) \in \mathbb{L}, \forall t \in \mathbb{T}$

$$p_{i,j,t} \leq S_{i,j}^{max}. \quad (6)$$

In Eq. (4), the power injected by the rooftop system is bounded by; a binary vector ( $I_i^{pg}$ ) that indicates if there is a PV system installed in the bus; the power system capacity ( $\beta_i^p$ ); and the maximum power ( $PG_t^{max}$ ) that can be injected by the system into a specific period  $t$  (see section 3.A).

The battery behaviour is represented through the follows constraints;  $\forall i \in \mathbb{B}, \forall t \in \mathbb{T}$

$$soc_{i,t+1} = soc_{i,t} + (\varphi ch_{i,t} - \frac{ds_{i,t}}{\varphi})\Delta t, \quad (7)$$

$$I_i^{bt} \beta_i^b SOC_t^{min} \leq soc_{i,t} \leq I_i^{bt} \beta_i^b SOC_t^{max}, \quad (8)$$

$$ch_{i,t} \leq M^{bt} w_{i,t}, \quad (9)$$

$$ds_{i,t} \leq M^{bt}(1 - w_{i,t}) - M^{bt}(1 - I^{bt}), \quad (10)$$

$$w_{i,t} \leq I^{bt}. \quad (11)$$

Eq. (7) indicates the state of charge of the battery, which is bounded in Eq. (8) by the battery capacity, multiplied by its minimum/maximum operating range and multiplied by a binary vector ( $I^{bt}$ ) which is 1 when a bus possesses a storage system installed. Likewise, Eq. (9) indicates the charge power of the battery, such that when it is charging,  $w_{i,t}$  takes value 1; otherwise, the battery is discharging through Eq. (10). If there is no battery installed ( $I^{bt} = 0$ ),  $w_{i,t}$  must be zero (see Eq.(11)), and the other battery constraints are also zero.

Flexible Demand, Therefore;  $\forall i \in \mathbb{B}, \forall t \in \mathbb{T}$

$$pl_{i,t} = PL_{i,t} + \sum_{d \in \mathbb{D}} \tau_{i,t}^d Pfd^d. \quad (12)$$

Therefore;  $\forall i \in \mathbb{B}, \forall d \in \mathbb{D}$

$$\sum_{d \in \mathbb{D}} \tau_{i,t}^d = Nfd_i^d. \quad (13)$$

The total electricity load in Eq. (12) is composed of unmanageable demand ( $PL_{i,t}$ ) and flexible demand ( $Pfd^d$ ), which could be activated at any time  $t$  depend on the generation and consumption level, in order to minimize the energy

## P2P Energy Trading Model for a Local Electricity Community V

purchased to the grid. Thus, the binary variable  $\tau_{i,t}^d$  is 1 when the flexible load is activated and zero otherwise, allowing different types of flexible loads activated in the same period  $t$ , such as air conditioner, wash, and dish machine. Eq (13) indicates the total numbers of hours that a type of demand must be activated at a certain time horizon.

The local energy market is modelled through the following set of constraints. Therefore;  $\forall i \in \mathbb{B}, \forall t \in \mathbb{T}$

$$pg_{i,t} + ds_{i,t} = p_{i,t}^{sc} + p_{i,t}^{sm} + p_{i,t}^{sg} + ch_{i,t}, \quad (14)$$

$$p_{i,t}^{sm} + p_{i,t}^{sg} \leq (pg_{i,t} + ds_{i,t} - pl_{i,t}) + M(1 - y1_{i,t}), \quad (15)$$

$$p_{i,t}^{sm} + p_{i,t}^{sg} \leq y1_{i,t} + M(1 - y2_{i,t}), \quad (16)$$

$$y1_{i,t} + y2_{i,t} = 1, \quad (17)$$

$$\sum_{(i,j) \in \mathbb{L}} p_{i,j,t} \leq p_{i,t}^{sm}, \quad (18)$$

$$\sum_{(j,i) \in \mathbb{L}} p_{j,i,t} \leq p_{i,t}^{bm}. \quad (19)$$

Eq. (14) represents the relation between i) the power injected from the generator plus the battery (power available to use), with ii) how to assign this power to: meet the load ( $p_{i,t}^{sc}$ ), sell the remaining energy to the local market ( $p_{i,t}^{sm}$ ) /grid ( $p_{i,t}^{sg}$ ), or charge the battery ( $ch_{i,t}$ ). Eqs. (15)-(17) represents the energy amount that can be sold by a user (peer) at a specific time. Specifically, Eqs. (15) and (16) explain: if the user has generation and/or energy stored, this energy must satisfy first its electricity load. Once the load is complete, the remaining energy can be sold in the local market; otherwise, the power sold to the grid or the market must be zero. Eq. (17) is composed of two sets of binary variables that allow the proper operation of the Eqs. (15) and (16) supported by  $M$ , which is a significant positive number. Thus,  $y1$  takes the value 1 when the generator's power plus the power injected from the battery is greater than the electricity load, and in the case when the load is greater than the power available to use,  $y2$  takes the value 1. Eq. (18) indicates that all the energy that leaves node  $i$  is energy sold to the market, and Eq. (19) that all the energy reaching node  $i$  is energy bought to the market.

Market clearing constraint;  $\forall t \in \mathbb{T}$

$$\sum_{i \in \mathbb{B}} p_{i,t}^{sm} = \sum_{i \in \mathbb{B}} p_{i,t}^{bm}. \quad (20)$$

Eq. (13) indicates that the total energy sold to the local market must be bought. Therefore, following the market constraints already explained, a user

VI Fernando García-Muñoz and Francisco Díaz-González Cristina Corchero

(peer) with a self-consumption system is under the following scenarios:

- |  |           |                                       |
|--|-----------|---------------------------------------|
| a) if $pg_{i,t} + ds_{i,t} > pl_{i,t}$ , | sell to   | Market: $p_{i,t}^{sm} = p_{i,t}^{bm}$ |
|  |           | Grid: Remaining                       |
| b) if $pg_{i,t} + ds_{i,t} < pl_{i,t}$ , | bought to | Market: $p_{i,t}^{bm} = p_{i,t}^{sm}$ |
|  |           | Grid: Remaining                       |
| c) if $pg_{i,t} + ds_{i,t} = pl_{i,t}$ , | nothing.  |                                       |

In the first scenario, if the self-generation is greater than the load, the remaining energy could be sold to the grid or the local market, such that the energy available to sell within the community must be equal to the market load. However, for selling within the market to make sense, the pricing should be under the following pattern:

$$\lambda_t^{sg} \leq \lambda_t^{sm} \leq \lambda_t^{bg}, \quad \lambda_t^{sm} = \lambda_t^{bm}. \quad (21)$$

Therefore, the user would prefer to sell its remaining energy to the market before the grid because the internal market price is always greater than  $\lambda_t^{sg}$ . On the other hand, the users always would choose to buy energy to the internal market than the grid because it is cheaper than  $\lambda_t^{bg}$ . Under this context, the objective function must be rewritten as follows:

$$z = \sum_{i \in \mathbb{B}} \sum_{t \in \mathbb{T}} \lambda_t^{bg} p_{i,t}^{bg} - \lambda^{sg} p_{i,t}^{sg} + \sum_{(i,j) \in \mathbb{L}} \sum_{t \in \mathbb{T}} p_{i,j,t}. \quad (22)$$

In Eq. (22), the local market's energy traded has been deleted because the energy sold and bought always are equal in amount and price.

### 3 Computational Results

This section presents the data used to test the model under two IEEE bus systems with their respective results. The first network, corresponding to the IEEE 5-bus system, is used as a slight case of study to facilitate the results explanations and show clearly the data type obtained from the model and its operation before being tested in a second case study corresponding to the 33 nodes distribution network. The two study cases compare the total energy bought when there is no energy traded among peers and when it is. The aim is to quantify the savings produced by the energy exchange among peers with PV and storage systems. The formulation has been programmed in Pyomo-Python using CPLEX as the solver.

#### 3.1 Data

The load profiles have been taken from [10], the energy price [11], and the PV power output from [12], where the weather conditions belong to Barcelona,

P2P Energy Trading Model for a Local Electricity Community VII

Spain. Fig 1 shows the relationship between these curves such that everyone has been normalized to be in function of the maximum power capacity. i.e., if the power capacity of the PV system is 10 kW, then every hour of the PV normalized curve (between 0 and 1) represents the power than can be injected into the system at that hour. Thus the PV curve in Fig 1 is the PG max vector used in the formulation. Likewise, the normalized curves belonging to the load profiles are multiplied by the maximum power load at every bus to obtain the load at every hour. The price to sell energy to the grid has been assumed in 1/3 of the buy price.

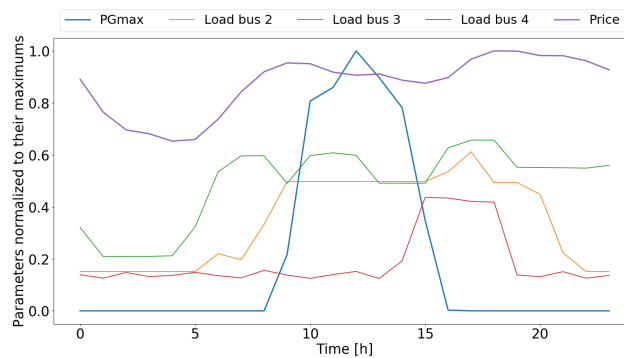


Fig. 1. Profiles used in the first case of study

3.2 IEEE 5 bus system

The small case study [16] considers five nodes, six lines, and three buses with load profiles where buses 2, 3, and 4 possess a maximum power of 7, 5, and 3.5 kW, respectively. Besides, node 2 and 4 have installed a rooftop PV system of 10 and 5 kW, and bus 4 has a storage device of 10 kWh with a power charge/discharge of 5 kW which start charged at 50%. Two types of flexible demand are included: a consumption of 1.5 and 2.5 kWh, which must be activated within the 24 hours time horizon.

Table 1 shows the results for bus 4 that includes self-generation and battery. Thus, it is easy to observe the following behaviour:

- Hour 1: The load is composed only by unmanageable demand that is fulfilled with energy from the battery, which means that the load is equal to the self-consumption.
- Hour 2-7: There is not battery discharged, and therefore the energy is bought to the grid.
- Hour 10-16: There is power generated from the PV system, which in hour 10 generate 1.1 kW, of which 0.5 kW are for self-consumption; the remaining

VIII Fernando García-Muñoz and Francisco Díaz-González Cristina Corchero

is summed to the 2.1 kW discharged from the battery to sell 2.7 kW to the market. In hour 13, the power generated reaches 5 kW, of which 3 kW belong to self-consumption composed of a fixed load of 0.5 kW and a flexible demand of 2.5 kW; the remaining 2 kW are used to charge the battery with 1.5 kW and sell to the market 0.5 kW.

- Hour 17-24: In the remaining hours, the battery supplies the energy to meet the load. Thus, the only hours when bus 4 buy energy to the grid is when the electricity price is the lowest (see Fig 1).

Fig 2 shows schematically how the nodes exchange energy into the local market at hour 12. Bus 3 is a consumer without flexible devices or PV system, while nodes 2 and 4 are prosumer, which sells the remaining energy to node 3, showing the energy flow in Fig 2.

Table 3 shows a final comparison between three different scenarios: **(A)** System without DERs penetration, **(B)** System with DERs but without energy traded among peers, and **(C)** System with DERs and energy traded. Thus, in case **(B)** the energy bought to the grid is 102.8 kW, corresponding to 67.68% of the total demand; however, when there are energy traded, the energy from the grid is 78.6 kW, 51.7% of the total load, which means that the community local market has reduced the grid dependence in 23.6%. In saving terms, the community electricity bill for 24 hours arise to 9.15€ in scenario **(A)**; however, under **(B)** scenario, the cost decreases to 5.68€ and considering energy traded among peers 4.79€, which means a 15.7% in saving regarding the scenario **(B)** and 47.6% of the scenario **(A)**.

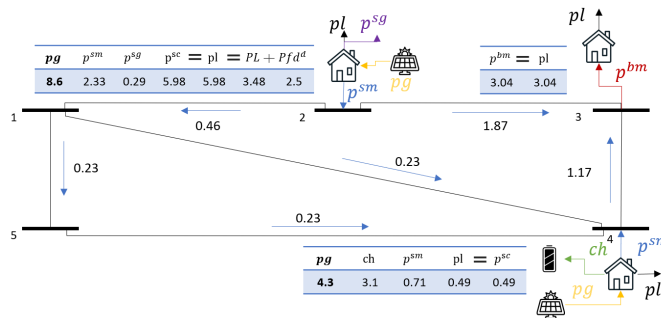


Fig. 2. IEEE 5 bus system: Energy traded, 12 am

### 3.3 IEEE 33 bus system

The second case of study considers the IEEE 33 bus system [15], which has been modified to includes a high DERs penetration, i.e., the PVs and Batteries power installed represents 61.8% and 70.9%, respectively, of the total power demanded.

P2P Energy Trading Model for a Local Electricity Community IX

**Table 1.** 5-test system case: Bus 4 results

Hour	$pg$	$p^{sc}$	$p^{bg}$	$p^{sg}$	$p^{bm}$	$p^{sm}$	$soc$	$ch$	$ds$	$pl$	$PL$	$Pfd$
1	0	0.5	0	0	0	0	5	0	0.5	0.5	0.5	0
2	0	0	0.4	0	0	0	4.5	0	0	0.4	0.4	0
3	0	0	0.5	0	0	0	4.5	0	0	0.5	0.5	0
4	0	0	0.5	0	0	0	4.5	0	0	0.5	0.5	0
5	0	0	0.5	0	0	0	4.5	0	0	0.5	0.5	0
6	0	0	0.5	0	0	0	4.5	0	0	0.5	0.5	0
7	0	0	0.5	0	0	0	4.5	0	0	0.5	0.5	0
8	0	0.4	0	0	0	0	4.5	0	0.4	0.4	0.4	0
9	0	0.5	0	0	0	0	4	0	0.5	0.5	0.5	0
10	1.1	0.5	0	0	0	2.7	3.4	0	2.1	0.5	0.5	0
11	4	1.9	0	0	0	1.5	1	0.6	0	1.9	0.4	1.5
12	4.3	0.5	0	0	0	0.7	1.5	3.1	0	0.5	0.5	0
13	5	3	0	0	0	0.5	4.3	1.5	0	3	0.5	2.5
14	4.5	1.9	0	0	0	0	5.7	2.6	0	1.9	0.4	1.5
15	3.9	0.7	0	0	0	2.1	8	1.1	0	0.7	0.7	0
16	1.7	1.5	0	0	0	0.2	9	0	0	1.5	1.5	0
17	0	1.5	0	0	0	0	9	0	1.5	1.5	1.5	0
18	0	1.5	0	0	0	0	7.3	0	1.5	1.5	1.5	0
19	0	1.5	0	0	0	0	5.7	0	1.5	1.5	1.5	0
20	0	0.5	0	0	0	0	4.1	0	0.5	0.5	0.5	0
21	0	0.5	0	0	0	0	3.5	0	0.5	0.5	0.5	0
22	0	0.5	0	0	0	0	3	0	0.5	0.5	0.5	0
23	0	0.4	0	0	0	0	2.4	0	0.4	0.4	0.4	0
24	0	0.5	0	0	0	0.5	1.9	0	0.9	0.5	0.5	0

**Table 2.** 5-test system case: Summary table results

	$pg$	$p^{sc}$	$p^{bg}$	$p^{sg}$	$p^{bm}$	$p^{sm}$	$sc$	$ds$	$pl$	$PL$	$Pfd$
(A)	0	0	151.9	0	0	0	0	0	151.9	131.9	20
(B)	73.7	49.1	102.8	26.7	0	0	8.4	10.4	151.9	131.9	20
(C)	73.7	47	78.6	2.4	26.4	26.4	8.9	10.9	151.9	131.9	20

The DN has 33 nodes, 32 lines, and 32 load points, where the load profiles used in Fig. 1 has been replicated to the 33 bus system.

Table 3 shows the comparison results for the same scenarios explained in the previous section. Thus, the internal market; traded 10% of the total load; the self-consumption round the 27% for scenarios (B) and (C); the batteries provide 8% of the energy to meet the load; and the scenario (C) shows a lower dependence from the external grid purchasing 12% less than the scenario with DERs but without energy traded. In terms of savings, scenario (C) continues been the most efficient because it paid 9.13% less than scenario (B) and 39.7% less than scenario (A). These results are aligned with the first case of study, and they are consistent with the expected values for an energy local trading market.

X Fernando García-Muñoz and Francisco Díaz-González Cristina Corchero

**Table 3.** 33-test system case: Summary table results

	$pg$	$p^{sc}$	$p^{bg}$	$p^{sg}$	$p^{bm}$	$p^{sm}$	$sc$	$ds$	$pl$	$PL$	$Pfd$
(A)	0	0	990.7	0	0	0	0	0	990.7	925.7	65
(B)	403	275.4	715.3	151.9	0	0	55.5	79.7	990.7	925.7	65
(C)	403	255.6	296.5	66.1	105.5	105.5	55.4	79.7	990.7	925.7	65

## 4 Discussion and Next Steps

The model presented in this paper allows computing the efficiency obtained when a community network with high DERs penetration exchange energy among peers to meet the load, minimizing the energy purchased to an external grid. Besides, the formulation proposed could favour creating local energy markets identifying and quantifying every user share, addressing one of the main barriers of this new market structures. However, the formulation presents several assumptions that could relax to improve significantly the model proposed. For example:

- Use the AC power flow equations to represents more realistic technical constraints.
- Consider the slack bus like interconnection point among peers to sell or buy energy to the grid, and size possible congestion level produced by the energy exchanged.
- Include electric vehicles and observe their role when they are connected and operate like flexible service to the users.
- Change the global internal trading price to a competitive price to move toward a decentralized market design, where the model proposed to act as a master problem to identify the energy amount that should be traded, and a subproblem could establish the final price for every user that could buy or sell energy into the local market.

## Nomenclature

- $i \in \mathbb{B}$  Set of buses.
- $t \in \mathbb{T}$  Set of time periods.
- $d \in \mathbb{D}$  Set of types of flexible demand resources.
- $(i, j) \in \mathbb{L}$  Set of lines, such that  $\mathbb{L} = \{(i, j); i, j \in \mathbb{B}\}$ .
- $PG_t^{max}$  Maximum active power available at the period  $t$  in [%].
- $PL_{i,t}$  Non-flexible active load of the bus  $i$  at the period  $t$  [kW].
- $V^{min}$  Minimum voltage allowed for the bus  $i$  [p.u.].
- $V^{max}$  Maximum voltage allowed for the bus  $i$  [p.u.].
- $S_{i,j}^{max}$  Maximum apparent power of the line between buses  $i$  and  $j$  [kVA].
- $SOC^{min}$  Minimum state of charge of battery [%].
- $SOC^{max}$  Maximum state of charge of battery [%].

## P2P Energy Trading Model for a Local Electricity Community XI

$\beta_i^p$	Maximum rated power of generator of the bus $i$ [kW].
$\beta_i^{bt}$	Capacity of the Battery of the bus $i$ [kWh].
$I_i^{pg}$	Binary parameters; 1 if bus $i$ has generation, 0 otherwise.
$I_i^{bt}$	Binary parameters; 1 if bus $i$ has battery, 0 otherwise.
$\varphi$	Efficiency of battery [%].
$M^{bt}$	Maximum charge/discharge for battery in a period [kW].
$\lambda_t^{bg}$	Electricity price bought to the grid at the period $t$ [kW].
$\lambda_t^{sg}$	Electricity price sold to the grid at the period $t$ [kW].
$\lambda_t^{bm}$	Electricity price bought to the market at the period $t$ [kW].
$\lambda_t^{sm}$	Electricity price sold to the market at the period $t$ [kW].
$Pfd^d$	Load for the flexible demand type $d$ [kW].
$Nfd_i^d$	Total number of hours that $Pfd^d$ should be active in a period of time.
$pg_{i,t}$	Active power injected from the generator in the bus $i$ at period $t$ [kW].
$v_{i,t}$	Voltage of the bus $i$ at the period $t$ [p.u].
$\theta_{i,t}$	Angle of the bus $i$ at the period $t$ [p.u].
$p_{i,j,t}$	Active power in line between buses $i$ and $j$ at the period $t$ [kW].
$ch_{i,t}$	Power absorbed by the battery of the bus $i$ at the period $t$ [kW].
$ds_{i,t}$	Power injected from the storage to the bus $i$ at the period $t$ [kW].
$soc_{i,t}$	State of charge of battery of the bus $i$ at the period $t$ [kWh].
$w_{i,t}$	Binary variable: 1 if the battery is charging in bus $i$ at period $t$ , 0 otherwise.
$p_{i,t}^{sc}$	Self-consumption energy by the bus $i$ at the period $t$ [kW].
$p_{i,t}^{bg}$	Energy bought to the grid by the bus $i$ at the period $t$ [kW].
$p_{i,t}^{sg}$	Energy sold to the grid by the bus $i$ at the period $t$ [kW].
$p_{i,t}^{bm}$	Energy bought to the market by the bus $i$ at the period $t$ [kW].
$p_{i,t}^{sm}$	Energy sold to the market by the bus $i$ at the period $t$ [kW].
$pl_{i,t}$	Total electricity load of bus $i$ at the period $t$ [kW].
$\tau_{i,t}^d$	Binary variable: 1 if the flexible demand type $d$ is activated, 0 otherwise.

## References

1. Paudel, A., Chaudhari, K., Long, C. & Gooi, H. Peer-to-peer energy trading in a prosumer-based community microgrid: A game-theoretic model. *IEEE Transactions On Industrial Electronics*. **66**, 6087-6097 (2019)
2. Guerrero, J., Chapman, A. & Verbič, G. Local energy markets in LV networks: Community based and decentralized P2P approaches. *2019 IEEE Milan PowerTech, PowerTech 2019*. pp. 1-6 (2019)
3. Park, D., Park, Y., Roh, J., Lee, K. & Park, J. A Hierarchical Peer-to-Peer Energy Transaction Model Considering Prosumer's Renewable Energy Preference. *IFAC-PapersOnLine*. **52**, 312-317 (2019), <https://doi.org/10.1016/j.ifacol.2019.08.228>
4. Wang, Z., Yu, X., Mu, Y. & Jia, H. A distributed Peer-to-Peer energy transaction method for diversified prosumers in Urban Community Microgrid System. *Applied Energy*. **260**, 114327 (2020), <https://doi.org/10.1016/j.apenergy.2019.114327>
5. Khorasany, M., Mishra, Y. & Ledwich, G. Market framework for local energy trading: A review of potential designs and market clearing approaches. *IET Generation, Transmission And Distribution*. **12**, 5899-5908 (2018)

## XII Fernando García-Muñoz and Francisco Díaz-González Cristina Corchero

6. Zhou, Y., Wu, J., Long, C. & Ming, W. State-of-the-Art Analysis and Perspectives for Peer-to-Peer Energy Trading. *Engineering*. **6**, 739-753 (2020), <https://doi.org/10.1016/j.eng.2020.06.002>
7. Tushar, W., Saha, T., Yuen, C., Morstyn, T., McCulloch, M., Poor, H. & Wood, K. A motivational game-theoretic approach for peer-to-peer energy trading in the smart grid. *Applied Energy*. **243**, 10-20 (2019), <https://doi.org/10.1016/j.apenergy.2019.03.111>
8. Paudel, A., Sampath, L., Yang, J. & Gooi, H. Peer-to-Peer Energy Trading in Smart Grid Considering Power Losses and Network Fees. *IEEE Transactions On Smart Grid*. **11**, 4727-4737 (2020)
9. Morstyn, T. & McCulloch, M. Multiclass Energy Management for Peer-to-Peer Energy Trading Driven by Prosumer Preferences. *IEEE Transactions On Power Systems*. **34**, 4005-4014 (2019)
10. OpenEI Open Energy Information. (2020), <https://openei.org/datasets/files/961/pub/>
11. Omie Iberian Electricity Market Operator. (2020), <https://www.omie.es/en/market-results/daily/daily-market/daily-hourly-price>
12. Commission, E. Photovoltaic Geographical Information System. (2019), <https://re.jrc.ec.europa.eu/pvg-tools/en/tools.html>
13. Mengelkamp, E., Staudt, P., Garttner, J. & Weinhardt, C. Trading on local energy markets: A comparison of market designs and bidding strategies. *International Conference On The European Energy Market, EEM*. (2017)
14. IRENA Electricity trading arrangements. (2020), <https://www.youtube.com/watch?v=UDv04q3U6e0>
15. Selvan, M. & Swarup, K. Distribution system load flow using object-oriented methodology. *2004 International Conference On Power System Technology, POW-ERCON 2004*. **2** pp. 1168-1173 (2004)
16. Saharuddin, N., Abidin, I., Mokhlis, H., Abdullah, A. & Naidu, K. A power system network splitting strategy based on contingency analysis. *Energies*. **11** (2018)

# Development and improvement of a data storage system in a microgrid environment with HomeAssistant and MariaDB

Oscar Izquierdo-Monge<sup>1</sup>, Gonzalo Martin-Jimenez<sup>1</sup>, and Paula Peña-Carro<sup>1</sup>

CEDER-CIEMAT, Autovía de Navarra A15 salida 56, 422290 Lobia (Soria), España,  
O.I-M.: oscar.izquierdo@ciemat.es; G.M-J.: gonzalomj96@gmail.com; P.P-C.:  
paula.pena@ciemat.es

**Abstract.** In a microgrid environment, it's suitable to store data obtained from the different devices that make up the microgrid in order to have the ability to perform a detailed data analysis later. This article will detail the process followed to store the data that has been collected through the monitoring and control software 'Home Assistant' in the microgrid of the CEDER-CIEMAT (Renewable Energy Center in Soria, Spain). The structure of the storage system created for a robust storage of data in the DBMS (Database Management System) MariaDB will be detailed and how to correct the different typical errors that are made in the development process of this storage system. Aspects the operation of the connection between Home Assistant and MariaDB, the configuration to establish communication with each other correctly and the organization of the different structures to be formed in the database created using the programming language SQL (Structured Query Language). It will detail the performance offered by this system together with the transformed data that has been generated for further analysis. Due to the emergence of new storage systems that are better adapted to the field of microgrids, the different alternatives that can be used will be described, which may replace the system developed to improve it.

**Keywords:** Microgrids, Data Storage, Home Assistant, MariaDB, Data Analytics, SCADA

## 1 Introduction

In recent years, IoT (Internet of Things) technology has become increasingly popular, this type of technology can be seen as it is applied in homes with the so-called domotics, applied to energy saving in the home, security and comfort, among others. It is also applied in modern cities with the 'Smart Cities' concept, facilitating mobility, improving the environment and the way of life for citizens. It can also be applicable to the industry to achieve greater efficiency in production and obtain analysis of the different processes that are carried out in order to obtain a series of improvements in the production process.

The term 'Internet of Things' has come to represent electrical or electronic devices, of varying sizes and capabilities, that are connected to the Internet. The

2 Oscar Izquierdo-Monge, Gonzalo Martin-Jimenez, Paula Peña-Carro

scope of the connections is ever broadening to beyond just machine-to-machine communication (M2M) [1]. All those devices are seamlessly integrated into the information network, and where the physical objects can become active participants in business processes. Services are available to interact with these 'smart objects' over the Internet, query their state and any information associated with them [2].

IoT technology can also be applied in the energy sector, obtaining various benefits and advantages, i.e. in energy supply, transmission and distribution, and demand. IoT can be employed for improving energy efficiency, increasing the share of renewable energy, and reducing environmental impacts of the energy use. Energy systems are on the threshold of a new transition era, the need for efficient use of energy calls for system-wide, integrated approaches to minimize the socio-economic-environmental impacts of energy systems. In this respect, modern technologies such as IoT can help the energy sector transform from a central, hierarchical supply chain to a decentralized, smart, and optimized system [3, 4]. The advancements in computational intelligence capabilities can evolve an intelligent IoT system by emulating biological nervous systems with cognitive computation, streaming and distributed analytics including at the edge and device levels [5].

Knowing the advantages that IoT technology has in the energy sector, as a logical consequence it is possible to apply it in an energy distribution and storage system, thus obtaining the concept of an intelligent electrical microgrid, which is defined as a local smaller electricity systems that can operate independently and separated from the main electricity grid. Microgrids provide improved security and availability for the electrical distribution system while reducing the carbon emissions [6]. a smart grid is an electricity network that can intelligently integrate the actions of all users connected to it – generators, consumers and those that assume both roles – in order to efficiently deliver sustainable, economic and secure electricity supplies. A smart grid employs innovative products and services together with intelligent monitoring, control, communication and self-healing technologies. Wired and wireless technology based integrated, robust and reliable communication network is needed for real time monitoring and control of microgrids [7, 8].

Once the connection of the microgrid has been made, with all the elements connected to each other and to be able to monitor the different variables in real time and to be able to have control over the devices, the next step to follow will be to store the acquired data in order to carry out a precise analysis subsequently. The data storage is controlled by a DBMS, with a stable infrastructure that allows to save large amounts of data with a fast read/write speed to be able to make queries to the database easily.

Traditional database systems used SQL database which has supported all the user requirements along with simplicity, robustness, flexibility, scalability, performance. But the main limitation they are facing is their static schema which is making RDBMS (Relational Database Management System) not suitable for IoT applications. On the other hand, NoSQL (non SQL) databases emerging in mar-

ket have claimed to perform better than SQL database. With the emergence of IoT and Big Data, NoSQL databases now represent an alternative to traditional relational databases in terms of simpler design and faster operations on large data volumes [9–11]. It is worth highlighting within the non-relational databases the real-time databases that are gaining increasing popularity in recent years, these databases save the values in time series (timestamps) and allow different functions to be performed with the data, all oriented to IoT applications [12].

The software and hardware used in this use case is detailed in section number 2, section 3 explains the operation of data storage in ‘Home Assistant’, section number 4 explains the connection between Home Assistant and MariaDB, in section 5 the various steps to follow for the configuration of the MariaDB server are detailed to start operating the database, then in section 6 the structure of the data stored by default in Home Assistant is exposed along with the transformation of these as convenient in section 7, in section 8 the results obtained thanks to the implementation of the database in the whole monitoring system and the benefits of storing data for subsequent analysis are exposed and finally in section 9 the conclusions are narrated, where the importance of having a robust database in microgrids will be exposed, in addition to the next line of work in the field of data storage in the center’s microgrid.

## 2 Materials and Methods

To carry out the work, the data storage system will be implemented in the CEDER-CIEMAT (Renewable Energy Center in Soria, Spain, as shown in figure 1) microgrid, data will be stored in a relational database such as MariaDB [13], where it will be periodically stored for later analysis.



Fig. 1. CEDER-CIEMAT location.

CEDER grid is connected to a 45 kV distribution network and transforms at its input to 15 kV. Eight transformation centres make up the grid, reducing the voltage to 400 V. The centre has various non-controllable renewable

4 Oscar Izquierdo-Monge, Gonzalo Martin-Jimenez, Paula Peña-Carro

(photo-voltaic and wind), controllable renewable (hydraulic turbine), and non-renewable (diesel generator) generation systems, several storage systems, mechanical (pumping system with tanks at different levels) and electrochemical (lithium-ion and Pb-acid batteries), as well as various consumption elements connected to each of the transformation centres monitored with grid analyzers (PQube) installed in the low voltage part of each of the transformation centres [14].

To carry out the tests it will be used a Raspberry Pi 4 Model B (Broadcom BCM2711, Quad core Cortex-A72 (ARM v8) 64-bit SoC @ 1.5GHz, LPDDR4-3200 SD RAM, 64 GB Micro-SD card, 5V DC) [15], obtaining all the data related to performance and consumption to be able to carry out an analysis with processing times. The system will be developed using two Raspberry computers, each with its corresponding dedicated software (Home Assistant and MariaDB), although this design decision is optional.

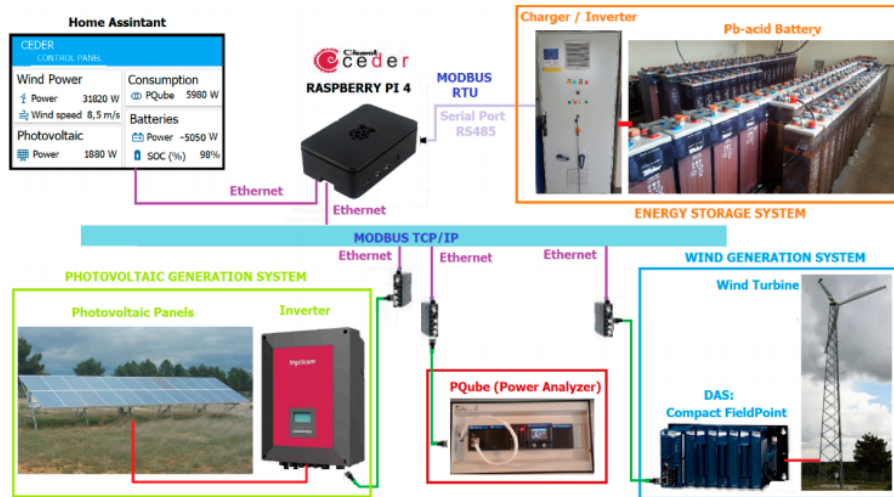


Fig. 2. Example of device connection in CEDER microgrid with Home Assistant.

For the monitoring and control of the different elements that make up the microgrid, the Home Assistant software [16] has been used., as shown in the diagram of the figure 2 This software allows to obtain the different values in real time of different elements and save them in a database in a simple way. Home Assistant can support more than 1000 devices, allowing to control and automate them, with a wide variety of extensions, security, smartphone support and power manager. For the development of this system, version 2021.8.8 of this software has been used.

For data storage, the DBMS MariaDB is used, a relational-type database that it's made by the original developers of MySQL and guaranteed to stay

open source. It is part of most cloud offerings and the default in most Linux distributions. It is built upon the values of performance, stability, and openness [13]. For the development of this system, version v10.3.29-MariaDB-0 + deb10u1 of this software has been used.

### 3 Data storage behavior in Home Assistant

In order to store the data that is being monitored by the Home Assistant software, it is necessary to have a database in order to achieve robust, reliable data storage that allows high-speed read/write operations.

Home Assistant stores the data thanks to the integration called 'recorder' by default the data is stored in its own database located in the configuration directory of the Home Assistant itself using SQLite as the database engine, this database is automatically generated in a file with the extension '.db'. Home Assistant uses SQLAlchemy, a Python SQL toolkit and Object Relational Mapper that provides the application with support for all types of operations in relational databases. This communication flow is explained in figure 3. With Home Assistant and SQLAlchemy, the supported relational databases are SQLite, MySQL, PostgreSQL, and MS SQL Server. In this use case, the MariaDB database will be used, since the default database, SQLite has several limitations such as limiting the maximum to 264 rows for a table or advanced and complex functions in SQL that are not supported, therefore that it will be mandatory to use the another database management system.

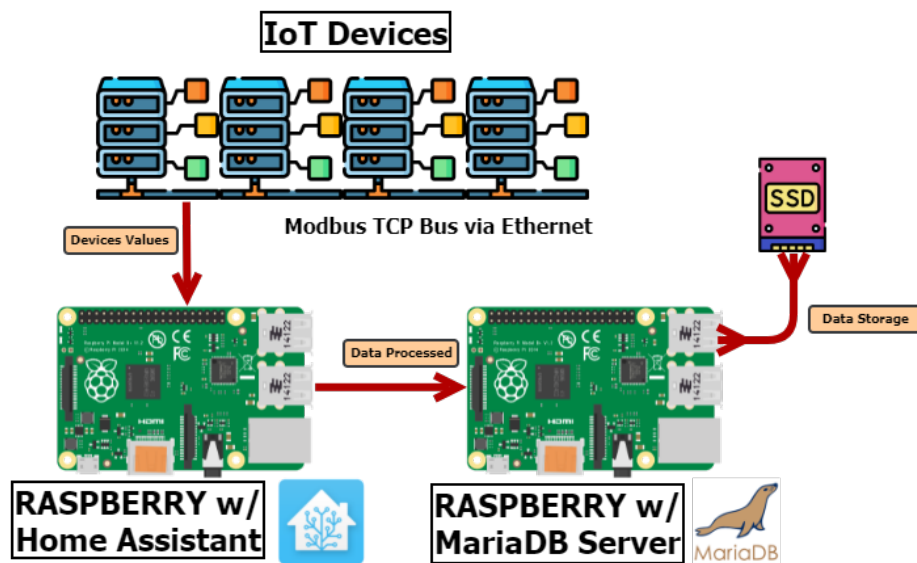


Fig. 3. Microgrid - Home Assistant - MariaDB flow connection.

6 Oscar Izquierdo-Monge, Gonzalo Martin-Jimenez, Paula Peña-Carro

This database can be installed both on the device/server on which Home Assistant is running as well as on another independent device/server, for this use case the implementation will be carried out through the second option, as it is advisable to build the system following the modularization-oriented micro-services architecture for better performance and security.

It is also advisable to use storage systems other than the microSD card that Raspberry uses by default, it is possible to connect an external hard drive through the USB inputs, even an external SSD (Solid-State Drive), this being the most recommended option and the one used in this use case. Different advantages are obtained with this system since the data read/write transmission speed is much higher compared to a microSD and the life expectancy and reliability is greater since microSD cards are not designed to perform operations constantly or to store large amounts of data.

#### 4 Setting up the connection between Home Assistant and MariaDB

To use MariaDB it is necessary to install the server of this software on a device, to connect it and be able to link it with Home Assistant it will be necessary to modify the configuration file.

```

recorder:
  db_url: mysql://cederuser:CEDER2021@127.0.0.1/cederdb?charset=utf8mb4
  purge_keep_days: 5
  exclude:
    event_types:
      - call_service
      - service_registered
      - component_loaded
      - panels_updated
      - platform_discovered
  include:
    entities:
      - sensor.meteo_ceder_temperatura
      - sensor.meteo_ceder_velocidad_viento
      - sensor.meteo_ceder_direccion_viento
      - sensor.meteo_ceder_humedad
      - sensor.meteo_ceder_radiacion_solar
      - sensor.meteo_ceder_radiacion_solar_par
      - sensor.meteo_ceder_lluvia

```

Fig. 4. Recorder Integration in the Home Assistant configuration file.

This file declares the connection with the IP address of the device where the database is located, the port it uses, the name of the database where it will operate, along with the username and password with the necessary permissions to perform the operations. An example of this configuration is shown in figure 4

In this configuration file, with the “recorder” integration we can also declare the variables that we want to be stored, thanks to this it is possible to separate the monitored variables and the subset of them that are going to be saved.

## Data storage system in a microgrid with HomeAssistant and MariaDB 7

With this connection we indicate that the database is of type MySQL and that the database called “cederdb” located at IP address 10.10.103.80 will be accessed, accessing with the user “cederuser” and its password “cederpass”. Once the “recorder” integration is configured, other integrations such as “loogbook” or “hystorygraph” will be enabled, which will allow the Home Assistant web environment to view the changes in the variables and historical graphs of the different variables. An example of a monitored variable is shown in the graph in the figure 5.

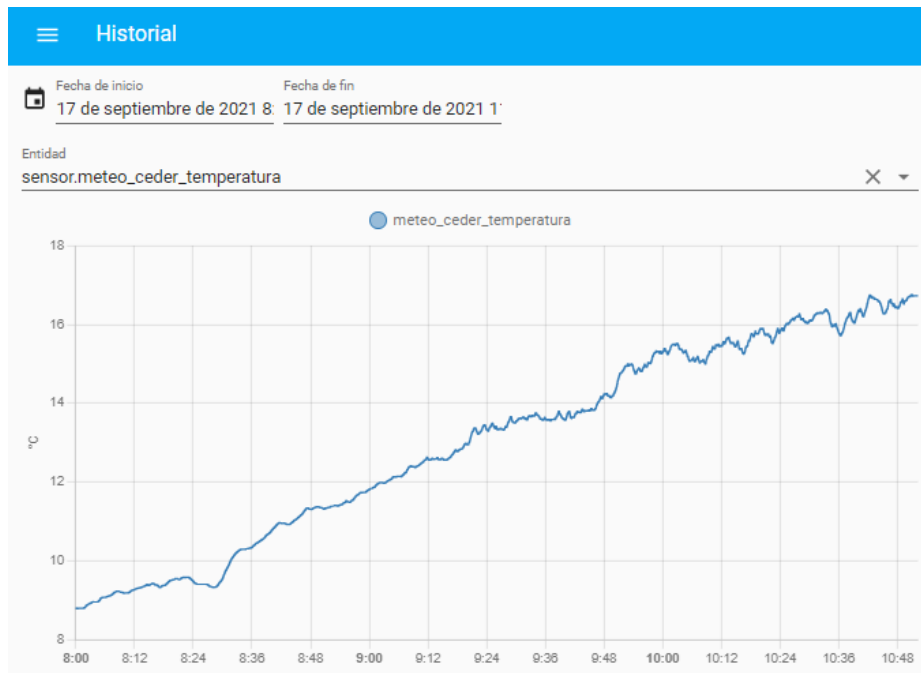


Fig. 5. History graph integration in Home Assistant.

## 5 Installation and configuration of the MariaDB server

In order to start using the database, it will be necessary to install the MariaDB server using the “apt” tool, in this case in its stable version v10.3.29-MariaDB-0 + deb10u1, in the repository, this package is called “mariadb-server”. You will also need a Python client that performs the operations such as “pymysql” or “mysqlclient”. When working as independent modules there can be no conflict between the version of Home Assistant and MariaDB, so there is no problem about which version each software uses for compatibility. Once the server is installed, the database and a user will be created, which will serve as access for the connection between the database and the Home Assistant application. To do

8 Oscar Izquierdo-Monge, Gonzalo Martin-Jimenez, Paula Peña-Carro

this using the command “sudo mysql -u root”, with which you access the mysql command line interpreter, three different commands will be executed:

A database schema is created, on which it is going to operate, with the name ‘homeassistant’ using the following command:

```
“$ CREATE DATABASE cederdb;”
```

A user is created with the name “cederuser” who can access from any device on the network and whose password is ”CEDER2021”. With this user you can access and operate Home Assistant with the database. To carry out this operation it is necessary to enter the following command:

```
“$ CREATE USER ‘cederuser’@‘*’ IDENTIFIED BY ‘cederpass’;”
```

Permissions are given to the “cederuser” user from any device on the network to perform any type of operation on any of the available schemes and tables by means of the following command:

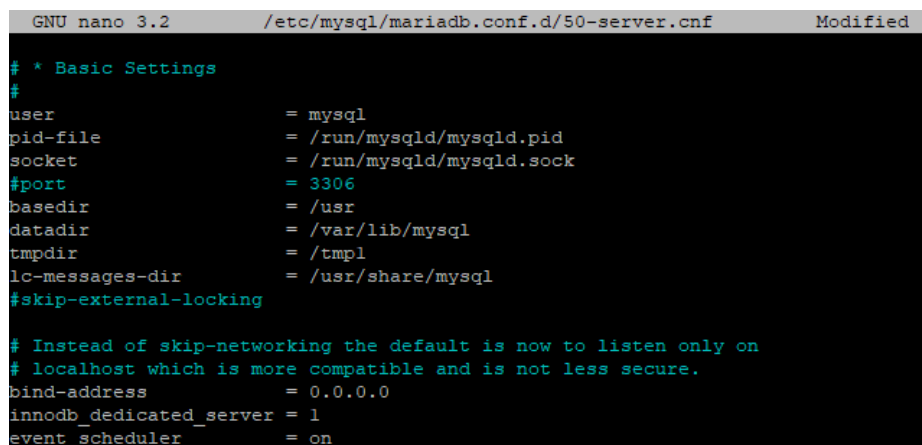
```
“$ GRANT ALL PRIVILEGES ON *.* TO ‘cederuser’@‘*’;”
```

And the privileges of the users will be updated by the command:

```
“$ FLUSH PRIVILEGES;”
```

The next step will be to configure the MariaDB server by modifying the configuration file, for this the ‘nano’ tool will be used, which is a text editor, indicating the path of the configuration file itself:

```
“/etc/mysql/mariadb.conf.d/50-server.cnf”
```



```
GNU nano 3.2 /etc/mysql/mariadb.conf.d/50-server.cnf Modified
# * Basic Settings
#
user = mysql
pid-file = /run/mysqld/mysqld.pid
socket = /run/mysqld/mysqld.sock
#port = 3306
basedir = /usr
datadir = /var/lib/mysql
tmpdir = /tmp
lc-messages-dir = /usr/share/mysql
#skip-external-locking

# Instead of skip-networking the default is now to listen only on
# localhost which is more compatible and is not less secure.
bind-address = 0.0.0.0
innodb_dedicated_server = 1
event_scheduler = on
```

Fig. 6. MariaDB configuration file.

Inside the configuration file, a variable will be modified and two new ones will be added: In order for the server to be accessible from any device on the network, it will be necessary to modify the variable “bind-address”, which by default its value is 127.0.0.1 (localhost), it will be changed to the value 0.0.0.0 so that the server is accessible for all devices on the network. It is also possible to add a list of IP addresses so that only certain devices can operate with the

database, indicating the desired list of IP addresses. There is a default example of this configuration on the config file of figure 6.

By means of the variable “innodbdedicatedserver” the server is indicated that the device that is running the server, in this case a raspberry, is only dedicated to running this database service, which will automatically assign some memory values, buffer and cache that allow to take advantage of the maximum efficiency of the device for the MariaDB server.

Regarding the execution of events on the MariaDB server, it is disabled by default, that is, we can only execute events through the command line, but not schedule them for a certain date and that they are executed at that moment, to enable this function it will be necessary create the variable “event\_scheduler” with a default value of “on”.

## 6 Structure of the default data storage in Home Assistant

By default, Home Assistant stores the data in the database to which it is automatically connected, this data has a certain structure optimized for recording and graphic representation in Home Assistant, but it is quite ineffective for a later analysis carried out with third-party software.

```
MariaDB [home_assistant]> describe states;
+-----+-----+-----+-----+-----+-----+
| Field          | Type          | Null | Key | Default | Extra          |
+-----+-----+-----+-----+-----+-----+
| state_id       | int(11)       | NO   | PRI | NULL    | auto_increment |
| domain        | varchar(64)   | YES  |     | NULL    |                |
| entity_id     | varchar(255)  | YES  | MUL | NULL    |                |
| state         | varchar(255)  | YES  |     | NULL    |                |
| attributes    | text         | YES  |     | NULL    |                |
| event_id      | int(11)       | YES  | MUL | NULL    |                |
| last_changed  | datetime     | YES  |     | NULL    |                |
| last_updated  | datetime     | YES  | MUL | NULL    |                |
| created       | datetime     | YES  |     | NULL    |                |
| context_id    | varchar(36)   | YES  |     | NULL    |                |
| context_user_id | varchar(36)  | YES  |     | NULL    |                |
| old_state_id  | int(11)       | YES  |     | NULL    |                |
+-----+-----+-----+-----+-----+-----+
12 rows in set (0.00 sec)
```

Fig. 7. Default data structure in Home Assistant

The structure of the stored data, described on figure 7 is quite ineffective for a later analysis of them, so we will proceed to transform this structure into a more adequate one. The structure provided is as follows:

An example of a tuple stored in this table is as follows:

10 Oscar Izquierdo-Monge, Gonzalo Martin-Jimenez, Paula Peña-Carro

```
id: 71530000
last_changed: 2021-08-14 02:12:34
last_updated: 2021-08-14 02:12:34
created: 2021-08-14 02:12:40
event_id: 71527383
old_state_id: 71527387
domain: sensor
entity_id: sensor.pqube7pepaiiiturbina500
state: 294
unitofmeasurement: W
friendlyname: PQUBE7PEPAIIITURBINA500
```

These tuples store three important values that will be used in the new structure, which are the name of the monitored variable (‘state\_id ’, in this case “sensor.pqube7pepaiiiturbina500”), the value of that variable (“state” , in this case 294 Watts/hour of active power) and the instant of time in which the variable has changed its value (“last\_updated”, in this case 2021-08-14 02:12:34); the other values are totally unnecessary for the treatment and analysis to be carried out, so they will be ignored in the new table structure created from it.

## 7 Data structure transformation

In the new structure, a new row will not be generated with each change in the value of a variable, but rather each row will correspond to one second in the given time, that is, each day we will have 86,400 rows, which correspond to the seconds that a day has . In each row the value of all the variables at that instant of time will be saved. The instants of time in which there has been no change in value will be filled in with the previous value of the specific variable.

In this new structure, only the values of the devices are stored every second in time, resulting in tuples with an identifier number, date and the values of all the devices at that instant of time.

From this table, a new one will be generated with the values in 15-minute averages, which will serve for a subsequent analysis of the data. These data in averages of 15 minutes will be saved forever in the database and the data will be eliminated from the table in seconds for better performance and efficiency in database storage.

The insertion of data in the new tables is carried out through events automatically, every day after 00:00 the necessary insertions and calculations will be made to introduce the data values of the previous day into the tables.

To operate with large amounts of data as is this case, it is necessary to use different mechanisms, so that the database engine uses all the hardware of the equipment, the equipment will be limited to the operation of the database service as It is indicated in the installation process and to handle the numerous queries made, “HASH” -type indexes specialized in equality queries will be used. With

Data storage system in a microgrid with HomeAssistant and MariaDB 11

all this, the database is capable of processing 2.5 million daily operations in 30 minutes.

## 8 Different methods of data analysis

Once the data is monitored and stored, it is time to perform an analysis on that data, for this, in this case the data will be exported through automated SQL queries daily in an Excel sheet to obtain a unified view of them.

These excel sheets can be modified using MACROS to obtain a transformation of these daily data into graphs and tables that offer a quick overview of the values obtained.

It is also possible to use other data analysis methods using business intelligence technology and the software associated with this technology, such as PowerBI, Tableau, Domo, Grafana, etc. With this software we will be able to connect with the database created and collect the data through queries to create graphs in a simple way.

## 9 Conclusions

Thanks to the inclusion of the database in the monitoring system, it is possible to use additional integrations offered by Home Assistant such as a record and time series graphs, this allows obtaining a quick visualization of the values of a variable without leaving the web environment by Home Assistant. Apart from this advantage, the data is automatically saved in a database in which it is possible to access a history of data since it has been stored. In the field of microgrids it is quite important to have historical data available to be able to make a concrete analysis of them in posterity.

The Home Assistant tool allows you to easily store the data, although it is designed to support a couple of weeks of data by default, it is possible to transform this data to save it in a database independent of the system that allows you to save the data historically without limits, Even so, Home Assistant offers different integrations that save the data in periods of time but do not allow to choose the way of grouping that data.

In recent years a good type of database has been used in the field of IoT technology, which are time series databases, you can find different managers such as InfluxDB, Prometheus, Timescale, DBGraphite, etc. This type of database is ideal for storing data in the field of microgrids since their main values to save are the value of a variable and the instant of time in which this variable has changed its value, in addition to a large number of advanced functions to perform statistical calculations, that is why the center will migrate data to this new time series DBMS to implement it in the already developed system and obtain a data reading/writing time greater and less use of storage space.

12 Oscar Izquierdo-Monge, Gonzalo Martin-Jimenez, Paula Peña-Carro

## References

1. Miraz, M.H., Ali, M., Excell, P.S., Picking, R.: A review on internet of things (iot), internet of everything (ioe) and internet of nano things (iont). In: 2015 Internet Technologies and Applications (ITA), pp. 219–224 (2015). DOI 10.1109/ITechA.2015.7317398
2. Weber, R.H., Weber, R.: Introduction, pp. 1–22. Springer Berlin Heidelberg, Berlin, Heidelberg (2010). DOI 10.1007/978-3-642-11710-7\_1
3. Hossein Motlagh, N., Mohammadrezaei, M., Hunt, J., Zakeri, B.: Internet of things (iot) and the energy sector. *Energies* **13**(2) (2020). DOI 10.3390/en13020494. URL <https://www.mdpi.com/1996-1073/13/2/494>
4. Liu, X., Ansari, N.: Toward green iot: Energy solutions and key challenges. *IEEE Communications Magazine* **57**(3), 104–110 (2019). DOI 10.1109/MCOM.2019.1800175
5. Bedi, G., Venayagamoorthy, G.K., Singh, R., Brooks, R.R., Wang, K.C.: Review of internet of things (iot) in electric power and energy systems. *IEEE Internet of Things Journal* **5**(2), 847–870 (2018). DOI 10.1109/JIOT.2018.2802704
6. Zubieta, L.E.: Power management and optimization concept for dc microgrids. In: 2015 IEEE First International Conference on DC Microgrids (ICDCM), pp. 81–85 (2015). DOI 10.1109/ICDCM.2015.7152014
7. Islam, M., Lee, H.H.: Microgrid communication network with combined technology. In: 2016 5th International Conference on Informatics, Electronics and Vision (ICIEV), pp. 423–427 (2016). DOI 10.1109/ICIEV.2016.7760039
8. Hatzigargyriou, N.: The microgrids concept. In: *Microgrids: Architectures and Control*, pp. 1–24 (2014). DOI 10.1002/9781118720677.ch01
9. Asiminidis, C., Georgiadis, I., Syndoukas, D., Kokkonis, G., Kontogiannis, S.: Performance evaluation on encrypted - non encrypted database fields containing iot data. In: *Proceedings of the 23rd International Database Applications and Engineering Symposium, IDEAS '19*. Association for Computing Machinery, New York, NY, USA (2019). DOI 10.1145/3331076.3331097. URL <https://doi.org/10.1145/3331076.3331097>
10. Rautmare, S., Bhalerao, D.M.: Mysql and nosql database comparison for iot application. In: 2016 IEEE International Conference on Advances in Computer Applications (ICACA), pp. 235–238 (2016). DOI 10.1109/ICACA.2016.7887957
11. Reetishwaree, S., Hurbungs, V.: Evaluating the performance of sql and nosql databases in an iot environment. In: 2020 3rd International Conference on Emerging Trends in Electrical, Electronic and Communications Engineering (ELECOM), pp. 229–234 (2020). DOI 10.1109/ELECOM49001.2020.9297028
12. Ming, D., Tian, X., Lei, W.: Research of real-time database system for microgrid. In: *The 2nd International Symposium on Power Electronics for Distributed Generation Systems*, pp. 708–712 (2010). DOI 10.1109/PEDG.2010.5545839
13. Mariadb foundation (2019). URL <https://mariadb.org/>
14. Izquierdo-Monge, O., Peña-Carro, P., Villafafila-Robles, R., Duque-Perez, O., Zorita-Lamadrid, A., Hernandez-Callejo, L.: Conversion of a network section with loads, storage systems and renewable generation sources into a smart microgrid. *Applied Sciences* **11**(11) (2021). DOI 10.3390/app11115012. URL <https://www.mdpi.com/2076-3417/11/11/5012>
15. Pi, R.: Raspberry pi 4 model b specifications. URL <https://www.raspberrypi.org/products/raspberry-pi-4-model-b/specifications/>
16. Home assistant. URL <https://www.home-assistant.io/>

# Wide-range time-domain simulation environment for stand-alone microgrids

Mario Araya-Carrillo<sup>1</sup>[0000-0001-9626-186X] and  
Carlos Meza<sup>1,2</sup>[0000-0002-7374-505X]

<sup>1</sup> Costa Rica Institute of Technology,  
30101 Cartago, Costa Rica

<sup>2</sup> Anhalt University of Applied Sciences  
06366 Köthen, Germany

**Abstract.** Microgrids represent a growing paradigm shift from centralized energy generation to a distributed model. However, given the relative novelty compared to traditional grids, there are still many unknown factors regarding the optimal design of this kind of system. In this paper, a mathematical model to describe microgrids is presented and a stand-alone microgrid simulation program for a wide range of time domains was proposed as a tool to facilitate the design process and study of these microgrids. The program was validated employing simulation of a stand-alone microgrid with photovoltaic generation and electrochemical energy storage. The program limitations are discussed, and further improvements are proposed to increase execution time performance.

**Keywords:** microgrid · photovoltaics · stand-alone

## 1 Introduction

Microgrids are systems that have attracted interest in recent years due to their potential advantages compared to centralized power generation, distribution, and consumption systems. Among the benefits of microgrids are their flexibility to operate as direct current (DC), alternating current (AC), or hybrid systems (AC and DC), thus facilitating the coupling of all types of energy sources with emphasis on clean and renewable sources [14], [19]. They also present lower energy losses during transmission since they follow an *in situ* generation model or are located at short distances from loads and can reduce the number of conversion stages along distribution lines [7], [10].

Microgrids can operate connected to the main power grid or in isolation. The latter is a viable option to achieve the electrification of rural areas due to their capacity for self-sufficiency. Microgrids represent an alternative in those places where the power grid does not meet the appropriate levels of reliability, stability, and quality of energy required [15]. Given these characteristics, isolated microgrids are an area of study that could have a high impact at a global level on the quality of life of people in regions far from metropolitan centers.

2 M. Araya-Castillo and C. Meza

Due to the hegemony of centralized AC systems, more research is still required in the area of isolated microgrids, especially those focused on DC, regarding their modeling and standardization [16,17]. Research topics of interest in microgrids are what is the ideal microgrid architecture for any specific application, what are the optimal voltage levels for power distribution buses, what type of control strategy (centralized or distributed, short or long term prediction) facilitates a more efficient use and higher availability of energy as assessed in [3,13], among others.

A cost-effective alternative to analyze and optimize microgrid design and operation is through numerical simulations of microgrid models. Research works such as [9], [8] and, [2] use simulations to optimize the design process of stand-alone microgrids. Those works provide important insight into the operation of microgrids over their steady-state operation. Nevertheless, they do not provide information about the transient response of the different elements connected to the microgrid. Information about transients is useful because there might be overshoots that may damage equipment or affect the operation of the whole system.

Given these factors, the design of a simulation program for electrical microgrids, in a wide range of time domains, is presented to evaluate and eventually optimize different architectures, loading conditions, energy balance, and control strategies. The novelty of the proposed work is that the obtained code for the microgrid mathematical model captures the system's behavior in a wide range of time domains. In other words, short-time transient events, as well as longer dynamic evolution are visible. In this way, it is possible to optimize the microgrid design and operation process before implementing it. As a first approach, the program is bounded within the context of isolated DC microgrids. A generalized mathematical model for microgrids is proposed and a validation process of the program is performed employing a comparison with a prevalidated circuit simulation software. The aim is to create a tool to speed up the microgrid simulation, analysis, and design process. Therefore, the execution time of the program was defined as a variable of interest, and the limitations of the program, as well as the possible solutions to improve its performance such as the hardware acceleration proposed in [5] are discussed. In this regard, the results obtained in this paper will serve to develop hardware-specific systems (digital twins) that allow to significantly reduce the simulation time of microgrids.

## 2 Microgrid mathematical model

This paper deals with the development of a wide-range time-domain simulation environment for a microgrid with a bus topology. This network configuration is the most widely used because it allows simple integration of the different components that make up a microgrid, e.g., power generators, storage, load. The elements of the microgrid are interconnected with each other through buses that can be direct current or alternating current as shown in the Figure 1, where, for simplicity, the power processing units, which are located between the sources

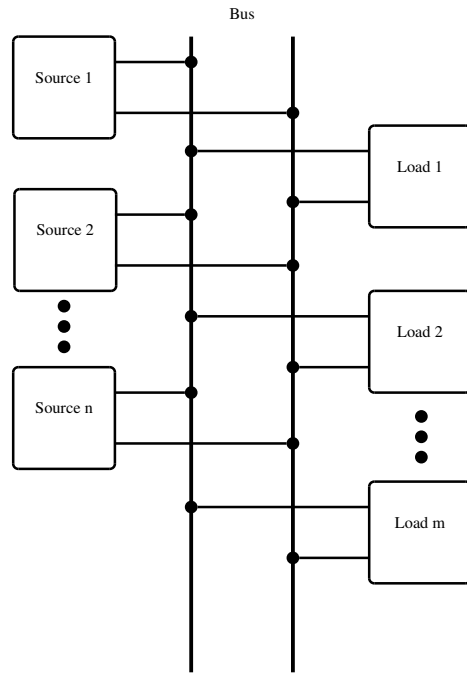


**Fig. 1.** Microgrid architecture

and the bus and between the loads and the bus, are omitted. It is also possible to have configurations of more than one bus such as the one shown in Figure 2.

From a mathematical modeling point of view, the incorporation of the buses can be represented by the following set of equations

$$v_{b_q} = v_{1_{b_q}} = v_{2_{b_q}} = \dots \tag{1}$$

$$\sum i_{j_{b_q}} = 0 \tag{2}$$

Where  $v_{b_q}$  represents the voltage on the  $q$ -th bus and  $v_{1_{b_j}}, v_{1_{b_j}}, \dots$ , are the voltages of the devices connected to that bus. Likewise,  $i_{j_{b_q}}$  represents the current contributed by the  $j$ -th device connected to the  $q$ -th bus.

In addition to the buses, the model considers the following microgrid components:

- power generators,
- energy storage systems (e.g. electrochemical batteries),
- power converters,
- electrical loads,
- control subsystems.

4 M. Araya-Castillo and C. Meza

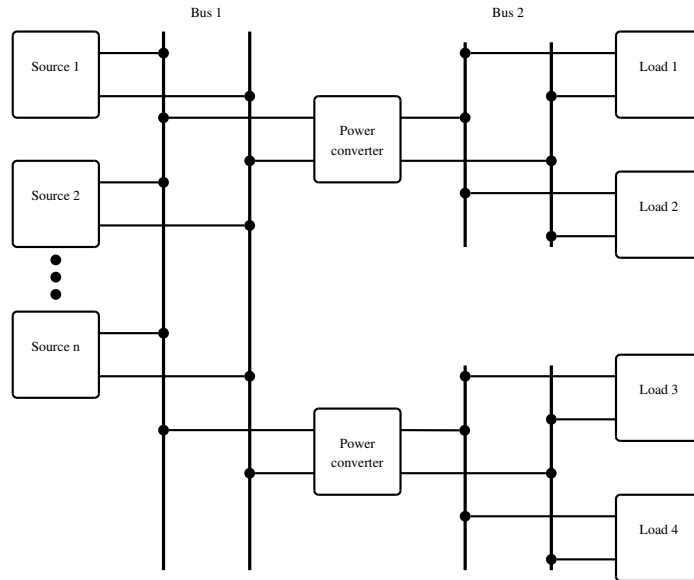


**Fig. 2.** Multi-bus microgrid architecture

The modeling was carried out by means of algebraic differential equations described as follows

$$\frac{dv_i}{dt} = f_i(v_1, v_2, \dots, v_n, i_1, i_2, \dots, i_m, u_k, \rho_i) \quad (3)$$

$$\frac{di_j}{dt} = f_j(v_1, v_2, \dots, v_n, i_1, i_2, \dots, i_m, u_k, \rho_j) \quad (4)$$

Where  $v_i$  and  $i_j$  represent the system voltages and currents associated with those elements that can store energy, i.e., capacitors and inductors, respectively. Thus, the open-loop microgrid can be represented with  $n + m$  first-order differential equations where  $n$  is the number of capacitive elements and  $m$  is the number of inductive elements. The rates of change of these voltages and currents are determined by a set of functions,  $f_i(\cdot)$  and  $f_j(\cdot)$ , which are related to the network topology and the characteristics of the sources and loads connected to the network. These functions depend on the electrical variables of the system and on a set of parameters  $\rho_i = \{\rho_{i1}, \rho_{i2}, \dots\}$  and  $\rho_j = \{\rho_{j1}, \rho_{j2}, \dots\}$  specific to the elements that make up the microgrid. It is important to clarify that these functions are discontinuous and for systems using photovoltaic energy they are also nonlinear. For example, the function that determines the current of a photovoltaic generator is shown in the equation 5, where  $v_{pv}$  is the voltage at the terminals of the generator, and  $A$ ,  $\Psi$  and  $\alpha$  are parameters.

$$f_{pv} = A - \Psi e^{\alpha v_{pv}} \quad (5)$$

The subsystems that make up the microgrid must be managed and controlled in such a way as to ensure energy balance and correct operation. Therefore, in addition to (3) and (4) there is also a set of equations that describe the dynamic performance of the control subsystems, i.e.

$$u_k = g_k \left( \frac{d^{n_u} u_k}{dt}, \frac{d^{n_u-1} u_k}{dt}, \dots, \frac{du_k}{dt}, \frac{d^{n_v} v_i}{dt}, \frac{d^{n_v-1} v_i}{dt}, \dots, \frac{dv_i}{dt}, v_i, \frac{d^{n_j} i_j}{dt}, \frac{d^{n_j-1} i_j}{dt}, \dots, \frac{di_j}{dt}, i_j, \rho_k \right) \quad (6)$$

Where  $u_k$  represents the  $k$ -th control signal for one of the elements of the microgrid that is generated by the control subsystem  $k$  and where  $\rho_k \{ \rho_{k1}, \rho_{k2}, \dots \}$  are its parameters. Note that, unlike the expressions in (3) and (4), the function  $g_k(\cdot)$  can depend on the derivatives of the input voltages, currents, and signals, which means that the expression (6) can be described as a system of  $n_u$  first-order differential equations.

The sources, loads and elements interconnecting the buses are managed by a power processing unit which, given their high efficiency, consist of power mosfet circuits that are switched in such a way that the desired conversion process is achieved. The control signals  $u_k$  control these power units and represent duty cycles that are converted to discontinuous signals by means of a pulse width modulator. The discontinuous signals, which have a switching frequency of between 100 kHz up to 1 MHz, are responsible for turning the transistors on and off. This activation process generates a ripple in the currents and voltages of the system that can provide useful information for its management, as indicated in [12]. If these equations are solved in real-time, then it is possible to visualize and analyze ripple signals at all points of the microgrid.

Nevertheless, the development of digital models of the electrical microgrids described by means of the equations (1), (2), (3), (4) and (6) presents important challenges, which are detailed below:

- The mathematical model of the microgrid can be described by a set of differential equations of order  $n + m + n_u$ , where even for a system with few generators and loads one can have a high order system. For example, a microgrid with two power sources and two independent loads can be described, in its simplest configuration, by a 6th order differential equation.
- The integration step for the numerical algorithm that must solve the system of algebraic differential equations must be at least 10 times smaller than the period of the carrier signal. That is, it must be equal to or less than 1 microsecond.
- The emulation time of the digital microgrid will depend on the characteristics of the connected generators and loads. For example, for a microgrid based on photovoltaic generators with resistive loads, the emulation time should be at least 10 minutes, in order to see all the transient processes of the load balance. It is also desirable to perform a 24 to 48 hour analysis to evaluate the load balance on predetermined days.
- Microgrids based on photovoltaic generators can be described by means of a set of first order difference equations and a set of algebraic equations. The

6 M. Araya-Castillo and C. Meza

number of differential equations depends on the number of elements, i.e., generators and loads, present in the grid. The numerical solution of this set of differential equations must focus on the parallelization of the processes.

- The storage and display of storage system data can represent a bottleneck for the emulation system for the following reasons:
  - There is a difference of several orders of magnitude between the period of the signals that could be displayed and the emulation time. For example, the ripple of the system currents and voltages is between 10 microseconds and 0.01 microseconds, while the emulation time could be from 10 minutes to 48 hours.
  - There are a large number of possible measurement points in the microgrid. For example, each generator and power processing unit set has at least 2 voltage and 2 current values that could be useful to visualize. The same amount can be considered for the loads.

### 3 Simulation approach

As stated previously, we are looking for a microgrid simulation program that can resolve the values of the system's electrical variables over a wide range of time domains; from the small microseconds and milliseconds scale to capture the ripple in currents and voltages and system transients, and on the other hand, a larger scale at the minutes, hours and days level to be able to observe characteristics of the system energy balance, the state of charge of storage elements and the response to different input vectors of the photovoltaic generation system and loads, i.e., to solve equations (1), (2), (3), (4) and (6).

The microgrid architecture proposed in [11] was taken as a reference as a basis for evaluating the performance of the simulation program as it was developed for scalable stand-alone microgrids for rural electrification with the use of photovoltaic generators. The architecture, shown in Figure 3, consists of  $n$  number of PV arrays as a power source, with a respective boost converter each. All boost converters feed a single high voltage distribution bus  $V_H$  with voltages between 360 V and 400 V. Connected to this bus are a  $m$  number of load branches each feeding a buck converter, called distribution nodes, with an intermediate voltage  $V_M$  between 45 V and 50 V, and these, in turn, feed a  $l$  number of buck converters, where each converter is a power management unit (PMU) connected to the load and storage system in the form of 12 V electrochemical batteries through a low voltage bus  $V_L$ .

Analyzing the most simple case of the chosen architecture, i.e., a single power source and a single loading branch as shown in Figure 4, it is relatively trivial to obtain the dynamic equations that describe the system. For this case, we obtain a system with the six first-order differential equations (7) to (13); without accounting for the equations of the switching control algorithms which may be of higher order. However, this is the smallest possible case, in reality, one can have multiple load branches and each of these can in turn have several PMUs with their respective loads. Thus, the number of elements that make up the

Wide-range time-domain simulation environment for stand-alone microgrids 7

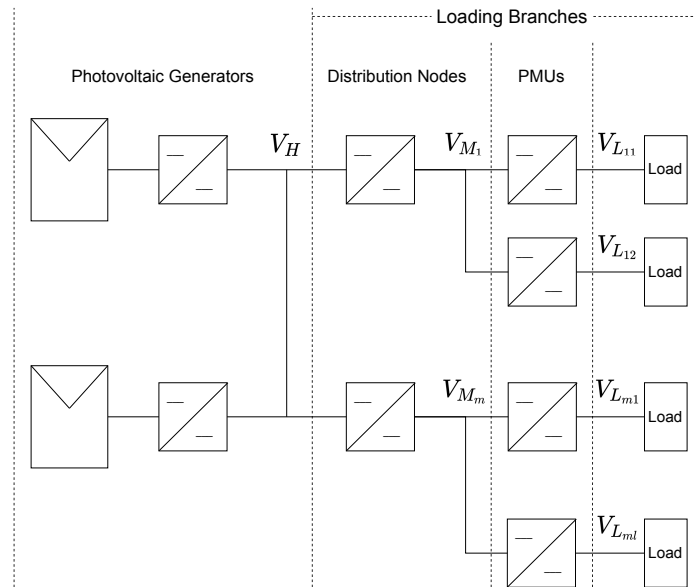


Fig. 3. Multi-bus microgrid architecture based on [11].

microgrid can grow by one or more orders of magnitude, along with the number of equations of the system. The task of obtaining all the dynamic equations could quickly become impractical.

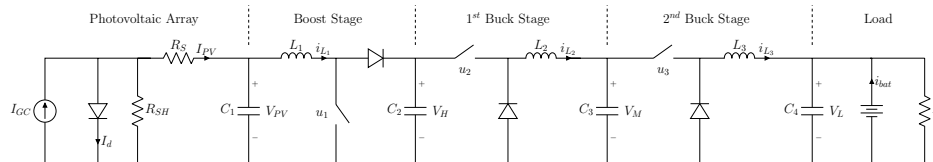


Fig. 4. Microgrid equivalent circuit with one photovoltaic source and one loading branch. Based on [11].

$$\frac{dV_{PV}}{dt} = \frac{i_{PV} - i_{L1}}{C_1} \tag{7}$$

$$\frac{di_{L1}}{dt} = \frac{V_{PV} - V_H(1 - u_1)}{L_1} \tag{8}$$

$$\frac{dV_H}{dt} = \frac{(1 - u_1)i_{L1} - u_2i_{L2}}{C_2} \tag{9}$$

8 M. Araya-Castillo and C. Meza

$$\frac{di_{L_2}}{dt} = \frac{u_2 V_H + V_M}{L_2} \quad (10)$$

$$\frac{dV_M}{dt} = \frac{i_{L_2} - u_3 i_{L_3}}{C_3} \quad (11)$$

$$\frac{di_{L_3}}{dt} = \frac{u_3 V_M - V_L}{L_3} \quad (12)$$

$$\frac{dV_L}{dt} = \frac{i_{L_3} + i_{bat} - i_R}{C_4} \quad (13)$$

In order to reduce the complexity of larger systems, it was deemed convenient to decompose and describe the microgrid through a series of blocks that represent the different elements that compose it (energy sources, power converters, loads, and energy storage). Code-wise, each block is represented as an object or a class composed of its electrical parameters and the dynamic equations that describe its behavior. In such a way that each block has a single dynamic equation and is interconnected with adjacent blocks according to the microgrid architecture. For each calculation iteration, the equations of all the blocks are solved separately and then the resulting currents and voltages are propagated to the neighboring blocks.

Therefore, the dynamic equations of the boost and buck power converters can be modeled with equations (14) and (15) respectively, and the voltage buses with equation (16) in accordance with the voltage equation of a capacitor. For the photovoltaic generators, the equivalent circuit equations of the 1D2R model [4] were used.

$$\frac{di_L}{dt} = \frac{V_{in} - (1 - u)V_{out}}{L} \quad (14)$$

$$\frac{di_L}{dt} = \frac{uV_{in} - V_{out}}{L} \quad (15)$$

$$\frac{dV_C}{dt} = \frac{i_{in} - i_{out}}{C} \quad (16)$$

### 3.1 Program sequence

The simulation program developed was implemented using Python language and structured in a linear way as shown in Figure 5. So that first the architecture of the microgrid to be simulated is defined, where all the objects/classes representing the different elements of generation, power converters, storage, and loads are created. Next, the simulation parameters corresponding to time variables and a constant integration step are defined. Then the initial state of the microgrid is established, in other words, the voltages and currents in the system, as well as the state of charge of the batteries.

## Wide-range time-domain simulation environment for stand-alone microgrids

9

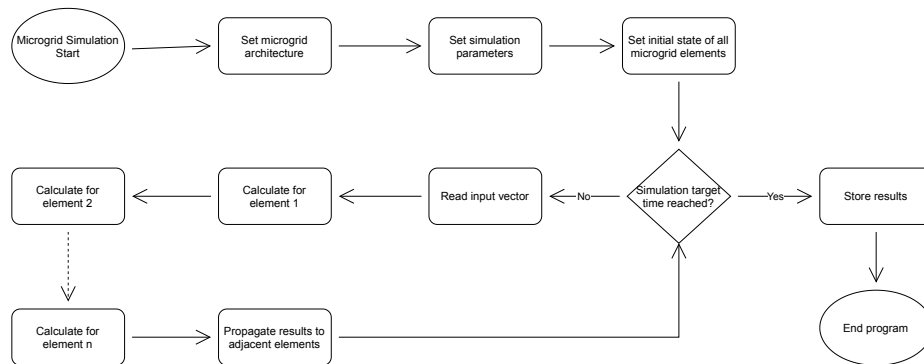


**Fig. 5.** Stand-alone DC microgrid simulation program flowchart.

The next stage starts the simulation process in a loop that stops when the final simulation time is reached. During the simulation, the program reads an input vector that includes the solar irradiance intensity and magnitude of the loads. It then proceeds to sequentially solve the dynamic equations of all the elements of the microgrid. For the solution of the equations, the explicit Euler integration method is used [6], which was chosen for its ease of calculation and also because it allows solving for each element of the microgrid individually for each iteration. Once all the elements of the microgrid have been solved for the current iteration, the results of each element are propagated throughout the microgrid and the next iteration is initiated.

Lastly, when the final simulation time is reached, the results are stored for further analysis.

## 4 Simulation results and discussion

In order to assess the program's capability, three different tests were conducted. First, a validation test to confirm that the program returns correct results. Then a demonstration of the ability to simulate signals in a wide range of time domains and finally a test to measure the time it takes for the program to simulate one second for microgrid configurations with differing number of elements.

### 4.1 Program validation

To validate the performance of the program, a comparison of the results obtained against the software PowerSim (PSIM) was carried out; this software was taken as a reference since it is designed for the simulation of power circuits and it is a prevalidated software for commercial use.

A simulation of the circuit previously shown in Figure 4 was performed for a time of 1 s and a with a step of  $0.1 \mu\text{s}$  to capture the transient period of microgrid start-up and subsequent stabilization.

10 M. Araya-Castillo and C. Meza

For the microgrid voltages, a maximum absolute error of 0.98 % was obtained for PSIM and 1.08 % for the Python-based program as shown in Table 1.

**Table 1.** Steady state voltage comparison for PSIM and Python simulations.

Parameter	Theoretical	PSIM	PSIM	Python	Python
	Steady State [V]	Result [V]	Error [%]	Result [V]	Error [%]
$V_{PV}$	179.71	181.48	-0.98	181.33	-0.91
$V_H$	359.42	362.94	-0.98	362.67	-0.90
$V_M$	44.93	45.36	-0.96	45.10	-0.38
$V_L$	11.23	11.29	-0.52	11.35	-1.08

In the case of the currents, a maximum absolute error of 0.78 % was obtained for PSIM and 1.12 % for the Python program as can be seen Table 2.

**Table 2.** Steady state current comparison for PSIM and Python simulations.

Parameter	Theoretical	PSIM	EPSIM	Python	Python
	Steady State [A]	Result [A]	Error [%]	Result [A]	Error [%]
$i_{L1}$	1.404	1.394	0.74	1.394	0.68
$i_{L2}$	5.616	5.574	-0.51	5.678	-1.12
$i_{L3}$	22.463	22.297	0.78	22.706	-1.08

For both cases, it is considered that the error of approximately 1 % achieved is acceptable since the solution method selected for its simplicity was not affected by the discontinuous equations caused by the high-frequency switching of the MOSFETs. Also, the error can be reduced by using a smaller integration step, although this would have an impact on the simulation's execution time.

Furthermore, by means of the voltage curves shown in Figure 6 it can be seen that the resulting behavior is similar for both programs. The oscillations during the transient in the curve generated by Python are larger in magnitude than those of PSIM. This is because the models simulated in Python are ideal and do not consider the internal resistance of the capacitors and inductors of the system. PSIM on the other hand, requires the configuration of minimum internal resistance, in the range of the milliohms to facilitate the convergence of the solver.

## 4.2 Time domains

To demonstrate the capability of the simulation program in different time domains, the aim was to study the behavior of the system on a small time scale, given by the switching frequency of the MOSFETs, and one of several orders of magnitude larger given by the state of charge of the battery in the circuit.

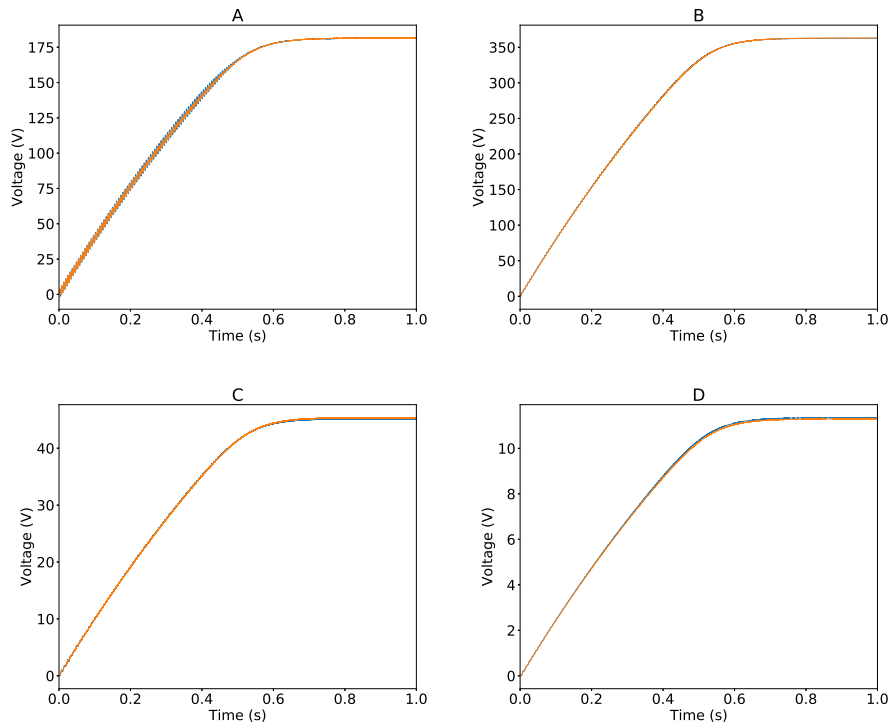


**Fig. 6.** Voltage curve comparison between Python (blue) and PSIM (orange) simulations. A)  $V_{PV}$  B)  $V_H$  C)  $V_M$  D)  $V_L$

The  $V_M$  bus ripple obtained was a sawtooth signal with an oscillation range of 0.04216 V in Python and 0.04208 V in PSIM, which corresponds to a difference of less than 0.2 %. In Figure 7 the results of both programs were normalized. It can be seen how both signals overlap in both magnitude and phase.

In order to demonstrate the change in the state of charge of the battery, the simulation time was extended to 10 minutes since a period of 1 s produces a negligible variation. The power consumed by the load was varied to see the effect on the charge/discharge rate of the battery. The simulation started with a load of 160 W, then increased to 630 W at  $t = 200$  s, and finally reduced to 80 W at  $t = 400$  s.

Figure 8 shows how the state of charge initially increases, indicating that the battery is charging. Then when the load increases at  $t = 200$  s, the PV generation is not sufficient to supply the required power, so the battery discharges to compensate for the missing power. Finally, the battery begins charging again at  $t = 400$  s.

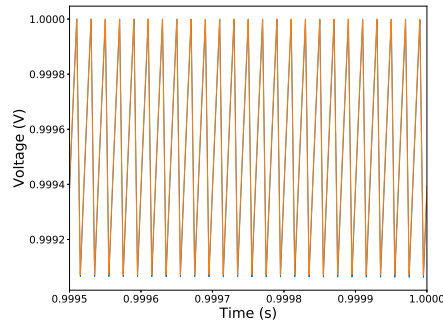


**Fig. 7.** Normalized voltage ripple of  $V_M$  bus at  $0.0995 \text{ s} \leq t \leq 1 \text{ s}$ . Python (orange) y PSIM (blue).

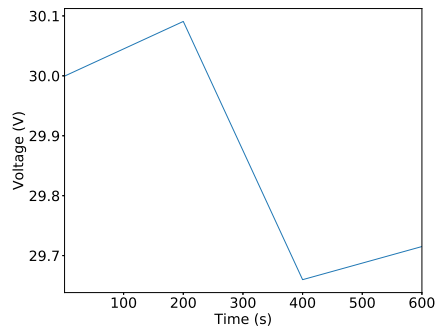


**Fig. 8.** State-of-charge (SOC) variation of the energy storage component. System load defined as 160 W at  $t = 0 \text{ s}$ , 630 W at  $t = 200 \text{ s}$ , and 80 W at  $t = 400 \text{ s}$ .

### 4.3 Simulation time

The performance of the developed program with respect to the execution time of the simulations was measured for three simulations with 1, 5, and 10 loading branches. In all three cases, a single PV array was set as the generator and a simulation time of 1 s was used as a benchmark. It was determined that for the selected microgrid architecture, simulating one second requires executing the program for a duration of 516 s for 1 loading branch. This time increases linearly with the number of elements in the microgrid as shown in Table 3, reaching up to 3788 s with 10 loading branches.

The execution time of the program, which is considered a vital factor presents a bottleneck, which is caused by three factors. Firstly, the program was written in Python, which is a high-level interpreter that is not optimized for applications that require high performance in a short time. To overcome this limitation, the

Wide-range time-domain simulation environment for stand-alone microgrids 13

**Table 3.** Execution time of microgrid simulations with varying number of elements.

Number of Load Branches	Number of Elements	Execution Time [s]
1	7	516
5	22	2172
10	42	3788

program can be translated into a lower abstraction level language, such as C, which allows better use of computational resources.

The second factor that contributes to the long execution time of the program is its linearity. The equations of the system are solved one after the other, so a reduction in execution time can be achieved by parallelizing the calculation process. This can be done by adapting the program to make use of multiple processor cores/threads. Hardware acceleration can also be used through the implementation of the program on a stand-alone FPGA board or in combination with specialized emulation equipment as used in [1, 18].

The third factor is a small integration step that forces the program to perform millions of iterations for each simulated second. The step can be increased, however, its maximum value depends on the switching frequency of the MOS-FETs and the transients of the system, so it is not considered an ideal solution. In addition, a larger step size may result in convergence issues in the solution of the dynamic equations of the microgrid due to stiffness since these are discontinuous. For these reasons, it is considered appropriate to address the first two factors.

## 5 Conclusions

A model was proposed to describe different microgrid architectures employing a series of algebraic differential equations dependent on the voltages and currents of the microgrid elements, a set of parameters specific to each element, and a set of equations to describe the dynamic behavior of the control subsystems.

A simulation program for isolated microgrids in a wide range of time domains was developed. The results of the program were validated by comparison with the results of the PSIM software. An absolute error of approximately 1 % was obtained and the ability to simulate the behavior of the selected microgrid architecture in both a domain in the range of microseconds as the ripple in the voltage curves, as well as in a domain in the range of several minutes in the case of the state of charge of the energy storage system was showcased.

The performance of the program was evaluated with respect to its execution time in simulations of microgrids with different number of elements. Time was found to increase linearly with the number of elements that make up the microgrid. Optimization measures proposed for the program included the modification of the sequential simulation of the microgrid elements in favor of a

14 M. Araya-Castillo and C. Meza

parallel simulation strategy or the acceleration of the computation using a hardware implementation.

## References

1. Abrishambaf, O., Faria, P., Gomes, L., Spínola, J., Vale, Z., Corchado Rodríguez, J.: Implementation of a real-time microgrid simulation platform based on centralized and distributed management. *Energies* 10, 806 (06 2017)
2. Alam, M., Kumar, K., Srivastava, J., Dutta, V.: A study on dc microgrids voltages based on photovoltaic and fuel cell power generators. In: 2018 7th International Conference on Renewable Energy Research and Applications (ICRERA). pp. 643–648. IEEE (2018)
3. Alzahrani, A., Ferdowsi, M., Shamsi, P., Dagli, C.H.: Modeling and simulation of microgrid. *Procedia Computer Science* 114, 392 – 400 (2017), complex Adaptive Systems Conference with Theme: Engineering Cyber Physical Systems, CAS October 30 – November 1, 2017, Chicago, Illinois, USA
4. Araújo, N., Sousa, F., Costa, F.: Equivalent models for photovoltaic cell—a review. *Revista de Engenharia Térmica* 19(2), 77–98 (2020)
5. Brenes, E.M., Meza, C.: An application-specific instruction set processor for microgrid simulation. In: 2019 IEEE 39th Central America and Panama Convention (CONCAPAN XXXIX). pp. 1–6 (2019)
6. Chakraverty, S., Mahato, N., Karunakar, P., Rao, T.: *Advanced Numerical and Semi-Analytical Methods for Differential Equations*. Wiley (2019)
7. Elsayed, A.T., Mohamed, A.A., Mohammed, O.A.: Dc microgrids and distribution systems: An overview. *Electric Power Systems Research* 119, 407–417 (2 2015)
8. Hu, G., Li, S., Cai, C., Wu, Z., Li, L.: Study on modeling and simulation of photovoltaic energy storage microgrid. In: 2017 4th International Conference on Information Science and Control Engineering (ICISCE). pp. 692–695. IEEE (2017)
9. Khadepaun, N.C., Shah, N., et al.: Operation of solar pv with pem fuel cell for remote hybrid microgrid. In: 2020 IEEE International Conference on Electronics, Computing and Communication Technologies (CONECCT). pp. 1–6. IEEE (2020)
10. Lasseter, R.H.: Microgrids. In: 2002 IEEE Power Engineering Society Winter Meeting. Conference Proceedings. vol. 1, pp. 305–308. IEEE (2002)
11. Madduri, P.A., Poon, J., Rosa, J., Podolsky, M., Brewer, E., Sanders, S.: A scalable dc microgrid architecture for rural electrification in emerging regions. In: 2015 IEEE Applied Power Electronics Conference and Exposition (APEC). pp. 703–708 (2015)
12. Meza, C., Ortega, R.: On-line estimation of the temperature dependent parameters of photovoltaic generators. *IFAC Proceedings Volumes* 46(11), 653–658 (2013)
13. Olivares, D.E., Cañizares, C.A., Kazerani, M.: A centralized energy management system for isolated microgrids. *IEEE Transactions on Smart Grid* 5(4), 1864–1875 (2014)
14. Planas, E., Andreu, J., Gárate, J.I., de Alegría, I.M., Ibarra, E.: Ac and dc technology in microgrids: A review. *Renewable and Sustainable Energy Reviews* 43, 726–749 (3 2015)
15. Tank, I., Mali, S.: Renewable based dc microgrid with energy management system. In: 2015 IEEE International Conference on Signal Processing, Informatics, Communication and Energy Systems (SPICES). pp. 1–5 (2015)

Wide-range time-domain simulation environment for stand-alone microgrids 15

16. Unamuno, E., Barrena, J.A.: Hybrid ac/dc microgrids—part i: Review and classification of topologies. *Renewable and Sustainable Energy Reviews* 52, 1251–1259 (12 2015)
17. Unamuno, E., Barrena, J.A.: Hybrid ac/dc microgrids—part ii: Review and classification of control strategies. *Renewable and Sustainable Energy Reviews* 52, 1123–1134 (12 2015)
18. Zhang, B., Fu, S., Jin, Z., Hu, R.: A novel fpga-based real-time simulator for microgrids. *Energies* 10(8) (2017)
19. Zhang, Y., Gatsis, N., Giannakis, G.B.: Robust energy management for microgrids with high-penetration renewables. *IEEE transactions on sustainable energy* 4(4), 944–953 (2013)

# A machine learning approach for detecting traffic incidents from video cameras

Guillermo Gabrielli<sup>1</sup>, Ignacio Ferreira<sup>1</sup>, Pablo Dalchiele<sup>1</sup>,  
Andrei Tchernykh<sup>2,3</sup>[0000-0001-5029-5212], and  
Sergio Nesmachnow<sup>4</sup>[0000-0002-8146-4012]

<sup>1</sup> Universidad de la República, Montevideo, Uruguay  
{guillermo.gabrielli, ignacio.ferreira, pablo.dalchiele}@fing.edu.uy

<sup>2</sup> CICESE, México  
chernykh@cicese.mx

<sup>3</sup> Institute for System Programming of the Russian Academy of Sciences, Russia

<sup>4</sup> Universidad de la República, Montevideo, Uruguay  
sergion@fing.edu.uy

**Abstract.** In the area of vehicular traffic analysis, many cities have surveillance devices (cameras) installed in different junctions as well as along roads, to obtain information on how vehicles behave in a certain area. To help in the process of preventing accidents, this article proposes a computer vision pipeline for detecting different types of dangerous/risky driving behavior. The pipeline includes object detection, tracking, speed normalization, and the application of computational intelligence, among other relevant features for pattern detection and traffic behavior analysis. The developed models are applied on videos from traffic cameras from eight different sites in the metropolitan area of the city of Montevideo. Three different algorithms were developed for detecting dangerous incidents in traffic in real time. Accurate results are reported for the case studies addressed in the experimental validation, reaching precision values up to 0.82 and recall values up to 0.91.

**Keywords:** vehicular traffic, road safety, image processing, computer vision, artificial intelligence, machine learning, neural networks, intelligent transport systems

## 1 Introduction

Nowadays, most modern cities have traffic surveillance cameras installed in different locations, to monitor traffic and gather information on how vehicles and pedestrian behave in specific areas [13]. Road safety is an important concept for the development of smart cities, since it allows citizens to live in a safe environment, reducing traffic jams and relevant social costs related to road accidents and pollution [16, 17]. It also contributes to the safety of the most vulnerable road users. In turn, road safety is also a key concept for the design and implementation of sustainable transportation systems [9] and for the Transit Oriented Development paradigm [10].

2 G. Gabrielli, I. Ferreira, P. Dalchiale, A. Tchernykh and S. Nesmachnow

Traffic surveillance is of capital importance to properly manage and operate complex transportation systems with high traffic density. Automatic systems capable of providing assistance for traffic monitoring and analysis allow human operators to focus on relevant issues, instead of constantly observing many videos from different sources [12]. Automatic systems also allow to significantly reduce problems related to global attention degradation and errors due to boredom and/or fatigue [6]. Thus, automatic intelligent systems provide operators and regulators the capability of responding to diverse traffic issues and situations.

Vehicle counting and reckless driving detection are very important for Intelligent Transportation Systems [20, 22]. The application of image processing and computer vision for developing detection algorithms has led to better results than traditional traffic surveillance methods, usually based on sensors [21]. Several recent studies have highlighted the importance of the subject and proposed smart methods for detecting traffic accidents or damaged vehicles that can indicate the occurrence of traffic incidents [15]. The detection of traffic incidents by automatic smart methods can save lives and improve traffic safety.

This article proposes a system to automatically detect usual traffic-related situations in metropolitan areas, from videos taken by road surveillance cameras. A flexible methodology is proposed, able to operate without human supervision. Computational intelligence and machine learning techniques are applied for detecting traffic incidents. Based on traffic camera videos, the system is capable of detecting reckless driving behavior in real time, taking advantage of high performance computing and Graphic Processing Units (GPU).

The proposed automatic system is based on a modular design consisting of a pipeline that includes object detection algorithms, tracking methods, labeling, image processing, and computing relevant metrics of the detected vehicles, pedestrians, and traffic infrastructure. Convolutional neural networks (CNN) are applied for object detection and learning patterns associated with reckless driving and pedestrian behavior. The system is targeted to execute on commodity hardware, to allow scaling to a large number of cameras without heavy expenses on hardware. The system is able to process video in real-time.

The developed system is validated and evaluated on a real case study using a dataset gathered from recordings of eight traffic cameras from the metropolitan area of the city of Montevideo, Uruguay. Selected areas were monitored in the city, to properly validate the reckless driving patterns and situations implemented in the system. Urban data analysis [14] is applied for the analysis of relevant data sources for the validation of the proposed system. Results of the evaluation demonstrate the effectiveness of the proposed system, according to standard metrics for detection and learning. Precision values up to 0.82 and recall values up to 0.91 were computed for the different problem instances solved.

The main contributions of this article are: the developed system, useful for traffic monitoring in modern smart cities; the pipeline applying image processing and computational intelligence for the detection of reckless driving behavior; ancillary applications for traffic image processing and labeling; and the evaluation of the proposed system on a real case study using real traffic data.

The article is organized as follows. Next section introduces the problem of automatic detection of traffic incidents and a review of the main related work. The proposed system for automatic traffic incidents detection is described in Section 3. The evaluation of the developed system for relevant case studies in Montevideo, Uruguay is reported in Section 4. Finally, Section 5 presents the conclusions and the main lines for future work.

## 2 Automatic detection of traffic incidents

This section presents an overview of the problem of automatic detection of traffic incidents and a review of relevant related works on the subjects of object detection and tracking and their application to automatic traffic monitoring.

### 2.1 Problem description

The problem consists in identifying traffic incidents so that the analysis of them using machine learning and computational techniques can be incorporated in an Smart Transport System for a Smart City, as outlined by Ristvej et al. [16]. According to that study, a Smart City Transport System should include a safe layer that incorporates the use of technology, planning, construction, traffic rules and supervision that allow to diminish the amount of traffic accidents, resulting in an improvement in transportation safety as well as integrity of traffic infrastructure. Another layer of the Smart Transport System relevant to this work is the Smart Layer, which consist of features like urban mass transport system connected with smart parking systems and smart traffic light and road signs.

Automatic detection of traffic incidents is essential to improve the productivity of the users and operators of the Smart City Transport System because it lessens their workload, allowing them to focus on reviewing the incidents and reasoning about the causes of them. As explained in Chavat et al. [6], current detection systems are based on operational centers that manually analyse the traffic incidents thus the importance of the development of a system that addresses the issue in an automated fashion.

In order to approach the automatic detection of traffic incidents, it is crucial to have a reliable way to detect vehicles and other objects of interest. Background subtraction have been used in the past to detect vehicles at low complexity, however it is vulnerable to false detections from illumination changes, e.g. from shadows and vehicle highlights, as well as from movement of unrelated objects like trees, while offering poor results when the object color does not significantly differ from the background. Handling different perspectives, due to differences on camera height, angle with respect to the horizon and camera parameters like focal length, often would require running multiple models to cover different views of the object. In the last years there has been considerable interest in deep learning methods, which use large scale models with multiple layers to learn from the data how to solve a given task without human intervention. For dealing with

4 G. Gabrielli, I. Ferreira, P. Dalchiale, A. Tchernykh and S. Nesmachnow

images and video, particularly for object detection and classification, CNNs provide a useful approach. CNNs are translation invariant and while not inherently rotational and scale invariant, given sufficient scene variation during training, they are robust to changes in camera perspective and object size. Furthermore, inference speed for CNN-based detectors is largely independent of the number of classes to detect and particularly of the number of objects in the image, which is a desirable property to achieve consistent speed for real-time processing.

## 2.2 Related work

A number of articles have presented automated systems applying image processing and computational intelligence for traffic analysis and incidents detection. Related works are reviewed next.

Regarding vehicle detection and classification, Zhou et al. [24] studied the application of the You Only Look Once (YOLO) and Alexnet CNN architectures for classification and feature extraction. YOLO obtained similar precision than a multi-scale Deformable Parts Model in a public dataset, whereas Alexnet using Support Vector Machines (SVM) outperformed Principal Component Analysis. Dey et al. [7] implemented a CNN on a System-On-a-Programmable-Chip for the analysis and categorization of traffic. The prediction accuracy of the CNN was improved by including a combination of transfer learning with re-training. Arinaldi et al. [2] applied Mixture of Gaussian (MoG) and Faster Recurrent CNN (FR-CNN) for collecting traffic statistics. The evaluation on a public dataset from MIT and real Indonesian road videos showed that FR-CNN was the best method for detection and classification of vehicles, because MoG did not performed well the separation of overlapping vehicles. Chauhan et al. [5] applied CNN for real-time traffic analysis using a YOLO network, pre-trained on the MS-COCO dataset and annotations. A mean average precision of 65–75% was reported for real scenarios from Delhi, India. Results highly depended on the camera position and the type of vehicle. These results provide a reference baseline for the accuracy of YOLO models improved with annotated data. Khazukov et al [11] proposed a system to measure traffic parameters such as vehicle counts and average speed. Vehicles are detected using YOLOv3 object detector and tracked using the SORT tracker [3], cameras are calibrated to eliminate distortion. Inverse Haversine method is used to calculate traveled distance and speed from coordinates. 6000 images containing 430,000 vehicles were collected from several cameras in the cities of Chelyabinsk and Tyumen (Russia), 80% was used for training and 20% for validation. Object detection mAP was 85% while Mean counting error was 5.5%. For speed estimation maximum error was 1.5 km/h while mean error was 0.57 km/h. Source code is available for a partial implementation using a tiny version of the model.

Regarding incidents detection, Uy et al. [18] applied genetic algorithms for detecting vehicles obstructing pedestrian crossings and ANN for recognizing the license plate number of offenders. Accurate results were reported (91.6% on 47 test images), but the methods were not highly robust against different vehicle positions respect to the camera. Ravindran et al. [15] proposed a supervised

learning algorithm using SVM trained with histogram of gradients and grey level co-occurrence matrix on several parts of cars (wheels, headlights and hood), to detect damaged cars and infer the occurrence of an accident. This work reported results of 80% precision, 83.75% recall and 81.83% accuracy. Zheng et al. [23] applied a CNN for traffic accidents severity prediction. The model was able to properly represent relevant features and found deep correlations between accident data, improving over previous models in the evaluation performed. Agrawal et al. [1] proposed a system for automatic detection of traffic accidents. Key frame detection is used to detect important frames, then vehicles are detected and the distance between vehicles is used to detect possible collision situations. Key frames are processed through a ResNet50 model to obtain features vectors. Then, K-means clustering is applied on the feature vectors to obtain five clusters per video, the centroids of each cluster are used to build a bag of visual words representation of the video, which is fed to a linear SVM classifier to output whether the video contains a collision or not. In the evaluation performed on a small set of 32 videos, the system achieved an average accuracy of 94.14%, outperforming similar works in the area.

Previous articles from our research group proposed different automatic systems applied to pattern detection in smart cities. Chavat et al. [6] applied computational intelligence for detecting harmful pedestrian movement patterns. The proposed system processed several video sources in real time by using a pipes and filters architecture for two main tasks: features extraction by object detection and tracking, and harmful patterns detection. The experimental evaluation was performed on PETS09-S2L1 videos from the Multiple Object Tracking Challenge (MOTChallenge) benchmark and real surveillance videos. The proposed system was competitive with MOTChallenge benchmark results, yet simpler than other proposed software methods. Winter et al. [20] developed a system for collecting and analyzing traffic data applying computational intelligence, using the modern object detection library Detectron2, by Facebook Research. A loosely-coupled pipeline architecture was applied for frame processing. The system was validated on videos from Montevideo, Uruguay, on daylight, nightlight, and different video qualities. The system obtained MOTA values up to 0.89 for tracking, average precision values of 0.90 and average recall of 0.97 for daylight scenarios.

### **3 The proposed system for automatic traffic incidents detection**

This section describes an overview of the developed pipeline for detecting events, and a brief description of each of its parts.

#### **3.1 System architecture**

The design of the proposed system is based on a modular architecture to implement an image processing and computational intelligence pipeline [6]. This design decision provides flexibility and extensibility to the developed system.

6 G. Gabrielli, I. Ferreira, P. Dalchiale, A. Tchernykh and S. Nesmachnow

Fig. 1 presents a diagram of the system architecture. The pipeline uses tagged information from a set of cameras. The information includes street lanes, intersections, and traffic lights tagged on every camera image. An initial geographic calibration is required to normalize the speed of vehicles. The object detector uses the frames of video to detect the vehicles, which are then feed to the object tracker module. The object detector used is YOLO version 3 algorithm (YOLOv3), whereas SORT [3] is used for object tracking, given its good performance and low complexity. The traffic light state module takes the video frames, as well as the tagged information, to generate a state (green, yellow, red or unknown) for each traffic light present in the screen, for each timestamp. By using the tracking information and the data tagged for the camera, the object history model is able to get information about the behavior of each vehicle (street movement, speed estimation, location, class, etc). After building the object history data and the traffic light state is detected, these two elements are feed to each event detector, which outputs at each timestamp, all vehicles fulfilling the condition of each specific event detected.

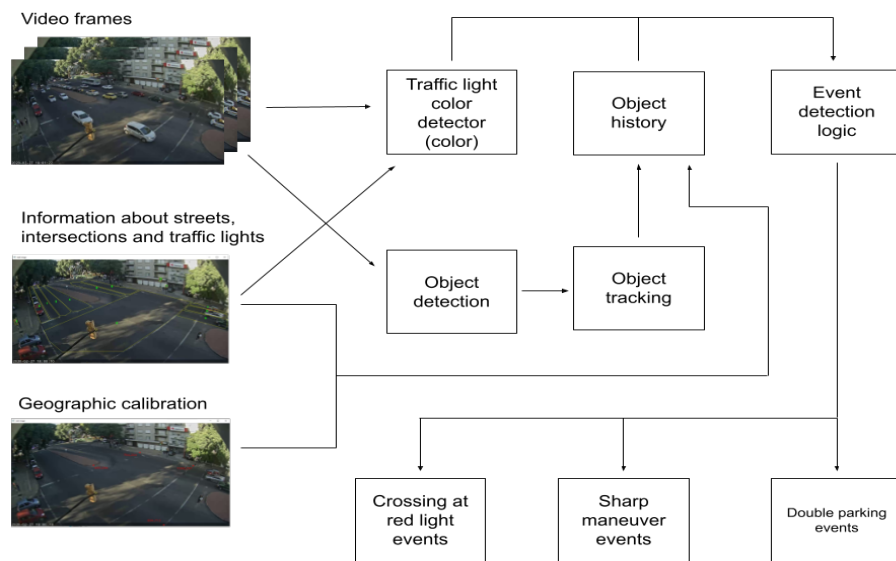


Fig. 1. System pipeline architecture.

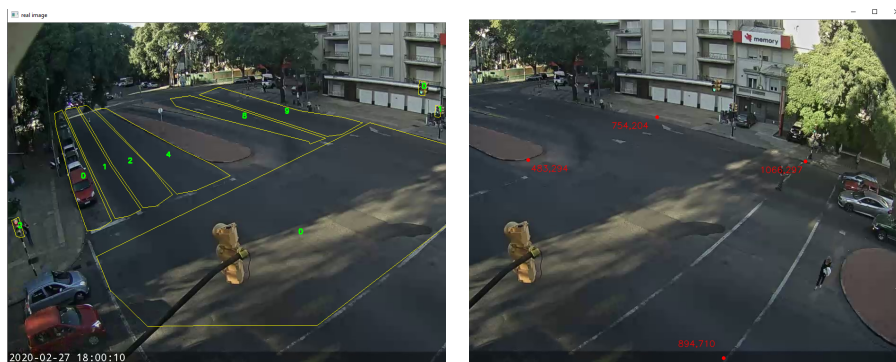
### 3.2 Tagging tools

Two ancillary tools were developed for assisting in the task of labeling data: a tool for labeling road infrastructure (lanes, lane groups, traffic lights, and intersections) and a tool for mapping screen coordinates (pixels) to real geographic coordinates (longitude and latitude). These ancillary tools are described next.

**Road infrastructure labeling tool.** This tool consists of a user interface (UI) that takes a frame of a camera and allows the user to draw the different

elements of the road infrastructure (e.g., lanes, traffic lights, intersections, etc.) and a second UI for creating several aggregations, e.g., by assigning traffic lights to lanes, lanes to lane groups, etc. The road infrastructure labeling tool is shown on Fig. 2. The aim of this tool is to ease the process of tagging the roads, lane groups, intersections and traffic lights in each camera using a simple UI.

**Geographic coordinates tagging tool.** This tool has as inputs a polygon with four points selected in Google Earth and a frame for the reference camera from the same location. The tool allows to tag each screen point to its matching geographical coordinate point. It is able to ease the process of getting this matching, which is necessary to calculate vehicle speeds accurately. The geolocation mapping and tagging tool is shown on Fig. 2.



(a) UI to draw lanes, traffic lights, inter- (b) UI to translate screen coordinates to  
sections and lane groups. geographic coordinates.

**Fig. 2.** Tagging tools.

### 3.3 Object detection

Object detection is performed using YOLOv3, which applies a convolutional neural network (CNN) to achieve real-time detection when running on GPU. In this article, with the goal of running on commodity hardware. The tiny variant with three yolo detection layers is used, with a five fold reduction in inference time and six fold reduction in number of operations, compared to the full YOLOv3 model. This YOLO variant, presented in Fig. 3, consist of 31 layers, 15 of which are part of the Darknet backbone (feature extractor).

YOLOv3 is a single-shot detector, i.e. the entire image is processed on a single step by the CNN, detecting bounding boxes and class probabilities at the same time. This approach avoids the overhead from running multiple steps and individual processing for each bounding box, which was required by previous works such as R-CNN [8]. Furthermore, information for a bounding box detection can be obtained from the entire image rather than only from its neighborhood. These features are processed on three scales,  $1/32$ ,  $1/16$ , and  $1/8$  of the original

8 G. Gabrielli, I. Ferreira, P. Dalchiale, A. Tchernykh and S. Nesmachnow

size, to detect large to small objects (a two yolo layer model would skip the 1/8 scale). The last layer (yolo) for each scale predicts a 3D tensor by encoding bounding box, objectness (a detection certainty estimation, from 0 to 1), and the probabilities of each class. Then, the non max suppression step filters the bounding boxes, and outputs the one with maximum objectness for each set of overlapping bounding boxes of the same class (according to a threshold).

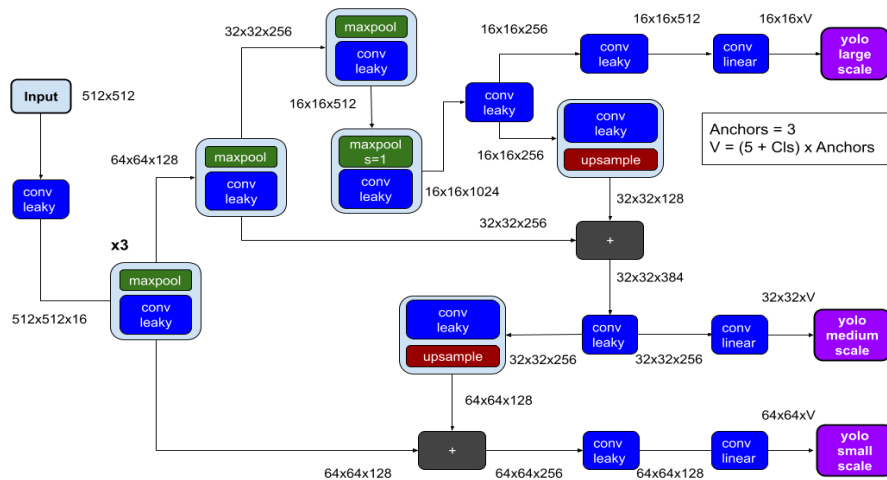


Fig. 3. YOLOv3 Tiny-3l Architecture for 512x512 resolution.

### 3.4 Object tracking

For tracking objects, the SORT method proposed by Bewley et al [3] was used. SORT is a framework to track previously detected objects, at very low complexity. The tracker uses Kalman filters to predict future bounding boxes from past ones, matching predictions to detections from the new frame using the Hungarian algorithm. Every detection is either given the identity that maximizes the Intersection over Union (IoU) metric or a new identity if no association is found.

### 3.5 Object history

Based on tagged information and detections, the object history tracks several different types of elements from an object in time. The elements tracked for each frame for each vehicle include:

- Positions for detected bounding boxes and geographic locations corresponding to each bounding box position (center).
- Estimated speeds.
- Current lane and lane group.
- Bounding box classes detected.

Speed calculation is performed using perspective transform. A set of four annotated points is used to create a perspective transformation matrix to translate image coordinates into geographic coordinates for any point of the image at ground level, resulting in a homography. A coordinate reference system (CRS) transformation is used to convert from WSG84 coordinates in degrees to the local CRS system (EPSG:32721) in meters using the PyProj library.

### 3.6 Traffic light color detector

Traffic light color is detected by finding ellipse (i.e., projected circle) shaped blobs within appropriate (Hue, Saturation, Value) ranges and maintaining a maximum aspect ratio. For each traffic light, either a color is emitted or 'undetermined' when it cannot be ascertained. In the latter case, an alternative traffic light can be used to infer the applicable color in certain cases, either a redundant traffic light or the one in the intersecting street.

### 3.7 Event detection logic

This section presents a general description of the implemented event detectors.

**Crossing at red light.** The event happens when a vehicle or pedestrian crosses the street while the traffic light is red. The event detection is performed slightly different according to the location on the image: detection for vehicles only happens while the vehicle is within an intersection, while detection for pedestrians must run both inside the street and within intersections. There are two subsystems according to the object location, detection for vehicle runs only on crossings while detection for pedestrians runs on both crossings and streets. As a first step, objects with speed below a certain threshold are excluded, to avoid detecting vehicles waiting at the red light or eager pedestrians waiting on the street.

To select the pedestrians who are crossing the street, only pedestrians whose trajectory makes an angle to the lane direction exceeding a threshold are considered (a value of 40 degrees was determined in preliminary experiments). In case the pedestrian is on an intersection, the nearest lane is used. Lane direction is computed by obtaining oriented bounding boxes and selecting the axis for each lane which maximizes the concatenated length for all of the lanes in a street.

**Sharp maneuver.** The procedure to detect if a vehicle is performing a sharp maneuver is as follows. First, the speed of the vehicle is computed, to determine if it exceeds the experimentally determined limit of 40 Km/h. Then, a low-pass filter is applied to smooth the noisy vehicle trajectory and two average movement vectors are calculated, using the first 15 and last 15 positions of the vehicle. If the angle between those vectors is between an (experimentally determined) range of 15 and 70 degrees, based on the histogram of turning angles of vehicles shown in Fig. 4, then the vehicle is considered to be likely doing a sharp maneuver. Finally, the object history is used to determine if the vehicle changed lane group, in which case it is turning the corner, thus not doing a sharp maneuver. Otherwise, it is considered to be doing a sharp maneuver.

10 G. Gabrielli, I. Ferreira, P. Dalchiale, A. Tchernykh and S. Nesmachnow

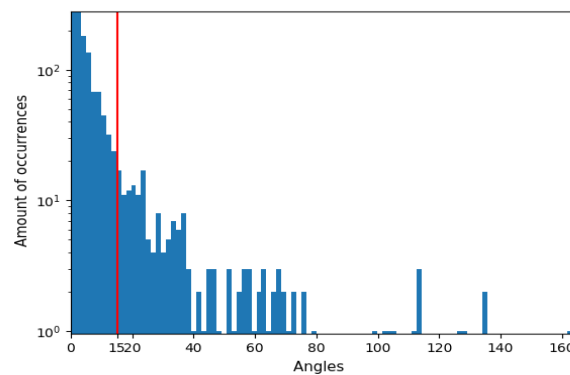


Fig. 4. Histogram of vehicles turning angles.

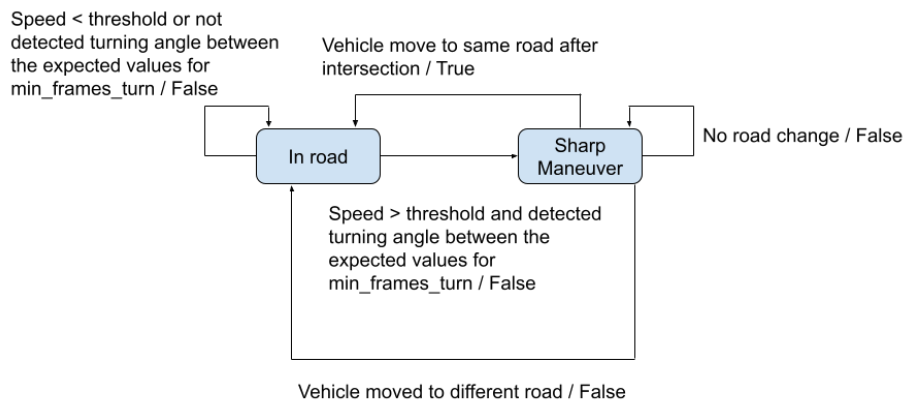


Fig. 5. State diagram for detecting sharp maneuver events.

**Double parking.** Double parking occurs when a vehicle parks in a lane that is adjacent to the parking lane (the lane that borders the sidewalk), blocking the flow of traffic.

To detect a double parking, first the vehicles whose bounding box is smaller than the fifth percentile of bounding box sizes of its class are excluded. Then, if any of the representative points of the vehicle, shown in Fig. 6, intersects a double parking, the vehicle is considered as being in a double parking. Next, the average speed is checked and if it is less than a minimum the vehicle is considered to be stopped. Finally, the ratio of detections on the parking lane over the total number of detections is computed. If this ratio is over a predefined threshold, the vehicle is considered properly parked. If not, the traffic light that grants way to the vehicle is checked and if it has been green the vehicle is considered to be likely double parked and a counter is increased. To discard spurious detections, the event is triggered once the counter exceeds a parameter.



(a) Vehicle with representative point at 0.1. (b) Vehicle with representative point at 0.25.

**Fig. 6.** Examples of vehicles with representative points with respect to the bottom of their bounding box.

## 4 Experimental evaluation

This section presents the validation of the proposed system in the events to be detected, the evaluation of the trained object detectors is also presented.

### 4.1 Evaluation methodology and metrics

**Object detection.** The evaluation dataset was generated using videos provided by the Mobility Management Center of Montevideo City Council. The videos were obtained from 8 different fixed cameras and one pivoting camera from the metropolitan area of Montevideo. Two subsets were used: the training dataset and the validation dataset.

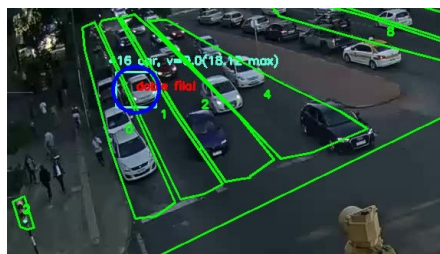
The training set contained 7200 frames from the eight real cameras plus the VisDrone2019 image dataset, whereas the validation set contained 2100 frames. The objects were tagged using interpolation in the CVAT object detection tagging tool. Pseudo labeling was also used in the training process to improve the results. The teacher model was not used in the final solution, because it hinders the operation in real time. Cameras used in the training set were excluded from the object detection validation set. mean Average Precision (mAP) was used as the main metric For the evaluation of the object detectors. Precision, Recall and F-Score were also computed.

**Event detection.** Usual metrics in literature were not suitable for evaluating the events in the given conditions, since they focus either only in the spatial dimension or only in the time dimension. Thus, approaches that evaluate events taking into account jointly the spatial and time dimension were reviewed, to develop a comprehensive metric. The analysis revealed that using IoU for detecting a match in two dimensions was the best approach. A threshold IoU value of 0.25 was used in the spatial dimension to match the vehicle to the ground truth, based on Bochinski et al. [4]. For the time dimension, Ward et al. [19] proposed using per frame event detections and then calculating Precision, Recall and F-score based on these detections. The proposed method for evaluating events combines both of these approaches into an evaluation metric for event detection.

12 G. Gabrielli, I. Ferreira, P. Dalchiele, A. Tchernykh and S. Nesmachnow

### 4.2 Validation scenarios

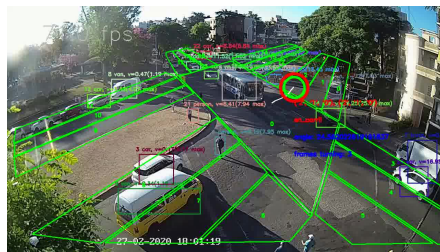
CVAT was used to generate the metadata to tag the events to be evaluated. For the sharp maneuvers event, both real time scenarios and synthetically generated ones were used, since few occurrences of the event were found in the studied videos. For the sharp maneuvers event, false positive tests were also added to have a better approximation of the number of false positives in a real video. Eleven tagged events were considered for each one of the studied events (sharp maneuvers and double parking). The scenarios were generated using different cameras to provide generalization. All videos are in MP4 format, with resolution 1280×720. Fig. 7 presents sample images of the considered scenarios for the sharp maneuver and double parking events. In turn, Table 1 summarizes the main properties of the analyzed videos.



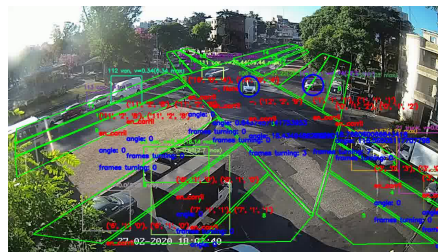
(a) Example of double parking test for camera BVAR\_RODO.



(b) Example of double parking test for camera 21\_BVAR.



(c) Synthetic test for sharp maneuver event detection. Vehicle ground truth location tag event detected shown with red circle.



(d) False positives test for sharp maneuver detection. Vehicle ground truth location tag event detected shown with red circle.

**Fig. 7.** Testing video scenarios.

**Table 1.** Main properties of the validation scenarios.

<i>event type</i>	<i>camera id</i>	<i>test type</i>	<i>start time</i>	<i>end time</i>
Double parking	BVAR_RODO	real	00:12	00:27
Double parking	21_BVAR	real	00:54	01:50
Sharp maneuver	21_BVAR	synthetic	01:06	01:20
Sharp maneuver	21_BVAR	false positives	02:00	03:00

### 4.3 Experimental results

**Object detection.** Table 2 reports the mAP results obtained on the validation of YoloV3 tiny object detection models with two and three yolo layers.

class	tiny model		
	2l auto	3ln	3l auto
AP car	50.68%	63.29%	<b>69.67%</b>
AP bus	53.00%	30.72%	<b>50.82%</b>
AP truck	12.57%	<b>20.97%</b>	19.24%
AP van	38.43%	16.27%	<b>46.11%</b>
mAP vehicles	38.67%	32.81%	<b>46.46%</b>

**Table 2.** AP for the most relevant classes and mAP for the tiny models: 2l auto (two yolo layers), 3ln and 3l auto (three yolo layers).

Results in Table 2 indicate that the 3l auto model computed significantly better mAP values than the other two models. The mean AP for the 3l model improved 7.79% over the 2l model, both trained using pseudo labeling, thanks to better small object detection. Pseudo labeling significantly improved mAP (by 13.65%) for the 3l model.

**Event detection.** Table 3 reports the results obtained for events detection. The parameters of the detectors were tuned to maximize the Recall, trying to not miss events, but without penalizing Precision much. The rationale behind this decision is that it is preferable to detect a false positive, which can be discarded by a human operator, than missing a reckless driving that may cause an accident.

Event	Precision	Recall	F-Score
Sharp maneuver	0.82	0.82	0.82
Crossing at red light	0.42	0.63	0.51
Double parking	0.59	0.91	0.72

**Table 3.** Precision, Recall and F-score for the studied events

Results in Table 3 show different values of Precision and Recall for the studied events. The low precision for crossing at red light event may be related to differences on camera lighting and the small size of traffic lights. For double parking event, precision was limited by false positives caused by imprecision on the assignment of traffic lights to lanes in complex intersections. The best results were computed for the sharp maneuver event, for which precision and recall were balanced and accurate. In this case, recall results can be improved by using a low pass filter that requires less previous data.

14 G. Gabrielli, I. Ferreira, P. Dalchiale, A. Tchernykh and S. Nesmachnow

## 5 Conclusions and future work

This article presented a system for detecting traffic incidents, applying computational intelligence and machine learning techniques. Based on traffic camera videos, the proposed system is capable of detecting in real time different types of reckless behavior carried out by drivers.

The developed system was conceived to be an efficient and flexible solution for traffic monitoring, by applying conceptually simple computational intelligence methods to be executed on commodity hardware. Accurate results were obtained for the sharp maneuver event (precision and recall values 0.82). In turn, for the double parking event, a 0.91 recall value was computed, and a reasonable precision (0.59). The experimental evaluation suggests that the proposed system is a viable solution for detecting reckless driving behavior, able to execute in real time, to be applied for traffic monitoring in the metropolitan area of Montevideo.

The main lines for future work are related to improve the processing speed and the accuracy of the proposed system. Multi-threading processing can be enhanced to improve computational efficiency, whereas applying batch inference and recent advances in object detection models can lead to better accuracy on events detection. Finally, developing an automated procedure for tagging information would diminish the calibration time per camera.

## References

1. Agrawal, A.K., Agarwal, K., Choudhary, J., Bhattacharya, A., Tangudu, S., Makhija, N., B, R.: Automatic traffic accident detection system using resnet and svm. In: 2020 Fifth International Conference on Research in Computational Intelligence and Communication Networks. pp. 71–76 (2020)
2. Arinaldi, A., Pradana, J., Gurusinga, A.: Detection and classification of vehicles for traffic video analytics. *Procedia Computer Science* 144, 259–268 (2018)
3. Bewley, A., Ge, Z., Ott, L., Ramos, F., Upcroft, B.: Simple online and realtime tracking. 2016 IEEE International Conference on Image Processing (2016)
4. Bochinski, E., Eiselein, V., Sikora, T.: High-speed tracking-by-detection without using image information. In: 2017 14th IEEE International Conference on Advanced Video and Signal Based Surveillance. pp. 1–6 (2017)
5. Chauhan, M., Singh, A., Khemka, M., Prateek, A., Sen, R.: Embedded CNN based vehicle classification and counting in non-laned road traffic. In: 10<sup>th</sup> Int. Conf. on Information and Communication Technologies and Development (2019)
6. Chavat, J., Nesmachnow, S., Tchernykh, A., Shepelev, V.: Active safety system for urban environments with detecting harmful pedestrian movement patterns using computational intelligence. *Applied Sciences* 10(24), 9021 (2020)
7. Dey, S., Kalliatakis, G., Saha, S., Kumar Singh, A., Ehsan, S., McDonald, K.: MAT-CNN-SOPC: Motionless analysis of traffic using convolutional neural networks on system-on-a-programmable-chip. In: NASA/ESA Conference on Adaptive Hardware and Systems (2018)
8. Girshick, R., Donahue, J., Darrell, T., Malik, J.: Rich feature hierarchies for accurate object detection and semantic segmentation. In: 2014 IEEE Conference on Computer Vision and Pattern Recognition. pp. 580–587 (2014)

9. Hipogrosso, S., Nesmachnow, S.: Sustainable mobility in the public transportation of montevideo, uruguay. In: *Smart Cities*, pp. 93–108. Springer International Publishing (2020)
10. Hipogrosso, S., Nesmachnow, S.: A practical approach for sustainable transitoriented development in montevideo, uruguay. In: *Smart Cities*. pp. 93–108 (2021)
11. Khazukov, K., Shepelev, V., Karpeta, T., Shabiev, S., Slobodin, I., Charbadze, I., Alferova, I.: Real-time monitoring of traffic parameters. *Journal of Big Data* 7(1), 84 (2020)
12. Kruegle, H.: *CCTV Surveillance, Second Edition: Video Practices and Technology*. Butterworth-Heinemann, Newton, MA, USA (2006)
13. La Vigne, N., Lowry, S., Markman, J., Dwyer, A.: Evaluating the use of public surveillance cameras for crime control and prevention. Tech. rep., Urban Institute, Justice Policy Center (2011)
14. Massobrio, R., Nesmachnow, S.: Urban Mobility Data Analysis for Public Transportation Systems: A Case Study in Montevideo, Uruguay. *Applied Sciences* 10(16), 5400 (2020)
15. Ravindran, V., Viswanathan, L., Rangaswamy, S.: A novel approach to automatic road-accident detection using machine vision techniques. *International Journal of Advanced Computer Science and Applications* 7 (2016)
16. Ristvej, J., Lacinák, M., Ondrejka, R.: On smart city and safe city concepts. *Mobile Networks and Applications* 25(3), 836–845 (2020)
17. Toh, C., Sanguesa, J., Cano, J., Martinez, F.: Advances in smart roads for future smart cities. *Proceedings of the Royal Society A: Mathematical, Physical and Engineering Sciences* 476(2233) (2020)
18. Uy, A., Quiros, A., Bedruz, R., Abad, A., Bandala, A., Sybingco, E., Dadios, E.: Automated traffic violation apprehension system using genetic algorithm and artificial neural network. In: *IEEE Region 10 Technical Conference*. pp. 2094–2099 (2016)
19. Ward, J., Lukowicz, P., Gellersen, H.: Performance metrics for activity recognition. *ACM TIST* 2, 6 (2011)
20. Winter, H., Serra, J., Nesmachnow, S., Tchernykh, A., Shepelev, V.: Computational intelligence for analysis of traffic data. In: *Smart Cities*, pp. 167–182 (2021)
21. Yang, H., Qu, S.: Real-time vehicle detection and counting in complex traffic scenes using background subtraction model with low-rank decomposition. *IET Intelligent Transport Systems* 12, 75–85 (2018)
22. Yang, Z., Pun-Cheng, L.: Vehicle detection in intelligent transportation systems and its applications under varying environments: A review. *Image and Vision Computing* 69, 143 – 154 (2018)
23. Zheng, M., Li, T., Zhu, R., Chen, J., Ma, Z., Tang, M., Cui, Z., Wang, Z.: Traffic accident's severity prediction: A deep-learning approach-based CNN network. *IEEE Access* 7, 39897–39910 (2019)
24. Zhou, Y., Nejati, H., Do, T., Cheung, N., Cheah, L.: Image-based vehicle analysis using deep neural network: A systematic study. In: *IEEE International Conference on Digital Signal Processing*. pp. 276–280 (2016)

# Exact approach for electric vehicle charging infrastructure location: a real case study in Málaga, Spain

Claudio Risso<sup>1</sup>[0000-0003-0580-3083], Christian Cintrano<sup>2</sup>[0000-0003-2346-2198],  
Jamal Toutouh<sup>2</sup>[0000-0003-1152-0346], and Sergio Nesmachnow<sup>1</sup>[0000-0002-8146-4012]

<sup>1</sup> Universidad de la República, Uruguay  
{crisso, sergion}@fing.edu.uy,  
<sup>2</sup> University of Málaga, Spain  
{cintrano, jamal}@lcc.uma.es

**Abstract.** This article presents an exact approach for solving the problem of locating electric vehicle charging stations in a city, whose goal is upon minimizing the distance citizens must span to charge their vehicles. Mixed integer programming formulations are presented for two variants of the problem: relaxed (i.e., without considering electrical constraints for the infrastructure) and full versions. The experimental evaluation is performed over a real-world case study defined in Málaga, Spain. Results show that the proposed approach can deal with the large number of variables (i.e., millions) of the problem, computing optimal solutions for all problem instances and variants addressed. The improvements in solutions quality over a previous metaheuristic approach applied to the same problem and application case are notorious.

**Keywords:** Electric vehicles · Infrastructure location · Sustainable mobility · Smart Cities · Combinatorial Optimization

## 1 Introduction

Sustainability has become a priority goal for society. Agreements and conventions, such as the Sustainable Development Goals, are shifting societies towards green-conscious ones. An important change is being experienced in road mobility because vehicles are shifting from inefficient combustion engines to more sustainable ones (i.e., hybrid or electric engines). Cars, scooters, and electric motorcycles are novel ways preferred by newer generations to move along the cities. Thus, electric vehicles (EV) have a great boom and socioeconomic impact [10].

Electric cars allow citizens to reduce gas emissions, if the electricity used to charge the cars is obtained from green sources. The number of kilometers that an electric car can drive without stopping is a decisive factor when deciding to opt for an electric car. Maximum kilometers would not be such a pressing problem if there were a good network of charging stations. Cities have not yet adapted to this new trend in transportation. Even though there are many plans to deploy networks of charging points for electric vehicles in the main cities of the world [8].

2 C. Risso, C. Cintrano, J. Toutouh, S. Nesmachnow

The selection of locations for these charging points has been studied by the Electric Vehicle Charging Stations Locations (EV-CSL) problem. The problem proposes determining the location of electric vehicle charging stations to optimize a quality of service metric, i.e., minimizing the sum of distances that citizens must walk to charge their vehicles. Our previous research addressed EV-CSL over a real scenario defined in Málaga city (Spain) [6]. A realistic instance was defined taking into account real information about the roads, the limitations of the power grid, and the location of the tentative charging point users. In turn, two metaheuristics were proposed to solve the problem.

This article presents a new version of the EV-CSL problem model, to better capture realistic features in terms of energy supply constraints. In turn, an exact method based on ILP is applied to solve the problem. The main contributions of the research reported in this article include: *i)* Providing a new improved mathematical formulation of EV-CSL; *ii)* Proposing a new exact approach to address EV-CSL based on ILP; *iii)* Designing new realistic instances and variations of the problem to evaluate the proposed approach; *iv)* Reporting a comparison among the solutions provided in previous research and the results computed by our approach; *v)* Discussing the different solutions obtained in terms of the quality of service and the distribution of the charging points.

The article is organized as follows. Next section introduces the optimization problem addressed in this research and its mathematical formulation. Section 4 describes the main details of the proposed optimization approach. The experimental evaluation is reported in Section 5, including discussion of the obtained results and their applicability in the real case study in Málaga. Finally, Section 6 presents the conclusions and formulates the main lines for future work.

## 2 Infrastructure location for electric vehicles charging

The mathematical formulation of the EV-CSL problem is defined attending to the elements and considerations described in the following subsections.

### 2.1 Problem Data

An instance of the EV-CSL problem is determined by the following data:

- The set of potential charging points  $S = \{s_1, s_2, \dots, s_M\}$  comprises those physical locations considered suitable for installing recharging infrastructure. The formulation makes no distinction between points, other than its location and the set of power stations within the distribution grid capable of feeding each point. Particularly, no difference is considered regarding the number of customers that can be served in parallel at any given point.
- The maximum number of charging points to be deployed all over the city,  $M_s$ . For the optimization problem to be realistic, it is assumed that  $M_s \ll M$ .
- The set  $C = \{c_1, c_2, \dots, c_N\}$  comprises clusters of clients, grouped according on their geographical proximity. For each cluster  $c \in C$ , the number  $u_c$  of

clients is known. Since clusters are pre-calculated so that their members are not widely separated from each other, the average distance  $d_{cs}$  between cluster  $c$  clients and every potential charging point  $s \in S$  is known in advance, and its variance is low regarding the average.

- There is a known bound  $D_c$  for the maximum distance that customers in cluster  $c \in C$  are willing to walk to charge their vehicles. So, only points  $s \in S$  where  $d_{cs} \leq D_c$  are considered to serve customers of the cluster  $c$ .
- $E = \{e_1, e_2, \dots, e_T\}$  is the set of power stations that might serve as source to feed charging points. For every pair  $e \in E$ ,  $s \in S$ , the reference distance  $d_{es}$  over the power grid necessary to connect  $e$  with  $s$  is known in advance. This correspondence imposes viability among connections because of electric constraints, such as: tension drops, thermal or stability limits the grid must comply with. A maximum extent  $D_e$  is assumed between each power station  $e \in E$  and those points  $s \in S$  to be connected to it. Only those  $(e, s)$  pairs where  $d_{es} \leq D_e$  are considered.
- A power-stations to charging-points assignment cannot lead to configurations that overload stations beyond their capacity. Every station  $e \in E$  has a specific limit  $mp_e$  to the number of charging points it can feed.

## 2.2 Design premisses and control variables

A feasible deployment of charging points must comply with a simple set of rules:

1. Every cluster of clients  $c \in C$  must count an effective charging point  $s \in S$  at a distance  $d_{cs}$  of at most  $D_c$ .
2. Every charging point to be installed must be fed from a unique power station  $e \in E$ , whose distance  $d_{es}$  is lower or equal to  $D_e$ .
3. The power-stations to charging-points assignment cannot press the number of charging points to be served by any station  $e \in E$  beyond its limit  $mp_e$ .
4. The objective to optimize accounts the accumulated distance between clients and their nearest charging points available. Hence, though a cluster  $c \in C$  could have more than one charging point within  $D_c$  range, only that at the nearest distance is considered to account in the QoS.
5. The number of charging-points is bound to a total limit  $M_s$ , so the election affects the whole and it must be globally coordinated.
6. Power limits at stations only concern with the number of charging points fed from them, not with the associated number of customers.

The main control variables of the problem regard with the selection of charging points to be installed. However, the formulation includes additional variables to capture other design concerns. The list of variables by kind is as follows:

- Boolean variables  $z_s$  indicate whether some charging point  $s \in S$  is to be installed or not, so they are as many as  $|S| = M$ .
- Boolean variable  $x_{cs}$  is active if and only if those clients in the cluster  $c \in C$  find their closest point of the charge at  $s \in S$ .

4 C. Risso, C. Cintrano, J. Toutouh, S. Nasmachnow

Constraint  $d_{cs} \leq D_c$  must hold to comply with distance limits, what is achieved by solely considering  $x_{cs}$  variables where  $d_{cs} \leq D_c$ . Let  $CS \subseteq C \times S$  be the a-priori computed set of *distance viable* clusters to charge-points assignments. Observe that the number  $|CS|$  of  $x_{cs}$  variables could be as high as  $M \times N$  ( $|S| = M, |C| = N$ ) in the limit. The value depends of the maximum allowed distance  $D_c$ , the higher the limit, the greater  $|CS|$ .

Variables described so far only concern with the physical placement of charging points. Electric grid constraints require additional variables:

- Boolean variables  $y_{es}$  capture the fact that station  $e \in E$  supplies power to charging point  $s \in S$ . Since the problem description also integrates distance limits amid these connections,  $(e, s)$  assignments fulfilling  $d_{es} \leq D_e$  are pre-filtered, whose outcome is referred to as  $ES \subseteq E \times S$ . The number  $|ES|$  of  $y_{es}$  variables could be as high as  $T \times M$  ( $|E| = T, |S| = M$ ) in the limit. Unlike the previous  $CS$  set, the number  $|ES|$  is fixed among instances to solve, since it is inherited by constraints coming from the power grid rather from some ultimately adjustable service goal, such as  $D_c$ .

Eqs. (1a)–(1g) expresses the mixed integer programming (MIP) for EV-CSL, i.e., finding the most efficient location for the electric vehicle charging infrastructure, in terms of the sum of distances between clusters and charging points.

$$\min_{x_{cs}, y_{es}, z_s} \sum_{cs \in CS} u_c d_{cs} \cdot x_{cs} \tag{1a}$$

subject to:

$$\sum_{cs \in CS} x_{cs} = 1, \quad \forall c \in C \tag{1b}$$

$$z_s \geq x_{cs}, \quad \forall cs \in CS \tag{1c}$$

$$\sum_{s \in S} z_s \leq M_s \tag{1d}$$

$$\sum_{es \in ES} y_{es} = z_s, \quad \forall s \in S \tag{1e}$$

$$\sum_{es \in ES} y_{es} \leq mp_e, \quad \forall e \in E \tag{1f}$$

$$x_{cs}, y_{es} \in \{0, 1\}, 0 \leq z_s \leq 1 \tag{1g}$$

The objective function (1a) directs the optimization towards the lowest per-customer combined distance between clusters and charging points. Given that the number of clients is fixed and it is assumed that they always recharge at the closest point available, the sum in Eq. (1a) is indeed a metric for the Quality of Service (QoS) of the infrastructure as presented earlier in this section.

Note that (1a) adds up to the distance that the whole of the customers should travel to recharge their vehicles. Without any other constraint, that number could be as low as zero when every  $x_{cs} = 0$ , which makes no sense, since no

charge point is provisioned in that case. To prevent that, (1b) forces every cluster  $c$  to have one assigned station within  $D_c$  range, because  $CS$  only contains  $(c, s)$  pairs where  $d_{cs} \leq D_c$  and there must be one and only one variable for which  $x_{cs} = 1$ . Whenever more than one station  $s$  is within  $D_c$  range, the optimization itself will choose that closest to  $c$ . Therefore, (1a) and (1b) combined guarantee that: i) every cluster  $c$  counts a charging point within  $D_c$  range; ii) each cluster is optimally assigned for a given set of charging points; and iii) after consolidated, that assignment achieves the lowest total distance for all clients combined.

Since installing a station accounts no cost, an optimal configuration would assign every cluster to the nearest station possible, what most certainly leads to configurations where the limit of stations  $M_s$  is exceeded. To prevent this violation, (1c) and (1d) are incorporated. Eqs. (1c) simply make a station  $s \in S$  to be installed whether any cluster  $c$  is going to use it, since a variable  $x_{cs} = 1$  is enough to force  $z_s = 1$ . Observe that although the integrality of  $z_s$  variables is intrinsic, it should not be explicitly imposed as it is with  $x_{cs}$  ones, which unlike  $z_s$  variables are declared as boolean in (1g).

The problem with variables and constraints defined so far only concerns with the physical placement of charging points, not with other limits imposed by the electric grid. Since it has less constraints, this subproblem clearly is a relaxation of the complete one, and its optimal solutions represent lower bounds of EV-CSL. Subtler is the fact that, since power station limits are set by the number of charge points assigned to them, not by the number of users, solutions to the previous relaxation might also be feasible in the complete problem, as long as the  $M_s$  limit is low when compared with  $mp_e$  values. This property is in fact exploded during the experimental evaluation, Section 5.

Power stations limits are incorporated into the problem, to get to the *full version*, as follows. Eqs. (1e) are equivalent to (1b), except that in this case, the assignment of a charging point  $s \in S$  to a power-station  $e \in E$  within  $D_e$  range (captured by variables in  $ES$  set) is triggered if and only if that point is to be installed (i.e. only if  $z_s = 1$ ). Finally, Eqs. (1f) guarantee that no station  $e \in E$  is assigned with a number of charging points higher than its limit  $mp_e$ .

### 3 Related Work

The optimal location of electric vehicle charging stations has been a relevant problem since the emergence of a renewed interest in electric transportation infrastructures, in the early 21st century.

Frade et al. [9] applied a maximal covering model to maximize the demand within a maximum desirable distance, assuming that coverage decays beyond that threshold distance. A MIP model was proposed, including a penalty term to prevent the installation of unnecessary supply points. The model was evaluated on four scenarios in Lisbon, Portugal, installing up to 324 supply points in 43 charging stations in a higher-demand scenario. Accurate covered demand results were computed, providing an acceptable level of service. Wagner et al. [16] proposed a business intelligence model for EV-CSL to maximize demand cover-

6 C. Risso, C. Cintrano, J. Toutouh, S. Nesmachnow

age, based on potential trip destinations of vehicle owners, defined using urban data analysis [12]. An iterative method was proposed to find optimal locations using penalties to define ranks for points of interest and a MILP model solved in CPLEX. The proposed model achieved promising results on two case studies from Amsterdam and Brussels. Chen et al. [5] proposed a MILP formulation for locating charging stations minimizing the total walking distance according to parking patterns estimated using real urban data. The model was evaluated on a case study on 218 zones of Seattle, USA. Results achieved good accessibility: locating 20 charging station the walking distance was 1.1 km (average) and 3 km (maximum), whereas almost 80% of the demand was fulfilled.

Cavadas et al. [4] proposed a MIP model for EV-CSL to maximize the satisfied demand subject to a maximum budget constraint, considering the activity patterns of travelers. A multi-period formulation was introduced to model time intervals within a day. The model was evaluated in a small real scenario in Coimbra, Portugal, with just nine stations and four charging points each, to be installed on 129 candidate locations. Accurate solutions were computed, improving over the real configuration of EV charging stations installed in the city. Brandstätter et al. [2] proposed an ILP model for EV-CSL to maximize economic benefits in a car-sharing system, considering stochastic demands. The model was validated on medium-size synthetic scenarios and real world instances from Vienna (up to 693 potential locations). For Vienna, the exact approach was only able to solve instances for eight central districts of the city, whereas an heuristic method was applied for larger problem instances. Solutions confirmed the economic viability of implementing a electric car-sharing system.

Çalik and Fortz [3] proposed a MILP formulation for EV-CSL to maximize the profit of a public one-way electric cars system. The model and two relaxations were studied for 63 instances in New York, USA, with 85 potential locations for installing non-identical charging stations. The impact of cost changes in the number of stations was studied. Bian et al. [1] proposed a GIS-based approach for EV-CSL to maximize the profit. GIS was applied to determine the probability for users to charge their EV in different areas, using relevant traffic information. The model was evaluated in a small case study in Västerås, Sweden, with 268 square zones. Two scenarios were studied, adding three and ten new charging stations to 40 already installed in the city. When adding three stations, the best option was selecting fast chargers in commercial areas, whereas slow chargers installed in residential areas were better when including ten stations.

Lin et al. [11] proposed MILP model based on Geographic Information System (GIS) to optimally select the location and the size EVCS in urban scenarios. The MILP model is defined to maximize the economical profits of installing new charging stations, which are computed according to the charging demand based on the traffic flow data, charging profiles, and city land-use classification. In order to compute the charging demand, the authors generated an aggregated charging demand profile of the EVs based on the real-world travel data in National Household Travel Survey and charging behaviors. These daily charging behaviors, for each charging type of location, are represented by 24 hourly charging demands.

GIS is employed to calculate the charging demand in different locations by taking into account traffic flow and land-use classifications (e.g., residential with villa, residential with apartment, working, etc.). In this study, it is assumed that a charging station will only serve the demands in specific given area. In turn, there is defined an acceptable walking distance from the charging station (parking lot) to the destination of the user. The researchers take into account the costs of a new station (which could include fast and slow chargers). Thus, the costs of a station consist of an aggregation of the economical costs of the equipment, installation, rent, maintenance and operation, and electricity consumption, which depend on the number and the type of chargers installed chargers. The optimization problem objective (the economical profits of deploying the new stations) is computed by subtracting the costs of locating the new charging station to the revenues of charging EVs. The proposed approach was evaluated over an area of 67 Km<sup>2</sup> of Västerås, Sweden. Västerås had a population of 119 372 people, there were 44 192 personal cars, and the city had 324 plug-in EVs charging stations. The authors defined 532 tentative charging stations. The experimental analyses evaluated only the proposed method over four scenarios: installing three, five, ten, and 15 new charging stations. The results show that the proposed approach was able to provide charging station locations that provided competitive profits.

The EV-CSL problem and related variants have been also solved using meta-heuristic approaches, due to the inherent complexity of specific variants using complex formulations or even simulations for solution evaluation.

In this line of work, this article contributes with an exact solution to EV-CSL, taking advantage of our expertise on location problems in the context of smart cities, including roadside infrastructure for vehicular networks [13], stations for public bicycles [6], bus stops [7], and waste bins [15], among other relevant problems. Our research demonstrates that a simple MILP formulation of EV-CSL can be solved with an exact method for medium-sized instances, and we solve a real-life scenario modeling the current reality in the city of Málaga.

## 4 The proposed optimization approach

This section elaborates upon the developments implemented to solve variants of the EV-CSL. The previous approach to solve this problem relied on meta-heuristics to find good-quality solutions for real-world instances [6]. Conversely, this work presents how exact methods have proven to be successful to solve the Mathematical Programming formulation for the previously studied instances, as well as over many others of such size.

A couple of tools were used along the development process. The optimization toolkit of MATLAB (release R2015a-8.5.0) was used in early stages of the work, mainly to validate the general formulation over a manually crafted test-set with relatively few variables. However, real-world instances solved in this article are far beyond capabilities of these tools. The number of  $x_{cs}$  variables could be as high as  $M \times N$ , which in some instances (e.g.  $D_c = 8000$  meters) reaches almost six and a half million integer variables.

8 C. Risso, C. Cintrano, J. Toutouh, S. Nesmachnow

To cope with the size of instances for the application case, IBM(R) ILOG(R) CPLEX(R) Interactive Optimizer 12.6.3.0 was used as the optimization tool. The total time to optimal required by this solver to find solution was always below two hours. As we see later in this document, total times were quite below that value in general. It is worth mentioning that by optimal we mean: within the default GAP tolerance, which is set to the default value for the MIP solver (i.e. 0.01%). The GAP corresponds to the relative difference between the best integer solution found and the best upper bound estimated up to that moment, namely  $(f(x) - bestBound)/f(x)$ , where  $x$  is a feasible solution,  $f(x)$  is its objective function value, and  $bestBound$  is the higher lowest bound found for the optimum value. For the interface between the large instance data-sets and the solver, we developed a C++ program to read data and convert them to CPLEX LP-format. Afterwards, those LP files were launched in computing resources of the National Supercomputing Center, Uruguay (Cluster-UY) [14].

## 5 Experimental validation

This section reports the experimental evaluation of the proposed exact approach for solving the EV-CSL problem over realistic instances in Málaga, Spain.

### 5.1 Methodology

The methodology applied in the experimental validation of the proposed exact methods is described next.

**Analysis.** Three relevant analysis are developed. First, the relaxed problem variant flexible (without including constraints defined by Eqs. (1e) and (1f)) is evaluated for a set of realistic instances, varying the maximum number of charging points to be deployed,  $M_s$ . Then, for the relaxed problem variant, results are compared with the corresponding previous EA applied to the problem [6]. Finally, the full (more realistic) problem variant, including the constraints that model the supply of the electrical grid (defined by Eqs. (1e) and (1f)) is studied.

**Metrics.** Relevant metrics are considered in the evaluation of the computed solutions. On the one hand, the objective function values account for the per-customer combined distance between clusters and their nearest charging point. On the other hand, other relevant QoS-related metrics are considered, such as the average and maximum distance a customer must travel for charging. In turn, the installation cost of the electric charging stations is also evaluated, according to a simplified cost model developed for the analysis. The cost model is based on real infrastructure installation costs (including the cost of the charger, civil infrastructure works, electrical installation, signaling, security, and legalization). A semi-rapid charger is considered, with a power of 22 kW and a cost of 10 500 €. In addition, the cost of the connection from the charging point to the corresponding electrical substation is added.

For the comparison with the previous EA for the problem, the GAP metric is used to evaluate the differences in the computed objective function values.

**Problem instances.** Two set of instances are considered in the evaluation of the proposed exact approach for EV-CSL:

- For the evaluation of the exact approach on both the relaxed and full versions, a constant threshold distance of  $D_c = 2500$  m is used, assumed as a reasonable distance citizens are willing to travel to charge their electric vehicles. Setting  $D_c$  fixes in turn the set of variables of the problem. The value of  $M_s$  varies from 20 to 80. Whenever Eqs. (1e) and (1f) are dismissed from the full version (Eqs. (1a)–(1g)), a relaxation is obtained, no matter what the dataset is. However, along the sequence of problem instances previously introduced and since  $D_c$  is fixed along them, as  $M_s$  increases, either version of the problem is in turn a relaxation of the previous problem instance. This is because the only difference between any instance and the following is on the right-hand side of Eq. (1d), which is exactly one unit larger than the previous. Hence, as  $M_s$  increases, the optimal objective can only decrease, and whatever solution for any prior instance previously tackled could be used as an initial feasible solution for the current, a property that whether used helps to improve the performance of the solver.
- For the comparison with results computed using the previous EA, instances reported in our previous work [6] are used. In these instances, both the values of  $M_s$  and  $D_c$  vary simultaneously, so no nesting exists among problems.

Regarding geographical information, both sets of instances were built considering real data for the city of Málaga. A total number of  $M_s = 33.550$  potential locations for charging points are considered. In turn, 363 clusters and 14 electric substations are considered. Fig. 1 presents the potential locations over the map of Málaga (green dots) and the electric substation location (blue squares).



Fig. 1: Potential locations for charging stations in Málaga

10 C. Risso, C. Cintrano, J. Toutouh, S. Nesmachnow

**Numerical results.** This section, discusses the results of the proposed exact approach for EV-CSL on the relaxed version and compares them against the results obtained by the previous EA [6]. Then, it presents the results provided by the proposed exact approach on the full version of the problem.

Tables 1 and 3 reports the results for the relaxed and full versions of the problem, Reported values are: the total distance between clusters and charging points ( $f_{\text{BEST}}$ ), the economical cost of deploying that solution in euros (cost), and the actual distance in meters between the clusters and the charging points in terms of average ( $d_{\text{AVG}}$ ) and maximum ( $d_{\text{MAX}}$ ) for each  $M_s$ .

Table 1: Experimental results for the relaxed version of the problem.

$M_s$	$f_{\text{BEST}}$	cost	$d_{\text{AVG}}$	$d_{\text{MAX}}$	$M_s$	$f_{\text{BEST}}$	cost	$d_{\text{AVG}}$	$d_{\text{MAX}}$
20	515866608	3802015	1155.18	2497	51	246365755	8366825	777.61	2497
21	492189525	3913565	1139.56	2497	52	243013759	8486655	774.47	2497
22	470795972	4086410	1119.10	2497	53	239713988	8599355	763.06	2497
23	453698051	4296630	1062.30	2498	54	236423096	8604645	750.37	2492
24	437985284	4414850	1043.62	2498	55	233256211	8734480	739.11	2492
25	422884012	4704420	1013.72	2498	56	230153919	8838900	735.58	2492
26	408509548	4857025	998.26	2497	57	227101656	8911580	734.37	2492
27	394495141	4984790	978.34	2497	58	224085462	9037620	732.75	2492
28	382545839	5075295	960.75	2497	59	221071931	9164695	731.14	2492
29	370970640	5271485	942.30	2497	60	218127562	9367325	728.73	2492
30	361019674	5377515	931.24	2497	61	215241637	9436900	724.12	2492
31	351748722	5435935	922.01	2497	62	212386123	9498885	721.73	2492
32	344195535	5614875	916.74	2497	63	209542491	9601005	718.49	2492
33	337185494	5733670	910.92	2497	64	206798841	9665290	716.24	2492
34	330720516	5863620	906.91	2497	65	204076876	9873555	713.29	2492
35	324414266	6036350	898.78	2497	66	201380990	10037430	710.68	2492
36	318213955	6255310	880.72	2497	67	198701745	10148520	707.70	2492
37	312456675	6412285	864.77	2497	68	196042267	10657280	700.38	2492
38	306745623	6554770	858.26	2497	69	193486949	11233430	689.48	2492
39	301057871	6720830	853.57	2497	70	190941050	10886245	695.55	2492
40	295633585	7005800	840.68	2497	71	188385732	11462395	684.65	2492
41	290469709	7155415	830.72	2497	72	185844597	11668130	682.38	2492
42	285334212	7285825	822.28	2497	73	183382962	11842355	671.34	2492
43	280187531	7377250	817.70	2497	74	180841827	12048550	669.07	2492
44	275197190	7442455	811.21	2497	75	178437781	12159640	665.95	2492
45	270522493	7608515	806.30	2497	76	176095511	12220015	661.18	2492
46	265941206	7696490	804.07	2497	77	173834250	12423335	654.85	2486
47	261403566	7777335	801.43	2497	78	171624251	12515910	653.24	2486
48	257424493	7871750	800.53	2497	79	169445056	12624010	643.01	2486
49	253503768	7982150	794.28	2497	80	167282054	12693930	638.27	2486
50	249922088	8107385	784.61	2497					

Results in Table 1 show that as the number of charging points increases ( $M_s$ ) the combined distance between clusters and charging points ( $f_{\text{BEST}}$ ) decreases, as expected.  $d_{\text{MAX}}$  is slightly below 2500m in all cases, so, optimal solutions tend to assign some clusters very close to the distance threshold.

Optimized location for electric vehicle charging infrastructure 11

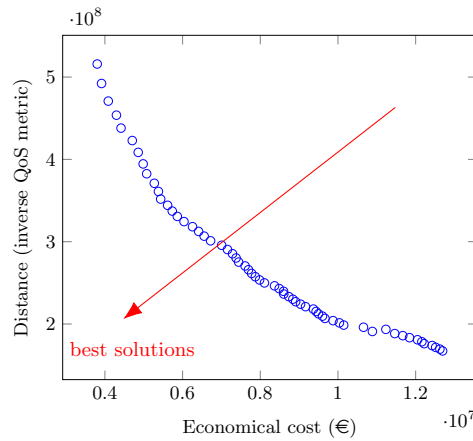


Fig. 2: Distance and the economical cost on the relaxed variation.

The reduction in the calculated  $f_{BEST}$  values when increasing  $M_s$  implies that citizens generally travel shorter distances to charge their cars. Values of  $d_{AVG}$  and  $d_{MAX}$  in Table 1 show that the average distances decrease as the number of charging points increases. However, not all citizens benefit when adding only one charging point. For this reason, the maximum distance values do not improve in the same way as the average (it is always close to threshold distance of  $D_c = 2500m$ ). This is illustrated in Fig. 3 that shows the distribution of the charging points through the real map of Málaga for different values of  $M_s$ . Even though the exact method distributes the charging points through the whole map as  $M_s$  increases, there are areas of the city that are not targeted because they have low population densities. This is mainly the objective to be optimized defined in Section 2 is the combined distance (see Eq. (1a)) that takes into account the population density of the clusters, and therefore, the method prioritizes the areas of the city with higher population densities.

Regarding the economical cost of deploying the solutions, Fig. 2 illustrates  $f_{BEST}$  values, i.e., the combined distance, given the economical cost as blue circles. This figure can be seen as a Pareto Front of an optimization problem in which the combined distance and the economical costs are two objectives to be minimized. Thus, the points close to the red row represent the solutions with the best trade-off between these two objectives. The figure shows that for solutions with fewer charging points (left side of the figure), a smaller economical investment gets a higher improvement in the QoS metric than when there are already a considerable number of stations (right side of the figure).

Even though the considered economical cost model takes into account the cost of the infrastructure of the charging point and the cost of wiring the charging point the cost behaves as a linear monotonic function increasing with respect to  $M_s$  because the cost of the infrastructure is significantly higher than the wiring cost and contributes much more to the cost of the proposed solution.

Results computed by the exact method are compared against the previous EA, for  $M_s = \{10, 20, 30, 40, 50\}$  [6]. Table 2 reports the mean GAP between the

12 C. Risso, C. Cintrano, J. Toutouh, S. Nesmachnow

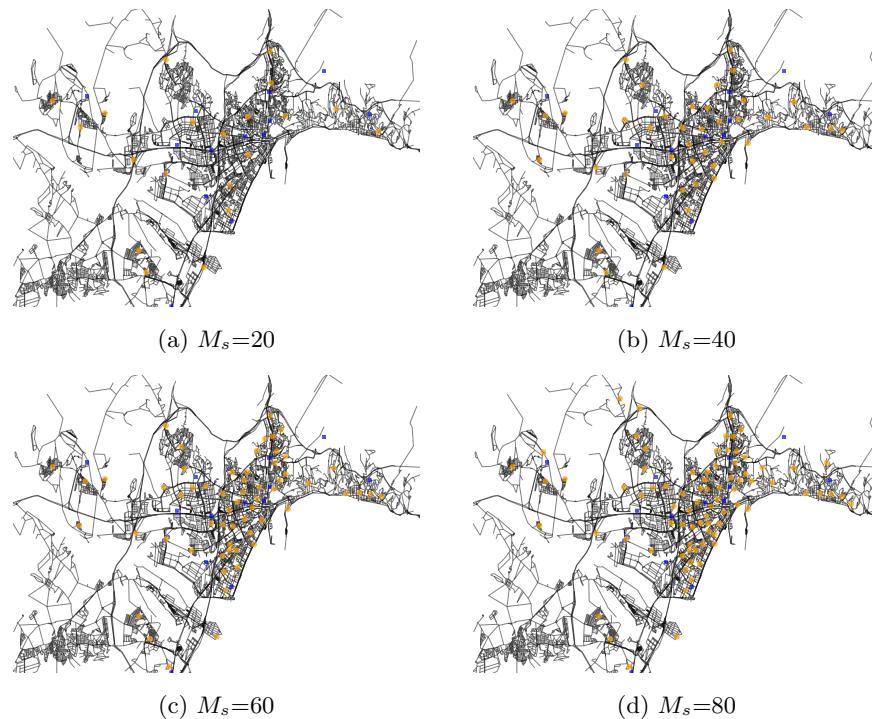


Fig. 3: Solutions computed by the proposed exact approach for the relaxed version of the problem over map of Málaga for different  $M_s$ .

exact solution and all computed solutions by the EA for the same  $M_s$ , and the best GAP, regarding the best EA solution. According to results in Table 2, the exact approach is better than the EA. The GAPs are always positive and they increase as  $M_s$  increases, takes advantage of installing more charging points.

Table 2: GAP between the proposed exact approach and the EA.

$M_s$	$D_c$ (m)	#variables	mean GAP	best GAP
10	8.000	6.298.967	1.90%	0.30%
20	7.000	5.394.820	6.63%	4.02%
30	6.500	4.932.345	10.72%	7.96%
40	6.000	4.453.698	13.91%	11.16%
50	5.000	3.482.353	17.74%	14.45%

Exact solutions are the same for the full version and the relaxed version of the problem for  $M_s$  from 20 to 59, because they fulfill the constraints. However, solutions found for the greater of values of  $M_s$  get slightly higher  $f_{BEST}$ , i.e., less competitive QoS. This behavior is because when the number of charging points in the instance does not exceed a given threshold (i.e.,  $M_s < 60$ ), the exact approach is able to locate the charging points in any place (as in the relaxed version of the problem), without exceeding power station limits. However, as  $M_s$  grows the exact approach distributes in a different way the charging points, because solutions for the relaxed version of the problem are not feasible (they do

Optimized location for electric vehicle charging infrastructure 13

not fulfill the power stations limit). Thus, the exact method in the full version locates the charging points in the way they are close to the high population areas but also the charging points are wired to different electric substations.

Table 3: Experimental results for the full version of the problem. Solutions when  $M_s < 60$  always match those reported in Table 1.

$M_s$	$f_{\text{BEST}}$	cost	$d_{\text{AVG}}$	$d_{\text{MAX}}$	$M_s$	$f_{\text{BEST}}$	cost	$d_{\text{AVG}}$	$d_{\text{MAX}}$
60	218186006	9234270	726.53	2492	61	215329466	9441040	724.06	2492
62	212473952	9503025	721.67	2492	63	209630320	9605145	718.43	2492
64	206886670	9669430	716.18	2492	65	204164705	9878155	713.23	2492
66	201485460	9989245	710.24	2492	67	199062686	10149210	702.93	2492
68	196482690	10369665	696.94	2492	69	194149274	10388870	692.76	2492
70	191808940	10638765	690.08	2492	71	189547679	10842545	683.74	2486
72	187337680	10935120	682.14	2486	73	185174678	11005040	677.40	2486
74	183092960	11431690	671.67	2496	75	181210543	11561180	667.88	2496
76	179358901	11665255	665.65	2496	77	177549296	11855350	662.02	2496
78	175741776	11946085	660.05	2496	79	173953074	12183330	655.01	2496
80	172232296	12439895	649.31	2496					

Fig. 4 shows the solutions deployed through the city for  $M_s = 60$  and  $M_s = 80$ . These two solutions distribute more the charging points over the city in comparison with the solutions computed for the flexible version of the problem (which concentrate most of the charging points in the same Downtown locations).

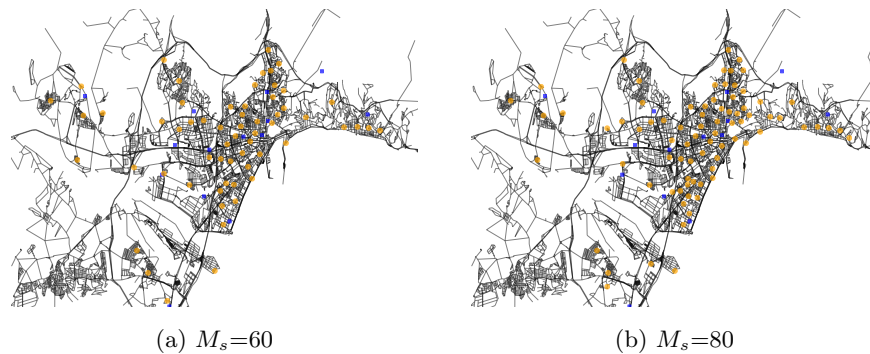


Fig. 4: Solutions computed by the exact approach for the full version of the problem over map of Málaga for different  $M_s$ .

Fig. 5 plots ( $f_{\text{BEST}}$ ) and economical cost results. Blue circles illustrate identical solutions for both versions of the problem, while gray squares represent different solutions. Whenever solutions in both versions do not match, that of the full version must be higher since the other is its relaxation. Those differences exist for  $60 \leq M_s \leq 80$  only, but they are relatively negligible, and in fact, it is necessary to zoom into that range to notice any difference as is in Fig. 6.

14 C. Risso, C. Cintrano, J. Toutouh, S. Nesmachnow

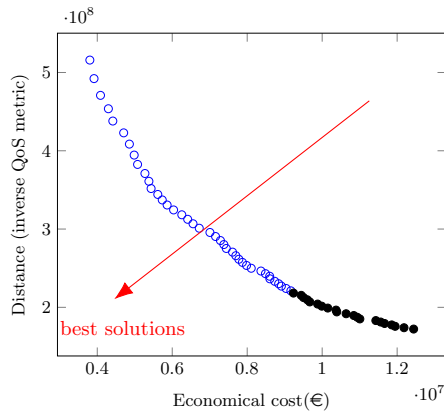


Fig. 5: Distance and the economical cost on restricted variation.

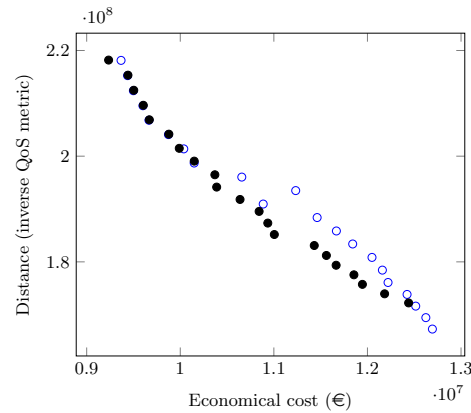


Fig. 6: Solutions of both problem variations ( $60 \leq M_s \leq 80$ ).

## 6 Conclusions and future work

Proposing efficient and effective networks of EV charging points has become a must in modern urban areas to allow easy adoption of sustainable mobility based on EVs. This article presented an exact optimization approach for solving a new variant of the EV-CSL problem defined on a real city, Málaga. This new variant is more realistic because it explicitly models the actual energy supply constraints and it takes them into account to compute the solutions.

Results of the experimental evaluation on a set of real-world instances of Málaga show that the proposed approach is competitive to address EV-CSL for the constrained and the flexible versions of the problem. The exact optimization approach based on ILP is able to automatically distribute the charging points along the city taking into account the real distribution of the tentative EV users, while optimizing the QoS of the whole charging points network.

Besides, the proposed exact approach has shown being more competitive than a GA proposed in previous research to address EV-CSL. It is able to improve the QoS by 17,74% in instances with 50 charging points.

The main lines for future work are related to improve the realism of the model by considering general citizen’s mobility behavior, the location of points of interest, and aspects related to the installation costs; to the definition of the EV-CSL problem by taking into account other objectives rather than QoS, such as installation costs; and to the definition of real instances over other cities.

*Acknowledgments* This research was partially funded by ANII and PEDECIBA (Uruguay), by the Universidad de Málaga, and by MCIN/AEI/10.13039/501100011033 under grant number PID 2020-116727RB-I00 (HUMove) .

## References

1. Bian, C., Li, H., Wallin, F., Avelin, A., Lin, L., Yu, Z.: Finding the optimal location for public charging stations—a gis-based milp approach. *Energy Procedia* **158**, 6582–6588 (2019)

2. Brandstätter, G., Kahr, M., Leitner, M.: Determining optimal locations for charging stations of electric car-sharing systems under stochastic demand. *Transportation Research Part B: Methodological* **104**, 17–35 (2017)
3. Çalık, H., Fortz, B.: Location of stations in a one-way electric car sharing system. In: 2017 IEEE Symposium on Computers and Communications (ISCC). pp. 134–139. IEEE (2017)
4. Cavadas, J., de Almeida Correia, G.H., Gouveia, J.: A mip model for locating slow-charging stations for electric vehicles in urban areas accounting for driver tours. *Transportation Research Part E: Logistics and Transportation Review* **75**, 188–201 (2015)
5. Chen, T.D., Kockelman, K.M., Khan, M.: Locating electric vehicle charging stations: Parking-based assignment method for seattle, washington. *Transportation research record* **2385**(1), 28–36 (2013)
6. Cintrano, C., Toutouh, J., Alba, E.: Citizen centric optimal electric vehicle charging stations locations in a full city: case of malaga. In: Conference of the Spanish Association for Artificial Intelligence. pp. 247–257. Springer (2021)
7. Fabbiani, E., Nasmachnow, S., Toutouh, J., Tchernykh, A., Avetisyan, A., Radchenko, G.: Analysis of mobility patterns for public transportation and bus stops relocation. *Programming and Computer Software* **44**(6), 508–525 (2018)
8. Falchetta, G., Noussan, M.: Electric vehicle charging network in europe: An accessibility and deployment trends analysis. *Transportation Research Part D: Transport and Environment* **94**, 102813 (2021). <https://doi.org/https://doi.org/10.1016/j.trd.2021.102813>, <https://www.sciencedirect.com/science/article/pii/S1361920921001164>
9. Frade, I., Ribeiro, A., Gonçalves, G., Antunes, A.P.: Optimal location of charging stations for electric vehicles in a neighborhood in lisbon, portugal. *Transportation Research Record* **2252**(1), 91–98 (2011)
10. Kumar, R.R., Alok, K.: Adoption of electric vehicle: A literature review and prospects for sustainability. *Journal of Cleaner Production* **253**, 119911 (2020). <https://doi.org/https://doi.org/10.1016/j.jclepro.2019.119911>, <https://www.sciencedirect.com/science/article/pii/S095965261934781X>
11. Lin, H., Bian, C., Li, H., Sun, Q., Wennersten, R.: Optimal siting and sizing of public charging stations in urban area. In: 2018 Joint International Conference on Energy, Ecology and Environment (ICEEE 2018) and International Conference on Electric and Intelligent Vehicles (ICEIV 2018). p. 7 (2018)
12. Massobrio, R., Nasmachnow, S.: Urban mobility data analysis for public transportation systems: A case study in montevideo, uruguay. *Applied Sciences* **10**(16), 5400 (2020)
13. Massobrio, R., Toutouh, J., Nasmachnow, S., Alba, E.: Infrastructure deployment in vehicular communication networks using a parallel multiobjective evolutionary algorithm. *International Journal of Intelligent Systems* **32**(8), 801–829 (2017)
14. Nasmachnow, S., Iturriaga, S.: Cluster-UY: Collaborative Scientific High Performance Computing in Uruguay. In: *Communications in Computer and Information Science*, pp. 188–202. Springer International Publishing (2019)
15. Rossit, D.G., Toutouh, J., Nasmachnow, S.: Exact and heuristic approaches for multi-objective garbage accumulation points location in real scenarios. *Waste Management* **105**, 467–481 (2020)
16. Wagner, S., Götzinger, M., Neumann, D.: Optimal location of charging stations in smart cities: A points of interest based approach (2013)

# Integration of Internet of Things Technologies in Government Buildings through Low-cost Solutions

Miguel Aybar-Mejía<sup>1</sup> [0000-0002-4715-3499], Deyslen Mariano-Hernández<sup>1</sup> [0000-0002-4255-3450],  
Jesús Coronado Marte<sup>1</sup> [0000-0002-9419-2626], Adrián Contreras<sup>1</sup> [0000-0002-2446-8738], Jimmy  
Arias<sup>1</sup> [0000-0003-1353-5429]

<sup>1</sup> Área de Ingeniería, Instituto Tecnológico de Santo Domingo.  
Santo Domingo, Dominican Republic.  
miguel.aybar@intec.edu.do

**Abstract.** Buildings have an untapped efficiency potential, being, on many occasions, government buildings present the most significant potential for energy savings. With the help of building energy management systems, this potential can be exploited, but due to the high cost that represents the implementation of these systems are not used in many buildings. This article aims to present a low-cost building energy management system based on Internet of Things technologies that can help take advantage of the efficiency potential that buildings have. The system implemented in this investigation consisted of a monitoring system that monitored different variables in real-time such as temperature, humidity, air quality, luminous intensity, and energy consumption. This system was implemented in a government building in the Dominican Republic, where the results showed opportunities for improvement. Many of these opportunities for improvement were impossible to know before the system implementation because there was no practical way to monitor them.

**Keywords:** Internet of things, IoT, energy efficiency, building energy management system, monitoring system.

## 1 Introduction

Energy efficiency is an issue that has gained critical pertinence in the preceding decade of the XXI century due to its significant environmental and economic role. Several nations have presented energy-effective techniques in their public-use buildings due to the increment in energy needs [1]. Energy efficiency levels have increased in the last years, but there is a critical unexploited energy efficiency potential in the building sector.

Buildings offer energy-saving opportunities with extraordinary potential since their performance level is far beneath current efficiency potentials [2]. The buildings sectors consumed 36% of the worldwide energy and almost 40% of CO<sub>2</sub> emission [3], [4].

Over the years, the search for systems to better manage energy has become mandatory. The development of energy management systems has been increasing due to

improving energy consumption [5]. The work of building energy management systems (BEMS) is known and significant since these systems can contribute to saving energy and reducing costs [6].

Internet of things (IoT) is a communication paradigm that imagines a future worldview where day-to-day existence items will be outfitted with a microcontroller and some communication protocol. For an IoT-based solution to be executed, it should be energy efficient, ready to communicate and share information across continued coverage [7].

The innovation of IoT has been generally evolved, and its utilization has been stretched out to buildings, security, business, social networks, and medical care. The innovations joining the IoT-based smart monitoring, for example, energy consumption [8] and environment monitoring, with human cooperation, have made a massive possibility inside a smart city setting to assist with working on human wellbeing and prosperity [9].

The sensor normalization in BEMS through IoT technologies and their coupling to more intelligent control systems are shaping the premise of smart buildings, giving better approaches to work on both reliability and performance [10].

There are successful studies that have integrated IoT technology into BEMS for the monitoring of different variables. Kelly et al. [11] presented an efficient implementation for IoT utilized for monitoring normal building conditions through a minimal expense pervasive detecting framework. Stavropoulos et al. [12] introduced a system for developing a university application, fusing an energy-effective sensor and actuator network, and a suitable Information Integration. Lehrer et al. [13] exhibited the efficacy of constant information observing and interactive information visualization in buildings to increase energy efficiency. Rahman et al. [14] proposed an architecture for a distributed blockchain-based IoT network for the smart building. Xing et al. [15] presented an intelligent energy-saving monitoring system for buildings based on the IoT.

This paper aims to present a methodology to implement a low-cost monitoring system based on IoT for building energy management systems in government buildings.

The rest of the paper is organized as follows. Section 2 shows the materials and methods used for the development of this research, Section 3 presents the case study, Section 4 discusses the results obtained by the systems, and Section 5 presents the conclusions.

## 2 Materials and Methods

Based on the literature review on studies using IoT and BEMS, which controllers were used were investigated. Before selecting the controller, the sensors were selected due to the need to know which types of sensors can measure variables such as temperature, humidity, air quality, light intensity, voltage, and the current was available.

Once the hardware to be used was selected, the components were programmed through Python. Additionally, the Firebase platform was used to develop the applica-

tion that would allow the monitoring system to be viewed in real-time and to record the measurements made by the sensors.

### 2.1 System Architecture

The architecture of the monitoring system is shown in Fig. 1. This research decided to create two subsystems using two single-board computers (SBC) to monitor the variables. One of the subsystems is in charge of the environmental variables, while the other subsystem is in charge of the electrical variables.

The environmental subsystem is composed of a single-board computer, a multiplexer for the I2C serial communication protocol, a light intensity sensor, and an environmental sensor to measure the variables of temperature, humidity, and air quality. In the case of the electrical subsystem, it is composed of an analog-to-digital converter, a voltage sensor, and a current sensor.

Both subsystems are connected wirelessly to the internal network of the building, which is connected to the internet. Through this connection, the monitoring system can be remotely viewed through a user interface.

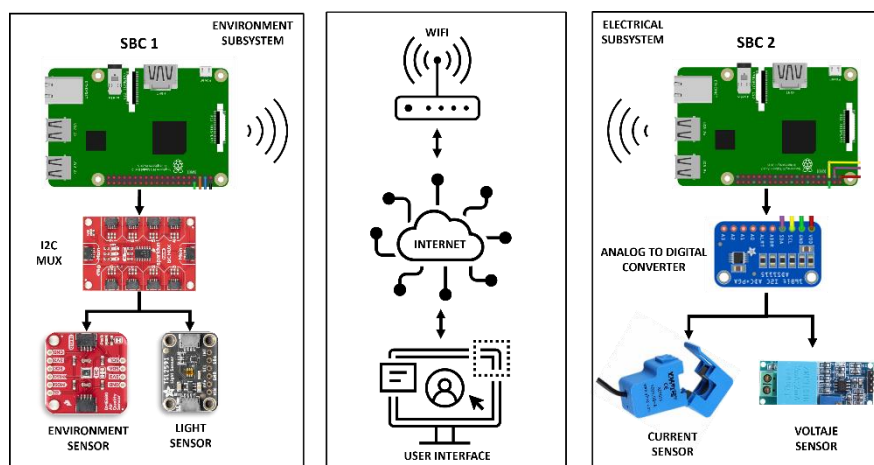


Fig. 1. Monitoring system architecture overview.

### 2.2 Hardware Description

The hardware selected for the monitoring system was the following:

- The SBC used was a Raspberry Pi 3B for both subsystems, which has a Quad-Core 1.2GHz Broadcom BCM2837 64bit CPU, 1GB RAM, BCM43438 wireless LAN and Bluetooth low energy onboard, and 40-pin extended GPIO.
- Sparkfun TCA9548A MUX is an 8 channel multiplexer that enables communication with multiple I2C devices with the same address.

- Adafruit TSL2591 is a digital light sensor configured to detect light ranges from 188  $\mu$ Lux up to 88,000 Lux.
- Sparkfun BME680, an environment sensor that allows measuring temperature, humidity, and indoor air quality. With an operating range of -40°C - 85 °C for temperature, 0% - 100% for humidity, and resolution of gas sensor resistance of 0.05% to 0.11%.
- Adafruit ADS1115, an analog-to-digital converter with 16-bit precision at 860 samples/second over I2C.
- YHDC SCT-013-000, a split-core current transformer that allows measuring a maximum current of 100 A.
- ANGEER ZMPT101B, a voltage sensor that can measure AC within 250V.

### 2.3 Software Programming

For the programming of the system, the steps shown in Fig. 2 were followed. First, the libraries required for the operation of the devices were imported. Second, the necessary functions for the connection of the devices were activated, such as activating the multiplexer ports. Third, the variables for all sensors were defined, and they were assigned to the controller's physical port. Fourth, the values received for the different sensors were normalized to be related to the measured variables. Fifth, the connection between the Firebase platform and the SBCs was made to store the data collected by the sensors and subsequently access them. Finally, a web application was programmed for users to view the data obtained by the monitoring system in real-time.

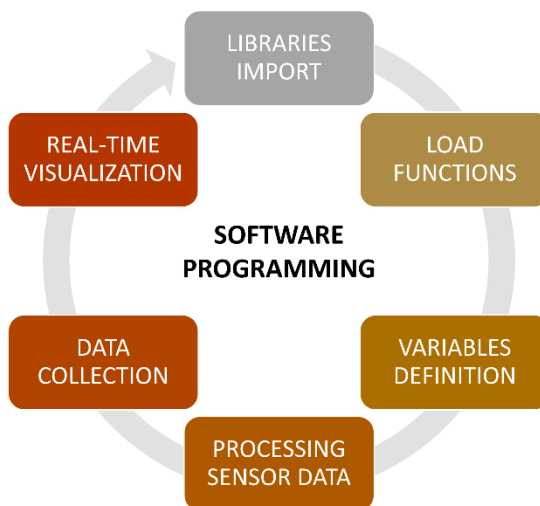


Fig. 2. Programming cycle of the monitoring system.

## 2.4 Real-Time Data Visualization

Through the Firebase platform, a web interface was created in which users could view in real-time the different variables recorded by the monitoring system. The user interface (see Fig. 3) consists of three display sections, (1) shows a trend graph of the selected variable, (2) shows a bar graph with the average value of each month, and (3) shows a table with the data recorded by the sensors.

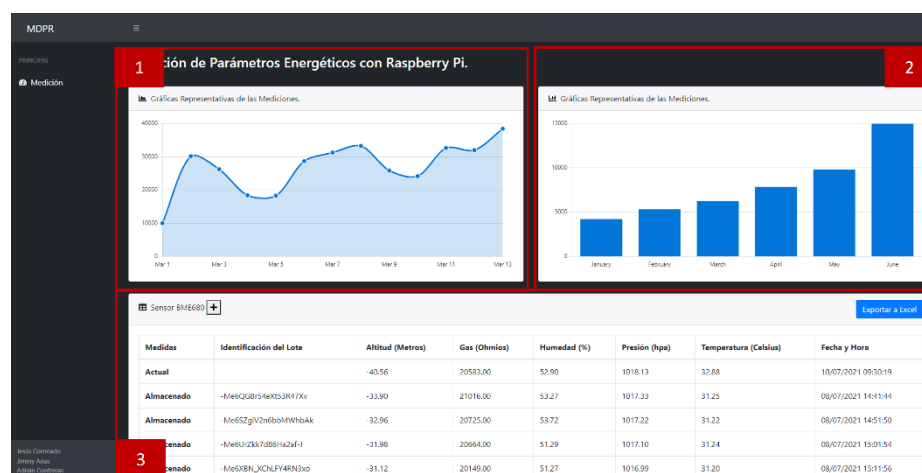


Fig. 3. Firebase user interfaces for real-time visualization.

## 3 Case of Study

### 3.1 General Description

In collaboration with the Ministerio de Trabajo (MT) of the Dominican Republic, a pilot application was carried out at the main headquarters. The MT is located at the following coordinates 18° 26'58.5 "N, 69° 55'37.8" W and has five levels of which, the first level is used for citizen service, and the other four are intended for offices (see Fig. 3).

For the case study, the customer service area located on the first level of the building was selected; the working hours of this area are Monday through Friday from 8:00 AM to 4:00 PM. This area was selected because it is the area with the highest circulation of people. The monitoring system was placed to measure the different variables during customer service hours to save energy and have better resources management.

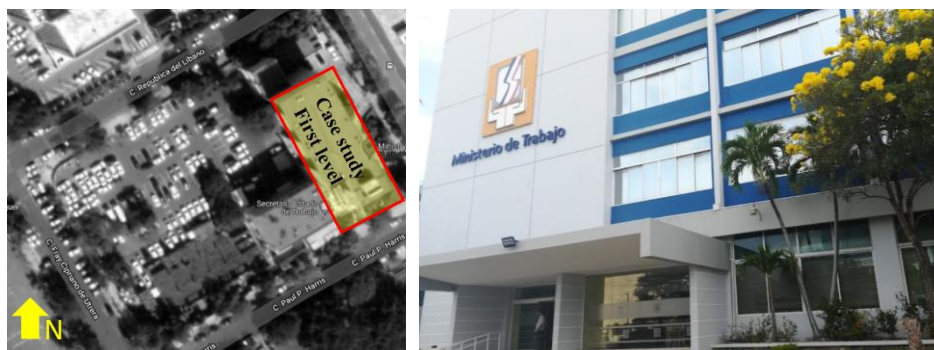


Fig. 4. Location of the building for the case study.

The data collection was carried out from June to July 2021. Fig. 4 presents the physical location of the subsystems, which were located in two different areas of the first level. The environmental subsystem was located in the customer service department, which has an area of 195 m<sup>2</sup>; the walls are made of cement with translucent windows that allow seeing the exterior of the building. For the air conditioning of the customer service area, two air conditioners units of five tons are used. The electrical subsystem was located next to the distribution panel that connects all the electrical loads, located in the first level's electrical room.

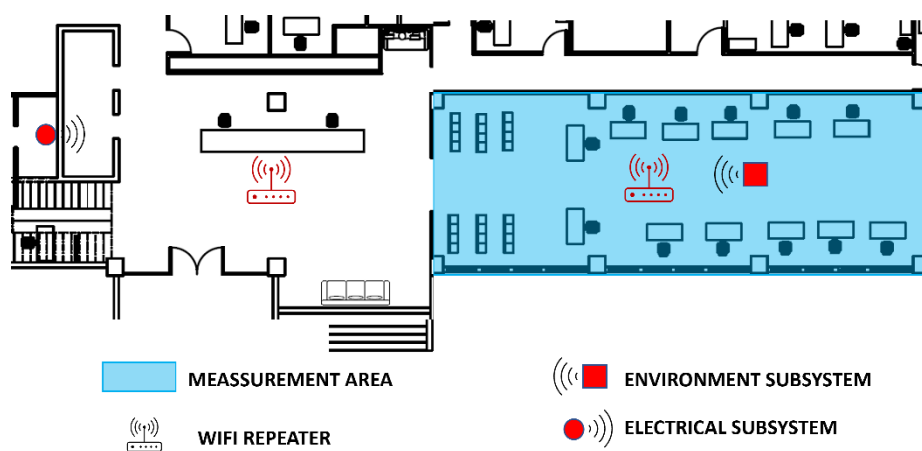


Fig. 5. The physical location of the environmental subsystem and the electrical subsystem.

#### 4 Results and Discussion

In the case of the air quality index, the higher the value, the higher the level of air pollution. According to the Air Quality Index Basics for Ozone and Particle Pollution [16], if the air quality value is 50 or below, the air quality is satisfactory. Fig. 6 shows

the data captured by the air quality sensor where it can be seen that the air quality index remains between 11-12 indicating good air quality.

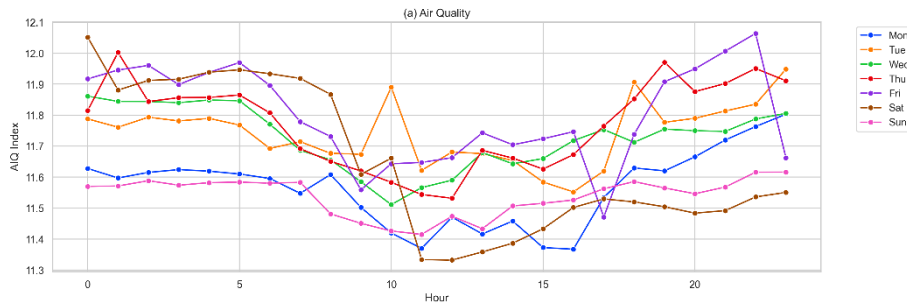


Fig. 6. Average air quality record for each hour of each day of the week.

Fig. 7 shows the values obtained from the temperature and humidity sensors, where it can be seen that the temperature during the operation of the system was between 30 °C and 33°C. It was verified if it was a system error, but after several validations, it was observed that within the area, there were problems with some windows that made the air conditioning units not achieve the desired temperature in the area.

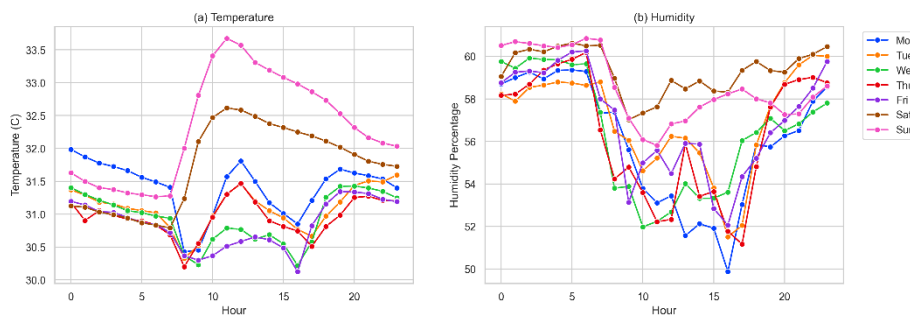
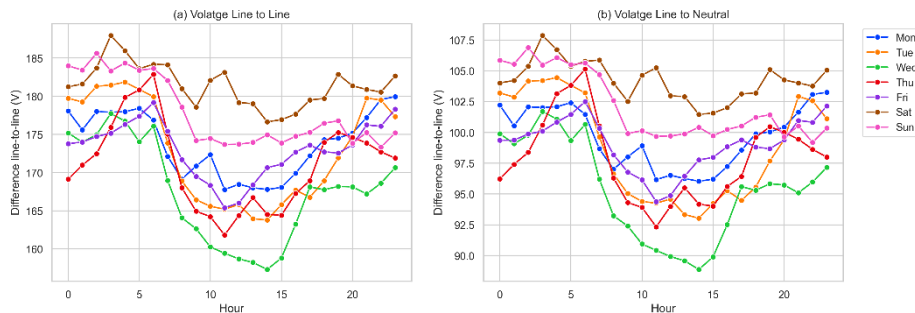


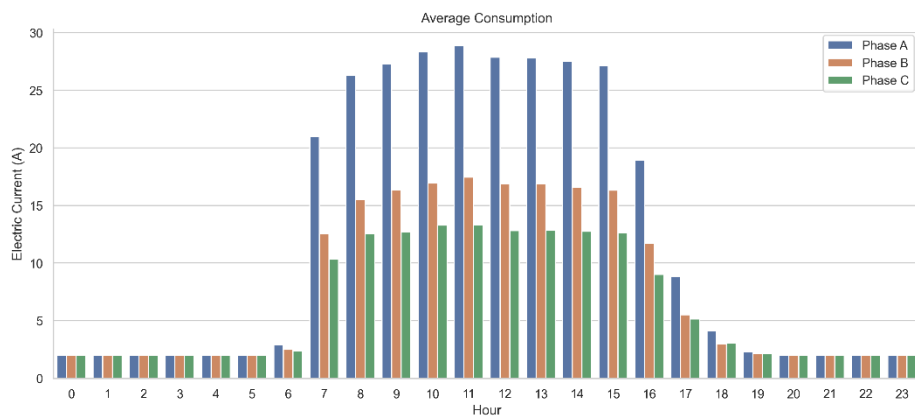
Fig. 7. (a) Average temperature and (b) average humidity for each hour of each day of the week.

Fig. 8 shows the recorded average voltage line to line values and phase voltage (line to neutral) with the study area. Both voltages present a voltage drop of approximately 20% of the nominal value. This voltage drop is far above the approved value of 3% that exposes the electric code of the Dominican Republic for charges interconnected in electrical panels [17]. In the same figure, it is seen as the voltage drop begins to increase as it starts the working day of the customer service area due to the electrical equipment that is used in that area.



**Fig. 8.** (a) Average voltage line to line and (b) Average voltage line to neutral for each hour of each day of the week.

Fig. 9 presents the values of electrical currents registered in each of the connected lines to the monitoring system. The behavior of the average current is observed for 24 hours. In the same way, an imbalance exists between phase A and the other phases (B-C) due to the excess load connected therein. This registered load imbalance is one of the factors that affects the voltage drop recorded in the study area.



**Fig. 9.** Average consumption of the three phases for each hour of each day of the week.

## 5 Conclusions

This case study demonstrated the advantages of applying an IoT system for energy management systems in government buildings. Although it is known that there are IoT technologies for EMS applications, but in the proposed case, it is present as an integrated system in government buildings that can use to record information on the state of energy quality and environmental conditions. The measurements showed the importance of using EMS systems in government buildings since they allow managers

and those in charge of building maintenance to detect areas where energy infrastructure improvements should be proposed.

Integrating the IoT system and the EMS allows seeing in real-time the consumption conditions of the building, allowing to detect energy consumption outside service hours, achieving a better demand management system within a specific area of any government building. This information served as a decision tool since they have presented some weaknesses in their energy system within the customer service area.

As future work remains, the integration of the IoT system to a 3G to 5G network allows, in case of failures or latency of the data network of the building, subsequent degradation, the system can continue to send the information to the database.

## Acknowledgment

Ministerio de Trabajo (MT) of the Dominican Republic for allowing this case study to be carried out in one of its service areas, in addition to the complementary information on the selected area.

## References

- [1] C. de la Cruz-Lovera, A.-J. Perea-Moreno, J.-L. de la Cruz-Fernández, J. Alvarez-Bermejo, and F. Manzano-Agugliaro, "Worldwide Research on Energy Efficiency and Sustainability in Public Buildings," *Sustainability*, vol. 9, no. 8, p. 1294, Jul. 2017, doi: 10.3390/su9081294.
- [2] Y. Sheiknejad, D. Gonçalves, M. Oliveira, and N. Martins, "Can buildings be more intelligent than users?- The role of intelligent supervision concept integrated into building predictive control," *Energy Reports*, vol. 6, pp. 409–416, Feb. 2020, doi: 10.1016/j.egy.2019.08.081.
- [3] Y. Sun, F. Haghighat, and B. C. M. Fung, "A review of the state-of-the-art in data-driven approaches for building energy prediction," *Energy Build.*, vol. 221, p. 110022, 2020, doi: 10.1016/j.enbuild.2020.110022.
- [4] A. Vishwanath, V. Chandan, and K. Saurav, "An IoT-Based Data-Driven Precooling Solution for Electricity Cost Savings in Commercial Buildings," *IEEE Internet Things J.*, vol. 6, no. 5, pp. 7337–7347, 2019, doi: 10.1109/JIOT.2019.2897988.
- [5] D. Bonilla, M. G. Samaniego, R. Ramos, and H. Campbell, "Practical and low-cost monitoring tool for building energy management systems using virtual instrumentation," *Sustain. Cities Soc.*, vol. 39, pp. 155–162, 2018, doi: <https://doi.org/10.1016/j.scs.2018.02.009>.
- [6] H. Doukas, K. D. Patlitzianas, K. Iatropoulos, and J. Psarras, "Intelligent building energy management system using rule sets," *Build. Environ.*, vol. 42, no. 10, pp. 3562–3569, 2007, doi: <https://doi.org/10.1016/j.buildenv.2006.10.024>.

- [7] T. J. Sheng *et al.*, “An Internet of Things Based Smart Waste Management System Using LoRa and Tensorflow Deep Learning Model,” *IEEE Access*, vol. 8, pp. 148793–148811, 2020, doi: 10.1109/ACCESS.2020.3016255.
- [8] A. R. Al-Ali, I. A. Zualkernan, M. Rashid, R. Gupta, and M. Alikarar, “A smart home energy management system using IoT and big data analytics approach,” *IEEE Trans. Consum. Electron.*, vol. 63, no. 4, pp. 426–434, 2017, doi: 10.1109/TCE.2017.015014.
- [9] M. Hossain, Z. Weng, R. Schiano-Phan, D. Scott, and B. Lau, “Application of IoT and BEMS to visualise the environmental performance of an educational building,” *Energies*, vol. 13, no. 15, p. 4009, Aug. 2020, doi: 10.3390/en13154009.
- [10] L. Linder, D. Vionnet, J.-P. Bacher, and J. Hennebert, “Big Building Data - a Big Data Platform for Smart Buildings,” *Energy Procedia*, vol. 122, pp. 589–594, 2017, doi: <https://doi.org/10.1016/j.egypro.2017.07.354>.
- [11] R. Bala and S. Aravind, “Towards the Implementation of IoT for Environmental vStatus Verification in Homes,” *Indian J. Public Heal. Res. Dev.*, vol. 10, no. 8, p. 591, 2019, doi: 10.5958/0976-5506.2019.01950.8.
- [12] T. G. Stavropoulos, A. Tsioliariidou, G. Koutitas, D. Vrakas, and I. Vlahavas, “System architecture for a smart university building,” *Lect. Notes Comput. Sci. (including Subser. Lect. Notes Artif. Intell. Lect. Notes Bioinformatics)*, vol. 6354 LNCS, no. PART 3, pp. 477–482, 2010, doi: 10.1007/978-3-642-15825-4\_64.
- [13] D. Lehrer and J. Vasudev, “Visualizing Energy Information in Commercial Buildings: A Study of Tools, Expert Users, and Building Occupants,” *Final Rep. to Calif. Energy Comm. Program.*, pp. 41-pp, 2011.
- [14] A. Rahman, M. K. Nasir, Z. Rahman, A. Mosavi, S. Shahab, and B. Minaei-Bidgoli, “DistBlockBuilding: A Distributed Blockchain-Based SDN-IoT Network for Smart Building Management,” *IEEE Access*, vol. 8, pp. 140008–140018, 2020, doi: 10.1109/ACCESS.2020.3012435.
- [15] L. Xing, B. Jiao, Y. Du, X. Tan, and R. Wang, “Intelligent Energy-Saving Supervision System of Urban Buildings Based on the Internet of Things: A Case Study,” *IEEE Syst. J.*, vol. 14, no. 3, pp. 4252–4261, 2020, doi: 10.1109/JSYST.2020.2995199.
- [16] AirNow, “AQI Basics | AirNow.gov,” 2019.
- [17] Superintendencia de Electricidad and I. D. de la C. Calidad, “Codigo Eléctrico Nacional de la República Dominicana. SIE-056-2016-MEMI,” Santo Domingo, Distrito Nacional, 2016. [Online]. Available: [https://sie.gob.do/images/sie-documentos-pdf/marco-legal/resoluciones-sie/2016/RESOLUCION\\_SIE-056-2016-MEMI\\_EMISION\\_CODIGO\\_ELECTRICO\\_NACIONAL\\_-1-\\_merged2\\_merged2.pdf](https://sie.gob.do/images/sie-documentos-pdf/marco-legal/resoluciones-sie/2016/RESOLUCION_SIE-056-2016-MEMI_EMISION_CODIGO_ELECTRICO_NACIONAL_-1-_merged2_merged2.pdf).

## Propuesta de Nuevas Tarifas con Opción de Precios por Tiempo de Uso para Clientes de la Cooperativa Eléctrica de San Pedro de Atacama en Chile

Jorge PÉREZ MARTÍNEZ<sup>1</sup> and Luis GARCÍA-SANTANDER<sup>2</sup>[0000-0002-6474-6528]

<sup>1</sup> Universidad de Concepción, Concepción. E. Larenas 219, CHILE

<sup>2</sup> Universidad de Concepción, Concepción. E. Larenas 219, CHILE  
jorgeperez2017@udec.cl luis.garcia@udec.cl

**Abstract.** En este trabajo se propone una alternativa tarifaria basada en el esquema de Precios por Tiempo de Uso (Time Of Use Pricing, TOUP), para los clientes de la Cooperativa Eléctrica de San Pedro de Atacama (CESPA) en el extremo norte de Chile. La propuesta considera el reemplazo de los actuales medidores electrónicos y electromecánicos por medidores inteligentes. Con esto se busca promover la Gestión De la Demanda (Demand Side Management, DSM), optimizando así tanto el uso de la energía eléctrica como el de la infraestructura disponible. La propuesta tarifaria reemplaza el régimen tarifario actual cimentado en tramos de consumo de energía y que no aporta incentivos para que los clientes realicen una eficiente gestión de su energía. La propuesta considera la conformación de franjas horarias y sus fórmulas tarifarias correspondientes, de modo de conseguir beneficios económicos tanto para los clientes como para la empresa eléctrica. Los casos de estudios consideran la operación de una planta Fotovoltaica (FV) de 2 MWp en el sistema eléctrico de CESPA, la que actualmente se encuentra en etapa de ejecución. Los resultados alcanzados reportan beneficios para todos los actores del mercado eléctrico. Para los clientes se alcanzan valores favorables de hasta un 19,1% de reducción mensual en las cuentas de electricidad, mientras que la empresa logra aumentos en sus ingresos mensuales promedios cercanos al 7,7%.

**Palabras clave:** TOUP, DSM, Medidores Inteligentes.

### 1 Introducción

Hasta el día de hoy, la mayoría de los hogares en Chile probablemente cuenta con un medidor electromecánico registrando el consumo eléctrico, y como bien se sabe, en estos equipos de medida la lectura del consumo eléctrico por parte de la empresa proveedora se realiza cada 30 días. Los precios de la energía que se establecen en las opciones tarifarias tradicionales son fijos durante las 24 horas del día, siendo éste el ejemplo para la tarifa residencial del sector regulado en Chile, denominada BT1 [1] y que también aplica para las tarifas por tramos de consumo en CESPA.

2

San Pedro de Atacama se encuentra aislada del sistema eléctrico nacional de Chile y por ende es CESPAs quien cumple el rol de generar y distribuir la energía eléctrica a los clientes tanto de San Pedro de Atacama como sus alrededores, asimilando el comportamiento de una microrred. Su planta de generación es térmica a base de Diésel y Gas Natural Licuado (GNL) con una capacidad instalada de 4 MW. Actualmente se encuentra en proceso de adjudicación la construcción de una planta FV de 2 MWp, la que permitirá diversificar la matriz energética actual y ampliar la capacidad total instalada a 6 MW. Según el registro de facturación del mes de febrero del 2020, CESPAs está encargada de proveer de energía eléctrica a un total 2.254 clientes, de los cuales 1.802 son clientes residenciales (80%) y 452 son clientes comerciales (20%). Todos ellos están adheridos a un régimen tarifario que está estructurado en 9 tramos de volumen de energía, donde el precio marginal se incrementa por la cantidad total de energía consumida, es decir, superado un cierto margen de consumo mensual, el precio de la electricidad se incrementa a un valor mayor por clasificarse en el siguiente tramo de consumo. La Tabla 1 muestra el régimen tarifario actual de CESPAs, el cual es una estructura plana que ofrece nulo incentivo, para que clientes realicen una real DSM.

**Tabla 1.** Estructura tarifaria actual de CESPAs.

Tramos	Rangos		Precio (\$/kWh)	Cargos Fijos	
	Desde (kWh/mes)	Hasta (kWh/mes)		Residencial (\$/mes)	Comercial (\$/mes)
<b>1</b>	0	120	196	2.500	5.000
<b>2</b>	121	240	220	2.500	5.000
<b>3</b>	241	360	257	2.500	5.000
<b>4</b>	361	480	273	2.650	5.200
<b>5</b>	481	600	291	2.750	5.350
<b>6</b>	601	720	307	3.250	5.450
<b>7</b>	721	840	324	3.500	5.700
<b>8</b>	841	1.080	341	3.750	5.950
<b>9</b>	1.081	99.999	357	4.000	6.200

La consecuencia del régimen tarifario actual de CESPAs se traduce finalmente en el perfil de demanda del sistema eléctrico. La Fig. 1 exhibe los perfiles de demanda en meses de diferentes estaciones como julio 2019 (invierno) y febrero 2020 (verano). Se observan cambios de hasta el doble entre la demanda mínima de 800 kW y la demanda máxima de 1.600 kW independiente de la estación del año.

Si se considera un cambio en los equipos de medición a medidores inteligentes [2], se puede entonces proponer a los clientes un conjunto de nuevas opciones tarifarias, que contemplen precios diferenciados según la hora del día en que esta sea consumida. Con precios horarios se incentiva a los clientes a consumir en las horas de menor costo. La incorporación de los medidores inteligentes permite considerar una Infraestructura de Medición Avanzada (Advanced Metering Infrastructure, AMI), la cual utiliza tecnología de comunicación bidireccional y la Internet de las Cosas (Internet of Things, IoT) para una periódica y sistemática medición, lectura, monitoreo y gestión de los consu-

mos eléctricos para grandes grupos de clientes. Es decir, promueve un mayor protagonismo de los clientes en la toma de decisiones como, por ejemplo, en la DSM por medio de tarifas horarias, lo que permite maximizar el recurso energético del sistema eléctrico.

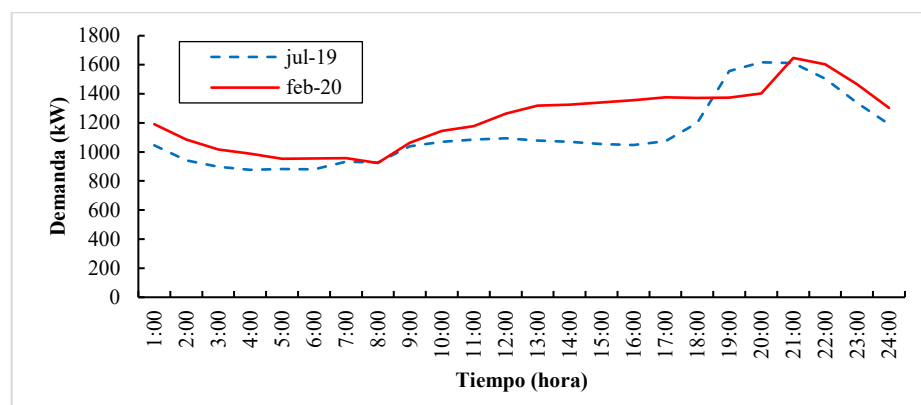


Fig. 1. Perfil de demanda promedio Julio 2019 (Invierno) y Febrero 2020 (Verano).

Este trabajo aprovecha la función de facturación horaria que pueden ser programada en los medidores inteligentes para con ello proponer un esquema de precios variables en el tiempo como lo es TOUP. El esquema de precio TOUP es una herramienta eficaz para implementar la DSM basada en precios para promover una adecuada gestión del perfil de demanda en los clientes [3]. De esa manera, con la presente propuesta se aspira a optimizar tanto el uso de la energía eléctrica como el de la infraestructura disponible, beneficiando tanto técnica como económicamente a la empresa CESP A y a sus clientes. El artículo se desarrolla como sigue. En la sección 2 se presenta una revisión bibliográfica de algunos de los esquemas tarifarios de tipo horarios o variables en el tiempo y que sirvieron para seleccionar la opción TOUP propuesta para los clientes de CESP A. En la sección 3 se modela la estructura TOUP, definiendo franjas horarias y niveles de precios para clientes residenciales y comerciales, junto con presentar las fórmulas tarifarias para cada uno de los cargos monetarios. En la sección 4 se exponen resultados con proyecciones económicas mensuales para los clientes y empresa CESP A al considerar la implementación de la propuesta tarifaria. En la sección 5 se presenta el análisis de los resultados, y finalmente en la sección 6 se muestran las conclusiones del trabajo.

## 2 Esquemas Tarifarios de Precios Variables en el Tiempo

Los esquemas tarifarios de precios variables en el tiempo se han discutido en la literatura desde hace bastante tiempo como una medida para aumentar la DSM a corto plazo en los sistemas eléctricos [4]. Esto se sigue naturalmente, porque el precio depende de la oferta y la demanda, y en este caso la DSM basada en precios, funciona de modo tal que optimiza la generación y consumo, para evitar la necesidad de inversiones costosas en la capacidad de producción y transmisión de los sistemas de energía.

4

La Fig. 2 muestra esquemas tarifarios variables en el tiempo. Estos son Precios en Tiempo Real (Real Time Pricing, RTP) donde los precios dependen directamente del mercado spot diario [5, 6], los Precios del Día Próximo (Day Ahead Pricing, DAP) donde los precios dependen del mercado del día antes de la subasta [7, 8], el esquema TOUP que es utilizado para la presente propuesta, los precios varían según las horas del día pero en niveles y períodos fijos [9, 10], y por último, el Precio Peak Crítico (Critical Peak Pricing, CPP) donde se pueden imponer precios más altos si el sistema está severamente restringido [11, 12]. Todas estas tarifarias son una opción diferente, a las tarifas planas donde los clientes pagan el mismo precio por la energía que consumen en cualquier momento, y, por tanto, no tienen ningún incentivo económico para modificar su perfil de uso.

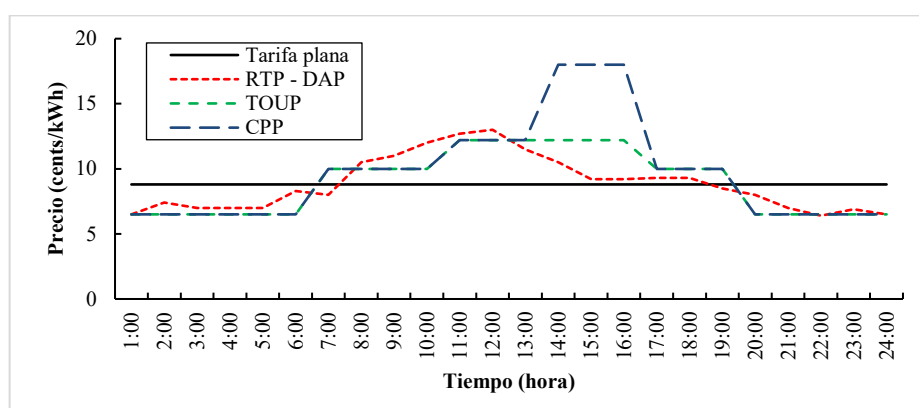


Fig. 2. Variación de precios según esquema tarifario [4].

## 2.1 RTP [5, 6]

La estructura tarifaria de RTP se articula en torno al precio real del mercado mayorista. Los clientes que tienen la capacidad de monitorear y participar activamente, ya sea reduciendo o cambiando su carga pueden aprovechar los bajos precios del mercado mayorista, de lo contrario, están sujetos a precios altos. Esto significa que los RTP suelen ser una base horaria en la que los precios se actualizan hora a hora. Es decir, RTP divide los precios en franjas de 24 horas, como se muestra en Fig. 2 donde se compara RTP y otras estructuras tarifarias variables en el tiempo con la tarifa plana. En cuanto a experiencias de implementación, este sistema ya se ha vuelto común en los países de la Unión Europea y Japón está siguiendo su ejemplo.

Por otro lado, cabe destacar que el esquema RTP es una opción ideal ya que vincula efectivamente las tarifas minoristas a los precios mayoristas fluctuantes. Sin embargo, el alto costo de instalación de un sistema para comunicar tarifas en tiempo real a los clientes y la falta de conocimiento entre los mismos son las principales barreras para implementar el esquema RTP que lo hace imposible en muchas áreas.

## 2.2 DAP [7, 8]

En esta estructura tarifaria a diferencia de RTP donde los precios se actualizan hora a hora (ver Fig. 2), con DAP, las empresas obtienen los precios del mercado por hora para las 24 horas del siguiente día operativo, cuando se despeja el mercado mayorista diario y los transmiten simplemente a los clientes sin margen. Los clientes de electricidad reaccionan a esta señal de precio, por ejemplo, cambiando su demanda de los períodos peak a los períodos no-peak. De esta forma se ayuda a reducir la relación entre el peak máximo y mínimo de la demanda eléctrica, aplanando la curva de carga. Un ejemplo claro de implementación de DAP ocurre en España donde se utiliza este esquema en el denominado Precio Voluntario para el Pequeño Consumidor (PVPC).

Por último, para implementar el esquema DAP en los clientes, se deben cumplir ciertas condiciones técnicas. Las infraestructuras de comunicación bidireccional y los medidores inteligentes son fundamentales. Además, conviene instalar controladores automatizados para gestionar de forma óptima el perfil de carga siguiendo la señal económica de DAP. Por lo mismo y al igual que RTP, el alto costo de instalación de un sistema para comunicar tarifas con precios del día próximo a los clientes y la falta de conocimiento entre los mismos son las principales barreras para implementarlo.

## 2.3 TOUP [9, 10]

Los programas TOUP son un híbrido entre una estructura de precios de tarifa plana y una estructura de RTP, ya que los precios varían a lo largo del día, pero a niveles y períodos fijos. Las tarifas de TOUP están predeterminadas para una vigencia mensual o trimestral y se basan en las tendencias generales de los precios al por mayor diarios y estacionales y no reflejan directamente los rápidos cambios de precios en el mercado mayorista. La mayoría de las estructuras de TOUP tienen dos o tres niveles (precio no-peak, precio medio-peak y precio peak) y donde la relación es de aproximadamente 2:1, 3:1, 4:1 e incluso 5:1 entre el precio peak y el precio no-peak. En Fig. 2 se muestra una estructura TOUP de tres niveles. En cuanto a la adopción del esquema TOUP en países y empresas del mundo, se puede decir que, actualmente es lejos el más empleado dentro de la categoría de tarifas con precios variables en el tiempo y la literatura lo respalda. Por ejemplo, se reportan experiencias en China, Reino Unido, Malasia y EE.UU.

Complementariamente, se puede decir que, para implementar el esquema TOUP no se necesitan tantos requerimientos técnicos y humanos como RTP y DAP, ya que aparte de la infraestructura AMI, sólo es necesario de instancias educativas o instructivas de parte de empresas para sus clientes, a modo de informar las novedades de este esquema tarifario, tales como franjas horarias y diferencias de precios entre ellas. Además, con un diseño adecuado, puede proporcionar una buena señal de precios a los clientes para beneficiar la operación del sistema eléctrico. Por tal motivo, el esquema TOUP es el seleccionado para introducir el concepto de tarifas con opción de precios variables en el tiempo para los clientes de CESP.

6

## 2.4 CPP [11, 12]

El esquema CPP es un mecanismo de precios dinámico basado en TOUP y RTP, ya que los precios varían a lo largo del día, pero a niveles e intervalos más estables. Al igual que TOUP, CPP tiene el mismo diseño de dos o tres niveles. Sin embargo, existe un precio de “peak crítico” adicional que excede el precio peak durante un número determinado de veces al año, incluso puede tener una relación de 15:1 entre los precios de un horario con peak crítico y no peak (ver ejemplo de Fig. 2).

Los precios de la energía en CPP, como diferencia adicional del esquema TOUP, es que la fijación de precios es más dinámica, pudiendo realizarse con anuncios de 24 horas de anticipación, y usualmente para pocas oportunidades al año. Y, las razones para declarar un día con peak crítico, pueden basarse por ejemplo en condiciones climáticas o algún desperfecto en la planta de generación que impida satisfacer a toda la demanda.

## 2.5 Experiencias en Países de Sudamérica

A nivel regional, se encuentran mayoritariamente aplicaciones con el esquema TOUP, que, dependiendo del país, son dirigidas a clientes residenciales y de mayor porte de consumo. En Tabla 2 se resumen dos experiencias sudamericanas en Brasil y Uruguay de implementación de tarifas TOUP junto con sus características fundamentales.

**Tabla 2.** Experiencias sudamericanas en tarifas horarias.

País	Tipo de Tarifa	Identificación Tarifaria	Componentes de Facturación	Segmento de Clientes
Brasil [13]	TOUP	Tarifa Blanca	<ul style="list-style-type: none"> <li>Energía (kWh)</li> </ul>	Residencial Rural Comercial Industrial
Uruguay [14]	TOUP	Doble Horario Triple Horario	<ul style="list-style-type: none"> <li>Energía (kWh)</li> <li>Potencia Contratada (kW)</li> </ul>	Residencial

## 3 Modelo de Estructura TOUP para CESPA

Aplicando la metodología TOUP, la empresa CESPA podrá considerar diferentes franjas horarias con precios diferentes para la energía, con ello los clientes tenderán a optimizar su consumo para reducir sus costos totales. Para ello, es necesario conocer primero que todo algunos principios de fijación de precios de energía de TOUP que fueron establecidos en [15] y así modelar la estructura de precios para los clientes de CESPA.

1. *Precio TOUP debe estar de acuerdo con el objetivo de DSM.* Significa que el precio de la energía de TOUP puede beneficiar a cualquiera o todos los clientes, las fuentes de energía y la sociedad, pero no puede dañar a ninguno de ellos.
2. *Principio de determinación de las particiones de franjas horarias.* Quiere decir que, las particiones de tiempo deben reflejar correctamente la curva de demanda característica del sistema, en especificado, el horario peak tiene que comenzar antes y terminar después de la presencia de la demanda máxima.
3. *Evitar riesgo de pérdidas en la empresa distribuidora.* Este punto invita a proteger el horario no-peak de menor costo económico para los clientes, para de esa forma no crear un desbalance en los beneficios de TOUP entre clientes y empresa.
4. *Principio determinante de la curva de respuesta del consumidor.* Significa que la respuesta del consumidor debe tenerse en cuenta para mejorar la señal precios en las tarifas TOUP.

Luego, hay que buscar y definir las franjas horarias y niveles de precios junto con los cargos y fórmulas tarifarias del esquema TOUP, siguiendo los principios estipulados.

### 3.1 Franjas horarias y Niveles de precios

No todos los clientes tienen el mismo perfil de demanda a lo largo del día. Por ello es imperativo tener diferentes franjas horarias y niveles de precios para cada tipo de cliente, y en CESPAs se tienen dos grupos de clientes, los residenciales y los comerciales. Para definir las franjas horarias y niveles de precios para cada grupo de clientes se realiza un análisis de la demanda eléctrica del sistema en un período de doce meses lo que permite conocer el perfil del consumo de los clientes para diferentes meses del año.

La Fig. 3 muestra el perfil de demanda promedio entre los meses de abril 2019 a septiembre 2019. Mientras que la Fig. 4, considera los meses de octubre 2019 a marzo 2020. Se separan en dos grupos los meses del año para analizar el efecto estacional entregando información adicional para el estudio.

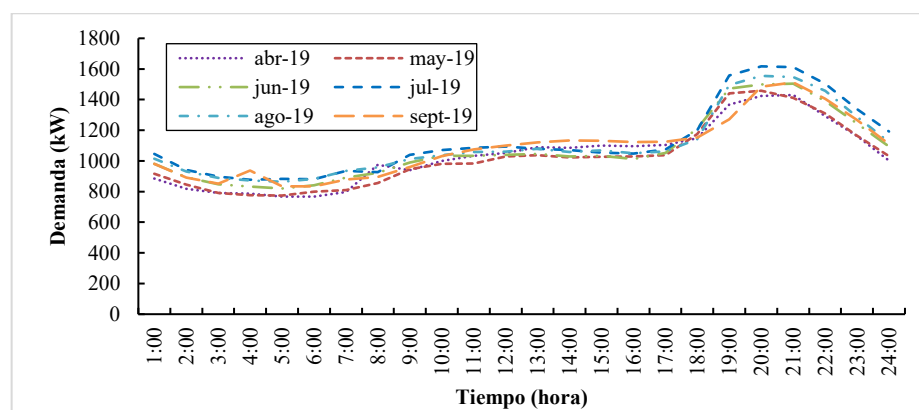


Fig. 3. Perfil de demanda promedio de Abr-19 a Sep-19.

8

De Fig. 3 se aprecia que el perfil de demanda entre los meses de abril 2019 a septiembre 2019 es muy similar en cada uno de estos meses y se divide en tres niveles distintos de potencia, demanda mínima, media y máxima respectivamente. La demanda mínima se hace presente entre las 24:00 y 07:00 horas y tiene un valor aproximado de 800 kW. En cuanto la demanda media aparece a continuación de la demanda mínima entre las 09:00 y 17:00 horas de cada mes y alcanza un valor superior a los 1.000 kW. Así también, podemos notar que la demanda máxima comienza aproximadamente a las 19:00 horas y finaliza a las 21:00 horas y en esta situación se obtiene a un valor notoriamente más grande de 1.600 kW en su punto más alto del mes de julio 2019.

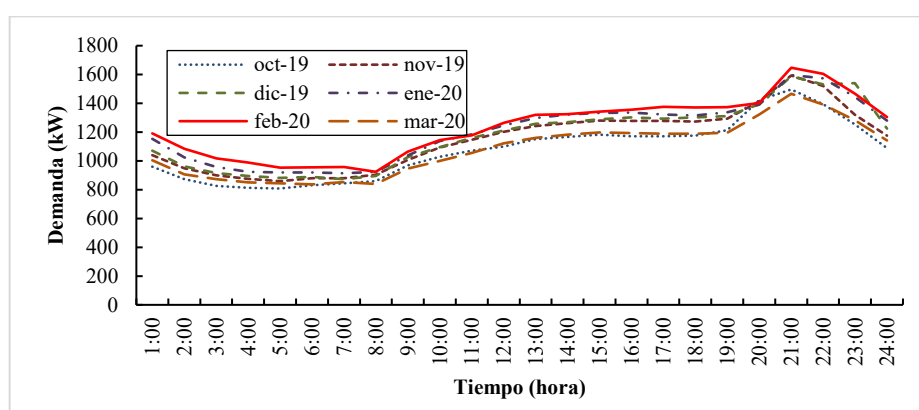


Fig. 4. Perfil de demanda promedio de Oct-19 a Mar-20.

De manera similar la Fig. 4 muestra los perfiles de demanda para el período de octubre 2019 a marzo 2020, al igual que el caso anterior se identifican tres zonas. En este caso la demanda media alcanza un valor promedio aproximado de 1.300 kW (13:00 a 20:00 horas), que se puede atribuir al efecto estacional con meses más ligados a la actividad del turismo en San Pedro de Atacama y al probable uso de artefactos de climatización por parte de los turistas que hacen que la demanda media sea más abultada. Mientras que la demanda máxima de 1.600 kW como en el mes de febrero 2020 comienza más tarde (20:00 a 22:00 horas), también a causa del efecto estacional donde en estos meses los días tienen más horas con luz natural. Por lo tanto, la demanda media y la demanda máxima se alcanzan en un horario más tardío. Las diferencias entre los valores mínimos y máximos son menos significativas que aquellos que se logran en los meses de abril 2019 a septiembre 2019.

Se hace importante destacar que los perfiles de demanda mostrados anteriormente se mantienen para cada día hábil, fines de semana y feriados. Las Fig. 3 y Fig. 4 representan la demanda total del sistema eléctrico, esto es consumo de clientes residenciales y comerciales, por lo que no es posible discriminar la demanda por separado. A partir de lo descrito en [16], se asume que la demanda máxima es ocasionada mayoritariamente por las actividades de los clientes residenciales. Y, De [17], se asume que el nivel de demanda media es propio de las actividades de clientes comerciales con perfiles de

carga de hoteles u hostales, centros comerciales como restaurantes y pequeños supermercados y oficinas de edificios. En Tabla 3 se plantean las opciones de franjas horarias y niveles de precios para clientes residenciales y en Tabla 4 para clientes comerciales.

En esta propuesta, cada grupo de clientes tendrá dos opciones para seleccionar en función del requerimiento de energía eléctrica. Por otro lado, por cada nivel de precios, existirá un cargo por energía consumida que se multiplicará por el consumo, en kWh, de cada franja horaria. Además, estos cargos reflejarán los valores de la energía y de la potencia que la empresa CESPА generará desde las tecnologías de generación y el costo de transportar la energía por las redes de distribución.

**Tabla 3.** Opciones de franjas horarias y niveles de precios para tarifas residenciales.

Opción TOUP	Nivel de precio	Franja horaria	
		abril - septiembre	octubre - marzo
Residencial A	Peak	18:00 – 22:59	19:00 – 22:59
	no-peak	23:00 – 17:59	23:00 – 18:59
Residencial B	Peak	19:00 – 23:59	20:00 – 23:59
	no-peak	24:00 – 18:59	24:00 – 19:59

**Tabla 4.** Opciones de franjas horarias y niveles de precios para tarifas comerciales.

Opción TOUP	Nivel de precio	Franja horaria	
		abril - septiembre	octubre - marzo
Comercial A	Peak	18:00 – 22:59	19:00 – 22:59
	medio-peak	08:00 – 17:59	08:00 – 18:59
	no-peak	23:00 – 07:59	
Comercial B	Peak	19:00 – 23:59	20:00 – 23:59
	medio-peak	09:00 – 18:59	09:00 – 19:59
	no-peak	24:00 – 08:59	

### 3.2 Fórmulas tarifarias

Las tarifas son fijadas garantizando precios que beneficien técnica y económicamente a los clientes, al sistema de energía en general y a la empresa CESPА. En Tabla 5 se exhiben las fórmulas para los precios unitarios por concepto de energía en kWh de las opciones tarifarias para clientes residenciales y de manera similar en Tabla 6 se proponen para los clientes comerciales.

**Tabla 5.** Fórmulas tarifarias para opciones TOUP residenciales.

Cargo por nivel de precio	Unidad	Fórmula	
Cargo por consumo de energía en horario peak	(\$/kWh)	$CPG_i^{HP} * FPD_i * FHP * FU$	(1)
Cargo por consumo de energía en horario no-peak	(\$/kWh)	$CPP_i^{HNP} * FU$	(2)

**Tabla 6.** Fórmulas tarifarias para opciones TOUP comerciales.

Cargo por nivel de precio	Unidad	Fórmula	
Cargo por consumo de energía en horario peak	(\$/kWh)	$CPG_i^{HP} * FPD_i * FHP * FU$	(3)
Cargo por consumo de energía en horario medio-peak	(\$/kWh)	$CPG_i^{HMP} * FPD_i * FHMP * FU$	(4)
Cargo por consumo de energía en horario no-peak	(\$/kWh)	$CPG_i^{HNP} * FPD_i * FU$	(5)

Para Tabla 5 y Tabla 6, en los horarios peak “HP”, medio-peak “HMP” y no-peak “HNP”. La variable CPG corresponde al costo promedio de generación que representa la inversión en la compra de combustibles y mantenciones para generar un kWh en las diferentes tecnologías de generación en CESP. La planta térmica tiene actualmente un costo de 114,9 (\$/kWh), y la futura planta solar FV tiene un CPG de 0,0684 (USD/kWh) [18], equivalentes a 53,5 (\$/kWh). La componente CPP, es el costo promedio de producción y a diferencia de CPG, corresponde a la inversión en la compra de combustibles y mantenciones y también, los gastos operaciones (sueldos de profesionales, técnicos y otros) en la producción de un kWh, y se aplica a la franja horaria no-peak de residenciales para prevenir riesgos de pérdidas económicas en la banda horaria más extensa de la propuesta TOUP. La variable FPD es el factor de pérdidas de distribución y se obtiene entre la energía generada y vendida, y no se aplica en las opciones residenciales para evitar un sobreprecio. Es importante resaltar que estas variables descritas en las ecuaciones (1) a (5), serán calculadas con relación al mes “i” anterior a aquel en que las tarifas resultantes serán aplicadas.

Por su parte FHP es el factor de horas peak. Corresponde a una relación de aproximadamente 2 a 5 veces entre el precio peak y el precio no-peak en las opciones TOUP residenciales y de 3 a 5 veces entre el precio peak y el precio no-peak en las opciones TOUP comerciales. La componente FHMP corresponde al factor de horas medio peak, y está dado por una relación de aproximadamente 2:1 entre el precio medio-peak y el precio no-peak en el caso de las opciones TOUP comerciales. Finalmente, la componente FU corresponde al factor de utilidad, que representa el margen de ganancia que la empresa proveedora CESP. va a obtener como mínimo por la comercialización de energía eléctrica, en este caso el 6% según la última modificación legislativa en Chile del año 2019 [19].

## 4 Resultados

En este apartado se muestran los resultados al aplicar la metodología propuesta. Se estudian escenarios de demanda considerando que la planta FV de 2 MW está operando junto a la actual planta térmica [20]. Los precios de energía eléctrica contemplan precios para las diferentes franjas horarias de las opciones TOUP de clientes residenciales y comerciales, considerando la variación de matriz energética dependiendo de la hora

del día. Además, las cifras son proyectadas bajo el supuesto que el esquema tarifario TOUP sustituye, en forma obligatoria las actuales tarifas por tramos de consumo en todos los clientes. Bajo estas condiciones, se cuantifican los ahorros y ganancia que provocará el esquema TOUP tanto para los clientes (residenciales y comerciales) como para la empresa eléctrica CESP.A.

#### 4.1 Precio de la Energía con las Opciones TOUP

La Fig. 5 resume la variación de precios por franjas horarias de la opción TOUP residencial A, tomando como ejemplo las tendencias de un mes como febrero 2020. Lo mismo se expone en Fig. 6, pero en la opción TOUP comercial A.

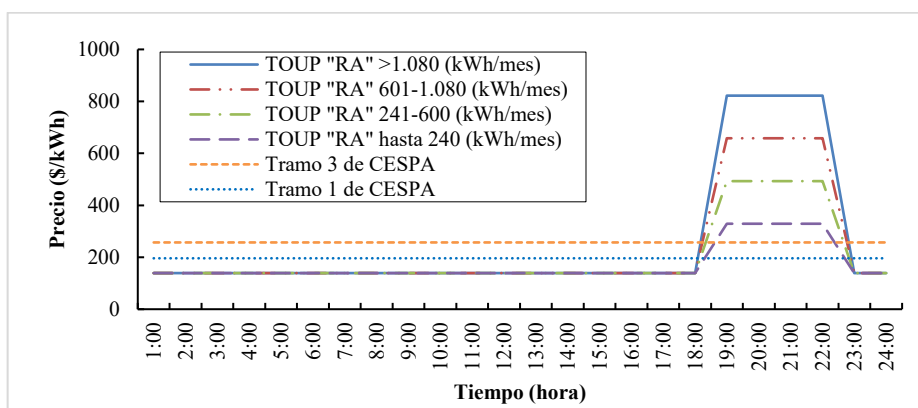


Fig. 5. Opción TOUP Residencial A vs Tramos de CESP.A en tendencias de Feb-20.

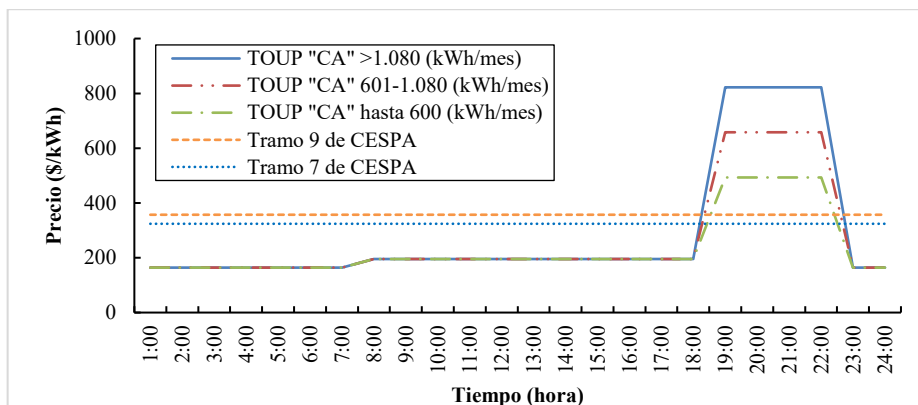


Fig. 6. Opción TOUP Comercial A vs Tramos de CESP.A en tendencias de Feb-20.

Tanto en Fig.5 como en Fig. 6, se tiene la existencia de una relación escalonada entre el precio peak y no-peak delimitado por el FHP de 2 a 5 veces y que varía de acuerdo con el volumen mensual de consumo en los clientes residenciales y comerciales.

#### 4.2 Variaciones para los clientes de CESPА con las opciones TOUP

En la proyección de ahorros para los clientes con las opciones TOUP, se suponen dos casos, el primero sin cambio de carga en los consumos de los clientes y un segundo con cambio de carga en dichos consumos. En este último caso, se supone en un 12% para los meses de abril a septiembre por contar con una hora peak más y en un 7% para los meses de octubre a marzo por contar con una hora peak menos, asumiendo en el primer grupo de meses, un mayor esfuerzo en los clientes para lograr una efectiva DSM. Esto se resume en Tabla 7 para los clientes residenciales y en Tabla 8 para los clientes comerciales, tomando en cuenta las tendencias de un mes como febrero 2020, donde una variación (+) implica aumento y una variación (-) implica reducción o ahorro en las cuentas de electricidad para los clientes.

**Tabla 7.** Variación en boletas para clientes residenciales con TOUP en tendencias de Feb-20.

Cliente Ejemplo de CESPА	Consumo (kWh/mes)	Boleta Real (\$)	horario peak (kWh/mes)	horario no-peak (kWh/mes)	Boleta TOUP Sin cambio (\$)	% Variación Sin cambio	Boleta TOUP Con cambio (\$)	% Variación Con cambio
Res1	120	23.520	35,6	84,4	23.402	-0,5%	22.928	-2,5%
Res2	142	31.240	42,1	99,86	27.693	-11,4%	27.131	-13,2%
Res3	358	92.006	106,2	251,8	87.287	-5,1%	84.648	-8,0%
Res4	439	119.847	130,3	308,7	107.036	-10,7%	103.801	-13,4%
Res5	491	142.881	145,7	345,3	119.714	-16,2%	116.096	-18,7%
Com1 C.	29	5.684	8,96	20,04	5.723	+0,7%	5.603	-1,4%
Com2 H.	229	50.380	51,15	177,85	41.461	-17,7%	40.779	-19,1%

**Tabla 8.** Variación en facturas para clientes comerciales con TOUP en tendencias de Feb-20.

Cliente Ejemplo de CESPА	Consumo (kWh/mes)	Factura Real (\$)	horario peak (kWh/mes)	horario medio-peak (kWh/mes)	horario no-peak (kWh/mes)	Factura TOUP Sin cambio (\$)	% Variación Sin cambio	Factura TOUP Con cambio (\$)	% Variación Con cambio
Com1 C.	29	5.684	9,0	15,5	4,5	8.188	+44,1%	7.991	+40,6%
Com2 H.	229	50.380	51,2	116,3	61,5	58.011	+15,1%	56.887	+12,9%
Com6 O.	601	184.507	107,7	381,3	112,0	163.589	-11,3%	159.983	-13,3%
Com7 C.	782	253.368	241,6	418,8	121,6	260.520	+2,8%	252.433	-0,4%
Com8 R.	1.078	367.598	333,0	577,3	167,7	359.131	-2,3%	347.983	-5,3%
Com9 H.	8.750	3.123.750	1.954	4.445	2.351	2.859.359	-8,5%	2.771.430	-11,3%

Además, con el fin de beneficiar a todos los clientes, se recomienda trasladar a los comerciales del tramo 1 y 2 (consumo  $\leq 240$  kWh/mes), hacia las opciones residenciales ya que, en primera instancia resultarían perjudicados (ver Tablas 7 y 8).

### 4.3 Variaciones para empresa proveedora CESPA con TOUP

Por otro lado, en la proyección de las ganancias, se supone un cambio de carga en el comportamiento del consumo total de los clientes del 12% para meses de abril a septiembre y 7% para meses de octubre a marzo como efecto de la señal de precios. Así también, las pérdidas del I<sup>2</sup>R se podrán reducir en aproximadamente un 1%. A partir de ello, y tomando como ejemplo el mismo mes de febrero 2020, en Tabla 9 se expone la variación de los ingresos para CESPA, sin trasladar a los comerciales de bajo consumo hacia las opciones residenciales, mientras que Tabla 10 exhibe lo propio, con trasladar a los comerciales de bajo consumo hacia las opciones residenciales.

**Tabla 9.** Variación en tendencias de Feb-20, sin trasladar a comerciales de  $\leq 240$  (kWh/mes).

Total por Ítem	Proyección TOUP		Real Obtenido		Variación (\$/mes)	% Variación
	(kWh/mes)	(\$/mes)	(kWh/mes)	(\$/mes)		
<b>Facturado</b>	607.078	166.456.673	607.078	201.107.119	<b>-34.650.446</b>	<b>-17,2%</b>
<b>Producción</b>	607.078	76.830.834	607.078	102.613.180	<b>-25.782.346</b>	<b>-25,1%</b>
<b>Pérdidas</b>	249.663	31.597.038	251.492	42.509.190	<b>-10.912.152</b>	<b>-25,7%</b>
<b>Ganancias</b>	-	58.028.801	-	55.984.749	<b>+2.044.052</b>	<b>+3,7%</b>
<b>Promedio Mensual en un Ciclo Anual</b>					<b>+7.096.955</b>	<b>+15,6%</b>

**Tabla 10.** Variación en tendencias de Feb-20, con trasladar a comerciales de  $\leq 240$  (kWh/mes).

Total por Ítem	Proyección TOUP		Real Obtenido		Variación (\$/mes)	% Variación
	(kWh/mes)	(\$/mes)	(kWh/mes)	(\$/mes)		
<b>Facturado</b>	607.078	162.714.216	607.078	201.107.119	<b>-38.392.903</b>	<b>-19,1%</b>
<b>Producción</b>	607.078	76.830.834	607.078	102.613.180	<b>-25.782.346</b>	<b>-25,1%</b>
<b>Pérdidas</b>	249.663	31.597.038	251.492	42.509.190	<b>-10.912.152</b>	<b>-25,7%</b>
<b>Ganancias</b>	-	54.286.344	-	55.984.749	<b>-1.698.405</b>	<b>-3,0%</b>
<b>Promedio Mensual en un Ciclo Anual</b>					<b>+3.461.460</b>	<b>+7,7%</b>

Complementariamente, se muestra el promedio mensual en un ciclo anual de la proyección de variación en el nivel de ingresos para la empresa CESPA, considerando las tendencias de los 12 meses estudiados inicialmente en los perfiles de demanda, de abril 2019 a marzo 2020. De esa forma, se considera también a los meses donde la empresa podrá ofertar una hora peak más de mayor costo, tomando en cuenta que, un mes como febrero (o cualquier otro de octubre a marzo), en la presente propuesta, el nivel de los ingresos será menor en relación con los meses de abril a septiembre.

### 4.4 Costo de Infraestructura AMI y Recuperación de Inversión

En Tabla 11 se expone el costo y tiempo estimado de recuperación de inversión por la infraestructura AMI necesaria para implementar las opciones TOUP. Para ello, se consulta con el proveedor de medidores inteligentes de la marca Aclara en Chile [21].

**Tabla 11.** Costo y recuperación de inversión para CESPA.

Mover comerciales $\leq 240$ (kWh/mes)	Inversión Total (\$)	Aumento Ganancias (\$/mes)	Tiempo Recuperación (mes)
No	423.707.400	7.096.955	60 meses
Sí	423.707.400	3.461.460	122 meses

## 5 Análisis de Resultados

Desde los resultados presentados, al analizar la variación de ahorros para los clientes en las tendencias de un mes como febrero 2020, se observa que al ser un mes favorable para los clientes por tener una hora peak menos de mayor precio, todos los residenciales sin y con cambio de carga lograrían una reducción mensual en sus boletas de electricidad, llegando hasta un 18,7% en el caso de los clientes del tramo 5 (ver Tabla 7). Mientras que, en los comerciales dependiendo de su volumen de consumo y perfil particular de su demanda, la mayoría también puede acceder a reducciones mensuales en sus facturas eléctricas, menos los clientes de clientes del tramo 1 y 2 (ver Tabla 8). Se recomienda trasladar a este grupo de clientes hacia las opciones residenciales para beneficiar a todos los usuarios, de esa manera, un comercial del tramo 2 pueda pasar de pagar un 12,9% más a pagar un 19,1% menos.

Así también, al analizar la variación en los ingresos para la empresa proveedora CESPA, se examina en el mismo mes de febrero 2020, y sin trasladar a los comerciales de bajo consumo hacia las opciones residenciales, la facturación total descendería en 17,2% por vender más barato, al mismo tiempo el costo total de producción bajaría en un 25,1% como efecto de los bajos costos de la generación FV, y también caería la valorización monetaria de las pérdidas en un 25,7%, lo que se proyecta en un aumento en las ganancias netas del 3,7% para este mes, pero esta cifra puede ser mucho mejor, si tomamos el promedio mensual en un ciclo anual, pudiendo la empresa ver un aumento favorable en su nivel de ingresos del 15,6% (ver Tabla 9). Y en caso de que la empresa acepte trasladar a los comerciales de bajo consumo hacia las opciones residenciales en las tendencias de un mes como febrero 2020, las ganancias se reducirían en un 3%, pero el promedio mensual en un ciclo anual se mantendría en positivo con un aumento en el nivel de los ingresos del 7,7% (ver Tabla 10).

## 6 Conclusiones

Se ha propuesto la metodología de TOUP para implementar nuevas opciones tarifarias para los clientes residenciales y comerciales de la empresa CESPA.

Los resultados alcanzados permiten obtener un menor costo mensual para la totalidad de los clientes y un mayor ingreso para la empresa proveedora CESPA.

Al aplicarse DSM los clientes alcanzan beneficios máximos de ahorros mensuales que van desde un 18,7% para los residenciales y de un 19,1% para los comerciales. Por su parte la empresa CESPA alcanza aumentos en sus ingresos en torno a un 7,7%. Y, además, CESPA podría recuperar la inversión en un tiempo máximo de 122 meses.

Una adecuada DSM permite trasladar entre un 7% y un 12% de la demanda máxima hacia otros bloques horarios, logrando suavizar la curva de la demanda total y optimizar el uso de la energía eléctrica y la infraestructura disponible en el sistema eléctrico.

## Referencias

- [1]. CNE.: Fija Fórmulas Tarifarias Aplicables a los Suministros Sujetos a Precios Regulados que se Señalan. Diario Oficial de la República, pp. 1-19, Santiago (2017).
- [2]. Alahakoon, D., Yu, X.: Smart Electricity Meter Data Intelligence for Future Energy Systems: A Survey. In IEEE Transac. on Indu. Informatics, vol. 12, no. 1, pp. 425-436 (2016).
- [3]. VanderKley, T., Negash, A., Kirschen, D.: Analysis of dynamic retail electricity rates and domestic demand response programs. In IEEE Conference on Technologies for Sustainability (SusTech), pp. 172-177, Portland (2014).
- [4]. Ghasemifard, M., Abbaspour, A., Parvania, M., M. Fotuhi-Firuzabad, M.: Incorporating time-varying electricity rates into day-ahead distribution system operation. In 14th International Conference on Environment & Electrical Engineering, pp. 193-198, Krakow (2014).
- [5]. Tachikawa, S., Yachi, T., Tanaka, T., Babasaki, T.: Economical evaluation of photovoltaic and battery systems under real-time pricing (RTP). In International Conference on Renewable Energy Research and Applications (ICRERA), pp. 264-268, Madrid (2013).
- [6]. Safdarian, A., Fotuhi-Firuzabad, M., Lehtonen, M.: Impacts of Time-Varying Electricity Rates on Forward Contract Scheduling of DisCos. In IEEE Transactions on Power Delivery, vol. 29, no. 2, pp. 733-741 (2014).
- [7]. Luo, G., Chen, Y., Zhao, Y., He, Y., Gong, C., Zhao, C.: Consensus-based Nodal Pricing Mechanism for Automated Demand Response Considering Congestion Management on Distribution Networks. In IEEE/IAS Industrial and Commercial Power System Asia (I&CPS Asia), pp. 575-580, Weihai (2020).
- [8]. Red Eléctrica Española, <https://www.ree.es/es/actividades/operacion-del-sistema-electrico/precio-voluntario-pequeno-consumidor-pvpc#>, last accessed 2021/04/01.
- [9]. Hussin, N. S., Abdullah, M. P., Ali, A. I. M., Hassan, M. Y., Hussin, F.: Residential electricity time of use (ToU) pricing for Malaysia. In IEEE Conference on Energy Conversion (CENCON), pp. 429-433 (2014).
- [10]. We Energies.: Plan de Precios Tiempo de Uso para Clientes Wisconsin, Wisconsin (2018).
- [11]. Huang, L., Xu, S., Wang, X., Huo, X., Zheng, H.: Dynamic optimized decision model of smart utilization for typical public building employing critical peak pricing. In China International Conference on Electricity Distribution (CICED), pp. 1-5, Xi'an (2016).
- [12]. Jose, A. A., Pahwa, A.: Economic evaluation of small wind generation ownership under different electricity pricing scenarios. In NAPS, pp. 1-4, Arlington TX (2010).
- [13]. ANEEL, <https://www.aneel.gov.br/tarifa-branca>, last accessed 2021/11/22.
- [14]. UTE, <https://portal.ute.com.uy/clientes/soluciones-para-el-hogar/planes-hogar/plan-inteligente>, last accessed 2021/11/22.
- [15]. Tang, Y., Song, H., Hu, F., Zou, Y.: Investigation on TOU pricing principles. In IEEE/PES Transmission & Distribution Conf. & Exposition: Asia & Pacific, pp. 1-9, Dalian (2005).
- [16]. Gruber, J. K., Prodanovic, M.: Residential Energy Load Profile Generation Using a Probabilistic Approach. In Sixth UKSim/AMSS European Symposium on Computer Modeling and Simulation, pp. 317-322, Malta (2012).
- [17]. He, L., Liu, N.: Load profile analysis for commercial buildings microgrids under demand response. 12th IEEE Conference on ICIEA, pp. 461-465, Siem Reap, Cambodia (2017).
- [18]. IRENA, <https://www.irena.org/costs/Power-Generation-Costs/Solar-Power>, last accessed 2020/12/01.
- [19]. Termómetro Antofagasta, <https://termometro.cl/2019/12/09/gobierno-logra-aprobar-ley-asegura-el-6-de-utilidades-a-empresas-distribuidoras-electricas/>, last accessed 2021/03/01.
- [20]. Ministerio de Energía, <http://solar.minenergia.cl/fotovoltaico>, last accessed 2020/12/01.
- [21]. Aclara, <https://www.aclara.com/chile/>, last accessed 2021/11/22.

## Smart Campus CIC-IPN

Ponciano J. Escamilla-Ambrosio<sup>[0000-0003-3772-3651]</sup>, Marco Antonio  
Ramírez-Salinas<sup>[0000-0002-9376-2893]</sup>, Jorge Iván Martínez-Badillo,  
Hugo Enrique Vega-Rivera, Maria Guadalupe Pulido-Navarro<sup>[0000-  
0002-5496-7044]</sup>.

Instituto Politécnico Nacional, Centro de Investigación en Computación, Ciudad de México,  
México

{pescamilla, mars}@cic.ipn.mx, gpulidon@hotmail.com

**Abstract.** In this paper, under the context of the development of Smart Cities, the Smart Campus CIC-IPN project is presented. The project is being implemented considering an Internet of Things architecture at the Computing Research Center of the National Polytechnic Institute. The development of the different subsystems in software and hardware elements that compose this approach are described. Those elements that we wish to implement in the future to lay the foundations of a comprehensive project aimed at developing a Smart Campus are also presented. As part of this project, the intelligent crosswalk is developed. This is a value proposition that seeks to improve the pre-existing pedestrian systems. On the other hand, advances in other projects are presented, such as the intelligent vehicular access control. Other subsystems that are still in the planning phase are described.

**Keywords:** Internet of Things, Smart Campus, Intelligent Pedestrian Passage, Intelligent Vehicular Access.

### 1 Introduction

From the moment that point-to-point connections took place and with it, the creation of the first computer network, the desire to expand beyond the frontiers of the way we communicate with other people, machines, and systems, has been the main driver of technological development and progress [1]. This project seeks to add to the efforts to expand the understanding of these barriers to transcend them and contribute to the national technological development in the field of the Internet of Things (IoT). Therefore, the main objective is to implement an IoT architecture where multiple subsystems work together efficiently leading to a Smart Campus at CIC-IPN.

The Internet of Things is the process of connecting everyday physical elements to the Internet: from common household objects, such as light bulbs and appliances, to healthcare resources, such as medical devices; it also includes wearables and personal items, such as smartwatches, and even traffic lights in cities. The term IoT refers to all physical device systems that receive and transfer data over wireless networks [2].

As evaluated by Porouhan and Premchaiswadi [3] and An et al. [4], the development of reliable and cutting-edge crosswalk systems, where new IoT technologies are applied, is still under development. These proposals aim to reduce the number of vehicular accidents and improve existing road systems' efficiency.

In addition to being IoT projects, Smart Campuses, as analyzed by Zhamanov et al. [5], are proposed as complementary solutions to improve the quality of life and efficiency of resources to increase the quality of life of all those inhabitants of Smart Cities.

In contrast to the previously mentioned works, which are presented as complementary and independent elements, the Smart Campus of CIC-IPN is presented as an integral IoT proposal where multiple subsystems are included.

To clarify the context of the present work, next definitions are presented:

### **Smart Cities**

Smart Cities are defined as the interconnection of systems that, by applying new technologies, seek to manage their resources, from the operation of public and private transportation to the efficient use of water and energy resources [6].

### **Smart Campus**

A Smart Campus seeks to bring and adapt the concept of a smart city to an educational ecosystem, which can benefit from the advantages and improvements that the IoT brings with it [7].

## **2 Smart Campus CIC-IPN Project**

The Smart Campus CIC-IPN project is a proposal whose improve traffic conditions, energy efficiency use, and adapting the development to the needs of the educational facilities of the Centro de Investigación en Computación (CIC, Computing Research Center) of the Instituto Politécnico Nacional (IPN, National Polytechnic Institute).

### **2.1 Smart Campus Elements**

The Smart Campus CIC-IPN concept contemplates the development of several subsystems, among which are the following:

- Intelligent pedestrian crossing (implemented).
- Intelligent traffic light (future work).
- Intelligent vehicle access control by facial recognition and vehicle license plate recognition (under development).
- Intelligent parking (future work)

Fig. 1 shows the general architecture of the Smart Campus CIC-IPN.

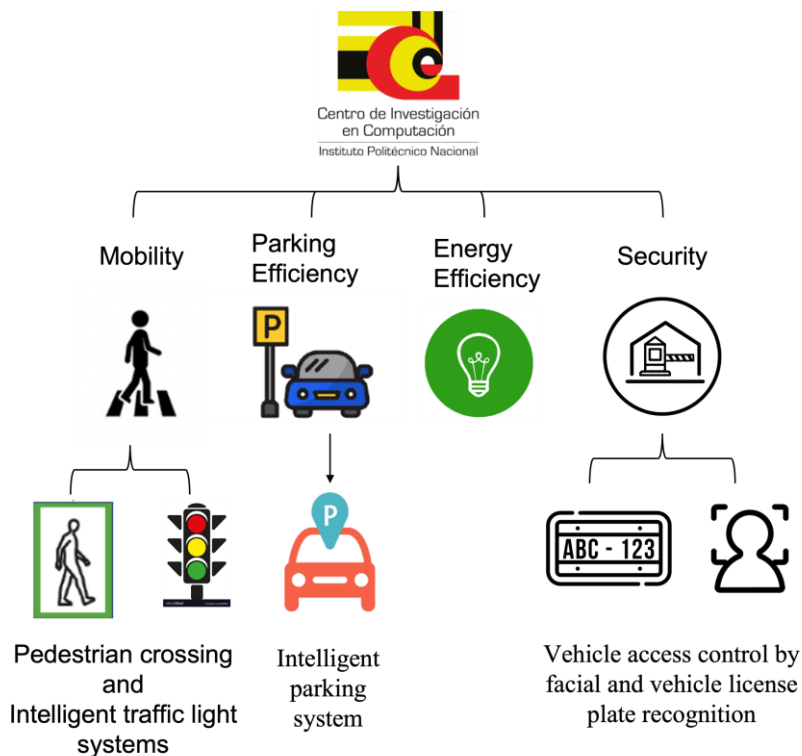


**Fig. 1.** General architecture of the smart campus IPN project.

The Smart Campus presented on this work, consists of 3 main subsystems: the intelligent pedestrian crossing, the intelligent parking and vehicular access control.

Firstly, the intelligent pedestrian crossing is composed of the crosswalk and the intelligent traffic light. The functionality of the former is explained below. The second will complement to the crosswalk, which will oversee detecting and tracking moving targets (future work).

Secondly, there is the intelligent parking, which consists of facial recognition access (on development).

Finally, the intelligent parking which is responsible for detecting and signaling available spaces within the parking lots (future work).

Energy efficiency is showed as a possible implementation according to the characteristics and possible scopes of the Smart Campus definition.

### 3 Intelligent Pedestrian Crossing System

#### Definition

A crosswalk is defined as the intersection area of the roadway enabled for pedestrians to cross and at which vehicle drivers or animals must stop to yield [8].

As part of the Smart Campus CIC-IPN project development program, an IoT-oriented crosswalk system was implemented at the crosswalk between the Escuela Superior de Cómputo (ESCOM, Computer Superior School) and the CIC, which seeks to improve the quality of vehicular traffic within the IPN facilities and the safety of its passers-by.

#### Location

The CIC is located at Av. Juan de Dios Bátiz s / n esq. Miguel Othón de Mendizábal, colonia Nueva Industrial Vallejo, Alcaldía Gustavo A. Madero, C.P. 07738, Mexico City, México. See Fig. 2. In its infrastructure, CIC has a building with a total constructed area of 9,768.8 m<sup>2</sup>, the property is 20 years old, it houses a total population of 383 users (before the pandemic). The building operates from Monday to Sunday, from 7:00 a.m. to 9:00 p.m., although it is an open-door building for its users, i.e., it is functional 24 hours a day, 365 days a year.



**Fig. 2.** Front view of the CIC.

The ESCOM is located at Av. Juan de Dios Bátiz s/n, colonia Nueva Industrial Vallejo, Alcaldía Gustavo A. Madero, C.P. 07738, Mexico City, Mexico, see Fig. 3. In its infrastructure, ESCOM has five buildings with a total built area of 17,172.71 m<sup>2</sup>. The property is 25 years old and has 386 fixed users and 2800 variable users (students). The operation of the building is from Monday to Saturday, from 07:00 am to 10:00 pm.



**Fig. 3.** Front view of the ESCOM.

The crosswalk where the intelligent was implemented is located between the CIC and ESCOM buildings (see Fig. 5 below).

### **3.1 Layers of the IoT Smart Crossing System**

The smart crosswalk is based on an IoT architecture composed of 3 layers. Perception layer, network layer and application layer. The elements and technologies that make up the smart crosswalk are explained below.

#### **IoT system layers**

##### **Perception layer**

- Outdoor multimedia content transmitter display, 1024 mm x 1024 mm with IP65 certification for outdoor use.
- Sonoff mini-internet-connected actuator device

##### **Network layer**

- Dual band Wifi 5 router.
- Mini PC with dual core Intel Celeron N2807 1.58 GHz processor, 2GB RAM, 500 GB hard drive, RJ-45 Gigabit ethernet port, 2 USB 2.0 ports and one USB 3.0 port. This PC had the hard drive replaced with a 250GB SSD, also the operating system was changed to Ubuntu.

**Application layer**

- Node-RED, programming tool for connecting hardware devices, API, and online services [9].
- Emqx broker, open source IoT MQTT messages based on the Erlang / OTP platform [10].
- Apache Server, open-source HTTP server for modern operating systems, including UNIX and Windows [11].
- Tasmota Firmware, custom firmware available for ESP8266 based devices [12].
- Protocols
- MQTT is a client-server publish/subscribe messaging transport protocol. [13].
- HTTP (Hypertext Transfer Protocol) is an application layer protocol for the transmission of hypermedia documents, such as HTML [14].

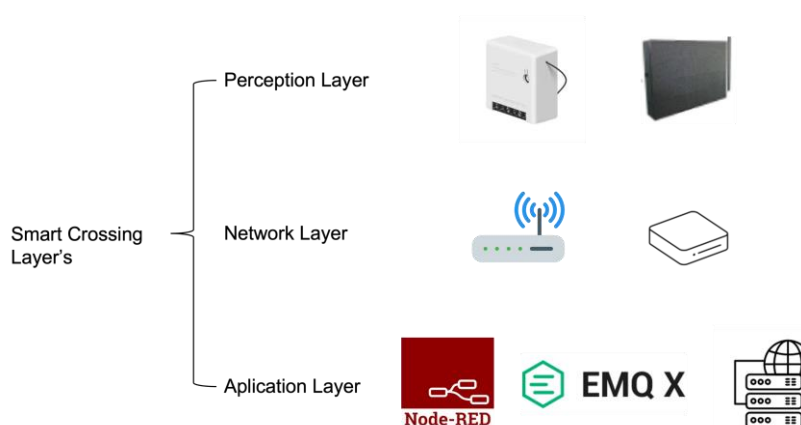


**Fig 4.** Smart Crossing Layer's.

**3.2 Operation**

The general functionality of the intelligent crosswalk is shown in Fig. 4. The pedestrian crossing request is made through two buttons placed on blue-painted pedestals at each end of the crossing. These buttons have an integrated Wifi device that sends the push signal to the network captured by a router. The request is processed in Node-Network [3], where a flow of nodes receives the request and activates a multimedia projection on three screens (see Fig. 5), located on each side of the crossing. The projection is an

animated traffic light, where the crossing of a white donkey (IPN's mascot) can be seen, and next to it, a 15-second counter allowing the pedestrian to cross. The projection of the traffic light is made through outdoor multimedia screens.

When there is no request from a pedestrian to cross the road, multimedia content is played on the screens (see Fig. 7). The multimedia content can be changed depending on what is needed to be projected. A particular node was developed and implemented for this purpose in Node-Red (see Fig. 6), which allows manipulating the duration and content to be projected, being able to project videos, images, etc. An integrated dashboard for the administration of the material to be projected on the screens is in the planning phase of development.

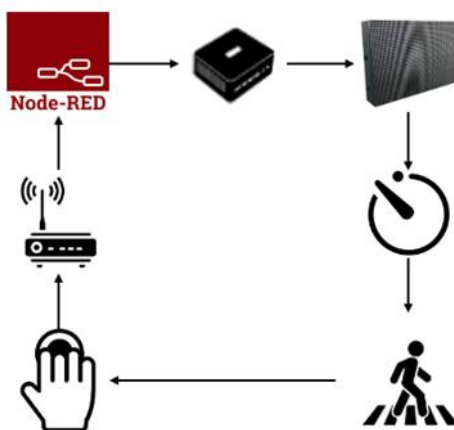


Fig. 5. Operation of the crosswalk.



Fig. 6. Screens placed at the crossing.

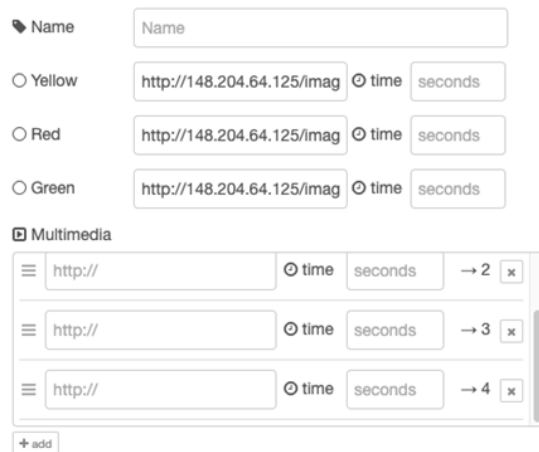


Fig. 7. Multimedia content node

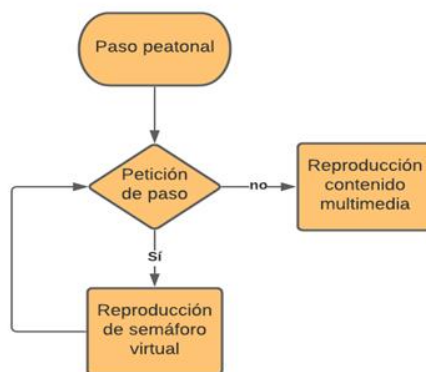


Fig. 8. System flow diagram.

#### 4 Intelligent Traffic Light System

The intelligent traffic light will be a complement to the existing crosswalk. It is desired to detect and predict the movement of pedestrians and vehicles using cameras mounted on each of the traffic light poles to determine the trajectory and movements of these. Hence, the system will be able to determine whether a pedestrian will use the crossing or not and, on the other hand, whether a vehicle must yield or not. It should be noted that the development of this subsystem is still in the planning phase because the best way to predict pedestrian or vehicle movement has not yet been determined.

## **5 Intelligent Vehicular Access Control System**

Access control consists of those permissions that an entity (person, vehicle, etc.) must make use of specific restricted or controlled resources.

Intelligent access control seeks to be a substantial upgrade to pre-existing access systems. It aims to integrate facial recognition and recognition of characters contained in the license plates of cars. Note: The resources required for the implementation of intelligent access and the choice of the best model to achieve facial recognition and recognition of characters contained in the license plates of cars have not yet been defined as multiple options are still under evaluation.

Is important to mention that all biometric and sensitive information, is properly trade. Users and employees, are aware of the destination and use of the information provided,

### **Location**

The intelligent access control will be located in the subway parking lot of the CIC's building (see Section 3, Fig. 2).

### **Operation**

The intelligent vehicular access control (see Fig. 9) will start with an actuator placed under the vehicle entry zone. When triggered, it will send an initialization signal via a Wi-Fi switch to the server, which will send the image request to the cameras placed at the side of the entry zone. These cameras will be placed so that the first one can capture the image of the vehicle's license plate, while the second one will capture the face of the incoming user to be sent to the server for processing. Subsequently, the characters in the license plate will be obtained, and the user will be identified using Python programming. It should be noted that duly registered users will be registered in a user control platform (still being planned). Once the images have been processed, the respective database will be searched to confirm that the user has the right to enter the building. Finally, the user will be allowed or denied access based on the previous point. The cases of authorization or denial of access are explained below.

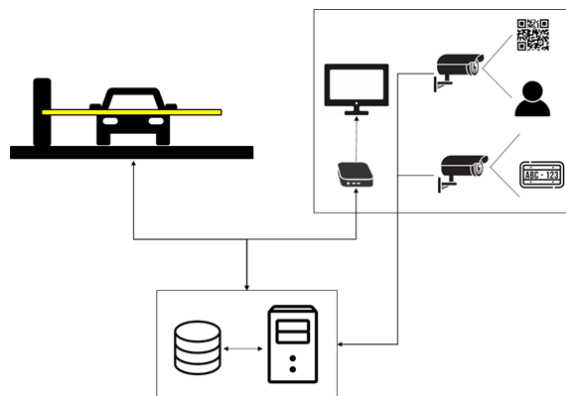


**Fig. 9.** Intelligent access operation diagram.

For the intelligent vehicle access control, multiple cases are contemplated in which access is allowed not only by using facial or license plate recognition. These access cases are described in Table 1 and described as follows:

**Table 1.** Parking access control cases for entry.

Case	User	Vehicle registration	Access code	Result
Regular user	V	V	F	V
Guest	F	V	V	V
User verification failed	F	F	V	V
User unknown	F	F	F	F

- Regular user case, where the user and the vehicle are successfully recognized and access to the parking lot is granted.
- Guest case where only the license plate is verified by the system, but the user has an access QR code. This case is contemplated when users are external to the registered users, and for some reason, enter the parking lot with the consent of the main user, owner of the vehicle.
- Case of failed user verification is when the user is duly registered, but for some reason has not been recognized by the system. The user will have the possibility to generate a unique access code to enter the parking lot.
- In the case of an unknown user where neither the user nor the vehicle has been recognized and there is no QR access code. In this case, access will be denied to the incoming user.

## 6 Intelligent Parking System

The intelligent parking will complement the intelligent vehicle access so that both together form a single intelligent parking solution.

The purpose of this will be to provide the user with a clear visualization of the available spaces in the different parking lots of the Smart Campus through visual guides placed in each one of the parking spaces. It should be noted that this system is still in the planning phase because it has not been possible to continue with the implementation of the immediately preceding subsystem, which is the vehicular access.

## 7 Conclusions

The Smart Campus project is an avant-garde proposal for the medium and long term, which seeks to increase the use of the road resources of the IPN and its schools. The project also brings with it the improvement of road quality that includes both pedestrians and drivers. By implementing state-of-the-art techniques and technology, the traffic safety of all those individuals that make up the Smart Campus is included as one of the main objectives.

One of the main challenges at the beginning of the project, was to plan and lay the groundwork for the project needs, because a complete infrastructure capable of sustain the growth and possible incoming additions was required. We had to migrate the web server services, MQTT broker among others, to a suitable server for the project. It was also necessary to configure and create a private network for the devices housed in the project. And finally, we design and create an appropriate data bases to store the amount of information we'll be recollecting along tests, monitoring and start up.

On the other hand, the possibility of collecting information according to the use of the campus facilities and the use of the different subsystems implemented will allow the evaluation of how the IPN resources are currently managed. This will allow the development and implementation of new and varied IoT subsystems oriented to new areas of daily life within the Campus. The Smart Campus concept can be applied to any desired area as mentioned initially, ranging from energy and water resources to perhaps measuring and monitoring the environmental quality of the educational classrooms. We believe that the development of this type of project will lay the foundations for a new era of development focused on the quality of life of those who inhabit a shared space considering the impact that human beings have on their environment. We hope that in the future, the awareness of our actions and how we affect our environment will allow us to change the excessive rate of consumption of resources that today dramatically affects our environment and, therefore, the planet.

## References

1. Madakam, S., Ramaswamy, R., Tripathi, S.: Internet of Things (IoT): A Literature Review. *Journal of Computer and Communications*, 3, 164-173, (2015).
2. Red Hat, <https://www.redhat.com/es/topics/internet-of-things/what-is-iot>, last accessed 2021/08/03.
3. Porouhan, P., and Premchaiswadi, W.: Proposal of a Smart Pedestrian Monitoring System based on Characteristics of Internet of Things (IoT), *International Conference on ICT and Knowledge Engineer-ing (ICT&KE)* 18, 1-4, (2020).
4. An, K., Jeong, Y. J., Lee, S., & Seo, D.: Smart Crossing System using IoT, *IEEE International Conference on Consumer Electronics (ICCE)*, 392-393, (2017).
5. Zhamanov, A., Sakhiyeva, Z., Suliyev, R., & Kaldykulova, Z.: IoT smart campus review and implementation of IoT applications into education process of university. *13th International Conference on Electronics, Computer and Computation (ICECCO)*, 1-4, (2017).
6. Batty, M., Axhausen, K., Giannotti, F., Pozdnoukhov, A., Bazzani, A., Wachowicz, M., Ouzounis, G., and Portugali, Y.: Smart cities of the future. *The European physical journal special topics*, 481-518, (2012).
7. Alghamdi, A. and Shetty, S.: Survey: toward a smart campus using the internet of things. *IEEE 4<sup>th</sup> International Conference on Future Internet of Things and Cloud*, 235-239, (2016).
8. *Diccionario Panhispánico del Español Jurídico*, <https://dpej.rae.es/lema/paso-de-peaton>, last accessed 2021/08/03.
9. Node-RED, <https://nodered.org/>, last accessed 2021/09/15.
10. EMQ, <https://www.emqx.com/en/about>, last accessed 2021/09/10.
11. APACHE HTTP SERVER PROJECT, <https://httpd.apache.org/>, last accessed 2021/09/03.
12. IoTRant, <https://iotrant.com/2018/10/18/what-is-tasmota-and-what-can-it-do-for-you/>, last accessed 2021/09/06.
13. MQTT, <https://mqtt.org/>, last accessed 2021/09/10.
14. Mozilla MDN Web Docs, <https://developer.mozilla.org/en-US/docs/Web/HTTP>, last accessed 2021/09/10.

# Visualization in Smart City Technologies

Teresa Cepero<sup>(✉)</sup>, Luis G. Montané-Jiménez<sup>(✉)</sup>, Edgard Benítez-Guerrero, and Carmen Mezura-Godoy

Universidad Veracruzana, Xalapa, México,  
marite\_cepero@live.com.mx, lmontane@uv.mx, edbenitez@uv.mx, cmezura@uv.mx

**Abstract.** Smart cities aim to use technology to connect people with information to make evidence-based decisions, use resources more efficiently, improve citizens' quality of life, and make cities more sustainable. Smart cities generate massive amounts of data due to a large number of embedded technology; although useful to achieve the city goals, these data are complex for people to manage. Data visualization is an efficient means to represent urban data and help people to understand the underlying information, uncover hidden patterns in data sets, and generate insights that support decision-making. This paper presents an overview of the usage of data visualization in smart city technologies, identifies the technologies used to visualize information, analyzes the visualization techniques, and offers an overview of the biggest challenges and future directions of visualization in smart cities systems.

**Keywords:** Visualization, Smart Cities, Dashboards, Literature Review

## 1 Introduction

Most cities are introducing technology into their infrastructure to gather data from the urban environment and their citizens that helps understand the city's situation. Real-time data from sensors capture environmental conditions such as noise, water, and air quality, as well as the dynamics that take place within the city, such as vehicular traffic. In addition to machine-generated data, people, processes, paperwork, business and government transactions can be a data source [48]. For example, government records and population surveys produce data on the size and characteristics of the population, such as demographics, employment statistics, crime rates, and well-being [51].

The transition from raw data to information has been simplified through technological tools. In particular, smart city technologies help integrate and analyze data from various sources to develop a comprehensive vision of the city [15]. Smart city platforms integrate the information of the urban environment elements to optimize the efficiency of the city's processes, activities, and services by joining various elements and key actors in an intelligent system [47]. In the face of the challenge of efficiently monitoring and interpreting large amounts of data, most smart city systems integrate visualizations to show the information in a visual and meaningful way to help users understand the information [28].

Smart city technologies enable the retrieve, analysis, and visualization of urban data in almost real-time [30]. However, data visualization in these environments represents a challenge, given the volume and diversity of the handled data. In recent years, there has been a technological and theoretical growth specialized in visualization in smart cities; however, the information is scattered. There have been reviews of the smart city literature [50,19,27], but these studies have focused on technology, data generation and analysis. Some studies [38,1,2,55] have addressed data visualization by reviewing some of the latest smart city projects; others have focused on visualizing a specific type of data or domain [63,43]. More analytical work is needed to integrate the dispersed knowledge of the field and provide an overview of the usage of visualization. In this paper, we present a literature review of visualization in smart city technologies that integrates and describes technological features, analyzes data visualization techniques, and offers an overview of the challenges in the field.

This document is organized as follows. Section 2 describes the methodology followed in the literature review. Section 3 presents the results of the study of data visualization in smart city technologies. Finally, in Section 4, the conclusions are presented.

## 2 Literature Review Methodology

This paper presents a structured literature review based on the guidelines proposed by Kitchenham [22]. The objectives of the study were to analyze the literature on visualization in smart city technologies, analyze the systems used to visualize information, review the visualization techniques most used to represent urban data, and offer an overview of the biggest challenges and future directions of visualization in smart city systems.

Based on the research objectives, the following keywords were defined as the most relevant for the research: information, data, visualization, decision support, urban data, and smart city. These keywords were used to create a search string connecting them and different synonyms of the words with the boolean operators “ AND ” and “ OR ”.

- (“information” OR “data”) AND (“visualization” OR “visualisation”) AND (“decision support” OR “decision making”) AND (“urban data” OR “smart city” OR “smart cities”)

The papers were searched using the search string in five specialized online databases: ScienceDirect, IEEE Xplore Digital Library, SpringerLink, ACM Digital Library, and Wiley. The search was made for titles, keywords, abstracts, and the body of the documents, without any specified time range. Table 1 shows the results of the resource identification process, 2 343 papers were found in total.

In order to evaluate the relevance of the identified papers, we selected articles in English or Spanish focused on data visualization in smart cities. The selection process was carried out in two stages. First, we selected a set of papers based on titles and abstracts. This first filtering of the documents helped establish which

**Table 1.** Results of the resource identification process

Databases	Identified papers	1st selection	2nd selection
ScienceDirect	1242	40	15
IEEE Xplore Digital Library	37	9	7
SpringerLink	540	37	10
ACM Digital Library	314	37	17
Wiley	210	2	2
<b>Total</b>	<b>2343</b>	<b>125</b>	<b>51</b>

studies were relevant and reduced the documents to 125. Based on the content analysis of the selected papers, another filtering was carried out to select the studies that help identify advances in information visualization in smart city technologies. This second stage reduced the total number of documents to 51 (see Table 1). Later, in the data extraction stage, an analysis of the literature was carried out based on the selected articles.

Based on the literature review, we analyzed the advances in data visualization for decision-making in cities, the visualization technologies used, visualization techniques used in smart city systems, and the challenges in the field. The next section presents the results of the analysis of the literature review of visualization in smart city systems.

### 3 Data Visualization in Smart City Technologies

The smart city concept aims to use information and communication technologies (ICT) to improve the functioning of cities and the quality of life of their citizens [4]. These cities are highly instrumented and interconnected, allowing the collection of data on multiple phenomena -both natural and social- through the use of satellites, sensors, cameras, smartphones, personal devices, the web, and other data-acquisition systems, including social networks as networks of human sensors [20,39,58].

The data generated in a city contributes to creating useful content for stakeholders, including local governments, businesses, citizens, and city visitors [23]. In order to get value from data, data analysis is necessary to extract useful information from the collected data, and visualization is key to conveying the information to stakeholders in an efficient way. For example, instead of viewing Madrid weather station logs and a list of geographic coordinates of places with free internet, a citizen might prefer to consult a dashboard that shows the weather forecast on a line chart and a map with the places with free WiFi.

In smart cities, technology is used to collect and analyze large-scale data in real-time, from which visualizations can be generated to monitor the city and make better decisions based on evidence [38,47]. Of the range of technologies used to make a city “smarter”, the most used technologies for visualizing urban data are smart city platforms, city dashboards, and the graphical interfaces of smart city systems.

### 3.1 Smart City Platforms

A smart city platform is a software that systematically collects, integrates, and analyzes urban data from different sources. This definition conveys the general concept of the smart city platform; however, there is no universally accepted definition. Some authors like [7,50,37,16] conceive the smart city platform as a middleware to build smart city applications. On the other hand, authors such as Ghosh [15] and Raj [44] define a smart city platform as software that collects and analyzes various data sources to generate information that promotes new knowledge that leads to better decision-making and optimized actions.

Smart city platforms provide information on the current situation in the city that is used to support short-term city management tasks. This short-term approach predominates in the literature and on the platforms available on the market (FIWOO, kaa, Thingsboard, and Ubidots) due to developments strongly oriented to real-time data sources, such as sensors and social networks. There are some attempts to analyze data from different time periods, such as Pettit's platform [40] that updates its information at different time intervals according to the updates of the data source, or the Zdravesk's platform [61] that collects data almost in real-time, in addition to monthly and annual information, such as economic indicators. However, so far, the main smart city development approach has been on real-time or near-real-time data [2].

The literature review shows that smart city platforms integrate and analyze data from various sources, and these platforms may or may not include data visualization. When the platform is designed as software that integrates and analyzes urban data to promote an understanding of the elements in a city [3,60,61,26,54,8], the smart city platform includes a user interface that displays the analyzed information. On the other hand, when the platform is designed as middleware [7,50,37,16], its architecture does not include a component to display the data -user interface-, but usually contemplates the connection to apps, dashboards, or other external systems to display the information.

### 3.2 City Dashboards

Another key smart city technology is the dashboard. A dashboard is a software characterized by having a predominantly visual interface that people use to monitor at a glance the most important information necessary to achieve one or more objectives [12]. The city dashboard or urban dashboard can have the mechanisms to collect, process, and analyze urban data [40], or access the information through services, such as a smart city platform. These integrate live data feeds from sensors, official and social media data into a single interface through data visualization [1].

The information contained in a dashboard varies in each city; however, the elements most commonly displayed in city dashboards are related to the following categories: transport, environment, statistics, economy, community, culture, and security [55]. Dashboards can present information from more than one category but not necessarily from all of them (see Fig. 1).

Based on a comprehensive analysis of city dashboards worldwide, Tong and Wu [55] summarize the six main characteristics of city Dashboards: recording, connectivity, sensing, interaction, adaptation, and integration. Recording refers to the process of saving all kinds of city data. Connectivity means creating seamless connectivity to the gathered data through all kinds of devices. Sensing refers to collecting data through sensors to perceive the city environment. Interaction refers to the way a user interacts with a system (and its data); this defines the content and structure of information presented; some ways of interaction are point selection, adding, zooming, and narrowing. Adaptation refers to the ability to personalize data products and services based on user needs. The integration enables integrating all kinds of information sources and services to display information on the dashboard [55].

City dashboards need data from the urban environment to display. There are multiple schemes (frameworks, indices, indicators, and rankings) of urban data to monitor and evaluate the performance of cities [52]. Most of these schemes are formed with a hierarchical structure of data, where each level is described by the results of the previous level. The hierarchical information structure of smart city schemes is commonly used for the analysis of urban data and its organization in dashboards. According to these organization, the relevant features of the city are organized into sections. Each section is defined by a series of composite indicators, which contain information from simple indicators.

Sharifi [52] analyzed the characteristics of 34 smart city schemes. The results of this study indicate that schemes have been developed under three approaches: market-oriented (to assess the competitive capacity of cities); research-based (schemes focused on the valuation of the smart city with scientific solidity); and schemes focused on the development of a smart city and the improvement of governance (to improve the understanding of data on smart city governance). Regarding the target audience of the schemes, the analysis shows that the target audience in decreasing order of frequency is: city authorities, police and decision-makers, the public, investors, smart city developers, and academia [52].

Data visualization through city dashboards serve to create a communication channel between data and people. So local authorities and citizens can easily explore data and take advantage of city information and infrastructure [55]. Yet, there has been little research concerning the optimum design for city dashboards that takes account of users' expectations and skills [59]. Professional designers and developers can improve city dashboard design to help citizens and government departments to monitor the city and foster technology adoption.

### 3.3 Smart City Systems

Smart city systems and apps process and analyze urban data to generate information that leads to developing an awareness of the current situation and acting based on it, taking optimized actions, and improving the provision of urban services [47,14]. Smart city systems have been proposed to address the challenges of different public services, such as traffic and transport control, air pollution



make activities more efficient, and users' information needs. With the aim of developing a next-generation parking management system, Dunne's projects [9] involve experts in transportation planning, computer science, urban planning, data analysis, and visualization in the design and development process.

In the last decade, research has focused on developing technologies that analyze urban data to optimize the monitoring of cities and improve the provision of services. A smart city platform is a software that systematically collects, integrates, and analyzes data generated in a city, which sometimes integrates data visualization. On the other hand, a city dashboard is a system that presents urban data visualizations to give an overview of the current situation in a city. Each city dashboard integrates different information according to the priorities of each city. Unlike city dashboards, smart city systems focus on a specific issue of a city, such as air quality monitoring, waste management, or monitoring of energy use in the city. The literature review of smart city systems [21,38,9,45,42,57,13,31] shows a wide use of data visualization to facilitate the monitoring of the data collected by sensors and different sources of information, detect patterns, and make decisions based on evidence.

### 3.4 Data Visualization Techniques

According to a study about smart city data, data can be classified as raw data -data collected from sensors, crowdsourcing, or city records- and enhanced data -data processed through analytics-. Data can also be classified according to their dynamism in static data related to the use of land, roads, and buildings; semi-dynamic related to cultural events, entertainment, and social networks; and dynamic, such as data collected by sensors used for weather and traffic [46]. Analyzing these data can be a difficult task for a person; visualization is an efficient mean to represent data and help people to understand the information [28].

The literature review shows that the use of traditional visualization techniques such as tables, bar charts, line charts, and scatterplots predominates in dashboard and smart city system interfaces, in addition to the wide use of maps to represent geospatial information. Table 2 presents the most common visualization techniques in smart city systems and their use.

Maps are the main technique used to represent data in smart city systems. According to a review of open data visualization by Eberhardt [10], the most commonly used map types are dot maps, pointer maps, route maps, choropleth maps, and heatmaps. These maps are used for a variety of purposes: for exploring the spatial dynamics of some attributes (dot maps and heatmaps), for easily locating elements and events in a city (maps with pointers), for understanding urban areas and comparing them (choropleth map), for analyzing transport routes and trajectories (route maps), among other uses. For all the advantages that maps offer to understand urban space, maps have been widely used to identify places of interest such as schools and restaurants; monitor the environment (water level, climate, air quality, etc.); and analyze public transport in the city.

Tables, bar charts, and line charts are other widely used visualization techniques in smart city systems. Tables are the second most used form of pre-

**Table 2.** Visualization techniques used in smart city systems

Technique	Usage	Papers
Map	-Exploring the spatial dynamics of an attribute	[38][30]
	-Locate elements and events of interest in the city	[57][28][34]
	-Understand the areas of the city and compare them	[30]
	-Monitor environmental variables	[57]
	-Analyze routes and trajectories	[6][45][53]
	-View the location of public transportation	[40]
	-View the location of sensors	[42]
	-Analyze changes in space over time	[63]
Choropleth map	-Represent information from predefined regions with clear boundaries. It is useful for making comparisons.	[17][24]
Flow map	-Show the movement of objects from one place to another.	[6][17]
Heatmap	-Analysis of the relationship between geographic characteristics and another measurement.	[38][6] [28] [40]
	-Presentation of quantitative values of two dimensions through a matrix using a color code.	[19][36]
Line chart	-Analyze the change in the values of different categories over time (time series).	[38][21][17][31] [19][36][60]
	-Analyze trends.	[30][49]
Bar chart	-Compare (quantitative) values by category.	[38][45] [17]
	-Present data by category.	[28][19][36]
Pie chart and Donut chart	-Show the percentage distribution.	[8][40]
Table	-Show the constituent parts that make up a whole.	[58][43]
	-Show data proportions.	[19][36]
Stacked Bar chart	-Show records.	[45][38][21]
	-Organize, relate and compare elements.	[40][42]
Scatterplot	-Show the composition of the data.	[8][19][43][35]
Buble chart	-Analyze the relationship between two variables.	[6][10][19][43]
Histogram	-Analyze the relationship between three variables.	[45][10][43][19]
	-Analyze the frequency or distribution of a variable over time.	[6][19][43]
Space Time Cube	-Analyze trajectories over time.	[38][63][6]
3D model	-Model the dynamic environment of a city.	[21]
	-Analysis of possible changes in the urban space.	[9]
Gauge chart	-Display the current value of an indicator relative to the best and worst target value of the indicator.	[30]
Treemap	-Show the hierarchical categories that make up a whole and their values.	[10][36]
Strip plot	-Show events over time.	[53]
Sankey Diagram	-Illustrate the flow of relationships, such as input vs output	[35]
Sunburst chart	-Show the composition of the organizational structure.	[58]
Spectrogram	-Overview of audio data.	[49]

sentation of information. The tabular display is a popular data representation technique due to the possibility of presenting multiple attributes and containing quantitative and qualitative data. However, analyzing the information contained in a table can be time-consuming and difficult, especially if the table is large; that is why in many of the smart city interfaces, the table is used to show a summary of the information - with a manageable number of records - or as an alternative to access more information on demand.

Bar charts and line charts summarize large data sets in an easy-to-interpret way. A bar chart is useful for comparing values by category - such as energy consumption by sector - while a line chart analyzes the change in values over time and detects any possible trends. Line charts are commonly used to analyze the evolution of indicators over time and present the values collected from sensors. For example, McArdle [30] used a line chart to plot Dublin home prices, population growth, and unemployment rates. On the other hand, [17] and Kim [21] used a line chart to display the hourly energy consumption records.

In addition to the traditional visualizations, new techniques have been developed to present multiple dimensions or variables. In recent years, efforts have focused on visualizing massive data with spatial and temporal properties [13,62,33,24,63,6]. For example, Moustaka [32] developed a visualization based on the Human DNA helix to represent the relationship between the different dimensions of a smart city. Fortini [13] proposed the Urban Transit Fingerprint visualization, which consists of a graph with associated geographic information, where different transport routes are represented. And Obie [33] presented a visualization to represent space-time attributes through a radial graph (to represent time) on top of a map (to represent space) and the color to describe the third attribute. Although these representations are exciting, animation techniques remain the most used strategy to represent changes in space and time [63,6].

To select a visualization technique, it is necessary to analyze the needs of the users and their goals to determine the objective of the visualization [36]. To perform this analysis, Grainger [18] proposed a framework for visualization in non-scientific professional contexts that offers a set of guidelines for a user-centered visualization design. The framework [18] is oriented to support the design process and does not offer sufficient guidance for selecting a type of visualization. On the other hand, Protopsaltis [43] proposed a set of rules for the selection of charts based on the number of variables (one, two, or multiple) and the objective of the visualization, which can be to analyze relationships, evaluate a distribution, compare data, and study a comparison. For example, Protopsaltis [43] recommends using scatterplots to analyze the relationship between two variables and using bubble charts for three variables. However, these guidelines are limited to statistical charts (bar chart, line chart, histogram, among others).

The revised visualization techniques enable synthesizing, organizing, and presenting the information collected in a city in a visual and meaningful way. Although data visualization libraries and tools currently facilitate the integration of visual representations in smart city technologies, there are still challenges to overcome to achieve greater growth and acceptance of smart city systems.

### 3.5 Discussion and Future Challenges

There are challenges in the different stages of the visualization process (see Fig. 3), from collecting data to implementing the visualizations and interpreting it. According to Eberhardt [10], access to data can be challenging. Although smart cities are characterized by integrating technology to collect data in real-time, there is a lot of information on paper that cannot be accessed. This historical or static data could be useful to complement real-time data [52].

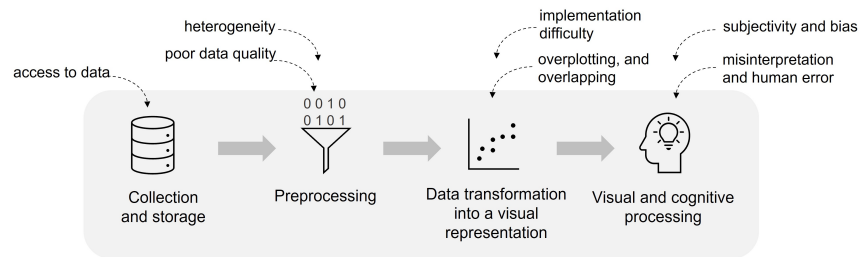


**Fig. 3.** Visualization challenges in smart city technologies.

In smart cities, there are different systems, services, and devices that generate and consume data [50]. Heterogeneity in data types and structures (unstructured, structured, and semi-structured) represents a challenge for cleaning, analyzing, and visualizing data [50,27,43]. In addition to heterogeneity, poor data quality is one of the most cited challenges in the literature [10,27,29]. If the data has not been cleaned, poor-quality data can lead to erroneous analysis and convey the wrong information through visualizations [29].

The large volume of data generated in a city can be difficult to display on a single screen due to space limitations and the perceptual capabilities of humans. Visualizing a large data set in a single chart can lead to data overloading, overplotting, and overlapping, making the visualization difficult to perceive and interpret [43]. Some possible solutions are reducing the size of points, making the points semi-transparent, binning the data into rectangles or hexagons, and showing a subset of points [5]. However, issues related to overplotting are still a common problem in big data visualization. That is why some researchers' efforts have focused on effectively visualizing big data.

Eberhardt [10] and Matheus et al. [29] report a gap between data visualization initiatives and stakeholders. There is low development and adoption of smart city systems due to a lack of technical knowledge, skills, and experience [10,11,29]. In order to bring smart city technologies closer to the citizens and government actors without technical knowledge, current projects incorporate interactive visualizations that enable dynamic data queries by visual manipulation (visual analytics). Visual analytics is the science that aims to provide techniques and tools for data analysis through visual interfaces [41]. Visualization and visual

analytics have been incorporated into most smart city systems since they allow efficient use of space and facilitate its use. However, implementing interactivity in visualizations can also be a challenge for developers of smart city systems [43].

Human intervention in the visualization process can involve some risks of subjectivity, bias, misinterpretation, and human error [29,43]. Although they are risks of human interaction, some of them can be caused by poor design and can be mitigated by creating effective visualization. In response to design and technology adoption challenges, studies of perceptual aspects and human-centered visualization design have increased in recent years.

The human-centered approach to smart city systems goes beyond visualization design. According to [56], the new generation of smart cities systems will be developed with a human-centered approach. These systems will serve to improve public services, meet the needs of citizens, improve governance, and promote sustainability. For the fulfillment of these objectives, visualization will help to see the problems, obtain key information, and choose better courses of action [56].

## 4 Conclusions and Future Work

This study presents a literature review of visualization in smart city technologies. This study analyzed visualization in smart city platforms, dashboards, and smart city systems and presented the most used visualization techniques and their use. The presented analysis of visualization techniques helps to see the options and may help designers and developers choose one method. The visualizations described are not infallible; a wrong visualization selection and poor design can lead to data misinterpretation and a bad user experience. To develop technological solutions that meet user needs and communicate information effectively and satisfactorily, we recommend iterative development -preferably user-centered- with evaluations at different stages of development to detect and correct possible design problems.

Visualization in smart cities is a growing area. Although some tools facilitate incorporating visualization in smart city systems, the visualization of massive data sets still requires more research, from strategies to visualize data effectively to the development of new algorithms and visualization methods for large-scale data. Analyzing the development of several smart city systems, we observed the lack of protocols for evaluating data visualization; some authors evaluate usability and others ease or difficulty of interpretation. That is why we consider the evaluation of visualizations an open issue. To facilitate the design of interactive visualizations in smart city systems, the analysis of city decision-makers' needs and the construction of a visualization framework are potential lines of research.

## References

1. Barns, S.: Smart cities and urban data platforms: Designing interfaces for smart governance. *City, Culture and Society* **12**, 5 – 12 (2018)

12 Cepero et al

2. Batty, M., Hudson-Smith, A., Hugel, S., Roumpani, F.: Visualising Data for Smart Cities, pp. 453–475. IGI Global (2018)
3. Bocconi, S., Bozzon, A., Psyllidis, A., Titos Bolivar, C., Houben, G.J.: Social glass: A platform for urban analytics and decision-making through heterogeneous social data. In: Proceedings of the 24th International Conference on World Wide Web. pp. 175–178. WWW '15 Companion, Association for Computing Machinery, New York, NY, USA (2015)
4. Camero, A., Alba, E.: Smart city and information technology: A review. *Cities* **93**, 84 – 94 (2019)
5. Chang, W.: R graphics cookbook: practical recipes for visualizing data. O'Reilly Media (2018)
6. Chen, W., Guo, F., Wang, F.Y.: A survey of traffic data visualization. *IEEE Transactions on Intelligent Transportation Systems* **16**(6), 2970–2984 (2015)
7. Cheng, B., Longo, S., Cirillo, F., Bauer, M., Kovacs, E.: Building a big data platform for smart cities: Experience and lessons from santander. In: 2015 IEEE International Congress on Big Data. pp. 592–599 (2015)
8. Chun, S.A., Lyons, K., Adam, N.R.: The smart city of newark, nj: data analytics platform for economic development and policy assessment. In: Anthopoulos, L. (ed.) *Smart City Emergence*, pp. 315 – 331. Elsevier (2019)
9. Dunne, C., Skelton, C., Diamond, S., Meirelles, I., Martino, M.: Quantitative, qualitative, and historical urban data visualization tools for professionals and stakeholders. In: Streitz, N., Markopoulos, P. (eds.) *Distributed, Ambient and Pervasive Interactions*. pp. 405–416. Springer International Publishing, Cham (2016)
10. Eberhardt, A., Silveira, M.S.: Show me the data! a systematic mapping on open government data visualization. In: Proceedings of the 19th Annual International Conference on Digital Government Research: Governance in the Data Age. dg.o '18, Association for Computing Machinery, New York, NY, USA (2018)
11. Evertzen, W.H.N., Effing, R., Constantinides, E.: The internet of things as smart city enabler: The cases of palo alto, nice and stockholm. In: *Digital Transformation for a Sustainable Society in the 21st Century*. pp. 293–304. Springer International Publishing, Cham (2019)
12. Few, S.: Dashboard confusion revisited. *Perceptual Edge* pp. 1–6 (2007)
13. Fortini, P.M.a., Davis, C.A.: Analysis, integration and visualization of urban data from multiple heterogeneous sources. In: Proceedings of the 1st ACM SIGSPATIAL Workshop on Advances on Resilient and Intelligent Cities. pp. 17–26. ARIC 18, Association for Computing Machinery, New York, NY, USA (2018)
14. Ghosh, D., Chun, S.A., Shafiq, B., Adam, N.R.: Big data-based smart city platform: Real-time crime analysis. In: Proceedings of the 17th International Digital Government Research Conference on Digital Government Research. pp. 58–66. Association for Computing Machinery, New York, NY, USA (2016)
15. Ghosh, P., Mahesh, T.: Smart city: Concept and challenges. *International Journal on Advances in Engineering Technology and Science* **1**(1), 25–27 (2015)
16. González-Briones, A., Chamoso, P., Casado-Vara, R., Rivas, A., Omatu, S., Corchado, J.M.: Internet of things platform to encourage recycling in a smart city, pp. 414–423. Elsevier (2019)
17. Gouveia, J.a.P., Seixas, J., Giannakidis, G.: Smart city energy planning: Integrating data and tools. In: Proceedings of the 25th International Conference Companion on World Wide Web. p. 345–350. WWW 16 Companion, International World Wide Web Conferences Steering Committee (2016)

18. Grainger, S., Mao, F., Buytaert, W.: Environmental data visualisation for non-scientific contexts: Literature review and design framework. *Environmental Modelling & Software* **85**, 299 – 318 (2016)
19. Habibzadeh, H., Kaptan, C., Soyata, T., Kantarci, B., Boukerche, A.: Smart city system design: A comprehensive study of the application and data planes. *ACM Comput. Surv.* **52**(2) (May 2019)
20. Harrison, C., Eckman, B., Hamilton, R., Hartswick, P., Kalagnanam, J., Paraszczak, J., Williams, P.: Foundations for smarter cities. *IBM Journal of research and development* **54**(4), 1–16 (2010)
21. Kim, S.A., Shin, D., Choe, Y., Seibert, T., Walz, S.P.: Integrated energy monitoring and visualization system for smart green city development: Designing a spatial information integrated energy monitoring model in the context of massive data management on a web based platform. *Automation in Construction* **22**, 51 – 59 (2012)
22. Kitchenham, B.: Procedures for performing systematic reviews. Tech. Rep. 0400011T.1, Keele University, Keele, UK (July 2004)
23. Lim, C., Kim, K.J., Maglio, P.P.: Smart cities with big data: Reference models, challenges, and considerations. *Cities* **82**, 86 – 99 (2018)
24. Liono, J., Salim, F.D., Subastian, I.F.: Visualization oriented spatiotemporal urban data management and retrieval. In: *Proceedings of the ACM First International Workshop on Understanding the City with Urban Informatics*. p. 21–26. UCUI '15, Association for Computing Machinery, New York, NY, USA (2015)
25. Liu, X., Nielsen, P.S.: Air quality monitoring system and benchmarking. In: Bellatreche, L., Chakravarthy, S. (eds.) *Big Data Analytics and Knowledge Discovery*. pp. 459–470. Springer International Publishing, Cham (2017)
26. Lv, Z., Li, X., Wang, W., Zhang, B., Hu, J., Feng, S.: Government affairs service platform for smart city. *Future Generation Computer Systems* **81**, 443–451 (2018)
27. Ma, M., Preum, S.M., Ahmed, M.Y., Tärneberg, W., Hendawi, A., Stankovic, J.A.: Data sets, modeling, and decision making in smart cities: A survey. *ACM Trans. Cyber-Phys. Syst.* **4**(2) (2019)
28. Marras, M., Manca, M., Boratto, L., Fenu, G., Laniado, D.: Barcelonanow: Empowering citizens with interactive dashboards for urban data exploration. In: *Companion Proceedings of the The Web Conference 2018*. pp. 219–222. WWW '18, International World Wide Web Conferences Steering Committee, Republic and Canton of Geneva, CHE (2018)
29. Matheus, R., Janssen, M., Maheshwari, D.: Data science empowering the public: Data-driven dashboards for transparent and accountable decision-making in smart cities. *Government Information Quarterly* **37**(3), 101284 (2020)
30. McArdle, G., Kitchin, R.: The dublin dashboard: Design and development of a real-time analytical urban dashboard. In: *First International Conference on Smart Data and Smart Cities; ISPRS Annals Photogrammetry, Remote Sensing and Spatial Information Sciences, III-4/W1*. pp. 19–25 (September 2016)
31. Ming, F.X., Habeeb, R.A.A., Md Nasaruddin, F.H.B., Gani, A.B.: Real-time carbon dioxide monitoring based on iot & cloud technologies. In: *Proceedings of the 8th International Conference on Software and Computer Applications*. pp. 517–521. ICSCA '19, Association for Computing Machinery, New York, NY, USA (2019)
32. Moustaka, V., Vakali, A., Anthopoulos, L.G.: Citydna: Smart city dimensions' correlations for identifying urban profile. In: *Proceedings of the 26th International Conference on World Wide Web Companion*. p. 1167–1172. WWW '17 Companion, International World Wide Web Conferences Steering Committee, Republic and Canton of Geneva, CHE (2017)

14 Cepero et al

33. Obie, H.O., Chua, C., Avazpour, I., Abdelrazek, M., Grundy, J., Bednarz, T.: Pedaviz: Visualising hour-level pedestrian activity. In: Proceedings of the 11th International Symposium on Visual Information Communication and Interaction. p. 9–16. VINCI '18, ACM, New York, NY, USA (2018)
34. Panagiotou, N., Zygouras, N., Katakis, I., Gunopulos, D., Zacheilas, N., Boutsis, I., Kalogeraki, V., Lynch, S., O'Brien, B.: Intelligent urban data monitoring for smart cities. In: Berendt, B., Bringmann, B., Fromont, É., Garriga, G., Miittinen, P., Tatti, N., Tresp, V. (eds.) Machine Learning and Knowledge Discovery in Databases. pp. 177–192. Springer International Publishing, Cham (2016)
35. Pardo-García, N., Simoes, S.G., Dias, L., Sandgren, A., Suna, D., Krook-Riekkola, A.: Sustainable and resource efficient cities platform – surecity holistic simulation and optimization for smart cities. *Journal of Cleaner Production* **215**, 701–711 (2019)
36. Peddoju, S.K., Upadhyay, H.: Evaluation of IoT data visualization tools and techniques, pp. 115–139. Springer (2020)
37. Petrolo, R., Loscri, V., Mitton, N.: Towards a smart city based on cloud of things, a survey on the smart city vision and paradigms. *Transactions on Emerging Telecommunications Technologies* **28**(1), 294–307 (2017)
38. Pettit, C., Widjaja, I., Russo, P., Sinnott, R., Stimson, R., Tomko, M.: Visualisation support for exploring urban space and place. In: ISPRS Annals of the Photogrammetry, Remote Sensing and Spatial Information Sciences. vol. 1, pp. 153–158 (2012)
39. Pettit, C., Bakelmun, A., Lieske, S.N., Glackin, S., Hargroves, K., Thomson, G., Shearer, H., Dia, H., Newman, P.: Planning support systems for smart cities. *City, Culture and Society* **12**, 13 – 24 (2018)
40. Pettit, C., Lieske, S.N., Jamal, M.: CityDash: Visualising a Changing City Using Open Data, pp. 337–353. Springer International Publishing (2017)
41. Pinto, A.L., Gonzales-Aguilar, A., Lima Dutra, M., Ribas Semeler, A., Deniszczwicz, M., Closel, C.: The Visualization of Information of the Internet of Things, chap. 5, pp. 117–137. John Wiley & Sons, Ltd (2017)
42. Popa, C.L., Carutasu, G., Cotet, C.E., Carutasu, N.L., Dobrescu, T.: Smart city platform development for an automated waste collection system. *Sustainability* **9**(11), 2064 (2017)
43. Protopsaltis, A., Sarigiannidis, P., Margounakis, D., Lytos, A.: Data visualization in internet of things: Tools, methodologies, and challenges. In: Proceedings of the 15th International Conference on Availability, Reliability and Security. ARES '20, Association for Computing Machinery, New York, NY, USA (2020)
44. Raj, P., Kumar, S.A.P.: Big Data Analytics Processes and Platforms Facilitating Smart Cities, chap. 2, pp. 23–52. John Wiley & Sons, Ltd (2017)
45. Ram, S., Wang, Y., Currim, F., Dong, F., Dantas, E., Sabóia, L.A.: Smartbus: A web application for smart urban mobility and transportation. In: 25th International Conference on World Wide Web Companion. pp. 363–368. WWW '16 Companion, International World Wide Web Conferences Steering Committee, Republic and Canton of Geneva, CHE (2016)
46. Rhazal, O.E., Tomader, M.: Study of smart city data: Categories and quality challenges. In: Proceedings of the 4th International Conference on Smart City Applications. SCA '19, Association for Computing Machinery, New York, NY, USA (2019)
47. Sachsenmeier, R., Marinescu, L., Oliveira, J., Silva, M., Verhijde, M.: Smart cities. In: Guide to Open Government, chap. 3, pp. 4 – 18. Lifelong learning program (2015)

48. Saggi, M.K., Jain, S.: A survey towards an integration of big data analytics to big insights for value-creation. *Information Processing & Management* **54**(5), 758 – 790 (2018), in (Big) Data we trust: Value creation in knowledge organizations
49. Sanaei, S., Majidi, B., Akhtarkavan, E.: Deep multisensor dashboard for composition layer of web of things in the smart city. In: 2018 9th International Symposium on Telecommunications (IST). pp. 211–215 (2018)
50. Santana, E.F.Z., Chaves, A.P., Gerosa, M.A., Kon, F., Milojevic, D.S.: Software platforms for smart cities: Concepts, requirements, challenges, and a unified reference architecture. *ACM Comput. Surv.* **50**(6) (Nov 2017)
51. Schunke, L.C., de Oliveira, L.P.L., Villamil, M.B.: Visualization and analysis of interacting occurrences in a smart city. In: 2014 IEEE Symposium on Computers and Communications (ISCC). pp. 1–7 (June 2014)
52. Sharifi, A.: A typology of smart city assessment tools and indicator sets. *Sustainable Cities and Society* **53**, 101936 (2020)
53. Steptoe, M., Krüger, R., Garcia, R., Liang, X., Maciejewski, R.: A visual analytics framework for exploring theme park dynamics. *ACM Trans. Interact. Intell. Syst.* **8**(1) (Feb 2018)
54. Suci, G., Necula, L., Usurelu, T., Rogojanu, I., Dițu, M., Vulpe, A.: Iot-based 3d visualisation platform for an efficient management of the smart city ecosystem. In: 2018 Global Wireless Summit (GWS). pp. 37–42 (2018)
55. Tong, X., Wu, Z.: Study of chinese city “portrait” based on data visualization: Take city dashboard for example. In: Marcus, A., Wang, W. (eds.) *Design, User Experience, and Usability: Designing Interactions*. pp. 353–364. Springer International Publishing, Cham (2018)
56. Trencher, G.: Towards the smart city 2.0: Empirical evidence of using smartness as a tool for tackling social challenges. *Technological Forecasting and Social Change* **142**, 117–128 (2019)
57. Trilles, S., Calia, A., Belmonte, Ó., Torres-Sospedra, J., Montoliu, R., Huerta, J.: Deployment of an open sensorized platform in a smart city context. *Future Generation Computer Systems* **76**, 221–233 (2017)
58. Vila, R.A., Estevez, E., Fillottrani, P.R.: The design and use of dashboards for driving decision-making in the public sector. In: *Proceedings of the 11th International Conference on Theory and Practice of Electronic Governance*. pp. 382–388. ICEGOV 18, ACM, New York, NY, USA (2018)
59. Young, G.W., Kitchin, R., Naji, J.: Building city dashboards for different types of users. *Journal of Urban Technology* **0**(0), 1–21 (2020)
60. Zaldei, A., Gualtieri, G., Camilli, F., Cavaliere, A., De Filippis, T., Di Gennaro, F., Di Lonardo, S., Dini, F., Gioli, B., Matese, A., Nunziati, W., Rocchi, L., Toscano, P., Vagnoli, C.: An integrated low-cost road traffic and air pollution monitoring platform to assess vehicles air quality impact in urban areas. In: 20th EURO Working Group on Transportation Meeting, EWGT. vol. 27, pp. 609 – 616 (2017)
61. Zdraveski, V., Mishev, K., Trajanov, D., Kocarev, L.: Iso-standardized smart city platform architecture and dashboard. *IEEE Pervasive Computing* **16**(2), 35–43 (2017)
62. Zhang, J., Chen, Z., Liu, Y., Du, M., Yang, W., Guo, L.: Space–time visualization analysis of bus passenger big data in beijing. *Cluster Computing* **21**(1), 813–825 (2018)
63. Zhong, C., Wang, T., Zeng, W., Müller Arisona, S.: *Spatiotemporal Visualisation: A Survey and Outlook*, pp. 299–317. Springer, Berlin, Heidelberg (2012)

# Smart City Vienna – Factors Driving Location Attractiveness

Pablo Collazzo<sup>1</sup> and Velislava Stoyanova<sup>2</sup>

<sup>1</sup> Danube University Krems, Dr.Karl Dorrek-Strasse 30, 3500 Krems, Austria  
pablo.collazzo@donau-uni.ac.at

<sup>2</sup> Lauder Business School, Hofzeile 18-20, 1190 Vienna, Austria  
velislava.stoyanova@lbs.ac.at

**Abstract.** As with firms, cities compete with each other. They compete to attract investments, eventually unlocking a virtuous circle that would bring in business and talent, and ultimately tax revenues to further enhance location attractiveness. In that quest, many cities are labelling themselves as ‘smart city’. Yet the meaning and scope of such label remains unclear. So do the ‘smart’ factors that drive relative attractiveness of urban locations. Bridging into the literature on entrepreneurial ecosystems, as arguably a strong entrepreneurial base boosts innovation and in turn location attractiveness, this study applies content analysis to interview outputs to Viennese startappers on their assessment of smart city factors, following Giffinger’s Smart City model. The findings suggest that infrastructure, quality of life and high-skilled labor largely explain the city of Vienna as the location of choice for new ventures. Implications are likely to be relevant for policymakers –at both national and local levels- and entrepreneurs alike, as they jointly shape urban competitiveness.

**Keywords:** Urban Competitiveness, Smart Cities, Entrepreneurial Ecosystems.

## 1 Introduction and Research Purpose

Cities account for 2 percent of the world’s surface, and are home to more than 50 percent of the global population (WEF, 2020). It is estimated that by 2030, approximately 60 percent of the planet will live in urban areas, with one out of three people living in a city of more than half a million inhabitants (United Nations, 2016). Those urban locations consume about 75 percent of the resources and energy worldwide, leading to the generation of ca. 80 percent of the planet’s greenhouse gases (Mohanty et al., 2016). The call to optimize resource usage while reducing greenhouse emissions urges cities to become ‘smarter’. The need to ensure an economic, social and ecological sustainability balance in the medium to long term, remains the main urban challenge in the 21st century (Finco and Nijkamp, 2001).

In order to compete globally, cities have to redevelop their infrastructure, by creating a desirable place for highly educated professionals to live and work in, attracting investors in new industries with high growth potential, while guaranteeing a sustainable tax revenue stream and continued domestic and foreign investments (Harrison et al. 2010). Competitiveness, driven by firms (Porter, 1990, 1998, 2000) is increasingly people-centered, no longer measured by economic metrics alone but factors such as living standard and quality of people (Esmailpoorarabi et al., 2016).

The smart city concept, advocating for technology-based efficiency gains for urban firms and people, could be arguably framed within the challenge of upgrading the business environment depicted by Porter's Diamond model (Porter, 1990, 2008).

In 2014, the city of Vienna launched its 'Smart City Vienna Framework Strategy', recently revised for the period 2019-2050, signalling its long-term commitment towards urban competitiveness. The pillars remain tackling the challenge of scarce resources and their efficient use, sustaining a high quality of life for future generations and fostering innovation in the city. Yet whether these are the factors that define the 'smartness' of a location, and in turn shape the urban development agenda, arguably calls for a broader buy-in of all relevant stakeholders. Among them, start-ups are likely to take center stage, hence this study intends to give them voice by collecting and assessing their smart city demands. Building on the ranking of smart city factors developed by Giffinger et al. in 2007 (see Appendix A), we explore whether such factors remain relevant through the lens of start-ups located in the Austrian capital, by applying content analysis to interviews conducted with local entrepreneurs.

## **2 Overview of Relevant Literature**

The smart city concept may be traced back to Van Bastelaer (1998) and Mahizhnan (1999), coined around information and communication technology applied to urban development. It has evolved to include the innovative drive of urban firms, along with metrics of education at the city level (Giffinger et al., 2007), and further into sustainability practices and eco-cities (Tsolakis and Anthopoulos, 2015). The multiple domains identified in the literature as defining features of a smart city, namely digital, virtual, knowledge-based, intelligent, cyber to wired to sustainable, eco and ubiquitous (Schuler, 2002; Schiewe et al., 2008; Schuurman et al., 2012; Moutinho, 2008; Yigitcanlar and Lee, 2014), have only fuelled the debate on the meaning and scope of smart cities. What seemingly remains somehow overlooked is that each city embarks in a journey of its own towards 'smartness', and should balance out the demands of multiple stakeholders – a complexity compounded by the changing nature of those demands over time.

The entrepreneurial ecosystem insight, developed by Isenberg (2011, 2014, 2016), is applied by Ahvenniemi et al. (2017), who argue that 'smart sustainable city' is not

the fuzzy label of a futuristic city, but an urban entrepreneurial ecosystem with the ambition to fight environmental problems, relying on information and communication technology (ICT) for urban planning and development.

The interplay of technology and sustainability at the city level is discussed by Höjer and Wangel (2014), as they claim that sustainable cities could be built without the help of ICT -technology is likely to enhance smartness but it does not necessarily contribute to the sustainability of cities. Hence only when smart technology is used to make urban areas more sustainable, the term smart sustainable city would apply.

In 2007, Giffinger et al. developed a ranking of mid-sized cities in Europe, which has since become a widespread yardstick to assess the attractiveness of urban regions. A remarkable contribution of their model is that it goes beyond large metropolises, to include smaller cities –with a population of around 500,000 inhabitants. The authors define a ‘smart city’ as a city well performing in a forward-looking way across six dimensions [Smart Economy, Smart Governance, Smart Mobility, Smart Living, Smart Environment and Smart People], built on the ‘smart’ combination of endowments and activities of self-decisive, independent and aware citizens (Giffinger et al., 2007).

The literature is not free from criticism to household names such as IBM, Siemens, Cisco or Microsoft, blamed for narrowing the narrative on smart cities down to commercial interests around their own devices and platforms (Söderström et al., 2014). While they have undoubtedly shaped the debate on smart cities, their impact has been more noticeable advocating for data sourcing and usage deregulation, making ICT a powerful efficiency driver for firms and people alike.

Nam and Pardo (2011) claim that the smart city concept is not significantly different than traditional urban innovations, while others argue that smartness at the city level should be a function of collective social and political priorities, rather than technological hypes (Hollands, 2008). Along the same lines, Coe et al. (2000) point out that ‘smart communities, community partnerships –not wires- are the fibers that bind the smart city’.

While ICT is the single recurrent component across smart city definitions, a more people-centered approach, building on sustainability, quality of life and economic efficiency –with ICT as a means rather than a goal- is increasingly gaining ground. That is reflected in the definition put forward by the International Telecommunications Union (ITU), the United Nations specialized agency in the field of ICT, as a result of a Focus Group on Smart, Sustainable Cities in 2014:

*"A smart sustainable city (SSC) is an innovative city that uses information and communication technologies (ICTs) and other means to improve quality of life, efficiency of urban operation and services, and competitiveness, while ensuring that it meets the needs of present and future generations with respect to economic, social and environmental aspects" (ITU, 2014).*

Bridging smart and sustainable enriches the approach of Giffinger et al. (2007), highlighting the relevance of the sustainability and competitiveness dimensions. And more importantly for this study, ITU's proposed definition is more in line with Vienna's Smart City Framework Strategy, as the city aims at offering 'the finest quality of life, combined with maximum resource preservation for all citizens by 2050'. Hence the upcoming analysis builds on ITU's understanding of a smart city.

### **3 Research Gap and Research Question**

As noted, the literature identifies a wide variety of domains – ICT, innovation, education, quality of life, sustainability, competitiveness- that jointly shape the smart city concept. While they are all arguably relevant, their relative importance is likely to be contingent on the needs and expectations of different stakeholders. Upon reconciling existing definitions of smart cities, this study applies Giffinger et al.'s 2007 categorization to ascertain the relative weight of its factors, through the outputs of interviews conducted with local entrepreneurs, who are ideally positioned to benefit from and scrutinize location attractiveness. Thus the research question we aim to answer is:

'According to local entrepreneurs, what factors out of Giffinger et al.'s Smart City model mostly impact the city of Vienna's location attractiveness?'

The research design and methodology follow.

### **4 Research Design and Methodology**

The study conducts a critical review of available definitions of the smart city concept, building on the literature summarized above, combined with qualitative content analysis on interviews of Vienna-based entrepreneurs, carried out between April and July 2021.

The collected data were assessed through a qualitative content analysis following Mayring (2010). The data were analyzed in a combination of the two qualitative techniques of summarizing and structuring (ibid). Non-content-carrying components, i.e., information that does not contribute towards answering the research question, was eliminated. The qualitative content analysis was completed by grouping and forming major categories. These main categories were used as a basis for structuring the generalized paraphrases that were produced in the course of summarizing. The content of the generalization obtained was returned into the main categories in order to determine which elements could be found in the respective main categories. These elements were ranked in order of importance. The weighting of importance was carried out through a subjective assessment based on the frequency of repetition, the emphasis of the responses and the direct assessment of the participants themselves. This building of categories based on frequency, allows some extent of quantification of the data (ibid).

All findings were analyzed, compared, structured and discussed in order to finally define the criteria that suggest the relative weight of Giffinger et al.'s factors.

## 5 Discussion of Findings

In the process of disentangling the meaning and scope of the smart city concept, we built on the literature reviewed above. Environmental issues are the more recurrent component of the reviewed definitions, with economy and people trailing closely, followed by quality of life. References to the economy in the smart city narrative are straightforward, given the economic essence of the term. As for people, the smart city concept is increasingly people-centered, as ICT-enabled efficiency gains should be aimed at improving living standards. Other topics depicting a relatively high frequency, such as infrastructure and energy, cannot be matched to Giffinger et al.'s model. ICT arguably unlocks a more comprehensive understanding of infrastructure in the smart city debate, as it typically improves mobility and transportation. Same for energy, which is often captured under the environmental dimension. The result is a challenging, at times overlapping mix of themes.

The validity of the findings above was examined by applying qualitative content analysis to the outputs of 54 interviews to city-based entrepreneurs, selected by convenience sampling. The choice of the city of Vienna as location for their start-up could be attributed to the perceived high quality of living along with a well-functioning, reliable infrastructure, closely followed by the availability of skilled labor. Yet both infrastructure and access to talent seem to be losing steam, the former largely as a result of ageing and missed opportunities on digitalization of transportation networks, the latter following a seemingly increasing gap between higher education curricula and labor market demands. Access to capital was granted a lower weight among the given smart city factors, which is consistent with the limited offer of private equity and venture capital funding in the city, as documented in the literature (Groh et al., 2018). Rather than funding alone, entrepreneurs seem to place more value to the broader entrepreneurial ecosystem they could tap into, particularly access to multiple business incubation and acceleration programs.

When revisiting Giffinger et al.'s model, it became apparent that the defining dimensions discussed in the literature and perceived by Vienna-based entrepreneurs are consistent with their 2007 Smart City model. Two potential adjustments emerged from the analysis, namely whether infrastructure and energy should be considered as stand-alone dimensions or rather embedded in the more cited mobility and environment factors. While both academic and policy references tend to use infrastructure and mobility fairly interchangeably –rather the former as factor and the latter as indicator- (Mohanty et al., 2016; Gong and Lyu, 2017; ITU, 2015), energy and environment seem to be less of a single dimension, since the urban environmental agenda is likely to encompass multiple sustainability challenges, with energy atop but not alone.

Another piece of evidence suggesting that Giffinger et al.'s model remains relevant, refers to the governance factor. Even if it did not come out clearly of our text mining exercise, it was indirectly mentioned by local entrepreneurs in the open-end exchange of the interviews, when referring to the tax burden and rigid labor market regulations faced by Austrian start-ups. A claim for a louder voice from entrepreneurs, and more of a bottom-up process in shaping the local entrepreneurial ecosystem, would be a reminder that the factors identified by Giffinger and his team are closely interconnected, such as people and governance.

## **6 Implications for Theory, Policy and Practice**

The overall conclusion of the study is that the smart city factors shaping Vienna's location attractiveness, applying the model developed by Giffinger et al. in 2007, remain largely current and relevant. Eventually infrastructure and energy could be meaningful extensions to the original model, which would account for our contribution to theory. Although infrastructure is often mimicked in the literature with mobility, entrepreneurs, i.e. users, do tell the difference between the hardware, the resource (the infrastructure itself) and the capability (the use of the asset, how it is designed to optimize resource efficiency), the latter being the sought-after 'smart' feature. Energy has in the meantime developed its own agenda within urban development, with many pressing issues on generation and consumption, which would merit dedicated measuring and monitoring, apart from broader environmental issues. Extending the original model with these two factors would arguably reconcile user (entrepreneur) perception with recent literature, better reflecting the 'smartness' that drives location attractiveness.

The contribution to policy of an empirically revised smart city model, would be contingent on the given city's urban agenda, which is likely to be significantly shaped by context-specific and time-specific stakeholder demands. However, increased awareness on the interplay of infrastructure and mobility, as well as the mounting pressure on energy issues, beyond broader environmental concerns, would signal policy makers current user priorities.

Following a similar rationale, practitioners, particularly those at the supply side of ICT platforms and devices potentially boosting efficiency, might benefit from this revised, entrepreneur-tested smart city model, disclosing perceptions and priorities of potential clients/users.

## **7 Limitations and Future Research**

Being a cross-sectional study, hence with its findings and implications only applicable to the data collection timeframe, future research might turn it into a longitudinal analysis, assessing evidence at different points in time. As a result, all relevant stakeholders,

including policymakers, practitioners and scholars, would be able to monitor performance and expectations, and adjust accordingly, towards enhanced location attractiveness.

Even if Giffinger et al.'s model has established itself among academics, corporates and policymakers as a proven framework to ascertain a city's 'smartness', this study relies on this single model. As an alternative to our approach to challenge the currency and boundaries of this model, future research might apply or develop other models on smart cities, broadening the scope of the analysis.

The data for this study were sourced from entrepreneurs, as it is claimed that they are at the core of strong entrepreneurial ecosystems, which in turn drive location attractiveness. Thus, further studies may draw from different stakeholders, e.g. (venture) capital providers, policymakers or private sector representatives, to name a few, in an effort to triangulate empirical evidence and explore convergent or divergent findings.

While this research was conducted on Vienna as geographical unit of analysis, the research design could be replicated in other cities, most likely leading to meaningful differences across locations.

## References

1. Ahvenniemi, H., Huovila, A., Pinto-Seppä, I., and Airaksinen, M. What are the differences between sustainable and smart cities? *Cities* 60, 234–245. <https://doi.org/10.1016/j.cities.2016.09.009> (2017).
2. Coe, A., Paquet, G., and Roy, J. E-Governance and Smart Communities: A Social Learning Challenge, Working paper 53, Faculty of Administration, University of Ottawa, (2000).
3. Esmailpoorarabi, N., Yigitcanlar, T. and Guaralda, M. Place quality and urban competitiveness symbiosis? A position paper, *Int. J. Knowledge-Based Development*, 7(1), 4–21. <https://doi.org/10.1504/IJKBD.2016.075444> (2016).
4. Finco, A. and Nijkamp, P. Pathways to urban sustainability, *Journal of Environmental Policy and Planning*, 3, pp. 289-302. <https://doi.org/10.1002/jep.94> (2001).
5. Giffinger R., Fertner C., Kramar H., Kalasek R., Pichler -Milanović N. and Meijers E., "Smart cities. Ranking of European medium-sized cities", Centre of Regional Science of Vienna. (2007)
6. Gong, W., Lyu, H. Sustainable City Indexing: Toward the Creation of an Assessment Framework for Inclusive and Sustainable Urban Industrial Development, UNIDO (2017).
7. Groh, A., H. Liechtenstein, K. Lieser and M. Biesinger. The Venture Capital and Private Equity Country Attractiveness Index 2018, Ninth Edition, IESE Business School (2018).
8. Harrison, C., Eckman, B., Hamilton, R., Hartswick, P., Kalagnanam, J., Paraszcak, J., and Williams, P. Foundations for Smarter Cities, *IBM Journal of Research and Development*, 54 (4). doi: 10.1147/JRD.2010.2048257 (2010).
9. Höjer, M., and Wangel, J. Smart Sustainable Cities Definition and Challenges, *Advances in Intelligent Systems and Computing*, Springer International Publishing, 333-349 (2014).

10. International Telecommunications Union. Smart sustainable cities: An analysis of definitions, Retrieved from: <https://www.itu.int/en/ITU-T/focusgroups/ssc/Documents/.../TR-Definitions.docx> (2014).
11. Isenberg, D. J. The Entrepreneurship Ecosystem Strategy as a New Paradigm for Economic Policy: Principles for Cultivating Entrepreneurship. Retrieved from The Babson Entrepreneurship Ecosystem Project website: [entrepreneurial-revolution.com/2011/05/11/the-entrepreneurship-ecosystem-strategy-as-a-new-paradigm-for-economic-policy-principles-for-cultivating-entrepreneurship/](http://entrepreneurial-revolution.com/2011/05/11/the-entrepreneurship-ecosystem-strategy-as-a-new-paradigm-for-economic-policy-principles-for-cultivating-entrepreneurship/) (2011a).
12. Isenberg, D. J. Introducing the Entrepreneurship Ecosystem: Four Defining Characteristics, *Forbes* (2011b).
13. Isenberg, D. J. What an Entrepreneurship Ecosystem Actually Is, *Harvard Business Review Digital Articles* (2014, May 12).
14. Isenberg, D. J. Applying the Ecosystem Metaphor to Entrepreneurship: Uses and Abuses, *The Antitrust Bulletin*, 61(4), 564–573 (2016).
15. Mahizhnan, A. Smart cities: The Singapore case, *Cities*, Vol. 16, No. 1, pp. 13-18, ISSN 0264- 2751, [https://doi.org/10.1016/S0264-2751\(98\)00050-X](https://doi.org/10.1016/S0264-2751(98)00050-X) (1999).
16. Mayring, P. Qualitative content analysis: theoretical foundation, basic procedures and software solution, URN: <http://nbn-resolving.de/urn:nbn:de:0168-ssoar-395173> (2014).
17. Mohanty, S., Choppali, U., Kougianos, E. "Everything you wanted to know about smart cities: The Internet of things is the backbone," in *IEEE Consumer Electronics Magazine*, vol. 5, no. 3, pp. 60- 70, doi: 10.1109/MCE.2016.2556879 (2016).
18. Moutinho, J. L. Building the information society in Portugal: lessons from the digital cities programme 1998-2000, In van Geenhuizen (Eds.), *Value-added partnering and innovation in a changing world* (2008).
19. Nam, T., and Pardo, T.A. Conceptualizing Smart City with Dimensions of Technology, People, and Institutions, *Proc. 12th Annual International Conference on Digital Government Research*. (2011).
20. Porter, M. E. The Competitive Advantage of Nations, *Harvard Business Review*, pp. 73-93. (1990).
21. Porter, M. E. Clusters and the New Economics of Competition, *Harvard Business Review*, pp. 77-90. (1998).
22. Porter, M. E. Location, Competition, and Economic Development: Local Clusters in a Global Economy, *Economic Development Quarterly*, February, pp. 15-34. <https://doi.org/10.1177/089124240001400105> (2000).
23. Porter, M. E. *On Competition*. 13th Ed. Boston, Massachusetts: Harvard Business School Press. (2008).
24. Schiewe, J., Krek, A., Peters, I., Sternerg, H., and Traub, K. P. HCU research group "Digital City": developing and evaluating tools for urban research, In: Ehlers et al. (Eds.) *Digital Summit on Geoinformatics*. (2008).
25. Schuler, D. Digital cities and digital citizens, In: M. Tanabe, P. van Besselaar, T. Ishida (Eds.), *Digital Cities II: Computational and Sociological Approaches*. LNCS, (2362), 71-85. Berlin, Springer. (2002).
26. Schuurman, D., Baacarne, B., De Marez, L., and Mechant, P. Smart ideas for smart cities: investigating crowdsourcing for generating and selecting ideas for ICT innovation in a city context. *Journal of Theoretical and Applied Electronic Commerce Research*, 7(3), 49-62. (2012).
27. Söderström, O., Paasche, T., and Klauser, F. Smart cities as corporate storytelling, *City*, 18 (3), 307-320. <https://doi.org/10.1080/13604813.2014.906716> (2014).

28. Tsolakis N., and Anthopoulos, L. Eco-cities: An Integrated System Dynamics Framework and a Concise Research Taxonomy, *Sustainable Cities and Society*, 17, 1-14. <https://doi.org/10.1016/j.scs.2015.03.002> (2015).  
 United Nations. *The World’s Cities in 2016*, Retrieved from [http://www.un.org/en/development/desa/population/publications/pdf/urbanization/the\\_worlds\\_cities\\_in\\_2016\\_data\\_booklet.pdf](http://www.un.org/en/development/desa/population/publications/pdf/urbanization/the_worlds_cities_in_2016_data_booklet.pdf) (2016).

29. Van Bastelaer, B. Digital cities and transferability of results, *Proceedings of the 4th EDC conference on digital cities*, Salzburg, pp. 61–70. (1998).

30. World Economic Forum. *Guidelines for City Mobility: Steering towards collaboration*, Retrieved from [https://www3.weforum.org/docs/WEF\\_Guidelines\\_for\\_City\\_Mobility\\_2020.pdf](https://www3.weforum.org/docs/WEF_Guidelines_for_City_Mobility_2020.pdf) (2020).

31. Yigitcanlar, T. and Lee, S. Korean ubiquitous-eco-city: A smart-sustainable urban form or a branding hoax? *Technological Forecasting & Social Change* 89, 100–114. (2014).

**Appendix A. Smart City Factors and Indicators**

<p><b>SMART ECONOMY</b> (Competitiveness)</p> <ul style="list-style-type: none"> <li>▪ Innovative spirit</li> <li>▪ Entrepreneurship</li> <li>▪ Economic image &amp; trademarks</li> <li>▪ Productivity</li> <li>▪ Flexibility of labour market</li> <li>▪ International embeddedness</li> <li>▪ <i>Ability to transform</i></li> </ul>	<p><b>SMART PEOPLE</b> (Social and Human Capital)</p> <ul style="list-style-type: none"> <li>▪ Level of qualification</li> <li>▪ Affinity to life long learning</li> <li>▪ Social and ethnic plurality</li> <li>▪ Flexibility</li> <li>▪ Creativity</li> <li>▪ Cosmopolitanism/Open-mindedness</li> <li>▪ Participation in public life</li> </ul>
<p><b>SMART GOVERNANCE</b> (Participation)</p> <ul style="list-style-type: none"> <li>▪ Participation in decision-making</li> <li>▪ Public and social services</li> <li>▪ Transparent governance</li> <li>▪ <i>Political strategies &amp; perspectives</i></li> </ul>	<p><b>SMART MOBILITY</b> (Transport and ICT)</p> <ul style="list-style-type: none"> <li>▪ Local accessibility</li> <li>▪ (Inter-)national accessibility</li> <li>▪ Availability of ICT-infrastructure</li> <li>▪ Sustainable, innovative and safe transport systems</li> </ul>
<p><b>SMART ENVIRONMENT</b> (Natural resources)</p> <ul style="list-style-type: none"> <li>▪ Attractivity of natural conditions</li> <li>▪ Pollution</li> <li>▪ Environmental protection</li> <li>▪ Sustainable resource management</li> </ul>	<p><b>SMART LIVING</b> (Quality of life)</p> <ul style="list-style-type: none"> <li>▪ Cultural facilities</li> <li>▪ Health conditions</li> <li>▪ Individual safety</li> <li>▪ Housing quality</li> <li>▪ Education facilities</li> <li>▪ Touristic attractivity</li> <li>▪ Social cohesion</li> </ul>

Source: Adapted from Giffinger et al. (2007).

# VIA: A Virtual Informative Assistant for Smart Tourism

M.C. López<sup>1</sup> ORCID: 0000-0002-2060-2047, D. Hernández<sup>1</sup> ORCID: 0000-0001-8922-354X, A.A. Navarro-Newball<sup>1</sup> ORCID: 0000-0002-4231-8661, and Edmond C. Prakash<sup>2</sup> ORCID: 0000-0002-4410-144X

<sup>1</sup> Pontificia Universidad Javeriana Cali, Colombia  
{mclopez09,davidher28,anavarro}@javerianacali.edu.co  
<sup>2</sup> Cardiff Metropolitan University, UK  
epakash@cardiffmet.ac.uk

**Abstract.** Tourism can be approached from the technological virtual continuum, calling it smart tourism which is related to cultural computing. To achieve that, we implemented an application for mobile devices to enrich the visit of locals and foreigners to the San Antonio neighbourhood in the city of Santiago de Cali, Colombia using concepts such as augmented reality, natural language processing and techniques such as speech-to-text, text-to-speech, skeletal animation and blend shapes. The main objective is to guide and inform about the neighbourhood in order to provide awareness of it as a heritage site. We developed the application following a software development cycle which included analysis, design, prototyping, implementation, and validation. Particularly, in validation, we performed unitary tests, functional tests and user tests. The resulting application was well received among participants in the test.

**Keywords:** Augmented Reality, Natural Language Processing, Speech-To-Text, Text-To-Speech, Skeletal Animation, Blend Shapes, Smart Tourism, Cultural Computing

## 1 Introduction

The city of Santiago de Cali, Colombia in favour of standing out as a special district, is betting on increasing sports, culture, tourism, and business markets. To the west of the city is one of the most typical neighbourhoods of the Cali culture and that is part of the development plan, San Antonio. Its creation and consolidation are closely linked to the construction of the chapel of San Antonio (representative temple of the neighbourhood) carried out almost 300 years ago, more precisely in the year 1746. Hostels, dance academies, restaurants, theatres, and monuments, are some of the many things that have emerged over the years and that today represent the idiosyncrasy of the citizens of Cali. In this sense, our project focuses on recognising that the methods used to provide information regarding the different events and places in the neighbourhood show some limitations. For example, some of the information is in the hands of private individuals and institutions; public media, such as posters, are unclear and scarce;

2 M.C. Leal et al.

and there is no bilingual information that is inclusive with international visitors. Therefore, we implemented an application to share and publicise the place through different designed and impactful ways using technology, in this case, with the use of augmented reality (AR) and natural language processing (NLP).

The architectural, anthropological, urban, and social heritage of the San Antonio neighbourhood is one of the fundamental pillars for locals and tourists to fall more and more in love with the city of Santiago de Cali, Colombia. Thus, all the history that characterises the neighbourhood should be known by all those who live among its streets daily, since it is a representative icon of the region. Recognising some of the oldest houses, keeping in mind events and fairs, differentiating the monuments, and distinguishing the hill where the church is located, would favour for the development of the place. Despite this, and after a field outing, it became clear that the way in which information about places and events in the neighbourhood that is provided is limited. There is no strategy to generate interest; the information is frequently outdated; the information posters are unclear or incomplete. In contrast, Boboc et al. [1] propose a system based on AR that shows an old church, now non-existent, in the place where it should have been located. Here, information is presented to visitors in a visual and interactive way, highlighting the importance of the place and its history. This suggests that the virtual continuum, which includes AR, mixed reality and virtual reality and its technologies, provide great information potential that could complement visits to the San Antonio neighbourhood.

Wei et al. [2] shows how interesting it was to expose the history of places, through comparative images with current and ancient facades. Perea-Tanaka et al. [3] expose interactive factors to attract the public's attention through AR. In addition, Sauter et al. [4] and Darwin et al. [5] provide their expertise with geolocation and how it contributes to certain functions such as using a map to locate users. Likewise, Wei et al. [6] and Cavallo et al. [7] present how AR can contribute to changing the behaviours in urban areas, generating greater tourism. Thus, our project recognises the importance of establishing actions to interact with an application by enhancing the use of AR. We propose an application for smart tourism, a Virtual Informative Assistant (VIA) that makes use of AR to provide information to locals and visitors to the San Antonio neighbourhood. To achieve this we: (1) identified, analysed and structured the information of the San Antonio neighbourhood that is used in a VIA; (2) developed an architecture for the VIA that allows to integrate the information obtained; (3) implemented the application of the VIA based on the proposed architecture and (5) evaluated the quality control and user experience of the implemented system. As Escobar and Margherita state [8], "Smart Tourism describes a plethora of advanced information and communication technologies applied in the tourism industry".

## 2 Analysis

To identify and define the places to be used in the VIA, a process was carried out in which the necessary information was obtained virtually and in person.

Initially, the San Antonio neighbourhood is recognised through tools such as TripAdvisor, Google Maps and Street View. Each of them offers different aspects to consider. For example, TripAdvisor, under its ideal of providing reviews of travel-related content, makes it possible to recognise the opinion of people who have visited the neighbourhood and its most representative places. While Google Maps and Street View allow to geographically locate and visually distinguish the neighbourhood in a way very close to reality. In this way, we selected different options of places in the San Antonio neighbourhood according to criteria such as opinions and valuation of locals and visitors, historical relevance reviewed on the web and location. Subsequently, we proceeded with a field outing and an approach to the owners that allowed to evaluate and confirm in person the choice made. The chosen places consist of a public place and two private places as follows. (1) St. Anthony's Church: it was built in 1786 and became public property in 1944. In addition, it was declared a national monument in 1997. (2) La Linterna (The Lantern): it is one of the oldest typographic printers in Colombia. Since 1938 this printing press has been providing its services in the San Antonio neighbourhood. (3) La Colina gathering place (The Hill) : it is recognised as the oldest store in the city of Cali, it was created in 1942. Initially it was catalogued as a neighbourhood store and with the passage of time it became a gathering icon on the tourist route of the city.

When conducting a survey to a group of 32 people, it was evident that San Antonio is considered one of the most representative neighbourhoods in Cali with an acceptance score of 8.93 out of 10. Here, participants have had enriching experiences with family and friends. Gastronomy, architecture and a cosy and bohemian atmosphere stand out. Of the three places chosen to be part of the VIA, only the church is known by 85% of people, while La Linterna and La Colina are known only by 7% and 41% of respondents respectively, which is interesting since the latter places have an important history within the neighbourhood and the city, that many do not know. Some of the respondents highlighted their experiences in La colina as: "Good music, beer and food." However, there were also confusions such as: "it is fun to listen to the storytellers with their magnificent stories as well as to dance some Andean dances," referring to the storytellers located in the church. Regarding La Linterna only 2 out of 32 of the respondents said they knew about it by saying: "I know the traditional posters they make," and: "they print for saying something, the old-fashioned way. It once came out in the newspaper." In this way, it is considered of great importance to highlight them in the application so that tourist and local users know about them and their most notable aspects. We proposed the work flow in Figure 1 accordingly.

### 3 Design

For the design section, the planning of the system architecture, the proposed data models, and the layout of the graphic interface of the VIA are presented.

4 M.C. Leal et al.

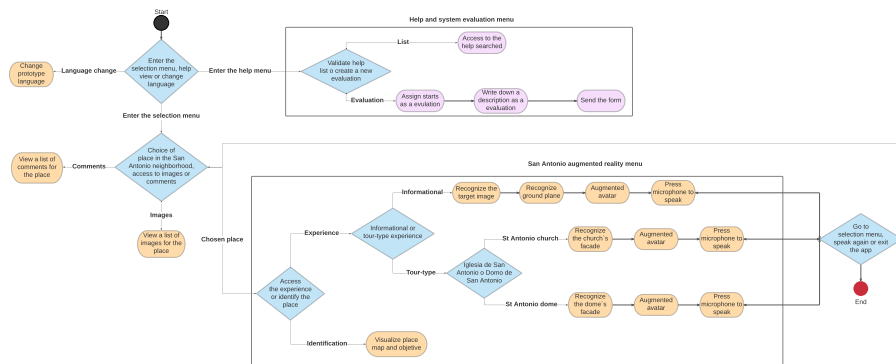


Fig. 1. Application flow.

### 3.1 Architecture

The architecture is a key piece in any technology project. In this case, we proposed to make use of an event-driven microservices architecture. This approach was chosen primarily because the system had a set of tools and services that communicated both locally and over the network. Therefore, using a low coupling and high cohesion architecture allowed the prototype to make use of memory and local processing, but also, make use of up to six different virtualised services on Microsoft Azure and Firebase servers. Here (Figure 2), a client layer and a service layer are defined. In addition, these layers communicate by means of an event handler that is based on the occurrence of events for the generation of transitions and requests.

### 3.2 Data Model

Emphasising the architecture presented in Figure 2 it is pertinent to say that we used three different types of databases. The first database works in an embedded way as a system of collecting visual objectives recognisable by the application. These objectives are stored in the database as sets of points recognisable by the camera at the time of deploying the system. In addition, it has an internal scheme in which it collects information about the images and areas, such as a recognition identifier, status, upload date and its augmentation level. The second schema used focuses on a knowledge database. This technology is implemented for the creation of a conversational layer with a virtual agent. Its approach is based on hosting a set of keys that are the possible questions from the users and, values that represent the possible answers of the agents. In short, a dictionary is proposed where all possible requests from users and responses from agents are defined. The third approach implemented is that of a schema-based non-relational database. This database hosts the data generated by users in sections of the VIA such as comments and the rating menu. In this sense, two schemes were proposed to model the information of the comments and the evaluations.

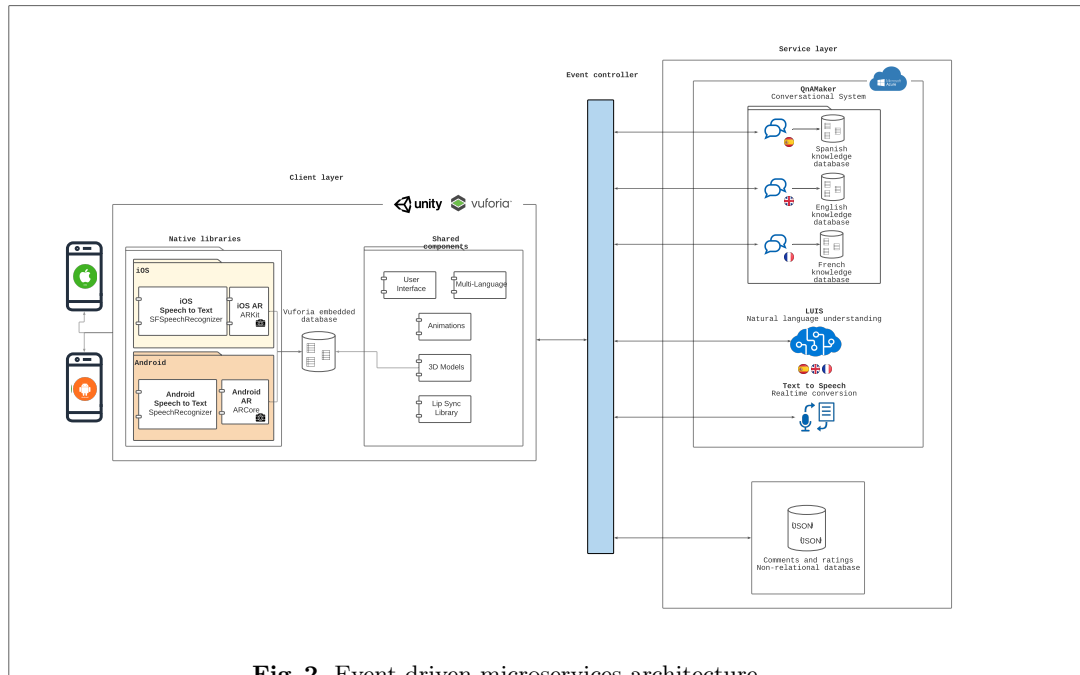


Fig. 2. Event-driven microservices architecture.

### 3.3 Prototyping

The graphical interface is a user’s first point of contact with the application, and it directly influences usability and therefore the experience gained. To visually characterize the VIA, two phases were executed. In the first phase, we designed the complete flow of the application and how it was articulated with the requirements of this (Figure 1). Also, we made an initial approach to the aesthetic design of the application. The second phase was carried out after the feedback in conjunction with users, therefore, the observations found were considered and final details were given to start with the implementation. It should be borne in mind that the VIA, being an application in AR, had two approaches to the design of its interface, which are the AR interface where a much more minimalist aspect is sought, and the interface of the application that provides relevant information to the user. Based on this, we initiated a design process with the help of the Figma tool. Figma is a design tool that allows creating interfaces and prototypes from vectors, therefore, it is modifiable in a short time. The main goal with the user interface design in this project was to provide a look that was intuitive, easy to use and provided a pleasant feeling in aesthetic terms for end users. For this, we followed the usability heuristics proposed by Jakob Nielsen [9] and the recommendations provided in the user evaluations. Five main interfaces were defined. Figure 3a shows the initial menu that allows the user to enter the help module and the places within San Antonio. Figure 3b shows the interface where the frequently asked questions and the assessment of user experience are

6 M.C. Leal et al.

listed, mainly for complaints and claims. Figure 3c shows the menu that allows entering the places along with a slider that shows relevant information and photos corresponding to the places. Figures 3d and 3e are the interfaces associated with the type of travelling and informative experience respectively.

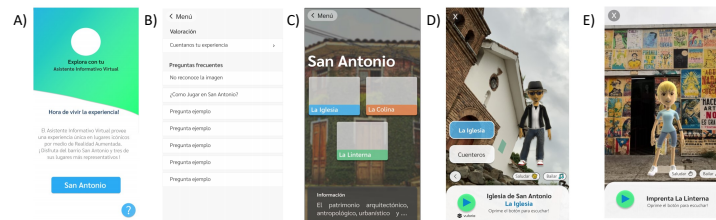


**Fig. 3.** User interfaces of the VIA.

## 4 Implementation

A video of the resulting VIA application can be watched [here](#). We used the Unity engine due to the connectivity it brings to each of the technologies used in the project, in addition to the knowledge and previous management of the tool and the C# programming language. Likewise, this engine was chosen since it supports the framework for the development of AR, Vuforia Engine. Its use allowed, for example, if the application runs on a Google Pixel 2 XL to take advantage of ARCore; while if the application is run on a device that does not support ARCore, it will use Vuforia VISLAM if and only if the device has the required sensors and has been calibrated by Vuforia. The same scenario applies to iOS devices. If the prototype is deployed on an iPhone X, it automatically leverages ARKit for all object and environmental recognition features. If this same prototype runs on an older iOS device (which does not support ARKit but has been calibrated by Vuforia) it will automatically use Vuforia VISLAM for dependent tasks [10].

This means that all the AR technologies used in this research are accessible through a wide set of devices with operating systems such as Android, iOS, and Windows, making use of a priority model. The VIA made use of target areas, target images and blueprint recognition for positioning avatars on real-life horizontal planes. For the construction of the target areas, a respective point cloud was mapped for one of the areas chosen as the basis of the research. To achieve this, the possibilities lay in the use of laser scanning technology such as Matterport, NavVis or Leica. However, this was implemented through a three-dimensional imaging system called Vuforia Area Target Creator. The areas created were the facade of the Church and the Dome of the San Antonio neighbourhood in Cali, Colombia. In addition, these objectives allowed to locate

the avatars in real size according to the scanned facades. Likewise, the avatars were created from a service for the parameterisation of each of its characteristics. Among them, gender, skin and hair tones, accessories such as glasses, clothing such as t-shirts, trousers, and shoes. These avatars were created as humanoids with the ability to be animated (Figure 4A). In addition, Blend shapes were used to create facial animations for lip sync simulation (Figure 4B). This was carried out through the SALSA Lip Sync lip sync library [11], that provided the ability to combine facial animations according to the audio that is played by means of activation in an interval that is parameterised from zero to one.



**Fig. 4.** Use of animation. A) Skeleton for avatar animation. B) Facial animation using blendshapes. Pronouncing letter O (left) and letter T (right)

After a research process based on the verification of current technological capabilities, the team recognised the existence of native classes to convert speech into text in the operating systems. Both can be configured with any of the languages supported by both operating systems, which made it possible to continue an implementation based on multiple languages, with the vocal interaction (Spanish, English, French) of the users. To achieve the implementation of native classes in cross-type development, the Unity development platform allows the use of a layer in which plugin-type components can be defined for native communications with the project's target operating systems. Based on this, speech conversion was adapted and based on an open-source project documented on the GitHub platform [12]. Its implementation focuses on the capabilities of Android and iOS operating systems to convert speech into text and text into speech through their native libraries. In addition, it implements a direct communication bridge with Unity. Therefore, for the speech-to-text technique, native connection files were implemented in programming languages such as Java for Android and Objective-C for iOS, making use of the SpeechRecognizer and SFSTextRecognizer libraries.

We had to focus the research on recognising how to carry out this type of interaction or voice control approach. We used artificial intelligence techniques to satisfactorily engage a user in a conversation or communication with the avatar. We proposed to reduce the problem of communication by voices, in a communication by text. With this, internally the system controls all the information as text inputs. Thus, the voice of the end users is captured and converted directly into text. Subsequently, when recognising what users said through the microphone, the next step focuses on studying the text to generate a response accordingly. To develop an application based on interactive and clear communi-

cation, we decided to make use of models for the recognition of the text and the understanding of requests or possible questions from users. These models were created through Microsoft Azure, exactly, through two cognitive cloud computing services, QnAMaker and Language Understanding (LUIS). This choice was made thanks to the keyword ranking and intent recognition capabilities of each of the tools. The models were trained from the server and through a user interface, which made it possible to use them through web services that allowed the generation of answers based on each of the questions asked by the end users of the application.

Because the prototype was built with a multicultural approach, on issues such as language, gender, and ethnicity of the avatars, it was also necessary to foray diversity into the speech of each of them. To achieve this, speech synthesis markup language (SSML) was used, which is an XML-based markup language that allowed to specify how input text is converted into synthesised speech from the Microsoft Azure text-to-speech cognitive service. Compared to plain text, SSML allowed us to adjust pitch, pronunciation, speech speed, volume, and other aspects of text-to-speech output. Normal punctuation marks, such as pause after a period or intonation when a sentence ends with a question mark, were handled automatically. A set of nine different types of voices were defined and associated with each avatar and the three languages of their domain. In addition, a method was developed to build the speech synthesis markup file at run time according to the avatar and the selected language in the system.

Emphasising the architecture developed for the VIA, we implemented an event handler. To do this, the approach used was based on the use of an event-driven finite state machine. The services used for the NLP were virtualised and accessed through the web using HTTP protocol through representational state transfer or REST requests. To achieve this, the virtualisation of each of the services was implemented through App Service, a Hosting service of Microsoft Azure and high compatibility with the technical features used in the project. The choice of this technology focused on its ability to host and execute in a dedicated and secure way of each of the services with the implementation of access tokens for its use. The communication was based on the sending and receipt of JSON type objects that were serialised and deserialised using the Newtonsoft JSON library.

## 5 Validation

In the validation process, all the activities related to quality tests are carried out. Therefore, the strategies used for the planning, execution and results are reflected together with their respective analysis and improvements within the functionalities that were considered pertinent. This, recognising that the environment in which the system had to be deployed required the timely classification of different types of tests, exactly three different categories.

First, we developed unitary tests before any other type of testing was performed. These were executed in each of the cycles in the testing phase as a first

step. To carry out the development of these tests, the Unity Test Framework (UTF) provided by the tool used to develop the Unity application was used, so the integration and use occurs naturally and quickly [13]. The main module for which the system was tested was AR. Therefore, test scripts were used. Through these, the deployment of Vuforia's AR camera was tested. Even the test framework creates an isolated environment in which to carry out tests both at run time and editing and generates an acceptance result or not.

Second, the product tests were aimed at making sure of the correct functioning of the application. Here, the functional tests allowed to validate the existence of the functional requirements in the system and that they effectively complied with the proposal. In this case the tests were carried out manually. In contrast, non-functional testing verifies requirements based on software quality attributes such as performance, portability, and usability. Performance testing is necessary to identify bottlenecks that may arise with respect to CPU usage, memory, or other factors, leading to high response times and excessive device resource usage. The Unity development platform provides within its tools the Unity Profiler. Profiler collects and displays data about application performance in terms of CPU, memory, and renderability; identifying the relationship of its high or low performance with the source code, scenes, and configurations of the application [14]. In addition, it allows access to Android and iOS. For this reason this tool was used to carry out the profiling of the application in the operating systems used. Vuforia defines a set of frames per second objectives for the correct functioning of the applications according to the devices and operating systems. Based on this, if the experience has a duration of more than ten minutes, the target number of frames would be 30 Frames per Second (FPS) for both Android and iOS. According to Figure 5 the number of frames per second is between 30 and 60 FPS, which demonstrates an expected operation based on what Vuforia proposed. In addition, when executing tasks with greater processing such as facial and body animation of avatars, the system demonstrated through the Unity Profiler to respond (communication with the CPU, not with the end user) in an average time not exceeding 30 ms. While in low processing tasks such as entering the selection menu, average response times of 17 ms were achieved. We concluded that, with respect to what Vuforia proposed, the characteristics found in this profiling follow the documented and expected standards for this type of application.

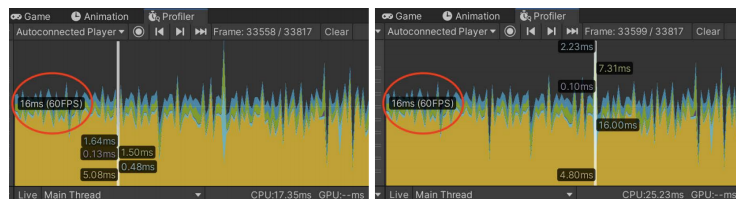


Fig. 5. Unity Profiler in VIA. Lower limit in ms (left). Upper limit in ms (right)

10 M.C. Leal et al.

Third, we performed user tests. We used the Think Aloud method to evaluate the first impression and the usability of the interface. We used informal summative evaluation for assessing user experience. With this approach [18], we were able to evaluate a smaller number of user participants and to present summary descriptive statistics. Considering that it was taken remotely and with only five people due to the COVID-19 pandemics; it was done using the WhatsApp messaging application as follows: (1) The participant was given a brief contextualisation of the project and the objective of the evaluation. (2) The link to the simulation of the prototype designed with Figma was shared. (3) After the users used the application, they sent the assessments regarding the interface and usability of the prototype openly, through text messages or voice notes. (4) All responses were gathered and analyzed to finally highlight the specific elements that need to be modified.

After carrying out the evaluation to five people, their assessments were collected and analysed to specify what were those comments in common and make an improvement. We found that: (1) Three of the five people suggested that the interaction with the avatars should be enriched, since this was the element that most caught their attention. (2) Four of the five people considered that the interface contained many colours and elements that made it look saturated. (3) Three of the five people mentioned that they would like to be able to know about other users' experiences using the app.

While opinions on this method tend to be subjective and qualitative, they allowed the team to identify changes and improvements. The way of communication between users and the VIA was modified, allowing them to start a conversation with the avatar, going beyond the automatic reproduction of audio that was initially proposed. Taking into account the saturation at the interface level identified in the evaluation, we made adjustments based on the Nielsen heuristics. Here, the aesthetic characteristics of colour and proportion were adjusted to the application's screens so that they did not generate discomfort to the end user. Continuing with the findings, we proposed to add the options to submit comments to the application. Although the option of providing a review, complaint or claim through the help module had already been raised, the comments would allow to satisfy the exposed need to recognise the experiences of other users. It is worth clarifying that the system does not contain user creation or login, since the idea is to access easily and quickly the place the user (visitor) wants to know. The comments are made anonymously, and the visitor has the possibility of adding a reaction and the text of the comment, and so, be able to know the experiences of others to add value to the application.

Considering that the objective of the application is to provide tourists and foreigners with an experience of learning places, specifically those chosen within the San Antonio neighbourhood, this evaluation was carried out to account for the effectiveness of the VIA in terms of satisfaction and usability for end users. We carried out a usability test, which consisted of three main elements: Tasks, Facilitator, and Participant. This type of test allowed us to observe and analyse the user's behaviour in front of the learning process with the system and how it is

positively or negatively affected through the user's facial and verbal expressions. This is intended to demonstrate the level of commitment that the user obtains in the time of initiation, transition, and progress [15]. Initiation behaviours are given by the first impression of the user, either observing others using it or when there is minimal interaction. Transition behaviours occur when the users finish performing some tasks and show their positive reaction to their experience and comfort with the response of the system. Progress behaviours are those that recognise a deep understanding of the system and possible future use. They are all part of a progressive set of reactions that contribute to demonstrating the acceptance of the application. Data collection was carried out in a joint test with visitors from the San Antonio neighbourhood, in the places of the Church of San Antonio and La Linterna. The evaluation took place in two moments, during the use of the application and after the use of the application. In this way, it was possible to evaluate the visitor's behaviour during the use of the application and subsequently their general appreciation of the system. We performed observation processes and questionnaires (Tables 3 and 4), to quantitatively measure the results of the test. During the use of the application, the facilitator oversaw guiding the users through the previously established tasks (Table 1). These tasks were read aloud to the participants as they progressed one by one, while each task was performed. The facilitator carried out an observation process following the plan established in Table 3, to convert the facial and verbal expressions evidenced by the user's behaviour into indicators (Table 2). On some occasions, the facilitator turned to the Think Aloud method to confirm interpretations of user behaviours. After the use of the software, we asked users to fill in a questionnaire (Table 4).

Based on the answers obtained in the questionnaire, we analysed the results obtained. As mentioned above, to carry out the evaluation, a usability test was used, in which the tasks allow to give a natural and orderly flow to the use of the application, in addition to covering at a general level all the functionalities and possible paths that it may have to obtain a complete analysis of the behaviour and acceptance by the end users. We proposed six tasks to be performed in the locations available in the VIA (Table 1). These tasks allowed to articulate the test objectively and precisely to be performed under realistic conditions of use. To perform the analysis of the results obtained in the test, we used an informal summative evaluation as exposed in Navarro-Newball et al. [16]. With this, it was possible to focus the measurement of the objectives based on indicators that show the acceptance and enjoyment by users when interacting with the application. To select these indicators the tests were made on real scenarios similar to Mekler et al. [17] and Navarro-Newball et al. [16], in addition to recommendations evidenced in [18]. An observation plan [16] was established to relate the indicators to the actions performed by the users while performing the tasks. These actions in turn were classified based on the different behavioural times evidenced by the test participants. Along with the strategy of the observation plan, a questionnaire was carried out adopting the recommendations of other questionnaire models, in this case the USE (usability, satisfaction and ease of

12 M.C. Leal et al.

use) [18]. To measure the results quantitatively by means of descriptive statistics, the questionnaire was evaluated on a differential semantic scale of 1 (little agreement) to 5 (completely agree).

To carry out the evaluation in the different places, we went to the San Antonio neighbourhood to have a scenario under real conditions. During application’s usage, participants could ask the VIA several questions. The project was trained with questions related to the three places and with questions out of context or of a general nature through a Microsoft owned database. The “chit-chat” small talk datasets are available for five pre-built personalities in nine languages [19]. Among the questions the user could ask VIA about the three places were: tell me about this place; what do you know about this place? and; what is this place? Accuracy of avata’s understanding of the questions seemed to be high and participants did not get any unanswered question, although further experiments could be done regarding this. Table 5 shows recorded scores of the semantic scale collected with the five participants, both in the observation plan (Table 3) made during the execution of tasks, and in the questionnaire (Table 4) resolved at the end of the test. Therefore, the values obtained were added and divided on the maximum score that could be achieved, considering the indicators that related to each task and question. In this way, we were able to show that the satisfaction (95%) and immersion (92%) was high. Users also provided positive feedback regarding the implementation of the application in the neighbourhood, highlighting how fun and useful it can be in the area, some mentioning that they did not know about La Colina and La Linterna. Linked to this is the fact that users intend to use the application in the future (88%), showing the viability of VIA. However, it would be worthwhile to continue working on the interface design to improve the ease of learning, since, although there were no drawbacks, as observed the indicator (86%) can be improved. This could be done through more test cycles.

Task	Objective	Location
1. Enter to (San Antonio church / La Linterna)	Enter the place.	Both
2. When was the San Antonio church built?.	Obtain information about the church	Church
3. ¿Qué se realiza en la Imprenta La Linterna?	Obtain information about La Linterna.	La Linterna
4. Watch the VIA dancing	Animate the VIA	Both
5. Where is (the church / La Colina) located?	Find address	Both
6. Send a comment about (the church / La Colina)	Send comment.	Both
7. Change the VIA’s language to English	Change the application’s language	Both

**Table 1.** The tasks for the evaluation tests.

Indicator	Description
A. Satisfaction	I would recommend the app to someone else. The app works the way the user wants it to work. It’s fun to use.
B. Better mood after using the app	The user feels satisfied and happy. Provides positive opinions.
C. Easy to use	It’s simple to use. The user uses the application intuitively.
D. Intention for future use	The user would use the app again.
E. Frustration	The user was frustrated by not being able to use the application correctly.
F. Immersion	The user concentrates on the application, learns to use it quickly.

**Table 2.** Usability and satisfaction indicators.

Action	Behaviour	Indicator
Performs the task	Initiation	C
Repeats Task	Transition	D
Shows positive emotions	Transition	A
Recommends the application	Transition	A
Shows negative emotions	Transition	E
Quickly identify next steps	Progress	C
Engages with the App	Progress	F
Better mood after using the app	Progress	B

Table 3. Observation plan.

Question	Indicator
Did you enjoy the activity ?	A
Did you enjoy the talk with the VIA?	F
Will you use the app again?	D
Would you recommend the app to a friend?	A
Do you think you could use the app without any instructions?	C
Do you think the app is easy to use?	C
Do you consider that the graphical Interface of the application is clear and adequate?	Usability

Table 4. Questionnaire for evaluation.

Indicator	Observation plan	Questionnaire	Total	Maximum score	Result (%)
A	47	24	71	75	95
B	22	n/a	22	25	88
C	43	43	86	100	86
D	23	21	44	50	88
E	0	n/a	0	25	0
F	24	22	46	50	92
Usability	N/A	24	24	25	96

Table 5. Results of recorded scores from the observation plan during the tasks and the questionnaire.

## 6 Conclusions and Further Work

Once the testing stage was finished we had evidence that the VIA application met the objectives. The presentation, animation, and voice of the three avatars proposed for the VIA application were well received (Table 5). To achieve this, we developed a VIA application that integrates technologies such as AR and NLP. Through these technologies, it was possible to communicate consciously and naturally about the three places chosen as the basis of the research in the San Antonio neighbourhood in Cali, Colombia, which promotes smart tourism based on new interaction technologies. Likewise, by approaching the research from the perspective of the end users, the implementation of three languages (Spanish, English, French) allowed the prototype to be used by both locals and foreigners. This validated the use of the VIA as a smart tourism and cultural computing application. In addition, the team in charge made use of environmental recognition technologies blending hardware and software, with which the

facades of places such as the Church of San Antonio and the Dome of San Antonio (Open air theatre at the church) were recreated virtually. This, in order to improve the user experience when deploying the avatars in AR, doing so with a recognition of the existing real infrastructure. On the other hand, the graphical interface defined for the VIA was implemented under the suggestion of the Nielsen usability heuristics, generating an aesthetic and user-friendly interface. Finally, thanks to the combination of different techniques and technologies, it was possible to reach a functional application accepted by an archetype of end users.

Considering the activities carried out within this project and the entire development research process that emerged, it is considered important as future work to continue with the growth of the VIA, improving and adding functionalities that positively benefit the tourist and commercial development of the city of Santiago de Cali. Undoubtedly, the city has places that are worth adding within the proposed approach, both within the Barrio San Antonio and outside it (eg: Cristo Rey, Gato Tejada, La Tertulia museum). Therefore, it is considered interesting to continue with the research process by the hand of local entities that seek to highlight the history and heritage of the city, also providing necessary information to enrich the knowledge databases. In the same way, it is important to follow an exhaustive evaluation process with end users, to identify enhancements that can be added to VIA to captivate the attention of the public and improve the user experience. In addition to this, functionalities would be integrated, directly related to suggestions of commercial establishments, with the aim of providing visibility to small and large entrepreneurs in the region who also allow them to create a business model for the scalability and maintenance of the same application. Finally, it will be important to consider privacy issues and contemplate the possibility to expand the application to Windows and/or the Web. Finally, this sort of VIA becomes very relevant in current pandemics and post pandemics scenario. The VIA may be able to provide more autonomy to visitors, helping to avoid crowds of tourist flocking near a human guide, thus, contributing to smart tourism. Additionally, technologies such as VIA favour complementing, reinterpreting and reunderstanding history in a friendly manner, without the need of destroying the heritage sites. This becomes relevant in an era when many monuments that could be augmented in the virtual space worldwide, are being destroyed and vandalised, as it has recently happened with the Cali's foundation monument.

## References

1. Boboc, R.G., Gîrbacia, F., Duguleană, M., Tavčar, A. A handheld Augmented Reality to revive a demolished Reformed Church from Braşov. In: Proceedings of the Virtual Reality International Conference - Laval Virtual 2017 (VRIC '17), Article 18, pp. 1–4, (2017). DOI:<https://doi.org/10.1145/3110292.3110311>
2. Wei, C., Chen, F., Chen, C., Lin, Y. Virtual and Augmented Reality to Historical Site Reconstruction: A Pilot Study of East Taiwan Old Railway Station. In: Pro-

- ceedings of the 2018 International Conference on Artificial Intelligence and Virtual Reality, pp. 42-46, (2018). DOI:<https://doi.org/10.1145/3293663.3293675>
3. Perea-Tanaka, C.F., Moreno, I., Prakash, E.C., Navarro-Newball, A.A. Towards tantalluc: Interactive mobile augmented reality application for the Museo de América in Madrid. In: 10th Computing Colombian Conference, pp. 164-171, (2015). doi: 10.1109/ColumbianCC.2015.7333427.
  4. Sauter, L., Rossetto, L., Schuldt, H. Exploring Cultural Heritage in Augmented Reality with GoFind! In: IEEE International Conference on Artificial Intelligence and Virtual Reality, pp. 187-188, (2018). doi: 10.1109/AIVR.2018.00041.
  5. Alulema, D., Simbaña, B., Vega, C., Morocho, D., Ibarra, A., Alulema, V. Design of an Augmented Reality-based Application for Quito's Historic Center. In: IEEE Biennial Congress of Argentina, pp. 1-5, (2018). doi: 10.1109/ARGENCON.2018.8646296.
  6. Wei, X., Weng, D., Liu, Y., Wang, Y. A tour guiding system of historical relics based on augmented reality. In: IEEE Virtual Reality, pp. 307-308, (2016). doi: 10.1109/VR.2016.7504776.
  7. Cavallo, M., Rhodes, G.A., Forbes, A.G. Riverwalk: Incorporating Historical Photographs in Public Outdoor Augmented Reality Experiences. In: IEEE International Symposium on Mixed and Augmented Reality, pp. 160-165, (2016). doi: 10.1109/ISMAR-Adjunct.2016.0068.
  8. Escobar S.D., Margherita E.G. (2021) Outcomes of Smart Tourism Applications On-site for a Sustainable Tourism: Evidence from Empirical Studies. In: Musleh Al-Sartawi A.M.A. (eds) The Big Data-Driven Digital Economy: Artificial and Computational Intelligence. Studies in Computational Intelligence, vol 974. Springer, Cham. [https://doi.org/10.1007/978-3-030-73057-4\\_21](https://doi.org/10.1007/978-3-030-73057-4_21)
  9. Nielsen, J., and Molich, R. Heuristic evaluation of user interfaces. In: Proc. ACM CHI'90 Conf. (Seattle, WA, 1-5 April), pp. 249-256, (1990).
  10. Vuforia Fusion. <https://library.vuforia.com/environments/vuforia-fusion>
  11. Crazy Minnow Studio. CMS. SALSA LipSync v2 suite. SALSA LipSync Suite - Online Documentation. [urlhttps://crazyminnowstudio.com/docs/salsa-lip-sync/](https://crazyminnowstudio.com/docs/salsa-lip-sync/)
  12. j1mmyto9. Speech-And-Text-Unity-iOS-Android. GitHub. <https://github.com/j1mmyto9/Speech-And-Text-Unity-iOS-Android>
  13. Unity Technologies. Unit testing. <https://docs.unity3d.com/Manual/testing-editortestsrunner.html>
  14. Unity Technologies. Profiler overview. <https://docs.unity3d.com/es/2021.1/Manual/Profiler.html>
  15. Barriault, C., Pearson, D. Assessing Exhibits for Learning in Science Centers: A Practical Tool. Visitor Studies, 13:1, 90-106 (2010). DOI: 10.1080/10645571003618824
  16. Navarro-Newball, A.A., Loaiza, D., Oviedo, C., Castillo, A., Portilla, A., Linares, D., Álvarez, G. Talking to Teo: Video game supported speech therapy. Entertainment Computing, 5:4, 401-412 (2014). <https://doi.org/10.1016/j.entcom.2014.10.005>.
  17. Mekler, E.D., Bopp, J.A., Tuch, A.N., Opwis, K. A systematic review of quantitative studies on the enjoyment of digital entertainment games. In: Proceedings of the SIGCHI Conference on Human Factors in Computing Systems, pp. 927-936, (2014). DOI:<https://doi.org/10.1145/2556288.2557078>
  18. Hartson, R., Pyla P. The UX Book. Agile UX Design for a Quality User Experience. Morgan Kaufmann, (2019).
  19. Microsoft. Personality Chat Datasets. <https://github.com/microsoft/botframework-cli/blob/main/packages/qnamaker/docs/chit-chat-dataset.md>

# A case study of smart industry in Uruguay: grain production facility optimization

Gabriel Bayá<sup>1</sup>[0000-0003-3193-6939], Pablo Sartor<sup>2</sup>[0000-0001-7076-3917], Franco Robledo<sup>1</sup>[0000-0003-4235-4221], Eduardo Canale<sup>1</sup>[0000-0002-1311-6497], and Sergio Nesmachnow<sup>1</sup>[0000-0002-8146-4012]

<sup>1</sup> Universidad de la República, Uruguay  
{gbaya, frobledo, canale, sergion}@fing.edu.uy

<sup>2</sup> Universidad de Montevideo, Uruguay  
psartor@um.edu.uy

**Abstract.** This article presents a Mixed-Integer Linear Programming model for cost optimization in multi-product multi-line production scheduling. The proposed model applies discrete time windows and includes realistic constraints. The model is validated on a specific case study from a real Uruguayan grain production facility. Results of the evaluation indicate that the proposed model improves over the current ad-hoc heuristic planning, reducing up to 10.4% the overall production costs.

**Keywords:** grain facility optimization · smart industry · Mixed-Integer Linear Programming · real case study.

## 1 Introduction

Intelligent systems for decision making are a valuable asset in production, especially under the novel Industry 4.0 paradigm [13]. The integration of new technologies and intelligent methods into classical industrial processes offers the capability of designing innovative processes and even business models. In any case, technological advances also enhance the application of traditional techniques aimed at improving business performance through efficiency. In agriculture, computational tools have been widely applied for crop planning and production [14]. Efficient and accurate models and algorithms to manage resources are crucial for improving competitiveness and minimizing operation costs.

This article presents a Mixed-Integer Linear Programming (MILP) optimization model for a capacitated multi-product multi-line production scheduling process. The model incorporates several constraints, which are frequently found on real applications. The problem is restated by using discrete time windows.

A specific case study of the proposed problem is analyzed: the optimization of the generalized production costs in a real grain production facility in Uruguay. The case study involves the batch production scheduling of 17 products spanning 16 weeks, 2 production lines, limited storage capacity and restrictions regarding product switching times and limited lifetime. Results of the application of the proposed model to the real case study demonstrate that significant improvements are obtained over an ad-hoc planning.

2 G. Bayá, P. Sartor, F. Robledo, E. Canale, S. Nesmachnow

The article is organized as follows. Next section describes the proposed grain facility optimization problem and the MILP formulation. Section 3 presents the real case study. The experimental evaluation is reported in Section 4, including a comparison with the ad-hoc planning, based on several common-sense rules, applied before the model was conceived.

## 2 The grain facility optimization problem

This section describes the grain facility optimization problem and its mathematical formulation.

### 2.1 Problem description

The problem concerns grain processing facilities, which must treat the seeds using resources such as machinery, workers, and storage capacity, in order to meet pre-planned delivery demands for each harvest. Several varieties of seeds are processed and delivered. Some of them expire a certain number of days after being processed, which imposes a restriction relating the production and withdrawal dates. Once the seeds are processed, they are stored in silos waiting to be withdrawn by clients, based on a planned list of withdrawals that were previously communicated in the planning phase. The production is carried out according to the withdrawals of the established products and the processing and storage capacities that the company has. To carry out the required processes on the seeds there are different production lines, which in turn have different processing capacities, commonly measured in tons per hour. These production lines must be supervised by operators during the period of time that they are operational. Since the machines are generally producing at maximum capacity, operator shifts are established and assigned to each of the lines. The number of shifts is set for every week, and remains the same within the same week. Every time a line ends the production of a certain product, it must be stopped and cleaned before proceeding with the processing of a different product. If the line stops after having met a certain demand and later returns to produce the same product, such cleaning is not necessary. The production process covers several weeks per year, and for each week a set of demanded products must be produced and withdrawn according to the previously specified conditions.

The problem models should minimize production costs, considering the number of production hours, the number of operator shifts and the amount of cleanings performed on the machines. In the same way, it must be ensured that the production is sufficient so the withdrawals can be fulfilled, the expiration periods of the products that expire are respected and the production not delivered immediately does not exceed the available storage facilities.

### 2.2 Problem formulation

The mathematical formulation of the proposed grain facility optimization problem considers the following sets and parameters:

Smart industry in Uruguay: grain production optimization 3

- $V_I$  is the set of products that expire.
- $V_T$  is the set of products that do not expire.
- $V$  is the set of all products,  $V = V_I \cup V_T$ .
- $L$  is the set of production lines.
- $S_f$  is the number of weeks in which production is scheduled.
- $M$  is the maximum number of withdrawals for each product.
- $C$  is the total storage capacity in tons.
- $\tau$  is the shelf life (in weeks) of products that expire.
- $N$  is the maximum number of shifts per week.
- $H_f$  is the number of productive hours in a shift.
- $\pi_l$  is productivity in tons/hour of the production line  $l \in L$ .
- $L_l$  is the cleaning time in hours of line  $l \in L$ .
- $R_v$  is number of batches of a product, when  $v \in V_I$ , if  $v \in V_T \rightarrow R_v=1$ .
- $S_v^r$  is the week in which the  $r$ -th withdrawal of product  $v \in V$  is located.
- $\delta_v^r$  is the demand for product  $v \in V$  in its  $r$ -th withdrawal,  $r = 1 \dots M$ .
- $d_v^s$  is the demand for product  $v \in V$  to withdraw in the week  $s$ .
- $D_s$  working days for each week  $s$  (e.g., 5 days from Monday to Friday, 5.5 days from Monday to Saturday noon, etc.).

In turn, the considered decision variables are:

- $x_{v,l}^{s,r} \in \mathbb{R}^+$ , the quantity of product  $v \in V$  produced in the line  $l \in L$  in the week  $s$  for the  $r$ -th withdrawal.
- $t_l^s \in \mathbb{Z}^+$ , the number of shifts to put in line  $l \in L$  in week  $s$ .
- $y_{v,l}^s = \begin{cases} 1 & \text{if and only if line } l \text{ is producing product } v \in V \text{ in the week } s \\ 0 & \text{otherwise} \end{cases}$
- $p_{v,l}^s = \begin{cases} 1 & \text{if and only if product } v \in V \text{ is the first product to be produced} \\ & \text{in week } s \text{ in } l \in L \\ 0 & \text{otherwise} \end{cases}$
- $u_{v,l}^s = \begin{cases} 1 & \text{if and only if product } v \in V \text{ is the last product to be produced in} \\ & \text{week } s \text{ in } l \in L \\ 0 & \text{otherwise} \end{cases}$
- $w_{v,l}^s = \begin{cases} 1 & \text{if product } v \in V \text{ ends the week } s \text{ and starts the week } s+1 \text{ in line} \\ & l \in L \\ 0 & \text{otherwise} \end{cases}$
- $c_l^s = \begin{cases} 1 & \text{if in the week } s, \text{ one cleaning of the line } l \in L \text{ is avoided} \\ 0 & \text{otherwise} \end{cases}$

Considering the previously defined constants and variables, the mathematical formulation of the problem as a Mixed-Integer Linear Programming (MILP) problem is presented in Eq. 1–16.

4 G. Bayá, P. Sartor, F. Robledo, E. Canale, S. Nesmachnow

$$\min P \sum_{l \in L} \sum_{s=1}^S t_l^s + Q \sum_{l \in L} \frac{1}{\pi_l} \sum_{v \in V} \sum_{r=1}^{R_v} x_{v,l}^{s,r} + R \sum_{l \in L} L_l \left( \sum_{s=1}^S \sum_{v \in V} y_{v,l}^s - \sum_{s=1}^{S-1} c_l^s \right) \quad (1)$$

$$\text{subject to } \sum_{z=S_v^r-\tau}^{S_v^r} \sum_{l \in L} x_{v,l}^{z,r} - \delta_v^r \geq 0, \forall v \in V_I, \quad r = 1 \cdots R_v \quad (2)$$

$$\sum_{z=1}^{S_v^r} \sum_{l \in L} x_{v,l}^{z,1} - \sum_{z=1}^{S_v^r} d_v^z \geq 0, \forall v \in V_T, \quad r = 1 \cdots M \quad (3)$$

$$\sum_{z=1}^s \sum_{v \in V} \sum_{l \in L} \sum_{r=1}^{R_v} x_{v,l}^{z,r} - \sum_{z=1}^s \sum_{v \in V} d_v^z \leq C \quad \forall s = 1 \cdots S \quad (4)$$

$$t_l^s \leq N \quad \forall l \in L, \quad \forall s = 1 \cdots S \quad (5)$$

$$d_v^s \cdot y_{v,l}^s - \sum_{r=1}^{R_v} x_{v,l}^{s,r} \geq 0 \quad \forall l \in L, \quad \forall v \in V, \quad \forall s = 1 \cdots S, \quad (6)$$

$$\sum_{r=1}^{R_v} x_{v,l}^{s,r} - y_{v,l}^s \geq 0 \quad \forall l \in L, \quad \forall v \in V, \quad \forall s = 1 \cdots S, \quad (7)$$

$$y_{v,l}^s - p_{v,l}^s \geq 0 \quad \forall l \in L, \quad \forall v \in V, \quad \forall s = 1 \cdots S, \quad (8)$$

$$\sum_{v \in V} p_{v,l}^s \leq 1 \quad \forall l \in L, \quad \forall s = 1 \cdots S, \quad (9)$$

$$y_{v,l}^s - u_{v,l}^s \geq 0 \quad \forall l \in L, \quad \forall v \in V, \quad \forall s = 1 \cdots S, \quad (10)$$

$$\sum_{v \in V} u_{v,l}^s \leq 1 \quad \forall l \in L, \quad \forall s = 1 \cdots S, \quad (11)$$

$$2w_{v,l}^s - u_{v,l}^s - p_{v,l}^{s+1} \leq 0 \quad \forall l \in L, \quad \forall v \in V, \quad \forall s = 1 \cdots S-1, \quad (12)$$

$$c_l^s - \sum_{v \in V} w_{v,l}^s \leq 0 \quad \forall l \in L, \quad \forall s = 1 \cdots S-1, \quad (13)$$

$$|V|p_{v,l}^s + |V|u_{v,l}^s + \sum_{v_1 \in V, v_1 \neq v} y_{v_1,l}^s \leq 2|V| \quad \forall l \in L, \quad \forall v \in V, \quad \forall s = 1 \cdots S, \quad (14)$$

$$\pi_l (D_s H_f t_l^s - L_l \sum_{v \in V} y_{v,l}^s - c_l^s) - \sum_{v \in V} \sum_{r=1}^{R_v} x_{v,l}^{s,r} \geq 0 \quad \forall l \in L, \quad \forall s = 1 \cdots S-1, \quad (15)$$

$$\pi_l (D_S H_f t_l^S - L_l \sum_{v \in V} y_{v,l}^S) - \sum_{v \in V} \sum_{r=1}^{R_v} x_{v,l}^{S,r} \geq 0 \quad \forall l \in L, \quad (16)$$

The objective function (Eq. 1) proposes minimizing the overall cost of production. The cost is composed of three different terms, which model the costs associated to labor, production, and cleaning. The generalized cost is defined as a number that summarizes these three cost sources for each production cycle.

The first term of the objective function represents the labor cost, which is proportional to the total number of shifts (of operators) to be used in production, for all available machines. The second term represents the costs associated to the time during which the machines produce, other than labor (e.g., energy and amortization). The third term represents the costs incurred every time a line is cleaned, other than labor (e.g., supplies and energy; the latter has a different hourly consumption than in the second term). Parameters  $P$ ,  $Q$ , and  $R$  are the unit conversion coefficients, which allows expressing the total cost (sum of all the terms of the objective function) in a single unit. The linear aggregation approach is appropriate since all costs are variable and directly proportional to the decision variables: labor cost is proportional to the number of shifts, energy, supplies and amortization costs are proportional to the operational hours and to the cleaning hours (at different rates).

Eq. 1–16 formulate the constraints of the optimization problem. Eq. 2 guarantees that there is sufficient production of inoculated products to be delivered, thus implying that production must be greater than demand. Since inoculated products have an expiration date, the model must ensure that the number of weeks elapsed since they were produced until they are delivered does not exceed parameter  $\tau$ . Eq. 3 ensures that the enough treated product are produced. As for Eq. 2, the production must be greater than the demand, but in this case the products can be produced at any moment of the production cycle. Eq. 4 rules the storage capacity. The first term of the left side of the inequality is the production of week  $s$  and the second term correspond to the deliveries in that week. The difference between production and delivery must be positive, thus ensuring that the products can be stored without exceeding the total capacity  $C$ . Eq. 5 limits the number of shifts for each of the production lines in each week.

Eq. 6–11 rule the activation of binary variables  $y_{v,l}^s$ ,  $p_{v,l}^s$ ,  $u_{v,l}^s$  y  $w_{v,l}^s$ , which act as auxiliary variables to calculate the number of cleanings avoided in the production lines. Eq. 6 and Eq. 7 work together to activate the variable  $y_{v,l}^s$  if and only if some quantity of a certain product  $v$  was produced on the line  $l$  in the week  $s$ . Eq. 8 indicates that the necessary condition for the variable  $p_{v,l}^s$  to be activated ( $v$  is the first product to be produced in the line  $l$  in the week  $s$ ) is that some quantity of product  $v$  has been produced in the week  $s$ . Eq. 9 guarantees the uniqueness of the first product produced in week  $s$  on line  $l$ , thus ensuring that the definition of the variable  $p_{v,l}^s$  is consistent. Eq. 10 and 11 are analogous to Eq. 8 and 9, but applied to the last product produced in the week. To guarantee the existence of a last product  $v$  to be produced on the line  $l$  in week  $s$ , there must be a production of said product  $v$  and it is also guaranteed that this last product is unique. Eq. 12 forces the variable  $w_{v,l}^s$  to take the value 1 only if the product  $v$  crosses the weekly border, that is, if it is the last of the week  $s$  and the first of the week  $s + 1$  for the production line  $l$ .

6 G. Bayá, P. Sartor, F. Robledo, E. Canale, S. Nesmachnow

Eq. 13 rules variable  $c_l^s$ , i.e., whether a cleaning is saved on production line  $l$  for week  $s$ . The sum of variables  $c_l^s$  has a negative sign in the objective function, therefore the model presses for this quantity to be the maximum possible. Eq. 14 ensures that if a certain product  $v$  is the first and the last of the week  $s$  for a production line  $l$ , no other product is produced on line  $l$  in the same week.

Eq. 15 expresses that the maximum production capacity of line  $l$  must be greater than that produced in the line for that week. The nominal production capacity of line  $l$  is subtracted from the necessary stop times and the cleanings saved are added, as a result of the correct sequencing of the products to be produced. Eq. 16 is analogous, to cover the last week, where there are no savings in cleaning, since no more productions are to be scheduled.

### 2.3 Related work

Several articles in the literature have proposed MIP models for solving grain production and/or delivering optimization problems.

Early works in the area applied MILP models for problems related to harvesting methods and machinery selection. Al-Soboh et al. [3] applied MILP for mixed cropping systems, computing an optimal spacing for planting navy bean. Ait Si Larbi et al. [1] proposed a MILP model for multi-stage optimization in agri-food supply chain, which outperformed a planning heuristic in a real case study in Algeria. Later, the authors [2] applied the AUML protocol specification to build an effective system for production and transportation. The proposed model was effective to compute accurate values of the optimized functions.

Bilgen and Ozkarahan [4] proposed a multi-period MILP model for minimizing costs of blending and shipping on the wheat supply chain. An hybrid deterministic/non-deterministic model was proposed by Granillo et al. [5] for minimizing the building cost of a distribution network farm. The model computed accurate solutions for the supply chain of barley in Mexico. Sanches et al. [10] applied a multi-period MIP model for the optimization of production scheduling of fruit beverages. The proposed approach computed accurate results under realistic assumptions for a case study in Brazil. Hosseini et al. [6] proposed a two-stage mixed-stochastic approach to deal with uncertainty on costs, demand, and supply in the wheat supply chain network. The proposed model outperformed a deterministic model in real case study in Iran.

León et al. [7] proposed a MILP formulation for minimizing the total cost of the bioethanol supply chain. Accurate results were computed to satisfy the demand in a case study considering corn and barley residues in México. The proposed MILP approach was robust and applicable to other similar problems.

Several articles related to food supply chain and logistics have applied MILP models for optimization. Soysal et al. [12] proposed a MILP model for beef industry, extended to minimize cost and greenhouse gas emissions in the transportation system. Mishra et al. [8] applied a nonlinear programming model to minimize refrigeration cost in the storage process of leafy greens. Shekarian et al. [11] proposed a MILP model for profit optimization in the soybean supply chain network, computing accurate results for a real case in Ontario.

### 3 Case study: Production optimization in a grain processing facility

The case study considered in this article corresponds to the production planning of a company that processes and sells soybeans. The main details of the scenario are presented in this section.

#### 3.1 Description of the case study

The company operates in Uruguay serving, among others, soy producers. Producers send orders for 17 different kinds of soybeans for the harvest, that must be processed and delivered according to a schedule that extends over a period of 19 weeks (the annual soybean harvest). The main problem that the company faces when the orders are received is the accurate planning of the production and preparing the deliveries in a timely manner.

The company has two production lines with 6.165 and 6.65 tons per hour respectively of processing capacity; both are able to produce any of the 17 products. Every time the machines finish processing a product, they must stop and be cleaned if a different product is to be processed next. The duration of stoppage and cleaning times of these production lines are 6 and 8 hours respectively. The period of time the machines are stopped to be cleaned is a time in which the company stops producing and therefore reducing this downtime is of paramount importance for improving the efficiency. The adequate quantity to produce, as well as the correct sequencing of the products that must enter the two production lines, helps reducing stoppages with the corresponding savings in time and associated costs. This strategy often implies producing a larger quantity of grains than withdrawals in particular weeks, which must therefore be stored. For this purpose, the company has a storage capacity of 2.700 tons of grain. Using machinery efficiently and taking advantage of storage silos, the company must produce and store enough grain to cover the withdrawals required by its customers.

Processed products can be divided into two classes, inoculated and treated. This adds an additional control that the company must resolve. Products within the class named as *inoculated* (7 out of the 17 products) have an expiration time. Such products therefore cannot be produced and stored too far in advance, due to their upcoming expiration date. In the considered case study the expiration time is two weeks, which is a major constraint for planning. In turn, there is no expiration time for products within the *treated* class (10 out of the 17).

The supervision of the machinery during production as well as cleaning are carried out by shifts of operators, who work 7.5 effective hours in every shift. Due to worker management policies, given a week  $w$  and a specific line  $l$ , the same number of shifts (1, 2 or 3) are performed from Monday to Friday (and half of it on the corresponding Saturday); the number of shifts can be set to different values for every combination of week and line  $(w, l)$ .

8 G. Bayá, P. Sartor, F. Robledo, E. Canale, S. Nesmachnow

### 3.2 Conception of the optimization model

This subsection describes the process for conceiving the optimization model.

The company raised the need to improve the scheduling efficiency to the research group. The main goal of the company was exploring intelligent planning methodologies such as the ones applied in smart logistics to improve over the costs obtained applying a non-formalized planning, following a basic set of intuitive criteria (this planning is referred as Plan-1 hereafter).

After several interviews, a first simple model of the problem was created as a spreadsheet, whose cells stores numbers equivalent to the decision variables  $x$  and  $t$  of the mathematical formulation presented in Section 2. The spreadsheet was organized with rows representing the weeks and columns representing pairs (product,line) as amounts of tons to produce. The simple model in the spreadsheet allowed manually changing values in the mentioned cells and showing the corresponding use of lines and storage capacities, and also displaying alerts in case of violated constraints.

The production plan for year 2020 was computed using the described spreadsheet and a heuristic procedure that is described in Section 4.3. The resulting plan is referred as *ad-hoc* plan and its was significantly better than the one of Plan-1 (i.e., providing a reduction of approximately 20% on the necessary number of cleaning cycles). The *ad-hoc* heuristic schedule is used as a reference baseline to compare the results computed by the proposed MILP model, as described in the next section.

## 4 Experimental evaluation

This section reports the experimental evaluation of the proposed approach for solving the real case study of production planning.

### 4.1 Evaluation methodology

The proposed formulation was implemented using the AMPL modelling program language and solved with IBM CPLEX Solver ver. 20.1.0.0. The hardware used for running this model was an Intel Core i9-9900K CPU @ 3.60GHz, 16 processors with 64 Gb. of RAM. Equipment OS is CentOS Linux release 7.7.1908. The default configuration of CPLEX was used for all parameters for all executions. A fixed effort stopping criterion is applied: CPLEX ends execution after reaching a predefined threshold on the execution time.

Two metrics were considered to evaluate the performance of the model: the execution time considered as threshold and the gap of the computed solution with respect to a certain lower bound calculated by the solver. The gap is related to the execution time, i.e., an inversely proportional relationship is observed, as increasing the total execution time of the model allows computing more accurate results. For the considered case study, several executions of the proposed model are performed considering as stopping criterion 1, 5, 30, 60, 120, 180, and 240 minutes, respectively.

## 4.2 Definition of the problem instance

The experimental evaluation of the proposed model was performed on a specific instance of the case study. The parameters that define the used instance are:

- $V_I = \{1 \dots 7\}$ ;  $V_T = \{8 \dots 17\}$ ;  $V = V_I \cup V_T$ ;  $\tau = 2$   
The products defined as inoculated in this instance are those specified with an index between 1 and 7, whereas products defined as treated have an index between 8 and 17. The  $\tau$  parameter specifies the shelf life of the inoculated products and it is set to 2 weeks.
- $L = \{1, 2\}$ ;  $\pi_l = \{6.165, 6.5\}$ ;  $L_l = \{6, 8\}$ , with  $l \in L$   
These parameters correspond to the set of machines available, their production capacity, and their cleaning times in hours respectively.
- $S_f = 19$ ;  $C = 2700$ ;  $N = 3$ ;  $H_f = 7.5$ ;  $D_s = 5.5 \forall s$   
The total number of weeks that the harvest lasts (parameter  $S_f$ ) is set to 19 weeks, the storage capacity of processed grains (parameter  $C$ ) is set to 2700 tons, the maximum number of operator shifts (parameter  $N$ ) is set to 3, and the number of productive hours in a shift (parameter  $H_f$ ) is set to 7.5. The number of working days for each week (parameter  $D_s$ ) is set to 5 days (i.e., from Monday to Friday and a half day at Saturday).
- The maximum number of withdrawals for each product (parameter  $M$ ) is set to 10.
- The number of batches corresponding to the inoculated products is  $R_v = \{6, 7, 8, 4, 5, 2, 2\}$  with  $v \in V_I$  and the treated products belonging to a single batch is  $R_v = 1 \quad \forall v \in V_T$

Demands are established by customers. Table 1 reports the planned demand for products and the week in which these products are to be withdrawn. Values in the table are the main input to the model, corresponding to the parameter  $d_v^s$  that describes the quantity of product  $v$  to be withdrawn in week  $s$ . Products 1–7 are inoculated (i.e., the limited lifetime constraint applies to them), while 8–17 are treated. From table 1 the last two parameters that define the problem instance are defined: the week in which the  $r$ -th withdrawal of product  $v$  is located ( $S_v^r$ ) and the demand for product  $v$  in its  $r$ -th withdrawal ( $\delta_v^r$ ).

## 4.3 Baseline solution for comparison

This subsection describes the heuristic procedure followed by the operations manager to create the baseline ad-hoc production plan, used to compare the results computed by the proposed model.

The heuristic applies the following procedure:

1. Set 3 shifts for all weeks in both lines and 0 tons to produce in every (week, line) combination.

10 G. Bayá, P. Sartor, F. Robledo, E. Canale, S. Nesmachnow

week	products																
	1	2	3	4	5	6	7	8	9	10	11	12	13	14	15	16	17
8									20	600	60					200	
9				80	140	100			60	600	120					200	
10			40	120	400	100			80	120	600	140	60	24		200	
11		160	200	120	600				80	120	400	40	140	24	60		40
12		240	400	120	360		120	200	120	40			200	60	80		120
13	36	240	440		300		120	200	40				140	60	60		80
14	60	160	440					400					20	48			40
15	80	160	280					400						24			
16	40	80	120											40			
17	100	40	80											80			
18	40																

**Table 1.** Demand ( $d_v^s$ , in tons) of products ( $v$ ) by week ( $s$ )

- Set the production of product  $p$  in week  $w$ , equal to the demand of  $p$  in  $w$ , always in the fastest line (several capacity overflow and/or storage overflow will appear).
- Repeat while possible: choose a week in which there is overflow on capacity and move any product to the other line, provided that it does not imply a capacity overflow on the latter.
- Repeat while possible: choose a week and a treated product ( $w, p$ ) for which there is capacity overflow or storage overflow, and move its production to earlier weeks (seeking to soften the capacity-need peaks).
- Repeat the previous step, over the inoculated products, anticipating production at most two weeks to respect the expiration dates constraint.
- Reduce all shifts as possible, as long as the reduction does not cause new capacity overflow to appear.

Finally, a visual inspection is performed, searching for other movements of products between lines and weeks trying to reduce shifts and cleanings without introducing capacity overflows or storage overflows until no further evident improvements arise. Preparing the spreadsheet and executing the above described steps took approximately 16 hours of human work (operations manager) and yielded a production plan that involved 319 shifts and 34 cleanings.

#### 4.4 Numerical results

Once the input parameters of the model have been specified, the solver is executed to find the solution for the proposed instance of the real case study. The solution found is described in Tables 2–4, which report the week and the quantity of products to be processed, in order to obtain the best computed production plan that meets the demand requirements and adjusts to both the production capacities of the machinery and the storage volume of the facilities.

Smart industry in Uruguay: grain production optimization 11

Table 2 presents the production schedule, reporting for each week, line, and product, the quantity to be produced, the hours the process will take, if a cleaning must be performed after the product has been processed and it can be avoided, and the stored stock of the product at the time of finalizing its production, subtracting the withdrawals for the week, if any.

<i>week</i>	<i>line</i>	<i>product</i>	<i>production (tons)</i>	<i>hours</i>	<i>cleans</i>	<i>cleans saved</i>	<i>stockpiled</i>
3	2	9	320	48.12	1	0	320
3	2	11	175.43	26.38	0	1	175.43
4	2	11	548.62	82.5	0	1	724.05
5	2	11	274.31	41.25	0	1	998.36
6	2	11	822.94	123.75	0	1	1821.3
7	2	11	274.31	41.25	0	1	2095.61
8	1	12	254.72	41.25	0	1	254.72
8	2	11	104.39	15.7	1	0	2200
8	2	10	360	54.14	1	0	360
8	2	16	252.15	37.92	0	1	252.15
9	1	12	105.28	17.05	1	0	300
9	1	6	200	32.39	1	0	200
9	1	14	168	27.21	1	0	168
9	1	4	179.73	29.11	0	1	179.73
9	2	16	347.85	52.31	1	0	400
9	2	5	421.89	63.44	0	1	421.89
10	1	4	260.27	42.15	1	0	360
10	1	3	297.03	48.1	1	0	297.03
10	1	13	109.94	17.8	0	1	109.94
10	2	5	822.94	123.75	0	1	1104.83
11	1	13	450.06	72.88	1	0	500
11	1	15	200	32.39	1	0	200
11	1	17	40	6.48	0	1	40
11	2	5	555.17	83.48	1	0	1260
11	2	2	214.56	32.27	0	1	214.56
12	1	17	240	38.87	1	0	240
12	1	7	240	38.87	1	0	240
12	1	8	200	32.39	0	1	200
12	2	2	426.76	64.17	1	0	481.33
12	2	3	342.97	51.58	0	1	400
13	1	8	600	97.17	1	0	600
13	1	1	116	18.79	0	1	116
13	2	3	769.15	115.66	0	1	769.15
14	1	1	60.38	9.78	1	0	140.38
14	1	2	182.96	29.63	0	1	184.28
14	1	14	192	31.09	1	0	192
14	2	3	274.31	41.25	0	1	603.46
15	1	2	254.72	41.25	0	1	279
15	2	3	316.54	47.6	1	0	480
15	2	8	400	60.15	1	0	400
16	1	2	1.00	0.16	1	0	120.00
16	1	1	179.62	29.09	1	0	180

**Table 2.** Production schedule (in tons) by week for the considered case study

12 G. Bayá, P. Sartor, F. Robledo, E. Canale, S. Nesmachnow

An important point to take into account, which is reported in Table 2, is the correct sequencing for each production line of the products to be processed within the same week. Every time the column *cleans saved* takes the value 1, the product (which was the last processed in the week for the line) continues its production as the first product in the following week, therefore avoiding a cleaning of the machine.

Table 3 summarizes for each production line, the total number of operator shifts used, the production amount and production hours, the cleanings required and cleanings avoided by optimization, and the total hours of effective cleaning.

<i>line</i>	<i>shifts</i>	<i>production (tons)</i>	<i>hours per line</i>	<i>cleanings</i>	<i>saved cleanings</i>	<i>cleaning hours</i>
1	20	4531.70	733.88	14	8	84
2	31	8024.30	1206.66	8	12	64
<i>total</i>	51	12556	1940.54	22	20	148

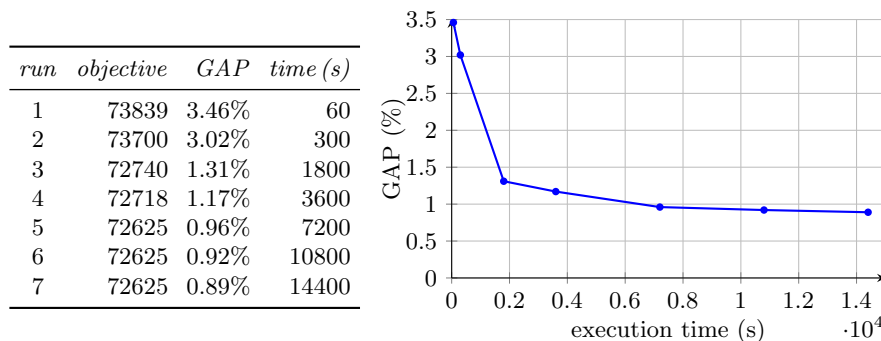
**Table 3.** Production and cleanings for the considered case study

Table 4 reports for each week of the harvest the total products stored (production minus withdrawals) and the storage capacity available in the facility.

<i>week</i>	1	2	3	4	5	6	7	8	9	10
<i>stored production (tons)</i>	0	0	495	1044	1318	2141	2415	2506	2629	2235
<i>available capacity</i>	2700	2700	2205	1656	1382	559	285	194	71	465
<i>week</i>	11	12	13	14	15	16	17	18	19	
<i>stored production (tons)</i>	1711	1101	870	412	439	339	39	0	0	
<i>available capacity</i>	989	1599	1830	2288	2261	2361	2661	2700	2700	

**Table 4.** Stored production and available capacity by week for the case study

Fig. 1 reports the results (value of the objective function and the percentage gap) of seven executions of the proposed model with different time limits.



**Fig. 1.** Numerical results and GAP evolution for the considered case study

The graph in Fig. 1 shows a decrease of the gap metric as the solver execution times increase. Convergence towards the global optimum is faster in the first minutes, becoming stagnant for execution times greater than two hours. The gap of 0.89% obtained after four hours of running the model can be taken as an excellent approximation to the global optimum.

Regarding the comparison with baseline method, Table 4.4 reports the values obtained by the existing heuristic method and the proposed method in CPLEX for three relevant metrics: number of shifts, number of cleanings needed, maximum storage used, and overall cost. Values of  $\Delta$  reports the improvements (reductions) of the proposed method.

	<i>heuristic</i>	<i>CPLEX</i>	$\Delta$	$\Delta\%$
shifts	58	51	7	12.1%
cleanings	34	22	12	35.3%
maximum storage used	3666	2629	1037	28.3%
overall cost	81070	72625	8445	10.4%

Results in Table 4.4 indicate that the proposed methods computed plans that reduced more than 12% the number of shifts, more than one third the number of cleanings, and more than 28% the maximum storage used. These results demonstrate the accuracy of the computed plans, which directly imply a better resource management, which is crucial for improving competitiveness and minimizing operation costs. Overall, the plan computed by the proposed model improved cost values 10.4% over the the heuristic planning and more than 30% over the original manual planning.

## 5 Conclusions and future work

The novel paradigm of Industry 4.0 has revitalized production in smart cities. Intelligent systems are now being applied for transforming traditional production processes into smart value chains. This way, Industry 4.0 developed new relationships in production systems, focused on improved interactions between manufacturers, suppliers and citizens, via efficient models and algorithms.

Inspired on the need to effectively plan production, organize deliveries, and manage storage in a seed sales and processing company, this article presented a mathematical model for the exact resolution of a typical production problem in the soybeans logistic chain. A MILP model was specified and implemented to optimize the overall production costs, including machine operating hours, number of assigned shifts, and stops for cleaning. The problem model includes several features from real-world production facilities, including multi-product, multi-line processing, machinery cleaning stops and storage of processed products. In turn, the formulation accounts for realistic constraints considering that demands can be met, all processed products can be stored if it is necessary, inoculated products are produced so that they do not expire before delivery and shifts do not exceed working hours.

14 G. Bayá, P. Sartor, F. Robledo, E. Canale, S. Nesmachnow

The proposed model was implemented in AMPL and solved using CPLEX20.0.0.1 in an Intel Core i9-9900K with 16 processors and 64 Gb. of RAM to optimize a real case study of a Uruguayan grain processing facility for the year 2020 soybean harvest, which previously applied manual and an heuristic method to plan production and deliveries.

The results obtained in the experimental evaluation indicated that an orderly production plan is obtained, with efficient storage capacity, notably reducing the number of stops for cleaning as well as the supervisory shifts used. Overall, the proposed model computed plans that improved more than 10% and more than 30% regarding cost over the manual and the heuristic planning, respectively. Furthermore, the computed plans also improved storage occupancy and costs of machinery cleaning supplies.

The main lines of future work include additional realistic features in the optimization model. Regarding the discretization applied to determine productions, moving from planning weeks to planning days will allow for a more accurate production planning, further optimization of supervisor shift costs, and improved storage management. In addition, introducing a silo farm for raw grains, shared to store the processed grains, will certainly reflect the current reality of grain production companies. The proposed model should be adapted to take in consideration these new features and related new constraints. All these considerations will imply more complex models and a direct increment on the computing demands of the exact resolution approaches, then developing efficient optimization approaches using high performance computing techniques and the infrastructure of National Supercomputing Center [9] is also a promising line for future work.

## References

1. Ait Si Larbi, E., Bekrar, A., Trentesaux, D., Bouziane, B.: Multi-stage optimization in supply chain: an industrial case study. In: 9<sup>th</sup> International Conference on Modeling, Optimization & Simulation (2010)
2. Ait Si Larbi, E., Ghani, B., Trentesaux, D., Bouziane, B.: Supply chain management using multi-agent systems in the agri-food industry. In: Borangiu, T., Trentesaux, D., Thomas, A. (eds.) *Service Orientation in Holonic and Multi-Agent Manufacturing and Robotics*, Studies in Computational Intelligence, vol. 544, pp. 145–155. Springer, Cham (2014)
3. Al-Soboh, G., Srivastava, A., Burkhardt, T., Kelly, J.: A mixed-integer linear programming (MILP) machinery selection model for navybean production systems. *Transactions of the ASAE* **29**(1), 81–84 (1986)
4. Bilgen, B., Ozkarahan, I.: A mixed-integer linear programming model for bulk grain blending and shipping. *International Journal of Production Economics* **107**(2), 555–571 (2007)
5. Granillo-Macias, R., Hernandez, I.J.G., Martinez-Flores, J.L., Caballero-Morales, S.O., Olivarez-Benitez, E.: Hybrid model to design a distribution network in contract farming. *DYNA* **86**(208), 102–109 (2019)
6. Hosseini, S., Ghatreh, M., Saadi, F.: Strategic optimization of wheat supply chain network under uncertainty: a real case study. *Operational Research* (2019)

7. León-Olivares, E., Minor-Popocatl, H., Aguilar-Mejía, O., Sánchez-Partida, D.: Optimization of the supply chain in the production of ethanol from agricultural biomass using mixed-integer linear programming (MILP): A case study. *Mathematical Problems in Engineering* **2020**, 1–25 (2020)
8. Mishra, A., Buchanan, R., Schaffner, D., Pradhan, A.: Cost, quality, and safety: A nonlinear programming approach to optimize the temperature during supply chain of leafy greens. *LWT – Food Science and Technology* **73**, 412–418 (2016)
9. Nesmachnow, S., Iturriaga, S.: Cluster-UY: Collaborative Scientific High Performance Computing in Uruguay. In: Torres, M., Klapp, J. (eds.) *Supercomputing, Communications in Computer and Information Science*, vol. 1151, pp. 188–202. Springer (2019)
10. Sanches, M., Morabito, R., Oliveira, M.: Otimização da programação da produção de bebidas à base de frutas por meio de modelos de programação inteira mista. *Gestão & Produção* **24**(1), 64–77 (2016)
11. Shekarian, S., Amin, S.H., Shah, B., Tosarkani, B.M.: Design and optimisation of a soybean supply chain network under uncertainty. *International Journal of Business Performance and Supply Chain Modelling* **11**(2), 176 (2020)
12. Soysal, M., Bloemhof-Ruwaard, J., van der Vorst, J.: Modelling food logistics networks with emission considerations: The case of an international beef supply chain. *International Journal of Production Economics* **152**, 57–70 (2014)
13. Ustundag, A., Cevikcan, E.: *Industry 4.0: Managing The Digital Transformation*. Springer International Publishing (2018)
14. Woodruff, D., Voß, S.: *Introduction to Computational Optimization Models for Production Planning in a Supply Chain*. Springer-Verlag (2006)

# Hybrid GRASP+VND for flexible vehicle routing in smart cities

Lucía Barrero, Rodrigo Viera, Franco Robledo,  
Claudio Risso, and Sergio Nesmachnow

Universidad de la República, Uruguay,  
{lucia.barrero,rodrigo.viera,frobledo,crisso,sergion}@fing.edu.uy

**Abstract.** This article presents a metaheuristic resolution approach for a variant of the Vehicle Routing Problem considering heterogeneous fleet and flexible time windows. This problem variant solved considers extended time windows for delivering products to customers, modeling a realistic situation for logistics in smart cities. The proposed metaheuristic follows an hybrid approach, combining well known search procedures. Accurate results are reported for problem instances built by extending existing benchmarks in the literature. The proposed model is competitive with previous results and was able to compute better solutions in ten problem instances

**Keywords:** smart logistics, vehicle routing, smart cities

## 1 Introduction

Vehicle routing is a classical optimization problem that has received a renewed interest due to the importance of logistics for the new Industry 4.0 paradigm. The capabilities of providing supply chains with accurate, coordinated, real-time tool for vehicle scheduling and routing is very relevant for acquiring decisive advantages on supply chain management and business [5, 3].

The term Vehicle Routing Problem (VRP) embraces a whole class of problems aimed at determining a set of routes for a fleet of vehicles that must visit and deliver products to a set of customers. The main goal of the problem is computing a minimum cost routing schedule for each vehicle to deliver products to customers according to their demands, operation times, and other constraints [8].

VRP is among the most studied combinatorial optimization problems in operations research. Unlike other traditional combinatorial optimization problems, like the the Traveling Salesman Problem (TSP), where exact solvers can be applied to optimally solve instances with thousand of customers, the VRP is intrinsically more complex, as instances with more than one hundred customers can be hard to solve [1].

This article focuses on a specific variant of the VRP that considers flexible time windows for delivering goods to customers. The flexibility allows modeling realistic scenarios and problem instances that account for situations where it is

2 L. Barrero, R. Viera, F. Robledo, C. Risso, S. Nesmachnow, A. Tchernykh

preferable for the route planner to use a reduced number of vehicles, even paying a penalization for late arrivals in certain customers.

In this line of work, this article presents an hybrid metaheuristic approach combining Greedy Randomized Adaptive Search Procedure (GRASP) and Variable Neighborhood Search (VNS) for solving the VRP with heterogeneous fleet and flexible time windows. The experimental evaluation of the proposed model is performed on realistic problem instances, specifically designed by extending existing VRP benchmarks from literature.

Accurate results are reported for the proposed hybrid metaheuristic model. Despite applying a simple pattern for exploration and exploitation of the search space, the combination of GRASP and VNS computed comparable results with baseline methods in the related literature, and improved existing results in ten problem instances.

The article is organized as follows. Section 2 describes the flexible vehicle routing problem in smart cities and presents its mathematical formulation. Section 3 summarizes relevant related works. Section 4 describes the hybrid algorithmic approach to solve the problem combining GRASP and VND. Section 5 reports the experimental evaluation on standard scenarios and problem instances. Finally, Section 6 presents the conclusions and formulate the main lines for future work.

## 2 Flexible vehicle routing in smart cities

This section describes the flexible vehicle routing problem and presents its mathematical formulation.

### 2.1 Problem description

The proposed problem is a specific variant of the VRP considering time windows for deliveries and heterogeneous vehicles (i.e., vehicles with different transportation capacities) [7]. The main goal is to compute solutions that minimize the cost, the objective function of the problem, which is related to the time needed to deliver the products to all customers.

The proposed problem variant relax the standard formulation by considering *flexible* time windows. Flexible time windows operates as follows: i) early arrivals (i.e., before the start of the time window for a customer) are penalized by adding the waiting time to the cost function, whereas ii) late arrivals (i.e., after the end of the time window for a customer) are allowed within a certain tolerance, and a penalty is added to the cost function in order to take into account the extra time (after the end of the time window). Introducing flexible time window provides the studied problem with many additional interesting solutions, by elastically computing different routes accounting for different attention times within the tolerance for each customer.

The mathematical formulation of the considered problem variant is detailed in the next subsection.

## 2.2 Mathematical Formulation

A linear programming formulation is defined for the Heterogeneous Flexible Vehicle Routing Problem with Time Windows (HFVRPTW).

The problem is defined on a complete graph  $G(V, A)$ , considering the following elements [2]:

- $V = \{0, 1, \dots, n\}$  is the set of nodes. Node 0 represents the deposit (an special node from where all vehicles start their routes), whereas nodes  $N = \{1, \dots, n\}$  represent the customers.
- $A = \{(i, j) : 0 \leq i, j \leq n, i \neq j\}$  is the set of edges that represent the connections between the nodes.
- $t_{ij}$  is the travel time associated with arc  $(i, j)$ .

All customers must be visited in a feasible solution. Each customer  $i \in N$  has specific attributes that provide known information for the problem formulation:

- $d_i$  is the fixed demand of customer  $i$ .
- $s_i$  represents the service time demanded by a vehicle while delivering products to the customer  $i$ .
- $[e_i, l_i]$  is the time window of customer  $i$ .  $e_i$  is the earliest time and  $l_i$  is the latest time of the time window for customer  $i$ . The considered time windows are of the *soft* type: a vehicle is allowed to reach the customer before the earliest time and also after the end of its time window. In both cases, the solution cost is penalized.
- $ot_i$  is the *overtime* allowed in customer  $i$  (i.e., the tolerance after the end of its time window).  $ot_i$  is computed as  $ot_i = (l_i - e_i) \times \omega$ , with  $0 \leq \omega \leq 1$  being a known constant value. Therefore, for each customer  $i$ , a new *flexible* time window is defined, of the form  $[e_i, l_i + ot_i]$ . The vehicle cost is penalized if it reaches the customer in the interval  $[l_i, l_i + ot_i]$ .

Specific information is also known for the deposit:

- $[e_0, l_0] = [E, L]$  is the time window of the deposit.
- $d_0 = s_0 = 0$ , because there is no demand or service time in the deposit.

The set of vehicles is modeled by set  $K = \{1, \dots, k\}$ . In turn,  $C$  represents the set of vehicle types and  $S_c$  is the set of vehicles of type  $c$  in  $C$ . For each vehicle of type  $c \in C$ , the following information is known:

- $q_c$  is the capacity of a vehicle of type  $c \in C$  (i.e., how many product the vehicle can transport when full).
- $f_c$  is the fixed cost of a vehicle of type  $c \in C$ .
- $\alpha_c$  is the variable cost of a vehicle of type  $c \in C$ .
- $n_c$  is the number of available vehicles of type  $c \in C$ .

The decision variables of the problem are:

- $x_{ij}^k$  is a binary variable that takes value 1 if vehicle  $k$  passes through edge  $(i, j)$  in the graph, and takes value 0 otherwise.

4 L. Barrero, R. Viera, F. Robledo, C. Risso, S. Nesmachnow, A. Tchernykh

- $a_{ik}$  is the time of arrival of vehicle  $k$  to customer  $i$ .
- $o_{ik}$  is the time that the vehicle  $k$  exceeds the time range of the customer  $i$  (referred as “the overtime of vehicle  $k$  in the customer  $i$ ”).

Other relevant elements include:

- $\rho$  is the penalty term associated with the overtime of a vehicle in a customer.
- $\omega$  is the (percentage) deviation allowed for the time windows of customers.  $\omega$  is used to define  $ot_i$  for each customer  $i$ .
- $M = \max(l_i + ot_i + t_{ij} + s_i - e_j), (i, j \in V)$  is the maximum possible time for a vehicle to move from customer  $i$  to customer  $j$ .

The mathematical formulation of the HFVRPTW is as follows:

$$\min \sum_{c \in C} f_c \sum_{k \in S_c} \sum_{j \in N} x_{0j}^k + \sum_{c \in C} \alpha_c \sum_{k \in S_c} \sum_{\substack{i, j \in V, \\ i \neq j}} t_{ij} x_{ij}^k + \sum_{k \in K, i \in N} o_{ik} * \rho \quad (1)$$

subject to:

$$\sum_{k \in K} \sum_{\substack{j \in V, \\ i \neq j}} x_{ij}^k = 1 \quad \forall i \in N \quad (2)$$

$$\sum_{j \in N} x_{0j}^k \leq 1 \quad \forall k \in K \quad (3)$$

$$\sum_{i \in N} x_{i0}^k \leq 1 \quad \forall k \in K \quad (4)$$

$$\sum_{i \in V} x_{ij}^k = \sum_{i \in V} x_{ji}^k \quad \forall j \in V, k \in K \quad (5)$$

$$\sum_{i \in N} d_i \sum_{\substack{j \in V, \\ i \neq j}} x_{ij}^k \leq q_c \quad \forall k \in S_c, c \in C \quad (6)$$

$$a_{ik} + s_i + t_{ij} - M(1 - x_{ij}^k) \leq a_{jk} \quad \forall k \in K, i \in N, j \in V, i \neq j \quad (7)$$

$$t_{0i} * x_{0i}^k \leq a_{ik} \quad \forall k \in K, i \in N \quad (8)$$

$$a_{ik} \leq (l_i + ot_i) \sum_{\substack{j \in V, \\ i \neq j}} x_{ij}^k \quad \forall k \in K, i \in N \quad (9)$$

$$e_i \sum_{\substack{j \in V, \\ i \neq j}} x_{ij}^k \leq a_{ik} \leq (l_i + ot_i) \sum_{\substack{j \in V, \\ i \neq j}} x_{ij}^k \quad \forall k \in K, i \in N \quad (10)$$

$$E \leq a_{0k} \leq L + ot_0 \quad \forall k \in K \quad (11)$$

$$\sum_{k \in S_c} \sum_{j \in N} x_{0j}^k \leq n_c \quad \forall c \in C \quad (12)$$

$$o_{ik} \geq \max(0, a_{ik} - l_i) \geq 0 \quad \forall k \in K, i \in V \quad (13)$$

$$a_{ik} \geq 0 \quad \forall k \in K, i \in N \quad (14)$$

$$x_{ij}^k \in \{0, 1\} \quad \forall k \in K, (i, j) \in A \quad (15)$$

The objective function of the problem (Eq. 1) proposes minimizing the total routing cost. Three terms are considered: the sum of fixed costs and the sum of variable costs of the vehicles that conform each route, as well as the sum of penalties for all those vehicles that arrives with overtime.

Eqs. 2–15 formulate the problem constraints, which corresponds to:

- The constraint in Eq. 2 guarantees that all customers are visited only once (by one vehicle).
- Eq. 3–5 are routing constraints, which forces that every used vehicle departs and returns to the depot using only one route: the vehicle cannot return from the same edge and the route must be a continuous path.
- Eq. 6 is a capacity constraint, establishing that for each route, the accumulated demand for any customer cannot exceed the capacity of the vehicle.
- The constraint in Eq. 7 establishes the precedence relationship between the arrival times of the vehicles to the customers in each route. This constraint is the linearization of  $x_{ij}^k(a_{ik} + s_i + t_{ij} - a_{jk}) = 0 \quad \forall k \in K, i \in N, j \in V, i \neq j$ .
- The constraint in Eq. 8 establishes the earliest arrival time at the first node of the path. Eqs. 9–11 impose the constraints set by the time windows for customers and the deposit, whereas the constraint in Eq. 12 limits the number of vehicles available for each type.
- Finally, the constraints in Eq. 13–15 restrict the values that the decision variables can take.

The proposed problem is a relaxation of the heterogeneous VRP with time windows proposed by Jiang et al. [7].

### 3 Related work

VRP is a classic optimization problem introduced by Dantzig and Ramser [4]. VRP can be defined as the problem of determining a series of delivery routes for a fleet of vehicles, departing from one or several depots, to deliver products to a set of geographically dispersed customers [6].

VRP is a problem with NP-Hard complexity, as a generalization of the Travelling Salesman Problem [9]. Solomon [16] studied the VRP with time windows and several heuristic methods for its resolution: i) an intuitive method that places all customers in a single route, disregarding the time windows, and after that divides the route into different shorter routes to fulfill the time windows constraints; ii) heuristics based on different movements to define neighborhoods (Nearest-Neighbor, Insertion, Sweep, and Time-Oriented Insertion); and iii) list heuristics, following a waiting time limit approach. In the comparative empirical evaluation, the Time-Oriented Insertion heuristic computed the best results.

6 L. Barrero, R. Viera, F. Robledo, C. Risso, S. Nesmachnow, A. Tchernykh

This method is based on selecting a seed customer between those most distant from the depot or those with the earliest time for delivering, and then building an initial route to those customers. After that, routes are building by adding other customers to the initial route, properly observing their time windows, until the vehicle capacity is reached or until the end of the delivering time period.

On the one hand, several exact methods have been proposed for different VRP variants. One of the most comprehensive related works was presented by Baldacci et al. [1], who proposed a framework to compute exact solutions to VRP problem, including the variant with time windows, based on modeling partition problems with additional constraints. Efficient results were reported in comparison with previous exact methods.

On the other hand, many articles have proposed heuristic and metaheuristic approaches [11] to solve different VRP variants. Regarding the VRP with time windows and heterogeneous fleet, Tabu Search (TS) methods have been applied by Semet and Taillard [15] and Rochat and Semet [14]. Yepes and Medina [18] applied probabilistic variable neighborhood local searches for the problem. The most relevant related work is by Jiang et al. [7], which proposed an exact formulation for the VRP with time windows and heterogeneous fleet and a two-stages heuristic method based on TS. The method computed accurate results, even for larger problem instances.

Many other articles have studied specific cases of the VRP with time windows and heterogeneous fleet, focused on the real routing applications; e.g. bi-objective multi-depot VRP [19], and heterogeneous VRP with time windows and a limited number of resources [10]. However, no recent articles have addressed the problem variant where flexible deadlines are considered, to account for the trade-off between cost and quality of service.

Our previous work [2] studied the flexible VRP variant with heterogeneous fleet and time windows. A MILP formulation was presented and an exact resolution approach was developed and implemented in CPLEX. The proposed exact model was able to solve 146 out of 148 problem instances, but just 16 of them to optimality. The exact approach was not evaluated with problem instances including 100 customers, due to the large execution times required.

The research reported in this article contributes to this line of work by developing an hybrid metaheuristic approach combining GRASP and VND to solve problem instances for which the previous exact method was unable to compute solutions in reasonable execution times.

#### **4 The proposed GRASP+VND for flexible vehicle routing**

This section describes the hybrid metaheuristic approach combining GRASP and VND to solve the HFVRPTW.

#### 4.1 Overall description

The proposed metaheuristic approach to solve the HFVRPTW follows an hybrid approach. Hybridization is a common technique for improving the search capabilities of metaheuristic algorithms [17]. In this context, hybridization refers to include problem-dependent knowledge in the search mechanism or combine several methods, trying to take advantage of the features of each one of them to improve the search efficiency and/or accuracy of the resulting hybrid method. The common approach is to organize the hybrid in a master method that controls the application of a given (or a set of) subordinate metaheuristics. The hybrid metaheuristic defines a new search pattern that determines when each algorithm is applied and how each algorithm reports its results to the other [11].

The pseudocode in Algorithm 1 presents the overall description of the proposed hybrid GRASP+VND metaheuristic for the HFVRPTW. A standard approach is applied: a solution is built using a constructive procedure, and a VND operator is applied for improving the solution.

---

#### Algorithm 1: Proposed GRASP+VND for the HFVRPTW

---

```

1 noImprov = 0
2 data ← ReadData()
3 vehicles ← SortVehicles(datos)
4 bestSol ←  $\phi$ 
5 for  $k = 1$  to maxIter do
6   | initSol ← Construction(data, vehicles)
7   | improvedSol ← VND(solucionInicial)
8   | if cost(bestSol) > cost(improvedSol) then
9   |   | bestSol ← improvedSol
10  | else
11  |   | noImprov = noImprov + 1
12  | end
13  | if noImprovement  $\geq$  maxIterWithoutImpr then
14  |   | break
15  | end
16 end
17 return bestSol

```

---

Two stopping criteria are considered in Algorithm 1: a fixed effort stopping criterion defined by a maximum number of iterations (maxIter) and a stagnation criterion defined by a maximum number of iterations without improvement (maxIterWithoutImpr) of the best best solution found.

Before starting the iterative process, function SortVehicles() sorts each of the vehicles types according to a specific criterion. For each dataset that defines a problem instance, two values are computed: the average customer demand  $\bar{d}$  and the average travel time  $\bar{t}$  between all nodes (depot and customers). Let  $q$  be the capacity of each type of vehicle, it is possible to compute the number of

8 L. Barrero, R. Viera, F. Robledo, C. Risso, S. Nesmachnow, A. Tchernykh

customers that can be attended by that type of vehicle, that is, the number of customers on the average route:  $customers = \lfloor q/\bar{d} \rfloor$ . Therefore, for each vehicle type, the average demand for the average route is  $demand = customers \times \bar{d}$ , and the average travel time for the average route is  $time = (customers + 2) \times \bar{t}$  (the +2 term accounts for two additional segments when departing from/returning to the depot). Using these data, and the fixed ( $f_c$ ) and variable costs ( $\alpha_c$ ) for the vehicle type, a specific metric for each type of vehicle is defined by Eq. 16. The different types of vehicles are added to a list  $K$  in increasing order of priority according to the defined metric.

$$\frac{f_c}{demand} + \alpha_c \times time \quad (16)$$

*Construction phase* Two stages are involved in the construction phase: vehicle selection and construction of the route for the selected vehicle.

For vehicle selection, a list of customers that have not yet been included in the solution is maintained. When creating a new route to be added to the solution, the available vehicle type with the highest priority is selected.

After that, a route is assembled for the selected vehicle, always including the depot as initial node. A list of candidate customers to be included as the next node is defined, checking that they generate a feasible route. Then, the incremental cost associated with each candidate is calculated as follows: being  $t$  the travel time from the current node of the route under construction to the candidate customer,  $at$  the arrival time to the candidate,  $ot_i$  the time that the time window of the candidate is exceeded,  $\rho$  the penalty for the late arrival, the incremental cost is calculated as  $incr(i) = \alpha * t + ot_i \times \rho + at_i$ . This incremental cost does not represent the real cost to be summed if that candidate is added to the route, since the time of arrival to the candidate is also weighted, trying to include as soon as possible in the route those customers with high priority (i.e., with the earliest time windows).

Once the incremental cost are computed, a restricted candidate list (RCL) is built by selecting from the candidate list those that verify  $incr(cand) \leq \min(incr) + \alpha(\max(incr) - \min(incr))$ , with  $\alpha = 0,2$  (computed in preliminary experiments). Then, an element from the RCL is randomly selected and added to the partial route, updating both the list of customers not included in the solution and the candidate set, and reevaluating the incremental costs. When the capacity of the vehicle is reached or the list of candidates is empty (i.e, there is no customer to add to the solution generating a feasible route), the current route is closed by adding the deposit. In case there are customers not visited, another vehicle is selected to create a new route.

Algorithm 2 describes the construction procedure. Function `Getcustomers` returns the set of customers for a problem instance and `GetCapacity` returns the capacity of a vehicle. Function `SelectVehicle`, given a list of vehicle types ordered according to the defined metric, returns an available vehicle of the type with the lowest metric and updates the availability for that type of vehicle. Function `CreateRoute` initializes a route by associating a vehicle and a path.

Given a route and a customer, function `IsFeasible` determines if is possible to add the customer at the end of the path of the route, by checking if the demand of the customer does not exceed the available capacity of the vehicle and that the arriving time to the customer is within its extended time window. Finally, function `SelectRandom` returns an element of the RCL, selected according to a uniform distribution probability.

*Local search phase* The local search phase applies a VND metaheuristic to explore different neighborhoods of the solution constructed in the previous phase. Five neighborhood structures are considered, four of them taken from the related literature: Exchange, Relocate, 2-opt, and 3-opt. They are explored in that order, according to their cardinality [13].

In addition, a new operator is applied: `fleet-opt`. The main goal of this operator is creating a neighborhood that allows exploring the allocation of vehicles on each route of a given solution. This way a fifth neighborhood is defined by applying the fleet-opt operator in two different ways:

- *A movement*: For all routes in the solution, pairs of two different routes  $p$  and  $q$  are selected. If their associated vehicles  $v_p$  and  $v_q$  are of different types, their are exchanged (route  $p$  is associated with vehicle  $v_q$  and route  $q$  is associated with vehicle  $v_p$ , as illustrated in Fig. 1(a).
- *B movement*: This movement requires knowing the available vehicles  $v_d$ , not included in the solution. For each route  $p$  of the solution, the associated vehicle  $v_p$  is replaced by each of the  $v_d$  with a different type, as illustrated in Fig. 1(b).

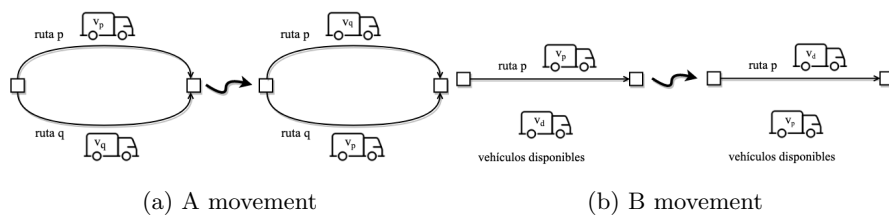


**Fig. 1.** Fleet-opt operator

The proposed fleet-opt neighborhood has a smaller cardinality than that of the other neighborhood structures, therefore, it is applied first.

The diagram in Fig. 2 describes the structure of the proposed VND metaheuristic algorithm applied as local search operator in the proposed algorithm and the order of exploration of each neighborhood.

10 L. Barrero, R. Viera, F. Robledo, C. Risso, S. Nesmachnow, A. Tchernykh

---

**Algorithm 2:** Construction phase of the proposed GRASP+VND for the HFVRPTW
 

---

```

1 solution  $\leftarrow \phi$ 
2 customers  $\leftarrow$  GetCustomers(datos) ▷ Initialize customers list
3 newRoute  $\leftarrow$  true ▷ Define new route initialization
4 while customers  $\neq \phi$  do
5   candidates  $\leftarrow \phi$  ▷ Initialize candidate list
6   if newRoute then
7     path  $\leftarrow$  depot ▷ Initialize path
8     vehicle  $\leftarrow$  SelectVehicle(vehicles) ▷ Select vehicle
9     q  $\leftarrow$  GetCapacity(vehicle) ▷ Initialize vehicle capacity
10    route  $\leftarrow$  CreateRoute(vehicles,path) ▷ Initialize route
11    newRoute  $\leftarrow$  false
12  end
13  for cust  $\in$  customers do
14    if IsFeasible(route, cust) then
15      candidates  $\leftarrow$  candidates  $\cup$  {cli} ▷ Insert candidate
16    end
17  end
18  if candidates  $\neq \phi$  then
19    for cand  $\in$  candidates do
20      incr(cand) ▷ Compute incremental cost
21    end
22     $i^{min} \leftarrow \min\{\text{incr}(\text{cand}) \mid \text{cand} \in \text{candidates}\}$ 
23     $i^{max} \leftarrow \max\{\text{incr}(\text{cand}) \mid \text{cand} \in \text{candidates}\}$ 
24    RCL  $\leftarrow \{\text{cand} \in \text{candidates} \mid \text{incr}(\text{e}) \leq i^{min} + \alpha(i^{max} - i^{min})\}$ 
25    customer  $\leftarrow$  SelectRandom(RCL)
26    path  $\leftarrow$  path  $\cup$  {customer} ▷ Add customer to path
27    Update(path,route) ▷ Update path in route
28    q = q - GetDemand(customer) ▷ Update capacity
29    customers  $\leftarrow$  customers  $\setminus$  {customer} ▷ Update customers list
30  end
31  if candidates =  $\phi$  OR q = 0 then
32    path  $\leftarrow$  path  $\cup$  {depot} ▷ Add depot to path
33    Update(path,route) ▷ Update path in route
34    Add(route,solution) ▷ Add route to solution
35    newRoute  $\leftarrow$  true
36  end
37 end
38 return solution

```

---

## 5 Experimental evaluation

This section reports the experimental evaluation of the proposed hybrid meta-heuristic algorithmic approach to solve the HFVRPTW.

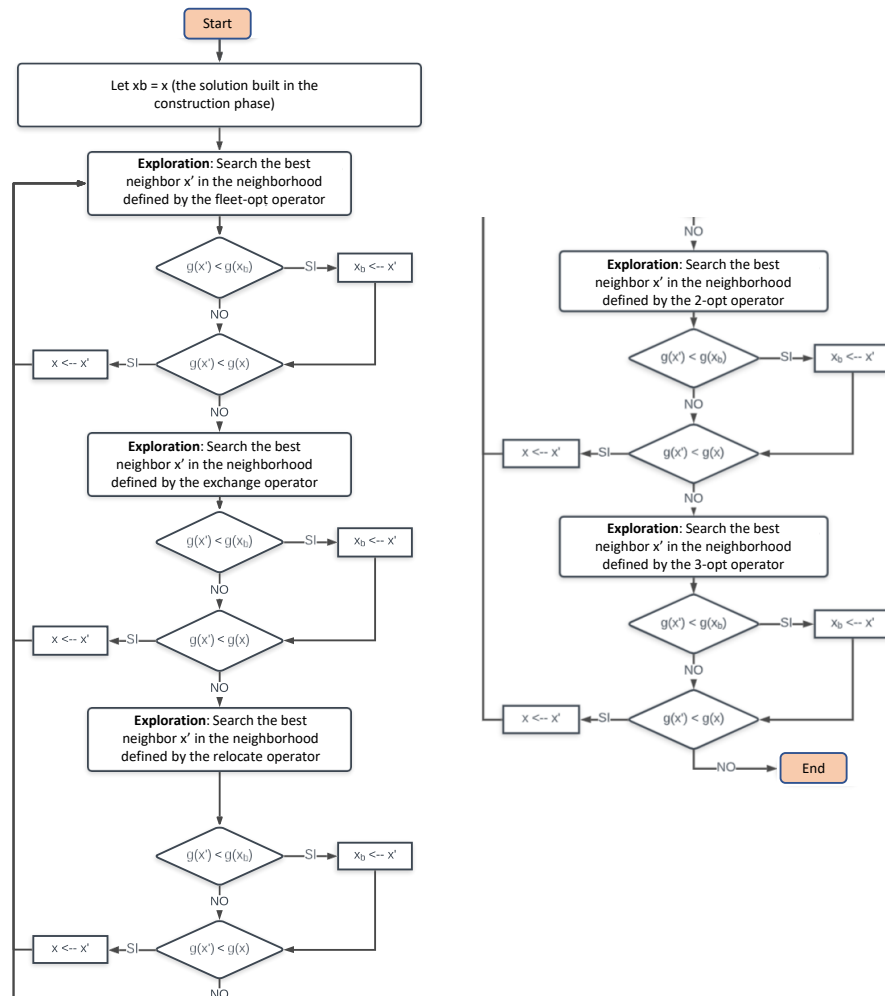


Fig. 2. Diagram of the proposed VND search

### 5.1 Problem instances

The evaluation of the proposed hybrid metaheuristic approach is performed using a set of benchmark instances built over existing ones for the classic VRP problem (with homogeneous vehicles) and including specific features of the proposed HFVRPTW model, namely heterogeneous vehicles and flexible time windows. These problem instances are described next.

Regarding topological data, the proposed dataset extends VRP benchmark with homogeneous vehicles by Solomon [16]. Information of these instances include: locations, demands, time windows, and service times of customers and the depot. The benchmark is organized in six classes:

- Classes C1 and C2 are defined considering grouped customers.

12 L. Barrero, R. Viera, F. Robledo, C. Risso, S. Nesmachnow, A. Tchernykh

- Classes R1 and R2 are defined considering evenly distributed locations on a square area,
- Classes RC1 and RC2 are defined considering both customers grouped and location distributed.

Problem instances with narrow windows and small vehicle capacities (classes C1, R1, and RC1) and also with wide time windows and large vehicle capacities (classes C2, R2, and RC2) are considered. Fixed and variable costs are defined as proposed by Jiang et al. [7]. The defined cost structure assigns higher fixed and variable costs to vehicles with larger capacities. Six new classes are generated: HC1, HC2, HR1, HR2, HRC1 and HRC2 (the ‘H’ stands for heterogeneous). Four classes (HC1, HC2, HR2, and HRC2) include two types of vehicles, with different capacities, costs, and different cost/capacity ratios. Other two classes (HR1 and HRC1) include three types of vehicles, with similar cost/capacity ratios. Regarding flexibility of customers and time windows, the value of  $\omega$  is set to 0.3, providing a reasonable level of flexibility for delivering products.

Table 1 reports the data of new heterogeneous problem instances. Information reported in the table include the number of vehicles, their type, capacities, and both fixed and variable costs.

<i>class</i>	<i>vehicle type</i>	<i># vehicles</i>	<i>capacity</i>	<i>fixed cost</i>	<i>variable cost</i>
HC1	A	20	100	30	1.0
	B	5	200	80	1.2
HC2	A	20	400	100	1.0
	B	5	500	140	1.2
HR1	A	10	50	80	1.0
	B	15	80	140	1.2
	C	10	120	250	1.4
HR2	A	10	300	45	1.0
	B	5	400	70	1.2
HRC1	A	10	40	60	1.0
	B	20	80	150	1.2
	C	10	150	300	1.4
HRC2	A	10	100	150	1.0
	B	5	200	350	1.2

**Table 1.** Data of the considered problem instances classes

## 5.2 Methodology

*Development and execution platform.* The proposed GRASP+VND metaheuristic was implemented in C. The experimental evaluation was performed in a HP ProLiant DL380 G9 with Intel Xeon Gold 6138 processor and 128 GB RAM, from National Supercomputing Center, Uruguay (Cluster-UY) [12].

*Parameters setting.* For the proposed GRASP+VND, parameter values for the stopping criteria were set to  $\text{maxIter} = 100$  and  $\text{maxIterWithoutImpr} = 20$ ,

after a preliminary analysis that concluded that this values allowed a proper exploration of the search space of the problem.

*Results comparison.* Results computed with the proposed GRASP+VND approach are compared with previous reference results by the TS of Jiang et al. [7] for non-flexible problem instances with 100 customers.

### 5.3 Numerical results of the hybrid metaheuristic approach

Table 2 reports the results computed for VRP instances with 00 customers and the comparison with the previous TS approach by Jiang et al. [7] for the non-flexible version of the problem. The gap metric reports the relative difference between the cost of solutions computed by GRASP+VND and the previous TS.

Results in Table 2 indicate that the proposed hybrid metaheuristic approach combining GRASP and VND is able to compute competitive results when compared with state-of-the-art results for the heterogeneous VRP with time windows. Although the average gap is over 14.1% for instances class HC1, significantly lower values were obtained for the other studied problem classes. The best results were computed for problem classes HR1 and HR2, where the gaps between the proposed GRASP+VND and the reference TS [7] were 0.93% and 1.68% respectively. In those problem classes, GRASP+VND computed nine better solutions (four in class HR1 and five in class HR2), with improvement up to 10.75% in problem instance HR202. In turn, another better solution was computed for problem instance HC207.

The best solutions computed for classes HR1 and HR2 suggest that the proposed hybrid metaheuristic approach is useful to solve both problem instances with narrow windows and small vehicle capacities, and also with wider time windows and large vehicle capacities, using different types of vehicles.

## 6 Conclusions and future work

This article presented an hybrid metaheuristic approach to solve the VRP with heterogeneous fleet and flexible time windows. The addressed problem variant considers extended time windows for delivering products to customers, and models interesting situations in smart cities, considering the renewed interesting on smart logistics under the Industry 4.0 paradigm.

An hybrid metaheuristic approach is applied to solve the problem. combining GRASP and VND, two well-known search procedures for optimization. Different operators and neighborhood structures are proposed for the search.

The experimental evaluation is performed on a set of problem instances with 100 customers, built by extending existing benchmarks in the literature. Regarding the quality of the computed solutions, the GRASP+VND approach was competitive when compared with a previous TS method applied to the non-flexible version of the problem and was able to compute better solutions in ten problem instances.

14 L. Barrero, R. Viera, F. Robledo, C. Risso, S. Nesmachnow, A. Tchernykh

<i>instance</i>	GVND	<i>TS</i> [7]	$\Delta cost$	<i>gap</i>	<i>instance</i>	GVND	<i>TS</i> ,[7]	$\Delta cost$	<i>gap</i>
HC101	2285.12	1885.33	399.79	17.50%	HR201	1661.63	1765.74	<b>-104.11</b>	<b>-6.27%</b>
HC102	2136.37	1890.66	245.71	11.50%	HR202	1387.66	1536.81	<b>-149.15</b>	<b>-10.75%</b>
HC103	2109.95	1908.04	201.91	9.57%	HR203	1240.21	1337.39	<b>-97.18</b>	<b>-7.84%</b>
HC104	2098.63	1809.78	288.85	13.76%	HR204	1111.87	1114.94	<b>-3.07</b>	<b>-0.28%</b>
HC105	2209.49	1854.73	354.76	16.06%	HR205	1375.37	1263.91	111.46	8.10%
HC106	2184.47	1880.64	303.83	13.91%	HR206	1263.93	1180.44	83.49	6.61%
HC107	2170.92	1839.52	331.4	15.27%	HR207	1191.44	1102.06	89.38	7.50%
HC108	2160.83	1826.49	334.34	15.47%	HR208	1072.93	1007	65.93	6.14%
HC109	2096.88	1799.22	297.66	14.20%	HR209	1242.66	1119.04	123.62	9.95%
					HR210	1243.48	1307.53	<b>-64.05</b>	<b>-5.15%</b>
					HR211	1127.61	1010.22	117.39	10.41%
<i>avg.</i>	-	-	306.47	14.14%	<i>avg.</i>	-	-	-	1.68%
HC201	1355.96	1313.28	42.68	3.15%	HRC101	6032.29	5703.97	328.32	5.44%
HC202	1380.24	1283.58	96.66	7.00%	HRC102	5841.77	5556.02	285.75	4.89%
HC203	1390.66	1259.97	130.69	9.40%	HRC103	5819.42	5438.89	380.53	6.54%
HC204	1274.94	1256.09	18.85	1.48%	HRC104	5728.36	5331.41	396.95	6.93%
HC205	1371.87	1325.84	46.03	3.36%	HRC105	5906.44	5705.79	200.65	3.40%
HC206	1382.84	1263.63	119.21	8.62%	HRC106	5898.69	5528.42	370.27	6.28%
HC207	1278.11	1307.35	<b>-29.24</b>	<b>-2.29%</b>	HRC107	5767.87	5451.31	316.56	5.49%
HC208	1331.29	1190.81	140.48	10.55%	HRC108	5733.73	5322.31	411.42	7.18%
<i>avg.</i>	-	-	-	5.16%	<i>avg.</i>	-	-	-	5.77%
HR101	4979.38	5125.52	<b>-146.14</b>	<b>-2.93%</b>	HRC201	4951.2	4501.65	449.55	9.08%
HR102	4752.87	4982.39	<b>-229.52</b>	<b>-4.83%</b>	HRC202	4766.55	4408.53	358.02	7.51%
HR103	4555.72	4661.22	<b>-105.50</b>	<b>-2.32%</b>	HRC203	4598.44	4321.87	276.57	6.01%
HR104	4393.14	4530.55	<b>-137.41</b>	<b>-3.13%</b>	HRC204	4511.08	4306.65	204.43	4.53%
HR105	4707.31	4570.39	136.92	2.91%	HRC205	4633.37	4452.88	180.49	3.90%
HR106	4564.32	4431.31	133.01	2.91%	HRC206	4696.54	4419.09	277.45	5.91%
HR107	4485.23	4391.14	94.09	2.10%	HRC207	4562.1	4343.55	218.55	4.79%
HR108	4410.89	4280.05	130.84	2.97%	HRC208	4442.41	4276.15	166.26	3.74%
HR109	4540.24	4339.86	200.38	4.41%					
HR110	4419.36	4272.25	147.11	3.33%					
HR111	4467.47	4366.32	101.15	2.26%					
HR112	4403.84	4252.71	151.13	3.43%					
<i>avg.</i>	-	-	-	0.93%	<i>avg.</i>	-	-	-	5.68%

**Table 2.** Results computed by the proposed GRASP+VND (GVND) and comparison with Jiang et al. [7] heterogeneous instances with 100 customers

The main lines for future work are related to extend the experimental validation of the proposed approach, by considering an extended set of problem instances and improving the exploration/exploitation procedures to compute better solutions. The problem model can also be extended to consider a multiobjective formulation to compute accurate trade-off solutions for the simultaneous optimization of the total cost and the quality of service offered to customers.

## References

1. Baldacci, R., Bartolini, E., Mingozzi, A., Roberti, R.: An exact solution framework for a broad class of vehicle routing problems. *Computational Management Science* **7**(3), 229–268 (2010)
2. Barrero, L., Viera, R., Robledo, F., Risso, C., Nesmachnow, S., Tchernykh, A.: Exact resolution of the vehicle routing problem with flexible time windows. In: *International Conference of Production Research*. pp. 658–672 (2020)
3. Brekalo, L., Albers, S.: Effective logistics alliance design and management. *International Journal of Physical Distribution & Logistics Management* **46**(2), 212–240 (2016)
4. Dantzig, G., Ramser, J.: The truck dispatching problem. *Management Science* **6**(1), 80–91 (1959)
5. Díaz-Madroño, M., Peidro, D., Mula, J.: A review of tactical optimization models for integrated production and transport routing planning decisions. *Computers & Industrial Engineering* **88**, 518–535 (2015)
6. Golden, B., Magnanti, T., Nguyen, H.: Implementing vehicle routing algorithms. *Networks* **7**(2), 113–148 (1977)
7. Jiang, J., Ng, K.M., Poh, K.L., Teo, K.M.: Vehicle routing problem with a heterogeneous fleet and time windows. *Expert Systems with Applications* **41**(8), 3748–3760 (2014)
8. Laporte, G.: Fifty years of vehicle routing. *Transportation Science* **43**(4), 408–416 (2009)
9. Lenstra, J., Rinnooy, A.: Complexity of vehicle routing and scheduling problems. *Networks* **11**(2), 221–227 (1981)
10. Molina, J., Salmeron, J., Eguia, I., Racero, J.: The heterogeneous vehicle routing problem with time windows and a limited number of resources. *Engineering Applications of Artificial Intelligence* **94**, 103745 (2020)
11. Nesmachnow, S.: An overview of metaheuristics: accurate and efficient methods for optimisation. *International Journal of Metaheuristics* **3**(4), 320–347 (2014)
12. Nesmachnow, S., Iturriaga, S.: Cluster-UY: Collaborative Scientific High Performance Computing in Uruguay. In: *Communications in Computer and Information Science*, pp. 188–202. Springer International Publishing (2019)
13. Pop, P., Fuksz, L., Marc, A.: A variable neighborhood search approach for solving the generalized vehicle routing problem. In: Polycarpou, M., de Carvalho, A., Pan, J., Woźniak, M., Quintian, H., Corchado, E. (eds.) *Hybrid Artificial Intelligence Systems*. pp. 13–24. Springer International Publishing, Cham (2014)
14. Rochat, Y., Semet, F.: A tabu search approach for delivering pet food and flour in switzerland. *Journal of the Operational Research Society* **45**(11), 1233–1246 (1994)
15. Semet, F., Taillard, E.: Solving real-life vehicle routing problems efficiently using tabu search. *Annals of Operations Research* **41**(4), 469–488 (1993)
16. Solomon, M.: Algorithms for the vehicle routing and scheduling problems with time window constraints. *Operations Research* **35**(2), 254–265 (1987)
17. Talbi, E.G.: A taxonomy of hybrid metaheuristics. *Journal of Heuristics* **8**(5), 541–564 (2002)
18. Yepes, V., Medina, J.: Economic heuristic optimization for heterogeneous fleet VRPHESTW. *Journal of Transportation Engineering* **132**(4), 303–311 (2006)
19. Zhou, Z., Ha, M., Hu, H., Ma, H.: Half open multi-depot heterogeneous vehicle routing problem for hazardous materials transportation. *Sustainability* **13**(3), 1262 (2021)

## Reactive power optimization on a smart microgrid

Óscar Izquierdo-Monge<sup>1</sup>, Elgar Lloret Pérez<sup>1</sup>, Paula Peña-Carro<sup>1</sup>, Gonzalo Martin Jimenez<sup>1</sup>, Luis Hernandez-Callejo<sup>2</sup>, Oscar Duque-Perez<sup>3</sup>; Angel Zorita-Lamadrid<sup>3</sup>

<sup>1</sup> CEDER-CIEMAT, Autovía de Navarra A15 salida 56, 422290 Lubia (Soria), Spain, O.I.M.: oscar.izquierdo@ciemat.es; E.L.P. elgardrummer@hotmail.com; P.P.C.: paula.pena@ciemat.es; G.M.J.: gonzalomj96@gmail.com;

<sup>2</sup> University of Valladolid, Campus Universitario Duques de Soria, 42004 Soria, Spain, luis.hernandez.callejo@uva.es

<sup>3</sup> University of Valladolid, Paseo del Cauce 59, 47011 Valladolid, Spain. O.D.P.: oscar.duque@eii.uva.es; A.Z.L.: zorita@eii.uva.es

**Abstract.** Reactive Power optimization on a microgrid is important for network stability, energy efficiency and electricity bill reduction. In this article, a reactive power study is carried out with the aim of reducing consumption in the smart microgrid of the CEDER (Renewable Energy Development Center). The study has taken measurements of reactive power with network analysers in each of the transformation centres to establish the initial state of the microgrid. The data was analysed which has led to the decision to install different capacitor banks (a robust, effective and low-cost method) in different transformer stations. Finally, another series of measurements was carried out to check the effectiveness of the measures adopted. This study has led to a considerable reduction in reactive power consumption, which implies a saving in the electricity bill, thus justifying the use of reactive power compensation devices.

**Keywords:** Smart microgrid, reactive power, power factor, capacitor bank.

### 1 Introduction

The traditional electricity grids, whose manageability has been based for years on the storage of fossil resources, have undergone significant advances due to the boom in renewable energy over the last few years, which have promoted new challenges for the integration and coordination of distributed generation systems (DGS). With the decline of fossil fuels and the necessary implementation of renewable sources in electricity generation, the inclusion of these generation systems, called distributed generation systems in the grid, play a very important role in reducing pollution, the reduction of transmission losses and the increased use of renewable sources in the production of electricity [1]. However, this approach generated other problems to solve such as the appearance of reverse power flow, voltage deviation and voltage fluctuation in the distribution

network due to the variation in the magnitude of the supply voltages and the imbalances that this produces in the power flows between the different power sources.

The integration of small generation sources in the same grid, whose production can be manageable and controllable, has made it possible to advance towards a new concept of electric grids known as microgrids. According to the definition of "The US department of energy's microgrid initiative" a microgrid [2] is defined as a group of interconnected loads and distributed energy resources within clearly defined electrical boundaries that act as a single controllable entity with respect to the grid. A microgrid enables the successful connection of different DGS [3], allowing the simultaneous inclusion of different generation systems, local loads and storage systems. The concept of smart microgrid is applied in the case where there is communication between the different elements of the grid, such that each of the grid elements can be managed in order to control the grid parameters and to make an efficient use of energy [4]. A microgrid can operate in two modes [5], allowing the microgrid to connect and disconnect from the grid, working in connection with the power grid through the Point of Common Coupling (PCC) or in island mode from the grid.

When the microgrid operator connects to the power grid, the microgrid provides the voltage and frequency references so that the generation systems operate correctly and there are no stability problems. When, it operates in island mode, the DGS must be able to respond quickly to changes in consumption to maintain stable voltage and frequency [6]. The microgrid will necessarily require storage systems to ensure the initial energy balance when the microgrid switches to island mode, ensuring frequency voltage references to the rest of the generation systems.

Some of the problems that can decrease power quality in the network are associated with instability produced by voltage and current harmonics, voltage sags, voltage spikes, voltage and current unbalances, and reactive power mismatches [7]. A study on the use of reactive power to evaluate losses in an electrical system [8] concludes that the measurement of reactive power absorbed by electrical loads is an effective procedure to measure the energy lost in single-phase systems, and in three-phase systems in the case where the loads are balanced, not being fulfilled in the more common case where the loads are unbalanced. Electric utilities measure reactive power absorbed by the receivers, taking into account its measurement in billing by means of the power factor [9] depending on the type of tariff [10]. This is why reducing reactive power consumption by compensating it will always be economically beneficial for the consumer, but it will not be a good indicator of the efficiency of the electrical system, since in some cases increasing the power factor may even increase losses in the electrical system.

Reactive power control improves the voltage profile and reduces network losses [11]. Reactive power compensation is analysed from two points of view [7], from the point of view of loads and voltage support. Balance of the loads is achieved by making the power factor as close to unity as possible. For voltage unbalance is necessary to reduce the fluctuations by installing devices that regulate the voltage, ensuring a fast and accurate response in each of the nodes of the network.

Energy storage methods reduce energy losses by increasing the power factor and providing improvements in voltage variations [12]. Proper design in the location of

storage systems reduces energy losses [13]. Inverters in generation systems have also been used for reactive power compensation locally and without additional costs, with fast response through high precision voltage regulation [14].

When we are looking for power factor improvement, capacitor banks (CB) are one of the most commonly used methods due to its simplicity of installation and low cost. The type of CB depends on whether the load is constant or time-varying [15]. Multi-stage CBs acting under the control of a switch, static (contactor) or electromagnetic (thyristor) are used in cases where the consumption is variable.

The correct choice in location and capacitance can increase the benefits of installing capacitor banks reducing costs and improving voltage quality [16]. The correct choice in the location of energy storage systems and capacitor banks has been studied for years, and its resolution by mathematical methods such as genetic algorithms and linear programming is in constant implementation. In a reactive power compensation problem, minimisation of energy losses, maximisation of voltage quality, and minimisation of the sum of losses associated with power and costs in the compensation installation are pursued [11].

In this paper, a study has been carried out to reduce the reactive energy consumption in the CEDER-CIEMAT smart microgrid in order to achieve savings in the electricity bill derived from these consumptions and avoid instabilities due to high reactive energy consumption at specific times.

The rest of the article is as follows: Section 2 deals with the materials and methods used to carry out the power consumption measurements: Section 3 shows the results in graphs before and after applying the reactive power compensation from the measurements obtained on the power consumptions in the transformer substations. Finally, conclusions and cited bibliography are presented.

## 2 Material and methods

The study was carried out on the smart microgrid of CEDER (Renewable Energy Development Centre), which belongs to the Centre for Energy, Environmental and Technological Research (CIEMAT), a Spanish Public Research Organization, currently under the Ministry of Science and Innovation. It is located in the locality of Lubia, province of Soria (Spain), and has an area of 640 ha with more than 13000 m<sup>2</sup> built in three separate areas as shown in Figure 1. [4]



**Fig. 1.** Location and distribution of buildings at CEDER.

CEDER's microgrid is supplied by a 45 kV distribution network and transforms at the substation at the entrance to the centre at 15 kV. It consists of eight transformer stations with multiple renewable generation systems and different storage systems, as well as several consumption elements connected to each transformer station [4]. The microgrid can operate either in ring or radial mode and has a length of about 4200 meters.

Figure 2 shows the distribution of the medium voltage between the transformer stations of the CEDER microgrid.

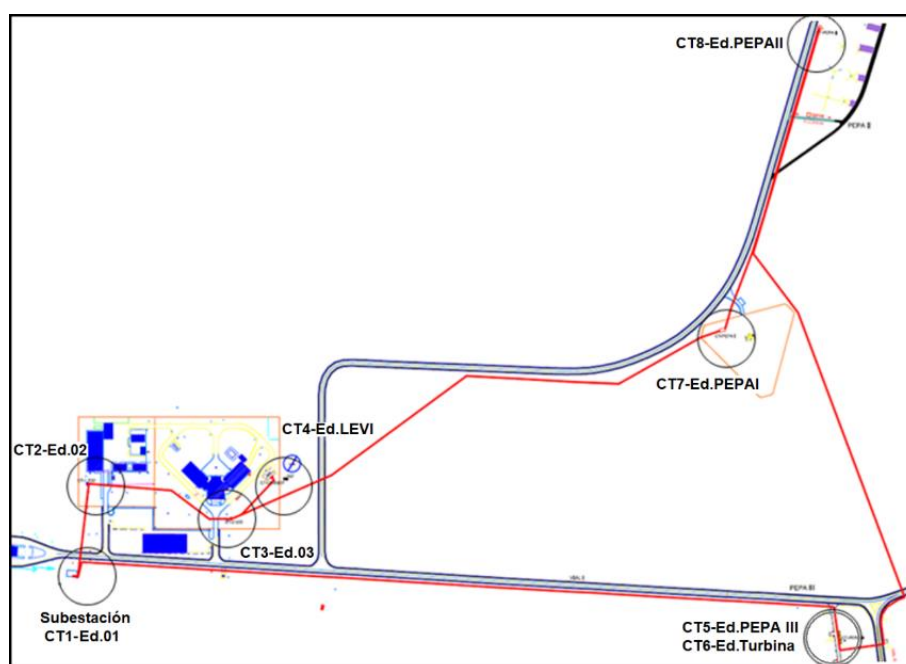


Fig. 2. Medium voltage distribution between CEDER's transformer stations.

There are installed grid analysers in the low voltage side of each transformer stations in order to perform different measurements (including reactive power). The power analyser used is the PQube 02 model from Power Standards Lab. Figure 3 shows the location of each of the grid analysers.

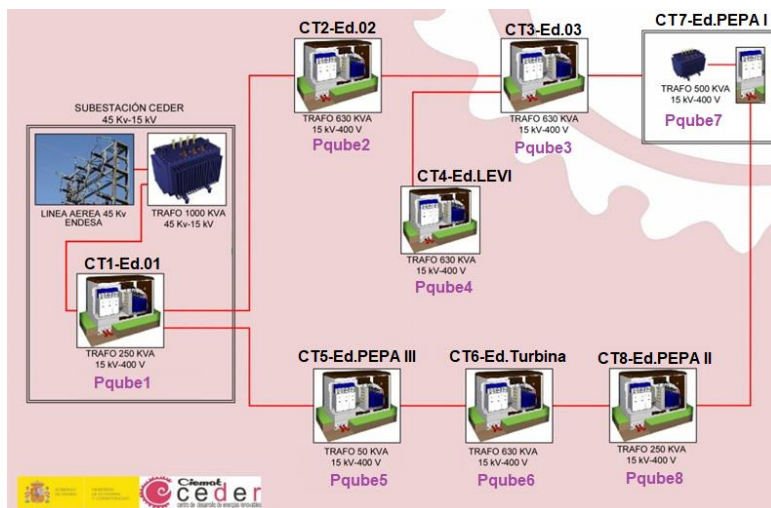


Fig. 3. Distribution of the grid analysers at CEDER facilities.

Each PQube is connected to CEDER's data network via Ethernet and communicate via the Modbus TCP/IP protocol, which allows their integration in the monitoring and control system of CEDER's electrical microgrid developed with Home Assistant as explained in [4]. The network analysers collect data with a frequency of 1 Hz. In order to be able to work for long periods, instead of using data per second, analysers collect data averaging each 15 minutes, which is the minimum unit of time that the electricity distribution company provides energy to CEDER. Figure 4 shows the network analyser.



Fig. 4. PQube grid analysers.

There are several transformer stations that have connected equipment that consumes reactive power. Some equipment consumes a lot of reactive power such as the electric generator connected to a 60 kW hydraulic turbine in CT6-Ed.Turbina and the various milling, crushing, drying and pelletizing equipment of the biomass plant connected to CT3-Ed.03. There is also other equipment in different buildings that consume reactive power, but lower amounts such as a motor/generator in CT7-PEPAI and some motor and compressor in CT2-Ed.02.

The rest of the transformation centres (CT1-Ed.01, CT4-Ed.LEVI, CT5-Ed.PEPAlII and CT8-Ed.PEPAlII) do not have any equipment that demands significant amounts of reactive power.

CEDER has a 6.1 TD electricity tariff named after June 1 2020 following the merger of tariffs 3.1 A and 6.1 [17]. It has a contracted voltage rate between 1 kV and 30 kV, and consists of 6 periods. The excess of reactive power consumed which applies an economic surcharge is the same in all periods, except in period 6 for which there is not surcharges. In order not to produce an excess of reactive power, this must not exceed 33% of the active power consumed in the period. To establish if it is necessary for this to be installed an electricity meter measure the reactive power every fifteen minutes. In case of exceeding 33% or if the power factor is between 0.8 and 0.95 the surcharge will be 0.04155 €/kVArh, and in case the reactive power excess is above 75% or the power factor is below 0.8 the billing term will be 0.062332 €/kVArh.

### 3 Results

A first measurement was made to check the reactive power consumption in each of the transformer stations and the general consumption of the micro-grid. The results, obtained are shown in the following figures.

Figure 5 shows the reactive power consumption in the transformation station which are connected the hydraulic turbine (CT6-Ed.Turbina) and its electric generator, during a day when the turbine is generating from 7:30 to 10:00 am. It can be seen that when the turbine produces 30 kW (-30 kW in Figure 5) the installation consumes slightly more than 40 kVAr.

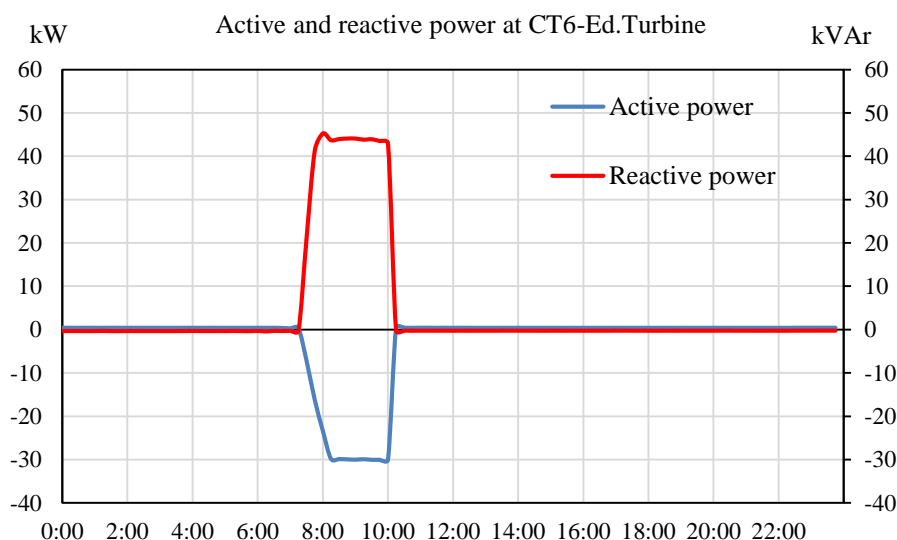


**Fig. 5.** Active and reactive power consumption CT6-Ed.Turbine.

Figure 6 shows the reactive power consumption at the turbine transformer station (CT6-Ed.Turbina) during February and March 2020. The turbine was scheduled to produce 30 kW every working day until March 8.

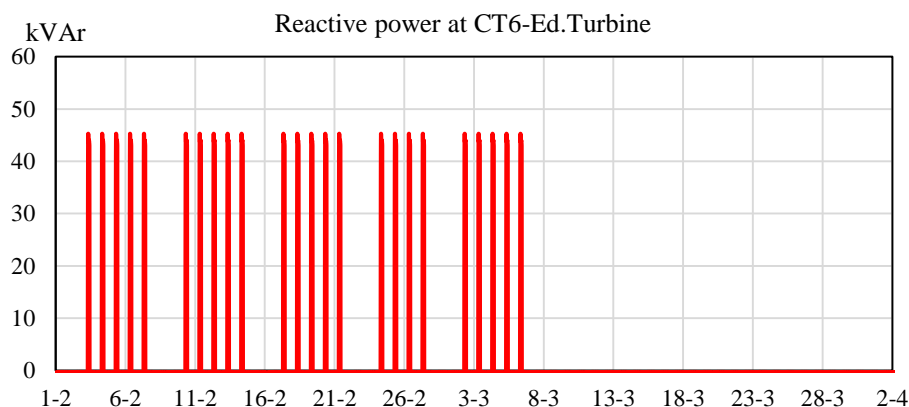


Fig. 6. Reactive power consumption CT6-Ed.Turbine.

Figure 7 shows the active and reactive power consumption in the transformation centre of the building which are connected to several grinding and crushing plants, a drying plant and a pelletizing plant (CT3-Ed.03) during a day when the grinding and crushing plant is in operation in three different jobs between 8:30 and 15:00. In the first and the third milling operation is similar and consumes around 20 kW of active power and slightly more than 30 kVAr of reactive power, while during the second job the consumptions are lower, producing around 10 kW of active power and 20 kVAr of reactive power.

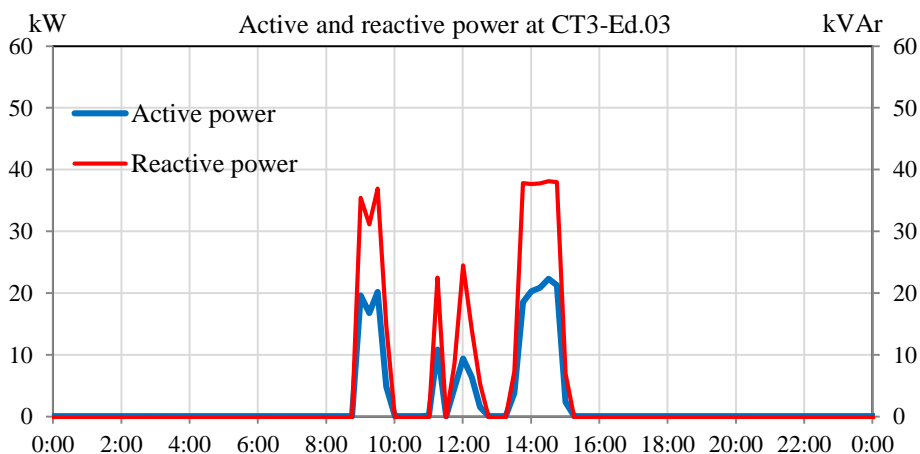
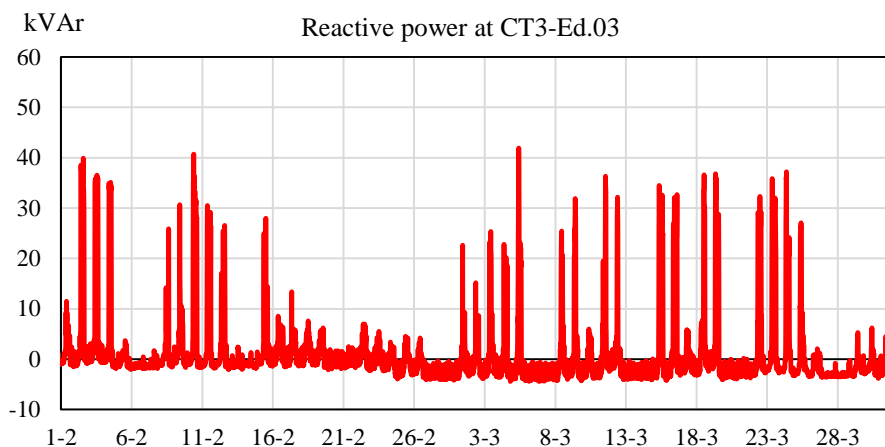


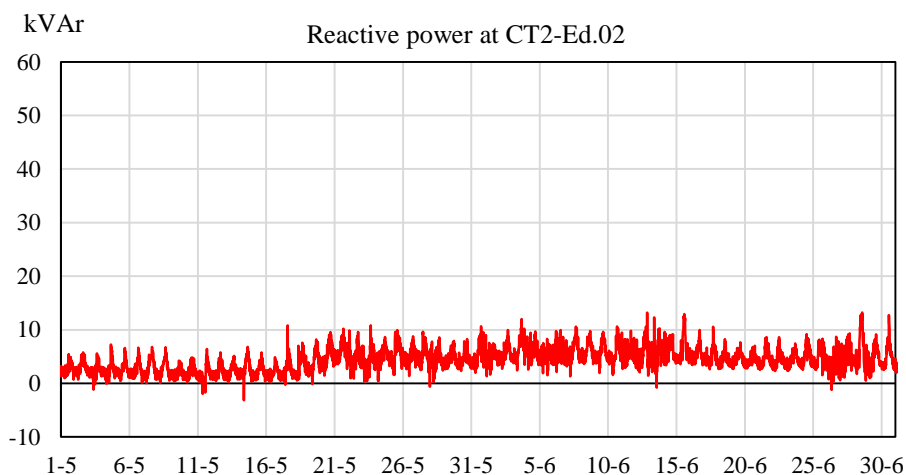
Fig. 7. Active and reactive power consumption CT3-Ed.03.

Figure 8 shows the reactive power consumption during the months of February and March 2020 in the CT3-Ed.03 transformation centre, where we can see the power consumption of other equipment in addition to the grinding plant.



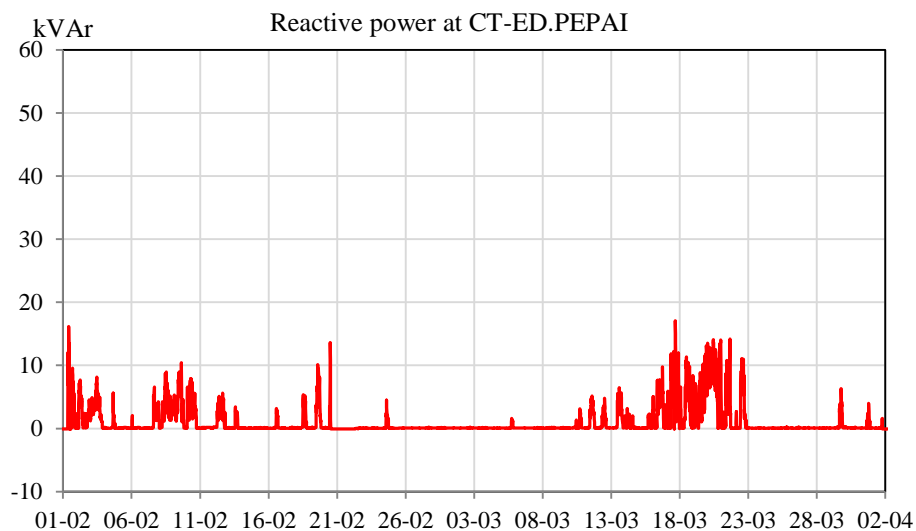
**Fig. 8.** Active and reactive power consumption CT3-Ed.03.

Figure 9 shows the reactive power consumption during the months of May and June 2020 in the CT2-Ed.02 transformer substation. It can be observed that some equipment starts and stops quite frequently. In addition, it produced a higher level of consumption from May 20, the day when some tests begin and new equipment that also consumes reactive power is turned on. Consumption before tests is from 6 kVAr to values higher than 10 kVAr during tests.



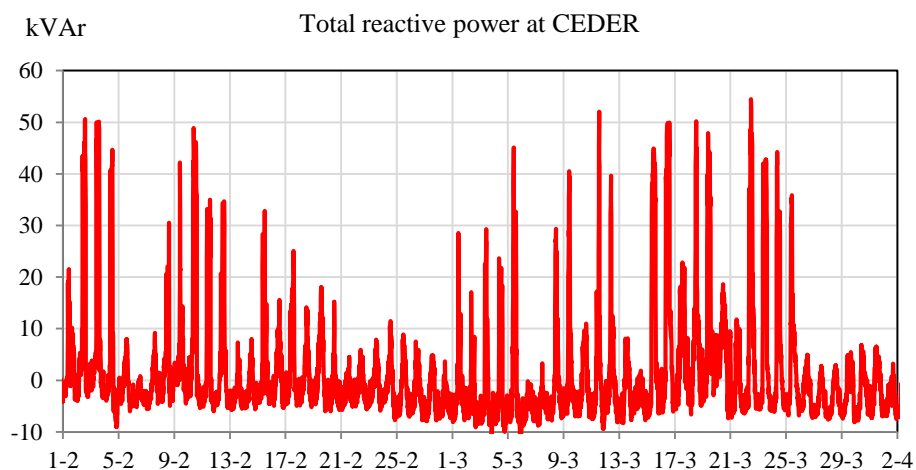
**Fig. 9.** Reactive power consumption CT2-Ed.02.

Figure 10 shows the reactive power consumption during the months of February and March 2020 in the CT7-PEPAI transformer substation.



**Fig. 10.** Reactive power consumption CT7-PEPAI.

Finally, Figure 11 shows the total reactive energy consumption of CEDER during two months. It can be seen that values higher than 40 kVAr are reached during many days, which implies paying an extra cost in the electricity bill in addition to the possibility of instability in the network at specific moments.



**Fig. 11.** Reactive power consumption at CEDER.

To reduce reactive power consumption by compensating it from the loads' point of view can be done by making the power factor as close to unity as possible.

The simplest and cheapest way to improve the power factor is to install capacitor Banks. For this reason, two equal banks of CIRCUTOR capacitors with constant reactive power (15 kVAr) have been installed in the CT7-PEPAI and CT2-Ed.02 transformer stations (see figure 12), where there are variable consumptions, but not very high.



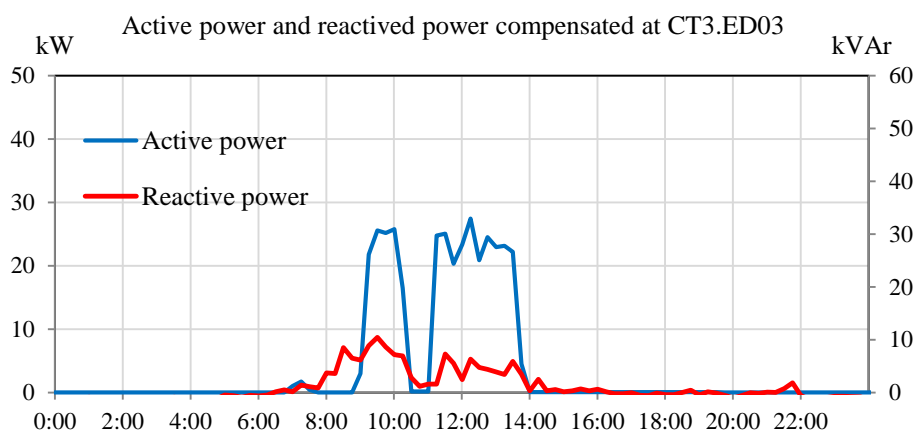
**Fig. 12.** Capacitor bank installed in CT7-PEPAI and CT2-Ed.02.

In addition, two automatic capacitor banks have been installed, operating in different stages at 400 V of the CIRCUTOR brand: an OPTIM 6 operating in 4 steps with a maximum compensation of 71.75 kVAr, at an approximate cost of 1,500 euros installed for CT6-Ed.Turbine and a two-stage OPTIM 9 P&P with a maximum compensation of 165 kVAr and an approximate cost of 3,500 euros for CT3-Ed.03 (see Figure 13). Both capacitor Banks are associated with the two equipment that consume the most reactive power at the centre, the turbine's electric generator and the biomass grinding and crushing plant, so that when they start consuming, the capacitor bank starts up to compensate the consumption.



**Fig. 13.** Capacitor bank installed in CT6-Turbine and CT3-Ed.03.

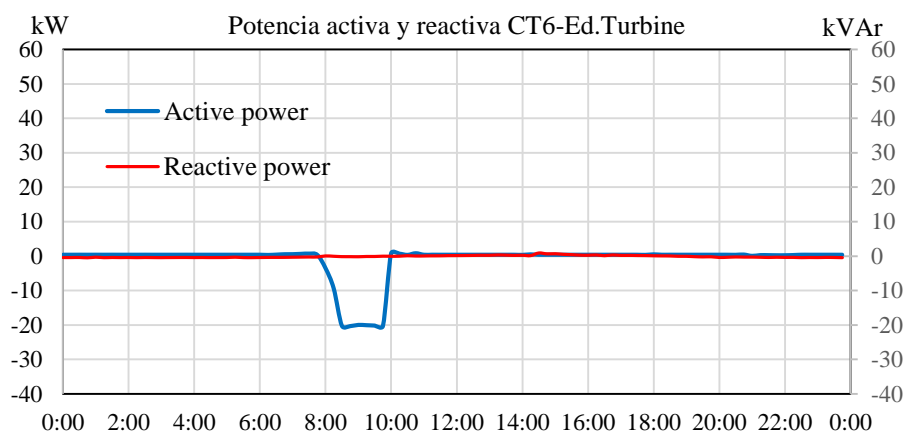
The results obtained in each of the transformer substations once the capacitor banks have been installed are as follows. Figure 14 shows how reactive power is compensated in the biomass grinding and crushing plant connected to CT3.Ed03 on June 3, 2021.



**Fig. 14.** Reactive power in CT3.Ed03 compensated with capacitor bank.

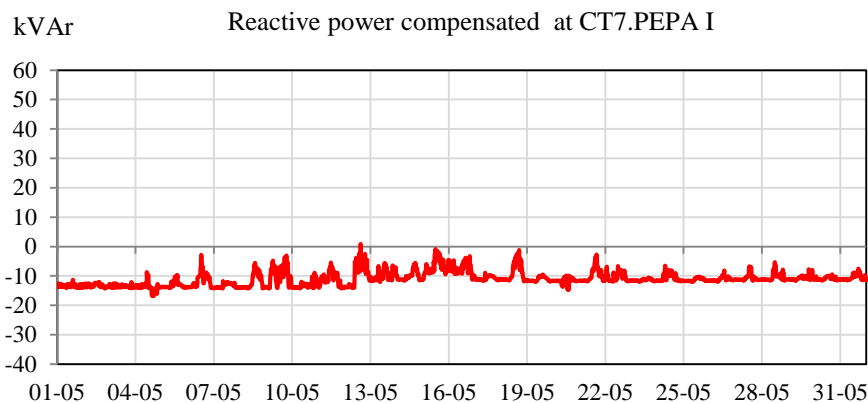
Before installing the capacitor bank, the reactive power consumed by the biomass grinding and crushing plant (between 20 and 35 kVAr) was the same as seen in the transformer station, however with the installation of the capacitor bank it's zero.

Figure 15 shows reactive power consumption of the turbine transformation centre (CT6-Ed.Turbine) once the capacitor bank associated is installed is practically zero, even though the turbine is in operation (May 31, 2021).



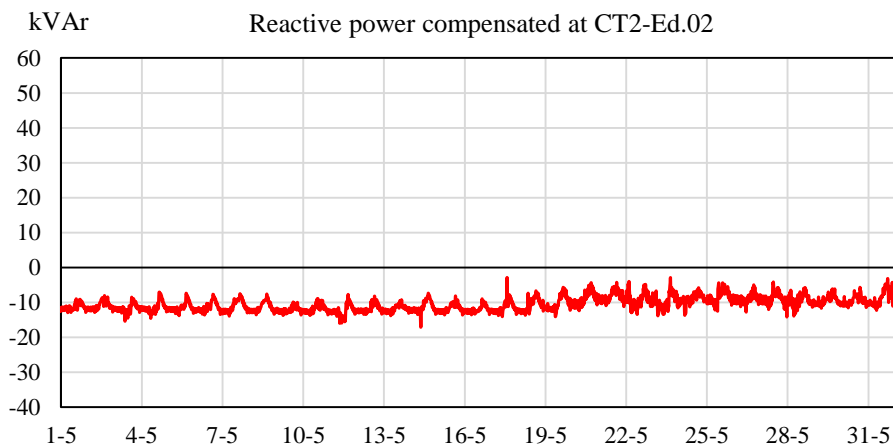
**Fig. 15.** Active and reactive power compensated with capacitors in CT6-Ed.Turbine.

Figure 16 shows the reactive power consumption in the CT7-PEPAI transformer substation once the capacitor bank is installed. Reactive power values before installing capacitor bank varied between 0 and 15 kVAr and it's now in negative values, so not only do we not consume reactive power in this transformer centre we also produce a surplus that is consumed in other centres.



**Fig. 16.** Reactive power compensated with capacitor bank in CT7-PEPA I.

In the CT2-Ed.02 transformer substation, the result in Figure 17, is very similar to what occurs in the CT7-PEPAI transformer substation which values are from 0 and 12 kVAr of reactive power to negative values between -6 and -13 kVAr.



**Fig. 17.** Reactive power compensated with capacitor bank in CT2-Ed.02.

Finally, Figure 18 shows the total reactive power consumption in CEDER for a period of two months once the four capacitor banks were installed. Before the installation of the capacitor banks there was always reactive power consumption at CEDER and peaks of up to 50 kVAr were reached. Currently, most of the time CEDER discharges reactive power to the distribution network instead of consuming it, and there are only sporadic peaks in reactive power consumption that do not exceed 24 kVAr.

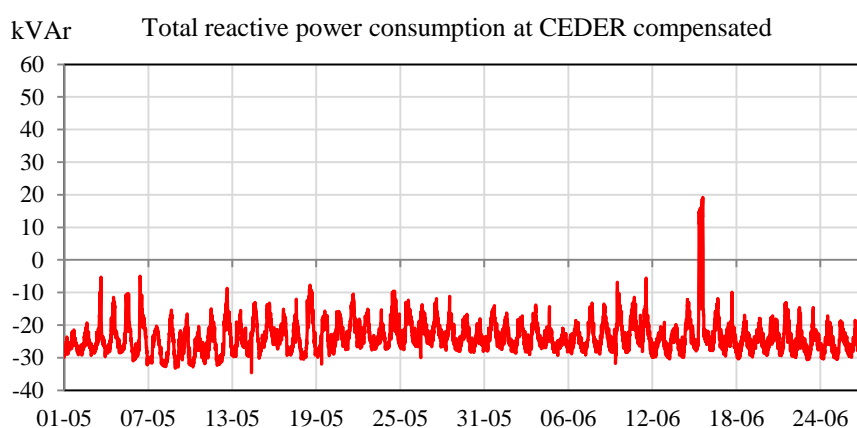


**Fig. 18.** Total reactive power consumption at CEDER compensated.

Table 1 shows a summary of the comparative data between two two-month periods of consumption at CEDER with and without capacitor banks.

**Table 1.** Summary of reactive power consumption in CEDER with and without capacitor bank

	Before capacitor banks	After capacitor banks
Average monthly reactive energy consumption	2523,8 kVArh	177,9 kVArh
Maximum monthly peak	63,48 kVAr	19,9 kVAr
Monthly average reactive energy > 33% of active power	1653,4 kVArh	0 kVArh
Monthly average reactive energy > 75% of active power	318,2 kVArh	0 kVArh
Average monthly bill cost	88,53 €	0 €

## 4 Conclusions

This paper presents a study to reduce the reactive energy consumption in the CEDER-CIEMAT smart microgrid in order to achieve savings in the electricity bill derived from these consumptions and to avoid instabilities in the same due to high consumption of reactive energy at specific times.

After initial measurements to determine the reactive power consumption in the microgrid and to identify the main consumers in the microgrid, it was decided to install four capacitor banks, two constant and two scalable, associated with the equipment with the highest reactive power consumption in CEDER.

Once installed, new reactive energy consumption measurements were taken and after their study it was found that the reactive energy consumption in the centre has been significantly reduced, which implies a monthly saving of around 100 € in the electricity bill. In addition, high consumption peaks derived from the use of the equipment with the highest reactive energy consumption have been eliminated and to which the two scalable capacitor banks have been associated, bringing the power factor close to unity.

In summary, by means of this reactive power study, it has been possible to locate the installations where there is a higher consumption of reactive power and an effective solution to reactive power compensation has been proposed. An analysis of network stability and harmonics has been left as future work.

## Acknowledgments

The authors thank the CYTED Thematic Network “INTELLIGENT CITIES FULLY INTEGRAL, EFFICIENT AND SUSTAINABLE (CITIES)” n° 518RT0558. This work has been supported by Spanish national project [RTC-2017-6712-3] of the Spanish Ministry of Science.

## References

1. H. Minxiao, S. Xiaoling, L. Shaobo, and Z. Zhengkui, “Transient analysis and control for microgrid stability controller,” in *2013 IEEE Grenoble Conference*, 2013, pp. 1–6, doi: 10.1109/PTC.2013.6652175.
2. D. T. Ton and M. A. Smith, “The U.S. Department of Energy’s Microgrid Initiative,” *Electr. J.*, 2012, doi: 10.1016/j.tej.2012.09.013.
3. C. Bordons, F. García Torres, and L. Valverde, “Gestión Óptima de la Energía en Microrredes con Generación Renovable,” *Rev. Iberoam. Automática e Informática Ind.*, vol. Vol. 12, N, doi: 10.1016/j.riai.2015.03.001.
4. O. Izquierdo-Monge, P. Peña-Carro, R. Villafafila-Robles, O. Duque-Perez, A. Zorita-Lamadrid, and L. Hernandez-Callejo, “Conversion of a Network Section with Loads, Storage Systems and Renewable Generation Sources into a Smart Microgrid,” *Applied Sciences*, vol. 11, no. 11. 2021, doi: 10.3390/app11115012.
5. F. Katiraei, M. R. Iravani, and P. W. Lehn, “Micro-grid autonomous operation during and subsequent to islanding process,” *IEEE Trans. power Deliv.*, vol. 20, no. 1, pp. 248–257, 2005. DOI 10.1109/TPWRD.2004.835051

6. CENER-Centro Nacional de Energías Renovables, “Introducción a las Micorredes” .
7. M. T. L. Gayatri, A. M. Parimi, and A. V Pavan Kumar, “A review of reactive power compensation techniques in microgrids,” *Renew. Sustain. Energy Rev.*, vol. 81, pp. 1030–1036, 2018, doi: <https://doi.org/10.1016/j.rser.2017.08.006>.
8. F. R. Quintela, R. C. Redondo, J. M. G. Arévalo, N. R. Melchor, and M. M. Redondo, “Uso de la energía reactiva para evaluar las pérdidas en el sistema eléctrico,” *Técnica Ind. Oct.*, 2006.
9. Ministerio de Industria Energía y Turismo de España, ITC 688/2011: Peajes de acceso y tarifas y primas de las instalaciones del régimen especial. 2011.
10. Ministerio de Interior, RD 1164/2001: Tarifas de acceso a las redes de transporte y distribución de energía eléctrica. 2001, p. 12.
11. C. Zhang and Y. Zeng, “Voltage and reactive power control method for distribution grid,” in *2013 IEEE PES Asia-Pacific Power and Energy Engineering Conference (APPEEC)*, 2013, pp. 1–6, doi: 10.1109/APPEEC.2013.6837313.
12. Y. Shen, D. Ke, Y. Sun, D. S. Kirschen, W. Qiao, and X. Deng, “Advanced Auxiliary Control of an Energy Storage Device for Transient Voltage Support of a Doubly Fed Induction Generator,” *IEEE Trans. Sustain. Energy*, vol. 7, no. 1, pp. 63–76, 2016, doi: 10.1109/TSTE.2015.2472299.
13. M. Qin, K. W. Chan, C. Y. Chung, X. Luo, and T. Wu, “Optimal planning and operation of energy storage systems in radial networks for wind power integration with reserve support,” *IET Gener. Transm. Distrib.*, vol. 10, no. 8, pp. 2019–2025, May 2016, doi: <https://doi.org/10.1049/iet-gtd.2015.1039>.
14. A. Cagnano, E. De Tuglie, M. Liserre, and R. A. Mastromauro, “Online Optimal Reactive Power Control Strategy of PV Inverters,” *IEEE Trans. Ind. Electron.*, vol. 58, no. 10, pp. 4549–4558, 2011, doi: 10.1109/TIE.2011.2116757.
15. A. Pană, F. Molnar-Matei, A. Băloi, A. Radulian, N. Mocioi, and G. Dumitrescu, “A smart solution for a smart grid: Unbalanced reactive power compensation,” in *2017 Electric Vehicles International Conference (EV)*, 2017, pp. 1–6, doi: 10.1109/EV.2017.8242116.
16. M. M. A. Salama and A. Y. Chikhani, “A simplified network approach to the VAR control problem for radial distribution systems,” *IEEE Trans. Power Deliv.*, vol. 8, no. 3, pp. 1529–1535, 1993, doi: 10.1109/61.252679.
17. España, *Boletín Oficial del Estado*. 2019, pp. 26798–26800.

## Modelado de llamado masivo remoto de medidor con requerimientos de alta disponibilidad para la operación de un CGM.

Fernando Vélez Varela<sup>1</sup>, Jorge Junior Garcia Ledesma<sup>2</sup>

<sup>1,2</sup> Universidad Santiago de Cali, Cali, Valle del Cauca, COLOMBIA  
Calle 5 # 62-00 Barrio Pampalinda

fernando.velez00@usc.edu.co<sup>1</sup>; jorge.garcia08@usc.edu.co<sup>2</sup>

**Abstract.** Las Empresas Comercializadores de energía específicamente los centros de gestión de medida del área de servicio eléctrico (CGM) se encuentran en una constante evolución de sus servicios, además de cumplir con las condiciones establecidas por entes gubernamentales quienes brindan a la sociedad ciertos parámetros mínimos de calidad en las prestaciones ofrecidas por cada Comercializador, a razón de estas directrices se implementan una serie de estrategias tecnológicas para cumplir dichas condiciones. Como primer mecanismo en el siguiente proyecto se presenta el modelado de una solución de llamado masivo, la cual considera en gran medida el escenario real de un CGM, como lo es variedad y volumen de usuarios. En consecuencia, los parámetros establecidos dentro del proyecto brindan un conjunto de conceptos imprescindibles para lograr una comprensión a detalle de la solución presentada, por lo tanto, se ejecutarán una serie de estrategias y programas las cuales tienen como base el llamado remoto e implementación de protocolos de seguridad en la información. El principal impacto de este papel es la propuesta de un nuevo marco de agrupamiento para la clasificación automática de las cargas eléctricas. El tiempo de cálculo del marco propuesto es menor que el de las técnicas de clasificación anteriores, lo que permite procesar una muestra completa de la compañía eléctrica en cuestión de minutos en una computadora personal.

**Keywords:** CGM, Telemetría, Medidor, llamado, nativo, marca, AC6000, SL7000, A1800, PHP, Smart Grids, Red, Tráfico de Datos, Big data.

### 1 Introducción

Las nuevas tecnologías derivadas del paradigma de las Smart Grids [1] han incrementado el control y seguimiento del consumo eléctrico por parte de clientes y empresas distribuidoras. Este nuevo escenario ha supuesto un crecimiento exponencial de la información disponible sobre la red y el consumo. Por tanto, estas tecnologías han propiciado la aparición de nuevos servicios y el aumento de la eficiencia y fiabilidad del suministro eléctrico. Para facilitar la interacción con otros sistemas, estos nuevos servicios deben poder analizar grandes cantidades de información en poco tiempo [2]. Para lograr este objetivo, los métodos de análisis y los diseños de modelado deben

construirse utilizando plataformas de big data [3] como Apache Hadoop [4], Spark. [5] o KumbiaPHP, C#. En el actual modelo de regulación del sector eléctrico, uno de los principales objetivos es mejorar el desempeño de la distribución, aumentando así el nivel de conocimiento sobre la demanda. La forma más común de evaluar la energía y la eficiencia es evaluar el comportamiento de la curva de carga de los clientes, incluidos los posibles desplazamientos en horas punta [6]. Los usuarios de sistemas eléctricos han desempeñado un rol pasivo en lo concerniente a la toma de decisiones operacionales y la planificación del servicio. Durante décadas ha bastado con instalar medidores análogos que registran el consumo de energía en un hogar para que luego se realice el cálculo del diferencial entre los periodos y se determine el costo de la factura respectiva. Se han presentado un par de hechos recientes que vienen transformando la concesión de sistemas eléctricos y por consiguiente la forma como se miden sus variables.

El primer hecho es que la seguridad energética del país en el corto y mediano plazo se encuentra amenazada. Lo anterior se debe a diversas circunstancias: el fenómeno del Niño, las fallas técnicas en plantas de generación, resulta indispensable optimizar los recursos para la prestación del servicio, pasando de un esquema tradicional (en el cual la generación se hace de forma centralizada y alejada de los centros de consumo) a un esquema híbrido en el que parte de la energía proviene de lugares cercanos al usuario, e incluso de su propia instalación. El conocimiento preciso de los patrones de consumo de los clientes representa un activo valioso para los proveedores de electricidad en los mercados competitivos. La idea principal es identificar perfiles de carga horaria de clientes (HLPs) [7] y desarrollar un conjunto de reglas para la clasificación automática de nuevos consumidores [8].

El segundo hecho innegable es la necesidad de aprovechar los avances de las tecnologías de la información y las comunicaciones para atender las nuevas demandas del sector. Así sería posible contar, en tiempo real, con información detallada sobre las variables del sistema eléctrico de potencia (que sería suministrada por medidores inteligentes). También, con miras a optimizar la prestación del servicio, convendría implementar las herramientas Big Data (datos masivos) para almacenar, procesar y analizar la información proveída por los usuarios. De igual manera, dada la vulnerabilidad de los sistemas eléctricos y la privacidad de los datos, resultaría necesario recurrir a los avances en el campo de ciberseguridad [4].

En la actualidad las Distribuidoras de energía o proveedores de Energía tienen que tener una medida exacta, correcta y real del consumo de cada cliente, para ofrecer un alto nivel de seguridad, de presencialidad y un buen concepto construido, que esté relacionado con lo dispuesto en su estructura de servicios que se le ofrece a cada cliente, esto es debido a la gran responsabilidad y exactitud con la que debe medir el consumo eléctrico, además de tener el respaldo de fallas (eventos, monitoreo, seguimiento, visualización de datos entre otros). Para aceptar a muchos usuarios que son determinados como clientes de hogar (vivienda), al igual que los que se definen como clientes empresariales (torres y centros comerciales), los cuales involucran múltiples características adicionales como la validación en tiempo real en el proceso de telemétrica en

consumo eléctrico y que por muchos motivos exigen niveles altos de veracidad y exactitud en la medida y operabilidad de algo más del 99% [9].

El telecontrol en empresas de distribución eléctrica se compone básicamente de tres partes que son:

- Equipos de telemedida.
- Comunicación.
- Puesto de control central y monitorización de datos.

Para tener esta exactitud no solo basta tener los equipos correctos como medidor y modem en equipos físicos, sino que también deben tener una serie de configuraciones, disposiciones de diseño y aplicación tecnológicas, que, sumadas al uso de los debidos protocolos lógicos, le dan respaldo, al consumo generado. Las redes eléctricas están en proceso de evolución a la vinculación de nuevas tecnologías, convirtiéndose en Smart Grids que permite articular la relación entre el sistema eléctrico y el consumidor final de energía y también determina el tipo de relación comercial y técnica entre los agentes involucrados [10].

Una infraestructura de medición inteligente (Advanced Metering Infrastructure - AMI) puede definirse como la integración de varias tecnologías que crean una conexión inteligente entre los operadores del sistema y los consumidores, para brindar a estos últimos la información que necesitan para tomar decisiones que redunden en mayores beneficios. Un sistema AMI integra elementos de hardware y de software, con base en un medidor inteligente, una infraestructura de comunicaciones integrada que permite intercambios bidireccionales de información y de registros en tiempo real. Todos los elementos del sistema interactúan entre sí de forma fiable, flexible y eficiente para permitir interacciones entre el usuario final y la empresa comercializadora. Los sistemas AMI están conformados por cuatro elementos básicos: Medidor inteligente, Concentrador de datos, Red de comunicaciones, Sistema de gestión de la información [11].

El medidor cuenta con funcionalidades que le permiten recolectar y transmitir los datos de consumo hacia los agentes involucrados (CGM).

En el caso colombiano se vienen adelantando acciones interesantes por parte de las empresas del sector, como la iniciativa sectorial Colombia Inteligente, conformada por diferentes empresas (XM, EPM, DICEL, CODENSA, EMCALI, CELSIA, EPSA, ELECTRICARIBE, EEB, ISAGEN).

Las funciones necesarias para la realización del telecontrol en las redes eléctricas de distribución en baja tensión son:

- Consulta. Visualización de los valores de los datos actuales y archivados diarios de carga consumida y las interrupciones realizadas.
- Órdenes. Definición de órdenes (umbrales, periodos horarios.), puesta al índice de las telelecturas.
- Traslado de alarmas. Configuración del número de llamadas a los destinatarios de la alarma, y notificación de estas.
- Ajuste. Definición de los datos de entradas/salidas.
- Diagnóstico. Herramientas informáticas de mantenimiento del software [12].
- Puesta en marcha. Definición de claves de acceso, configuración de las tarjetas de entradas/salidas y de las tarjetas de comunicaciones.
- Registro de corrientes de falla.

- Operador del sistema:
  - Sistemas de medición fasorial - PMU.
  - Monitoreo, medida y control exhaustivo del sistema (“wide”).
- Empresas de transmisión:
  - Gestión de activos (monitoreo constante, diagnóstico y detención de fallas)
  - Incorporación de tecnologías (Sistemas Flexibles de Transmisión AC – FACTS, Dispositivos superconductores de alta temperatura, Líneas de Alta Tensión DC – HVDC Líneas de Ultra Alta Tensión AC – UHVAC).

Empresas de generación:

- •Energías limpias (ciclo combinado con gasificación integrada de carbón, ciclo combinado de gas natural, etc.)
- •Energías no convencionales (nuclear) y no convencionales renovables (eólica, solar, geotérmica, undimotriz, mareomotriz, termal oceánica, biomasa, biogás, etc.) [13].

Los protocolos han sido incluidos en un solo programa para el propósito, el cual se enmarca en un objetivo evolutivo, se usan para aprovechar el máximo desempeño este aplicativo. Esto se hace con base en el conocimiento que de estos se tiene y de las potencialidades que se pueden tener de acuerdo con la necesidad específica para busca lograr un excelente nivel de eficiencia. Llamador es el sistema de gestión comercial y está a disposición de las compañías de distribución eléctrica. Tiene integrado telemetría, telegestión y facturación electrónica, lo que facilita en gran medida su trabajo y su contacto con las comercializadoras eléctricas y con los consumidores finales [14].

Esto determina el hallazgo de una solución modular y escalable, que facilita el trabajo de las compañías eléctricas en cuestiones de: accesibilidad, explotación de datos, planes de despliegue, órdenes de servicio, gestión de expedientes (fraudes, verificaciones de equipos de medida, anomalías), lecturas (para definir calendarios, grupos, itinerarios), gestión del cobro, etc [15].

## 2 Marco Teórico

Para el desarrollo de este trabajo se tendrán en cuenta los objetivos de desarrollo sostenido (ODS). Trabajo decente y crecimiento económico que expresa preocupaciones totales acerca de la implementación de las legislaciones y los compromisos internacionales sobre trabajo decente (fomento del trabajo productivo, la protección de derechos laborales, obtención de ingresos adecuados, la protección y seguridad social, y el diálogo social) y las normas dispuestas por la CREG e instalaciones relacionadas con pruebas de conectividad con medidores de energía eléctrica, más lo adquirido en conocimientos en relación con la práctica y procesos del tema [16].

El aplicativo llamador es un aplicativo que permitirá el acoplamiento de diversas marcas de medidores para la obtención de la información o consumo. Este aplicativo o página web estará amarrado a usuarios y contraseñas suministrada para el personal calificado para dicha tarea. Cada usuario tendrá permisos distintos para el manejo de la aplicación [17] [18].

A continuación se mostrará el login del aplicativo web y dentro de sus características y diferentes apartados (Ver Fig. 1):



Fig. 1: login. Fuente: Los Autores

En este escenario de aplicación de transmisión de datos de equipos eléctricos, se analiza el método de transmisión de datos basado en la tecnología Message Queue Server Telemetry Transport (MQTT) (Ver Fig. 2).

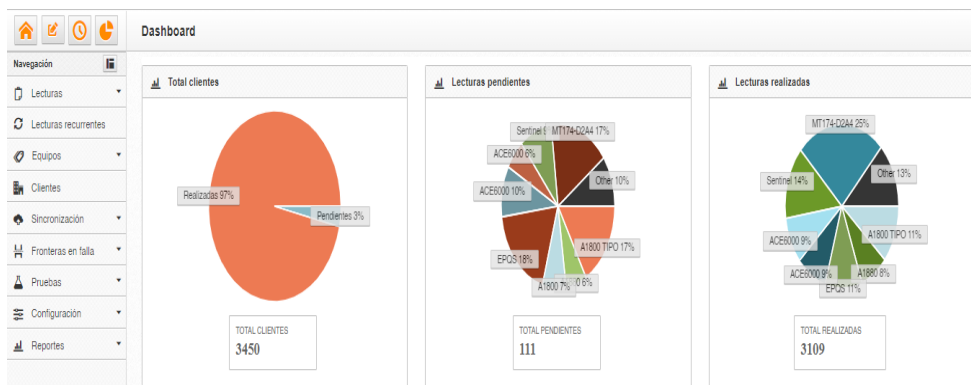


Fig. 2. Menú aplicativo web. Fuente: Los Autores

Se implementará una arquitectura de tres capas conocida como modelo vista controlador (MVC) que es un patrón de diseño que separa la interfaz del usuario, la lógica de control y los datos en distintos componentes. La interfaz de usuario estará en el servicio web y la lógica del control estará en el dispositivo móvil (modem) mientras que los datos estarán del lado servidor [19].

La lógica de control es la encargada de enviar las peticiones ingresadas por el personal que llama en la vista al servicio web, el cual se comunica con los distintos

componentes y procesa las peticiones. El modelo genera una respuesta que retorna al control a través del servicio web donde será procesada y mostrada [20].

Se hará uso del Proceso Unificado, el cual se fundamenta en el uso de las mejores prácticas como el desarrollo iterativo, el seguimiento a los requerimientos, el uso de arquitecturas que permiten la reutilización de código y la verificación de calidad del producto (Ver Fig. 3).

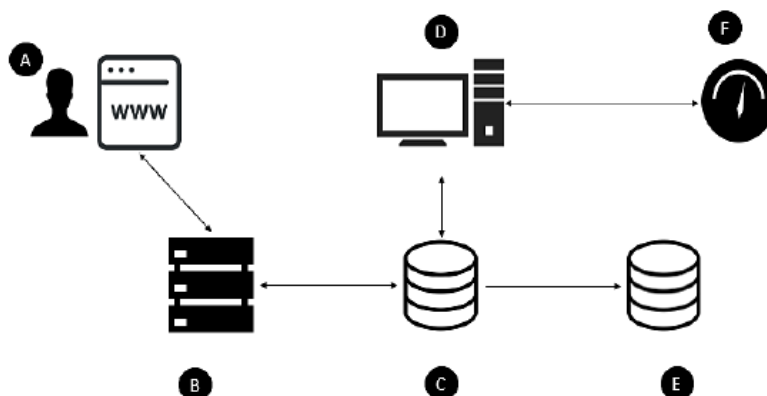


Fig. 3. Diagrama de casos. Fuente: Los Autores

### Marco Normativo

Las aplicaciones desarrolladas en este proyecto no generaran interferencia a otras aplicaciones instaladas la aplicación hará uso de redes móviles o inalámbricas para la transferencia de información relacionada la propiedad intelectual de este proyecto estará sujeta a las normas vigentes establecidas por la CREC.

### Comunicación

Dada la forma de una red de distribución eléctrica urbana y las distancias entre los puntos periféricos y el puesto central que oscilan entre unos centenares de metros y decenas de kilómetros, el precio del medio físico requerido para la comunicación (p. Ej. cable, fibra óptica o radio) puede ser muy importante. Por ello es fundamental seleccionar la solución más económica para cada caso [21] [22].

### Principio de funcionamiento

El cometido principal de la aplicación es posibilitar el telemando de estado de los circuitos ubicados en los distintos centros de transformación. Con este fin se incluye el interfaz hombre / máquina que permite seleccionar una RTU remota, dentro de la misma, uno de los interruptores y de éste una de las dos órdenes de maniobra (apertura o cierre).

Tras las correspondientes confirmaciones de seguridad de la maniobra a ejecutar, el sistema envía la trama al equipo de telemando correspondiente. Esta trama lo suficientemente larga, descriptiva y completa para que la maniobra pueda ser ejecutada por el sistema y así se pueda plasmar en una matriz horaria [16] [21].

### Red telefonía interna o pública

En los casos que se dispone de línea telefónica, se ofrece la solución de trabajar por medio de enlace telefónico vía MODEM o INTERNET. En esta forma de transmisión, se llama desde el control central, abriendo el canal de comunicación justo para el tiempo de la consulta y, una vez terminada la transmisión, se abandona la línea. Al igual que en el caso de enlace por radio, se trata también en este caso de un enlace punto a punto que puede servir también de conexión entre zonas enmalladas. La transmisión, si bien es punto a punto, permite enlazar redes, intercalando repetidoras [2] [4].

### Infraestructura de comunicación

La transmisión de la información desde el medidor hacia el sistema de gestión se puede realizar por dos vías diferentes:

1) De forma directa desde el medidor hasta el centro de gestión.

2) A través de un concentrador de datos que recibe la información de un grupo de medidores y la transmite al centro de gestión. En ambos casos, se utilizan medios de comunicación tanto cableados como inalámbricos. La infraestructura de comunicaciones también incluye las herramientas, recursos y métodos necesarios para garantizar la ciberseguridad de la información en el sistema.

### Sistema de gestión de la medida

Está conformado por dos bloques generales:

1) Gestión de la medida - medidor, el cual se encarga de la recepción y transmisión de datos desde y hacia el equipo.

2) Meter Data Management (MDM), que cumple las funciones de almacenamiento y procesamiento de información. El lazo interno dentro del Sistema de Gestión de la Medida representa los datos relacionados con la operación y que circulan permanentemente en la infraestructura de comunicaciones.

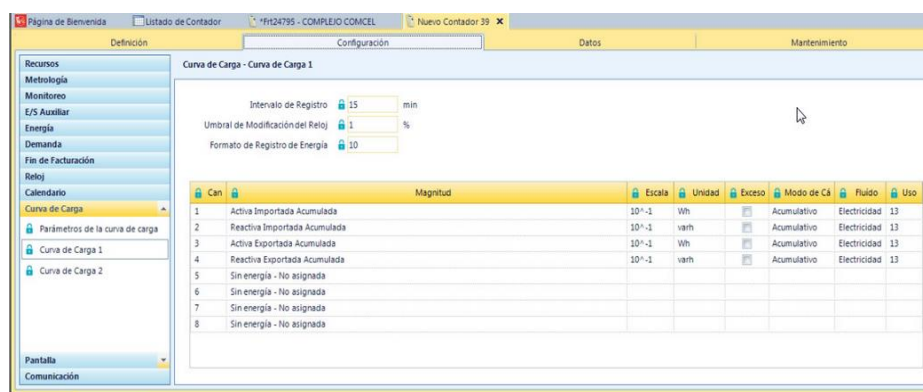


Fig. 4: Proceso de llamado (tiempo real). Fuente: Impresión tomada de programa nativo ACEPILOT

Cabe resaltar que los datos de respuesta deben coincidir obligatoriamente con los de petición (mismo medidor y contraseñas de seguridad). Para la realización de la prueba se usa el llamador con sus parámetros y configuraciones el cual permite generar la

conexión remota de manera rápida y con ella validar si es correcto la información que se tiene vs la que se programó el medidor inteligente [23].

#### **Almacenamiento**

Este estado permite la agrupación de la curva de carga y plasmarla en una matriz horaria que permite ver el consumo real de cada cliente diario y así validar su consumo corte entre otros. El almacenamiento de datos tanto del cliente (nombre, dirección etc.) como el almacenamiento de los consumos), brindando al cliente un historial puntual ya sea diario semana, mensual o anual. Estableciendo un escenario de conformidad y seguridad.

#### **Protocolo**

Se utilizaron los siguientes protocolos:

- ANSI/ISA-101.01-2015: Es abordar la filosofía, el diseño, la implementación, la operación y el mantenimiento de las HMI para los sistemas de automatización de procesos, a lo largo de su ciclo de vida.
- Protocolos TCP/IP: define cuidadosamente cómo se mueve la información desde el remitente hasta el destinatario. En primer lugar, los programas de aplicación envían mensajes o corrientes de datos a uno de los protocolos de la capa de transporte de Internet, UDP (User Datagram Protocol) o TCP (Transmission Control Protocol). Estos protocolos reciben los datos de la aplicación, los dividen en partes más pequeñas llamadas paquetes, añaden una dirección de destino y, a continuación, pasan los paquetes a la siguiente capa de protocolo, la capa de red de Internet.

#### **Normativa**

La normativa asociada a los sistemas de Telecontrol contemplada por la IEC es la siguiente:

- IEC 60870-2-1 (1995-12), IEC 60870-2-2 - Ed. 1.0, IEC/TR 60870-1-1(1988-12). Especifica las condiciones de funcionamiento cuando el equipo de telecontrol se encuentra operando. Da una visión general de los elementos funcionales contribuyendo a la escogencia de la estructura básica y la configuración del sistema de telecontrol. Enfatiza los problemas característicos de los procesos geográficamente dispersos, como la influencia dominante de los lazos de telecomunicaciones, las restricciones de ancho de banda y la razón señal/ruido. Esta norma es una descripción básica.
- IEC-60870-4 (1990-04). Es un tratado que contiene las características afectan el desempeño de los sistemas de telecontrol y enuncia las características de las aplicación y funciones de procesamiento. Establece un grupo de reglas que fijan unos requerimientos de desempeño de los sistemas de telecontrol.
- IEC/TR3 60870-1-3 (1997-04). Contiene los términos relativos a las técnicas de telecontrol y otros términos necesarios para el entendimiento e los estándares asociados al telecontrol.
- IEC-60870-5-5(1995-06), IEC 60870-5-101 (2003-02), IEC-60870-5-104(2000-12) y IEC-60870-5-101-104. Aplica a los equipos de telecontrol y sistemas con transmisión por codificación serial de datos para monitorear y controlar procesos geográficamente dispersos. Define un grupo de estándares para la interoperabilidad entre equipos compatibles de telecontrol.

- IEC 60870-6-502 (1995-12). Especifica el protocolo para el uso de aplicación-servicio-elemento- elemento de telecontrol. Como soporte para el intercambio de datos de proceso entre sistemas de telecontrol. Menciona los protocolos de telecontrol compatibles con estándares ISO y recomendaciones ITU-T.
- IEC-60870-6-501(1995-12). Define los servicios que provee una aplicación de telecontrol específica en aplicación-servicio-elemento-aplicación de telecontrol, para el intercambio de datos de proceso en sistemas telecontrolados. incluye protocolos y telecontrol compatibles con los estándares ISO y las recomendaciones ITU-T.
- IEC/TR3 60870-1-4 (1994-07). Esta norma es un reporte técnico que contiene un tutorial con las técnicas de transmisión, equipos y protocolos que se usan en sistemas de telecontrol. Es una guía de orientación para el uso de los estándares definidos en las series de IEC 60870-5 y 60870-6.
- IEC 60870-1-2(1989-11) - IEC60870-5-3(1992-09). Esta norma aplica a los equipos y sistemas de telecontrol con transmisión por codificación serial de datos para monitorear y controlar procesos geográficamente dispersos. Especifica reglas para la estructuración de tramas de datos en sistemas de telecontrol.

### 3 Metodología

Consiste en implementar un aplicativo de llamado masivo (todo tipo de medidores) disminuyendo costos grandes de aplicativos nativos entre otros. Se diseñará una serie de pasos para el manejo de datos primordiales para el llamado como marca de medidores y módems la configuración de estos entre otros (Ver Fig. 5).

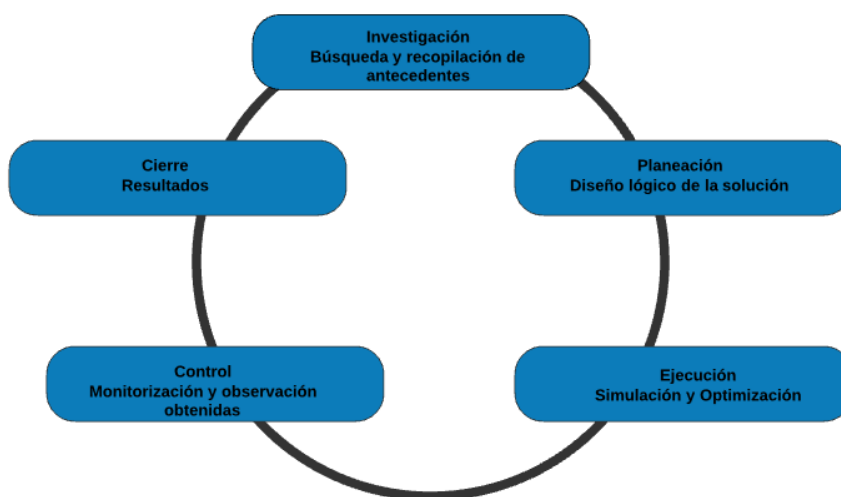


Fig. 5. Proceso Metodológico. Fuente: Los Autores

### **Actividades y Tareas**

Diseño. Recolección de requerimientos, creación de drivers, bosquejo de la solución, definición de equipos a utilizar y definición de direccionamiento a utilizar.

Simulación. Simulación de los equipos, Simulación conexiones de los equipos, Simulación conexión de modem (con ruteo), creación del equipos y configuración.

Pruebas. Verificación modem, verificación medidora, verificación de instalación de modem (cableado a medidor), verificación de conectividad entre equipos de comunicación y verificación entre equipos modem medidor.

### **Plan de proyecto**

**Etapa 1 – Investigación.** Búsqueda y recopilación de antecedentes:

Se hará uso de bases de datos, registros de investigaciones y otros sistemas de información, grupos o entidades reconocidas científicamente para la obtención de contenido similar al del proyecto que aporte al direccionamiento de este. Cabe resaltar que el aporte de los conocimientos nos ayudará a tener las distintas bases y códigos para el llamado de cada medidor (este código es suministrado por el fabricante de cada medidor por un costo determinado comercialmente). De igual manera se resalta el conocimiento adquirido en semestres anteriores e investigación de la nueva temática relacionada con el proyecto: Modelado de llamado masivo remoto de medidor con requerimientos de alta disponibilidad para la operación de un CGM.

**Etapa 2 – Planeación.** Periodo de planeación.

Teniendo en cuenta las exigencias que se han definido en la etapa anterior, se discuten las posibles vías de solución al problema, se realizan los diseños de programación (página, escenarios y despliegue de servicios para darle un consumo más acertado a lo descargado y modelado a presentar. Adicionalmente, se ponen en marcha las técnicas enseñadas. A la vez, se elige el contenido relevante que estaría disponible a través del modelado.

**Planeación – Diseño.** Al dar inicio con la recolección de datos, se obtienen los primeros resultados necesarios para concluir con los objetivos del proyecto, los cuales son la identificación de equipos (medidores) y protocolos implementados, además de la vista general y específica del código del proveedor de servicios. Se obtiene el diseño de la solución, la cual consta de un código definido y con las necesidades establecidas en cada uno de los equipos (medidores). Realizando una distribución de tareas paso a paso las cuales se determinaron de la siguiente manera: Se lleva a cabo la recolección de requerimientos, bosquejo de la solución, definición de equipos a utilizar, definición de código a utilizar, definición de direccionamiento a utilizar, descarga de curva o datos envió de información, transferencia applicativa a BD, impresión de datos.

**Etapa 3 – Ejecución.** Durante el ciclo de ejecución, tras haber determinado la topología final, se procede a establecer el código fuente, y desarrollar arquitectura haciendo uso de buenas prácticas en la implementación de protocolos, basándose en la variedad de tipos de clientes y mediadores quienes tendrán sus requerimientos adecuados a sus necesidades, dentro de estos se destacan clientes quienes ocupan servicios de alta tensión o baja , no obstante cabe resaltar el balanceo de paquetes y tráfico de información, siendo la estrategia base para el despliegue del proyecto.

**Ejecución – Simulación.** Teniendo el apoyo del diseño de la topología se pasa al emulador o servidor de prueba, con la parte de la simulación de equipos, se utilizan código PHP para el entorno web diseñando diversas ventanas de búsqueda, petición, de configuración de medidores, routers, Simcards de distintos operadores, Modems y switches que permitirán manejar todos los protocolos establecidos con anterioridad, se conectan los equipos teniendo en cuenta que el llamado solo trabaja con conexiones de red inalámbrica, en este caso se trabaja por conexión de red de telefonía 4G y de 5G dependiendo de la necesidad del usuario, por lo cual para realizar este llamado se necesita diversos módems de salida (distinto operador) para llamar a cada medidor y solicitar la trama de información. Una vez configuración del modem, y ya conectados los equipos, entramos a la programación del medidor y después de eso se pasa a la parte de configuración de seguridad y reconocimiento de medidor el cual se puede decir que es la más robusta de todo el proceso. ya que el programa debe reconocer el cliente encriptar la información, obtener la curva de carga transformarla en matriz horaria, plasmar esta información en un archivo de Excel y texto y posteriormente pasarla a la base de datos [24].

Al realizar la ejecución de la simulación se tuvieron en cuenta una serie de puntos desarrollados en el siguiente orden:

- Código de consulta, código de petición, drivers (fabricante), modelos o marca de medidor para la parte de telemetría.
- Simulación de los equipos, simulación conexiones de los equipos (red 4G y 5G), simulación de protocolos de seguridad en los equipos del cliente, simulación en equipos de medición, simulación en equipos nativos, configuración en equipos modem y medidor

Se inicia con la activación de las interfaces en los distintos equipos, para esto se necesita estar en las redes de internet de la empresa y tener consigo ya los permisos de ingreso al aplicativo web establecidos, el MPLS da la libertad de configurar de manera interna y utilizar este como medio de transporte para paquetes de datos, se pueden utilizar protocolos de enrutamiento como OSPF, BGP entre otros dependiendo de la necesidad y requerimiento del usuario, esto se hace con el fin de generar las redes y hacer que haya comunicación entre los diferentes equipos, también es importante asignar los direccionamientos en los equipos finales.

Teniendo la todo configurada de esta manera se puede pasar a la parte de configuración del modem, se establece los equipos y se establece la configuración del llamado en BD para que esta se refleje en el sistema, posteriormente se configuran los equipos (medidores) y por último los equipos en BD.

**Etapa 4 – Control.** En esta etapa, se concluyen todas las actividades relacionadas con el modelamiento del sistema, se tiene en cuenta la infraestructura a nivel de capa física de datos y de red, para posteriormente realizar la simulación a pruebas y revisiones de desempeño con el fin de visualizar los resultados y verificar el cumplimiento del alcance del proyecto.

**Etapa 5 – Cierre.** Para finalizar el proyecto, se expone el modelo y se somete a escenarios similares a entornos real, así realizando un análisis y seguimiento del comportamiento del proyecto.

## 4 Desarrollo

Para la recolección de resultados, se tuvo en cuenta el proceso de comparación de resultados en diferentes entornos, conclusiones, en este caso, el servidor se encarga de alojar la aplicación Web, dicha aplicación está desarrollada en .net (Drivers), PHP bajo el framework de KUMBIA y se ejecuta bajo apache, que viene incluido en la instalación realizada XAMPP.

Se debe tener en cuenta que, la aplicación web permite la realización de las siguientes tareas:

- Registro de canales, clientes y medidores., exportación de reportes, sincronización de medidores, programación de lecturas.
- Servicio de lectura. Este servicio esta Implementado en lenguaje C#; Se debe tener en cuenta que, para el funcionamiento de este servicio, el equipo en el cual se ejecute debe poseer las siguientes implementaciones: Cliente de Oracle (ODAC); Acceso a la red de la empresa; Tablas de enrutamiento (necesarias para la comunicación vía TCP/IP con los medidores).; Archivo de configuración llamado del aplicativo, en el cual se configura el usuario, contraseña e IP de la base de datos del aplicativo.

Este aplicativo contendrá:

- El estado de lectura (conectando, descargando, errores, etc.), roles de medidores (principal o respaldo), sincronización, inserción a BD, procedimiento para lectura de consumos.
- Para llevar a cabo un proceso de lectura, el usuario debe generar una lectura programada a través de la página web. Luego de esto, el sistema ejecuta el siguiente procedimiento, es decir, se debe hacer un registro de lectura en una tabla, perteneciente a la base de datos del aplicativo, el servicio de lectura detecta la creación de una nueva lectura, utilizando tablas de enrutamiento y los parámetros de configuración introducidos a través de la aplicación web, se comunica el medidor especificado, el medidor retorna la información solicitada, el servicio almacena los datos en tablas, perteneciente a la base de datos para esto, utilizar una sentencia INSERT INTO A través de un dblink ubicado en un trigger especificado de la tabla en al cual se van a guardar los datos, se envía los consumos al aplicativo.

**Desarrollo de los estados de lectura.** Durante el proceso de lectura, se deben considerar algunas variables que permiten determinar el estado del proceso. Dichos campos son las siguientes:

- ESTADO: Determina si la lectura se programó recientemente (estado 0), está pendiente (estado 1) o ya se realizó (estado 2).
- LECT\_ESTADO: El servicio de lectura puede realizar múltiples lecturas al mismo tiempo gracias a los múltiples hilos que se crearon para el llamado. para evitar que varios hilos intenten realizar una misma lectura se creó este estado. Está en 1 cuando la lectura está siendo procesada por un hilo o está en 0 cuando ningún hilo la está procesando.

Existen otros estados aparte de programada, pendiente y realizada. El más importante de ellos es Fallida (estado 3). Este estado se da cuando el servicio ya se intentó comunicar con un medidor, pero la lectura falló y se cumplió la cantidad de intentos de conexión máximas permitidas (configuradas por cada medidor en la aplicación web). Los demás estados son propios de cada driver e indican el progreso de la comunicación y lectura de los medidores, por ejemplo: comunicando, descargando perfil de carga, conectando con medidor, error de conexión con modem etc.

Cuando el servicio de lectura está realizando la comunicación con un medidor y la comunicación falla por algún motivo, este se encarga de cambiar el estado de la lectura a 1 (pendiente), sumar 1 en el campo NUMERO\_INTENTOS y establece la fecha en la cual se debe volver a intentar, comunicar 15 minutos después de la actual.

Cuando se cumplan el número de intentos máximos de comunicación, ya no se volverá a intentar llamar el medidor a no ser que la relancen en la aplicación web.

#### **Paso de consumos**

- Cuando se realiza exitosamente la comunicación con un medidor y se descarga la información de los consumos, estos se ingresan a una tabla dispuesta para esto, la cual tiene un trigger de inserción que llama al procedimiento por\_ingresa\_intervalo creado en el aplicativo. Este llamado a dicho procedimiento lo realiza a través del dblink (Ver Fig. 6).
- La tabla dispuesta, va a almacenar los intervalos de consumo verticalmente, cada fila de la tabla corresponde a un intervalo. Lo anterior, es diferente al aplicativo realizado la cual almacena todos los 96 (4 por cada hora) intervalos que componen un día de consumo en un solo registro.

#### **Inserción de mediciones**

- El servicio de lecturas inserta directamente en la tabla MEDICIONES haciendo un INSERT INTO, pero antes de realizar esta inserción, elimina lo que ya tiene registrado ese medidor en la fecha de consumo. Lo anterior implica que, se va a guardar los consumos que se hayan traído con la última lectura realizada. Se debe tener en cuenta que el anterior proceso no se presenta en el aplicativo, debido a que la información es almacenada hasta que sea eliminada manualmente de la tabla ME\_PRECONS. El aplicativo tendrá el acceso a diversas informaciones como se mostrarán en las siguientes Fig. 7 y 8. Desde el aplicativo se logrará ver la conexión eléctrica de los medidores y su configuración interna validando las fallas o estados guardados por el medidor. Poder validar la conectividad al modem.

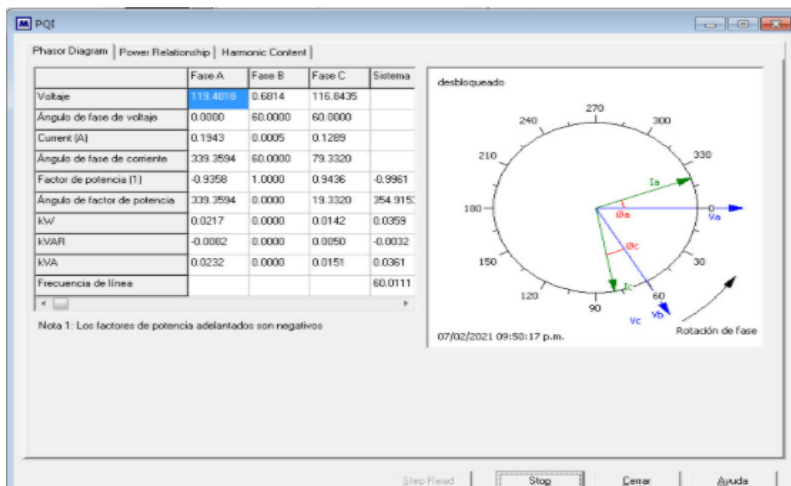


Fig. 6: Tiempo Real. Fuente: Impresión tomada de programa nativo METERCAT

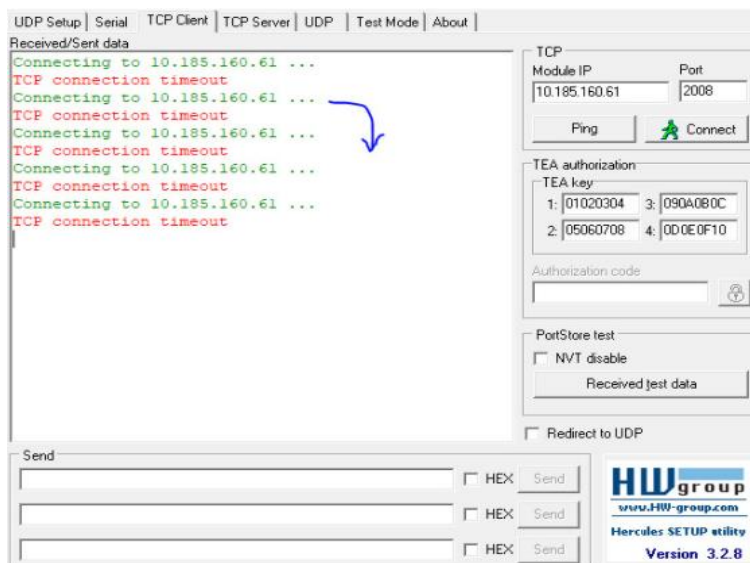


Fig. 7: Conectividad Modem. Fuente: Impresión tomada de programa nativo HERCULES

Se podrá validar la conexión entre modem llamador – modem medidor con esto aseguramos que la configuración y código se encuentra correcto, tanto como el ruteo para el llamado (Ver Fig. 8).



Con esto se puede hacer una transformación a una matriz horaria por medio del programa siguiendo normas como solo los canales Wh y vard entre otros, y así cierta trama que compone una hora se multiplica por un factor determinado de cada cliente y eso es plasmado como matriz horaria. El aplicativo está diseñado para realizar estas funciones. La metodología para realizar este cambio tiene fallas tanto lógicas como físicas por ejemplo si se rompe la trama principal el servicio cae ya que no hay información concreta ni información de respaldo, no hay estrategias de convergencia y dependiendo de la cantidad curva es la alteración de dicha matriz. Para brindar una solución a la problemática presentada en el primer escenario, es un requisito fundamental la implementación o toma de la hora descargada en la curva de carga, a partir de este punto se despliegan las demás estrategias lógicas para asegurar la alta fiabilidad de la información (Ver Fig. 10).

Fecha	Cliente	Cod. SIC	01:00	02:00	03:00	04:00	05:00	06:00	07:00
01/09/21	EV-000100001	Frt00027	1,960.20	1,932.15	1,935.45	1,933.14	1,936.77	1,932.15	1,930.17
02/09/21	EV-000100001	Frt00027	1,956.57	1,958.22	1,955.91	1,952.28	1,957.89	1,955.58	1,955.91
03/09/21	EV-000100001	Frt00027	1,845.36	1,856.25	1,851.96	1,848.66	1,843.38	1,837.44	1,807.74
04/09/21	EV-000100001	Frt00027	1,777.71	1,774.41	1,775.07	1,774.74	1,771.11	1,771.11	1,770.78
05/09/21	EV-000100001	Frt00027	1,732.83	1,746.36	1,740.42	1,734.15	1,692.57	1,694.55	1,696.20
06/09/21	EV-000100001	Frt00027	1,820.94	1,768.14	1,647.69	1,652.31	1,654.29	1,654.62	1,739.43
07/09/21	EV-000100001	Frt00027	1,855.26	1,833.15	1,887.93	1,897.83	1,889.58	1,888.59	1,911.69
08/09/21	EV-000100001	Frt00027	1,860.54	1,826.55	1,825.56	1,819.29	1,771.44	1,776.06	1,811.04
09/09/21	EV-000100001	Frt00027	1,950.30	1,947.66	1,942.05	1,946.67	1,945.02	1,940.07	1,927.53
10/09/21	EV-000100001	Frt00027	1,762.53	1,759.89	1,755.93	1,750.32	1,709.40	1,693.56	1,704.78
11/09/21	EV-000100001	Frt00027	1,968.78	1,968.45	1,966.80	1,965.81	1,967.79	1,962.84	1,968.12
12/09/21	EV-000100001	Frt00027	1,929.18	1,914.33	1,919.61	1,927.20	1,952.61	1,950.30	1,950.96
13/09/21	EV-000100001	Frt00027	1,956.24	1,967.79	1,974.06	1,973.40	1,973.73	1,971.75	1,972.74

**Fig. 10:** Mediciones de Escenario 1, referencia de marcas horarias. **Fuente:** Los Autores

**Segundo Escenario:** Interconexión de nodos (módem), conexión de módem (medidor) y modem llamador. En el segundo escenario se tiene una topología un poco más compleja la cual involucra nodos de dialogo que permitan informar sobre la conexión a los respectivos artefactos como modem y medidor) (Ver Fig. 11).

A pesar de tener una topología con un nivel considerable de robustez se siguen presentando inconvenientes tanto físicos como lógicos, llegado el caso de que haya una ruptura en alguna conexión entre modem y medidor que transportan la información, en este punto crítico cabe la posibilidad de que se genere una pérdida del servicio, por esta razón las conexiones del modem a medidor son en primera instancia la solución directa a fallas físicas dentro del despliegue. Se presentan una serie de inconvenientes físicos y lógicos, debido a la interconexión entre los modem a medidor ya que poseen un camino físico y lógico de interconexión entre ellos, además para el paso de la información es necesario realizar una configuración según sea la necesidad. No obstante, dentro de las estrategias desarrolladas, las soluciones lógicas determinan la capacidad de alta disponibilidad establecidas desde la capa de enlace de datos.

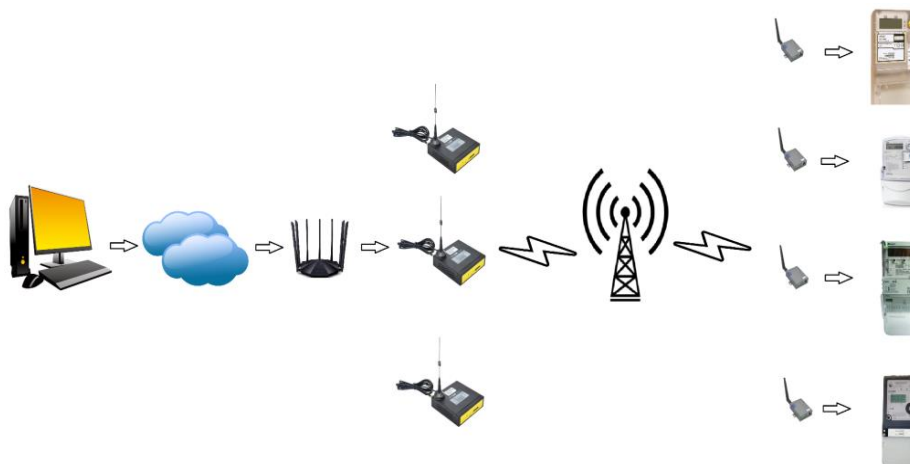


**Fig. 11:** Topología Escenario 2. **Fuente:** Los Autores

**Tercer Escenario:** Interconexión entre un Modem y Modem.

Enfocando redes más complejas como lo son las redes de los proveedores de servicio de internet y telefonía, se presentan con mayor frecuencia problemáticas masivas a la hora de revisar la disponibilidad y calidad en los distintos servicios que viajan sobre la red. Por lo cual el aplicativo no tiene como indicarnos si el problema es de red o si el problema es de conexión lógica (modem medidor) (Ver Fig. 12).



**Fig. 12:** Topología Escenario 3. **Fuente:** Los Autores

**Solución planteada.** La solución está basada en la implementación de estrategias basadas e integradas principalmente en el sistema, el cual es un mecanismo que permite validar el tipo de error que se tiene en el llamado a cada uno de ellos, esta solución brinda fiabilidad cuya prioridad es la sustentación de alta disponibilidad en conjunto con la calidad del llamado. Se plantean una serie de soluciones basadas en .net el cual es simple cuadros de diálogos de información dependiendo de la trama o error encontrado en el llamado de los medidores. Teniendo las redes en un determinado estado, el llamado del cliente tiene un modelo del mensaje de conexión entre dispositivos y con el aplicativo, que es el siguiente (Ver Fig. 13).

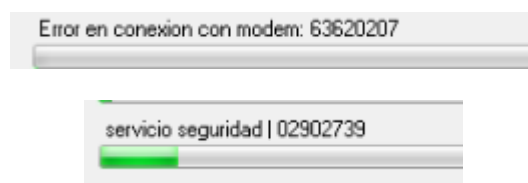


**Fig. 13:** Códigos de Salidas en la solución Planteada. **Fuente:** Los Autores

Este diseño basado en .net como se puede apreciar en la figura anterior, se considera como una buena solución en contra de vicisitudes que puedan afectar el desempeño lógicos y físicos de la red. Gran parte de la solución planteada depende de las tecnologías las cuales se configuran en cada uno de los nodos brindando una dinámica en la comunicación entre pares.

## 6 Conclusiones

Actualmente se tienen muchas tecnologías que permiten ofrecer calidad sobre el servicio prestado, gracias a esto se puede garantizar la información real de cada cliente, privilegios, adaptabilidad a los cambios por parte del cliente etc.

Las redes cumplen en gran parte las problemáticas que se presentan en el día a, así mismo es una herramienta valiosa para administrar los índices por los cuales estos son controlados por la ley.

Los Comercializadoras que deseen migrar a esta tecnología en sus redes lo pueden hacer de la manera menos traumática, esto es debido a que el aplicativo permite un esquema jerárquico respecto a las capas de enlace de datos. De esta manera se garantiza el aprovechamiento de las tecnologías actuales.

Las redes GPRS implementada permiten aplicar ingeniería de tráfico, con lo cual se garantiza que la red pase de ser un simple elemento para transportar paquetes a una red versátil y adaptable.

Para los clientes las migraciones de sus servicios a una red de transporte de información son transparente, se percibe el cambio en la calidad de servicio esto es, debido a que la tecnología proporciona una conmutación en base a etiquetas, motivo por el cual no se ve la claridad de la información y precisión con las tramas de red, ofreciendo un transporte rápido y eficiente.

## 7 Recomendaciones

Las Comercializadoras que quieran migrar o implementar el aplicativo en sus redes eléctricas deben tener en cuenta los siguientes:

- Tener claro los requerimientos: Cada empresa debe verificar la alcanzabilidad y estrategia de negocio que está ofreciendo en el mercado actualmente, una vez teniendo esto claro se debe verificar si la implementación es una opción viable como solución para sus requerimientos.

- Comprender en profundidad los requerimientos de la red: Cada empresa debe determinar el alcance del negocio la cual está determinada por el comportamiento actual del mercado (red telefónica).
- Personal capacitado: Deben contar con el personal capacitado para operar dichas redes de manera correcta, con el fin de sacar el máximo provecho a todos los beneficios que ofrecen este tipo de soluciones, cabe resaltar que es extenso lo que hace que el personal tenga que estar en constante capacitación y actualizaciones.
- Proyección a futuro: Debido a que el mundo de las telecomunicaciones es versátil, las empresas deben adaptarse para sobrevivir en el mercado, el aplicativo es una excelente opción y permite extender el portafolio de servicios de empresa.

## Referencias

- [1] M. Tuballaa y M. Abundob, «Volume 59, June 2016, Pages 710-725.» *A review of the development of Smart Grid technologies*, p.  
<https://usc.elogim.com:2119/science/article/pii/S1364032116000393>, 22 January 2016..
- [2] B. Fanga, X. Yina, Y. Tana, C. Li, Y. Gao y J. Li, «The contributions of cloud technologies to smart grid.» ScienceDirect, p.  
<https://usc.elogim.com:2119/science/article/pii/S1364032116000629>, 30 January 2016..
- [3] P. D. Diamantoulakis, V. M. Kapinas y G. K. Karagiannidis, «Big Data Analytics for Dynamic Energy Management in Smart Grids.» ScienceDirect, p.  
<https://usc.elogim.com:2119/science/article/pii/S2214579615000283>, online 28 April 2015.
- [4] R. Hafen, T. Gibson, K. Kleesevan Dam y T. Critchlow, «Chapter 1 - Power Grid Data Analysis with R and Hadoop.» ScienceDirect, p.  
<https://usc.elogim.com:2119/science/article/pii/B9780124115118000013>, 5 December 2013..
- [5] S. R, B. G. H.B, S. K. S, P. Poornachandran y S. K.P., «Apache Spark a Big Data Analytics Platform for Smart Grid.» ScienceDirect, p.  
<https://www.sciencedirect.com/science/article/pii/S2212017315003138>, 17 November 2015..
- [6] A. Silva Ferreira, C. Oliveira Fontes, C. Mattos, T. Cavalcante, J. Eduardo y M. S., «Pattern recognition as a tool to support decision making in the management of the electric sector. Part II: A new method based on clustering of multivariate time series.» ScienceDirect, p.  
<https://usc.elogim.com:2119/science/article/pii/S0142061514007285#!>, 27 December 2014.
- [7] G. Chicco, . R. Napoli, F. Piglion y P. Postolache, «Load pattern-based classification of electricity customers.» IEEE XPLORE, p.

- <https://ieeexplore.ieee.org/abstract/document/1295037/authors#authors>, 2 May 2004.
- [8] M. Halkidi y M. Vazirgiannis, «A density-based cluster validity approach using multi-representatives» ScienceDirect, p.  
<https://usc.elogim.com:2119/science/article/pii/S0167865508000020>, 12 January 2008..
- [9] D. Arturo , G. Begovich y R. R. Meza, «Equipo biomédico con telemetría diseñado para las áreas rurales.» Científica, vol. 10, núm. 4, p.  
<https://www.redalyc.org/articulo.oa?id=61410405>, Científica 2006, 10 (4).
- [10] J. Salido, A. Lillo, Ó. Déniz y M. Bueno, «CtrWeb: Una herramienta de programación para telecontrol de sistemas físicos educativos.» ScienceDirect, p.  
<https://usc.elogim.com:2119/science/article/pii/S1697791211700115>, 12 November 2011..
- [11] . W. Figueredo y . L. E. Aparicio Pico, «Estructura de datos XTCE en sistemas CubeSat/XTCE Data Structure in CubeSat Systems/Estrutura de dados XTCE em sistemas Cubesat.» Revista Científica(Issue 40), p.  
<https://go.gale.com/ps/i.do?id=GALE%7CA649853616&sid=googleScholar&v=2.1&it=r&linkaccess=abs&issn=01242253&p=IFME&sw=w&userGroupName=anon%7E854d2cb,Jan-April 2021> .
- [12] S. V. Hurtado Gil , «UML-based Scheme for Software Architecture Representations.» S&T Sistema y Telemedida, p.  
[https://webcache.icesi.edu.co/revistas/index.php/sistemas\\_telematica/article/view/918,2006-07-28](https://webcache.icesi.edu.co/revistas/index.php/sistemas_telematica/article/view/918,2006-07-28).
- [13] F. Carrera, «seguridad informática Política INFOSEC Nacional.» p.  
[https://books.google.es/books?hl=es&lr=&id=cQk\\_Ms6MUfEC&oi=fnd&pg=PA9&dq=protocolos+de+seguridad+inform%C3%A1tica&ots=Z16k9PvBzK&sig=qtk5CUYX4TRA1BSiTjGcbLCRSQ#v=onepage&q=protocolos%20de%20seguridad%20inform%C3%A1tica&f=false, \(Junio de 2003\).](https://books.google.es/books?hl=es&lr=&id=cQk_Ms6MUfEC&oi=fnd&pg=PA9&dq=protocolos+de+seguridad+inform%C3%A1tica&ots=Z16k9PvBzK&sig=qtk5CUYX4TRA1BSiTjGcbLCRSQ#v=onepage&q=protocolos%20de%20seguridad%20inform%C3%A1tica&f=false, (Junio de 2003).) .
- [14] J. R. Arana , L. Villa y O. Polanco , «implementación del control de acceso a la red mediante los protocolos de autenticación, autorización y auditoría.» univalle, p.  
[https://revistaingenieria.univalle.edu.co/index.php/ingenieria\\_y\\_competitividad/article/view/2626,2013-01-08](https://revistaingenieria.univalle.edu.co/index.php/ingenieria_y_competitividad/article/view/2626,2013-01-08).
- [15] F. Biscarri, I. Monedero, A. García y J. Ignaci, «Electricity clustering framework for automatic classification of customer loads.» Sciencedirect, p.  
<https://usc.elogim.com:2119/science/article/pii/S095741741730372X?via%3Dihub#bib0014,23 May 2017>.
- [16] A. Trejo Nieto, «CRECIMIENTO ECONÓMICO E INDUSTRIALIZACIÓN EN LA AGENDA 2030: PERSPECTIVAS PARA MÉXICOECONOMIC GROWTH AND INDUSTRIALIZATION ON THE 2030 AGENDA: PROSPECTS FOR MEXICOLA CROISSANCE ÉCONOMIQUE ET INDUSTRIALISATION DANS L'AGENDA 2030: PERSPECTIVES POUR LE MEXIQ.» ScienceDirect, p.

<https://usc.elogim.com:2119/science/article/pii/S0301703617300056>, 25 January 2017.

- [17] R. Cazali y R. Antonio, «Desarrollo de una aplicación de monitoreo de routers 3G en sistemas de telemedida, para su gestión y mantenimiento,» Universidad de San Carlos de Guatemala, p. <http://www.repositorio.usac.edu.gt/7015/>, 2017.
- [18] C. C. Cordoba Poveda, D. A. Barbosa Cortes y D. L. Castañeda Tibaquira, « Sistema de telemetría para medición de elevaciones y depresiones,» p. [https://www.academia.edu/40583201/Sistema\\_de\\_telemetr%C3%ADa\\_para\\_medici%C3%B3n\\_de\\_elevaciones\\_y\\_depresiones](https://www.academia.edu/40583201/Sistema_de_telemetr%C3%ADa_para_medici%C3%B3n_de_elevaciones_y_depresiones), 03/01/2018.
- [19] M. H. Quishpe P., «Telemetría o telectura para los medidores de agua potable en el Centro de (DMQ),» p. <https://repositorio.iaen.edu.ec/handle/24000/215>, mar-2008.
- [20] H. Jame y A. Sanchez, «Lecturas de medición de agua por telemetría y su Trasmisión inalámbrica en Zipaquirá,» p. <https://repository.unimilitar.edu.co/handle/10654/20935>, 23 de noviembre de 2018.
- [21] A. Olaya, H. D. Bohórquez y A. R. Barrios, «CardioResyncApp: Un aplicativo móvil para recolectar datos de investigación en Cardiología» ScienceDirect, p. <https://usc.elogim.com:2119/science/article/pii/S0120563320300474>, 10 September 2020.
- [22] S. Quincozes, E. Tubino y J. Kazienko, «MQTT Protocol: Fundamentals, Tools and FutureDirections,» IEEE, p. <https://latam.ieceer9.org/index.php/transactions/article/view/211/286>, SEPTEMBER 2019.
- [23] G. J. Araque y R. Barba, «Unidades de Medición Fasorial - PMU,» Revista Técnica "energía", Edición No. 6, p. <http://revistaenergia.cenace.gob.ec/index.php/cenace/article/view/227>, 2010-01-31.
- [24] L. Bolivar, L. Guerrero , F. G y & Polanco,, Diseño e implementación de una red IPv6 para transición eficiente desde IPv4., Ingeniería y Competividad, (Vol. 14, Issue 2), (2012).
- [25] G. P. Arevalo y J. L. Rodriguez, «Implementacion de un sistema de supervision y monitorizacion del consumo de energia electrica y agua potable,» Universidad Politecnica, pp. <https://dspace.ups.edu.ec/bitstream/123456789/12676/1/UPS-CT006492.pdf>, Julio 2016.

## Cooling effect of urban green infrastructures by remote sensing data: case study in 7 cities of the northern hemisphere

P. Andrés-Anaya<sup>1</sup>[0000-0001-7708-3260], S. del Pozo<sup>1</sup>[0000-0003-4869-3742], M. Sánchez-Aparicio<sup>1</sup>[0000-0002-7931-9561], E. González-González<sup>1</sup>[0000-0002-8025-2464], J. Martín-Jiménez<sup>1</sup>[0000-0003-4383-9386] and S. Lagüela<sup>1</sup>[0000-0002-9427-3864]

<sup>1</sup> University of Salamanca, Ávila 05003, Spain  
70265257g@usal.es

**Abstract.** Urban areas around the world are expanding at high speed, which implies a transformation of the landscape and the climate of cities that alters all population. One of the major problems related to mass urbanization is the appearance of the Urban Heat Island (UHI) effect, which is characterized mainly by the accumulation of heat during daytime, due to the artificial construction materials in the environment, and its emission at nighttime. Therefore, this work aims to study the behaviour of different surfaces in 7 cities of the North hemisphere. The objective is to demonstrate the importance of the implementation of Urban green covers, due to its cooling effect in reducing the Land Surface Temperature (LST). It has been concluded that the season is a determining factor, with Summer being the one with the greatest variation of LST in the green covers. On the other hand, results shown that latitude and the type of green spaces influence the variation of LST, with large green spaces being more decisive for cooling than urban areas with small green spaces, such as Las Vegas with the use of green zones without obstacles. This last difference, in the type of green cover, is decisive to address more in-depth the mitigation of heat: daytime, with extensive areas of vegetation such as parks, or nighttime, with the use of small green cover such as grass and green roofs.

**Keywords:** Urban green covers, land covers, Land Surface Temperature, UHI, Local Climate Zones

### 1 Introduction

The playful variability, the wide labour supply and the different residential options make large cities in developing countries the perfect locations for hundreds of people to decide to live in them. This increase in the population in urban nuclei causes a continuous growing urbanization [1], resulting in numerous problems such as the increase in the Land Surface Temperature (LST hereinafter) [2], the increase in air temperature [3], the presence of air and [4] [5] light pollution [6], and the loss of forest mass [7]. All these inconveniences can lead to short and long-term health problems for the population [8], such as respiratory, cardiovascular, or mental health problems.

The phenomenon derived from the increase in surface and air temperatures is known as Urban Heat Island (UHI hereinafter), which refers to the urban microclimate with higher soil and air temperatures than rural areas [9]. The effect of UHI is noticeable at night, when the wide difference in daytime / nighttime temperatures can be measured. There are different circumstances for which UHIs are more notable: urban planning and unfavourable construction elements, such as construction materials with high radiation absorption and low albedo [10]; the lack of green surfaces [11]; or adverse weather conditions, such as lack of wind or high global radiation during the day [12]. Numerous studies have shown that the use of green roofs in cities mitigates the UHI effect [13] [14] (Fig. 1), even forming the Urban Cool Island (UCI) [15]. Despite the numerous studies that demonstrate the mitigation of UHI by the use of green areas, there is still much to be quantified and varied depending on the type of plant cover (type of plant species, phenological status, height, distribution, etc.) and urban environment (type of construction material, urban map, etc.). The most similar studies in this regard have been carried out using the Local Climate Zones (LCZ) [16]. This type of study is very important and presents high variability, since not all cities have the same climatic or urban characteristics. To carry out such a wide and heterogeneous study, remote sensing methodologies are used, which allow multitemporal studies to be carried out in different geographical areas in a very short time and without the need for displacement.

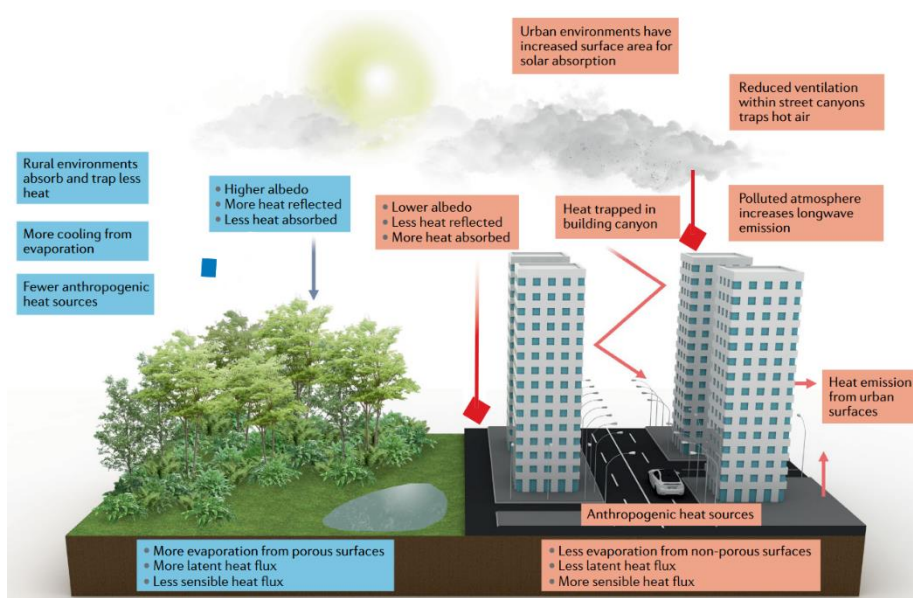


Fig. 1. Cooling and warming mechanisms contributing to urban heat islands [14].

This paper aims to carry out a small-scale study in different cities of the Northern Hemisphere, estimating the day-night temperature differences of different green areas within the city and its peripheral urban area. Specifically, the study has been carried out

through the analysis of LST, which is a parameter proportional to air temperature [17]. Images from the Landsat 8 satellites (OLI and TIRS sensors) and Terra (ASTER sensor) have been used.

## 2 Materials and Methods

### 2.1 Study cases

The present study is based on 7 representative big cities of the Northern Hemisphere (Fig. 2), spread over different continents and in different seasons of the year, depending on the availability of simultaneous satellite images without cloud cover (Table 1). Regarding the latitude and altitudes of the selected cities: Guadalajara Mx. is the southernmost city and with the highest altitude (1566 m), Indore is a city located to the south with an altitude (550 m) that is around the average of those analysed (515 m), Wuhan and Paris are the lowest (37 and 35 m, respectively) and are located at an intermediate latitude in the case of Wuhan and further north in the case of Paris. Las Vegas and Madrid are located at a latitude that is around the average of those analysed and at an altitude that is also around the average (610 and 820 m high, respectively). Finally, Strasbourg is the most northern city analysed and has an altitude of 140 m.



**Fig. 2.** Location of the 7 study cities: Strasbourg (France), Guadalajara (Mexico), Indore (India), Las Vegas (USA), Madrid (Spain), Paris (France) and Wuhan (China).

**Table 1.** Cities, coordinates and dates of study. \* Decimal degrees World Geodetic System 1984 (WGS 84)

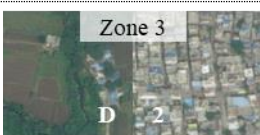
City - Country	Latitude*	Longitude*	Date Terra - Landsat8	Season
Paris - France	48,858	2,320	09/07/2019 - 04/07/2019	Summer
Strasbourg - France	48,584	7,750	22/06/2018 - 26/06/2018	Summer
Madrid - Spain	40,416	-3,703	19/06/2020 - 18/06/2020	Spring

			02/09/2018 - 02/09/2018	Summer
Las Vegas - USA	36,167	-115,148	08/11/2019 - 08/11/2019	Autumn
			08/07/2021 - 08/07/2021	Summer
Wuhan - China	30,595	114,299	03/11/2017 - 30/10/2017	Autumn
Indore - India	22,720	75,868	26/04/2015 - 17/04/2015	Spring
			12/10/2015 - 10/10/2015	Autumn
Guadalajara - Mexico	20,672	-103,338	26/05/2018 - 23/05/2018	Spring
			13/02/2019 - 19/02/2019	Winter

For each city, 4 different vegetation zones and their corresponding peripheral urban zones have been studied, making a total of 56 study zones (Table 2). Each study area corresponds to an area of 3,24 ha within the urban nucleus.

**Table 2.** Study areas within the selected cities and distances between them. Each area has an indication of the LCZ where it is classified, according to Table 4.

City - Country	Zones and LCZ	Distance (m)	Zones and LCZ	Distance (m)
Paris - France	Zone 1 D 5	468	Zone 3 A 4	818
	Zone 2 A 5	467	Zone 4 A 8	428
Strasbourg - France	Zone 1 B 2	375	Zone 3 B 4	446
	Zone 2 D 2	358	Zone 4 B 4	515
Madrid - Spain	Zone 1 A 2	1107	Zone 3 A 2	856
	Zone 2 B 4	582	Zone 4 A 5	587

Las Vegas - USA		637		655
		819		557
		2586		525
		1003		1671
Indore - India		531		572
		452		733
		570		640
		800		460

## 2.2 Materials

For the daytime LST (LSTd) calculation, in this project, 4 products from two NASA satellites are used, while the nighttime LST (LSTn) calculation is already done by NASA through a Tier 2 product. These final materials will be further analysed and compared to their respective Local Climate Zones (LCZ).

**Bands 4, 5 and 10 from Landsat 8.** For the calculation of LSTd, the two sensors on board NASA's Landsat 8 satellite have been used: the Operational Land Imager (OLI) sensor and the Thermal Infrared Sensor (TIRS) [18]. The bands used for this project are mentioned in Table 3. Bands 4 and 5 are used for the calculation of the NDVI while band 10 provides the necessary thermal information for the LST product.

**Table 3.** Landsat 8 level 1 products for LSTd calculation.

Bands	Wavelength (µm)	Spatial Resolution (m)	Sensor
Band 4 - RED	0,64-0,67	30	OLI
Band 5 - NIR	0,85-0,88	30	
Band 10 - TIRS	10,60-11,19	100 (resamplet at 30)	TIRS

**MOD05\_L2.** The Moderate Resolution Imaging Spectroradiometer (MODIS) is found aboard NASA's Terra and Aqua satellites. This sensor offers level 2 products already processed, such as the image MOD05\_L2 from the Terra satellite, corresponding to the image of total precipitable water vapor [19]. This product is necessary for the calculation of LSTd, it has a spatial resolution of 1km and a temporal resolution of 1 day.

**AST08.** The Advanced Spaceborne Thermal Emission and Reflection Radiometer (ASTER) is an instrument on board NASA's Terra satellite. Like MODIS, it offers level 2 products such as AST08, which corresponds to the Surface Kinetic Temperature product [20]. It has a spatial resolution of 90m and a temporal resolution on demand, hence the low number of images available.

**Local Climate Zones (LCZ).** LCZs are a classification used for zoning urban morphology for various applications, among which is the study of UHI [16]. The LCZs present 17 standard classifications shown in Table 4, which describe different urban classes and land covers [21] that present characteristics or properties that are homogeneous among them, such as LST or air temperature. This classification helps to explain the different effects of UHI within the same city.

**Table 4.** Description of LCZ as defined by [21].

Built series	Land cover series
LCZ 1: Compact high-rise	LCZ A: Dense trees
LCZ 2: Compact mid-rise	LCZ B: Scattered trees
LCZ 3: Compact low-rise	LCZ C: Bush, scrub
LCZ 4: Open high-rise	LCZ D: Low plants
LCZ 5: Open mid-rise	LCZ E: Bare rock or paved
LCZ 6: Open low-rise	LCZ F: Bare soil or sand
LCZ 7: Lightweight low-rise	LCZ G: Water
LCZ 8: Large low-rise	

LCZ 9: Sparsely built  
 LCZ 10: Heavy industry

---

### 2.3 Methods

The LST calculation, based on satellite data, differs between LSTd and LSTn because there is a lack of data from the optical spectrum at night due to the lack of solar radiation. The methodologies followed for both computations are explained below.

**LSTd.** The methodology used in the calculation of LSTd through satellite data is the one used in [22]. This follows a combined strategy of single-channel methodologies (Eq. 1) taking into account the levels of thermal radiation and the product MOD05\_L2 for its classification.

$$LST = \gamma[\varepsilon^{-1}(\psi_1 \cdot L_{sensor\ i} + \psi_2) + \psi_3] + \delta \quad (1)$$

Through this combined strategy from Landsat8 data, an LSTd product is obtained with a spatial resolution of 30m and a temporal resolution of 16 days.

**LSTn.** As mentioned in the materials section, in the case of LSTn, the use of the direct level 2 satellite product AST\_08 [19] is chosen. This product is obtained from five TIR bands with which it uses the Temperature / Emissivity Separation (TES) algorithm. This algorithm is based on estimating the emissivity of the TIR bands using the Normalized Emissivity Method (NEM).

## 3 Results

To quantify the implication that green infrastructures have in mitigating the urban heat island effect, the daytime and nighttime surface temperatures (LSTd and LSTn) of nearby green and built-up areas were analysed for the sample of the 7 chosen cities. Specifically, 4 urban green infrastructures and 4 urban built-up areas per city were analysed as represented in Fig. 3. Therefore, a total of 28 green areas and 28 built-up areas with different LCZ typologies were analysed.

The 3,24 ha evaluated per zone correspond to an area of interest of 180 m x 180 m. Since the LSTd and LSTn satellite products have different spatial resolutions (30 m and 90 m respectively), the LSTd will be evaluated based on the average of 36 LST values and the LSTn based on the average of 4 LST values, 6x6 px in the first case and 2x2 px in the second, (Fig. 3).

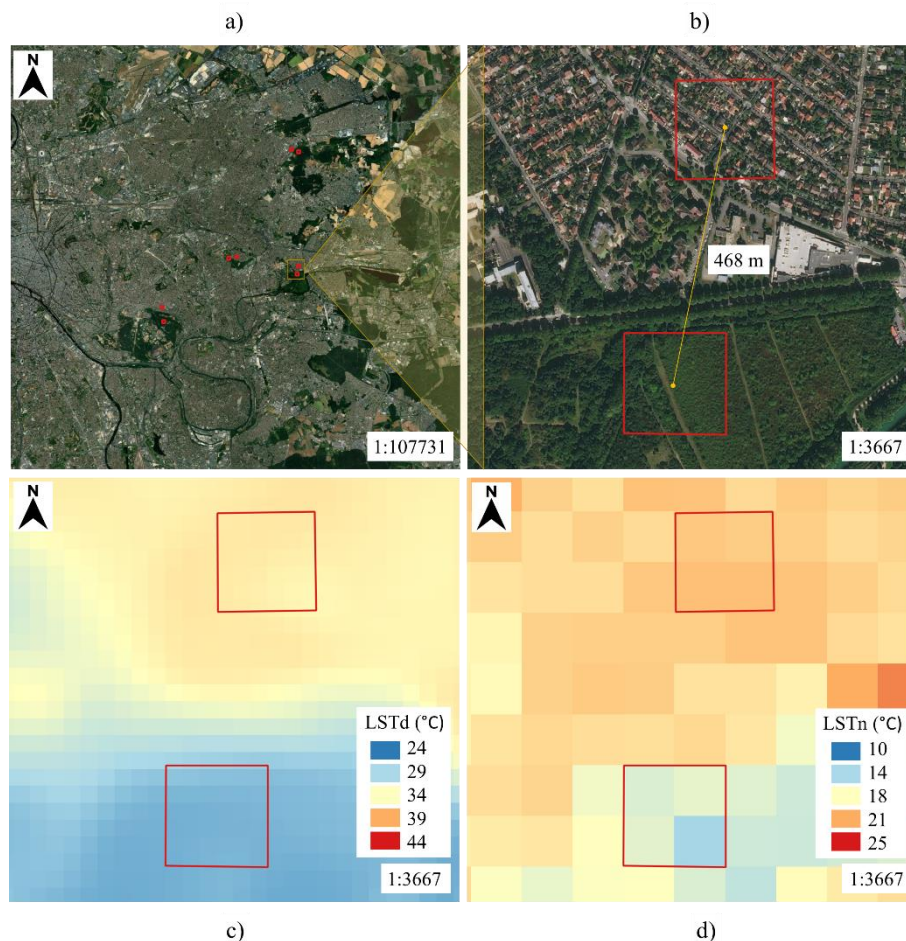


**Fig. 3.** Representation of the analysed areas by city showing: a) the proximity between the vegetation and built-up per area of interest, b) the RGB image (from google maps), c) the LSTd and d) the LSTn products.

Table 5 collects the set of LSTd and LSTn data obtained from the 8 areas analysed per city (4 vegetation areas and 4 built-up areas) for the specified seasons of the year.

**Table 5.** LSTd and LSTn data for the analysed areas and cities specifying the date of the satellite products used. V\*= urban vegetation area, B\*=urban built-up area.

City	Area	LSTn (°C)			Date	LSTd (°C)			Date
		V*	B*	$\Delta LST_{V-B}$		V*	B*	$\Delta LST_{V-B}$	
Paris	1	15,55	20,20	4,65	09/07/2019	27,17	35,12	7,95	04/07/2019
	2	17,53	19,58	2,05		29,69	34,97	5,28	
	3	19,18	21,85	2,67		27,00	36,10	9,10	
	4	16,60	21,15	4,55		25,90	40,40	14,50	

Strasbourg	1	14,55	17,48	2,93	22/06/2018	29,19	35,09	5,90	26/06/2018
	2	12,63	16,03	3,40		27,09	35,63	8,54	
	3	11,30	17,83	6,53		29,05	34,22	5,17	
	4	9,90	17,48	7,58		28,24	32,60	4,36	
Madrid	1	21,83	23,93	2,10	19/06/2020	27,42	37,81	10,39	18/06/2020
	2	21,33	24,80	3,47		28,80	36,48	7,68	
	3	21,65	23,48	1,83		29,4	38,19	8,79	
	4	21,43	23,7	2,27		28,04	35,82	7,78	
Las Vegas	1	20,80	26,53	5,73	02/09/2018	45,58	49,76	4,18	02/09/2018
	2	20,98	28,00	7,02		38,26	48,69	10,43	
	3	20,93	28,7	7,77		40,85	46,64	5,79	
	4	22,85	29,23	6,38		37,79	48,94	11,15	
	1	28,19	36,1	7,91	08/07/2021	48,25	62,68	14,43	08/07/2021
	2	28,51	36,25	7,74		49,66	61,57	11,91	
	3	28,76	36,91	8,15		50,03	59,49	9,46	
	4	29,98	38,19	8,21		47,87	63,71	15,84	
1	8,12	9,87	1,75	08/11/2019	25,5	29,89	4,39	08/11/2019	
2	8,85	12,52	3,67		24,32	28,34	4,02		
3	7,70	10,52	2,82		27,20	26,83	0,37		
4	8,77	11,6	2,83		25,22	28,23	3,01		
Wuhan	1	15,26	16,66	1,40	03/11/2017	17,59	20,61	3,02	30/10/2017
	2	15,41	16,84	1,43		17,17	19,64	2,47	
	3	14,35	16,50	2,15		19,43	18,51	0,92	
	4	15,09	16,53	1,44		15,88	20,69	4,81	
Indore	1	28,77	30,83	2,06	26/04/2015	47,34	49,80	2,46	17/04/2015
	2	28,85	30,43	1,58		46,10	50,65	4,55	
	3	26,18	29,81	3,63		46,04	50,38	4,34	
	4	27,00	30,03	3,03		42,41	46,81	4,40	
	1	24,72	27,57	2,85	12/10/2015	40,08	42,94	2,86	10/10/2015
	2	25,27	26,35	1,08		37,29	43,43	6,14	
	3	23,37	26,72	3,35		39,55	43,56	4,01	
	4	24,15	25,67	1,52		37,82	43,03	5,21	
Guadalajara Mexico	1	21,48	27,14	5,66	26/05/2018	33,20	43,50	10,30	23/05/2018
	2	22,55	25,42	2,87		40,29	45,55	5,26	
	3	20,00	24,10	4,10		41,73	45,47	3,74	
	4	23,44	24,19	0,75		39,53	44,48	4,95	
Guadalajara Mexico	1	15,4	18,45	3,05	13/02/2019	26,52	32,57	6,05	19/02/2019
	2	14,8	18,02	3,22		30,83	33,78	2,95	
	3	12,62	16,77	4,15		38,38	32,84	5,54	
	4	15,59	18,09	2,50		32,79	33,71	0,92	

Even though the same LCZ typologies had not been studied for each city, for vegetation and built-up areas respectively, the low standard deviation values between the LSTd and LSTn values respectively, allow to average the 4 LSTd and LSTn values per type of coverage (vegetal and built-up) by city and season in order to perform the subsequent analysis. Results are shown in Table 6 and 7.

**Table 6.** Average daytime LST by surface coverage (whether vegetation or built-up), city and season of the year analyzed. V\*= urban vegetation area, B\*=urban built-up area.

LSTd (°C)							
City	Season	LSTd V*	Std LSTd V*	LSTd B*	Std LSTd B*	$\Delta$ LST <sub>V-B</sub>	Std
Paris	Summer	27,4	1,6	36,6	2,5	9,21	3,8
Strasbourg	Summer	28,4	1,0	34,4	1,3	6,0	1,8
Madrid	Spring	28,4	0,9	37,1	1,1	8,7	1,3
	Summer	49,0	1,1	61,9	1,8	12,9	2,8
Las Vegas	Summer	40,6	3,6	48,5	1,3	7,9	3,4
	Autumn	25,6	1,2	28,3	1,3	2,9	1,8
Wuhan	Autumn	17,5	1,5	19,9	1,0	2,8	1,6
Indore	Spring	45,5	2,1	49,4	1,8	3,9	1,0
	Autumn	38,7	1,3	43,2	0,3	4,6	1,4
Guadalajara Mx	Spring	38,7	3,8	44,8	1,0	6,1	2,9
	Winter	32,1	4,9	33,2	0,6	3,9	2,4

**Table 7.** Average nighttime LST by surface coverage (whether vegetation or built-up), city and season of the year analyzed. V\*= urban vegetation area, B\*=urban built-up area.

LSTn (°C)							
City	Season	LSTn V*	Std LSTn V*	LSTn B*	Std LSTn B*	$\Delta$ LST <sub>V-B</sub>	Std
Paris	Summer	17,2	1,5	20,7	1,0	3,5	1,3
Strasbourg	Summer	12,4	1,9	17,2	0,8	5,1	2,3
Madrid	Spring	21,5	0,2	24,0	0,6	2,4	0,7
	Summer	28,9	0,8	36,9	1,0	8,0	0,2
Las Vegas	Summer	21,4	1,0	28,1	1,2	6,7	0,9
	Autumn	8,4	0,5	11,1	1,2	2,8	0,8
Wuhan	Autumn	15,0	0,5	16,6	0,2	1,6	0,4
Indore	Spring	27,7	1,3	30,3	0,5	2,6	0,9
	Autumn	24,4	0,8	26,6	0,8	2,2	1,1
Guadalajara Mx	Spring	21,9	1,5	25,2	1,4	3,4	2,1
	Winter	14,6	1,4	17,8	0,7	3,2	0,7

After analysing Tables 6 and 7, it can be highlighted that the mean variation of LST between vegetation and built-up urban covers for the cities analysed was 3,8°C (standard deviation of 2,0°C) when comparing them at nighttime ( $\Delta LST_{nV-B}$ ), and 6,3°C (standard deviation of 3,1°C) when comparing them at daytime ( $\Delta LST_{dV-B}$ ).

The city with the greatest thermal variation between vegetation and built-up urban covers both at daytime and nighttime was Las Vegas, with 7,9°C and 5,8°C, respectively. This may be due to the influence that solar radiation has in lower latitudes as well as the influence that the urban morphology has on heat trapping.

Analysing the thermal behaviour by season, it was observed that the greatest LST variation between vegetation and built-up urban covers, both day and night, occurred in summer, with an average of 5,8°C at night and 9,0°C during the day. In spring, the  $\Delta LST_{nV-B}$  and  $\Delta LST_{dV-B}$  was 2,8°C and 6,2°C respectively. Regarding autumn, the  $\Delta LST_{nV-B}$  and  $\Delta LST_{dV-B}$  was 2,2°C and 3,4°C, without being possible to analyze winter because only Guadalajara-Mexico was studied for this season.

## 4 Conclusions

The quantitative analysis of the implication that vegetation cover has in mitigating the urban heat island effect (UHI) has been possible thanks to the availability of Earth Observation data. Specifically, both day and night land surface temperatures (LST) have been analysed from 7 large cities of the northern hemisphere: Paris, Strasbourg, Madrid, Las Vegas, Wuhan, Indore, and Guadalajara (Mexico). For this, satellite data offered by the NASA have been used. Specifically, LST images at night (already processed from ASTER) and other kind of satellite data (water vapor, and images of the red, near infrared and thermal infrared bands) that allow obtaining images with daytime LST values have been analysed.

Four urban vegetation areas and four urban built-up areas were analysed per city. Therefore, the thermal behaviour of a total of 28 urban vegetation areas and 28 urban built-up areas were analysed for different seasons.

The results show that there is a great influence of the vegetation on both the daytime and nighttime temperatures. A LST variation between vegetation and built-up covers of 3,8°C at night (with a standard deviation of 2,0°C) and 6,3°C (with standard deviation of 3,1°C) during the day was obtained as average for the 7 cities.

In addition, it is shown that the LST variation between vegetation and built-up covers depends not only on latitude (due to the way the sun rays strike) but also on the season analysed. The thermal variation becomes more intense in summer, when the vegetation plays a more important role in the attenuation of high temperatures, reaching variations of 5,8°C at night and 9°C during the day by average.

From the LST standard deviation values obtained, it is derived that during the night the LSTs are more homogeneous than during daytime, as was to be expected in the absence of the influence of solar radiation.

It is also concluded that the city with the greatest variation in LSTs between vegetation and built-up covers among the analysed, both at daytime (7,9°C) and nighttime

(5,8°C), was Las Vegas. In this sense, multiple factors such as latitude, urban morphology, and coverage typology (LCZs), among others, may be affecting the temperature. In this case, vegetation covers with LCZ D were analysed, which, due to the absence of obstacles, allows a greater temperature drop than in the case of LCZ A or B.

Although all types of vegetation cover help to mitigate high day and night temperatures, the implication that city parks (LCZ A and B) would have in mitigating UHIs would be more diurnal. On the other hand, the implication that landscaped areas with grass or green roofs (LCZ D) would have in mitigating UHIs would be more diurnal.

## References

1. Aboulnaga, M. M., Elwan, A. F., Elsharouny, M. R.: Climate Change Impacts on Urban Areas and Infrastructure. In *Urban Climate Change Adaptation in Developing Countries*, pp. 49-75. Springer, Cham (2019).
2. Mukherjee, F., Singh, D.: Assessing land use–land cover change and its impact on land surface temperature using LANDSAT data: A comparison of two urban areas in India. *Earth Systems and Environment*, 4(2), 385-407 (2020).
3. Paranunzio, R., Ceola, S., Laio, F., Montanari, A.: Evaluating the effects of urbanization evolution on air temperature trends using nightlight satellite data. *Atmosphere* 10(3), 117 (2019).
4. Mayer, H.: Air pollution in cities. *Atmospheric environment*, 33(24-25), 4029-4037 (1999).
5. European Environment Agency: Air quality in Europe – 2020 report, <https://www.eea.europa.eu/publications/air-quality-in-europe-2020-report>, last accessed 2021/10/04
6. Lamphar, H.: Spatio-temporal association of light pollution and urban sprawl using remote sensing imagery and GIS: A simple method based in Otsu's algorithm. *Journal of Quantitative Spectroscopy and Radiative Transfer*, 251, 107060 (2020).
7. De la Barrera, F., Henríquez, C.: Vegetation cover change in growing urban agglomerations in Chile. *Ecological Indicators*, 81, 265-273 (2017).
8. Santamouris, M.: Recent progress on urban overheating and heat island research. Integrated assessment of the energy, environmental, vulnerability and health impact. Synergies with the global climate change. *Energy and Buildings*, 207, 109482 (2020).
9. Oke, T. R.: The energetic basis of the urban heat island. *Quarterly Journal of the Royal Meteorological Society* 108(455), 1-24 (1982).
10. Taha, H.: Urban climates and heat islands: albedo, evapotranspiration, and anthropogenic heat. *Energy and buildings* 25(2), 99-103 (1997).
11. Tiwari, A., Kumar, P., Kalaiarasan, G., Ottosen, T. B.: The impacts of existing and hypothetical green infrastructure scenarios on urban heat island formation. *Environmental Pollution*, 274, 115898 (2021).
12. Morris, C. J. G., Simmonds, I., Plummer, N.: Quantification of the influences of wind and cloud on the nocturnal urban heat island of a large city. *Journal of Applied Meteorology and Climatology*, 40(2), 169-182 (2001).
13. Heidt, V., Neef, M.: Benefits of urban green space for improving urban climate. In *Ecology, planning, and management of urban forests* (pp. 84-96). Springer, New York, NY (2008).
14. Wong, N. H., Tan, C. L., Kolokotsa, D. D., Takebayashi, H.: Greenery as a mitigation and adaptation strategy to urban heat. *Nature Reviews Earth & Environment*, 2(3), 166-181 (2021).

15. Yang, X., Li, Y., Luo, Z., Chan, P. W.: The urban cool island phenomenon in a high-rise high-density city and its mechanisms. *International Journal of Climatology*, 37(2), 890-904 (2017).
16. Del Pozo, S., Landes, T., Nerry, F., Kastendeuch, P., Najjar, G., Philipps, N., Lagüela, S.: Evaluation of the Seasonal Nighttime Lst-Air Temperature Discrepancies and Their Relation to Local Climate Zones (lcz) in Strasbourg. *ISPRS-International Archives of the Photogrammetry, Remote Sensing and Spatial Information Sciences*, 43, 391-398 (2021).
17. Del Pozo, S., Landes, T., Nerry, F., Kastendeuch, P., Najjar, G., Philipps, N., Lagüela, S.: UHI estimation based on ASTER and MODIS satellite imagery: first results on Strasbourg City, France. *ISPRS-International Archives of the Photogrammetry, Remote Sensing and Spatial Information Sciences*, 43, 799-805 (2020).
18. Roy, D. P., Wulder, M. A., Loveland, T. R., Woodcock, C. E., Allen, R. G., Anderson, M. C., ..., Zhu, Z.: Landsat-8: Science and product vision for terrestrial global change research. *Remote sensing of Environment*, 145, 154-172 (2014).
19. Gao, B., Kaufman, Y. J.: MODIS atmosphere L2 water vapor product. NASA MODIS adaptive processing system, Goddard Space Flight Center, USA (2015).
20. NASA, LP DAAC. ASTER Level 2 Surface Temperature Product. Retrieved from, (2001). [https://doi.org/10.5067/ASTER/AST\\_08.003](https://doi.org/10.5067/ASTER/AST_08.003), last accessed 2021/10/04
21. Cai, M., Ren, C., Xu, Y., Lau, K. K. L., Wang, R.: Investigating the relationship between local climate zone and land surface temperature using an improved WUDAPT methodology—A case study of Yangtze River Delta, China. *Urban Climate*, 24, 485-502 (2018).
22. Sánchez-Aparicio, M., Andrés-Anaya, P., Del Pozo, S., Lagüela, S.: Retrieving Land Surface Temperature from Satellite Imagery with a Novel Combined Strategy. *Remote Sensing*, 12(2), 277 (2020).

## A mathematical model to regulate the density of natural gas based on its composition

Jorge Mírez<sup>[0000-0002-5614-5853]</sup> and Eduardo Calle<sup>[0000-0003-3279-5162]</sup>

<sup>1,2</sup> Universidad Nacional de Ingeniería, Lima, Peru;

<sup>1</sup>jmirez@uni.edu.pe

<sup>2</sup>ecallec@fip.uni.edu.pe

**Abstract.** This paper presents a mathematical model of an automatic system to maintain the constant density of natural gas. This is done by calculating the density of natural gas in the reservoir based on its composition, which is ideally measured online at the outlet of the reservoir. It is assumed that the composition changes over time and the variations in the density of the gas resulting from the change in the composition are studied. To keep the density of natural gas constant, a control system is proposed and implemented, using as a compensator for the density of natural gas, a reservoir whose storage volume is determined under different case studies. This article has the potential to be used in the natural gas industry, as well as in related applications, such as biomass plants used as a source of electrical or thermal energy in the concepts of distributed generation, microgrids or SmartGrids.

**Keywords:** Control, natural gas, biomass.

### 1 Introduction

El gas natural es una fuente primaria de energía del mundo. Natural gas had a remarkable year in 2018, with a 4.6% increase in consumption accounting for nearly half of the increase in global energy demand. Since 2010, 80% of growth has been concentrated in three key regions: the United States, where the shale gas revolution is in full swing; China, where economic expansion and air quality concerns have underpinned rapid growth; and the Middle East, where gas is a gateway to economic diversification from oil. Natural gas continues to outperform coal or oil in both the Stated Policies Scenario (where gas demand grows by over a third) and the Sustainable Development Scenario (where gas demand grows modestly to 2030 before reverting to present levels by 2040). Nevertheless, Natural gas consumption was already falling over the first months of 2020 in major markets even before the Covid-19 pandemic, mainly due to historically mild temperatures in the northern hemisphere. Supply did not adjust to this drop in consumption, resulting in a considerable build-up of gas in storage. Demand was projected to decrease in 2020, with most of the declines in power generation [13].

2

Global biomass electricity capacity expanded 8.5 GW in 2019, the second-highest level of annual additions on record. China accounted for 60% of last year’s new capacity, primarily made up of energy-from-waste projects. The next-largest market, Japan, was one-tenth of the size of the Chinese market Major deployment of biomass power projects is concentrated in relatively few countries, with just ten nations accounting for 90% of new capacity in 2019. Of these, China, Brazil, Japan and the United Kingdom have been the most affected by the pandemic, so potential exists for some project delivery delays. Nevertheless, with forestry activity ongoing and ports operational, widespread supply disruptions of biomass fuels (e.g. wood chips and pellets) for existing projects have not been observed. [14]. A pesar de los embates de la pandemia, se espera que la capacidad nueva de bioenergía se incremente en los próximos años, como se muestra en Fig. 1.

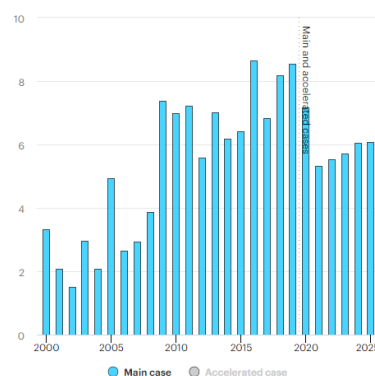


**Fig. 1.** Bioenergy capacity net additions, main and accelerated case, World, 1990-2025 [15].

Renewable power overall needs to continue increasing 7% annually over 2019-30 to meet the Sustainable Development Scenario (SDS) level. However, the growth of renewable electricity generation was lower in 2019 (6.5%) than in 2018 (7%), meaning that stronger deployment of all renewable technologies will be necessary, including hydropower, which represented 60% of global renewable generation in 2019 [16]. Entre las tecnologías prometedoras está la biomasa que ha presentado un incremento a nivel mundial en capacidad instalada desde 9,519 MW en el 2010 a 19,381 MW en el 2019 and has significant potential to boost energy supplies in populous nations with rising demand, such as Brazil, India and China. The biogas can be directly burned for heating or power generation, or it can be converted into oil or gas substitutes [17]. Sin embargo, la producción local de biogás no asegura que el porcentaje de metano sea alto y constante pues va a depender de condiciones medioambientales así como de los materiales que se usen para la producción de biogás. Por lo tanto, en el presente paper se propone: la implementación de una instalación mixta de biogás – gas natural con medida de la composición del biogás producido localmente, para con ello calcular la densidad y poder calorífico, valores que van a alimentar al sistema de control que compensará un decremento en la calidad del biogás mediante la inyección de un por-

centaje de gas natural almacenado en recipientes o como parte de un suministro continuo en tubería. Esta propuesta tiene el potencial de optimizar el uso de biogás y de gas natural, en entornos de producción local de biogás que están en concordancia con las actuales tendencias de microgrids y Smart Grids.

## 2 Mathematical model

### 2.1 Density of natural gas based on its composition

The reservoir energy that drives petroleum fluids towards wells is directly related to the prevailing reservoir pressure. Since both reservoir pressure and temperature control fluid properties, these are discussed first. In fact, hydrocarbon fluid composition, pressure, and temperature determine whether the fluid would initially exist in a single phase (oil or gas) or in two phases (oil with a gas cap). It is common practice to determine the reservoir pressure and temperature at discovery, and to conduct pressure surveys periodically or even continuously at various wells during the life cycle of the reservoir. Most reservoir engineering studies, including reservoir simulation, require knowledge of the reservoir pressure response as a function of time and location during production and shutdown of the wells. A robust pressure monitoring program may readily point to reservoir drive mechanisms, effectiveness of fluid injection, and suspected heterogeneities in the rock, among other factors. Modern reservoir monitoring practices employ downhole sensors that continuously provide a wealth of pressure and rate data [5].

Natural gas is a mixture of  $n$  components  $c_i$  which is extracted from the earth's crust at a reservoir temperature  $T_{res}$  and at a reservoir pressure  $P_{res}$  [1].

The composition of natural gas can be determined using techniques such as gas chromatography [3,4].

Each component has a composition mole fraction  $cmf_i$ , from which its molecular weight can be found for each component  $W_i$ , critical pressure  $p_{c_i}$  and the critical temperature  $T_{c_i}$ . The sum of the  $cmf_i$  of all components of natural gas is equal to 1.

With the after mentioned variables, the molar weight  $M_W$  was calculated by using (1), pseudo-critical pressure  $p_{pc}$  using (2) and the pseudocritical temperature  $T_{pc}$  using (3) [1].

$$M_W = \sum_{i=1}^n W_i \cdot cmf_i \quad (1)$$

$$p_{pc} = \sum_{i=1}^n p_{c_i} \cdot cmf_i \quad (2)$$

4

$$T_{pc} = \sum_{i=1}^n T_{c_i} \cdot cmf_i \quad (3)$$

With molar weight  $M_W$ , specific gravity  $\gamma_g$  was calculated by using (4) [1].

$$\gamma_g = \frac{M_W}{28.97} \quad (4)$$

From pseudocritical pressure  $p_{pc}$ , pseudocritical temperature  $T_{pc}$ , reservoir temperature  $T_{res}$  and the reservoir pressure  $P_{res}$ ; pseudo-relative pressure  $p_{pr}$  and the pseudorelative temperature  $T_{pr}$  was calculated by using (5) and (6) respectively [1].

$$p_{pr} = \frac{p_{res}}{p_{pc}} \quad (5)$$

$$T_{pr} = \frac{T_{res} + 460}{T_{pc}} \quad (6)$$

The Dranchuk and Abou-Kassem equation of state gives por result for  $T_{pr}=1.0$  and  $p_{pr} > 1.0$ . The form of Dranchuk and Abou-Kassem equation of state by determination of gas deviation factor  $z$  is represented en (7) [1]

$$z = 1 + c_1(T_{pr})\rho_r + c_2(T_{pr})\rho_r^2 - c_3(T_{pr})\rho_r^5 + c_4(\rho_r, T_{pr}) \quad (7)$$

$$\rho_r = 0.27 \cdot \frac{p_{pr}}{z \cdot T_{pr}} \quad (8)$$

$$c_1(T_{pr}) = A_1 + \frac{A_2}{T_{pr}} + \frac{A_3}{T_{pr}^3} + \frac{A_4}{T_{pr}^4} + \frac{A_5}{T_{pr}^5} \quad (9)$$

$$c_2(T_{pr}) = A_6 + \frac{A_7}{T_{pr}} + \frac{A_8}{T_{pr}^2} \quad (10)$$

$$c_3(T_{pr}) = A_9 \left( \frac{A_7}{T_{pr}} + \frac{A_8}{T_{pr}^2} \right) \quad (11)$$

$$c_4(\rho_r, T_{pr}) = A_{10} \left( 1 + A_{11} \cdot \rho_r^2 \right) \left( \frac{\rho_r^2}{T_{pr}^3} \right) \cdot \exp(-A_{11} \cdot \rho_r^2) \quad (12)$$

where the constants  $A_1 - A_{11}$  are as:  $A_1 = 0.3265$ ;  $A_2 = -1.0700$ ;  $A_3 = -0.5339$ ;  $A_4 = 0.01569$ ;  $A_5 = -0.05165$ ;  $A_6 = 0.5475$ ;  $A_7 = -0.7361$ ;  $A_8 = 0.1844$ ;  $A_9 = 0.1056$ ;  $A_{10} = 0.6134$  and  $A_{11} = 0.7210$ .

Finally, the density of the reservoir gas  $\rho_g$  was calculated using by (13) where  $R'$  is the gas constant equal to 10.73 [1].

$$\rho_g = \frac{28.97 \cdot \gamma_g \cdot p_{res}}{z \cdot R' \cdot T_{res}} \tag{13}$$

To calculate  $z$ , in this work we will use the Matlab [2] solve command from MathWorks Inc. to solve equation (7) using the algorithm shown in Fig. 2.

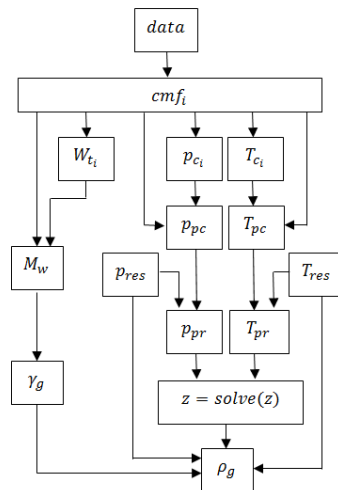


Fig. 2. Sequence of calculation to obtain reservoir gas density from collected composition data.

The algorithm shown in Fig. 2 has been implemented in Matlab [2] software.

### 2.2 Control system for constant density

Control systems in a multidisciplinary field covering many areas of engineering and sciences. Control systems exist in many systems of engineering, sciences, and in human body. Control means to regulate, direct, command, or govern. A system is a collection, set, or arrangement of elements (subsystems). A control system is an interconnection of components forming a system configuration that will provide a desired system response. Hence, a control system is an arrangement of physical components connected or related in such a manner as to command, regulate, direct, or govern itself or another system [6]

In Fig. 3 the control system is shown, the objective of which is to keep the reservoir (or source) density constant at the output of the control system  $\rho_{go}$ . For this, the measurement of the reservoir (or source) density is carried out at the input of the control system  $\rho_{gi}$  and  $\rho_{go}$ . The readings obtained are fed back to the System Control Controller (SCC) that processes the information and acts on the valve of the reservoir gas line  $v_g$  and on the valve of the Natural Gas Deposit (NGD)  $v_d$  that contains a natural gas of constant composition over time and that is mixed with the natural gas of

6

the reservoir to obtain a natural gas of constant density. Inlet mass flow  $m_{gi}$ , exit  $m_{go}$  and that is dispatched from the warehouse  $m_d$  of the control system, will be analyzed in Chapter III.

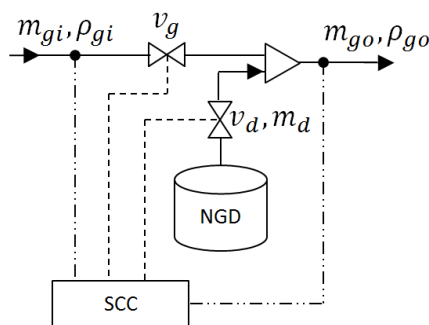


**Fig. 3.** Control system to obtain constant density of the gas to study.

The feedback (as the detailed in Fig. 3) is using to decrease the sensitivity of the system to plant variations, enable adjustment of the system transient response, reject disturbances, and reduce steady-state tracking errors [7].

For the calculation of natural gas volume  $V_d$  coming out of the tank NGD, has been considered to develop the calculations for a unit of volume and with the same conditions of the incoming gas to be regulated, using the Ec. (14) where  $\rho_d$  is the density of the natural gas contained in the tank NGD

$$V_d = V_{gi} \frac{\rho_d (\rho_{go} - \rho_{gi})}{\rho_{gi} (\rho_d - \rho_{go})} \tag{14}$$

### 2.3 Effect of density change in the transport of the biogas-natural gas mix

The behavior of the liquids that flow through the pipe is known that its density remains constant due to a weak dependence of this property with pressure, this simplifies the equations to describe the phenomena. However, this assumption is not valid when the fluid is understandable where the decrease in pressure since frictional head losses cause the decrease in gas density [18]

On the other hand, the variation of the gas density causes in the compressors, effects on the turbocharger pressure ratio, compressor head, system resistance, the turbocharger flow and power. Any change in molecular weight, T, k, or Z will change the ratio of the pressure produced. Gas velocity will change will change with gas density since a gas is compressible. Effect on the resistance of the system this is affected by a change in density that causes a variation in the friction drop in pipes, fittings and vessels. The effect on turbocharger flow causes a change in the operating point of each compressor stage in a multistage compressor, that depending on the impeller selection, this change could have an adverse affect on the operation of a dynamic

compressor causing surge and corresponding high vibration, temperature, flow changes, etc. The dynamic compressor required power increases directly with gas density up to the choke flow or stonewall region of the performance curve, and, in the choke flow region, the head produced by the compressor approaches zero since the gas velocity is equal to its sonic velocity. Finally all these effects cause a mismatch in compressor stage mismatching which can cause significant mechanical damage to the compressor train [19]

### 3 Simulations and analysis

Simulations are made according to the following criteria:

(a) It is assumed that the composition of natural gas will be methane  $\text{CH}_4$ , ethane  $\text{C}_2\text{H}_6$ , propane  $\text{C}_3\text{H}_8$ , butane  $\text{C}_4\text{H}_{10}$ , pentane  $\text{C}_5\text{H}_{12}$  and hexane  $\text{C}_6\text{H}_{14}$ ; which together are most of a typical natural gas composition as can be seen in [8] and in the research criteria of [9].

(b) In [8] using a combination of mixture components, a randomized test matrix of experiments generated with methane  $\text{CH}_4$  entre 80 % - 100 % (by volume), ethane  $\text{C}_2\text{H}_6$  entre 0 % - 15 % (by volume) and propane  $\text{C}_3\text{H}_8$  between 0 % - 20 % (by volume). As a purely mathematical exercise in order to verify the operation of the control system and the quantification of random variables, the equations have been considered (14) - (19 using the command *rand()* of Matlab [2] which generates uniformly random numbers between 0 and 1, and;  $m$  is the number of test states to simulate. Has been considered  $m$  equal to 30, and that a subject of study is to evaluate the delivery of natural gas at constant flow during a determined period of time that we will call "state", which would allow the algebraic management of the supply.

$$\text{CH}_4 = 0.80 + 0.2 \times \text{rand}(1, m) \quad (14)$$

$$\text{C}_2\text{H}_6 = 0.07 \times \text{rand}(1, m) \quad (15)$$

$$\text{C}_3\text{H}_8 = 0.05 \times \text{rand}(1, m) \quad (16)$$

$$\text{C}_4\text{H}_{10} = 0.05 \times \text{rand}(1, m) \quad (17)$$

$$\text{C}_5\text{H}_{12} = 0.02 \times \text{rand}(1, m) \quad (18)$$

$$\text{C}_6\text{H}_{14} = 0.01 \times \text{rand}(1, m) \quad (19)$$

(c) The properties of the natural gas components to be used are shown in Table 1.

**Table 1.** Physical properties of the paraffin hydrocarbons and other compounds.

Compound	Molecular Weight $W_t$	Critical Pressure $p_c$ , psia	Critical Temperature $T_c$ , °R
Methane	16.04	673.1	343.2
Ethane	30.07	708.3	549.9

8

Propane	44.09	617.4	666.0
Butane	58.12	529.1	734.6
Pentane	72.15	489.8	846.2
Hexane	86.17	440.1	914.2

(d) The composition of natural gas in NGD will be of high quality in methane as in [10,11,12]. Is considered a  $\rho_d$  equal to 0.04 lb/cu.ft

### 3.1 Normalization of natural gas composition

Since Equations (14-19) generate random numbers, the sum can exceed the value 1, therefore, it is necessary to perform a normalization in order to keep the total sum of all the percentages of the gas components at 1 natural. An example of normalized and non-normalized methane is shown in Fig. 4 considering  $m = 30$ .

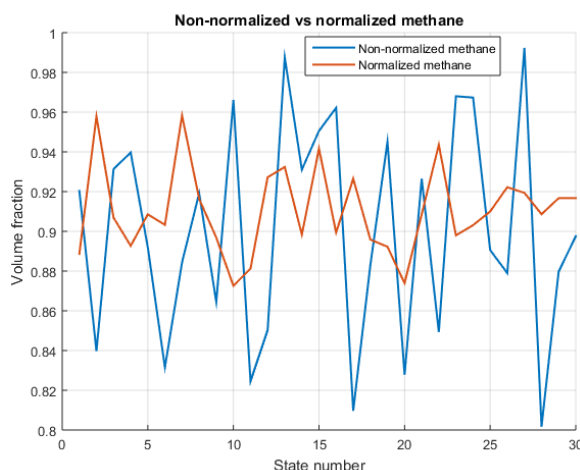


Fig. 4. Evolution of CH<sub>4</sub> non-normalized and normalized volume fraction per state.

Is assumed as reservoir pressures and temperature: 3250 psi and 213 ° F, which can be modified for other study cases.

With the normalized composition of natural gas for each of the m states; the molar mass, the pseudocritical pressures and temperatures, the pseudo-relative pressures and temperatures are determined, and then the gas deviation factor is calculated (see Fig. 5) and gas density (see Fig. 6), as well as the pure natural gas volume (see Fig. 7) and cumulative volume of pure natural gas from NGD deposit (see Fig. 8).

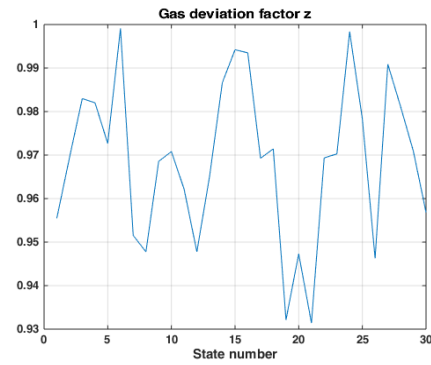


Fig. 5. Evolution of gas deviation factor  $z$  per state.

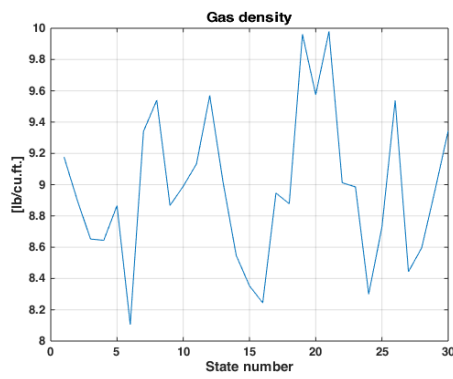


Fig. 6. Evolution of gas density [lb/cu.ft.] per state.

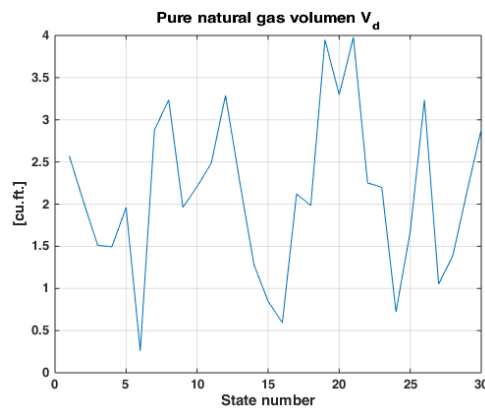


Fig. 7. Evolution of the pure natural gas volumen per state.

10

### 3.2 Volume of natural gas in the NGD

The calculation determines the discharge of pure natural gas from the NGD and its accumulation. NGD will have to be reloaded after a certain time. The local production of natural gas (for example, in biodigesters located within the metropolises) allows to reduce the natural gas coming from the subsoil.

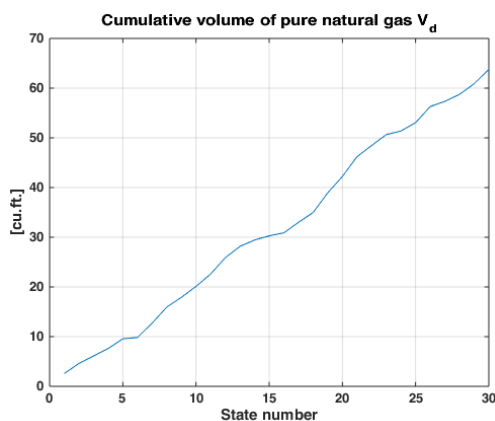


Fig. 8. Evolution of the cumulative volume of pure natural gas per state.

## 4 Discussion

The calculation of the gas deviation factor, considered an interactive and laborious process, has been developed and tested for a scenario of states that evolve in ordinary time. It is a topic of interest to answer in future research the duration of each state, however, it must be changing to meet varying demand during the day and quasi-constant during the night. A reduction in the consumption of natural gas from the subsoil is possible from production at the ground surface level and locally, from biodigesters, very possible given that there is an increasing world population and fits into the concepts of smart cities for the production, use and management of heat (in heating systems or similars) and electricity (in microturbines or similars), and that in this regard, can be extended to concepts such as distributed generation and microgrids. For the practical implementation of the system, it is enough to have the pressure and temperature characteristics of the natural gas source and its composition using measurement systems with real-time data reading, capture and processing with an adequate sensors-computer-machine-human.

## Acknowledgment

The authors thank the following projects and institutions: (a) CYTED Thematic Network “Ciudades Inteligentes Totalmente Integrales, Eficientes y Sostenibles

(CITIES)” N° 518RT0558; (b) too thanks to the support and motivation provided by the Federal University of Maranhão (UFMA), CEMAR, CP ELETÔNICA, CNPq – Brazil, and MEIHAPER CYTED.; (c) Group of Mathematical Modeling and Numerical Simulation (GMMNS) y Center of Communications and Information Technologies (CTIC) in National University of Engineering (UNI), Lima, Peru, for the use of facilities for research development; (d) Project: "Modeling and numerical simulation in oil reservoirs", supported by the Faculty of Petroleum, Gas and Petrochemical Engineering of the Universidad Nacional de Ingeniería, Lima, Peru, and to; (e) Miss Fabiola García Herrera by technical support

## References

1. B. C. Craft, M. F. Hawkins. "Applied Petroleum Reservoir Engineering". 2<sup>nd</sup> ed., New Jersey, USA: Prentice Hall, 1991.
2. MathWorks Inc. Matlab & Simulink Software. Available: <http://www.mathworks.com>
3. D. J. Abbott, J. P. Bowers, S. R. James. "The impact of natural gas composition variations on the operation of gas turbines for power generation". *6th International Conference The Future of Gas Turbine Technology*, Brussels, Belgium, Oct 17-18,2012.
4. Nino Ripepi, Kyle Louk, Joseph Amante, et. al. "Determining coalbed methane production and composition from individual stacked coal seams in a multi-zone completed gas well". *Energies*, 2017, 10, 1533; DOI:10.3390/en10101533
5. Abdus Satter, Ghulem M. Iqbal, James L. Buchwalter. "Practical Enhanced Reservoir Engineering – Assisted with Simulation Software". Tulsa, Oklahoma, USA: PennWell Corporation, 2008.
6. Rao V. Dukkipati. "Analysis and Design of Control Systems using Matlab". New Delhi, India: New Age International Limited, Publishers, 2006.
7. Robert H. Bishop. "Modern Control Systems Analysis and Design using Matlab". Reading, Massachusetts, USA: Addison-Wesley Publishing Company, 1993.
8. R. M. Flores, V. G. McDonell, G. S. Samuelsen. "Impact of Ethane and Propane Variation in Natural Gas on the Performance of a Model Gas Turbine Combustor". *Journal of Engineering for Gas Turbines and Power*. 2003, Vol. 125, pp. 701-708.
9. Craig Freeman, George J. Moridis, Gerard Eric Michael, Thomas Alwin Blasingame "Measurement, Modeling, and Diagnostics of Flowing Gas Composition Changes in Shale Gas Wells". 2012 SPE Latin America and Caribbean Petroleum Engineering Conference, , Mexico City, Mexico. DOI <https://doi.org/10.2118/153391-MS>
10. Bin Huang, Erjiang Hu, Zuohua Huang, et. al. "Cycle-by-cycle variations in a spark ignition engine fueled with natural gas-hydrogen blends combined with EGR". *International Journal of Hydrogen Energy*, 2009, 34, 8405-8414.
11. R. M. Flores, M. M. Miyasato, V. G. McDonell, G. S. Samuelsen. "Response of a Model Gas Turbine Combustor to Variation in Gaseous Fuel Composition". *J. Eng. Gas Turbines Power*. Oct 2001, 123(4): 824-831. <https://doi.org/10.1115/1.1377011>
12. M. Reyes, F. V. Tinaut, A. Melgar, et. al. "Characterization of the combustion process and cycle-to-cycle variations in a spark ignition engine fuelled with natural gas/hydrogen mixtures". *International Journal of Hydrogen Energy*, 2016, 41, 2064-2074.
13. International Energy Agency – IEA. "Gas". Available in: <https://www.iea.org/fuels-and-technologies/gas>

12

14. International Energy Agency – IEA. “Renewables 2020 – Analysis and forecast to 2025”. Available in: <https://www.iea.org/reports/renewables-2020/hydropower-bioenergy-csp-and-geothermal#abstract>
15. International Energy Agency – IEA. “Renewables 2020 Data Explorer – Explore electricity, heat and transport data from Renewables 2020”. Available in: <https://www.iea.org/articles/renewables-2020-data-explorer?mode=market&region=World&product=Bioenergy>
16. International Energy Agency – IEA. “Renewable Power”. Available in: <https://www.iea.org/reports/renewable-power>
17. International Renewable Energy Agency – IRENA. “Bioenergy”. Available in: <https://www.irena.org/bioenergy>
18. P. C. Narváz, “Solución de redes de flujo para gases usando el modelo de balance de nodos y el método de linealización de ecuaciones”, Ing. Inv., no. 44, pp. 56-62, Sep. 1999. Available in: <https://revistas.unal.edu.co/index.php/ingainv/article/view/21300/22269>
19. William Forsthoffer. “Forsthoffer's Rotating Equipment Handbooks - Compressors”. 1st Edition. New York, USA: Elsevier Inc, 2005. ISBN 1-85617-469-7

## Microclimatic Studies and Scenarios Simulation with ENVI-Met – A Case Study from a Residential Neighborhood in Bragança (Portugal)

Marcos Costa<sup>1</sup>, Artur Gonçalves<sup>1</sup>[0000-0002-4825-6692], António Castro Ribeiro<sup>1</sup>[0000-0002-8280-9027], Felipe Romero<sup>2</sup>[0000-0002-9971-2387]

<sup>1</sup> Centro de Investigação de Montanha (CIMO), Instituto Politécnico de Bragança, Campus de Santa Apolónia, 5300-253 Bragança, Portugal.

ajg@ipb.pt

<sup>2</sup> Instituto de la Construcción de Castilla y León, Valladolid, Spain.

**Abstract.** As cities are increasingly denser, there is a major change in the radiation balance and heat exchanges. Therefore, cities tend to be warmer than their surroundings, thus generating the Urban Heat Island Effect (UHI). With the growing pressure from climate change, it is increasingly necessary to carry out studies that can address outdoor thermal Comfort, and provide useful indications for urban design. This research, developed within the framework of the cross-border project INTERREG POCTEP ENERUSER, took place in a residential Neighborhood in Bragança (Portugal), with the aim of evaluating the local microclimate and the potential benefits of vegetation integration, using both local meteorological measurements and microclimate simulations. On-site meteorological monitoring took place in four locations, on June 2020, using Delta Ohm 32.1 and 32.3 Thermal Microclimate Data Loggers. For microclimate simulations, ENVI-Met software was used, as it provides 3D simulations of local microclimatic conditions and is widely used for urban micro-scale analysis. Monitoring data was used for parametrization and validation. An alternative scenario was considered with the introduction of trees in parking lots and changes in soil sealing. Results indicate that there is a good correlation between local data, from monitoring, and the data obtained through simulation. The simulation of the alternative scenario estimated a thermal comfort improvement due to a decrease in temperature of up to 2°C, most relevant at the hottest period of the day, therefore suggesting thermal benefits from the introduction of trees in the studied neighborhood, as proposed in the ENERUSER project.

**Keywords:** ENVI-met; simulation; thermal comfort; urban microclimate.

### 1 Introduction

Cities can be considered complex systems, opened to energy and mass flows, in a continuous change. The growing demographic, socioeconomic and cultural importance of cities makes environmental issues increasingly relevant for public authorities and researchers [1]. According to the United Nations [2], the urban population will increase from 3.9 billion to 6.4 billion inhabitants by 2050, with urban areas hosting 64% of the total global population.

2

The first study devoted to urban climate dates back to 1818 when L. Howard demonstrated that temperatures in inner London were higher than those in nearby rural areas, although there was some awareness of this phenomenon before this date [3]. There is a growing concern about global warming, a phenomenon that is occurring at a faster than expected [4]. At the current pace global warming would reach 1.5°C between 2030 and 2052 [5], this forecast shows that there is a risk of thermal stress in cities, threatening human health (Scherer et al. cit in. [6]).

The study of outdoor thermal comfort has gained increased relevance among the scientific community and, therefore, there is the need for the development of innovative methods to better understand the data collected. These studies depend on the time of year in which they are carried out, given the variation in weather conditions, which influence thermal comfort. In this regard, cities should adopt mitigation measures, thus reducing issues related to comfort [7]. Currently, researchers use computer models to represent the urban environment, these models are also important to verify the effectiveness of mitigation measures [8]. For the evaluation of the urban microclimate, several models are proposed in the literature, which are based on theoretical foundations. Model selection and application of tools have been one of the main challenges for both research and planning [9].

This paper presents a research integrated in the INTERREG POCTEP EnerUSER Transnational Project. This particular study intends to assess the outdoor thermal comfort in Bairro da Misericórdia, in Bragança (Portugal), through the combination of climate modeling, with ENVI-Met, and on site monitoring.

## 2 Methods

Urban climate modelling requires an extensive survey of urban parameters, such as the characteristics of the buildings, the green spaces (existing vegetation), and the pavements, in order to proceed with the construction of scenarios. Variables such as air temperature, wind direction, wind speed and relative humidity should also be monitored at the study sites, and then integrated into a microclimatic scenario, while serving to validate that same scenario. Starting from the base scenario, in this study, alternative scenarios for the improvement of thermal comfort will also be presented.

### 2.1 Case Study

The present study focuses on the Bairro da Providência, close to the Local Hospital (ULS NE), as shown in Fig. 1. This neighborhood consists of 12 buildings grouped into six pairs. These buildings are multi-family, with four apartments per building. In addition to housing buildings, this neighborhood includes storage buildings, as well as parking spaces and paved sidewalks, with some areas with vegetation, mostly located near the main road.



Fig. 1. Study Area.

## 2.2 On-Site Data Collection

On-site data collection, for integration on ENVI-met, included the height and distance between building façades, using the digital laser meter Ld500 Stabila. Other elements were also characterized including the vegetation, surfaces, and buildings materials. The height of the trees was measured with the aid of a telescopic pole, which extended up to eight meters, for taller the digital meter was used. Regarding the width of the crowns, a measuring tape was used to record two perpendicular measurements, one in the north-south direction and the other in the east-west direction.

## 2.3 ENVI-met Model Definition

The software used in this study was ENVI-met, created by Michael Bruse of the University of Mainz [10]. ENVI-met allows for the definition of three-dimensional scenarios, with which urban microclimate is simulated, based on surface-air interactions. This software calculates the energy balance by estimating variables such as radiation, temperature, humidity, among others [11].

4

ENVI-met is considered a computational fluid dynamics modeling software (CFD) [12]. This software is notable for its high temporal and spatial resolution, as well as its advanced 3D interface. This software is based on the fundamental laws of fluid dynamics and thermodynamics [13]. It can be applied in areas such as urban climatology, architecture, building design, and urban planning.

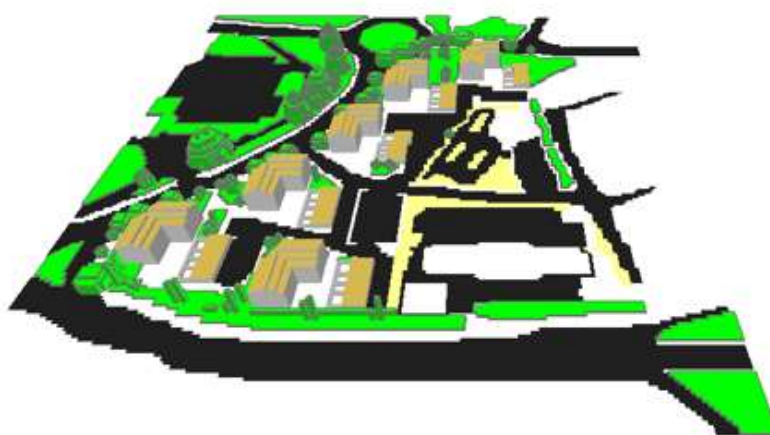


**Fig. 2.** Base Scenario based on the initial neighborhood configuration

The software version used in this study was the 4.4.4. It includes databases for pavements, building materials and vegetation. For this work, the study area was transformed into a simulation scenario with dimensions of 200 x 200 x 30 cells, with a resolution of 1 m<sup>3</sup>. After an initial 2D representation, buildings and trees were projected to its measured height. As the ENVI-met database is limited, and most of the vegetation found in the study site is not available in the software, most of the trees were design in 3D using 3D m<sup>3</sup> blocks. Once every element was defined, the initial scenario was completed reproducing with as much exactitude as possible the prevailing urban design characteristics (Fig. 2). In order to assess the potential benefits of the introduction of Nature Based Solutions on this neighborhood, a new scenario was developed (Fig. 3).

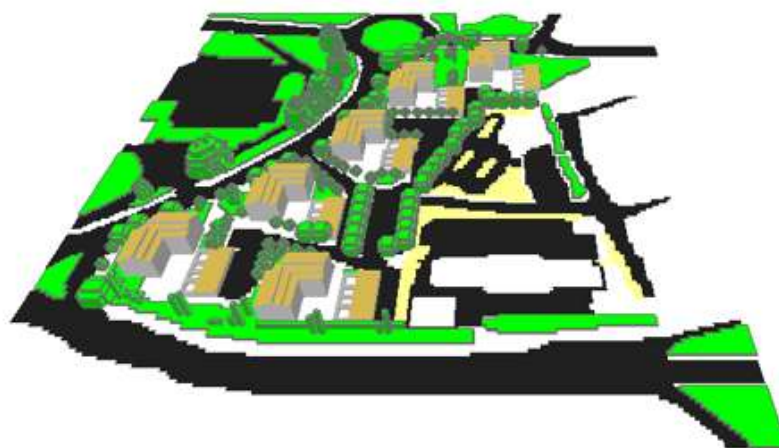


Fig. 3. Neighborhood Greening Alternative Scenario

#### 2.4 Meteorological Data Collection

The collection of micrometeorological data was carried out on June 18, 2020, a warm spring day. Delta Ohm 32.1 and 32.3 micrometeorological monitoring stations were used, with sensors for measuring air velocity, mean radiant temperature (from globe temperature), air temperature, and relative humidity. In the case of the Delta Ohm 32.1 station, in addition to the sensors mentioned, it also featured wet and dry bulb thermometers. Sensors and data loggers shown in Fig. 4.

The devices were programmed to take measurements every five minutes during the two hours: for sunrise (4:00-6:00 UTC), morning (10:00-12:00 UTC). In the afternoon (14:00-16:00 UTC) and at sunset (19:00-21:00 UTC), the devices were reprogrammed to take measurements every two minutes. Equipment was placed 1.5 m above the ground.

6



Fig. 4. Measurement Equipments

In Fig. 5, the four measurement points are presented: point 1, placed over a stone pavement, next to the grass, without shade; point 2, located in a car park where the pavement is asphalt and where there was no shade; point 3, on the sidewalk, with cement pavement, where there was no vegetation in the surroundings, nor shadows; finally, point 4, located in a shady place over grass. The main objective underlying the choice of these locations was the diversity of conditions, taking into account the pavements, vegetation, and construction elements.



Fig. 5. Measuring locations (1 to 4 from left to right)

Data from local measurements were used to define the entry data for ENVI-Met simulation (Table 1).

**Table 1.** Entry data for ENVI-Met simulation (UTC time)

<b>Day</b>	18-06-2020
<b>Minimum Air Temperature (°C)</b>	7.40 (05h20)
<b>Maximum Air Temperature (°C)</b>	28.50 (14h32)
<b>Minimum Relative Humidity (%)</b>	18.40 (15h14; 15h16)
<b>Minimum Relative Humidity (%)</b>	99.70 (04h35)
<b>Average Wind Speed (m/s)</b>	0.86->04h00-06h00 1.50->10h00-12h00 2.10->14h00-16h00 1.45->19h00-21h00
<b>Average Wind Direction (Degrees)</b>	82->04h00-06h00 333->10h00-12h00 52->14h00-16h00 56->19h00-21h00

Data recorded through local monitoring were analyzed using the R statistical analysis tool. The software allowed several analyzes including Pearson correlation, boxplots, as well as ANOVA tests. Due to the limited extent of this article, it will focus on the analysis of air temperature and on the modeling of the 16:00-17:00 period.

### 3 Results

Fig. 6 shows the air temperature box-plots for the four points, for the different measurement periods. The air temperature was lower at sunrise, while the highest temperatures were reached in the afternoon, with point 3 being the place with the highest air temperature and point 4 with the lowest. As expected, air temperature is lowest at sunrise and sunset. Temperatures reached their pic in the afternoon, the moment in which temperatures were higher in points 1 and 3, and lower in point 4. Results are consistent with the spots that should generate warmer thermal environments because of the presence of low albedo materials (cement and asphalt); nonetheless, point 3 had a slightly lower temperature than expected considering its surface materials. This difference could be attributed to the fact that point 3 was located in a more open area of the neighborhood that could favor ventilation and convection.

8

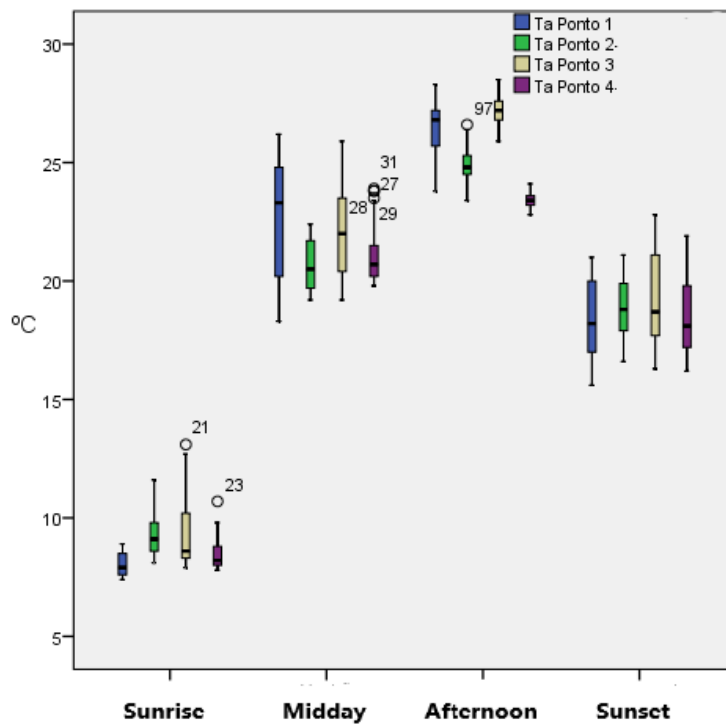


Fig. 6. Box plot for temperature distribution on the different measurement periods

Data from local measurements were integrated as inputs in ENVI-Met. The results from modeling for the 16:00-17:00 period are presented in Fig. 7. Temperature ranged from 24.74°C and 28.40°C, with a 3.66°C range across the study area. Differences across the simulation can be attributed to the differences in the thermal environment and the differences in shaded areas. Lower temperatures were simulated for the shaded areas near the tree lines at the edges of the neighborhood, while higher temperatures were found at spots exposed to solar radiation with low albedo surfaces.

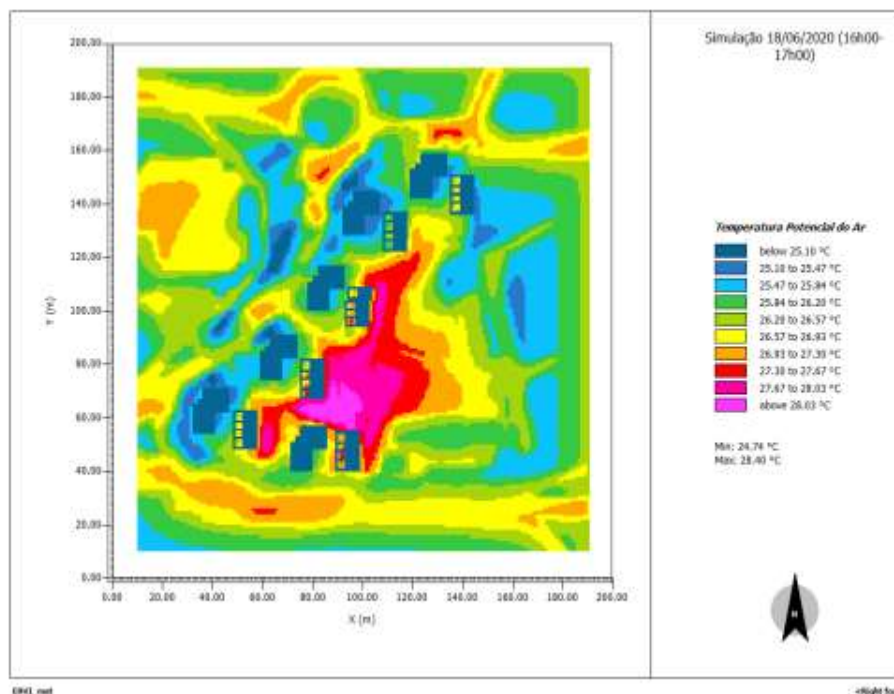


Fig. 7. Air temperature simulation for the 17:h00 to 18:00 period

Through Pearson's correlation, it was possible to measure the correlation between the two data sets, the temperature recorded by measurements and the temperature estimated by simulation (Table 2). Results show a positive and very strong correlation in the four points, as the values approach 1.

Table 2. Pearson correlation coefficients for the relation between measured and modelled air temperature

	Ta Point 1 (ENVI-met)	Ta Point 2 (ENVI-met)	Ta Point 3 (ENVI-met)	Ta Point 4 (ENVI-met)
Ta Point 1	0.983	-	-	-
Ta Point 2	-	0.984	-	-
Ta Point 3	-	-	0.968	-
Ta Point 4	-	-	-	0.990

Despite this strong correlation, a detailed analysis allowed for the identification of some differences between the two datasets, which are more significant in the sunrise period, especially in the first hour (5:00-6:00), when the simulation exceeded the measurements by 3oC in all measurement points. On the other periods, differences are lower as the simulation is more accurate. Coltri et al. [14] also identified the overestimation of results related to air temperature, although with greater incidence both in the morning and

10

in the afternoon. Chow et al. (2012, cit. in [9]) also reported an overestimation of temperature values at night and an underestimation during the day.

The results from the simulation for 17:00 – 18:00 (Fig. 8) show a relevant change from the base scenario. To better understand the simulated impact from the introduced changes.

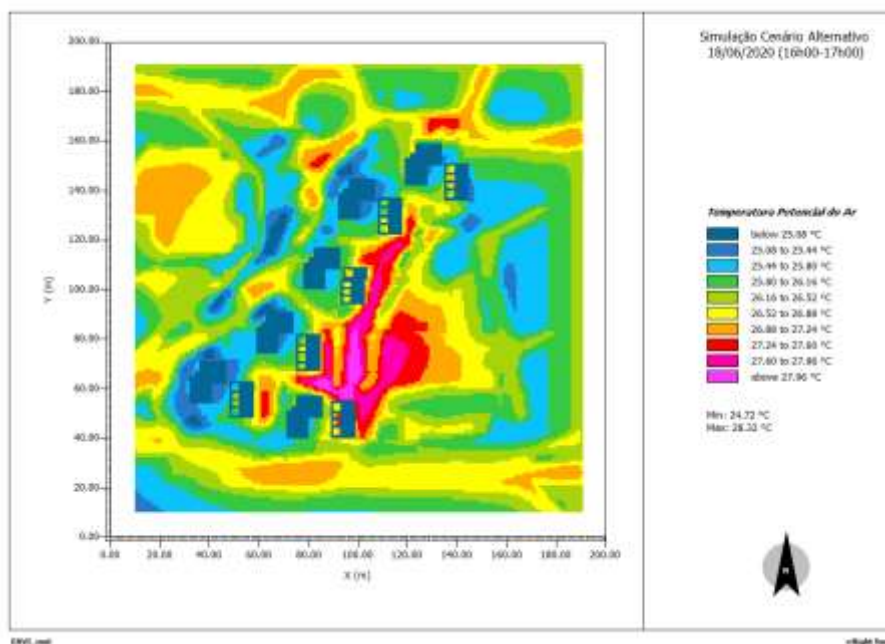
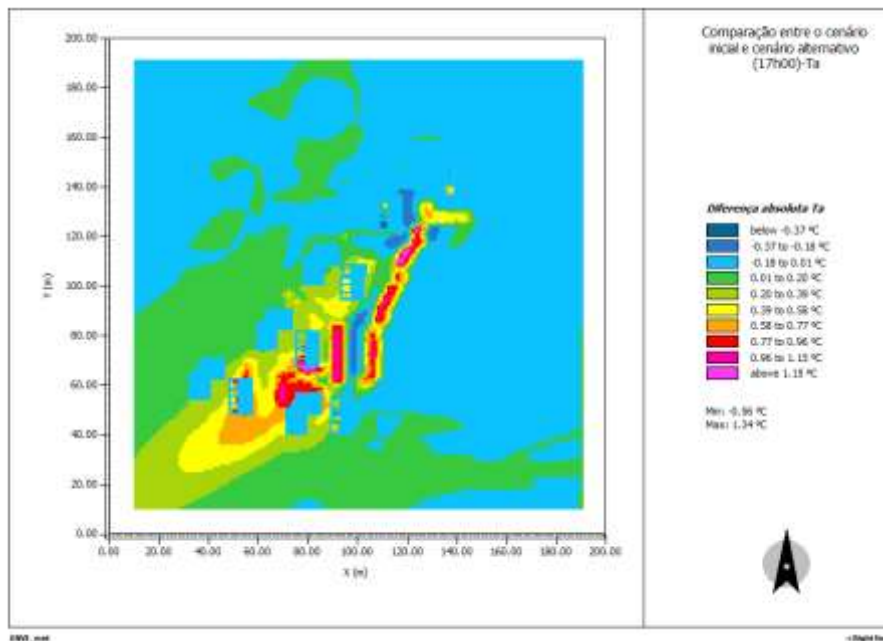


Fig. 8. Air temperature simulation for the 17:h00 - 18:00 period.

As Fig. 9 presents the differences between the base scenario and the alternative scenario, the maximum temperature decrease was  $-1.34^{\circ}\text{C}$  and a temperature increase at certain points of  $0.56^{\circ}\text{C}$ . As expected, with the introduction of arboreal vegetation, ENVI-Met estimated a decrease in air temperature in almost the entire study area. The increase in tree density can also lead to decreased ventilation, which in turn can determine specific temperature increases, due to lower convection processes, in places with low albedo surfaces. Yilmaz et al. [15] reached identical conclusions.



**Fig.9.** Comparison between the estimated results for the base scenario (Sc1) and the alternative scenario (Sc2) for 16:00 to 17:00 period (Sc1-Sc2).

#### 4 Conclusions

This study combined on-site data collection with software simulation to provide data regarding microclimate in a residential neighborhood. Measurements provided valuable information regarding the air temperature differences across the study area, with differences that were attributed to the physical environment surrounding the location of the sensors, including the differences in surface materials and vegetation.

Modelling results show a good correlation between measured and modelled data. However, the simulated air temperature was clearly overestimated for the sunrise period. The maps created by ENVI-Met simulation allowed for the identification of the most critical points on the base scenario, thus providing essential elements for the definition of an alternative scenario, with the introduction of additional trees. The resulting simulation estimates an air temperature reduction of up to 2oC and localized increases in temperature.

This study should be seen as an example of the potential for microclimate simulation as a tool that can provide valuable information for urban design, as it can help to simulated microclimate conditions and/or to project new developments.

## Acknowledgments

This work has been developed in the context of the INTERREG POCTEP project ENERUSER (ref. 0640\_ENER\_USER\_2\_E.). The funding program is not responsible for the opinions expressed by the authors.

The authors are grateful to the Foundation for Science and Technology (FCT, Portugal) and FEDER under Programme PT2020 for financial support to CIMO (UIDB/00690/2020).

## References

1. Andrade, H., 2012. “O Clima Urbano - Natureza, escalas de análise e aplicabilidade”, *Finis-terra*, 40(80), 67–91. <https://doi.org/10.18055/finis1479>
2. UN (2018) World Population Prospects: 2018 Revision. United Nations.
3. Ganho, N., 2019. “Clima urbano e a climatologia urbana : fundamentos e aplicação ao ordenamento urbano”. *Cadernos de Geografia* nº 18. Universidade de Coimbra.
4. Brysse, K., Oreskes, N., O’Reilly, J., & Oppenheimer, M. (2013). “Climate change prediction: Erring on the side of least drama?” *Global Environmental Change*. <https://doi.org/10.1016/j.gloenvcha.2012.10.008>
5. IPCC., 2019. “Aquecimento Global de 1,5°C: Relatório especial do Painel Intergovernamental sobre Mudanças Climáticas (IPCC) sobre os impactos do aquecimento global de 1,5°C acima dos níveis pré-industriais e respetivas trajetórias de emissão de gases de efeito estufa”. IPCC, 28. <https://www.ipcc.ch/site/assets/uploads/2019/07/SPM-Portuguese-version.pdf>
6. Jänicke, B., Meier, F., Hoelscher, M. T., & Scherer, D., 2015. “Evaluating the effects of façade greening on human bioclimate in a complex Urban environment.” *Advances in Meteorology*, 2015(May). <https://doi.org/10.1155/2015/747259>
7. Mao, J., Fu, Y., Afshari, A., Armstrong, P. R., & Norford, L. K., 2018. “Optimization-aided calibration of an urban microclimate model under uncertainty”. *Building and Environment*, 143(July), 390–403. <https://doi.org/10.1016/j.buildenv.2018.07.034>
8. Crank, P. J., Sailor, D. J., Ban-Weiss, G., & Taleghani, M., 2018. “Evaluating the ENVI-met microscale model for suitability in analysis of targeted urban heat mitigation strategies”. *Urban Climate*, 26(September), 188–197. <https://doi.org/10.1016/j.uclim.2018.09.002>
9. Yang, Yujun, Zhou, D., Wang, Y., Ma, D., Chen, W., Xu, D., & Zhu, Z. Z., 2019. “Economic and outdoor thermal comfort analysis of greening in multistory residential areas in Xi’an”. *Sustainable Cities and Society*, 51(July), 101730. <https://doi.org/10.1016/j.scs.2019.101730>
10. Huttner, S., Bruse, M., & Dostal, P. (2008). “Using ENVI-met to simulate the impact of global warming on the microclimate in central European cities”. *5th Japanese-German Meeting on Urban Climatology*, 18(18), 307–312.
11. Paas, B., & Schneider, C., 2016. “A comparison of model performance between ENVI-met and Austal2000 for particulate matter”. *Atmospheric Environment*, 145, 392–404. <https://doi.org/10.1016/j.atmosenv.2016.09.031>
12. Ayyad, Y. N., & Sharples, S., 2019. “Envi-MET validation and sensitivity analysis using field measurements in a hot arid climate.” *IOP Conference Series: Earth and Environmental Science*, 329(1). <https://doi.org/10.1088/1755-1315/329/1/012040>

13. Tsoka, S., Tsikaloudaki, A., & Theodosiou, T., 2018. "Analyzing the ENVI-met microclimate model's performance and assessing cool materials and urban vegetation applications—A review". *Sustainable Cities and Society*, 43(August), 55–76. <https://doi.org/10.1016/j.scs.2018.08.009>
14. Coltri, P. P., Pinto, H. S., Gonçalves, R. R. do V., Zullo Junior, J., & Dubreuil, V., 2019. "Low levels of shade and climate change adaptation of Arabica coffee in southeastern Brazil". *Heliyon*, 5(2), e01263. <https://doi.org/10.1016/j.heliyon.2019.e01263>
15. Yilmaz, S., Mutlu, E., & Yilmaz, H., 2018. "Alternative scenarios for ecological urbanizations using ENVI-met model". *Environmental Science and Pollution Research*, 25(26), 26307–26321. <https://doi.org/10.1007/s11356-018-2590-1>

## Analysis of mathematical models for location of electric vehicle charging stations: state of the art

Fernanda Helena Amaro Verneque<sup>1</sup>, Pedro Henrique González<sup>2</sup> and Vanessa de Almeida Guimarães<sup>1</sup>

<sup>1</sup> Centro Federal de Educação Tecnológica Celso Suckow da Fonseca, Angra dos Reis/RJ, Brazil

<sup>2</sup> Centro Federal de Educação Tecnológica Celso Suckow da Fonseca, Rio de Janeiro/RJ, Brazil

fernanda.verneque@aluno.cefet-rj.br

pegonzalez@eic.cefet-rj.br

vanessa.guimaraes@cefet-rj.br

**Abstract.** In recent years, electric vehicles have received special attention due to environmental concerns and possible oil shortages. These vehicles are pointed out as promising alternatives to reduce fossil fuel consumption and contribute to reducing the emission of greenhouse gases. In order for the mass adoption of these vehicles to be possible, there must be a minimum of charging infrastructure and, as the initial investment of these projects is high, it is necessary to use models with optimal location. This study proposes to map the literature published in the Web of Science (WoS) database until the year 2019, focusing on studies on location models for electric vehicle charging stations. As a result, it was found that the works on location could be classified according to the type of problem they are analyzing, three main groups were found: Maximum Coverage, Flow Capture and P-Median. The research showed some characteristics about the three types of Problems found in the studies.

**Keywords:** Optimization; Charging stations; Electric vehicles.

### 1 Introduction

In recent years, there has been an increase in growth about sustainable development, ways to reduce the impact on the environment and ensure the quality of life of future generations have been studied (Tan et al., 2013). When the divisions of energy consumption are analyzed, the transportation sector stands out, consuming about 31.2% of the total energy available in Brazil in 2020 (EPE, 2021) and 32.7% in 2019 (EPE, 2020). The sector was also responsible for emitting about 179.8 Mt CO<sub>2</sub>-eq, corresponding to 45.1% of total emissions in 2020 (EPE, 2021) and 45.4% in 2019 (EPE, 2020). It should be noted that the increase in greenhouse gas emissions and air pollutants are harmful to the environment and people's health (Vries et al., 2015). Thus, the

transport sector contributes to the increase in global warming potential and the scarcity of natural resources (Verneque et al., 2020). For these reasons, the transport sector has been pressured to adopt green and sustainable strategies (Krishna *et al.*, 2012).

One of the strategies that have gained momentum to make the transport sector eco-friendly is the replacement of Internal Combustion Vehicles (ICEV) by Electric Vehicles (EVs) (Vries et al., 2015). Such changes happened because EVs are more energy-efficient and have lower operating costs when compared to ICEVs (Zheng et al., 2016 and Vries et al., 2015). On the other hand, one of the main difficulties in accepting these vehicles is the driving range, which corresponds to the maximum distance vehicles can travel without recharge (Zheng et al., 2016). The range of EVs has increased year on year. In 2016 it was around 160km and by 2020, there were already EVs with a range between 402km and 643km (Office of Energy Efficiency and Renewable Energy, 2020). To stimulate and facilitate the use of EVs, it is essential to have a network of on-site charging stations that ensure that vehicles can reach most of their destinations without running out of fuel (Pagany et al. 2018 e Vries et al., 2015). As the initial investment in these recharge stations is high and restricted, it is important to choose its locations carefully (Vries et al., 2015).

Some studies, such as Pagany et al., 2018 and Hosseini et al., 2015 point out that municipal, state and federal governments must make a joint effort to ensure an appropriate recharging infrastructure and facilitate the introduction of EVs to the market. Some countries, such as the United States, China, Spain, the United Kingdom, the Dominican Republic and others have invested efforts to increase the number of EVs in their countries (Onata et al., 2019 e Zheng et al., 2018).

This work aims to survey the scientific literature published in the Web of Science database, evidencing the main characteristics of the optimization models of the location of recharging stations for electric vehicles.

From this section, the present work is divided into four sections: Section 2 reviews the literature on the context of models of optimization of the location of EVs, Section 3 presents the methodological procedures adopted in the research, Section 4 brings the main results and discussions, and Section 5 brings the main contributions and conclusions about this work.

## 2 Theoretical Reference

Given the considerable impact of the transport sector on a country's emissions and energy consumption, the concept of eco-friendly transport has been proposed as a critical element to reduce environmental impacts, such as dependence on oil and GHG emissions (JUN et al., 2019; FENG et al., 2019), air pollution, climate change and negative impacts on people's lives, especially concerning respiratory diseases (VERNEQUE et al., 2020). EVs can reduce CO<sub>2</sub> contributions of the transportation sector in case the majority of the electric power used in EVs originates from renewable sources (Sanchari et al., 2018). EVs' other benefits are low noise, minimal maintenance, and lower operating cost (Sanchari et al., 2018). Such characteristics have motivated many countries to promote the use of EVs for public and private transportation.

Thanks to that, vehicle manufacturers and policymakers are boosting their attention and actions related to electric vehicles, developing technologies such as full battery-electric (BEV) and plug-in hybrid electric (PHEV) models, which are attractive options to help reach environmental, societal and health objectives (IEA, 2021).

China, for example, has implemented several subsidies policies, credit taxes and infrastructure improvements to motivate consumers and new manufacturers to adopt/invest in this technology (Zheng et al., 2016). Sanchari et al., 2018 and Zheng et al., 2016 show that, since 2010, the USA has offered a tax credit of \$2,500 to \$7,500 as an incentive to purchase PHEVs and BEVs. Besides, Shao et al., 2017 present a discount scheme adopted in Romania and Spain (MOVELE plans): the governments offer a 25% discount rate on EV's purchase price. The UK government has also implemented a similar discount scheme since January 2011

In Figure 1, we can see the evolution of the world stock of EVs from 2010 to 2019.

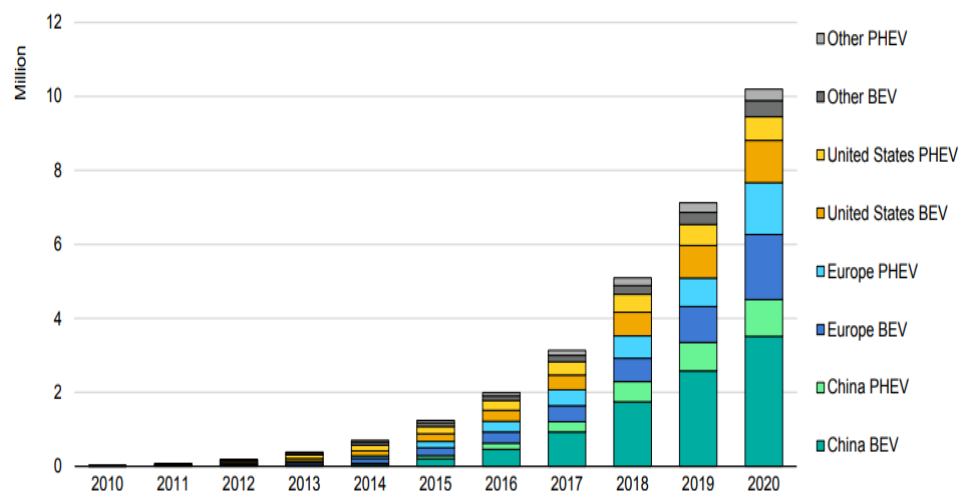


Fig. 1. Global electric car stock 2010 – 2020

Fonte: IEA, 2021

Although all these implemented policies and the potential benefits of EVs still have a barrier to mass adoption of these vehicles, in 2019, the EV's sales represented only 2.6% of all vehicles sales globally (IEA, 2020).

### 3 Methodological Procedures

To perform the literature review proposed in this paper, we use a statistical technique combined with Cytometrics. According to Gregolin et al. (2005), Cytometrics

seeks to understand a structure, evolution and, as determined by the field of study, establish relationships between scientific, technological, economic and social development. Table 1 presents the search parameters we use in our search. We choose the Web of Science (WoS) as a database because of its satisfactory coverage and scope and because it has been used in works with similar methodologies, as in Guimarães, Azevedo and Ferreira (2018) and Guimarães et al. (2020). Table 1 present the parameters of the search.

**Table 1.** Description of the search criteria in WoS database

Criteria	Description
Topics	TS1 = ("optimization")
	TS2 = ("electromobility") AND ("transport*")
	TS3 = ("electric vehicl*") OR ("eletric car*") OR ("electric car*") OR ("eletic vehicl*")
	TS4 = ("recharg* statio*") OR ("charg* statio*") OR ("charg* point*") OR ("electric vehicl* supply equipment") OR ("electric vehicl* charging station*") OR ("electric recharg* point*") OR ("recharg* point*") OR ("electronic charg* station*")
Database	TS1 AND (TS2 OR TS3) AND TS4 Web of Science
Refinements	All WoS area until 2019.
search	19/09/2020 at 16:20 GMT-3

The keywords were combined to search for optimization works associated with vehicle charging stations and electric vehicles (not just electric cars), considering direct transport applications.

With the preliminary results of the search, a new filter was made: a subset of works was created, papers that had a direct relationship between optimization from the selected keywords related to the search area.

Then, we selected the papers that have location optimization from the analyses of the abstract. The flowchart of this methodologic procedure can be seen in figure one with the respective number of papers in each filter. This procedure was necessary because we are interested in the papers that work with optimization models for charging station placement.

#### 4 Results

In the literature found on the optimization of the location of charging stations, it was possible to identify three groups of optimization problems: Maximum Coverage Location Problem (MCLP), Flow Capture Location Problem (FCLP) and p-Median Problem (PMP).

The MCLP aims to locate a certain number of charging stations, maximizing the total area covered. In this type of problem, all paths within the coverage region are considered covered (Du et al., 2016 e Dong et al., 2019).

The FCLP is characterized by the capture of flows and the objective is to maximize the number of vehicles that find at least one recharge facility in its path (Xiang et al., 2017; Hosseini et al., 2015; Islam et al., 2016).

In the last group of studies, the p-Median Problem (PMP) locates facilities minimizing the total distances traveled between the EV and the station.

Regarding the type of problem analyzed, we can see Table 2, in which the works were separated according to the type of problem and the general optimization objective was identified. Although in Table 3 we can see the type of variables, EV, charge type and where the study apply the method.

#### **4.1 Maximum Coverage Location Problem**

In Du et al. (2016), the authors present a new charging station planning model for EVs considering operators, drivers, vehicles, traffic flow and network power altogether, using real-time data to solve the MCLP. Already in Feng et al. 2019 they find the optimal location of charging stations by optimizing traffic conditions, operators, drivers and the electrical network in real time.

In Asamer et al. (2016), the authors formulate the MCLP problem as Mixed Integer Linear Programming and solve it with a generic algorithm, considering construction costs, power losses, etc. An analysis of six scenarios is also performed using the following parameters: Station development cost; Cost of charging losses; Cost of network losses; Cost of rent for five years; Cost of electrification. These parameters are varied in each of the scenarios.

A model of maximum demand coverage is proposed by Laporte et al. (2014) in order to minimize the number of slow charging stations in a given district. The model considers that all stations have the same coverage radius and can meet the same demand around them regardless of having different numbers of chargers, focusing only on the network topology.

A heuristic algorithm to solve the set coverage model is proposed by Hosseini et al. (2015) to find the location of recharging stations considering station capacity, recharging time and waiting time. The model is tested on two networks, theoretical and real, and provides a good travel plan, especially for tourism trips, where it could be adapted to a maximum coverage model with pre-defined activities.

#### **4.2 Flow Capture Location Problem**

In Chu et al. (2014), for example, the authors consider half of the follow-up between two nodes as possible candidates for the location of the stations. In addition, preference is always given to the centroids of each region. A comparison between solution models is performed in Kazemi-Karegar et al. (2014) using: I - Interactive mixed-integer linear program, II - Greedy Approach, III - Effective MILP and IV - Chemical Reaction Optimization. The results show that each method has its own characteristics

and is suitable for different situations depending on the solution quality requirements, algorithmic efficiency, problem size, algorithm nature and the existence of prerequisites in the system (Kazemi-Karegar et al., 2014). For example, with respect to the quality of the solution, the methods can be classified as  $I = III > IV > II$ .

In Cui et al. 2018a they investigate the problem of locating stations with different numbers of chargers with different recharge speeds.

In Cai et al. (2015), the authors determine the location and size of the charging station along with the charging technology for a given budget. As input to the model solution, we have the initial charge amount, the total budget and the maximum and minimum amount of network chargers. The model is solved considering the lowest total cost. The model also considers the minimization of time, which is composed of: travel time, time to prepare the recharge and recharge time.

**Table 2.** Classification of papers according to the type of problem analyzed

<b>Authors</b>	<b>Approach</b>	<b>Objective Function</b>	<b>Constraint</b>
Cui et al., 2018a	FCLP	Minimize the total travel time	Budget; Station and link capacity, Electricity; Charging delay
Feng et al., 2019	MCLP	Minimize the total construction cost	Charging waiting time; Traffic efficiency; Safety of power grid;
Du et al, 2016	MCLP	Minimize the total construction cost	Distance between charging station and EV; Number of chargers in a station; Number of stations in a link;
Chu et al, 2014	FCLP	Minimize the total construction cost	Charging capacity; Distance of the shortest path from nodes;
Kazemi-Karegar et al., 2017	FCLP	Minimize the total cost	Number of EV that can be charged by a connector during 24 h.
Asamer et al., 2016	MCLP	Maximize the coverage area	Number of new stations to be build; Coverage area;
Cui et al., 2018b	PMP	Minimize the total travel time	Budget; Station and link capacity, Electricity; Charging delay
Bian et al., 2018	FCLP	Maximize the total profits of new stations in the study area	Demand; Assignment; Number of chargers; Number of charging stations.
Cai et al., 2015	FCLP	Minimize the total distance that can't be completed only with electricity	Distance between charging station and EV;
Lin et al., 2013	PMP	Maximize the path coverage and minimize the total cost	Budget; Distance between charging station and EV;
Laporte et al, 2014	FCLP	Maximize the coverage area and	Traffic flow; Traveling distance; Drive range

		minimize the total cost	
Bowen et al., 2019	MCLP	Maximize the coverage area	Drive range; Coverage radius;
Hosseini et al., 2015	MCLP	Minimize the total construction cost and the total travel time	Station Capacity; Amount of charge
Xiang et al, 2017	FCLP	Minimize the total construction cost	Capacity of charging station; distance between the drive and the station
Islam et al, 2016	PMP	Minimize the total cost	Budget; Distance between charging station and EV;

**Table 3.** Main features of the analyzed papers

Authors	Model	Variable	Linear?	Method	EV type	Charging type	Data	Case Study
<i>Cui et al., 2018a</i>	O	D	Yes	Branch Cut (GAMS + CPLEX)	BEV	All	S	Nguyen–Dupius
Du et al, 2016	O	D	Yes	Genetic algorithm	Plug-in	All	S	Beijing
Chu et al, 2014	O	D, C	Yes	Branch and Bound; Greedy Approach; Branch and Cut; Chemical Reaction Optimization	All	All	S	Hong Kong
Kazemi-Karegar et al., 2017	O	D	Yes	Genetic algorithm	All	All	S	Tehran North-West zone
Asamer et al., 2016	O	C	Yes	Do not say	BEV	All	R	Vienna

<i>Cui et al., 2018b</i>	O	D	Yes	Branch Cut (GAMS + CPLEX)	BEV	All	S	Nguyen-Dupius / Sioux Falls
Cai et al., 2015	O	D	Yes	Branch Cut (GAMS + CPLEX)	Plug-in	All	S	Beijing
Lin et al., 2013	O	D	Yes	Branch and Bound	All	All	S	Beijing
Laporte et al., 2014	O	D	Yes	Branch and Cut	All	Slow	S	Denmark,
Bowen et al., 2018	O	D, C	Yes	Only say that runs on MATLAB	All	All	R	Beijing
Hosseini et al., 2015	B	D, C	Yes	Branch and Cut	All	All	S	Penghu County
Xiang et al, 2017	O	D	Yes	Particle swarm optimization)	All	All	S	Nanjing
Islam et al, 2016	O	D	Yes	Binary gravitational search algorithm	Plug-in	All	S	Bangi

Note: It presents the type of the model (O - single objective, B - Bi-objective and M - multi-objective), the optimization objectives, if the variable are deterministic (D) or stochastic (E) and the type of data, (R) to real data and (S) to Statistical. It also presents the solution model, the type of vehicle and station analyzed and if the paper do some study case.

The study presented by Bowen et al. (2019) uses a flow-based set coverage model considering budget constraints, various types of charging stations and vehicle routing behavior. In the model, various types of charging stations, slow, fast and battery change, are considered at each location along a path, all of which are candidates. According to location, cost, recharge efficiency and time, the optimal location is selected.

Xiang et al. (2017) introduce the FCLP with a set of sub-paths for each path between an origin and a destination so that in each of the sub-paths, there is at least one charging station. Thus, the entire flow of paths is captured. The model performed well when considering different load levels due to the existence of sub-paths also in round trips, which are composed of: travel time, time to prepare the recharge and recharge time.

### 4.3 p-Median Problem

Cui et al. (2018b) determine the possible locations for an exclusive charging station for a fleet of electric taxis. The places considered with high potential for installing the station are those with high demand. The study considered the scenario where the entire city of Venice could be served by electric taxis. Similarly, Lin et al. (2013) use vehicle route data to find the ideal station location for public charging stations in order to maximize the efficiency of the miles traveled.

A location model for battery exchange for electric buses is proposed in Islam et al. (2016) based on the PMP model and solves the problem with Particle Swarm Optimization. Existing bus stops in the network are used as potential charging station locations and are selected based on demand, bus line, coverage area. Another side of choosing locations is selecting locations close to substations to ensure that the nominal capacity of the substation or transformer meets the charging demand of the batteries, avoiding unnecessary expansions and capacity increases.

## 5 Final Considerations

This research showed that within the works found, it is possible to verify the different approaches that are being studied, such as rotation and location of the charging station, batteries, chargers, among other accessories for the EVS. In general, it was verified that three types of problems are usually used to model charging stations optimization problems: Maximum Coverage, Flow Capture, and P-Median.

Regarding the limitations of this study, only articles published in the WoS database until the end of 2019 were mapped. Therefore, publications indexed only in databases such as Scopus and Scielo were not considered. Furthermore, it is important to highlight that the chosen keywords can influence the search results.

As a suggestion for future work, a more comprehensive analysis can be made, considering other databases to more clearly validate the results obtained and raise new research topics relevant to the topic. In addition, more specific analyzes can be made on the mathematical models and solution techniques developed, so it would be possi-

ble to propose new models and support tools for the decision-making process in this area.

## References

1. Asamer, J., Puchinger, J., Reinthaler, M., Ruthmair, M., Straub, M., 2016, "Optimizing charging station locations for urban taxi providers", *Transportation Research A-Policy and Practice*, Vol. 85, pp. 233-246.
2. Bowen, Z., Haorui, J., Manhao, I., Xin, Z., 2018, "Improved Set Covering Location Model for Charging Facility Deployments", *International Conference on Artificial Intelligence Applications Technologies*, Vol. 435.
3. Cai, H., Shahraki, N., Turkay, M., Xu, M., 2015, "Optimal locations of electric public charging stations using real world vehicle travel patterns", *Transportation Research part D-Transport and Environment*, Vol. 41, pp. 165-176.
4. Cui, S. H., Zhang, C. P., Zhao, H., 2018 a, "Locating Charging Stations of Various Sizes with Different Numbers of Chargers for Battery Electric Vehicles", *Energies*, Vol. 11, pp. 3056-3078.
5. Cui, S. H., Wen, H J., Zhang, C P., Zhao, H, 2018 b, "Locating Multiple Size and Multiple Type of Charging Station for Battery Electricity Vehicles", *Sustainability*, Vol. 10, pp. 3267-3288.
6. Chu, X W., Lam, A Y S., Leung, Y W, 2014, "Electric Vehicle Charging Station Placement: Formulation, Complexity, and Solutions", *IEEE Transaction on Smart Grid*, Vol. 5, pp. 2846-2856. (Chu, X., W. et al., 2014)
7. Du, H. M., Gao, Z. Y., Zheng, J. F., Zhu, Z. H, 2016, "Charging station location problem of plug-in electric vehicles", *Journal of Transportat Geography*, Vol. 52, pp. 11-22.
8. EPE (Empresa de Planejamento Energético), 2020, "Balaço Energético Nacional. Relatório (2020)" Disponível em: < <https://www.epe.gov.br/pt/publicacoes-dados-abertos/publicacoes/balanco-energetico-nacional-2020>> . Acessado em 19/08/2021
9. EPE (Empresa de Planejamento Energético), 2021, "Balaço Energético Nacional. Relatório (2021)" Disponível em: < <https://www.epe.gov.br/pt/publicacoes-dados-abertos/publicacoes/balanco-energetico-nacional-ben>> . Acessado em 19/08/2021
10. Feng G., Kong, W., Li, K., Luo, Y., Peng, H.: Optimal location planning method of fast charging station for electric vehicles considering operators, drivers, vehicles, traffic flow and power grid. (2019). *Energy* 186
11. Gregolin, J., Höffmann, W., Faria, L., Quoniam, L., Queyras, J., Fratucci L., Cesar G., 2004, "Análise da produção científica a partir de indicadores bibliométricos". *Indicadores de Ciência, Tecnologia e Inovação em São Paulo* v. 5.
12. Guimarães, V. A., Lima, R. P. C., Azevedo-Ferreira, M. A., González, P. H., 2020, "Carbon regulation policies in transport: a review". In: *Proceedings of the III Ibero-American Conference on Smart Cities*. Costa Rica.
13. Guimarães, V. A., Ribeiro, G. M., Ferreira, M. A, 2018, "Mapping of the Brazilian scientific publication on facility location". *Pesquisa operacional*, Vol. 38, pp. 307-330.
14. Hosseini, M., MirHassani, S A, 2015, "Selecting optimal location for electric recharging stations with queue", *KSCE Journal of Civil Engineering*, Vol. 19, pp. 2271-2280.
15. IEA: *Global EV Outlook 2021* (2021), <https://iea.blob.core.windows.net/assets/ed5f4484-f556-4110-8c5c-4ede8bcba637/GlobalEVOutlook2021.pdf>, last accessed 29/09/21.
16. Islam, M M., Mohamed, A., Shareef, H, 2016, "Optimal siting and sizing of rapid charging station for electric vehicles considering Bangi city road network in Malaysia", *Turkish Journal of Electrical Engineering and Computer Sciences*, Vol. 24, pp. 3933-3948.
17. Kazemi-Karegar, H., Rajabi-Ghahnavieh, A., Sadeghi-Barzani, P, 2014, "Optimal fast charging station placing and sizing", *Applied Energy*, Vol. 125, pp. 289-299.

18. Krishna, P., Krishna, K., Kuladeep, M., Kumar, G.: The Importance of Transport and Logistics Services in Green Supply Chain Management. *International Journal of Innovative Technology and Exploring Engineering* 1(6), (2012)
19. Laporte, G., Madsen, O B G., Norrelund, A V., Olsen, A., Wen, M, 2014, "Locating replenishment stations for electric vehicles: application to Danish traffic data", *Journal of the Operation Research Society*, Vol. 65, pp. 1555-1561.
20. Lin, C C., Wang, Y W, 2013, "Locating multiple types of recharging stations for battery-powered electric vehicle transport", *Transportation Research part E-Logistics and Transportation Review*, Vol. 58, pp. 76-87.
21. Office of energy efficiency & renewable energy: Median Driving Range of All-Electric Vehicles Tops 250 Miles for Model Year 2020. Disponível em: <<https://www.energy.gov/eere/vehicles/articles/fotw-1167-january-4-2021-median-driving-range-all-electric-vehicles-tops-250#:~:text=The%20median%20EPA%20estimated%20range,Protection%20Agency%2C%20Fuel%20Economy%20website>> Acessado em 25/08/2021
22. Onata, N., Kucukvarb, M., Aboushaqraha, N., Jabbara, R.: How sustainable is electric mobility? A comprehensive sustainability assessment approach for the case of Qatar. *Applied Energy* 250, 461-477 (2019).
23. Tan, C W., Tie, S F., 2013, "A review of energy sources and energy management system in electric vehicles", *Renewable and Sustainable Energy Reviews*, v. 20, pp. 82–102
24. Sanchari D., Karuna k., Pinakeswar M., Tammi K., 2018, "Review of recent trends in planning for electric vehicles", *Wiley Interdisciplinary Reviews-Energy and Environment*, Vol. 7.
25. Verneque F., Azevedo-Ferreira M., Guimarães, V. de A., 2021, " The role of the electrical vehicle in sustainable supply chains: a review", III Ibero-American Congress of Smart Cities ICSC-CITIES 2020
26. Vries H., Duijzer E., 2015, "Incorporating driving range variability in network design for refueling facilities", *Omega*, Vol. 69, pp. 102-114.
27. Zheng, X., Lin, H., Liu, Z., Li, D., Llopis-Albert, C., Zeng, S.: Manufacturing Decisions and Government Subsidies for Electric Vehicles in China: A Maximal Social Welfare Perspective. *Sustainability*, 1-38 (2018)
28. Xiang, Y., Zhang, Y, 2017, "Optimal Location of Charging Station of Electric Bus in Battery Replacement Mode", *International Symposium for Intelligent Transportation and Smart City*, Vol. 62, pp. 113-125. (Xiang, Y. et al., 2017)

## Solar-driven drinking water supply in rural areas: Jutiapa (El Salvador) experience

Alfonso García Álvaro <sup>[1, 2]</sup>, Sara Gallardo Saavedra <sup>[2]</sup>, Raúl Muñoz Torre <sup>[1]</sup>, Alberto Redondo Plaza <sup>[2]</sup>, Diego Fernández Martínez <sup>[2]</sup>, Víctor Alonso Gómez <sup>[2]</sup>, Ignacio de Godos Crespo <sup>[1, 2]</sup>\*

<sup>1</sup>University of Valladolid, Institute of Sustainable Process, Valladolid, Spain,

<sup>2</sup>School of Forestry, Agronomic and Bioenergy Industry Engineering (EiFAB), Soria, Spain

\*Corresponding author

### Abstract.

Implementation of drinking water systems is limited in rural areas with reduced electrical connectivity. Water extraction from groundwater wells powered by solar light offers a sustainable and low-cost solution easy to replicate. Under an international cooperation program, a complete unit of drinking water supply was designed and installed in Jutiapa (El Salvador) providing high quality water for at least 160 families. Selection of equipment and sizing was based on the simulation of available solar energy and equipment consumption performed by specific software. This approach indicates that solar power installed should be slightly oversized to ensure water supply, although that configuration will result in energy losses. In the light of the results battery accumulation is not recommended since water storage tanks can match energy availability and water requirements. The resulting design will serve as prototype for similar communities in the area, therefore the know-how generated will be made available to municipalities through the collaboration with NGOs (Non-Governmental Organizations).

**Keywords:** Distributed generation, Drinking water, Renewable Energies, Rural areas, Innovation in cooperation

## 1 Introduction

### 1.1 Drinking water supply challenge

771 million people worldwide still lack elementary water services, that means safe drinking water and sanitation systems. Among these, 80 percent live in rural areas and nearly half live in the least developed countries [1]. Which means a large population at health risk due to consumption of untreated water containing pathogens, chemicals or undesired materials. This issue has been addressed in the Sustainable Development Goals (SDG) set up by United Nations in 2015 under SDG number 6: Clean Water and

2

Sanitation [2]. The solutions provided by the organizations and the different stakeholders involved in the water sector include improvements in the information about water resources, optimized financing of local communities and innovation in the technologies applied. In case of drinking water systems placed in rural areas of emergent nations the implementation of water facilities is limited not only by the economic resources of municipalities but by general development of the areas. Isolated rural areas of extended areas of Africa and Latin America are barely connected to the electrical grids [3]. Therefore, conventional drinking water facilities, which requires electricity for pumps, mixers and filtration units are rarely implemented. In this sense, distributed generation technologies based on renewable energy coupled to small scale water treatment units can provide a new model for drinking water supply [4]. In case of rural communities (100 to 500 inhabitants) with access to groundwater reservoirs, photovoltaic panels coupled to pumping and filtering devices are a doable alternative with very low capital and operational costs.

### **1.2. The case study in Jutiapa (El Salvador)**

In case of El Salvador, only 50 % of inhabitants of the rural areas have access to clean drinking water and only 38 % have a piped connection at home [5]. However, groundwater reservoirs are relative common and wells are easily constructed by local communities. During last decades drinking water facilities powered by oil or diesel generators have been installed in small isolated rural communities, with the involvement of NGOs and cooperation programs. Substitution of fuel generators by photovoltaic panels reduces GHG emissions and oil dependency, ensuring water supply even in very low-income communities.

Financed by the Spanish Agency of International Development Cooperation (AECID) a demonstration unit for drinking water supply for 160 families was developed and installed in Jutiapa (El Salvador). Solar panels were used for the energy required by pumping, filtration and water treatment previous to its distribution. Simulation of consumption and available solar energy was performed under the local climatic conditions considering available commercial panels. This approach allowed for the development of a model system that can be easily used for installations design in similar communities.

## 2 Materials and Methods

### 2.1 Jutiapa community and water demand

The demonstration unit is placed in Jutiapa, Department of Cabañas (El Salvador). Four villages with a total population of 545 inhabitants, mainly dedicated to farming activities, were lacking of drinking water at home. The agglomerations are located between the coordinates 13°57'13'' (North), 13°56'20'' (South), 88°48'34'' (East) and 88°49'05'' (West). Calculation of water requirement were done according to the standards value reported by UN of 90 liters per person and day. Population variation was considered for a period of 20 years taking into account the average annual increase of the region (0.06 %). Although small manufacture industries are located in the area, water demand was only calculated considering domestic consumption.

The groundwater reservoir is available through a 100 m depth well placed at 500 meters from distribution tank (99 m<sup>3</sup>). Raw water characteristics are depicted in table 1. Most of the parameters were within the allowable limits for human consumption. However, heterotrophic plate count was far above the recommended values (100 UFC/ml). In this sense, the water treatment was designed to accomplish the elimination of microorganisms present in the water (see section 2.2).

**Table 1.** Groundwater characteristic in Jutiapa (El Salvador) reservoir

Parameter	Value
pH	7.7
Sodium (mg/l)	<10
Total Suspended Solids (mg/l)	370
Sulfates (mg/l)	24
Turbidity (NTU)	0.49
Heterotrophic plate count (UFC/ml)	4,400
Alkalinity (mg/l)	220

### 2.2 Installation for drinking water supply

The design of the water treatment unit driven by solar light was based in conventional groundwater extraction from wells (see figure 1). A submergible pump introduced into the well extracts water at average flow of 49 m<sup>3</sup>/d, according to the possible water consumption of the community. A sand filter is connected to the pipe in order to remove suspended solids and microorganisms. Hypochlorite is dosed by a specific pump before distribution tank with a volume of 99 m<sup>3</sup>, this treatment will remove heterotrophic bacteria present in water. A net of pipes delivers water to family houses from the tank. Solar panel connected to an inverter supply the energy to all the equipment.

4

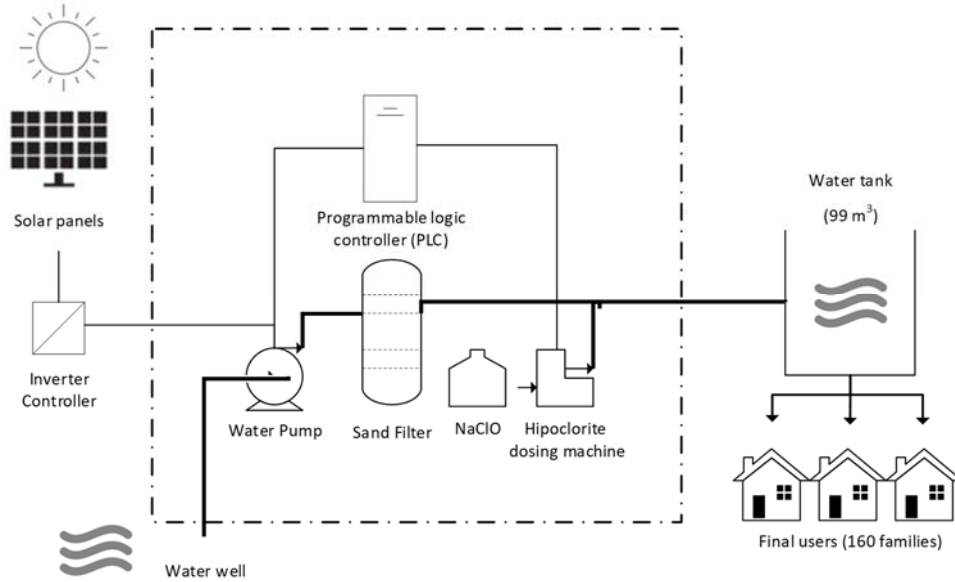


**Figure 1.** Equipment diagram of the water treatment unit.

### 2.3 Simulations of conditions

PVSyst V7.2.2 software was used to estimate the power requirements. Solar irradiation availability in the selected area was estimated with Meteonorm software.

### 2.4 Photovoltaic system description

The photovoltaic (PV) solar module chosen is a generic model 385 W peak power with Si-mono technology and a size of 0.992 m width per 1.962 m length composed by 72 cells. The PV field orientation is tilted 19/0°. The specifications are depicted in table 2 Technical specifications of solar module 385Wp general device. IV diagram at different irradiation levels is showed in the figure. The maximum power delivered by the panel are 359 W, for an irradiation of 1000 W/ m<sup>2</sup>, 287.6 W for an irradiation of 800 W/m<sup>2</sup> 215.2 W for an irradiation of 600 W/m<sup>2</sup>, 142.2 W for an irradiation of 400 W/m<sup>2</sup> and 69.3 W for an irradiation of 200 W/m<sup>2</sup>

**Table 2.** Technical specifications of solar module 385Wp general device. 1.

Reference temperature	25 °C	Reference irradiance	1000 W/m <sup>2</sup>
Open circuit voltage	50.0 V	Short-circuit current	9.83 A
Max. power point voltage	41.4 V	Max. power point current	9.32 A
Maximum power	385.5 W	Isc temperature coefficient	3.9 mA/°C

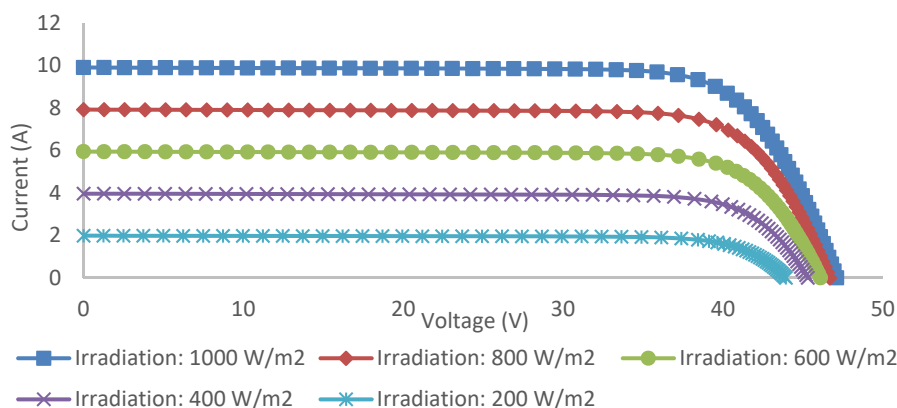


**Figure 2.** Performance of the PV module 385 Wp general device under different irradiation conditions Intensity values (A) in X axis and voltage (V) y axis.

The inverter chosen is a generic model MPPT-AC (Maximum Power Point Tracker – Alternating Current), 5.5 kW nominal power. The specifications are the next (see table 3 and figure 3):

6

**Table 2.** Technical specifications of inverter 5.5 kW general device.

Nominal Power	5500 W	Minimum MPP Voltage	290 V
Power threshold	55 W	Maximum MPP Voltage	480 V
Maximum efficiency	95.0%	Maximum Input Current	8.4 A

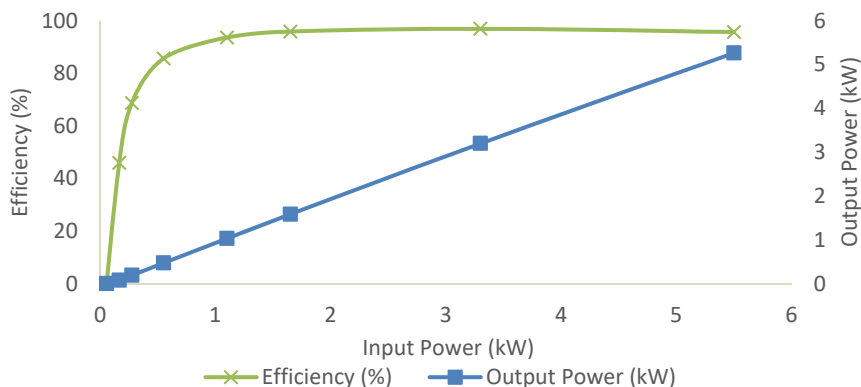


**Figure 3.** Performance of the inverter 5.5 kW general device under different input power conditions.

A submersible pump with a centrifugal multistage technology and an AC motor of 5.5 kW was selected for water extraction from well. The pump operation conditions for a constant water flow 49 m<sup>3</sup> per day are shown in table 3 and figure 4.

**Table 3.** Operation conditions of submersible pump 5.5 kW generic model.

	Head minimum	Head nominal	Head maximum
	1020 KPa	1246 KPa	1413 KPa
Flowrate (m <sup>3</sup> /h)	12.00	8.00	4.00
Requirement power (W)	5863	4944	3737
Efficiency (%)	58.0	56.0	42.0

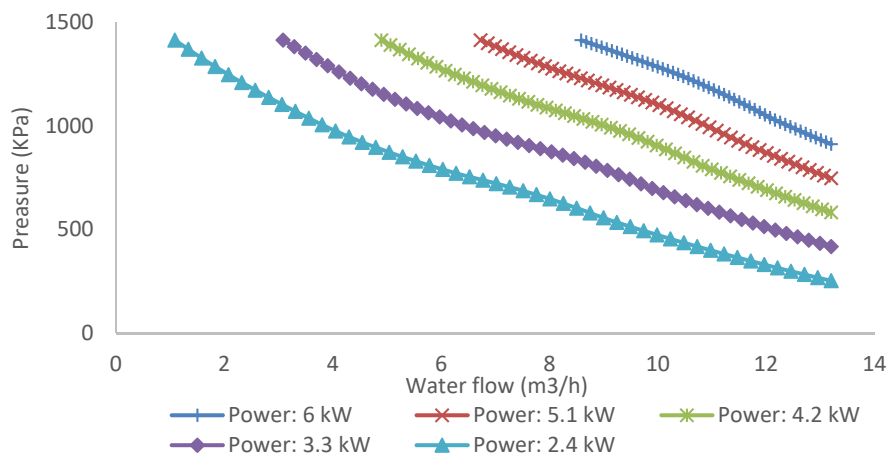


**Figure 4.** Water flow capacity of the submersible pump 5.5 kW generic device under different pressure conditions.

A System operating control device adjusts the operation parameters according to the water level at the tank. Well pump is controlled by a float buoy with an output signal. transmitted through radio waves by two antennas. It was decided to use large water storage tank (99 m<sup>3</sup>) to serve as an energy accumulator instead of electric energy storage batteries, which involved operational and installation costs that could be hardly be borne in rural areas of El Salvador.

Prior to the selection of equipment and sizing of devices three different scenarios were simulated corresponding to different number of PV solar modules: 1, 2 and 3, corresponding to 21, 24 and 30 modules, respectively.

### 3 Results and Discussion

According to the meteorological data available, monthly effective irradiance ranged between 148.2 and 201.4 kWh/m<sup>2</sup>, while the temperature is between 24.9 and 26.09 °C (see figure 5). In spite of the seasonal fluctuations of the rainfall, the level of the ground-water reservoir should be sufficient for the required supply; this fact was verified with the local authorities.

8



**Figure 5.** Meteo conditions (Irradiance and temperature) per month in Jutiapa (El Salvador).

In order to check the suitability of the proposed scenarios according to the water needs throughout the year the percentage of compliance was studied (see figure 6). In this sense, water supply could be compromised in case of scenario 1, with the lower level of installed power, resulting in a compliance value of 84.5% of the required water. Percentage of compliance was increased at higher levels of installed power: 93.2% and 98.7%, in scenario 2 and 3, respectively.

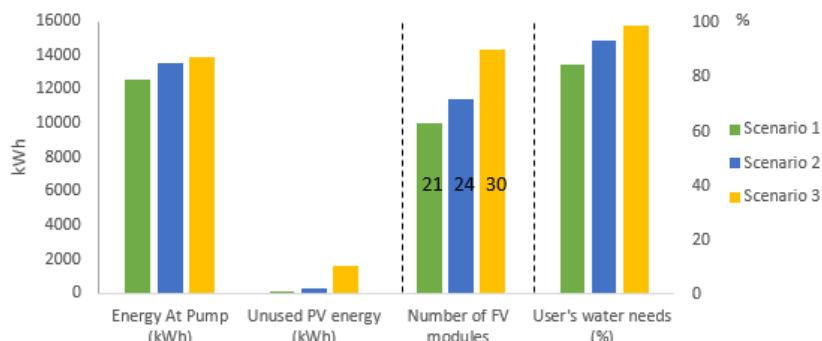


**Figure 6.** Balances and main results in the three scenarios

On the other hand, efficiency of the system, measured in terms of energy lost, presented the opposite behavior (see figure 7). In this sense, the system must be configured for optimum operational and environmental performance. Scenario 1 presented the better PR value (System Performance Ratio) with 73.9 %. Energy losses resulted in considerable reduced performance in scenario 2, 69.5 %, and scenario 3, 57.2%. The low PR data in scenario 3 is due unused energy involved in pumping at moments of low water demand.

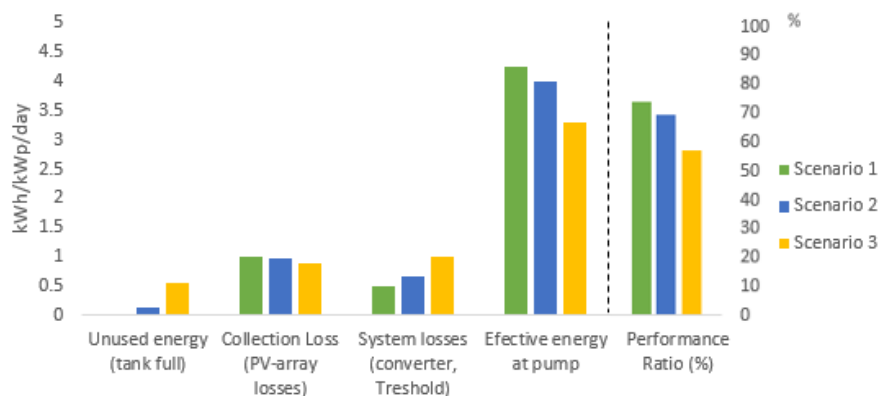


**Figure 7.** Normalized productions (per installed kWp) in the three studied scenarios

Accumulated energy losses in the PV-system was studied. The loss diagram (see figure 8) provides a insight look into the quality of the PV system scenarios, identifying the main sources of losses. The array losses start from the rough evaluation of the nominal energy, using the global effective irradiance. Then it gives the detail of the PV model behaviour according to the environmental and equipment parameters.

The main factor of losses the system is the water pump due to a efficiency of 49.40%. The summarized energy losses are shown in table 4. Beside this, the efficiency of the solar panels present a high impact with a 19.80% of energy production from the global irradiation (standard value).

**Table 4.** Effective energy in each process step per scenario. Loss diagram.

	Scenario 1	Scenario 2	Scenario 3
Global horizontal irradiation (kWh/m <sup>2</sup> )	2042	2042	2042
Effective irradiation on collectors (m <sup>2</sup> )	41	47	58
Array nominal energy (kWh)	16479	18833	23541
Array virtual energy at MPP (kWh)	14079	16091	20113
Electrical Looses (kWh)	12571	13816	15474
Operating electrical energy at pump (kWh)	12555	13500	13880
Hydraulic energy at pump (kWh)	5757	6413	6859
Water volume pumped (m <sup>3</sup> )	15112	16670	17648
User's water needs (%)	84.5	93.2	98.7

10

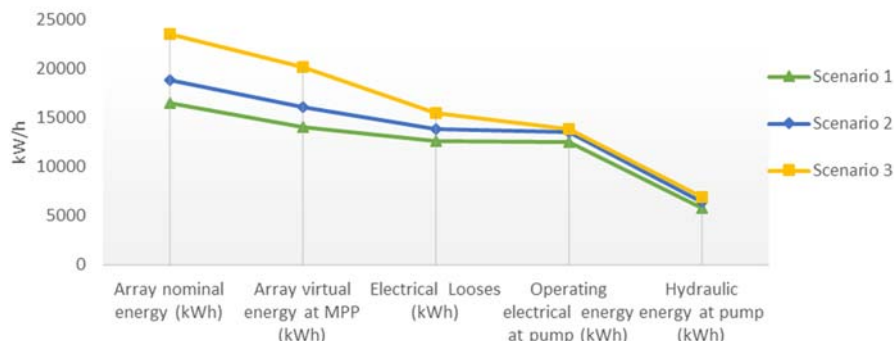


Figure 8. Effective energy in each process step per scenario. Loss diagram.

Similar works in the field of photovoltaic water pumping have reported comparable systems in isolated conditions in other regions of Asia and Africa [6], [7]. Naval et al. (2021) also proposes a pumping system based on photovoltaic energy since the increase in the cost of energy of the water pumping facilities puts at risk the economic sustainability of the recent investments in the modernization of the systems. To address this problem, the application of renewable technologies for the production of electricity is essential, and photovoltaic energy is especially attractive due to its reduced cost and recent technological advances [8]. Viability of photovoltaic-based water systems has been reported for irrigation and domestic supply in urban and rural regions of countries with high solar irradiation levels where a considerable part of the rural population lives in remote areas [9].

The use of software simulations allows to design the equipment and shows impact of the different parameters affecting performance results of the system [10]. In this sense, reducing the power of the pumping device results in higher efficiency decreasing the energy losses. However, water supply can be compromised at moments of low irradiation level. In this solar panel devices should slightly oversized in order to ensure water supply along the year. Current prices of solar panels allow rural communities to install sufficient capacity to solve this problem. Batteries are not recommended since large storage tanks will match solar energy availability and water requirements without excess of installation and operational cost.

#### 4 Acknowledgments

This study is being carried out from March 2021 thanks to a grant from AECID (Spanish Agency of International Development Cooperation) within the framework of cooperation and innovation (grant number 020/ACDE/00026).

### Declaration of competing interest

The authors declare that they have no known competing financial interests or personal relationships that could have appeared to influence the work reported in this paper.

### References

- [1] UN-Water, “Summary Progress Update 2021 : SDG 6 — water and sanitation for all,” *UN-Water Integr. Monit. Initiat.*, pp. 1–58, 2021, [Online]. Available: <https://www.unwater.org/new-data-on-global-progress-towards-ensuring-water-and-sanitation-for-all-by-2030/>.
- [2] N. Ferri, “United nations general assembly,” *Int. J. Mar. Coast. Law*, vol. 25, no. 2, pp. 271–287, 2010, doi: 10.1163/157180910X12665776638740.
- [3] IEA, “No Title,” *IEA (2020), SDG7 Data Proj. IEA, Paris* <https://www.iea.org/reports/sdg7-data-and-projections>.
- [4] J. Marsden, “Distributed generation systems: A new paradigm for sustainable energy,” *2011 IEEE Green Technol. Conf. Green 2011*, no. May 2011, 2011, doi: 10.1109/GREEN.2011.5754858.
- [5] M. Ballesteros, V. Reyes, and Y. Astorga, “Groundwater in Central America: Its importance, development and use, with particular reference to its role in irrigated agriculture,” *Agric. Groundw. Revolut. Oppor. Threat. to Dev.*, pp. 100–128, 2007, doi: 10.1079/9781845931728.0100.
- [6] I.Togola. “Solar energy use water supply of rural areas in East Africa”, [PhD. Thesis], 2003
- [7] Kazem, H.A., Al-Waeli, A.H.A., Chaichan, M.T. et al. Design, measurement and evaluation of photovoltaic pumping system for rural areas in Oman. *Environ Dev Sustain* 19, 1041–1053 (2017). <https://doi.org/10.1007/s10668-016-9773-z>
- [8] Natalia Naval, Jose M. Yusta, Optimal short-term water-energy dispatch for pumping stations with grid-connected photovoltaic self-generation, *Journal of Cleaner Production*, Volume 316, 2021, 128386, ISSN 0959-6526, <https://doi.org/10.1016/j.jclepro.2021.128386>
- [9] Olga V. Shepovalova, Alexander T. Belenov, Sergei V. Chirkov, Review of photovoltaic wa-ter pumping system research, *Energy Reports*, Volume 6, Supplement 6, 2020, Pages 306-324, ISSN 2352-4847, <https://doi.org/10.1016/j.egy.2020.08.053>.
- [10] Rakhi Sharma, Shivanshu Sharma, Sumit Tiwari, Design optimization of solar PV water pumping system, *Materials Today: Proceedings*, Volume 21, Part 3, 2020, Pages 1673-1679, ISSN 2214-7853, <https://doi.org/10.1016/j.matpr.2019.11.322>.

# A study of polystyrene biodegradation through the use of mealworm larvae with application in waste treatment in cities

Maura Arminda Jara Ramos<sup>1</sup>[0000-0002-8638-146X] and Jorge Mirez<sup>2</sup>[0000-0002-5614-5853]

<sup>1</sup> Universidad Andina Néstor Cáceres Velásquez, Juliaca, Peru  
hema.ambiental.3.7@gmail.com

<sup>2</sup> Universidad Nacional de Ingeniería, Lima, Peru  
jmirez@uni.edu.pe

**Abstract.** The experimental biodegradation of expanded polystyrene called "Tecnopor" using mealworm larvae (*Tenebrio Molitor*) under controlled conditions in the city of Juliaca, Peru (3,825 m. Altitude) is reported in this paper. Indicators such as percentage of degradation, consumption capacity and environmental factors of temperature and humidity are presented. The observation period was 47 days with three groups of larvae that resulted in a percentage of biodegradation of the expanded polystyrene of between 8 % to 40 %, therefore, with adequate feeding and constant monitoring, it is an alternative to reduce contamination. and improve environmental quality since Tecnopor is non-biodegradable and has a long degradation period in the environment.

**Keywords:** Biogradation, biomass, expanded polystyrene, *Tenebrio Molitor*.

## 1 Introducción

In the present, the industry that manufactures plastic materials in their interest to satisfy their consumers have created containers of Tecnopor material that is manufactured based on expanded polystyrene. This is used as a container for food and when discarded, these containers go directly to the garbage, generating negative damage to the environment. In the industrial sector, expanded polystyrene is in high demand due to its low cost and malleability as it is used as containers and packaging, however, its degradation is slow and persists in the environment for a period of 1000 years [1,2].

In [3] the life cycle of *T. molitor* in the city of Chaco Argentina is reported, under experimental conditions (laboratory) for this, *T. molitor* larvae were collected in a container with a capacity of 2000 cm<sup>3</sup> and they were reared until adult phase grouping them into two groups of 114 and 96 specimens in the egg phase. As they changed to the larval stage, they were placed in a container labeled 250 cm<sup>3</sup>. In addition, in each phase they switched to the next they were separated and the food they were supplied in small pieces of vegetables, fruits and corn grains. The study was carried out with a maximum and minimum temperature of (22.4 °C ± 5 °C) and humidity of (74.2 % ± 20 %) recorded with a SIAP THG-3 thermohygrograph. The development time of

2

each phase was calculated by recording the data on a daily basis and also the mortality of these. The monitoring was carried out for 14 months and the results were obtained. The egg phase occurred approximately 11.5 days of the females, the duration of the larval phase is the longest, therefore it is more than a month [3].

In [4] the percentage of degradation of different plastics when used as food for *T. molitor* larvae is determined; 4 groups of 11 larvae are used, with 13g. of weight, to later assign plastics as food to each group, so each group was given 25g. of plastic material leaving it as food for a month and a half in a suitable climate (environmental conditions). After 45 days, the mass measurement and counting of the larvae was carried out, obtaining as a result that the percentage of degradation, in the 1st polystyrene sample was 96% and the final quantity of larvae is 10, in the 2nd sample of diapers 68%, the final number of larvae is 8, and; in the 3rd sample of garbage bag, 64% and the final quantity of larvae equal to 8, finally, in the 4th sample of Styrofoam, 84%, and the final quantity is 8 larvae.

In [5] the potential for use of the mealworm in the degradation of polystyrene is determined. For this, three tests were carried out: (a) One of the treatments was used polystyrene in the form of a bed of reduced particles of a size less than or equal to 0.5 cm of Tecnopor with a total weight of 30 g, made by rubbing against another fragment of Tecnopor, because in this way, these small fragments come off in the form of circumferences that measure no more than 0.4 cm. (b) The 2nd treatment polystyrene was used as a bed with a weight of 30 g. and a measure greater than 1 cm and less than or equal to 5 cm made by dividing with the hands of pieces of polystyrene greater than one centimeter. (c) And the 3rd treatment was used as a base or saved substrate with a determined weight of 30g. The results indicate that the 1 cm polystyrene blocks facilitate feeding to *T. Molitor*.

In [6] the ubiquity of polystyrene digestion and biodegradation within yellow mealworms (larvae of *T. Molitor* Linneo Coleoptera: Tenebrionidae) is studied to evaluate whether *T. Molitor* can survive eating foam made of polystyrene (PS). Responses in 22 countries indicated that *T. Molitor* consumed PS foam in North America (Canada, Mexico, USA); Asia (Cambodia, Japan, Indonesia, Iran, Israel, South Korea, Thailand); Europe (Finland, France, Poland, Slovenia, Spain, Turkey, United Kingdom); Africa (Nigeria, South Africa) and islands. Based on these results, chewing and ingesting PS is an adaptive behavior intrinsic to yellow *T. molitor*. Students at Marshall School (Duluth, MUNSA) reported 33 mg of degraded PS per 100 worms. For *T. Molitor*, survival at 32 days fed with PS, exceeded 80% for wheat flour with PS plus bran. The degradation was for *T. molitor* fed only with bran (88-90%), and PS only (83-92%) than for those not fed (69-76%). Being, the highest observed, in *T. Molitor* fed with PS plus bran (95%) during a period of 34 days. In the 98-day trials fed only PS it coincided with those fed PS plus saved during the initial incubation phase (95.5% versus 98.0%), then it fell to low levels. Investigations revealed that *T. Molitor* fed only PS did cannibalism in the order of between  $11.8 \pm 1.1\%$ , and  $11.5 \pm 4.9\%$  fed only PS. PS contains only hydrogen and carbon, and does not provide adequate nutrition (N, P, N, a, K elements, amino acids, etc.) for long-term survival and growth, therefore the addition of bran alleviated this restriction. In the absence of

bran, they survived by consuming dead *T. Molitor* and its molts (about 12% of the original population).

In [7] they analyze the biodegradation process of plastic with the larvae of the *T. molitor* beetle under the biological characterization methodology describing the breeding and biodegradation bioassay of plastics. They report that the consumption of polystyrene (Icopor) is higher than that of low-density polyethylene (plastic bag). Being the productivity percentage for sample 1 and 2 of Icopor of 5% and 8%, unlike samples 3 and 4 of the plastic bag, they presented a productivity percentage of 0.5% and 1.5%. In addition, sample 1 of Icopor started with 25 larvae and ended with 3, with a consumption of 0.1g, unlike sample 2, which started with 30 larvae and ended with 7, with a consumption of 0.16g. And for samples 3 and 4 of the plastic bag, which started with 25 and 30 larvae and ended with 9 and 7 larvae, a consumption of 0.01g and 0.02g was obtained.

In [8] the biodegradation of Tecnopor by the mealworm (larva) is investigated to determine to what extent it contributes to the production of compost. As results they obtained that the consumption of Tecnopor in 8 days is 0.0903g. and 4 days is 0.0416 g. For average biomass variation, the 8-day treatment is -0.1681 g., 4 days is -0.0848 g. And for the average excreta in 8 days it is 0.0843 g. and 4 days is 0.0307 g.

According to [9], the physical composition of the solid waste known as municipal, is found in the Characterization of Tecnopor in a percentage of the districts: Juliaca (1.54%), San Miguel (2.11%), Cabanillas (1.68%), Cabana (0.92%), and Caracoto (2.67%) and total of 1.78% of Tecnopor of 20 common residues generally found.

Population growth has led to easy consumerism with the use of Tecnopor plates and glasses, since these objects are polystyrene polymers that are used in disposable containers and that at the same time it is an object that generates a negative impact on the environment creating a series of problems to the biotic environment.

From a quantitative approach, the inappropriate use of polystyrene involves negative effects in different sectors: as in the health sector through its use in food that causes diseases; also due to contamination of water, soil, air and landscape pollution.

What motivates to investigate on the amount of degradation of the polystyrene (Tecnopor) using larvae of *Tenebrio Molitor* under controlled conditions, which is justified in the technical, economic, social and environmental aspects. In the technical aspect, creating a treatment plant with the use of larvae would be a good option since this research provides data and evidence that could be a solution. In the economic aspect, the use of the larvae will bring with it an economic decrease compared to large plants, which is why the degradation of the polystyrene would be an alternative, likewise to obtain fertilizers. In the social aspect, this research brings the opportunity for residents of the city of Juliaca to propose this degradation system, not only that but to coordinate with the municipalities to reduce these polystyrene materials (Tecnopor). On the other hand, it is necessary to become aware of the affectation, since the inhabitants tend to get sick as the day goes by, for this it would be necessary to train the population in order to give our new generations a healthy environment. Likewise, the social is favored by obtaining an environmental culture in people, in such a way that the quality of life changes, creating a change in attitude and participation in the population. And in the environmental aspect, the degradation of polystyrene is an alterna-

4

tive for its reduction in the environment, since the worm (*Tenebrio Molitor*) has the ability to degrade these materials considering part of its food chain in a certain percentage. On the other hand, the environmental part also benefits from the degradation of polystyrene, since this would lead to greater conservation of natural resources, as well as the reduction of sources of contamination, since the population has discarded what they no longer consume. and during his evolution he tends to opt for the easy.

## 2 Theoretical Framework

### 2.1 *Tenebrio Molitor*

*T. Molitor* is a hexapod insect that corresponds to the family "Tenebrionidae", it belongs to the genus *Tenebrio*, they are of the coleoptera order and are in the *Molitor* species. They are found in warehouses or mills [4,11].

*Tenebrio Molitor* are larvae of two species of dark beetles; *tenebrio Linnaeus* (yellow mealworm beetle) and *tenebrio obscurus Fabricius* which is less common beetle is small dark. *T. molitor* goes through a life cycle, egg, larva, pupa, and beetle. The larvae hatch from eggs, they are 3 mm long, they are whitish after a few days these larvae produce a hard exoskeleton, contain chitin and take a yellowish color, an adult larva has a weight of 0.2 g. and it is 25 and 35 mm long, the pupa 12 to 18 mm long and has a creamy white color. The *T. Molitor* (mealworm) is widely spread throughout the world. The *tenebrio molitor* are originally from Europe [10].

The development of the life cycle of *T. Molitor* lasts between 4 to 5 months in 4 phases and they develop at an optimal temperature of 28 ° C and the stages or phases of the life cycle of *Tenebrio Molitor* are: Egg Phase: It has a phase of incubation for 10 days; Larva Phase: During its growth at maturity it changes its skin, this in a period of 2 to 3 months; Pupa Phase: It has a triangular shape, during 20 days it passes to the hardened phase, usually static and arched, and; Beetle Phase: They are born with an ivory tone, during 2 to 3 days it changes to a brownish black tone. They live for approximately 2 to 3 months. And at 10 days oviposition begins, giving 4 to 5 months to complete its life cycle. The larval stage has 6 prolegs, a dark and small head, it is orange-yellow in color. And in the adult phase it has wings with elongated stripes, it is reddish brown, almost persistently shiny black [5].

The *T. Molitor* avoid light and prefer dark and quiet places, when the temperature remains between 22 to 28 °C the *tenebrio* live, grow and reproduce without any problem and no harmful parasites were registered but it is estimated that the mite acts as predator [12]. The live *tenebrionum* is composed of 62% water, 20% protein, 13% fat and 2% fiber, while the dried larvae are composed of 53% protein, 28% fat, 6% fiber, and 5% water. Its chemical composition can vary according to its diet, stage of development and habitat [13].

The larvae serve as food for fish, birds, broilers, reptiles, amphibians and mammals. Nowadays these organisms are a protein alternative. Corn tortillas with *tenebrionum* can be made for human consumption. And the production of feces, serves for compost). Likewise, it is excellent food for fish, whether in the form of flour or live [14]. The *tenebrio* are considered a pest because they are flour consumers, since they

represent 50% production losses. But in human and animal nutrition, they are an excellent source of protein [15].

## 2.2 Expanded Polystyrene

PS (Polystyrene) also called thermoplastic has many desirable properties such as: transparency, ease of coloring and ease of production and has good thermal and mechanical properties, it is light, brittle and softens at a temperature lower than 100 ° C. Polystyrene has lower density, has good thermal stability and low economic cost, but some of the physical properties of polystyrene can be unfavorable and these can be brittle and rigid. The disadvantages that it presents can be solved by copolymerizing the styrene with other polymers and monomers [16,17].

PS is a polymer that has no shape (amorphous) and in the market it is marketed in four different qualities and shapes [16, 18] including expanded polyethylene. Expanded polystyrene has a content of 95 % air and 5 % polystyrene, these are easy to mold into different shapes and the one that has the greatest use are containers and packaging, containers such as disposable cups and plates, and lower-density products. , the physical characteristics of expanded polystyrene call it suitable and light, for electromagnetics in these packages are used since they have high resistance to impacts and humidity and these are white and have porosity. This type of polystyrene is used in the manufacture of PS (polystyrene) foam, obtaining polystyrene is by molding in which steam is used where pentane ( $\text{CH}_3$ ) is present as a foaming agent. [1,17].

## 3 Experiments and Results

### 3.1 Description of experiment

The technique used was experimental observation, whose procedure to determine the percentage of degradation of polystyrene (Tecnopor) used as food for the larva mealworm (T. Molitor) is as follows:

First: Expanded polystyrene (Tecnopor) pieces were made from recycled packaging of disposable plates and cases for electronic television devices, CD cases. To later be consumed by the Tenebrio Molitor larvae and be a protective means while they adapt to the temperature of Juliaca.

Second: To measure the size of the larvae, a rule was used considering the size of each larva, likewise the temperature of the day was taken into account.

Third: T. Molitor larvae are counted and then placed in test containers. For this, the samples were labeled as, M1-1; M1-2; M2-1; M2-2; M3-1; M3-2, which was distributed the larvae in six lids and a container that was only in a disposable plate container.

Fourth: T. Molitor larvae were weighed, likewise the expanded polystyrene "Tecnopor" was weighed. These data were obtained every 10 days until the end of the Larva phase, which lasted for 47 days. the amount you consume was obtained.

Fifth: The "Tecnopor" expanded polystyrene pieces were placed in the container so that the larvae are in anti-cold conditions and with days the larvae are already

6

adapted. We proceeded with the placement of samples of *T. Molitor* larvae in the six container containers, to then measure the temperature and humidity of each sample.

Sixth: The thermohydrometer was placed in the lids to be able to obtain the result of temperature and humidity in the environment where the *T. Molitor* larvae were kept. The temperature and humidity readings were then recorded. This was done during the 12 hours of the 47 days.

### 3.2 Results

It is experienced for 47 days, with 1,400 larvae, an average maximum temperature of 18 °C with a standard deviation of 0.74, and; the average minimum temperatures was 16.15 °C and with a standard deviation of 1.26 °C (see Fig. 1). Similarly, the average relative humidity was 45.6% with a standard deviation of 3.54 (see Fig. 2).

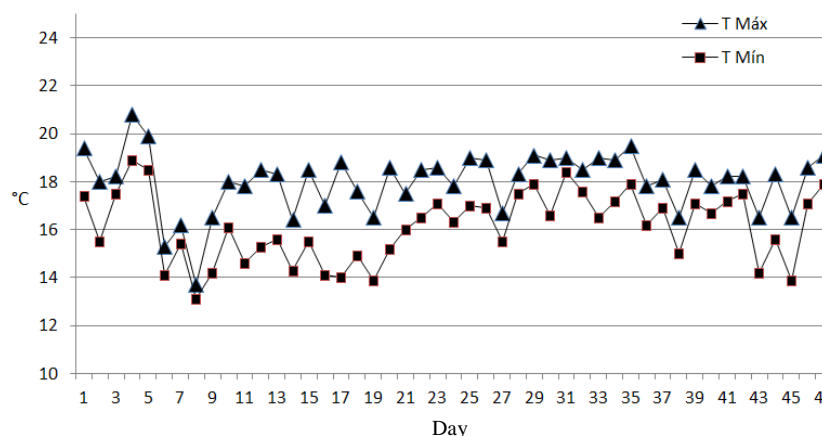


**Fig. 1.** Evolution of the maximum ambient temperature (T Max) and minimum (T Min) during the development days of the experiment.

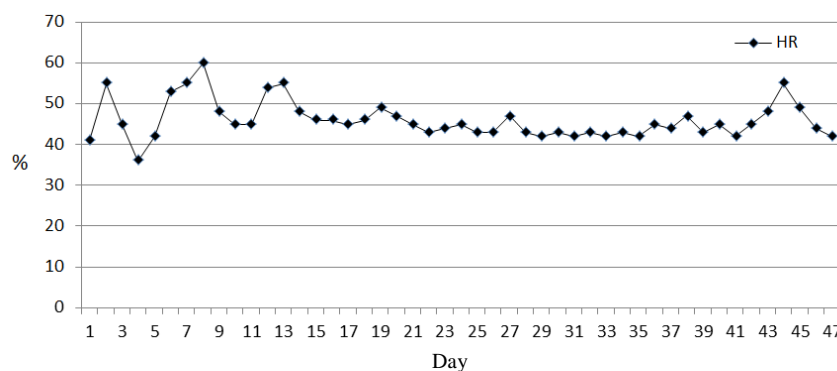


**Fig. 2.** Evolution of ambient relative humidity (RH) during the development days of the experiment.

**Results 1.** Weight of polystyrene (Tecnopor) for each sample during 47 days of interaction with larvae.

In Table 1 is showed the results obtained after 47 days; the polystyrene consumed is on average 0.4 g in the M1 samples, 0.5 g in the M2 samples and 0.75 g in the M3 samples.

**Table 1.** Weights of polystyrene (Tecnopor) for each sample during 47 days of larvae of "Tenebrio Molitor".

N°	Number of larvae	Sample	Weight 1 (Day 1)	Weight 2 (Day 10)	Weight 3 (Day 20)	Weight 4 (Day 30)	Weight 5 (Day 40)	Weight 6 (Day 47)
1	100	M1-1	2.8	2.8	2.7	2.6	2.5	2.4
2		M1-2	2.9	2.8	2.7	2.6	2.5	2.5
3	250	M2-1	4.3	4.2	4.1	4.0	3.9	3.8
4		M2-2	4.3	4.2	4.1	4.0	3.9	3.8
5	350	M3-1	6.7	6.5	6.4	6.3	6.1	5.9
6		M3-1	6.8	6.5	6.4	6.3	6.2	6.1

**Results 2.** Weight of the "Tenebrio Molitor" larvae for each sample during the 47 days.

In Table 2 is showed the results obtained after 47 days about the weight of the larvae. This has increased an average of 0.5 g in samples M1, 0.65 g in samples M2 and 0.80 g in samples M3.

**Table 2.** Weights of the "Tenebrio Molitor" larvae during the 47 days with different amounts of samples.

N°	Number of larvae	Sample	Weight 1 (Day 1)	Weight 2 (Day 10)	Weight 3 (Day 20)	Weight 4 (Day 30)	Weight 5 (Day 40)	Weight 6 (Day 47)
1	100	M1-1	6.80	6.90	7.00	7.10	7.20	7.30
2		M1-2	5.70	5.80	5.90	6.10	6.20	6.20
3	250	M2-1	16.20	16.30	16.40	16.50	16.70	16.80
4		M2-2	17.40	17.50	17.80	17.90	18.00	18.10
5	350	M3-1	23.40	23.70	23.80	23.90	24.00	24.20
6		M3-1	22.80	23.00	23.20	23.30	23.40	23.60

**Results 3.** Disposable plate Tecnopor degradation from 300 larvae.

This result, of the 300 larvae was made as food to the recycled polystyrene of a disposable plate, likewise, three 135 g bears were fed flour, Quaker oats, and fruits to rehydrate such as apple, banana, these each weighed 100 g, during all 47 days.

**Table 3.** Consumption of reused polystyrene from disposable plate.

Nº	Number of larvae	Sample	Polystyrene Starting Weight (Day 1)	Final polystyrene weight (Day 47)	Polystyrene consumption [g]
1	300	Unique	10.20	7.40	2.80

**Table 4.** Variación de la masa de larvas.

Nº	Number of larvae	Sample	Starting weight [g] (Day 1)	Final weight [g] (Day 47)	Variation of the weight of larvae [g]
1	300	Unique	28.30	24.90	-3.40

#### 4 Discussion

Environmental factors influence the development of each stage, also considering that the city of Juliaca, Peru is located at 3,825 meters of altitude. The size and color of *Tenebrio Molitor* larvae change according to feeding.

Dividing the results obtained in Table 1 by the number of larvae in each sample, the reduction in the weight of expanded polystyrene made by each larva is 0.004 g / larva (for M1), 0.002 g / larva (for M2) and 0.0021428 g / larva (for M3) in 47 days. The difference can be explained by the use of containers of the same dimensions for all samples, therefore, in sample M1 there is a smaller stacking of larvae than in sample M3. Dividing the results of Table 2 by the number of larvae in each sample, it is obtained that the increase in weight of the larvae during the 47 days is 0.005 g / larva (for M1), 0.0026 g / larva (for M2) and 0.0022857 g / larvae (for M3) in 47 days (see Fig. 3)

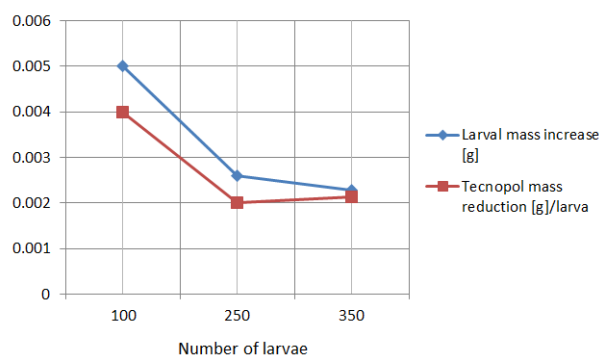


**Fig. 3.** Evolution of the mass of larvae and technopol according to the number of sample larvae.

In the degradation of the Tecnopor recycled polystyrene disposable plate, a higher percentage was degraded than that of the six samples, since this sample was combined with feeding and constant monitoring.

## Acknowledgment

The authors thank the following projects and institutions: (a) CYTED Thematic Network “Ciudades Inteligentes Totalmente Integrales, Eficientes y Sostenibles (CITIES)” N° 518RT0558; (b) too thanks to the support and motivation provided by the Federal University of Maranhão (UFMA), CEMAR, CP ELETÔNICA, CNPq – Brazil, and MEIHAPER CYTED.; (c) Group of Mathematical Modeling and Numerical Simulation (GMMNS) y Center of Communications and Information Technologies (CTIC) in National University of Engineering (UNI), Lima, Peru, for the use of facilities for research development; (d) Project: "Modeling and numerical simulation in oil reservoirs", supported by the Faculty of Petroleum, Gas and Petrochemical Engineering of the Universidad Nacional de Ingeniería, Lima, Peru, and to; (e) Miss Fabiola García Herrera by technical support.

## References

1. Alarcon Lozada, Susan Indira. “Recuperación del Poliestireno Expandido (EPS) con aceite esencial de naranja, Lima 2017”. Tesis para obtener el Título Profesional de Ingeniero Ambiental. Facultad de Ingeniería. Universidad César Vallejo, Peru. Disponible en: [https://repositorio.ucv.edu.pe/bitstream/handle/20.500.12692/3564/Lozada\\_ASI.pdf?sequence=1&isAllowed=y](https://repositorio.ucv.edu.pe/bitstream/handle/20.500.12692/3564/Lozada_ASI.pdf?sequence=1&isAllowed=y)
2. Leon Almaraz, R., & Ramirez Cruz, M. A.: Síntesis, caracterización y aplicación del PS entrecruzado a partir de residuos de PS. In: Revista Iberoamericana de Polímeros. Vol. 8(2), Marzo 2007. Disponible en: <https://reviberpol.files.wordpress.com/2019/08/2007-leon.pdf>
3. Damborsky, M., Bar, P. S. T., & Oscherov, M. E. (2000). Ciclo de Vida de Tenebrio molitor (Coleoptera, Tenebrionidae) en Condiciones Experimentales. Comunicaciones Científicas y Tecnológicas. UNNE 6, (UNNE 6), 35–38.
4. Flores Vasquez, K. P., & Molina Cerron, F. Degradación de Polímeros con Tenebrio molitor. XXVII Congreso de Investigación CUAM-ACMOR. Disponible en: <https://dspace.umad.edu.mx/bitstream/handle/11670/261/7%20Secundaria%20%20Degradaci%3%b3n%20polimeros%20extenso.pdf?sequence=1&isAllowed=y>
5. Coh May, A., Arroyo Chan, J. E., & Canche Contreras, U. A. (2017). Evaluar el potencial de uso del Tenebrio Molitor en la degradacion del poliestireno. ExpoCiencia Campeche 2017. Disponible en: <https://docplayer.es/88392493-Evaluar-el-potencial-de-uso-del-tenebrio-molitor-en-la-degradacion-del-poliestireno.html>
6. Yang, Sang-Sang, Ubiquity of polystyrene digestion and biodegradation within yellow mealworms, larvae of Tenebrio molitor Linnaeus (Coleoptera: Tenebrionidae). Chemosphere. Volume 212, December 2018, Pages 262-271. Disponible: <https://www.sciencedirect.com/science/article/abs/pii/S0045653518315509?via%3Dihub>
7. Dolly Natalia Álvarez Estepa, Lina Marcela Botache Laguna. Biodegradación de plástico con larvas de coleóptero Tenebrio Molitor como un aporte interdisciplinar a la biotecnolo-

10

- gía ambiental. Trabajo de Grado para optar por el título de Licenciada en Biología. Universidad Pedagógica Nacional. Colombia. 2020. Disponible en: [http://repository.pedagogica.edu.co/bitstream/handle/20.500.12209/12205/Biodegradacion\\_de\\_Plastico\\_con\\_Larvas\\_Tm%20%282%29.pdf?sequence=1&isAllowed=y](http://repository.pedagogica.edu.co/bitstream/handle/20.500.12209/12205/Biodegradacion_de_Plastico_con_Larvas_Tm%20%282%29.pdf?sequence=1&isAllowed=y)
8. Daviran Yance, Peter Albert. Biodegradación de la Espuma de Poliestireno por la larva del Tenebrio molitor para la producción de Abono. Tesis para obtener el Título Profesional de Ingeniero Ambiental. Universidad César Vallejo. 2017. Disponible en: [https://repositorio.ucv.edu.pe/bitstream/handle/20.500.12692/22578/Daviran\\_YP.pdf?sequence=1&isAllowed=y](https://repositorio.ucv.edu.pe/bitstream/handle/20.500.12692/22578/Daviran_YP.pdf?sequence=1&isAllowed=y)
  9. Municipalidad de San Román, Región Puno, Perú. PIGARS - MPSJ. (2018). Plan Integral de Gestión Ambiental de Residuos Sólidos PIGARS de la Provincia de San Roman. Juliaca, Peru. Disponible en: <http://munisanroman.gob.pe/portal/sites/default/files/2020-02/Plan%20SOL%20Final%20Nov%202020%2015-01.pdf>
  10. Mariod, A. A., Saeed Mirghani, M. E., y Hussein, I. (2017). Chapter 50 - Tenebrio molitor Mealworm Unconventional Oilseeds and Oil Sources (pp. 331-336): Academic Press.
  11. Fereshteh M. Saeizad, Dewanand Makhan. The first record of Tenebrio molitor Linnaeus, 1758 from Iran, Semnan, Damghan, Cheshmeh-Ali (Coleoptera: Tenebrionidae). Calodema, 286: 1-3 (2013). DOI: 10.13140/RG.2.2.36673.35689
  12. Leonardo Argueta Reyes, Glenda Karina Ramos Meléndez. Contenido de Proteína, Grasa, Calcio, Fósforo en larvas del escarabajo molinero (Coleoptera: Tenebrionidae: Tenebrio molitor L.) alimentadas con diferentes sustratos y fuentes de agua; para ser utilizadas como alimentación de animales silvestres. Tesis para optar el Grado de Licenciado en Medicina Veterinaria y Zootecnia. Universidad de El Salvador. 2013. Disponible en: <https://ri.ues.edu.sv/id/eprint/3536/1/13101364-1.pdf>
  13. Luis Carlos Medrano Vega. Larvas de gusano de harina (Tenebrio molitor) como alternativa proteica en la alimentación animal. Tesis para optar el Título de Zootecnista. Universidad Nacional Abierta y a Distancia – UNAD. Colombia. 2019. Disponible en: <https://repository.unad.edu.co/bitstream/handle/10596/28001/lcmedranov.pdf?sequence=1&isAllowed=y>
  14. Ramos-Elorduy, Julieta; Costa Neto, Eraldo Medeiros; Ferreira dos Santos, Jéssica; et.al. Estudio comparativo del valor nutritivo de varios coleoptera comestibles de México y pachymerus nucleorum (Fabricius, 1792) (Bruchidae) de Brasil. Interciencia, vol. 31, núm. 7, julio, 2006, pp. 512-516. Disponible en: <https://www.redalyc.org/pdf/339/33911807.pdf>
  15. Iliana A. Herrera-Sotoa, Sergio Soto-Simentala, Juan Ocampo-López, et. al. Producción y usos de Tenebrio molitor. Boletín de Ciencias Agropecuarias del ICAP, Vol. 6, No. 12 (2020) 1-4. DOI: <https://doi.org/10.29057/icap.v6i12.5712>
  16. Reynaldo León Almaraz, Mario Albero Ramírez Cruz. Síntesis, caracterización y aplicación del PS entrecruzado a partir de residuos de PS. Rev. Iberoamer. Polím., 8(2), 112-137 (2007). Disponible en: <https://dialnet.unirioja.es/servlet/articulo?codigo=2291747>
  17. M. E. Solís Jara, J. H. Lisperguer Muñoz, L. F. Arencibia Silva. Compuestos Mixtos Poliestireno y Pino Radiata. Revista Cubana de Química. Vol. XVII, No. 3, 2005. Disponible en: <https://www.redalyc.org/pdf/4435/443543687101.pdf>
  18. M. T. Acevedo-Morantes, M. Brieva-Sarmiento, y A. Realpe-Jimenez, «Effect of the molding temperature and cooling time on the residual stresses of crystal polystyrene», DYNA, vol. 81, n.º 187, pp. 73-80, sep. 2014.

## Analysis of the orography for the study of the technical feasibility of urban electric buses in Ávila

J. Martín-Jiménez<sup>1</sup>[0000-0003-4383-9386], S. Del Pozo<sup>1</sup>[0000-0003-4869-3742], M. Sánchez-Aparicio<sup>1</sup>[0000-0002-7931-9561], E. González-González<sup>1</sup>[0000-0002-8025-2464], P. Andrés-Anaya<sup>1</sup>[0000-0001-7708-3260] and S. Lagüela<sup>1</sup>[0000-0002-9427-3864]

<sup>1</sup> University of Salamanca, Ávila 05003, Spain  
joseabula@usal.es

**Abstract.** Lately, there is an increase in the use of electric vehicles, especially in public means of transport with battery electric buses (BEBs). These vehicles present certain limitations regarding the maximum slopes they can overcome, which are lower than those of conventional vehicles. In addition to the inclined terrain, the orography of the routes is one of the factors which most influences the consumption and autonomy of electric buses. In this article, airborne LiDAR point clouds are used, which are freely accessible according to the INSPIRE directive, with the consequent reduction of economic and time costs. From these point clouds, the digital elevation model is calculated. This model, together with the tracing of bus routes, serve to carry out the calculation of the longitudinal profile and the analysis of slopes. In particular, the analysis of the electric bus routes of the city of Ávila (Spain) is developed as this city presents an orography with extremely steep slopes. The conclusions show that it is feasible to undertake the electrification of urban bus routes, even in demanding orography situations, such as those found in the referred city.

**Keywords:** Battery Electric Buses, LiDAR, Orography, INSPIRE, Urban Buses, Public Transport.

### 1 Introduction

As it is necessary to reduce greenhouse gas emissions and air pollution, the new public transport directives in urban centers are moving towards the incorporation of low emission vehicles. With the increase in battery capacity and the feasibility of battery recharging, electric vehicles are becoming the best candidates to fulfill this task. But, before making a change of urban vehicles, we need to analyze the viability of their electrification. In order to do so, the orography of the routes and their maximum slope are one of the most important factors to be considered [1].

Some previous studies analyze how speed [2] or the driving profile [3] influence the autonomy and the duration of batteries. Although these factors influence the results, extreme slopes may make the use of electric vehicles unfeasible for some routes. To calculate the slope inclination, other previous approaches use GPS in current vehicles

to collect information on the routes before performing the slope calculation [4]. To obtain the slopes of routes, a mobile mapping system (MLS) can be used although this would require complex equipment and a greater data gathering time. In order to avoid this, the approach followed starts from the use of freely available airborne LiDAR point cloud data, with the savings that this implies. Thus, the digital model of elevations is obtained, the longitudinal profiles of the routes are generated and the slopes are analyzed to propose an orography factor that adjusts the nominal autonomy indicated by the vehicle manufacturer.

## 2 Urban buses in the city of Ávila

Ávila (Figure 1) is a city of just over 60,000 inhabitants. It is Spain's highest capital city, which is located at 1,131 meters above sea level [5] and on a hill on the banks of the Adaja river. It is a medieval city with a number of narrow streets and steep slopes. All these features condition, among other things, that the buses contemplated in this study are 10.62 meters long so that steering wheel turns are possible at some critical points [6].



Fig. 1. City of Avila

### 2.1 City bus routes

The urban bus system in the city of Ávila is made up of six routes represented in the plan in Figure 2. Routes 3 and 5 are circular while the rest of them have a return trip route [7]. There are also some special services on specific dates which are out of the scope of this study.

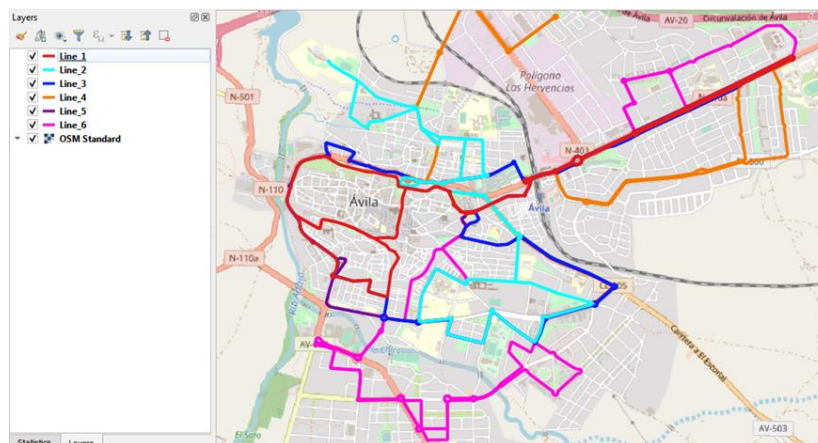


Fig. 2. Route plan

### 3 Materials and Methods

#### 3.1 Data Sources

For this study, on the one hand, the spatial data provided by the National Geographic Institute of Spain (Instituto Geográfico Nacional, IGN hereinafter) are considered, specifically the LiDAR point clouds from photogrammetric flights. These data collections are carried out according to the rules of the INSPIRE directive (Infrastructure for Spatial Information in Europe) [8], so that this same methodology can be applied to other places where LiDAR data are available. On the other hand, information on the urban transport routes is provided by the city municipality and by the bus service concession company.

#### **Geospatial Data: Spanish National Geographic Institute.**

The LiDAR point cloud can be downloaded online from the IGN website [9]. These points are classified according to the ASPRS (American Society for Photogrammetry and Remote Sensing) [10], which facilitates the creation of the Digital Elevation Model (*DEM* hereinafter). The LiDAR data used are from the second flight round, with a minimum point cloud density of 1 point / m<sup>2</sup> and an elevation accuracy (RMSE<sub>z</sub>) of between 0.15 and 0.20 m [11].

#### **Route data.**

In addition to the data from the point clouds to obtain the DEM, the information provided by the municipality and the concession company shows, on the one hand, some cases in which the paths of the routes are georeferenced 2d polyline whereas, in other cases, the information given allows its georeferencing. On the other hand, we also know the number of journeys that need to be made per route during weekdays and weekends

along with the kilometers for each journey and route, the distances to the bus garage and the number of buses per line (Figure 3).

Line	Travel	Km	Working days			Saturday			Sunday			
			Trips	Total Km	Bus garage	Buses	Trips	Km	Buses	Trips	Km	Buses
1	Go	5.68	45	255.60 km	3.44 km	3	37	210.16 km	3	19	107.92 km	2
	Return	7.47	43	321.21 km	3.44 km		35	261.45 km		19	141.93 km	
	daily total km			597.45 km				492.25 km			263.61 km	
2	Go	7.81	19	148.39 km	2.20 km	1						
	Return	4.92	19	93.48 km	2.20 km							
	daily total km			246.27 km								
3	Circular	14.28	28	420.24 km	5.10 km	2	20	306.00 km	2	20	306.00 km	2
4	Go	7.74	25	193.50 km	2.34 km	2	20	154.80 km	2	16	123.84 km	2
	Return	8.71	25	217.75 km	2.34 km		20	174.20 km		16	139.36 km	
	daily total km			420.61 km				338.36 km	2		272.56 km	1
5	Circular	14.51	28	426.68 km	5.10 km	2	20	310.60 km	2	20	310.60 km	2
6	Go	9.44	41	387.04 km	5.10 km	3	29	273.76 km	3	16	151.04 km	2
	Return	11.13	41	456.33 km	5.10 km		28	311.64 km		15	166.95 km	
	daily total km			873.97 km				616.00 km	2		338.39 km	1

Fig. 3. Data of lines, routes and buses

### 3.2 Methodology

Firstly, we create the DEM and the longitudinal profile of the routes. Secondly, we carry out the analysis of the orography of each route to obtain the associated orography factor.

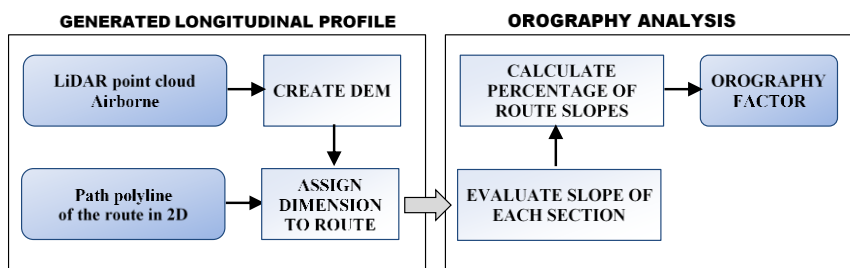


Fig. 4. Process Flow Diagram

#### Create the DEM from the LiDAR point cloud

The starting points are classified according to ASPRS, table 1 [10].

Table 1. Classes defined by ASPRS

Class	Meaning
0	Unclassified
1	Not qualified
2	Ground
3	Low vegetation



Once the vertices are added, they are all selected, and the elevation of the model is assigned to them (Figure 7).

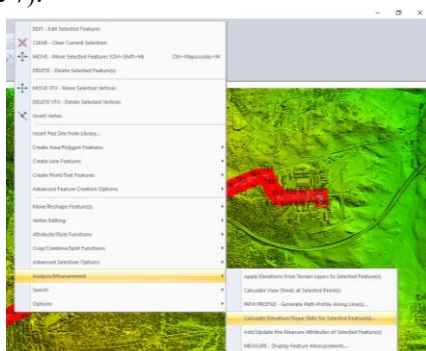


Fig. 7. Menu to assign elevation to the vertices of the path

Then we proceed to create the longitudinal profile.

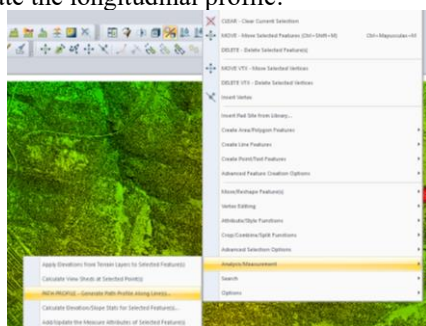


Fig. 8. Longitudinal profile calculation tool

From the menu for viewing the calculated longitudinal profile, it can be exported to a comma-delimited text format, to continue processing the information from the spreadsheet.

**Categorize sections according to slopes**

To perform the analysis of each section, the inclination of slopes is considered according to the following ranges: slopes greater than 8%, average slope between 4% and 8%, gentle slope between 1 and 4%, flat section between - 1% and 1%, slight decrease between -1% and -4%, average decrease between -4% and -8%, steep decrease greater than -8%.

To obtain the orography factor, we consider the percentage of steep climbs, medium climbs and gentle climbs of routes with relation to its total length. The orography factor

is thus dependent on the interval of the percentage of climbs indicated below (Figure 9).

% Slope up		Factor
From	To	
0%	5%	<b>0.05</b>
5%	15%	<b>0.10</b>
15%	25%	<b>0.20</b>
25%	30%	<b>0.30</b>
30%	35%	<b>0.40</b>
>	35%	<b>0.50</b>

Fig. 9. Orography factor according to percentage.

#### 4 Results and Discussion.

##### Creation of the DEM from the LiDAR point cloud

With the point clouds, the digital elevation model is calculated. Figure 10 shows the result with the trajectories of the overlapping routes.



Fig. 10. Digital Elevation Model with overlapping routes.

##### Attainment of the longitudinal profile.

The path of each line does not have a Z coordinate. The height of the DEM point corresponding to each point of the path is taken, so that the longitudinal profiles of each

route are obtained in their outward and return paths. As lines 3 and 5 are circular, there is only one profile for them. The profiles of all the routes are included in Figure 11.

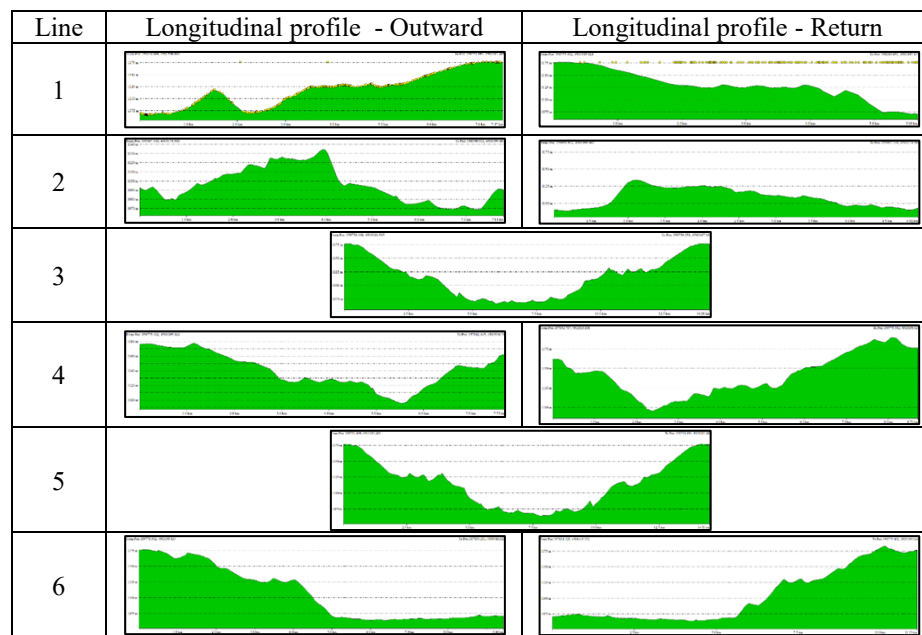


Fig. 11. Longitudinal profiles of the routes

**Categorization of sections according to slopes.**

For each section of the route, its slope is calculated, the sections are classified by grouping them for the indicated slope intervals. The percentage of routes found in each type of segment is calculated according to the exposed methodology (Figure 12).

From	To	Type of segment	Line 1	Line 2	Line 3	Line 4	Line 5	Line 6
>	8%	<i>Steep slope</i>	2.11%	4.56%	0.92%	1.02%	0.14%	0.11%
4%	8%	<i>Middle slope</i>	16.27%	6.94%	6.18%	10.01%	7.80%	7.45%
1%	4%	<i>Soft Slope</i>	44.37%	25.18%	30.59%	25.36%	30.71%	18.76%
-1%	1%	<i>Flat</i>	17.37%	22.89%	23.93%	25.48%	24.84%	46.12%
-4%	-1%	<i>Smooth Descent</i>	10.96%	30.54%	29.77%	27.65%	28.12%	19.87%
-8%	-4%	<i>Middle Descent</i>	4.81%	6.65%	8.55%	9.93%	7.35%	7.00%
<	-8%	<i>Steep Drop</i>	4.11%	3.23%	0.00%	0.55%	1.04%	0.69%

<b>% Total Slope up</b>	<b>62.74%</b>	<b>36.68%</b>	<b>37.68%</b>	<b>36.39%</b>	<b>38.65%</b>	<b>26.31%</b>
<b>Orography Factor</b>	<b>0.50</b>	<b>0.50</b>	<b>0.50</b>	<b>0.50</b>	<b>0.50</b>	<b>0.30</b>
<b>Maximum uphill slope</b>	<b>11.30%</b>	<b>9.50%</b>	<b>10.63%</b>	<b>9.81%</b>	<b>9.67%</b>	<b>8.60%</b>
<b>Maximum downhill slope</b>	<b>-10.74%</b>	<b>-9.96%</b>	<b>-9.16%</b>	<b>-9.65%</b>	<b>-9.75%</b>	<b>-8.85%</b>

Fig. 12. Summary of lines and slopes

For all lines except for line 6, the calculated orography factor corresponds to the most demanding of 0.5. Besides, the maximum slope is 11.30% for line 1.

**Autonomy analysis on the proposed bus model.**

The proposed bus model is an Irizar ie bus 10 m model. with a nominal autonomy of 250km and a maximum allowed slope of 18% [6].



**Fig. 13.** Irizar bus ie bus 10 m

All lines require a maximum slope lower than that supported by the model indicated. By applying the orography factor, the manufacturer's nominal autonomy is reduced to have a confidence interval on roads with extremely inclined profiles. In Figure 14, the routes which exceed the nominal autonomy are highlighted in red; those below the adjusted autonomy are found in green; and, those that are within the interval between the nominal and the adjusted autonomy are indicated in orange. For the lines analyzed, the autonomy of line 6 would be sufficient to operate on Sunday without an opportunity charging during the route. For the rest of the lines, it would be necessary to consider increasing the capacity of the batteries, or contemplating one intermediate recharge a day.

Line	Km by bus Work days	Km by bus Saturday	Km by bus Sunday	Autonomy Nominal	Factor of Orography	Reduction of autonomy	Autonomy adjust
1	199.15	164.08	131.81	250	0.50	125	125
2	246.27			250	0.50	125	125
3	210.12	153.00	153.00	250	0.50	125	125
4	210.31	169.18	136.28	250	0.50	125	125
5	213.34	155.30	155.30	250	0.50	125	125
6	291.32	205.33	169.20	250	0.30	75	175

**Fig. 14.** Application of the orography factor to adjust the autonomy

## 5 Conclusions

With the proposed methodology, it is possible to obtain the longitudinal profile of the bus lines from open data from LiDAR point clouds. With the analysis of sections of the profiles, it is feasible to obtain the maximum slope and the percentage of sections of climbs. These data allow us to analyze whether the performance of the battery electric bus models can satisfy the needs required in the routes to be electrified. In the study carried out for the city of Ávila, it is concluded that urban bus electrification is possible. Although the city presents demanding slopes, these are not higher than the maximum inclines which that market models can satisfy. In addition, the present study provides information on the need to use larger capacity batteries and opportunity charging.

## Reference

1. Anita GRASER, A., ASAMER, J., DRAGASCHNIG, M., How to Reduce Range Anxiety? The Impact of Digital Elevation Model Quality on Energy Estimates for Electric Vehicles, Austrian Institute of Technology GmbH, (2014).
2. Warren Vaz, Arup K.R. Nandi, Robert G. Landers, Umit O. Koylu, Electric vehicle range prediction for constant speed trip using multi-objective optimization, *Journal of Power Sources*, Volume 275, 435-446, (2015).
3. Margarida C. Coelho, Marco B. Luzia, Evaluating the energy performance of a SUV hybrid electric vehicle, *Transportation Research Part D: Transport and Environment*, Volume 15, Issue 8, 443-450, (2010).
4. Kai Liu, Toshiyuki Yamamoto, Takayuki Morikawa, Impact of road gradient on energy consumption of electric vehicles, *Transportation Research Part D: Transport and Environment*, Volume 54, 74-81, (2017).
5. Ciudad de Ávila, <https://es.wikipedia.org/wiki/%C3%81vila>, last accessed 2021/10/05.
6. Irizar ie bus, <https://irizar-emobility.com/vehiculos/irizar-ie-bus>, last accessed 2021/10/05.
7. Plano de líneas AvilaBus, <https://avila.avanzagrupo.com/lineas-y-horarios/plano-de-las-lineas>, last accessed 2021/10/05.
8. Kocsis, S. Estandarización de datos geográficos: La directiva europea INSPIRE. *EUR. J. Geogr.* 79–89 (2011).
9. Instituto Geográfico Nacional Centro de Descargas del CNIG (IGN), <https://centrodedescargas.cnig.es/CentroDescargas/index.jsp>, last accessed 2021/10/05.
10. Plan Nacional de Ortofotografía Aérea, <https://pnoa.ign.es/caracteristicas-generales>, last accessed 2021/10/05.
11. Sánchez-Aparicio M, Del Pozo S, Martín-Jiménez JA, González-González E, Andrés-Anaya P, Lagüela S. Influence of LiDAR Point Cloud Density in the Geometric Characterization of Rooftops for Solar Photovoltaic Studies in Cities, *Remote Sensing*, 12(22):3726, (2020).
12. Global Mapper, <https://www.blumarblegeo.com/global-mapper/>, last accessed 2021/10/05.

# Embedded System for automating manual inventory survey process of street lighting with a I2C photometric sensor network

Luis Ricardo Delgado Cortés<sup>1</sup>[0000-0003-1164-7689] and Saúl Esquivel-García<sup>2</sup>[0000-0001-8939-2298]

Posgrado CIATEQ, Av. del Retablo 150, Col.  
Constituyentes-Fovissste, Querétaro 76150, México  
luis.ricardo.delgado.cortes@gmail.com eg.saul@gmail.com

**Abstract.** Currently, most companies dedicated to managing public lighting infrastructure manually perform the process to determine the quantity, lighting technology and physical condition of luminaires and poles. This process carries some problems inherent to its manual execution such as increased costs in large areas, logistics issues and personnel management, but, mainly, a bad acquisition of the required data derived from the human factor that performs the process (i.e., taking wrong sensor information or incomplete inventory survey) that can cause economic losses due to energy consumption to the electricity companies.

This article presents an alternative proposal that involves hardware and firmware on existing systems to automate the inventory survey of public lighting based on an embedded system with a network of photometric sensors and geolocation focused on the acquisition of ambient light and light color data with a restricted sampling frequency, environmental data and inertial measurement data proposing a certain set of sensors and organizing the data obtained in a log file for further processing. The results obtained in the field tests are presented and discussed.

**Keywords:** Street lighting, inventory survey, embedded system, microcontroller, photometric sensor

## 1 Introduction

### 1.1 Background

Public lighting is an indispensable service in any urban area regardless of its size. Urban development is constantly growing, and street lighting also must grow along with the urban area. Managing this service is not an easy task and for this there are companies whose turn is exclusively the provision of public lighting management services, services that range from keeping an inventory control of the public lighting infrastructure, updating it to modern lighting technologies such as LED luminaires, as well as keeping it in optimal conditions to lighting maps, intelligent lighting, energy saving, among others. These companies carry out a process called inventory survey of

public lighting or also known colloquially as census of luminaires that consists of collecting information on the number of luminaires that exist, their location, as well as their physical conditions and such process, at present day, continues to being performed manually by most companies. This process requires organized personnel that are hired in the form of crews of 4 technicians that are given pre-established routes to carry out the inventory survey. The manual process of inventory surveying in general is as follows:

- The zones and routes to be followed by the crews are established to cover the area of interest of the city.
- Crews are given their personal protection equipment, a tablet, a lux meter and a crane to make the journey through the streets.
- Upon arrival at the area of interest, the crew search and stops at each of the luminaires following the previously defined route.
- In each luminaire, the staff identifies the geolocalization of the luminaire, type of light head and pole, type of pick arm, height, physical conditions, lighting technology, makes measurements of the lighting levels and enters all this information in a digital form on the tablet.
- With the tablet, photographs of evidence of the pole and luminaire are taken.
- A stamp is placed to identify that the luminaire has already been checked.
- After the data is taken and in case the luminaire or pole presents any defect or needs its lighting technology to be updated, a report is raised for a maintenance team to carry out the necessary repairs or changes.

This process is complicated as the volume of infrastructure to be managed grows as is the case of large cities and can become a challenge as problems arise in logistics, human resources, costs, time to complete, etc.

With the development of electronic technologies applied to embedded systems and wireless communications, public lighting management companies began applying these technologies to reduce energy consumption through remote monitoring of luminaires in specific areas of a city. This technology typically uses photometric sensors and microcontrollers to acquire sensor data, as well as wireless communication modules to send the information to a remote monitoring terminal or web page.

The present article presents an embedded system with a network of photometric sensors, an environmental sensor, an inertial motion sensor, a high-precision GPS and a real-time clock to automate the manual process of the inventory survey of public street lighting extracting only the variables of interest and organizing the information in a format required format.

## **2 State of the art**

### **2.1 Commercial solutions**

There are systems developed by commercial companies that have the similarity of implementing modules with photometric sensors and a microcontroller, along with wireless communication modules that are mounted on each of the luminaires in the area of interest and allow remote monitoring / control of the luminaires.

One of these systems is based on a microprocessor that runs a Java VM along with an integrated sensor board including a light sensor [1] that was developed for prototyping wireless sensor networks projects could be used for an application in which the module is installed on the lighting pole near the luminaire to acquire real time measurements of the illumination levels and controlling the power on/power off the luminaire remotely for energy saving purposes. The main disadvantages of this system are that it's already discontinued, it was not developed for street lighting monitoring (it's a development module that could be used for anything else), their application approach is monitoring specific areas (such as industrial buildings or shopping centers) and having to install a module for each luminaire which increases the costs in areas with a high number of luminaires.

Another commercial solution is based on the integration of consumer electronics modules: a conventional luxmeter, a high precision vehicular GPS and digital cameras mounted on the top of a car fixed on a tower-form mechanical structure [2]. However, this solution does not implement a microcontroller to acquire and organize the data and it's not processed by a specialized software to generate a virtual map of the street lighting infrastructure, instead, all the acquired data that is delivered to the client is inside of Excel spreadsheets with links to the photographs taken and AutoCAD files containing the map plot of the lighting infrastructure.

### **2.2 Related papers**

In 2014, Sumeet Kumar of the Massachusetts Institute of Technology (MIT) in his PhD thesis [3], developed a mobile prototype to map the lighting levels in the streets and public lighting infrastructure of a city automatically using an embedded system based on the Arduino Mega development card, TEMT6000T ambient light sensors, an inertial motion sensor and a high-precision GPS, along with another system based on high-definition cameras with wide-angle lenses. He also developed a software that can identify the "hot spots" of lighting by filtering the noise of other light sources and discarding false positives in the measurements to finally build a map where you can visualize the lighting levels and the lighting infrastructure based on the measurements of both systems that integrate the complete system called "CASP" (Car-mounted Autonomous Street light scanning Platform). He also explored the distribution of photometric sensors throughout the system.

The mechanical structure of the system is a bar on which both sensors and cameras are mounted. This bar is installed on the roof of a vehicle that is driven through the areas of interest to be mapped.

Although the prototype was successfully tested, it did not escalate to the point of developing the system beyond a prototype, it was not commercialized and there are still areas of future work and exploration to improve the system:

1. Analyze other photometric sensor options than can obtain more information. In the same way, explore the use of other types of sensors that provide extra information to guarantee the reliability of the system.
2. Change the microcontroller to another that offers better performance or fits better for the application, as well as modify the overall architecture of the system.
3. Design a new structure that will house the system to protect it from the environment but won't interfere with measurements.
4. Modify the way in which the data obtained by the sensors will be transferred to a custom developed software to process this data and map the inventory of public lighting, either by means of and wireless protocol, direct USB connection to a laptop and / or by SD memory storage.

In 2015, a team in association with a local electricity company developed a mobile system for automating the manual process of detecting and classifying street lighting infrastructure combining hardware and software based on a neural network [4]. The version presented on the paper consists of an electronic board with the light sensors and a DSP that communicates via Bluetooth to a tablet managed by an operator for transferring the acquired sensor data. This tablet also communicates via USB to a digital camera for taking pictures of the luminaires of interest. This information is then downloaded to a PC via a wireless communication.

This article does not focus on the data acquisition of the sensors, instead, it explains in more details the software that processes the data with a neural network and the data acquisition interface developed for the tablet (Android OS).

### 3 System Architecture

#### 3.1 System requirements

According to the functional requirements for this prototype’s version, the system has a restricted sample rate of minimum 4 to 5 photometric measurements per second. In order to comply with this requirement, each board of the sensor network is controlled by an Atmega328 microcontroller that obtains the required measurements and store them on its internal memory until the main board sends a digital signal that triggers an event to send the information to the Raspberry Pi. This information also needs to be stored in a log file since it will be an entry file for the software that will process the acquired data.

Log file storage is not required to be stored in an external memory unit, it can be extracted directly from the Raspberry Pi or by any means.

#### 3.2 System components

The architecture was developed based on the functional requirements and the previous research/development. Each set of photometric sensors are controlled by an Atmega328 microcontroller using the I2C communication protocol and the sensors of the main board are controlled by a Atmega2560 microcontroller using the I2C and UART communication protocols. All the system’s boards are connected to Raspberry Pi for organizing the collected data in a specific required format via the UART protocol. The system is composed of 2 types of boards, 5 boards containing photometric sensors and a microcontroller to acquire data named “Photometric sensor boards”, and a board named “Main Board” that contains an ambiental sensor, an inertial movement unit, a high-precision GPS, a Real-Time Clock and a microcontroller to acquire data. In figure 1, the components of each board are displayed in more details:

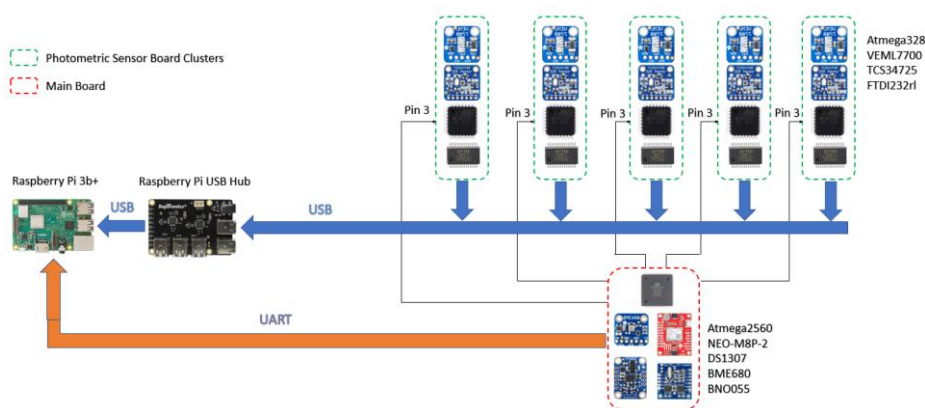


Fig. 1. System’s general architecture

The system is contained by a wooden case prototype mounted over the roof of the car. This case holds the Raspberry Pi, the USB hub and the cables that connect the system altogether with the systems boards, the main board and 5 photometric sensor boards distributed along the case. The reason why it is mounted over a car is to receive directly the light generated by the streetlighting while the car is on movement, thus, automating the manual survey process. In figure 2, there's a 3D model representing of how the system's case is mounted over a vehicle.



**Fig. 2.** 3D representation of the system mounted on a car

### 3.3 Main Board Architecture

The ATmega2560 microcontroller controls and acquires data of the GPS, Real-Time Clock, BME680 and BNO055 sensors and store the information in its internal memory. After acquiring the data, it organizes and sends it to the Raspberry Pi which triggers a digital control sequence on the photometric boards to make them send their acquired data to the Raspberry Pi. A block diagram representing the general architecture of the main board is presented in figure 3 as well as table 1 describing the components and measurements.

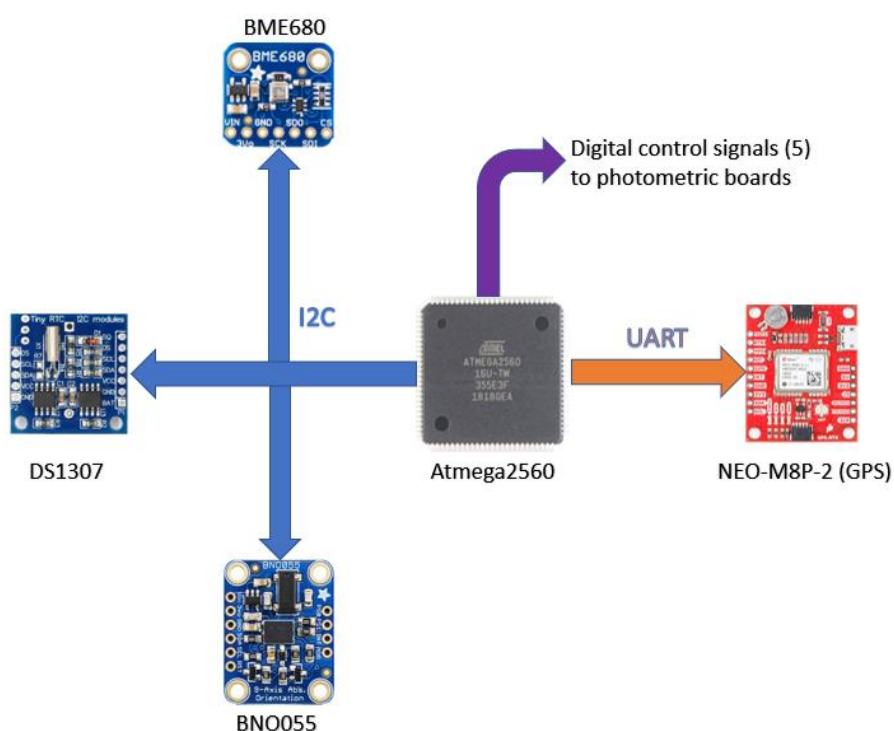


Fig. 3. Main board architecture block diagram

Table 1. Sensor and components of the main board

Sensor/Component	Description	Measurements
NEO-M8N-2P	High precision GPS	Geolocalization
DS1307	Real-Time Clock	Timestamp
BME680	Ambiental Sensor	Temperature, Pressure, Humidity
BNO055	Inertial Movement Unit	X, Y and Z orienta-

ATmega2560	Microcontroller	tion Data Acquisition
------------	-----------------	--------------------------

### 3.4 Photometric Sensor Board Architecture

It consists of a ATmega328 microcontroller that controls and acquires data of the VEML7700 and TCS34725 sensors. It sends its obtained information to the Raspberry Pi when the main board sends a digital control signal. In figure 4, it's represented the general photometric board architecture in a block diagram. Also, in table 2 the components and measurements of this board are listed.

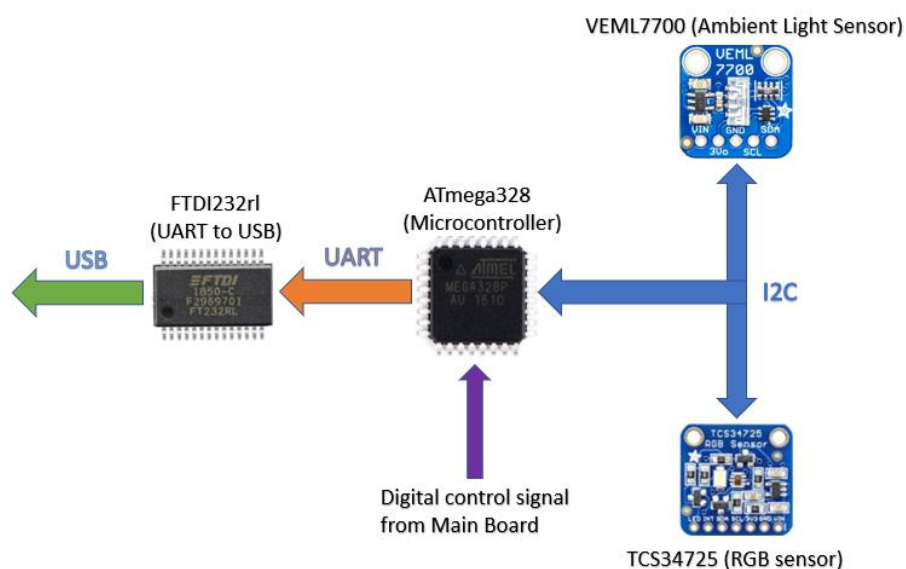


Fig. 4. Photometric sensor board architecture block diagram

Table 2. Sensor and components of the photometric sensor board

Sensor/Component	Description	Measurements
VEML7700	Lecture Notes	Lux, White
TCS34725	RGB Sensor	Red, Green, Blue, Clear
ATmega2328	Microcontroller	Data Acquisition

## 4 Automation of the manual inventory survey process

### 4.1 System's Algorithm

As the system is composed of several components, each of the boards have their own source code which allows them to acquire and organize data in a parallel way. The general steps or algorithm the system follows is represented in the figure 5 and later described in steps.

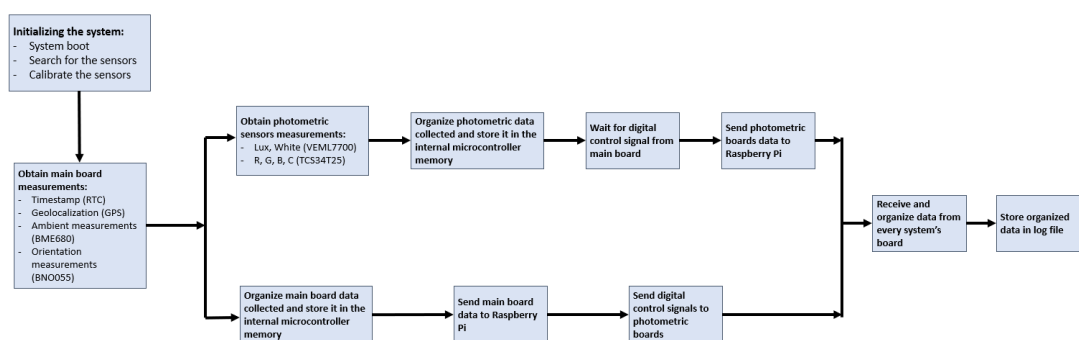


Fig. 5. System's general algorithm block diagram

- At system's power up, the Raspberry Pi starts its booting process.
- Initialization of main board and photometric boards (sensor calibration).
- Raspberry Pi executes logger script and waits for incoming data.
- Main board and photometric boards data acquisition in parallel.
- Main board sends its data to Raspberry Pi.
- Main board sends trigger signal to photometric boards.
- Photometric boards send its information to Raspberry Pi.
- Raspberry Pi organizes data received.
- Data saved in log file.

#### 4.1.1 Main Board Data Acquisition

The main board communicates with its sensors via the I2C and UART (for the GPS) protocols. It accesses specific registers of the sensors by sending them a command (specified in the sensor's datasheet) to acquire timestamp, geolocalization, temperature, pressure, humidity, X orientation, Y orientation and Z orientation. Each sensor has its own address and specific registers to retrieve the required measurements and they are partitioned in the MSB and LSB registers to obtain the complete information. The I2C communication is set to function in the fast mode which has a 400 Kbit/s speed.

With the GPS it's different, since the communication protocol is UART, once it has connected to the mobile network, it will start sending all its information in the NMEA (National Marine Electronics Association) protocol. The microcontroller then filters only the required information from the NMEA output string.

After completing data acquisition from all the sensors and GPS, it will reorganize them in a string with a specific order (table 4) and send it to the Raspberry Pi. The last step is to send a digital control signal to each photometric board so they can send their acquired data.

```
Hour:Minutes:Seconds,Day/Month/Year;$GNRMC,$GNVTG,$GNGGA,  
$GNGSA,$GPGSV,$GLGSV,$GNGLL;Temperature,Pressure,Humidity  
;X_orientation,Y_orientation,Z_orientation;
```

#### 4.1.2 Photometric Boards Data Acquisition

Each sensor has its own address and registers to retrieve the required data. After the microcontroller is done obtaining the required data and arranging them in a string with a specific order which can be seen in the string below and it's the same for every photometric board.

```
ClusterNumber,Lux,White,ColorTemperature,R,G,B,C;
```

#### 4.1.3 Connection of Photometric Sensor Boards and Main Sensors Board

The digital control signal generated by the main board in order to communicate with the photometric boards and indicate them it's time to send their information, consists of pulling 5 digital pins (table 7) from low to high in a sequential way starting with the first photometric cluster, passing through clusters 2, 3, 4 and finally cluster 5. The main board will then pull the 5 digital pins from high to low and start obtaining again its data.

#### 4.1.4 Connection of Raspberry Pi with The Main Board and Photometric Boards

The way the main board and the photometric boards communicate with the Raspberry Pi is via an USB port connected to a hub. The reason for using USB ports to communicate is because the Raspberry Pi does not have all the necessary UART or I2C modules to connect with the 5 photometric boards. It has 4 USB ports, but they can be extended using a USB hub as seen in figure 6.

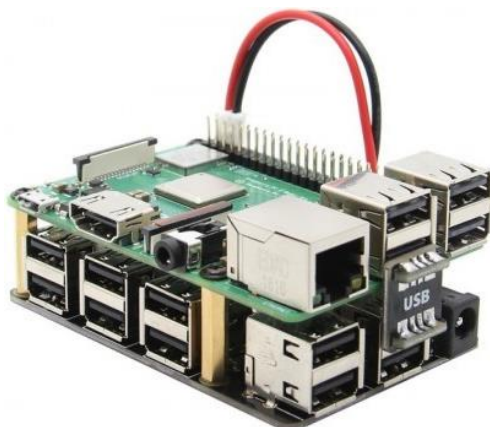


Fig. 6. Raspberry Pi USB hub [5]

#### 4.1.5 Format of Acquired Data

Every measurement is separated by a comma and every sensor is separated by a semi-colon. The only measurement that is separated with a different character is the timestamp which uses a colon. The following string represents the acquired data:

```
20:07:21,24/11/2020;$GNRMC,061944.40,A,2038.49005,N,10325.56848,W,1.973,,241119,,A*77$GNVTG,,T,,M,1.973,N,3.654,K,A*35$GNGGA,061944.40,2038.49005,N,10325.56848,W,1,07,1.10,1604.0,M,16.8,M,,*4F$GNGSA,A,3,30,17,19,06,13,07,01,,,,,2.14,1.10,1.83*1E$GPGSV,4,1,13,01,15,041,12,02,10,204,21,03,03,092,,06,42,182,19*73$GLGSV,2,1,07,76,35,113,,77,59,029,,78,20,335,,81,20,216,19*6C;BME680,30.48,849.62,49.14;BNO055,359.94,21.31,26.38;Cluster1,4178.53,7898.11,2267,80,101,113,140;Cluster2,4783.96,8139.91,2538,90,97,107,200;Cluster3,4929.44,9029.8,2600,100,98,109,219;Cluster4,4800,8564,2526,117,104,100,220;Cluster,5024.7,8998,2636,112,102,120,215;
```

#### 4.1.6 Organizing Data in Raspberry Pi

In order to receive and organize the incoming data from all the system's boards, a python script was developed to read data from the USB port connected to the USB hub. This script reads the strings received and store them in the log file with a line break at the end. The script is executed every time the Raspberry Pi finishes its booting process with the help of a crontab, but it can be executed directly from the terminal whenever it's necessary. The Raspberry Pi is connected to a laptop via an ethernet

cable using the VNC software so the operator of the system can visualize in real time the logging process. When the automated street lighting survey process of a specific area is terminated, the operator stops the execution of the python script and extracts the log file for further processing.

### 5 Results

This prototype was tested outside the laboratory by mounting it in a car and taking a special route that was selected based on the street lighting infrastructure of the zone. The results were uploaded to a web platform to validate the GPS data of the followed route and to visualize in an organized way the data acquired from the sensors as it can be seen in figure 7 and figure 8. The platform converts the NMEA GPS data to a format used in online map services like google maps for a more comfortable visualization.

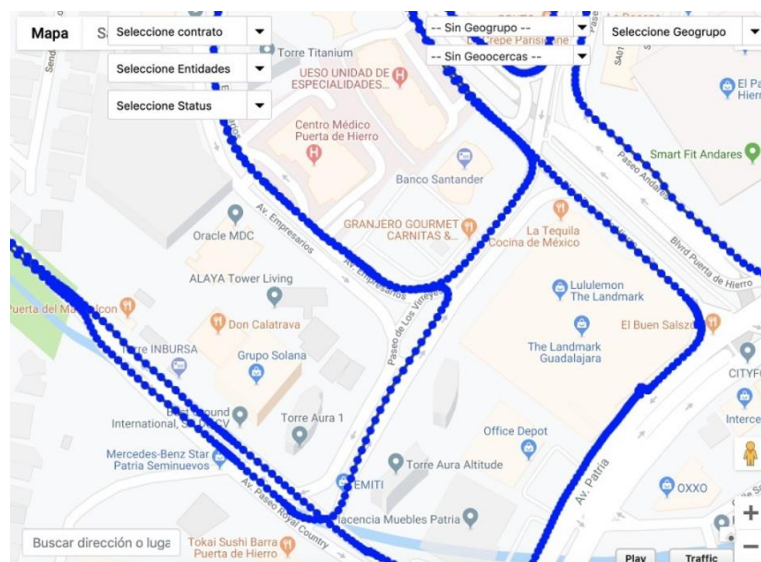


Fig. 7. GPS data represented in a map

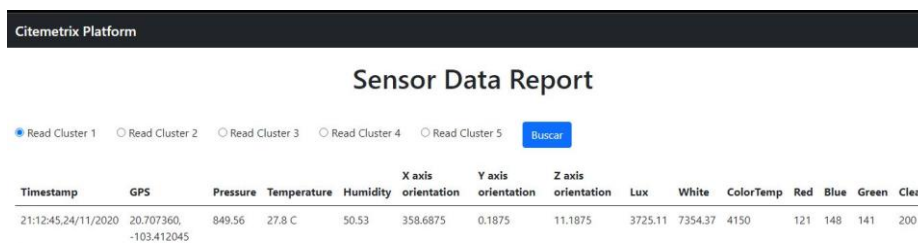


Fig. 8. Sensor’s data visualized in web platform

According to an interview with a former technician that worked performing this manual process, the routes they follow are divided by zones in which there's a street limitation similar to a geofence. Each zone takes up 3 to 4 days to be mapped and they approximately map 80 – 100 luminaires every work day of 8 hours. Depending on the size of the zone, a combination of 2 or 3 zones results in a neighborhood and a combination of several neighborhoods results in a municipality. So, in urban areas like big cities, the higher the number of municipalities, the higher the time that will take to get the complete inventory survey of street lighting infrastructure. In figure 9 there's a chart representing the comparison of time taken by the manual process vs the automated process based on field tests performed.

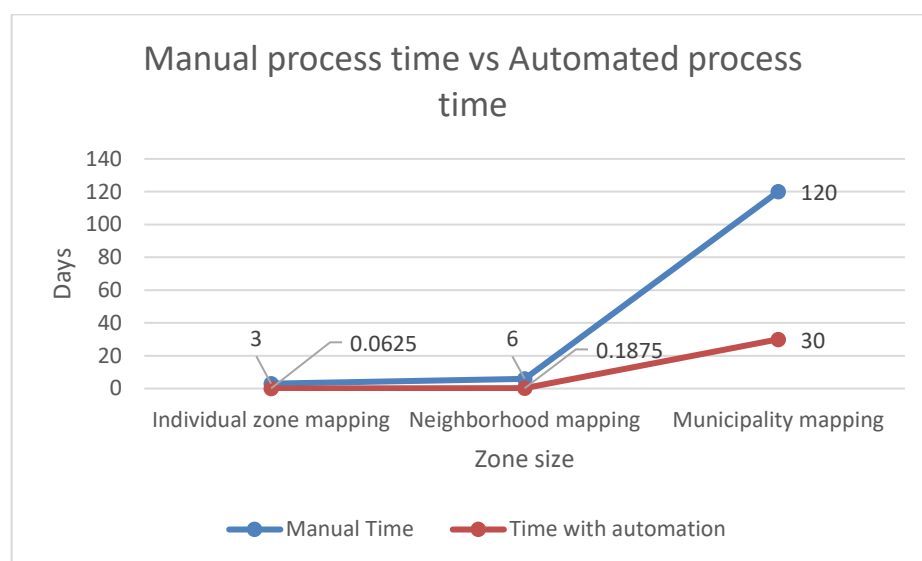


Fig. 9. Manual process vs Automated process time graph

Even though the field tests were only individual zone mapping (the rest of the mapping was calculated based on the individual zone markers), the automated process performed by the prototype is much faster than the manual process performed by technicians since it's mounted over a vehicle with a 50km/hr. average speed, no stopping and the results will later be processed to get the same information the technicians obtain.

## 6 Conclusion & Discussion

### 6.1 Conclusion

The manual process of street lighting inventory survey requires data acquisition of every single luminaire of interest in a determined zone which makes it a repetitive and

a very time-consuming process as well as facing problems that are inherent from the human intervention. Implementing this solution can not only help to reduce the amount of time taken to map a zone but also reduce the amount of the human resources required by half.

For example, by having a precise map of the street lighting infrastructure, the quality of the public street lighting service improves by enabling faster decisions making regarding on predictive and corrective maintenance of luminaires that need it which can help reduce the insecurity levels of zones with deficient illumination. Energy efficiency is another plus that this solution gives since it maps with precision the actual luminaire infrastructure with illumination technology and thus, helps electricity companies to calculate a more precise energy consumption marker that could help implementing energy saving controls and reduce electricity shortages in zones with higher volume of luminaires. Implementing embedded applications to automate the manual street lighting survey process is a big contribution to the development of smart cities since it goes hand in hand with improvements in public services area, specifically in the street lighting infrastructure that will give this service a better quality for the citizens and will lead updating outdated lighting technologies to smart LED urban lighting and consequently a beneficial environmental impact

## 6.2 Future work

This prototype presented is still on development and there are improvements to be made. Some of the future work (but not limited to) is listed next:

- Add a Human-Machine Interface like a touchscreen on the Raspberry Pi and/or a web interface for better control of the system and interaction with the operators.
- Add digital cameras to take pictures of the pole and luminaire.
- Faster data acquisition frequency. (add percentage or quantitative marker)
- Wireless communication module to send the log file / sensor measurements to the web platform.
- Improve the materials of the mechanical case to make them water and vibration proof.

This a proposal for automating the manual survey process of street lighting, at the end, another proposal can be implemented.

## References

1. Kumar, S.: Mobile Sensor Systems for Field Estimation and "Hot Spot" Identification. MIT Ph.D. Thesis (2014).
2. Sun Spot World: Program the world! (Mirrored) Homepage.  
<http://sunspotdev.org/>, last accessed 2021/11/25
3. Lumidim de México Censos de alumbrado público.  
<http://www.lumidim.com/Pdf/2014/CensosLumidim.pdf>, last accessed 2021/11/25

4. Soares G., Almeida A., Mendes R., Teixeira E., Braga H et al.: On the Use of Light Sensors and Pattern Recognition Techniques for Automated Detection of Street Lighting Lamps. *Sensing Technology: Current Status and Future Trends III*. 79 – 104 (2015)
5. Teknistore. [https://www.teknistore.com/es/raspberry-pi-y-orange-pi/23839-x150-9-port-usb-hub--power-supply-expansion-board-for-raspberry-pi.html?mobile\\_theme\\_ok](https://www.teknistore.com/es/raspberry-pi-y-orange-pi/23839-x150-9-port-usb-hub--power-supply-expansion-board-for-raspberry-pi.html?mobile_theme_ok), last accessed 2021/10/1

# Building Smart City Based on the Big Data, Computer Analytics, Public Demand, and Governance

Alexander Shemetev<sup>[0000-0003-0563-3491]</sup> and Martin Pelucha<sup>[0000-0003-2024-5964]</sup>

Prague University of Economics and Business, Prague, Czech Republic  
aleksandr.shemetev@vse.cz, pelucham@vse.cz

**Abstract.** Researchers in the field of smart cities fall into two broad categories: philosophical approach and case studies. At the same time, none of the categories is suitable for defining smart cities or creating strategies for their development (this paper provides logic for this point). This study offers a unified concept for understanding smart cities (and verifies it with global demand). Determination of the specificity of the development of agglomerations transpires through the use of big data and modern technologies of computer analytics (A.I.). This research proposes the application of cluster analysis based on machine learning to determine the specifics of each city/town. Such an analysis allows working with both missing, distorted, and partially inaccurate data. This approach determines clusters of similar cities to which researchers can apply similar digital technologies to draw up a high-quality development strategy. It will gradually lead an intelligent urban environment up in the global hierarchy to the top of international centers (like Tokyo, London, Beijing, or New York).

**This research focuses** on creating a shared understanding of the concept of a smart city as a digital urban environment with seven components (smart transportation, innovative infrastructure, intelligent law enforcement, intelligent emergency management, innovative medicine, competent public administration, and municipal management, and intelligent city planning). This research suggests these modules to be the very minimum a city must have to become really "smart." An additional goal of the study is to form a unified concept of a smart city with the regions for gathering the appropriate data. Clustering analysis should help solve the data inconsistency and distortion problem while implementing the SCA-matrix should help solve the A.I. black box problem in managing the smart city.

**Keywords.** A.I., classification of smart cities, cluster analysis, components of smart city, development strategy of smart cities, global demand in the parts of the smart city, MLT clustering, smart city

## 1 Introduction

Researchers of smart cities fall into two broad categories: philosophical approach and case studies. At the same time, none of the categories is suitable for defining smart cities or creating strategies for their development (Lisdorf, 2020). This study offers a unified concept for understanding smart cities. Determination of the specificity of the development of agglomerations transpires through the application of big data and modern technologies of computer analytics (A.I.). The results of computer analytics can be used to manage the development of each city within the framework of smart technologies and create a proper development strategy. This research proposes to use

cluster analysis based on machine learning to determine the specifics of each city/town. Such an analysis allows working with both missing, distorted, and partially inaccurate data. This approach determines a cluster of similar cities to which similar smart technologies can be applied to draw up a high-quality development strategy. It will gradually lead smart cities up in the global hierarchy (ideally, up to the international centers like Tokyo, London, Beijing, or New York).

**This research focuses** on creating a shared understanding of the concept of a smart city as a digital urban environment with seven components (smart transportation, innovative infrastructure, intelligent law enforcement, intelligent emergency management, innovative medicine, competent public administration, and municipal management, and intelligent city planning). This research suggests these modules to be the very minimum a city must have to become really "smart." Thus, the study attempts to estimate the components of smart cities' concept to validate the areas to find the proper indicators. An additional goal of the study is to form a unified concept of a smart city with the regions for gathering the appropriate data. Clustering analysis should help solve the data inconsistency and distortion problem while implementing the SCA-matrix should help solve the A.I. black box problem in managing the smart city.

## 2 Literature overview and discussion

Researchers of smart cities fall into two broad categories: philosophical approach and case studies. Advocates of the philosophical approach strive to comprehend the phenomenon of smart cities. They often provide abstract descriptions<sup>1</sup>. Such descriptions often have been made in the broadest sense. Consequently, it is frequently challenging to plant something into practice when following this way. Case studies are an alternative to the philosophical approach. The most advanced experience of a smart city is selected and described within the framework of this concept. The logical conclusion of this approach is that each specific case applies to all smart cities, and following this path will make each standard city as intelligent as possible. The most advanced case study research focuses on the practical application of the concept of smart cities. At the same time, their examinations stream into lists of exciting projects and ideas worldwide (Lisdorf, 2020). Thus, this is the same case-study approach in its essence.

However, cities are not comparable to each other. There are regional centers at the international level. Such an agglomeration is both a local, national, and global center (for example, London, New York, Tokyo, or Beijing). Regional centers at the global level are units of the previous step of the hierarchy. These are essential agglomerations for many regions worldwide (Vienna, Moscow, or Zurich). There are national/regional centers as well. These agglomerations are crucial for the entire nation inside its territory

<sup>1</sup> For example (Ratti & Claudel, 2016): "Optimization inflected with humanization means neither metropolitan-scale computers nor a network-enabled wild west. It is the convergence of bits and atoms: systems and citizens." [definition of smart city].

(for example, Prague, Warsaw, or Kyiv). Regional centers are significant agglomerations for the whole region (for example, Yakutsk, Saint Petersburg, or Yekaterinburg are centers of their areas in Russia). Micro-regional centers are essential agglomerations for several local communities. For instance, Nizhny Tagil is a center of a part of the Sverdlovsk area [its regional center is the Yekaterinburg agglomeration]. The local centers are essential parts of the local communities (for example, Gornoural'skii is an important center for the local communities of an area that is a small part of the mentioned Nizhny Tagil area in Russia). Figure 1 represents this concept in more detail.

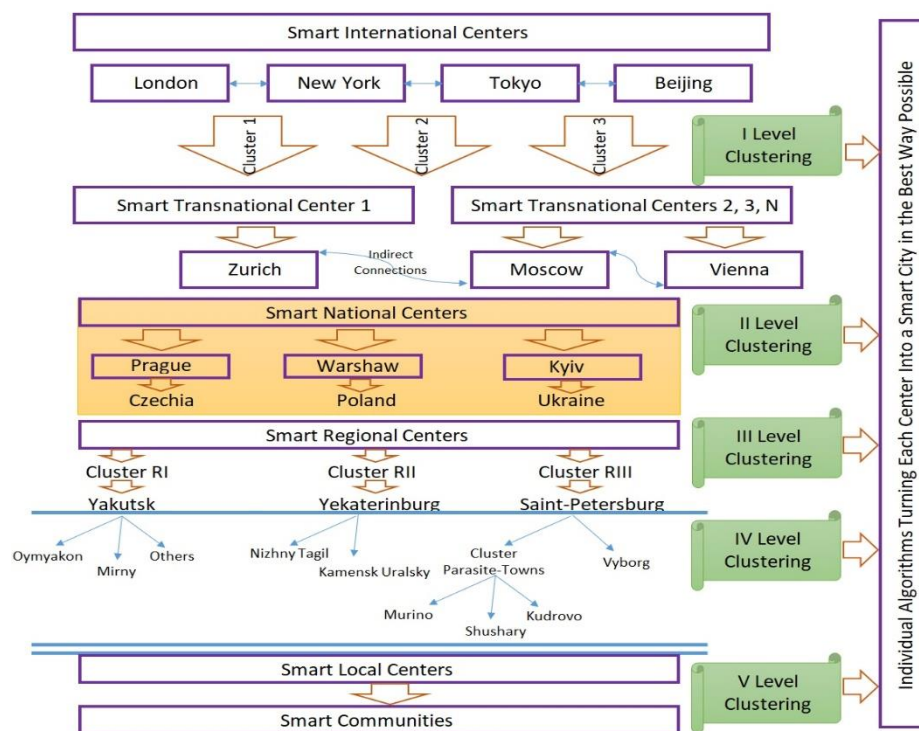


**Fig. 1.** The concept of smart cities by their hierarchy in the modern global world<sup>2</sup>

Therefore, modern cities are already rather agglomerations with adjacent regions (Gordon & McCann, 2000). Such agglomerations often become the drivers of the

<sup>2</sup> Notes to fig. 1. Source: own processing. It contains some examples of towns and cities. Parasite towns are the living places that do not have sufficient infrastructure for supporting the needs of their population (like medicine, workplaces, social spaces, schools, etc.). Thus, such towns fully depend on the greater centers (like Saint Petersburg). The smart city management for such towns should differ from managing the smart city of its center, this research assumes. Therefore, they should create separate clusters.

successful economic development of areas. Researchers and analysts usually apply rating approaches to evaluate the effectiveness of such agglomerations: experts utilize one or several indicators to rank cities or regions; thus, the most innovative cities are often on the top of such ratings (Huggins et al., 2014).

The very concept of smart cities originated relatively recently. Researchers often use it in a narrow sense. The smart city is a center for applying modern technology to improve infrastructure issues, energy supply, utility management, and environmental issues (Caragliu et al., 2011). The gradual development of science (Organisation for Economic Co-operation and Development, 2019) has led to implementing innovative technologies to improve the lives of citizens within agglomerations within various spheres (government, healthcare, social services, culture). Meanwhile, the whole line of thought regarding the concept of a smart city comes down to either an abstract philosophical concept or to discuss a list of exciting solutions from around the world (like case studies (Lisdorf, 2020)).

Meanwhile, it is vital to understand the mechanisms behind the development of smart cities at the international level. Neither a philosophical approach nor listing the sound elements (case study) can help in this process. Understanding such mechanisms allows analysts to develop intelligent strategies for growing cities, considering their movement up the hierarchy of agglomerations (see Fig. 1). Thus, it becomes possible to strategically plan the future development of settlements, taking into account the most modern technologies.

### **3 Methodology**

#### **3.1 Solving the data inconsistency and distortion problem**

The main problem in studying smart cities is the general data inconsistency. There is no universal standard for collecting data from every city that is (or claims to be) smart. Moreover, there is no indivisible methodology for the registration of any events within different metropolitan areas. Thus, each city collects data on its own, analyzes it, selects the most appropriate methods for collecting, storing, and analyzing data, and makes its own management decisions.

Consequently, it is impossible to collect a high-quality single database for all indicators of even a significant part of cities and agglomerations. It means that it is impossible to apply the methodology of standard econometrics or statistics. It is impossible to take indicators that have been assessed differently with different methods, given that even the choice of variables and ratios differs for each city, and then perform a qualitative econometric or statistical analysis (Babecký & Campos, 2011; Babecky & Havranek, 2014; Hanushek & Woessmann, 2016).

This research adopts a different approach. It proposes applying machine learning technologies based on big data (Leite, 2017; Yee, 2015) to classify agglomerations correctly. At the second stage, we suggest implementing artificial intelligence technologies to identify common patterns in urban development (the most straightforward way is clustering). The third stage is making management decisions based on A.I. data.

The simplest method to implement clustering is the k-means. This methodology implies random primary points and then puts additional points so that the distance within each point in its cluster is minimal. The spread of each point to the following clusters is maximal. As new clustering points do not seem optimal, the machine learning (MLT) algorithm ends the clustering by the k-means method.

### 3.2 Solving the A.I. black box problem by implementing the SCA-matrix

Methodologically, this study assumes that the S.C.A. matrix can assess the risk for each indicator; this S.C.A. matrix should include the results of big data processing by artificial intelligence. Similar technology allows discovering the black box in financial data<sup>3</sup> (Shemetev, 2018, 2019). This Matrix is a variation of the A-matrix (Shemetev, 2012, 2013) adjusted for intelligent cities. This research represents the Fisher intervals (Fisher, 1936; Gorban et al., 2018; Yu & Yang, 2001) for interpreting the overall scheme:

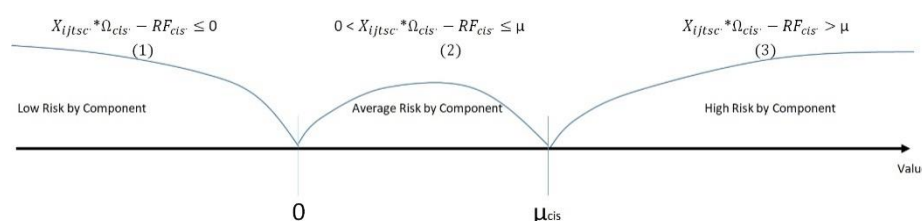


**Fig. 2.** Evaluation of the components of the S.C.A. matrix output for smart cities<sup>4</sup>

Applying this algorithm for processing big data helps in the black box problem in artificial intelligence and machine learning systems.

<sup>3</sup> The books mentioned in this part were created by the A.I. algorithm designed by the author that applied similar S.C.A. matrix of data processing for controlling the results.

<sup>4</sup> Own processing. Notes: i – specific indicator; j – specific city; t – specific period of time; s – value of the step (version of algorithm for evaluation); c – specific cluster (obtained from cluster analysis with the MLT [for example, with the mentioned k-means method]); RF – suggested risk free parameter for a specific indicator; μ - the upper bounder of the extra-risk for a specific parameter (the values above indicate significant risk for the parameters); Ω - the risk threshold of the parameter.

### 3.3 Determining the general demand from citizens for various elements of the smart city system

Public demand is the core source of information for estimating the criteria of smart cities. The analysis of the search queries can determine the trends and levels of the public interest in different aspects. It is possible to determine how the public interest changes in each specific component of the smart city system by observing these trends (Fig. 5 – 9). This research proposes a code in the programming language R for determining the public interest within each element of the smart city concept. This code should soon appear in the programming package in R (Shemetev, 2020). This algorithm represents the data at 100 percent of the maximum (for data privacy).

## 4 Results and discussion

Lisdorf (2020) provides the complete concept of an ideal smart city (based on matching and comparing almost all the available scientific literature on smart cities). The diagram below represents his concept:

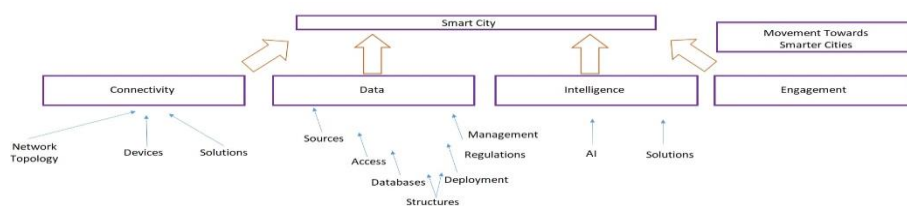


Fig. 3. Lisdorf (2020) concept of the smart cities in a single scheme<sup>5</sup>

At the same time, a smart city is more of a digital urban environment. This research offers a different idea of the smart city (Fig. 4).

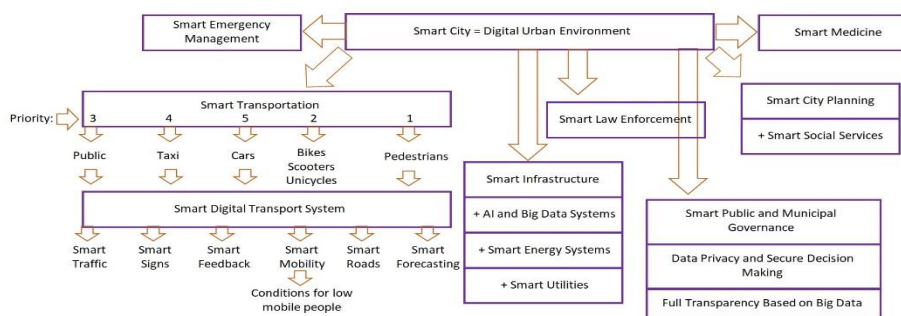


Fig. 4. Concept of the smart city and its main components<sup>6</sup>

<sup>5</sup> Own processing based on Lisdorf (2020) concepts.

<sup>6</sup> Own processing

Its first component is **smart transportation**.

The first subcategory is **smart public transport**. Each resident of such a city should have access to the geolocation of each vehicle in real-time; an easy and friendly interface to find out the entire route of each vehicle; a navigation system for the users of public transport to make a reasonable choice of carrier, taking into account the situation on the roads in the city; an intelligent selection system of public transport by traffic, taking into account the current and projected interest in it at each moment; a method for intercepting control of public transport data for emergency services and the police (as well as intercepting public transport traffic by these services); a system for predicting public transport breakdowns based on big data and artificial intelligence.

The second subcategory of smart transport should be **an intelligent taxi**. Every taxi car and every driver must have a registration in the public transport system. Special technical devices must control the time spent behind the wheel of each taxi driver. It is also desirable to monitor the health status of each taxi driver in real-time. Each taxi car must be integrated into an intelligent city transport system that should help taxis choose the correct route, considering the situation on the roads (and an overall situation in the city [like disasters, strikes, reconstructions, alerts]). This system should track the movement of taxis through taxi companies, service stations, repair and preventive operations for taxi cars. Such data makes it possible to create a system for predicting malfunctions and incidents on the roads with taxis (to minimize them). A particular system should monitor the speed of a taxi and violation of traffic rules by taxi drivers in real-time. Such a component of the innovative city system will make the city safer and more civilized (judging by the traffic on the roads).

The third subcomponent of the system should be **the intelligent traffic system**. A "smart traffic" method should work, selecting a route for each car/bike/scooter/pedestrian, taking into account the road situation in real-time (and in the predicted future). There must be a unified traffic integration system for cars, following which drivers receive more bonuses than by following a typical navigator. Such a system should be able to switch traffic signals, automatically change lanes, and change the meanings of road signs, taking into account the quantity and quality of routes built by users and taking into account the situation on the roads.

**This subsystem should consist of three components: cars, mobility devices** (bicycles, scooters, unicycles), and **pedestrians** (taking into account their mobility status). So, for example, if a pedestrian with limited mobility has a connection to a single city system online, the system should build a route for such person and keep traffic lights on green lights longer when such a pedestrian crosses vital traffic lanes. Also, such a system will allow for the correct distribution of traffic from bicycles (and scooters) and cars to minimize conflicts of interest on the roads. All this should be done in 2 modes: in the current time and prognostically.

The fourth subsystem of intelligent transport is a **system of smart roads and smart signs**. Signs are static in modern cities. Cities rarely implement dynamic road signs.

Meanwhile, connecting all signs to the intelligent city system makes sense so that each sign is dynamic. The size of the sign should change (for example, in conditions of heavy fog, the signs should increase in size and be brighter), the values on the sign (for example, the maximum allowed speed on the signs should fall in conditions of rain/ice/fog), as well as complexness of signs. For instance, A.I. can convert some roads into one-way roads by changing signs to relieve traffic in rush hour conditions. It can be helpful in a commuting environment. Suppose everyone moves to the city center in the morning. In that case, A.I. can automatically convert all signs for one-way traffic along the main highways (providing several exit routes for cars that travel from the center along different edges). In the evening, A.I. can convert the same roads to move sideways from the city center to the edges to avoid traffic jams. The intelligent city system must select signs to maximize road safety and efficiency in traffic capacity.

The fifth subcomponent of a smart transport system is a **system for the smart collection of user feedback**. Each user should be able to provide feedback on the problems of smart transport. For example, if a user sees a pothole on the road, this person should photograph it and immediately send it to be considered for city services. Systems for collecting and processing big data and artificial intelligence must ensure that road services correct all deficiencies on time and efficiently. Otherwise, they should automatically charge fines for employees who perform their duties least effectively compared to similar employees (by analyzing their reactions to feedback<sup>7</sup>).

The second critical component of an innovative city system is **the smart infrastructure module**. Artificial intelligence based on big data must decide whether government (or other) intervention is needed. For example, suppose two people have official registration in some apartment, and water and electricity are consumed for 16 people. In that case, the automatic system should request that such an apartment can have unregistered persons. Another example: people can forget to turn off the gas or iron in some flats. The intelligent city system should notify local services about the need to help such people install special sensors in their apartments, promptly contacting emergency services in the shortest possible time if signs of an emergency are detected. Selecting such notable groups is also possible based on cluster analysis (see the methodology section). Smart infrastructure must include capabilities for artificial intelligence and data storage. It should also include intelligent energy-saving systems for supply and heating. All of this operates hand in hand with smart utility management.

The third component of the smart city system is the **smart law enforcement module**. Exploring big data can predict both crime and potentially dangerous crime scenes. As a result, it is possible to change the city's infrastructure to prevent certain crimes proactively. For example, it may be a decision to demolish part of the infrastructure that blocks the area's visibility where crimes can potentially be committed. A.I. can also strengthen patrols based on data on potential crimes in a particular area. Smart cameras

<sup>7</sup> This experience corresponds with the unique Pudong experiment in China (the innovative smart city system that have reactions up to 120 times faster than similar systems in U.S. or E.U. in fixing the problems.

and facial recognition systems can help police catch criminals in hot pursuit (following local privacy laws). The crime prediction system can recommend routes to citizens by-passing potentially dangerous areas of a smart city. In addition, the global interest in law enforcement services remains high over time (Fig. 5).

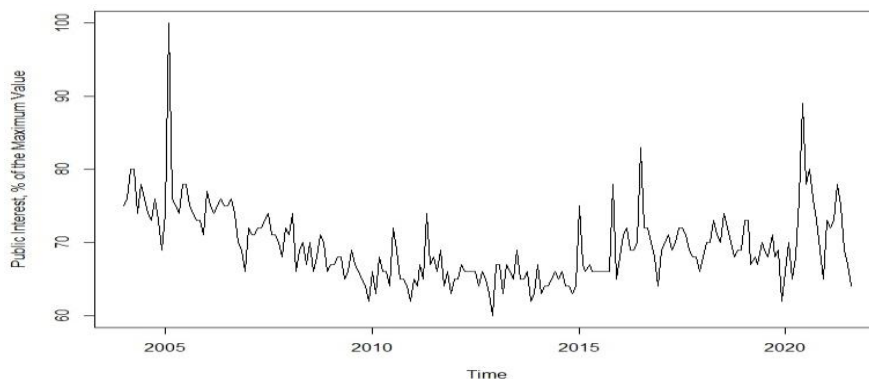


Fig. 5. Global interest in the law enforcement services over time, 01.2004 – 08.2021<sup>8</sup>

The fourth essential component of a smart city is **smart emergency management**. The system should automatically assess the danger and the number of forces to eliminate the consequences of such a situation. The system should block areas of the city with emergencies to make it easier for special equipment and personnel to eliminate the results of an emergency. The long and gradual decline of the global interest in emergency services [2005 – 2020] reversed (Fig. 6) to some increase in the public interest in the times of pandemics [2020-2021]. People looking for emergency services over the internet should receive them from the smart city's infrastructure rather than from direct "googling."

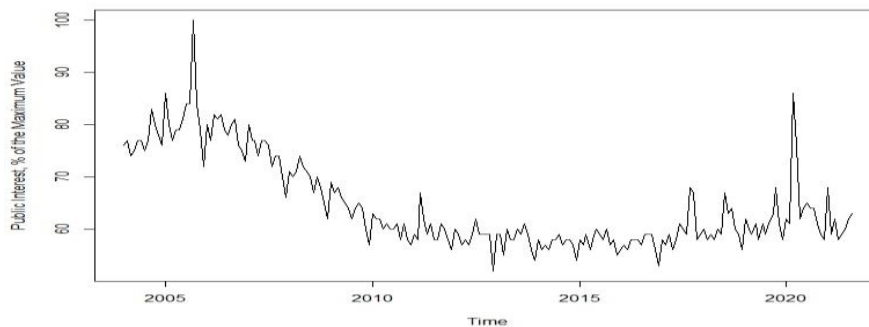


Fig. 6. Global interest in emergency services over time, 01.2004 – 08.2021<sup>9</sup>

<sup>8</sup> Own processing by the algorithm described in the methodology section.

<sup>9</sup> Own processing by the algorithm described in the methodology section.

The fifth component of the intelligent city system is the **smart city planning module**. Artificial intelligence based on big data should modulate city districts, for example, the more qualified distribution of building permits. Machines can use international databases and consider the most similar cases of successful designs of the most similar quarters of cities globally, considering the terrain and specifics. Thus, this should help solve the dilemma of Corbusier in city planning (Corbusier, 1971). Intelligent urban planning has strong links with the competent delivery of social services. It is challenging to plan an urban environment if essential social services are lacking (for example, if there is no quality urban environment, including schools, hospitals, social places, administrative centers, kindergartens). The global interest in urban and regional planning has gradually been increasing since 2014 (Fig. 7).

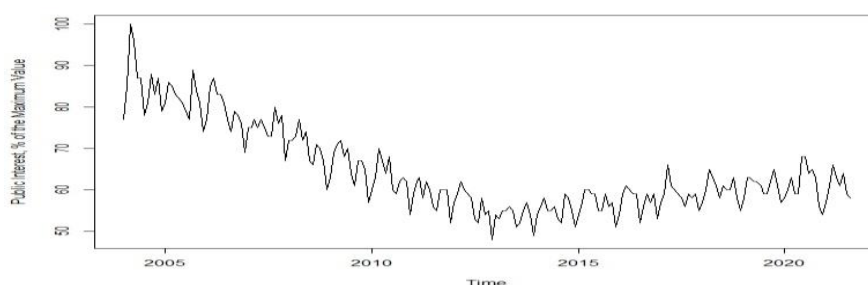


Fig. 7. Global interest in the urban and regional planning over time, 01.2004 – 08.2021<sup>10</sup>

The sixth essential component of a smart city is **smart medicine**. These components should analyze the risks to citizens' health and do everything possible to prevent an increase in these risks. This system can be embedded with points of collection of medical data, analyze the levels of the epidemiological situation, mobility of citizens, and existing threats. The global interest in public healthcare (Fig. 8) usually increases in crises (2009-2011; 2020-2021). The adequately developed infrastructure of a smart city could help people find the proper medical services.

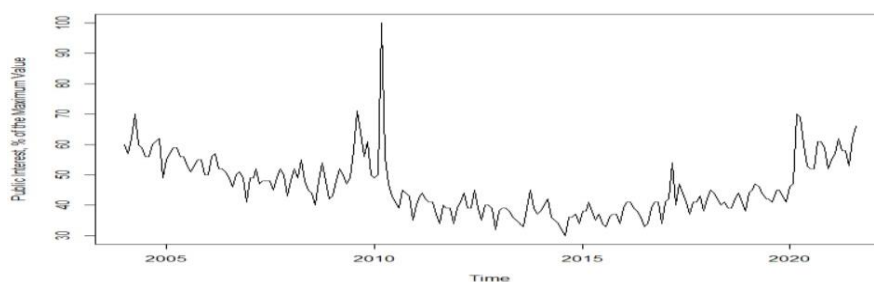


Fig. 8. Global Interest in Public Healthcare over Time, 01.2004 – 08.2021<sup>11</sup>

<sup>10</sup> Own processing by the algorithm described in the methodology section.

<sup>11</sup> Own processing by the algorithm described in the methodology section.

Public demand for smart medicine increases in times of crisis. The recent pandemic has also sparked a surge in demand for intelligent medicine.

The seventh critical component is **smart public and municipal governance**; it is one of the widely studied modules of the intelligent city system. There are many concepts for the implementation of this module nowadays. All models form two categories: those that value privacy most (Estonia) and those that value control most (for example, China). All countries have non-categorical distribution on a scale between these two levels. The overall interest in the services from the national and local authorities is usually constantly high over time (Fig. 9).

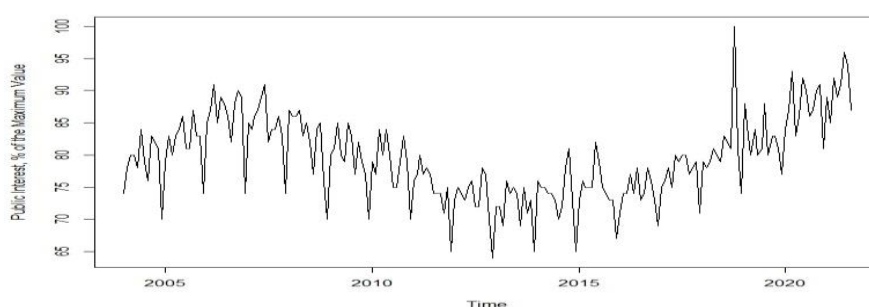


**Fig. 9.** Global interest in the services from state and local governments over time, 01.2004 – 08.2021<sup>12</sup>

There is a seasonal component in demand for public and municipal services. The minimum request is during the Christmas period. Bursts in spring and fall are typical. The need for assistance from the state and local authorities may decrease in summer during the vacation period. This category has had the most significant growth trend in recent years (against the background of other components of the intelligent city system).

This approach departs from both philosophical interpretation and case study. The technology implementation can be any. It can be some blockchain to maximize privacy (a comparative example can be Estonia). On the contrary, it can be a single database with no confidentiality (China is a comparative example). The proposed concept of a smart city will not change if researchers apply it to defining a smart city as a digital urban environment. Various cases of technology application are, in fact, only tools for the development of smart cities, this study suggests.

## 5 Conclusion

A smart city is an infrastructural phenomenon where technologies apply big data for computer analysis and city governance in at least seven innovative city components

<sup>12</sup> Own processing by the algorithm described in the methodology section.

suggested in this research. These components are smart transportation, innovative infrastructure, intelligent law enforcement, intelligent emergency management, innovative medicine, competent public administration, municipal management, and thoughtful city planning. This research focuses on creating a shared understanding of the concept of a smart city as a digital urban environment with seven elements. The additional contribution of this research is estimating the overall public interest and its trends in the smart city components. This research suggests these modules to be the minimum for a city to become "smart" (our study of the global demand verifies these components as vital). Thus, the study attempts to estimate the features of the smart city concept to validate the areas to find the proper indicators. Clustering analysis should help solve the data inconsistency and distortion problem while implementing the SCA-matrix should help solve the A.I. black box problem in managing the smart city. This analysis expresses an approach to define, monitor, and predict the degree of intelligence of a city. It can control the situations when the preliminary data has distortions or is unavailable for some core components.

## 6 Acknowledgment

The project funded this research is 19/2021 (IG507011, Faculty of Economics, Prague University of Economics and Business [V.S.E., Czech Republic]).

## 7 References

- Babecký, J., & Campos, N. F. (2011). Does reform work? An econometric survey of the reform-growth puzzle. *Journal of Comparative Economics*. <https://doi.org/10.1016/j.jce.2010.11.001>
- Babecky, J., & Havranek, T. (2014). Structural reforms and growth in transition. *Economics of Transition*. <https://doi.org/10.1111/ecot.12029>
- Caragliu, A., del Bo, C., & Nijkamp, P. (2011). Smart cities in Europe. *Journal of Urban Technology*. <https://doi.org/10.1080/10630732.2011.601117>
- Corbusier, L. (1971). *The city of to-morrow and its planning, 1887-1965*. M.I.T. Press.
- Fisher, R. A. (1936). The Use of Multiple Measurements in Taxonomic Problems. *Annals of Eugenics*, 7(2), 179–188. <https://doi.org/10.1111/j.1469-1809.1936.tb02137.x>
- Gorban, A. N., Golubkov, A., Grechuck, B., Mirkes, E. M., & Tyukin, I. Y. (2018). Correction of AI systems by linear discriminants: Probabilistic foundations. *Information Sciences*, 466, 303–322. <https://doi.org/10.1016/j.ins.2018.07.040>
- Gordon, I. R., & McCann, P. (2000). Industrial clusters: Complexes, agglomeration and/or social networks? *Urban Studies*. <https://doi.org/10.1080/0042098002096>
- Hanushek, E. A., & Woessmann, L. (2016). Knowledge capital, growth, and the East Asian miracle. *Science*. <https://doi.org/10.1126/science.aad7796>
- Huggins, R., Izushi, H., Prokop, D., & Thompson, P. (2014). The global competitiveness of regions. In *The Global Competitiveness of Regions*. <https://doi.org/10.4324/9780203799130>

- Leite, W. (2017). Propensity Score Matching. In *Practical Propensity Score Methods Using R*. <https://doi.org/10.4135/9781071802854.n5>
- Lisdorf, A. (2020). Demystifying Smart Cities: Practical Perspectives on How Cities can Leverage the Potential of New Technologies. In *Journal of Global Information Technology Management*. APRESS. <https://doi.org/10.1080/1097198x.2021.1954322>
- Organisation for Economic Co-operation and Development. (2019). *Smart Cities and Inclusive Growth*.
- Ratti, C., & Claudel, M. (2016). *The city of tomorrow: sensors, networks, hackers, and the future of urban life*. Yale University Press. <https://www.amazon.com/City-Tomorrow-Sensors-Networks-Hackers/dp/0300204809>
- Shemetev, A. (2012). *Complex financial analysis and bankruptcy prognosis and also financial management-marketing manual for self-tuition book* (1st-st ed.). Zodchy. [https://books.google.cz/books/about/Complex\\_financial\\_analysis\\_and\\_bankruptc.html?id=iViOsALV23QC&redir\\_esc=y](https://books.google.cz/books/about/Complex_financial_analysis_and_bankruptc.html?id=iViOsALV23QC&redir_esc=y)
- Shemetev, A. (2013). *Alexander Shemetev's financial softs as an innovative approach to management decisions making at an example of financial analysis of the three leading Russian business Gamers for the last 12 years (in Russian)*. FinSoft.Systems. <https://cutt.ly/fIRZGTd>
- Shemetev, A. (2018). *FinSoft.Systems performing financial analysis: RSBU, GAAP, IFRS. The leading Russian companies. Analysis for the last 20 years (by one button click)*. (FinSoft.Systems (ed.); 1st ed.). FinSoft.Systems. <https://cutt.ly/AIRX9un>
- Shemetev, A. (2019). *FinSoft.Systems creating financial analysis: RSBU, GAAP, IFRS: The European companies. In just few minutes (by one button click)*. <https://cutt.ly/nlRCGU6>
- Shemetev, A. (2020). *R Package alexandershemete*. FinSoft.Systems. <https://github.com/Alexandershemete/alexandershemete>
- Yee, T. W. (2015). *Erratum: Vector Generalized Linear and Additive Models*. [https://doi.org/10.1007/978-1-4939-2818-7\\_19](https://doi.org/10.1007/978-1-4939-2818-7_19)
- Yu, H., & Yang, J. (2001). A direct LDA algorithm for high-dimensional data — with application to face recognition. *Pattern Recognition*, 34(10), 2067–2069. [https://doi.org/10.1016/s0031-3203\(00\)00162-x](https://doi.org/10.1016/s0031-3203(00)00162-x)

# Diseño colaborativo de servicios inclusivos en ciudades inteligentes con mapas interactivos

Iván García-Magariño<sup>1,2</sup>, Juan Pavón<sup>1,2</sup>, Rubén Fuentes-Fernández<sup>1,2</sup>, and Jorge J. Gómez-Sanz<sup>1,2</sup>

<sup>1</sup> Grupo de investigación en Aplicaciones Sociales e Interdisciplinares basadas en Agentes (GRASIA),

Universidad Complutense de Madrid, Madrid 28040, España  
igarciam@ucm.es, jpavon@ucm.es, rfuentes@ucm.es, jjgomez@ucm.es,  
WWW home page: <https://grasia.fdi.ucm.es/>

<sup>2</sup> Instituto de Tecnología del Conocimiento, UCM, Madrid 28040, España

**Resumen** En el diseño de servicios de ciudades inteligentes se tiene cada vez más en cuenta la inclusividad, dando lugar a lo que se denomina Ciudad Inteligente Inclusiva (CII). Sin embargo, muchas de las soluciones que se implementan no cumplen realmente con las necesidades de los ciudadanos con discapacidad, generalmente por no tenerles en cuenta durante la captura de requisitos y posteriormente durante las pruebas de los servicios de ciudad inteligente. Para abordar un diseño más inclusivo es necesario, por tanto, contar con la participación ciudadana. En este sentido proponemos un par de herramientas para sistemas concebidos como conjunto de localizaciones coherentemente conectadas conteniendo ciertos elementos. La primera es una herramienta online distribuida y escalable que permite a los ciudadanos contribuir activamente al diseño de los servicios de CII. Esta herramienta permite visualizar las decisiones de los ciudadanos sobre los servicios propuestos y sus localizaciones en un mapa dinámico casi en tiempo real. Esta herramienta se complementa con otra que permite a los diseñadores seleccionar las ubicaciones adecuadas como combinaciones de opiniones de los ciudadanos, con suficiente flexibilidad para considerar funciones de similitud específicas. Se muestra su aplicabilidad con un caso de estudio concreto de servicio para emergencias pandémicas.

**Keywords:** Ciudad inteligente, diseño inclusivo, participación ciudadana, herramienta de colaboración

## 1. Introducción

La mayoría de los ayuntamientos y comunidades están planteándose la transformación de las ciudades con servicios inteligentes, y recientemente hay una sensibilidad hacia la inclusión de sectores con necesidades especiales, como puede ser personas con discapacidad o con menores recursos [2]. No obstante, muchas de las soluciones que se implementan no son aplicables o usables por estos sectores específicos de la población, generalmente por no tenerles en cuenta durante

2      García Magariño et al.

la captura de requisitos y posteriormente durante las pruebas de los servicios de ciudad inteligente. Para abordar un diseño más inclusivo es necesario, por tanto, contar con la participación ciudadana. En este trabajo defendemos que una ciudad inteligente inclusiva implica, entre otras cosas, el desarrollo de tecnologías que permitan a todas las personas, independientemente de su condición, obtener una mejor calidad de vida diaria, una mayor participación en su comunidad y una plena accesibilidad a todos los espacios y servicios desplegados. Concretamente en el caso de las personas con discapacidad, la aplicación amplia de sus derechos como cualquier ciudadano, y una vida más autónoma.

La transformación de las ciudades en ciudades inteligentes inclusivas (CII) requiere tener en cuenta muchos aspectos, como los diferentes tipos de discapacidad (por ejemplo, visuales, auditivas o cognitivas, como las que adolecen las personas con Parkinson o Alzheimer), los dominios de actuación (por ejemplo, la movilidad, la señalización o el consumo de recursos) y la perspectiva de los distintos actores (por ejemplo, la administración, los arquitectos, los trabajadores sociales, los ciudadanos o los ingenieros de software). Basta con recorrer hoy día un kilómetro en cualquiera de nuestras ciudades para identificar muchas dificultades que pueden encontrarse las personas con discapacidad, las personas mayores o las mujeres embarazadas tanto en edificios públicos, el transporte público o las calles [2].

Para abordar un diseño más inclusivo es necesario, si queremos entender bien los requisitos de los distintos colectivos, contar con la participación ciudadana. En este sentido proponemos una herramienta online distribuida y escalable que permita a los ciudadanos contribuir activamente al diseño de los servicios de CII. En la concepción de esta herramienta se ha considerado que el despliegue de soluciones de servicios de CII implica la instalación de dispositivos como sensores y actuadores, o elementos arquitectónicos o de transporte en el entorno urbano. Así pues, uno de los aspectos clave es situar adecuadamente estos elementos para la prestación de servicios. Por ello la herramienta permite asignar en un mapa interactivo dichos elementos y las opiniones de los ciudadanos al respecto, pudiéndose analizar posteriormente la información aportada.

A continuación se presenta, en la sección 2 una revisión de trabajos relacionados, que motiva la necesidad de herramientas como nuestra propuesta. Para ello planteamos un marco de trabajo de diseño colaborativo de servicios de CII, que se describe en la sección 3. Este marco de trabajo se ha experimentado con varios casos de estudio, y se presenta uno de ellos en la sección 4, así como resultados de dicha experimentación. Finalmente, la sección 5 discute los aspectos más relevantes de este trabajo y plantea algunas de las futuras líneas de investigación.

## **2. Herramientas para la participación ciudadana en el diseño de ciudades inteligentes**

Son numerosos los trabajos que proponen directrices para el diseño de las CII, pero no muchos abordan aspectos de inclusividad, como la accesibilidad,

o la participación ciudadana activa a lo largo del proceso de desarrollo de las soluciones.

En algún caso, como en [8] se analizan varios enfoques de diseño de CII en distintos países para proponer un modelo que sea aplicable a las particularidades de las ciudades indias, centrado en la recogida de datos de Internet de las Cosas (IoT), dispositivos vestibles y teléfonos inteligentes, para conformar perfiles digitales que se consideren CII. Sin embargo, dicho modelo no está soportado por una herramienta que permita involucrar a los ciudadanos en el diseño de la CII, como hace el presente trabajo.

Algún esfuerzo se ha realizado para proporcionar herramientas visuales que promuevan la participación pública inclusiva para involucrar a los ciudadanos en el diseño de las ciudades. En [1] se hace una revisión de las herramientas visuales que permiten evaluar de forma colaborativa el impacto ambiental y así apoyar los procesos de toma de decisiones de las autoridades. Algunas de las herramientas que se describen permiten ayudar en nuevos diseños sobre fotos aéreas, o utilizando mapas interactivos en los que los usuarios colocan objetos físicos, o basándose en sistemas de información geográfica (SIG) como base para la evaluación del impacto ambiental. No obstante, estas herramientas se centran más en el impacto medioambiental que en la inclusión de las ciudades inteligentes, como en el presente trabajo.

Aunque existe una gran preocupación por hacer que las ciudades inteligentes sean inclusivas, por ejemplo en lo que respecta a las necesidades de las personas con discapacidad, la literatura sobre el diseño urbano colaborativo todavía carece de herramientas online adecuadas para involucrar a los ciudadanos en el diseño de servicios inclusivos. Este trabajo aborda esta laguna de la literatura como se explica en las siguientes secciones.

### **3. Marco de trabajo para la participación ciudadana en el diseño de ciudades inteligentes inclusivas**

Tal vez los ingenieros estemos acostumbrados a utilizar diagramas para especificar nuestros diseños y trabajar sobre ellos, pero el ciudadano en general no. Es necesario por tanto encontrar algún tipo de elemento de representación del objeto de discusión, en este caso los servicios de CII. En este sentido, el marco de trabajo propuesto plantea el uso de herramientas visuales que atraigan más fácilmente la atención de los ciudadanos participantes en el proceso de desarrollo. Estas herramientas deben proporcionarse en línea para fomentar la participación ciudadana, sin necesidad de instalar ningún software adicional que pudiera desanimar a los potenciales participantes.

La Figura 1 muestra el marco de trabajo propuesto, donde puede observarse que los ciudadanos pueden colaborar en el diseño de las CII colocando los servicios y sus dispositivos asociados en determinados escenarios mediante una herramienta interactiva que trabaja sobre un mapa de la zona donde se quiere implantar la solución. Por otra parte, los diseñadores de la solución de CII dispondrán de otra herramienta que analiza la información recolectada por

4 García Magariño et al.

la anterior herramienta para combinar automáticamente los diseños propuestos basándose en funciones de clustering o de similitud específica.

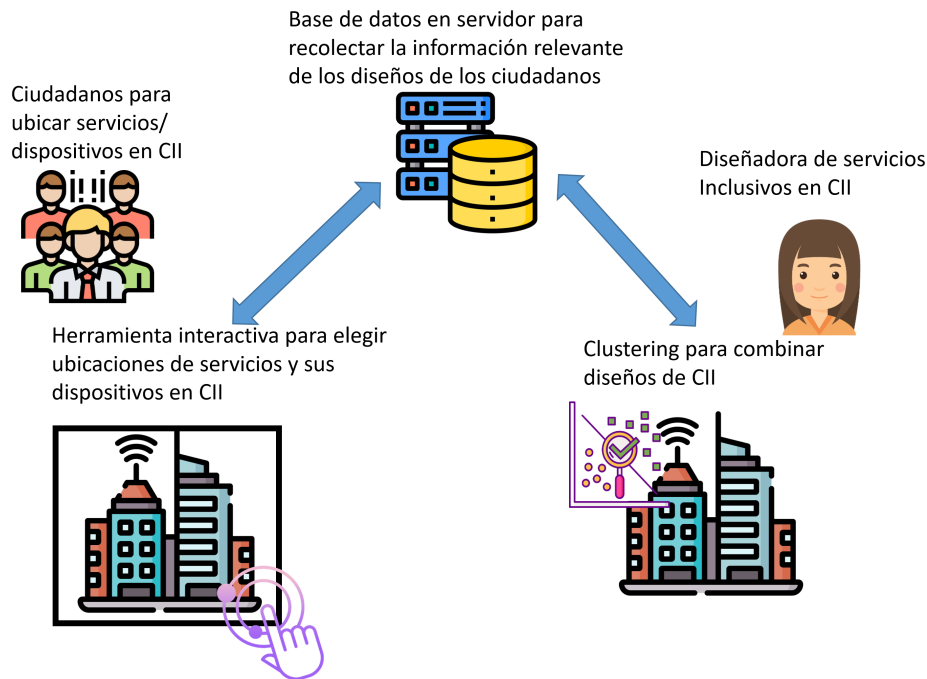


**Figura 1.** Visión general del marco de trabajo de diseño participativo de CII

El marco de trabajo admite el desarrollo de herramientas en línea para decidir los lugares adecuados y la cantidad de diferentes tipos de sensores, dispositivos o servicios en cualquier entorno interior o exterior de una CII. En particular, se pide a los usuarios que tengan en cuenta en la medida de lo posible la inclusión de las personas con discapacidad (por ejemplo, con sillas de ruedas, o con discapacidad visual o auditiva).

La creación de cada escenario se basa en la selección de una determinada fotografía como fondo y de determinados iconos para representar los sensores/dispositivos/ servicios que deben colocarse en la fotografía para indicar el lugar. Para separar al máximo la programación de las imágenes de los casos, hemos utilizado un mecanismo numerado de denominación de escenarios e imágenes, de modo que las acciones de los ciudadanos se limitan a seleccionar las imágenes adecuadas y a organizarlas con los nombres apropiados. Utilizamos esta técnica porque una similar nos permitió trabajar de forma eficiente y en colaboración con investigadores médicos en nuestro anterior sistema para el desarrollo de aplicaciones de m-salud (FAMAP) [3].

Para los diseñadores se ofrece la posibilidad de realizar el clustering de los diferentes lugares de servicios recogidos de los usuarios. Para ello, utiliza un módulo programado en Python que procesa los datos recogidos en la base de datos a través de un script PHP. El framework utiliza la librería de Python Scikit-learn [9] para el algoritmo de clustering K-Means.

Así es posible aplicar diferentes mecanismos para generar un diseño popular a partir de diferentes propuestas ciudadanas. Una forma de hacerlo es aplicando el clustering con el algoritmo K-means [5] y luego utilizar los centros de estos clusters como las posiciones estimadas. Esto se aplica a todas las posiciones sugeridas para cada tipo de servicio. Para ello el diseñador debe probar varios números de conglomerados y elegir el número de conglomerados que tenga sentido en el contexto dado.

Otra opción es tratar cada diseño como un diseño completo y coherente que debe ser analizado en su totalidad y de forma consistente. Así, cada diseño se considerará como un vector de posiciones de cada tipo de servicio. A continuación, cada diseño se compara con todos los demás calculando la suma de las distancias al cuadrado con respecto a otros diseños. De este modo, el sistema elegirá un diseño coherente que sea el más parecido a todos los demás, y se asegurará de que el diseño sea coherente, ya que fue diseñado inicialmente como un diseño completo. Además, el diseño seleccionado es el más cercano a todas las posibilidades en la medida en que la función de distancia sobre la similitud está correctamente seleccionada.

Las funciones de similitud de los lugares diseñados deben considerar los siguientes aspectos:

1. En el mismo servicio, la distancia no debería depender del orden de las ubicaciones en cada diseño, ya que una permutación de la representación interna de un conjunto de ubicaciones es el mismo conjunto de ubicaciones.
2. Si el sistema permite al usuario seleccionar un número variable de ubicaciones, entonces el sistema debe ser capaz de comparar conjuntos de ubicaciones de diferentes tamaños.
3. Los diferentes servicios pueden considerarse por separado o junto con otros servicios, teniendo en cuenta la posible dependencia entre los diferentes servicios. Esto varía en función del contexto CII seleccionado y de los servicios seleccionados.

Para mejorar el primer aspecto, se pueden ordenar las ubicaciones en todos los diseños antes de la comparación, de modo que el orden original de cada diseño no influya en el resultado de la función de similitud.

En cuanto a la comparación de diseños con diferentes tamaños, se pueden considerar varias opciones. El diseñador puede establecer el número o rango de servicios disponibles y luego ver los resultados de cada diseño. Así el algoritmo sólo considerará como candidatos los diseños que estén dentro de ese rango, y la comparación se realizará sobre todos los diseños. En los diseños con un número excesivo de ubicaciones, sólo considerará las más cercanas a los servicios comparados. Además, el diseñador puede definir una función de similitud adecuada

6 García Magariño et al.

que pueda aplicarse de forma coherente sobre diseños con diferente número de ubicaciones.

El tercer problema se aborda dando al diseñador cierto grado de libertad en la definición de la función de similitud. El diseñador puede escribir una nueva función de similitud y utilizarla teniendo en cuenta las particularidades del dominio y la dependencia entre servicios. En caso de ser servicios independientes, la comparación puede calcularse por separado y, opcionalmente, ponderarse para considerar la relevancia. Estas ponderaciones se pueden votar y promediar entre todos los diseñadores.

Con estas herramientas los diseñadores puedan crear nuevos escenarios con sólo indicar una imagen de fondo e imágenes que representen los servicios, y nombrar a todos ellos de una manera particular, es decir “b.jpg” o “b.png” para el fondo y “s0.png”, “s1.png”, ..., “sN.png” para cualquier número de servicios. Esto debe colocarse en una carpeta con un nombre/número y luego se accederá a este servicio indicando este nombre/número en el parámetro “escenario” de la URL del sitio web.

Las posiciones almacenadas en la base de datos se calculan con distancias proporcionales a la anchura de la imagen de fondo, por lo que las ubicaciones se representan de forma coherente independientemente del dispositivo utilizado por los usuarios.

#### 4. Diseño colaborativo de una ciudad inteligente para emergencias por pandemias

Como ejemplo de aplicación del marco de trabajo y herramientas asociadas se plantea el diseño de algún servicio que ayude a la gestión de emergencias en situaciones de pandemia, estableciendo en ella hospitales temporales, residencias para cuarentenas y lugares para hacer pruebas de virus en lugares estratégicos. La herramienta interactiva permite establecer los mejores lugares para tales fines, permitiendo al usuario pulsar los botones de iconos para crear nuevos servicios y arrastrarlos a los lugares preferidos en el mapa.

En la figura 2 se muestra esta herramienta interactiva que utiliza el mapa de Madrid para este tipo de diseño. Este estudio de caso está disponible en su sitio web <sup>3</sup>.

La pandemia de Covid-19 ha planteado muchos enfoques diferentes para controlar la transmisión del virus, que van desde los mecanismos impulsados por el hombre hasta los impulsados por la tecnología [7]. En España, la forma de restringir la movilidad ha cambiado según la comunidad autónoma, los distritos y las ciudades. Las soluciones tomadas/diseñadas no suelen tener en cuenta la opinión de los ciudadanos, en parte por la dificultades para consultarlos masivamente cuando los periodos de tiempo son cortos. La herramienta propuesta podría ser útil para el diseño colaborativo de ciudades inteligentes para que sean

<sup>3</sup> <http://euphoria.fdi.ucm.es/placeISC/index.php?scenario=1&lan=es> (último acceso 30/09/2021)

Diseño colaborativo de servicios inclusivos en ciudades inteligentes

7

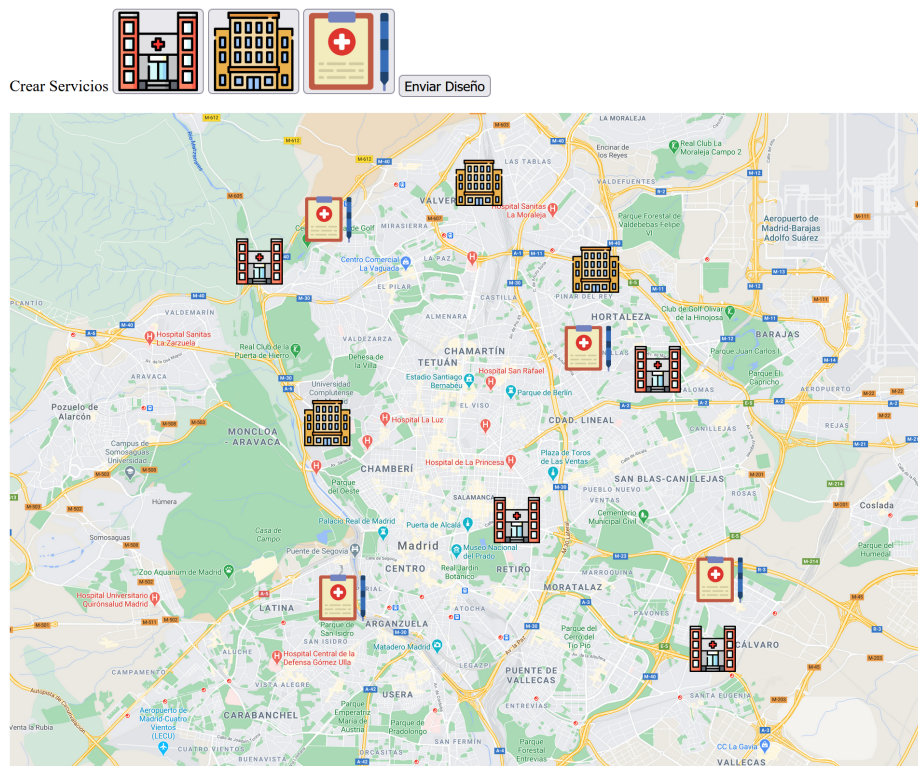


**Figura 2.** Herramienta interactiva para el diseño de una ciudad inteligente para emergencias pandémicas.

8 García Magariño et al.

robustas contra las pandemias y las soluciones propuestas bien aceptadas por sus ciudadanos.

La figura 3 presenta una de las soluciones usadas, concretamente la colocación de dispensadores de gel hidroalcohólico y el análisis de clustering de las posiciones seleccionadas de los dosificadores de gel hidroalcohólico. Este gráfico muestra todas las posiciones. La posición de cada cluster se representa con un color diferente. Para cada análisis de clustering, probamos diferentes números de clusters en el rango de tres a siete, y presentamos el análisis más relevante que tuvo sentido.



**Figura 3.** Análisis de clustering de las ubicaciones de los dispensadores de gel.

La imagen del análisis de clustering de los dispensadores de gel muestra líneas verticales de posiciones. Esto es razonable ya que la fotografía de la biblioteca tenía grandes ventanas y los lugares razonables coinciden con los únicos espacios de columna entre las ventanas.

## 5. Discusión y conclusiones

El marco de trabajo propuesto proporciona una base para recopilar masivamente propuestas ciudadanas que contribuyan a un diseño más eficaz e inclusivo de soluciones en CII. Las herramientas facilitan la identificación y combinación de diseños populares que satisfagan las preferencias de la mayoría de usuarios en la medida de lo posible. Sin embargo, el diseño colaborativo suele requerir varias rondas de propuestas y debates entre los diseñadores, como se suele

proponer en el proceso Delphi, como se puede observar, por ejemplo, en su aplicación como herramienta de apoyo a la toma de decisiones para la gestión del parque inmobiliario en las ciudades [6]. De hecho, existen ejemplos de plantillas de cuestionarios, y hay algunas herramientas que proponen parcialmente el proceso Delphi en determinados contextos, como nuestra propuesta para evaluar la relevancia de los documentos con un sistema multiagente (MAS) [4]. El inconveniente del proceso Delphi es que puede ralentizar el proceso de diseño en el caso de un gran número de participantes, y sería realmente difícil esperar un acuerdo completo entre todas las partes. Incluso en este contexto, sería útil combinar automáticamente los diseños recogidos con un mecanismo como los propuestos en el presente artículo. En este sentido, nuestro modelo podría incluir un mecanismo de comunicación sobre los diseños.

Cabe destacar que la puesta en marcha de un caso de estudio concreto ya implica la toma de algunas decisiones de antemano, como los servicios concretos que se ofrecerán, así como el dominio. Una primera fase consistirá en recabar de los ciudadanos qué servicios son los más deseados por el ciudadano de una ciudad para considerar su inclusión en la misma. Un cuestionario abierto podría permitir a los ciudadanos proponer servicios para tener una amplia colección de servicios en los que haya al menos algunos ciudadanos interesados. De hecho, en una segunda fase, la gran variedad de servicios puede ser votada para considerar sólo los más populares.

La experimentación muestra una adecuada interacción en la determinación del diseño en términos de tiempos de respuesta, gracias a la ejecución local en los dispositivos de los usuarios de la mayor parte del procesamiento. El análisis de clustering también muestra tiempos de respuesta razonables.

Tenemos previsto seguir integrando esta herramienta interactiva para la selección de servicios inclusivos en diferentes escenarios de las CII en el proceso completo de decisión del diseño de las CII en su conjunto. Por ejemplo, planeamos integrar esta herramienta con novelas interactivas que hemos desarrollado recientemente, para combinar la introducción de servicios con el diseño de CII indicando las ubicaciones de los dispositivos. También estamos considerando la oportunidad de utilizar Twitter como herramienta externa para comentar los diferentes diseños combinados, para aumentar el impacto y la participación, ya que esta red social ya tiene muchos usuarios que están conectados entre sí de una manera coherente.

## Referencias

1. De Oliveira, A.R., Partidário, M.: You see what I mean?—A review of visual tools for inclusive public participation in EIA decision-making processes. *Environmental Impact Assessment Review* **83** (2020) 106413
2. de Oliveira Neto, J.S., Kofuji, S.T.: Inclusive smart city: an exploratory study. In: *International Conference on Universal Access in Human-Computer Interaction*. Volume 9738 of *Lecture Notes in Computer Science.*, Springer (2016) 456–465
3. García-Magariño, I., Bedia, M.G., Palacios-Navarro, G.: FAMAP: a framework for developing m-Health Apps. In: *World conference on information systems and tech-*

10      García Magariño et al.

- nologies. Volume 745 of *Advances in Intelligent Systems and Computing.*, Springer (2018) 850–859
4. García-Magariño, I., Gómez-Sanz, J.J., Pérez-Agüera, J.R.: A complete-computerised delphi process with a multi-agent system. In: *International Workshop on Programming Multi-Agent Systems*. Volume 5442 of *Lecture Notes in Computer Science.*, Springer (2008) 120–135
  5. Hofmeyr, D.P.: Degrees of freedom and model selection for k-means clustering. *Computational Statistics & Data Analysis* (2020) 106974
  6. Jiménez-Pulido, C., Jiménez-Rivero, A., García-Navarro, J.: Sustainable management of the building stock: A Delphi study as a decision-support tool for improved inspections. *Sustainable Cities and Society* **61** (2020) 102184
  7. Kummitha, R.K.R.: Smart technologies for fighting pandemics: The techno-and human-driven approaches in controlling the virus transmission. *Government Information Quarterly* (2020) 101481
  8. Malhotra, C., Manchanda, V., Bhilwar, A., Basu, A.: Designing inclusive smart cities of the future: the Indian context. In: *Solving Urban Infrastructure Problems Using Smart City Technologies*. Elsevier (2021) 631–659
  9. Pedregosa, F., Varoquaux, G., Gramfort, A., Michel, V., Thirion, B., Grisel, O., Blondel, M., Prettenhofer, P., Weiss, R., Dubourg, V., et al.: Scikit-learn: Machine learning in Python. *the Journal of machine Learning research* **12** (2011) 2825–2830

## Post-pandemic redesign of downtown streets for people. The Bahía Blanca city experience.

Yamila S. Grassi<sup>1</sup>[0000-0002-9655-4643] and Mónica F. Díaz<sup>1-2</sup>[0000-0002-6680-8067]

<sup>1</sup> Planta Piloto de Ingeniería Química - PLAPIQUI (UNS-CONICET), Camino La Carrindanga 7000, Bahía Blanca (8000), Argentina

<sup>2</sup> Departamento de Ingeniería Química, Universidad Nacional del Sur (UNS), Avenida Alem 1253, Bahía Blanca (8000), Argentina  
ygrassi@plapiqui.edu.ar

**Abstract.** Sustainable urban mobility in a city encourages active mobility and public transportation. Rethinking better use of streets will reduce vehicular congestion and pollutant emissions, discouraging private car use and promoting pedestrian traffic and sustainable mobility. As a result of the lifestyle changes brought about by the COVID-19 pandemic, government authorities have begun to evaluate improvements in urban mobility, prioritizing projects that reappraise public spaces. In Bahía Blanca, before the pandemic, interventions such as semi-pedestrianization and the construction of bicycle and bus lanes were already underway. However, in the pandemic times, changes in public spaces have been reappraised with the aim of developing an environmentally friendly and people-centered urban mobility. Therefore, the sidewalks widening and the more recent creation of the so-called urban living rooms, as well as the permissions for the construction of parklets, have been favored by the social distancing measure adopted to avoid massive contagions. In addition, active mobility was also reinforced during the pandemic with the construction of new bicycle paths. Undoubtedly, the pandemic situation has given cities the opportunity to rethink the manner in which citizens travel around and the way in which urban public spaces are used.

**Keywords:** Active Mobility, Streets for People, Bahía Blanca City, Tactical Urbanism.

### 1 Introduction

Sustainable urban mobility is accompanied by a new prioritization of city street space, encouraging active mobility and public transport [1, 2]. As the number of vehicles rises in the city, the vehicular flow increases, leading to traffic jams and higher levels of urban air pollution. Therefore, this situation triggers a rethinking of the urban mobility form, tending to be more environmentally friendly and people-centered [3]. For this reason, more and more cities are trying to change the balance of their streets to discourage motorized traffic, especially private cars [4, 5, 3]. Through the change in the way that urban streets are used, there is an attempt to move towards what is known as “street for people” or “complete street” instead of “streets only for motorized traffic” [6, 7, 8].

The COVID-19 pandemic, which began in late 2019 in China, has brought deep changes to the daily lives of people around the world. This has allowed citizens to consider the possibility of living in a more sustainable and smarter city. Moreover, it has made it possible for urban planners to redesign city streets and create more space for pedestrians and cyclists, while respecting the rules of social distancing [9]. Thereby, supporting the mobility trend that involves focusing on travelling people in a more sustainable and healthy way, thus reducing congestion and urban air pollution [10]. Consequently, the construction of pedestrian-only lanes, micromobility, a paradigm shift that encourages shared mobility, as well as a strong engagement with public transport to reinforce it, emerged as goals of many cities during this pandemic situation. Undoubtedly, as Kakderi et al. mention, the COVID-19 crisis will generate important opportunities for urban planning and mobility [11].

Bahía Blanca is a medium-sized Argentine port city with 301,572 inhabitants, according to the last census of 2010, and has approximately one motor vehicle for every two people [12]. It is located in the southwest of the province of Buenos Aires and given the city size, many of the pre-pandemic activities were centered in the city downtown area. As the pandemic situation progresses, there are more habits that may continue over time, such as telecommuting and reducing the number of trips needed between different parts of the city [13, 14]. This paper describes the changes observed in daily life in the microcenter of the city. Some amendments were spontaneous and others were promoted by the local hall, both in response to the new socio-economic situation. The impact of these changes could be evaluated by following indicators in short and medium term periods. It is known that the restrictions have modified the local daily life and the way of commuting. Consequently, a greater number of people have started to use alternative means of transport, such as bicycles or e-scooters [15]. As a result of the pandemic situation and the implementation of measures against COVID-19 infection, the government has begun to prioritize projects to reappraise public space. In this context, measures such as social distancing have led the local authorities to carry out interventions in urban streets, such as widening sidewalks for pedestrian traffic or allowing the construction of parklets for shops. However, all these initiatives are intended to take root in the city and discourage the use of private cars in the city's downtown area. After the pandemic passes, the goal of cities should not be to return to the “old normality”, but to build a better, more sustainable and environmentally friendly one, which is associated with the concept of smart environment [16, 17]. In particular, this paper shows the experience of urban spaces transformations in the downtown area of Bahía Blanca City towards a “new post-pandemic normality”.

## 2 The Bahía Blanca experience

Cities around the world have taken measures to increase the outdoor space available for people, create safer streets that prioritize public transport and active mobility, and involve citizens in the process [3]. Furthermore, the aim is not only to deal with the pandemic and support public health, but also to rethink the streets and public spaces for a future post-pandemic city [16]. In this sense, these actions not only decrease motorized vehicle traffic on the streets, but also provide environmental, health and safety benefits [7]. Figure 1 shows the location of the most outstanding interventions

that have been carried out in the microcenter of the city, most of them in a pandemic situation. Note that the bus lanes were not included in Figure 1 in order to avoid color overlaps and to make the image as clear as possible. Please consider that “Plaza Rivadavia” is the main square, surrounded by the microcenter of the city.

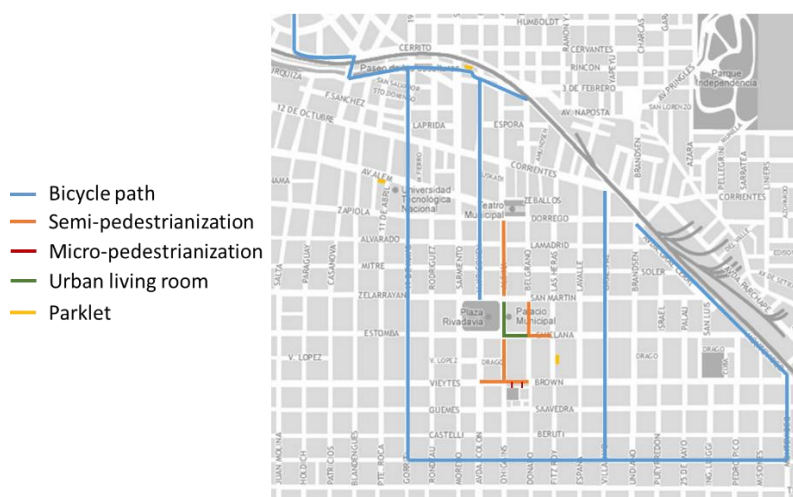


**Fig. 1.** Location of the different interventions carried out in the micro and macro center of Bahía Blanca City (no bus lanes were included because of overlapping).

In each subsection below, the most relevant modifications carried out in the micro and macro center of Bahía Blanca City are discussed, as well as the concept and interventions of bicycle paths, semi-pedestrianization, sidewalk widening, micro-pedestrianization, urban living rooms, parklets and bus lanes.

### 2.1 Bicycle paths

Bicycle paths can be defined as separate lanes for bicycles or similar non-motorized vehicles, physically separated from other traffic lanes [18]. The construction of bicycle paths in Bahía Blanca City has been carried out in stages, and segments of the network are still awaiting to be constructed [18, 19]. Furthermore, each stage has had its own particularities, such as the location within the street and the form of protection for the cyclist. In Figure 2, it can be seen how physical barriers have been implemented to protect cyclists, such as concrete stops, or the parked vehicles. Moreover, all the bicycle paths that have been built in the city so far are two-way, allowing traffic to circulate in both directions. According to municipal and own assessments [15, 20, 21], bicycle paths are becoming more and more used. However, the evolution should continue to be evaluated in terms of the purpose of their use (commute or recreational) as well as whether there is a certain seasonality in the increase in the number of bicycles that use the city's bicycle paths.

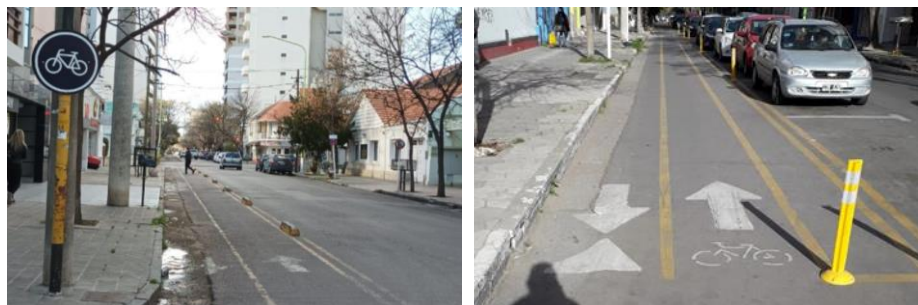


**Fig. 2.** Depending on the stage of the bicycle path, two types of physical barriers have been used to protect the cyclists, concrete stops (left) or parked vehicles (right). Source: Own.

### 2.2 Pedestrianization, sidewalk widening and urban living rooms

It is well known that pedestrian zones are of utmost importance in cities, especially to encourage active mobility, improve the environment, as well as to allow safe and comfortable pedestrian circulation [22]. In 2009, the semi-pedestrianization of O'higgins Street was carried out in Bahía Blanca (see Figure 3). From 2011 to 2018, the semi-pedestrianization of Alsina Street was carried out in order to generate new meeting spaces and improve pedestrian circulation (see Figure 4). The semi-pedestrianization consisted of widening sidewalks, installation of LED lighting, street furniture, sidewalks at street level, corner ramps and docks for loading and unloading of goods [23, 24]. Figures 3 and 4 show how the sidewalks are wider now and only two lanes of traffic are allowed to circulate, avoiding stopping in these areas. Moreover, in Figures 3 and 4 the widening generated in the intervened areas has been indicated by using red arrows; in consequence, it can be realized the original sidewalks were too narrow.



**Fig. 3.** Semi-pedestrianization on O'higgins Street. The red arrow indicates the widening of the originally narrow sidewalks. Source: Own.

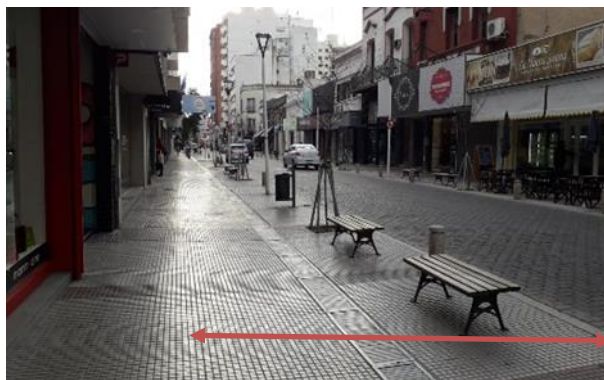


**Fig. 4.** Semi-pedestrianization on Alsina Street. The red arrow indicates the widening of the originally narrow sidewalks. Source: Own.

Despite the fact that semi-pedestrianization started prior to the pandemic with the objective of promoting and improving pedestrian movement in the downtown area, during the period 2020-2021 a greater number of interventions have been carried out. For instance, sidewalk widening (see Figure 5), urban living rooms (see Figure 6) as well as micro-pedestrianization (see Figure 7) have been implemented. Consequently, pedestrians were gaining ground on the streets of the microcenter of the city. While the COVID-19 pandemic was progressing, all the measures presented were taken in order to comply with social distancing [25].

One of the initial measures implemented during 2020 was the sidewalk widening. In this case, one of the lanes of the street is separated by the use of plastic poles to provide pedestrians with more space to walk safely. In this sense, people can circulate on both the original sidewalk and the widening (see Figure 5).



**Fig. 5.** The pictures show the widening of the sidewalk on Brown Street (left) and Chiclana Street (right) demarcated with paint and plastic poles. Source: Own.

In order to make more attractive places for pedestrian transit, some sectors that had initially been intervened with the sidewalks widening, were transformed into what is known as urban living rooms. This concept is associated with the so-called tactical urbanism and was implemented both on Alsina Street, just in City Hall’s block (in front of Rivadavia Square), and on the second block of Chiclana Street (see Figure 6). The

improvements include an artistic intervention on the pavement that is part of this new space. In addition, planters with plants have been placed and there are plans to add benches for seating [26, 27].



**Fig. 6.** Pictures of the so-called urban living rooms in Alsina Street (left) and Chiclana Street (right). Source: Own.

Finally, the area surrounding the Municipal Market, where some groceries and food stores are located, has been intervened. In order to reappraise this area of the city's downtown, small streets belonging to the sector were pedestrianized (see Figure 7). The micro-pedestrianization, so called because it involves short segments of streets, favors open-air meeting space for citizens [28].



**Fig. 7.** The pictures show the before (left) and after (right) of the micro-pedestrianization of one of the streets next to the Municipal Market. Source: La Nueva [29, 30].

### 2.3 Parklets

Parklets are temporary facilities that increase public space for people to reconnect with others in their community and the environment. As defined by Birdsall, a parklet is a "space for people to park themselves" [31]. In mid-August 2020, a city ordinance was approved allowing merchants to install the so-called parklets [32]. The purpose of having a parklet is to expand sidewalk space, initially to provide more space for businesses, in order to comply with the social distancing imposed by the pandemic. In addition, the idea of discouraging the use of private cars in the micro and macro center areas is promoted by this modality [33], occupying the space destined for private parking. It should be noted that the idea of parklets is that they can be used by anyone passing through the area. For this reason, and because the economic investment is made

by the merchants, there are still not many constructions of this type that have been installed in the city [31, 32]. Figure 8 shows the parklets installed in the city.

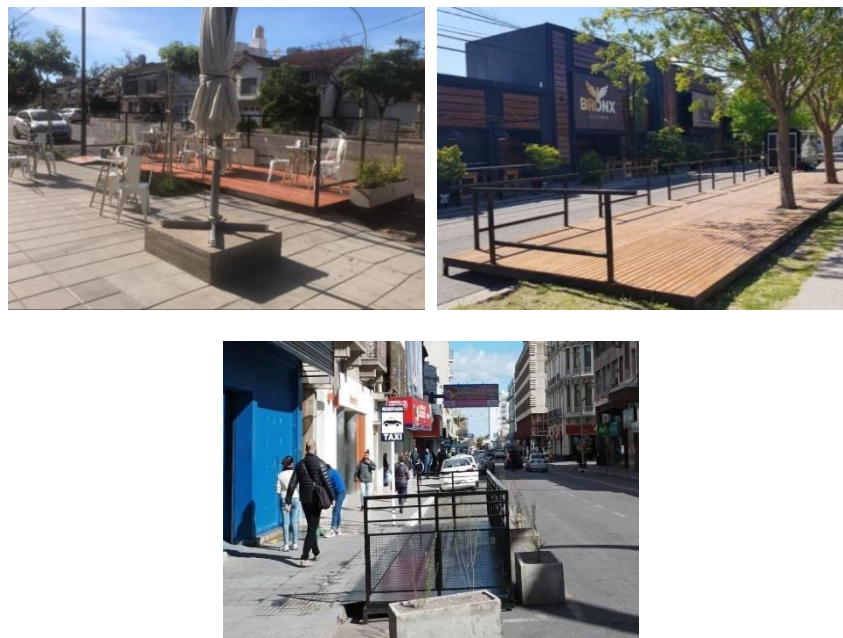


**Fig. 8.** Parklets installed at different local stores. Source: La Nueva (top left) [34], Frente a Cano (top right) [35] and own (bottom).

#### 2.4 Bus Lanes

The preferential lanes for public-passenger transport began to be implemented in the city in 2017, under municipal ordinance No. 18792 and its subsequent amendments [36]. These lanes are exclusively for urban passenger buses; no private vehicles of any kind can circulate, although ambulances, police, firefighters and civil defense are allowed to circulate in case of emergencies. The delimitation of bus lanes makes it possible to speed up the passing of urban passenger buses through the city's downtown area, thus reducing travel time. Therefore, the polluting and greenhouse gas emissions generated by public transportation can be reduced. In addition, given that urban traffic is becoming more and more chaotic due to the increase in the number of vehicles, all the reorganization measures taken will reduce traffic congestion. Figure 9 shows the delimitation of the preferential lane for public transport, with the corresponding signs and infographics painted on the asphalt.



**Fig. 9.** Delimitation of preferential lanes for buses with the corresponding infographics and signs.  
Source: Own.

### 3 Discussions and conclusions

The crisis generated by the COVID-19 pandemic has become the starting point for a deep change in urban organization; in particular, in urban mobility, not only in the way we move around the city, but also in the conception we have of the streets and who should circulate on them, as well as public spaces. At this point, cities should take advantage of this moment to implement sustainable mobility plans, rethinking the way we move around the city and use urban public spaces. Consequently, this paper presented the experience of transforming the urban environment of the microcenter of Bahía Blanca City, Argentina.

The measures implemented to counteract COVID-19 contagions made it possible to prioritize projects that reappraised public space, improving the city's resilience for the future, moving towards a city with less traffic and more outdoor activities. In addition, the implementation of pre-existing measures in the city were accelerated, such as the installation of new bicycle paths. While the measures that correspond to the development of tactical urbanism seek to improve conditions that encourage the pedestrianization of areas, as well as discourage the use of private motorized transport, among other things. These interventions must be planned and designed with a long-term vision to encourage a permanent, healthier and more sustainable urban design [37].

In this work, several modifications that have been carried out in the microcenter of the city of Bahía Blanca were presented. It should be noted that at the beginning some modifications were not supported by a part of the society [38, 39]. This was not only because they did not agree with them or considered them unnecessary, but also because of the expense they could generate for the municipality, as well as considerations that have not been taken into account at the time of the interventions such as the accessibility for people with disabilities, among others [30]. It is well known that changes are not always simple and, as Vargas Tobar mentions, "tactical urbanism will be a good strategy as long as it is adapted to the Latin American reality" [40]. In particular, we consider that the interventions presented in this work should be a first stage for the city's microcenter, being that new phases that include the different Bahía Blanca neighborhoods should be considered. It may be noted that, during the strictest lockdown of the pandemic, according to Google reports [41], citizens began to move more in the surroundings close to their homes. As a result, necessities were purchased nearby,

because large neighborhoods of the city have small centers. Such is the case of Villa Mitre, Noroeste, Villa Rosas, and the area of 14 de Julio Street, which are located at 3, 4, 5 and 7 kilometers from the city's microcenter, respectively. Therefore, taking advantage of this pandemic situation and encouraging the growth of these mini urban centers will further promote the goal of minimizing motorized traffic in the downtown area. The development of what could be called a polycentric city will gradually reduce the need for transfers and the use of private transportation.

Finally, and as a consequence of the situation produced by the COVID-19 pandemic, the interventions generated aim to achieve a more humane and sustainable city, displacing the private car as the focus of the streets and promoting more outdoor spaces for restaurant trade [14]. It is challenging to measure both the impact and usefulness of the main interventions presented in this paper. One way of evaluation could involve the analysis of the citizen's opinions, which may be associated with economic issues and local customs. On the other hand, by carrying out vehicle counts and characterizing them, it would be possible to stand an analysis of the variation in the number of private motorized vehicles. In this way, it would be possible to know if the final objective of reducing the private motorized vehicles at the city's microcenter has been achieved. In consequence, as future works, more in-depth and updated analysis would be necessary to arrive at more robust conclusions regarding the impact generated. It is known that modifications of urbanism have the power to alter the expectations of citizens about the urban environment, as well as to present an alternative way of urban life, showing what the city could, or should, be [42].

## Acknowledgement

We would like to thank architect María Álvarez Raineri for her help in clarifying some urban planning concepts.

## References

1. Singh, D., Pérez, V., Hernández C., Velázquez, M.: Movilidad pública, activa y segura. Reflexiones sobre la movilidad urbana en tiempos de COVID-19. *Prácticas de Oficio. Investigación y Reflexiones en Ciencias Sociales*, 1(25), 67-84 (2020).
2. Koszowski, C., Gerike, R., Hubrich, S., Pohle, M., Wittwer, R.: Active mobility: bringing together transport planning, urban planning, and public health. In: Müller B., Meyer G. (eds) *Towards User-Centric Transport in Europe. Lecture Notes in Mobility*, pp. 149-171. Springer, Cham (2019). doi:10.1007/978-3-319-99756-8\_11.
3. Nieuwenhuijsen, M., Khreis, H.: Car free cities: Pathway to healthy urban living. *Environment International*, 94, 251-262 (2016). doi:10.1016/j.envint.2016.05.032.
4. Pase, F., Chiariotti, F., Zanella, A., Zorzi, M.: Bike Sharing and Urban Mobility in a Post-Pandemic World. *IEEE Access*, 8, 187291-187291 (2020). doi:10.1109/ACCESS.2020.3030841.
5. Sarmiento, O., Díaz del Castillo, A., Triana, C., Acevedo, M., González, S., Pratt, M.: Reclaiming the streets for people: Insights from Ciclovías Recreativas in Latin America. *Preventive Medicine*, 103, S34-S40 (2017). doi:10.1016/j.ypmed.2016.07.028.

6. Bertolini, L.: From “streets for traffic” to “streets for people”: can street experiments transform urban mobility? *Transport Reviews*, 40(6), 734-753 (2020). doi:10.1080/01441647.2020.1761907.
7. Calloway, D., Faghri, A.: Complete Streets and Implementation in Small Towns. *Current Urban Studies*, 8, 484-508 (2020). doi:10.4236/cus.2020.83027.
8. Lydon, M., García, A.: *Tactical Urbanism. Short-term action for long-term change*. Island Press, Washington (2015).
9. Honey-Rosés, J., Anguelovski, I., Chireh, V., Daher, C., Konijnendijk van den Bosch, C., Litt, J., Mawani, V., McCall, M., Orellana, A., Oscilowicz, E., Sánchez, U., Senbel, M., Tan, X., Villagomez, E., Zapata, O., Nieuwenhuijsen, M.: The impact of COVID-19 on public space: an early review of the emerging questions – design, perceptions and inequities. *Cities & Health*, 1-17, (2020). doi:10.1080/23748834.2020.1780074.
10. Cohen, B.: Tres paradigmas de movilidad para 2020–2030 (2019/12/26). <https://iambiente.es/2019/12/tres-paradigmas-de-movilidad-para-2020-2030/>, last accessed 2021/08/18.
11. Kakderi, C., Oikonomaki E., Papadaki, I.: Smart and Resilient Urban Futures for Sustainability in the Post COVID-19 Era: A Review of Policy Responses on Urban Mobility. *Sustainability*, 13, 6486 (2021). doi:10.3390/su13116486.
12. Grassi, Y., Brignole, N., Díaz, M.: Vehicular fleet characterisation and assessment of the on-road mobile source emission inventory of a Latin American intermediate city. *Science of the Total Environment*, 792, 148255 (2021). doi:10.1016/j.scitotenv.2021.148255.
13. Mouratidis, K., Peters, S., van Wee, B.: Transportation technologies, sharing economy, and teleactivities: Implications for built environment and travel. *Transportation Research Part D: Transport and Environment*, 92, 102716 (2021). doi:10.1016/j.trd.2021.102716.
14. Mardones-Fernández de Valderrama, N., Luque-Valdivia, J., Aseguiolaza-Braga, I.: La ciudad del cuarto de hora, ¿una solución sostenible para la ciudad post-COVID-19? *Ciudad y Territorio – Estudios Territoriales*, 52(205), 653-664 (2020). doi:10.37230/CyTET.2020.205.13.1.
15. Grassi, Y., Brignole, N., Díaz, M.: Pandemic impact on air pollution and mobility in a Latin American medium-size city. *International Journal of Environmental Studies*, (2021). doi:10.1080/00207233.2021.1941662.
16. Barbarossa, L.: The post pandemic city: Challenges and opportunities for a non-motorized urban environment. An overview of Italian cases. *Sustainability*, 12(17), 7172 (2020). doi:10.3390/su12177172.
17. Alderete, M.: Determinants of smart city commitment among citizens from a middle city in Argentina. *Smart Cities*, 4, 1113–1129 (2021). doi:10.3390/smartcities4030059.
18. Universidad Tecnológica Nacional - Regional Bahía Blanca: Informe Técnico Ciclovías – MBB 2015. <http://www.bahiablanca.gov.ar/wp-content/uploads/2015/07/3.-Informe-Tecnico-UTN-Web.pdf>, last accessed 2021/07/14.
19. La Nueva, newspaper: Comenzaron a trazar una nueva ciclovía en el eje Viamonte-Darregueira (2020/11/04). <https://www.lanueva.com/nota/2020-11-4-12-38-0-comenzaron-a-trazar-una-nueva-ciclovía-en-el-eje-viamonte-darregueira>, last accessed 2021/07/14.
20. La Nueva, newspaper: El municipio midió el uso de la ciclovía de 19 de mayo que había despertado polémica (2020/10/27). <https://www.lanueva.com/nota/2020-10-27-6-30-49-el-municipio-midio-el-uso-de-la-ciclovía-de-19-de-mayo-que-habia-despertado-polemica>, last accessed 2021/07/14.
21. La Nueva, newspaper: A un mes de habilitadas, las ciclovías ganan espacios y adeptos (2020/10/03). <https://www.lanueva.com/laciudad/nota/2020-10-3-7-0-24-a-un-mes-de-habilitadas-las-ciclovías-ganan-espacios-y-adeptos>, last accessed 2021/07/14.

22. Uzunoglu, K., Uzunoglu, S.: The Importance of Pedestrianization in Cities- Assessment of Pedestrianized Streets in Nicosia Walled City. *European Journal of Sustainable Development*, 9(2), 589-614 (2020). doi:10.14207/ejsd.2020.v9n2p589.
23. La Nueva, newspaper: Se inaugura hoy la obra de peatonalización de O'Higgins, (2009/11/17). <https://www.lanueva.com/nota/2009-11-17-9-0-0-se-inaugura-hoy-la-obra-de-peatonalizacion-de-o-higgins>, last accessed 2021/07/16.
24. Municipalidad de Bahía Blanca: Semipeatonalización del centro: se firmó acuerdo para intervenir Alsina, entre Soler y Dorrego, (2017/06/06). <https://www.bahia.gob.ar/2017/06/06/semipeatonalizacion-del-centro-se-firmo-acuerdo-para-intervenir-alsina-entre-soler-y-dorrego/>, last accessed 2021/07/16.
25. Municipalidad de Bahía Blanca: Mayor espacio para circulación peatonal: comenzó el ensanchamiento de veredas en el microcentro, (2020/05/14). <https://noticias.bahia.gob.ar/2020/05/14/mayor-espacio-para-circulacion-peatonal-comenzo-el-ensanchamiento-de-veredas-en-el-microcentro/>, last accessed 2021/07/16.
26. La Nueva, newspaper: Colocaron 59 macetones con plantas en Alsina y seguirán por otras calles del centro, (2021/05/19). <https://www.lanueva.com/nota/2021-5-19-11-0-0-colocaron-59-macetones-con-plantas-en-alsina-y-seguiran-por-otras-calles-del-centro>, last accessed 2021/07/16.
27. Telefé Bahía Blanca: Colocaron macetas en Chiclana al 100 para delimitar el ensanchamiento de la vereda, (2021/06/06). <https://bahia.telefe.com/locales/colocaron-macetas-en-chiclana-al-100-para-delimitar-el-ensanchamiento-de-la-vereda/>, last accessed 2021/07/16.
28. Municipalidad de Bahía Blanca: Peatonalización de calle Anchorena: comienza la puesta en valor de la zona del Mercado Municipal, (2020/10/06). <https://noticias.bahia.gob.ar/2020/10/06/peatonalizacion-de-calle-anchorena-comienza-la-puesta-en-valor-de-la-zona-del-mercado-municipal/>, last accessed 2021/07/20.
29. La Nueva, newspaper: Callecitas del mercado: una zona histórica de la ciudad que busca reinventarse, (2020/03/14). <https://www.lanueva.com/nota/2020-3-13-10-49-0-callecitas-del-mercado-una-zona-historica-de-la-ciudad-que-busca-reinventarse>, last accessed 2021/08/20.
30. La Nueva, newspaper: "No les pedimos un puente de Madison, les pedimos que corran algunas cosas", (2020/11/12). <https://www.lanueva.com/nota/2020-11-12-18-3-0--no-les-pedimos-un-puente-de-madison-les-pedimos-que-corran-algunas-cosas>, last accessed 2021/08/20.
31. Birdsall, M.: Parklets. *ITE Journal*, 37, 37-39 (2013).
32. Telefé Bahía Blanca: Los locales gastronómicos de la ciudad podrán ampliar sus veredas (2020/08/14). <https://bahia.telefe.com/locales/los-locales-gastronomicos-de-la-ciudad-podran-ampliar-sus-veredas/>, last accessed 2021/07/16.
33. Frente a Cano: Plataformas Urbanas Removibles (o parklets) (2020/08/13). <http://www.frenteacano.com.ar/noticia/224536>, last accessed 2021/07/16.
34. La Nueva, newspaper: Bahía ya tiene su primera plataforma gastronómica y "hay más comerciantes interesados", (2020/10/30). <https://www.lanueva.com/nota/2020-10-30-10-59-0-bahia-ya-tiene-su-primera-plataforma-gastronomica-y-hay-mas-comerciantes-interesados>, last accessed 2021/08/30.
35. Frente a Cano: Mientras tanto se colocó otra plataforma urbana (2021/04/20). <http://www.frenteacano.com.ar/noticia/234143>, last accessed 2021/08/30.
36. Municipalidad de Bahía Blanca: Ordenanza 18762 - Implementando en la ciudad de Bahía Blanca el Régimen de Carriles Preferenciales para el Transporte Público de Pasajeros, (2016/11/17). <https://www.bahia.gob.ar/decretosyresoluciones/ordenanza/18762/>, last accessed 2021/08/20.

37. Rojas-Rueda, D., Morales-Zamora, E.: Built Environment, Transport, and COVID-19: a Review. *Current Environmental Health Reports*, 8, 138-145 (2021). doi: 10.1007/s40572-021-00307-7
38. La Nueva, newspaper: Opiniones y quejas por las ciclovías: las respuestas desde el Municipio, (2020/02/28). <https://www.lanueva.com/nota/2020-2-28-8-20-0-opiniones-y-quejas-por-las-ciclovias-las-respuestas-desde-el-municipio>, last accessed 2021/07/19.
39. Telefé Bahía Blanca: Ensanchamiento de veredas: ¿se adaptan los bahienses? (2020/06/17). <https://bahia.telefe.com/locales/ensanchamiento-de-veredas-se-adaptan-los-bahienses/>, last accessed 2021/07/19.
40. Vargas Tobar, Y.: Urbanismo táctico en el contexto de ciudades no resueltas. El caso de la ciudad de Barranquilla, Colombia. *Módulo Arquitectura CUC*, 24, 97-116 (2020). doi:10.17981/mod.arq.cuc.24.1.2020.06.
41. La Nueva, newspaper: Según Google, hubo un fuerte descenso de la movilidad en Bahía Blanca, (2020/10/25). <https://www.lanueva.com/nota/2020-10-25-7-0-53-segun-google-hubo-un-fuerte-descenso-de-la-movilidad-en-bahia-blanca>, last accessed 2021/07/19.
42. Sandler, D.: Grassroots urbanism in contemporary São Paulo. *Urban Design International*, 25(1), 77-91 (2020). doi:10.1057/s41289-020-00108-8.

## Technological Intelligence in Small Cities

Norela Mora<sup>1</sup>[0000-0002-4875-785X]

<sup>1</sup> Universidad Politécnica de Valencia, Camino de Vera, s/n 46022, Spain  
nomoce@doctor.upv.es

**Abstract.** The need for the benefits of innovation to permeate mainly towards the less advantaged sectors of the population has directed attention towards small cities or towns in transition towards sustainability. The aim of this research is to enable small cities to manage their assets efficiently, investing in socio-technological innovation and creativity as a way to promote sustainable and inclusive development. A methodological guide for the development of energy and water management strategies allows small cities to provide intelligence by efficiently appropriating available technologies aimed at improving the quality of life of the population, which necessarily leads to greater care for the environment and the reduction of social inequality. Towns or small cities must offer smart solutions to the challenges of contemporary urban and rural life, solutions that improve the quality of life of their citizens and the economic viability of the city. Therefore, it is not enough to apply modern ICTs to towns to make them smart. Efforts should extend to improving the ability of a given people to attract and advance their own innovation potential.

**Keywords:** Transition to sustainability. Sustainable development. Small Smart Cities. Technological and Inclusive Innovation. Technological intelligence.

### 1 Introduction

Today, more than 50 per cent of the world's population lives in urban areas, and this figure has been increasing significantly, taking into account that only 34 per cent of the world's population lived in urban areas in 1960. This is already known in Western Europe, where approximately 80% of the population will live in urban areas by 2020.

This reality gives cities a new commitment. How do they become more innovative, participatory, connected urban spaces with sustainable places without neglecting the quality of life of the populations?

The answer can be translated into several denominations, among which are: smart and/or sustainable cities; new technology communities; etc.

One thing is for sure, the intention that underlies any of these situations is to make the city a community that can be friendly in the village and for the village. The concept of "smart cities" has come to dominate both fields, both academic literature and public

2

policy. Several projects around the world are being conceived and implemented, with different characteristics, motivations, levels of maturity, governance models and funding sources. However, the goal has always been the use of information and communication technologies for a simpler urban life.

However, how can we define a Smart City? The International Data Corporation defines a Smart City as a city that has declared its intention to use information and communication technologies to transform its *modus operandi* into one or more of the following areas: energy; environment; governance; mobility, buildings and services. The main objective of a Smart City is to improve the quality of life of its citizens by guaranteeing sustainable economic growth (Lopes, I.M, Oliveira, P, 2017). This growth implies a growing demand for resources for buildings and infrastructure in urban areas. The term "Smart City" was developed only very recently. One approach to exact definition and optimal interpretation is "intelligent development." although what "smart" means to the city and its inhabitants is controversial. Each smart city design has a different approach to what "smart" or "smarter city" means and how to proceed with its specific development (Maier, 2016).

Increasing urbanization generates enormous challenges for contemporary cities, mainly that of economic efficiency and environmental sustainability. Smart city initiatives are aimed at solving these major challenges through the use of technologies and innovation, and are an opportunity for cities to rethink the way they provide their services to citizens. According to the European Parliament, smart cities can be identified and classified according to six main axes or dimensions: smart governance, smart economy, smart mobility, smart environment, smart people, and, finally, smart living. Therefore, a city can be defined as "smart" when investments in human and social capital and in transport and ICT infrastructures contribute to sustainable economic development and improve the quality of life, with a rational management of natural resources, through participatory government (Villarejo, 2015).

In short, increasing urbanization presents innumerable challenges for local governments that must develop their policies for the future taking into account the increasing number of urban inhabitants. Sustainable urbanization requires cities to generate better income and employment opportunities, expand the infrastructure needed for water and sanitation, energy, transport, information and communications; ensure equal access to services; reducing the number of people living in slums; and preserve natural assets within the city and its surroundings (United Nations, 2015).

In general terms, the concept of smart and sustainable cities or territories refers to an extensive and efficient use of technologies available in particular ICTs aimed at improving the quality of life of the population, which should inevitably lead to greater care for the environment and the reduction of social inequality. This is compatible with the concept of inclusive innovation, which roughly raises the need for innovation benefits to permeate mainly towards the less favored sectors of the population (Alvarado, 2017).

According to Givens, J.W and Lam, D. (2018) research for development in smart cities has been growing rapidly. Smart cities promise a new era of efficient, sustainable and safe living. The tools and technologies aimed at driving better public decision-making in everything, from where we live to how we work. While the world is rapidly urbanizing, a large percentage of the population still lives in smaller, rural communities. Smart City solutions as defined here are process-driven and not limited by population or geography metrics; are the application of technology and data available to improve the quality of life. Smaller communities can also be smart, and excluding or ignoring them widens inequality, limits use cases, and slows innovation.

## **2 Intelligence for small cities**

The development of a smart city is an iterative process in which cities are constantly improving their efforts to apply appropriate technologies and data. This fits very well within other results-oriented city frameworks, such as sustainable development or resilience. For example, the UN Brundtland report (1987) defines sustainability in terms of meeting the needs of current generations without endangering future generations. Smart cities can be the means to achieve sustainable development, providing the technology to achieve the goals and the data to measure whether they have been met.

Although little attention has been paid to the potential of small cities to become smarter, the definition of smart cities does not exclude the possibility. Indeed, there are almost no references to populations, sizes, densities or minimum urbanities in almost any of the definitions of smart cities. In fact, these definitions allow intelligent solutions at any scale, from people who have technology and data to improve their daily decision-making, to neighbors who meet through their community associations to address cleaning or block surveillance tasks, to regional networks that include large metropolitan areas and even, extensions across national borders.

Universities, similar in size and scale to many small cities, have become natural testing grounds for smart solutions. They have operational control and ownership over many city-like functions, from transportation to infrastructure. They also have substantial advantages over most small cities, including resources, expertise, and streamlined governance. According to Givens, J.W and Lam, D. (2018) to meet sustainability and energy goals, some universities have developed high-performance buildings and created the space to welcome the development of autonomous vehicles, such as Mcity from the University of Michigan. The success of these initiatives demonstrates the potential of smart solutions for smaller cities, but also the challenges that most such cities will face, as they lay far behind universities, especially in terms of resources, initiative and expertise.

4

Local governments of all sizes have degrees of autonomy and independence to develop their smart community, but their needs and priorities are very different from those of an urban metropolis.

As evidenced above, the Smart concept covers large cities and some of its efforts that focus on small towns have been developed in universities, but it is true that there are many small municipalities far from large cities that seek to take advantage of technological innovations for the benefit of their citizens and the environment.

## **2.1 Small Smart Cities**

The generation of research projects aimed at the development of Small Smart Cities raise the need for the benefits of innovation to permeate mainly towards the less favored sectors of the population, in which unmet basic needs such as access to basic services such as electricity and drinking water are still detected. To date, research on smart cities has focused primarily on urban congested areas. It is increasingly important to consider intermediate and sparsely populated regions, such as towns and rural areas, as spaces for digital innovation (Hosseini et al. 2018).

In a world of ever-changing (corporate) environments, disruptive digital technologies and very diverse citizen needs, the concept of smart cities has become a widely discussed topic (Hollands 2008). In general, smart cities are seen as a promising response to the urgent challenges of the twenty-first century, such as air pollution, immigration and sociodemographic problems (Klein et al., 2017). The penetration of smart cities thanks to digital technologies gives this generation the unprecedented opportunity to fundamentally reorganize urban infrastructures, whether transport or food and water supply, in much smarter ways (Ramaswami et al., 2016). Consequently, the use of modern information and communication technologies (ICTs) fosters people's exchange and connection, which can provide multiple opportunities for innovative business models (Schaffers et al., 2011).

According to the European Union's statistics office, urban areas can be represented by the so-called degree of urbanisation (DEGURBA) which divides urban areas into cities (densely populated areas), towns and suburbs (areas of intermediate nature), and rural areas (sparsely populated areas) (Eurostat 2017). Until now, research on smart cities and smart solutions has focused predominantly on densely populated areas, leaving behind towns, suburbs and rural areas. Roberts et al. (2017, p.372) note that "digital technology remains a niche topic in rural studies."

In addition, research on rural areas and development takes a strong agricultural focus and hardly considers digital technologies from an overall community and business perspective (Roberts et al., 2017). Low levels of research and development in predominantly rural areas (Toedtling and Trippel 2005) aggravate this problem, although

digital technologies and smart solutions could provide promising solutions for the future development of towns (Roberts et al., 2017).

However, recent literature even highlights the paramount importance of smart strategies and innovation in rural areas (Provenzano et al., 2016). This new focus on the social periphery is becoming increasingly important, for example, a significant proportion of the European Union's population lives in sparsely populated areas (in what are known as villages). According to DEGURBA, 28% of European residents live in these sparsely populated areas (Eurostat 2017). As Porter et al. (2004) claim that these peoples have enormous economic potential, although the gap between sparsely populated and densely populated areas is widening. Other studies have revealed that the recent success of populist candidates in democratic elections can be attributed, at least in part, to determining factors such as economic distress (Rothwell and Diego-Rosell 2016; Monnat 2016), as there is a quantifiable relationship between personal economic well-being and election results (Glasgow and Weber 2005).

Importantly, policy and research should not only consider the challenges and problems of large-scale smart cities. According to DEGURBA, one fifth of the German population lives in sparsely populated areas. This corresponds to a total of 17 million people (Eurostat 2017). A wide range of public (research) projects has illustrated the importance of digital innovations in regions where residents are more spatially dispersed. Exemplary research projects include "Smart Rural Areas" (Hess et al., 2015) or the Living Lab initiatives (Schaffers et al., 2011). However, it is worth noting that rural areas differ from cities in terms of their specific characteristics, challenges and problems. These include (but are not limited to) significantly reduced amounts of research and development, as well as the consequent grievances of little or no innovation, underdeveloped industries, missing knowledge providers, and almost no innovation assistance from administrations (Tödtling and Trippel 2005). Moreover, when looking at the digital policy agenda, rural areas tend to be more "passive and static, in contrast to the mobility of urban, technological and globalization processes" (Roberts et al. 2017, p.372). Several "domains such as teleworking, health services, logistics, mobility, agriculture, trade or education" (Hess et al., 2015, p.164) are plagued by these problems. Therefore, our definition of smart village refers to Giffinger et al. (2007) as a rural village or area that is intermediate or sparsely populated, but provides adequate and future-oriented ICT solutions to improve various domains related to economy, people, governance, mobility, environment or life.

Of course, peoples require innovation to harness the potential of digitalization. However, like cities, villages also face a complex range of specific local challenges based on their various characteristics, such as geographical, economic, social and ecological conditions. Neirotti et al. (2014) summarize such variables as factors of local context that are crucial for the development of all types of urban areas. However, solutions based on innovative digital technologies are discussed in the broad context of smart cities, which means that they do not necessarily fit the requirements of cities. Hess et al. (2015) argue that villages, compared to smart cities, have their own

6

challenges in the future since, for example, they do not have a wide availability of infrastructure services that bring individual challenges to different application domains such as logistics, mobility or education, therefore, the context must be understood. In addition, unlike villages, cities exhibit more complex structures in terms of the number of different stakeholders from various domains who must participate in smart projects (Nam and Pardo 2011). But, once again, cities can better take advantage of economies of scale and multiple business model opportunities thanks to the connection of many participants and stakeholders (Schaffers et al., 2011), while villages are characterized by smaller sizes and more dispersed populations.

Smart villages must offer smart solutions to the challenges of contemporary urban and rural life, solutions that improve the quality of life of their citizens and the economic viability of the city. Therefore, it is not enough to apply modern ICTs to people to make them smart. Efforts should extend to improving the ability of a given people to attract and advance their own innovation potential (Hosseini et al. 2018).

### **3 Context**

The term "smart cities" has been widely used in recent years. The main objective of the smart cities initiative is to enable cities to efficiently manage their assets, invest in innovation and creativity as a way to promote sustainable and inclusive urban development. When addressing an area as promising as it is emerging, it is important to know if all cities can fit into this concept, regardless of their size or location, thus promoting social equity throughout the territory (Lopes et al. 2017).

#### **3.1 The Portuguese Smart Cities Network RENER**

One of the main reasons for this research work aimed at finding out if a small/medium-sized inland city can be considered a smart city. The Portuguese smart cities network covers 46 municipalities that function as places of experimentation and development of urban solutions. This idea of sharing experiences between municipalities has already reached Spain with the creation of the Iberian smart cities network, which is currently made up of 111 cities.

RENER invested in the thematic expansion of its action, incorporating other areas such as energy efficiency, renewable energies, water and waste management, governance and citizenship, culture and tourism, all in the sense of a holistic model of smart cities.

#### **3.2 Methodology for intelligence assessment in small and medium-sized cities**

The need to develop policies that improve energy and environmental sustainability, as well as technological innovation is the basis for increasing the intelligence of cities

around the world. In the European Union, protocols were developed to measure the intelligence of cities through indicators. However, these indicators are designed for large cities and do not fit the case of small cities in a satisfactory way. Therefore, a methodology is developed to evaluate intelligence through indicators that is applicable to small and medium-sized cities. The choice of indicators is consistent with the ISO 37120 standard and is inspired by the environmental indicators used in the EU Sustainable Energy Action Plan. The proposed methodology could be seen as an expansion of governance strategies that have already been partially adopted by many cities. The methodology has been applied to 3 municipalities in northern Italy (Dall'O et al. 2017). The interest in the promotion of a Smart City protocol for small and medium-sized municipalities is given by the reasons mentioned below:

- Most projects regarding smart cities refer to large cities (e.g. Milan, Turin, Rome, Venice, Naples, etc.), however the majority of the Italian population is concentrated in small and medium-sized cities: 23% of the Italian population lives in cities with more than 100,000 inhabitants, 47.5% lives in cities of less than 20,000 inhabitants, while 31.3% live in cities with less than 10,000 inhabitants.
- It is not possible to apply the same smartness indicators used for the assessment of large cities to small and medium-sized cities. The Intelligence Assessment in these cases must be adapted and/or modified in order to meet real needs;
- Small and medium-sized cities have the opportunity to support the development of groups of citizens driven by critical thinking, whose role it is necessary to promote environmentally friendly projects, such as sustainable mobility strategies (i.e. roads equipped for electric cars, bicycle tracks, bicycles, car sharing, etc.);
- Information and Communication Technologies (ICT) has a significant contribution practically in contact with companies, citizens and other actors, as well as the provision of services that allow them to limit travel to large urban centers;
- Several small and long-term cities have committed to promoting the SEAP (Sustainable Energy Action Plan) within the framework of the Covenant of Mayors. The implementation of Smart City models can constitute a strategy to expand the governance strategies already adopted (Dall'O et al. 2017).

### 3.3 Personalized Digital Innovation for Rural Areas

The aim is to develop a first approach to digital innovation in a field that has so far hardly been considered. The authors conduct a case study, which demonstrates the applicability and effectiveness of their approach to innovation in a small town in southern Germany and derives the first important lessons learned. Therefore, the concept of an innovation ecosystem reveals a promising solution to face the challenges of the investigated city (Hosseini et al. 2018).

According to Hosseini et al. (2018) a problem-solving perspective is adopted (Nickerson and Zenger 2004) where they take the problems and challenges of smart

8

cities as the basic unit of analysis. In line with Nickerson and Zenger (2004), as well as Felin and Zenger (2014), it is argued that a reasonable method of solution can be determined by understanding and analyzing the complexity of a problem. Therefore, a multi-phase research process is followed (Fig. 5) inspired by design science research (Hevner 2007; Hevner et al. 2004). It consists of three phases: (I) considering the justifying knowledge of the problem domain and finding "problem adjustment factors" within the current scientific work on the subject, (II) developing an innovation process to derive an adequate solution after an exploratory search process, and (III) evaluating the applicability and effectiveness of the resulting innovation process to apply it to a small city.

### **3.4 Smart University: University of Alicante**

The University of Alicante, a young, plural and welcoming university, is endowed with a magnificent campus that can be comparable to most small, medium and even large Spanish cities in terms of the use and use of technologies. With a population of inhabitants formed by a diverse group of students, workers and visitors highly qualified and technologically trained that can exceed 40,000 citizens and infrastructures similar to those of any city with streets, accesses and roads, parking lots, buildings, luminaires, communications infrastructures, water and waste management, warehouses, workshops, laboratories, health center, Sports facilities, restaurants, gardens and parks, our university faces the same challenges and needs as modern cities. That is why from the university we understand that it is necessary to bet on an innovation project towards the cities of the future, which serves both for the university itself and to export to any other city (Maciá et al. 2016).

Within the university framework, the concept of Smart City, transferred to its entire community and its environment, results in the Smart University, and maintains the main objective of improving the quality of life of its community by applying IN A global, intensive and sustainable way THE IT (Information Technologies) under the principle of service to citizens. For a university of this size, it is essential to achieve the same levels of quality of life as those expected for a Smart City. Undoubtedly, the university environment is complex, sensitive and prepared enough to be more than representative of a medium-sized city, but with the great advantage of greatly minimizing the impact of the factors that can currently prevent this type of proposal from being viable in our cities. That is why it is a controlled environment, in which economic, sustainability, construction or development policies are decided locally and do not depend on external factors, although they follow criteria similar to national or international policies and strategies. In short, it is the "perfect model" of a Smart City and an ideal scenario for short-term results to be achieved, in addition to serving as a guide example and case study to address viable projects in our cities (Maciá et al. 2016).

## **4 Technical Intelligence for the transformation of the city**

### **4.1 Methodological proposal for the integration of green technologies creating Small Smart Cities**

The development of this methodology allows those responsible for the management of small cities to consider the need to evolve towards an efficient and sustainable city with technological intelligence that promotes the characteristics of each city, creating quality services for the intelligent management of water and energy.

Success lies in cooperation between the authorities and all economic and social actors, with crucial involvement of citizens. In this way, sustainability theories can become realities (Madrid Network et al. 2012).

A good part of the interest that a city arouses depends on how attractive its natural and environmental conditions are, both the urban environment itself, and the immediate environment that surrounds them. The intrinsic characteristics of a city influence the citizen when assessing its environmental attractiveness, although these may not be enough if there is no efficient management behind it. In this context, the strategy of a Smart City will be effective by assuming the intrinsic characteristics of a territory, trying to enhance its environmental attractions and mitigating or neutralizing its weaknesses, through appropriate management and environmental protection measures (Bentué, 2016).

Development is a double-edged sword. Poverty reduction, economic development and the construction of more egalitarian societies are collective achievements that in turn entail new and greater environmental and social challenges and therefore the need to reconcile the various objectives of development to keep us on the path of sustainable development. The success of economic growth requires realizing the potential that ecosystems have to meet the demands for water and energy that are essential for life and for the production and consumption processes in which water and energy intervene as non-replicable inputs (UN, 2014).

Considering together the challenges of water and energy represents a unique opportunity to create a logo in favour of the preservation of the environment to guarantee these services. A transition from the use of non-renewable resources to a greater use of renewable resources is necessary, from supply-only policies to policies to improve the use and management of available resources and from a policy of infrastructure construction to one where there is a better balance of infrastructures and conservation of ecosystems that allow the production of water and energy services to continue (UN, 2014).

A Small Smart City - SSC proposes an integrated approach where technology improves the efficiency of the city's operations, the quality of life of its citizens and the growth of the local economy through the development of energy and water management

10

estates while maintaining the balance of infrastructures and conservation of ecosystems.

According to Maciá (2016) "*The Smart Environment field focuses on the use of Green IT (Green Computing and Information Technology) to develop an intelligent environment, capable of optimizing natural resources, preserving and protecting the environment, reducing gases and waste in a sustainable way, and of controlling and rationalizing energy consumption*", this area allows generating strategies to convert the project of an SSC into opportunities for citizens, private companies and public entities.

To achieve the desired objectives, Smart Environment focuses on the following areas to which we can provide intelligence from IT solutions:

**Energy (SmartGrid)** . Consumo and energy efficiency

**Water (SmartWater)** . Control, management and optimization of water.

In short, the urban scale of a small city is ideal to promote a sector of eco-technological urban solutions, bringing together the private initiative with the public and civil society, promoting pilot projects of territorial development and urban, social, economic and environmental rehabilitation. The needs of creation, renovation and maintenance of infrastructures and services that this growth will generate can end up becoming an extraordinary destructive force for the planet if they are not addressed from a design from the beginning of the villages, an intelligent urban design combined with the sensible application of clean technologies. If we combine new ways of life and consumption habits, with intelligent urban design and with the application of green technologies for sustainable development, we can build a new generation of intelligent infrastructures and services. To provide intelligence to small cities, some transversal axes characteristic of a Smart City must be integrated, which are detailed below:

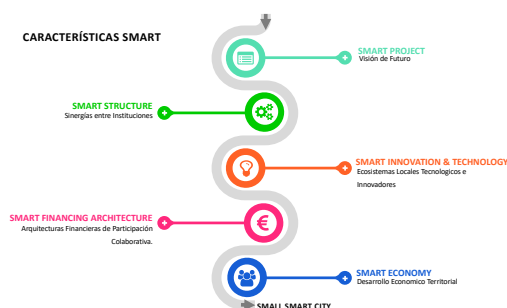


**Fig. 1.** Characteristics of an SSC.

**Smart Project.** Vision of the future in a small city that allows the design and territorial development based on an integral urban regeneration in aspects such as energy technologies and drinking water production as a commitment to the Small Smart City

with a vision of the future. Permanent process of creation, maintenance and improvement of living conditions and basic structures in order to enable all human beings to well-being within the limits of ecosystems (Sustainable Development Summit, Madrid 2006). The ultimate goal is to achieve the "sustainable city", a city whose economic, social and ecological components are harmoniously associated.

**Smart Structure.** Synergies between institutions, citizens and the private sector in order to generate integrated governance models through Smart City projects, sustainable development and transformation of city into green city, with sustainable strategies linked to the territory, produce progress and well-being for citizens. Carrying out a city project with the scope and approach proposed here requires an intelligent structure of **leadership, momentum and management**. Leadership at the local level is increasingly relevant for the growth of territorial innovation ecosystems, open and collaborative, which facilitate, encourage and promote the physical and knowledge infrastructures that constitute it as an intelligent, effective and attractive territory, and make the difference of the city as a place conducive to investment and the development of innovative economic activities.

**Smart Innovation & Technology.** Local ecosystems where collaboration between industry, government organizations and citizens allows to create a new generation in which the application and appropriation of ICTs generates sustainable development and spaces, where technological innovation is also social innovation. Innovation is the only strategy that ensures long-term sustainability, responding to the challenges of socio-economic development at the scale of the territory and promoting a greener and more sustainable economy.

**Smart Financing Architecture.** Financial architectures with formulas of public-private participation and innovative public procurement to generate economic sustainability. Public Private Partnerships (PPPs) are of particular interest to Smart City projects as it allows risks and benefits to be shared. CPP contracts are a tool that guarantees the execution and exploitation of projects while ensuring the private sector involved in them a competitive economic return. In addition, they favor innovation and allow accelerating the development of new services, of higher quality and with a greater social impact.

**Smart Economy.** New high-value economic activity based on innovation and clean technologies in the transition to the green economy. Develop a territorial economy to promote and strengthen economic development processes at the territorial level, with a focus on human development, that is, development with economic efficiency, inclusive, equitable and sustainable character. Generate national policies, territorial economic development strategies; promoting the creation and operation of Local Economic Development Agencies.

12

## 5 Conclusion

The modern human being, immersed in technology and the beauty of its versatility, has stopped looking at the past without knowing that it not only allows us to reflect on the future, but is also the reason for the evolution and existence of current technology. Therefore, it is not enough to apply modern ICTs to people to make them smart. Efforts should extend to improving the capacity of a people by appropriating their innovation capabilities.

The SSC will be a reference model to explain the interactions between the technological progress driven by the different digital vectors, the cultural change in the patterns of social behavior and industrial organization and the transformation of the management of public services. In this scenario of the appearance of innovations of different signs, both technical and institutional, we seek to establish a framework to understand in an organized and integral way a possible horizon to make the promises of personalization, optimization, adaptation in real time a reality... in the day-to-day functioning of public services and the decisions that organize and shape small cities.

It is a model that is part of a broader dynamic of change in any social sphere, from the economy and industrial development to social habits or the development of new practices of democratic deepening (Martín Patino, 2017). This research aims to shed light on the conceptual bases and their practical applications. The methodological proposal for the creation of Small Smart Cities allows to provide intelligence to small cities, solve their basic needs, guiding the action of companies, institutions and social organizations interested in contributing to urban and social development, reflecting on their deepest meanings, not only from the point of view of the digital transformation of the city, but also from its implications in society and in the aspiration to move towards cities on a human scale that offer quality of life to the population.

The SSC seeks to generate the city's own capacities, as indicated by Martín Patino, 2017, transforming individual and collective capacities to intervene in public and private affairs in a different way, through fewer or new intermediaries that can potentially create new balances with power. The distribution and access to information, forms of collective organization, the creation of projects at local level or mediation in public debates. Collective action, self-organization or co-creation are rejuvenated dynamics of this condition of the connected city at street level, and foundational elements of approaches sensitive to the social and human elements of the transformative role of smart technology.

The SSC will be even smarter than the big cities since they will be built from the experience of the past and the reflection of the future, in search of the conservation of natural assets as an inheritance for future generations. The strategy of a Small Smart City will be made effective by assuming the intrinsic characteristics of a city, and

strengthening them to their maximum potential, with a focus on building from its beginnings.

## References

1. Lopes, I. M, Oliveira, P. : *Can a small city be considered a smart city?* CENTERIS - International Conference on Project Management / HCist - International Conference on Health and Social Care Information Systems and Technologies. Procedia Computer Science Volume: 121 Pages: 617-624 (2017)
2. Maier, S.: *Smart Energy Systems for Smart City Districts: Case Study Reininghaus District.* ENERGY SUSTAINABILITY AND SOCIETY Volume: 6 Article number: 23 (2016).
3. Villarejo, H.: *Smart Cities: A commitment of the European Union to Improve Urban Public Services.* Journal of European Studies: University of Valladolid, Institute of European Studies. Spain (2015).
4. Givens, J.W, Lam, D.: *Small and Smart: Why and How Smart City Solutions Can and Should be Adapted to the Unique Needs of Smaller Cities.* NEW GLOBAL STUDIES Volume: 12 Number: 1 Special Issue: SI Pages: 21-36 (2018).
5. United Nations: *World Urbanization Prospects: The 2014 Revision,* Department of Economic and Social Affairs, Population Division, New York. Available in: <http://esa.un.org/unpd/wup/Publications/Files/WUP2014-Report.pdf> (2015).
6. Mckinsey GLOBAL INSTITUTE: *Mapping the economic power of cities.* Available in: <http://www.mckinsey.com/global-themes/urbanization/urban-world-mapping-the-economic-power-of-cities> (2011).
7. Alvarado, R.: *Smart and sustainable city: towards an inclusive innovation model.* University of Guadalajara Virtual University System Mexico. Year 7, number 13, September 2017-February 2018. e-ISSN: 2007-3607. DOI: <http://dx.doi.org/10.18381/Pk.a7n13.299>. JEL code: O32, O33 (2017).
8. Hollands, R. G.: Will the real smart city please stand up? Intelligent, progressive or entrepreneurial? *City*, 12(3), 303–320. <https://doi.org/10.1080/13604810802479126> (2008).
9. Giffinger, R., Fertner, C., Kramar, H., Kalasek, R., Pichler- Milanović, N., & Meijers, E.: *Smart cities: Ranking of European medium-sized cities.* Vienna, Austria: Centre of Regional Science (SRF), Vienna University of Technology. Available at [http://www.smart-cities.eu/download/smart\\_cities\\_final\\_report.pdf](http://www.smart-cities.eu/download/smart_cities_final_report.pdf) (2007).
10. Maciá, F., Berná, J., Sanchez, J., Fonseca, I., Guilló, A.: *Smart University: Towards a more open university.* Alicante, Spain: University of Alicante. ISBN:978-84-267-2328-4. (2016).
11. Hosseini, S., Frank, L., Fridgen, G., Heger, S.: *Do Not Forget About Smart Towns: How to Bring Customized Digital Innovation to Rural Areas.* Augsburg: Germany. Fraunhofer FIT Project Group Business and Information Systems Engineering (BISE), University of Augsburg. The online version of this article (<https://doi.org/10.1007/s12599-018-0536-2>). (2018).
12. Klein, B., Koenig, R., Schmitt, G.: *Managing urban resilience.* *Inform Spektr* 40(1):35–45. <https://doi.org/10.1007/s00287-016-1005-2> (2017).
13. Ramaswami, A., Russell, AG., Culligan, PJ., Sharma, KR., Kumar, E.: *Meta-principles for developing smart, sustainable, and healthy cities.* *Sci* 352(6288):940–943. <https://doi.org/10.1126/science.aaf7160> (2016).
14. Schaffers, H., Komninos, N., Pallot, M., Trousse, B., Nilsson, M., Oliveira, A.: *Smart cities and the future internet: towards cooperation frameworks for open innovation.* *Fut Internet* 6656:431–446 (2011).

14

15. Eurostat: Degree of urbanisation. <http://ec.europa.eu/eurostat/web/degree-of-urbanisation>. Accessed 15 Oct 2017.
16. Roberts, E., Anderson, BA., Skerratt, S., Farrington, J.: A review of the rural-digital policy agenda from a community resilience perspective. *J Rural Stud* 54:372–385 (2017).
17. To'dtling, F., Tripl, M.: One size fits all? Towards a differentiated regional innovation policy approach. *Res Policy* 34(8):1203–1219. <https://doi.org/10.1016/j.respol.2005.01.018> (2005).
18. Provenzano, V., Arnone, M., Seminara, MR.: Innovation in the rural areas and the linkage with the quintuple helix model. *Proceed Soc Behav Sci* 223:442–447. <https://doi.org/10.1016/j.sbspro.2016.05.269> (2016).
19. Porter, ME., Ketels, CHM., Miller, K., Bryden, R.: Competitiveness in rural US regions: learning and research agenda. US Economic Development Administration (EDA), Washington, D.C (2004).
20. Rothwell, JT., Diego-Rosell, P.: Explaining nationalist political views: the case of Donald Trump. Working Paper (2016).
21. Monnat, SM.: Deaths of despair and support for Trump in the 2016 presidential election. Pennsylvania State University Department of Agricultural Economics Research Brief, pp 1–8 (2016).
22. Hess, S., Naab, M., Trapp, M., Magin, D., Braun, S.: The importance of mobile software ecosystems in smart rural areas. In: 2015 2nd ACM International Conference on Mobile Software Engineering and Systems, pp 164–165 (2015).
23. Neirotti, P., de Marco, A., Cagliano, AC., Mangano, G., Scorrano, F.: Current trends in smart city initiatives: some stylised facts. *Cities* 38:25–36. <https://doi.org/10.1016/j.cities.2013.12.010> (2014).
24. Nam, T., Pardo, TA.: Conceptualizing smart city with dimensions of technology, people, and institutions. In: Bertot J, Nahon K, Chun SA, Luna-Reyes L, Atluri V (eds) the 12th Annual International Digital Government Research Conference, pp 282–291 (2011).
25. Hevner, AR.: A three cycle view of design science research. *Scand J Inf Syst* 19(2):87–92 (2007).
26. Hevner, AR., March, ST., Park, J., Ram, S.: Design science in information systems research. *MIS Q* 28(1):75–105 (2004).
27. Nickerson, JA., Zenger, TR.: A knowledge-based theory of the firm—the problem-solving perspective. *Organ Sci* 15(6):617–632. <https://doi.org/10.1287/orsc.1040.0093> (2004).

## **Desarrollo de un sistema tecnológico para el monitoreo de cultivos de agricultura familiar en transición agroecológica de la provincia del Sumapaz Colombiano.**

Roberto Ferro Escobar<sup>1</sup> & Danilo Alberto Vera Parra<sup>2</sup>

<sup>1</sup> Doctor en Ingeniería Informática de la Pontificia Universidad de Salamanca, España. Director de la Red de Investigaciones de Tecnología Avanzada y Director del Instituto de Investigación e Innovación en Ingeniería i3+ de la Universidad Distrital Francisco José de Caldas.

Bogotá Colombia  
rferro@udistrital.edu.co

<sup>2</sup> Estudiante de Maestría en Gestión Estratégica de Proyectos de la Universidad Pedagógica y Tecnológica de Colombia. Funcionario de la Red de Investigaciones de Tecnología Avanzada de la Universidad Distrital Francisco José de Caldas.

Bogotá Colombia  
social.rita@correo.udistrital.edu.co

**Resumen.** Este artículo expone el proceso y resultados de un proyecto de investigación de carácter público financiado por el Gobierno de Colombia a través del Ministerio de Ciencia, Tecnología e Innovación. En él se ha desarrollado un sistema tecnológico para el monitoreo, manejo y determinación de la diversidad funcional de arvenses asociadas a agricultura familiar en transición agroecológica de la provincia del Sumapaz Colombiano. El sistema está compuesto por una aplicación móvil, una plataforma web y una red de sensores para la medición de factores climáticos. La herramienta en su conjunto analiza información recolectada sobre abundancia, riqueza y diversidad funcional de arvenses, permitiendo la generación de diagnósticos y formulación de tratamientos sobre los hallazgos presentes en los cultivos. Nuestro proyecto se destaca como un aporte al cumplimiento de los objetivos de desarrollo sostenible de la región, particularmente a los objetivos número 11 y 12 teniendo en cuenta que las familias que intervienen se caracterizan por estar incorporando prácticas sostenibles con el fin de reducir el uso de insumos y fertilizantes químicos. Así mismo, este proyecto fortalecerá la discusión del evento, al ser una experiencia desarrollada con todos los estándares de transparencia en contratación pública bajo la relación Universidad – Estado - Sociedad.

**Palabras clave:** Entorno inteligente, TIC, Sostenibilidad.

### **1 Planteamiento del problema**

Los sistemas productivos agropecuarios familiares de países tropicales actualmente atraviesan una situación crítica, la afectación y el cambio en la distribución y diversidad de especies vegetales en zonas de bosque está llevando a transformaciones del paisaje, aumentando la probabilidad de que los suelos estén más áridos (Bastos et al, 2016). Los

problemas se agravan con los cambios inesperados del clima (altas precipitaciones y sequías prolongadas) como parte del cambio climático, con efectos diferentes según la zona de vida; por ejemplo, en zonas de trópico húmedo, los suelos se saturan de agua, lo cual está ocasionando problemas en la disponibilidad de forrajes, pérdida de especies tanto animales como vegetales por inundación de áreas extensas de tierra, compactación y erosión de suelos, entre otros (Villanueva et al., 2009).

Las situaciones descritas anteriormente son debido en parte, a que la mayoría de productores agropecuarios se caracterizan por hacer mal uso de los recursos naturales y adicionalmente por causar problemas ambientales tales como la deforestación, ampliación de la frontera agrícola, monocultivos en especial pastos, quemados que conllevan a la erosión, pérdida de la diversidad y contaminación de las fuentes hídricas (Arboleda et al., 2013). Es por esto, que tanto los sistemas agrícolas, pecuarios y agropecuarios se están convirtiendo en un problema ecológico, están atentando contra la sostenibilidad de los ecosistemas (Arboleda et al., 2013), e igualmente sobre la soberanía alimentaria y la calidad de vida de la población rural (Muñoz-Espinosa et al., 2016). En América Latina y el Caribe, la ganadería vacuna es una de las principales aplicaciones de la tierra (FAO 2008), en donde una parte considerable de esta actividad se caracteriza por sus bajos niveles de productividad y rentabilidad, así como por la generación de efectos ambientales negativos como los que se mencionaron anteriormente, convirtiéndose en una de las grandes causas de la pérdida de especies vegetales, ocurriendo igualmente en la región del Sumapaz (FAO, 2010). De la misma manera Harvey et al. (2008), indican, que en América latina se vienen presentando incrementos muy significativos en las tasas de deforestación, acompañados de procesos de degradación de suelos, fragmentación de paisajes, pérdidas de biodiversidad y reducción del nivel de ingresos.

Por lo que concierne a Colombia los sistemas de producción se han generado a partir del cambio en el uso del suelo, la deforestación de bosques, erradicación y eliminación de gran cantidad de especies vegetales útiles en la producción animal y propagación de pastos en forma de monocultivo ocasionando la pérdida de la fertilidad del suelo, baja calidad de las pasturas, incremento de las emisiones de los gases de efecto invernadero (GEI) y la baja productividad de las fincas (Navas, 2007). Autores como Ramírez et al. 2005 señalan que los sistemas de producción animal en el trópico se basan en el uso de gramíneas forrajeras en monocultivos que causan degradación de las especies nativas y disminuyen la sostenibilidad de estos sistemas. Esto lo corrobora Macip et al. (2013) quienes mencionan que la transformación de los ambientes naturales hacia ambientes manejados como cultivos o pastizales conlleva a un impacto directo en la abundancia de las especies que ahí habitan y por consiguiente en la productividad de los sistemas.

Al respecto, en la provincia del Sumapaz no son ajenos todos estos problemas mencionados. La Cámara de Comercio de Bogotá (CCB), indicó que para el 2008 cerca del 28,6% del área total de la región; alrededor de 52.523 ha., estaban cubiertas por pastos (manejados o naturales), ocupadas por una población bovina de tan solo 43.669 cabezas, lo que representa 1,2 hectáreas por animal. De igual manera la FAO, (2010) señala

la ineficiencia que presenta la ganadería en la región del Sumapaz, indicando que la capacidad de carga era para esa época de apenas 1,5 animales por hectárea.

Estos datos revelan el inadecuado uso que se da a los recursos naturales, destacándose que cada vez más tierras con vocación agrícola están siendo destinadas para la ganadería, dejando así a la provincia como una de las menos competitivas a nivel agropecuario frente a las demás provincias del departamento de Cundinamarca. Sumado a este contexto, la mayoría de los productores subestiman el recurso vegetal local, ya que desconocen la gran variedad de arvenses que se encuentran en la zona y con ello el uso potencial que podrían tener estas en el agroecosistema.

La provincia del Sumapaz representó en el 2005 el 6.6 % del PIB de Cundinamarca, que a su vez presentó el 5.23% del PIB Nacional, siendo el municipio de Fusagasugá el del PIB más alto (61.1 %), seguido por Silvania (8.9 %) del total provincial. La vocación productiva se encuentra asociada a la construcción, el transporte, a la actividad agrícola en general y a la pecuaria especialmente en los subsectores bovinos (carne y leche), porcinos, y avícolas (postura y engorde) La producción agrícola semestral es de minifundio y atiende básicamente la seguridad alimentaria de los habitantes de los municipios que ocupan el ADR y los excedentes de la producción se comercializan principalmente con Bogotá (MINAGRICULTURA, 2010).

Según las evaluaciones agrícolas municipales del Ministerio de Agricultura en el año 2010 el área total agrícola del ADR fue de 19.007 Has cosechadas, equivalentes al 6,99% del área agrícola de Cundinamarca y al 0,49% del área agrícola nacional (Fig. 1).

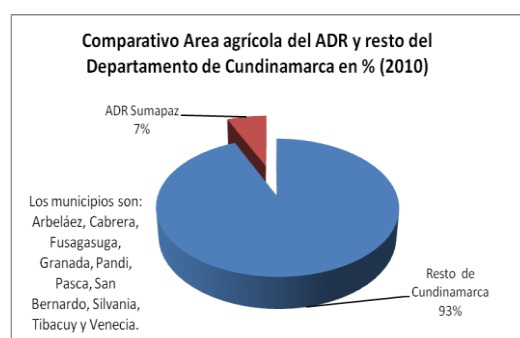


**Fig 1.** Comparativa área agrícola. Fuente: MINAGRICULTURA, 2010.

La mayor parte de los cultivos semestrales son de seguridad alimentaria y de gran importancia para los pobladores, como son: papa, maíz, arveja y frijol. En cultivos semi-permanentes están: mora, granadilla, gulupa, lulo, Maracuyá y Uchuva; los cultivos

permanentes: café, tomate de árbol, aguacate, banano y Pitahaya. Sin embargo, las producciones mencionadas (en más del 80%), se caracterizan por la aplicación excesiva de agroquímicos y plaguicidas, quema de residuos sólidos, implementación de monocultivos, así como la producción pecuaria intensiva (ICA, 2010).

En la provincia del Sumapaz existe una crisis agrícola, ya que prevalecen los sistemas de producción convencional y no se han implementado estrategias participativas permanentes y continuas con las familias campesinas. En los POTs de los municipios se contemplan políticas públicas encaminadas “hacia el uso sostenible de los recursos naturales”, pero en realidad estas no se articulan con la situación actual de la región, así como es evidente la falta de políticas orientadas hacia la implementación de sistemas agroecológicos.

## **2 Desarrollos tecnológicos referentes**

Hoy en día la producción familiar debe ser eficiente, productiva y sostenible Roa et al. (s.f.), teniendo en cuenta la conservación y la buena gestión de los recursos naturales en especial el vegetal. Por esta razón, es necesario cambiar el manejo de las producciones hacia sistemas más sostenibles (Zapata et al., 2017), que representan, en teoría y práctica, una opción importante para la producción alimentaria en Latinoamérica, con un mejoramiento significativo del sistema (Clavero y Suárez, 2016), de igual manera es necesario empezar a optar por la generación de servicios ambientales (Zapata et al., 2018) y la identificación de especies arvenses adaptadas a cada zona, para ser incluidas en los sistemas de producción agropecuarios, siendo éstas, alternativas de producción que mejoran y superan la producción convencional.

Investigaciones como las de Sosa et al., (2015); Chamorro et al., (2015); Hernandez-Melo (2016); Arboleda et al., (2016); Cano et al., (2016); Ortiz et al., (2017); Russi et al., (2017), se enfocaron en la identificación, evaluación y caracterización de especies arvenses con potencial forrajero, encontrando que existe en las unidades de producción ubicadas en regiones del trópico alto y trópico bajo colombiano, especies con alto potencial para la producción animal, resaltando la gran diversidad genética que se puede encontrar y el aporte que ésta brinda para el desarrollo productivo. Además, hallaron que existen especies con más de seis usos aprovechables.

Por lo expuesto anteriormente es indispensable empezar a valorar la diversidad vegetal con potenciales usos (forrajero, medicinales, alelopáticas, etc), ya que si se sigue desaprovechando y perdiendo, habrá una gran limitación en la producción, y la capacidad de respuesta ante las nuevas necesidades será nula (Toral et al, 2018), esto demuestra la importancia que presenta la prospección y colecta de materiales nativos y/o naturalizados (Toral et al, 2018), con el fin de rescatar estos recursos y otras especies de interés. Murgueitio, (2017) también resalta que es de vital importancia utilizar especies nativas para garantizar su adaptabilidad y formar de esta manera ecosistemas sostenibles integrados para cada zona.

Respecto a los desarrollos tecnológicos que se integran a las dinámicas agrícolas para dar solución a problemas puntuales, es importante hacer una revisión de los más importantes y cercanos a nuestro objetivo de investigación.

Agricultura Inteligente o Smart Farming es el nombre que recibe la implementación de Tecnologías de la Información y Comunicación (TIC) en la agricultura, la cual tiene sus bases conceptuales en Smart Cities, lo cual se ha llegado incluso a abordar como la tercera revolución verde. Estas implementaciones incluyen sistemas de gestión de la información, georreferenciación, agricultura de precisión, automatización, entre otras. La universidad de California Davis (UC Davis) realiza un proyecto de investigación en el cual integran sistemas de última tecnología en cámaras para reconocer por medio de fotografías aéreas el estrés de los cultivos que es producido por la presencia de plagas. Las fotografías son tomadas por drones y el análisis se hace por medio de la luz que arrojan los cultivos, la cual es diferente en el caso de cultivos sanos a cultivos estresados por la presencia de ácaros e insectos. Realizando una analogía con los seres humanos para entender de manera más sencilla el proyecto, las plantas sufren “fiebre” cuando están siendo atacadas por plagas y esto se refleja en cambios de color que en principio no pueden ser detectados por el ojo humano ya que nuestro sistema no cuenta con una sensibilidad al cambio de color tan avanzada. Por otra parte, el análisis toma en cuenta los cambios en las características de reflectancia brindando la posibilidad de generar un diagnóstico asociado al factor causante del estrés.

Recientemente, al prototipo le fue agregado un sistema de iluminación para poder mejorar el monitoreo durante horas de la noche, permitiendo eliminar sombras que interfieren en los análisis de imágenes y mejorar el proceso de procesamiento durante la noche para poder ofrecer resultados a los cultivadores en horas de la mañana. Por último, el equipo de investigadores está trabajando en un prototipo que pueda ser instalado en rieles para poder realizar monitoreo desde el suelo donde las cámaras, la captura de datos y su almacenamiento serán manejadas de manera autónoma por un software. Continuando con los prototipos que incluyen drones, el Centro de Investigación Científica y de Educación Superior de Ensenada (CICESE) en Tepic, México, desarrolla un sistema que incluye tres (3) software para la detección, análisis y diagnóstico de plagas en cultivos de Sorgo. El primero identifica patrones de la plaga del plugón amarillo que afecta este tipo de cultivos, a partir de imágenes capturadas con drones que son enviadas al segundo software, el cual conforma una base de datos contando con un sistema inteligente de agricultura para generar un diagnóstico. Por último, el tercer software cuenta con una biblioteca de información agrícola que le permite emitir alertas y sugerir acciones que mejoran el diagnóstico.

Por su parte, un equipo de investigadores de la Ciudad de Veracruz creó un dispositivo capaz de identificar enfermedades analizando tan solo un fragmento de un centímetro cuadrado de la hoja de la planta. Este dispositivo tiene el nombre de Biocorder, recibe el fragmento de planta y realiza un análisis químico de sus componentes, sus creadores indican que a nivel humano es similar a una biometría hemática en la cual se identifican células presentes en la sangre por medio de una muestra. Al igual que los sistemas de

identificación de imágenes tomadas con drones, este dispositivo detecta las enfermedades en los cultivos antes de que sea identificado por el ojo humano.

En Perú, el Centro de Diagnóstico del Servicio Nacional de Sanidad Agraria informó a finales del año 2017 que a partir del año 2018 implementaría una nueva técnica para acelerar el proceso de reconocimiento de plagas y disminuir los tiempos de diagnóstico por medio del código de barras del ADN del insecto que ataca el cultivo. Los tiempos de reconocimiento se logran disminuir de entre uno y tres meses a una semana ya que se trabaja con material genético obtenido de muestras en cualquier estado de desarrollo del insecto y no con insectos adultos como se trabaja con el método tradicional.

El 29 de agosto de 2017 el diario EL TIEMPO titulaba en su edición digital “Ya utilizan drones para monitorear cultivos de palma africana”. En este artículo se realiza seguimiento al proyecto que lidera el Grupo de Investigación y Desarrollo Aeroespacial (Gida), en compañía del Departamento de Ingeniería Mecánica y Mecatrónica y Departamento de Ingeniería Agrícola de la Universidad Nacional. El proyecto utiliza cámaras multispectrales que por medio de drones capturan fotografías aéreas para monitorear las condiciones en las que se encuentran los cultivos de palma africana.

Se puntualiza que este sistema no es nuevo, pero su aplicación en Colombia sí lo es, razón que lo hace llamativo por sus posibilidades de replicarse en otros escenarios. Al igual que en los proyectos europeos, las cámaras logran detectar ondas de luz que no son percibidas por el ojo humano, generando índices de seguimiento para establecer posible presencia de plagas en los cultivos o en segmentos del mismo. Se explica en este artículo que la idea de los investigadores es construir índices propios para este tipo de cultivos que conlleven a optimizar la gestión en el campo y evitar situaciones adversas que se puedan presentar con la presencia de enfermedades y plagas.

Desde la Universidad Nacional de Colombia, sede Palmira, se desarrolló el proyecto de investigación y desarrollo tecnológico llamado “Diseño de herramientas de tecnología móvil para parcelas vitícolas del municipio de Ginebra” por medio del cual se desarrolló una aplicación móvil que reporta plagas y enfermedades en uva Isabella, producto cultivado en esta zona del país, siendo Ginebra el municipio con mayor extensión de este tipo de cultivos.

MipUN es el nombre de la aplicación móvil y está dirigida a agricultores, este sistema recopila información de cultivos con datos puntuales como su nombre común, científico, familia, clase, entre otras. Así mismo, cuenta con información de las plagas más comunes que afectan a los cultivos de uva Isabella, también ofrece información de variables a tener en cuenta para la siembra del mismo, como por ejemplo humedad, altitud, calidad de los suelos, temperatura ideal, luz, humedad, entre otros.

Adicionalmente a las aplicaciones o sistemas que se han visto hasta el momento, recientemente ha llamado la atención de diferentes medios la introducción de la tecnología conocida como internet de las cosas o IoT por sus siglas en inglés en el campo

colombiano, la cual acerca a las personas a elementos de uso cotidiano. Al igual que se identificaban prácticas de inmersión de actividades de las ciudades inteligentes en Europa y otros países en el agro, se da un proceso similar en Colombia con el internet de las cosas, sustento conceptual de las Smart Cities, entre otras.

El pasado 27 de febrero de 2018 el diario El Espectador titulaba en uno de sus artículos de su portal web, “Internet de las cosas da sus primeros pasos en el agro colombiano”. Allí se realiza una entrevista a Andrés Sánchez, CEO de identidad IoT, el cual explica el potencial que estas tecnologías tienen en el campo colombiano.

Manifiesta que la implementación se ve reflejada en la agricultura de precisión, la cual ofrece a los cultivadores herramientas con las cuales hacer seguimiento en tiempo real de variables meteorológicas, así como de factores que afecten sus cosechas y pongan en riesgo su productividad. Identidad IoT inició una solución de agricultura de precisión en fincas cafeteras del municipio de Chinchiná, Caldas. Allí realizarán monitoreo de cultivos de café tipo Caturro con el fin de evaluar variables como humedad, precipitaciones, temperatura, entre otras. Esto por medio de la instalación de 10 sensores que permitirán analizar si las variaciones en las variables medidas inciden en la proliferación de plagas o enfermedades en las cosechas.

### 3 Metodología de trabajo en campo

Antes de iniciar el proceso de desarrollo de la aplicación móvil se debió realizar un trabajo de muestreo y análisis de laboratorio de las arvenses encontradas en la zona de estudio, para posteriormente tipificarlas y generar un insumo ideal para la programación tecnológica.

Para la realización de este proyecto se vincularon 12 familias que se encuentran ubicadas en los Municipios de Fusagasugá, Silvania y Pasca. La diversidad florística fue analizada mediante los índices de diversidad índice de Shannon-Wiener ( $H'$ ) que es una medida de la heterogeneidad  $H' = -\sum p_i \ln(p_i)$ ,  $E = H' / \ln(S)$ , el índice Simpson ( $D$ ), que es una medida de la dominancia que se enfatiza en las especies más comunes y reflejan más la riqueza de especies.  $D = \sum [n_i(n_i - 1) / N(N-1)]$  (Melo y Vargas 2003) Dónde:  $H'$  = Diversidad de Shannon,  $p_i = (n_i / N)$  = abundancia proporcional (relativa),  $E$  = Uniformidad de Shannon,  $S$  = Número total de especies en el muestreo,  $N$  = Número de individuos totales,  $n_i$  = Número de individuos de iésima especie (Melo y Vargas 2003)

Para comparar la similitud florística cualitativa entre las las zonas se calculó el coeficiente de similitud de Jaccard, basado en la presencia/ausencia de especies, mediante el uso el programa estadístico PAST 3.0. versión libre y para las pruebas de normalidad y de inferencia se utilizó la versión libre del programa InfoStat/L.

#### 4 Resultados y tipificación

En el área evaluada, se registraron 96 especies pertenecientes a 32 familias y 3 clases taxonómicas, Liliopsida, Magnoliopsida y Pteridopsida (Tabla 1). La clase Liliopsida o monocotiledonea presento 3 familias, con 17 especies en total, 11 para la familia Poaceae, tres de la familia Cyperaceae y tres de la familia Commelinaceae. De las Magnoliopsidas se registraron 27 familias, destacándose las familias Asteraceae con 18 especies, seguida de Lamiaceae con 8 especies y Amarantaceae con 5; familias como Polygonaceae, Solanaceae, Brassicaceae, malvaceae y Plantaginaceae presentaron 4 especies cada una (Figura 1), mientras que de la clase Pteridopsida solo se encontraron 2 especies en dos familias Polypodiaceae (1) y Pteridaceae (1).

**Tabla 1.** Listado de especies encontradas en 12 unidades agrícolas del Sumapaz

Especie	Familia.	Localidad											
		Huerto Eduardo	Sabarain	Crisanto	La esperanza don Alberto	San nedro	Alto de Rosas	Doña gloria	Doña Flor	Lote 1 tibacuy	Floriberto	El recreo Tibacuy	El arbolito Sardinias
Hypoestes phyllostachya Baker	Acanthaceae												5
Iresine diffusa Humb. & Bonpl. ex Willd.	Amarantaceae												6
Alternanthera cf albotomentosa Suess	Amarantaceae												
Amaranthus dubius Mart. ex Thell.	Amarantaceae				2								
Cyathula achyranthoides (Kunth) Moq.	Amarantaceae	8											
Dysphania ambrosioides (L.) Mosyakin & Clemants	Amarantaceae												
Spananthe paniculata Jacq.	Apiaceae												
Hydrocotyle bonplandii A.Rich.	Araliaceae							0					
Acmela sp	Asteraceae			5							5	5	
Acmella oppositifolia (Lam.) R.K.Jansen	Asteraceae		5										
Ageratum conyzoides (L.) L.	Asteraceae		6										

Artemisia vulgaris L.	Asteraceae	0 3	5																		
Aspilia aurantiaca Griseb.	Asteraceae												1							5 6	
Bidens pilosa L.	Asteraceae	2	7	9																3 5	4
Cotula australis (Sieber ex Spreng.) Hook.f.	Asteraceae						0														
Emilia fosbergii Nicolson	Asteraceae																				
Erechtites valerianifolia (Link ex Wolf) Less. ex DC.	Asteraceae																				
Erigeron bonariensis L.	Asteraceae	5		0	2		5														
Galinsoga parviflora Cav.	Asteraceae	3	5				1														
Galinsoga quadriradiata Ruiz & Pav.	Asteraceae	3					8								0					5	
Jaegeria sp	Asteraceae						5														
Pseudelephantopus spicatus (B.Juss. ex Aubl.) Rohr ex C.F.Baker	Asteraceae	1 0																			5
Sigesbeckia cf orientalis L.	Asteraceae	2 7																			2
Sonchus asper (L.) Hill	Asteraceae			3					9 0	0	4										
Synedrella nodiflora (L.) Gaertn	Asteraceae												7								
Taraxacum campylodes G.E.Haglund	Asteraceae	4																			
Impatiens balsamina L.	Balsami- naceae																				0
Tecoma stans (L.) Juss. ex Kunth	Bignonia- ceae																				
Capsella bursa-pastoris (L.) Medik.	Brassica- ceae								0												
Cardamine sp.	Brassica- ceae																				
Lepidium bipinnatifolium Desv.	Brassica- ceae				5																
Raphanus raphanistrum L.	Brassica- ceae		5		8										2						
Astrephia chaerophylloides (Sm.) DC	Caprifolia- ceae	8 6																			







## 5 Desarrollo de aplicación móvil

Teniendo como insumo principal la tipificación de arvenses que se realizó, el proyecto se encuentra en un punto en el que se procederá a realizar el desarrollo de la aplicación móvil que será manejada por las familias en transición agroecológica con el fin de contar con una herramienta que los acompañe en el proceso de identificación y tratamiento de arvenses.

El desarrollo seguirá los siguientes procedimientos:

**Fase de Análisis.** Se deben analizar los requerimientos funcionales y no funcionales del aplicativo, se define la tecnología y lenguajes de programación a usar, se definen los roles de usuario y estandarización a utilizar en el diseño de la aplicación.

**Diseño gráfico.** Inicialmente se hace el modelado de visual mediante un prototipo funcional del aplicativo y del sitio web en un software de diseño de apps móviles (Adobe XD, illustrator o figma). El prototipo funcional conlleva los siguientes pasos.

- a) Wireframes como modelos bases para guía del diseño de la aplicación.
- b) Diseño propuestas visuales de los layouts siguiendo los estándares de desarrollo móvil y estándar definido en la fase de análisis.
- c) Unificar los diseños mediante un prototipo funcional ejecutando en navegador o en aplicación nativa.
- d) Documentación completa de procesos y diseños.

**Diseño del software.** En la fase de diseño del software se realizan y documentan procesos referentes a diagramas UML, diseño de la base de datos con modelo entidad relación y demás anexos pertenecientes al diseño del software, una vez documentado esta fase se procede a comenzar con el desarrollo Frontend de la aplicación.

**Fase de desarrollo.** En la fase de desarrollo del Frontend se recolectan los diseños y el prototipo previamente realizado en la fase de diseño gráfico, de allí se mediante el entorno de desarrollo seleccionado se da inicio con la parte visual de la aplicación, desarrollando cada una de las vistas de la aplicación móvil, de manera alterna se llevará acabo la creación de toda la base de datos a utilizar en el proyecto, de manera que sea completamente administrable y sin problemas de seguridad o duplicidad de datos.

Teniendo esos procesos avanzados en su mayor parte, se procede a realizar la conexión entre las dos partes verificando funcionalidad del sistema con cargue de datos, consultas, almacenamiento y demás funcionalidades.

Una de las partes más importantes de la aplicación móvil es poder crear una algoritmo selector e identificador de arvenses, para ellos se debe usar la documentación previamente analizada en el documento de identificación de arvenses. En esta fase de debe de

tener en cuenta todas y cada una de las posibilidades que se tienen para dicha identificación.

En este proceso se debe crear la página web para poder visualizar los datos entregados por la estación meteorológica y en conjunto se deben hacer las conexiones pertinentes para lograr el correcto funcionamiento y conexión con la estación.

Fase de implementación y pruebas. En esta fase se deben realizar un test completo de la aplicación, verificando temas de experiencia de usuario e interfaz de usuario, así mismo como la funcionalidad de todos los módulos y conexiones mediante un simulador.

Realizar manuales de usuario y manuales técnicos que ayuden a comprender el funcionamiento y uso de la aplicación.

Posteriormente llega el despliegue de la aplicación y su publicación por Google play, y generando links de descarga para el uso.

## 6 Resultados esperados

- a) Determinación de la diversidad de arvenses y usos potenciales en los sistemas agrícolas familiares.
- b) Caracterización cualitativa de metabólicos secundarios relevantes en arvenses dominantes.
- c) Caracterización socio económica de la población participante en el proyecto.
- d) Transferencia de conocimiento por medio de la participación en eventos académicos internacionales
- e) Monitoreo de variables meteorológicas

## Referencias

Arboleda, D., Tombe, A., Morales-Velasco, S., & Vivas-Quila, N. J. (2016). Propuesta para el establecimiento de especies arbóreas y arbustivas con potencial forrajero: en sistemas de producción ganadera del trópico alto colombiano. *Biotecnología en el Sector Agropecuario y Agroindustrial*, 11(1), 154-163.

Baldosano, H. Y., Castillo, B., Elloran, C. D. H., & Bacani, F. T. (2015). Effect of Particle Size, Solvent and Extraction Time on Tannin Extract from *Spondias purpurea* Bark Through Soxhlet Extraction. In *Proceedings of the DLSU Research Congress* (Vol. 3).

Bertin, C., Yang, X., & Weston, L. A. (2003). The role of root exudates and allelochemicals in the rhizosphere. *Plant and soil*, 256(1), 67-83.

Clavero, T & Suarez, J (2016). Limitaciones en la adopción de los sistemas silvopastoriles en Latinoamérica. *Pastos y Forrajes*, 29 (3)

FAO. (2011). Marco estratégico de mediano plazo de cooperación de la FAO en agricultura familiar en América latina y el caribe 2012-2015.

FAO. (2014) Año internacional de la agricultura familiar (AIAF).

FAO-BID, (2007). Políticas para la agricultura familiar en América Latina y El Caribe. Eds. Soto-Baquero, F.; Fazzone, M. R.; Falconi, C. Santiago de Chile. Oficina regional de la FAO para América Latina y el Caribe.

Hernandez V., Melo, M. J., & Plazas, G. (2016). Malezas asociadas a los cultivos de cítricos, guayaba, maracuyá y piña en el departamento del Meta, Colombia. *Revista de Ciencias Hortícolas*, 9(2), 247-258.

Huidobro, M (2011). La tecnología de proximidad NFC. *Antena de telecomunicación*, ISSN 2481-6345, N°. 183 (SEP), 2011, págs. 64-66.

IPCC. (2007), Cambio climático y biodiversidad.

Muñoz-Espinosa, M., Artieda-Rojas, J., Espinosa-Vaca, S., Curay-Quispe, S., Pérez-Salinas, M., Nuñez-Torres, O., & Carrasco-Silva, A. (2016). SUSTAINABLE FARMS: INTEGRATION OF AGRICULTURAL SYSTEMS. *Tropical and Subtropical Agroecosystems*, 19(2).

Orozco, Óscar Arley, & Llano Ramírez, Gonzalo. (2016). Sistemas de información enfocados en tecnologías de agricultura de precisión y aplicables a la caña de azúcar, una revisión. *Revista Ingenierías Universidad de Medellín*, 15(28), 103-124.

Ortí, C. B. (2011). Las tecnologías de la información y comunicación (TIC). *Univ. Val., Unidad Tecnol. Educ.*, (951), 1-7.

PND, (2014). PROGRAMA DE AGRICULTURA FAMILIAR.

Sánchez Duarte, Esmeralda (2008). LAS TECNOLOGÍAS DE INFORMACIÓN Y COMUNICACIÓN (TIC) DESDE UNA PERSPECTIVA SOCIAL *Revista Electrónica Educare*, vol. XII, 2008, pp. 155-162 Universidad Nacional Heredia, Costa Rica.

Seguí, M. J (2012). Aplicaciones prácticas de NFC. *Revista de investigación 3 Ciencias*

Toral, O. C., Navarro, M. & Reino, J. (2018) Prospection and collection of species of interest for livestock production in two Cuban provinces. *Pastos y Forrajes*, 38. (3):157-163

Wambui, C., A. Abdulrazak, & Q. Noordin. (2006). Performance of growing goats fed urea sprayed maize stover and supplemented with graded levels of *Tithonia diversifolia*. *J. Anim. Sci.* 19:992-996.

Zapata, Á., Murgueitio, E., Zuluaga, A. F., Ibrahim, M., & Mejía Avila, C. (2017). Efecto del pago por servicios ambientales en la adopción de sistemas silvopastoriles en paisajes ganaderos de la cuenca media del río La Vieja, Colombia.

